Evolution of cranial shape variation in strepsirhine primates

Thesis submitted in fulfilment of the degree of Doctor of Philosophy in Biological Anthropology

Department of Anthropology

University College London

Gemma Price

2015

I, Gemma Price confirm that the work presented in this thesis is my own. Where information has been derived from other sources, I confirm that this has been identified in the thesis.

– Acknowledgements –

I would like to thank my supervisors Dr. Christophe Soligo and Dr. Anjali Goswami for all of their excellent guidance and support over the past 5 years. I would also like to thank Dr. Jeroen Smaers for all of his help relating to, and the use of, his method. I am grateful to the following people for kindly granting access to primate osteological collections: Roberto Portela Miguez and Louise Tomsett (Natural History Museum, London), Jacques Cuisin (Muséum national d'Histoire Naturelle, Paris), Dr. Frieder Meyer and Nora Lange (Museum für Naturkunde, Berlin), Darrin Lunde (Smithsonian Institution National Museum of Natural History, Washington DC). I also thank my funding bodies, the Natural Environment Research Council and University College London, for allowing me to pursue this degree and research project.

A heartfelt thank you to my lovely friends and colleagues in the Aiello Lab at UCL, they have shown me such kindness and support (but never made tea).

Finally, the biggest thank you goes to my friends and family, who have stood by me with endless encouragement and patience, I simply could not have done this without them. Jacqui Caine, Kt Brinsmead-Stockham and Nick Thompson all deserve a special mention, as, of course, do my wonderful Mum and Dad, I will be forever grateful and forever in their debt.

– Abstract –

The strepsirhine cranium has received relatively little attention compared to that of its haplorhine sister clade. Where it has been subject to investigation, studies have tended to focus on a narrow range of species and/or include limited sample sizes. The current study investigates the evolution of the extant strepsirhine cranium using large sample sizes and a broad taxonomic range, focusing on modularity, allometry and phylogenetic signal to better understand the evolutionary pathways that have shaped its morphology. The data consist of 60 3D morphological landmarks, collected using a Microscribe MX, from the crania of 1633 adult strepsirhine specimens, across 20 genera and 30 species.

The effect of reduced sample size on estimates of size and shape parameters was investigated for six species and found to be constant across taxa. Estimates of size parameters remained accurate, while estimates of shape parameters and of the angles between allometric trajectories became increasingly inaccurate as sample size was reduced. Further analyses were therefore limited to species with sample size above 20.

Common patterns of modularity and allometry were found both within and across species. The cranium is best divided into two modules (face, neurocranium), and within those into a further six modules (face, orbit, oral, zygomatic, vault, base). Strepsirhines follow the general mammalian allometric pattern, with smaller taxa having a more paedomorphic appearance, although some differences were apparent between lorisiforms and lemuriforms. Strong phylogenetic signal is present in all cranial modules, as measured by Pagel's λ and Blomberg's *K*, with evidence that signal is strongly linked to size. Overall, the evolutionary pathways of the strepsirhine cranium are shown to be conserved, with comparative data suggestive of stabilising selection in extant lineages. Where species have diverged from the common pattern, this is attributed to selection for specialised diet or variation in activity pattern.

– Contents –

– Tables –

– Figures –

Chapter 4: The presence and influence of modularity in the crania of the Strepsirhini

Chapter 5: Allometric patterns in the cranium of the Strepsirhini

Chapter 6: Phylogenetic signal and models of evolution in the strepsirhine cranium

– Chapter 1 –

Introduction and literature review

1.1. Overview

This research investigates strepsirhine cranial morphology, using geometric morphometric (GMM) and phylogenetic comparative techniques. Three key, inter-relating, morphological topics, namely modularity, allometry and phylogenetic signal are explored in detail, with the aim of increasing the understanding of the evolutionary development of the cranium, across a broad range of strepsirhine taxa. In addition, the influence of reduced sample size on a range of geometric morphometric size and shape parameters is examined and interpreted with regard to this research and wider GMM studies. The four main data chapters are outlined below:

The effect of reduced sample size in geometric morphometric studies of size and shape

The influence of reduced sample size on estimates of commonly used GMM shape parameters is investigated in all family groups (except the Lepilemuridae), including: mean size, standard deviation of size, total shape variation, mean shape, variation in mean shape, variation in allometric trajectories and the percentage of shape variance explained by size.

Size parameters and total shape variance were found to be largely unaffected by reduced sample size, but the accuracy of other parameters was significantly reduced. Results were consistent across all taxa. The findings are discussed with regard to this research and their wider implications.

The presence and influence of modularity in the crania of the Strepsirhini

Four different modularity hypotheses are investigated, at both an intra- and inter-species level, including two, three, and two separate six module hypotheses. Hypotheses were tested using RV_M coefficient scores; within module correlation and overall integration were also investigated at an intra-species level.

Results indicate low overall integration and high levels of modularity across taxa. The most strongly supported modularity hypothesis was the six module model

(Goswami, 2006a), with modules corresponding to the dentition and face were found to be the most strongly integrated.

Allometric patterns in the crania of the Strepsirhini

Intra- and inter-species analyses were conducted to assess the relationships between size (centroid size) and shape (Principal Components) for the whole cranium and for cranial modules, the relationships between overall cranial size and the size of cranial modules, the percentage of shape change attributed to variation in size, and interspecies differences in allometric scaling.

Allometric scaling patterns are found to be conserved, both within and between species. However, lemuriforms are shown to respond more sensitively to size differences for traits in the face and lorisiforms shown to respond more sensitively for traits in the vault. Where species diverged from the common allometric trajectory, this is sometimes attributed to selection for a specialised diet. In comparison to other primate species the percentage of shape variation attributed to allometric scaling in strepsirhines is relatively low. A new re-sampling method, intended to incorporate intra-species variation within inter-species analysis is also tested and found to produce more conservative results than analyses based on species means.

Phylogenetic signal and models of evolution in the strepsirhine cranium

A range of models of evolution are investigated to determine which model best explains evolutionary shape change across the Strepsirhini; the models investigated include Brownian motion, Pagel's λ, kappa, delta (Pagel, 1999), the Ornstein-Uhlenbeck model (Felsenstein, 1988; Uhlenbeck & Ornstein, 1930), and the Independent Evolution model (Smaers & Vinicius, 2009). Independent Evolution was the best supported model of evolution; the data also suggest that trait change has largely followed a Brownian motion model.

In addition, the strength of phylogenetic signal within the strepsirhine cranium and cranial modules was assessed using Pagel's λ (Pagel, 1999) and Blomberg's *K* (Blomberg *et al.*, 2003). Robust phylogenetic signal was found for all cranial modules, both in terms of λ and *K* values.

Ancestral trait values, as estimated by the Independent Evolution model, were subsequently used to create 'evo-maps' depicting the rate and direction of shape change across the phylogenetic tree of the study species. These maps are used for identifying homologous and homoplastic traits.

To conclude, a review of the above results is presented and the interplay between the four subject areas (sample size, modularity, allometry and phylogenetic signal) is discussed, both in the context of understanding the evolutionary development of the strepsirhine cranium and the extent to which the results can be extrapolated to other taxa.

1.2. Literature review

1.2.1. The Strepsirhini

Encompassing lemurs, lorises and galagos, the Strepsirhini are a diverse group in terms of their taxonomy, geography and ecology (Gould *et al.,* 2011; Nekaris & Bearder, 2011). While lemurs are found only in Madagascar and on the nearby Comoros Islands, lorises and galagos inhabit the African mainland and South East Asia (Gould *et al.,* 2011; Nekaris & Bearder, 2011). Groves (2005) recognises 88 species of strepsirhines across 23 genera, while Mittermeier *et al.* (2008) argue for at least 99 species across 15 genera for the lemuriforms alone, and Nekaris and Bearder (2011) record at least 34 species of lorisiforms. Strepsirhines include specialised faunivores, folivores and gummivores, range in size from the smallest living primate, Madame Berthe's mouse lemur (*Microcebus berthae*) at ~30g, to the indri (*Indri indri*) at ~6.7kg, and have been recorded following nocturnal, diurnal and cathemeral activity patterns (Gould *et al.,* 2011; Mittermeier *et al.,* 2008; Nekaris & Bearder, 2011).

Within the Lemurs (Lemuriformes) there are five families: the Cheirogaleidae, Daubentoniidae, Indriidae, Lepilemuridae and Lemuridae, while the lorisiforms are divided into the Galagonidae and the Lorisidae (Nekaris & Bearder, 2011). The taxonomy of the Strepsirhini used here is summarised in Table 1.

Table 1: Classification of the Strepsirhini, following Nekaris & Bearder (2011) and Gould *et al.* (2011).

Infraorder	Family	Genus	Species	Common name
Lemuriformes	**Cheirogaleidae**	*Allocebus*	*trichotis*	hairy-eared dwarf lemur
		Cheirogaleus	*adipicaudatus*	Southern dwarf lemur
			crossleyi	Crossley's grester dwarf lemur
			major	greater dwarf lemur
			medius	fat-tailed dwarf lemur
			minusculus	lessor iron-grey dwarf lemur
			ravus	large iron-grey dwarf lemur
			sibreei	Sibree's dwarf lemur
		Microcebus	*arnholdi*	Arnhold's mouse lemur
			berthae	Berthe's mouse lemur
			bongolavensis	Bongolava mouse lemur
			danfossi	Danfoss' mouse lemur
			griseorufus	grey-brown mouse lemur
			jollyae	Jolly's mouse lemur
			lehilahytsara	Goodman's mouse lemur
			lokobensis	Lokobe mouse lemur
			macarthurii	MacArthur's mouse lemur
			mamiratra	Claire's mouse lemur
			margotmarshae	Margot Marsh's mouse lemur
			mittermeieri	Mittermeier's mouse lemur
			murinus	grey mouse lemur
			myoxinus	pygmy mouse lemur
			ravelobensis	golden-brown mouse lemur
			rufus	brown mouse lemur
			sambiranensis	sambirano mouse lemur
			simmonsi	Simmon’s mouse lemur
			tavaratra	Northern rufous mouse lemur
		Phaner	*furcifer*	fork-marked mouse lemur
	Daubentoniidae	*Daubentonia*	*madagascariensis*	aye-aye
	Indriidae	*Avahi*	*betsileo*	Betsileo woolly lemur
			cleesei	Bemaraha woolly lemur
			laniger	Eastern woolly lemur
			meridionalis	Southern woolly lemur
			mooreorum	Moore's woolly lemur
			occidentalis	Western woolly lemur
			peyrierasi	Peyriera’s woolly lemur
			ramanantsoavani	Ramanantsoavana's woolly lemur
			unicolor	unicolor avahi
		Indri	*indri*	indri
		Propithecus	*candidus*	silky sifaka
			diadema	diademed sifaka

		verreauxi	Verreaux's sifaka
Lemuridae	*Eulemur*	*cinereiceps*	gray-headed lemur
		collaris	collard brown lemur
		coronatus	crowned lemur
		flavifrons	blue-eyed black lemur
		fulvus	brown lemur
		macaco	black lemur
		mongoz	mongoose lemur
		rubriventer	red-bellied lemur
	Hapalemur	*aureus*	golden bamboo lemur
		gilberti	Gilbert's bamboo lemur
		griseus	lesser bamboo lemur
		meridionalis	southern lesser bamboo lemur
		simus	greater bamboo lemur
	Lemur	*catta*	ring-tailed lemur
	Varecia	*variegata*	ruffed lemur
		rubra	red ruffed lemur
Lepilemuridae	*Lepilemur*	*aeeclis*	Aeecl's sportive lemur
		ahmansoni	Ahmanson's sportive lemur
		ankaranensis	Ankarana sportive lemur
		betsileo	Betsileo sportive lemur
		dorsalis	grey-backed sportive lemur
		edwardsi	Milne-Edwards sportive lemur
		fleuretae	Fleurete's sportive lemur
		grewcocku	Grewcock's sportive lemur
		hollandorum	Holland's sportive lemur
		hubbardi	Hubbard's sportive lemur
		jamesi	Jame’s sportive lemur
		leucopus	white-footed sportive lemur
		manasamody	Manasamody sportive lemur
		microdon	small-toothed sportive lemur
		milanoii	Daraina sportive lemur
		mustelinus	weasel sportive lemur
		otto	Otto's sportive lemur
		petteri	Petter's sportive lemur
		randrianasoli	Randrianasoli's sportive lemur
		ruficaudatus	red-tailed sportive lemur
		sahamalazensis	Sahamalaza's sportive lemur
		scottorum	Scott's sportive lemur
		seali	Seal's sportive lemur
		septentrionalis	northern sportive lemur
		tymerlachsoni	Hawk's sportive lemur
		wrighti	Wright's sportive lemur

Lorisiformes	**Galagonidae**	*Euoticus*	*alleni*	Allen's bushbaby
			cocos	Kenya coastal bushbaby
		Galago	*demidoff*	Demidoff's dwarf bushbaby
			elegantulus	Southern needle-clawed bushbaby
			gallarum	Somali lesser bushbaby
			granti	Mozambique lesser bushbaby
			matschiei	spectacled bushbaby
		Galagoides	*moholi*	Southern lesser bushbaby
			nyasae	Malawi lesser bushbaby
			orinus	Taita Mountain dwarf bushbaby
			pallidus	northern needle-clawed bushbaby
			rondoensis	Rondo dwarf bushbaby
			senegalensis	Senegal lesser bushbaby
			thomasi	Thoma's dwarf bushbaby
			zanzibaricus	Zanzibar lesser bushbaby
		Otolemur	*crassicaudatus*	thick-tailed greater bushbaby
			garnettii	Garnett's (small-eared) greater bushbaby
			monteiri	silver greater bushbaby
	Lorisidae	*Arctocebus*	*aureus*	golden angwantibo
			calabarensis	Calabar angwantibo
		Loris	*tardigradus*	slender loris
		Nycticebus	*bengalensis*	Bengal slow loris
			coucang	greater slow loris
			javanicus	Javan slow loris
			menagensis	Bornean slow loris
			pygmaeus	pygmy slow loris
		Perodicticus	*potto*	potto

1.2.2. Strepsirhine phylogenetic relationships

A good understanding of species phylogenetic relationships is necessary before the evolutionary forces behind their behavioural, ecological and morphological diversity can be explicated. Fortunately, thanks to a wealth of molecular data, the phylogenetic relationships of the Strepsirhini have now largely been resolved (Finstermeier *et al.*, 2013; Horvath *et al.*, 2008; Masters *et al.*, 2007; Matsui *et al.,* 2009; Perelman *et al.*, 2011; Roos *et al.,* 2004; Springer *et al.*, 2012; Steiper & Seiffert, 2012; Yoder & Yang, 2004). A composite phylogeny of the strepsirhine species used in this research is shown in Figure 1. As a result, it is possible to address several, previously outstanding, questions about strepsirhine phylogenetics. Such questions include, whether both the lemuriforms and lorisiforms are

monophyletic clades (Masters *et al.*, 2007; Mittermeier *et al.*, 2008)? Furthermore, are the Galagonidae and the Lorisidae also monophyletic (Masters *et al.*, 2007)?
The striking physical similarities shared between the Cheirogaleidae and lorisiforms has previously caused confusion with regard to the closeness of their phylogenetic relationship (Rasmussen & Nekaris, 1998), and relationships within both the lemuriforms and the Lorisidae have been unclear (Rasmussen & Nekaris, 1998; Yoder, 1997). Finally, whether Tarsiiformes belong to the strepsirhine or to the haplorhine primate clade has been the subject of much debate (Jameson *et al.*, 2011).

Monophyly has been confirmed in all cases; in lemuriforms, lorisiforms, the Galagonidae and the Lorisidae (Masters *et al.*, 2007; Matsui *et al.*, 2009; Mittermeier *et al.*, 2008; Yoder, 1997), although there remains some dispute over the inclusion of *Daubentonia* within the lemuriforms (Groves, 2005; Mittermeier *et al.*, 2008; Perelman *et al.*, 2011; Roos *et al.*, 2004).

Several robust patterns have emerged with regards to the relationships within the Lemuridae, with *Varecia* strongly supported as basal to the family and *Hapalemur* and *Lemur* consistently found to be sister taxa, which together form a sister group to *Eulemur* (DelPero *et al.,* 2006; Finstermeier *et al.*, 2013; Matsui *et al.*, 2009; Pastorini *et al.,* 2002; Perelman *et al.*, 2011; Roos *et al.*, 2004; Wyner *et al.,* 2000; Yoder & Irwin, 1999). *E. rubriventer* has been shown to be the sister taxon to *E. fulvus* and in turn *E. mongoz* was found to be the sister taxon to the *E. fulvus/E. rubriventer* clade (DelPero *et al.*, 2006) and *E. macaco* sister to the *E. mongoz/E. fulvus/E. rubriventer* clade (Finstermeier *et al.*, 2013).

Debate has existed as to whether the Lorisidae species found in Africa (*Perodicticus* and *Arctocebus*) are more closely related to each other than they are to Asian species (*Nycticebus* and *Loris*), or if instead the slender species (*Arctocebus* and *Loris*) share a more recent common ancestor with each other than with the robust species (*Perodicticus* and *Nycticebus*) (Yoder, 1997). However, recent studies based on molecular data, have repeatedly found in favour of the African clade/Asian clade scenario (Masters *et al.*, 2007; Matsui *et al.*, 2009; Roos *et al.*, 2004).

In the past, the monophyly of both the lemuriforms and the lorisiforms had been called into question by a proposed close relationship between the Cheirogaleidae and the lorisiforms, based on shared physical characteristics, including an, apparently derived,

organisation of the intra-cranial blood supply (Cartmill, 1975; Charles-Dominique, 1970). However, molecular studies have revealed that they are not closely related and so any similarities are attributed to parallel evolution (Matsui *et al.*, 2009; Yoder, 1994). An alternative explanation is that both sets of taxa have retained the primitive primate form, which would require subsequent incidences of parallel evolution in remaining strepsirhine and haplorhine species for the trait, and therefore seems the less parsimonious of the two explanations (Matsui *et al.*, 2009; Yoder, 1994).

There has been considerable discussion concerning the alignment of tarsiers; specifically, whether they should be placed within the strepsirhine clade or within the haplorhine clade, as morphological data were inconclusive (Arnason *et al.*, 2002; Jameson *et al.*, 2011; Matsui *et al.*, 2009). Recent genetic data, however, appear to confirm tarsiers affiliation with the haplorhines (Jameson *et al.*, 2011).

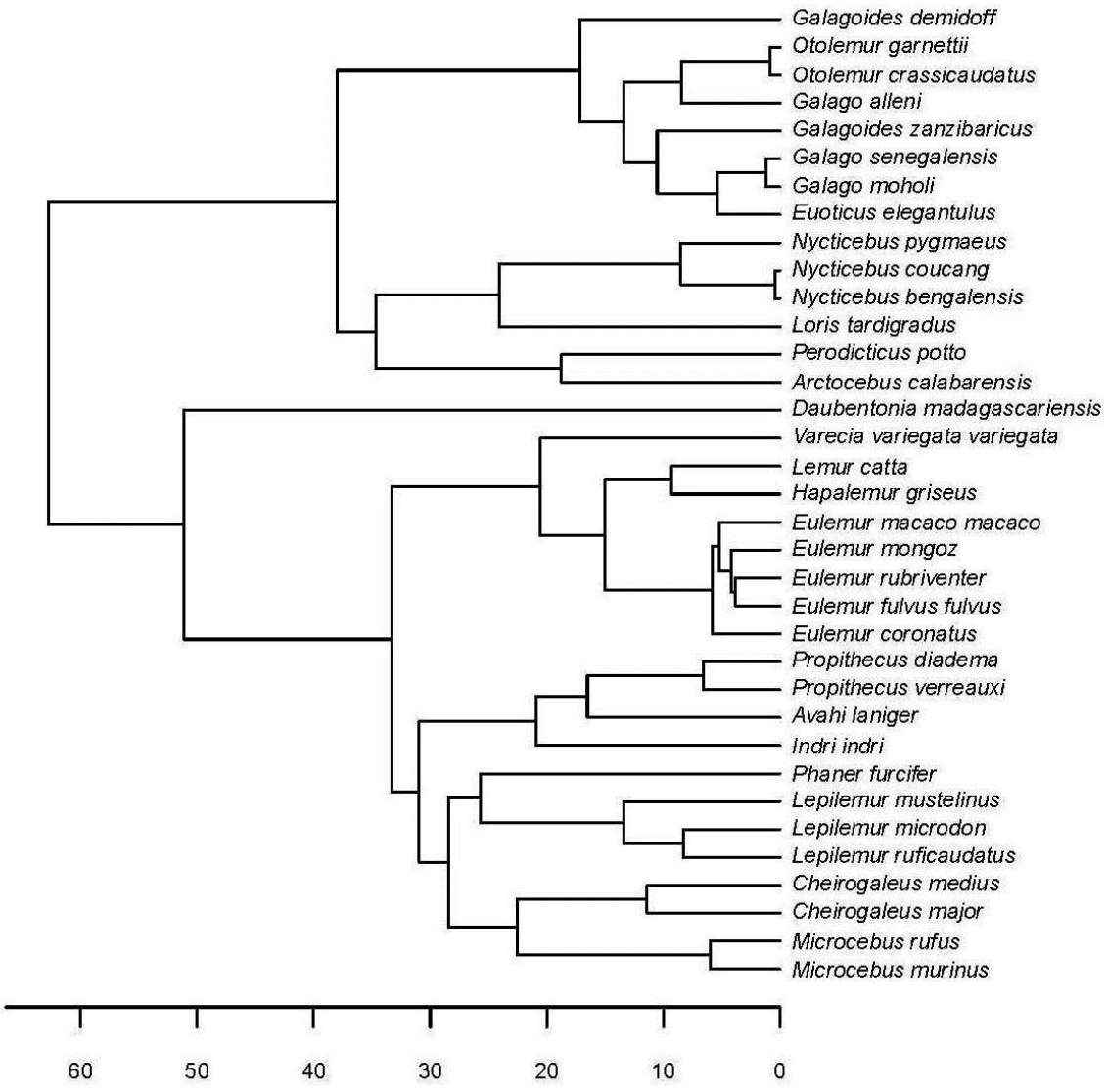

Figure 1: Phylogenetic relationships of the strepsirhine species for which data were collected for this research, based on the composite tree taken from the 10K Trees project (Arnold *et al.,* 2010)

1.2.3. The evolutionary history of the Strepsirhini

The evolutionary history of the Strepsirhini remains something of an enigma. Among the key questions still under discussion are the age and location of their origin, which families represent their direct ancestors (Bennett & Goswami, 2012; Fleagle, 2013 Martin, 1993; Martin *et al.*, 2007) and the manner and pattern in which they dispersed around the globe (Godfrey *et al.,* 2010; Seiffert *et al.,* 2003; 2005; 2010; Tavaré *et al.*, 2002).

1.2.3.1. The primate fossil record

A direct reading of the fossil record would place the origin of primates at 57 million years ago (mya), as this is when fossils of primates of undoubted modern aspect (often classified as euprimates) first appear North America, Europe and Asia (Martin *et al.,* 2007; Ni *et al.,* 2004). However, this offers only a minimum date for primate origins and fails to take into account the patchy nature of the fossil record (Martin *et al.*, 2007). Statistical analysis has estimated that only between 4-7% of the primate species that have ever existed are known in fossil form (Martin, 1993; Tavaré *et al.,* 2002). Moreover, there is a substantial gap of between 4-6 million years, during the Oligocene, for which no primate representatives have been recorded at all (Seiffert, 2006).

Ancestral links have been suggested between fossil Eocene primates and extant species, with Adapiformes typically being linked to strepsirhines and Omomyiformes to haplorhines (Bennett & Goswami, 2012; Fleagle, 2013). An alternate argument holds that Adapiformes and Omomyiformes occupy a separate radiation, which diverged from the lineage of crown-group primates prior to the split of strepsirhines and haplorhines (Martin, 1993; Martin *et al.*, 2007).

The strepsirhine fossil record is particularly sparse, with potential crown group fossils consisting of limited Lorisidae taxa from Eocene North Africa (Seiffert *et al.,* 2003; 2005; 2010) and subfossil Lemurs, which date from 26,000-500 years ago (Godfrey *et al.,* 2010). No earlier fossils have been found for the lemuriforms; their extensive ghost lineage therefore represents a further significant gap in the fossil record (Tavaré *et al.*, 2002).

The fossil species *Bugtilemur mathesoni* was recovered from Oligocene deposits, dated as 30 my old, in the Bugti Hills of Pakistan, and consists of only a few isolated teeth (Marivaux *et al.*, 2001). The morphology of the lower canine was originally argued to confirm the

presence of a tooth-comb, a trait that is a key identifying feature of extant strepsirhines (Marivaux *et al.*, 2001). Additional similarities in cheek teeth morphology lead to *Bugtilemur* being closely aligned with cheirogaleids, particularly *Cheirogaleus* (Marivaux *et al.*, 2001), although *Bugtilemur* is estimated to be much smaller than *Cheirogaleus,* with a much shorter and broader tooth-comb (Tattersall, 2007). Should this phylogenetic placement within the lemuriforms be accurate, *Bugtilemur* would be the only example of a lemuriform primate found outside of Madagascar. This would have distinct implications for the interpretation of the geographic origin of the extant Lemurs, hinting at possibility of an Asian origin for the strepsirhines (Marivaux *et al.*, 2001).

However, the alignment of *Bugtilemur* with the cheirogaleids has been questioned on the basis of both the interpretation of the morphology and phylogenetic analysis (Godinot, 2006). Specifically, the lower canine has been argued to be shorter and at a different angle than in extant lemuriforms and, crucially, lorisiform taxa. As such, it is unparsimonious to have the species embedded within the lemuriform clade, yet with a more primitive tooth-comb morphology than would be expected in the last common ancestor (LCA) of lemuriforms and lorisiforms (Godinot, 2006; Seiffert *et al.*, 2003). The reclassification of *Bugtilemur* as an adapiform has thus been argued for (Godinot, 2006). This is further supported by the discovery of *Muangthanhinius siami*, a fossil primate from the late Eocene, found on the Thai Peninsula (Marivaux *et al.,* 2006). *Muangthanhinius* is classified as an adapiform and shares aspects of its dental morphology with *Bugtilemur* (Marivaux *et al.,* 2006). Following this scenario, the morphological similarities between *Bugtilemur* and the cheirogaleids are judged to be homoplasies (Godinot, 2006).

The timing of the evolution of the tooth-comb in strepsirhine primates is unclear; parsimony suggests that it was present in the LCA of lorisiforms and lemuriforms, which molecular data has placed between 50 and 69mya (Chatterjee *et al.,* 2009; Finstermeier *et al.*, 2013; Jameson *et al.*, 2011; Perelman *et al.*, 2011; Pozzi *et al.*, 2014; Springer *et al.*, 2012; Wilkinson *et al.*, 2010; Yoder & Yang, 2004). Evidence of a tooth-comb first appears in the fossil record 37mya and is associated with *Karanisia clarki*, a species from the Egyptian Fayum known from isolated teeth and jaw fragments (Seiffert *et al.*, 2003). On account of its tooth morphology, *Karanisia* was initially placed within the Lorisidae clade, but further analysis, with an expanded fossil sample, has resulted in it being reclassified as either a stem lorisiform or a stem strepsirhine (Seiffert *et al.*, 2005). Another fossil species

Saharagalago misrensis, from the same deposits, is suggested to belong to the Galagonidae (Seiffert *et al.*, 2003). This is taken as the earliest physical evidence for the split between lorises and galagos and also as support for an Afro-Arabian origin for the lorisiform clade (Seiffert *et al.*, 2003). *Wadilemur*, like *Saharagalago*, is also from the Egyptian Fayum and is thought to be aligned with the Galagonidae (Seiffert *et al.*, 2005). Although dated later than *Saharagalago* (~35mya), *Wadilemur* does add support for an Eocene divergence of lorises and galagos (Seiffert *et al.*, 2005).

1.2.3.2. Molecular divergence dates

Molecular sequence data from extant species can provide a substantial amount of information about the evolutionary history of taxa. These data, combined with mathematical models of evolution, can be used to estimate species divergence dates. Traditionally, the mathematical models use the fossil record to set initial estimates of node ages for phylogenetic trees, as a means of calibrating molecular substitution rates, as rates can vary both within and between groups (Wilkinson *et al.*, 2010). There are three main problems that can affect the validity of using fossil evidence to calibrate molecular rates: first, the selection of unsuitable fossils; second, the incompleteness of the fossil record for some taxa; and finally, the incorrect placement of fossils within the phylogeny. Therefore the fossils used, as well as the genetic data used, can affect the resulting divergence date estimates (Wilkinson *et al.*, 2010; Yoder & Yang, 2004).

By their very nature, dates generated using the molecular clock method tend to be significantly earlier than those based on a direct reading of the fossil record (Chatterjee *et al.,* 2009; Finstermeier *et al.*, 2013; Jameson *et al.*, 2011; Martin *et al.,* 2007; Ni *et al.,* 2004; Perelman *et al.*, 2011; Pozzi *et al.*, 2014; Springer *et al.*, 2012; Wilkinson *et al.*, 2010; Yoder & Yang, 2004). Using molecular data, estimates for the divergence of the LCA of extant primates have been found ranging from >87.2 – 63mya (Finstermeier *et al.*, 2013; Jameson *et al.*, 2011; Perelman *et al.*, 2011; Pozzi *et al.*, 2014; Springer *et al.*, 2012; Wilkinson *et al.*, 2010; Yoder & Yang, 2004). A statistical method to control for fossil preservation rates also predicted a divergence date within this range (85mya) (Tavaré *et al.*, 2002). Thus, all estimates are substantially earlier than the first euprimate fossils at 55my (Martin *et al.*, 2007; Ni *et al.*, 2004). These earlier molecular estimates would place the LCA of extant primates within the Cretaceous and prior to the Cretaceous-Tertiary (K-T) boundary. It had previously been proposed that primates

may have originated, and exploded in diversity, after the K-T boundary, because they were filling empty ecological space, left vacant by the extinction of the dinosaurs (Martin *et al.*, 2007). While molecular clock analyses suggest an earlier origin, it is still likely that the initial radiation of primates was also subject to partial extinction around the K-T boundary, resulting in a, post K-T boundary, tertiary radiation (Martin *et al.*, 2007).

An Eocene (56.9 - 49.8mya) date has been estimated for the divergence of lemuriforms and lorisiforms (Chatterjee *et al.,* 2009; Finstermeier *et al.*, 2013; Jameson *et al.*, 2011; Springer *et al.*, 2012; Wilkinson *et al.*, 2010), but this is not without dispute, with other molecular clock analyses arriving at earlier dates of 68.7 – 66.3mya (Perelman *et al.*, 2011; Pozzi *et al.*, 2014; Yoder & Yang, 2004). The LCA of the lorisiform clade has been dated to 40-34.5mya (Finstermeier *et al.*, 2013; Matsui *et al.*, 2009; Perelman *et al.*, 2011; Springer *et al.*, 2012; Yoder & Yang, 2004), remarkably close to the date given for the galago *Saharagalago* from the Egyptian Fayum (Seiffert, 2012; Seiffert *et al.*, 2003).

1.2.3.3. Geographic origin

While euprimates are found in North America, Europe and Asia, and potentially North Africa, from 55mya, they appear to arrive fully formed and the molecular data implies that the lineage stretches much further back in time (Martin *et al.*, 2007). Locating the geographic origin and subsequent dispersal routes of primates, and more specifically strepsirhine primates, is dependent upon the accuracy of divergence dates, as it has direct implications for the position of continental plates, the direction of ocean currents and the environmental conditions experienced (Martin *et al.*, 2007). In addition, the identification of fossil species plays a critical role in placing strepsirhine ancestors at certain geographic locations at certain dates; the reassessment of species phylogenetic positions can therefore alter the support for different models of primate origins and dispersal (Godinot, 2006).

There are three key competing locations for the geographic origin of primates, namely Continental Asia, Africa and Indo-Madagascar (Miller *et al.,* 2005). The position of each of these landmasses has altered considerably since the proposed evolution of primates in the Cretaceous (Finstermeier *et al.*, 2013; Jameson *et al.*, 2011; Perelman *et al.*, 2011; Pozzi *et al.*, 2014; Springer *et al.*, 2012; Wilkinson *et al.*, 2010; Yoder & Yang,

2004). The African-Arabian landmass has been geographically isolated for at least ~120 million years, since it split with the South American plate (Rögl, 1997). It proceeded to drift northwards until its eventual collision with Eurasia ~20mya (Rögl, 1997). Madagascar split from the African mainland ~165mya, but remained attached to in the Indian subcontinent until 88mya (Storey *et al.*, 1995). Madagascar reached its current position, ~400km off the east coast of the African mainland, ~121mya (Rabinowitz *et al.,* 1983), while the Indian subcontinent collided with Asia ~56-66mya (Beck *et al.*, 1995).

The theory that the LCA of euprimates originated in Africa, including the lineage leading to the modern strepsirhines, with early lemuriforms dispersing to Madagascar and Lorisidae ancestors to Asia, is known as the African origin hypothesis (Roos *et al.*, 2004). Modelling of palaeo-geographic and palaeo-oceanographic conditions suggests that it would have been possible for ancestral lemuriforms to have reached Madagascar from the African Mainland during the Eocene, by travelling on floating vegetation (Ali & Huber, 2010). It has been further suggested that these primates may have been able to survive the ocean crossing, from Mainland Africa to Madagascar, due to their low metabolic rates or their ability to go into a state of torpor (Ali & Huber, 2010). It is argued that many of the mammalian lineages found on the Island must be the result of Eocene dispersals from mainland Africa as they share no features with the Island's late Cretaceous inhabitants, with each colonisation being the result of a single dispersal event (Roos *et al.*, 2004). This could be seen to tie in with the Eocene divergence dates for the lemuriform and lorisiform clades (Chatterjee *et al.*, 2009; Finstermeier *et al.*, 2013; Jameson *et al.*, 2011; Springer *et al.*, 2012; Wilkinson *et al.*, 2010).

The idea that land bridges may have enabled taxa to disperse from the African mainland to Madagascar has been proposed as an alternative hypothesis (Ali & Huber, 2010). This explanation is problematic: first, it is difficult to explain how plate tectonics would have enabled this to happen; second, a great number of species would have been expected to cross into Madagascar, with their arrival correlated with the purported existence of these bridges, and, third, fossil data do not support this mass dispersal. The rafting hypothesis, in contrast, can account for the limited number of mammalian families that now inhabit the Island, the seemingly random arrival dates for these families, and the otherwise perplexing absence of large-bodied mammals (Ali & Huber, 2010).

For lorisiforms, the African origin hypothesis appears to be a parsimonious explanation for both extant and fossil species; both galagos and lorises are found in Africa today, while only lorises are found in Asia (Yoder, 1997). Furthermore, the earliest fossil galagos and a potential stem lorisiform are found in North Africa and are dated to near the estimated time of the lorisiform/lemuriform split (Seiffert *et al.*, 2003; 2005). As with lemurs, the Lorisidae are proposed to have dispersed out of Africa either across land bridges (Yoder, 1997) or by rafting on vegetation, in this case across the Tethys Sea (Kappeler, 2000). Although, the earliest true Lorisidae found in Asia date from the Miocene (Jacobs, 1981; Rasmussen & Nekaris, 1998) and, as such, could be concordant with the collision between Eurasia and Afro-Arabia (Rögl, 1997) and dispersal by land (Yoder, 1997), this dispersal has been argued to have occurred earlier, at ~42mya in line with molecular divergence dates for African and Asian Lorisidae (Roos *et al.*, 2004). Fossil evidence of faunal exchange between Afro-Arabia and Eurasia from ~49mya provides some support for this earlier dispersal date (Seiffert, 2012). The rafting hypothesis is invoked on the basis that the Lorisidae, like lemuriforms (Ali & Huber, 2010), have relatively low metabolic rates, in comparison to other primates (Rasmussen & Izard, 1988), which may have enabled them to survive the crossing (Kappeler, 2000).

The closest common ancestors of primates are Scandentia and Dermoptera, both of which are found in Asia, thereby highlighting it as a parsimonious location for primate origins (Beard, 1998). In addition, primates have recently been identified as belonging to the Euarchontoglires clade, rather than the endemic African clade, the Afrotheria (Murphy *et al.*, 2001; Martin *et al.*, 2007). Scandentia and Dermoptera also belong to the clade, as do Rodentia and the Lagomorpha; the first appearance of all of these orders in the fossil record implies a Laurasian origin for the Euarchontoglires (Springer *et al.,* 2011), Laurasia having formed from the continents that now make up the northern hemisphere, after the break-up of Pangaea in the Late Triassic-Early Jurassic (Manspeizer, 1994). The Asian origin model holds that strepsirhine ancestors subsequently dispersed into Afro-Arabia during the Eocene (Seiffert, 2012). This is in line with the north African fossils *Karanisia* and *Saharagalago*, which date from that period (Seiffert *et al.*, 2003; Steiper & Seiffert, 2012). Subsequently lemuriforms dispersed to Madagascar and at a later date the effects of global cooling may have pushed the crown Galagonidae to more southern latitudes (Seiffert, 2007).

The Indo-Madagascar hypothesis (also referred to as the Indian-Ark hypothesis) suggests a Gondwanan ancestry for primates, with their early evolution largely confined to Indo-Madagascar (Miller *et al.*, 2005). Its validity is therefore dependent on a Cretaceous dating for primate origins (Miller *et al.*, 2005). It is proposed that a large proportion of mammalian ancestors became isolated on the Indian subcontinent after its separation from Africa in the early Cretaceous, including Artiodactyla, Perissodactyla and the Adapidiformes and Omomyiformes. The subsequent collision of the Indian subcontinent and the Asian Mainland near the Paleocene-Eocene boundary enabled the previously isolated taxa, including primate ancestors, to migrate to the northern continents (Krause & Maas, 1990). This would be congruent with the apparent sudden appearance of euprimates in the northern continents at this time, a phenomenon that other factors, such as the environmental change linked to the Paleocene-Eocene thermal maximum, fail to fully explain (Soligo, 2007). This scenario would also explain the presence of lorises in Asia (Miller *et al.*, 2005). However, it also implies separate dispersals of galagos and African lorises, as well as the subsequent extinction of bushbabies in Asia. While additional fossil evidence for an Indo-Madagascar origin is lacking, it is also true that the sampling of appropriately aged sediments has been extremely limited (Miller *et al.*, 2005). However, Madagascar separated from the Indian subcontinent ~88mya (Storey *et al.*, 1995), prior to all dates given for the LCA of crown group strepsirhines and certainly for those given for the divergence of lemuriforms (Chatterjee *et al.*, 2009; Finstermeier *et al.*, 2013; Jameson *et al.*, 2011; Springer *et al.*, 2012; Wilkinson *et al.*, 2010), leaving the question of how the diverse array of Lemurs arrived on the Island unanswered.

1.2.4. Socioecology of the Strepsirhini

1.2.4.1. Lemuriformes

Numerous molecular analyses have confirmed the lemuriforms to be the sister clade of the lorisiforms (Finstermeier *et al.*, 2013; Matsui *et al.*, 2009; Perelman *et al.*, 2011; Roos *et al.*, 2004; Springer *et al.*, 2012; Steiper & Seiffert, 2012; Yoder & Yang, 2004). Lemurs are often referred to as a classic example of an adaptive radiation, and the high level of diversity that they exhibit has been attributed to their lack of competition with other mammalian groups (Martin, 1990). In addition to the lemuriforms, only four other mammalian groups inhabit the Island of Madagascar (Eupleridae, the Tenrecidae, Rodentia and Chiroptera), as a result, the primates on Madagascar tend to fill niches

that are occupied by other mammalian groups on the African mainland (Martin, 1990). Within this diversity, there are several general trends: as size increases there is usually a move from an animal- to a plant-based diet, a shift from nocturnal to diurnal activity period, and from less to more gregarious behaviour (Martin, 1990).

1.2.4.1.1. Cheirogaleidae

The family Cheirogaleidae includes four genera: *Microcebus, Allocebus, Cheirogaleus* and *Phaner* (Gould *et al.*, 2011). All species are quadrupedal, typically with an elongated body and short limbs (Mittermeier *et al.*, 2008). The Cheirogaleidae are also all nocturnal, sleeping in either tree holes or in nests during the day and, when necessary (e.g., during times of food shortage), some species are able to go into torpor for extended periods of time (Mittermeier *et al.*, 2008).

The mouse lemurs (*Microcebus*) include the smallest of all primates, *M. berthae*, at just 30g, while the heaviest of the genus is *M. ravelobensis* at 72g (Gould *et al.*, 2011). All *Microcebus sp.* are branch runners and their small size allows them to exploit fine branches and lianas (Martin, 1990). They are fairly widespread across Madagascar, in comparison to other lemur genera (Mittermeier *et al.*, 2008; Rasolooarison *et al.,* 2000), but many species have only recently been described, based on differences at the genetic level, as they can be hard to distinguish morphologically (Gould *et al.*, 2011).

The home ranges of several conspecifics are likely to overlap, with male home ranges larger than those of females (Martin, 1990). But, mixed reports are available with regard to mouse lemur social organisation, most indicate that they are solitary while foraging, but gregarious at sleeping sites (Radespiel, 2000; Radespiel *et al.*, 1998). Sleeping groups may consist of many females and one male or be multi-male/multi-female (Schwab, 2000). One exception is *M. berthae*, which is thought to sleep and forage alone; a behaviour that has been suggested to be an anti-predator strategy for this smallest of primates (Schwab, 2000). All *Microcebus* are omnivorous, with their diets consisting of fruit, invertebrates, leaves, flowers, nectar and tree sap (Gould *et al.*, 2011; Martin, 1990).

The other large group within the Cheirogaleidae are the dwarf lemurs (*Cheirogaleus*). *C. medius* is found in the Western dry forests of Madagascar, while *C. major* occupies the rainforests in the east of the Island (Groves, 2000). *Cheirogaleus* is omnivorous, consuming fruit, nectar, leaves, pollen and insects (Fietz & Ganzhorn, 1999). Though

larger than mouse lemurs, they are still relatively small at 150-600g; but their body mass can fluctuate considerably depending on the season (Mittermeier *et al.*, 2006; 2008). Especially for *C. medius*, which can double its weight over the period of a few weeks, a large proportion of this extra body fat is stored in their tails, which can triple in size (Fietz & Ganzhorn, 1999). This increase in body mass occurs prior to the onset of hibernation or torpor (Fietz & Ganzhorn, 1999). Both *C. medius* and *C. major* are able to go into torpor (Wright & Martin, 1995), which is thought to be a method for coping with limited food supplies, especially fruit, during the dry season (Fietz & Ganzhorn, 1999; Wright & Martin, 1995). Dwarf lemur social organisation has not been fully determined, but field studies suggest that it varies widely between species, with *C. major* recorded as being largely solitary (Petter *et al.*, 1977), while *C. medius* has been found living in pair-bonded family groups (Müller, 1999). As with the mouse lemurs, the dwarf lemurs travel quadrupedally along the tops of branches, although with less leaping and at a slower pace than *Microcebus* (Mittermeier *et al.*, 2008).

1.2.4.1.2. Daubentoniidae

The Daubentoniidae includes only one extant species, the nocturnal aye-aye (*Daubentonia madagascariensis*) (Gould *et al.*, 2011). Weighing in at ~2.5kg (Feistner & Sterling, 1995), the aye-aye is found throughout Madagascar's coastal forests, although population densities are often low, especially in the south-west of the Island (Quinn & Wilson, 2004). It displays many adaptations for locating and obtaining its specialised diet of larvae, seeds and fungi (Sterling, 1994); these include, continually growing incisors, which are used either to gnaw through the bark of a tree or to access seeds (Sterling, 1994). They also have claws rather than nails on all digits except the hallux, which it uses to aid its exclusively quadrupedal locomotion. An attenuated middle digit, on each hand, is used for percussive foraging (Martin, 1990; Ramsier & Dominy, 2012; Sterling, 1994); this involves the rapid tapping of the digit against bark to locate prey species beneath. The aye-aye also has enhanced auditory sensitivity to the particular frequencies produced by this tapping action (Ramsier & Dominy, 2012). This extended digit is also used to scoop up both larvae and nectar (Sterling, 1994). The aye-aye both forages and sleeps alone, with females maintaining exclusive home ranges, while male home ranges overlap with both females and other males, which can make for aggressive encounters (Gould *et al.*, 2011). Phylogenetically the aye-aye has consistently been shown to be basal to all other lemuriforms (DelPero *et al.*, 2006; Horvath *et al.*, 2008; Perelman *et al.*, 2011; Roos *et al.*, 2004; Yoder, 1997; Yoder & Yang, 2004) .

There has been debate over its inclusion within Lemuriformes and for a time it was placed within its own infraorder, the Chiromyiformes (Groves, 2005; Perelman *et al.*, 2011; Roos *et al.*, 2004). This has since been revised; with the aye-aye placed back within the Lemuriformes (Mittermeier *et al.*, 2008).

1.2.4.1.3. Indriidae

There are three extant genera within the Indriidae, ranging in size from the smallest, *Avahi laniger* at ~1kg, to *Propithecus sp.,* which vary from 3- 5kg, and finally *Indri indri,* which is the largest strepsirhine at ~6.7kg (Gould *et al.*, 2011). The Indriidae are found throughout Madagascar in both deciduous forests and rainforests, but individual species are generally confined to specific regions (Mittermeier *et al.*, 2008). All species are united in their diet and locomotion; they are folivorous (although they will incorporate fruit and flowers when they are seasonally available) and move around the forest using vertical-clinging and leaping, keeping their body upright and using their powerful and elongated hindlimbs to propel themselves between vertical supports (Mittermeier *et al.*, 2008). When they do descend to the ground they travel using a distinctive bipedal hopping (Gould *et al.*, 2011; Martin, 1990). The smaller *Avahi* is nocturnal, while the larger genera, *Propithecus* and *Indri*, are diurnal (Mittermeier *et al.*, 2008). The Indriidae are also varied in their social structure, with *A. laniger* and *I. Indri* forming pair-bonded family units, while *Propithecus sp.* live in multi-male, multi-female groups (Mittermeier *et al.*, 2006). *Indri* is distinguished from the other Indriidae taxa by its rudimentary tail, in place of the more common long tail, and its loud morning 'song', which can be heard up to 3 miles away (Mittermeier *et al.*, 2006).

1.2.4.1.4. Lemuridae

The Lemuridae includes four genera*: Hapalemur, Lemur, Eulemur* and *Varecia*, all (with the exception of *Eulemur*) are diurnal (Gould *et al.*, 2011; Mittermeier *et al.*, 2008). Cathemeral activity patterns have been recorded for all *Eulemur* species (Colquhoun, 1998; Curtis *et al.*, 1999; Kapperler & Erkert, 2003; Schwitzer *et al.,* 2007).The family are found throughout Madagascar, but, with the exception of *E. fulvus*, intra-species distribution is less wide ranging. *E. fulvus* subspecies are distributed in a halo around the Island's coast (Gould *et al.*, 2011; Martin, 1990).

The smallest of the family is *Hapalemur*, which range in size from 700g to 2.5kg (Mittermeier *et al.*, 2008). Members of the genus are all vertical clingers and leapers, with their hindlimbs moderately longer than their forelimbs (Mittermeier *et al.*, 2008). They are distinguished from the other Lemuridae taxa by their comparatively shorter snout and their specialised bamboo diet (Mittermeier *et al.*, 2008). Giant bamboo contains cyanide, which *Hapalemur* is able to ingest in large quantities without harm (Tan, 1999). The precise mechanism by which *Hapalemur* detoxify cyanide is unclear, but traces of cyanide in their urine implies that it is absorbed by their gastrointestinal tract and is excreted by their kidneys (Yamashita *et al.,* 2010). The social structure of the bamboo lemurs is varied, with both bonded pairs and multi-male/multi-female groups found across intra- and inter-species levels (Grassi, 2001).

Lemur catta is the only extant species of the genus *Lemur*, although *Eulemur coronatus , E. fulvus, E. macaco, E. mongoz* and *E. rubriventer* were originally classified as *Lemur*, but were removed to their own *Eulemur* genus based on morphological traits (Groves & Eaglen, 1988). This has since been backed up by molecular data (DelPero *et al.*, 2006; Finstermeier *et al.*, 2013; Matsui *et al.*, 2009; Pastorini *et al.*, 2002; Perelman *et al.*, 2011; Roos *et al.*, 2004; Wyner *et al.*, 2000; Yoder & Irwin, 1999). *L. catta* is found in south and southwest Madagascar, in arid-adapted, scrub, and spiny forests (Gould *et al.*, 2011; Jolly, 2004). They are omnivores and their flexibility allows them to live in very seasonal habitats that are prone to drought (Jolly, 2004). On average species body mass is 2.2kg and they live in large multi-male, multi-female social groups (Jolly, 2004). Their gregariousness has been suggested to be an anti-predation strategy that is required due to the species' semi-terrestrial form of locomotion (Jolly, 2004).

Eulemur sp. are arboreal quadrupeds, that range in size from 1.2-2.5kg (Gould *et al.*, 2011). All species follow a cathemeral activity pattern and, with the exception of *E. fulvus*, all exhibit sexual dichromatism (Mittermeier *et al.*, 2008). Most species live in multi-male/multi-female groups with the exception of *E. rubriventer* which form pair-bonded family groups, and *E. mongoz* which has been recorded in both pair-bonded and larger mixed sex groups (Gould *et al.*, 2011). *Eulemur* is omnivorous, although fruit does make up a large proportion of the diet for most species (Gould *et al.*, 2011). *E. mongoz* is again the exception, as it is highly reliant on nectar, particularly during the dry season (Curtis & Zaramody, 1999). Unlike other lemuriforms, where species are largely confined to distinct

areas of the Island, *E. fulvus* are found in a full halo around the island (Gould *et al.*, 2011). As a result, they are sometimes found in sympatry with each other, consequently some hybrids within the *Eulemur* genus have been noted. Specifically, between *E. fulvus* and *E. macaco* (Goodman & Schütz, 2000) and *E. fulvus* and *E.* mongoz (Pastorini *et al.,* 2009; Whitesides *et al.*, 2001). It may also be because of this widespread distribution that so many sub-species, at least 5, of *E. fulvus* are recognised (Gould *et al.*, 2011).

Found in the eastern rainforests of Madagascar, *Varecia* is the largest of the Lemuridae, with a body mass of 3-4.5kg (Mittermeier *et al.*, 2008). They, like many of the other Lemuridae are found in both pair-bonded family groups and multi-male/multi-female groups (Britt, 2000; Gould *et al.*, 2011). They are highly frugivorous and because of this they are thought to play a crucial role within the ecosystem as seed dispersers. However, they also consume a wide number of fall-back foods, such as flowers, leaves and nectar, when fruit is unavailable (Britt, 2000).

1.2.4.1.5. Lepilemuridae

There has previously been some debate as to whether the Lepilemuridae warrant classification as a separate family, or whether they should be included within the Lemuridae, however, molecular data supports a distinction (Horvath *et al.*, 2008; Ishak *et al.,* 1988). While there is only one genus within the Lepilemuridae (*Lepilemur*), the number of recognised species has recently been increased to 26, as a result of molecular analyses (Gould *et al.*, 2011; Mittermeier *et al.*, 2008). Species within the Lepilemuridae are consistently nocturnal and range in size from 600-800g (Gould *et al.*, 2011). They follow a largely folivorous diet, which allows them to exist in different types of forest habitat, across Madagascar (Jungers *et al.*, 2002). They are vertical clingers and leapers and have the characteristic elongated hindlimbs that allow for this mode of locomotion (Mittermeier *et al.*, 2008). Reports of their social organisations have varied across species, with some (*L. mustelinus*) classified as solitary, foraging and sleeping alone (Martin, 1990; Rasoloharijaona *et al.,* 2008), while others (*L. ruficaudatus* and *L. edwardsi*) are pair-bonded and thought to be territorial (Rasoloharijaona *et al.*, 2006). This variation in social structure is thought to be the result of the different environmental pressures imposed by dry forest and rainforest habitats (Rasoloharijaona *et al.*, 2008).

1.2.4.1.6. Giant lemurs

Until relatively recently, giant lemur species existed on Madagascar (Fleagle *et al*., 2010). In total, 16 species, across 9 genera, are known from subfossil remains, representing three principal families: the Palaeopropithecidae (koala-lemurs), Megaladapidae (sloth-lemurs) and Archaeolemuridae (monkey-lemurs) (Fleagle *et al.*, 2010; Mittermeier *et al.,* 2006). The position of the giant lemurs within the lemuriform phylogenetic tree has not been fully resolved. However the megaladapids have been linked with either the Lepilemuridae (Montagnon *et al.,* 2001) or the Lemuridae (Karanth *et al.,* 2005), while the Palaeopropithecidae and the Archaeolemuridae are thought to be more closely related to the Indriidae (Godfrey & Jungers, 2003; Orlando *et al.*, 2008).

Size estimates for the extinct species range from 10-160kg, making them larger than any of the extant lemuriforms (Godfrey *et al.*, 2010). Based on their postcranial skeleton and their large size, it is thought that giant lemurs, unlike their smaller extant counter parts, were slow moving, using either terrestrial quadrupedalism, suspension or slow climbing forms of locomotion (Fleagle, 2013; Godfrey & Jungers, 2003). They are thought to have predominantly been diurnal folivores, filling a now empty niche as seed dispersers for specific plant species (Crowley *et al.,* 2011).

Radiocarbon dating of the subfossils has produced dates ranging from 26,000 to 500 years ago (Godfrey *et al.*, 2010), but their extinction, along with nearly all of Madagascar's mega-fauna, is ultimately thought to have coincided with the arrival of humans on the Island (~2,000 years ago) and has been linked to anthropogenic effects, such as unsustainable hunting, habitat destruction and aridification (Godfrey & Jungers, 2003; Gould *et al.*, 2011; Perez *et al.*, 2005).

1.2.4.2. Lorisiformes

Widely dispersed throughout Africa (excluding Madagascar), Asia and South East Asia, the primate species that make up the lorisiforms are exclusively nocturnal and largely arboreal (Nekaris & Bearder, 2011). In this they differ from the lemuriforms, which contain nocturnal, diurnal and cathemeral species, and both arboreal and terrestrial species (Gould, 2011). These differences may arise because, unlike lemuriforms, the lorisiforms share their habitats with diurnal monkeys and apes. It is probably because of

their nocturnal and arboreal behaviour that relatively little is known about this group in comparison with other primate taxa (Martin, 1990).

It has been suggested that lorises and galagos diverged from their LCA due to the uptake of two different foraging strategies; galagos are swift hunters, while lorises remain still and so unseen by prey (Rasmussen & Nekaris, 1998).. These strategies can be linked to a long line of integrated evolutionary changes, which include anatomy, physiology, mode of locomotion, reproduction, social behaviour and life history, which ultimately resulted in separate families (Rasmussen & Nekaris, 1998).

1.2.4.2.1. Galagonidae

Also commonly known as bushbabies, galagos are found across sub-Saharan Africa (with the exception of southern South Africa) and, as such, inhabit a broad range of ecosystems: tropical rainforest, montane forests, woodland, subtropical and near-desert conditions among them (Rasmussen & Nekaris, 1998). Species are often found in sympatry with one another, although where this occurs, the different species are thought to occupy different strata of the forest (Nekaris & Bearder, 2011). They can appear morphologically similar, weighing between 55g-2kg, with a brown pelage, and this may explain why so few species were initially recognised (Bearder *et al.*, 2003). Much of the recent identification of *Galago* species has been through bioacoustic studies (Bearder, 1999), based on the principles of the mate-recognition species concept, and reinforced by genetic analyses (DelPero *et al.*, 2000; Masters & Lubinsky, 1988; Roos *et al.*, 2004).

Despite their similar morphology, galago species display marked differences in diet and locomotion. Although most species are omnivorous and all consume some gum, smaller species, such as *G. demidoff* at 45-72g, consume a greater proportion of insects, medium-sized species, such as *E. elegantulus* at 270-360g, consume a greater proportion of gum, and the larger species, such as *O. crassicaudatus* at 604g-1.06kg, are more frugivorous (Charles-Dominique, 1977; Nekaris & Bearder, 2011). The Galagonidae use their tooth-comb to help them scrap or gouge exudates from trees and even have a sublingua, a 'second tongue' underneath their main tongue, which has a serrated edge, to help them clean gum from their tooth-comb (Nekaris & Bearder, 2011). Galagos all have long tails and relatively elongated tarsal bones, which allow them to move quickly and to jump across gaps in the canopy, usually by vertical clinging and leaping. But, again, their specific

form of locomotion is largely dependent on their size: the smaller species tend to employ quadrupedal running, climbing and jumping, while larger taxa require sturdier branches, and move in a quadrupedal, more 'monkey like' fashion. Some taxa are strictly arboreal (*Galagoides* sp. and *Euoticus* sp.), while others sometimes come down to the ground, using either quadrupedal running (*O. crassicaudatus*) or bipedal hopping (*O. garnettii* and *G. moholi*) (Nekaris & Bearder, 2011). Some variation is also seen in social organisation, but in general galagos are thought to be solitary foragers, with matrilocal females sharing sleeping sites. Males are dispersed, with larger home ranges that overlap those of groups of females (Mueller & Thalmann, 2000; Nekaris & Bearder, 2011).

1.2.4.2.2. Lorisidae

The Lorisidae are found in a wide range of habitats, including montane-, rain- and bamboo forests, which is perhaps unsurprising given their extensive geographical distribution (Nekaris & Bearder, 2011). Both Africa and Asia can boast a robust (*Perodicticus* and *Nycticebus*, respectively) and a slender (*Arctocebus* and *Loris*, respectively) lorisid, which, despite appearing on separate continents, share many physical characteristics (Yoder, 1997). The African lorises are found in the central African rainforests (*Arctocebus*) and in a band across sub-Saharan Africa, from Nigeria, Cameroon and Gabon in the west to Kenya in the East (*Potto*). The Asian *Nycticebus* are distributed throughout south-east Asia, while *Loris* is found only in India and Sri Lanka (Groves, 1998; Nekaris & Bearder, 2011). The Lorisidae range in size from 100g-2.1kg and, interestingly, *Potto* appear to adhere to Bergmann's Rule (if altitude is taken as proxy for temperature), with larger specimens occupying higher altitudes and the smaller forms located in lower-lying coastal habitats (Ravosa, 2007).

All Lorisidae are slow in their movements and possess a suite of morphological traits that enable them to remain still for extend periods of time, including: highly mobile wrist and ankle joints; shortened second digits on their hands and feet; and 'retia mirabilia', which is an adaptation of the arteries and veins that allows the limbs to be provided with a constant supply of oxygen and for waste products to be removed, without the need for movement in the muscles (Nekaris & Bearder, 2011; Rasmussen & Nekaris, 1998). This stillness helps to camouflage the Lorisidae, which is useful both when hunting prey and as protection from predators (Nekaris & Bearder, 2011; Rasmussen & Nekaris, 1998). Lorises do not leap and instead bridge gaps in the canopy by 'cantilevering' with their long flexible bodies, branches

must therefore first be tested to ensure that they are strong enough to support the loris, hence the 'slow' in their common name (Nekaris & Bearder, 2011).

Diets are varied across species; *Potto* is found to have a predominantly fruit based diet, but does also consume prey species, including arthropods, bats and birds (Charles-Dominique, 1977). *Nycticebus* is a prolific 'gouger', with a diet that is heavily reliant on gum (~60%), with their specialised grip allowing them to cling on to the tree trunk or branch for extended periods of time while they feed (Nekaris, 2014; Starr & Nekaris, 2013; Wiens, 2002). Some of this gum is highly toxic to other animals, and can blister the skin or even kill humans (Wiens *et al.,* 2006). Slow lorises are thought to be an important pollinator, with nectar contributing a further 28% of their diet (Wiens, 2002), accessed with their specially adapted, very long tongue and short, broad sublingua (Starr & Nekaris, 2013; Wiens, 2002). Fruit and invertebrates make up the remainder of their diet (Wiens, 2002). The smaller *N. pygmaeus* also relies on nectar and gum (Streicher, 2005; Tan & Drake, 2001). *Loris* are faunivorous and are tolerant of many highly toxic prey species, with different species also supplementing their diet with fruit, gum and nectar, to varying extents (Nekaris & Rasmussen, 2003).

Convergent orbits mean that the visual fields overlap; this allows for stereoscopic or binocular vision (Cartmill, 1992). Asian lorises have the most convergent orbits of all strepsirhines; it has been suggested that this convergence was selected for to aid the capture of prey in *Loris* (Cartmill, 1992) and the selection of flowers, in the swaying terminal branches, in *Nycticebus* (Cartmill, 1992; Nekaris, 2014; Sussman, 1991).

Due to their nocturnal, arboreal, slow moving and camouflaged nature, it has been difficult to study the social structure of the Lorisidae (Nekaris & Bearder, 2011). The limited data available report a single-male/single-female social structure for both *Potto* (Charles-Dominique, 1977; Müller & Thalmann, 2000) and *Nycticebus* (Wiens & Zitzmann, 2003), while *Loris* is thought to have a multi-male/multi-female organisation, with one or more adult males sharing sleep sites with females (Nekaris, 2003).

One unique characteristic of the *Nycticebus* genera is their ability to produce venom through the combination of oil from their brachial arm glands and their saliva, making them the only venomous primate (Nekaris *et al.,* 2013). While their venom is strong enough to

kill small animals, and can cause anaphylactic shock in humans, it is not thought that it originally evolved to kill prey (Nekaris *et al.*, 2013). Instead, it has been suggested that, as the venom mimics that of cobras (*Naja sp.*), it may have developed during the Miocene as a Mullerian mimicry anti-predation strategy (Nekaris *et al.*, 2013). Now, in addition to predation and anti-predation, the venom is also used as defence against parasites and conspecifics (Nekaris *et al.*, 2013).

1.2.5. Strepsirhine morphology

1.2.5.1. Strepsirhine diagnostic traits

The diverse taxa contained within the Strepsirhini are distinct among primates in their retention a nasal region with a moist nose and an unfused mandibular symphysis (Fleagle, 2013; Nekaris & Bearder, 2011) and a relatively small cranial vault (Fleagle, 2013). Strepsirhines are derived from other primates with regard to their sloping talofibular facet (Fleagle, 2013; Nekaris & Bearder, 2011); their tooth-comb (Martin, 2003), which is made up of the lower incisors and canines (with the exception of *Daubentonia* and the *Indriidae*), and the associated reduced upper incisors, and is employed for grooming and in some cases for accessing tree exudates (Fleagle, 2013; Gould *et al.*, 2011; Martin, 2003); a postorbital bar, which helps to protect and stabilise the eyes against the movement of large chewing muscles, particularly the temporalis muscle (Kirk, 2003); and a grooming claw on the second digit of their feet (in most species all other digits have nails) (Kirk, 2013; Soligo & Müller, 1999).

1.2.5.2. Strepsirhine dental formulae

Dental formulae vary across taxa: for the Lemuridae and Cheirogaleidae, as well as the Galagonidae and the Lorisidae, it is 2.1.3.3 (Godfrey, 2005; Gould *et al.*, 2011); the Indriidae have lost a premolar in both their upper and lower dentition and as such their dental formula matches that of Old World Monkeys (OWM), and apes (2.1.2.3), in addition, only incisors and not canines are included in the tooth-comb (Gould *et al.*, 2011): As a family, the Lepilemuridae are derived in lacking permanent upper incisors, which are replaced by a 'plucking pad', an adaptation to their unique style of folivory (Jungers *et al.*, 2002), giving them the dental formula 0.1.3.3/2.1.3.3. Finally, the aye-aye has the most unusual dentition of all primates, with an upper dental formula of 1.0.1.3 and a lower of 1.0.0.3; furthermore, the incisors are rodent-like, in that they grow at a constant rate throughout their lifetime (Gould *et al.*, 2011).

1.2.5.3. Sexual dimorphism

Lemuriforms have been shown to be sexually monomorphic, both in terms of body size and cranium length (Jenkins & Albrecht, 1991; Kappeler, 1990). This is also true for the larger bodied sub-fossil lemurs (Godfrey *et al.,* 1993). Lorises have also been shown to be largely sexually monomorphic, with the exception of *Nycticebus pygmaeus* (Kappeler, 1991). Galagos do show some sexual dimorphism in terms of body weight, but this is minimal (<1:1.18) (Kappeler, 1991). In addition, any sexual dimorphism within the Strepsirhini has been shown to be significantly less than the sexual dimorphism found in the Haplorhini, and has thus been described as relative monomorphism (Kappeler, 1990; Thorén *et al.,* 2006).

It is hypothesised that the relative sexual monomorphism seen in strepsirhines is largely a consequence of their social organisation (Jenkins & Albrecht, 1991; O'Mara *et al.,* 2012). Sexual dimorphism may not be advantageous in multi-male/multi-female societies where it is not possible to monopolise breading partners; it is also thought to have little adaptive advantage in pair-bonded of solitary species (Jenkins & Albrecht, 1991; Martin, 1980). These three social structures cover the principal social organisations described for strepsirhines (Charles-Dominique, 1977; Gould *et al.*, 2011; Martin, 1990; Müller, 1999; Müller & Thalmann, 2000; Nekaris, 2003; Nekaris & Bearder, 2011; Petter *et al.,* 1977; Radespiel, 2000; Radespiel *et al.,* 1998; Rasoloharijaona *et al.,* 2008; Wiens & Zitzmann, 2003) and have also been shown to correspond to a lack of sexual dimorphism in some haplorhine species (Martin, 1980).

1.2.5.4. Morphological diversity in the strepsirhine cranium

In comparison to haplorhines, extant strepsirhines have been noted for their relatively low level of cranial diversity (Fleagle *et al.,* 2010). Extant haplorhines are both more speciose (~300) and more geographically diverse than stepsirrhines, occupying every continent with the exception of Australia and Antarctica (Wilson & Reeder, 2005). However, in view of strepsirhines' still extensive biogeographical distribution and their ecological and behavioural diversity, this comparative lack of morphological variation is surprising (Fleagle *et al.,* 2010). The relatively recent extinction of a large percentage of the Lemurs, specifically the larger of the taxa, which possessed some distinctive cranial morphologies, does have an impact on these findings (Fleagle *et al.*, 2010; Godfrey & Jungers, 2002). When subfossil taxa (*Megaladapis edwardsi, Paleopropithecus maximus* and *Archaeolemur majori*) are

included in the analysis, they increase the amount of morphological diversity contained within the strepsirhine clade, but it is still significantly lower than that found for haplorhines (Bennett & Goswami, 2012). It is possible that the inclusion of additional subfossil taxa would continue to increase the level of diversity within the strepsirhine clade. However, there is a counter-argument that other primate groups have experienced similar periods of high extinction (e.g., the hominids); extensive fossil taxa would therefore be need to be included for both clades, and such data is not necessarily available in the fossil record (Fleagle, 2013; Fleagle *et al.*, 2010).

In an analysis of shape variation in haplorhines and strepsirhines, PC2 was positively associated with the overall size of the cranium and the relative length of the snout and the palate and negatively associated with the height of the neurocranium (Fleagle *et al.*, 2010; Figure 2). Strepsirhines had particularly limited variation in PC2. For haplorhines, a large amount of the variation along this axis was driven by the morphology of sexually dimorphic males (Fleagle *et al.*, 2010). Strepsirhines are generally sexually monomorphic (Godfrey *et al.*, 1993; Jenkins & Albrecht, 1991; Kappeler, 1990; Kapperler, 1991), which may go some way to explaining their limited morphological diversity in comparison to haplorhines (Fleagle *et al.*, 2010). An additional cause, for the relatively low morphological diversity found across strepsirhines, may have been the morphological landmarks used in the analyses; only 18 (Fleagle *et al.*, 2010) or 33 (Bennett & Goswami, 2012) landmarks were used to ensure homology across primate species. This could have resulted in a failure to capture the full diversity of strepsirhine morphology (Fleagle *et al.*, 2010).

1.2.5.5. Primate cranial morphology

In studies of cranial morphology across extant primates, the main axis of shape variation (PC1) represents variation in the overall size of the cranium, as well as variation in relative neurocranial volume, orbital convergence, orbital frontation, orbit size, superior-inferior face depth and cranial base flexion (Figure2) (Bennett & Goswami, 2012; Fleagle *et al.*, 2010). This shift in morphology separates strepsirhines from haplorhines (Fleagle *et al.*, 2010). The addition of subfossil lemur taxa to the analysis narrows the morphological distance between strepsirhines and haplorhines, but the separation between the clades remains (Bennett & Goswami, 2012). This morphological separation is thought to be indicative of a significant event in primate evolution (Kay *et al.,* 1997). The precise reasons for this morphological reorganisation are not known, but it has been suggested that it could

be linked to a move towards a diurnal activity pattern and a subsequent reliance on vision for hunting prey in anthropoids (Ross, 1996; 2000). Moreover, within haplorhines, hominoids are also separated from cercopithecoids and platyrrhines, implying a second shift in morphology during the evolution of the great apes (Fleagle *et al.*, 2010).

Eulemur and *Varecia* are shown to be positioned at the extreme negative of this axis, with small neurocrania, relatively long, flat faces and laterally facing orbits, while great apes occupy the extreme positive of the axis, with their large neurocrania and convergent orbits (Fleagle *et al.*, 2010). Within stepsirrhines, the indriids, lorisoids and *Daubentonia* plot close to the anthropoids; this is likely to be the result of their relatively short faces, globular neurocrania and convergent orbits (Fleagle *et al.*, 2010).

In this instance, PC1 is correlated with size. However, while the small strepsirhines are found at the opposite end of the shape axis to the larger great apes, the Callitrichidae, which are similar in size to most of the Strepsirhini, have a relatively high score for PC1 and plot within the anthropoid primates. So, while size is a significant factor in the shape change, it is not the only factor (Fleagle *et al.*, 2010).

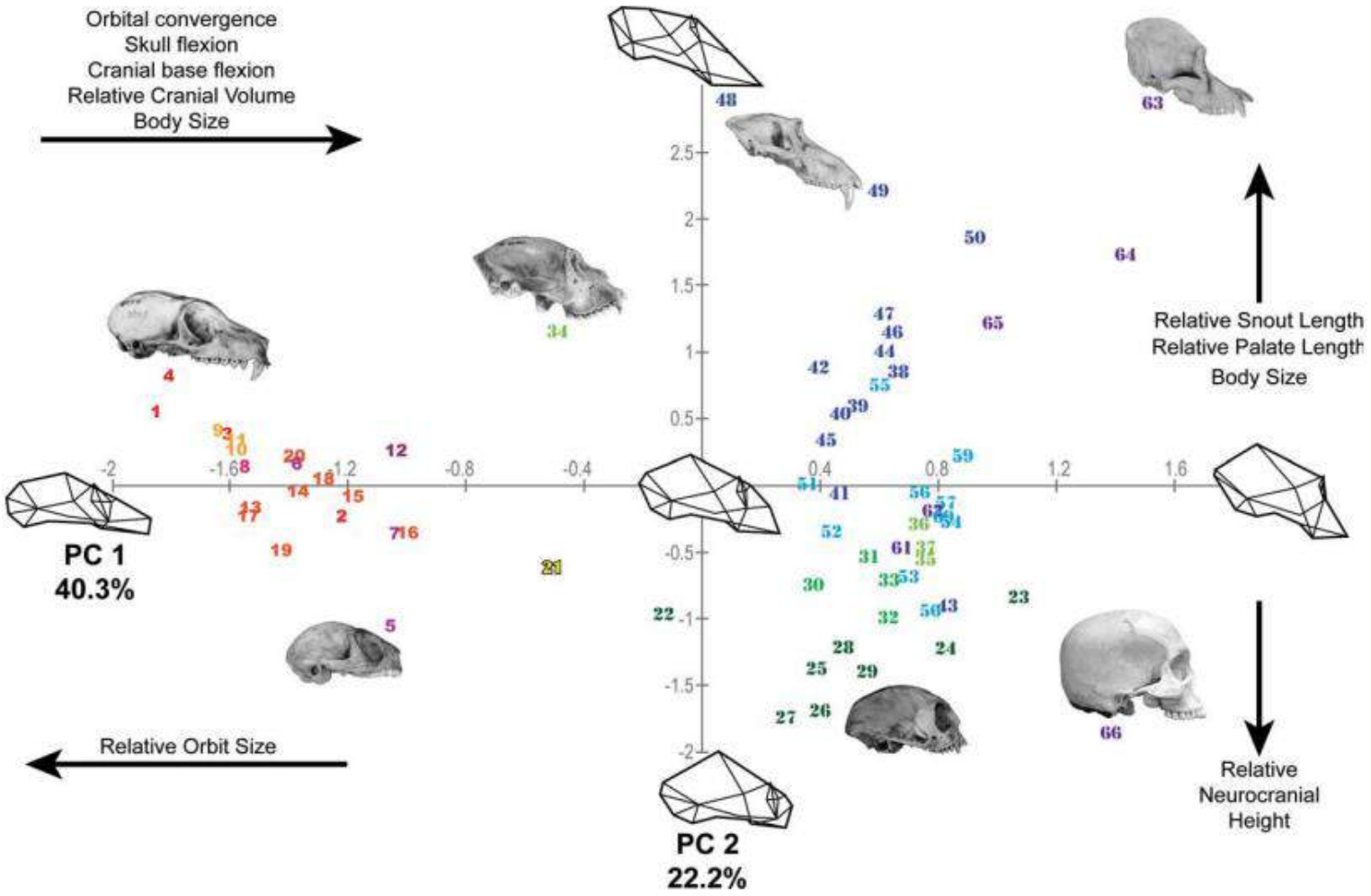

Figure 2: PCA of male primates demonstrating the extremes of primate cranial morphology, with both extant crania, and wireframes of the principal component axes, as well as the aspects of cranial morphology most highly correlated with each component. Numbers of individual taxa follow Taxon Code in Table 1 in Fleagle *et al.* (2010). Colours reference major primate groups. Red, lemurids; light purple, indriids; maroon, daubentoniids; light orange, cheirogaleids; dark orange, lorisoids; yellow, tarsiids; light green, atelids; dark green, cebids; light blue, colobines; dark blue, cercopithecines; dark purple, hominoids (from Fleagle *et al.* 2010, Fig 3, p. 569).

1.2.5.5.1. The primate orbit

The influence of allometric scaling has been noted as having a particular effect on orbit size and orientation, both of which vary dramatically across primate species, which in turn has wider implications for the morphology of the cranium overall (Fleagle *et al.*, 2010). Orbit size is negatively allometric in relation to body size in primates (Baab *et al.,* 2014). The relatively larger eyes in smaller species can accommodate a similar number of retinal cells as the eyes of larger species and therefore attain similar visual acuity (Kirk, 2006). In addition, nocturnal faunivorous primates have relatively larger orbits than diurnal primates (Kirk, 2006). The enlargement of the eye results in a larger retinal image (Ross, 2000) and as such, the relatively larger orbits of nocturnal faunivores may be an adaptation for better visual acuity in the context of visually locating and tracking prey (Kirk, 2006).

Orbital convergence is the extent to which both the right and the left orbit face in the same directions (i.e., when both orbits face forward there is high orbital convergence, but when orbits are laterally place on the cranium and therefore face in opposite directions orbital convergence is low) (Fleagle *et al.*, 2010). Larger taxa tend to have higher levels of orbital convergence than smaller taxa. In part, this may simply be attributed to the fact that forward facing orbits can more easily be accommodated on a larger face (Martin, 1990; Ross, 1995). But, it has also been linked with a need for increased stereoscopic vision, achieved through the overlapping of the eyes' visual fields, to aid the capture of prey species (Cartmill, 1992).

The postorbital bar, common to all primates, has been suggested to be an adaption to either aid in the resistance of stress exerted on the primate face during mastication (Greaves, 1985; 1991) or to provide stability to the lateral edge of the orbit during mastication (Ravosa *et al.,* 2000). The latter explanation is based on the Visual Predation Hypothesis (Cartmill, 1974, 1992); orbital convergence moves the lateral edge of the orbit away from the plane of the temporal fossa and into a position where the eye is likely to experience greater interference from the chewing muscles during mastication. The postorbital bar is therefore thought to protect the lateral edge of the eye, so that visual acuity is maintained during mastication and the animal can go on foraging (Ravosa *et al.*, 2000). Analysis of the amount of strain exerted on facial bones during mastication shows that the primate face should be able to withstand these stresses without the need for a

postorbital bar, therefore finding in favour of an explanation that requires visual acuity to be maintained during chewing (Heesy, 2005; Ravosa *et al.*, 2000).

1.2.5.5.2. The primate brain and cranial vault

Encephalisation varies across primate species; anthropoid primates are highly encephalised, about twice as much as the 'average' modern mammal (Jerison, 1973; Preuss, 2009), while strepsirhine primates lack the elevated degree of encephalisation found in haplorhine primates and, once fully matured, are not notably more encephalised in comparison to other mammalian groups (Isler *et al.*, 2008; Jerison, 1973; Kirk, 2013; Preuss, 2009), although at birth, brain mass constitutes ~12% of body mass in primates, including strepsirhines, and only ~6% for the majority of other mammals (Sacher, 1982). Brain size is inextricably linked to the shape of the primate cranial vault and in haplorhines the cranial base (Ross & Ravosa, 1993; Smith, 1994; see below), and in line with their relatively low levels of encephalisation, strepsirhines are noted as having a relatively small cranial vault (Fleagle, 2013). Within strepsirhines, a negative allometric relationship between brain and body size has been found for the Lemurs, with *Daubentonia madagascariensis* notable for having the largest brain in relation to body size and *Indri indri* the smallest (MacLean *et al.,* 2009).

The Social Brain Hypothesis has been a well-supported explanation for the high levels of encephalisation seen in haplorhine primates, both in terms of relative brain size and the relative size of the neocortex (Dunbar, 1992, 2002; Dunbar & Shultz, 2007b). The theory suggests that relatively larger brains evolved to cope with the expanding size and complexity of primate social groups (Dunbar, 2002). However, it seems that the positive correlation between group size and relative brain size may be one that is unique to haplorhine primates. In birds and other mammalian orders (Chiroptera, Carnivora and Artiodactyla), pair-bonding monogamy is instead associated with relatively large brain size (Dunbar & Shultz, 2007a). This relationship is explained as a need for greater cognitive ability as species move away from loose social aggregations to more complex individual relationships (Dunbar & Shultz, 2007b). Strepsirhine primates show no significant correlation between relative brain size and group size, differing from both haplorhine primate and non-primate mammals, although only relative brain size and not the relative size of the neocortex could be tested (MacLean *et al.*, 2009). These results indicate that the inter-individual relationships of strepsirhines living in large groups may be less complex

than those experienced by haplorrhines (Genty & Roeder, 2006; Nakamichi & Koyama, 1997). In addition, a pair-bonded social structure, which has been recorded for many strepsirhine taxa (Britt, 2000; Gould *et al.*, 2011; Mittermeier *et al.,* 2006; Müller, 1999; Rasoloharijaona *et al.,* 2006), does not appear to have had a significant impact on their relative brain size (MacLean *et al.*, 2009)

A correlation has been found between both activity pattern and diet and relative brain size in lemurs; cathemeral species have relatively larger brains than diurnal, but not nocturnal, species and frugivorous species are shown to have relatively larger brains than their folivorous counterparts (MacLean *et al.*, 2009). The relatively larger brain size associated with cathemerality has been linked to a need for greater flexibility in behaviour (Curtis *et al.,* 1999; MacLean *et al.*, 2009). Frugivory has been suggested to require greater visual sensitivity, specifically the ability to distinguish the colours of fruits from the rest of the forest flora (Barton, 1998), and/or a need for spatial and temporal memory to locate food sources (Milton, 1981). It has further been argued that frugivorous diets provide more energy and require less processing than folivorous diets, leaving more energy available to develop and support a larger brain (Aiello & Wheeler, 1995). Although, one point to take into consideration when interpreting these results, is that the data were not controlled for influence of phylogenetic relationships, with which both diet and activity patterns are correlated (MacLean *et al.*, 2009).

1.2.5.5.3. The primate cranial base

The cranial base provides the structure around which the face and brain develop, and acts as the junction between the cranial and postcranial skeleton, neural connections and circulatory system (Lieberman *et al.,* 2000). Due to the close association of the cranial base with both the face and the brain, significant correlations, in terms of size and shape, are expected to exist between them (Lieberman *et al.*, 2000; Ross & Ravosa, 1993). This has been confirmed for haplorhine primates, for which brain size, relative to basicranial length, was significantly correlated with basicranial flexion (Ross & Ravosa, 1993; Smith, 1994). The haplorhine face, specifically the orientation of the orbits and upper face is also closely related with the angle of the anterior cranial base (McCarthy & Lieberman, 2001; Ross & Ravosa, 1993). However, neither relationship was significant for strepsirhine primates (McCarthy & Lieberman, 2001; Ross & Ravosa, 1993; Smith, 1994). The absence of a relationship between brain size and basicranial flexion in strepsirhines may in part be

explained by their lack of encephalisation in comparison to haplorhine primates (Isler *et al.*, 2008; Jerison, 1973; Kirk, 2013; Preuss, 2009)**.** These differences in cranial organisation and integration between the two clades again indicate a significant shift in morphology at the beginning of haplorhine evolution (Fleagle *et al.*, 2010).

1.2.6. Strepsirhine conservation status

Among the Strepsirhini, it is the lemuriforms which face the greatest threat of extinction (IUCN, 2015; Schwitzer *et al.*, 2013). A recent assessment of the Malagasy taxa placed 91% of species (94 out of a recognised 103 species) into one of the International Union for Conservation of Nature's (IUCN) threat categories; i.e., either 'critically endangered', 'endangered', or 'vulnerable' (IUCN, 2015; Schwitzer *et al.*, 2013). In addition, in a list of the world's 25 most endangered primates, six of the species named are lemuriforms, namely, *Microcebus berthae, Eulemur flavifrons, Varecia rubra, Lepilemur septentrionalis, Propithecus candidus* and *Indri indri* (Schwitzer *et al.*, 2014).

Mass deforestation and habitat fragmentation are the principal causes of the threat to the lemuriforms, with an estimated 90% of the Island's natural vegetation already lost, largely due to agriculture and logging (Ganzhorn *et al.*, 2000; Harper *et al.,* 2007; Wilmet *et al.,* 2014). This has been exacerbated by the high growth rate of the human population and frequent incidences of political instability (Mittermeier *et al.*, 2008). Lemurs are facing a further threat from humans, as they have become a target for bushmeat hunters (Jenkins *et al.*, 2011; Jones *et al.,* 2008). This is a fairly recent problem, as traditionally it was considered taboo to eat them; however increased population mobility has meant the local taboos are being broken down (Jenkins *et al.*, 2011; Jones *et al.,* 2008).

The lorisiform primates are also threatened, but to a lesser extent than the lemuriforms, possibly as a result of their more extensive geographic distribution. Nine species of the Lorisidae and four of the Galagonidae have been classified as either 'critically endangered', 'endangered', or 'vulnerable' according to the ICUN 's Red List (IUCN, 2015), while both *Galagoides rondoensis* and *Nycticebus javanicus* are included on the list of the World's 25 most endangered primate species (Schwitzer *et al.*, 2014). The key threats to lorisiforms are, again, habitat destruction and fragmentation (Perkin *et al.,* 2008; Thorn *et al.,* 2009) and, for the Lorisidae in particular, capture for the pet trade (Nekaris & Jaffe, 2007; Thorn *et al.*, 2009).

1.3. Rationale

Strepsirhines are a richly diverse group, geographically, behaviourally and morphologically (Fleagle, 2013; Gould *et al.*, 2011; Nekaris & Bearder, 2011) while also physically distinct from other mammal and other primate taxa (Fleagle, 2013; Kirk, 2013). As such, they offer a prime opportunity for the exploration of evolutionary topics using GMM techniques, especially as the phylogenetic relationships between species are now largely resolved (Finstermeier *et al.*, 2013; Horvath *et al.*, 2008; Masters *et al.*, 2007; Matsui *et al.*, 2009; Perelman *et al.*, 2011; Roos *et al.*, 2004; Springer *et al.*, 2012; Steiper & Seiffert, 2012; Yoder & Yang, 2004).

However, to date studies of the Strepsirhini, and specifically their cranial morphology, have been limited. Where strepsirhines have been studied, particularly with regard to modularity, allometry and phylogenetic signal, there has been a tendency to either incorporate a limited number of strepsirhine species within a wider group of taxa (Goswami, 2006a; Goswami & Polly, 2010b; Shoshani *et al.,*1996), or to focus on only a narrow range of species within strepsirhines, generally within one family (Ravosa & Daniel, 2010; Ravosa *et al.,* 2010; Viguier, 2002) or in some cases one genus (Ravosa, 1998; Ravosa, 2007).

Furthermore, even fewer of these studies have used GMM analyses and those that have had been limited to fairly small sample sizes (Baab *et al.*, 2014; Lebrun *et al.,* 2010; Viguier, 2002). Shape parameters frequently used in GMM studies have been found to be increasingly inaccurate at reduced samples sizes in other primate groups (Cardini & Elton, 2007), but, comparable analyses have not been conducted for strepsirhines. This is therefore an opportunity to address questions that have previously been unexamined for the strepsirhine clade, using a large and broad sample and GMM techniques, with the aim to lay a solid foundation for investigating the evolutionary pressures and pathways that have resulted in the cranial morphology and diversity of extant stepsirrhines.

1.4. Specific aims

To investigate the effect of reduced sample size in geometric morphometric studies of size and shape, across a broad range of strepsirhine taxa.

To assess modularity in the strepsirhine cranium, gaining an understanding of how this is structured and how it influences the evolutionary pathways available for strepsirhine morphological evolution.

To understand the allometric patterns present in the strepsirhine cranium and how these vary both across cranial modules and across species.

To test a re-sampling method that incorporates intra-species variation into inter-species analysis and to compare it with a method that uses species average data.

To assess the strength of phylogenetic signal present in the strepsirhine cranium and how the strength of this signal varies across cranial modules.

To explore which statistical model of evolution best explains the data, with regard to the morphology of the strepsirhine cranium, and to use this to identify both homologies and homoplasies present in strepsirhine morphology.

– Chapter 2 –

Materials and methods

The specimens, data and general methods used throughout the following research are summarised below. Where additional methods are used, which are specific to a particular chapter, they are outlined within that chapter.

2.1. Specimens

Data were collected from the crania of 1633 strepsirhine specimens, across 7 families, 20 genera and 30 species (see Table 2 for details of species and sample sizes and Figures 6 and 7 for details of their phylogenetic relationships), housed in the collections of: the Natural History Museum, London, UK; Muséum National d'Histoire Naturelle, Paris, France; Museum für Naturkunde, Berlin, Germany; and the Smithsonian Institution National Museum of Natural History, Washington DC, USA. Only adult specimens were included, as determined by fully erupted dentition. Museum documentation was used for species identification. The majority of specimens were wild caught (N=1577) with date and location, or at least country, of origin available for most (N=1218), the remaining specimens (N=56) were raised in captivity. The inclusion of captive specimens and those for which location data were not available allowed for larger samples and the inclusion of a wider range of species. The general lack of sexual dimorphism in strepsirhines (see Chapter 1) means that the male, female and indeterminate specimens of each species, were able to be pooled, resulting in more robust sample sizes.

Table 2: Species sampled, with sample sizes, where M= males, F= females, I=indeterminate and N= total sample size. Museums from which specimens were collected are also indicated; A= Smithsonian Institution National Museum of Natural History, Washington DC, USA, B= Natural History Museum, London, UK, C= Muséum National d'Histoire Naturelle, Paris, France and D= Museum für Naturkunde, Berlin, Germany.

Infraorder	Family	Genus	Species	M	F	I	N	Location
Lemuriformes	Cheirogaleidae	*Cheirogaleus*	*major*	11	2	12	**25**	B, C, D
			medius	13	5	11	**29**	B, C, D
		Microcebus	*murinus*	28	24	20	**72**	A, B, C, D
			rufus	10	8	11	**29**	A, B, C, D
		Phaner	*furcifer*	4	3	3	**10**	B, C, D
	Daubentoniidae	*Daubentonia*	*madagascariensis*	6	1	5	**12**	A, B, C
	Indriidae	*Avahi*	*laniger*	9	6	7	**23**	B, C, D
		Indri	*indri*	18	10	11	**39**	B, C, D
		Propithecus	*diadema*	14	5	9	**28**	A, B, C, D
			verreauxi	12	17	14	**43**	A, B, C, D
	Lemuridae	*Eulemur*	*coronatus*	3	4	0	**7**	B, D
			fulvus	78	54	44	**176**	A, B, C, D
			macaco	22	22	11	**55**	A, B, C, D
			mongoz	13	17	27	**57**	A, B, C, D
			rubriventer	9	9	9	**27**	A, B, C, D
		Hapalemur	*griseus*	9	8	10	**27**	A, B, C, D
		Lemur	*catta*	9	5	20	**34**	A, B, C, D
		Varecia	*variegata*	10	5	24	**39**	A, B, C, D
	Lepilemuridae	*Lepilemur*	*microdon*	6	8	2	**16**	B, C
			mustelinus	3	1	1	**5**	B, D
			ruficaudatus	4	8	13	**25**	B, C, D
Lorisiformes	Galagidae	*Euoticus*	*elegantulus*	16	11	7	**34**	A, B, D
		Galago	*alleni*	10	4	10	**24**	A, B, C, D
			moholi	30	38	5	**73**	A, B, D
			senegalensis	97	75	3	**175**	A, B, C, D
		Galagoides	*demidoff*	39	16	4	**59**	A, B, D
			zanzibaricus	11	14	0	**25**	A, B
		Otolemur	*crassicaudatus*	46	35	20	**101**	A, B, D
			garnettii	47	42	6	**95**	A, B, D
	Lorisidae	*Arctocebus*	*calabarensis*	8	2	1	**11**	A, B, C, D
		Loris	*tardigradus*	10	11	6	**27**	A, B, C, D
		Nycticebus	*bengalensis*	7	6	9	**22**	A, B, C
			coucang	25	23	21	**69**	A, B, C, D
			pygmaeus	7	1	3	**11**	B, C
		Perodicticus	*potto*	59	38	32	**129**	A, B, C, D

2.2. Data

Data originally comprised 65 3D morphological landmarks collected using a Microscribe MX digitizer (accurate to <0.05mm), largely based on the composition outlined by Cardini *et al,* (2007). The landmarks encompass the nasal aperture, orbit and palate as well as the zygomatic, frontal, parietal, temporal, occipital and sphenoid bones. Where landmarks described midpoints between two other landmarks, this distance was measured with a tape measure and marked using museum putty (this is easily removed afterwards and leaves no mark). All specimens included in the analysis displayed a full complement of landmarks (i.e., any broken or damaged specimens were excluded from the sample). Landmarks were collected only from the left side of the cranium to avoid redundant information, except in cases when the left side of the cranium was damaged, in which case landmarks were collected from the right side.

Landmarks were assessed for repeatability; data were collected from the same specimen of *Eulemur fulvus* on five separate occasions and tested in two ways. First, graphically; the data were subjected to Generalised Procrustes Analyses (GPA; see below) and Principal Component Analyses (PCA; see below) using the programme MorphoJ (Ver. 1.06b; Klingenberg, 2014). PCA partitions shape change into discrete packets of variation. Performing PCA on repeats of the same specimen highlights any change in shape between those repeats, which would indicate a lack of landmark repeatability. MorphoJ provides a visualization of the change in the landmarks associated with each Principal Component (PC; Figure 3). For PC 1, which represents the greatest proportion of shape change, landmark 28, which describes the widest point on the parietal, showed considerable variation and therefore lack of repeatability compared to the other landmarks.

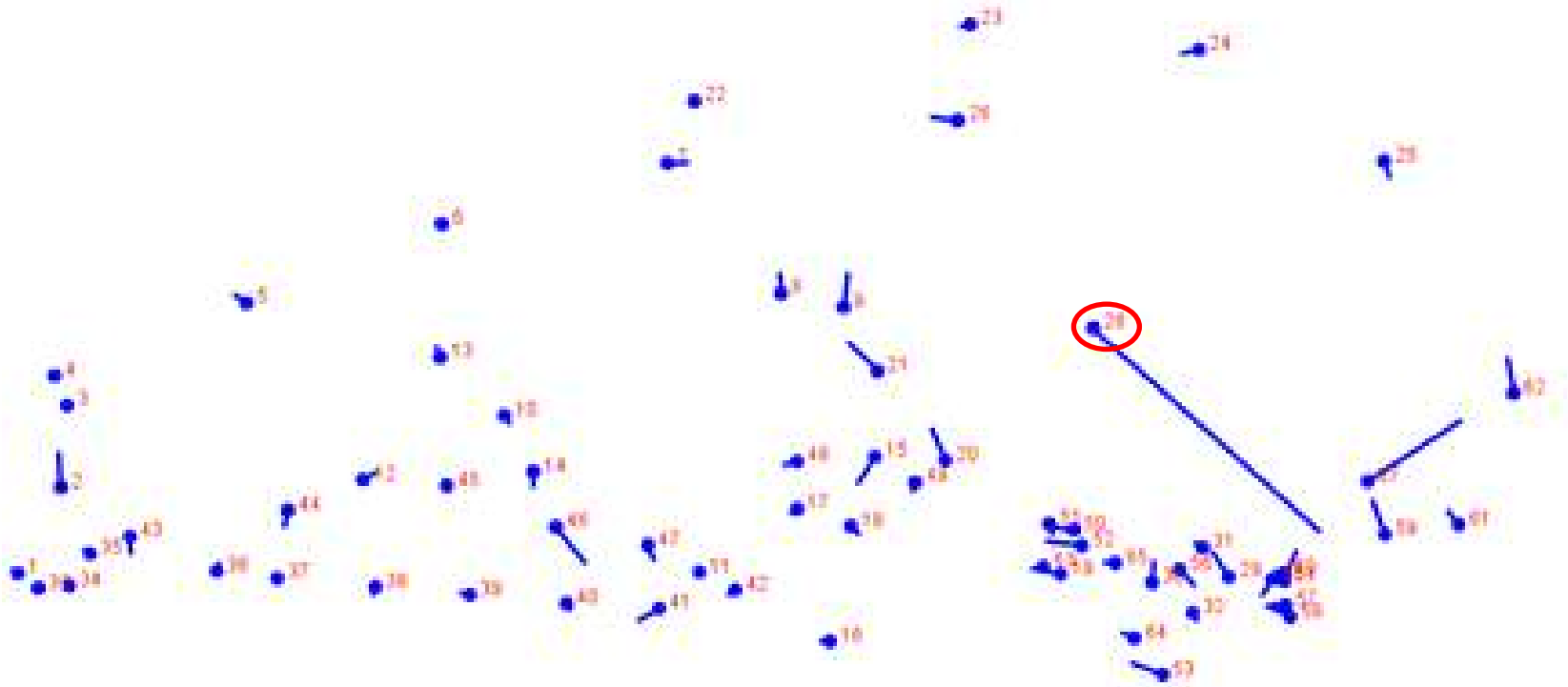

Figure 3: Visualisation of PC1 for all 65 landmarks based on the repeated sampling of a single *E. fulvus* specimen. Showing axis 1 against axis 2 (lateral view).

Second, landmark repeatability was tested quantitatively; again the repeat data collected from a single *E. fulvus* specimen was subjected to GPA to remove any non-biological components of shape change. The average standard deviation for each landmark (each x-y-z coordinate) was then calculated. These results are compared to each other, to see if certain landmarks show greater variation than others (Table 3). They are also compared to the standard deviation of corresponding landmarks calculated from species level (*Eulemur fulvus*) and genera level (*Eulemur* sp.) data sets (Table 4).

Table 3: Average standard deviation of each landmark for repeats of *E. fulvus*, shown in descending order.

Landmark	*Eulemur fulvus* repeats	Landmark	*Eulemur fulvus* repeats	Landmark	*Eulemur fulvus* repeats
28	0.008422	47	0.001182	6	0.000711
27	0.004095	48	0.001176	37	0.000706
9	0.002645	32	0.001101	11	0.000680
7	0.002453	41	0.001064	36	0.000667
46	0.002442	44	0.001056	23	0.000663
21	0.001959	29	0.001043	19	0.000655
26	0.001956	61	0.000974	65	0.000654
53	0.001832	60	0.000941	50	0.000622
20	0.001668	25	0.000924	13	0.000613
52	0.001583	2	0.000914	34	0.000584
18	0.001558	45	0.000882	57	0.000561
59	0.001530	40	0.000879	3	0.000555
30	0.001438	38	0.000859	64	0.000555
56	0.001388	55	0.000858	35	0.000533
62	0.001385	8	0.000856	22	0.000533
14	0.001365	49	0.000819	4	0.000518
54	0.001342	63	0.000813	5	0.000493
43	0.001316	39	0.000782	51	0.000480
12	0.001312	24	0.000780	1	0.000471
15	0.001279	31	0.000771	16	0.000435
58	0.001274	10	0.000766	33	0.000301
42	0.001189	17	0.000736		

Table 4: Average standard deviation of each landmark at specimen, species and generic level, for *E. fulvus.*

Landmark	*Eulemur fulvus* repeats	*Eulemur fulvus*	*Eulemur*	Difference between *E. fulvus* repeats and all *E. fulvus*
1	0.000471	0.003111	0.003392	0.002640
2	0.000914	0.002594	0.003000	0.001680
3	0.000555	0.002958	0.003322	0.002403
4	0.000518	0.003334	0.003496	0.002816
5	0.000493	0.003080	0.005453	0.002587
6	0.000711	0.004499	0.004986	0.003788
7	0.002453	0.005390	0.005774	0.002937
8	0.000856	0.004564	0.004625	0.003708
9	0.002645	0.004884	0.005261	0.002239
10	0.000766	0.003587	0.003931	0.002820
11	0.000680	0.004654	0.004703	0.003974
12	0.001312	0.003521	0.003473	0.002208
13	0.000613	0.003661	0.003616	0.003048
14	0.001365	0.003851	0.004085	0.002486
15	0.001279	0.002845	0.003066	0.001566
16	0.000435	0.004598	0.004219	0.004162
17	0.000736	0.003802	0.003812	0.003067
18	0.001558	0.004213	0.004334	0.002655
19	0.000655	0.003910	0.004109	0.003255
20	0.001668	0.005073	0.005414	0.003406
21	0.001959	0.004636	0.004907	0.002678
22	0.000533	0.004685	0.004818	0.004152
23	0.000663	0.005487	0.005646	0.004824
24	0.000780	0.004439	0.004567	0.003659
25	0.000924	0.004769	0.005069	0.003845
26	0.001956	0.009143	0.009216	0.007187
27	0.004095	0.006395	0.006567	0.002300
28	0.008422	0.010574	0.010314	0.002152
29	0.001043	0.002112	0.002285	0.001069
30	0.001438	0.003301	0.003223	0.001863
31	0.000771	0.002437	0.002536	0.001666
32	0.001101	0.002531	0.002604	0.001430
33	0.000301	0.002746	0.002938	0.002445
34	0.000584	0.002756	0.002805	0.002172
35	0.000533	0.003491	0.003418	0.002958
36	0.000667	0.002537	0.002576	0.001870
37	0.000706	0.002368	0.002463	0.001662
38	0.000859	0.002310	0.002451	0.001451
39	0.000782	0.002508	0.002610	0.001727
40	0.000879	0.002689	0.002866	0.001810
41	0.001064	0.002877	0.002999	0.001813
42	0.001189	0.003115	0.003363	0.001926

43	0.001316	0.002910	0.003129	0.001594
44	0.001056	0.002562	0.002669	0.001506
45	0.000882	0.003188	0.003255	0.002305
46	0.002442	0.006751	0.006971	0.004309
47	0.001182	0.004121	0.004133	0.002939
48	0.001176	0.005673	0.005726	0.004497
49	0.000819	0.004195	0.004245	0.003376
50	0.000622	0.003323	0.003246	0.002701
51	0.000480	0.003081	0.003413	0.002601
52	0.001583	0.003541	0.003718	0.001957
53	0.001832	0.003504	0.003739	0.001672
54	0.001342	0.002920	0.003001	0.001578
55	0.000858	0.003174	0.003089	0.002316
56	0.001388	0.002602	0.002558	0.001215
57	0.000561	0.002686	0.002679	0.002124
58	0.001274	0.002835	0.002930	0.001561
59	0.001530	0.002816	0.002837	0.001286
60	0.000941	0.002886	0.002793	0.001945
61	0.000974	0.003842	0.003706	0.002868
62	0.001385	0.004467	0.004461	0.003082
63	0.000813	0.003334	0.003419	0.002521
64	0.000555	0.002589	0.002716	0.002034
65	0.000654	0.002375	0.002526	0.001721

The quantitative analysis confirms what was shown in the graphical representation (Figure 3); landmark 28 lacks repeatability. Its standard deviation is more than double that of the next most variable landmark. As a result landmark 28 was removed from all further analyses. No landmarks were found to vary more in the same specimen than in the *E. fulvus* or *Eulemur* sp. data set.

Four additional landmarks were removed, as they were not homologous across all species: landmark 7, the supraorbital notch; 33, mesial incisor I1 septum; 34, mesial incisor I2 septum; and 36, mesial premolar P2 septum. The remaining 60 landmarks were found to be repeatable and were homologous for all specimens. Landmark numbers were reassigned and they are described in Table 5 and Figure 4.

Table 5: Final landmark composition

Landmark number	Landmark description
1	Nasospinale, inferior-most mid-line point
2	Piriform aperture, point of greatest width
3	Piriform aperture, meeting point of nasal and premaxilla
4	Rhinion, anterior-most mid-line point
5	Halfway point between rhinion and nasion
6	Nasion, frontal-nasal suture, mid-line point
7	Frontomalare orbitale, where frontozygomatic suture meet the inner orbit
8	Frontomalare temporale, where frontozygomatic suture meets the lateral part of the zygomatic
9	Zygomaticomaxillary superior, the anterior-superior point where the orbital rim meets the zygomaticomaxillary suture
10	Zygomaticomaxillary inferior, the lateral point of the zygomatic on the zygomaticomaxillary suture
11	Zygomatic foramen, inferior-most point
12	Infraorbital foramen, inferior-most point
13	Nasolacrimal foramen, inferior-most point
14	Optic foramen, inferior-most point
15	Ventral most point on the palatine
16	Point of maximum curvature of anterior of the zygomatic arch
17	Zygomaticotemporal suture on the lateral part of the zygomatic arch, superior-most point
18	Zygomaticotemporal suture on the lateral part of the zygomatic arch, inferior-most point
19	Junction of the sphenoid, zygomatic and parietal
20	Junction of the zygomatic, frontal and parietal
21	Midpoint between the nasion and bregma
22	Bregma, the junction of the coronal and sagittal sutures
23	Midpoint between the bregma and lambda
24	Lambda, the junction of the sagittal and lamboid sutures
25	Junction of the superior temporal crest and the coronal suture
26	Asterion, junction of the temporal, parietal and occipital bones
27	External auditory meatus, posterior-most point
28	External auditory meatus, anterior-most point
29	External auditory meatus, superior-most point
30	External auditory meatus, inferior-most point
31	Mesial canine C1 septum
32	Mesial premolar P3 septum
33	Mesial premolar P4 septum
34	Mesial molar M1 septum
35	Mesial molar M2 septum
36	Mesial molar M3 septum
37	Septum at the end of dentition, mid-point
38	Incisive foramen, posterior-most point
39	Mid-point between landmarks 38 and 40
40	Junction of the maxilla and palatine, on the mid-line
41	Greater palatine foramen, posterior-most/lateral-most point
42	Posterior edge of the palatine, posterior-most point
43	Nasal spine, posterior-most point
44	Junction of the presphenoid and basisphenoid, on the midline
45	Junction of the basisphenoid and basioccipital, on the midline
46	Petrous apex, junction of the petrous, basisphenoid and basioccipital
47	Foramen lavelli, anterior-most/medial-most point

48	Petrous, greatest central projection
49	Jugular foramen, distal-most point
50	Jugular foramen, medial-most point
51	Mid-point between the junction of the basisphenoid and basioccipital, and the basion
52	Basion, anterior-most point of the foramen magnum
53	Occipital condyle, anterior-most point
54	Occipital condyle, posterior-most point
55	Hypoglossal canal, most medial point
56	Opisthion, posterior-most point of foramen magnum
57	Inion, posterior-most point of the cranium, on the midline
58	Point of greatest curvature in the interior of the posterior process of the temporal bone
59	Postglenoid process, tip
60	Glenoid fossa, deepest point

Figure 4: Landmark configuration as shown on a *Eulemur fulvus* specimen.

2.2.1. Sample error

Two different methods were used to establish if the data would be affected by individual sampling error. First, Procrustes distances (see below) were calculated between all possible pairs of *E. fulvus* repeats of the same specimen. These distances were then compared to the distances between all possible pairs of *E. fulvus* specimens. Procrustes distances were calculated using the final configuration of 60 landmarks. Procrustes distances between the repeats of the same specimen were shown to be considerably lower than those between different specimens, giving confidence that intra-observer error would not have a detrimental influence on further analyses (Lockwood *et al.,* 2002). Figure 5 shows the Procrustes distances between the repeats and between different specimens of *E. fulvus.*

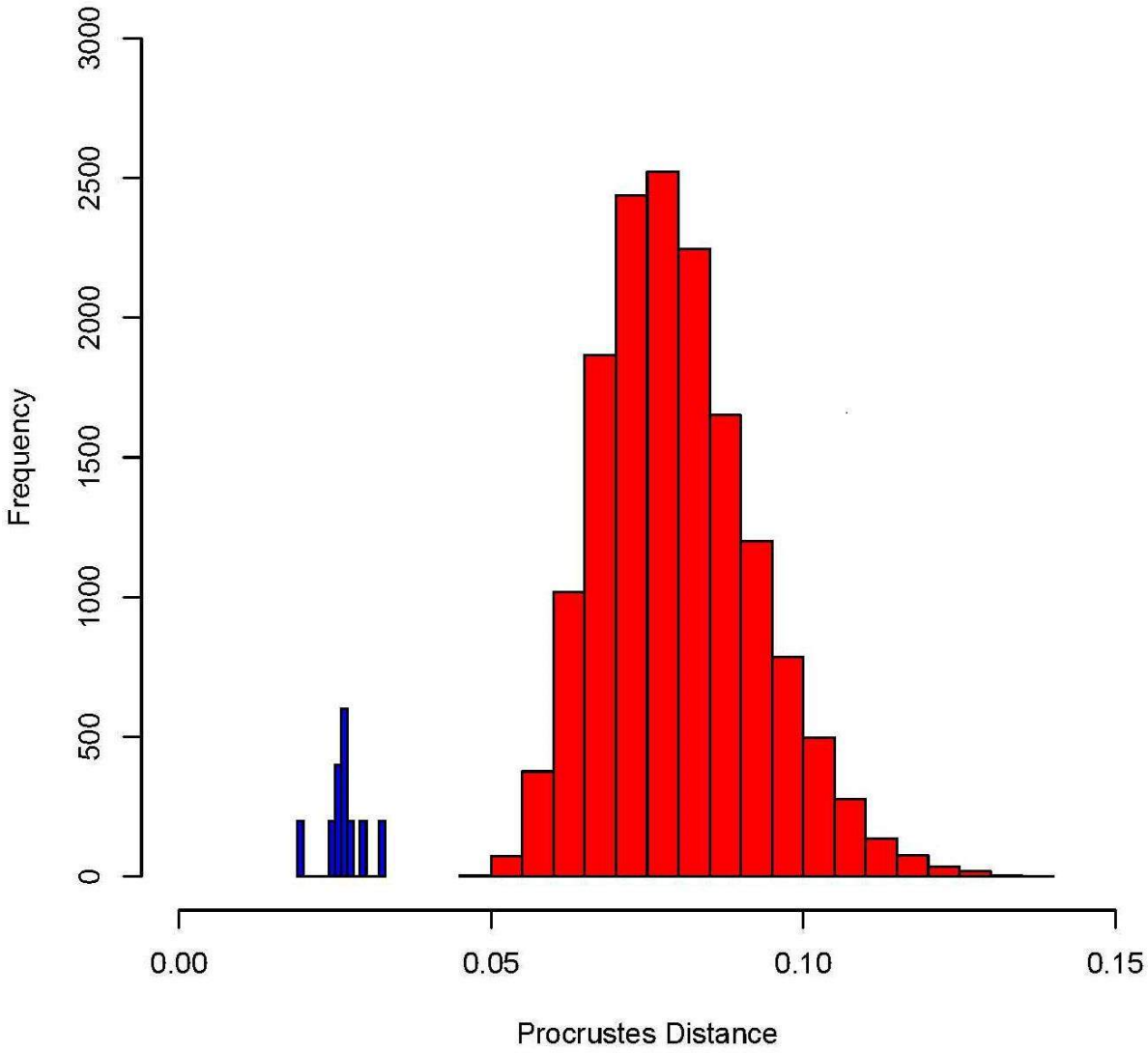

Figure 5: Procrustes distances between all pairs of repeats of the same *E. fulvus* specimen (blue) and between all pairs of *E. fulvus* specimens (red). The frequency of Procrustes distances between repeats have been increased (*200) for illustrative purposes.

Second, the amount of variation between repeats of the same specimen of *E. fulvus* was compared to the amount of variation between all specimens of *E. fulvus* and expressed as a percentage of the total variation that could be accounted for by measurement error.

$$\% \text{ measurement error} = 100 * \frac{\text{Within-specimen variance}}{\text{Within-specimen variance} + \text{between specimen variance}}$$

Where 'within-specimen variance' is the average standard deviation between the corresponding Procrustes residuals of the repeat specimen of *E. fulvus*, 'between-species

variance' is the average standard deviation between the corresponding Procrustes residuals of all *E. fulvus* specimens (Polly, 2001). The percentage measurement error for *E. fulvus* was 22.3%; this is higher than found by Polly (2001), who records a percentage measurement error of 15% for *Sorex* sp. Comparison of the results suggests that the difference is accounted for by low within-species variation.

2.2.2. Phylogenetic trees

It is sometimes necessary to incorporate species' evolutionary history into analyses, whether to control for it or to identify evolutionary trends (Felsenstein, 1985). To do this, species phylogenetic relationships need to be known. Fortunately, primate phylogenetic relationships have been heavily studied and many are fully resolved; here, the phylogeny for the study species is taken from the 10K Trees Project (Arnold *et al.,* 2010). Composite phylogenies (including branch lengths) of selected species are available to download from the Project website (Figure 6 and 7). Trees are generated through a Bayesian phylogenetic analysis of the available genetic data, taken from GenBank, encompassing eleven mitochondrial and six autosomal genes (Arnold *et al.*, 2010; Sanderson *et al.,* 2008).

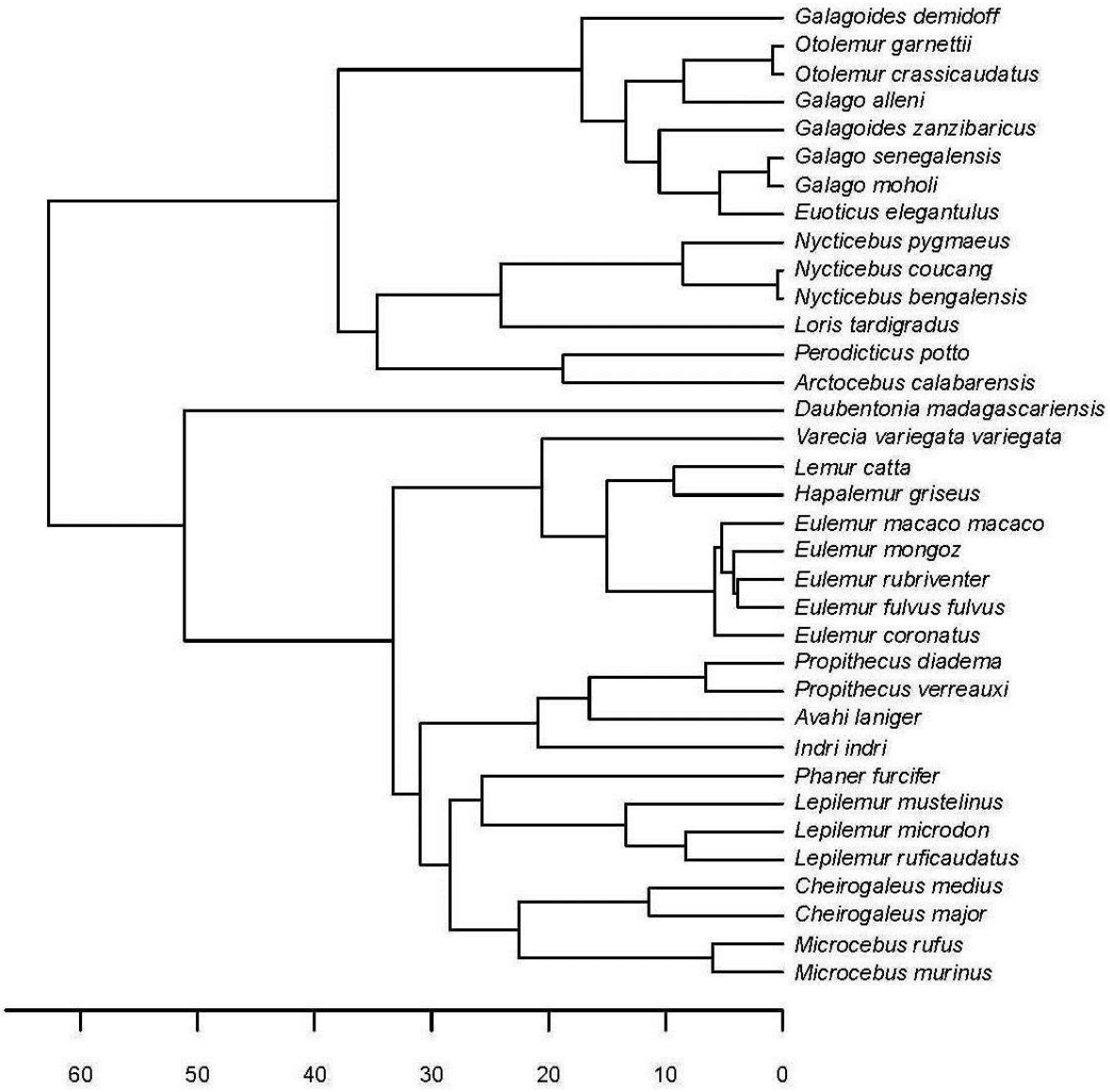

Figure 6: Composite phylogenetic tree of strepsirhine species for which data was collected (Arnold *et al.*, 2010) .

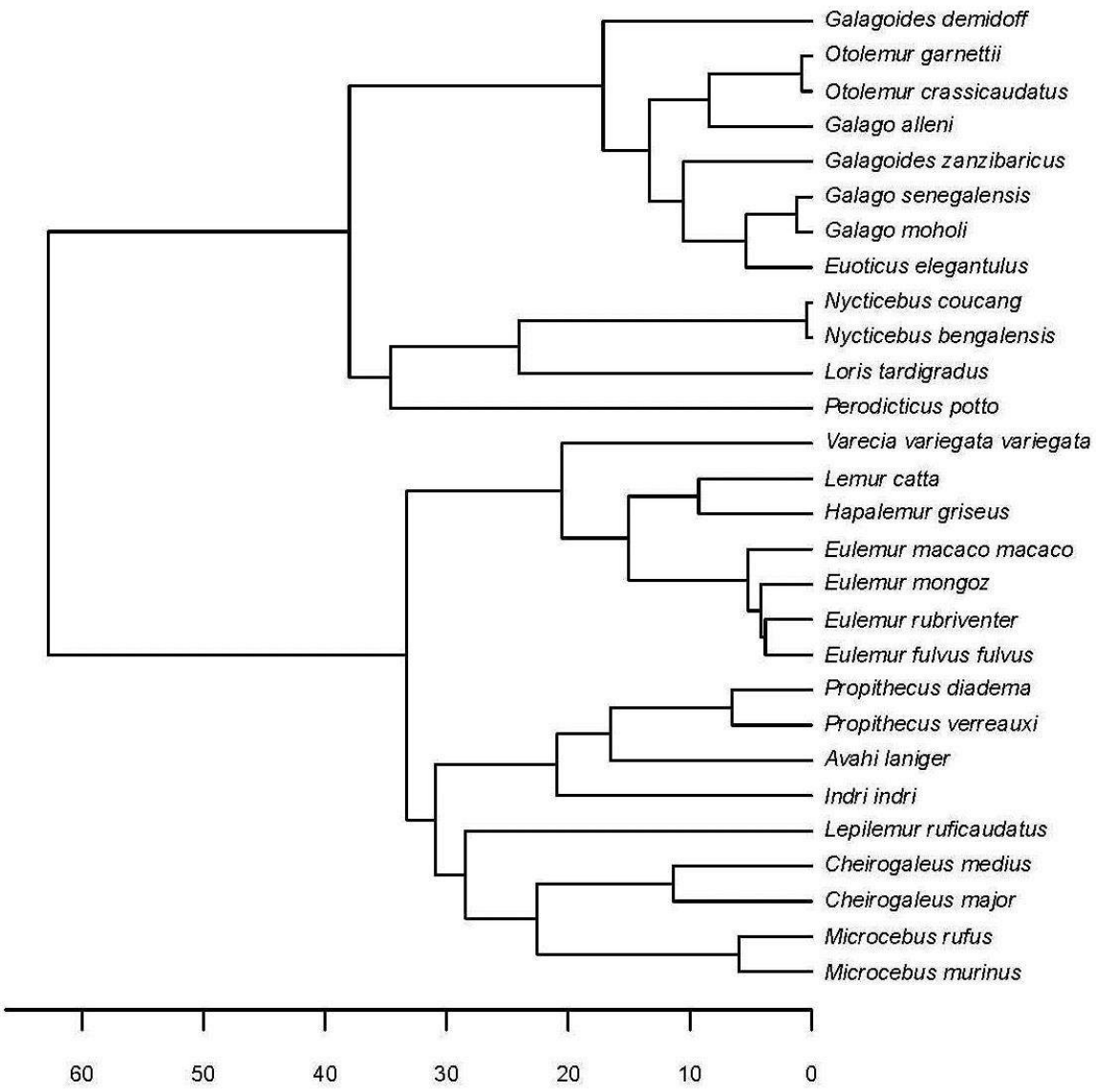

Figure 7: Composite phylogenetic tree of strepsirhine species used in further analyses; species with low sample size (<20) were excluded (Arnold *et al.*, 2010).

2.3. Analyses

2.3.1. Geometric morphometrics (GMM)

Broadly defined, morphometrics is concerned with variation in shape and the covariation of shape with other variables (Bookstein, 1997; Cooke & Terhune, 2015).Traditionally, morphometric data included linear distance measures, angles or ratios (Rohlf & Marcus, 1993). While this approach is by no means without merit, it does not enable the retention of the full geometry of landmarks (Cooke & Terhune, 2015; O'Higgins, 2000). In addition, it tends to treat measurements as being independent of one another rather than as part of an integrated structure (Cooke & Terhune, 2015; O'Higgins, 2000). The more recent Geometric Morphometric (GMM) approach aims to overcome these problems . It uses

Cartesian landmark coordinates to describe form, with landmark data collected in either 2D or 3D (Mitteroecker & Gunz, 2009). Landmarks were initially based on recognised features of the skeleton, which are homologous for the sample population, and, if possible, for wider taxa (Mitteroecker & Gunz, 2009). Three types of landmarks have been described: Type 1, the discrete junction of two tissues or sutures; Type 2, the maximum point of curvature or the projecting most or deepest most point of a trait; Type 3, either endpoints or points that are determined by the location of other traits, for example, the midpoint between landmark A and landmark B (Bookstein, 1997; Cooke & Terhune, 2015).

Advances in the area have also seen the development of semi-landmarks and the use of mathematically (rather than biologically) homologous landmarks (Gunz & Mitteroecker, 2013; Klingenberg, 2008). Data collection tools have also become more sophisticated over time, and a range of options are now available, including Microscribe digitisers, surface laser scanners and computerised tomography (CT) scans (Cooke & Terhune, 2015).

GMM methods have been used to investigate an increasing number of topics, including between species variation and the presence of phylogenetic signals (Cardini & Elton, 2008a; Couette *et al.,* 2005; Fleagle *et al.,*2010; Lockwood *et al.,* 2004; Viguier, 2002); variation within species, with a focus on sexual dimorphism or differences associated with geography (Cardini *et al.*, 2007; Wood *et al.*, 2007); studies of ontogenetic development (Rohlf, 1998; Viðarsdóttir *et al.,* 2002); fluctuating asymmetry (Lovatt & Hoelzel, 2011; White & Searle, 2008); and modularity and morphological integration (Fabre *et al.,* 2014; Goswami & Polly, 2010b), as well as retro-deformation and fossil reconstruction (Angielczyk & Sheets, 2007; Gunz *et al.,* 2009; Lawing & Polly, 2010). At the heart of all of these topics is the desire to obtain a greater understanding of evolutionary pathways and mechanisms.

A number of computer programmes are available for the collection and analysis of GMM data. For this particular study, 3D coordinates are collected in Microsoft Excel and analysed using MorhoJ (Ver. 1.06b) (Klingenberg, 2014) and R (Ver. 3.2) (Team, 2015), with code written in Tinn-R (Faria *et al.,* 2013).

2.3.2. Generalised Procrustes Analysis (GPA)

Superimposition is usually the first step in GMM analysis, its purpose is to remove differences in position and rotation as well as isometric size variation (although the analysis

can be performed without correcting for size if necessary; Cardini & Elton, 2008a). The most commonly used method is Generalised Procrustes Analysis (GPA), which translates landmark configurations to the origin, scales them to a centroid size (CS) of 1, where CS is a measure of the distribution of the landmarks around the centroid, calculated as the square root of the sum of the squared distances of all landmarks from the centroid (Cardini & Elton, 2008a), and aligns translated and scaled configurations by minimising the sum of squared distances between their corresponding landmarks (O'Higgins, 2000). After they have been subjected to GPA, landmarks are then referred to as Procrustes coordinates or Procrustes residuals, these residuals describe the deviations of individual specimens from the mean landmark configuration (Cooke & Terhune, 2015). The Procrustes residuals represent the 'shape' of the specimens, that is, the geometric variation that remains after position, rotation and scale have been removed (Cooke & Terhune, 2015). 'Form' is used to refer to the combined shape and size of a specimen (Cooke & Terhune, 2015).

2.3.3. Procrustes Distance (PRD)

The shape difference between two specimens, or between the mean shapes of two populations, can be quantified by the Procrustes distance. This is calculated as the square root of the sum of squared distances between corresponding pairs of landmarks after GPA (Cardini & Elton, 2007; 2008a; Cooke & Terhune, 2015). Procrustes distance can also be calculated as sin(Riemannian distance); GPA aligns shapes to correspond to the surface of a sphere with unit radius and Riemannian distance refers to the great circle distance - the distance between points on a sphere (Dryden & Mardia, 1993; Kendall, 1984; Rohlf, 1999).

2.3.4. Principal Component Analysis (PCA)

Principal Components Analysis (PCA) is used to transforms a large number of correlated variables into a smaller number of uncorrelated variables (Principal Components or PCs), which most effectively explain the variance within a given set of data (Cooke & Terhune, 2015). This is done by a singular value decomposition of the variance-covariance matrix, with the resulting eigenvectors becoming the PCs. The corresponding eigenvalues describe the amount of variance that is explained by each PC axis (Cooke & Terhune, 2015). The first PC accounts for the greatest percentage of variance within the data set, PC2 accounts for the greatest proportion of the remaining variance, and so on until the full amount of variance within the data has been explained (Cooke & Terhune, 2015). Where

geometric morphometric data are concerned, PCs will represent an aspect of change in shape (Field, 2003), with specimen's PC scores describing their position along each axis of change (Cooke & Terhune, 2015).

2.3.5. Controlling for non-independence of data

Data from different species is statistically non-independent due to their shared ancestry; the more closely they are related the more their data would be expected to co-vary. There are two principal ways to control for this: phylogenetic independents contrasts and phylogenetic least squares analysis (Symonds & Blomberg, 2014):

2.3.5.1. Phylogenetic Independent contrasts

Independent contrasts analysis controls for phylogenetic covariance by applying a Brownian motion model of evolution to the phylogenetic tree of the species concerned (Felsenstein, 1985). The tip values, typically the species mean values, are transformed into raw contrast values at each internal node, which are calculated as the difference between the species trait values (Symonds & Blomberg, 2014). If branch lengths are known, then the contrast values can be weighted by daughter branch length, to incorporate the length of time over which divergence has had the chance to occur (Symonds & Blomberg, 2014). The raw contrasts must then be standardised, to ensure that they meet the statistical requirement of having a normal distribution with equal variance, this is done by dividing them by their standard deviation (i.e., the square root of the sum of their branch lengths) (Symonds & Blomberg, 2014).

2.3.5.2. Phylogenetic Generalised Least Squares (PGLS) analysis.

Phylogenetic Generalised Least Squares (PGLS) (Grafen, 1989; Martins & Hansen, 1997) works like a weighted regression analysis, where data is increasingly 'down-weighted' in accordance with the closeness of the phylogenetic history of the species to which it pertains. The 'weight' is calculated using the variance-covariance matrix, with the level of covariance expected to correspond with the level of shared evolutionary history (Symonds & Blomberg, 2014). The matrix diagonal (variance) will therefore be the total length of the tree from route to tip, while the off diagonals (covariance) are the total branch lengths shared by each combination of species pairs (Symonds & Blomberg, 2014). This 'phylogeny based' matrix is then applied to a Generalised Least Squares (GLS) analysis (Symonds & Blomberg, 2014).

Although independent contrast analysis and PGLS deal with the problem of data non-independence using slightly different approaches, their results, in their basic form, are the same (Blomberg *et al.,* 2012; Symonds & Blomberg, 2014).

2.3.6. Analysis of Covariance (ANCOVA)

ANCOVA is a combination of regression analysis and analysis of variance (ANOVA) (Crawley, 2005). ANOVA is a method for assessing whether the means of 3 or more populations are equal (Field, 2003). It is a way to determine the effect of an independent variable on a dependent variable, while controlling for one or more continuous variables, known as covariates or control variables. Covariates are variables, other than the principal independent variable, which may, nevertheless, have an influence on the experimental outcome (Field, 2003). In essence an ANCOVA works like a hierarchical regression, first, control variables are regressed against the dependent variable. Group means are then adjusted for the dependent variable, so that all groups effectively have the same mean for control variables. The independent and newly adjusted dependent variable scores are then regressed against one another to measure what effect the independent variable has after the effect of the control variable has been removed (Field, 2003). The nature of the ANCOVA calculation means that it has two important assumptions: the independent and control variable must be uncorrelated, and the regression slopes, for the control variable against the dependent variable, must be homogenous across groups (Field, 2003).

2.3.7. Modelling evolution- The Independent Evolution (IE) method

The ancestral reconstruction of character states can be used to fill gaps in the fossil record, where the record is lacking or where the traits in question are soft tissue and therefore do not fossilise (Smaers & Vinicius, 2009). Models of ancestral reconstruction are based on several assumptions: that there is a correct representation of the phylogenetic relationships between species; that the history of evolutionary change is preserved within the phylogeny of the extant taxa (or available fossils); and that the model of evolution used to calculate the rate(s) of change is a valid representation of how the trait in question has actually evolved (Pagel, 1999; Smaers & Vinicius, 2009).

One of three main models of evolution, Brownian motion (BM) (Pagel, 1999), Ornstein-Uhlenbeck (OU) (Felsenstein, 1988; Uhlenbeck & Ornstein, 1930) or Independent Evolution (IE) (Felsenstein, 1988; Smaers & Vinicius, 2009), are usually used when reconstructing

ancestral states. BM is a random walk model, which mimics genetic drift; traits evolve with a mean change of zero and with an unknown and constant variance (Pagel, 1999). Under the OU model, trait change is again determined by random walk, but traits are tied to selective optimum values, traits which wander away from the optimum will be pulled back, with a force proportion to the distance that they have strayed (Blomberg *et al.,* 2003; Felsenstein, 1988). The BM and OU model are explained in detail in Chapter 6.

The IE method is a relatively recent implementation of Felsenstein's (1988) Adaptive Peak model of evolution and is therefore introduced here in more detail. It assumes that a population is continually trying to reach an 'adaptive peak'(Smaers & Vinicius, 2009). The location of the peak can drift, over time, through phenotypic space, resulting in a change in the favoured phenotype. Each internal node may have a different adaptive peak. Wherever the peak goes, the wider population will follow (Smaers & Vinicius, 2009). The IE model can be seen as incorporating both BM and OU models of evolution under certain circumstances. When the peak remains static and is the same across all nodes of the tree, then the model can be seen to be like BM (Smaers & Vinicius, 2009). When the peak is static, but shows a pattern of increasing or decreasing phenotypic values across the nodes of the tree, then the model can be seen to be 'pulling' the population towards a selective peak in a similar way to the OU model (Smaers & Vinicius, 2009).

Gradual models, such as BM, assume that trait change occurs by an absolute amount, per unit time (Pagel, 1999). The problem is that absolute change can be disproportionate Smaers & Vinicius, 2009). Consider body weight, a 1kg change in body weight represents a much greater trait divergence to a mouse lemur than it does to a gorilla. The Independent Evolution model avoids this problem by using measures of relative, rather than absolute, change (the IE distance metric). The relative change is calculated as 'the change between ancestor and descendant divided by their average' (Smaers & Vinicius, 2009, p. 995). It uses an eight step algorithm to reconstruct ancestral states, based on the morphology of the extant taxa of a given phylogeny (Figure 8).

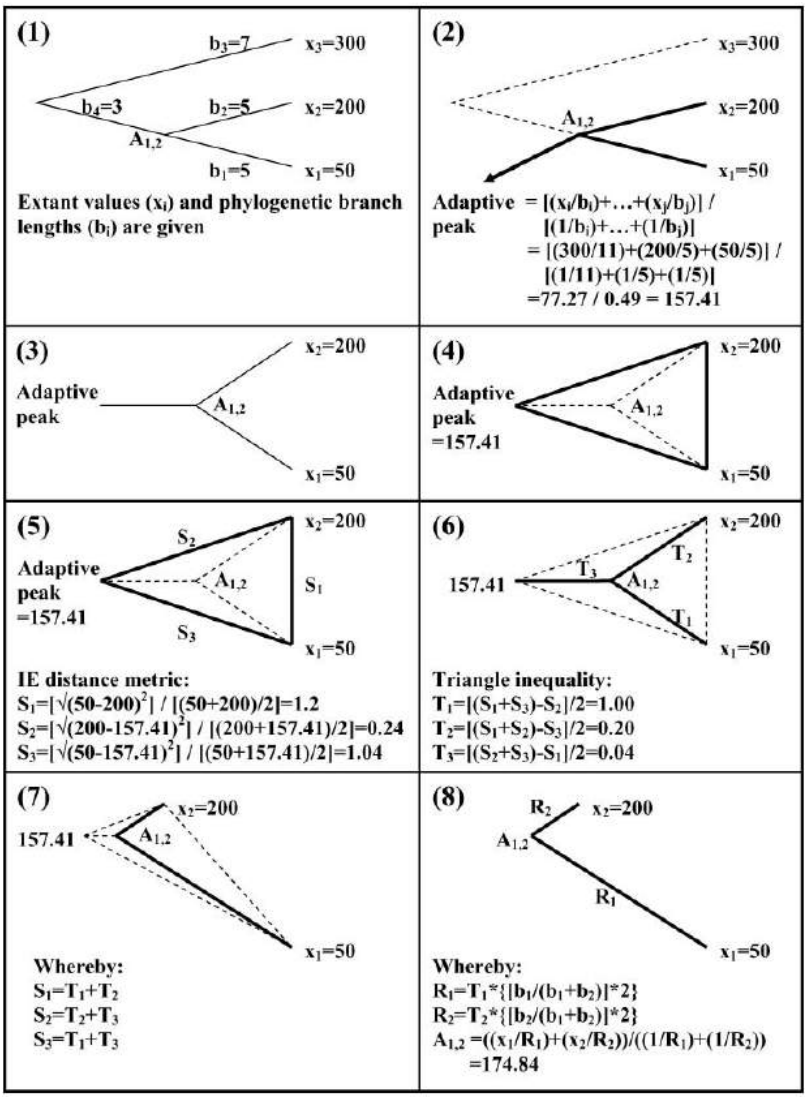

The IE method to investigate the continuous trait *×*, for the two extant species 1 and 2 and for their common ancestor ($A_{1,2}$).

1) A group of species is selected, which includes species 1 and 2, with a known phylogeny, known branch lengths at every node and data relating to trait *×* for the terminal species.
2) An 'adaptive peak' (AP) is calculated (see below) at internal node $A_{1,2}$ from data relating to all of the terminal species.
3) The AP replaces all branches of the tree which are ancestral to $A_{1,2.}$ The tree is then unrooted creating a star phylogeny including AP, $\times_1$, and $\times_2$.
4) The star phylogeny is considered as a triangle, where the barycentre of the triangle represents $A_{1,2,}$ and values $\times_1$, $\times_2$, and AP are represented by the tips of the triangle.

Figure 8: The IE procedure for estimating ancestral states, where; *×* represents a continuously defined biological trait; ×i represents the extant value of trait *×* for species i; bi represents the phylogenetic branch length for species i; Ai,j represents the ancestral value for species $\times_i$ and $\times_j$; *S* represents the relative phenetic distances between the tips of the triangle (thus representing the sides of the triangle); *T* represents the relative phenetic distance from *A* to the tips of the triangle; *R* represents relative branch-specific evolutionary change of trait *×* (from Smaers & Vinicius, 2009, p. 995 -7).

5) The IE distance matric between $\times_1$, $\times_2$, and AP is used to calculate the sides of the triangle (S_1, S_2 and S_3).
6) The Ptolemean property of triangle inequality is used to calculate the distance from $A_{1,2,}$ to the three tips $\times_1$, $\times_2$, and AP (T_1, T_2 and T_3) based only on the triangle sides.
7) The resting distances from $A_{1,2}$ to tips $\times_1$, $\times_2$, and AP represent the relative phenetic distances between ancestor ($A_{1,2}$) and descendants ($\times_1$ and $\times_2$), taking the AP into account.
8) The distance between $A_{1,2}$ and $\times_1$ and $\times_2$, (T_1 and T_2) are weighted for their phylogenetic branch lengths, creating a rate of change ('*R*-value') for the branch of each descendant of ancestor $A_{1,2.}$ *R*-values, representing the relative branch specific evolutionary change of a trait, are then used to estimate $A_{1,2}$ according to Felsenstein's (1985) algorithm. N.B. with equal phylogenetic branch lengths in sister branches, the weight for both phenetic branch lengths equals unity.

The IE algorithm is first used at the tip taxa and then recursively, towards the root of the evolutionary tree. The adaptive peak for each internal node is calculated as the sum of all terminal nodes divided by the patristic difference between the terminal node and the internal node in question (where the patristic difference in calculated as the sum of the lengths of the branches connecting the two nodes), divided by the sum of the inverse patristic difference of all of the terminal nodes.

Figure 8 (cont.)

In essence, the IE method uses all possible biological information to calculate the adaptive peak, giving greater weight to data from species more closely related to the ancestor, than those more distantly related (Smaers & Vinicius, 2009). Support for the IE approach comes from its ability to predict both body and brain size in primate, bat and carnivoran ancestors with relative accuracy (Smaers *et al.,* 2012).

2.3.8. Evo-maps

Evo-maps are a graphical representation of the rate of change trait change across a phylogenetic tree, as determined by the method of Independent Evolution (IE; Figure 9). They enable the identification of branches associated with strong selection for a particular trait (Smaers *et al.,* 2013). Within the image, the size of the trait (e.g. centroid size or Principal Component score), is indicated by the size of the circle at the ancestral node or branch tip. The thickness of the branches is representative of the rate of trait change, where thin branches are indicative of low rate change and thick branches of high rate change. Branches are turned red and green to indicate positive and negative rates of evolution respectively, positive rates of evolution represent an increase in the trait and negatives rates a decrease in the trait. Black branches indicate quantitatively small levels of trait change (Smaers *et al.,* 2012).

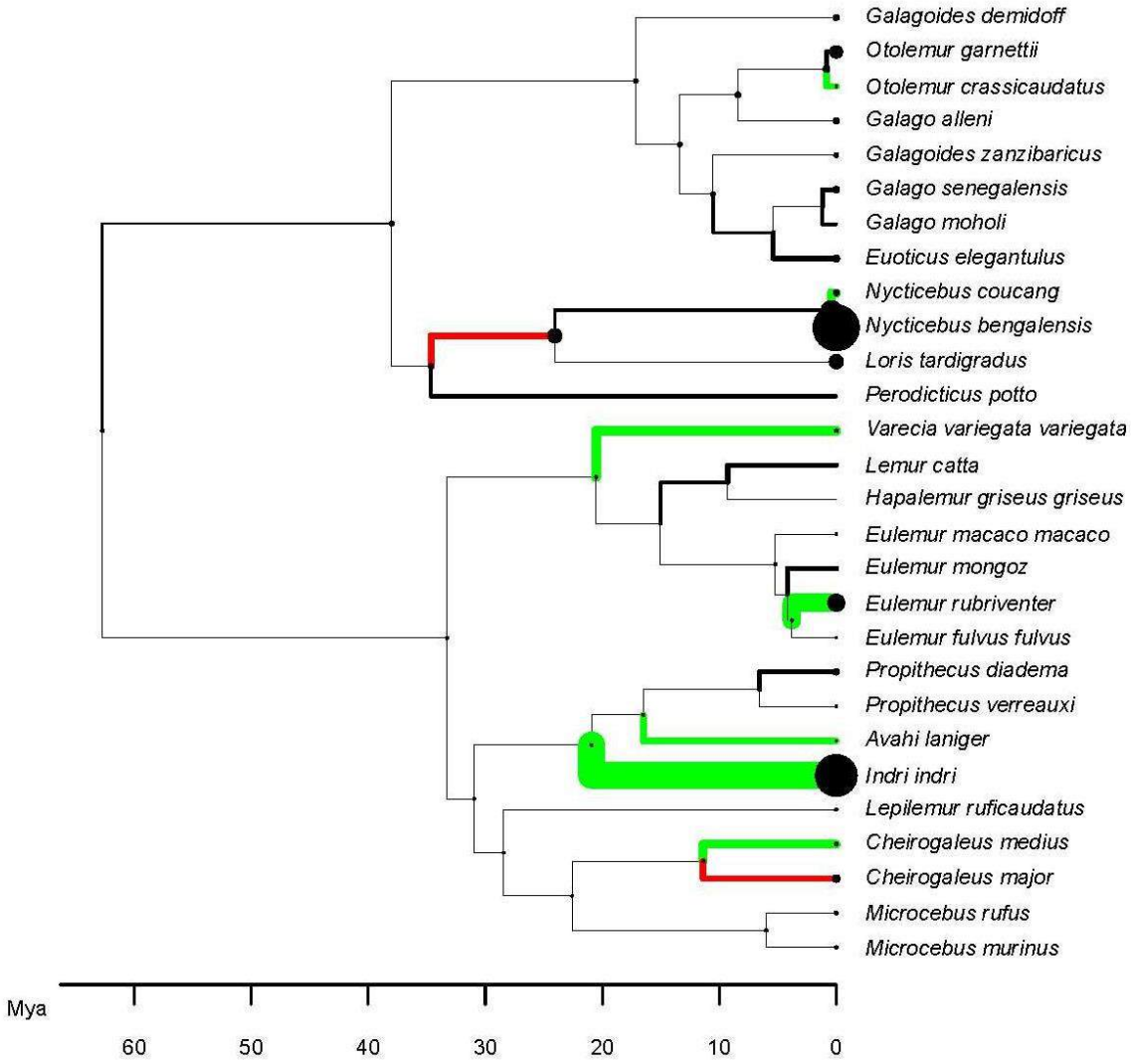

Figure 9: An example of an evo-map, illustrating the size of a trait (as indicated by the relative size of the black circles at the branch tips and ancestral nodes), the rate of trait change (as indicated by the thickness of branches, the thicker the branch the faster the rate change) and the direction of shape change (as indicated by the colour of the branches, red indicates an increase in the trait and green a decrease, black indicates little to no change in the trait), across the strepsirhine evolutionary tree.

– Chapter 3 –

The effect of reduced sample size in geometric morphometric studies of size and shape

3.1. Abstract

Paleontological, systematic, and comparative studies now commonly use 3D geometric morphometric approaches to quantify size and shape, but sample size in such studies is often small (Cardini & Elton, 2007). The accuracy of estimates of skull size and shape parameters has been shown to be differentially affected by decreasing sample size in *Cercopithecus aethiops* (Cardini & Elton, 2007). Here this analysis is extended to a sample of six strepsirhine species (*Eulemur fulvus, Galago senegalensis, Microcebus murinus, Nycticebus coucang, Otolemur crassicaudatus* and *Perodicticus potto*), to test whether the effect of limited sample size varies between taxa.

Three-dimensional landmark data, comprising 60 cranial landmarks, were collected from 722 specimens. A thousand random sub-samples were generated for each species, at each sample size, with sub-sample sizes ranging from five specimens to bootstrapping of the full sample, increasing in increments of five. A range of size and shape parameters (mean size; standard deviation of size; total shape variation; mean shape; variation in mean shape; variation in allometric trajectories and the percentage of shape variance explained by size) were calculated for each sub-sample size and compared to the corresponding parameters for the original species sample and, where appropriate, to inter-specific comparisons.

All six species showed very similar patterns of results; while size parameters and total shape variance hold up remarkably well when sample sizes are small (N=5), other parameters do not. Both mean shape and variance of mean shape are strongly affected when sample size is <40. This is especially a problem when studying intra-species populations and could also have implications for studies that seek to construct phylogenies using mean shape. Small sample sizes also result in an over-estimation of the angles between allometric trajectories and the amount of shape variance that is attributed to the influence of size, for both within-species (between males and females) and between-species calculations.

3.2. Introduction

Paleontological, systematic, and comparative studies of population or ontogenetic morphological variation, in extant or fossil taxa, now commonly use 3D geometric morphometric methods to quantify size and shape. Sample sizes in these studies usually reflect the number of specimens that are available within the logistic restraints of the research programme, rather than a predetermined ideal size. In a review of geometric morphometric studies, 50% were found to have an average sample size of N<30, and most had at least one species with N<10 (Cardini & Elton, 2007). However, a number of studies have suggested that small sample size can affect the reliability of results of morphometric research (Baab *et al.*, 2014; Cardini & Elton, 2007; Cobb & O'Higgins, 2004; Rohlf, 2003; Polly, 2005). It would therefore be useful to understand the ways in which the different measures of shape and size, which are commonly used in geometric morphometric studies, are affected by small sample size; as well as whether any effects of sample size are species specific or if they follow a common pattern for genera, families or even orders.

Previous work to assess the effect of sample size, in geometric morphometric studies, modelled the impact of small sample size for oblique and isosceles triangles (Rohlf, 2003). The size of errors was found to rise steeply once sample size fell below N=200. When N<100 errors could be 2-6 times greater than when N=500 (Rohlf, 2003). However, it is difficult to extrapolate from those simple shapes to the effect that sample size may have in the case of complex organic shapes characterised by substantially larger numbers of landmarks and constrained by biologically determined shape variation.

Analysis on the effect of sample size on intra-species shape variation in the molar teeth of *Sorex araneus* showed that sample sizes of N<15 severely affected the accuracy of results when using a matrix correlation approach, and when using Common Principal Component Analysis, accuracy was compromised when N<30 (Polly, 2005).

Sample size has also been shown to have an impact when calculating the angle between ontogenetic trajectories for species of *Pan* (Cobb & O'Higgins, 2004). When samples consisted of fewer than 20 adult and 20 juvenile specimens, estimates of angles varied considerably from those obtained from the larger, observed sample. The implications of this are perhaps most pressing for experiments that aim to predict and compare trajectories for fossil species, when only very few samples are usually available.

Cardini and Elton (2007) tested the effect of small sample size on different size and shape parameters, using geometric morphometric data consisting of 86 3D landmarks from almost 400 specimens of *Cercopithecus aethiops*. They found that mean centroid size (CS) estimates remained reasonably accurate even when N=10, which was attributed to a small coefficient of variation in size for this species and for the genus as a whole. Estimates of standard deviation of size were less accurate than those for mean centroid size, especially when N<40, which could have implications for studies that aim to compare the amount of variation in size between populations. Estimates of shape variation within a sample were, like mean size, found to remain accurate even when N=10. In contrast, estimates of mean shape did not fare well in small sample sizes. When N<30, distances between sub-sample mean shapes and the observed mean shape were 1.8 - 4 times as large as the average distance between the observed and average bootstrapped mean shapes. In addition, when N<30 the distance between sub-sample and the observed shapes for *C. aethiops*, could account for up to 37% of the interspecific distance between *C. aethiops* and *C. mitis* (Cardini & Elton, 2007). Similarly, angles between allometric trajectories are severely affected by small sample size, both when comparing intra-species trajectories (between male and female *C. aethiops*) and inter-species trajectories (between *C. aethiops* and *C. mitis*). In both cases, angles were up to 1.5 times larger than the observed angle when N<70 and almost 3 times larger when N=10 (Cardini & Elton, 2007).

A recent study (Baab *et al.*, 2014) on the effect of sample size on geometric morphometric analyses in the Lemuridae confirmed that the accuracy of mean shape estimates is reduced as sample size decreases for these species. The error in intra-species mean shape was shown to account for account for between 10 - 22% of inter-species distance for inter-generic comparisons when N=10, between 15 – 31% when N= 5 and 20 – 43% when N=3 (Baab *et al.*, 2014). Although it should be noted that the largest observed sample in the study was still a relatively small N=21 (Baab *et al.*, 2014).

Having seen how sample size variation can affect the accuracy of shape estimates in *C. aethiops* and, to a more limited extent, in some species of Lemuridae, it is important to establish if the same pattern holds true for other species (Baab *et al.*, 2014; Cardini & Elton, 2007). A broader understanding of the effects of variation in sample size on the results of geometric morphometric studies will help in determining the study's significance and in assessing the robusticity of their conclusions.

In the present study, the analyses by Cardini and Elton (2007) are extended to large samples of six species of strepsirhine primates, to test whether altering sample size affects the estimates of size and shape parameters, commonly used in geometric morphometric studies, in the same way as in *C. aethiops*. The use of multiple species also allows for multiple comparisons between phylogenetically more or less closely related taxa, thereby providing context with which to assess intra-species comparisons. Random sub-samples of different sizes were generated for each species. A range of size and shape parameters corresponding to those tested by Cardini and Elton (2007; mean size, standard deviation of size, total shape variance, mean shape, variation in mean shape, variation between allometric trajectories and the percentage of shape variation attributed to size) were calculated for each sub-sample and compared to the corresponding parameters for the entire observed species sample and, where appropriate, to interspecific comparisons.

3.2.1. Aims

To investigate the effect of reduced sample size in geometric morphometric studies of size and shape, across a broad range of strepsirhine taxa.

3.3. Materials and methods

3.3.1. Data collection

The sample consisted of 721 strepsirhine skulls from six species: *Eulemur fulvus, Galago senegalensis, Microcebus murinus, Nycticebus coucang, Otolemur crassicaudatus* and *Perodicticus potto*. These species were selected on the basis that large sample sizes were available for all of them (Table 6). The full landmark configuration was used in the analyses (See Methods chapter for landmark details of data collection and landmark configuration).

Table 6: species and sample sizes used in the analyses

	Number of specimens			
Species	**Males**	**Females**	**Indeterminate**	**Total**
Eulemur fulvus	78	54	44	176
Galago senegalensis	97	75	3	175
Microcebus murinus	28	24	20	72
Nycticebus coucang	25	23	21	69
Otolemur crassicaudatus	46	35	20	101
Perodicticus potto	59	38	32	129

3.3.2. Analysis

Specimens were subjected to Generalised Procrustes Analysis (GPA; see Chapter 2) and their resulting Procrustes scores and CS were used in the subsequent analysis. The shape and size parameters investigated are based on those used by Cardini and Elton (2007), making the results for the strepsirhine species in the present study comparable to those of *C. aethiops and C. mitis*. The parameters include:

(1) Mean size

Calculated as the mean CS of a given sample.

(2) Standard deviation of size

Calculated as the standard deviation (SD) around the mean CS of a given sample.

(3) Mean shape (i.e., the mean configuration of all specimens in a sample after GPA)

Procrustes distances (PRDs) were used to measure the distance between the observed mean shape and the mean shapes of the randomly generated sub-samples. PRDs were calculated as the sin(Riemannian distance). In GMM shapes correspond to points on a hemisphere, with unit radius, distance can therefore be considered in terms of great circle distance rho (ρ). This is also the angle between the vectors from the centre of the hemisphere to the two points being compared, which, as shown by Kendall, is a Riemannian distance (Dryden, 2013; Kendall, 1984; Rohlf, 1999).

(4) Variance in mean shape

To calculate mean shape variance, mean shapes were generated for each of 1000 sub-samples for sample size N. These mean shapes were then again subjected to GPA and the amount of variation around them was measured as the root mean square of rho, where rho is Kendall's Riemannian distance to the mean shape.

(5) Total shape variance

Calculated as the sum of variance in all Procrustes coordinates.

(6) The angle between allometric trajectories of males and females for each species and between species.

To investigate the effect of sample size on estimating allometric trajectories, multivariate regressions were run for all Procrustes coordinates onto size (log centroid size; ln CS). Within each species, the allometric trajectories for males

and females were calculated separately and the angle between the two vectors was then derived from the dot product of the regression coefficients ($a \cdot b = a_x*b_x + a_y*b_y = |a|*|b|*\cos(\theta)$). Parallel (or almost parallel vectors) will result in small angles and divergent vectors in large angles. The angles generated by sub-samples can then be compared to those generated by the original sample (Cardini & Elton, 2007; Mitteroecker *et al.,* 2004). Intra-species allometric trajectories were only investigated for *E. fulvus, G. senegalensis, O. crassicaudatus* and *P. potto*. *M. murinus* and *N. coucang* were excluded as, once split by sex, sample sizes were too small to ensure accuracy of the observed parameters. Inter-species allometric trajectories were investigated for each pair combination of all six species.

(7) The percentage of shape variance explained by size.
Calculated as 100 x [1 – (shape variance of the regression residuals/total shape variance)].

In line with Cardini and Elton (2007), each parameter was first calculated for the observed sample, for each species. Then 1000 random sub-samples were generated for each of the six species, at each sample size, with sample sizes ranging from five specimens to bootstrapping of the full sample, increasing in increments of five. This extends Cardini and Elton's sampling strategy to the lower sub-sample size of five to further determine the effect of the very low samples that frequently constrain analyses of fossil data.

For example, to investigate the effect of sample size on estimating the mean size of *E. fulvus*, the mean CS is calculated for the observed sample of 176 specimens. A sub-sample is then generated, with five specimens selected at random, with replacement, from the observed sample. The mean CS of this sub-sample is calculated. This is done a further 999 times and the overall mean size for all 1000 sub-samples of N=5 calculated. The process is then performed for sub-samples of N= 10, 15, 20, and so on, up to N=176 (i.e., bootstrapping of the full sample). The difference in CS estimates generated by the observed sample and the sub-samples can be expressed as a ratio and compared to the difference between the size estimates generated by the observed and the bootstrapped sample (Figure 10).

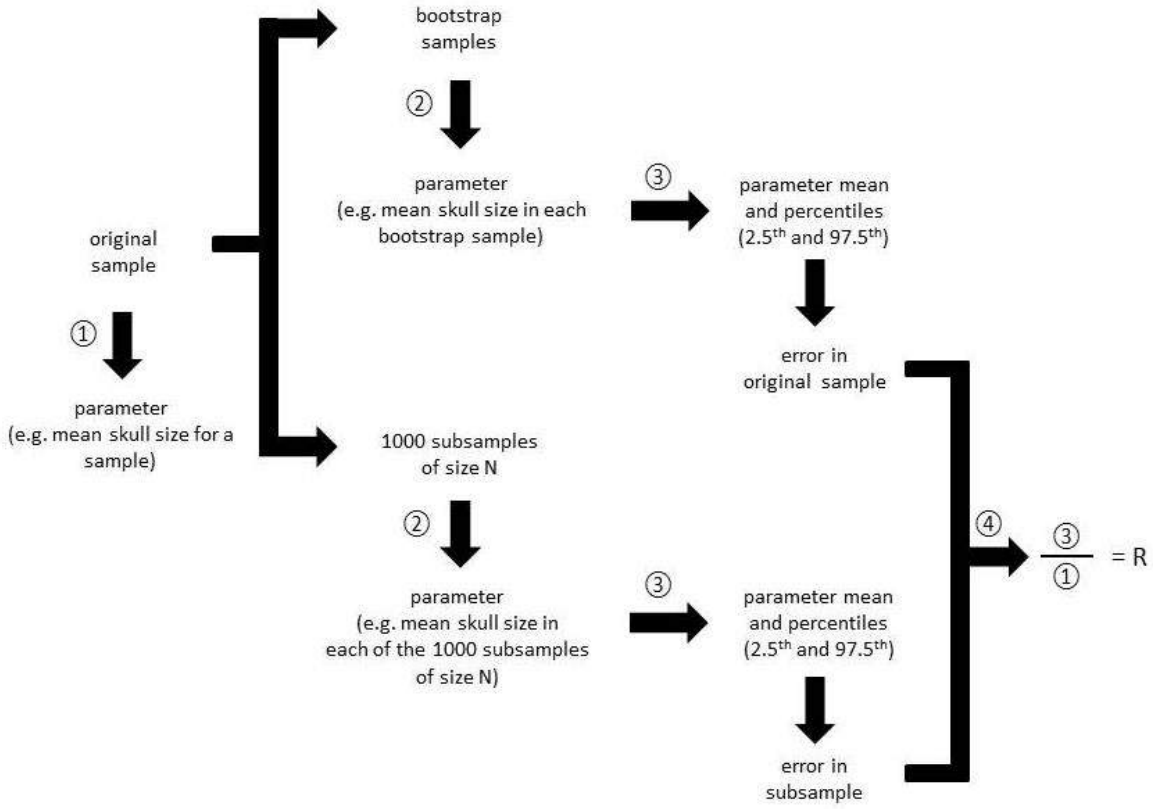

Figure 10: Diagram depicting the steps of the analysis for calculating and comparing parameters at different sample sizes, R = ratio between sub-sample and the original or bootstrapped parameter (based on Cardini & Elton, 2007, Figure 1, p. 123).

3.3.2.1. Ratios

Following Cardini and Elton (2007), ratios (R) are used to make the results comparable and easier to interpret. $R = P_N/P_{obs}$ where P_N is the parameter as calculated from the repeats of sub-samples of a given size and P_{obs} is the parameter as calculated from the observed sample for that species. In the case of mean shape and the variation in mean shape, $R_D = D_N/D_{obs}$, where D_{obs} is either the PRD between bootstrapped means and the observed mean (this provides a measure of the uncertainty around the original mean; therefore if $R_D = 2$, the distance of mean shapes in the sub-sample to the observed mean shape would be on average twice as large as the uncertainty in the estimate of the observed mean shape, or, for inter-species analyses, the PRD between the observed mean shape for two species. The average of *R* and the 2.5th and 97.5th percentiles were calculated as a function of sample size. This is illustrated with profile plots. A horizontal profile plot implies that small samples retain the ability to accurately describe a parameter (i.e.,, mean estimates of P_N are close to P_{obs} irrespective of N), while a non-horizontal plot suggests that sample size variation affects the mean accuracy of parameter estimation. Close and almost parallel percentile

lines indicate precision in parameter estimation at different sample sizes (i.e., P_N estimates cluster close to the average for a given sample size), while a large distance between the percentile lines and the average line, and a progressive increase in that distance indicate an increasing lack of precision in parameter estimation (i.e.,, while the mean of sub-sample estimates may accurately reflect the correct population mean, a randomly drawn sub-sample may substantially differ from the actual population mean (Cardini & Elton, 2007).

It should be noted that testing size and shape parameters in this way relies on the assumption that the observed sample is large enough to generate accurate results for the wider population, and therefore also representative of the species across its complete geographic range. Museum specimens often originate from the same date and geographic location. In this case the data were collected from four different museums (Three in the case of *O. crassicaudatus*), which might be an indicator of different points of origin, and more importantly, where data were available for geographic origin, a range of locations was evident.

3.4. Results

The effect of limited sample size varied between parameters, but not between taxa.
All species produced similar results for all parameters, for simplicity, results tables are only shown for *E. fulvus* (results for the remaining five species can be found in Appendix 1). Profile plots are shown for all of the species tested for each parameter.

3.4.1. Size

The accuracy of estimates of size parameters (i.e., mean size and standard deviation of size, calculated using the observed sample, the bootstrapped samples and the sub-samples) are shown in Table 7 and Figure 11. Mean size variation (where CS is used as a proxy for size) was minimally affected by sample size, even when sub-samples contained only five individuals. For *E. fulvus,* the mean estimate of mean size of N=5 had a 0% percentage error and 95% of the samples taken had a percentage error of less than +/- 3.4% (see Table 8 for other species % error, when N=5).

The mean standard deviation of size was also minimally affected by sample size, only when N<15 do modest differences become apparent. However, the range of mean standard deviations becomes much larger than that for the bootstrapped sample when sub-samples are made-up of fewer than 20 individuals. For *E. fulvus,* the range is 2.8 times larger when

N=20, 4 times larger when N=10 and 5.5 times larger when N=5 (Table 7). This is further illustrated by the percentage error for *E. fulvus* when N=5, the mean SD had an 11.4% percentage error, however this was shown to rise up to 69.2% and 80.7% for the 2.5th and 97.5th percentiles, respectively (Table 9).

Table 7: *E. fulvus* mean size (CS) and SD of size for observed, bootstrap and random sub-samples.

E. fulvus	Sample size	Mean CS	Percentile		SD of CS	Percentile	
			2.5th	97.5th		2.5th	97.5th
Observed	176	206.76	_	_	8.48	_	_
Bootstrap	176	206.77	205.50	207.99	8.44	7.29	9.61
Sub-samples	175	206.77	205.37	207.98	8.44	7.35	9.62
	170	206.75	205.42	208.00	8.45	7.30	9.60
	165	206.75	205.44	208.06	8.44	7.30	9.62
	160	206.77	205.38	208.06	8.42	7.29	9.64
	155	206.76	205.48	208.06	8.39	7.14	9.71
	150	206.76	205.42	208.09	8.46	7.30	9.76
	145	206.75	205.40	208.07	8.38	7.12	9.68
	140	206.78	205.35	208.22	8.43	7.12	9.73
	135	206.74	205.22	208.17	8.42	7.19	9.73
	130	206.77	205.40	208.17	8.42	7.12	9.82
	125	206.73	205.22	208.15	8.41	7.08	9.72
	120	206.77	205.18	208.37	8.45	7.05	9.71
	115	206.78	205.26	208.34	8.41	7.07	9.77
	110	206.81	205.30	208.43	8.42	6.91	9.92
	105	206.76	205.10	208.36	8.45	6.90	9.90
	100	206.77	205.21	208.52	8.41	6.83	9.90
	95	206.71	205.13	208.36	8.42	6.87	10.01
	90	206.73	204.84	208.46	8.42	6.91	10.05
	85	206.80	205.03	208.55	8.40	6.76	10.05
	80	206.81	204.79	208.61	8.36	6.64	10.08
	75	206.77	204.87	208.62	8.40	6.57	10.22
	70	206.79	204.64	208.67	8.41	6.67	10.17
	65	206.76	204.67	208.81	8.33	6.36	10.26
	60	206.82	204.52	208.81	8.40	6.45	10.39
	55	206.70	204.44	208.99	8.40	6.33	10.54
	50	206.74	204.51	208.89	8.40	6.34	10.49
	45	206.73	204.34	209.13	8.30	6.06	10.65
	40	206.78	204.22	209.18	8.38	6.08	10.85
	35	206.76	203.89	209.35	8.32	5.83	10.73
	30	206.77	203.64	209.92	8.30	5.67	11.18
	25	206.83	203.38	210.31	8.31	5.32	11.64
	20	206.78	203.02	210.52	8.27	5.11	11.81
	15	206.83	202.24	210.67	8.09	4.51	12.36
	10	206.78	201.20	211.53	8.12	4.00	13.25
	5	206.94	199.60	213.71	7.87	2.61	15.33

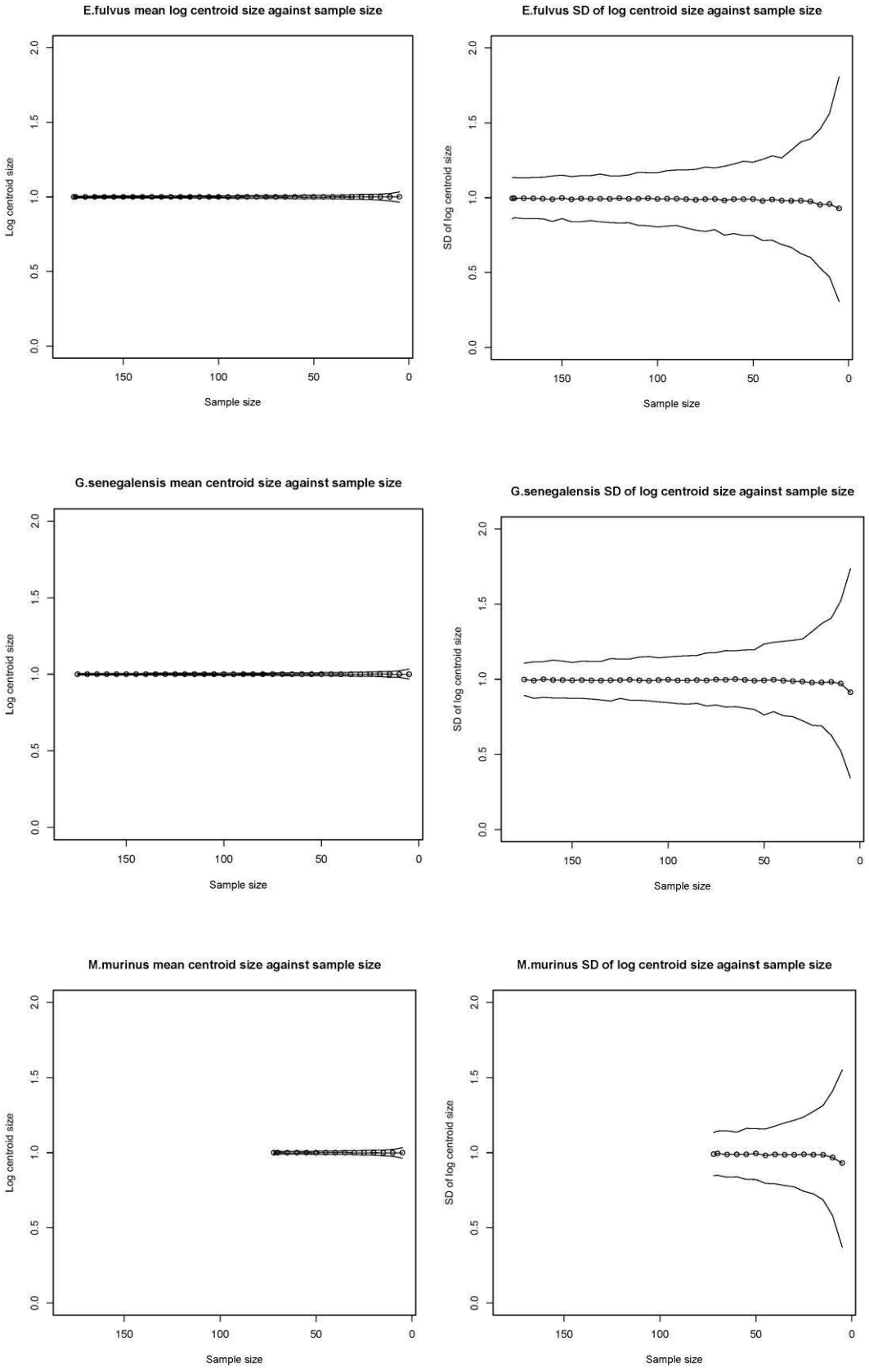

Figure 11: Profile plots of R for species mean size and standard deviation of size. Average and percentiles of the parameter are shown for the bootstrap samples and then for increasingly smaller sub-samples (N=100, 95, 90...10, 5).

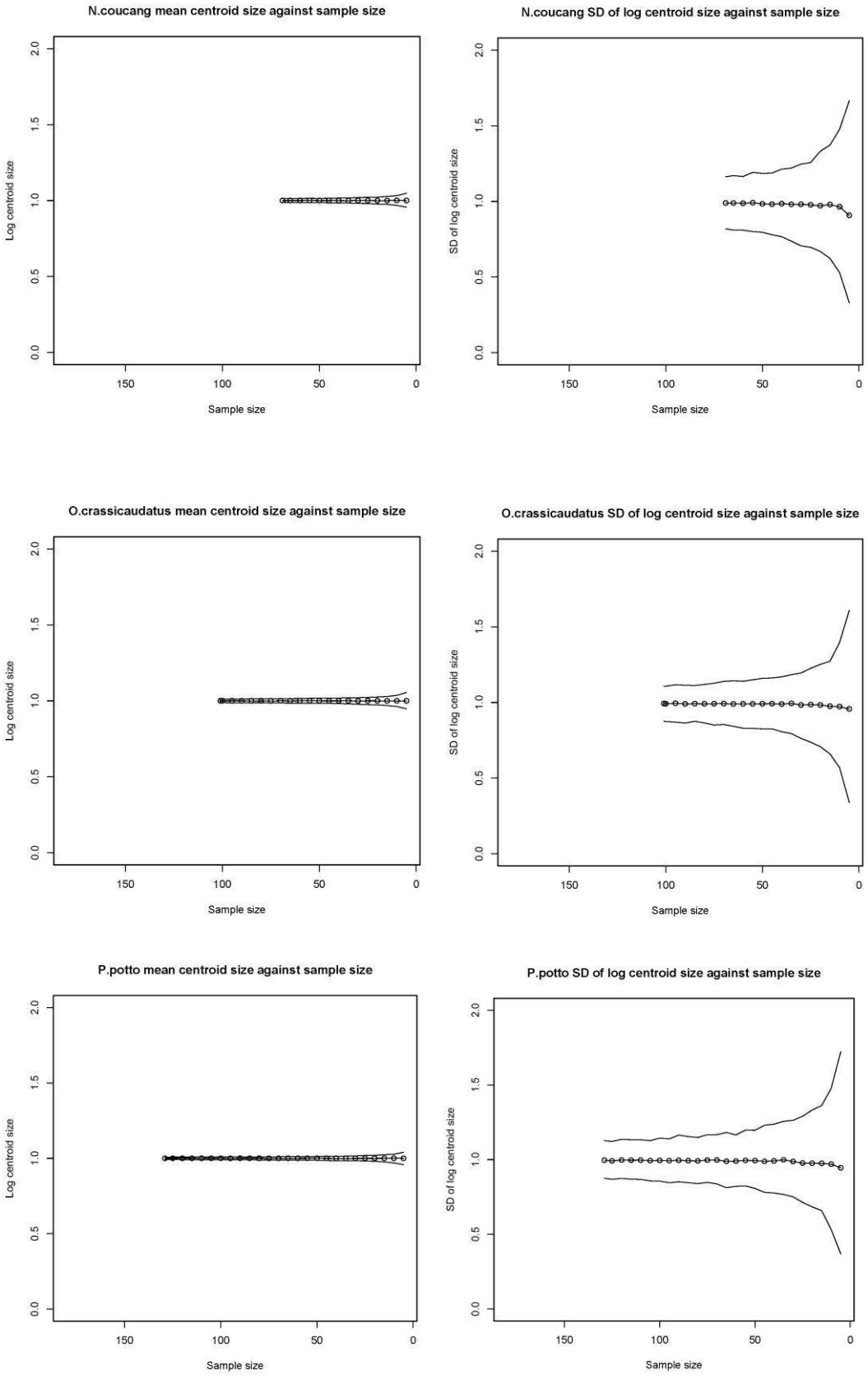

Figure 11 (Cont.)

Table 8: Percentage error of estimates of mean CS, for the mean, 2.5th and 97.5th percentiles for the 1000 sub-samples of N=5.

Species	% error		
	Mean	2.5th percentile	97.5th percentile
Eulemur fulvus	0.0	3.4	3.4
Galago senegalensis	0.0	3.1	3.3
Microcebus murinus	0.0	3.6	3.3
Nycticebus coucang	0.0	4.3	4.8
Otolemur crassicaudatus	0.0	5.3	5.5
Perodicticus potto	0.0	4.2	4.0

Table 9: Percentage error of estimates of standard deviation of ln CS, for the mean, 2.5th and 97.5th percentiles for the 1000 sub-samples of N=5.

Species	% error		
	Mean	2.5th percentile	97.5th percentile
Eulemur fulvus	11.4	69.2	80.7
Galago senegalensis	8.7	65.2	73.2
Microcebus murinus	6.9	62.8	54.9
Nycticebus coucang	9.3	66.9	66.5
Otolemur crassicaudatus	4.3	66.0	58.3
Perodicticus potto	5.4	63.1	72.2

3.4.2. Shape

The accuracy of mean shape estimates, characterised as PRDs between sub-sample mean shapes and the observed mean shape, as well as the variation in mean shapes, are shown in Table 10 and Figure 12. Small sample sizes result in large PRDs between sub-sample mean shapes and the observed mean shapes. For *E .fulvus,* distances between the observed mean shape and the sub-sample mean shapes were 2.1 times larger than the distance between the observed mean and the bootstrapped sample when N=40, 4.2 times larger when N=10 and 5.9 times larder when N=5. At N=5 percentage error for the average mean shape was 493.8%, for *E. fulvus*, rising to 639.9% for the 95th percentile (Table 11).

Table 10: Mean PRDs from the sample mean shapes to the observed mean shape and the variance in mean shape for *E. fulvus.*

E. fulvus	Sample size	Mean PRD	95th percentile	Mean shape variance
Observed	176	_	_	_
Bootstrap	176	0.004318	0.005371	0.004423
Sub-samples	175	0.004368	0.005483	0.004414
	170	0.004402	0.005374	0.004470
	165	0.004501	0.005699	0.004550
	160	0.004574	0.005606	0.004627
	155	0.004631	0.005824	0.004690
	150	0.004697	0.005782	0.004774
	145	0.004789	0.005918	0.004835
	140	0.004885	0.006055	0.004957
	135	0.004998	0.006264	0.005052
	130	0.005065	0.006355	0.005144
	125	0.005192	0.006541	0.005176
	120	0.005264	0.006538	0.005300
	115	0.005383	0.006767	0.005429
	110	0.005514	0.006853	0.005568
	105	0.005623	0.006969	0.005690
	100	0.005788	0.007108	0.005840
	95	0.005958	0.007420	0.005991
	90	0.006102	0.007548	0.006096
	85	0.006247	0.007816	0.006307
	80	0.006493	0.008037	0.006554
	75	0.006665	0.008324	0.006725
	70	0.006883	0.008525	0.006970
	65	0.007178	0.009084	0.007231
	60	0.007479	0.009307	0.007544
	55	0.007758	0.009600	0.007811
	50	0.008180	0.010087	0.008291
	45	0.008587	0.010802	0.008726
	40	0.009146	0.011329	0.009177
	35	0.009690	0.012018	0.009843
	30	0.010516	0.013127	0.010586
	25	0.011595	0.014688	0.011667
	20	0.012945	0.016020	0.013072
	15	0.015064	0.019023	0.015042
	10	0.018338	0.023138	0.018428
	5	0.025639	0.0319069	0.02618478

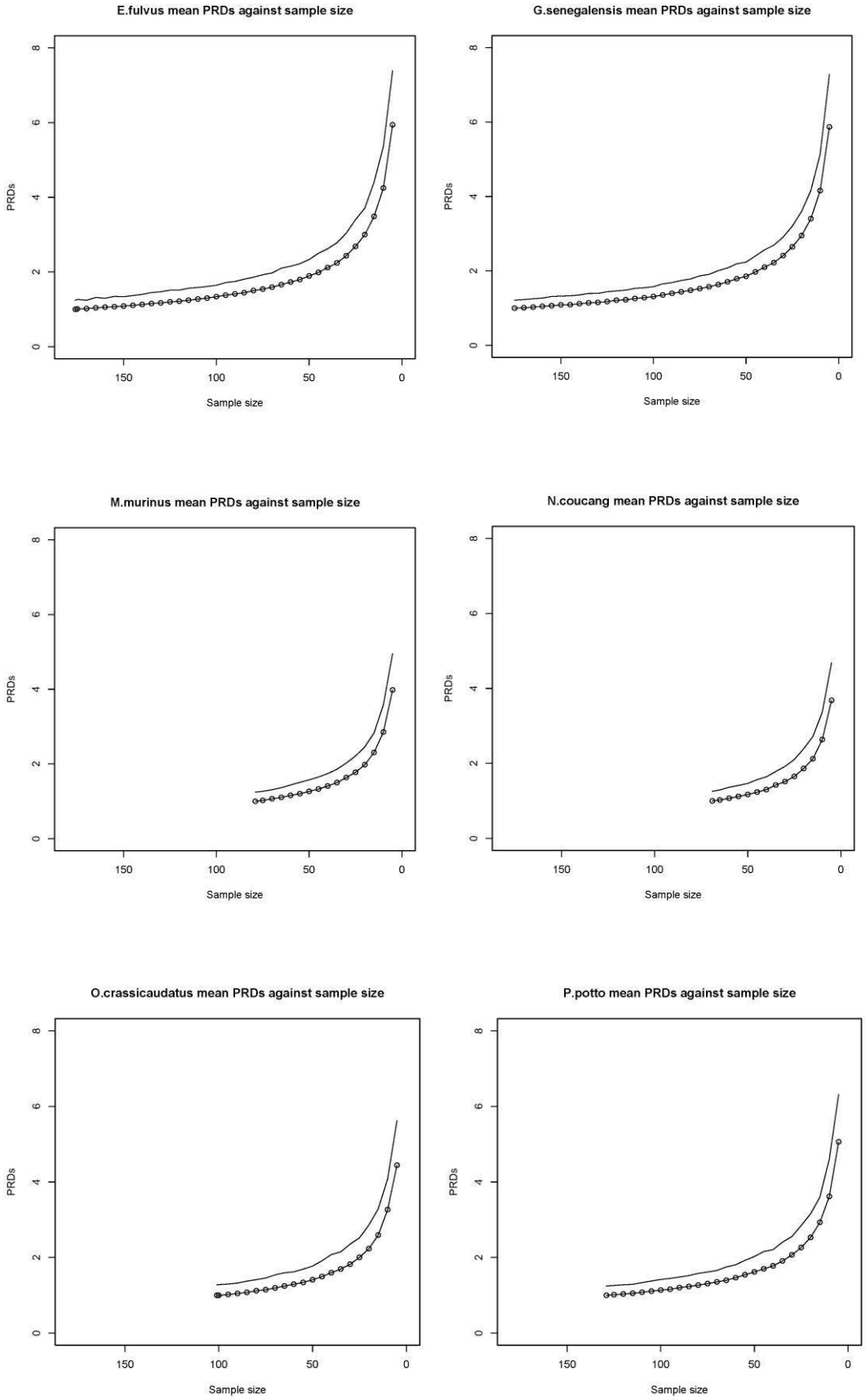

Figure 12: Profile plots of R_D, showing sampling error in mean shapes relative to within-species variation. Average and percentiles of the parameter are shown for the bootstrap samples and then for increasingly smaller sub-samples (N=100, 95, 90...10, 5).

Table 11: Percentage error of estimates of intra-species mean shape, for the mean and 95th percentile for the 1000 sub-samples of N=5.

Species	% error	
	Mean	95th percentile
Eulemur fulvus	493.8	639.9
Galago senegalensis	486.6	627.5
Microcebus murinus	298.1	395.4
Nycticebus coucang	268.0	468.6
Otolemur crassicaudatus	344.2	462.3
Perodicticus potto	406.1	531.3

The PRDs for inter-species mean shapes are shown in Table 12. The estimations of error in intra-species mean shape, as a ratio of inter-species differences in mean shape, are shown in Figure 13. The smallest inter-species distance was found between *N. coucang* and *P. potto*. For *P. potto,* the error in mean shape estimates was shown to be 5.1% of the inter-species distance when N=40, 17.0% when N=10 and 26.4% when N=5. The effect is reduced when the inter-species distance being used for comparison is larger. The largest inter-species distance was between *G. senegalensis* and *P. potto*. The error in mean shape estimates for *G. senegalensis* was 2.4% of this inter-species distance when N=40, 6.8% when N=10 and 10.5% when N=5. For the error in mean shape as percentage of inter-species distance for all pairs of species, at N=5, see Table 13.

Table 12: PRDs for between species mean shapes

PRDs between species mean shapes						
Species	*E.fulvus*	*G.senegalensis*	*M.murinus*	*N.coucang*	*O.crassicaudatus*	*P.potto*
E.fulvus		0.162158	0.139226	0.137194	0.100254	0.133255
G.senegalensis			0.115235	0.139445	0.108268	0.167056
M.murinus				0.098030	0.112022	0.114896
N.coucang					0.115912	0.084936
O.crassicaudatus						0.120261
P.potto						

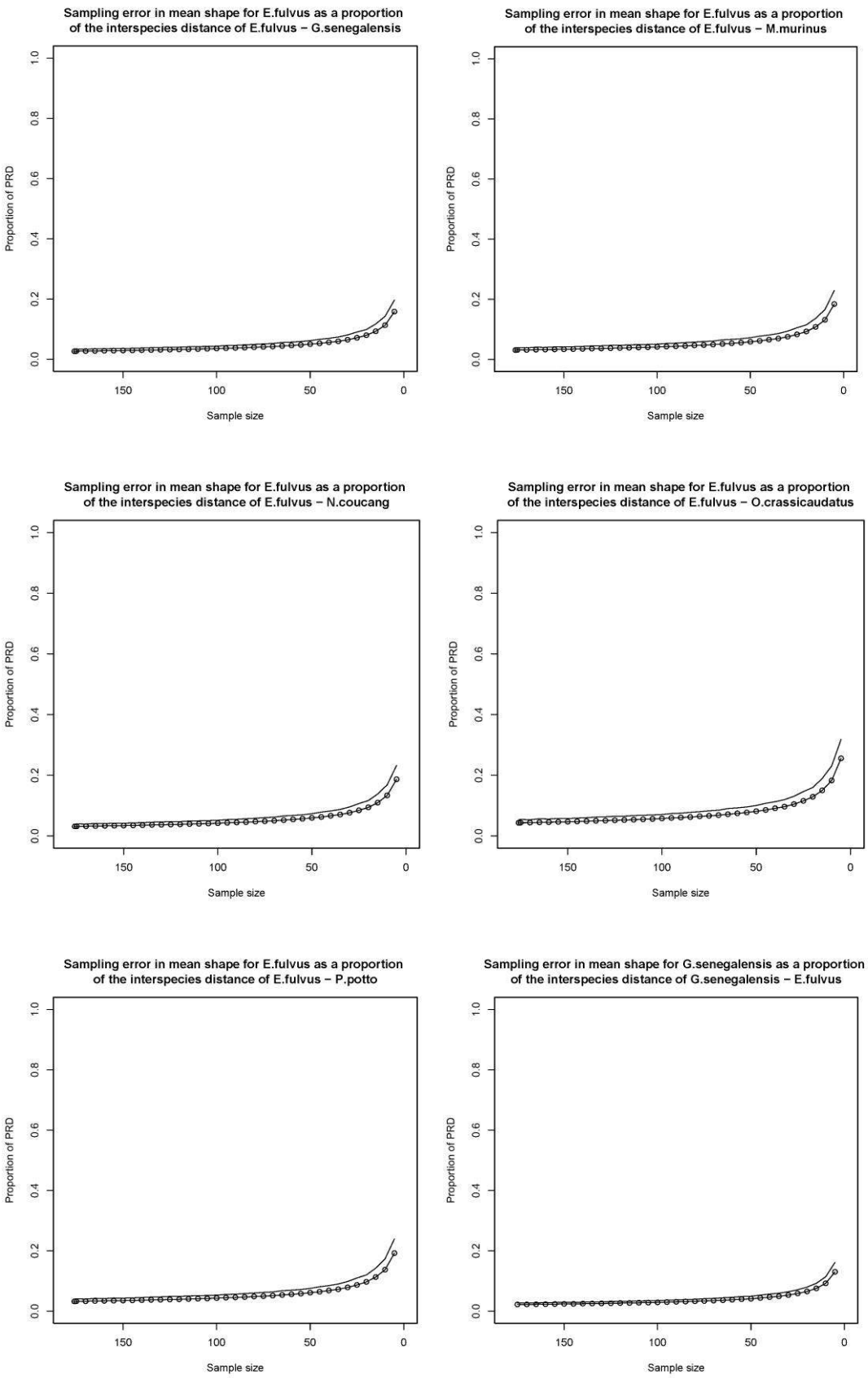

Figure 13: Profile plots of R_D showing sampling error in mean shapes as a percentage of inter-species distances. Average and percentiles for the parameter are shown for the bootstrap samples and then for increasingly smaller sub-samples (N=100, 95, 90...10, 5).

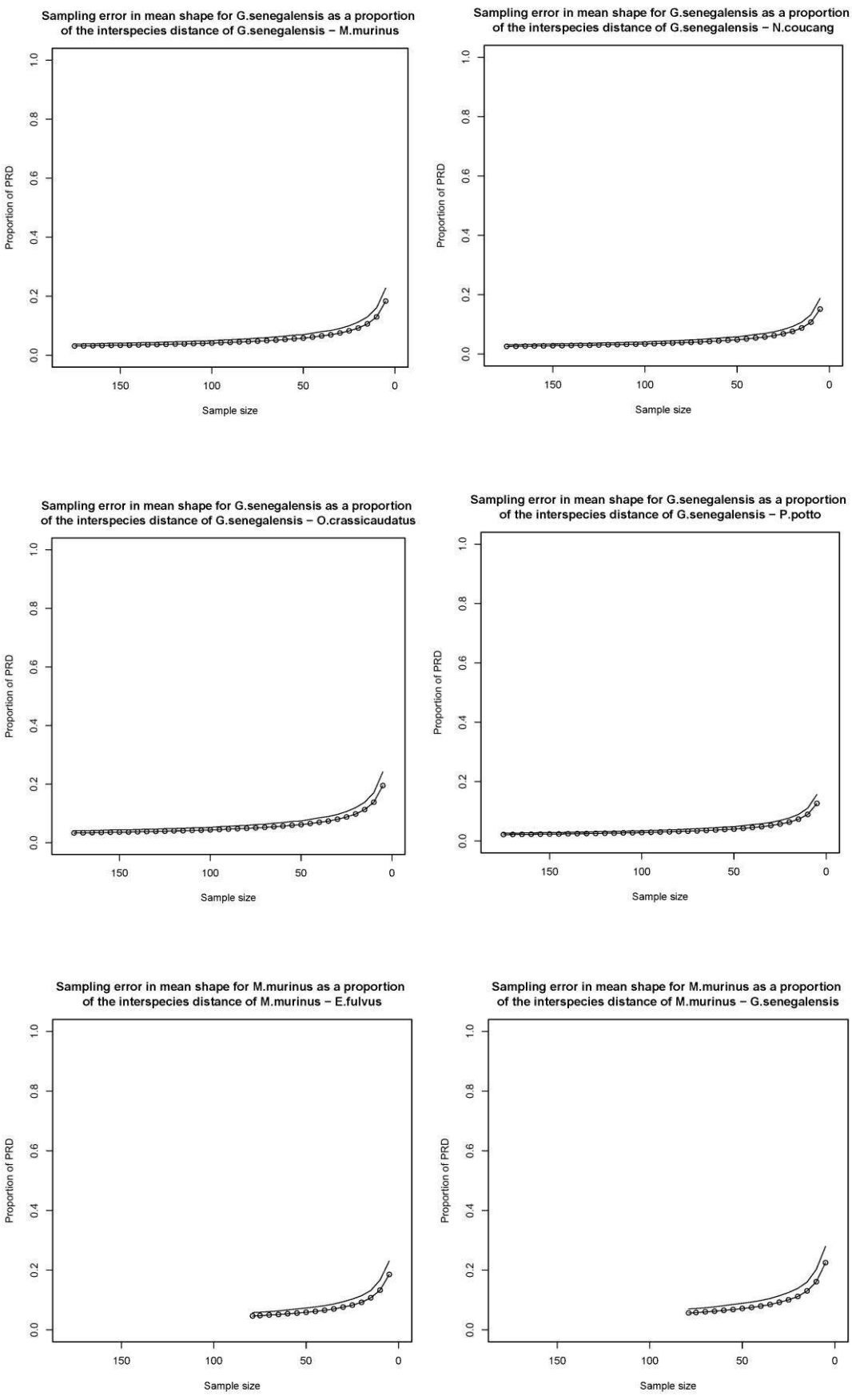

Figure 13 (Cont.)

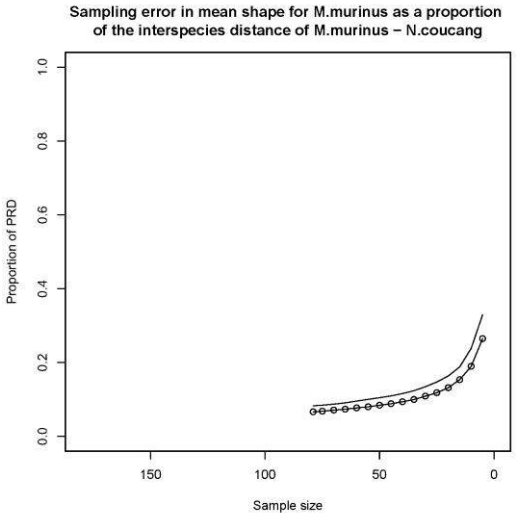

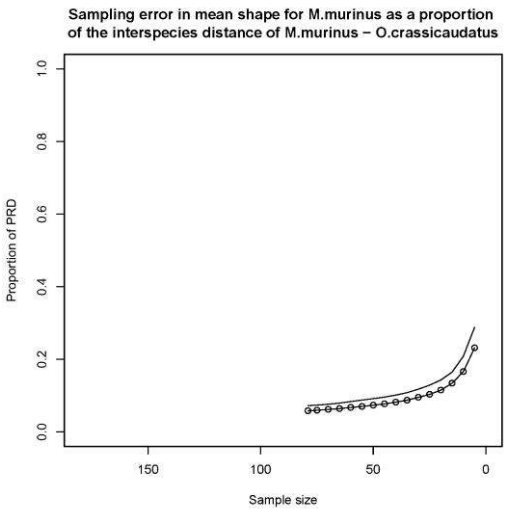

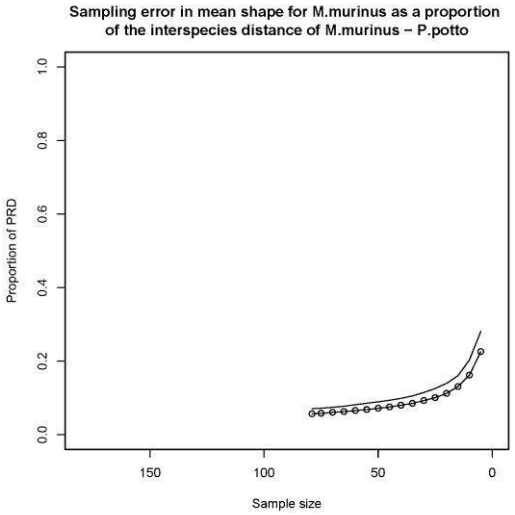

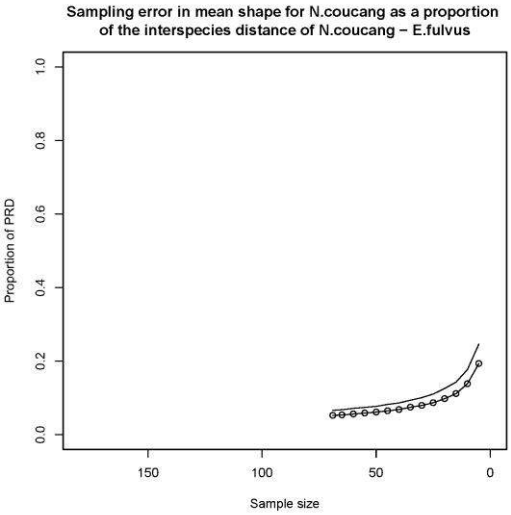

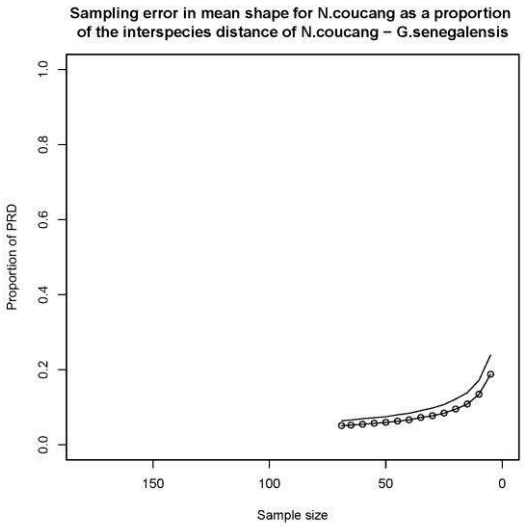

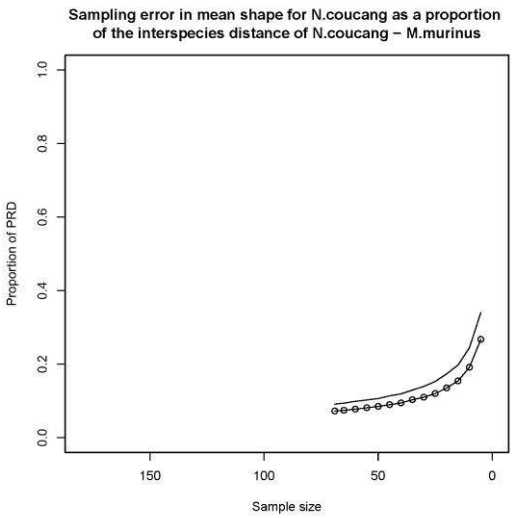

Figure 13 (Cont.)

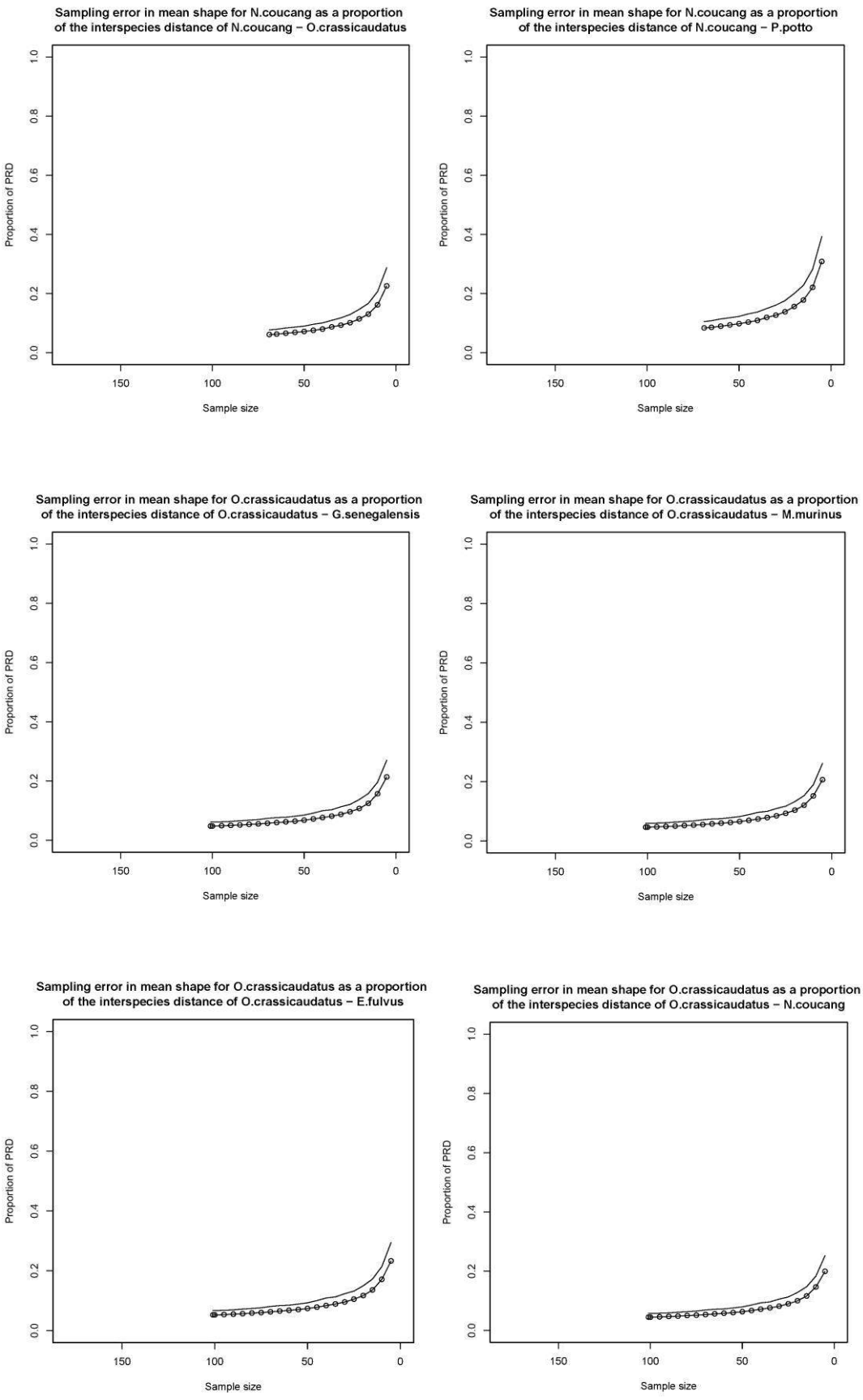

Figure 13 (Cont.)

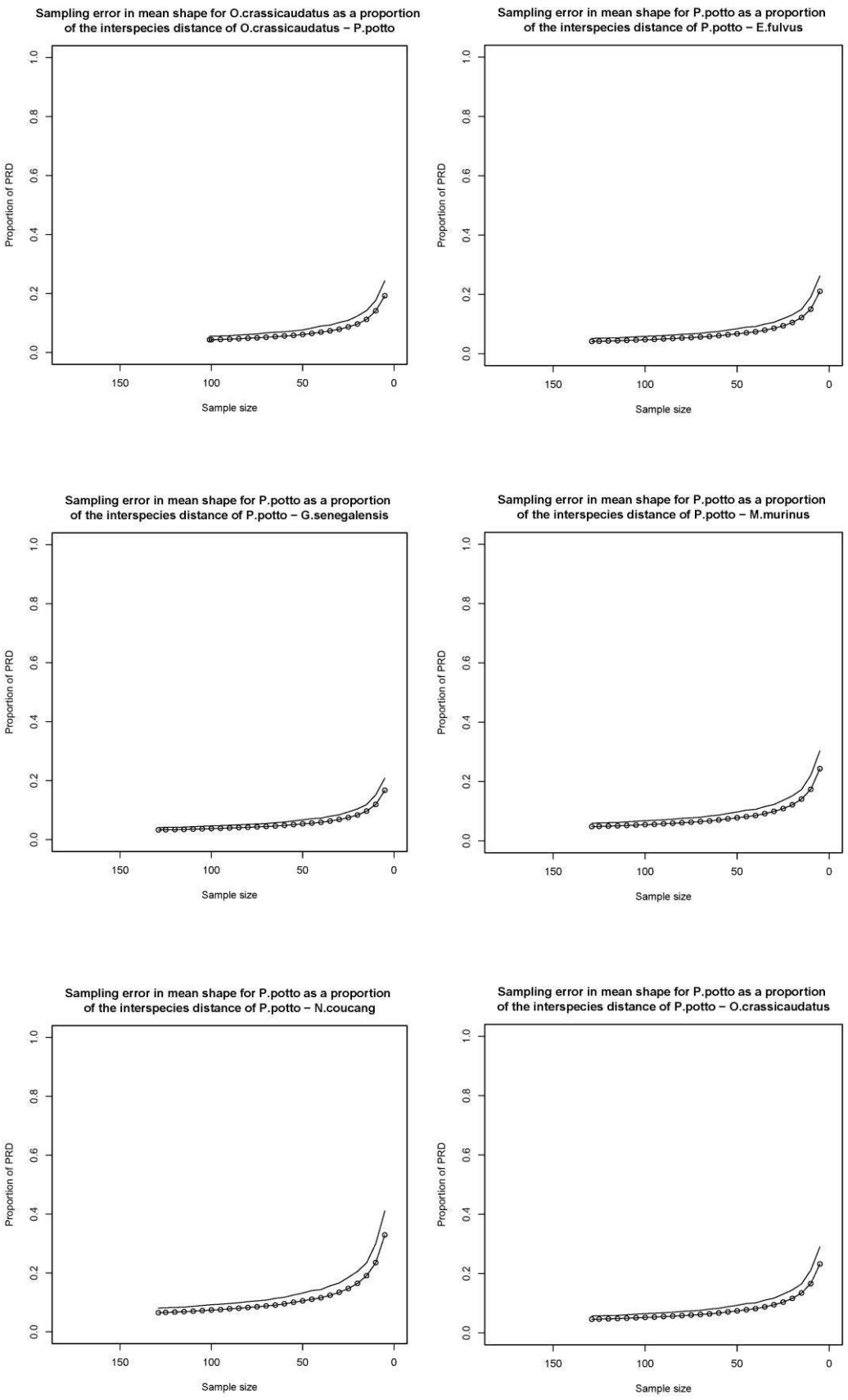

Figure 13 (Cont.).

Table 13: Error in species mean shape as a percentage of inter-species PRD when N=5. Unshaded rows report the mean of all 1000 N=5 sub-samples and shaded rows the 95th percentile.

Species	Error in mean shape as % of inter-species PRD					
	Eulemur fulvus	*Galago senegalensis*	*Microcebus murinus*	*Nycticebus coucang*	*Otolemur crassicaudatus*	*Perodicticus potto*
Eulemur		13.1	12.6	15.5	21.3	16.0
fulvus		17.0	19.8	20.1	27.5	20.7
Galago	10.8		15.2	12.6	16.2	10.5
senegalensis	13.9		19.8	16.2	20.9	13.5
Microcebus	14.0	16.9		19.8	17.3	16.9
murinus	18.4	22.4		26.3	23.0	22.4
Nycticebus	13.9	13.7	19.5		12.2	22.5
coucang	19.1	18.8	26.8		22.6	30.9
Otolemur	17.9	16.6	16.0	11.5		14.9
crassicaudatus	24.0	22.2	21.5	15.4		20.0
Perodicticus	16.8	13.4	19.5	26.4	18.6	
potto	21.0	16.8	24.4	32.9	23.3	

Variance in estimates of species mean shape becomes increasingly large at small sample sizes (Figure 14). For *E. fulvus* when N=40 the variance in estimates of mean shape is 2.1 times larger than that reported for the bootstrapped sample. When N=10, this increases to 4.2 times larger, and to 5.9 times larger when N=5, mirroring the results of error in mean shape. The percentage error when N=5 is 492. See Table 14 for the percentage error of the variance of mean shape when N= 5 for other species.

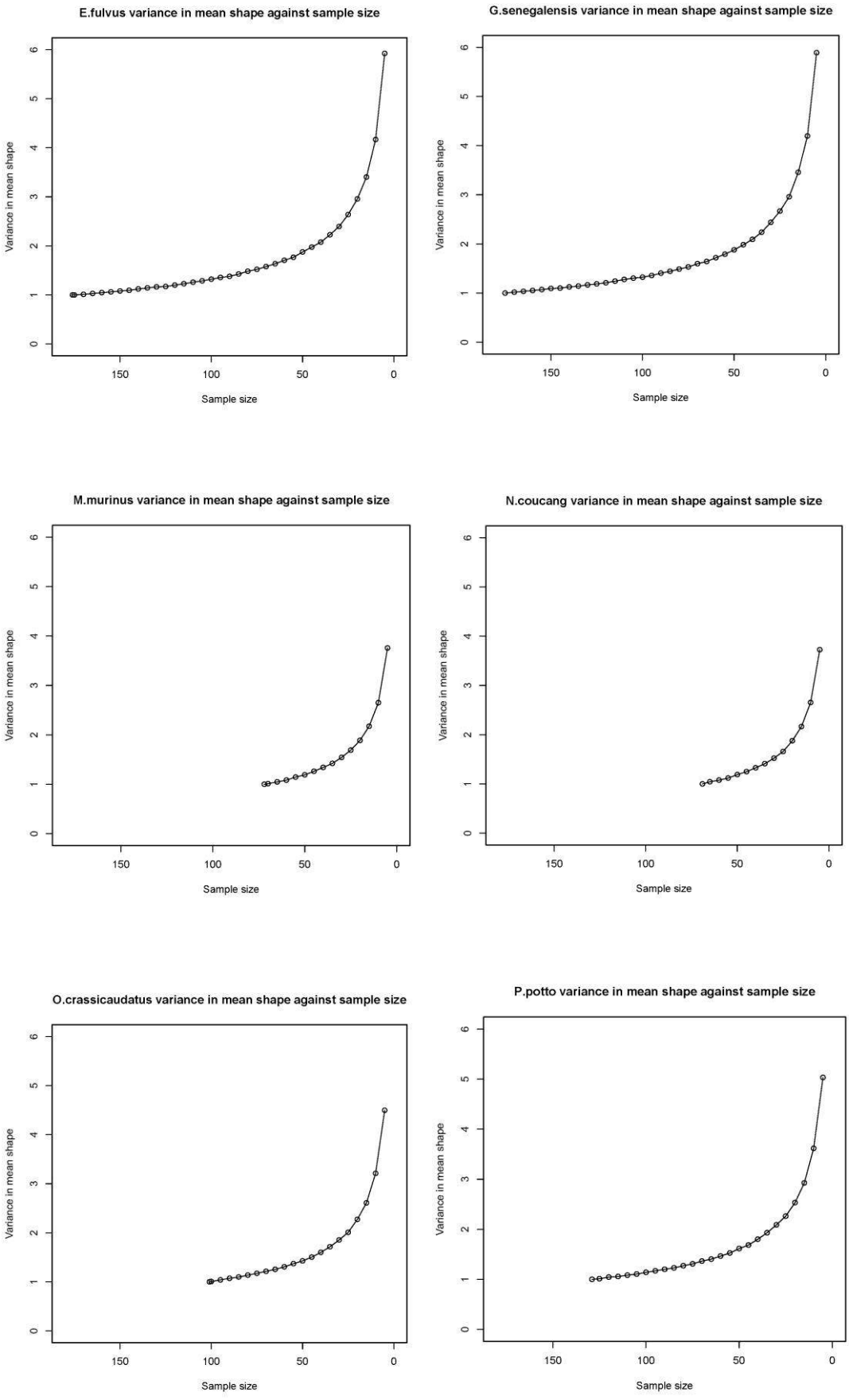

Figure 14: Profile plots of R showing variance in mean shapes. Variance in mean shapes is shown, from left to right, for the bootstrap samples and then for increasingly smaller sub-samples (N=100, 95, 80...10, 5).

Table 14: Percentage error of estimates of variance in mean shape when N=5.

Species	% error Mean
Eulemur fulvus	492.0
Galago senegalensis	478.3
Microcebus murinus	276.8
Nycticebus coucang	272.5
Otolemur crassicaudatus	349.6
Perodicticus potto	403.1

The accuracy of total shape variance, calculated for the observed sample, the bootstrapped samples and the sub-samples are shown in Table 15 and Figure 15. Unlike mean shape and variance in mean shape, estimates of total shape variance in a sample remain relatively accurate even at small sample sizes, and when N=5 the percentage error was only 0.1% for *E. fulvus* (although this increased to 30.0% and 41.3% for the 2.5th and 97.5th percentile respectively; Table 16).

Table 15: *E. fulvus* total shape variation: observed, bootstrap and random sub-samples.

E. fulvus	Sample size	Mean Total shape variation	2.5th percentile	97.5th percentile
Observed	176	0.003394	_	_
Bootstrap	176	0.003373	0.003196	0.003562
Sub-samples	175	0.003372	0.003188	0.003550
	170	0.003379	0.003213	0.003564
	165	0.003373	0.003196	0.003549
	160	0.003377	0.003194	0.003576
	155	0.003376	0.003197	0.003588
	150	0.003372	0.003179	0.003570
	145	0.003378	0.003184	0.003581
	140	0.003369	0.003168	0.003584
	135	0.003381	0.003173	0.003594
	130	0.003374	0.003162	0.003609
	125	0.003378	0.003170	0.003594
	120	0.003378	0.003160	0.003592
	115	0.003377	0.003164	0.003615
	110	0.003382	0.003161	0.003611
	105	0.003386	0.003156	0.003642
	100	0.003374	0.003142	0.003626
	95	0.003380	0.003136	0.003635
	90	0.003378	0.003127	0.003641
	85	0.003381	0.003112	0.003652
	80	0.003374	0.003111	0.003671
	75	0.003381	0.003107	0.003671
	70	0.003378	0.003119	0.003681
	65	0.003378	0.003098	0.003692
	60	0.003379	0.003083	0.003690
	55	0.003382	0.003027	0.003685
	50	0.003374	0.003049	0.003722
	45	0.003377	0.003037	0.003776
	40	0.003370	0.002985	0.003738
	35	0.003372	0.002972	0.003802
	30	0.003383	0.002960	0.003827
	25	0.003366	0.002918	0.003859
	20	0.003365	0.002875	0.003929
	15	0.003375	0.002782	0.004074
	10	0.003361	0.002681	0.004243
	5	0.003389	0.002376	0.004795

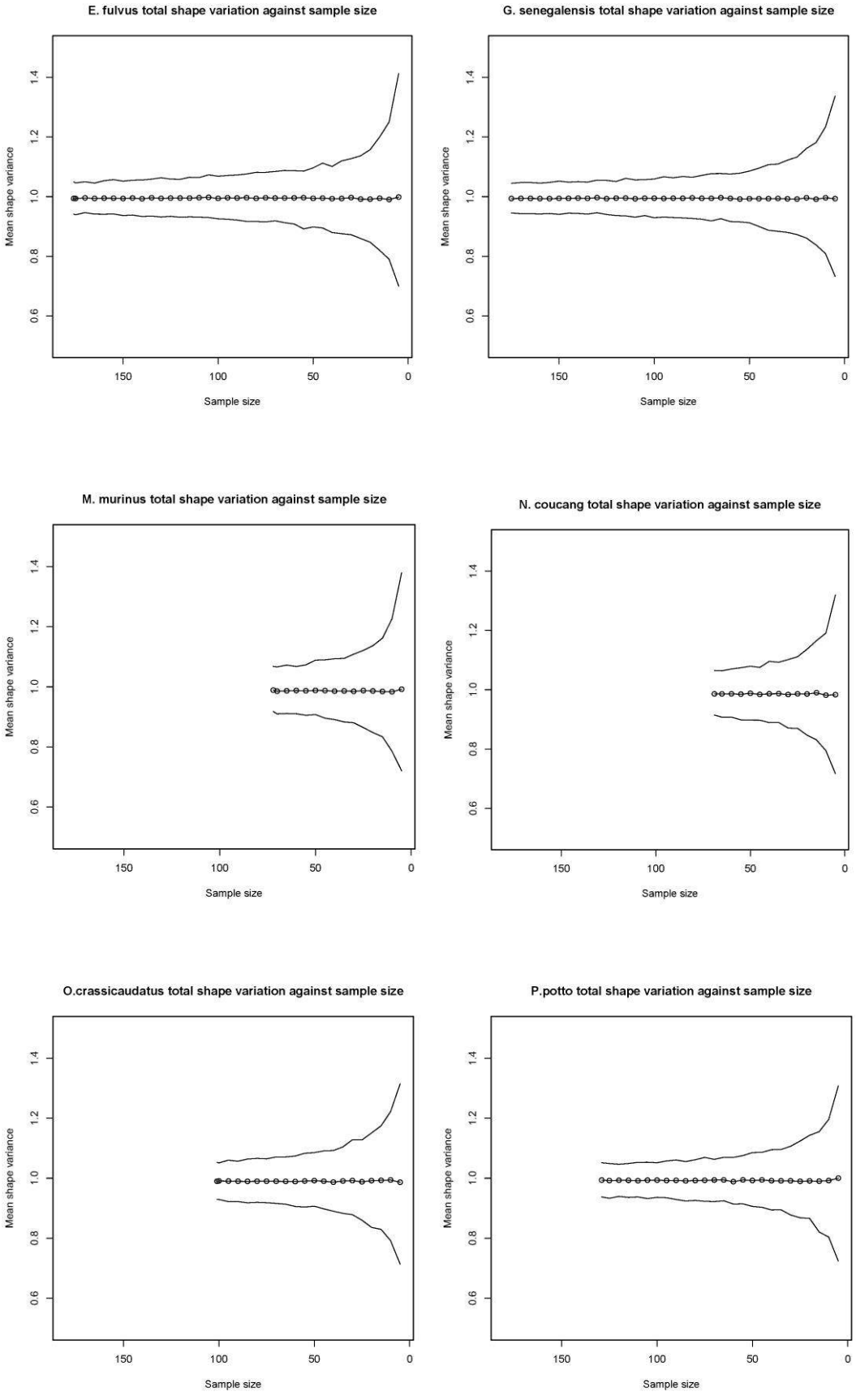

Figure 15: Profile plots of R for the total shape variation for each species. Average and percentiles of R for total shape variation are shown for the bootstrap samples and then for increasingly smaller sub-samples (N=100, 95, 90…10, 5).

Table 16: Percentage error of estimates of total shape variance for the mean, 2.5th and 97.5th percentile of all 1000 sub-samples of N=5.

Species	% error		
	Mean	2.5th percentile	97.5th percentile
Eulemur fulvus	0.1	30.0	41.3
Galago senegalensis	0.7	26.7	33.8
Microcebus murinus	0.8	28.0	38.0
Nycticebus coucang	1.7	28.2	32.1
Otolemur crassicaudatus	1.4	28.7	31.5
Perodicticus potto	0.0	27.6	30.8

3.4.3. Allometric trajectories

Estimates of angles between intra-species (males versus females) allometric trajectories increase rapidly as sample sizes are reduced (Table 17; Figure 16). When N=40 mean estimates of the angle between allometric trajectories of males and females of *E. fulvus* were up to 1.6 times larger than observed in the full sample, 3 times larger when N=10 and 4.2 times when N=5, with a percentage error of 319.1% (Table 18).

Table 17: Variation in angles (degrees) between static allometric vectors of group males and females for *E. fulvus.*

***E. fulvus* within species (male vs female)**				
N		**Vector angle**		
Group		**Mean**	**Percentile**	
Males	**Females**		**2.5th**	**97.5th**
Observed				
79	54	13.59	_	_
Bootstrap samples				
79	54	19.42	15.55	24.79
Random sub-samples				
54	54	20.16	16.06	25.74
50	50	20.61	16.25	26.90
45	45	21.43	16.69	28.32
40	40	22.21	17.21	29.23
35	35	23.34	17.63	30.75
30	30	24.51	18.32	33.50
25	25	26.66	19.28	36.98
20	20	29.12	20.32	40.95
15	15	33.57	21.90	46.94
10	10	40.23	25.54	58.10
5	5	56.95	34.26	82.11

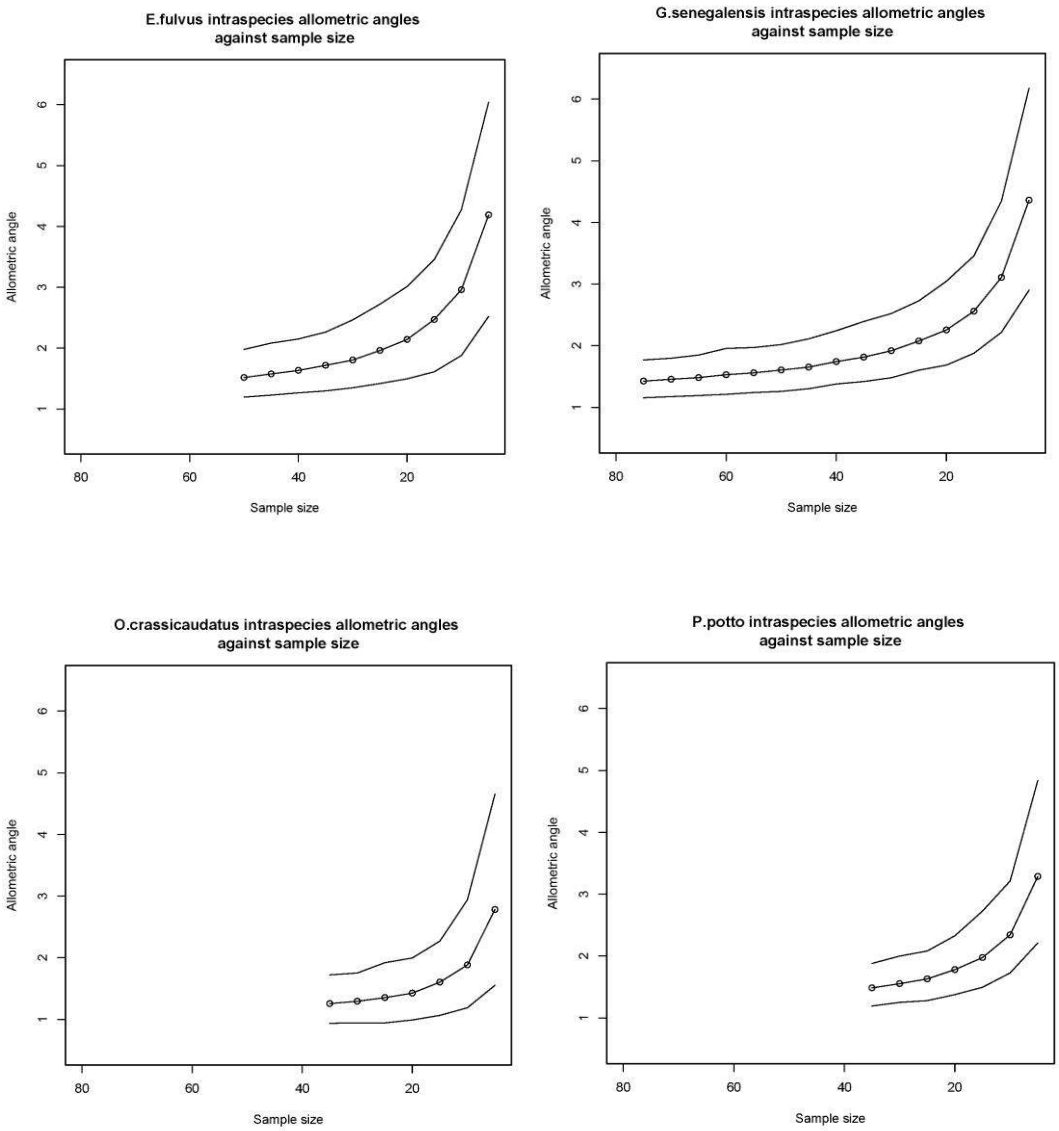

Figure 16: Profile plots of R for angles between male and female static allometries. Average and percentiles of the parameter are shown for increasingly smaller sub-samples (N=100, 95, 90…10, 5). Sample sizes are equal between groups, i.e., a sample size of N=20 describes 20 male and 20 female specimens.

Table 1: Percentage error of estimates of intra-species allometric angles (males vs females) for the mean, 2.5th and 97.5th percentile of all 1000 sub-samples of N=5.

Species	% error		
	Mean	2.5th percentile	97.5th percentile
Eulemur fulvus	319.1	152.1	504.2
Galago senegalensis	336.0	189.9	517.5
Otolemur crassicaudatus	178.2	55.3	365.3
Perodicticus potto	228.0	121.0	383.6

Estimates of angles between the allometric trajectories of different species are affected in the same way as the intra-species angles between male and female trajectories, becoming increasingly larger than the observed angle as sample sizes are reduced (Table 19-23; Figure 17). At N=40, the mean estimate of the angle between the allometric trajectories of two species was up to 1.8 times that of the observed, when N=10 it was up to 2.8 times that of the observed and up to 3.8 times when N=5 (Table 24).

Table 19: Variation in angles (degrees) between static allometric vectors of *E. fulvus* and *G. senegalensis*.

Inter-species*: E. fulvus, G. senegalensis*				
N		**Vector angle**		
Group		**Mean**	**Percentile**	
E. fulvus	***G. senegalensis***		**2.5th**	**97.5th**
Observed				
176	175	23.92	_	_
Bootstrap samples				
176	175	25.19	22.12	28.79
Random sub-samples				
175	175	25.19	22.17	28.52
170	170	25.23	22.13	28.90
165	165	25.19	22.03	29.08
160	160	25.31	22.11	29.28
155	155	25.37	22.05	29.40
150	150	25.36	21.99	29.24
145	145	25.40	22.04	29.61
140	140	25.46	22.19	29.52
135	135	25.53	22.06	29.44
130	130	25.58	22.22	29.83
125	125	25.84	22.09	30.06
120	120	25.70	22.10	30.31
115	115	25.82	22.23	30.84
110	110	26.01	21.89	30.61
105	105	26.07	22.10	30.61
100	100	26.09	22.20	30.86
95	95	26.20	22.19	31.36
90	90	26.42	22.40	31.15
85	85	26.54	22.29	31.88
80	80	26.75	22.34	32.28
75	75	26.88	22.25	32.81
70	70	26.94	22.09	33.06
65	65	27.29	22.16	33.70
60	60	27.64	22.83	34.29
55	55	27.87	22.64	34.62
50	50	28.22	22.90	34.99
45	45	28.69	23.10	35.94
40	40	29.37	23.13	37.51
35	35	30.33	23.77	38.66
30	30	31.04	24.04	40.13
25	25	32.18	25.19	42.66
20	20	33.93	25.37	45.00
15	15	37.15	27.31	48.90
10	10	43.01	30.15	58.55
5	5	56.43	36.86	77.60

Table 20: Variation in angles (degrees) between static allometric vectors of *E. fulvus* and *M. murinus.*

Inter-species*: E. fulvus, M. murinus*				
N		**Vector angle**		
Group		**Mean**	**Percentile**	
E. fulvus	***M. murinus***		**2.5th**	**97.5th**
Observed				
176	72	15.54	_	_
Bootstrap samples				
176	72	19.05	16.41	22.51
Random sub-samples				
70	70	20.55	17.35	24.68
65	65	20.83	17.38	24.78
60	60	21.11	17.59	25.84
55	55	21.69	17.95	26.86
50	50	22.28	18.19	27.99
45	45	22.67	18.36	28.10
40	40	23.46	18.87	30.08
35	35	24.51	19.55	30.77
30	30	25.84	20.62	33.33
25	25	27.52	21.32	35.96
20	20	29.93	22.40	39.79
15	15	34.02	24.78	45.91
10	10	40.42	28.35	55.96
5	5	55.65	36.42	77.08

Table 21: Variation in angles (degrees) between static allometric vectors of *E. fulvus* and *N. coucang*.

Inter-species*: E. fulvus, N. coucang*				
N		**Vector angle**		
Group		**Mean**	**Percentile**	
E. fulvus	***N. coucang***		**2.5th**	**97.5th**
Observed				
176	69	16.78	_	_
Bootstrap samples				
176	69	19.20	14.55	24.85
Random sub-samples				
65	65	20.82	15.29	28.16
60	60	21.12	15.41	28.81
55	55	21.47	15.28	28.64
50	50	21.93	15.91	30.28
45	45	22.48	16.22	31.08
40	40	23.15	16.52	31.77
35	35	23.78	17.05	33.30
30	30	24.99	17.44	35.27
25	25	26.49	18.12	37.10
20	20	28.54	19.71	40.92
15	15	31.77	21.28	45.09
10	10	37.84	24.23	53.60
5	5	52.25	31.52	76.10

Table 22: Variation in angles (degrees) between static allometric vectors of *E. fulvus* and *O. crassicaudatus*.

Inter-species*: E. fulvus, O. crassicaudatus*				
N		**Vector angle**		
Group		**Mean**	**Percentile**	
E. fulvus	***O. crassicaudatus***		**2.5th**	**97.5th**
Observed				
176	101	15.13	_	_
Bootstrap samples				
176	101	16.92	14.04	20.58
Random sub-samples				
100	100	17.58	14.04	22.45
95	95	17.77	14.15	22.93
90	90	17.95	14.36	23.30
85	85	18.12	14.24	23.22
80	80	18.15	14.33	23.73
75	75	18.48	14.52	24.60
70	70	18.68	14.77	24.80
65	65	19.04	14.74	25.64
60	60	19.26	14.92	26.36
55	55	19.71	15.12	26.88
50	50	20.19	15.28	27.33
45	45	20.61	15.37	28.44
40	40	21.15	15.82	29.09
35	35	21.83	16.16	30.88
30	30	22.92	16.53	32.97
25	25	24.37	16.86	35.10
20	20	26.06	17.79	37.69
15	15	29.31	19.37	43.09
10	10	34.96	21.78	52.92
5	5	49.40	28.65	71.13

Table 23: Variation in angles (degrees) between static allometric vectors of *E. fulvus* and *P. potto.*

Inter-species*: E. fulvus, P. potto*				
N		**Vector angle**		
Group		**Mean**	**Percentile**	
E. fulvus	***P. potto***		**2.5th**	**97.5th**
Observed				
176	129	17.89	_	_
Bootstrap samples				
176	129	19.75	15.95	25.16
Random sub-samples				
125	125	20.33	15.97	25.85
120	120	20.37	15.97	25.88
115	115	20.45	16.18	25.97
110	110	20.61	16.09	26.53
105	105	20.63	16.03	26.51
100	100	20.99	16.23	27.76
95	95	21.02	16.12	27.26
90	90	21.10	16.24	27.84
85	85	21.44	16.66	28.28
80	80	21.72	16.44	28.58
75	75	21.81	16.33	28.77
70	70	21.86	16.45	28.77
65	65	22.31	16.73	29.39
60	60	22.75	16.98	30.48
55	55	23.18	16.76	32.18
50	50	23.58	17.54	31.80
45	45	24.12	17.39	32.97
40	40	24.69	18.10	34.05
35	35	25.46	18.08	34.69
30	30	26.62	18.47	36.53
25	25	28.79	19.94	40.45
20	20	30.83	21.10	43.59
15	15	34.22	22.78	48.73
10	10	40.69	26.02	59.05
5	5	54.78	34.38	76.60

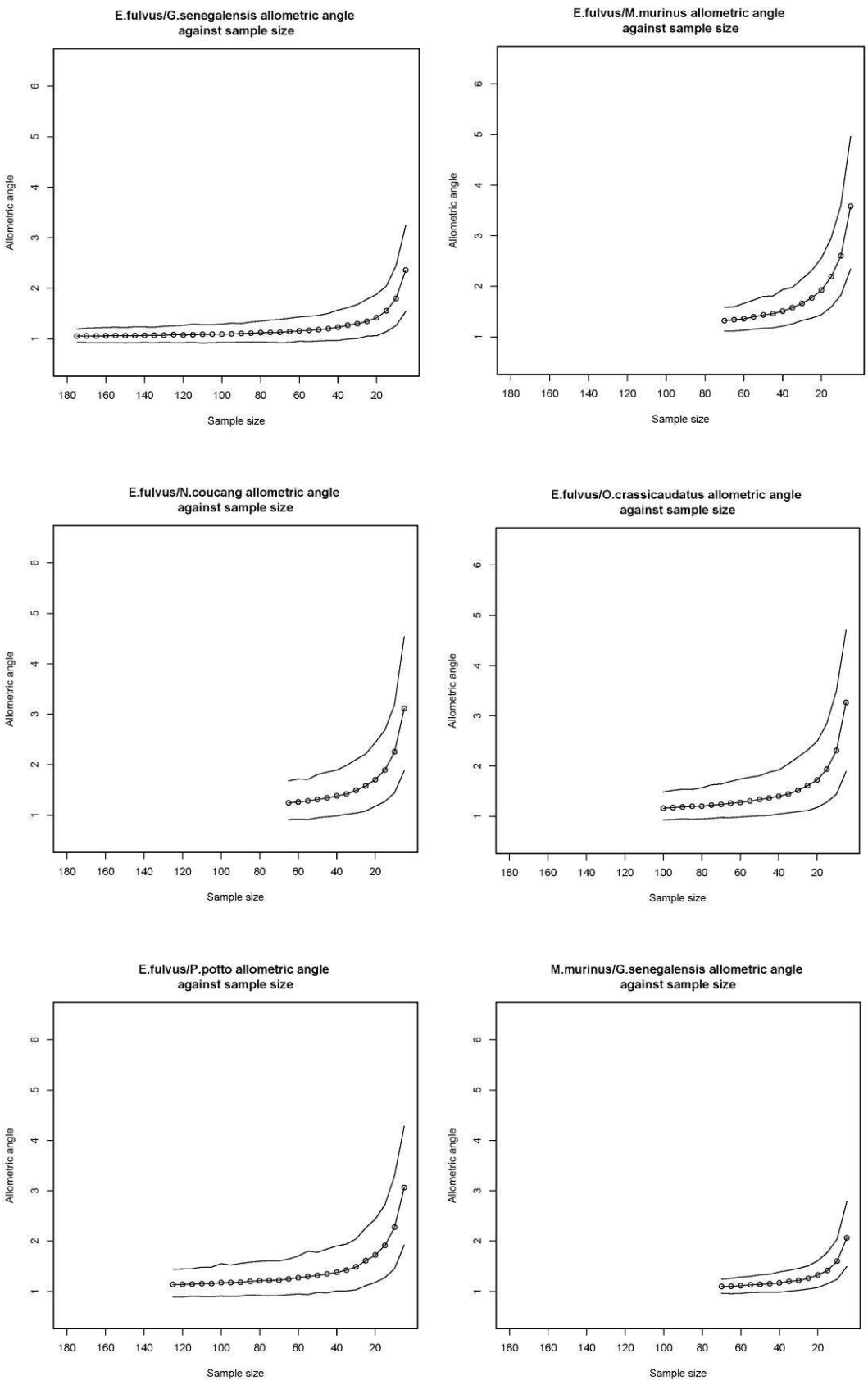

Figure 17: Profile plots of R for angles between species static allometries. Average and percentiles of the parameter are shown for increasingly smaller sub-samples (N=100, 95, 90…10, 5). Sample sizes are equal between groups, i.e., a sample size of N=20 describes 20 specimens from species A and 20 from species B.

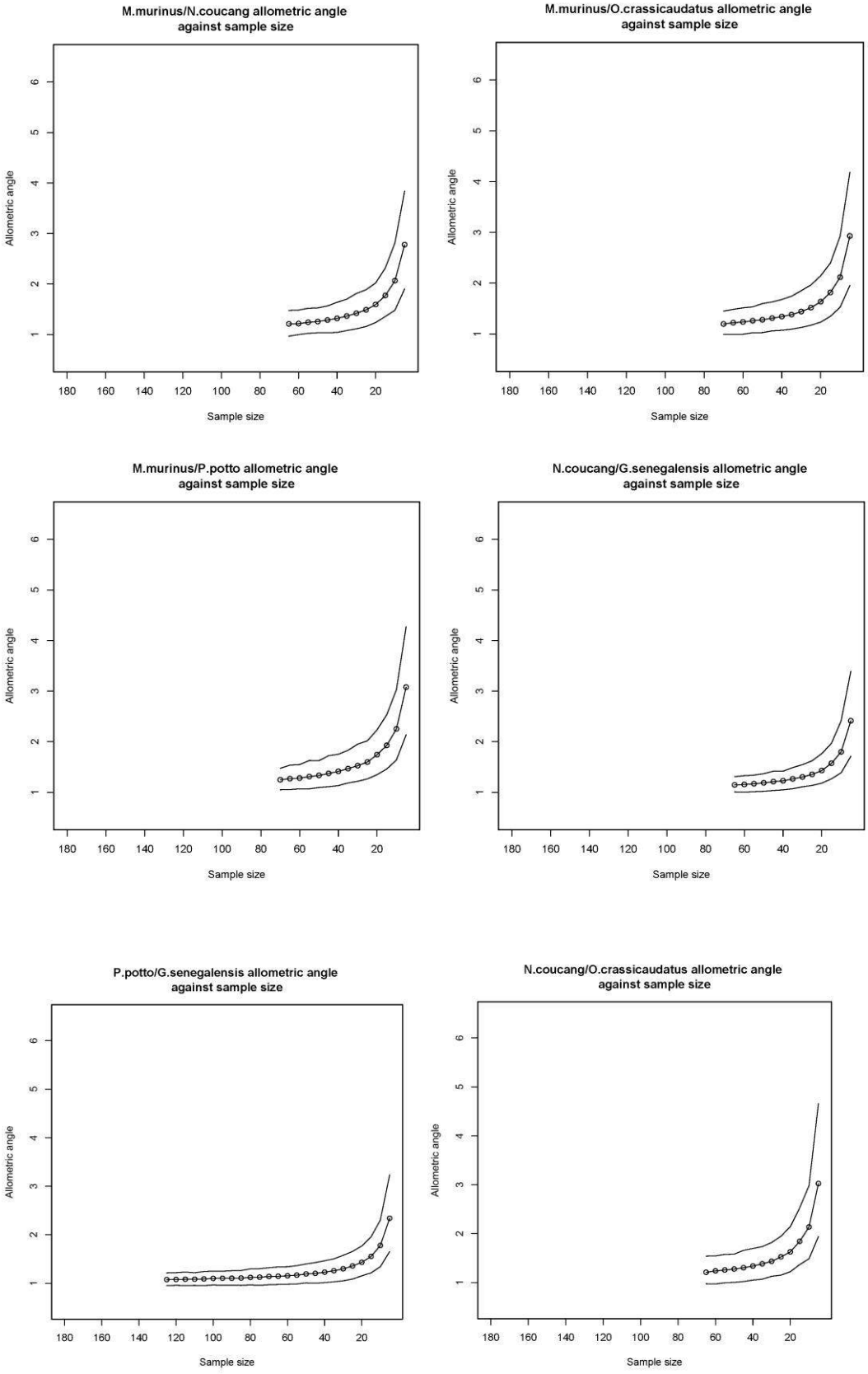

Figure 17 (Cont.)

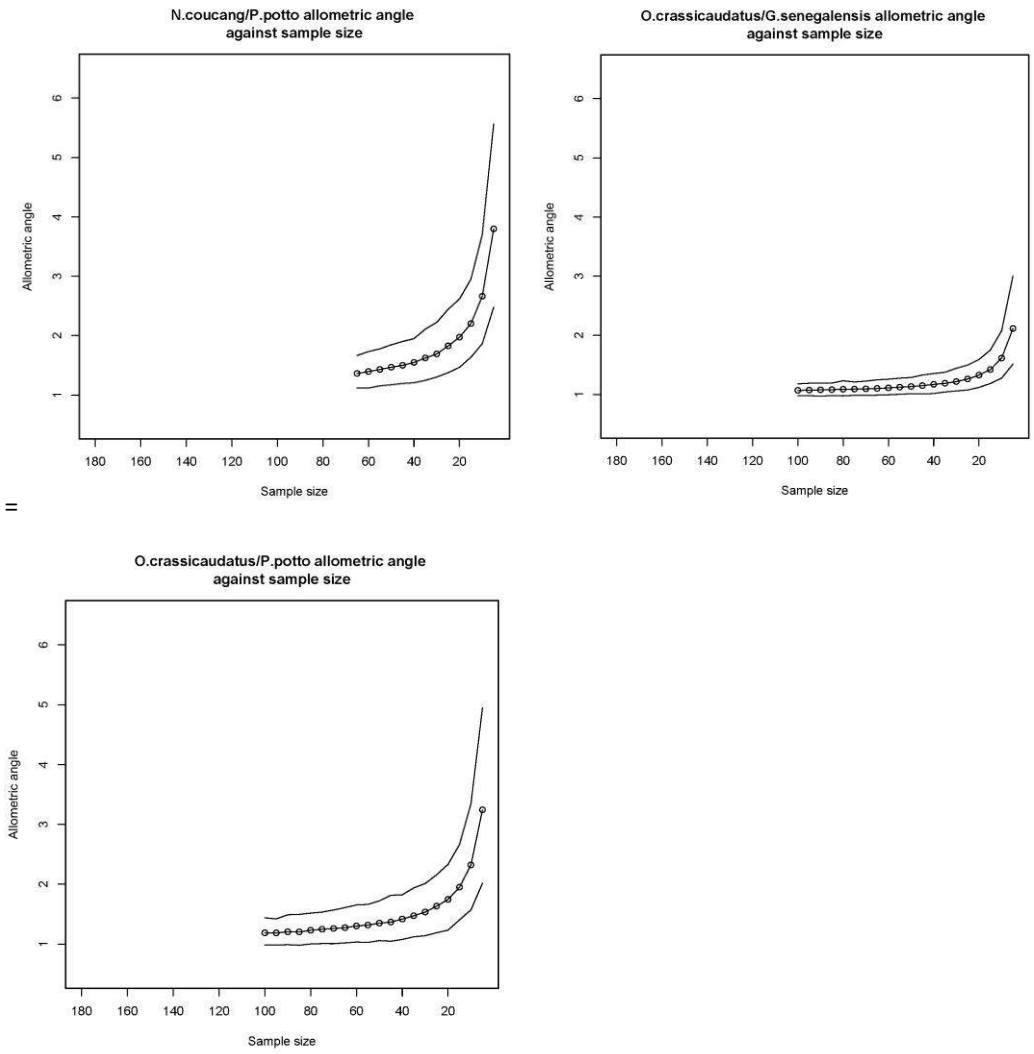

Figure 17 (Cont.)

Table 24: Percentage error of estimates of inter-species allometric angles for the mean (unshaded rows), 2.5th and 97.5th percentile (shaded rows) for the 1000 sub-samples of N=5.

Species	% error					
	Eulemur fulvus	*Galago senegalensis*	*Microcebus murinus*	*Nycticebus coucang*	*Otolemur crassicaudatus*	*Perodicticus potto*
Eulemur		135.9	257.5	211.4	226.5	206.2
fulvus		54.1 - 224.4	134.4 - 396.0	87.8 - 353.5	89.4 - 370.1	92.2 - 328.2
Galago			106.1	141.3	111.4	133.8
senegalensis			49.4 - 178.6	71.1 - 239.3	51.2 - 200.4	65.3 - 223.2
Microcebus				177.8	192.8	207.7
murinus				90.3 - 283.8	95.3 - 365.8	113.5 - 327.2
Nycticebus					202.3	279.4
coucang					94.0 - 365.8	24.8 - 111.0
Otolemur						224.3
crassicaudatus						101.5 - 394.8
Perodicticus						
potto						

3.4.4. Percentage of shape variation explained by size

As with angles between allometric trajectories, the percentage of shape variation explained by size is exaggerated in small sample sizes. For *E. fulvus* when N=40,mean estimates of the percentage of shape variation explained by size are 1.7 times that of the observed shape variation explained by size (Table 25; Figure 18). When N=10, this increases to 4.8 times that of the observed and 9.2 times when N=5. Variation around the mean estimate also increases as sample size decreases. For *E. fulvus* sub-samples of N=40, the range is 1.7 times larger than the variation around the bootstrapped mean of the whole sample, increasing to 6.1 times larger when N=10 and 9.2 times larger when N=5. The percentage error for *E. fulvus* when N=5 was 655.8% for the mean value, and ranged from 21.6% to 1085.3% for the 2.5th and 97.5th percentiles, respectively (Table 26).

Table 25: Mean percentage of shape variation explained by size for *E. fulvus*: observed, bootstrap and random sub-samples.

E. fulvus	Sample size	% shape variance caused by size	2.5th percentile	97.5thpercentile
Observed	176	3.87	-	-
Bootstrap	176	4.42	3.17	5.95
Sub-samples	175	4.41	3.12	6.13
	170	4.47	3.18	6.06
	165	4.44	3.12	6.05
	160	4.52	3.16	6.23
	155	4.56	3.18	6.21
	150	4.51	3.07	6.19
	145	4.53	3.13	6.31
	140	4.54	3.08	6.30
	135	4.60	3.16	6.44
	130	4.65	3.12	6.44
	125	4.67	3.18	6.65
	120	4.71	3.10	6.55
	115	4.75	3.14	6.74
	110	4.73	3.11	6.72
	105	4.83	3.16	6.84
	100	4.86	3.13	7.22
	95	4.88	3.10	6.93
	90	4.98	3.14	7.21
	85	5.00	3.18	7.22
	80	5.06	3.13	7.39
	75	5.23	3.27	7.58
	70	5.30	3.23	8.12
	65	5.38	3.18	7.97
	60	5.59	3.28	8.59
	55	5.59	3.28	8.46
	50	5.90	3.45	9.42
	45	6.09	3.48	9.59
	40	6.50	3.65	10.48
	35	6.79	4.03	10.76
	30	7.20	4.10	11.81
	25	8.13	4.29	13.86
	20	9.03	4.99	15.40
	15	11.02	5.86	18.85
	10	15.10	8.49	25.34
	5	29.25	17.25	45.87

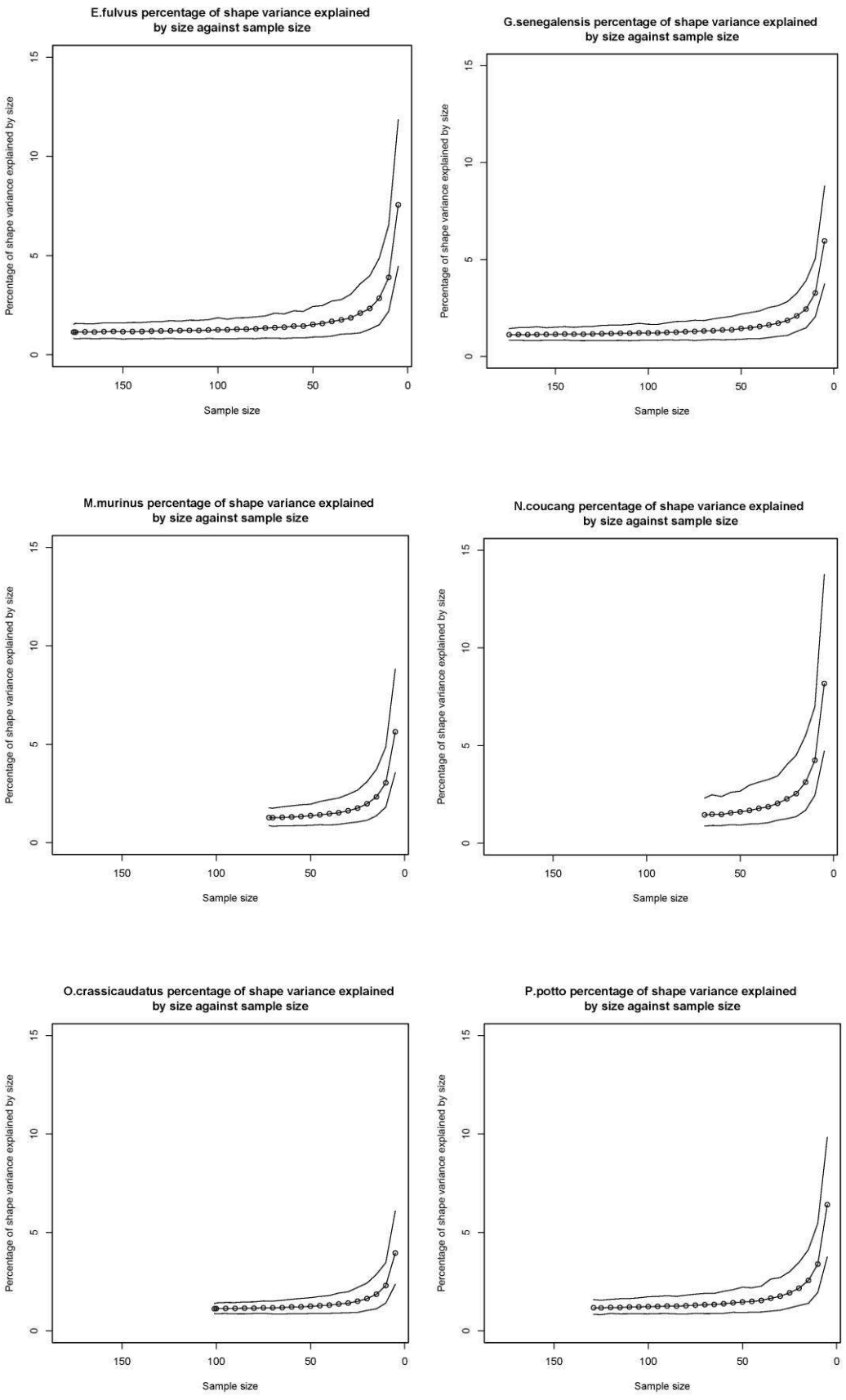

Figure 11: Profile plots of R showing the mean percentage of shape variance explained by size. Average and percentiles of the parameter are shown, from left to right, for the bootstrap samples and then for increasingly smaller sub-samples (N=100, 95, 90…10, 5).

Table 2: Percentage error of shape variation explained by size for the mean, 2.5th and 97.5th percentile for the 1000 sub-samples of N=5.

Species	% error		
	Mean	2.5th percentile	97.5th percentile
Eulemur fulvus	655.8	216.5	1085.3
Galago senegalensis	495.1	273.8	778.6
Microcebus murinus	463.3	256.0	782.4
Nycticebus coucang	717.4	371.7	1276.2
Otolemur crassicaudatus	295.2	136.2	509.1
Perodicticus potto	540.4	275.4	882.9

3.5. Discussion

The accuracy of size and shape parameters across different sample sizes varies distinctly, depending on the parameter in question. However, within each parameter, the effect of limited sample size does not vary substantially between samples. For all the parameters, the results largely mirror those found for guenons (Cardini & Elton, 2007), suggesting that the patterns may also apply to the order primates as a whole.

3.5.1. Size

Mean estimates of size parameters remain remarkably consistent, even at very small sample sizes. Mean size (CS) remained relatively accurate even at N=5, where mean size estimates were no worse than about 2 - 9mm smaller or larger than the observed size. These values are comparable to those reported for *C. aethiops* (Cardini & Elton, 2007) and translate into a maximum expected errors of 5.5% (based on 95% confidence intervals) when estimating mean size (Table 7 and 8). In the case of *C. aethiops*, the small expected error was attributed to a small coefficient of variation (CV=100 x SD/mean; where SD and mean are the standard deviation of size and the arithmetic mean of size, respectively) in the sample (4.8% for females, 6.8% for males; Cardini & Elton, 2007). Similarly low scores characterised the strepsirhine species analysed here (*E. fulvus*: 4.1%; *G. senegalensis*: 3.6%; *M. murinus*: 3.8%; *N. coucang*: 5.3%; *O. crassicaudatus*: 6.0%; *P. potto*: 4.7%).

As with guenons (Cardini & Elton, 2007), the mean of estimates of the SD of size remain relatively accurate at all but the very smallest sample sizes. However, the range of SD estimates increases substantially with decreasing sample size. This could be a problem if one wished to compare the amount of variation in size found between populations.

Based on current data, the effects of variable sample size on estimates of size parameters do not seem to be affected by size or taxonomy, as both the smallest (*M. murinus*) and the largest (*E. fulvus*) strepsirhines, as well as the larger still haplorrhine *C. aethiops* (Cardini & Elton, 2007), produced similar results.

3.5.2. Shape

As with mean size, mean estimates of total shape variation remain constant even when sample sizes are small. However, the range of estimated shape variance around the mean increases steadily with decreasing sample size, and begins to grow more rapidly once N<20, with a percentage error of up to +/- 25% for the 95th percentile when N=5. These results suggest that for the species analysed here, a sample size of N≥20 can produce an accurate estimation of the shape variation within the larger population (assuming that the observed samples used here are accurate representations of species variation, with specimens taken from throughout the species distribution in the wild), but at lower sample sizes some, caution is needed.

The accuracy of mean shape estimates deteriorates swiftly as sample size decreases. Even at N=40 the distance between the sub-sample mean and observed mean shape are 2.1 times the distance between the bootstrapped mean and the observed mean. At N=10, this distance was up to 4.2 times as large, and 5.9 times when N=5. Comparable results were found for *C. aethiops* (Cardini & Elton, 2007). *E. fulvus* and *G. senegalensis* appear to perform less well in terms of accuracy for this calculation (although all species follow the same pattern). This is due, at least in part, to these taxa having the largest observed sample sizes (N=176 and N=175 respectively), since larger observed samples result in narrower ranges of bootstrap replicate values (Table 10; Figure 12; Appendix 1): thus the ratio, *R*, of sub-sample relative to the observed sample values will automatically be higher. In line with this, *N. coucang* has the smallest observed sample size (N=69) and shows the least pronounced effect at the smallest sub-samples. If using mean shape to compare the variation in shape between populations, relatively large sample sizes would be recommended for each population, particularly for populations or species which are similar to each other in shape.

Mean shape is also sometimes used as a basis on which to construct phylogenies, in such cases the accuracy of the resultant phylogeny would be dependent on the extent of intra-species variation in mean shape compared to inter-species distances (setting aside for the

moment, the question of whether or not morphology contains phylogenetic signal. The closest inter-species distance was seen between *N. coucang* and *P. potto*, both members of the Lorisidae and with an estimated divergence time of approximately 37mya (Perelman *et al.*, 2011). The largest distance was observed between *G. senegalensis* and *P. potto* (which have an estimated divergence date of 40mya), although this was closely followed by *E. fulvus* and *G. senegalensis*, which is perhaps more expected, if shape difference reflects phylogenetic distance, as they diverged around 69mya (Perelman *et al.*, 2011), live on different continents and belong to different superfamilies (Fleagle, 2013) (See Chapter 6 for further discussion on the presence of phylogenetic signal in the strepsirhine cranium). When inter-species distance is smaller (i.e., between *N. coucang* and *P. potto*), error in intra-species mean shape estimates was found to be up to 23% as large as the inter-species distance when N=10, and 30.8% when N=5. However, when inter-species distance was at its largest (i.e., between *G. senegalensis* and *P. potto*) it could only account for 9% of inter-species distance when N=10, or 12.6% when N=5.

Cardini and Elton (2007) found that, for samples of fewer than 30 specimens, error in intra-species mean shape could account for up to 37% of the inter-species distance between *C. aethiops* and *C. mitis*. This inflated effect, in comparison to the strepsirhines tested here, may be the result of lower inter-species distances, rather than higher intra-species variation; *C. aethiops* and *C. mitis* are estimated to have diverged approximately 8mya (Perelman *et al.*, 2011; Tosi *et al.,* 2005), much more recently than any of the strepsirhine species in the analysis.

Baab *et al.* (2014) also found that intra-species distance between the observed and the sub-sample mean shape increased as sample size was reduced. When N=3, error in mean shape accounted for up to 43% of inter-species distances, between species from different genera (*Propithecus verreauxi – Indri indri*). This increased to as much as 91% of inter-species distance when species were from the same genus (*E. fulvus – E. macaco*). In addition, Baab *et al.'s* analyses were conducted with a maximum observed sample size of N=21. This may still be too small to gain an accurate estimate of mean shape. Here, for *E. fulvus,* a sample size of N=20 was found to have PRD of 3 times that of the bootstrapped sample of 176. As such, error in mean shape may account for an even higher proportion of inter-species distance.

The percentage of inter-species distance accounted for by intra-species error reduces as sample size increases, so both inter-species distances and sample size should be taken into account when conducting analyses based on mean shapes. Moreover, this highlights the difficulties of trying to construct phylogenies for fossil taxa from minimal data. While no solution to this problem is evident, we can at least be aware of the possible implications and limitations.

Cardini and Elton (2007) point out that inaccuracy in mean shape would also cause problems for studies of disparity. For example, partial disparity is calculated based on the distance between species mean and the overall mean of all species (Zelditch *et al.,* 2012), small sample sizes would therefore be expected to result in errors.

3.5.3. Allometry

Estimates of angles between static allometric trajectories lose accuracy as sample sizes become smaller, while the range around mean estimates increases as sample size is reduced. This is true for both intra-species (male versus female) and inter-species calculations. This inaccuracy is manifested as angles being grossly overestimated at smaller sample size. This explains why bootstrapped mean angles are consistently found to be larger than observed angles; in bootstrapped samples, some specimens may be represented more than once, making them effectively smaller than the observed sample.

The same pattern of results was found for *C. aethiops* (intra-species) and for *C. aethiops* and *C. mitis* (inter-species), although the intra-species angle for the observed sample for *C. aethiops* (23.4^{o}) was larger than any found for the strepsirhine species (Cardini & Elton, 2007). This is expected, as *C. aethiops* show strong sexual dimorphism in shape, which is lacking in the strepsirhines (Cardini & Elton, 2007; Jenkins & Albrecht, 1991; Kappeler, 1990, 1991; Thorén *et al.,* 2006).

Ideally, to minimize error in static allometric angle calculations, relatively large sample sizes should be used. Where this is not possible, especially when working with fossil species, we can at least be aware that differences are likely to be inflated when working with small sample sizes. Ontogenetic trajectories were not found to be as strongly affected by sample size as static trajectories, and a sample size of N=20 was found to be sufficient for *Pan* (Cobb & O'Higgins, 2004). However, it should be noted that in this instance only one of the

two samples was randomized, with the other sample consisting of all of the available specimens; this may have resulted in an underestimation of adequate sample size.

Mirroring the pattern seen for static allometric angles, the percentage of shape variance explained by size (CS) is also grossly overestimated at small sample sizes. The range of estimates around the mean of the parameter also becomes larger at small sample sizes. As such, similar care should be taken to maximise sample sizes and to recognize that results could be artificially inflated.

3.6. Conclusion

The effect of sample size, while constant across species, genera and family, is not constant across parameters of shape and size. Mean estimates of mean size, SD of size and total shape variance all remain accurate at small sample sizes ($N \geq 5$). Although, the range of estimates of SD of size does increase as sample size decreases and this should be considered when interpreting relevant calculations. Estimates of mean shape and of variance in mean shapes do not perform well at small samples sizes and large sample sizes are required for confidence in the accuracy of result. The influence of size over shape can be substantially overestimated at small sample sizes, both within and between species, and, once again, large sample sizes are recommended for these calculations.

– Chapter 4 –

The presence and influence of modularity in the crania of the Strepsirhini

4.1. Abstract

Cranial modularity, the subdivision of the skull into groups of correlated traits, based on shared function or developmental pathways, has been argued to be consistent in structure across the mammalian clade (Goswami, 2006a; Porto *et al.,* 2009). However, while the structure of modularity may be stable, the strength of correlation within those modules may vary between genera or even species (Goswami & Polly, 2010a). Modularity can either constrain or facilitate the evolution of the skull, and can determine the pathways which morphological change must follow (Goswami & Polly, 2010a).

Within (for 28 species with sample size >20) and between species analyses were conducted to examine which of four models of modularity best explained modularity in the strepsirhine cranium, based on RV_M coefficient scores. For each of these models, within-module correlation was also assessed at the intra-species and inter-species level. In addition, eigenvalue relative standard deviation scores were calculated for each species, after adjusting for the effect of sample size, as a measure of overall within-species integration with the skull.

Nearly all intra-species and inter-species level results indicate low overall integration and high levels of modularity within the strepsirhine cranium. The most strongly supported model of modularity was a six module hypothesis based on Goswami (2006a). Modules corresponding to the dentition and face were found to be the most strongly correlated. *Hapalemur griseus* differed from the general pattern; this result is likely linked to selection for a specialised diet. The consistent pattern of modularity in strepsirhines could be viewed as an underlying cause of homoplasy in the clade, with strong correlations within-modules limiting the directions available for morphological change.

4.2. Introduction

4.2.1. What is modularity?

'Morphological integration' and 'modularity' describe the covariation of traits within an organism. Integration is the encompassing or overarching pattern of covariation, and modularity, the partitioning of integration into subsets, is usually based on a shared function or developmental history (Goswami & Polly, 2010a; Klingenberg, 2013). Modules are identified in two ways: first, through a strong integration between traits within a module, detectable through their covariation, and second, through (semi-)autonomy from other modules or traits outside of that module (Goswami & Polly, 2010a). Modules identified quantitatively have been shown to corresponded to real-life biological components (Olson & Miller, 1951) and numerous studies have set out to unearth the link between patterns of modularity and their underlying functional or development cause (Ackermann & Cheverud, 2000, 2004; Cheverud, 1995; Drake & Klingenberg, 2010; Goswami, 2006a; Goswami & Polly, 2010b; Klingenberg *et al.,* 2004; Marroig *et al.,* 2004; Mitteroecker & Bookstein, 2008; Porto *et al.*, 2009; Ross, 2013; Villmoare *et al.*, 2014; Wagner *et al.,* 2007). Furthermore, studies are beginning to explore the link between phenotypic and genetic modularity, with some correlation found between the two (Cheverud, 1996; Cheverud *et al.*, 2004; Klingenberg *et al.*, 2004; Mitteroecker, 2009; Stock, 2001).

Modularity can be viewed as hierarchically structured; the mammalian skeleton, for example, can be separated into the limb and axial skeleton, the axial skeleton into cranial and postcranial modules and the skull into cranial and mandibular modules (Pavlicev *et al.*, 2008). Different hypotheses of modularity have been proposed for the cranium itself, depending on the depth of modularity in question, as well as its theoretical cause and the traits concerned (Cheverud, 1995; Drake & Klingenberg, 2010; Goswami, 2006a; Lieberman *et al.*, 2000; Singh *et al.*, 2012).

4.2.2. Models of modularity

The facial skeleton, comprising the nasal, lacrimal and maxillary bones and the zygomatic processes, has been separated from the rest of the cranium (Collard & Wood, 2001), as it follows a somatic growth pattern. Somatic growth patterns have been described as a 'S' shaped curves; in humans, for example, this would mean a rapid rate of growth in infancy, which slows during childhood, only to increase again during adolescence. In contrast, the

neurocranium follows a neural growth pattern. A neural growth pattern shows rapid growth and near developmental completion at an early age (humans will have completed 95% of their neural growth by eight years of age) (Premkumar, 2011). Due to these differences in growth patterns, the face continues to grow for an extended period of time compared to the neurocranium, and it has been proposed that this may make it more susceptible to environmental influences, especially those related to diet (Collard & Wood, 2001; Lieberman *et al.*, 2000; Singh *et al.*, 2012).

The neurocranium can be further separated into two parts, namely, the cranial base and the cranial vault, based on differences in the ossification processes of the two regions (Singh *et al.*, 2012). The growth of the vault occurs by intramembranous ossification, while growth of the basicranium occurs through endochondral ossification (Hall, 2005). The main difference between the two modes is that intramembranous ossification directly converts mesenchymal tissue into bone, whereas endochondral ossification first converts the mesenchymal cells into cartilage, which is subsequently replaced by bone (Gilbert, 2014). The basicranium may therefore be influenced by somatic growth factors, due to the effect of hormones on cartilage growth (Hall, 2005).

The facial skeleton itself, can be broken down into smaller, specific modules linked to shared developmental history or function. Cheverud (1995) identifies oral, zygomatic and nasal modules. The oral module includes the area surrounding the oral cavity and supporting the teeth. The zygomatic module is comprised of the zygomatic arch and the temporal fossa where the masseter and temporalis muscles attach. These muscles, which are responsible for mastication, are crucial for the development of bone tissue in the region. The nasal module lies between the oral module and the orbit and is largely formed in response to the growth of the cartilaginous nasal septum (Moore, 1981). Cheverud (1995) also divides the neurocranium into the cranial vault and base, due to their different growth patterns, as previously discussed, and the orbit, which forms in response to the growth of the eye.

Goswami (2006a), like Cheverud (1995), divides the cranium into six modules, but instead of using a priori reasoning based on function or development, the modules were determined through cluster analysis, performed on landmark covariance matrices. Cluster analysis will produce clusters regardless of the strength of the covariation; therefore, the

resulting clusters were only considered to be significant if the mean correlation among landmarks within each cluster was significantly greater than 0, as determined by Fisher's *z*-transformation and Students *t*-test (Goswami, 2006a). The modules returned consistently corresponded to the zygomatic-pterygoid (including the zygomatic arch, the sphenoid bones, the pterygoid region, and the anterior cranial base), the orbit (which incorporates landmarks from both the face and the neurocranium), the cranial vault, cranial base (composed principally of the endochondral bones) and oral regions, with the oral region divided into anterior oral-nasal module (including the facial skeleton and anterior dentition) and a posterior molar module (comprising landmarks from the molars, palate and anterior zygomatic).

4.2.3. The evolution of modularity

Despite addressing different levels of the modularity hierarchy, models of mammalian cranial modularity are similar in their basic structure (Porto *et al.*, 2009). Researchers have argued that the pattern of modularity within the mammalian skull has remained, more or less, constant for at least the last 65 million years, with the main changes occurring only in the strength of the covariance within and between established modules (Porto *et al.*, 2009). Basal mammals are reported to have higher overall cranial integration and lower integration within-modules, while more derived mammals, such as primates, show lower overall integration and greater levels of within-module covariation (Porto *et al.*, 2009).

Selection for the covariation of traits is argued to have occurred along lines of shared developmental history and/or shared functionality (where traits act together to perform a physiological function that is discrete in relation to other functional modules) (Wagner *et al.*, 2007). It has been suggested that, if cranial modules have formed as the result of shared developmental history, they are more likely to be homologous, conversely, modules that are the result of shared functionality they are more likely to be homoplastic responses to similar environmental pressures (Ackermann, 2005).

Investigation into the ontogenetic development of modularity in the hominoid cranium, following the modularity pattern proposed by Cheverud (1995), reveals that, while the traits in the oral module are strongly correlated throughout ontogeny, traits relating to the zygomatic module began to increase in their correlation after infancy. The nasal module either increased or decreased in its level of internal correlation over ontogenetic

time depending on species, and those species with strong correlation in the nasal module tended to have weak correlation in the oral module and vice versa (Ackermann, 2005). However, in general, within-module correlations increased in all species over ontogenetic time following a shared pattern of modularity, suggesting that cranial modularity results from a common developmental history or a common function during development (Ackermann, 2005).

In the case of therian mammals, a developmental explanation appears to be a better fit than a functional one (Goswami, 2006a). All six of the modules in therians identified through cluster analysis (Goswami, 2006a), correspond to functional units. The anterior oral-nasal and molar modules make up the cranium's primary masticatory apparatus; the zygomatic-pterygoid region also plays a role in mastication, as it contains the muscle attachment sights for the jaw; the orbit and vault protect and support the eyes and brain respectively; and the basicranium supports the braincase, while also acting as the attachment point between the cranial and post cranial skeleton. However, the oral-nasal, molar and cranial base modules show stronger within-module integration than the orbit, zygomatic or cranial vault modules, and there is no clear functional explanation as to why this might be (Goswami, 2006a). Developmentally, however, the three strongly integrated modules are all derived from a single tissue origin and are all produced by a single mode of ossification, albeit via different modes depending on the module; the anterior oral-nasal and molar modules develop through intramembranous ossification and the cranial base through endochondral ossification (Kuratani, 2005). In contrast, the three weaker modules are more developmentally complex, comprising tissues from different origins and/or formed using different modes of ossification (Goswami, 2006a). However, in most cases authors have struggled to disentangle the developmental from the functional routes, as they are often co-aligned (Cardini & Elton, 2008a; Cheverud, 1995; González-José *et al.*, 2004; Singh *et al.*, 2012) although see (Drake & Klingenberg, 2010).

At a proximal level, modularity is thought to be caused by pleiotropy; when one gene (or mutation, or a group of interacting genes) affects multiple traits (Wagner & Zhang, 2011). Natural selection is presumed to favour the formation of phenotypic effects among traits that serve the same function over those employed in disparate functions (Marroig *et al.*, 2004). Modularity is adaptive in at least two key ways; first, the covariation of traits within-modules allows for coordinated evolution while maintaining functionality (Porto *et al.*,

2009) and second, the semi-autonomous relationship between-modules allows them to evolve in a semi-independent fashion, thereby avoiding interference to other modules and their functions (Wagner *et al.*, 2007).

4.2.4. The behaviour of different cranial modules

Different modules have been predicted to behave in different ways, largely based on their particular development or function. The cranial base plays a role in multiple functions, including providing support for the brain and being the point of interaction between the skull and postcrania and, as a result, it has been argued that it should be a strongly integrated module (Lieberman *et al.*, 2000). Within primates, the cranial base has been shown to be both highly integrated and to have significantly low levels of variation, although it should be noted that, while this pattern was found to be true for primates in general, only 58% of the species tested were actually found to have such strong within-module trait correlations, suggesting variation in module strength within the order (Goswami & Polly, 2010b)

Precisely which landmarks make up the 'cranial base' has been a point of disagreement between researchers. Cheverud (1995) follows Lieberman *et al.* (2000) in attributing all landmarks on the cranial base, which are posterior to the posterior point of the nasal spine, to the 'cranial base module'. In contrast, Goswami (2006a) assigns only those landmarks on the cranial base posterior to the basisphenoid-basioccipital suture to the 'cranial base' module. The more anteriorly placed cranial base landmarks are classed as belonging to a 'zygomatic-pterygoid' module, which shows much lower within-module integration than the more posteriorly placed cranial base module (Goswami, 2006a).

Closer examination of the cranial vault has found it to be significantly less integrated in primates than it is in carnivorans (Goswami, 2006a). This difference has been attributed to selection for the uncoupling of traits in the primate cranial vault, to allow for the greater level of encephalisation they have undergone during their evolution, in comparison to carnivorans (Cheverud, 1996).

The strength and variation of the facial module(s) has predominantly been examined in relation to diet. Within carnivorans, a correlation between diet and cranial integration, hypothesised to be caused by the functional integration of traits primarily involved in

mastication, was found for arctoid carnivorans (bears, racoons and weasels), but not for feliforms or canids (Goswami, 2006b). The impact of diet on the strength of module integration may therefore be clade, or even species, dependent, as shown for capuchin monkeys (*Cebus* sp.). Capuchin species whose diets include hard-object foods, either as stable or fall-back foods, where shown to experience higher integration within facial modules than those species with a softer diet (Makedonska *et al.*, 2012). As the ability to process hard object foods increases in importance, it may be advantageous to evolve strongly integrated functional modules for this specialist form of mastication, while also decoupling those traits from the rest of the cranium (Makedonska *et al.*, 2012).

4.2.5. Evolution through modularity

The partitioning of the skull into modules should facilitate the overall evolution of the skull by enabling change to occur more readily than if the entire cranium was affected by every adaptation, in every trait (Goswami & Polly, 2010a). However, the covariation of traits within-modules could either constrain or facilitate evolution. Strong integrations within a module could reduce the ability of any single trait to adapt independently to environmental pressure. Alternatively, strong connections could help to coordinate and therefore facilitate the adaptation of that module (Goswami & Polly, 2010a).

In primates, modules with high degrees of integration (the anterior oral-nasal region, molar, and cranial base) were found to have lower levels of disparity across taxa compared to modules with low levels of integration (the orbit, zygomatic-pterygoid, and cranial vault) (Goswami *et al.*, 2014). It has therefore been argued that modularity may work to constrain evolutionary change, and thereby serve to maintain functional/developmental units (Goswami *et al.*, 2014).

Further modelling of the effects of integration suggest that, while it did not affect the rate, it did effect the direction of evolution, by limiting the pathways that it can take (Goswami *et al.*, 2014). This could potentially cause high levels of convergence in distantly related taxa; i.e., homoplasy. However, it can also work to increase morphological distances between taxa. Simulations demonstrated that correlations among traits did not necessarily limit variation, in terms of the area of morphospace occupied; rather, it rearranged the variation so that, instead of being randomly dispersed

throughout morphospace, it fell along particular axes. This can result in extreme morphologies and a greater range between end morphologies (Goswami *et al.*, 2014).

4.2.6. Modularity in the primate cranium

Previously, the presence and strength of modularity has generally been estimated by the comparison of correlation matrices (Ackermann, 2005; Cheverud, 1995; Marroig & Cheverud, 2001). Matrices are generated for theoretical modules, based on function and development; usually following the two-module - face and cranium - model or the Cheverud (1995) six-module model, outlined above. When two traits are assigned to the same module a value of one is entered in the integration matrix, when two traits are assigned to different modules than a value of zero is entered. The correlation between this theoretical matrix and the observed correlation matrix is then assessed using a Mantel's test (Ackermann, 2005; Cheverud, 1995; Marroig & Cheverud, 2001). For this, the theoretical matrix will be randomised and its correlation with the unaltered theoretical matrix measured. The process is repeated numerous times to generate a distribution of matrix correlation scores, based on the null hypothesis of no structural similarity among matrices. The correlation of the observed and unaltered theoretical matrices is then assessed against this distribution; the percentage of correlations greater than or equal to the observed correlation indicate the probability of obtaining that observed correlation (Ackermann, 2005; Cheverud, 1989; Marroig & Cheverud, 2001)

Across New World Monkey (NWM) genera, facial traits are generally found to be more strongly correlated than the traits of the neurocranium (Marroig & Cheverud, 2001) and, of the six modules proposed by Cheverud (1995), the oral module has the highest within-module correlation (Marroig & Cheverud, 2001)**.** The exceptions to this rule are *Saguinus, Callimico* and *Aotus,* which show the reversed pattern of weaker modularity in the face in comparison the neurocranium (Ackermann & Cheverud, 2000; Marroig & Cheverud, 2001). This has been linked to the lack of sexual dimorphism in all three of these genera (Ackermann & Cheverud, 2004; Rehg & Leigh, 1999; Wright, 1994), which in turn has been attributed to their pair-bonded or polyandrous social structures (Ackermann & Cheverud, 2004; Fernandez-Duque, 2011; Goldizen, 2003; Porter, 2001). This could imply that sexual selection on facial traits has resulted in their strong correlation, or lack of, in the case of *Saguinus, Callimico* and *Aotus* (Ackermann & Cheverud, 2004). In addition, *Aotus*, the owl monkey, is the only nocturnal anthropoid species and, as such, is derived in having

specific morphological adaptations associated with night vision, such as enlarged orbits (Wright, 1994). These changes could have called for a restructuring of the functional relationships of the cranium, as evident here in *Aotus* alternative pattern of modularity (Ackermann & Cheverud, 2004; Marroig & Cheverud, 2001)**.**

A similar modularity structure has also been recorded for Old World monkeys (OWMs; *Macaca, Papio* and *Cercocebus*), with the cranium divided into facial and neurocranial modules (Cheverud, 1982, 1989; Hallgrímsson *et al.,* 2004). Moreover, investigations into seven *Papio* species revealed the oral module to be relatively highly correlated in all of the taxa (Cheverud, 1989).

All great apes also show very high overall cranial integration and, as with NW and OWM, the oral module is particularly highly correlated (Ackermann, 2005). However, hominoids also have strong integration in the zygomatic region and, to a lesser extent, the nasal region (Ackermann, 2005). These are the modules which are primarily associated with mastication, and this may indicate a shift in cranial organisation at the divergence the hominoids. Such a shift could be the result of adaptations to a changing diet or to selection for increased body size and the subsequent influence of allometric scaling (Ackermann, 2005).

This apparently overarching pattern of modularity within primates could possibly be extended to help with the interpretation of fossil taxa. For example, *Homo rudolfensis* has a mosaic of *Homo* and *Paranthropus* features; a large, *Homo* like vault, but robust facial and dental features that resemble *Paranthropus* (Ackermann & Cheverud, 2004; Leakey *et al.*, 2012; Wood & Collard, 1999). The decoupling or semi-autonomous nature of the face and neurocranial modules would have enabled each module to evolve relatively independently, according to the selection pressures acting upon them, resulting in *H. rudolfensis* 'mosaic' nature (Ackermann & Cheverud, 2004).

4.2.6.1. Modularity in the strepsirhine cranium

Strepsirhine primates have previously been somewhat overlooked in terms of modularity analysis. They were, however, included in a recent study, which used Anatomical Network Analysis (AnNA) (Esteve-Altava *et al.,* 2015). AnNA uses methods from network theory to identify patterns within morphology. In this context, modules are defined based on

connectivity patterns rather than co-variation; bones within a module will have more contacts with other bones within the module than with bones outside of it (Esteve-Altava *et al.*, 2015). Following this system, strepsirhine craniums were divided into four modules: mid-facial, palatal, premaxillary and neurocranial Esteve-Altava *et al.*, 2015). In comparison to the other strepsirhine taxa studied (*Loris, Nycticebus* and *Propithecus*), which were conserved in terms of their patterns of modularity, *Lemur* was found to have a derived structure for the premaxillary and mid-facial modules (Esteve-Altava *et al.*, 2015).

4.2.7. Modularity and allometry

Allometry, the size related component of shape variation, has been shown to inflate levels of overall integration and thereby mask modularity (Goswami & Polly, 2010a; Marroig & Cheverud, 2004). However, allometric covariation can also act to increase levels of trait correlation within-modules. In saki monkeys (*Pithecia* sp.) modules were found to be differentially affected by allometry, with it playing a greater role in the integration of facial traits than neurocranial ones (Marroig & Cheverud, 2004). Data from capuchin monkeys further support the importance of allometry for integration of facial traits; it plays a canalising role in the facial modules of hard object feeding capuchins, meaning that it allowed phenotypes to remain robust despite small variations in either genotype or environmental conditions (Makedonska *et al.*, 2012). It therefore seems prudent to investigate modularity both controlling for and not controlling for allometric scaling (principal components analyses only controls for the effect of isometric size) to gain a clearer impression of its role (Goswami & Polly, 2010a).

4.2.8. Why is important to understand modularity?

A knowledge of how modularity is structured, whether it differs between taxa, how modules arise, the proximal mechanisms behind them and how they affect the rate and direction of evolution are key for understanding and interpreting the evolution of morphology. Moreover, the developmental and functional complexity of the cranium makes it arguably the best model through which to investigate the causes and consequences of integration and modularity (Makedonska, 2014).

4.2.9. Aims

To assess modularity in the strepsirhine cranium, gaining an understanding of how this is structured and how it influences the evolutionary pathways available for strepsirhine morphological evolution.

4.3. Materials and methods

4.3.1. Sample

The sample consisted of 1560 strepsirhine crania from 28 species across 15 genera and 6 families (Table 27). These species were selected on the basis that all sample sizes were N>20. Several methods of modularity analysis are used here and they are predicted to be differentially effected by sample size. The RV_M coefficient has been shown to decrease as sample size increases (Fruciano *et al.*, 2013); for intra-species analyses of this coefficient values are only compared within species not between them, for different models of modularity, thereby avoiding the problem of sample size. RV_M is also calculated at family and suborder level using species mean shapes; species mean shape was shown to be strongly affected by sample size, but this was tempered when viewed in comparison to differences between species (see Chapter 3). This, in conjunction with only using samples were N>20, should help to minimise the effect.

Moreover, previous research has used a sub-sampling approach to investigate the effect of small sample size on the estimation of landmark correlations. Estimations from sub-samples remained close to that for the observed data (N=41 for *Macaca fuscata fuscata* crania), when N was as low as 14 (Goswami & Polly, 2010a; see also Goswami, 2006b; Polly, 2005). Furthermore, matrix correlations between subsamples and the original data were higher than the mean unadjusted matrix correlation calculated for eight different *Macaca* species, even at N=10 (de Oliveira *et al.,* 2009; Goswami & Polly, 2010a). As such, between-species difference in modularity structure should be detectable even at very low sample sizes (Goswami and Polly, 2010a).

Finally, eigenvalue standard deviation has been shown to be strongly affected by sample size. To correct for this, a resampling method was employed a, so that eigenvalue standard deviation is estimated at N=20 for all species.

Table 27: Species and sample size included in analyses

Family	Genus	Species	Sample size
Cheirogaleidae	*Cheirogaleus*	*major*	25
		medius	29
	Microcebus	*murinus*	72
		rufus	29
Galagidae	*Galago*	*alleni*	24
		demidoff	59
		elegantulus	34
		moholi	73
		senegalensis	175
		zanzibaricus	25
	Otolemur	*crassicaudatus*	101
		garnettii	95
Indriidae	*Avahi*	*laniger*	23
	Indri	*Indri*	39
	Propithecus	*diadema*	28
		verreauxi	43
Lemuridae	*Eulemur*	*fulvus*	175
		macaco	55
		mongoz	57
		rubriventer	27
	Hapalemur	*griseus*	27
	Lemur	*catta*	34
	Varecia	*variegata*	39
Lepilemuridae	*Lepilemur*	*ruficaudatus*	25
Loridae	*Loris*	*tardigradus*	27
	Nycticebus	*bengalensis*	22
		coucang	69
	Perodicticus	*potto*	129

4.3.2. Analysis

4.3.2.1. Modularity hypotheses

Specimens were subjected to Generalised Procrustes Analysis (GPA; see Methods Chapter) and their resulting Procrustes scores were used in the subsequent analyses. The full landmark composition was used to test the fit of four different modularity hypotheses. These hypotheses were: (1) a two-module model dividing the face and cranial vault (including the cranial base), (here refereed to 2* model); (2) a three-module model (the Singh model)including face, cranial vault, and cranial base modules, based on Singh (2012); (3) a six-module model (the Cheverud model), including a face, orbit, oral, zygomatic, cranial vault and cranial base modules, based on Cheverud (1995) - as Cheverud's model is based on inter-landmark distances, landmarks were assigned to the modules to which the majority of their distances were associated; and (4) another six-module model based on Goswami (2006a), which also includes face, orbit, oral, zygomatic, cranial vault and cranial

base modules (the Goswami model). For simplicity, modules in different models have been given the same name, but do not necessarily include the same landmarks. The four hypotheses are outlined in Table 28. In each hypothesis, each landmark only appears in one module.

Table 18: Landmarks associated with the four module hypotheses; 2* model, Singh model, Cheverud model and Goswami model.

No.	Landmarks	2* modules	Singh 3 * modules	Cheverud 6* modules	Goswami 6* modules
1	Nasospinale, inferior-most mid-line point	face	face	face	face
2	Piriform aperture, point of greatest width	face	face	face	face
3	Piriform aperture, meeting point of nasal and pre-maxilla	face	face	face	face
4	Rhinion, anterior-most mid-line point	face	face	face	face
5	Halfway point between rhinion and nasion	face	face	face	face
6	Nasion, frontal-nasal suture, mid-line point	face	face	face	orbit
7	Frontomalare orbitale, where frontozygomatic suture meets the inner orbit	face	face	orbit	orbit
8	Frontomalare temporale, where frontozygomatic suture meets the lateral part of the zygomatic bone	face	face	vault	orbit
9	Zygomaticomaxillary superior, the anterior-superior point where the orbital rim meets the zygomaticomaxillary suture	face	face	oral	orbit
10	Zygomaticomaxillary inferior, the lateral point of the zygomatic on the zygomaticomaxillary suture	face	face	zygomatic	orbit
11	Zygomatic foramen, inferior-most point	face	face	oral	orbit
12	Infraorbital foramen, inferior-most point	face	face	oral	orbit
13	Nasolacrimal foramen, inferior-most point	face	face	orbit	orbit
14	Optic foramen, inferior-most point	face	face	orbit	orbit
15	Ventral most point on the palatine	face	face	oral	zygomatic
16	Point of maximum curvature of anterior of the zygomatic arch	face	face	zygomatic	zygomatic
17	Zygomaticotemporal suture on the lateral part of the zygomatic arch, superior-most point	face	face	zygomatic	zygomatic
18	Zygomaticotemporal suture on the lateral part of the zygomatic arch, inferior-most point	face	face	zygomatic	zygomatic
19	Junction of the sphenoid, zygomatic and parietal bones	vault	vault	zygomatic	vault
20	Junction of the zygomatic, frontal and parietal bones	vault	vault	zygomatic	vault
21	Midpoint between nasion and bregma	vault	vault	vault	vault
22	Bregma, the junction of the coronal and sagittal sutures	vault	vault	vault	vault
23	Midpoint between the bregma and lambda	vault	vault	vault	vault
24	Lambda, the junction of the sagittal and lamboid sutures	vault	vault	vault	vault
25	Junction of the crest and suture on the frontal bone	vault	vault	vault	vault

26	Asterion, junction of the temporal, parietal and occipital bones	vault	vault	vault	vault
27	External auditory meatus, posterior-most point	vault	vault	vault	base
28	External auditory meatus, anterior-most point	vault	vault	vault	base
29	External auditory meatus, superior-most point	vault	vault	vault	base
30	External auditory meatus, inferior-most point	vault	vault	vault	base
31	Lateral canine C1 septum	face	face	oral	oral
32	Lateral premolar P2 septum	face	face	oral	oral
33	Lateral premolar P3 septum	face	face	oral	oral
34	Lateral molar M1 septum	face	face	oral	oral
35	Lateral molar M2 septum	face	face	oral	oral
36	Lateral molar M3 septum	face	face	oral	oral
37	Septum at the end of dentition, mid-point	face	face	oral	oral
38	Incisive foramen, posterior-most point	face	face	oral	face
39	Mid-point between landmarks 38 and 40	face	face	oral	face
40	Junction of the maxilla and palatine, on the mid-line	face	face	oral	face
41	Greater palatine foramen, posterior-most/lateral-most point	face	face	oral	oral
42	Posterior edge of the palatine, posterior-most point	face	face	oral	face
43	Nasal spine, posterior-most point	vault	base	base	Molar
44	Junction of the presphenoid and basisphenoid, on the midline	vault	base	base	zygomatic
45	Junction of the basisphenoid and basioccipital, on the midline	vault	base	base	zygomatic
46	Petrous apex, junction of the petrous, basisphenoid and basioccipital	vault	base	base	zygomatic
47	Foramen lavelli, anterior-most/medial-most point	vault	base	base	zygomatic
48	Petrous, greatest central projection	vault	base	base	base
49	Jugular foramen, distal-most point	vault	base	base	base
50	Jugular foramen, medial-most point	vault	base	base	base
51	Mid-point between the junction of the basisphenoid and basioccipital, and the basion	vault	base	base	base
52	Basion, anterior-most point of the foramen magnum	vault	base	base	base
53	Occipital condyle, anterior-most point	vault	base	base	base
54	Occipital condyle, posterior-most point	vault	base	base	base
55	Hypoglossal canal, medial most point	vault	base	base	base
56	Opisthion, posterior-most point of foramen magnum	vault	vault	base	base
57	Inion, posterior-most point of the cranium on the mid-line	vault	vault	vault	vault
58	Point of greatest curvature in the interior of the posterior process if the temporal bone	vault	base	zygomatic	zygomatic
59	Postglenoid process, tip	vault	base	base	zygomatic
60	Mandibular fossa, deepest point	vault	base	base	zygomatic

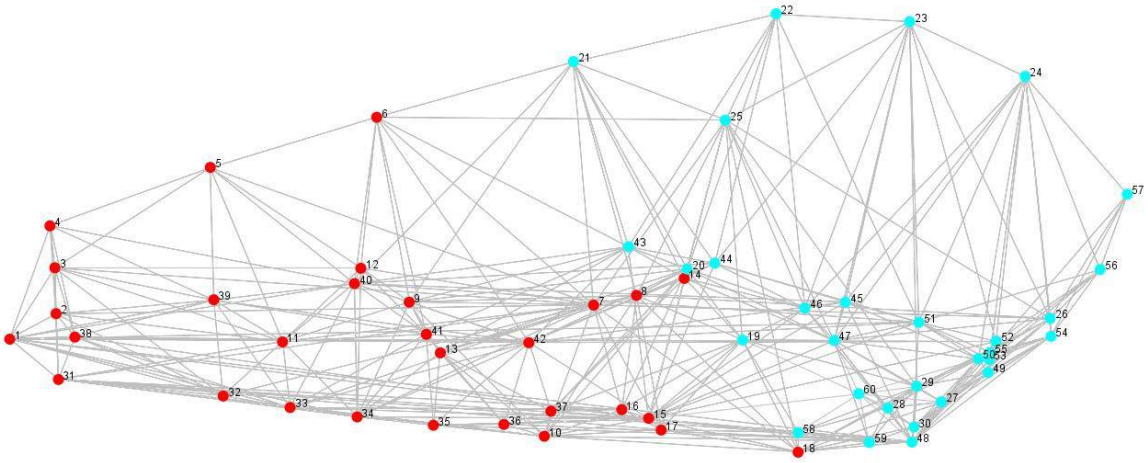

Figure 19: Modularity structure for the 2* model, as shown for *Varecia variegata*. Face module landmarks are shown in red and vault module landmarks in light blue.

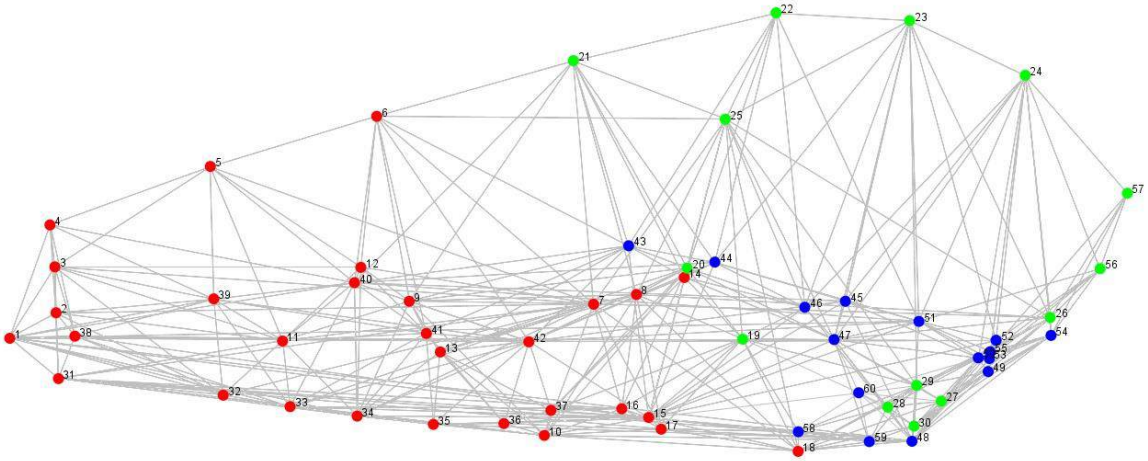

Figure 20: Modularity structure for the Singh model, as shown for *Varecia variegata*. Face module landmarks are shown in red, vault module landmarks in green and base module landmarks in dark blue.

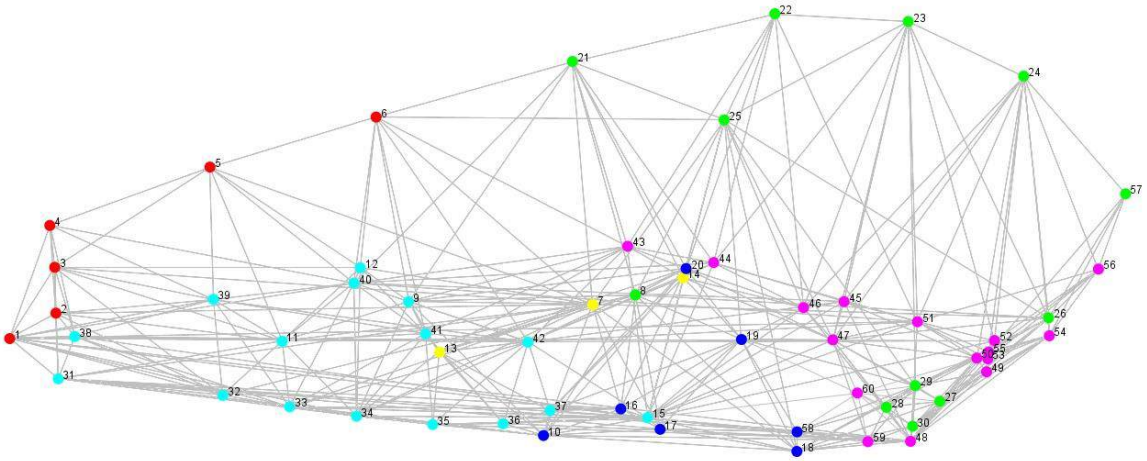

Figure 21: Modularity structure for the Cheverud model, as shown for *Varecia variegata*. Face module landmarks are shown in red, orbit module landmarks in yellow, oral module landmarks in light blue, zygomatic module landmarks in dark blue, vault module landmarks in green and base module landmarks in purple.

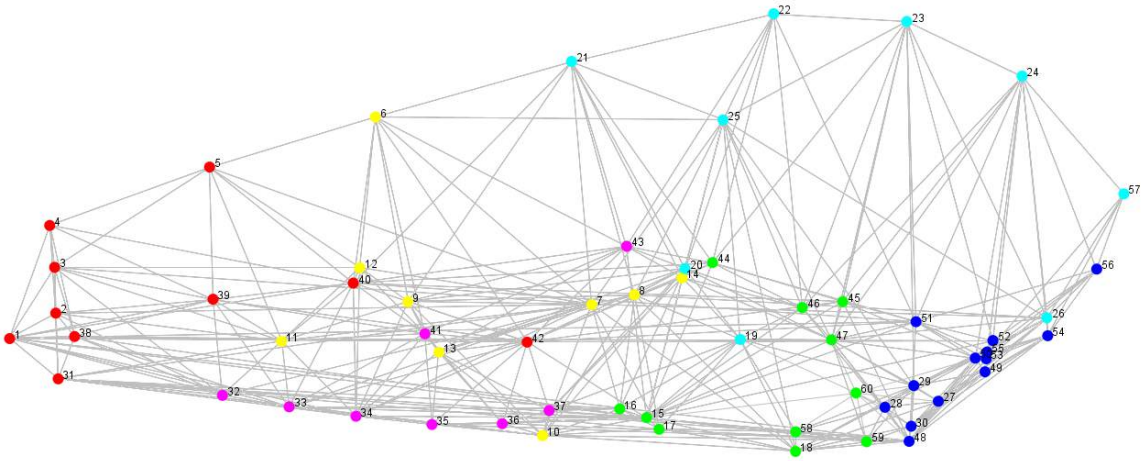

Figure 22: Modularity structure for the Goswami model, as shown for *Varecia variegata*. Face module landmarks are shown in red, orbit module landmarks in yellow, oral module landmarks in purple, zygomatic module landmarks in green, vault module landmarks in light blue and base module landmarks in dark blue.

4.3.2.2. RV_M coefficient

The validity of these models was tested using the multi-set *RV* coefficient (RV_M), which is a measure of the covariation between-modules. If the hypothesis accurately defines the pattern of modularity present in the cranium, then covariation between-modules should be low. However, if the hypothesis cuts across valid modules, covariation between the proposed subsets is predicted to be stronger, due to the integration between the true modules (Klingenberg, 2009). The *RV* coefficient ranges from 0-1, where 0 would represent a perfect fit of modularity with covariance only within and not between-modules (Goswami & Polly, 2010a). The strength of the covariation between the proposed modules is assessed by comparing it to the amount of covariation between alternative, randomly generated, modules (Klingenberg, 2009).

The *RV* coefficient is calculated as follows (Escoufier, 1973):

$$\mathbf{S} = \begin{bmatrix} \mathbf{S}_1 & \mathbf{S}_{12} \\ \mathbf{S}_{21} & \mathbf{S}_2 \end{bmatrix}$$

Where $\mathbf{S}_1$ and $\mathbf{S}_2$ are the covariance matrices within the two subsets of landmarks and $\mathbf{S}_{12}$ and $\mathbf{S}_{21}$ are the covariance matrices between the two subsets. The *RV* coefficient is therefore:

$$RV = \frac{\text{trace}\,(\mathbf{S}_{12}\mathbf{S}_{21})}{\sqrt{\text{trace}\,(\mathbf{S}_1\mathbf{S}_1)\,\text{trace}\,(\mathbf{S}_2\mathbf{S}_2)}}$$

The *RV* coefficient can be seen as roughly analogous to the squared correlation coefficient in that 'trace($\mathbf{S}_{12}$ $\mathbf{S}_{21}$)' is the sum of the squared covariances between two modules and therefore a measure of the total (squared) covariation and 'trace($\mathbf{S}_1$ $\mathbf{S}_1$)' and 'trace($\mathbf{S}_2$ $\mathbf{S}_2$)' are the sums of the squared variances and covariance's within those two modules and are therefore a measure of the (squared) variation within the modules (Klingenberg, 2009).

When a hypothesis consists of more than two modules, the multi-set *RV* coefficient (RV_M) is used; this is the average *RV* coefficient between all pairs of proposed modules, calculated as:

$$RV_M = \frac{2}{k(k\text{-}1)} \sum_{i=1}^{K\text{-}1} \sum_{j=i+1}^{K} RV(i,j)$$

Where *k* is the number of variables and '*RV*(*i,j*)'refers to the *RV* coefficient for sets *i* and *j* (Klingenberg, 2009).

In each case, the statistical significance of the covariation between the proposed modules is determined by way of permutation tests. The *RV* or RV_M for the hypothesised modules are compared to those for 10,000 randomly generated, non-spatially contiguous, alternative models with the same number of modules and the same number of landmarks within each module. Testing all possible partitions is not computationally feasible for configurations that contain more than about 20 landmarks (Klingenberg, 2009). In such cases, 10,000 random partitions is recommended; this is predicted to provide a good indication of the distribution of the RV_M coefficient. If the modularity hypothesis under scrutiny is supported, it should have a low, if not the lowest, RV_M coefficient score compared to the alternative models. The proportion of permutation tests in which the covariation score matches or exceed the original score is taken as the significance value for the test (Klingenberg, 2009).

RV_M coefficients can only be used to measure the fit of modularity hypotheses within species, RV_M coefficient scores cannot be compared between species, as it has been shown to be affected by sample size (Fruciano *et al.*, 2013).

4.3.2.3. Intra-species modularity

RV_M was calculated individually for all 28 species, for all four modularity hypotheses. These scores were also calculated using the residuals from the regression of log centroid size on to Procrustes scores, to control for allometry.

4.3.2.4. Inter-species modularity

RV_M was calculated for all 28 species together, for all four of the modularity hypotheses, and for each of the 5 family groups (Cheirogaleidae, Galagidae, Indriidae, Lemuridae and Lorisidae (as there was only one species - *Lepilemur ruficaudatus* - representing the Lepilemuridae, this family could not be included in the inter-species analyses). Each species

was represented by its species average shape. A number of different variations of this test were conducted:

a) Not controlling for either phylogeny or size.
b) Not controlling for phylogeny, but controlling for size, by using the residuals of the regression of species log centroid size onto species average shapes (Procrustes scores).
c) Controlling for phylogeny, by mapping species average shapes (Procrustes scores) onto the composite phylogenetic tree for either all 28 species, or the corresponding family tree from the 10K trees website (Arnold *et al.,* 2010), to generate independent contrasts, while not controlling for size. This was conducted first using un-weighted and then again with weighted squared-change parsimony, based on branch lengths (Maddison, 1991) (see Methods chapter).
d) Controlling for phylogeny (both un-weighted and weighted by branch length) and size.

4.3.2.5. Average within-module correlations – Intra-species

The average within-modules correlation between traits (landmarks) was calculated, for each species, for all four models of cranial modularity. Correlation matrices, of absolute values, were generated to correspond to each module, and their average correlation calculated. This was then performed again using the residuals of size regressed onto principal component scores, to control for allometric size.

4.3.2.6. Average within-module correlations – Inter-species

Species average scores for within-module correlation were subsequently used in an ANOVA to investigate whether there was a significant difference in within-module correlation scores between-modules at the inter-species level. This process was then repeated using species average within-module correlation scores that had been controlled for size.

4.3.2.7. Measuring integration using eigenvalue standard deviation

The level of integration across the cranium as a whole can be measured using the eigenvalue relative standard deviation (Cheverud *et al.,* 1989; Pavlicev *et al.*, 2009). Eigenvalues describe how much of the variation in a data set is explained by each Principal Component (PC; see Methods chapter). If there is strong integration in the cranium, then most of the landmarks would be expected to covary with each other, and the majority of

variation would be expected to be contained within the first few PCs. If this is the case eigenvalue variance, and, therefore, standard deviation will be high. However, if the cranium is organised into modules, then the variance should be more evenly distributed among the eigenvalues, resulting in lower variance and therefore, standard deviation (Goswami & Polly, 2010a).

Eigenvalues were calculated separately for each species, using the correlation matrix of their Procrustes scores. Correlation matrices were favoured over covariation matrices as they are scaled to equal variance, with the correlation coefficient ranging from 0-1. They therefore contain only information about the strength and pattern of the relationships between traits, which are the elements under investigation, and not information about the magnitude of the variances (Goswami & Polly, 2010a; Pavlicev *et al.*, 2009).

The relative standard deviation of eigenvalues is calculated as:

$$SD_{rel}(\lambda) = \frac{\sqrt{Var(\lambda)}}{\sqrt{N-1}} = r$$

Where N is the number of traits (landmarks).

Eigenvalue distribution can be significantly affected by sample size, especially when overall integration is low (Haber, 2011; Pavlicev *et al.*, 2009); sample sizes were therefore standardised to N=20 for each species. To do this 1000 subsamples of N=20 were randomly generated (without replacement) for each species; the eigenvalue standard deviation was calculated for each subsample and the average of all 1000 taken as the value for that species. Eigenvalue relative standard deviation was also calculated using the residuals of log centroid size regressed against Procrustes scores, to control for the effects of allometry.

In addition, the eigenvalue relative standard deviation score was used as the phylogenetic tip value for the corresponding species, and the level of integration was then mapped back across the phylogenetic tree, using the composite phylogeny from 10K trees (Arnold *et al.*, 2010). Estimates of the rate of evolution of integration are calculated using Independent Evolution (IE), following an Adaptive Peak (AP) model (See Methods Chapter). This approach allows for the independent estimation of rates on individual branches (Smaers *et*

al., 2012). Rates can be interpreted as the proportional amount of change along that particular branch length. Positive rates of change are inferred for an increase in a trait; i.e., an increase in integrations and therefore a decrease in modularity. Negative rates of change are inferred as a decrease in a trait; i.e., a decrease in integration and therefore an increase in modularity (Smaers *et al.*, 2012).

4.4. Results

4.4.1. RV_M coefficients – Intra-species modularity

In general, the 2* and Singh models result in higher RV_M coefficient scores than the Cheverud and Goswami models, suggesting that there is more covariation between-modules in the two- and three- module models than in the six-module models (Table 29). However, this is not necessarily the case, as different numbers of parameters are involved in the calculations. Permutations tests are therefore used to test the support for each model instead; for all 1000 permutations, the number of modules generated is equal to the number in the model being tested (Table 29) (Goswami & Polly, 2010a). The most strongly supported models were the 2* model and the Goswami model (Table 29). The 2* model was the most strongly supported in 10 of the taxa (9 when allometry was controlled for) and the Goswami model was the most strongly supported in 14 of the taxa (13 when allometry was controlled for). In comparison, the Singh model and the Cheverud model were the most strongly supported models in only 3 (4 when controlled for size) and 4 (3 when controlled for size) of the taxa, respectively. *Galago* sp. were found to consistently support the Goswami model, while *Eulemur* sp. tend to *s*upport the Singh model, however, no family level patterns were found. In general, controlling for the allometric effects of size decreases the strength of support shown for each model, but this is not a clade-wide pattern.

Table 29: Intra-species modularity scores for each of the four modularity models. Scores shaded in grey are controlled for size, underlined scores denotes *p*<0.05, *denotes most strongly significant *p* value for each species in each condition.

Genus	Species	2* modules		Singh 3 x modules		Cheverud 6* modules		Goswami 6* modules	
		RV_M	*p* value	RV_M	*p* value	RV_M	*p* value	RV_M	*p* value
Cheirogaleus	*major*	0.6442	0.0100	0.5489	0.0287	0.3787	0.0169	0.4160	0.0035*
		0.6377	0.0055*	0.5398	0.0107	0.3496	0.0266	0.4198	0.0098
Cheirogaleus	*medius*	0.6357	0.1325	0.5119	0.0325*	0.3526	0.0560	0.3956	0.1171
		0.6269	0.0777	0.5130	0.0647	0.3345	0.012*	0.3137	0.012*
Microcebus	*murinus*	0.4561	0.0000*	0.3756	0.0006	0.2367	0.0007	0.2646	0.0000*
		0.4344	0.0000*	0.3481	0.0001	0.2332	0.0100	0.2536	0.0033
Microcebus	*rufus*	0.5681	0.0000*	0.5482	0.0054	0.3756	0.0003	0.4009	0.0000*
		0.5934	0.0003	0.5383	0.0142	0.3737	0.0137	0.3906	0.0000*
Galago	*alleni*	0.6135	0.0063	0.5704	0.0789	0.3661	0.0006	0.3880	0.0000*
		0.5938	0.0083	0.5465	0.0920	0.3567	0.0017*	0.3567	0.0017*
Galago	*demidoff*	0.5382	0.0000*	0.4660	0.0107	0.2564	0.0000*	0.3173	0.0000*
		0.5259	0.0061	0.4192	0.0092	0.2446	0.0003	0.2824	0.0001*
Galago	*elegantulus*	0.5418	0.539	0.4919	0.8411	0.2970	0.1443	0.3536	0.6628
		0.5562	0.5596	0.4968	0.851	0.3033	0.24419	0.3537	0.6067
Galago	*moholi*	0.5037	0.0008	0.4441	0.0243	0.2788	0.0060	0.2989	0.0003*
		0.4516	0.0001	0.3633	0.0005	0.2423	0.0129	0.2553	0.0000*
Galago	*senegalensis*	0.3956	0.0028	0.3190	0.037	0.1734	0.0008	0.1858	0.0000*
		0.3456	0.0000*	0.2822	0.0163	0.1513	0.0004	0.1623	0.0000*
Galago	*zanzibaricus*	0.5997	0.0083	0.5386	0.1027	0.3892	0.0704	0.3847	0.0001*
		0.6029	0.0107	0.5393	0.1128	0.3959	0.1085	0.3941	0.0002*

Otolemur	*crassicaudatus*	0.3974	0.0032*	0.3616	0.1102	0.2777	0.3390	0.2607	0.0064
		0.3488	0.0017*	0.3191	0.0846	0.2497	0.4117	0.2298	0.0071
Otolemur	*garnettii*	0.3679	0.0000*	0.3454	0.0334	0.2356	0.0067	0.2499	0.0000*
		0.3141	0.0000*	0.2977	0.092	0.1815	0.0014	0.1946	0.0000
Avahi	*laniger*	0.6334	0.1528	0.5418	0.1668	0.3204	0.0000*	0.4066	0.0740
		0.6262	0.1282	0.5407	0.1598	0.3208	0.0000*	0.4061	0.0645
Indri	*Indri*	0.5285	0.0000*	0.4617	0.008	0.3013	0.0007	0.3433	0.0035
		0.5265	0.0000*	0.4599	0.0124	0.2992	0.0012	0.3455	0.0080
Propithecus	*diadema*	0.5244	0.0000*	0.4794	0.0005	0.3368	0.0002	0.3828	0.0011
		0.5249	0.0001*	0.4771	0.0001	0.3352	0.0008	0.3793	0.0017
Propithecus	*verreauxi*	0.5277	0.0031	0.4654	0.0849	0.3084	0.0381	0.3257	0.0030*
		0.5290	0.0137	0.4676	0.1735	0.3045	0.0712	0.3171	0.0037*
Eulemur	*fulvus*	0.2814	0.0008	0.2144	0.0000*	0.1437	0.0001	0.1858	0.0128
		0.2768	0.0007	0.2035	0.0001*	0.1389	0.0003	0.1794	0.0334
Eulemur	*macaco*	0.4095	0.0308	0.3065	0.004*	0.2171	0.0105	0.2668	0.2294
		0.4118	0.0197	0.3048	0.0018*	0.2221	0.014	0.2679	0.2015
Eulemur	*mongoz*	0.5201	0.0001*	0.4167	0.0005	0.3199	0.0466	0.3558	0.0506
		0.4535	0.0001	0.3562	0.0000*	0.2688	0.0283	0.3053	0.0934
Eulemur	*rubriventer*	0.4771	0.0727	0.4411	0.0916	0.3414	0.0402*	0.4045	0.4423
		0.4778	0.0147	0.4254	0.0145*	0.3365	0.0313	0.3519	0.3409
Hapalemur	*griseus*	0.6460	0.1058	0.5791	0.2048	0.4316	0.2992	0.4278	0.0028*
		0.5945	0.1784	0.4981	0.0932	0.4610	0.3206	0.3816	0.0190*
Lemur	*catta*	0.6146	0.0308	0.5092	0.0104	0.3691	0.0316	0.3988	0.0031*
		0.6504	0.1332	0.5105	0.0129	0.3731	0.0681	0.3979	0.0099*

Varecia	*variegata*	0.5800	0.1704	0.4801	0.1731	0.3680	0.4352	0.3777	0.2400
		0.5429	0.2025	0.4323	0.0958	0.3394	0.5106	0.3622	0.5172
Lepilemur	*ruficaudatus*	0.7232	0.0806	0.6115	0.0391	0.4499	0.1101	0.4503	0.0002*
		0.7145	0.3561	0.5955	0.1863	0.4139	0.1189	0.4451	0.0366*
Loris	*tardigradus*	0.7353	0.0605	0.7035	0.6619	0.4385	0.0131*	0.5095	0.0279
		0.6683	0.0362	0.6092	0.4139	0.3840	0.0090*	0.4619	0.1673
Nycticebus	*bengalensis*	0.5670	0.0426*	0.5047	0.2505	0.3648	0.4646	0.3859	0.3654
		0.5859	0.0643	0.5476	0.6164	0.3784	0.4859	0.4030	0.4489
Nycticebus	*coucang*	0.3723	0.0000*	0.3400	0.0246	0.2124	0.0055	0.2294	0.0009
		0.3614	0.0000*	0.3242	0.0083	0.2090	0.0074	0.2295	0.0024
Perodicticus	*potto*	0.3804	0.0000*	0.3416	0.0152	0.2025	0.0026	0.1894	0.0000*
		0.3455	0.0001	0.3042	0.0118	0.1864	0.0041	0.1748	0.0000*

4.4.2. RV_M coefficients – Inter-species modularity

Inter-species RV_M coefficient results mirrored those of the intra-species analysis, in that the 2* model and the Goswami model were the most strongly supported of the four models tested, regardless of the specific conditions of the analyses (i.e., whether or not allometric size and phylogenetic relationships where controlled for). Controlling for size had minimum effect on the results, in that they remained highly significant in both conditions. Controlling for phylogenetic relationships led to higher significance values for modularity, both using weighted and un-weighted branch lengths (Table 30).

Table 30: Inter-species modularity scores for each of the four modularity models. Scores shaded in grey are controlled for size, underlined scores denotes *p*<0.05, *denotes most strongly significant *p* value for each condition.

All species	2* modules		Singh 3 x modules		Cheverud 6* modules		Goswami 6* modules	
	RV_M	*p* value	RV_M	*p* value	RV_M	*p* value	RV_M	*p* value
Not phylogenetically corrected, not size corrected	0.7522	0.0010	0.7156	0.0049	0.5620	0.0011	0.5472	0.0000*
Not phylogenetically corrected, size corrected	0.6094	0.0000*	0.5952	0.0001	0.4840	0.0177	0.4238	0.0000*
Phylogenetically corrected, not weighted, not size corrected	0.6829	0.0000*	0.7281	0.0000*	0.5786	0.0001	0.5689	0.0000*
Phylogenetically corrected, not weighted, size corrected	0.6499	0.0000*	0.6459	0.0002	0.5697	0.0080	0.5167	0.0000*
Phylogenetically corrected, weighted by branch length, not size corrected	0.6256	0.0000*	0.6775	0.0001	0.5537	0.0002	0.5306	0.0000*
Phylogenetically corrected, weighted by branch length, size corrected	0.5724	0.0000*	0.5846	0.0000*	0.5158	0.0002	0.4771	0.0000*

At the family level, the Goswami model was repeatedly the most strongly supported (Table 31-35). Correcting for allometric scaling resulted in only minor differences in the recovered patterns of modularity and there appears to be no overall or family level pattern. Controlling for the phylogenetic relationships within a family (whether weighted or un-weighted) does tend to reduce the strength or the significance of the modularity, but again the impact on the results is minimal (Table 31-35). The only real exception to this pattern was for the Lemuridae, where, although the Goswami module was still the most strongly supported of the four models tested, overall the family were shown to have lower levels of modularity than the other strepsirhine groups, and modularity did not reach significant levels at all once both allometric size and genetic relationships were controlled for (Table 34).

Table 31: Inter-species modularity scores, for the Cheirogalidae, for each of the four modularity models. Scores shaded in grey are controlled for size, underlined scores denotes *p*<0.05, *denotes most strongly significant *p* value for each condition.

Cheirogalidae	2* modules		Singh 3 x modules		Cheverud 6* modules		Goswami 6* modules	
	RV_M	p value	RV_M	p value	RV_M	p value	RV_M	p value
Not phylogenetically corrected, not size corrected	0.7691	0.0000*	0.7821	0.0326	0.5568	0.0123	0.5802	0.0000*
Not phylogenetically corrected, size corrected	0.5172	0.0001*	0.4614	0.0561	0.2930	0.0585	0.2963	0.0001*
Phylogenetically corrected, not size corrected, not weighted by branch length	0.8813	0.0063	0.8944	0.0373	0.8351	0.0735	0.8168	0.0005*
Phylogenetically corrected, not size corrected, weighted by branch length	0.8505	0.0016	0.8703	0.0221	0.8236	0.0796	0.7980	0.0004*
Phylogenetically corrected, size corrected, not weighted by branch length	0.9520	0.0302	0.9661	0.1660	0.9477	0.4760	0.8916	0.0001*
Phylogenetically corrected, size corrected, weighted by branch length	0.9291	0.0307	0.9490	0.1620	0.9367	0.4937	0.8735	0.0021*

Table 32: Inter-species modularity scores, for the Galagidae, for each of the four modularity models. Scores shaded in grey are controlled for size, underlined scores denotes *p*<0.05, *denotes most strongly significant *p* value for each condition.

Galagidae	2* modules		Singh 3 x modules		Cheverud 6* modules		Goswami 6* modules	
	RV_M	*p* value	RV_M	*p* value	RV_M	*p* value	RV_M	*p* value
Not phylogenetically corrected, not size corrected	0.8403	0.0000*	0.8422	0.0314	0.6436	0.0227	0.6804	0.0000*
Not phylogenetically corrected, size corrected	0.5131	0.0002	0.4536	0.0706	0.2697	0.0078	0.2861	0.0000*
Phylogenetically corrected, not size corrected, not weighted by branch length	0.7725	0.0001	0.8131	0.0025	0.6528	0.0000*	0.7392	0.0000*
Phylogenetically corrected, not size corrected, weighted by branch length	0.7962	0.0000*	0.8187	0.0030	0.6510	0.0001	0.7461	0.0004
Phylogenetically corrected, size corrected, not weighted by branch length	0.8334	0.0248	0.8276	0.0576	0.6905	0.0046	0.7132	0.0003*
Phylogenetically corrected, size corrected, weighted by branch length	0.8941	0.0954	0.8707	0.2165	0.6860	0.0010*	0.7543	0.0033

Table 33: Inter-species modularity scores, for the Indriidae, for each of the four modularity models. Scores shaded in grey are controlled for size, underlined scores denotes *p*<0.05, *denotes most strongly significant *p* value for each condition.

Indriidae	2* modules		Singh 3 x modules		Cheverud 6* modules		Goswami 6* modules	
	RV_M	*p* value	RV_M	*p* value	RV_M	*p* value	RV_M	*p* value
Not phylogenetically corrected, not size corrected	0.7614	0.0005	0.7112	0.0192	0.5327	0.0397	0.5396	0.0000*
Not phylogenetically corrected, size corrected	0.6723	0.0015	0.5804	0.0071	0.3922	0.0065	0.4492	0.0010*
Phylogenetically corrected, not size corrected, not weighted by branch length	0.9499	0.0390	0.9491	0.1304	0.8991	0.1987	0.8225	0.0000*
Phylogenetically corrected, not size corrected, weighted by branch length	0.9363	0.0722	0.9349	0.2295	0.8481	0.1222	0.8022	0.0001*
Phylogenetically corrected, size corrected, not weighted by branch length	0.9991	0.1491	0.9999	0.4233	1.0000	0.9436	0.9996	0.0141*
Phylogenetically corrected, size corrected, weighted by branch length	0.9999	0.1561	0.9999	0.2033	0.9999	0.7749	1.0000	0.0073*

Table 34: Inter-species modularity scores, for the Lemuridae, for each of the four modularity models. Scores shaded in grey are controlled for size, underlined scores denotes *p*<0.05, *denotes most strongly significant *p* value for each condition.

Lemuridae	2* modules		Singh 3 x modules		Cheverud 6* modules		Goswami 6* modules	
	RV_M	*p* value	RV_M	*p* value	RV_M	*p* value	RV_M	*p* value
Not phylogenetically corrected, not size corrected	0.6297	0.0000*	0.5179	0.0020	0.4384	0.2326	0.4145	0.0001
Not phylogenetically corrected, size corrected	0.3607	0.0008	0.2581	0.0000*	0.1932	0.0278	0.2149	0.0244
Phylogenetically corrected, not size corrected, not weighted by branch length	0.9709	0.0632	0.9590	0.0542	0.9383	0.2950	0.9067	0.0012*
Phylogenetically corrected, not size corrected, weighted by branch length	0.9538	0.0312	0.9211	0.0120	0.9026	0.2909	0.8480	0.0003*
Phylogenetically corrected, size corrected, not weighted by branch length	0.9703	0.5372	0.9233	0.2782	0.8894	0.6016	0.9203	0.8399
Phylogenetically corrected, size corrected, weighted by branch length	0.9768	0.7052	0.9310	0.2732	0.9081	0.7280	0.9056	0.5505

Table 35: Inter-species modularity scores, for the Lorisidae, for each of the four modularity models. Scores shaded in grey are controlled for size, underlined scores denotes *p*<0.05, *denotes most strongly significant *p* value for each condition.

Lorisidae	2* modules		Singh 3 x modules		Cheverud 6* modules		Goswami 6* modules	
	RV_M	*p* value	RV_M	*p* value	RV_M	*p* value	RV_M	*p* value
Not phylogenetically corrected, not size corrected	0.7478	0.0002	0.7435	0.1170	0.5638	0.1440	0.4921	0.0000*
Not phylogenetically corrected, size corrected	0.6654	0.0008	0.6283	0.0983	0.4248	0.0763	0.3804	0.0000*
Phylogenetically corrected, not size corrected, not weighted by branch length	0.9075	0.0002	0.9335	0.0095	0.9339	0.2572	0.8930	0.0001*
Phylogenetically corrected, not size corrected, weighted by branch length	0.9433	0.0011*	0.9571	0.0345	0.9135	0.1016	0.9267	0.0112
Phylogenetically corrected, size corrected, not weighted by branch length	0.9999	0.8960	0.9999	0.2727	0.9998	0.4201	0.9996	0.0220*
Phylogenetically corrected, size corrected, weighted by branch length	0.9924	0.1271	0.9898	0.1416	0.9793	0.1373	0.9794	0.0239*

4.4.3. Average within module correlations – Intra-species

For the 2* model, traits within the face and vault showed little difference and no consistent across species pattern with regard to the strength of their within-module correlations. Results for the Singh model show the vault to be the most highly correlated module, even after the effects of size have been controlled for (Table 36).

For the Cheverud model, the face was consistently found to be the most highly correlated module, with the only clear exceptions being *Microcebus rufus*, *Galago alleni* and G. *moholi.* The traits within the vault and the zygomatic modules are also relatively strongly correlated (Table37).

For the Goswami model, the oral module was overwhelmingly the most strongly correlated. The few exceptions to this pattern include *Hapalemur griseus* and *Lepilemur ruficaudatus,* for which the face was the most strongly integrated module; *Galago zanzibaricus*, for which the vault was the most strongly integrated module; and *Galago alleni,* for which the base was the most strongly integrated module. In general, the orbit and zygomatic modules had lower within-module integration than the other four modules.

All species showed stronger overall within-module correlation for the Goswami model, rather than the Cheverud model (Table37).

The effect of size varies between both species and modules. The vault and the base modules, from Cheverud and Goswami models, both show a decrease in the average within- module correlation when allometric size is controlled for. This is the case for nearly all of the species, with only limited exceptions. In contrast, the orbit modules, of the two six-module models, tend to increase in correlation when size is controlled for, although this is a weaker pattern than is seen for the vault and base. The face module shows no specific overarching or family level pattern, and of all the modules it is the least affected by size (Table 37).

The effect of size on the oral module differs between models. For the Goswami model, the relationship with size is family specific; while controlling for size decreases the average within-module correlation for the Cheirogaleidae, Lemuridae and Galagidae, it increases it for the Lorisidae and the Indriidae. For the Cheverud model, however, the oral module has no particular relationship with size (Table 37).

Table 36: Average within-module correlation for each species, for the 2* and Singh modularity models, number of landmarks within each module are shown in brackets. Shaded rows indicate that allometry has been controlled for.

Species		2*		Singh		
		face (30)	vault (30)	face (30)	vault (14)	base (16)
Cheirogaleus	*major*	0.190	0.202	0.190	0.218	0.203
		0.194	0.200	0.194	0.210	0.205
Cheirogaleus	*medius*	0.182	0.176	0.183	0.195	0.184
		0.179	0.180	0.178	0.193	0.185
Microcebus	*murinus*	0.140	0.140	0.140	0.150	0.147
		0.139	0.128	0.139	0.135	0.139
Microcebus	*rufus*	0.194	0.202	0.194	0.214	0.206
		0.192	0.184	0.192	0.198	0.192
Galago	*alleni*	0.202	0.231	0.202	0.268	0.215
		0.204	0.218	0.204	0.246	0.210
Galago	*demidoff*	0.156	0.157	0.156	0.184	0.149
		0.152	0.136	0.152	0.160	0.130
Euoticus	*elegantulus*	0.168	0.179	0.168	0.191	0.185
		0.170	0.179	0.170	0.193	0.178
Galago	*moholi*	0.150	0.150	0.150	0.168	0.149
		0.144	0.129	0.144	0.149	0.130
Galago	*senegalensis*	0.112	0.114	0.112	0.128	0.113
		0.105	0.112	0.105	0.125	0.110
Galago	*zanzibaricus*	0.201	0.203	0.201	0.220	0.206
		0.204	0.205	0.204	0.220	0.213
Otolemur	*crassicaudatus*	0.152	0.143	0.152	0.170	0.143
		0.151	0.129	0.151	0.149	0.136
Otolemur	*garnettii*	0.147	0.139	0.147	0.151	0.142
		0.135	0.129	0.135	0.143	0.134
Avahi	*laniger*	0.208	0.203	0.203	0.207	0.208
		0.207	0.204	0.207	0.208	0.208
Indri	*Indri*	0.182	0.174	0.182	0.183	0.179
		0.184	0.174	0.184	0.182	0.181

Propithecus	*diadema*	0.198	0.201	0.198	0.232	0.204
		0.197	0.201	0.197	0.237	0.200
Propithecus	*verreauxi*	0.176	0.163	0.176	0.182	0.159
		0.171	0.161	0.172	0.176	0.160
Eulemur	*fulvus*	0.210	0.137	0.120	0.153	0.142
		0.119	0.126	0.119	0.141	0.137
Eulemur	*macaco*	0.150	0.153	0.150	0.174	0.155
		0.150	0.154	0.150	0.176	0.158
Eulemur	*mongoz*	0.189	0.163	0.189	0.171	0.180
		0.174	0.151	0.174	0.159	0.167
Eulemur	*rubriventer*	0.189	0.202	0.190	0.225	0.202
		0.188	0.203	0.188	0.228	0.202
Hapalemur	*griseus*	0.213	0.198	0.213	0.219	0.188
		0.213	0.177	0.213	0.187	0.183
Lemur	*catta*	0.199	0.189	0.199	0.218	0.188
		0.195	0.188	0.195	0.220	0.187
Varecia	*variegata*	0.189	0.193	0.189	0.194	0.216
		0.178	0.181	0.178	0.184	0.212
Lepilemur	*ruficaudatus*	0.200	0.204	0.200	0.216	0.195
		0.192	0.196	0.192	0.206	0.188
Loris	*tardigradus*	0.230	0.233	0.230	0.257	0.222
		0.235	0.206	0.235	0.230	0.201
Nycticebus	*bengalensis*	0.196	0.195	0.196	0.210	0.205
		0.201	0.201	0.201	0.214	0.205
Nycticebus	*coucang*	0.139	0.146	0.139	0.169	0.143
		0.141	0.145	0.141	0.170	0.141
Perodicticus	*potto*	0.126	0.145	0.126	0.174	0.134
		0.125	0.134	0.125	0.162	0.129

Table 37: Average within-module correlation for each species, for the Cheverud and Goswami modularity models, number of landmarks within each module are shown in brackets. Shaded rows indicate that allometry has been controlled for.

Species	Cheverud						Goswami					
	face (6)	orbit (3)	oral (16)	zygo (7)	vault (12)	base (16)	face (10)	orbit (9)	oral (8)	zygo (11)	vault (9)	base (13)
C. major	0.231	0.212	0.200	0.221	0.220	0.206	0.202	0.188	0.257	0.204	0.235	0.205
	0.240	0.217	0.203	0.222	0.216	0.208	0.208	0.191	0.257	0.211	0.211	0.203
C. medius	0.241	0.183	0.194	0.197	0.192	0.187	0.199	0.177	0.273	0.188	0.205	0.193
	0.250	0.176	0.188	0.202	0.193	0.190	0.202	0.180	0.243	0.191	0.201	0.191
M. murinus	0.184	0.140	0.166	0.150	0.157	0.149	0.157	0.142	0.248	0.139	0.176	0.148
	0.186	0.140	0.158	0.149	0.142	0.140	0.156	0.142	0.220	0.130	0.159	0.140
M. rufus	0.203	0.215	0.203	0.211	0.214	0.216	0.209	0.189	0.245	0.201	0.230	0.212
	0.187	0.222	0.200	0.202	0.195	0.202	0.199	0.193	0.230	0.185	0.220	0.207
G. alleni	0.267	0.199	0.207	0.222	0.278	0.217	0.226	0.211	0.274	0.204	0.256	0.283
	0.256	0.214	0.210	0.220	0.257	0.211	0.217	0.213	0.271	0.196	0.225	0.279
G. demidoff	0.227	0.161	0.180	0.171	0.204	0.148	0.169	0.155	0.258	0.158	0.195	0.186
	0.227	0.165	0.169	0.172	0.174	0.128	0.167	0.156	0.231	0.156	0.166	0.166
E. elegantulus	0.214	0.195	0.166	0.214	0.194	0.190	0.178	0.187	0.204	0.178	0.206	0.201
	0.217	0.193	0.169	0.215	0.195	0.184	0.175	0.186	0.207	0.179	0.206	0.203
G. moholi	0.172	0.127	0.157	0.200	0.181	0.147	0.138	0.149	0.212	0.170	0.197	0.157
	0.173	0.128	0.148	0.191	0.161	0.132	0.134	0.150	0.195	0.152	0.161	0.147
G. senegalensis	0.163	0.116	0.122	0.164	0.138	0.115	0.122	0.131	0.178	0.126	0.143	0.137
	0.164	0.125	0.110	0.161	0.134	0.113	0.121	0.124	0.159	0.121	0.142	0.136
G. zanzibaricus	0.255	0.185	0.196	0.253	0.226	0.201	0.213	0.219	0.220	0.226	0.234	0.205
	0.255	0.191	0.199	0.248	0.227	0.207	0.218	0.218	0.221	0.225	0.236	0.209
O. crassicaudatus	0.221	0.166	0.145	0.187	0.177	0.144	0.170	0.151	0.213	0.156	0.179	0.151
	0.226	0.183	0.140	0.193	0.160	0.133	0.170	0.152	0.203	0.149	0.159	0.142
O. garnettii	0.224	0.150	0.149	0.170	0.160	0.144	0.170	0.142	0.241	0.155	0.168	0.149
	0.225	0.139	0.138	0.148	0.152	0.135	0.172	0.130	0.222	0.146	0.163	0.139
A. laniger	0.282	0.222	0.223	0.230	0.223	0.212	0.206	0.227	0.264	0.194	0.213	0.221
	0.285	0.223	0.230	0.237	0.221	0.212	0.208	0.231	0.270	0.194	0.210	0.225

I. Indri	0.248	0.176	0.204	0.192	0.187	0.179	0.226	0.184	0.257	0.164	0.192	0.182
	0.249	0.182	0.205	0.191	0.184	0.180	0.224	0.181	0.264	0.166	0.188	0.183
P. diadema	0.288	0.218	0.206	0.214	0.238	0.203	0.238	0.195	0.262	0.186	0.260	0.206
	0.289	0.228	0.200	0.223	0.243	0.200	0.241	0.199	0.233	0.194	0.266	0.200
P. verreauxi	0.274	0.183	0.182	0.181	0.177	0.163	0.217	0.190	0.213	0.154	0.206	0.174
	0.254	0.166	0.181	0.182	0.170	0.163	0.214	0.182	0.221	0.156	0.199	0.174
E. fulvus	0.212	0.115	0.132	0.142	0.160	0.147	0.167	0.117	0.206	0.128	0.175	0.150
	0.213	0.116	0.126	0.143	0.151	0.139	0.165	0.117	0.200	0.125	0.163	0.142
E. macaco	0.250	0.166	0.162	0.171	0.184	0.158	0.204	0.149	0.218	0.143	0.194	0.167
	0.251	0.172	0.159	0.172	0.185	0.159	0.206	0.155	0.199	0.146	0.197	0.170
E. mongoz	0.304	0.233	0.182	0.195	0.183	0.176	0.227	0.183	0.247	0.184	0.181	0.176
	0.299	0.240	0.168	0.181	0.173	0.165	0.217	0.176	0.227	0.165	0.163	0.170
E. rubriventer	0.269	0.207	0.199	0.232	0.225	0.204	0.215	0.193	0.267	0.202	0.238	0.207
	0.276	0.184	0.200	0.227	0.225	0.203	0.217	0.187	0.279	0.200	0.241	0.211
H. griseus	0.303	0.171	0.216	0.204	0.227	0.190	0.264	0.203	0.259	0.191	0.241	0.213
	0.308	0.202	0.211	0.195	0.196	0.181	0.274	0.212	0.241	0.185	0.185	0.201
L. catta	0.330	0.141	0.194	0.206	0.236	0.193	0.243	0.185	0.244	0.187	0.214	0.219
	0.338	0.123	0.190	0.203	0.239	0.190	0.247	0.174	0.240	0.187	0.216	0.220
V. variegata	0.262	0.178	0.201	0.203	0.197	0.220	0.239	0.174	0.244	0.193	0.211	0.210
	0.270	0.199	0.187	0.189	0.192	0.212	0.223	0.178	0.231	0.193	0.204	0.192
L. ruficaudatus	0.300	0.213	0.189	0.215	0.223	0.203	0.275	0.215	0.213	0.182	0.254	0.213
	0.257	0.221	0.188	0.208	0.215	0.195	0.239	0.201	0.218	0.181	0.228	0.213
L. tardigradus	0.275	0.202	0.242	0.247	0.265	0.219	0.247	0.212	0.288	0.221	0.249	0.260
	0.278	0.218	0.257	0.241	0.240	0.197	0.250	0.219	0.306	0.200	0.226	0.219
N. bengalensis	0.266	0.222	0.193	0.216	0.215	0.206	0.225	0.195	0.231	0.217	0.230	0.204
	0.273	0.231	0.200	0.213	0.221	0.208	0.238	0.200	0.235	0.221	0.236	0.208
N. coucang	0.197	0.167	0.156	0.150	0.177	0.145	0.161	0.141	0.225	0.137	0.171	0.185
	0.195	0.171	0.157	0.151	0.179	0.145	0.160	0.143	0.230	0.137	0.170	0.180
P. potto	0.256	0.148	0.131	0.160	0.195	0.136	0.176	0.136	0.176	0.155	0.185	0.176
	0.255	0.148	0.130	0.153	0.181	0.132	0.176	0.133	0.178	0.143	0.166	0.175

4.4.4. Average within module correlation— Inter-species

Using species average scores, at an inter-species level, the strength of within-module correlation was found to be significantly different between-modules (not controlling for size, $F(16,459)=12.77$, $p=0.000$; controlling for size, $F(16,459)=11.49$, $p=0.000$). Both the Cheverud face module and the Goswami oral module were again found to have relatively strong within-module correlations. For the Goswami oral module, this strength was diminished once size had been controlled for. However, overall, controlling for the allometric influence of size made little difference to the results (Figure 23, 24).

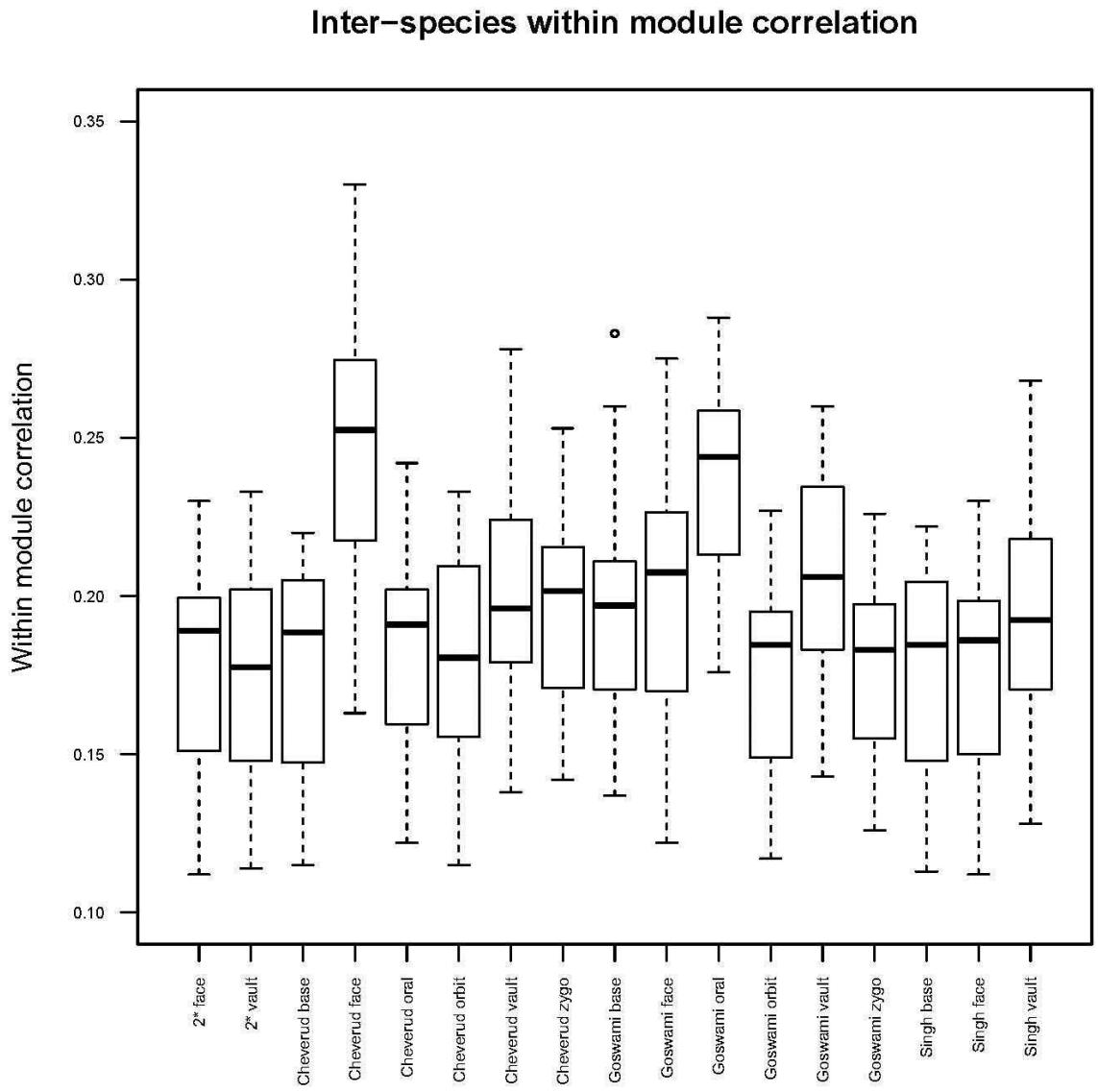

Figure 23: Within-module correlation scores, for each module at an inter-species level, using species average scores.

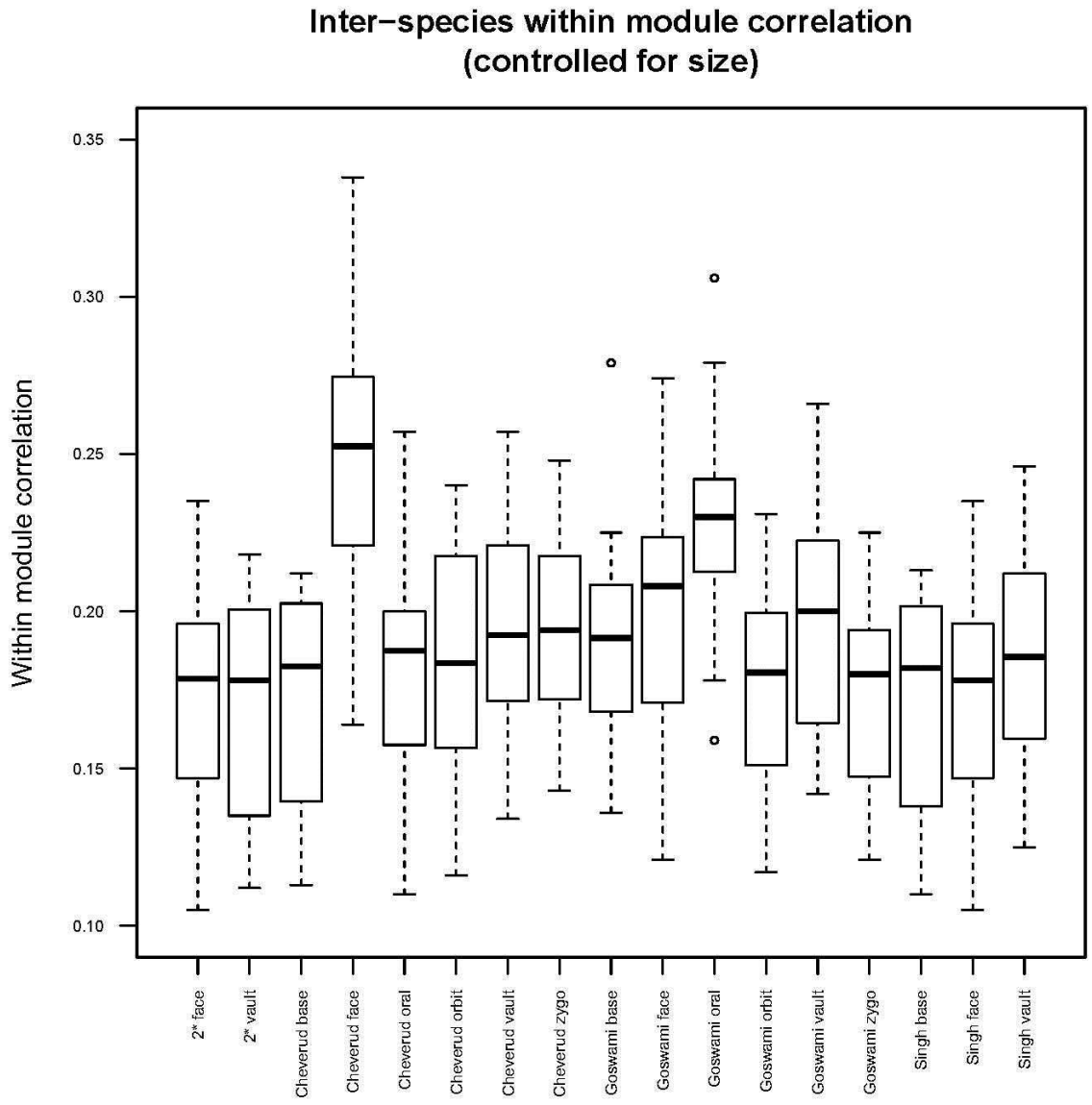

Figure 24: Within-module correlation scores, for each module at an inter-species level, using species average scores controlled for size.

4.4.5. Eigenvalue standard deviation – Intra-species modularity

To remove the effect of sample size on eigenvalue relative standard deviation, samples were standardised for N=20, by generating 1000 sub-samples of N=20 for each species and calculating the eigenvalue relative standard deviation of each of the sub-samples and taking the average. Figure 25 shows the mean values and variance of the average eigenvalue relative standard deviations of each of the 1000 sub-samples generated for each species, and demonstrates that by using this method, eigenvalue relative standard deviation is no longer correlated with sample size (see Table 27 for species sample size). In Figure 26, eigenvalue standard deviation is based on the residuals of log centroid size onto

Procrustes scores, to control for the effects of allometry. The results follow the same pattern, but find slightly less variation between species' results.

Average relative eigenvalue standard deviations, both before and after controlling for size are shown in Table 38. Minimal differences are found between species standard deviation values. However, *Loris tardigradus* stands out as having a higher eigenvalue relative standard deviation than all of the other species. The higher the standard deviation of eigenvalues, the higher the overall integration and lower the modularity of the cranium is predicted to be (Goswami & Polly, 2010a).

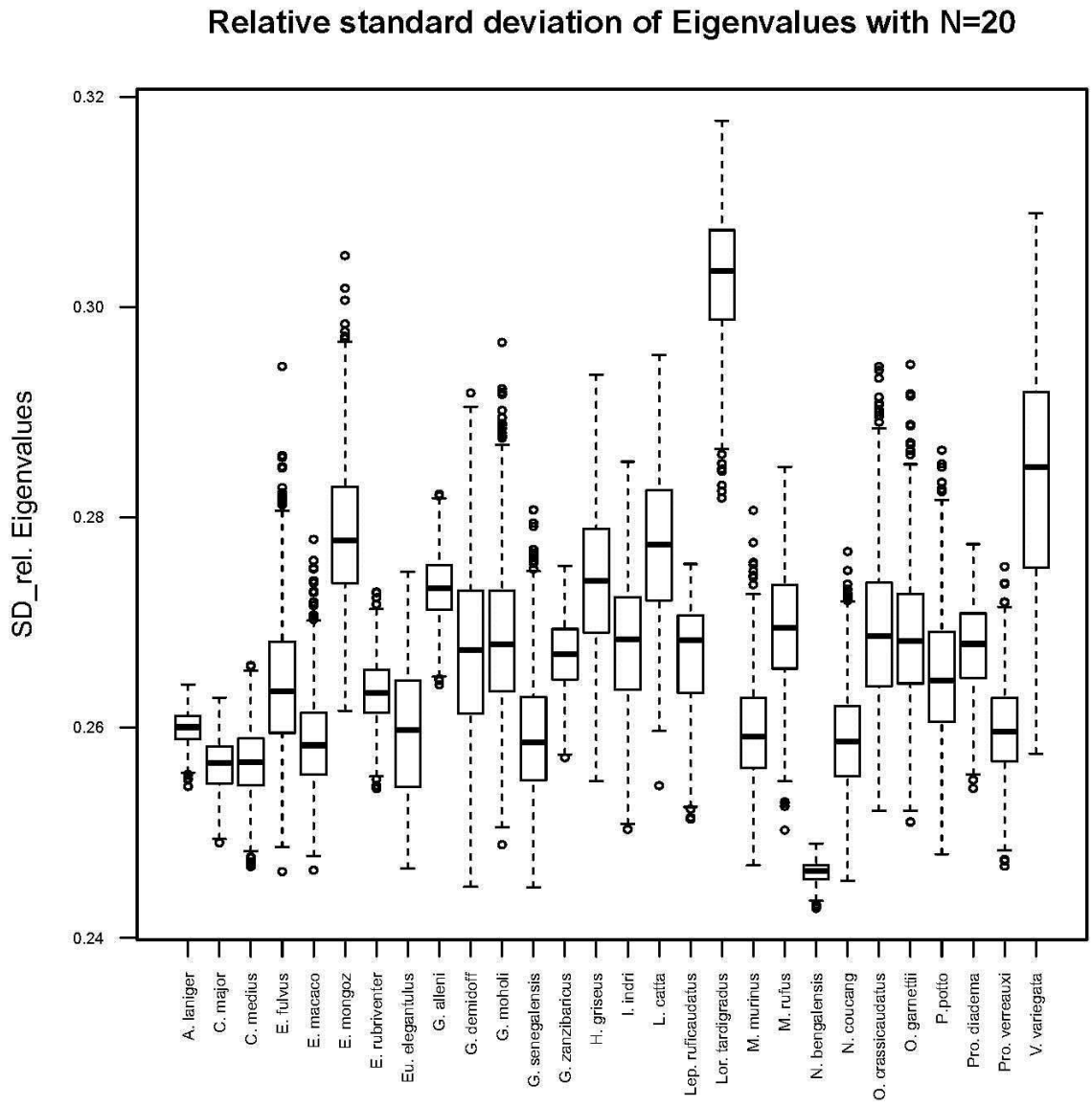

Figure 23: Relative standard deviation of eigenvalues for 1000 sub-samples of each species when N=20.

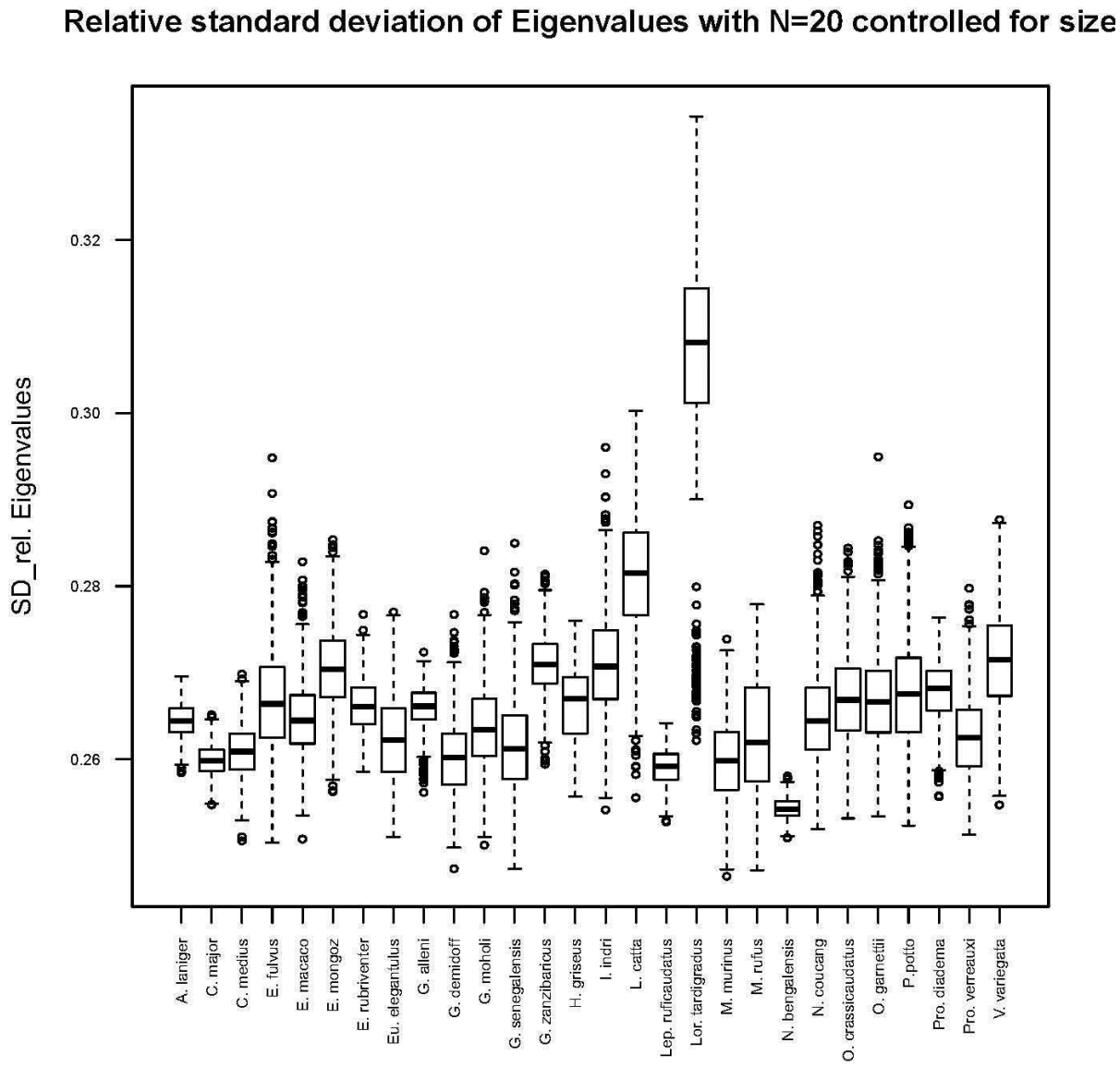

Figure 24: Relative standard deviation of eigenvalues for 1000 sub-samples of each species when N=20, based on the residuals of size regressed on to Procrutes coordinates to control for allometry.

Table 38: The relative standard deviations of eigenvalues for 1000 subsamples of N=20 for each species.

Genus	Species	Average relative eigenvalue standard deviation	Average relative eigenvalue standard deviation (controlled for allometric size)
Cheirogaleus	*major*	0.2565	0.2598
Cheirogaleus	*medius*	0.2566	0.2609
Microcebus	*murinus*	0.2591	0.2599
Microcebus	*rufus*	0.2694	0.2625
Galago	*alleni*	0.2733	0.2660
Galago	*demidoff*	0.2672	0.2603
Galago	*elegantulus*	0.2602	0.2624
Galago	*moholi*	0.2681	0.2637
Galago	*senegalensis*	0.2592	0.2616
Galago	*zanzibaricus*	0.2668	0.2710
Otolemur	*crassicaudatus*	0.2700	0.2671
Otolemur	*garnettii*	0.2688	0.2670
Avahi	*laniger*	0.2599	0.2644
Indri	*Indri*	0.2683	0.2712
Propithecus	*diadema*	0.2675	0.2678
Propithecus	*verreauxi*	0.2604	0.2626
Eulemur	*fulvus*	0.2635	0.2669
Eulemur	*macaco*	0.2590	0.2648
Eulemur	*mongoz*	0.2778	0.2704
Eulemur	*rubriventer*	0.2634	0.2662
Hapalemur	*griseus*	0.2740	0.2662
Lemur	*catta*	0.2780	0.2813
Varecia	*variegata*	0.2838	0.2715
Lepilemur	*ruficaudatus*	0.2668	0.2591
Loris	*tardigradus*	0.3032	0.3065
Nycticebus	*bengalensis*	0.2462	0.2543
Nycticebus	*coucang*	0.2590	0.2650
Perodicticus	*potto*	0.2649	0.2677

Figures 27 and 28 are evo-maps of eigenvalue relative standard deviation, not controlling and controlling for size, respectively. Node and tip values, as represented by black circles, appear identically sized due to the similarity in eigenvalue standard devoation across species. No overall direction of change or family level patterns are revealed through the evo-maps; instead, the greatest change is shown to have occurred in *L. tardigradus. L. tardigradus* has increased in eigenvalue relative standard deviation, and therefore increased in overall cranial integration since its last common ancester with *Nyticebus. Nyticebus* appears to have has decreased in overall cranial integration since this split, however, this change is lost once allometry is controlled for.

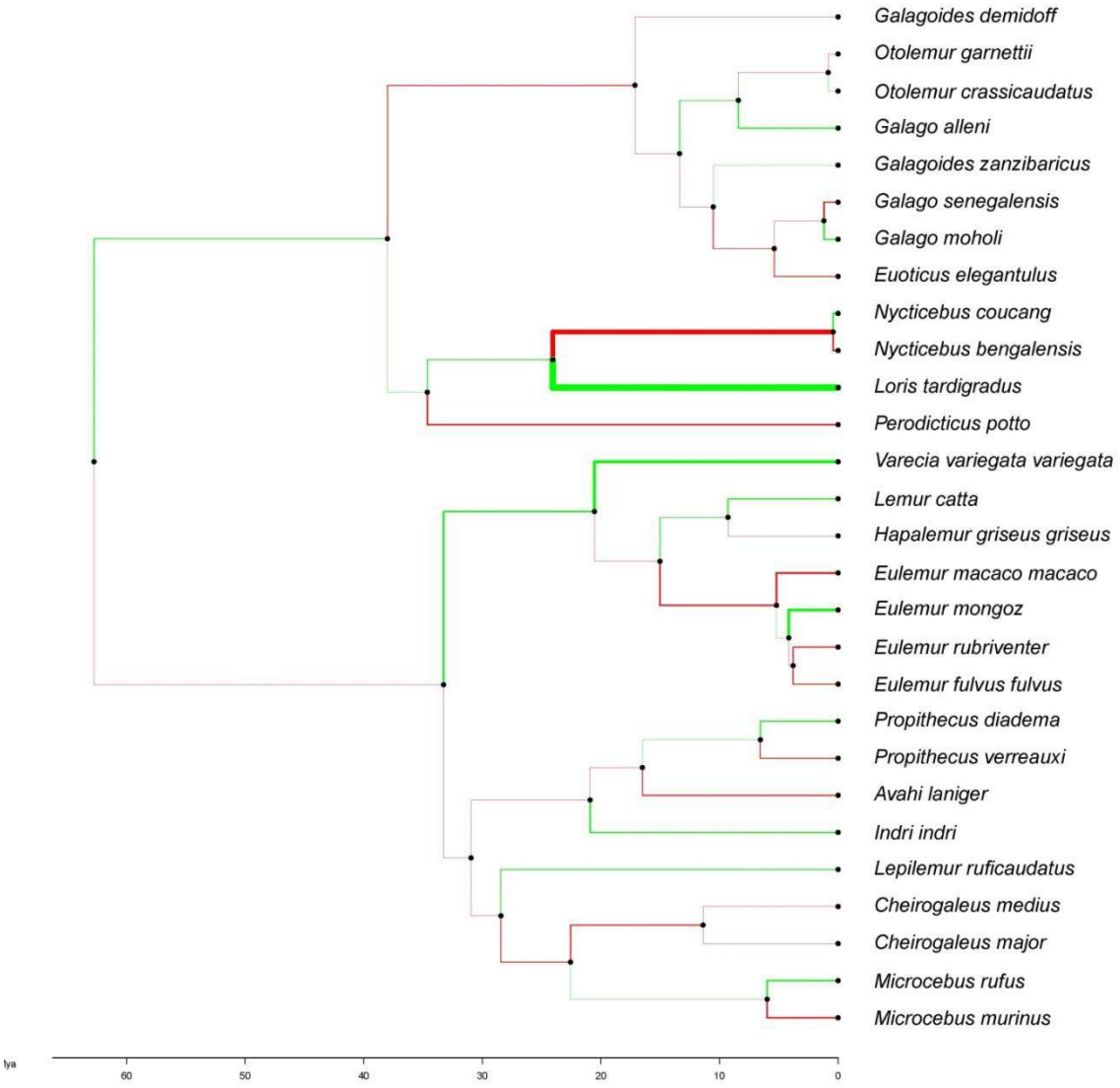

Figure 25: Evo-map of the mean relative standard deviation of eigenvalues, where green indicates an increase in standard deviation and therefore an increase in overall integration and a decrease in modularity and red a decrease in standard deviation and therefore a decreased in overall integration and an increase in modularity. The thickness of the line represents the magnitude of the increase or decrease and the size of the circles at the tips and nodes is representative of the strength of the trait for that species/ancestor.

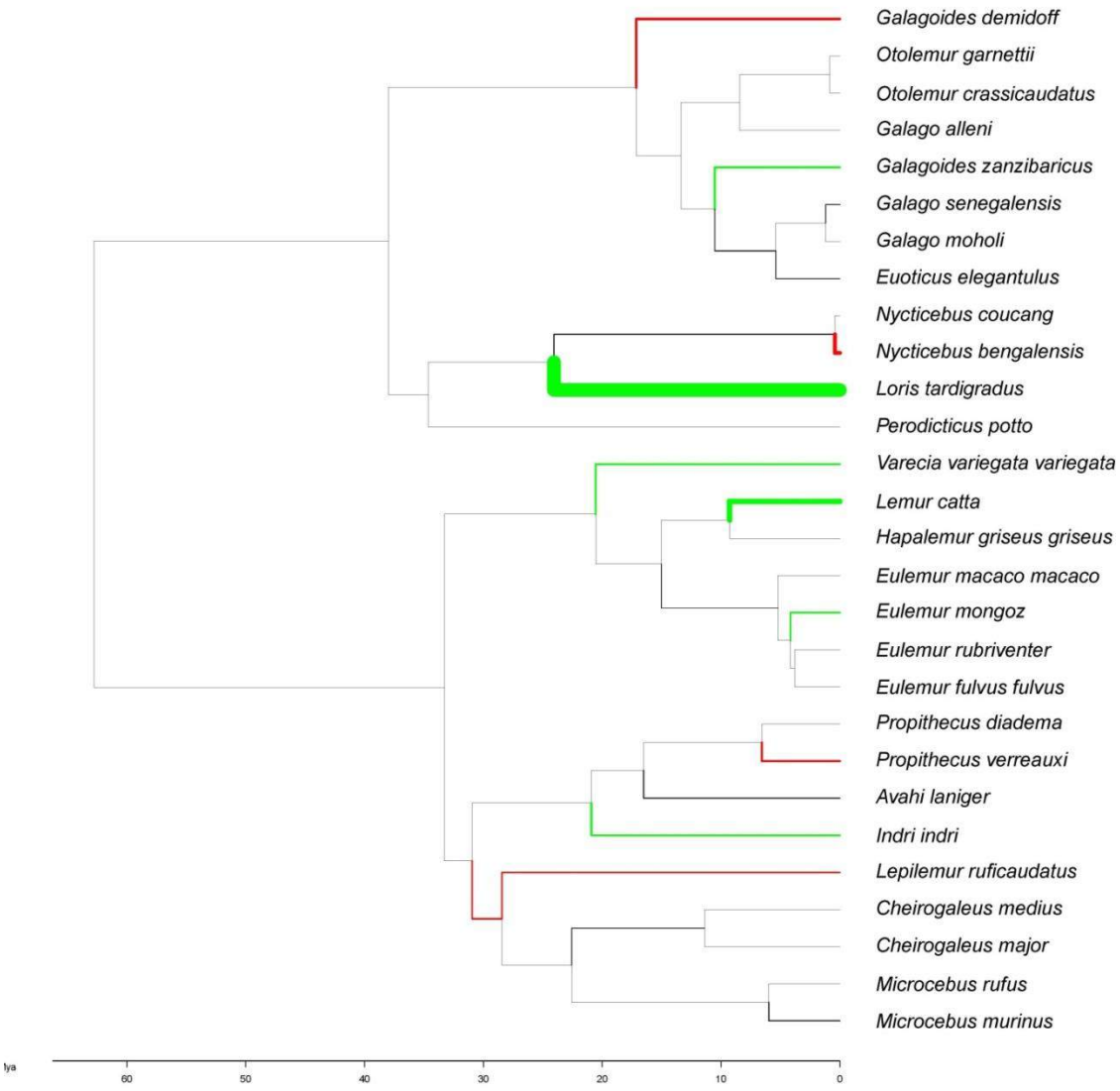

Figure 26: Evo-map of the mean relative standard deviation of eigenvalues, when allometry is controlled for, where green indicates an increase in standard deviation and therefore an increase in overall integration and a decrease in modularity and red a decrease in standard deviation and therefore a decreased in overall integration and an increase in modularity. The thickness of the line represents the magnitude of the increase or decrease and the size of the circles at the tips and nodes is representative of the strength of the trait for that species/ancestor.

4.5. Discussion

4.5.1. Models of modularity – Intra-species modularity

The four models of modularity that were tested (2* modules, the Singh (3 modules; Singh, 2012), the Cheverud (6 modules; Cheverud, 1995) and the Goswami (6 modules; Goswami, 2006a), examine different levels of the modularity hierarchy (Pavlicev *et al.*, 2008). The 2* and the Singh model focus on the shallower levels, with fewer larger modules, while the Cheverud and Goswami models take a deeper level approach, with smaller, more targeted modules (Table28).

Of the two shallower-level models, the 2* model was the more strongly supported. It was found to be the best model of modularity for 10 out of the 28 species and 9 when allometric size was controlled for (Table 29). The Singh model, in contrast, was the most strongly supported in only 3 out of 28 species and 4 when size was controlled for (Table 29). The 2-module division of the face and the neurocranium into separate modules, based on their different growth patterns (the face follows a somatic growth pattern while the neurocranium follows a neural growth pattern), can consequently be concluded as a valid model of modularity. However, the further subdivision of the cranium into the vault and base (Singh *et al.*, 2012) based on their different modes of ossification (intramembranous for the vault and endochondral for the base), is less well supported. Only *Eulemur* sp. show greater support for the Singh model over the 2* model, this could indicate a possible reorganisation of modularity in the last common ancestor of *Eulemur* sp. (Table 29).

Out of the two deeper level models, it is the Cheverud model, rather than the Goswami model, that is more closely aligned with the Singh model. This is largely due to the incorporation of the external auditory meatus into the vault module and the anterior onset of the cranial base in the Cheverud model (Table 28). Perhaps because of these similarities, the Cheverud model, like the Singh model, is not as well supported. It was found to be the best estimate of modularity (when both controlling and not controlling for allometric size) for only two species: *Avahi laniger* and *Loris tardigradus* (Table 29). The Goswami model, in contrast, was the best fit for 14 out of 28 species (and 13 when allometric size was controlled for; Table 29).

While the modules in the two deeper level models share the same names, the distribution of landmarks between the modules varies (Table 28). Cheverud (1995) includes the

landmarks of the external auditory meatus within the vault module, while Goswami (2006a) attributes them to the base. Goswami also shortens the cranial base module, only including landmarks that are posterior to the suture of the basioccipital synchondrosis, while more anteriorly placed landmarks on the base of the cranium are placed within the zygomatic module (Goswami, 2006a). Cheverud (1995) maintains that the anterior basicranial landmarks are part of the base module. Another key difference is in the definition of the orbit module, which in the Cheverud model only contains three landmarks (the frontomalare orbital, the nasolacrimal foramen and the optic foramen), whereas the Goswami model includes an additional six facial landmarks close to or surrounding the orbit. Finally, Cheverud (1995) attributes several of the landmarks from the palate to the oral module, while Goswami (2006a) places them in the face module.

Given that the modules in the Cheverud model are designed specifically with primates in mind (Cheverud, 1995), while the modules in the Goswami model were based on mammalian modularity in a much broader sense (Goswami, 2006a), the Cheverud model might have been expected to be a better 'fit' for strepsirhine primates. However, it has been argued that the basic structure of modularity has remained constant since it arose in basal mammals, with only the magnitude of the relationships within-modules changing (Porto *et al.*, 2009). As such, a model based specifically on primates may not have an advantage over one based on mammals. In addition, while the Cheverud modules are based on *a priori* reasoning linked to development and function, the Goswami modules were generated through cluster analysis. If the basic structure is the same, but the assignment of landmarks is slightly altered, then it seems reasonable that a bottom-up approach based on quantitative data, like Goswami's (2006a), will provide a better model. Moreover, Cheverud (1995) himself found that the levels of correlation within his modules were not especially high, for New World primates, and levels within the orbit module were actually negatively correlated.

4.5.2. Models of modularity – Inter-species modularity

The same pattern found at the intra-species level, where the 2* and Goswami models were the most strongly supported, was also found at the inter-species level, when all species were included, and remained true when size and phylogenetic relationships were controlled for (Table 30). As the pattern is so robust at the species level, it is not surprising that controlling for phylogeny did little to alter the results.

However, while the 2* module and Goswami model were the most strongly supported, all four models were found to be a significant fit (Table 30). It has been argued that this lack of distinction between models may reflect a real biological effect, in that developmental and functional interactions may form overlapping layers that influence trait correlations (Goswami & Polly, 2010a). This has been described as being analogous to reusing a scroll on which the impression of the previous script obscures the meaning of the new message and, as such, has been termed the "palimpsest model" of cranial evolution (Hallgrímsson *et al.*, 2009).

At the family level, the Goswami model was again the most strongly supported for all of the families, and controlling for size or phylogenetic relationships had only minimal effects (Table 31-35). The only family to show any noticeable difference was the Lemuridae, for which, although the Goswami model was still the most strongly supported, all four models were less successful at explaining modularity than they were for the other strepsirhine families (Table 34). The intra-species analyses gives a clue as to why this might be: *Eulemur* were the only group for which the Cheverud model was found to be favourable over the Goswami model; none of the models were significantly supported for *V. variegata*, while for the remaining family members (*H .griseus* and *L. catta*) the Goswami model was supported (Table 29). The result of both this mixed support and the lack of support for the models within species may be behind the results seen at the family level. Esteve-Altava *et al.*, (2015) found the Lemuridae, specifically *Lemur,* to have a derived pattern of modularity in comparison to other strepsirhines, particularly for the face and orbit regions, according to an assessment of their AnNA connectivity modules. Taken together, this could indicate a reorganisation of the modularity structure in the Lemuridae clade, however, the cause of this reorganisation is unclear. One possibility is that it is linked to the greater level of terrestriality in the Lemuridae than other strepsirhines (Jolly, 2004). An alternative, although less parsimonious, explanation could be that these results signify the retention of a primitive modularity structure in the Lemuridae, due to a lack of selection pressure on the family.

The strong evidence for modularity across species is inline with incidences of mosaic evolution that have been reported for other species (Ackermann & Cheverud, 2004); with the semi-autonomous nature of modules enabling them to evolve relatively independently of each other (Ackermann & Cheverud, 2004; Leakey *et al.*, 2012; Wood &

Collard, 1999). As such, modules can be differentially effected by allometry (both between-modules and between-species), as seen in chapter 5.

4.5.3. Within-module correlations

The strength of within-module correlations differed depending on the model or module in question (2*, Singh, Cheverud or Goswami), but, across species, the pattern of module strength or weakness was largely consistent (Table 36, 37; Figure 23, 24). This suggests a suborder wide arrangement of trait correlations, in line with the results from the RV_M coefficient analysis (Tables 29-30).

In general, controlling for the effects of allometry had minimal effect on the strength of module correlation at the intra-species level (Table 36, 37). However, for the Singh module, for some species, once allometry was controlled for, the module with the strongest within-module correlation ceased to be the vault and became the face. This suggests that size plays an important role in the integration of the vault, and possibly less of an important role in the integration of the face. This was further supported by the results from the two six-module models, for which correlation within the vault and base modules was generally shown to decrease when size was controlled for, suggesting that allometry plays a role in the integration of these modules. This could be due to the integrating role of these modules, especially the cranial base, for the whole cranium (Lieberman *et al.,* 2000); as the size of the cranium increases or decreases then so must the size of these modules to maintain the overall functionality of the cranium. In contrast, the strength of correlation within the orbit was shown to increase once size had been controlled for. This could indicate selection for correlation in the orbit unlinked to, or masked by, size. Interestingly, there is no evidence of increased correlation in the orbit for species with high orbital convergence or frontation (i.e., the Lorisidae) (Ross, 1995), compared to those without. Size also has a very limited effect on within-module correlation when investigated at an inter-species level; the main exception was the Goswami face module, for which allometry increased the internal trait correlations (Figure 23, 24). This could be explained if size is seen as a proxy for diet; across species size is closely associated with diet, with smaller species being insectivorous or gummivorous and larger species omnivorous, frugivorous, or folivourous (Gould *et al.,* 2011; Jolly, 2004; Mittermeier *et al.,* 2008; Nekaris & Bearder, 2011). Increased modularity could therefore be selected for to maintain functionality while adapting facial morphology to changing diets.

Results for the 2* model show little distinction between the two modules, with no trend for greater within-module correlation in one over the other, either in general or at a family level (Table 36). This is in contrast to results for NWM, OWM and apes, which all had greater correlation in the face than the neurocranium, when the cranium was divided into only two modules (Ackermann, 2005; Ackermann & Cheverud, 2000; Marroig & Cheverud, 2001). The only exceptions to this pattern in haplorhine primates were *Saguinus, Callimico* and *Aotus* which showed greater correlation in the neurocranium than the face (Marroig & Cheverud, 2001). It was suggested that this reversal in pattern was due to the lack of sexual dimorphism in the three genera (Ackermann & Cheverud, 2004; Marroig & Cheverud, 2001; Rehg & Leigh, 1999; Wright, 1994). Strepsirhines are also generally sexually monomorphic (Godfrey *et al.,* 1993; Jenkins & Albrecht, 1991; Kappeler, 1990, 1991; Thorén *et al.,* 2006); if high correlation in facial traits is the result of sexual selection, then this could also explain the absence of this pattern in strepsirhine primates (Marroig & Cheverud, 2001). Viewed from the opposite direction, strepsirhines may have higher integration in the vault than is generally found in haplorhine primates, rather than lower correlation within the face, thereby equalising the strength of modularity in their face and vault module; due to methodological difference the values are not directly comparable (Marroig & Cheverud, 2001). It has been argued that the correlation of traits in the neurocranium may have been weakened in haplorhine primates, as an adaptation for their high levels of encephalisation (Cheverud, 1996). Strepsirhines, in contrast, have relatively low levels of encephalisation (Isler *et al.*, 2008; Jerison, 1973; Kirk, 2013; Preuss, 2009), so the relaxation of within-module correlation in the neurocranium may not have been necessary.

For the Singh model, the vault was consistently the most strongly integrated module (Table 36). To find that the vault is more strongly integrated than the base is somewhat contradictory to what might be expected, as the primate cranial vault (including strepsirhines) has previously been shown to have lower integration than the cranial base, at the intra-species level (Goswami 2006a). These findings were argued to be the result basicranium's neural development and because of the multiple functional roles that the plays in the cranium (Porto *et al.*, 2009). The stronger integration in the vault, in comparison with the cranial base, was further supported by the results from both the Cheverud and Goswami models (Table 37), despite their differences in module composition. One possible explanation for this is that, while the vault largely develops

through intramembranous ossification, the base develops through endochondral ossification, meaning that cartilage is produced as a precursor to bone tissue. As a result, the cranial base is subject to the somatic effects of growth hormones acting on the cartilage (Gilbert, 2014; Hall, 2005). The lesser degree of encephalisation in strepsirhine primates, and so possible greater correlation in the vault, could also, again, play a part (Isler *et al.*, 2008; Jerison, 1973; Kirk, 2013; Preuss, 2009).

While this may partially explain why the vault is found to be more strongly integrated than the base, it does not clarify why these results differ from those found in previous work (Goswami, 2006a). A slight methodological difference between the two studies is the most likely explanation for these contrasting results. Here within-module correlations are calculated using scalar correlations (i.e., using each *x*, *y* and *z* coordinate), while Goswami (2006a) uses vector correlations (i.e., the whole landmark). If landmarks have variation that is scattered along a single dimension and it is at or near 90 degrees from the angle of variation for another landmark, using vector correlations could result in an underestimation of the covariance. In principle this is unlikely to cause a problem (variation is usually spherical in distribution), but if it would happen anywhere, the vault is the most likely place, given how the midline and side sutures are placed.

For the Cheverud model, the face module consistently has the highest average within-module correlation; this was in contrast to the Goswami model, for which the oral module is the most strongly correlated (Table 37). The distribution of landmarks between the face and oral modules could explain the difference between the two (Table 28). In the Goswami model, the majority of the landmarks in the oral module are associated with the spacing of the premolars and molars. The only non-dental landmarks in the module are the greater palatine foramen and the posterior tip of the nasal spine, with most other palatine landmarks attributed to the face module. A strong correlation between dental landmarks is not unexpected; the teeth must be appropriately spaced to fit within the jaw and correspond to the lower dentition, in addition to being functionally able to bite/gouge/chew the specific food source(s) of the organism. In the Cheverud model, the organisation is reversed; the face module is limited to the piriform aperture and nasion, and thus might be expected to be highly correlated based on both shared development and function (Cheverud, 1995), while the palatine landmarks are attributed to the oral module, thereby decreasing the correlation within that module.

The finding that the face is the most strongly correlated module of the Cheverud model (Table 37; Figure 23, 24) is also in contrast to previous findings for anthropoids, for which, following the Cheverud model, the oral module was the most strongly correlated module (Ackermann, 2005; Ackermann & Cheverud, 2000; Marroig & Cheverud, 2001).

Another major difference between the two six-module models is in their definition of the cranial base; while the Cheverud model includes the anterior landmarks from the cranial base, Goswami (2006a) proposes that the base module begins more posteriorly, at the basioccipital synchondrosis, with the anterior landmarks placed within the zygomatic module (Table 28). Between the two base modules, it is the Goswami module that tends to have the stronger correlation. However, the Cheverud model tends to show stronger correlation within the zygomatic module, in comparison to the Goswami zygomatic module (Table 37).

Previous work, on which the Goswami model is based, but which uses a different configuration of landmarks, found the equivalent of the face, oral and base modules to be strongly integrated, while the orbit, zygomatic and vault modules were weakly integrated for primates (Goswami, 2006a; Goswami & Polly, 2010b). This is matched here, in that the face and oral modules are found to be strongly correlated and, in comparison, the orbit and zygomatic modules are weakly correlated (Table 37). For these modules, it could be argued that strong within-module integration is found in modules that originate from a single tissue origin and a single mode of ossification, whereas weak integration is found in modules that develop from more than one type of tissue and/or more than one mode of ossification (Kuratani, 2005), although, in other cases, untangling the functional and developmental pathways of modules has proven impossible, as they are so closely intertwined (Cardini & Elton, 2008a; Cheverud, 1995; Singh *et al.*, 2012). However, as previously discussed for this and the other three models, the vault, rather than the base module, was found to be strongly integrated (Table 37), despite the base forming from one mode of ossification and one tissue type and the vault having a more complex developmental route (Gilbert, 2014; Hall, 2005).

In addition, Goswami (2006a) found the face module to have the strongest within-module correlation, in a broad range of species, including strepsirhine primates. In this analysis, the

oral module was repeatedly found to be more strongly integrated than the face. This difference may be attributed to the choice of landmarks; in Goswami (2006a), two landmarks were taken from the canine (medial and labial points) and these were assigned to the face module. In this study, only one landmark was taken from the canine (most superior, anterior point) and following Goswami (2006a) was assigned to the face module. Two landmarks from the same tooth would be expected to significantly covary, thereby increasing the within-module correlation for the face module. Other strongly correlated dental landmarks cause the oral module to be strongly correlated in both studies.

The results *H. griseus* for within-module correlations stand out, as the face module was found to be the most strongly correlated module in all four models (Table 36, 37). It has been argued that hard object feeders, or those species with a specialised diet, should have either a highly integrated face, to maintain function while adapting to evolutionary pressures linked to their diet, or have a weakly integrated face, to allow for plasticity in response to diet (Goswami, 2006a; Makedonska *et al.*, 2012). *H. griseus,* which has a specialised, bamboo-based, diet (Gould *et al.,* 2011), appears to have followed the former path. Other species (such as *E. elegantulus, G. moholi* and *O. crassicaudatus*), that follow a gummivorous diet, that might be classed as both specialist and hard-object feeding, due the necessary gouging and scraping of bark to access the sap (Charles-Dominique, 1977; Nash, 1986; Nash *et al.,* 1989; Wiens, 2002), or *L. tardigradus,* which is highly faunivorous (Nekaris & Rasmussen, 2003), did not report particularly strong or weak correlations within the face module compared to other cranial modules (Table 36, 37).

4.5.4. Eigenvalue relative standard deviation— Intra-species modularity

Differences in the level of overall cranial integration between species were limited, as shown by the lack of variation in eigenvalue relative standard deviation, once sample size had been controlled for (Table 38; Figure 25, 26). In addition, relative overall integration (where a value of 0 would represent no integration and 1 complete integration) was low in all species, ranging from 0.246-0.303, or 0.253-0.307 when allometric scaling is controlled for (Pavlicev *et al.*, 2009). This is in keeping with the RV_M coefficient scores for both intra and inter-species (Table 29, 30), which reveal a consistent pattern of modularity, with a six module model the most strongly supported, both within and between species (i.e., low integration). These low levels of overall cranial integration are in line with those reported for Japanese macaques (*Macaca fuscata fuscata*) (Goswami & Polly, 2010a).

Evo-maps (Figure 27, 28) reveal that the greatest change in modularity occurs in *L. tardigradus* (*N. bengalensis* also shows a strong change in the opposite direction, but this disappears once allometric size has been controlled for). The relatively high integration and therefore, implied low modularity seen in *L. tardigradus* (Table 38), combined with consistently high average within-module correlation scores for the species, across all modules, for all models, suggest that their high within-module correlation scores may be the result of strong correlation between all landmarks, both within and between the proposed modules (i.e., high overall integration). However, RV_M scores for the species where significant for some of the models tested, but unusually the best fitting model was the Cheverud model. Why *L. tardigradus* have reverted to a more overall integrated structure, with decreased modularity is unclear, but possible explanations may lie in their extremely faunivorous diet (Nekaris & Rasmussen, 2003) and their high levels of orbital frontation and convergence (Nekaris, 2005; Ross, 1995).

Within the Lemuridae, *V. variegata* and *L. catta* (and to some extent *E. mongoz*) show a reduction in modularity (Figure 27, 28). This is reflected in the RV_M scores for both species and for the Lemuridae family at the inter-species level (Table 29, 34). *V. variegata,* especially, shows a lack of modularity, with none of the four models significantly estimating modularity structure for the species. *V. variegata* and *L. catta* are the largest species within the Lemuridae (Gould *et al.,* 2011), which could suggest that overall integration is necessary to maintain functional integration of the cranium when it is under selection for an increased size. However, the effect remains even after allometry has been controlled for.

4.6. Conclusion

Within stepsirrhines, there is a common pattern of low overall integration and high modularity. In general, the same models of modularity are supported across species and, where species differ from this pattern, it can be linked to selection for morphological adaptations linked to a specialised diet. A quantitative, bottom-up approach for the allocation of landmarks to modules, rather than an a priori, top-down approach based on functional and developmental reasoning, generates a more strongly supported model (Cheverud, 1995; Goswami, 2006a). The relative strength of modules followed a different pattern for strepsirhine primates than has been recorded for haplorhines (Ackermann, 2005; Ackermann & Cheverud, 2000; Marroig & Cheverud, 2001), suggesting a possible

reorganisation of the cranium at the origin of haplorhines (Fleagle *et al.*, 2010). There are several possible, interlinking, reasons for this reorganisation; namely a change towards diurnal frugivorey in haplorhines (Strier, 2007), resulting in a greater reliance on sight over smell, an increase in size and greater levels of encephalisation (Fleagle, 2013; Strier 2007). In terms of the skull, this results in a more orgnathic face, more convergent orbits, the relocation if the mandible to inferior rather than anterior to the face (which together with greater orbital convergence results in the need for full orbital closure, to protect the eyes from the movement of the temporalis muscle) and the expansion of the vault (Fleagle, 2013).

The presence of modularity across the strepsirhine cranium and that of other primates (Ackerman, 2005; Ackerman & Cheverud, 2000; Cheverud, 1989; esteve-Altava *et al.,* 2015; Hallgrimsson *et al.,* 2004; Marriog & Cheverud, 2001) can help to explain the mosaic evolution also seen in primates (Ackermann & Cheverud, 2004; Leakey *et al.*, 2012; Wood & Collard, 1999) as the semi-autonomous relationship between-modules should allow them to evolve in a semi-independent fashion (Wagner *et al.*, 2007).

Previous research has shown levels of disparity across mammalian taxa to be lower in modules with high within-module integration than in those with low levels integration (Goswami *et al.,* 2014); suggesting that modularity is working to constrain morphological change. It would be interesting to apply a similar analysis to the strepsirhine data used in this research; if modularity again works to constrain the direction in which morphological change can occur, then the common strepsirhine pattern found here could be a significant underlying cause of homoplasy, which contributes so much noise to the primate paleontological record (Hall, 2007; Lockwood & Fleagle, 1999; Williams, 2007). Alternatively, it could also work to drive strepsirhine morphology to extreme forms, all-be-it along a narrow trajectory, as suggested by previous model simulations (Goswami *et al.*, 2014).

– Chapter 5 –

Allometric patterns in the cranium of the Strepsirhini

5.1. Abstract

Allometric pathways have been described as 'the line of least resistance' (Marroig & Cheverud, 2010), selected maintain integration and functionality in the skull as size varies. Conserved allometric patterns have been recorded for primates and the wider class Mammalian alike. Here, allometry is investigated for strepsirhine primates.

Intra- and inter-species analyses were conducted with a sample of 28 species, each with a sample size of N>20, to asses: relationships between size and shape for the whole cranium and for cranial modules, the relationships between overall cranial size and the size of cranial modules, the percentage of shape change attributed to variation in size and interspecies differences in allometric scaling.

Overall, allometric patterns (the axis of shape change associated with size) were conserved, both within and across species, and, with the exception of the orbit module, in line with the wider mammalian trend. Allometric scaling (the amount of shape change per unit of size change) is also relatively conserved across strepsirhine species, but the lemuriforms respond more sensitively to size differences for traits in the face, while the lorisiforms respond more sensitively for traits in the vault. Such conserved allometric pathways are considered to be a substantial source of homoplasy within strepsirhines.

Where species are seen to diverge from the common allometric trajectory, this could sometimes be attributed to selection for a specialised diet. The percentage of shape change that was the result of variation in size was relatively low in strepsirhines in comparison to other primate radiations, leaving scope for further research in to the causes of the residual variation.

For inter-species analyses, a new resampling method was used, in addition to the more traditional approach of using species averages, with an aim of incorporating intra-species variation into inter-species analysis. In comparison to the species average method, the resampling approach generated more conservative results, making it less likely to find in favour of significant inter-species allometry

5.2. Introduction

5.2.1. What is allometry?

Allometry is the size related component of shape variation (Goswami & Polly 2010a). As opposed to isometric variation, where shape change is proportional to size, allometric variation involves an unequal scaling of shape and size (Pilbeam & Gould, 1974). In addition, 'allometry' can also be used to refer to unequal relationships between component size, such as brain and body size (Gould, 1974).

Frédéric Cuvier was the first to comment on the unequal relationship between species brain and body size (Gayon, 2000), but it was Eugéne Dubois, in 1897, that initially proposed a quantitative formula to account for the across species pattern of brain size ($'e'$ for encephalisation) relative to body size ($'s'$ for soma) (Dubois, 1897, p. 368).

$$e = c.s^r$$

Where, e is the weight of the brain, c is the coefficient of cephalisation and r is the exponential constant (Dubois, 1897; Gayon, 2000). Louis Lapicque (1898) went on to apply Dubois' formula at an intra-species level. This work, combined with that of Albert Pézard (1918) and Christian Champy (1924), who both applied the principle of relative growth to secondary sexual characteristics, paved the way for Julian Huxley, who in 1924 released a seminal paper in which he stated a law for 'heterogonic growth', as allometry was then known.

$y = bx^k$ (Later amended to $y = bx^\alpha$ by Huxley & Teissier, 1936)

Where y is the size of the allometrically affected region, x is body size, k is a constant ratio of differential growth and b is a constant set at the value of y when $x = 1$ (Gayon, 2000; Huxley, 1924). The crucial theoretical feature of the formula is that k is a ratio between growth rates and not size (Gayon, 2000). The terms 'allometry' and 'isometry' were introduced in a joint paper by Huxley and Georges Teissier (1936). There was disagreement between Huxley and Teissier over whether the constant b was biologically significant, with Tiesser arguing for and Huxley against (Gayon, 2000).

Thus far, allometry had largely been considered to be non-adaptive; this idea was challenged by Norman Newell when he suggested that both α and b were modifiable by natural selection and that, under certain conditions, the consistency of α could also be accounted for by natural selection (Gayon, 2000; Newell, 1949). Newell went on to tutor

Stephen J. Gould, who would be pivotal in the further advancement of allometric theory, including in the link between allometry and adaptive evolution and in the outlining of the different forms of allometry and the interaction between them (Gould, 1966, 1971, 1974). For Gould, size was the main source of adaptive change, with allometric scaling a necessary consequence to maintain the functionality of the organism; however, once these changes have occurred, both parameters α and b will be subject to natural selection (Gayon, 2000).

Allometric scaling is still thought to be crucial in maintaining the functional elements of the skull as it varies in size, throughout both ontogeny and evolution (Cardini & Polly, 2013; Emerson & Bramble, 1993). The covariation of size and shape is similar to modularity (see Chapter 4), in that it can be seen as the result of genetic pleiotrophy due to shared developmental pathways or shared functional duties (Cardini & Polly, 2013).

Allometry has another similarity with modularity (see Chapter 4), in that it can be viewed as 'nested' or hierarchical in structure, so that the pattern, strength and taxonomic broadness of the effect may differ depending on the level being studied (Lockwood & Fleagle, 1999). Three different kinds of allometric relationships can be considered, similar to those first outlined by Gould (1966): ontogenetic, static and evolutionary. Ontogenetic allometry deals with the covariation of size and shape throughout the developmental stages of a given species, while static allometry focuses only on one particular ontogenetic stage of one particular species. Finally, evolutionary allometry describes allometric patterns across species, while, again, keeping the ontogenetic stage constant (Fleagle, 1985; Klingenberg, 1998; Lockwood & Fleagle, 1999).

Here the focus is on static and evolutionary allometry, but the three types are inextricably linked. Static and ontogenetic allometries correspond closely with one another, indicating that differences between individuals largely result from changes in ontogenetic processes (Klingenberg, 1996; Klingenberg & Zimmermann, 1992). Static and evolutionary allometry (Klingenberg & Zimmermann, 1992; Leamy & Atchley, 1984; Schluter, 1996), and ontogenetic and evolutionary allometry (Klingenberg & Zimmermann, 1992) share similar patterns. These correlations reflect the process of allometric change, with variation in ontogenetic growth patterns resulting in changes to static allometry, variation in static allometry is then subject to natural selection, resulting in evolutionary change (Klingenberg, 1998). When all three types of allometry were examined, ontogenetic and

static allometries were more strongly correlated to one another than either was to evolutionary allometry (Klingenberg & Zimmermann, 1992). This has been argued to be the result of the differential selection of traits across species affecting the interspecific evolutionary pattern (Klingenberg, 1998).

5.2.2. How and why does change in size occur?

The size of an organism or trait can be altered through changes in two different developmental components; a change in rate of growth and/or a change in period or growth. Collectively, these factors are referred to as heterochrony (Klingenberg, 1998). It has been proposed that cranial shape scales with size to maintain the functions of the skull, thus implying that there is selection for a change in size and that size is more plastic than shape.

Cope's rule describes an evolutionary trend for phylogenetic linages to increase in body size over time (Churchill *et al.,* 2015; Cope, 1896; Rensch, 1948).This selection for an increase in body size is often linked to adaptive benefits such as greater defence against predation, increased chance of survival during periods of environmental stress, and the ability to exploit a larger range of food sources (Churchill *et al.,* 2015). Though this increase in size is unlikely to continue unchecked, due to competitive pressures for the newly occupied niche, anatomical limitations or even the clade's eventual extinction (Hone & Benton, 2005). However, fossil primates (Omomyiformes, Adapiformes and Anthropoidea) show no inherent trend towards an increase in size over evolutionary time. It has been proposed that competition between the omomyiformes and the adapiformes, during the Eocene, may have constrained any evolutionary changes in size for both radiations (Soligo, 2006).

Changes in size within a population may also occur for additional environmental reasons; principally access to, and the abundance of, food resources (Elton *et al.,* 2010). For example, a link has been established between rainfall - assumed to be a proxy for the abundance of food resources - and size in vervet monkeys (*Cercopithecus aethiops*) (Cardini *et al.,* 2007) and red colobus monkeys (*Procolobus*) (Cardini & Elton, 2009a; b).

Size has been shown to be more plastic than shape and has been described as the 'line of least resistance' for change (Marroig & Cheverud, 2005). In fruit flies (*Drosophila*), where conditions are more easily manipulated and generational turnover is more rapid than in

primates, size responds more quickly to changes in resources than shape (Breuker *et al.,* 2006). In addition, complex developmental regulations have been shown to constrain the response of shape (Debat *et al.,* 2009). Allometry can be viewed both as a constraint on evolution, as it restricts the direction in which shape change can occur, and as facilitator, as it accelerates morphological differences along those pathways of least resistance (Cardini & Polly, 2013).

5.2.3. The mammalian allometric pattern

There is a common mammalian growth pattern, in which juveniles have relatively small faces and relatively large cranial vaults. The facial skeleton then proceeds to grow at a faster rate than the vault, so that the cranium reaches dolichocephaly, where the cranium is the length that would be predicted based on its width (Cardini & Polly, 2013). A pattern reminiscent of this ontogenetic allometry has also been recorded as a static/evolutionary allometric pattern in adult mammals (Cardini & Polly, 2013). The relationship between the size of the cranial vault and the length of the face is shown to range from a proportionally short face and large vault in small mammals to a proportionally long face and small vault in large mammals (Cardini & Polly, 2013). This covariation has been found in mammalian clades that share a common ancestor deep in the Eutherian tree (i.e., the Cetarctiodactula: Antilopinae and Cephalophinae; Chiroptera: Pteropodinae; Carnivoria: Herpestinae; and Rodententia: Sciurinae) (Cardini & Polly, 2013), suggesting that it might be a pattern common to all placental mammals. A large component of the cranial shape diversity seen in mammals could therefore be due to their differences in size (Cardini & Polly, 2013; Parsons *et al.,* 2011).

For primates specifically, allometry has, again, been shown to be a significant determinant of cranial morphology. In papionins, the first Principal Component (PC) of shape change (PC1) had a strong significant relationship with size (measured as the logarithm of centroid size; ln(CS)), across all genera (*Cercocebus, Lophocebus, Macaca, Mandrillus, Papio* and *Theropithecus*), suggesting a papionin-wide allometric trend. PC1 summarised 62% of the total cranial variation and represented relatively small orbits, small superiorly/inferiorly compressed crania and prognathic faces in large taxa and relatively large orbits, more globular neurocrania and more orthognathic faces in smaller taxa, in line with the wider mammalian trend (Singleton, 2002) (see also Collard & O'Higgins, 2001; Frost *et al.,* 2003).

Unlike in other Old World Monkeys (OWMs), the principal axis of shape change associated with size for guenons does not include the shortening or elongation of the muzzle (Cardini & Elton, 2008b). For the guenon *Cercopithecus aethiops* static allometry is responsible for 20% of shape difference between taxa at the subspecies level, demonstrating both the extent to which size can affect shape and also that *C. aethiops* sub-species are not simply allometrically-scaled versions of each other, with up to 80% of shape difference between subspecies attributed to other causes (Elton *et al.,* 2010; Schluter, 1996). Red colobus monkeys (*Procolobus*) show the same size related shape change witnessed in other mammals and primates, ranging from small paedomorphic forms, with short faces and large globular cranial vaults, such as *P. kirkii* and *P. rufomitratus*, to the larger, long faced and relatively smaller vaulted form of *P. tholloni* (Cardini & Elton, 2009a).

Studies of allometry in New World Monkey (NWMs) have returned conflicting results; no significant correlation was found between body mass and shape for the Atelidae, Cebinae, Aotinae, Callitrichinae or Pitheciidae, despite a significant correlation between body mass and centroid size having been established for the taxa (Perez *et al.,* 2011). These findings are in direct contradiction to reports of a conserved allometric pattern for NWMs (Marroig & Cheverud, 2005), both across and within genera, with allometric size variation accounting for 20-40% of total shape variation within-species and up to 92.8% across genera. This phenotypic correlation of size and shape was further underpinned by a conserved genetic pattern. It is argued that the diversification in size amongst NWMs may have been linked to diversification in diet. Morphological changes to the crania of NWMs away from this allometric line of least evolutionary resistance have occurred, but at a slower pace and with less dramatic morphological impact than those that are the result of selection for size (Marroig & Cheverud, 2005). Both studies (Marroig & Cheverud, 2005; Perez *et al.,* 2011)bused a geometric morphometric approach and control for non-independence between species, so why they have reached such opposing conclusions is unclear.

Further support for a common allometric pattern in NWMs comes from data on capuchin monkeys (*Cebus*); the regression of shape onto size finds size and shape to be significantly correlated, with size differences accounting for 16% of total shape variance (Cáceres *et al.,* 2014). However, the Cebidae appear to show almost the reverse of the common allometric pattern seen in other primates (Cardini & Elton, 2009a; Collard & O'Higgins, 2001; Frost *et al.,* 2003; Singleton, 2002), with larger size being associated with a larger neurocranium,

wider zygomatic arches and shorter muzzles (Cáceres *et al.,* 2014). Furthermore, unlike colobus and vervet monkeys (Cardini & Elton, 2009a; Cardini *et al.,* 2007) there was no correlation found between cranium size and climate in capuchins (Cáceres *et al.,* 2014). It has been argued that, in such circumstances, size differentiation maybe driven by niche exploitation, due to living sympatrically with other species (Ravosa *et al.,* 2010). Finally for NWMs, species of saki monkey (*Pithecia*) geographically separated from each other by the Amazon River, and which show a distinctive inter-species split in size, nevertheless share a common allometric pattern, responsible for 38% of their total shape variation (Marroig & Cheverud, 2004).

Homo sapiens do not follow the generalised mammalian static allometric trend of a more prognathic face and less globular vault with increasing size (Cardini & Polly, 2013). It has been speculated that strong selection for encephalisation, combined with an increasing reliance on processed food, led to a reduction in the need for masticatory power, which may have allowed *H. sapiens* to break away from this particular allometric constraint.

5.2.4. Allometric scaling

Papionins, as a group, share a common allometric trend, however there are significant differences in scaling patterns between genera (Singleton, 2002). *Macaca, Mandrillus, Papio* and *Theropithecus* share a common slope and elevation, for PC1 against size, as do *Cercocebus* and *Lophocebus*, but the slope and elevation of these two groups are significantly different from each other. In physical terms, this means that the mangabeys (*Cercocebus* and *Lophocebus*) have a more globular neurocranium and a less prognathic face than baboons of equal size (Singleton, 2002). Interestingly, *Cercocebus* and *Lophocebus* were previously thought to be sister taxa, based on their morphology, until genetic data aligned *Cercocebus* more closely with *Mandrillus*. Their morphological similarity is therefore attributed to parallel evolution, due to similar allometric trajectories (Singleton, 2002). However, contrasting results have been reported, in which both *Mandrillus* and *Papio,* and *Cercocebus* and *Lophocebus* differ in their allometric scaling patterns (Collard & O'Higgins, 2001). The two studies differ in the species they include for each genus and Collard and O'Higgins (2001) include data from juvenile specimens, while Singleton (20002) examines only adult crania; both factors could have contributed to their divergent results (Frost *et al.,* 2003).

A common allometric trajectory has also been found in guenons; in this instance, it was highly conserved across all species, despite marked differences in their phenotypic means (Cardini & Elton, 2008b). Moreover, the correlation between shape and size was stronger than that between shape and ecology, or shape and phylogeny, and controlling for allometric scaling increased the correlation between guenon morphological and genetic distance (Cardini & Elton, 2008b). The results suggest that guenons are more allometrically conserved across species than the Papionins. It has been suggested that this is linked to their constrained facial morphology in general, and specially their short faces. NWM are similarly conserved in terms of their allometric scaling, both across genera (Marroig & Cheverud, 2005) and species (Cáceres *et al.,* 2014).

5.2.5. Allometry in the Strepsirhini

The Lemuridae have the greatest variation in body size of all primate groups, past and present, once subfossil species are taken into account (Ravosa & Daniel, 2010), ranging from 20g – 200kg (Fleagle, 2013). Phylogenetically-controlled principal components analysis of this group found that PC1 contained 33.3% of the total shape variation and represented a prognathic face with a low (superiorly/inferiorly compressed) and narrow (bilaterally compressed) neurocranium at one extreme, and an orthognathic face with a high and broad neurocranium at the other (Baab *et al.,* 2014). For a wide range of mammals, including primates, this pattern of morphological change has been the result of allometric scaling (Cardini & Elton, 2009a; Cardini & Polly, 2013; Collard & O'Higgins, 2001; Frost *et al.,* 2003; Singleton, 2002). However, for the Lemurs this shape change was not significantly correlated with size (ln(CS); Baab *et al.,* 2014), although it is worth noting that the subfossil lemurs *Megaladapis* and *Hadropithecus* appear to have had a strong influence on the regression results; both are large species that fall at opposite ends of PC1 (Baab *et al.,* 2014). Instead, for the Lemurs, PC2, which describes a deflected posterior neurocranium, a reduction in orbit size in larger specimens and a more level neurocranium with an increase in orbit size in smaller specimens, is significantly correlated with size, with 69% of the shape change accounted for by PC2 (14.6% of the total shape variation) attributed to variation in size (Baab *et al.,* 2014). It should be noted, however, that this analysis (Baab *et al.,* 2014) on the lemuriforms was used species averages from very small samples (1<N>21). Small sample sizes significantly affect the accuracy of mean shape, with subsamples of N<5 generating a mean shape that is up to six times greater in Procrustes distance to the observed mean shape of the same species, compared to a bootstrap

sample, with an error that could account for up to 23% of inter-species distances (see Chapter 3).

Analysis of ontogenetic allometry patterns in the Lemuridae (Ravosa & Daniel, 2010), found that there was a conserved pattern of allometric scaling across species (*Eulemur coronatus, E. mongoz, E. macaco, E. rubriventer, E. fulvus, Lemur catta, Varecia variegata, Avahi laniger, Propithecus tattersalli, P. verreauxi, P. diadema, Indri indri, Mesopropithecus globiceps, M. pithecoides* and *Babakotia radofilai*). Furthermore, the majority of differences in cranium shape were the result of differential extensions of ontogenetic growth; it was therefore argued that speciation, for extant and subfossil species, has occurred largely through selection for size (Ravosa & Daniel, 2010). In the few instances where this pattern was not maintained (*Hapalemur* and *Pachylemur*) it was attributed to specific selection for dietary adaptations requiring a greater shift than that which could be achieved through allometric scaling alone (Ravosa & Daniel, 2010). While *Hapalemur* is well known for its bamboo based diet, the diet of the extinct *Pachylemur* is still subject to speculation: with suggest that it ate tough fibrous foods, in keeping with the reported adaptations to its cranial morphology (Ravosa, 1992), while others maintain, based on analysis of its dentition, that it had a largely frugivorous diet, with some folivory (Godfrey *et al.,* 2004; Jungers *et al.,* 2002).

In support of the argument that dietary specialisation is one of the key causes for shape to break away from allometric vectors, dietary category accounts for a significant proportion of morphological change in extant Lemurs, when size is controlled for (Baab *et al.,* 2014). However, this was only true prior to the necessary application of Bonferroni's correction, after which the result was no longer significant (Baab *et al.,* 2014).

Within lemurs, selection for a highly nectivorous diet appears to be the most likely cause for a change in allometric pattern (Muchlinski & Perry, 2011). Specific candidates are *E. mongoz*, which has been recorded, year-round, spending up to 80% of its foraging time feeding on nectar (Sussman, 1991; Sussman & Raven, 1978), and *V. variegata*, which depending on the season, spend 25-72% of its foraging time exploiting nectar (Kress, 1993; Kress *et al.,* 1994). Nectar feeding species have previously been shown to have increased cranium and palate lengths (Dumont, 1997). Within lemurs nectar feeders which are classed as 'non-destructive', a category to which both *E. mongoz* and *V. variegata* belong,

have relatively long craniums, palates and dental rows in relation to body size, when compared to taxa with different dietary characteristics, including destructive nectar feeders (Muchlinski & Perry, 2011). This implies that those species that rely heavily on nectar as a food source have developed mutualistic relationships with some of Madagascar's native plant species (Muchlinski & Perry, 2011; Sussman, 1991). Yet there is difficulty in attributing morphological changes to diet for lemuriforms, as species dietary preferences often significantly overlap with one another, with the majority of species consuming a wide variety of food types (Gould *et al.,* 2011; Muchlinski & Perry, 2011).

Galagoides have also been shown to be morphologically divergent as a result of selection for size. Again, exceptions to this trend have been linked to specialist feeding techniques, in this case the gouging of gum from tree bark (Ravosa *et al.,* 2010). The majority of species within the Galagidae are largely faunivorous or folivorous, with some, but not all occasionally feeding on gum (Fleagle, 2013). *Euoticus*, however, is known to frequently use gouging to extract gum. When gouging, the upper anterior teeth are anchored into trees while the lower anterior teeth are used to hack through bark to access the gum (Charles-Dominique, 1977; Nash, 1986; Ravosa *et al.,* 2010). Other species, namely *Galago moholi* and *Otolemur crassicaudatus*, are known to regularly use an alternative, less strenuous, technique, known as scraping. This involves using only the lower dentition to scour the bark (Charles-Dominique, 1977; Nash, 1986; Nash *et al.,* 1989). *Euoticus* and *Otolemur* both exhibit a change in morphology that breaks away from the allometric pattern. These changes are largely restricted to the mandible and are thought to enable an increased gape, useful when extracting gum (Ravosa *et al.,* 2010; Vinyard *et al.,* 2003).

O. garnetti displays the same allometric pattern as *O. crassicaudatus,* but has not been recorded as being a frequent gum feeder. It is possible that this is a synapomorphy, which has simply not yet been lost in *O. garnetti* (Ravosa *et al.,* 2010). However, it should be noted that, the data on *O. garnetti's* feeding behaviour come from sites where the gum producing trees (*Acacia*) are not present (Nash, 1986). Further data, from different *Acacia*-inhabited, field sites are therefore required before significant gummivory by *O. garnetti* can be ruled out. Unlike *Euoticus* and *Otolemur, G. moholi* is gummivorous, but does not show the same change in its morphology (Ravosa *et al.,* 2010). It is possible that *G. moholi's* small size results in allometric scaling that is more conducive to an increased gape (Ravosa *et al.,* 2010).

For the Lorisidae, as with the Lemuridae and the Galagidae, selection for body size differentiation seems to be the primary determinant of cranial shape variation (Ravosa, 1998; 2007). However, *Nycticebus pygmaeus* is not simply a scaled version of *N. coucang*; instead it has morphological differences, such as a relatively narrower interorbital margin, which are maintained even when allometric scaling is accounted for (Ravosa *et al.,* 1998). The smaller morphology of *N. pygmaeus* is considered to the be derived for *Nycticebus*, possibly evolved to avoid competition with sympatric, larger-bodied *Nycticebus* species (Fleagle, 2013; Ravosa, 1998). For other species of the Lorisidae, alternative environmental factors have been associated to selection for changes in size. Specifically, latitude - as a proxy for temperature - (*N. coucang*) and altitude (*Perodicticus potto*) have been correlated with size differences (Ravosa, 1998; Ravosa, 2007).

In the Galagidae, different size morphs can be found living in sympatry. This suggests that, for them, as with *N. pygmaeus* (Ravosa, 1998), size divergence may be linked to niche exploitation (Charles-Dominique, 1977; Nash, 1986; Nash *et al.,* 1989; Ravosa *et al.,* 2010).

5.2.6. Allometry in cranial modules

As seen in Chapter 4, there is an argument that the primate skull can be broken down into modules, based on shared functions or developmental histories. The best supported models of modularity for strepsirhines divide the cranium into either face and vault modules, or into smaller face, orbit, oral, zygomatic, vault and base modules, following the modularity hypothesis of Goswami (2006a) (Table 28). The nature of modularity is that traits within a module show greater covariance with one another than with traits outside of that module. Morphological change within modules can therefore be (semi-)autonomous in relation to the rest of the cranium and, as a result, differences may arise in allometric patterns, both across modules and across species (Goswami & Polly 2010a).

The brain and the eye reach full size relatively quickly in Eutherian mammals (Marroig & Cheverud, 2004). As a result, the orbit, vault and cranial base should not be subjected to the effects of growth hormones to the same extent as the slower growing areas of the cranium, such as the face and oral cavity (Marroig & Cheverud, 2004). If static allometry is representative of ontogenetic growth, then traits associated with the face would be expected to be more positively allometric relative to any traits associated with the

neurocranium (Marroig & Cheverud, 2004). The general allometric trend found in primates is in line with these predictions (Cardini & Elton, 2008b; Collard & O'Higgins, 2001; Elton *et al.,* 2010; Fleagle *et al.,* 2012; Frost *et al.,* 2003; Singleton, 2002), although, they are not necessarily met for strepsirhines (Baab *et al.,* 2014; Fleagle *et al.,* 2012).

5.2.7. Size-versus-size allometry

As well the effect of size on shape, allometry can also be examined in terms of the effect of overall size on the size of other traits, referred to here as 'size-versus-size' allometry. Where this relationship is a 1:1 ratio, then overall size and the trait in question are scaling with isometry; but, where this ratio is unequal, then the overall size and the trait can be said to scale with positive or negative allometry accordingly (Gould, 1974).

One key example of size-versus-size allometry, which has been frequently studied in primates, is the relationship between overall size (or body weight) and brain size (Emerson & Bramble, 1993). At an inter- and intra-species level, brain and body size scale with negative allometry, although slope values vary depending on taxonomic level being studied (Emerson & Bramble, 1993). Species with a relatively large brain in relation to their body size (i.e., plot above the line) are said to be encephalised (Clutton-Brock & Harvey, 1980; Gould, 1974; Martin & Harvey, 1985; Martin, 1984; Smaers *et al.,* 2012; Williams, 2002). Haplorhine primates, and especially the Hominidae, are encephalised, buts the relative brain size of strepsirhine primates is in line with that of other mammalian taxa (Kirk, 2013; Martin, 1990).

In cranial morphology, a positive, size-versus-size, allometric trend has been recorded for primates, with cranium, face and palate length scaling with positive allometry, in most, if not all, platyrrhines, cercopithecoids and hominoids (Fleagle *et al.,* 2012). However, when tested, lemuroids and lorisoids showed no significant relationship between these lengths and overall size (Fleagle *et al.,* 2012). Instead, relative orbit size and cranial volume were correlated with size in stepsirrhines. This difference in allometric pattern is argued to be the result of a cranial reorganisation during the origins of the anthropoidea (Fleagle *et al.,* 2012).

Particular attention has been paid to the orbit, which is reported to scale with negative allometry to body size, so that smaller primates have relatively large orbits in comparison

to larger primates (Baab *et al.,* 2014; Schultz, 1940). Furthermore, nocturnal primates have relatively larger eyes than diurnal primates, with cathemeral species falling somewhere between the two (Kirk, 2006; Martin, 1990; Ross, 1995), although for Malagasy strepsirhines, this pattern is only valid when cranial length, rather than body mass, is used as a proxy for size (Jungers *et al.,* 2002). Orbit size is not a precise predictor of eye size (eye size actually scales with negative allometry to orbit size), but there is a strong correlation between the two, so that larger orbit size can be interpreted as larger eye size. Larger eyes are thought to have been selected for an increased sensitivity to light, due to larger corneas and pupils (Kirk, 2006). In strepsirhines this pattern is slightly more complicated, as faunivorous species have larger orbits than folivorous or frugivorous species, regardless of their activity pattern (Kirk, 2006).

In addition, orbital convergence correlates negatively with relative orbit size; that is, small primates have relatively large but more laterally placed orbits, while larger primates have relatively small more anteriorly placed orbits (Lieberman, 2000). However, some small nocturnal primates, such as tarsiers and lorises, prove to be an exception to this rule (Lieberman, 2000). In strepsirhines, there is also a negative correlation between orbital frontation (how vertically orientated they are) and convergence (Ross, 1995).

5.2.8. Allometry as a cause of homoplasy

Allometry has been identified as a central cause of homoplasy among primates; with patterns of allometric scaling shared across species and genera and allometric scaling restricting the evolutionary pathways available for cranial shape change (Cardini & Polly, 2013). It follows that species will be likely to produce parallel responses when faced with similar environmental pressures, resulting in homoplasies, which can cloud phylogenetic signal (Hall, 2007).

The presence of such homoplasies can be seen in the phylogenetic history of *Cercocebus* and *Lophocebus* where, as previously discussed, a shared allometric scaling pattern is seen to cloud inferred phylogenetic signal (Singleton, 2002). Similarly, phylogenies generated from papionin craniodental morphometric data were not in accord with the accepted molecular phylogenies for the clade (Collard & Wood, 2001). However, when the same data were first treated to remove any allometrically linked components of shape change, the resulting trees reflected the molecularly determined relationships (Gilbert & Rossie, 2007).

However, allometric shape change is not necessarily all unhelpful noise when it comes to uncovering phylogenetic relationships. Even if allometric traits do evolve in parallel, this pattern would be expected to be specific to different groups. In this sense, allometry could be viewed as a character, which might reveal clues to the relationships between taxa at higher taxonomic levels (Lockwood & Fleagle, 1999). In addition, it is predicted that the influence of size over shape will decay over evolutionary time, as the covariation of shape traits are weakened or modified due to selective pressures (Cardini & Elton, 2008b). The length of evolutionary branches may therefore be a factor in the extent to which allometrically-caused homoplasies obscure phylogenetic signals (Cardini & Elton, 2008b).

5.2.9. The importance of understanding allometry

Within primates, size has a significant impact on cranial shape, with a large proportion of morphological differences attributed to the effects of allometric scaling (Cardini & Elton, 2008b; Collard & O'Higgins, 2001; Elton *et al.,* 2010; Fleagle *et al.,* 2012; Frost *et al.,* 2003; Singleton, 2002). This raises important questions in terms of understanding species' morphology, such as: a) when and why is greater or smaller size selected for?, b) How does shape respond to changes in size so that the integration and functionality of the cranium is maintained, and do different modules of the cranium react differently?, c) To what extent are patterns of allometric scaling shared among taxa, and how might that inform our knowledge of phylogenetic relationships or the homoplasies that might obscure them?, and, finally, d) What selection pressures are strong enough to cause shape change to break away from this evolutionary line of least resistance (Marroig & Cheverud, 2005; Ravosa, 1998)? By exploring these questions, we can hopefully achieve greater clarity on the causes and pathways of morphological evolution.

5.2.10. Aims

To understand the allometric patterns present in the strepsirhine cranium and how these vary both across cranial modules and across species.

To test a re-sampling method that incorporates intra-species variation into inter-species analysis and to compare it with a method that uses species average data.

5.3. Materials and methods

5.3.1. Sample

The sample consisted of 1560 strepsirhine craniums, from 28 species, across 15 genera and 6 families (Table 39). Species were selected on the basis that they had sample sizes of N>20, as analysis of the effect of sample size on GMM studies found that shape parameters can be inaccurately estimated when smaller sample sizes are used (see Chapter 3).

Table 39: Species and sample sizes used in analyses

Family	Genus	Species	Sample size
Cheirogaleidae	*Cheirogaleus*	*major*	25
		medius	29
	Microcebus	*murinus*	72
		rufus	29
Galagidae	*Euoticus*	*elegantulus*	34
	Galago	*alleni*	24
		moholi	73
		senegalensis	175
	Galagoides	*demidoff*	59
		zanzibaricus	25
	Otolemur	*crassicaudatus*	101
		garnettii	95
Indriidae	*Avahi*	*laniger*	23
	Indri	*Indri*	39
	Propithecus	*diadema*	28
		verreauxi	43
Lemuridae	*Eulemur*	*fulvus*	175
		macaco	55
		mongoz	57
		rubriventer	27
	Hapalemur	*griseus*	27
	Lemur	*catta*	34
	Varecia	*variegata*	39
Lepilemuridae	*Lepilemur*	*ruficaudatus*	25
Lorisidae	*Loris*	*tardigradus*	27
	Nycticebus	*bengalensis*	22
		coucang	69
	Perodicticus	*potto*	129

5.3.2. Analyses

Allometry is first investigated in the cranium as a whole, both within and between species. In addition, modules belonging to the two most strongly supported modularity hypotheses for strepsirhines, namely the 2* module model and the Goswami 6 module model (see Chapter 4), are investigated separately, again, both within and between species.

Data for all analyses were first subject to Generalised Procrustes Analysis (GPA; see Chapter 2), which corrects for isometric size, but, crucially, not for allometric changes in shape caused by size (Singleton, 2002).

To investigate the interactions between cranial size and shape, 'size' was estimated as centroid size (CS) and 'shape' was measured using Principal Components (PCs). In geometric morphometrics, CS is defined as the square root of the sum of squared distances of a set of landmarks from their centroid (Slice *et al.*, 1996). Centroid size is the logical choice for a proxy for size in this case, as it is the basis for the Procrustes calculation: moreover, body mass or postcranial measurements which might otherwise be used (Singleton, 2002) are unavailable for these cranial data. The logarithm of centroid size (ln(CS)) is used to ensure that size is comparable across taxa (Mitteroecker *et al.,* 2004). Principal Components Analysis (PCA) was performed on Generalised Procrustes Analysis (GPA) scores to identify the main directions of shape change (Field, 2003) (see Chapter 2). The first 13 PCs were used in all analyses, as they represent the vast majority of change in cranial shape: in most instances, the remaining PCs each explained less than 1% of total shape variation, and never more than 3%.

Previously, species mean scores have been used in inter-species allometry analyses (Baab *et al.,* 2014), potentially resulting in a loss of information relating to intra-species variation. Here the use of species averages is compared with a new resampling approach, designed to include the effect of within-species variation in between species analyses. This new approach selects data from one specimen from each species at random. The specified regression analyses is then performed on that temporary data set, while controlling for phylogenetic relatedness using multi-Independent Contrast analyses (see Chapter 2). This process is repeated 1000 times and the mean model parameters are reported.

5.3.2.1. Intra-species allometry

Intra-species allometry was examined using standard major axis regression. This accounts for the uncertainty in both the *x* and the *y* variable; therefore, rather than calculating the line to minimise the perpendicular distance between the line and the data points, as with major axis regression, it is calculated to minimise the area of triangles formed between the line and data points. Three different approaches were used for each species:

1) PC scores, both for the entire cranium and for each individual module against the size of the overall cranium.
2) PC scores for each individual module against the size of the corresponding modules.
3) The size of each module against the size of the entire cranium.

   Slope values for each species were then evo-mapped across the strepsirhine evolutionary tree, using an Independent Evolution (IE) approach, to illustrate where taxa have moved towards positive or negative allometry (See Chapter 2 for a full explanation of the IE method and evo-mapping procedure).

New GPA and PC were calculated for each species/model.

5.3.2.2. Inter-species allometry

Inter-species allometry, across all 28 species, was first examined using species average size and shape results, where GPA and PCs were calculated using all specimens. Phylogenetic Least Squared Analysis (PGLS) was used to control for the effects of phylogenetic relatedness (see Chapter 2). The three approaches used in the intra-species analyses (above) were again followed. All inter-species analyses were then repeated using the resampling approach described above and controlling for phylogenetic relatedness using multi-Independent Contrast Analysis (see Chapter 2).

5.3.2.3. Percentage of shape change caused by variation in size

The percentage of shape change that can be attributed to size variation was calculated by multiplying the R^2 from the regression analyses, where R^2 is the amount of shape variance explained by size for that PC (Nagelkerke, 1991), by the percentage of shape change explained by the associated PC. Again, this was done for PCs 1-13 relating to the whole cranium and for those PCs describing shape change for the modules of the 2* and Goswami modularity models (see Chapter 4) at an intra- and inter- species level.

5.3.2.4. Inter-species differences in allometric scaling

To test whether species had significant differences in their allometric scaling patterns, ANCOVAs were performed on each possible species pair, where the PC is the dependent variable, the log of centroid size the covariate and species the independent variable. This was done for PCs 1-5 relating to the whole cranium and for the modules of the 2* and Goswami modularity models (see Chapter 4). PC 1-5 were selected as, cumulatively, they explained at least 60% of the total shape variation; with higher PCs individually accounting for only small proportions of variation, often less than 5%.

To illustrate which species share the same allometric trajectories and which do not, using data from all specimens, each PC 1-5 was regressed against ln(CS), while controlling for phylogenetic relationships. The same calculation was then performed using the same size and PC score, but for each species separately. The value of the 'all species' slope was then subtracted from the value of each within-species slope, to quantify the differences between each species' allometric scaling pattern and the inter-species pattern. This was done for the whole cranium and each of 2* and Goswami model modules. These results were then evo-mapped across the strepsirhine evolutionary tree using an Independent Evolution (IE) approach, to show where, when, and in what direction on the tree inter- and intra-specific allometric scaling patterns diverge from each other (see Chapter 2 for a full explanation of the IE method and evo-mapping procedure).

5.4. Results

5.4.1. Intra-species allometry – shape verses size

Here, summary tables list only those PCs that possess a significant relationship with size (Table 40-48). The direction of the correlation is given and the change in shape associated with an increase in size is described. The percentage of shape variation attributed to change in size is also recorded. Changes in shape that are significantly correlated with size are illustrated using wireframe diagrams, with one example given for each family, selected to best illustrate the general allometric pattern for each module (Figure 29-37). Full results of the intra-species regressions for PCs 1-13 against ln(CS), for all modules can be found in Appendix 2. Full results of the percentage of shape change caused by size for PCs 1-13 for all modules can be found in Appendix 4.

For the whole cranium (Table 40; Figure 29), allometry was concentrated in the first 3 PCs. PCs are calculated separately for each species, so the shape change described by each PC can differ from species to species; however, across all species, the over-riding pattern associated with size is a shorter snout and a more globular vault for smaller specimens and a longer snout and a less globular vault for larger specimens, in line with the typical mammalian pattern (Cardini & Polly, 2013). The external auditory meatus also tends to be more posteriorly positioned in larger specimens.

Table 40: Description of shape change associated with increasing size at an intra-species level for the whole cranium. The direction of allometry and the percentage of the shape change that can be attributed to size are indicated for each PC. Only PCs found to be significantly correlated with size (p<0.003) are reported.

Species	PC	+ / - allometry	Shape change associated with PC as size increases	% of shape change associated with size
Cheirogaleus major	1	-	Longer snout, less globular vault, relatively smaller more posteriorly positioned external auditory meatus.	6.39
Microcebus murinus	1	-	Shorter snout, less globular vault, longer and straighter zygomatic arch, relatively smaller, more posteriorly positioned external auditory meatus.	2.85
	2	+	Longer snout, more globular vault, more anteriorly positioned meeting of the superior temporal crest and the coronal suture.	1.55
Microcebus rufus	2	-	Longer snout, less globular vault, relatively smaller more posteriorly positioned external auditory meatus, relatively longer palate, more posteriorly placed zygomatic arch.	7.94
Euoticus elegantulus	2	-	Less globular vault, a more posteriorly positioned meeting of the superior temporal crest and the coronal suture, vault more angled at inion.	3.17
Galago alleni	2	-	Longer snout, less globular vault, more angled inion, relatively smaller and more posteriorly/superiorly positioned external auditory meatus, relatively longer palate, more posteriorly/laterally positioned zygomatic arch.	4.53
Galago moholi	1	+	Less globular vault, relatively longer zygomatic arch.	6.79
Galago senegalensis	1	-	Less globular vault, more laterally positioned zygomatic arch.	1.37
	2	-	Relatively posteriorly positioned nasion and bregma.	0.10
Galagoides demidoff	1	+	Longer snout, less vertical upper face, less globular vault, more angled at inion.	5.77
Otolemur crassicaudatus	1	-	Longer snout, less globular vault, more anteriorly positioned meeting of the superior temporal crest and the coronal suture, relatively long bregma to lambda distance, relatively short lambda to inion distance.	2.16
	3	-	Less globular vault, a longer and more laterally positioned zygomatic arch, relatively smaller external auditory meatus positioned more posteriorly/superiorly/medially.	5.94
Otolemur garnettii	1	-	More anteriorly positioned meeting of the superior temporal crest and the coronal suture, more posteriorly positioned lambda, more laterally positioned zygomatic arch, external auditory meatus positioned more posteriorly and medially.	4.94

	2	+	Less vertical upper face, less globular vault, vault more angled at inion.	0.32
	3	-	More medially positioned meeting point of the superior temporal crest and the coronal suture.	2.01
Indri indri	2	+	Longer snout, less globular cranium, smaller angle between basion and opisthion.	2.12
Propithecus diadema	2	-	Shorter snout, less globular vault, more medial position of the meeting of the superior temporal crest and the coronal suture.	4.88
Propithecus verreauxi	1	+	Relatively longer snout, less globular vault.	0.73
	3	-	Longer and more superiorly positioned snout, less globular vault.	1.77
Eulemur fulvus	1	-	Relatively longer palate, less globular vault, more posteriorly positioned bregma, more medially positioned meeting of the superior temporal crest and the coronal suture.	1.47
	2	-	Relatively longer snout more anteriorly positioned palate and less globular vault.	1.00
	3	-	More superiorly positioned snout, relatively longer palate, less globular vault.	0.50
Eulemur macaco	7	+	Relatively less globular and longer vault.	0.81
Eulemur mongoz	1	-	Longer snout with a less vertical upper face.	6.76
Eulemur rubriventer	2	+	Less globular vault, more medially positioned meeting of the superior temporal crest and the coronal suture.	6.64
Hapalemur griseus	1	+	Longer snout, less vertical upper face and a less globular vault.	10.48
Lemur catta	1	+	More globular vault, more medially positioned meeting of the superior temporal crest and the coronal suture.	5.15
Varecia variegata	2	-	Longer snout, less vertical upper face, longer palate, less globular vault	7.71
Lepilemur ruficaudatus	1	+	Longer snout and palate, less globular vault, more posteriorly positioned meeting of the superior temporal crest and the coronal suture.	11.53
Loris tardigradus	1	-	More superiorly positioned snout, less globular vault, more laterally positioned zygomatic arch and external auditory meatus.	17.59
Nycticebus coucang	3	+	Relatively longer palate, more superiorly and laterally positioned zygomatic arch.	1.29
Perodicticus potto	1	+	Less vertically positioned upper face, less globular vault, more laterally positioned zygomatic arch, more posteriorly positioned external auditory meatus.	2.73

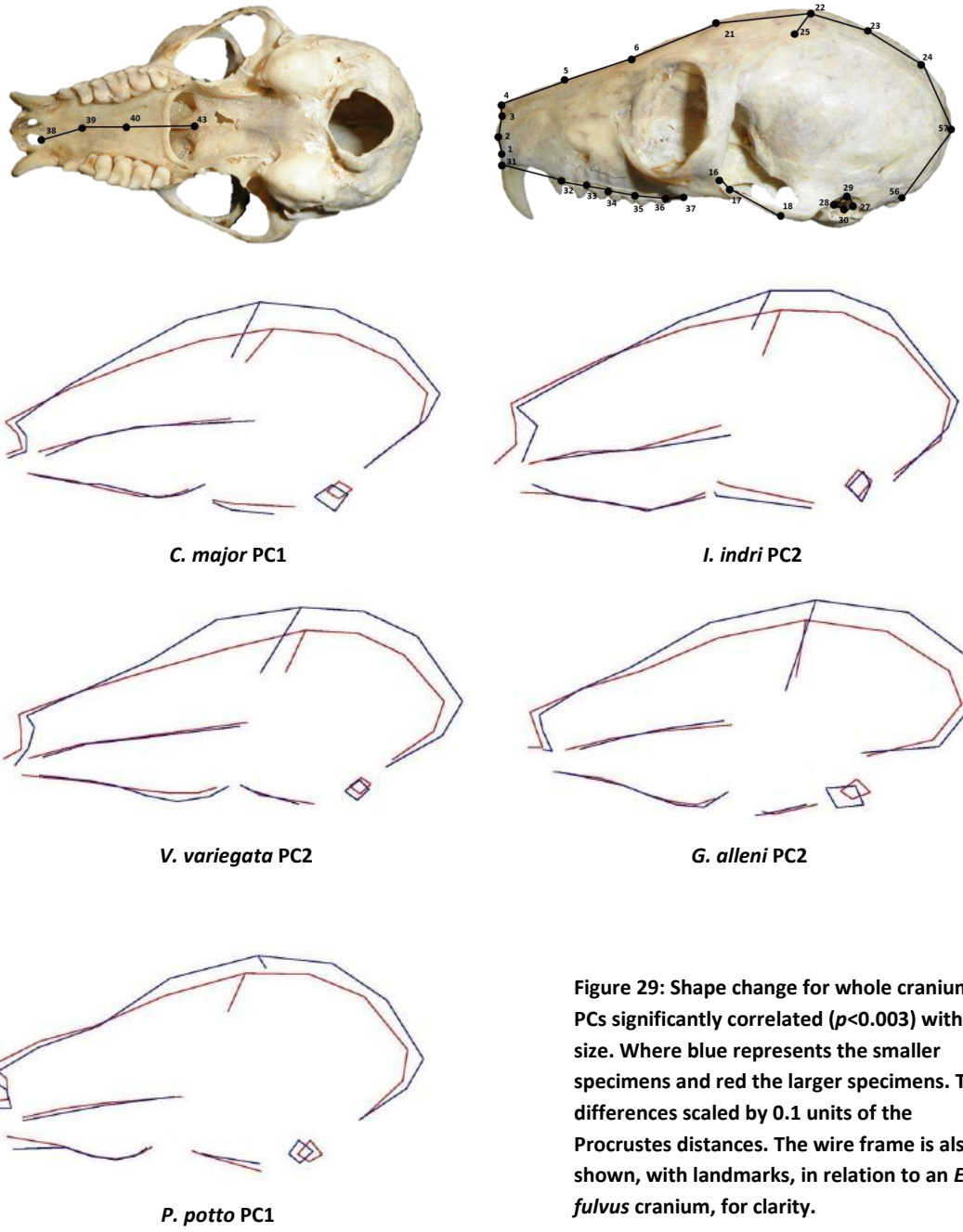

***C. major* PC1**

***I. indri* PC2**

***V. variegata* PC2**

***G. alleni* PC2**

***P. potto* PC1**

Figure 29: Shape change for whole cranium PCs significantly correlated (p<0.003) with size. Where blue represents the smaller specimens and red the larger specimens. The differences scaled by 0.1 units of the Procrustes distances. The wire frame is also shown, with landmarks, in relation to an *E. fulvus* cranium, for clarity.

For the 2* model face module, trends in allometric shape change across species were straighter zygomatic arches with relatively longer zygomaticotemporal sutures and more superiorly positioned zygomaticomaxillary sutures in larger specimens (Table 41; Figure 30). But these trends were not as strong or clear across species as those identified for the whole cranium. The other principal shape change was in the angle of the facial sutures, but the allometric relationship of this trait varied, both across families and genera. The relationships between shape and size were largely the same, regardless of whether the size

of the whole cranium or the size of the face module was used as the independent variable (Table 41).

Table 41: Description of shape change associated with increasing size at an intra-species level for the 2* model face module. The direction of allometry and the percentage of the shape change attributed to size, measured both as the size of the whole cranium and as the size of the face module, are indicated for each PC. Only PCs found to be significantly correlated with size (p<0.003) are reported.

Species	PC	+ / - allometry	Shape change associated with PC as size increases	% shape change associated with	
				whole cranium size	module size
Microcebus murinus	4	-	Superiorly positioned snout, relatively longer zygomaticotemporal suture, straighter zygomatic arch, more superiorly positioned frontozygomatic suture and more posteriorly positioned zygomaticomaxillary suture, indicating a smaller orbit.	1.74	1.89
Microcebus rufus	7	-	Relatively longer zygomaticotemporal suture, more posteriorly positioned zygomatic arch.	1.51	1.34
Galago alleni	3	+	More inferiorly positioned snout, more laterally placed zygomatic arch.	4.05	Not significant
Galago moholi	2	+	Relatively longer zygomaticotemporal suture, straighter zygomatic arch, more anteriorly positioned and vertically orientated zygomaticomaxillary suture.	1.45	1.24
Galago senegalensis	2	+	More posteriorly positioned zygomatic arch, more posteriorly positioned frontozygomatic suture.	2.50	2.64
	3	-	More anteriorly placed frontozygomatic suture, more inferiorly positioned zygomaticomaxillary suture.	0.79	0.88
	4	+	Superiorly positioned snout, inferiorly positioned palate and dentition, more horizontally orientated frontozygomatic suture.	Not significant	0.44
	7	-	More posteriorly positioned end of dentition, more anteriorly positioned frontozygomatic suture, more inferiorly positioned zygomatic arch.	0.50	0.32
Otolemur crassicaudatus	2	-	Relatively longer zygomaticotemporal suture, straighter zygomatic arch, more anteriorly positioned frontozygomatic suture, more horizontally orientated zygomaticomaxillary suture.	4.21	4.77
	4	-	Relatively longer zygomaticotemporal suture, more vertically orientated zygomaticomaxillary suture.	1.76	1.99
Otolemur garnettii	1	-	More vertically orientated zygomaticomaxillary suture, more anteriorly positioned frontozygomatic suture.	8.88	7.75
	2	+	Superiorly positioned frontozygomatic suture, more posteriorly positioned zygomatic arch.	1.04	8.88
Propithecus verreauxi	1	+	More superiorly positioned snout, more inferiorly positioned palate, more vertically oriented zygomaticomaxillary and frontozygomatic sutures.	Not significant	2.96
	2	+	More horizontally orientated zygomaticomaxillary suture.	2.26	3.92
Eulemur fulvus	1	-	More posteriorly and laterally positioned greater palatine foramen.	Not significant	0.64
	9	-	More posteriorly positioned frontozygomatic suture.	0.18	0.26

Eulemur macaco	3	+	Superiorly positioned zygomatic arch, more vertically positioned zygomaticomaxillary suture; as size decreases, the frontozygomatic suture becomes superior at the posterior end, rather than the anterior end, which is otherwise the norm.	2.51	2.1
	4	+	Superiorly positioned snout, inferiorly positioned palate and dentition, more horizontally orientated frontozygomatic suture.	1.21	1.24
Eulemur mongoz	1	+	Relatively longer snout, less vertically orientated upper face, more inferiorly positioned frontozygomatic suture.	5..37	6.19
	5	-	Relatively shorter and less vertically orientated upper face, more posteriorly positioned zygomaticomaxillary suture, more inferiorly positioned frontozygomatic suture, indicating a smaller orbit.	1.71	1.54
Eulemur rubriventer	2	+	Shorter distance between the rhinion and midpoint between rhinion and nasion, relatively longer zygomaticotemporal suture, more superiorly positioned zygomaticomaxillary suture.	3.66	4.27
Lemur catta	2	+	Relatively longer snout, superiorly positioned zygomaticomaxillary suture.	Not significant	2.69
Varecia variegata	2	-	Relatively shorter and more vertically orientated zygomaticomaxillary suture, more inferiorly positioned frontozygomatic suture.	6.38	6.79
Lepilemur ruficaudatus	1	+	Relatively longer snout, less vertically orientated upper face, relatively longer palate and dentition, relatively shorter zygomaticomaxillary suture, more inferiorly positioned frontozygomatic suture.	9.71	11.86
Loris tardigradus	1	+	Inferiorly positioned snout, more vertically orientated zygomaticomaxillary suture, more laterally positioned zygomatic arch.	6.70	Not significant
	2	+	Relatively longer and more vertically orientated frontozygomatic suture, relatively longer zygomaticotemporal suture.	4.03	5.36
Nycticebus coucang	9	+	Relatively longer snout, relatively longer zygomaticotemporal suture.	0.66	0.68
Perodicticus potto	2	-	Relatively longer dentition, relatively longer zygomaticomaxillary suture, relatively longer zygomaticotemporal suture.	1.11	0.83
	6	+	Inferiorly positioned frontozygomatic suture, superiorly positioned and relatively longer zygomaticotemporal suture.	0.88	0.89
	11	+	Superiorly positioned zygomaticomaxillary suture, more vertically orientated zygomatic arch.	0.31	0.39

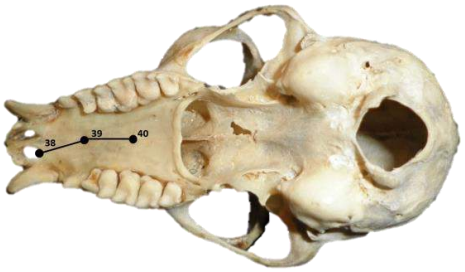

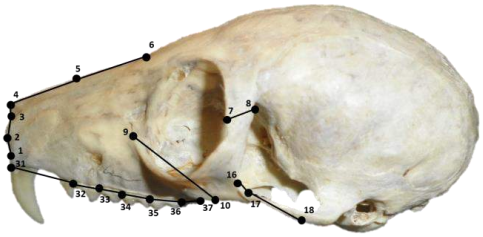

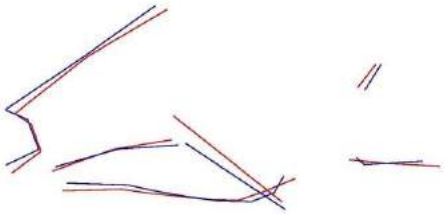

***M. murinus* PC4**

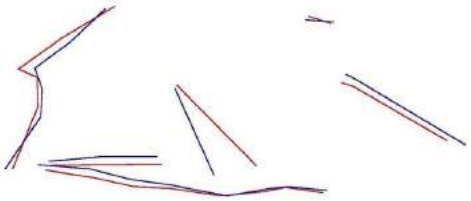

***P. verreauxi* PC2**

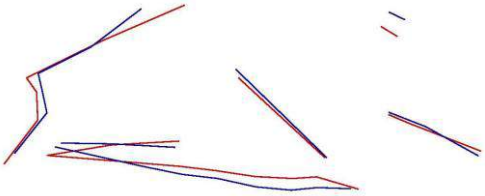

E. mongoz PC1

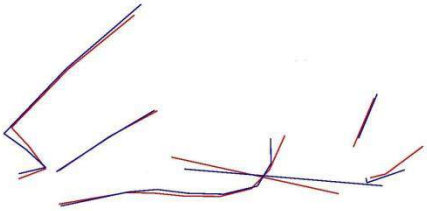

***G. moholi* PC2**

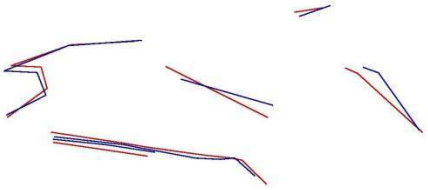

***P. potto* PC2**

Figure 30: Shape change for 2* Model face module PCs significantly correlated (*p*<0.003) with size. As with Figure 29.

Intra-species analysis of the vault module of the 2* model demonstrates several shared aspects of allometric shape change across species (Table 42; Figure 31), the strongest being a less globular vault as size increases. This longer, flatter vault is most often achieved through a relatively longer distance from lambda to inion and a relatively shorter distance from inion to opisthion, although the Indriidae go against this pattern, with a shorter distance between lambda and inion. As size increases there is also a trend for a more posterior meeting of the superior temporal crest and the coronal suture. Other changes in shape include the position of the asterion, the meeting point of the sphenoid, zygomatic and parietal bones, and the meeting point of the zygomatic, parietal and frontal bones, which vary between family and genera as to how they correspond with specimen size.

It is possible to see a shared pattern of allometric shape change within genera, particularly between *Galago moholi,* and *G. senegalensis* (PC1) and *Eulemur fulvus* and *E. macaco* (PC4; Figure 31). However, the traits which are shared, especially those shared by *Galago* species, are also found in other genera.

In general, the same pattern was found, within-species, whether vault shape was regressed against the size of the whole cranium or against the size of the vault module. However, the relationship between vault shape and vault size was significant less often than the relationship between relationship between vault shape and the size of the whole cranium (Table 42).

Table 12: Description of shape change associated with increasing size at an intra-species level for the 2* model vault module. The direction of allometry and the percentage of the shape change attributed to size, measured both as the size of the whole cranium and as the size of the vault module, are indicated for each PC. Only PCs found to be significantly correlated with size (p<0.003) are reported.

Species	PC	+ / - allometry	Shape change associated with PC as size increases	% shape change associated with	
				whole cranium size	module size
Cheirogaleus medius	3	-	Less globular vault, relatively smaller external auditory meatus.	3.85	3.01
Microcebus murinus	2	-	Less globular vault, more posteriorly positioned meeting of the superior temporal crest and the coronal suture, more posteriorly positioned asterion, marginally inferiorly positioned external auditory meatus.	1.54	Not significant
	4	-	Marginally more globular vault, relatively larger external auditory meatus.	0.78	Not significant
Microcebus rufus	2	+	Less globular vault, more angled at inion.	6.91	7.91
Galago moholi	1	-	Less globular vault, more medially positioned meeting of the superior temporal crest and the coronal suture.	5.06	1.45
Galago senegalensis	1	-	Less globular vault, more medially positioned meeting of the superior temporal crest and the coronal suture.	3.45	2.05
	3	-	Less globular vault, relatively longer cranial base.	0.48	0.35
	12	-	Superiorly positioned anterior vault, less globular posterior vault.	0.13	0.13
Galagoides demidoff	1	+	Less globular vault, relatively longer distance between lambda and inion, relatively shorter distance between inion and opisthion.	6.73	1.87
Galagoides zanzibaricus	1	-	Less globular vault, relatively longer distance between lambda and inion, relatively shorter distance between inion and opisthion, more anteriorly positioned meeting point of sphenoid, zygomatic and parietal bones, more anteriorly positioned meeting point of zygomatic, frontal and parietal bones.	6.03	Not significant
Otolemur crassicaudatus	1	+	More anteriorly positioned meeting of the superior temporal crest and the coronal suture.	1.75	2.26
	4	+	Relatively shorter distance between bregma and lambda, more inferiorly positioned meeting point of sphenoid, zygomatic and parietal bones, more inferiorly positioned meeting point of zygomatic, frontal and parietal bones.	2.28	2.4
Otolemur garnettii	3	-	Relatively longer distance between bregma and lambda, relatively smaller external auditory meatus.	2.28	2.7
	8	-	Relatively shorter distance between bregma and lambda, relatively shorter distance between lambda and inion, relatively longer distance between inion and opisthion.	Not significant	0.27
Indri indri	7	-	Less globular vault, relatively shorter distance between lambda and inion.	1.17	Not significant
Propithecus diadema	2	-	Less globular vault, relatively longer distance between bregma and lambda, relatively shorter distance between lambda and inion, relatively longer distance between ionion and opisthion.	3.48	4.3

Eulemur fulvus	1	-	Less globular vault, more anteriorly positioned meeting of the superior temporal crest and the coronal suture more inferiorly positioned meeting point of sphenoid, zygomatic and parietal bones, more inferiorly positioned meeting point of zygomatic, frontal and parietal bones.	2.4	Not significant
	4	+	Less globular vault, relatively greater distance between bregma and lambda, more superiorly positioned meeting point of sphenoid, zygomatic and parietal bones, more superiorly positioned meeting point of zygomatic, frontal and parietal bones.	0.82	0.7
Eulemur macaco	4	+	Less globular vault, relatively greater distance between bregma and lambda, more superiorly positioned meeting point of sphenoid, zygomatic and parietal bones, more inferiorly positioned meeting point of zygomatic, frontal and parietal bones.	Not significant	1.42
Eulemur rubriventer	1	-	Less globular vault, relatively shorter distance between bregma and lambda, more medially positioned meeting of the superior temporal crest and the coronal suture.	7.22	Not significant
Lemur catta	1	-	More posteriorly positioned meeting of the superior temporal crest and the coronal suture, more anteriorly positioned asterion, more anteriorly positioned meeting point of sphenoid, zygomatic and parietal bones, more anteriorly positioned meeting point of zygomatic, frontal and parietal bones.	6.27	Not significant
Varecia variegata	1	+	More anteriorly positioned meeting of the superior temporal crest and the coronal suture.	Not significant	5.73
Lepilemur ruficaudatus	1	-	Less globular vault, more medially positioned meeting of the superior temporal crest and the coronal suture.	5.00	4.48
Loris tardigradus	1	-	Les globular vault, more anteriorly positioned external auditory meatus, more medially positioned meeting of the superior temporal crest and the coronal suture.	16.55	15.45
Perodicticus potto	1	+	More anteriorly positioned meeting of the superior temporal crest and the coronal suture, more superiorly positioned meeting point of sphenoid, zygomatic and parietal bones, more superiorly positioned meeting point of zygomatic, frontal and parietal bones.	1.06	1.34
	3	-	Less globular vault, more inferiorly positioned asterion.	1.11	0.75
	4	-	Less globular vault, relatively shorter distance between bregma and lambda, relatively longer distance between lambda and inion, relatively shorter distance between inion and opisthion.	0.49	Not significant

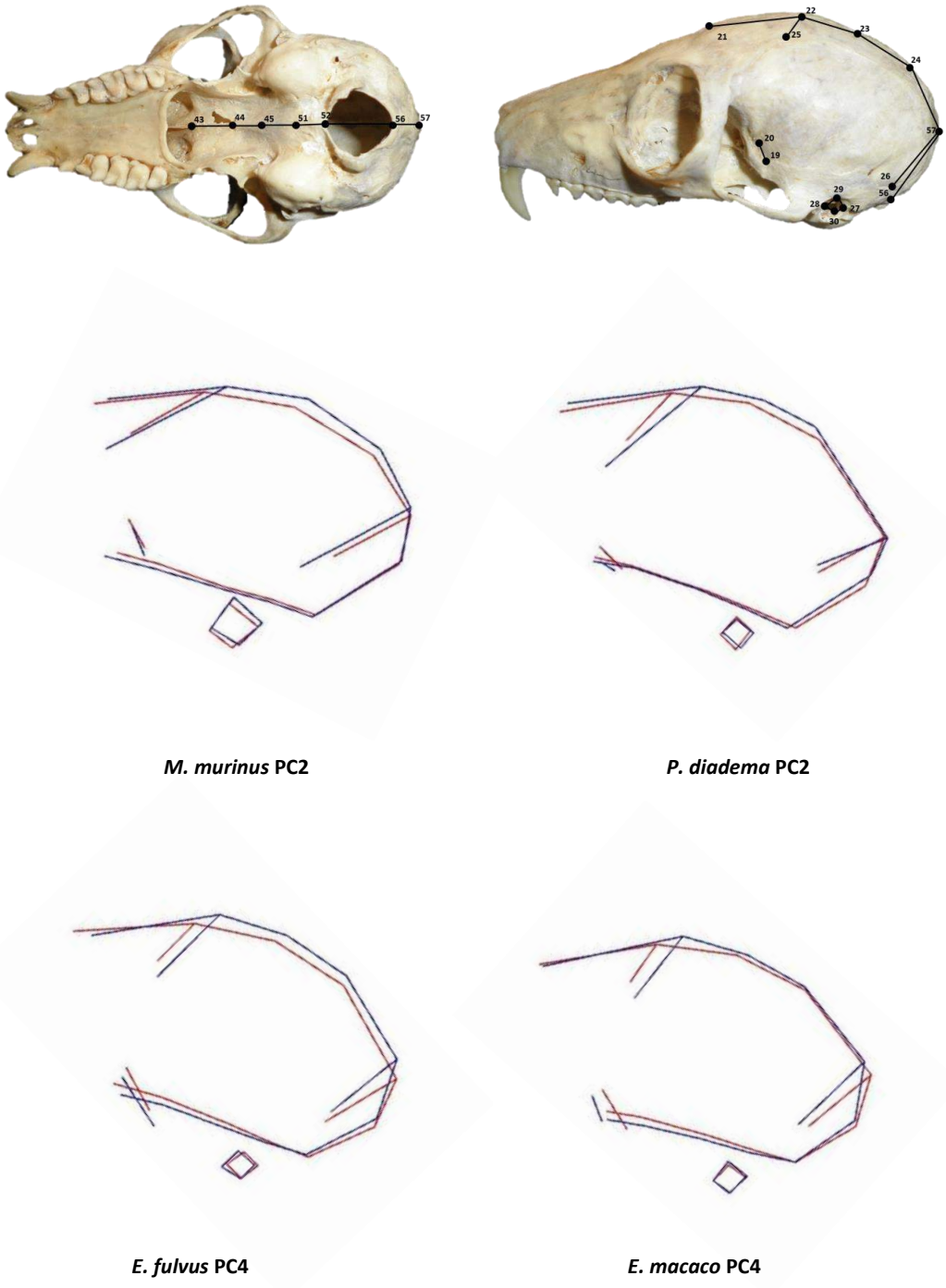

Figure 31: Shape change for 2* Model vault module PCs significantly correlated (*p*<0.003) with size. As with Figure 29.

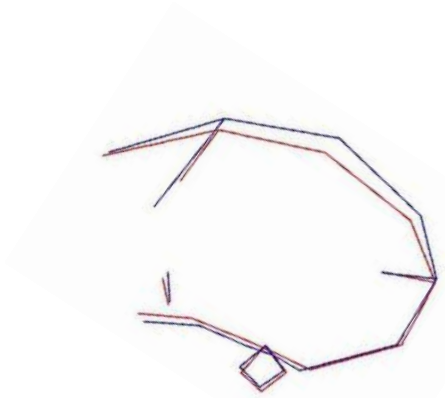

***G. moholi* PC1**

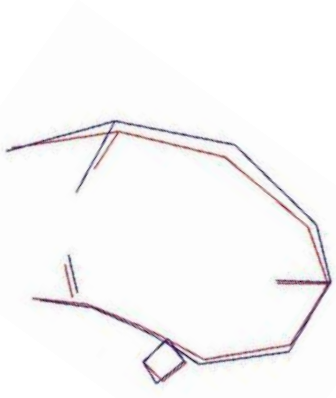

***G. senegalensis* PC1**

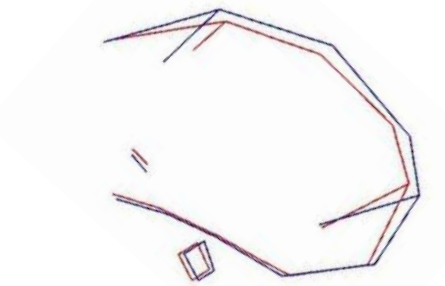

***L. tardigradus* PC1**

Figure 31 (Cont.)

For the Goswami model face module (Table 43; Figure 32), there are two consistent traits across species associated with larger size: specifically, an inferiorly positioned snout (but see *P. verreauxi*) and an inferior positioning of the canine septum. With the exception of these trends, the shape changes associated with allometric scaling are varied across families and genera. The regression of face PCs against the size of the face module were significant for more species than the regression of face PCs against overall cranium size (Table 43); this was also true for the 2* model face module (Table 41).

Table 43: Description of shape change associated with increasing size at an intra-species level for the Goswami model face module. The direction of allometry and the percentage of the shape change attributed to size, measured both as the size of the whole cranium and as the size of the face module, are indicated for each PC. Only PCs found to be significantly correlated with size (p<0.003) are reported.

Species	PC	+ / - allometry	Shape change associated with PC as size increases	% shape change associated with	
				whole cranium size	module size
Cheirogaleus medius	4	+	Relatively shorter distance between rhinion and the midpoint between rhinion and nasion, relatively longer palate.	3.19	3.23
Microcebus rufus	2	+	Inferiorly positioned snout, relatively longer and superiorly positioned palate.	Not significant	4.95
Galago alleni	1	+	More anteriorly positioned nasospinale, relatively larger piriform aperture, less vertically orientated upper face.	8.96	Not significant
Galago senegalensis	3	-	Relatively longer distance between rhinion and the midpoint between rhinion and nasion.	0.83	0.58
	4	+	Inferiorly positioned snout, more anteriorly and superiorly positioned nasospinale.	0.02	Not significant
	5	+	Inferiorly positioned widest part of piriform aperture, relatively longer and superiorly positioned palate.	Not significant	0.59
	7	-	Inferiorly and posteriorly positioned nasospinale, reactively shorter palate.	0.40	0.34
Galagoides demidoff	1	-	Inferiorly positioned snout, more anteriorly and superiorly positioned nasospinale, more posteriorly positioned palate.	Not significant	6.04
Otolemur crassicaudatus	4	+	Longer snout.	1.56	0.98
Otolemur garnettii	1	-	More inferiorly positioned canine septum, relatively longer distance between rhinion and midpoint between rhinion and nasion.	2.33	1.67
	3	-	Relatively shorter distance between rhinion and the midpoint between rhinion and nasion, relatively longer palate, more inferiorly positioned canine septum.	1.24	1.42
Propithecus verreauxi	1	-	More anteriorly and superiorly positioned snout, more posteriorly positioned nasospinale, relatively shorter palate.	6.00	6.92
	2	-	Relatively larger piriform aperture.	Not significant	3.45
Eulemur macaco	2	-	More inferiorly positioned canine septum, more posteriorly positioned meeting point of the maxilla and palatine along the midline.	Not significant	3.93
	8	+	Relatively taller but narrower piriform aperture, superiorly positioned snout.	Not significant	0.65
Lemur catta	2	+	Longer snout, more posteriorly positioned nasospinale.	4.89	4.05
Varecia variegata	1	+	More inferiorly positioned snout, relatively smaller piriform aperture, more superiorly positioned canine septum.	Not significant	5.69
Nycticebus coucang	2	-	Inferiorly positioned canine septum.	Not significant	1.69
Perodicticus potto	11	+	Less vertically orientated upper face.	0.23	0.23

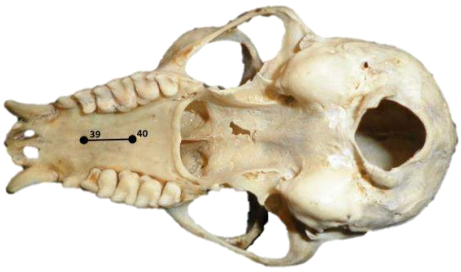

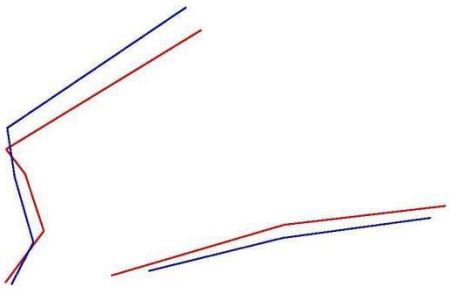

***M. rufus* PC2**

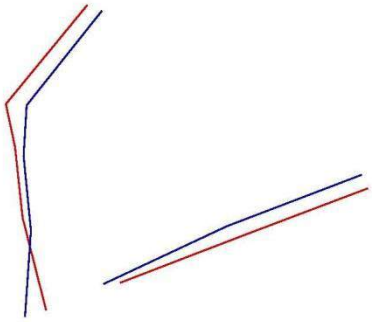

***P. verreauxi* PC1**

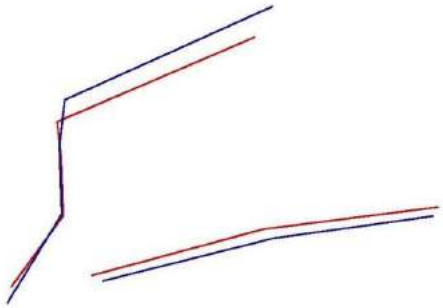

***V. variegata* PC1**

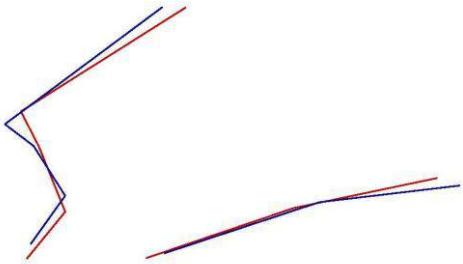

***G. alleni* PC1**

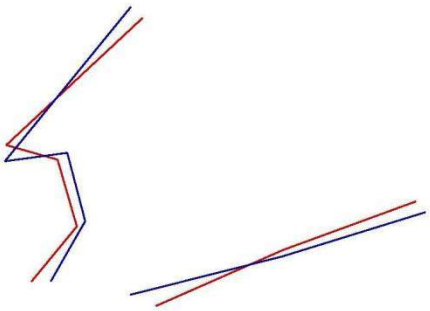

***P. potto* PC11**

Figure 32: Shape change for Goswami Model face module PCs significantly correlated (p<0.003) with size. As with Figure 29.

The shape change for the Goswami model orbit module shows very few consistent relationships between size and traits across species (Table 44; Figure 33). While the zygomatic foramen tended to be more anteriorly positioned, and the infraorbital foramen more posteriorly positioned, in larger specimens (possibly portraying the longer face associated with larger size), the relationship of other traits with size, including the position of the nasion, optical foramen and nasolacrimal foramen, as well as the length, position and orientation of the zygomaticomaxillary and frontozygomatic sutures, varied across species, with no evident family- or genera-wide patterns.

Shape change was significantly related to the size of the whole cranium more often than it was related to the size of the orbit module (Table 44).

Table 44: Description of shape change associated with increasing size at an intra-species level for the Goswami model orbit module. The direction of allometry and the percentage of the shape change attributed to size, measured both as the size of the whole cranium and as the size of the face module, are indicated for each PC. Only PCs found to be significantly correlated with size (p<0.003) are reported.

Species	PC	+ / - allometry	Shape change associated with PC as size increases	% shape change associated with	
				whole cranium size	module size
Cheirogaleus medius	5	+	More anteriorly positioned zygomatic and infraorbital foramen, relatively shorter zygomaticomaxillary suture, relatively longer and more vertically orientated frontozygomatic suture.	2.57	Not significant
Galago alleni	3	+	Relatively wider angle between nasion-optical foramen-nasolacrimal foramen, more inferiorly positioned zygomaticomaxillary suture, more posteriorly positioned infraorbital foramen, more anteriorly positioned zygomatic foramen, relatively shorter frontozygomatic suture.	3.32	Not significant
Galago moholi	8	-	More inferiorly and posteriorly positioned optical foramen, more anteriorly positioned zygomatic foramen, more vertically orientated frontozygomatic suture.	0.43	Not significant
Galago senegalensis	1	-	Relatively longer and more horizontally orientated zygomaticomaxillary suture, more anteriorly positioned frontozygomatic suture.	1.55	1.56
	2	-	More superiorly positioned nasion, more anteriorly positioned zygomatic foramen, relatively shorter and more horizontally orientated zygomaticomaxillary suture, more vertically orientated frontozygomatic suture.	1.68	1.32
	5	-	More anteriorly positioned zygomatic suture, more superiorly positioned nasolacrimal foramen, more anteriorly positioned frontozygomatic suture.	0.80	Not significant
	7	-	More anteriorly positioned optical foramen, more superiorly and anteriorly positioned nasolacrimal foramen, more posteriorly positioned frontozygomatic suture.	Not significant	0.72

	11	-	More anteriorly and superiorly positioned optical foramen, more posteriorly and inferiorly positioned nasolacrimal foramen, more superiorly positioned infraorbital foramen, more vertically orientated zygomaticomaxillary suture.	Not significant	0.11
Otolemur crassicaudatus	2	+	More anteriorly positioned zygomatic foramen, superiorly orientated optical foramen, more posteriorly orientated nasolacrimal foramen.	4.58	4.79
	3	+	More posteriorly positioned infraorbital foramen, more superiorly and posteriorly positioned nasion, more inferiorly and anteriorly positioned optical foramen, more inferiorly positioned nasolacrimal foramen, more anteriorly positioned and horizontally orientated frontozygomatic suture.	1.52	1.19
	4	+	More inferiorly and posteriorly positioned optical foramen, more posteriorly positioned zygomatic foramen, relatively longer zygomaticomaxillary suture, more anteriorly positioned and horizontally orientated frontozygomatic suture.	0.66	Not significant
Otolemur garnettii	1	-	More anteriorly and inferiorly positioned posterior point of zygomaticomaxillary suture, more superiorly and posteriorly positioned frontozygomatic suture.	5.66	Not significant
	2	-	Relatively wider angle between nasion-optical foramen-nasolacrimal foramen.	3.60	3.69
	5	-	More posteriorly positioned infraorbital foramen, relatively longer and more vertically orientated zygomaticomaxillary suture, more anteriorly positioned nasion, more anteriorly and inferiorly positioned optical foramen, more posteriorly and inferiorly positioned nasolacrimal foramen.	0.89	0.87
Propithecus diadema	11	+	Relatively wider angle between nasion-optical foramen-nasolacrimal foramen, more vertically orientated zygomaticomaxillary suture, relatively longer and more horizontally orientated frontozygomatic suture.	0.56	0.49
Eulemur mongoz	2	-	More anteriorly positioned zygomatic foramen, relatively shorter zygomaticomaxillary suture, relatively shorter frontozygomatic suture, more inferiorly positioned nasion, more posteriorly positioned optical foramen, more superiorly positioned nasolacrimal foramen.	Not significant	2.12
Eulemur rubriventer	1	-	Relatively smaller angle between nasion-optical foramen-nasolacrimal foramen, more posteriorly positioned zygomaticomaxillary suture, more inferiorly positioned frontozygomatic suture.	9.36	11.66
Varecia variegata	2	-	More anteriorly positioned zygomatic foramen, more posteriorly positioned infraorbital foramen, more anteriorly and posteriorly positioned nasion, more posteriorly positioned nasolacrimal foramen, relatively and more vertically orientated zygomaticomaxillary suture.	7.21	6.94
Loris tardigradus	5	+	More anteriorly positioned zygomatic foramen, more posteriorly positioned infraorbital foramen, more vertically orientated zygomaticomaxillary suture relatively shorter and more horizontally orientated frontozygomatic suture.	2.26	2.08

Nycticebus coucang	10	-	More anteriorly positioned zygomatic foramen, more posteriorly positioned infraorbital foramen, more vertically orientated zygomaticomaxillary suture relatively longer and more horizontally orientated frontozygomatic suture, more superiorly positioned nasion, more posteriorly positioned optical foramen.	0.26	Not significant
Perodicticus potto	2	+	More inferiorly and posteriorly positioned zygomaticomaxillary foramen, relatively longer and more vertically orientated zygomaticomaxillary suture, relatively shorter and more horizontally orientated frontozygomatic suture, more anteriorly and inferiorly positioned nasion.	1.96	2.23
	4	+	Relatively wider angle between nasion-optical foramen-nasolacrimal foramen, more anteriorly positioned zygomatic foramen, more posteriorly positioned infraorbital foramen, relatively longer and more vertically orientated zygomaticomaxillary suture, more superiorly positioned frontozygomatic suture.	1.09	1.29
	5	+	More posteriorly positioned infraorbital foramen, more anteriorly positioned nasion, more superiorly positioned optical foramen.	0.67	0.47

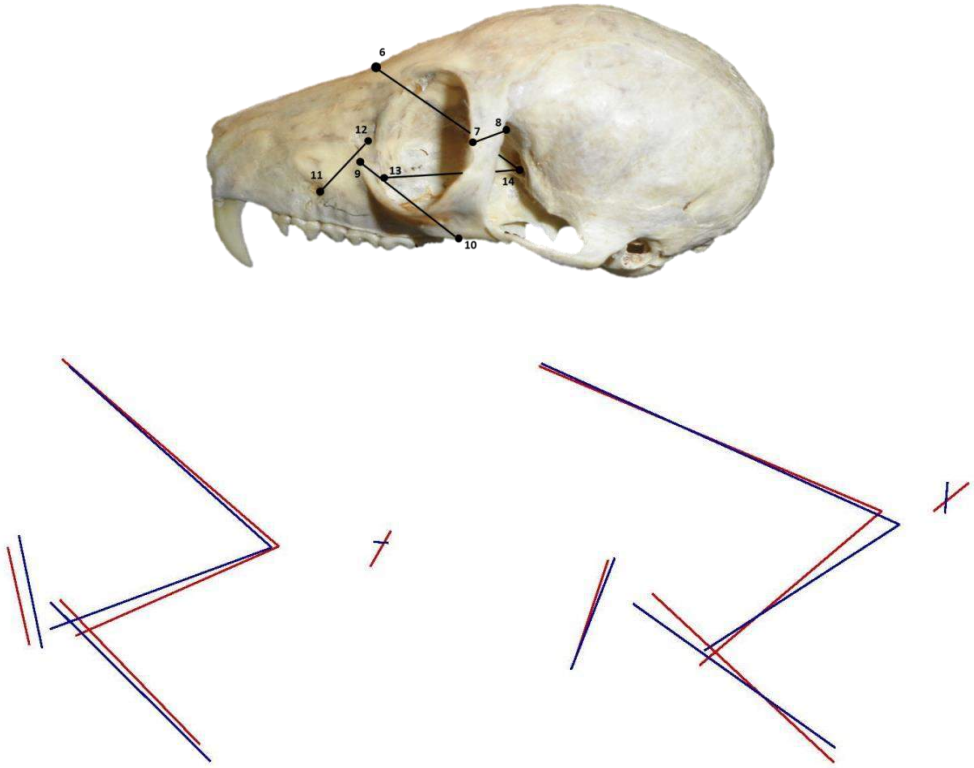

***C. medius* PC5** ***P. diadema* PC11**

Figure 33: Shape change for Goswami Model orbit module PCs significantly correlated (p<0.003) with size. As with Figure 29.

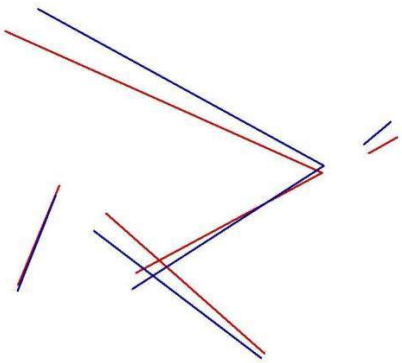

***E. rubriventer* PC1**

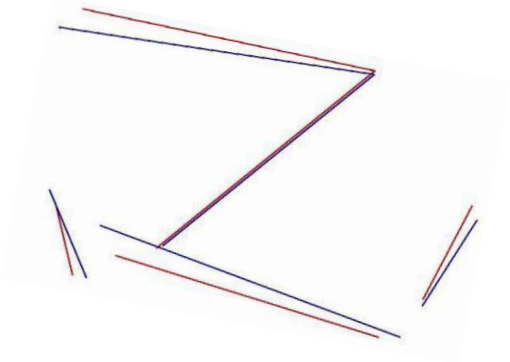

***G. senegalensis* PC2**

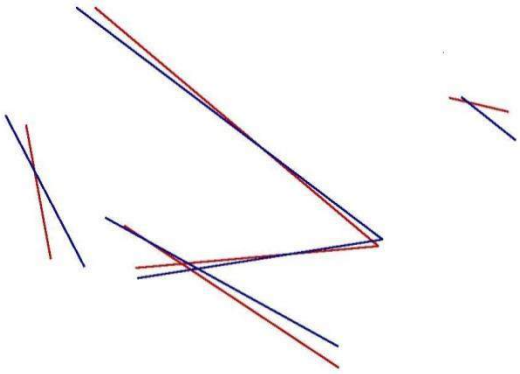

***L. tardigradus* PC1**

Figure 33 (Cont.)

A strong across species trend is seen in the allometric scaling of the Goswami oral module (Table 45; Figure 34), with a more lateral placement of the anterior end of the dentition (mesial P3), the posterior end of the dentition positioned more closely to the midline, a more lateral placement of the greater palatine foramen and a more posteriorly positioned tip of the nasal spine are seen as size increases. While this shape change is common across most species (excluding the Lorisidae), the shape change associated with size is even more similar within families. Specifically within the Lemuridae, which all closely follow the above pattern, and the Lorisidae, which have a more anteriorly positioned end of dentition, a more anteriorly placed greater palatine foramen, and a more posteriorly positioned tip of the nasal spine. Shape change was more often significantly related to the size of the oral module, rather than the size of the whole cranium. Again this pattern was stronger within the Lemuridae and the Lorisidae (Table 45).

Table 45: Description of shape change associated with increasing size at an intra-species level for the Goswami model oral module. The direction of allometry and the percentage of the shape change attributed to size, measured both as the size of the whole cranium and as the size of the face module, are indicated for each PC. Only PCs found to be significantly correlated with size (p<0.003) are reported.

Species	PC	+ / - allometry	Shape change associated with PC as size increases	% shape change associated with	
				whole cranium size	module size
Cheirogaleus medius	2	-	Mesial P3 septum more laterally positioned, more medially positioned end of dentition, more laterally positioned greater palatine foramen, more posteriorly positioned tip of nasal spine.	Not significant	6.10
Microcebus murinus	2	+	More medially positioned end of dentition, more laterally positioned greater palatine foramen, more posteriorly positioned tip of nasal spine.	4.66	12.09
Galago moholi	3	+	Relatively shorter distance between mesial P3 septum and end of dentition, more posteriorly positioned greater palatine foremen, more posteriorly positioned tip of nasal spine	1.38	Not significant
Galago senegalensis	2	-	More posteriorly positioned greater palatine foramen, more posteriorly positioned tip of nasal spine.	Not significant	5.40
	3	-	Mesial P3 septum more laterally positioned, more medially positioned end of dentition, more laterally positioned greater palatine foramen, more posteriorly position tip of nasal spine.	1.45	1.07
	6	+	More medially positioned mesial P3 septum, mesial P4 septum and end of dentition, molar 1 septum and molar 2 septum positioned more laterally.	0.29	Not significant
Otolemur crassicaudatus	2	-	Molar 1 septum and end of dentition more anteriorly and medially positioned, more posteriorly positioned tip of nasal spine.	5.73	8.05
	4	+	End of dentition positioned more anteriorly and more laterally, more laterally positioned greater palatine foramen, more medially positioned tip of nasal spine.	0.50	Not significant
Otolemur garnettii	1	-	More posteriorly positioned greater palatine foramen.	5.14	7.83
	2	-	Mesial P3 septum more laterally positioned, more medially positioned end of dentition, more laterally positioned greater palatine foramen, more posteriorly position tip of nasal spine.	5.67	5.23
Indri indri	1	-	More posteriorly positioned greater palatine foramen, more posteriorly positioned tip of nasal spine.	Not significant	24.20
Propithecus verreauxi	2	-	Mesial P3 septum and mesial P4 septum more laterally positioned, more medially positioned molar 3 septum and end of dentition, more posteriorly positioned greater palatine foramen, more posteriorly positioned tip of nasal spine.	Not significant	5.69
Eulemur fulvus	2	-	Mesial P3 septum and mesial P4 septum more laterally positioned, more medially positioned molar 3 septum and end of dentition, more posteriorly and laterally positioned greater palatine foramen, more posteriorly positioned tip of nasal spine.	Not significant	8.62
Eulemur macaco	2	+	Mesial P3 septum and mesial P4 septum more laterally positioned, more medially positioned molar 3 septum and end of dentition, more posteriorly and laterally positioned greater palatine foramen, more posteriorly positioned tip of nasal spine.	Not significant	8.86

Eulemur mongoz	3	-	Mesial P3 septum more laterally positioned, more medially positioned end of dentition, more medially positioned greater palatine foramen, tip of nasal spine more laterally positioned.	1.73	2.11
Lemur catta	1	-	Mesial P3 septum more laterally positioned, more medially positioned end of dentition, more anteriorly positioned greater palatine foramen, more posteriorly positioned tip of nasal spine.	Not significant	16.63
Varecia variegata	2	-	Mesial P3 septum more laterally positioned, more medially positioned end of dentition positioned, more posteriorly positioned greater palatine foramen, more posteriorly positioned tip of nasal spine.	Not significant	3.36
Loris tardigradus	2	-	More medially positioned end of dentition, more posteriorly positioned tip of nasal spine.	9.34	15.33
Nycticebus bengalensis	1	+	More anteriorly positioned end of dentition, more anteriorly positioned greater palatine foramen, more posteriorly positioned tip of nasal spine.	Not significant	17.44
Nycticebus coucang	1	+	More anteriorly positioned end of dentition, more anteriorly positioned greater palatine foramen, more posteriorly positioned tip of nasal spine.	Not significant	9.13
Perodicticus potto	1	+	More anteriorly positioned end of dentition, more anteriorly positioned greater palatine foramen, more posteriorly positioned tip of nasal spine.	Not significant	9.71
	8	-	More laterally positioned molar 1 septum.	0.31	0.19

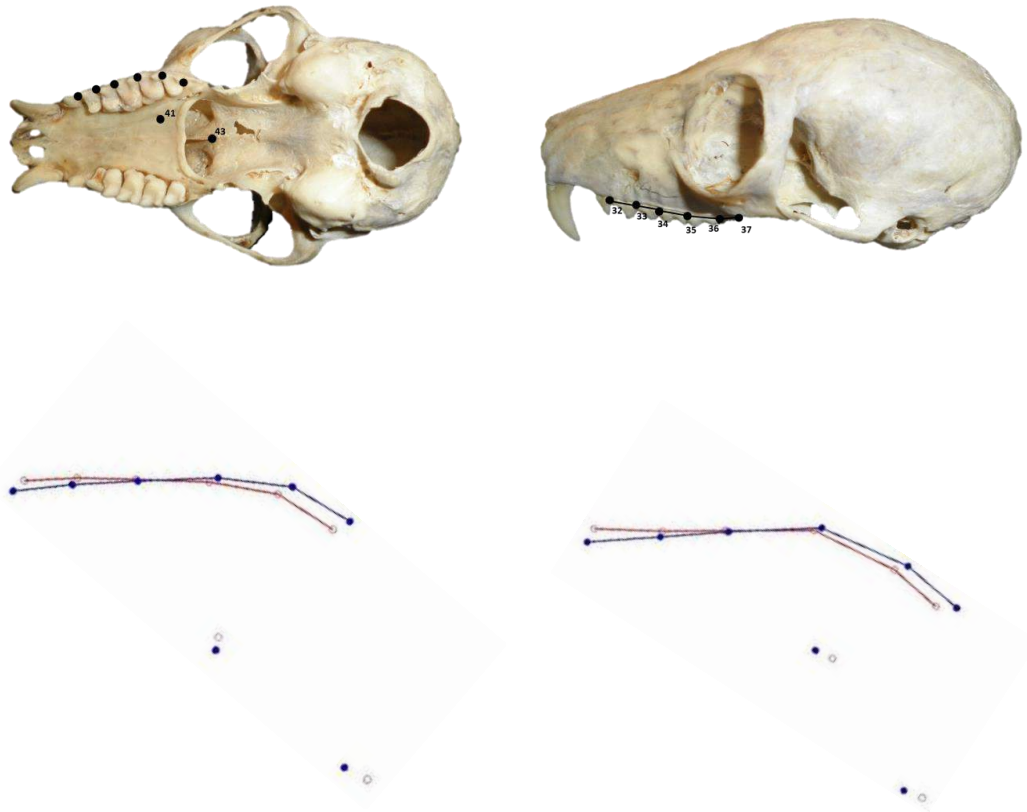

***M. murinus* PC2** ***P. verreauxi* PC2**

Figure 34: Shape change for Goswami Model oral module PCs significantly correlated (p<0.003) with size. As with Figure 29. For this module the wireframe shows an inferior view, with individual landmarks marked so that the greater palatine foreman and tip of the nasal spine (where shape change is concentrated)

***E. fulvus* PC2**

***O. crassicaudatus* PC2**

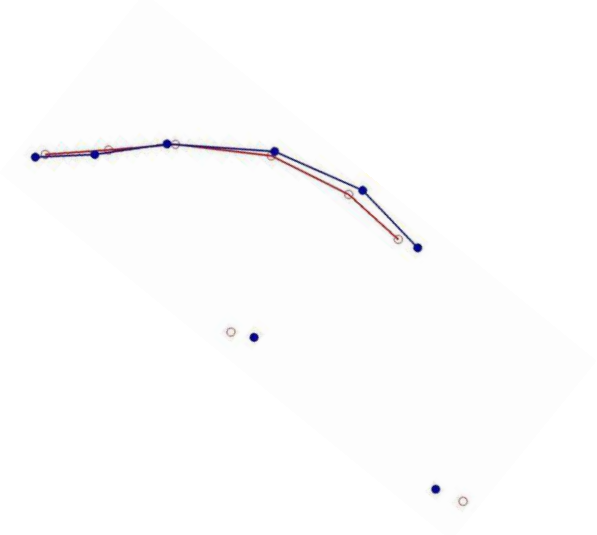

***N. bengalensis* PC2**

Figure 34 (Cont.)

Within the Goswami model zygomatic module (Table 46; Figure 35), there are some characters that appear to behave in the same way across species as size increases; the cranial base becomes narrower, the distance between the meeting point of presphenoid-basisphenoid and basisphenoid-basioccipital, in the midline, becomes longer (although see *O. garnettii*), and the foramen lavelli is positioned more laterally. With the exception of these more general trends, the other traits associated with the module (the position of the petrous apex, tip of the post-glenoid fossa and the mandibular fossa, and the length and position of the zygomaticotemporal suture) vary in their relationship to size across both families and genera.

While the general pattern and direction of the relationship between shape and size was similar for both whole cranium size and zygomatic module size, the relationship with PCs is rarely significant for both size variables simultaneously (Table 46). There were no apparent reoccurring trends across species for shape change significantly associated with size (Table 46).

Table 46: Description of shape change associated with increasing size at an intra-species level for the Goswami model zygomatic module. The direction of allometry and the percentage of the shape change attributed to size measured both as the size of the whole cranium and as the size of the face module, are indicated for each PC. Only PCs found to be significantly correlated with size (p<0.003) are reported.

Species	PC	+ / - allometry	Shape change associated with PC as size increases	% shape change associated with	
				whole cranium size	module size
Microcebus murinus	1	+	Relatively narrower base, as indicated by smaller distance between mandibular fossa and the midline, more posteriorly positioned petrous apex and foramen lavelli.	Not significant	2.92
Microcebus rufus	2	-	Relatively longer distance between meeting point of presphenoid-basisphenoid and basisphenoid-basioccipital in the midline, more laterally positioned foramen lavelli, more posteriorly positioned mandibular fossa.	Not significant	4.86
Galago moholi	1	-	Relatively longer zygomaticotemporal suture, relatively straighter zygomatic arch, more medially positioned tip of postglenoid process.	3.04	Not significant
Galago senegalensis	2	-	Relatively shorter zygomaticotemporal suture, relatively more curved zygomatic arch, more laterally positioned tip of postglenoid process.	Not significant	0.51
Euoticus elegantulus	2	-	Relatively narrower base, as indicated by smaller distance between mandibular fossa and the midline, more posteriorly positioned petrous apex, relatively shorter zygomaticotemporal suture, more curved zygomatic arch, more laterally and anteriorly positioned tip of postglenoid process.	Not significant	3.92
Otolemur crassicaudatus	1	-	Relatively shorter zygomaticotemporal suture, relatively less curved zygomatic arch, more posteriorly positioned tip of postglenoid process and mandibular fossa, more medially positioned posterior-most point on curvature of anterior margin of zygomatic process of temporal bone.	2.65	Not significant
	2	+	Relatively narrower base, as indicated by smaller distance between mandibular fossa and the midline and relatively shorter distance between petrous apex and foramen lavelli, relatively longer zygomaticomaxillary suture.	3.12	Not significant
	6	+	Relatively longer distance between meeting point of presphenoid-basisphenoid and basisphenoid-basioccipital in the midline, more posteriorly positioned foramen lavelli, more posteriorly positioned tip of postglenoid process.	Not significant	0.55
Otolemur garnettii	1	+	Relatively narrower base, as indicated by smaller distance between mandibular fossa and the midline, relatively shorter distance between meeting point of presphenoid-basisphenoid and basisphenoid-basioccipital in the midline, more medially positioned tip of postglenoid fossa, more laterally positioned zygomatic arch.	5.83	6.21

	6	-	Relatively narrower base, as indicated by smaller distance between mandibular fossa and the midline, relatively shorter distance between meeting point of presphenoid-basisphenoid and basisphenoid-basioccipital in the midline, more anteriorly placed petrous apex, more posteriorly placed foramen lavelli, more posteriorly placed mandibular fossa.	0.66	0.81
	9	-	More anteriorly and laterally positioned petrous apex, more posteriorly positioned mandibular fossa and tip of postglenoid process, more medially positioned posterior-most point on curvature of anterior margin of zygomatic process of temporal bone.	0.48	Not significant
Propithecus diadema	4	+	Relatively longer distance between meeting point of presphenoid-basisphenoid and basisphenoid-basioccipital in the midline, more anteriorly positioned petrous apex, more posteriorly positioned foramen lavelli, more medially positioned zygomaticomaxillary.	4.16	2.95
Eulemur fulvus	2	+	Relatively shorter distance between meeting point of presphenoid-basisphenoid and basisphenoid-basioccipital in the midline, more medially positioned tip of postglenoid fossa and mandibular fossa, zygomaticomaxillary suture positioned more laterally.	Not significant	0.80
	8	-	Relatively narrower base, as indicated by smaller distance between mandibular fossa and the midline, more medially positioned tip of postglenoid process, posterior-most point on curvature of anterior margin of zygomatic process of temporal bone more laterally positioned, petrous apex and foramen lavelli more posteriorly positioned.	0.45	0.68
	9	-	Relatively longer distance between meeting point of presphenoid-basisphenoid and basisphenoid-basioccipital in the midline, more anteriorly positioned petrous apex, more medially positioned mandibular fossa and tip of postglenoid process, posterior-most point on curvature of anterior margin of zygomatic process of temporal bone more laterally positioned.	0.18	Not significant
	11	-	More posteriorly positioned petrous apex, more posteriorly positioned foramen lavelli, more medially positioned tip of postglenoid process.	0.15	Not significant
Eulemur mongoz	1	-	Relatively longer distance between meeting point of presphenoid-basisphenoid and basisphenoid-basioccipital in the midline, more posteriorly positioned petrous apex, more posteriorly and laterally positioned foramen lavelli, relatively more curved zygomatic arch.	5.63	Not significant
	2	+	More anteriorly positioned petrous apex, relatively longer zygomaticotemporal suture.	Not significant	2.93
Loris tardigradus	4	-	Relatively narrower base, as indicated by smaller distance between mandibular fossa and the midline, more anteriorly positioned petrous apex, more posteriorly positioned foramen lavelli, more posteriorly positioned tip of postglenoid fossa.	Not significant	2.95
Perodicticus potto	2	-	Relatively narrower base, as indicated by smaller distance between mandibular fossa and the midline, more anteriorly positioned petrous apex, more posteriorly positioned foramen lavelli, more posteriorly and medially positioned tip of postglenoid fossa, relatively longer and more medially positioned zygomaticotemporal suture.	Not significant	0.92

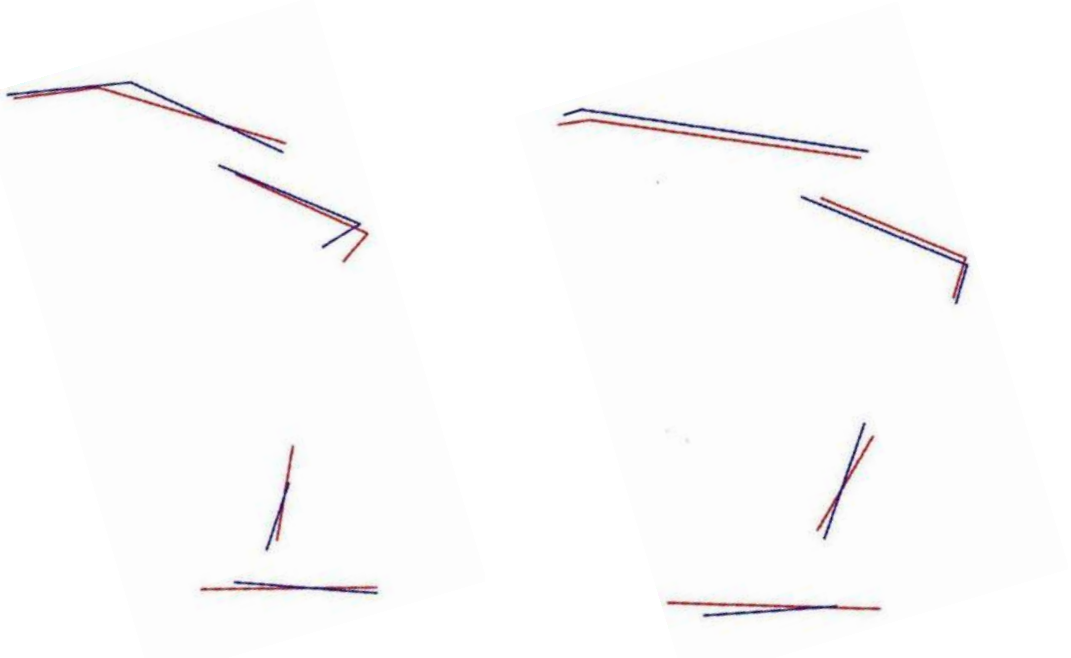

***M. rufus* PC2** ***P. diadema* PC4**

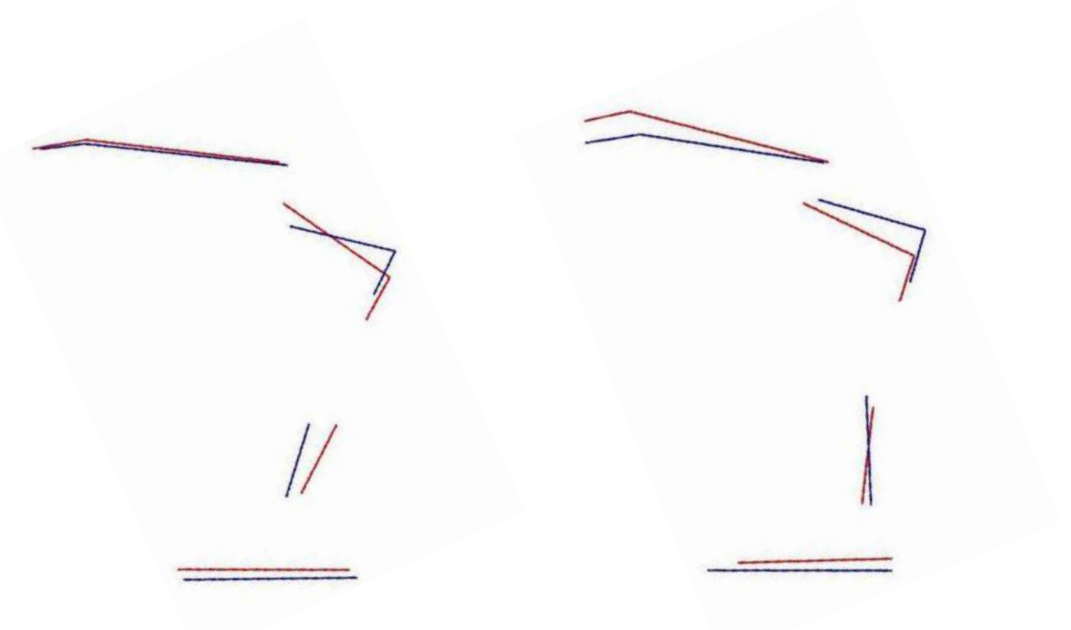

***E. fulvus* PC8** ***O. garnettii* PC1**

Figure 35: Shape change for Goswami Model zygomatic module PCs significantly correlated with size. As with Figure 29. For this module the wireframe shows an inferior view.

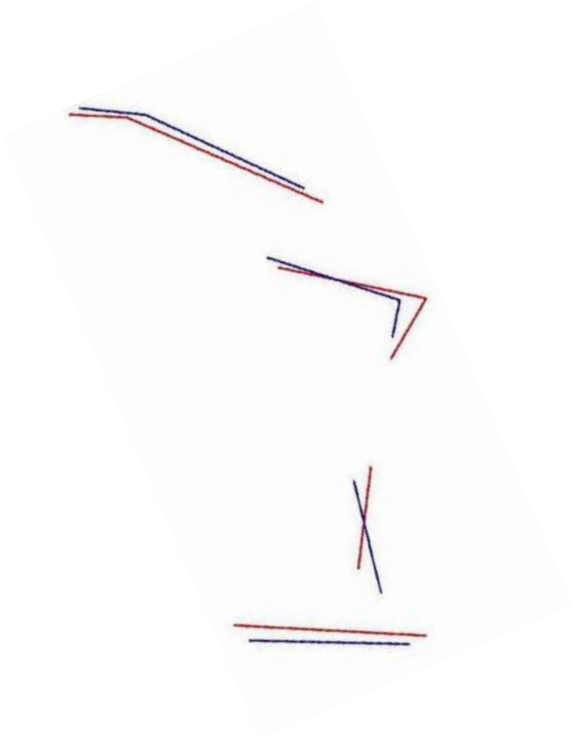

***L. tardigradus* PC8**

Figure 35 (Cont.)

The allometric shape change seen in the vault module, as defined by the Goswami model (Table 47; Figure 36), follows the general mammalian trend (Cardini & Polly, 2013), also seen in the whole cranium (Table 40; Figure 29) and 2* model vault module (Table 42; Figure 31), where an increase in size results in a less globular vault. Other shared trends across species associated with increased size include a more medially positioned meeting of the superior temporal crest and the coronal suture, which could potentially correspond to the narrower cranium recorded in larger specimens for the Goswami zygomatic module above, although there are exceptions (see *I. indri, E. macaco* and *P. potto).* With greater size, the asterion also tends to be more posteriorly located, although again there are exceptions (*O. garnettii* and *A. laniger*). Other traits, such as the position of bregma, lambda and inion and the position of the meeting points of the sphenoid, zygomatic and parietal bone, and of the zygomatic, frontal and parietal bone, varied in their relationship with size across families and genera.

Within families and genera, some species have very similar patterns of shape change related to size, specifically the Cheirogaleidae (*Microcebus* sp.), the Galagidae (*G. senegalensis* and *G. demidoff*) and the Indriidae (*I. indri* and *P. diadema*). In addition, both the Cheirogaleidae and the Galagidae have more significant relationships between vault

shape and overall skull size than between vault shape and the size of the size of the vault module, while the reverse is true for the Indriidae (Table 47).

Table 47: Description of shape change associated with increasing size at an intra-species level for the Goswami model vault module. The direction of allometry and the percentage of the shape change attributed to size, measured as both the size of the whole cranium and as the size of the vault module, are indicated for each PC. Only PCs found to be significantly correlated with size (p<0.003) are reported.

Species	PC	+ / - allometry	Shape change associated with PC as size increases	% shape change associated with	
				whole cranium size	module size
Microcebus murinus	1	+	Less globular vault, more anteriorly positioned basion, more posteriorly positioned inion, more posteriorly positioned asterion, more medially positioned meeting of the superior temporal crest and the coronal suture.	3.64	Not significant
Microcebus rufus	2	+	Less globular vault, more anteriorly positioned basion, more posteriorly positioned inion, more posteriorly and superiorly positioned asterion, more medially positioned meeting of the superior temporal crest and the coronal suture, more superiorly positioned meeting point of sphenoid, zygomatic and parietal bone, more superiorly meeting point of zygomatic, frontal and parietal bone.	5.87	8.59
Galago moholi	1	+	Less globular vault, more superiorly and medially positioned meeting of the superior temporal crest and the coronal suture, more inferiorly positioned meeting point of sphenoid, zygomatic and parietal bone, inferiorly positioned meeting point of zygomatic, frontal and parietal bone.	7.80	Not significant
Galago senegalensis	1	+	Less globular vault, more medially positioned meeting of the superior temporal crest and the coronal suture, more inferiorly and anteriorly positioned meeting point of sphenoid, zygomatic and parietal bone, more inferiorly and anteriorly positioned meeting point of zygomatic, frontal and parietal bone.	6.25	Not significant
Galago demidoff	1	+	Less globular vault, more posteriorly positioned inion, more posteriorly and medially positioned meeting of the superior temporal crest and the coronal suture, more posteriorly and superiorly positioned asterion, more anteriorly positioned meeting point of sphenoid, zygomatic and parietal bone, more anteriorly positioned meeting point of zygomatic, frontal and parietal bone.	5.11	Not significant
Otolemur crassicaudatus	1	+	More anteriorly and distally positioned meeting of the superior temporal crest and the coronal suture, more superiorly positioned meeting point of sphenoid, zygomatic and parietal bone, more superiorly meeting point of zygomatic, frontal and parietal bone.	3.15	9.08
	3	-	Less globular vault, more posteriorly positioned inion, more medially positioned meeting of crest and suture on frontal bone, more posteriorly and medially positioned asterion, more superiorly and anteriorly positioned meeting point of sphenoid, zygomatic and parietal bone, more superiorly and anteriorly meeting point of zygomatic, frontal and parietal bone.	1.26	1.14

Otolemur garnettii	2	+	Less globular vault, more posteriorly positioned lambda, superiorly positioned inion, more anteriorly and medially positioned meeting of the superior temporal crest and the coronal suture, more superiorly and medially positioned meeting point of sphenoid, zygomatic and parietal bone, more superiorly and medially meeting point of zygomatic, frontal and parietal bone.	1.69	Not significant
	3	-	More globular vault, inferiorly positioned inion, more anteriorly positioned meeting point of crest and suture on the frontal bone, more anteriorly positioned asterion, more anteriorly positioned meeting point of sphenoid, zygomatic and parietal bone, more anteriorly meeting point of zygomatic, frontal and parietal bone.	0.75	1.80
Avahi laniger	1	+	More posteriorly and inferiorly positioned lambda, more anteriorly positioned inion, more anteriorly and medially positioned meeting of the superior temporal crest and the coronal suture, more anteriorly and superiorly positioned asterion, more posteriorly and superiorly positioned meeting point of sphenoid, zygomatic and parietal bone, more posteriorly and superiorly meeting point of zygomatic, frontal and parietal bone.	Not significant	9.91
Indri indri	1	-	More anteriorly and laterally positioned meeting of the superior temporal crest and the coronal suture, more posteriorly and superiorly positioned meeting point of sphenoid, zygomatic and parietal bone, more posteriorly and superiorly meeting point of zygomatic, frontal and parietal bone.	Not significant	7.14
Propithecus diadema	1	-	More anteriorly positioned meeting of the superior temporal crest and the coronal suture, more posteriorly and superiorly positioned meeting point of sphenoid, zygomatic and parietal bone, more posteriorly and superiorly meeting point of zygomatic, frontal and parietal bone.	Not significant	14.47
Eulemur fulvus	1	+	More inferiorly and posteriorly positioned bregma, more posteriorly and medially positioned meeting of the superior temporal crest and the coronal suture, more anteriorly and inferiorly positioned meeting point of sphenoid, zygomatic and parietal bone, more anteriorly and inferiorly meeting point of zygomatic, frontal and parietal bone.	5.32	Not significant
Eulemur macaco	3	-	More anteriorly and laterally positioned meeting of the superior temporal crest and the coronal suture, more posteriorly and superiorly positioned meeting point of sphenoid, zygomatic and parietal bone, more posteriorly and superiorly meeting point of zygomatic, frontal and parietal bone.	Not significant	2.04
Lemur catta	1	+	More posteriorly and medially positioned meeting of the superior temporal crest and the coronal suture, more anteriorly, inferiorly and medially positioned meeting point of sphenoid, zygomatic and parietal bone, more anteriorly, inferiorly and medially meeting point of zygomatic, frontal and parietal bone.	9.84	Not significant
	3	+	Less globular vault, more anteriorly positioned bregma, more posteriorly positioned lambda, more anteriorly positioned meeting point of sphenoid, zygomatic and parietal bone, more anteriorly meeting point of zygomatic, frontal and parietal bone.	Not significant	3.85

	10	-	Less globular vault, more posteriorly placed bregma, more inferiorly placed inion, more anteriorly and medially positioned meeting of the superior temporal crest and the coronal suture, more posteriorly and superiorly positioned asterion, more posteriorly, superiorly and distally positioned meeting point of sphenoid, zygomatic and parietal bone, more posteriorly, inferiorly and distally positioned meeting point of zygomatic, frontal and parietal bone.	0.41	Not significant
Loris tardigradus	2	-	Less globular vault, more posteriorly and medially positioned meeting of the superior temporal crest and the coronal suture, more posteriorly and inferiorly positioned asterion, more anteriorly and superiorly positioned meeting point of sphenoid, zygomatic and parietal bone, more anteriorly and inferiorly positioned meeting point of zygomatic, frontal and parietal bone.	9.25	Not significant
Perodicticus potto	1	+	More anteriorly and distally positioned meeting of the superior temporal crest and the coronal suture, more superiorly positioned meeting point of sphenoid, zygomatic and parietal bone, more superiorly positioned meeting point of zygomatic, frontal and parietal bone.	Not significant	3.85

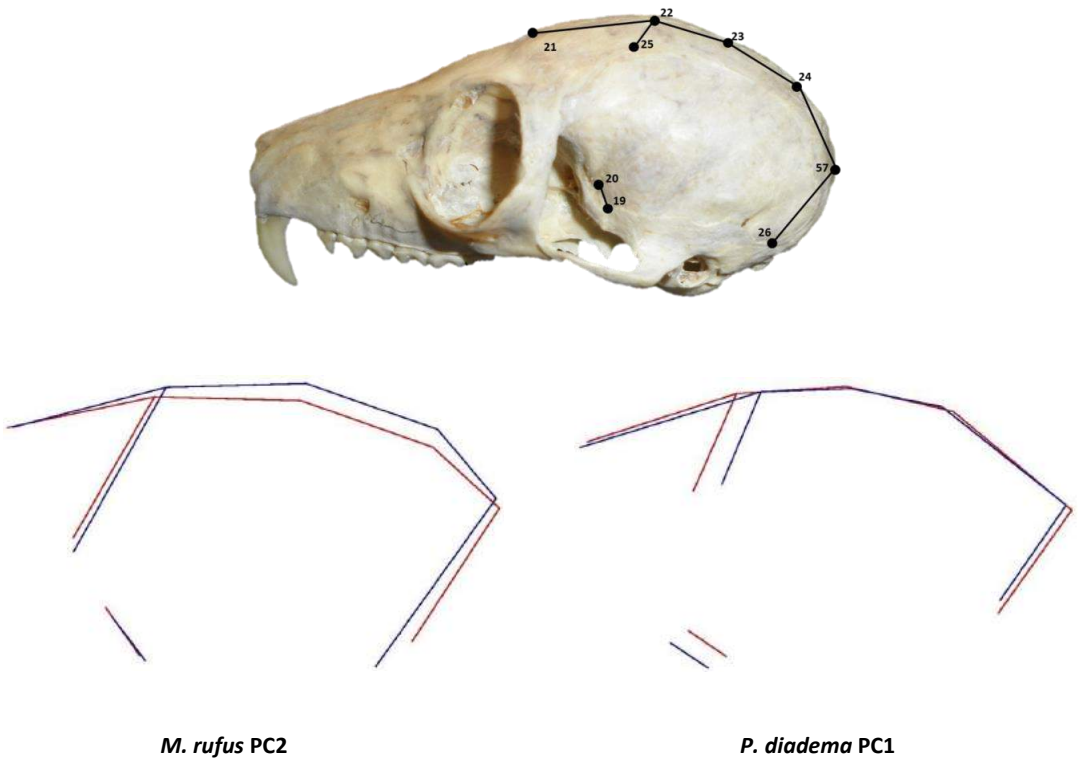

***M. rufus* PC2** ***P. diadema* PC1**

Figure 36: Shape change for Goswami Model vault module PCs significantly correlated with size. As with Figure 29.

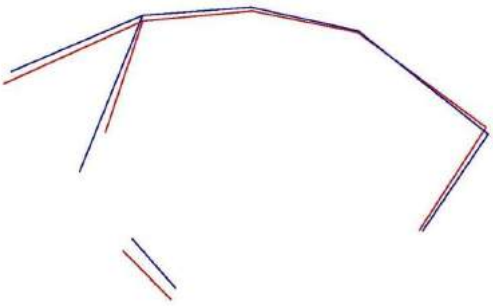

***L. catta* PC1**

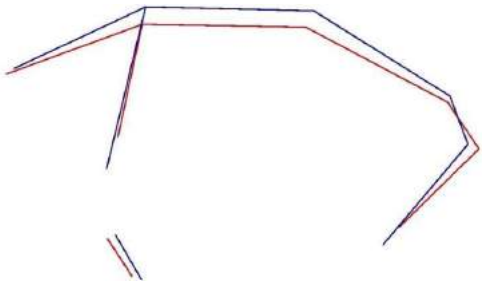

***G. demidoff* PC1**

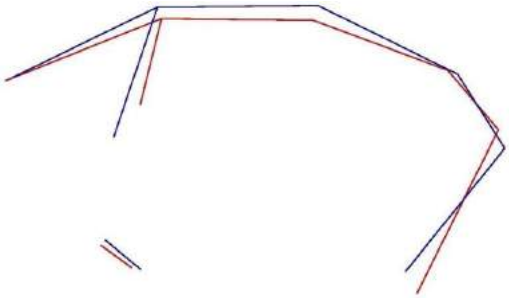

***L. tardigradus* PC2**

Figure 36 (Cont.)

The base module of the Goswami model has some traits that change in the same way across species in relation to size (Table 48; Figure 37). As size increases the external auditory meatus becomes relatively smaller (but see *N. coucang*) and, in many cases, more posteriorly positioned; this is in line with results found for the whole cranium. Also, as size increases, the distance between the basion and the opisthion is relatively smaller (but see *M. murinus*). This is achieved through both a more posteriorly positioned basion and a more anteriorly positioned opisthion. The position of the occipital condyle also shows a similar relationship with size across species; specifically, the anterior-most point is positioned more medially and the posterior-most point is positioned more distally. This trend is particularly strong among the Galagidae. The positioning of the basion, opisthion and the occipital condyle could be seen to indicate a smaller anterior-posterior, but larger medial-distal, size of the foramen magnum, as size increases. In contrast, the size, position and orientation of the jugular foramen, varies across families and genera. The relationship between the shape of the base module and size is similar, whether size is taken as the size of the overall cranium or the size of the base module (Table 48).

Table 48: Description of shape change associated with increasing size at an intra-species level for the Goswami model base module. The direction of allometry and the percentage of the shape change attributed to size, measured as both the size of the whole cranium and as the size of the vault module, are indicated for each PC. Only PCs found to be significantly correlated with size (p<0.003) are reported.

Species	PC	+ / - allometry	Shape change associated with PC as size increases	% shape change associated with	
				whole cranium size	module size
Cheirogaleus medius	1	-	Relatively smaller and more posteriorly positioned external auditory meatus, more anteriorly positioned jugular foramen.	Not significant	6.63
Microcebus murinus	2	-	Relatively smaller external auditory meatus, more posteriorly positioned jugular foramen, more inferiorly positioned opisthion, more superiorly positioned basion.	2.71	1.64
	3	+	Relatively smaller external auditory meatus, relatively longer distance between basion and opisthion, relatively smaller jugular foramen, more superiorly and posteriorly positioned opisthion, more anteriorly positioned basion, more medially positioned anterior-most point of occipital condyle.	1.42	Not significant
	4	-	Relatively smaller jugular foramen, more superiorly and medially positioned posterior-most point of occipital condyle, more superiorly and anteriorly positioned opisthion, more inferiorly and posteriorly positioned basion.	Not significant	0.96
Microcebus rufus	1	+	Relatively smaller external auditory meatus, more posteriorly positioned and larger jugular foramen, more anteriorly and superiorly positioned opisthion, more medially positioned anterior-most point of occipital condyle, more distally positioned posterior-most point of occipital condyle.	5.89	5.35
Galago moholi	1	+	Relatively smaller external auditory meatus, more anteriorly positioned jugular foramen, more medially placed optical foramen.	Not significant	4.85
Galago senegalensis	1	+	Relatively smaller external auditory meatus, more anteriorly positioned jugular foramen, more medially positioned anterior-most point of occipital condyle, more distally positioned posterior-most point of occipital condyle.	1.55	7.69
	8	-	More laterally positioned jugular foramen, more medially positioned anterior-most point of occipital condyle, more distally positioned posterior-most point of occipital condyle.	0.30	Not significant
Galago demidoff	7	-	Relatively smaller external auditory meatus, more medially placed jugular foramen, more medially positioned anterior-most point of occipital condyle, more distally positioned posterior-most point of occipital condyle.	Not significant	0.63
Otolemur crassicaudatus	2	+	Relatively smaller and more laterally positioned external auditory meatus, more anteriorly positioned jugular foramen, more medially positioned anterior-most point of occipital condyle, more distally positioned posterior-most point of occipital condyle.	1.86	3.91
Otolemur garnettii	2	-	Relatively shorter distance between basion and opisthion, more medially positioned anterior-most point of occipital condyle, more laterally positioned jugular foramen.	3.59	1.20
	3	-	Relatively smaller and more laterally positioned external auditory meatus, more anteriorly positioned jugular foramen, more medially positioned anterior-most point of occipital condyle, more distally positioned posterior-most point of occipital condyle.	1.08	3.19

Propithecus diadema	2	+	Relatively larger external auditory meatus, relatively shorter distance between basion and opisthion, more medially positioned anterior-most point of occipital condyle, more anteriorly positioned and laterally orientated jugular foramen.	4.39	Not significant
Eulemur fulvus	2	-	Relatively shorter distance between basion and opisthion, more posteriorly positioned basion, more anteriorly positioned opisthion, more posteriorly positioned anterior-most point of occipital condyle, more medially positioned posterior-most point of occipital condyle, more medially positioned jugular foramen.	0.62	Not significant
Eulemur macaco	3	-	More posteriorly and laterally positioned external auditory meatus, relatively shorter distance between basion and opisthion, more posteriorly positioned basion, more anteriorly positioned opisthion, more posteriorly positioned anterior-most point of occipital condyle, more distally positioned posterior-most point of occipital condyle, more medially and anteriorly positioned jugular foramen.	1.93	1.63
Loris tardigradus	1	-	Relatively smaller external auditory meatus, Relatively shorter distance between basion and opisthion, more posteriorly positioned basion, more anteriorly positioned opisthion, more medially positioned anterior-most point of occipital condyle, more distally positioned posterior-most point of occipital condyle, more medially and anteriorly positioned jugular foramen.	15.50	18.88
Nycticebus bengalensis	2	-	Relatively smaller external auditory meatus, relatively shorter distance between basion and opisthion, more posteriorly positioned basion, more anteriorly positioned opisthion, more medially positioned occipital condyle, more medially positioned jugular foramen.	Not significant	7.67
Nycticebus coucang	1	+	More posteriorly positioned external auditory meatus, relatively shorter distance between basion and opisthion, more posteriorly positioned basion, more anteriorly positioned opisthion, relatively shorter occipital condyle, more distally positioned posterior-most point of occipital condyle, more medially positioned and relatively shorter jugular foramen.	3.66	6.99
	2	-	Relatively larger external auditory meatus, relatively shorter distance between basion and opisthion, more posteriorly positioned basion, more medially positioned anterior-most point of occipital condyle, more distally positioned posterior-most point of occipital condyle, more medially and anteriorly positioned jugular foramen.	Not significant	2.63

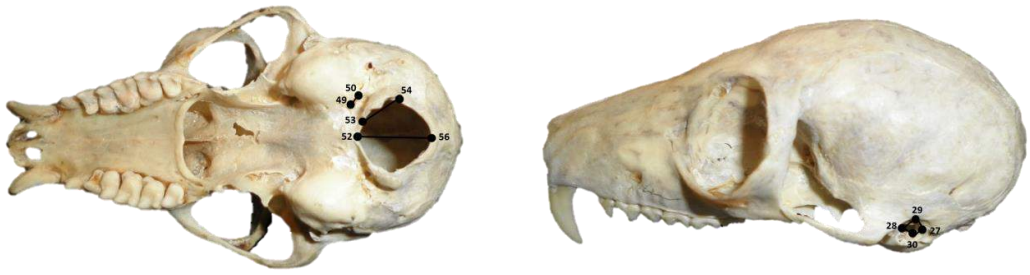

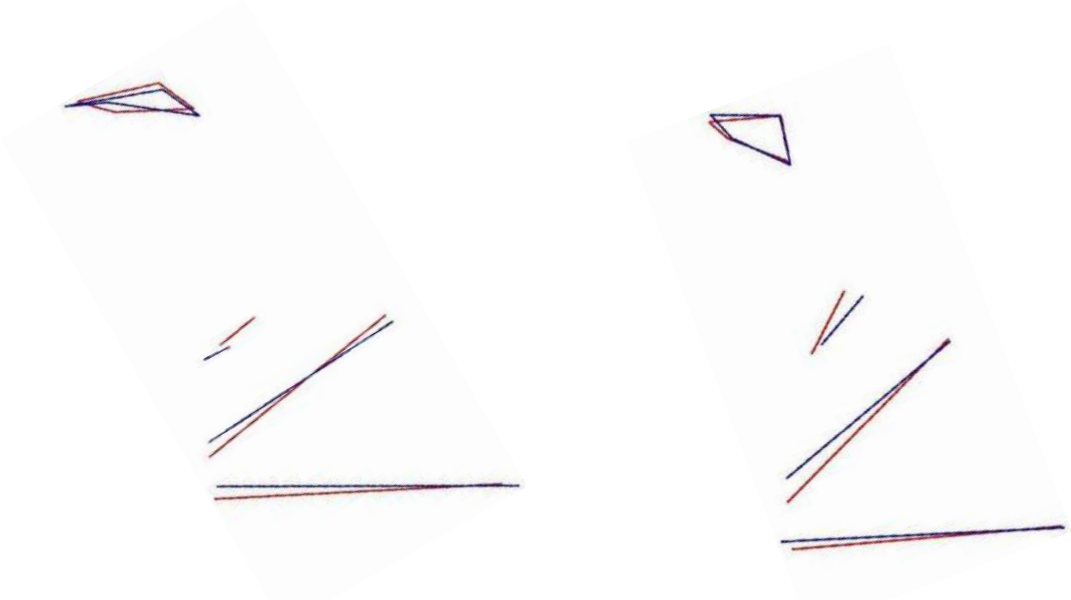

***M. rufus* PC1** ***P. diadema* PC2**

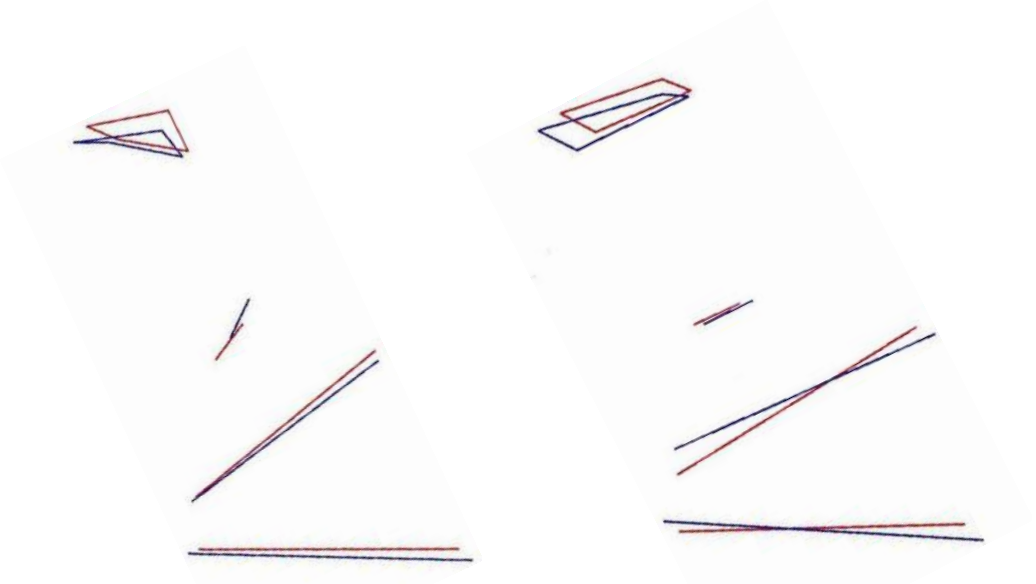

***E. macaco* PC3** ***O. crassicaudatus* PC2**

Figure 37: Shape change for Goswami Model base module PCs significantly correlated (p<0.003) with size. As with Figure 29. For this module the wireframe shows an inferior view.

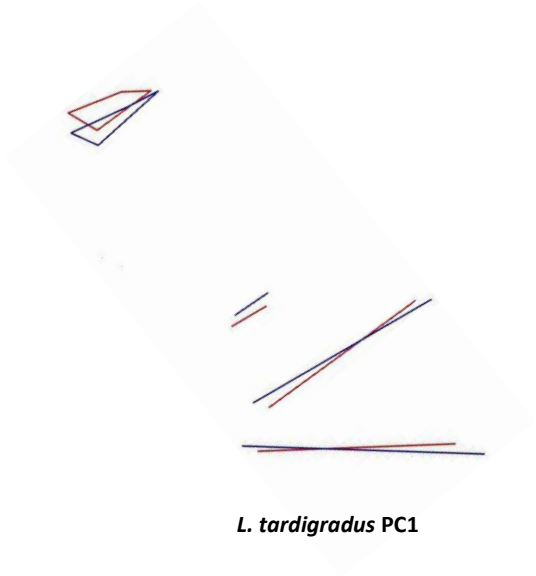

***L. tardigradus* PC1**

Figure 37 (Cont.)

5.4.2. Intra-species allometry – size-versus-size

Tables 49-56 show the results for intra-specific size-versus-size allometry, giving the slope, confidence intervals for the slope, as well as the R^2 value; incidences of significant positive and negative allometry are also indicated. Figures 38-45 show evo-maps of the intra-species slope values, where green indicates a move towards more positive allometry and red a move towards more negative allometry. In addition, the thickness of the branches represents the rate of change along that branch and the size of the circles at the tip and at the ancestral nodes is indicative of the size of the trait; i.e., the steepness of the slope.

Patterns of within-species size against size allometry were common across species, with both face modules (2* and Goswami) showing a strong trend for positive allometry (Table 49, 51) and both vault modules strong trends for negative allometry (Table 50, 55).

For the remaining Goswami modules, the orbit was shown only to be negatively allometric for *E. mongoz* and positively allometric for *G. moholi, G. zanzibaricus, M. rufus* and *P. potto*, against the general inter-species primate trend for negative size-versus-size allometry in the orbit (Kirk, 2006; Martin, 1990). Significant allometry in the oral and zygomatic modules is positive (with the exception of *L. tardigradus* for the oral module). The base module was also positively allometric, with the exception of the genus *Otolemur*.

The evo-map for the Goswami face module illustrates a general move towards more positive allometry along terminal branches. The exceptions to this are *O. crassicaudatus*

and *E. rubriventer,* where terminal branches show a move towards more negative allometry. The evo-map for the Goswami oral module shows an infra-order level split between the lorisiforms and the lemuriforms; lorisiforms, with the exception of *G. moholi*, move towards more negative allometry and the lemuriforms, with the exception of *Lepilemur ruficaudatus* and *P. verreauxi*, towards more positive allometry. For the other cranial modules, specific patterns at the infra-order or family level are not evident.

Table 2: Results of Intra-species allometry for the 2* model face module, where ln(CS) of the module was regressed against ln(CS) of the whole cranium. Where the relationship was found to be significantly different from isometry, the allometric direction is indicated.

Species	Slope	Lower CI	Upper CI	R^2	Allometry
Cheirogaleus major	1.13	1.02	1.25	0.943	+
Cheirogaleus medius	0.98	0.91	1.04	0.972	
Microcebus murinus	1.12	1.02	1.22	0.862	+
Microcebus rufus	1.24	1.12	1.38	0.933	+
Euoticus elegantulus	1.00	0.89	1.13	0.883	
Galago alleni	1.17	1.04	1.32	0.926	+
Galago moholi	1.25	1.17	1.34	0.920	+
Galago senegalensis	1.01	0.97	1.06	0.925	
Galagoides demidoff	1.15	1.05	1.26	0.890	+
Galagoides zanzibaricus	1.09	0.93	1.28	0.858	
Otolemur crassicaudatus	1.07	1.02	1.11	0.954	+
Otolemur garnettii	1.03	0.98	1.08	0.946	
Avahi laniger	0.86	0.72	1.01	0.860	
Indri indri	1.11	0.96	1.28	0.808	
Propithecus diadema	0.88	0.78	1.00	0.908	
Propithecus verreauxi	1.21	1.09	1.35	0.882	+
Eulemur fulvus	1.14	1.09	1.18	0.928	+
Eulemur macaco	1.03	0.93	1.13	0.869	
Eulemur mongoz	1.19	1.13	1.26	0.962	+
Eulemur rubriventer	0.99	0.86	1.13	0.888	
Hapalemur griseus	1.02	0.93	1.13	0.942	
Lemur catta	1.20	1.09	1.31	0.930	+
Varecia variegata	1.09	1.04	1.16	0.972	+
Lepilemur ruficaudatus	1.32	1.22	1.43	0.965	+
Loris tardigradus	1.05	0.97	1.14	0.963	
Nycticebus bengalensis	0.96	0.86	1.08	0.937	
Nycticebus coucang	1.07	1.02	1.12	0.967	+
Perodicticus potto	1.17	1.11	1.23	0.909	+

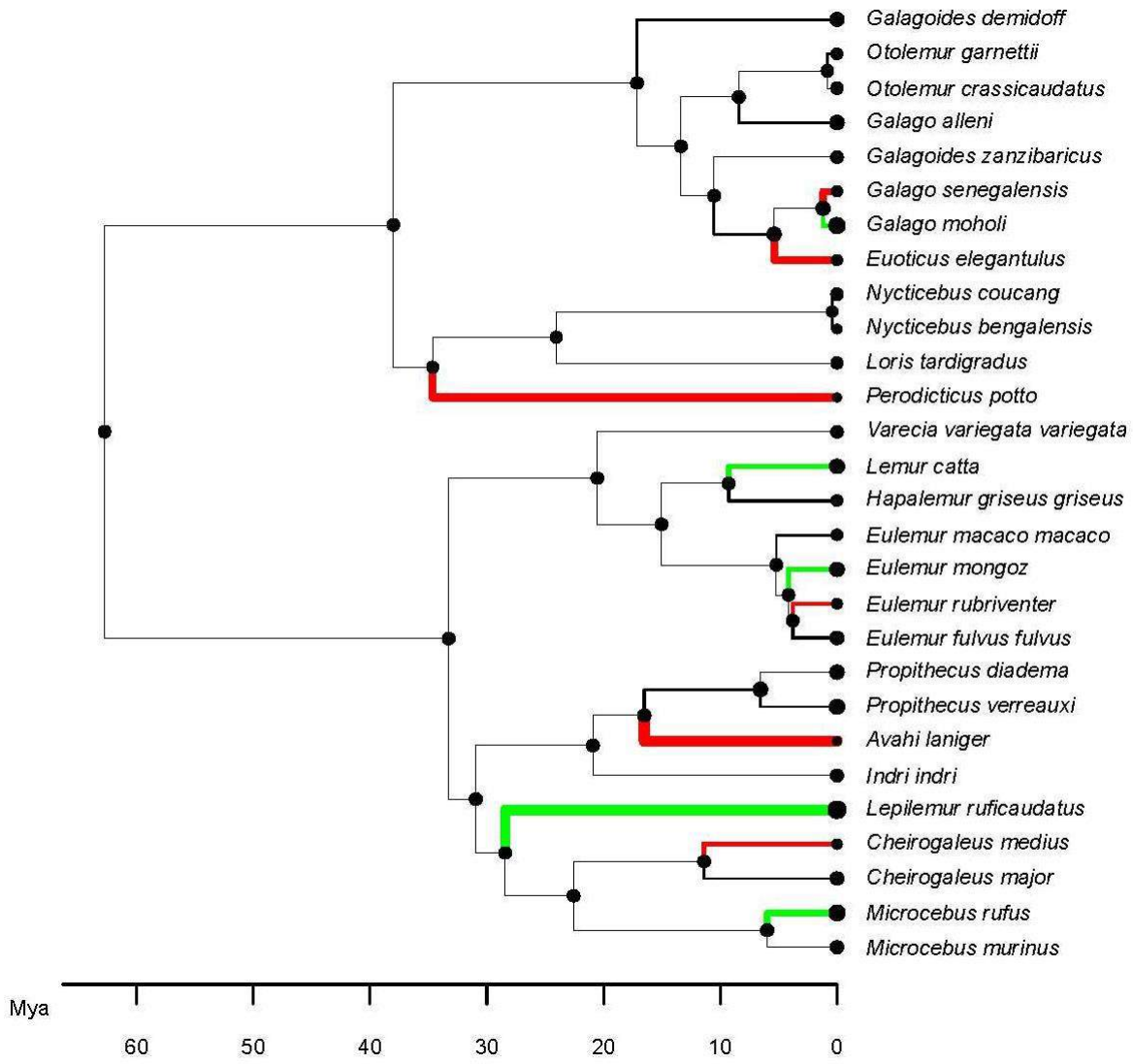

Figure 38: Evo-map of intra-species allometric slope values for the 2* model face module, where ln(CS) of the module was regressed against the ln(CS) of the whole cranium. Green indicates a change towards more positive allometry along that branch and red a change towards more negative allometry.

Table 50: Results of Intra-species allometry for the 2* model vault module, where ln(CS) of the module was regressed against the ln(CS) of the whole cranium. Where the relationship was found to be significantly different from isometry, the allometric direction is indicated.

Species	Slope	Lower CI	Upper CI	R^2	Allometry
Cheirogaleus major	0.74	0.59	0.93	0.717	-
Cheirogaleus medius	0.93	0.82	1.05	0.897	
Microcebus murinus	0.75	0.66	0.84	0.751	-
Microcebus rufus	0.65	0.55	0.76	0.832	-
Euoticus elegantulus	0.92	0.78	1.10	0.772	
Galago alleni	0.67	0.56	0.80	0.830	-
Galago moholi	0.74	0.64	0.84	0.682	-
Galago senegalensis	0.96	0.91	1.02	0.845	
Galagoides demidoff	0.81	0.70	0.93	0.705	-
Galagoides zanzibaricus	1.05	0.84	1.31	0.737	
Otolemur crassicaudatus	0.75	0.70	0.80	0.898	-
Otolemur garnettii	0.89	0.83	0.95	0.886	-
Avahi laniger	1.15	0.91	1.45	0.734	
Indri indri	0.81	0.65	1.01	0.574	
Propithecus diadema	0.99	0.81	1.20	0.766	
Propithecus verreauxi	0.77	0.64	0.92	0.673	-
Eulemur fulvus	0.84	0.77	0.92	0.635	-
Eulemur macaco	1.03	0.87	1.23	0.587	
Eulemur mongoz	0.85	0.76	0.95	0.833	-
Eulemur rubriventer	0.96	0.73	1.26	0.551	
Hapalemur griseus	0.69	0.56	0.83	0.770	-
Lemur catta	0.74	0.63	0.88	0.793	-
Varecia variegata	0.72	0.59	0.88	0.627	-
Lepilemur ruficaudatus	0.66	0.54	0.80	0.791	-
Loris tardigradus	0.85	0.78	0.92	0.957	-
Nycticebus bengalensis	1.05	0.86	1.28	0.822	
Nycticebus coucang	0.94	0.86	1.02	0.879	
Perodicticus potto	0.88	0.82	0.94	0.828	-

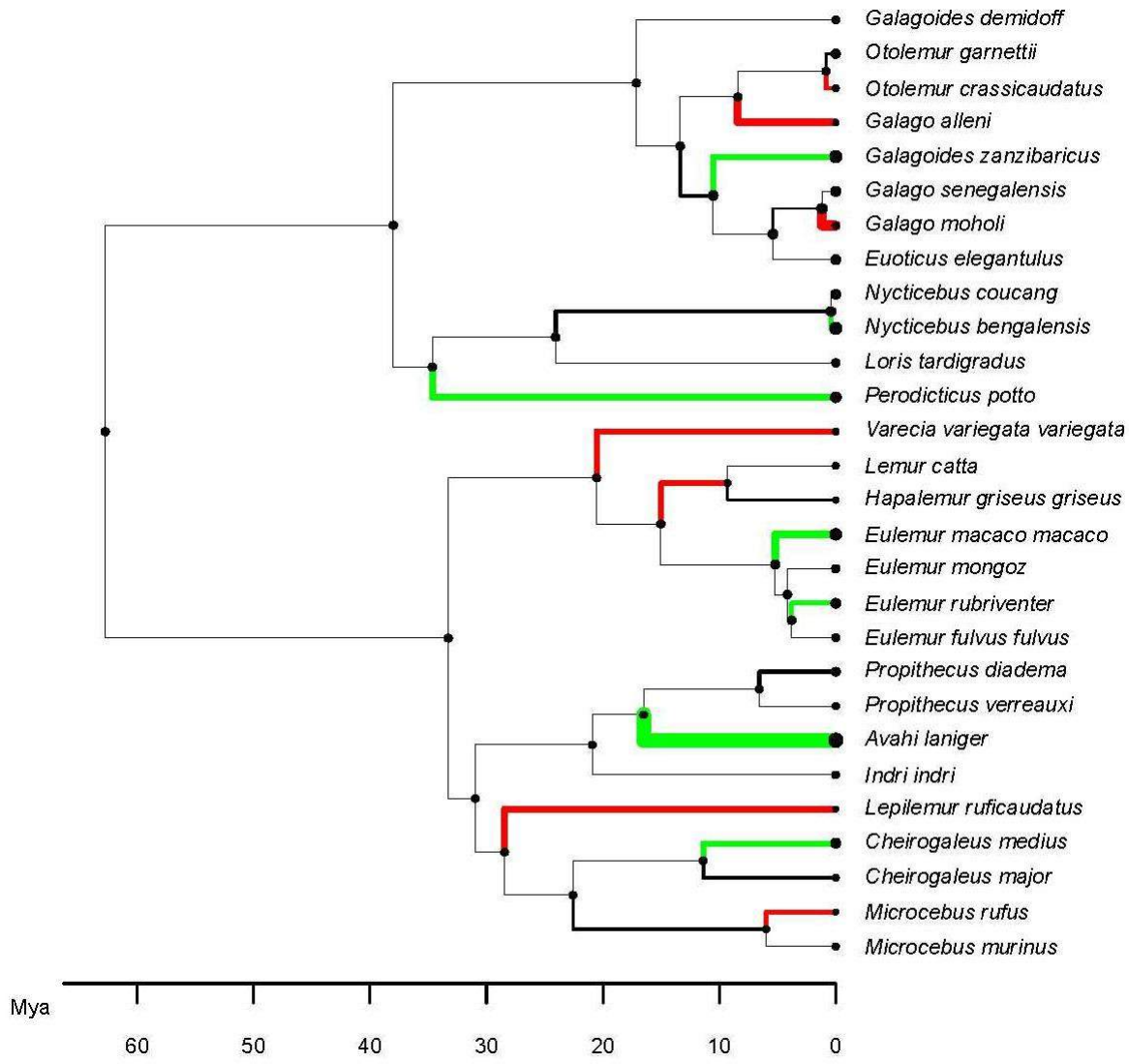

Figure 39: Evo-map of intra-species allometric slope values for the 2* model vault module, where ln(CS) of the module was regressed against the ln(CS) of the whole cranium. As with Figure 38.

Table 51: Results of Intra-species allometry for the Goswami model face module, where ln(CS) of the module was regressed against the ln(CS) of the whole cranium. Where the relationship was found to be significantly different from isometry, the allometric direction is indicated.

Species	Slope	Lower CI	Upper CI	R^2	Allometry
Cheirogaleus major	1.07	0.88	1.32	0.778	
Cheirogaleus medius	1.10	0.95	1.26	0.876	
Microcebus murinus	1.33	1.15	1.53	0.641	+
Microcebus rufus	1.35	1.11	1.63	0.762	+
Euoticus elegantulus	1.40	1.14	1.71	0.678	+
Galago alleni	1.37	1.11	1.68	0.776	+
Galago moholi	1.26	1.12	1.41	0.772	+
Galago senegalensis	1.06	0.98	1.14	0.743	
Galagoides demidoff	1.42	1.23	1.65	0.694	+
Galagoides zanzibaricus	1.05	0.76	1.45	0.426	
Otolemur crassicaudatus	1.07	1.00	1.14	0.891	+
Otolemur garnettii	1.21	1.12	1.30	0.872	+
Avahi laniger	1.27	0.96	1.68	0.605	+
Indri indri	1.65	1.28	2.12	0.414	+
Propithecus diadema	1.00	0.80	1.24	0.709	
Propithecus verreauxi	1.77	1.45	2.17	0.584	+
Eulemur fulvus	1.33	1.24	1.42	0.784	+
Eulemur macaco	1.48	1.25	1.76	0.615	+
Eulemur mongoz	1.69	1.50	1.91	0.801	+
Eulemur rubriventer	1.11	0.86	1.43	0.604	
Hapalemur griseus	1.49	1.29	1.73	0.872	+
Lemur catta	1.23	1.06	1.43	0.822	+
Varecia variegata	1.46	1.28	1.66	0.843	+
Lepilemur ruficaudatus	1.64	1.38	1.95	0.834	+
Loris tardigradus	1.01	0.83	1.22	0.772	
Nycticebus bengalensis	0.95	0.75	1.19	0.753	
Nycticebus coucang	1.24	1.15	1.35	0.892	+
Perodicticus potto	1.31	1.20	1.43	0.770	+

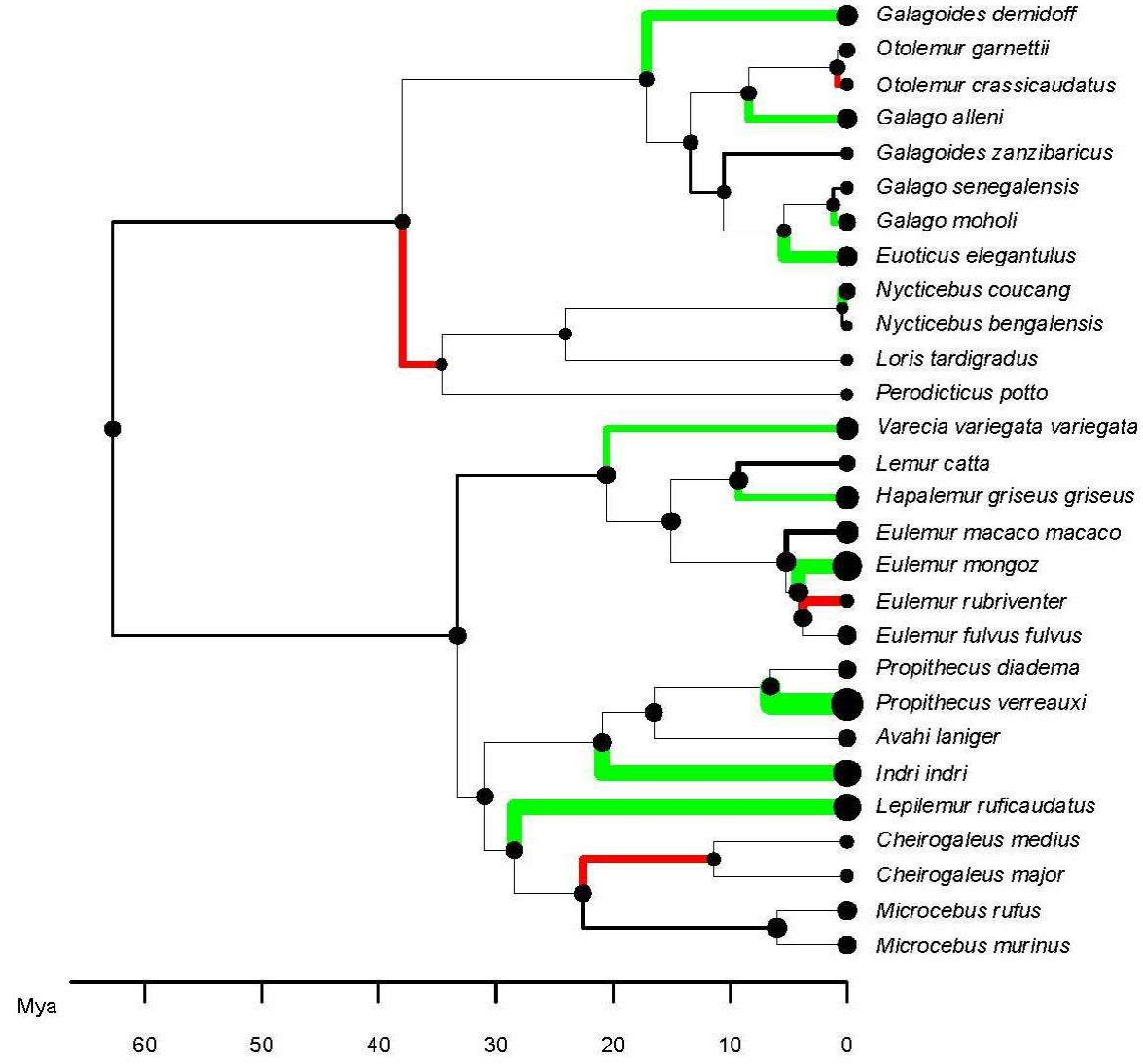

Figure 40: Evo-map of intra-species allometric slope values for the Goswami model face module, where ln(CS) of the module was regressed against the ln(CS) of the whole cranium. As with Figure 38.

Table 52: Results of Intra-species allometry for the Goswami model orbit module, where ln(CS) of the module was regressed against the ln(CS) of the whole cranium. Where the relationship was found to be significantly different from isometry, the allometric direction is indicated.

Species	Slope	Lower CI	Upper CI	R^2	Allometry
Cheirogaleus major	1.17	0.98	1.41	0.823	
Cheirogaleus medius	0.88	0.77	1.01	0.874	
Microcebus murinus	1.01	0.87	1.16	0.642	
Microcebus rufus	1.25	1.10	1.42	0.897	+
Euoticus elegantulus	0.96	0.77	1.20	0.614	
Galago alleni	1.07	0.92	1.23	0.893	
Galago moholi	1.25	1.13	1.37	0.833	+
Galago senegalensis	1.06	0.99	1.14	0.761	
Galagoides demidoff	1.08	0.93	1.26	0.676	
Galagoides zanzibaricus	1.34	1.10	1.64	0.784	+
Otolemur crassicaudatus	1.03	0.97	1.10	0.904	
Otolemur garnettii	0.94	0.87	1.01	0.875	
Avahi laniger	0.95	0.68	1.33	0.416	
Indri indri	1.01	0.84	1.22	0.679	
Propithecus diadema	1.09	0.90	1.33	0.754	
Propithecus verreauxi	1.16	1.01	1.33	0.807	
Eulemur fulvus	1.04	0.97	1.12	0.791	
Eulemur macaco	1.06	0.90	1.24	0.640	
Eulemur mongoz	0.82	0.73	0.93	0.801	-
Eulemur rubriventer	1.02	0.82	1.26	0.721	
Hapalemur griseus	0.83	0.64	1.07	0.616	
Lemur catta	0.96	0.84	1.09	0.871	
Varecia variegata	0.92	0.77	1.09	0.731	
Lepilemur ruficaudatus	0.92	0.81	1.05	0.915	
Loris tardigradus	1.04	0.94	1.17	0.927	
Nycticebus bengalensis	0.84	0.68	1.03	0.805	
Nycticebus coucang	0.97	0.89	1.06	0.861	
Perodicticus potto	1.10	1.02	1.17	0.842	+

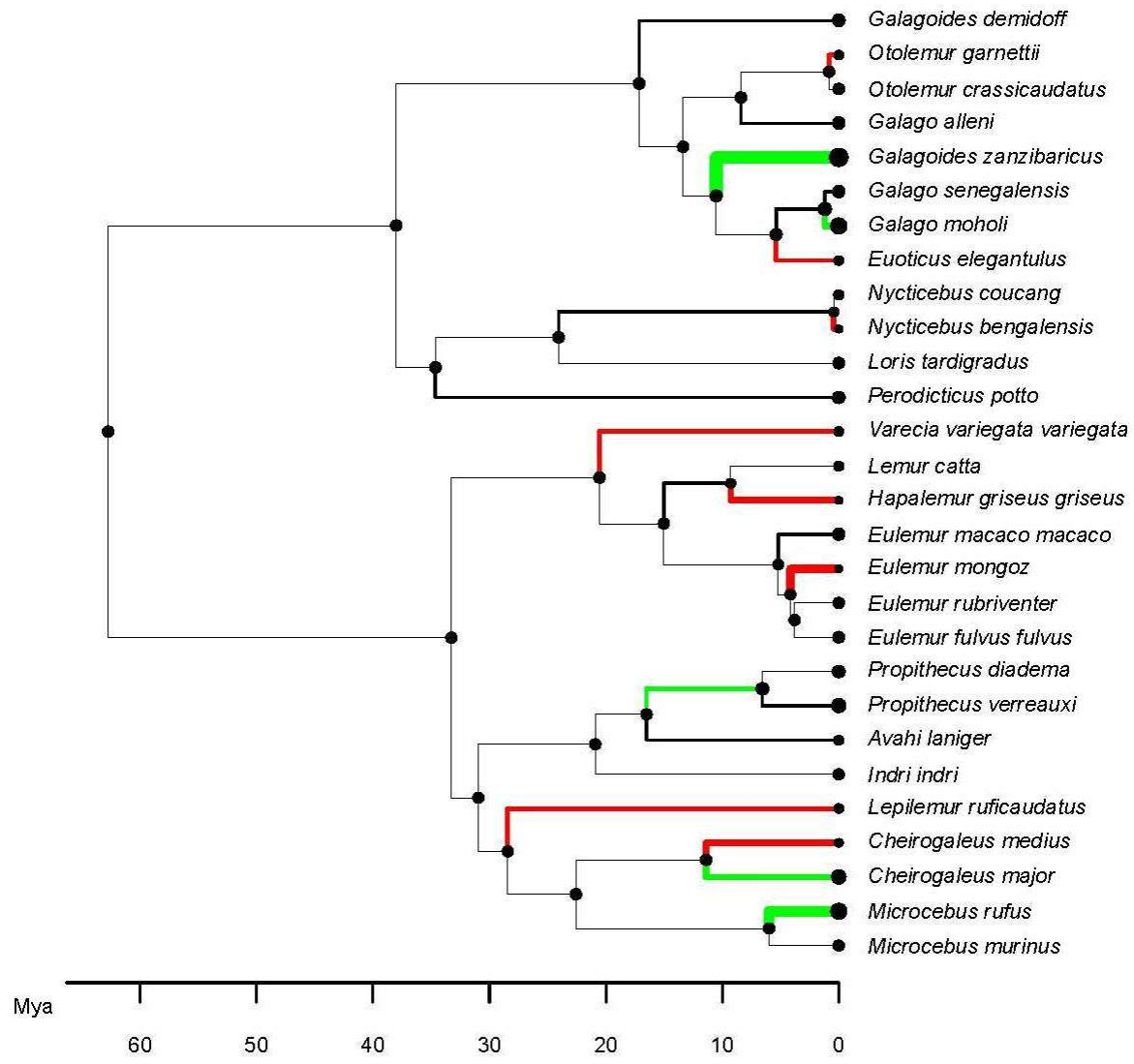

Figure 41: Evo-map of intra-species allometric slope values for the Goswami model orbit module, where ln(CS) of the module was regressed against the ln(CS) of the whole cranium. As with Figure 38.

Table 53: Results of Intra-species allometry for the Goswami model oral module, where ln(CS) of the module was regressed against the ln(CS) of the whole cranium. Where the relationship was found to be significantly different from isometry, the allometric direction is indicated.

Species	Slope	Lower CI	Upper CI	R^2	Allometry
Cheirogaleus major	1.18	0.90	1.56	0.571	
Cheirogaleus medius	1.47	1.18	1.83	0.678	+
Microcebus murinus	1.67	1.42	1.96	0.540	+
Microcebus rufus	1.44	1.19	1.74	0.770	+
Euoticus elegantulus	1.16	0.86	1.57	0.264	
Galago alleni	1.23	0.88	1.74	0.380	
Galago moholi	1.43	1.24	1.64	0.651	+
Galago senegalensis	1.10	0.98	1.24	0.377	
Galagoides demidoff	1.07	0.87	1.32	0.384	
Galagoides zanzibaricus	1.08	0.75	1.56	0.242	
Otolemur crassicaudatus	1.00	0.90	1.12	0.705	
Otolemur garnettii	0.87	0.77	0.98	0.685	
Avahi laniger	1.39	0.98	1.99	0.365	
Indri indri	1.45	1.14	1.85	0.469	+
Propithecus diadema	0.98	0.75	1.28	0.552	
Propithecus verreauxi	1.05	0.85	1.31	0.509	
Eulemur fulvus	1.53	1.37	1.72	0.400	+
Eulemur macaco	1.68	1.39	2.03	0.514	+
Eulemur mongoz	1.33	1.13	1.56	0.652	+
Eulemur rubriventer	1.22	0.98	1.51	0.714	
Hapalemur griseus	1.20	0.96	1.51	0.689	
Lemur catta	1.30	1.06	1.59	0.682	+
Varecia variegata	1.21	0.99	1.47	0.643	
Lepilemur ruficaudatus	1.09	0.87	1.37	0.727	
Loris tardigradus	0.86	0.74	0.99	0.868	-
Nycticebus bengalensis	1.31	0.94	1.81	0.488	
Nycticebus coucang	1.48	1.31	1.68	0.742	+
Perodicticus potto	1.59	1.42	1.79	0.557	+

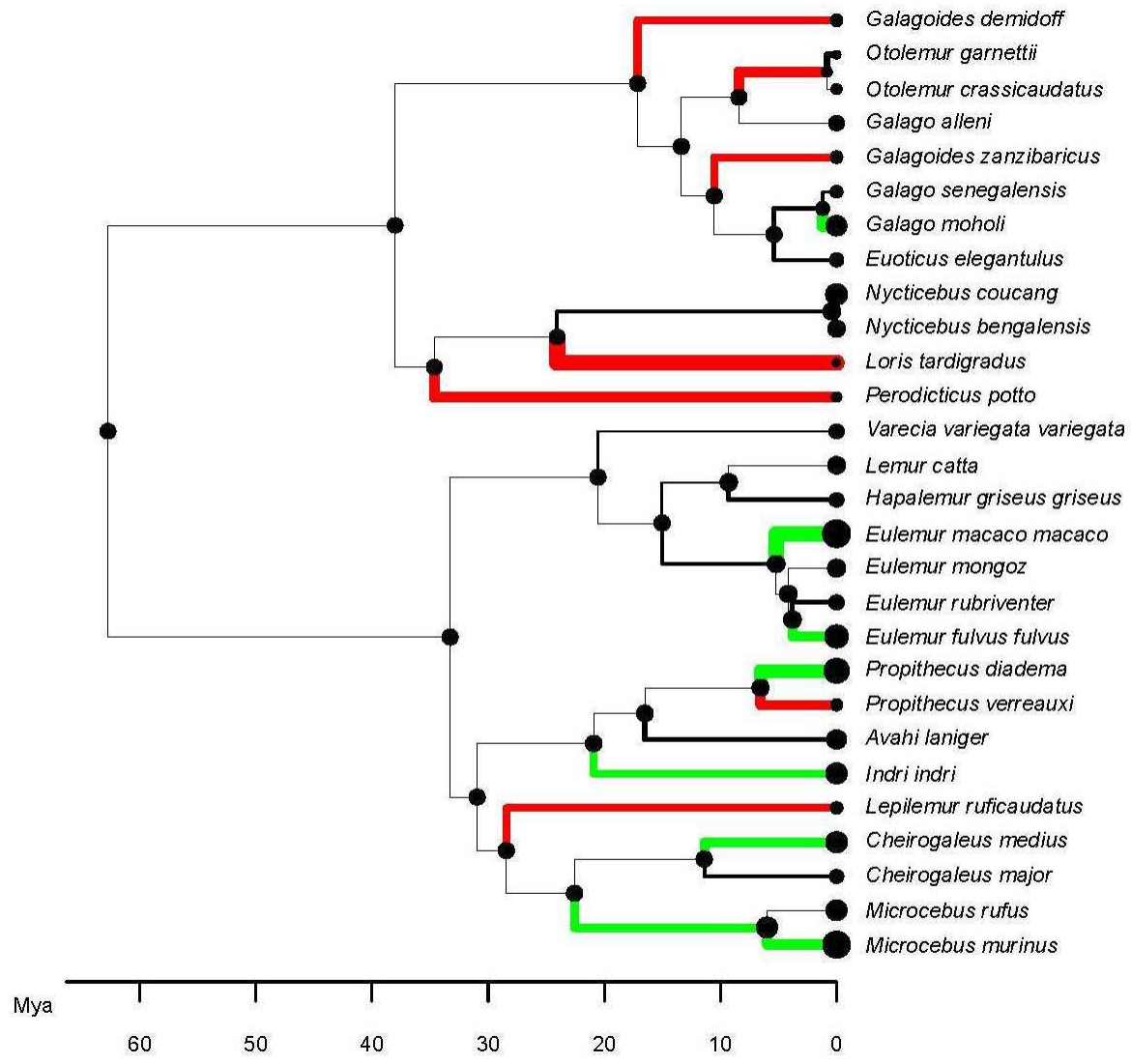

Figure 42: Evo-map of intra-species allometric slope values for the Goswami model oral module, where ln(CS) of the module was regressed against the ln(CS) of the whole cranium. As with Figure 38.

Table 54: Results of Intra-species allometry for the Goswami model Zygomatic module, where ln(CS) of the module was regressed against the ln(CS) of the whole cranium. Where the relationship was found to be significantly different from isometry, the allometric direction is indicated.

Species	Slope	Lower CI	Upper CI	R^2	Allometry
Cheirogaleus major	1.55	1.31	1.85	0.834	+
Cheirogaleus medius	1.18	0.99	1.40	0.812	
Microcebus murinus	1.47	1.29	1.68	0.703	+
Microcebus rufus	1.18	1.02	1.37	0.857	+
Euoticus elegantulus	1.36	1.07	1.73	0.544	+
Galago alleni	1.24	1.00	1.55	0.749	+
Galago moholi	1.31	1.16	1.49	0.714	+
Galago senegalensis	1.43	1.33	1.54	0.760	+
Galagoides demidoff	1.35	1.16	1.57	0.662	+
Galagoides zanzibaricus	1.73	1.38	2.18	0.716	+
Otolemur crassicaudatus	1.28	1.19	1.38	0.866	+
Otolemur garnettii	1.46	1.37	1.55	0.916	+
Avahi laniger	1.40	1.09	1.79	0.701	+
Indri indri	1.22	1.00	1.50	0.613	+
Propithecus diadema	1.29	1.08	1.53	0.816	+
Propithecus verreauxi	1.17	0.98	1.40	0.678	
Eulemur fulvus	1.23	1.12	1.34	0.665	+
Eulemur macaco	1.34	1.14	1.58	0.642	+
Eulemur mongoz	1.03	0.91	1.17	0.781	
Eulemur rubriventer	1.64	1.26	2.15	0.569	+
Hapalemur griseus	1.03	0.89	1.19	0.880	
Lemur catta	1.22	1.03	1.44	0.782	+
Varecia variegata	1.04	0.87	1.24	0.715	
Lepilemur ruficaudatus	0.99	0.81	1.21	0.781	
Loris tardigradus	1.33	1.25	1.42	0.976	+
Nycticebus bengalensis	1.34	1.13	1.58	0.867	+
Nycticebus coucang	1.20	1.09	1.32	0.849	+
Perodicticus potto	1.46	1.35	1.58	0.797	+

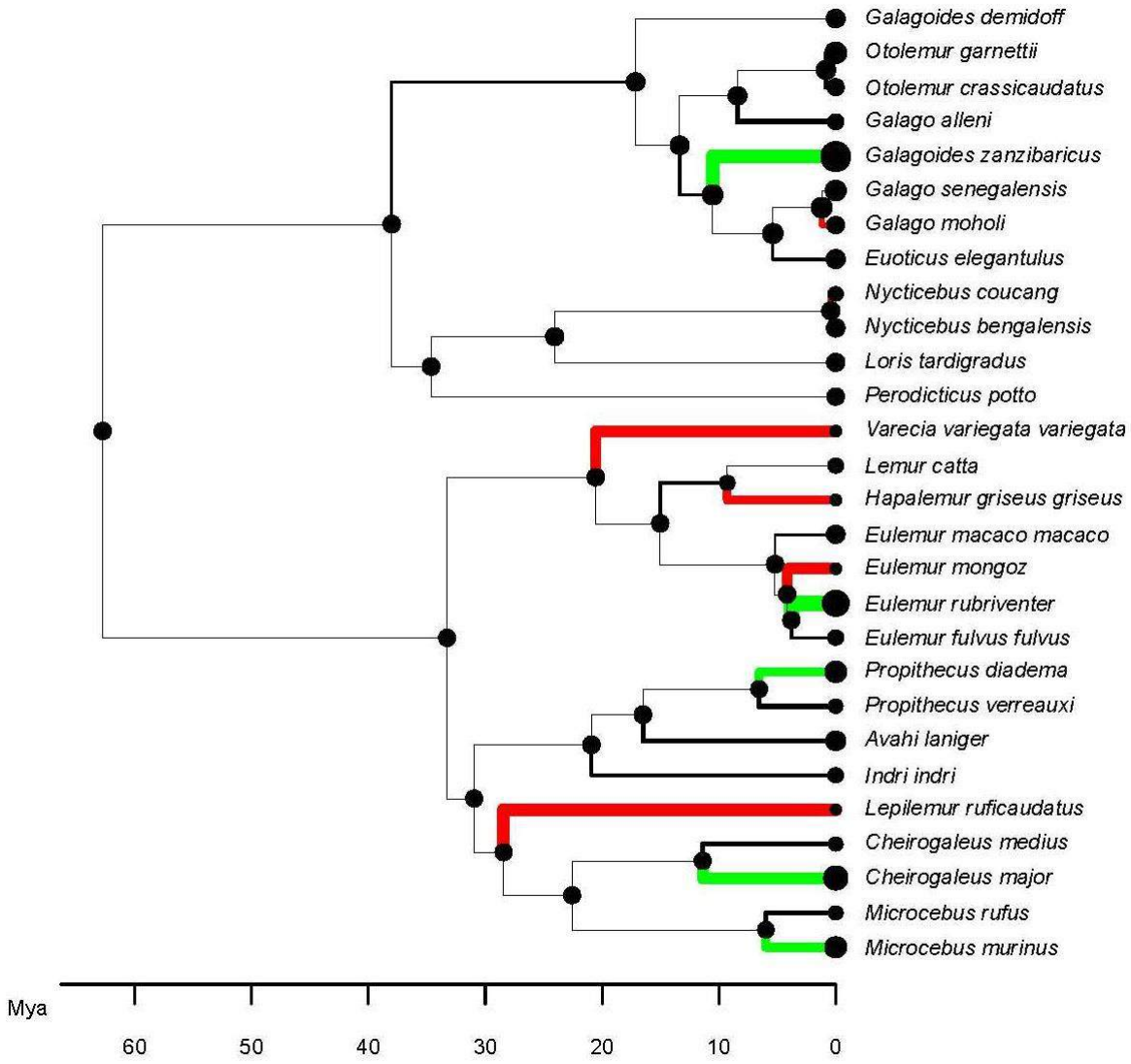

Figure 43: Evo-map of intra-species allometric slope values for the Goswami model zygomatic module, where ln(CS) of the module was regressed against the ln(CS) of the whole cranium. As with Figure 38.

Table 55: Results of Intra-species allometry for the Goswami model vault module, where ln(CS) of the module was regressed against the ln(CS) of the whole cranium. Where the relationship was found to be significantly different from isometry, the allometric direction is indicated.

Species	Slope	Lower CI	Upper CI	R^2	Allometry
Cheirogaleus major	0.71	0.53	0.96	0.500	-
Cheirogaleus medius	1.01	0.81	1.26	0.689	
Microcebus murinus	0.85	0.72	1.00	0.508	
Microcebus rufus	0.74	0.57	0.95	0.570	-
Euoticus elegantulus	1.04	0.80	1.35	0.468	
Galago alleni	0.52	0.37	0.74	0.370	-
Galago moholi	0.77	0.64	0.92	0.420	-
Galago senegalensis	1.06	0.98	1.16	0.671	
Galagoides demidoff	0.84	0.67	1.04	0.329	
Galagoides zanzibaricus	0.91	0.67	1.25	0.467	
Otolemur crassicaudatus	0.78	0.71	0.85	0.786	-
Otolemur garnettii	1.02	0.93	1.12	0.781	
Avahi laniger	1.36	1.02	1.81	0.583	
Indri indri	0.96	0.74	1.25	0.359	
Propithecus diadema	1.05	0.79	1.39	0.502	
Propithecus verreauxi	0.77	0.60	0.99	0.356	-
Eulemur fulvus	0.92	0.82	1.03	0.418	
Eulemur macaco	1.11	0.90	1.37	0.416	
Eulemur mongoz	0.92	0.80	1.05	0.760	
Eulemur rubriventer	1.14	0.80	1.62	0.234	
Hapalemur griseus	0.71	0.53	0.95	0.503	-
Lemur catta	0.78	0.61	1.01	0.493	
Varecia variegata	0.73	0.57	0.93	0.452	-
Lepilemur ruficaudatus	0.57	0.44	0.75	0.591	-
Loris tardigradus	0.62	0.54	0.71	0.888	-
Nycticebus bengalensis	1.01	0.69	1.48	0.298	
Nycticebus coucang	0.94	0.83	1.06	0.750	
Perodicticus potto	0.90	0.81	1.01	0.570	

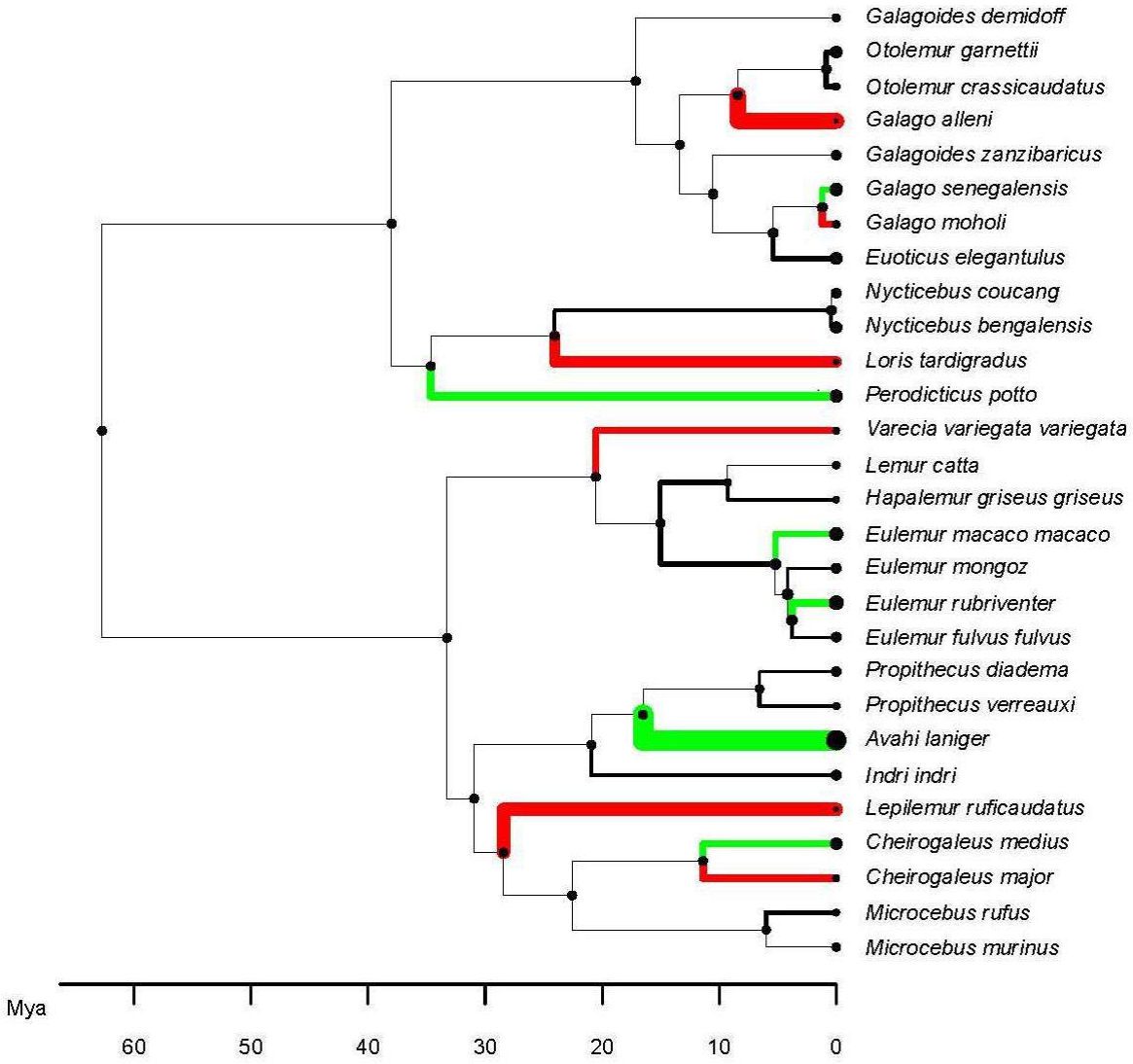

Figure 44: Evo-map of intra-species allometric slope values for the Goswami model vault module, where ln(CS) of the module was regressed against the ln(CS) of the whole cranium. As with Figure 38.

Table 3: Results of Intra-species allometry for the Goswami model base module, where ln(CS) of the module was regressed against the ln(CS) of the whole cranium. Where the relationship was found to be significantly different from isometry, the allometric direction is indicated.

Species	Slope	Lower CI	Upper CI	R^2	Allometry
Cheirogaleus major	0.95	0.66	1.37	0.231	
Cheirogaleus medius	1.18	0.95	1.46	0.704	
Microcebus murinus	0.94	0.78	1.14	0.382	
Microcebus rufus	0.79	0.59	1.06	0.441	
Euoticus elegantulus	1.46	1.13	1.90	0.461	+
Galago alleni	1.13	0.75	1.69	0.112	
Galago moholi	1.16	0.98	1.37	0.478	
Galago senegalensis	1.35	1.21	1.49	0.530	+
Galagoides demidoff	1.01	0.84	1.21	0.516	
Galagoides zanzibaricus	1.27	0.97	1.67	0.593	
Otolemur crassicaudatus	0.81	0.72	0.91	0.673	-
Otolemur garnettii	0.84	0.73	0.97	0.525	-
Avahi laniger	1.66	1.17	2.36	0.373	+
Indri indri	0.95	0.72	1.24	0.336	
Propithecus diadema	1.17	0.93	1.47	0.663	
Propithecus verreauxi	1.22	0.99	1.51	0.544	
Eulemur fulvus	0.97	0.87	1.10	0.391	
Eulemur macaco	1.31	1.06	1.61	0.432	+
Eulemur mongoz	0.97	0.83	1.13	0.681	
Eulemur rubriventer	1.10	0.79	1.54	0.325	
Hapalemur griseus	0.84	0.63	1.12	0.512	
Lemur catta	0.87	0.69	1.09	0.607	
Varecia variegata	0.88	0.69	1.11	0.491	
Lepilemur ruficaudatus	1.01	0.73	1.38	0.448	
Loris tardigradus	1.07	0.94	1.23	0.891	
Nycticebus bengalensis	1.66	1.26	2.17	0.654	+
Nycticebus coucang	1.43	1.23	1.66	0.633	+
Perodicticus potto	1.45	1.27	1.65	0.434	+

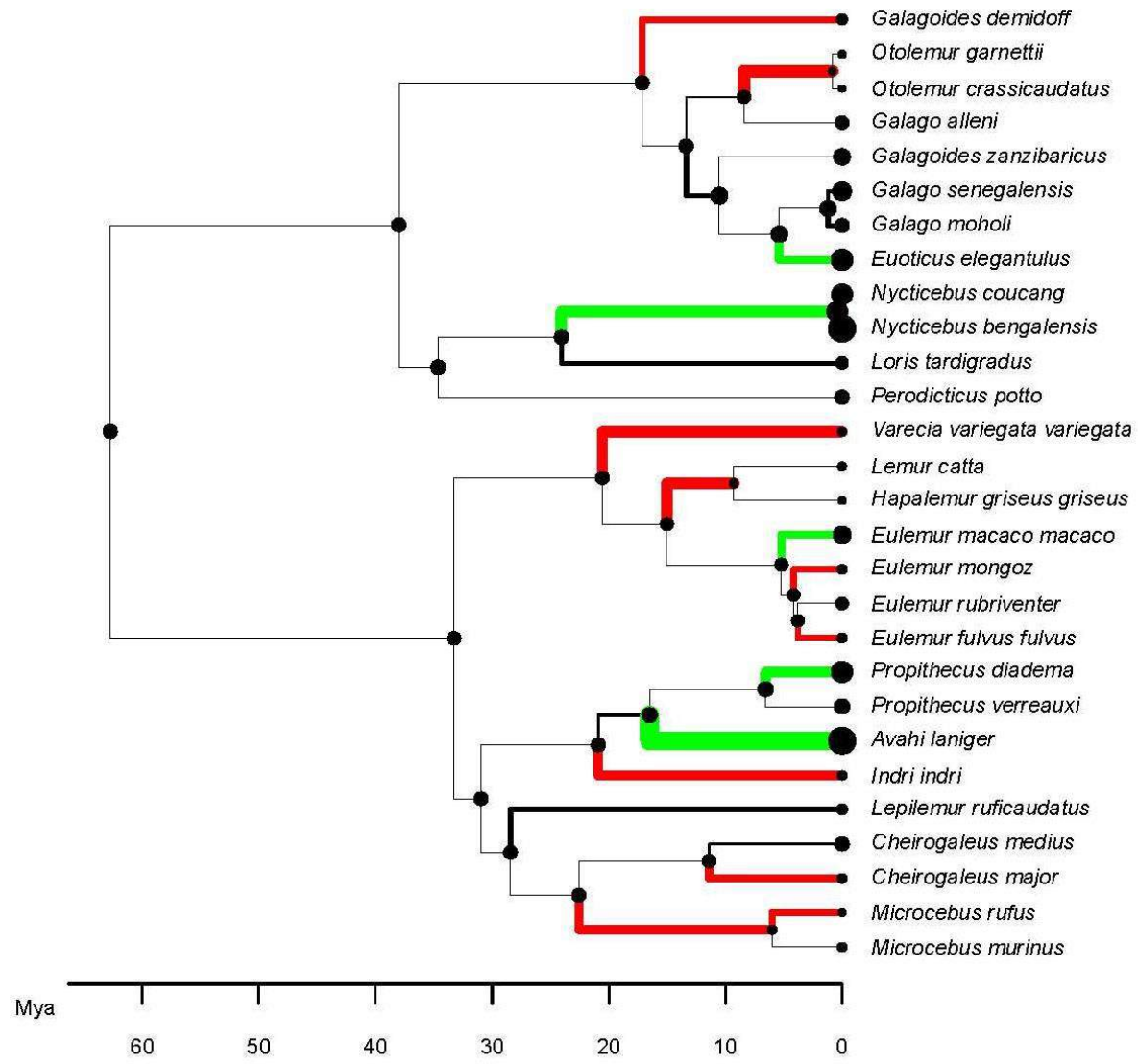

Figure 45: Evo-map of intra-species allometric slope values for the Goswami model base module, where ln(CS) of the module was regressed against the ln(CS) of the whole cranium. As with Figure 38.

5.4.3. Inter-species allometry – shape-versus-size

Some of the same changes in the vault that were associated with an increase in size at an intra-species level were again associated with increased size at an inter-species level. For the whole cranium and the 2* model, the vault was less globular as size increased. However, the other allometric traits seen at the intra-species level for the 2* model vault module were not mirrored at the inter-species level.

For the Goswami model, there were again traits associated with increased size at the inter-species level that matched those results seen at the intra-species level; namely a more posteriorly positioned inter-orbital foramen; a more laterally positioned mesial P3 septum; a more medially positioned end of dentition, a more laterally positioned greater palatine foramen, a more posteriorly positioned tip of the nasal spine; a greater distance between the meeting point of the presphenoid-basisphenoid and the meeting point of the basioccipital synchondrosis in the midline; a more posteriorly positioned foramen lavelli; a less globular vault; a relatively smaller external auditory meatus; and a relatively shorter distance between basion and opisthion.

Very similar patterns in allometric shape change were seen whether shape was regressed against the size of the whole cranium or against the size of the corresponding module. The pattern of results was also similar whether the regression was based on the species average results or on the resampling results. However, the resampling approach produced more conservative results; finding significant relationships between shape and size on fewer occasions than the species averages approach.

Here a summary table (Table 57) list only those PCs that had a significant relationship with size at an inter-species level. The direction of the correlation is given and the change in shape associated with an increase in size is described. The percentage of shape attributed to change in size is also recorded. For each module, the changes in shape significantly correlated with size, are illustrated using wireframes (Figure 46-53). Full results of the inter-species regressions for PCs 1-13 against ln(CS), for all modules is in Appendix 3. Full results of the percentage of inter-species shape change caused by size for PCs 1-13 for all modules is in Appendix 5.

Table 57: Description of shape change associated with increasing size for the whole cranium and each of the 2* model and Goswami model modules at an inter-species level. The direction of allometry and percentage of the shape change attributed to size, measured both as the size of the whole cranium and as the size of the corresponding module, are indicated for each PC. In this column, those results not shaded report the percentage of shape change attributed to size when species average results are used, while shaded results, report the percentage of shape change attributed to size when the resampling method is used. Only PCs found to be significantly correlated with size (p<0.003) are reported.

Module	PC	+ / - allometry	Shape change associated with PC as size increases	% shape change associated with	
				whole cranium size	module size
Whole cranium	1	-	Less globular vault, more angled at inion, more anteriorly positioned nasospinale, relatively longer palate, relatively longer dentition from canine septum to posterior end of 3rd molar, relatively longer and more medially positioned zygomaticotemporal suture, relatively smaller and more medially and posteriorly positioned external auditory meatus.	23.92	-
				19.77	-
	4	+	Relatively shorter and more superiorly positioned snout, less globular cranium, more posteriorly and medially positioned meeting of the superior temporal crest and the coronal suture, relatively longer palate, relatively longer and more laterally positioned zygomaticotemporal suture, relatively smaller and more medially and posteriorly positioned external auditory meatus.	3.94	-
				3.14	-
2* model - face	1	+	More anteriorly and inferiorly positioned nasospinale, relatively longer palate, relatively longer dentition from canine septum to posterior end of 3rd molar, more posteriorly position infraorbital foramen, more vertically orientated zygomaticomaxillary suture, relatively shorter and more horizontally orientated frontozygomatic suture, relatively longer zygomaticotemporal suture.	21.23	21.51
				18.12	18.40
	4	+	Less vertically orientated upper face, more horizontally orientated zygomaticomaxillary suture with a more posteriorly and superiorly positioned posterior-most point, more anteriorly positioned frontotemporal suture.	3.94	3.79
				3.03	2.93
2* model - vault	1	+	Less globular vault, relatively shorter distance between bregma and lambda, relatively longer distance between lambda and inion, more medially positioned meeting of the superior temporal crest and the coronal suture, relatively smaller external auditory meatus, more inferiorly positioned asterion, more anteriorly positioned meeting point of zygomatic, frontal and parietal bones.	20.42	19.56
				16.40	15.82
	3	-	More superiorly positioned bregma, more inferiorly positioned inion, more medially and posteriorly positioned meeting of the superior temporal crest and the coronal suture, more anteriorly and inferiorly positioned meeting point of sphenoid, zygomatic and parietal bone, more anteriorly and inferiorly positioned meeting point of zygomatic, frontal and parietal bone, relatively smaller external auditory meatus.	3.85	4.27
				Not significant	Not significant
Goswami model - orbit	1	+	More anteriorly positioned nasion, more posteriorly positioned optical foramen, more posteriorly and inferiorly positioned nasolacrimal foramen, more inferiorly positioned zygomatic foramen, more posteriorly positioned infraorbital foramen, more vertically orientated zygomaticomaxillary suture with a more anteriorly and inferiorly positioned posterior-most point, relatively shorter and more horizontally orientated frontotemporal suture.	8.30	Not significant
				Not significant	Not significant

	3	+	Relatively wider angle between nasion-optical foramen-nasolacrimal foramen, more posteriorly positioned nasion, more posteriorly positioned nasolacrimal foramen, more anteriorly positioned zygomatic foramen, relatively shorter and more anteriorly positioned frontotemporal suture.	5.83	4.75
				Not significant	Not significant
	12	+	More posteriorly positioned nasion, more anteriorly and superiorly positioned optical foramen, more posteriorly and superiorly positioned nasolacrimal foramen, more inferiorly positioned zygomatic foramen, more posteriorly and superiorly positioned anterior-most end of zygomaticomaxillary suture, relatively longer and more horizontally orientated frontotemporal suture.	0.26	0.25
				Not significant	Not significant
Goswami model - oral	3	-	More anteriorly and laterally positioned mesial P3 septum , more medially positioned 3rd molar septum and end of dentition, more laterally and posteriorly positioned greater palatine foramen, more medially and posteriorly positioned tip of nasal spine.	4.76	5.58
				Not significant	Not significant
Goswami model - zygomatic	1	-	Relatively longer distance between meeting point of presphenoid-basisphenoid and basioccipital synchondrosis in the midline, relatively narrower base, as indicated by smaller distance between glenoid fossa and the midline, more laterally and anteriorly positioned petrous apex, more posteriorly positioned foramen lavelli, more posteriorly positioned tip of postglenoid process and glenoid fossa, relatively longer and more medially orientated zygomaticotemporal suture.	23.67	25.29
				20.75	21.72
	4	-	More anteriorly positioned meeting point of presphenoid-basisphenoid in the midline, more anterior basioccipital synchondrosis in the midline, more posteriorly positioned petrous apex, more posteriorly and laterally positioned foramen lavelli, more posteriorly positioned glenoid fossa, more laterally positioned tip of postglenoid process, relatively shorter zygomaticotemporal suture.	Not significant	2.66
				Not significant	Not significant
Goswami model - vault	1	-	Relatively shorter distance from bregma to lambda, relatively longer distance from lambda to inion, more medially positioned meeting of the superior temporal crest and the coronal suture, more inferiorly positioned asterion, more inferiorly positioned meeting point of sphenoid, zygomatic and parietal bone, more inferiorly meeting point of zygomatic, frontal and parietal bone.	19.07	16.99
				13.59	Not significant
Goswami model - base	2	-	Relatively smaller external auditory meatus, relatively shorter distance between basion and opisthion, more posteriorly positioned basion, more anteriorly positioned opisthion, more posteriorly positioned anterior-most point of occipital condyle, relatively shorter occipital condyle, more medially positioned hypoglossal canal.	7.05	8.46
				Not significant	5.65

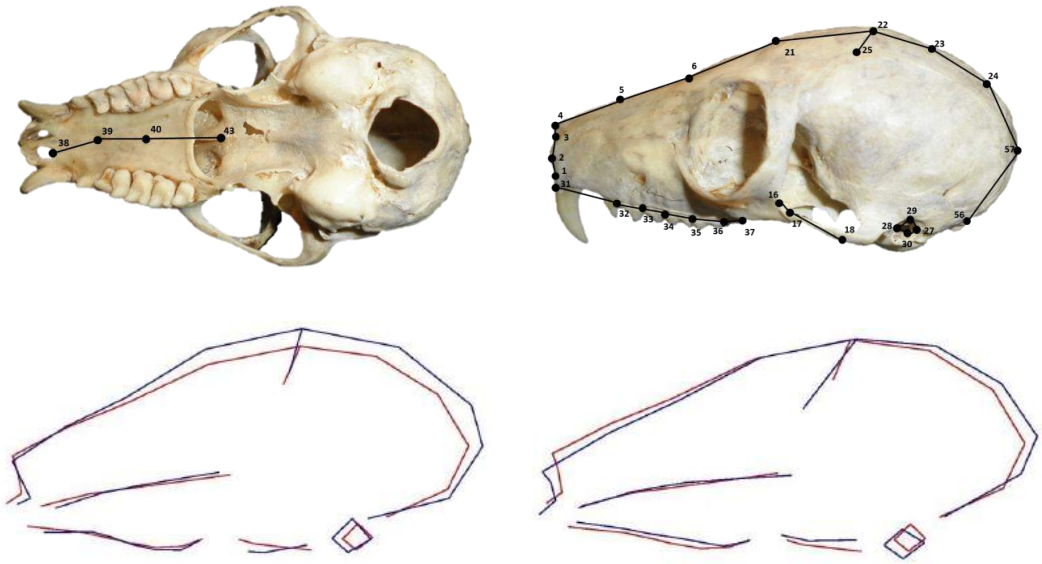

PC1 PC4

Figure 46: Inter-species shape change in the whole cranium for PCs significantly correlated (*p*<0.003) with size. Where blue represents the smaller specimens and red the larger specimens. The difference scaled by 0.1 units of the Procrustes distances. The wire frame is also shown, with landmarks in relation to an *E. fulvus* cranium, for clarity.

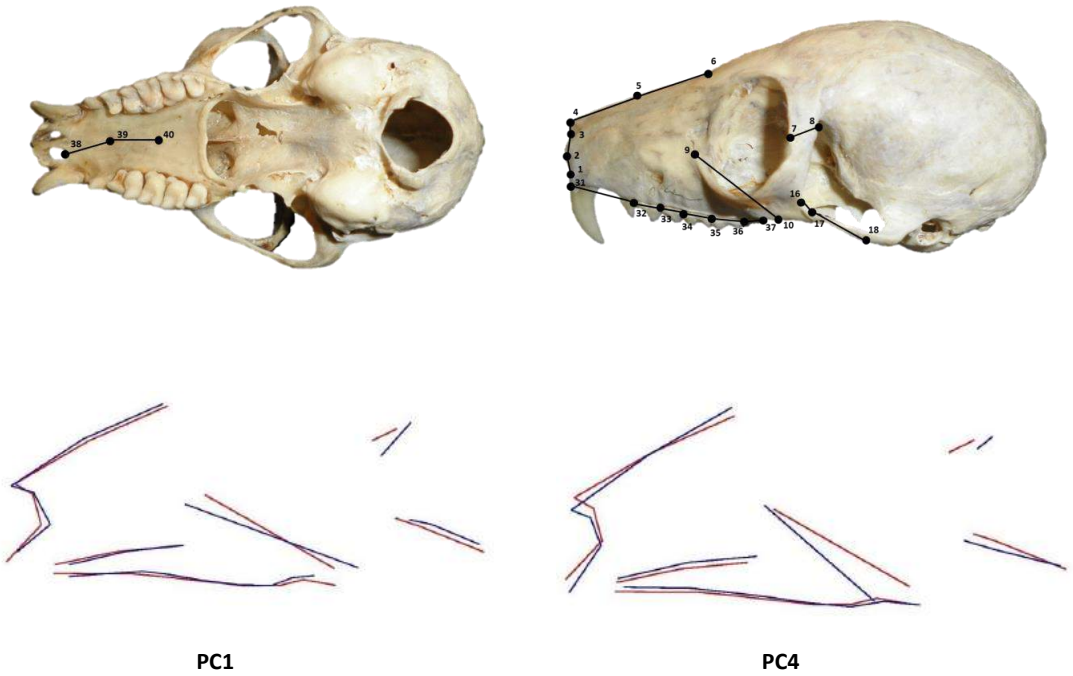

PC1 PC4

Figure 47: Inter-species shape change in the 2* model face module for PCs significantly correlated (*p*<0.003) with size. As with Figure 46.

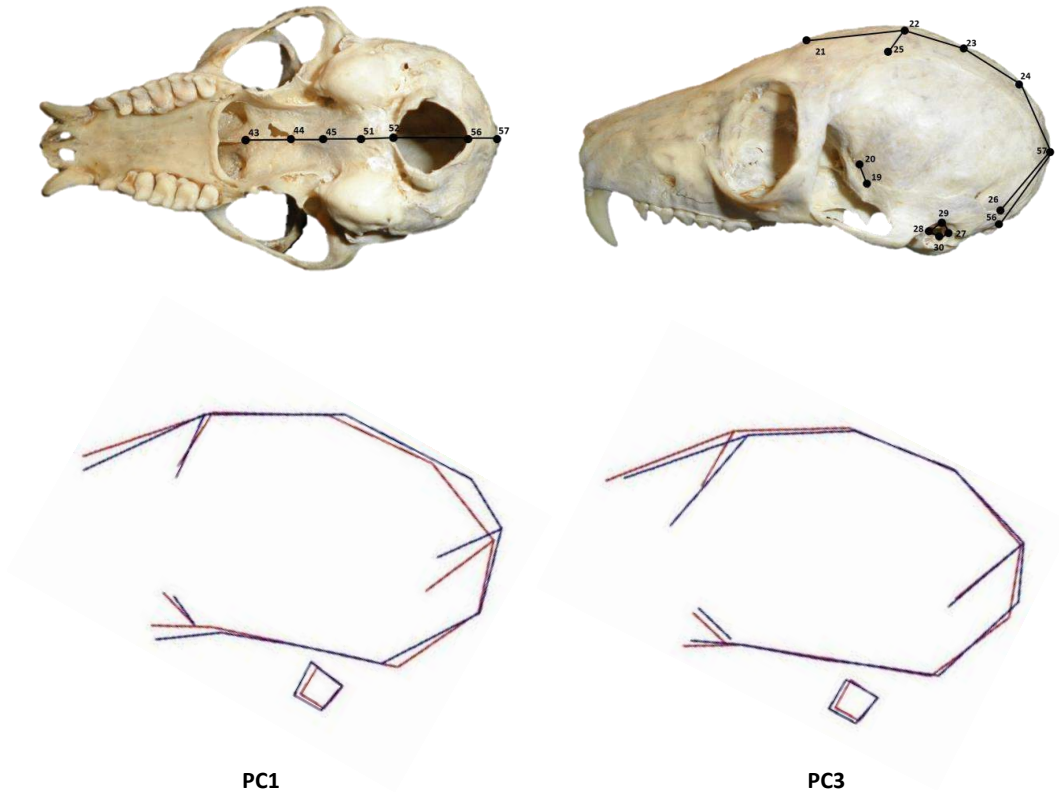

Figure 48: Inter-species shape change in the 2* model vault module for PCs significantly correlated (*p*<0.003) with size. As with Figure 46.

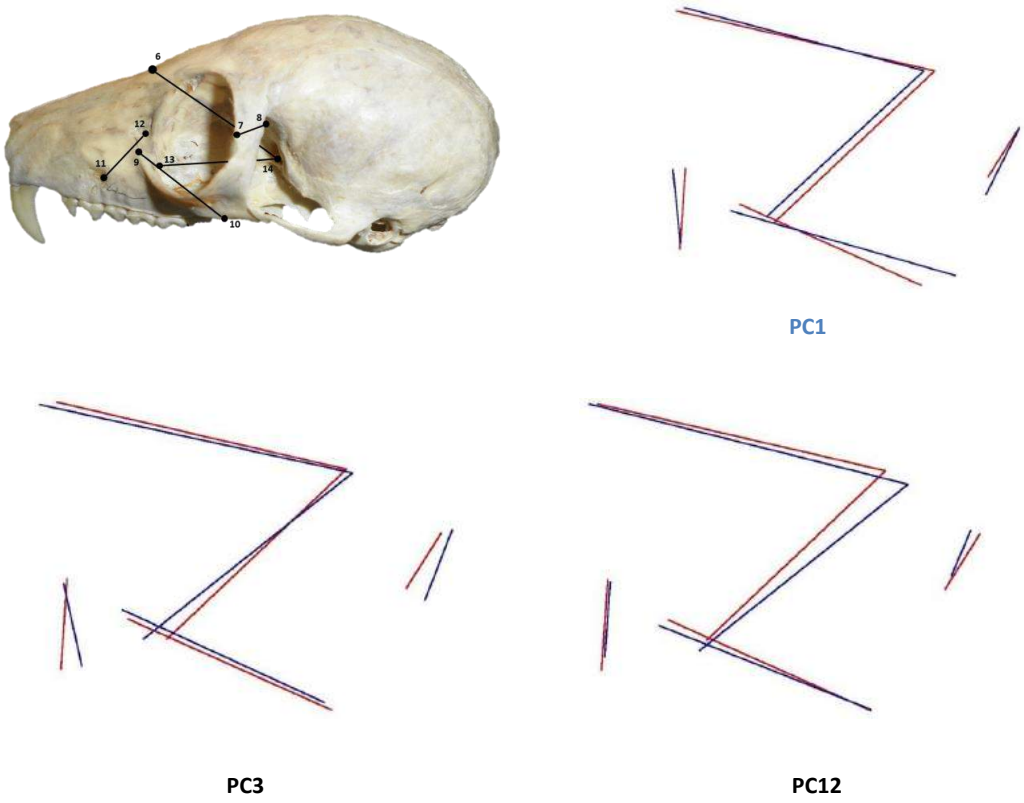

Figure 49: Inter-species shape change in the Goswami model orbit module for PCs significantly correlated (*p*<0.003) with size. As with Figure 46.

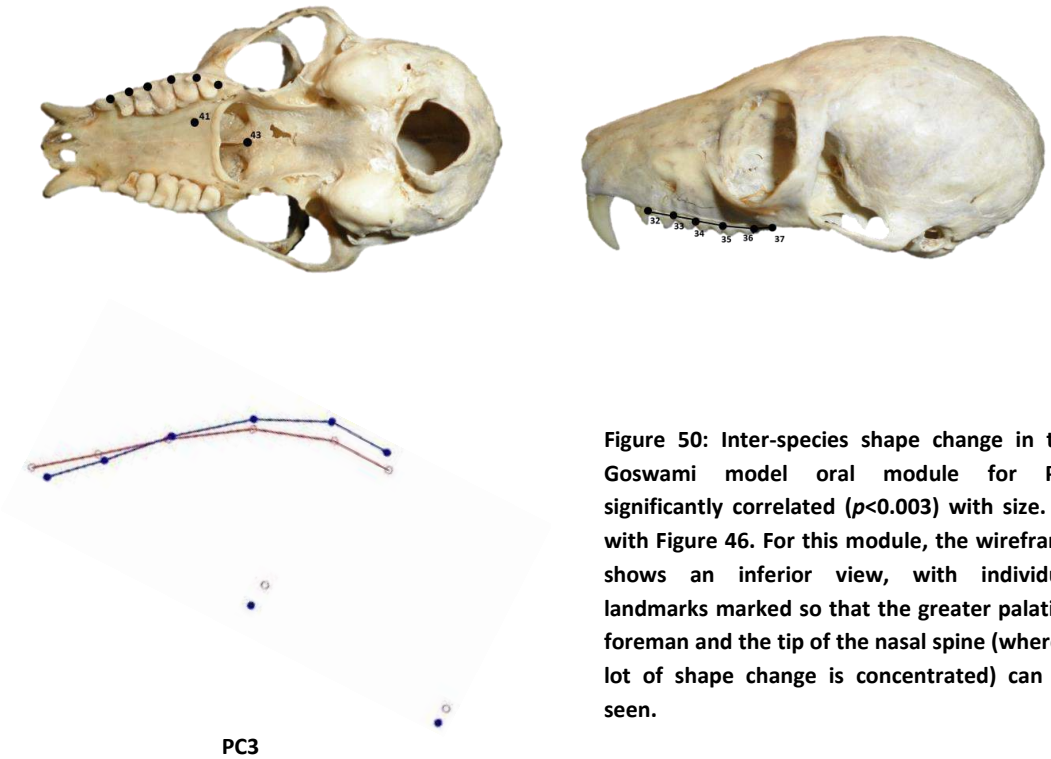

Figure 50: Inter-species shape change in the Goswami model oral module for PCs significantly correlated (*p*<0.003) with size. As with Figure 46. For this module, the wireframe shows an inferior view, with individual landmarks marked so that the greater palatine foreman and the tip of the nasal spine (where a lot of shape change is concentrated) can be seen.

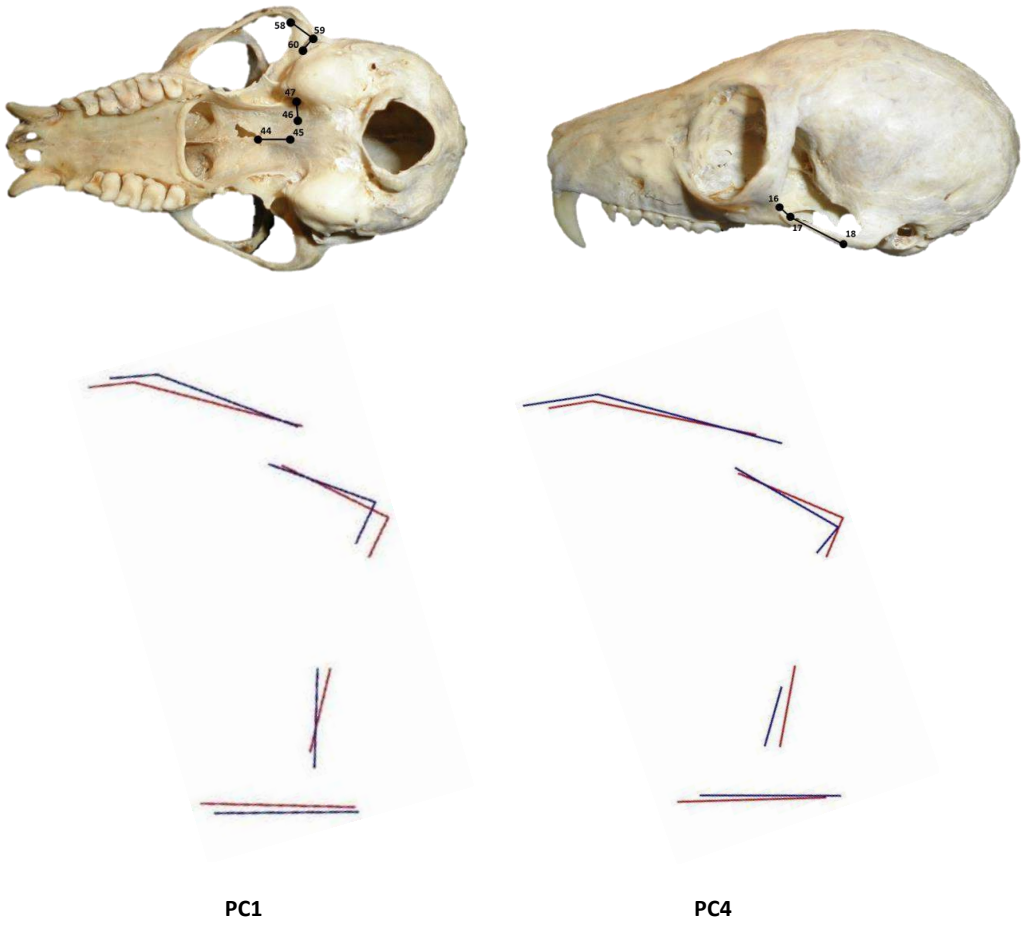

Figure 51: Inter-species shape change in the Goswami model zygomatic module for PCs significantly correlated (*p*<0.003) with size. As with Figure 46. For this module, the wireframe shows an inferior view.

Figure 52: Inter-species shape change in the Goswami model vault module for PCs significantly correlated (*p*<0.003) with size. As with Figure 46.

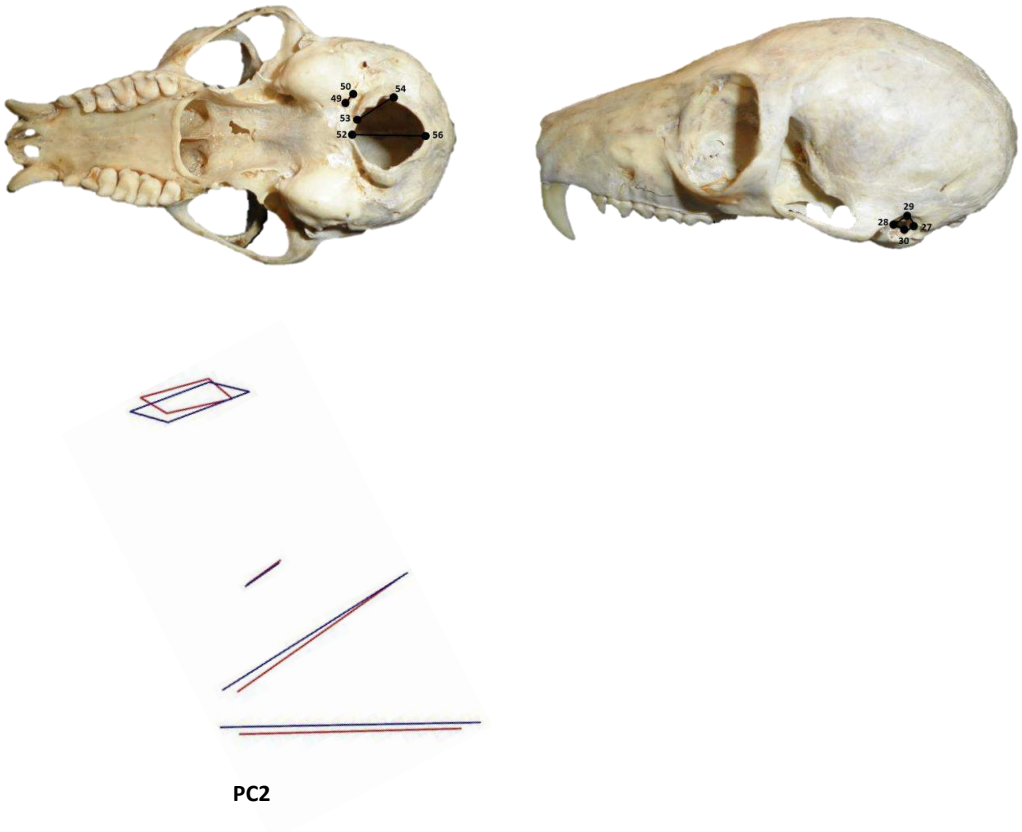

Figure 53: Inter-species shape change in the Goswami model base module for PCs significantly correlated (*p*<0.003) with size. As with Figure 46. For this module, the wireframe shows an inferior view

5.4.4. Inter-species allometry – size-versus-size

Inter-species relationships between module size and overall size (Table 58) were alike for the species average and the resampling method; however, they did not always mirror the trends shown at an intra-species level. While both vault modules (2* and Goswami model) showed negative allometry, neither of the respective face models showed significant allometry, and neither did the Goswami zygomatic module. In direct contrast to the intra-species results, the Goswami orbit and base module were negatively allometric. The oral module, however, remained in line with the intra-species results, being positively allometric.

Table 58: Results of Inter-species allometry for all of the 2* and Goswami model modules, where ln(CS) of the module was regressed against the ln(CS) of the whole cranium. Where the relationship was found to be significantly different from isometry, the allometric direction is indicated. Unshaded rows are the results using the SPECIES AVERAGE method and shaded rows are the results using the RESAMPLING method.

Module	Slope	Lower CI	Upper CI	R^2	Allometry
2* model - face	1.02	0.99	1.05	0.99	
	1.02	0.98	1.06	0.99	
2* model - vault	0.86	0.81	0.91	0.98	-
	0.87	0.81	0.93	0.97	-
Goswami model - face	1.05	0.97	1.12	0.97	
	1.02	0.95	1.10	0.96	
Goswami model - orbit	0.87	0.82	0.93	0.98	-
	0.88	0.82	0.94	0.97	-
Goswami model - oral	1.09	1.01	1.15	0.97	+
	1.08	1.00	1.16	0.96	+
Goswami model - zygomatic	1.03	0.96	1.10	0.97	
	1.02	0.94	1.09	0.96	
Goswami model - vault	0.83	0.78	0.89	0.97	-
	0.84	0.77	0.91	0.95	-
Goswami model - base	0.80	0.73	0.88	0.95	-
	0.80	0.71	0.89	0.92	-

5.4.5. Inter-species differences in allometric scaling – ANCOVA results

ANCOVAs were conducted for all combinations of species pairs to highlight which species, in particular, differed in their relationships between shape and size. Summary tables are shown below (Tables 59-67); for full results tables see Appendix 6. The results reveal that significant differences were often associated with specific species. For example, for the analysis of the whole cranium, *G. senegalensis, O. garnettii* and *E. mongoz* repeatedly have significantly different relationships between shape and size, compared to other species of the Strepsirhini, including, at times, each other. In fact, *G. senegalensis* differs from other

species in its allometric scaling in nearly all of the modules examined, with the exceptions of the base and zygomatic modules of the Goswami model. This includes significant differences even with closely related species such as *G. moholi* and *G. zanzibaricus*, to which it might be expected to be phenotypically similar.

Other species are seen to repeatedly differ in their allometric scaling pattern only for specific modules. For example, *Microcebus, Otolemur* and *Varecia variegata* repeatedly differ from other species for the Goswami zygomatic module, the Goswami orbit module and the 2* vault module, respectively. As a general rule, significant differences in allometric scaling were more likely to be seen across families then within them.

Table 59: ANCOVA results, showing inter-species differences in the relationship of size-versus-shape for the whole cranium, where numbers represent PCs for which results were significant (p<0.0001) for that species pair.

Whole cranium	*Cheirogaleus major*	*Cheirogaleus medius*	*Microcebus murinus*	*Microcebus rufus*	*Galago alleni*	*Galagoides demidoff*	*Euoticus elegantulus*	*Galago moholi*	*Galago senegalensis*	*Galagoides zanzibaricus*	*Otolemur crassicaudatus*
C. major											
C. medius											
M. murinus											
M. rufus											
G. alleni											
G. demidoff											
E. elegantulus											
G. moholi											
G. senegalensis				2	1	1		1			
G. zanzibaricus											
O. crassicaudatus											
O. garnettii				2	1						
A. laniger											
I. Indri									2		
P. diadema											
P. verreauxi						5					5
E. fulvus									2		5
E. macaco											
E. mongoz				4				4	2		
E. rubriventer						5					
H. griseus		1							1		1
L. catta						5		5	2, 5		5
V. variegata									1, 2, 4		
L. ruficaudatus									2		
L. tardigradus						5					5
N. bengalensis											
N. coucang				4				4	4		
P. potto									1		

Table 59 (Cont.)

Whole cranium	*Otolemur garnettii*	*Avahi laniger*	*Indri indri*	*Propithecus diadema*	*Propithecus verreauxi*	*Eulemur fulvus*	*Eulemur macaco*	*Eulemur mongoz*	*Eulemur rubriventer*	*Hapalemur griseus*	*Lemur catta*
C. major											
C. medius											
M. murinus											
M. rufus											
G. alleni											
G. demidoff											
E. elegantulus											
G. moholi											
G. senegalensis											
G. zanzibaricus											
O. crassicaudatus											
O. garnettii											
A. laniger											
I. Indri	2										
P. diadema											
P. verreauxi											
E. fulvus	2										
E. macaco											
E. mongoz	2			2		4					
E. rubriventer											
H. griseus	1										
L. catta	2							5		1	
V. variegata	2										
L. ruficaudatus	2			2							
L. tardigradus						2		2			2
N. bengalensis											
N. coucang						2, 4		2			
P. potto						5		2			5

Table 59 (Cont.)

Whole cranium	*Varecia variegata*	*Lepilemur ruficaudatus*	*Loris tardigradus*	*Nycticebus bengalensis*	*Nycticebus coucang*	*Perodicticus potto*
C. major						
C. medius						
M. murinus						
M. rufus						
G. alleni						
G. demidoff						
E. elegantulus						
G. moholi						
G. senegalensis						
G. zanzibaricus						
O. crassicaudatus						
O. garnettii						
A. laniger						
I. Indri						
P. diadema						
P. verreauxi						
E. fulvus						
E. macaco						
E. mongoz						
E. rubriventer						
H. griseus						
L. catta						
V. variegata						
L. ruficaudatus						
L. tardigradus	2	2				
N. bengalensis						
N. coucang		2				
P. potto		2	5			

Table 60: ANCOVA results, showing inter-species differences in the relationship of size-versus-shape for the 2* model face module, where numbers represent PCs for which results were significant (p<0.0001) for that species pair.

2x model FACE	*Cheirogaleus major*	*Cheirogaleus medius*	*Microcebus murinus*	*Microcebus rufus*	*Galago alleni*	*Galagoides demidoff*	*Euoticus elegantulus*	*Galago moholi*	*Galago senegalensis*	*Galagoides zanzibaricus*	*Otolemur crassicaudatus*
C. major											
C. medius											
M. murinus											
M. rufus											
G. alleni											
G. demidoff											
E. elegantulus											
G. moholi											
G. senegalensis			1	4	1						
G. zanzibaricus					1						
O. crassicaudatus											
O. garnettii		3	2	3		2		3			2
A. laniger											
I. Indri									2, 3		
P. diadema											
P. verreauxi											
E. fulvus									1 , 4	1	
E. macaco									1	1	
E. mongoz								1	1, 2, 4	1	1
E. rubriventer											
H. griseus									1	1	
L. catta									1	1	5
V. variegata									1, 2, 4	1	
L. ruficaudatus									1, 2	1	
L. tardigradus											2, 5
N. bengalensis			2								
N. coucang											
P. potto									1, 3		

Table 60 (Cont.)

2x model FACE	*Otolemur garnettii*	*Avahi laniger*	*Indri indri*	*Propithecus diadema*	*Propithecus verreauxi*	*Eulemur fulvus*	*Eulemur macaco*	*Eulemur mongoz*	*Eulemur rubriventer*	*Hapalemur griseus*	*Lemur catta*
C. major											
C. medius											
M. murinus											
M. rufus											
G. alleni											
G. demidoff											
E. elegantulus											
G. moholi											
G. senegalensis											
G. zanzibaricus											
O. crassicaudatus											
O. garnettii											
A. laniger											
I. Indri	2, 3										
P. diadema											
P. verreauxi	3										
E. fulvus	2 , 3										
E. macaco	3		2								
E. mongoz	1, 2, 3						2				
E. rubriventer											
H. griseus											
L. catta											
V. variegata	2						2				
L. ruficaudatus	2						2				
L. tardigradus	3		2			2		2			
N. bengalensis											
N. coucang	3							2			5
P. potto	3		2					2			

Table 60 (Cont.)

2x model FACE	*Varecia variegata*	*Lepilemur ruficaudatus*	*Loris tardigradus*	*Nycticebus bengalensis*	*Nycticebus coucang*	*Perodicticus potto*
C. major						
C. medius						
M. murinus						
M. rufus						
G. alleni						
G. demidoff						
E. elegantulus						
G. moholi						
G. senegalensis						
G. zanzibaricus						
O. crassicaudatus						
O. garnettii						
A. laniger						
I. Indri						
P. diadema						
P. verreauxi						
E. fulvus						
E. macaco						
E. mongoz						
E. rubriventer						
H. griseus						
L. catta						
V. variegata						
L. ruficaudatus						
L. tardigradus	2	2				
N. bengalensis						
N. coucang						
P. potto		2				

Table 61: ANCOVA results, showing inter-species differences in the relationship of size-versus-shape for the 2* model vault module, where numbers represent PCs for which results were significant (p<0.0001) for that species pair.

2x model VAULT	*Cheirogaleus major*	*Cheirogaleus medius*	*Microcebus murinus*	*Microcebus rufus*	*Galago alleni*	*Galagoides demidoff*	*Euoticus elegantulus*	*Galago moholi*	*Galago senegalensis*	*Galagoides zanzibaricus*	*Otolemur crassicaudatus*
C. major											
C. medius											
M. murinus											
M. rufus											
G. alleni											
G. demidoff											
E. elegantulus											
G. moholi											
G. senegalensis											
G. zanzibaricus											
O. crassicaudatus		4							2		
O. garnettii									2		
A. laniger											
I. Indri				3							
P. diadema											
P. verreauxi											
E. fulvus											3
E. macaco											
E. mongoz											
E. rubriventer											
H. griseus											
L. catta											
V. variegata		4	4				4	4	4	4	4
L. ruficaudatus											
L. tardigradus									1		1, 2, 4
N. bengalensis											
N. coucang											4
P. potto				3					3		

Table 61 (Cont.)

2x model VAULT	*Otolemur garnettii*	*Avahi laniger*	*Indri indri*	*Propithecus diadema*	*Propithecus verreauxi*	*Eulemur fulvus*	*Eulemur macaco*	*Eulemur mongoz*	*Eulemur rubriventer*	*Hapalemur griseus*	*Lemur catta*
C. major											
C. medius											
M. murinus											
M. rufus											
G. alleni											
G. demidoff											
E. elegantulus											
G. moholi											
G. senegalensis											
G. zanzibaricus											
O. crassicaudatus											
O. garnettii											
A. laniger											
I. Indri											
P. diadema											
P. verreauxi											
E. fulvus											
E. macaco											
E. mongoz											
E. rubriventer											
H. griseus											
L. catta											
V. variegata	4		4	4	4	4	4	4			
L. ruficaudatus											
L. tardigradus	1, 2, 6							5			
N. bengalensis											
N. coucang						3					
P. potto						3					3

Table 61 (Cont.)

2x model VAULT	*Varecia variegata*	*Lepilemur ruficaudatus*	*Loris tardigradus*	*Nycticebus bengalensis*	*Nycticebus coucang*	*Perodicticus potto*
C. major						
C. medius						
M. murinus						
M. rufus						
G. alleni						
G. demidoff						
E. elegantulus						
G. moholi						
G. senegalensis						
G. zanzibaricus						
O. crassicaudatus						
O. garnettii						
A. laniger						
I. Indri						
P. diadema						
P. verreauxi						
E. fulvus						
E. macaco						
E. mongoz						
E. rubriventer						
H. griseus						
L. catta						
V. variegata						
L. ruficaudatus						
L. tardigradus	4					
N. bengalensis						
N. coucang	4					
P. potto	4		3			

Table 62: ANCOVA results, showing inter-species differences in the relationship of size-versus-shape for the Goswami model face module, where numbers represent PCs for which results were significant (p<0.0001) for that species pair.

Goswami model FACE	*Cheirogaleus major*	*Cheirogaleus medius*	*Microcebus murinus*	*Microcebus rufus*	*Galago alleni*	*Galagoides demidoff*	*Euoticus elegantulus*	*Galago moholi*	*Galago senegalensis*	*Galagoides zanzibaricus*	*Otolemur crassicaudatus*
C. major											
C. medius											
M. murinus											
M. rufus											
G. alleni											
G. demidoff											
E. elegantulus					1						
G. moholi											
G. senegalensis					1	2					
G. zanzibaricus											
O. crassicaudatus						4					
O. garnettii				1	1	2					
A. laniger											
I. Indri											4
P. diadema											
P. verreauxi				1	1	2		1	1		1
E. fulvus						2					
E. macaco				1	1			1			
E. mongoz											
E. rubriventer											
H. griseus											
L. catta											
V. variegata											5
L. ruficaudatus											
L. tardigradus											
N. bengalensis											
N. coucang				1	1						
P. potto											

Table 62 (Cont.)

Goswami model FACE	*Otolemur garnettii*	*Avahi laniger*	*Indri indri*	*Propithecus diadema*	*Propithecus verreauxi*	*Eulemur fulvus*	*Eulemur macaco*	*Eulemur mongoz*	*Eulemur rubriventer*	*Hapalemur griseus*	*Lemur catta*
C. major											
C. medius											
M. murinus											
M. rufus											
G. alleni											
G. demidoff											
E. elegantulus											
G. moholi											
G. senegalensis											
G. zanzibaricus											
O. crassicaudatus											
O. garnettii											
A. laniger											
I. Indri											
P. diadema											
P. verreauxi			2								
E. fulvus			2								
E. macaco											
E. mongoz					1						
E. rubriventer											
H. griseus											
L. catta											
V. variegata					1, 5		1				
L. ruficaudatus											
L. tardigradus											
N. bengalensis											
N. coucang											
P. potto											

Table 62 (Cont.)

Goswami model FACE	*Varecia variegata*	*Lepilemur ruficaudatus*	*Loris tardigradus*	*Nycticebus bengalensis*	*Nycticebus coucang*	*Perodicticus potto*
C. major						
C. medius						
M. murinus						
M. rufus						
G. alleni						
G. demidoff						
E. elegantulus						
G. moholi						
G. senegalensis						
G. zanzibaricus						
O. crassicaudatus						
O. garnettii						
A. laniger						
I. Indri						
P. diadema						
P. verreauxi						
E. fulvus						
E. macaco						
E. mongoz						
E. rubriventer						
H. griseus						
L. catta						
V. variegata						
L. ruficaudatus						
L. tardigradus						
N. bengalensis						
N. coucang						
P. potto		3				

Table 63: ANCOVA results, showing inter-species differences in the relationship of size-versus-shape for the Goswami model orbit module, where numbers represent PCs for which results were significant (p<0.0001) for that species pair.

Goswami model ORBIT	*Cheirogaleus major*	*Cheirogaleus medius*	*Microcebus murinus*	*Microcebus rufus*	*Galago alleni*	*Galagoides demidoff*	*Euoticus elegantulus*	*Galago moholi*	*Galago senegalensis*	*Galagoides zanzibaricus*	*Otolemur crassicaudatus*
C. major											
C. medius											
M. murinus											
M. rufus											
G. alleni											
G. demidoff											
E. elegantulus											
G. moholi											
G. senegalensis				3							
G. zanzibaricus											
O. crassicaudatus				3		3		3			
O. garnettii				3							
A. laniger											
I. Indri			2			2			2		2
P. diadema											
P. verreauxi											3
E. fulvus											3
E. macaco											
E. mongoz											
E. rubriventer					5				2		3
H. griseus											
L. catta											3
V. variegata											
L. ruficaudatus											
L. tardigradus											3
N. bengalensis											
N. coucang											3
P. potto									4		

Table 63 (Cont.)

Goswami model ORBIT	*Otolemur garnettii*	*Avahi laniger*	*Indri indri*	*Propithecus diadema*	*Propithecus verreauxi*	*Eulemur fulvus*	*Eulemur macaco*	*Eulemur mongoz*	*Eulemur rubriventer*	*Hapalemur griseus*	*Lemur catta*
C. major											
C. medius											
M. murinus											
M. rufus											
G. alleni											
G. demidoff											
E. elegantulus											
G. moholi											
G. senegalensis											
G. zanzibaricus											
O. crassicaudatus											
O. garnettii											
A. laniger											
I. Indri	2										
P. diadema											
P. verreauxi											
E. fulvus	3		2								
E. macaco											
E. mongoz	4										
E. rubriventer	2, 5										
H. griseus											
L. catta											
V. variegata	4										
L. ruficaudatus											
L. tardigradus			2								
N. bengalensis			2						2		
N. coucang			2								
P. potto						4		4			

Table 63 (Cont.)

Goswami model ORBIT	*Varecia variegata*	*Lepilemur ruficaudatus*	*Loris tardigradus*	*Nycticebus bengalensis*	*Nycticebus coucang*	*Perodicticus potto*
C. major						
C. medius						
M. murinus						
M. rufus						
G. alleni						
G. demidoff						
E. elegantulus						
G. moholi						
G. senegalensis						
G. zanzibaricus						
O. crassicaudatus						
O. garnettii						
A. laniger						
I. Indri						
P. diadema						
P. verreauxi						
E. fulvus						
E. macaco						
E. mongoz						
E. rubriventer						
H. griseus						
L. catta						
V. variegata						
L. ruficaudatus						
L. tardigradus						
N. bengalensis						
N. coucang						
P. potto	4					

Table 64: ANCOVA results, showing inter-species differences in the relationship of size-versus-shape for the Goswami model oral module, where numbers represent PCs for which results were significant for that species pair.

Goswami model[i] ORAL	*Cheirogaleus major*	*Cheirogaleus medius*	*Microcebus murinus*	*Microcebus rufus*	*Galago alleni*	*Galagoides demidoff*	*Euoticus elegantulus*	*Galago moholi*	*Galago senegalensis*	*Galagoides zanzibaricus*	*Otolemur crassicaudatus*
C. major											
C. medius											
M. murinus											
M. rufus											
G. alleni											
G. demidoff											
E. elegantulus											
G. moholi											
G. senegalensis											
G. zanzibaricus											
O. crassicaudatus											
O. garnettii						2					
A. laniger											
I. Indri				1		1		1			1
P. diadema											
P. verreauxi											
E. fulvus											
E. macaco											
E. mongoz			4						2		4
E. rubriventer											
H. griseus											
L. catta											
V. variegata											
L. ruficaudatus											
L. tardigradus											
N. bengalensis											
N. coucang											
P. potto											

Table 64 (Cont.)

Goswami model ORAL	*Otolemur garnettii*	*Avahi laniger*	*Indri indri*	*Propithecus diadema*	*Propithecus verreauxi*	*Eulemur fulvus*	*Eulemur macaco*	*Eulemur mongoz*	*Eulemur rubriventer*	*Hapalemur griseus*	*Lemur catta*
C. major											
C. medius											
M. murinus											
M. rufus											
G. alleni											
G. demidoff											
E. elegantulus											
G. moholi											
G. senegalensis											
G. zanzibaricus											
O. crassicaudatus											
O. garnettii											
A. laniger											
I. Indri	1										
P. diadema											
P. verreauxi											
E. fulvus											
E. macaco											
E. mongoz	2, 4										
E. rubriventer											
H. griseus			1								
L. catta											
V. variegata											
L. ruficaudatus											
L. tardigradus	4										
N. bengalensis											
N. coucang											
P. potto	1										

Table 64 (Cont.)

Goswami model ORAL	*Varecia variegata*	*Lepilemur ruficaudatus*	*Loris tardigradus*	*Nycticebus bengalensis*	*Nycticebus coucang*	*Perodicticus potto*
C. major						
C. medius						
M. murinus						
M. rufus						
G. alleni						
G. demidoff						
E. elegantulus						
G. moholi						
G. senegalensis						
G. zanzibaricus						
O. crassicaudatus						
O. garnettii						
A. laniger						
I. Indri						
P. diadema						
P. verreauxi						
E. fulvus						
E. macaco						
E. mongoz						
E. rubriventer						
H. griseus						
L. catta						
V. variegata						
L. ruficaudatus						
L. tardigradus						
N. bengalensis						
N. coucang						
P. potto						

Table 65: ANCOVA results, showing inter-species differences in the relationship of size-versus-shape for the Goswami model zygomatic module, where numbers represent PCs for which results were significant (p<0.0001) for that species pair.

Goswami model Zygomatic	*Cheirogaleus major*	*Cheirogaleus medius*	*Microcebus murinus*	*Microcebus rufus*	*Galago alleni*	*Galagoides demidoff*	*Euoticus elegantulus*	*Galago moholi*	*Galago senegalensis*	*Galagoides zanzibaricus*	*Otolemur crassicaudatus*
C. major											
C. medius											
M. murinus	3										
M. rufus											
G. alleni											
G. demidoff											
E. elegantulus											
G. moholi											
G. senegalensis			3								
G. zanzibaricus											
O. crassicaudatus			3	4					4		
O. garnettii			3	4					4		
A. laniger											
I. Indri											
P. diadema											
P. verreauxi											
E. fulvus											
E. macaco											
E. mongoz			3								
E. rubriventer											
H. griseus											
L. catta											
V. variegata											3
L. ruficaudatus											
L. tardigradus			3								
N. bengalensis											
N. coucang											
P. potto			3						4		

Table 65 (Cont.)

Goswami model ZYGO	*Otolemur garnettii*	*Avahi laniger*	*Indri indri*	*Propithecus diadema*	*Propithecus verreauxi*	*Eulemur fulvus*	*Eulemur macaco*	*Eulemur mongoz*	*Eulemur rubriventer*	*Hapalemur griseus*	*Lemur catta*
C. major											
C. medius											
M. murinus											
M. rufus											
G. alleni											
G. demidoff											
E. elegantulus											
G. moholi											
G. senegalensis											
G. zanzibaricus											
O. crassicaudatus											
O. garnettii											
A. laniger											
I. Indri											
P. diadema											
P. verreauxi											
E. fulvus											
E. macaco											
E. mongoz											
E. rubriventer											
H. griseus											
L. catta											
V. variegata											
L. ruficaudatus											
L. tardigradus											
N. bengalensis											
N. coucang											
P. potto											

Table 65 (Cont.)

Goswami model ZYGO	*Varecia variegata*	*Lepilemur ruficaudatus*	*Loris tardigradus*	*Nycticebus bengalensis*	*Nycticebus coucang*	*Perodicticus potto*
C. major						
C. medius						
M. murinus						
M. rufus						
G. alleni						
G. demidoff						
E. elegantulus						
G. moholi						
G. senegalensis						
G. zanzibaricus						
O. crassicaudatus						
O. garnettii						
A. laniger						
I. Indri						
P. diadema						
P. verreauxi						
E. fulvus						
E. macaco						
E. mongoz						
E. rubriventer						
H. griseus						
L. catta						
V. variegata						
L. ruficaudatus						
L. tardigradus						
N. bengalensis						
N. coucang						
P. potto						

Table 66: ANCOVA results, showing inter-species differences in the relationship of size-versus-shape for the Goswami model vault module, where numbers represent PCs for which results were significant (p<0.0001) for that species pair.

Goswami model VAULT	*Cheirogaleus major*	*Cheirogaleus medius*	*Microcebus murinus*	*Microcebus rufus*	*Galago alleni*	*Galagoides demidoff*	*Euoticus elegantulus*	*Galago moholi*	*Galago senegalensis*	*Galagoides zanzibaricus*	*Otolemur crassicaudatus*
C. major											
C. medius											
M. murinus											
M. rufus											
G. alleni											
G. demidoff											
E. elegantulus											
G. moholi											
G. senegalensis				3							
G. zanzibaricus											
O. crassicaudatus									1, 2		
O. garnettii											
A. laniger						1			1		
I. Indri									2		
P. diadema				3					5		5
P. verreauxi											
E. fulvus											
E. macaco									5		
E. mongoz											
E. rubriventer											
H. griseus											
L. catta				3							
V. variegata						1			1, 2		
L. ruficaudatus											
L. tardigradus			1						1		1
N. bengalensis											
N. coucang											
P. potto									2		

Table 66 (Cont.)

Goswami model VAULT	*Otolemur garnettii*	*Avahi laniger*	*Indri indri*	*Propithecus diadema*	*Propithecus verreauxi*	*Eulemur fulvus*	*Eulemur macaco*	*Eulemur mongoz*	*Eulemur rubriventer*	*Hapalemur griseus*	*Lemur catta*
C. major											
C. medius											
M. murinus											
M. rufus											
G. alleni											
G. demidoff											
E. elegantulus											
G. moholi											
G. senegalensis											
G. zanzibaricus											
O. crassicaudatus											
O. garnettii											
A. laniger											
I. Indri											
P. diadema	5										
P. verreauxi											
E. fulvus											
E. macaco	5										
E. mongoz											
E. rubriventer											
H. griseus											
L. catta											
V. variegata											
L. ruficaudatus											
L. tardigradus	1			5		1					
N. bengalensis											
N. coucang											
P. potto											

Table 66 (Cont.)

Goswami model VAULT	*Varecia variegata*	*Lepilemur ruficaudatus*	*Loris tardigradus*	*Nycticebus bengalensis*	*Nycticebus coucang*	*Perodicticus potto*
C. major						
C. medius						
M. murinus						
M. rufus						
G. alleni						
G. demidoff						
E. elegantulus						
G. moholi						
G. senegalensis						
G. zanzibaricus						
O. crassicaudatus						
O. garnettii						
A. laniger						
I. Indri						
P. diadema						
P. verreauxi						
E. fulvus						
E. macaco						
E. mongoz						
E. rubriventer						
H. griseus						
L. catta						
V. variegata						
L. ruficaudatus						
L. tardigradus	1					
N. bengalensis						
N. coucang						
P. potto						

Table 67: ANCOVA results, showing inter-species differences in the relationship of size-versus-shape for the Goswami model base module, where numbers represent PCs for which results were significant (p<0.0001) for that species pair.

Goswami model BASE	*Cheirogaleus major*	*Cheirogaleus medius*	*Microcebus murinus*	*Microcebus rufus*	*Galago alleni*	*Galagoides demidoff*	*Euoticus elegantulus*	*Galago moholi*	*Galago senegalensis*	*Galagoides zanzibaricus*	*Otolemur crassicaudatus*
C. major											
C. medius											
M. murinus											
M. rufus											
G. alleni											
G. demidoff											
E. elegantulus											
G. moholi											
G. senegalensis											
G. zanzibaricus					3						
O. crassicaudatus											
O. garnettii											
A. laniger				5							
I. Indri											
P. diadema											
P. verreauxi											
E. fulvus					3				3		2
E. macaco											
E. mongoz											2
E. rubriventer											
H. griseus											
L. catta											
V. variegata											
L. ruficaudatus											
L. tardigradus											
N. bengalensis											
N. coucang											
P. potto											

Table 67 (Cont.)

Goswami model BASE	*Otolemur garnettii*	*Avahi laniger*	*Indri indri*	*Propithecus diadema*	*Propithecus verreauxi*	*Eulemur fulvus*	*Eulemur macaco*	*Eulemur mongoz*	*Eulemur rubriventer*	*Hapalemur griseus*	*Lemur catta*
C. major											
C. medius											
M. murinus											
M. rufus											
G. alleni											
G. demidoff											
E. elegantulus											
G. moholi											
G. senegalensis											
G. zanzibaricus											
O. crassicaudatus											
O. garnettii											
A. laniger											
I. Indri											
P. diadema											
P. verreauxi											
E. fulvus	2	3									
E. macaco											
E. mongoz	2										
E. rubriventer											
H. griseus											
L. catta											
V. variegata											
L. ruficaudatus											
L. tardigradus											
N. bengalensis											
N. coucang											
P. potto						3					

Table 67 (Cont.)

Goswami model BASE	*Varecia variegata*	*Lepilemur ruficaudatus*	*Loris tardigradus*	*Nycticebus bengalensis*	*Nycticebus coucang*	*Perodicticus potto*
C. major						
C. medius						
M. murinus						
M. rufus						
G. alleni						
G. demidoff						
E. elegantulus						
G. moholi						
G. senegalensis						
G. zanzibaricus						
O. crassicaudatus						
O. garnettii						
A. laniger						
I. Indri						
P. diadema						
P. verreauxi						
E. fulvus						
E. macaco						
E. mongoz						
E. rubriventer						
H. griseus						
L. catta						
V. variegata						
L. ruficaudatus						
L. tardigradus						
N. bengalensis						
N. coucang						
P. potto						

5.4.6. Inter-species differences in allometric scaling – evo-maps

Here, evo-maps are used to illustrate where inter- and intra-species allometric patterns diverge from each other. Where branches are shown in green or red, intra-specific scalars are larger or smaller than the corresponding inter-specific scalar, respectively. In addition, the thickness of the branch represents the rate of change along that branch and the size of the circles at the tip and at the ancestral nodes are indicative of the size of the trait (in this instance, the size of the difference between the slope of the intra-species regression of shape against size and the inter-species slope of the same regression). To save space, evo-maps are only shown for PCs judged to be the most interesting for each of the modules investigated (Figures 54-65), the remaining evo-maps, for PCs 1-5 for all modules are given in Appendix 7.

For the whole cranium differences between intra- and inter-species slopes were small for PC1 (Figure 54). This suggests that, for the greatest proportion of shape change among strepsirhine species, larger species tend to be scaled up versions of smaller species following a common allometric trend.

For the 2* model, PC1 for the face module shows a general trend for a larger allometric scalars in species of Lemuridae, with the exception of *C. major*. *G. zanzibaricus* stands out as having a smaller scalar (Figure 55). PC 1 for the vault module shows a split between the Lemuriformes and the Lorisiformes, with the lemur showing smaller and the Lorises and Galagos (with the exception of *Otolemur*) larger scalars (Figure 56).

For the Goswami model, differences between intra- and inter-species scaling are relatively small for the face and zygomatic modules (Figure 58, 62). However, large differences are seen in the orbit module, specifically for PC1, where *A. laniger, I. indri* and *G. zanzibaricus* have smaller scalars (Figure 59), and for PC3, where *A. laniger* has a larger scalar (Figure 60). For the oral module, there is no particular pattern at family or species level for PC1, but *E. rubriventer* and *I. indri* follow steeper scaling patterns and *H. griseus* has the lowest scalar of any species (Figure 61). For PC1, for the vault module, there is again a split between the Lemuriformes and the Lorisiformes (Figure 64), similar to that found for the 2* vault module (Figure 56). However, here the direction of scaling differences is reversed, with lemurs following steeper scaling patterns (with some exceptions in the Indriidae) and the lorises and galagos following lower scaling coefficients. For PC2 of the vault module, *V.*

variegata and *I. indri* have lower scalars (Figure 64). No family or genera level pattern is seen for PC1 of the base modules, but *G. alleni* and *A. laniger* are both identified as the species with the lowest scaling coefficients for that module (Figure 65).

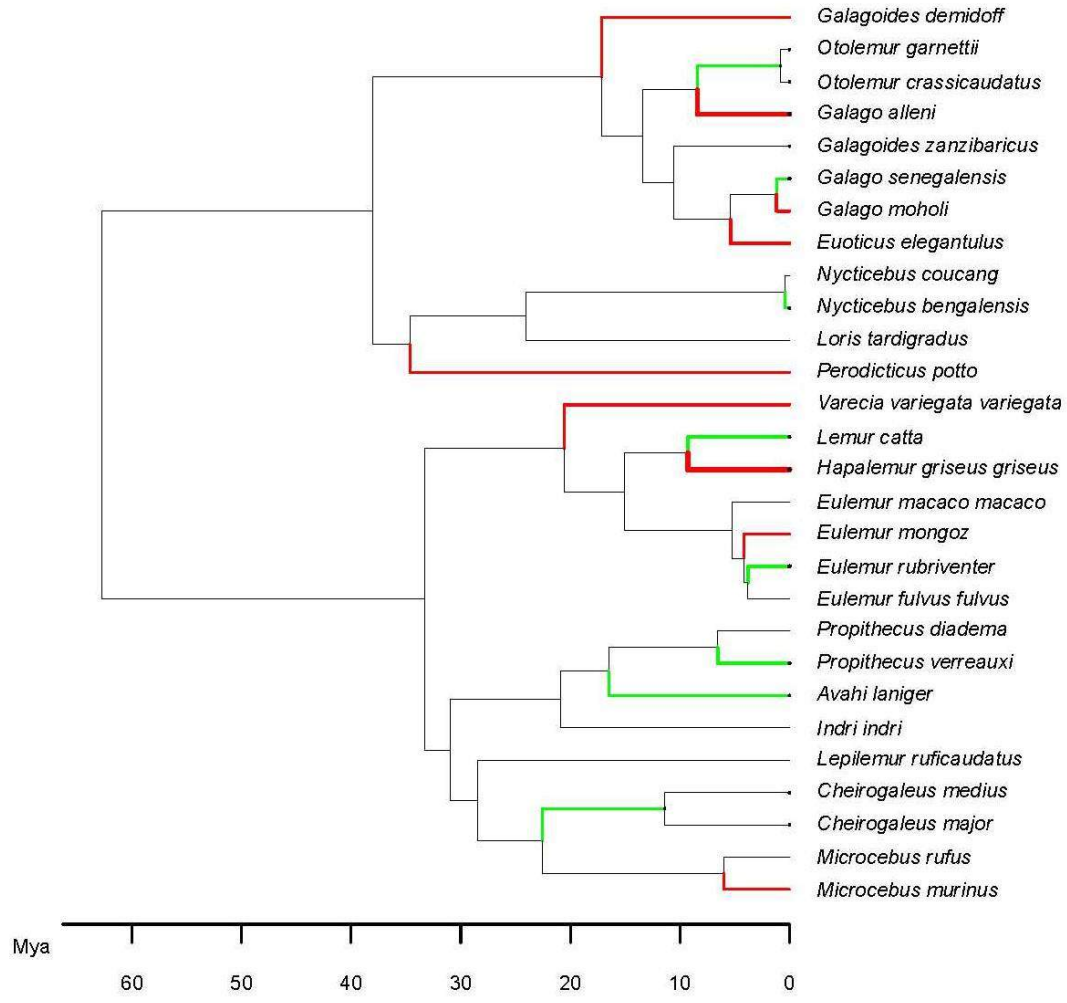

Figure 54: Evo-map of intra-species allometric scaling, in comparison to inter-species allometric scaling, for the whole cranium for PC1. Where green indicates that the intra-species allometric slope is more positive than the inter-species allometric slope and red that it is more negative.

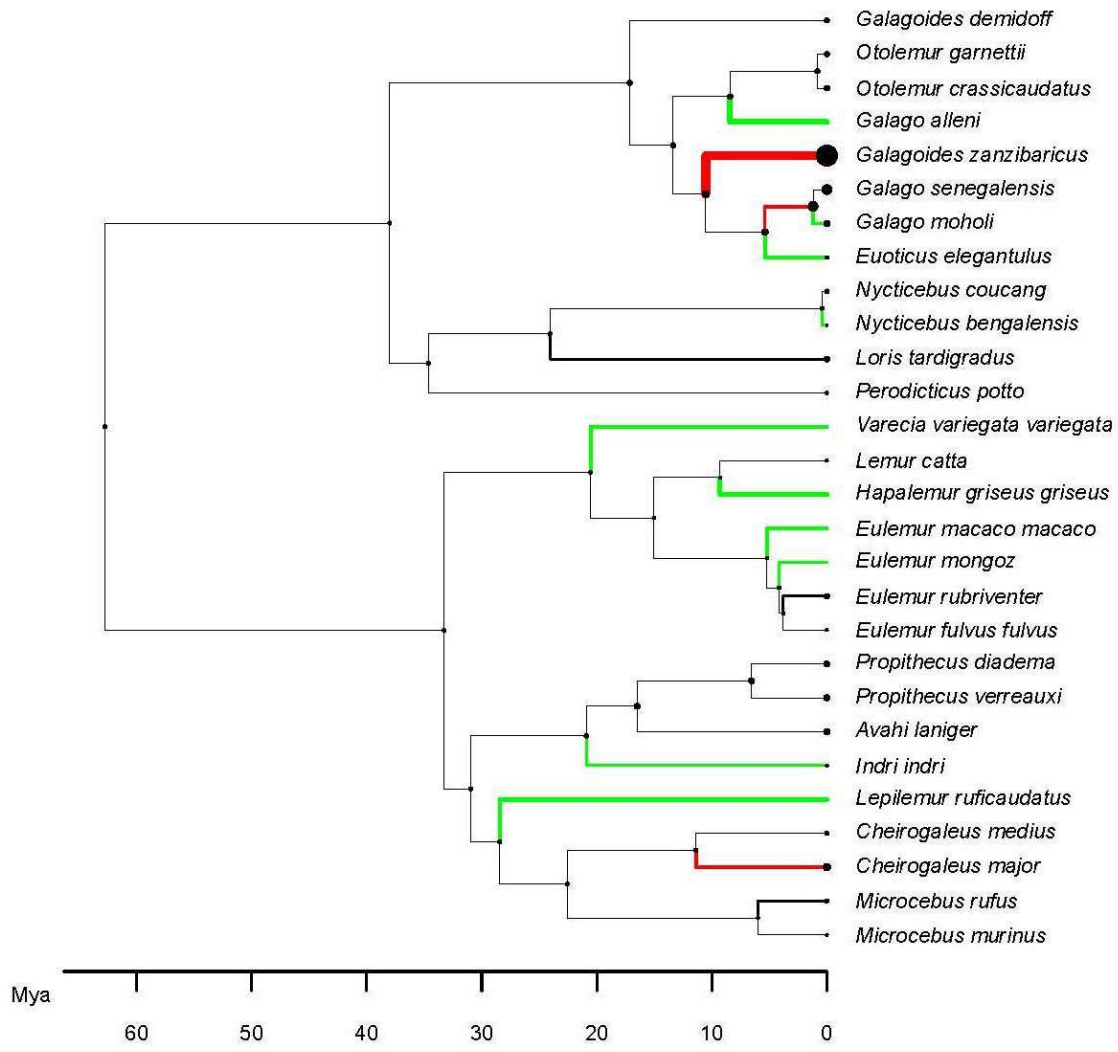

Figure 55: Evo-map of intra-species allometric scaling, in comparison to inter-species allometric scaling, for the 2* model face module for PC1. As with Figure 54.

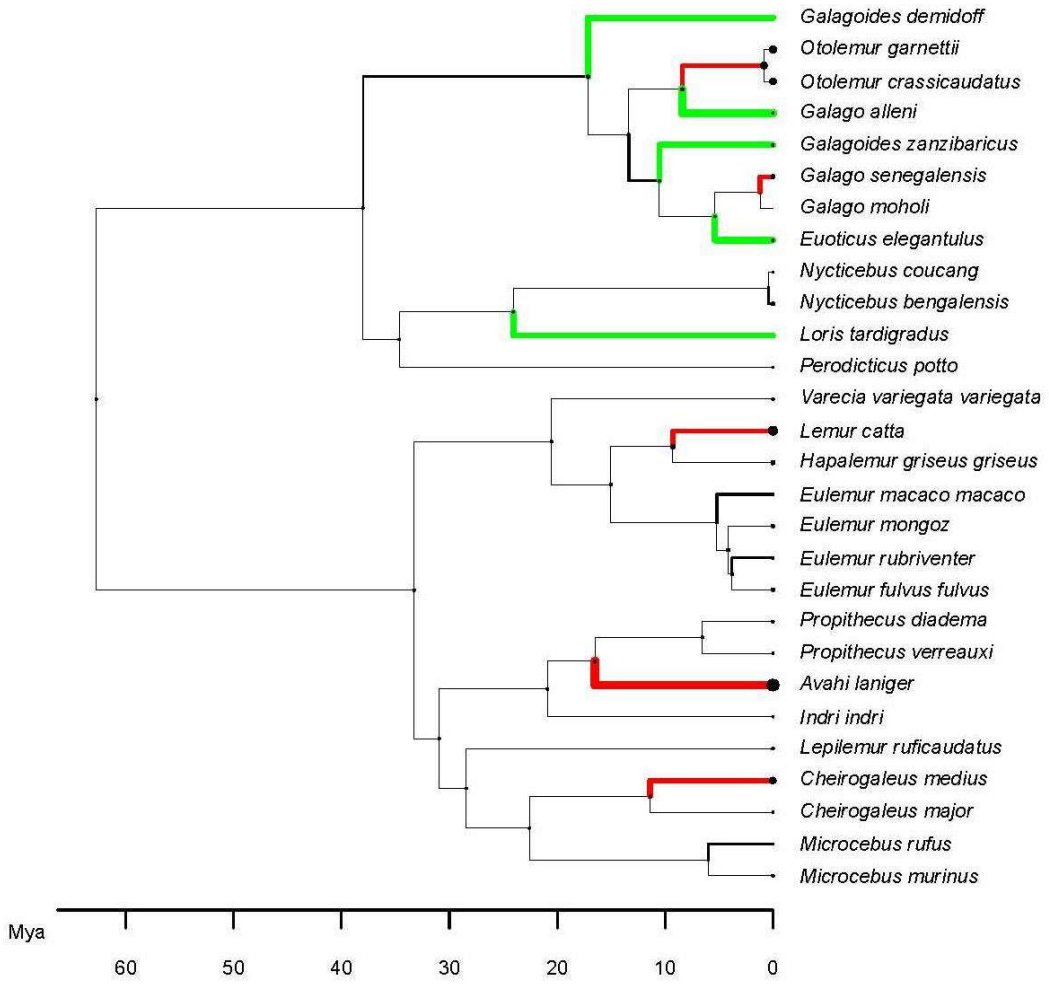

Figure 56: Evo-map of intra-species allometric scaling, in comparison to inter-species allometric scaling, for the 2* model vault module for PC1. As with Figure 54.

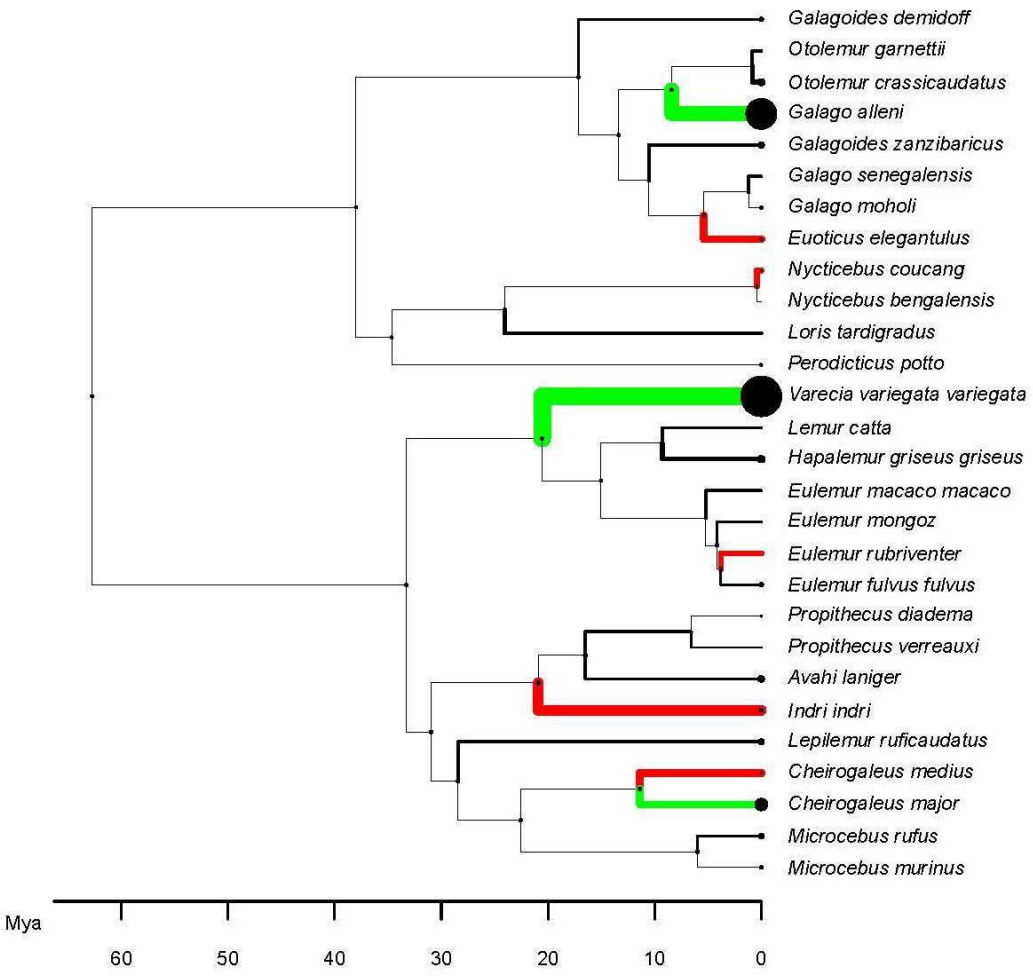

Figure 57: Evo-map of intra-species allometric scaling, in comparison to inter-species allometric scaling, for the 2* model vault module for PC4. As with Figure 54.

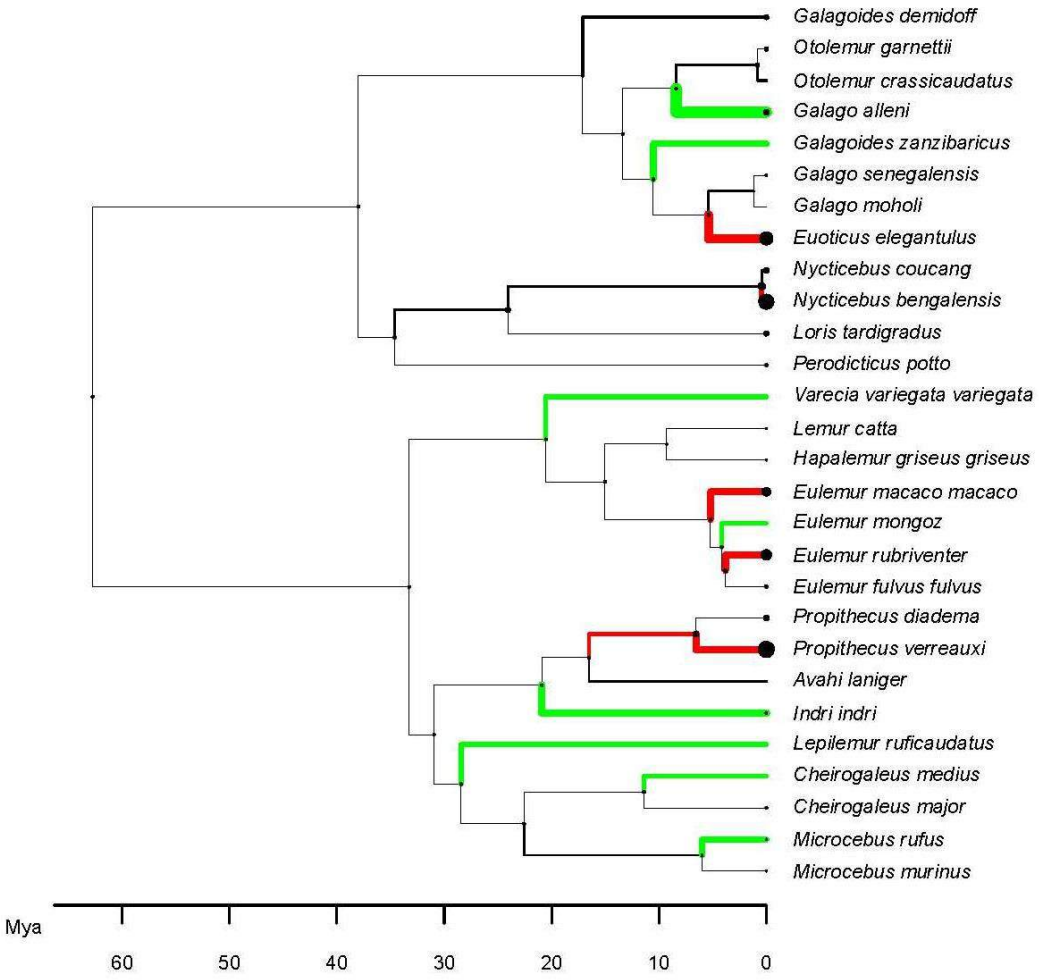

Figure 58: Evo-map of intra-species allometric scaling, in comparison to inter-species allometric scaling, for the Goswami model face module for PC1. As with Figure 54.

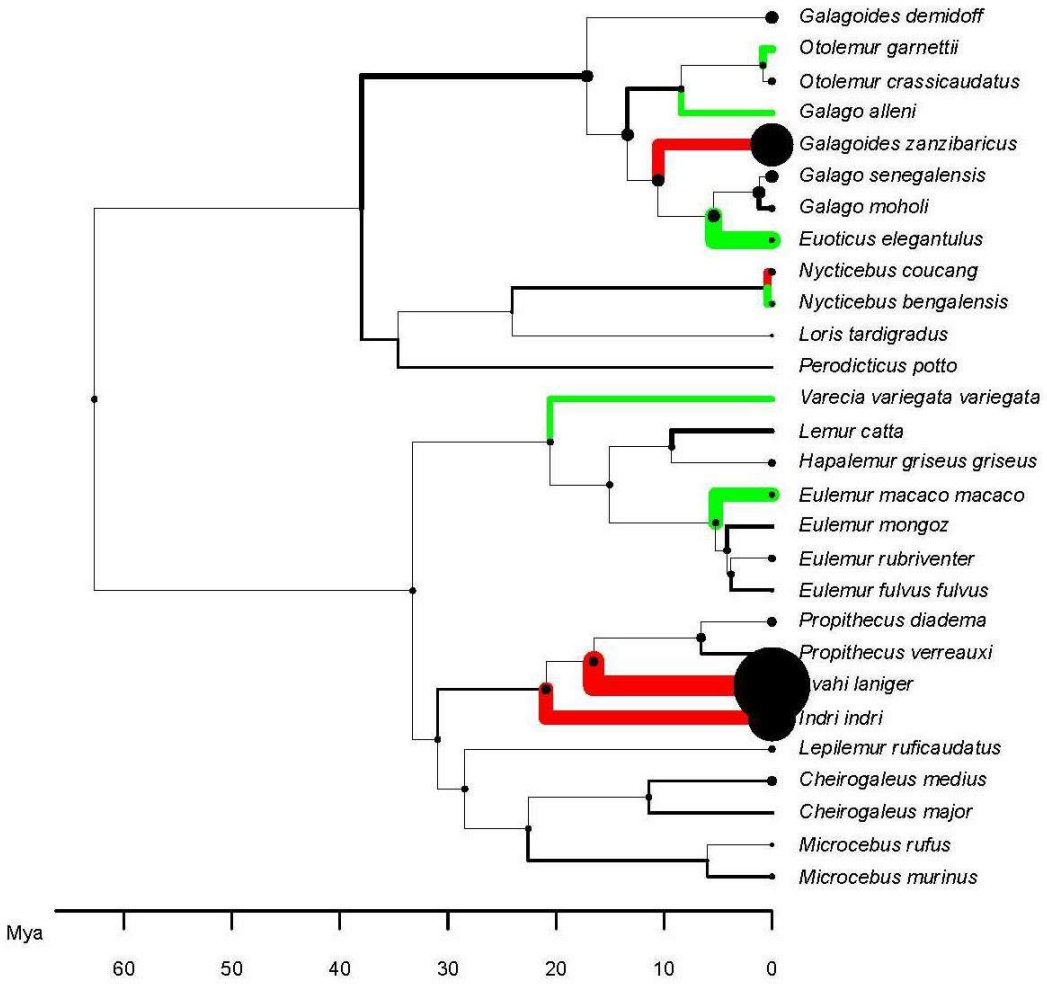

Figure 59: Evo-map of intra-species allometric scaling, in comparison to inter-species allometric scaling, for the Goswami model orbit module for PC1. As with Figure 54.

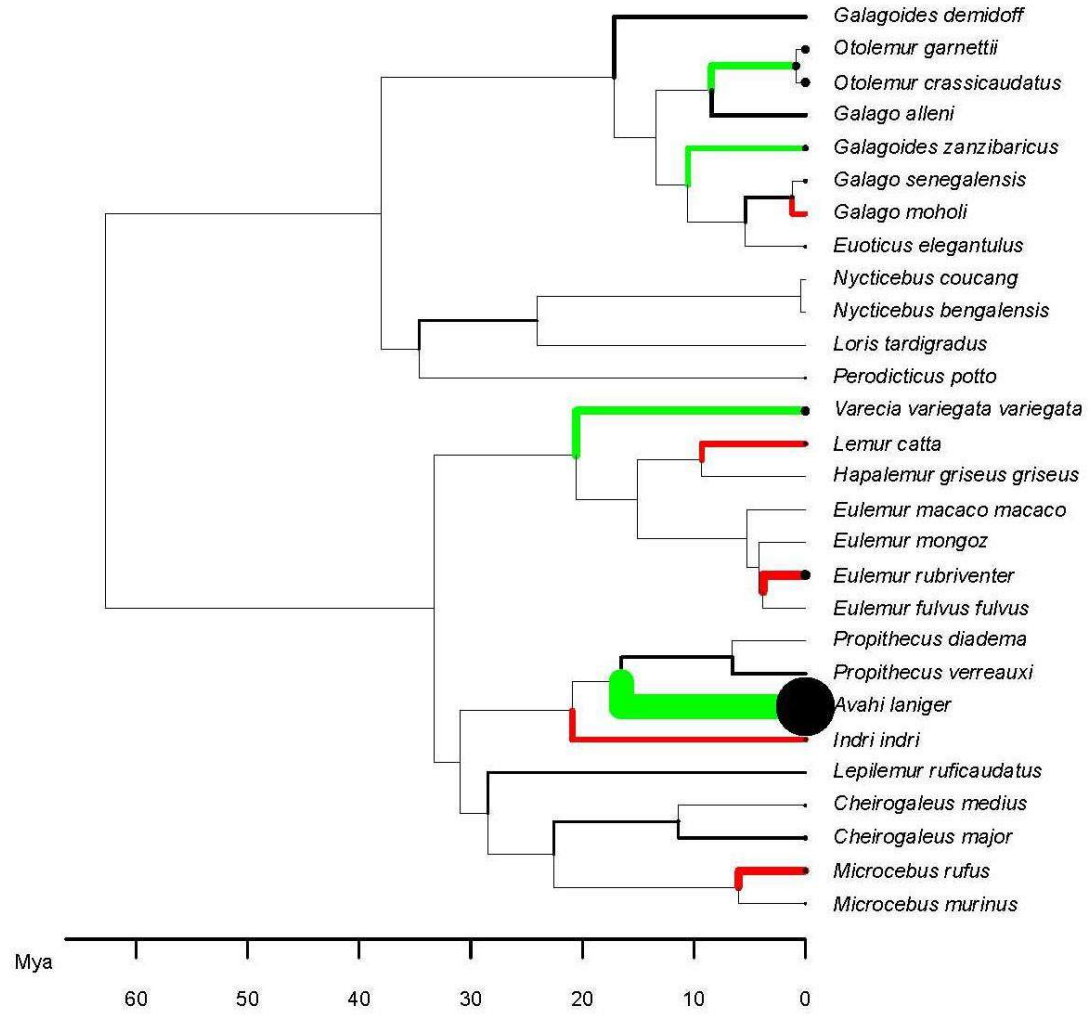

Figure 60: Evo-map of intra-species allometric scaling, in comparison to inter-species allometric scaling, for the Goswami model orbit module for PC3. As with Figure 54.

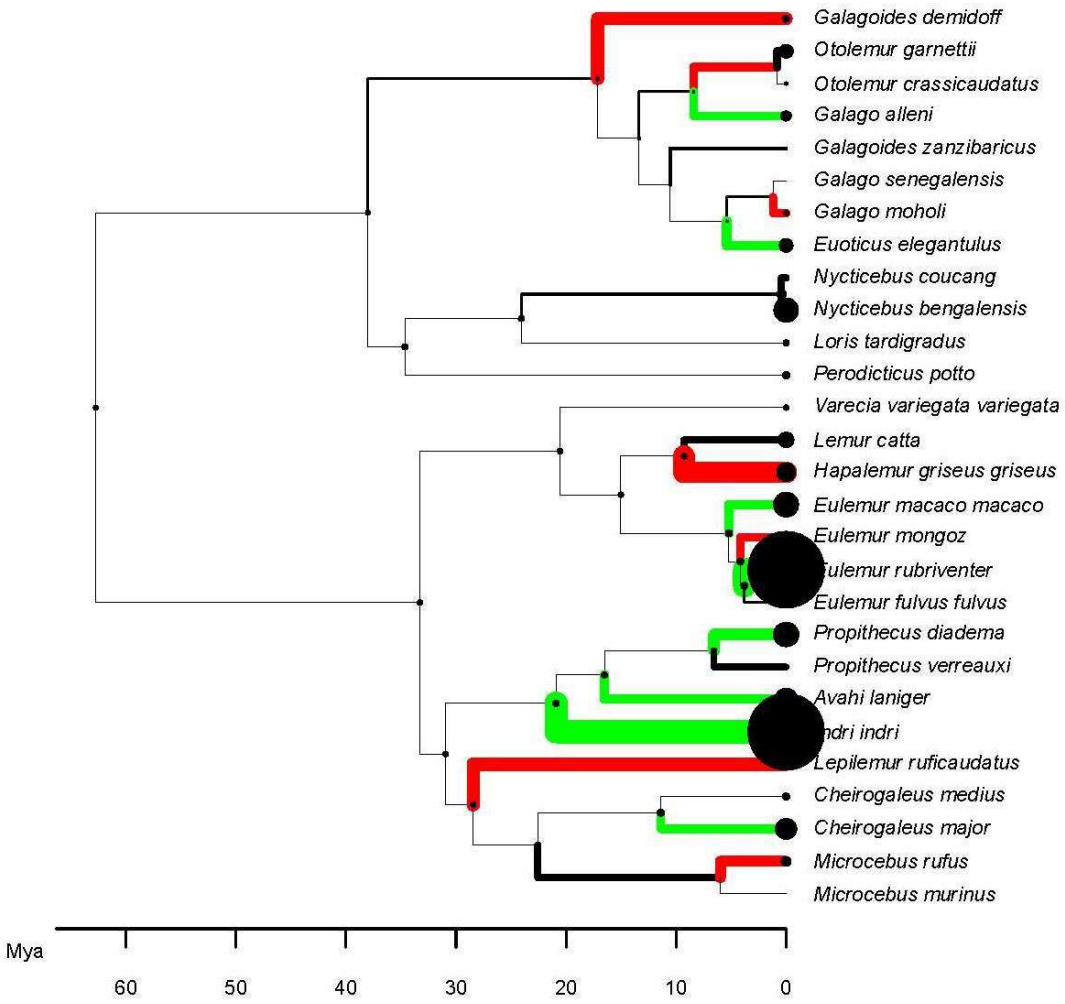

Figure 61: Evo-map of intra-species allometric scaling, in comparison to inter-species allometric scaling, for the Goswami model oral module for PC1. As with Figure 54.

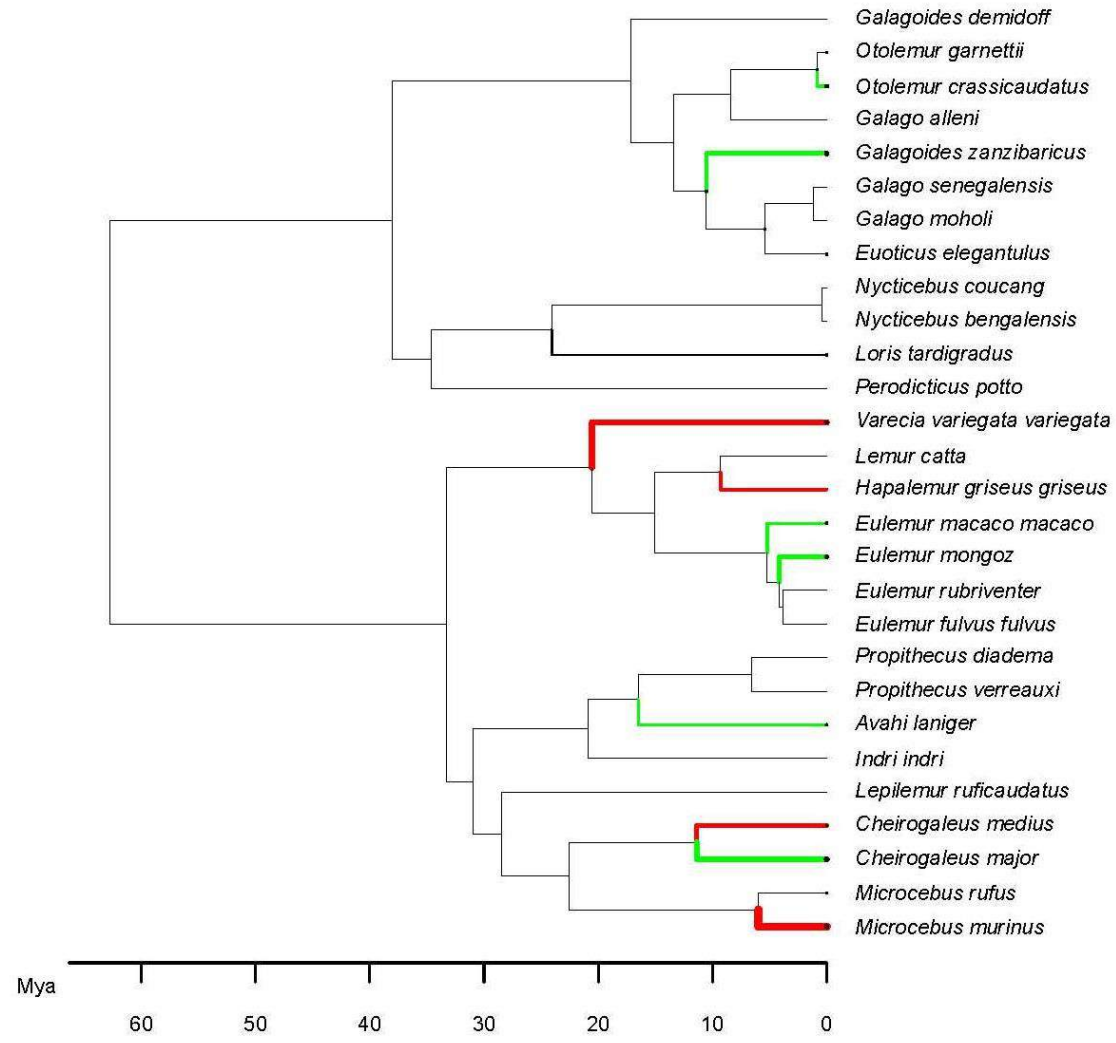

Figure 62: Evo-map of intra-species allometric scaling, in comparison to inter-species allometric scaling, for the Goswami model zygomatic module for PC3. As with Figure 54.

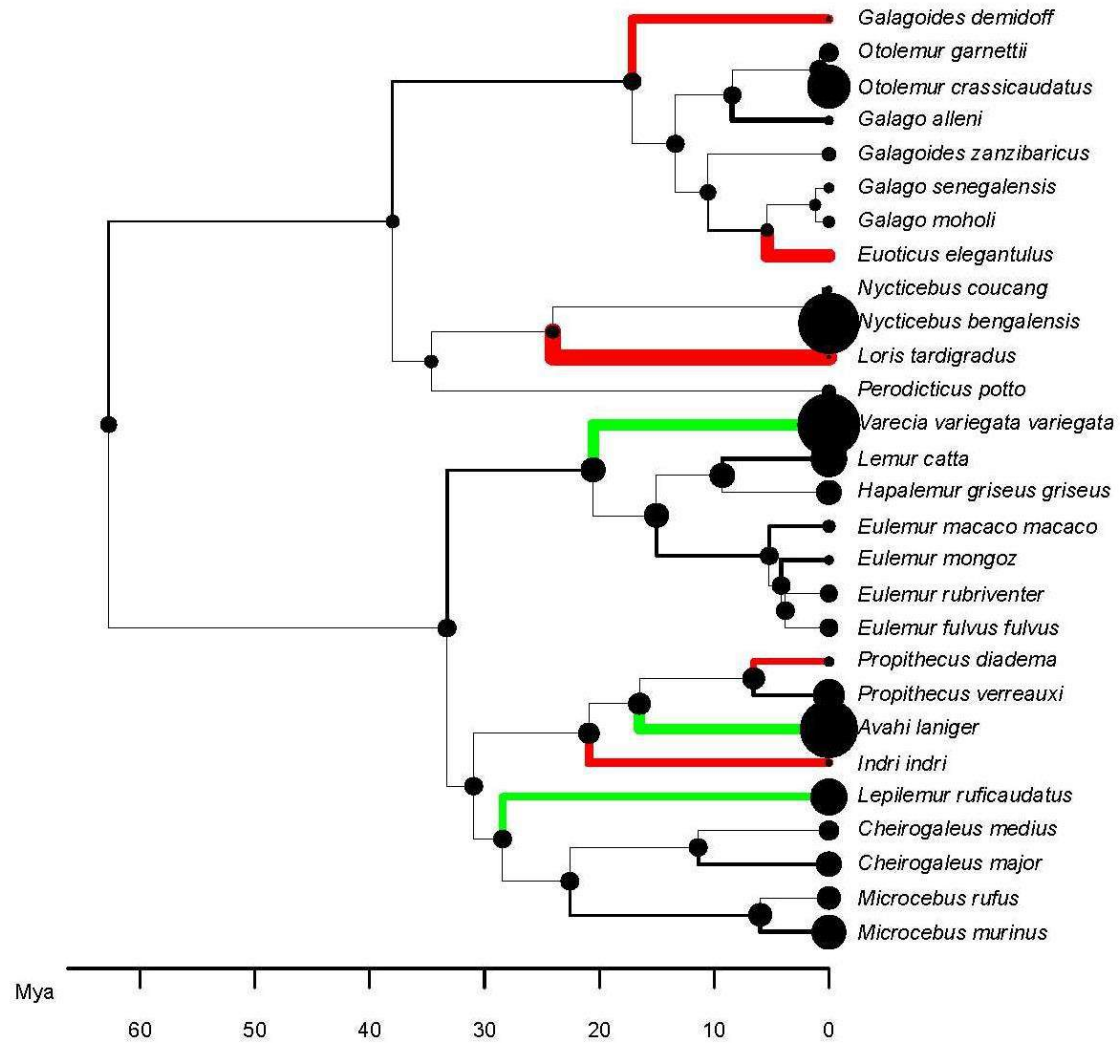

Figure 63: Evo-map of intra-species allometric scaling, in comparison to inter-species allometric scaling, for the Goswami model vault module for PC1. As with Figure 54.

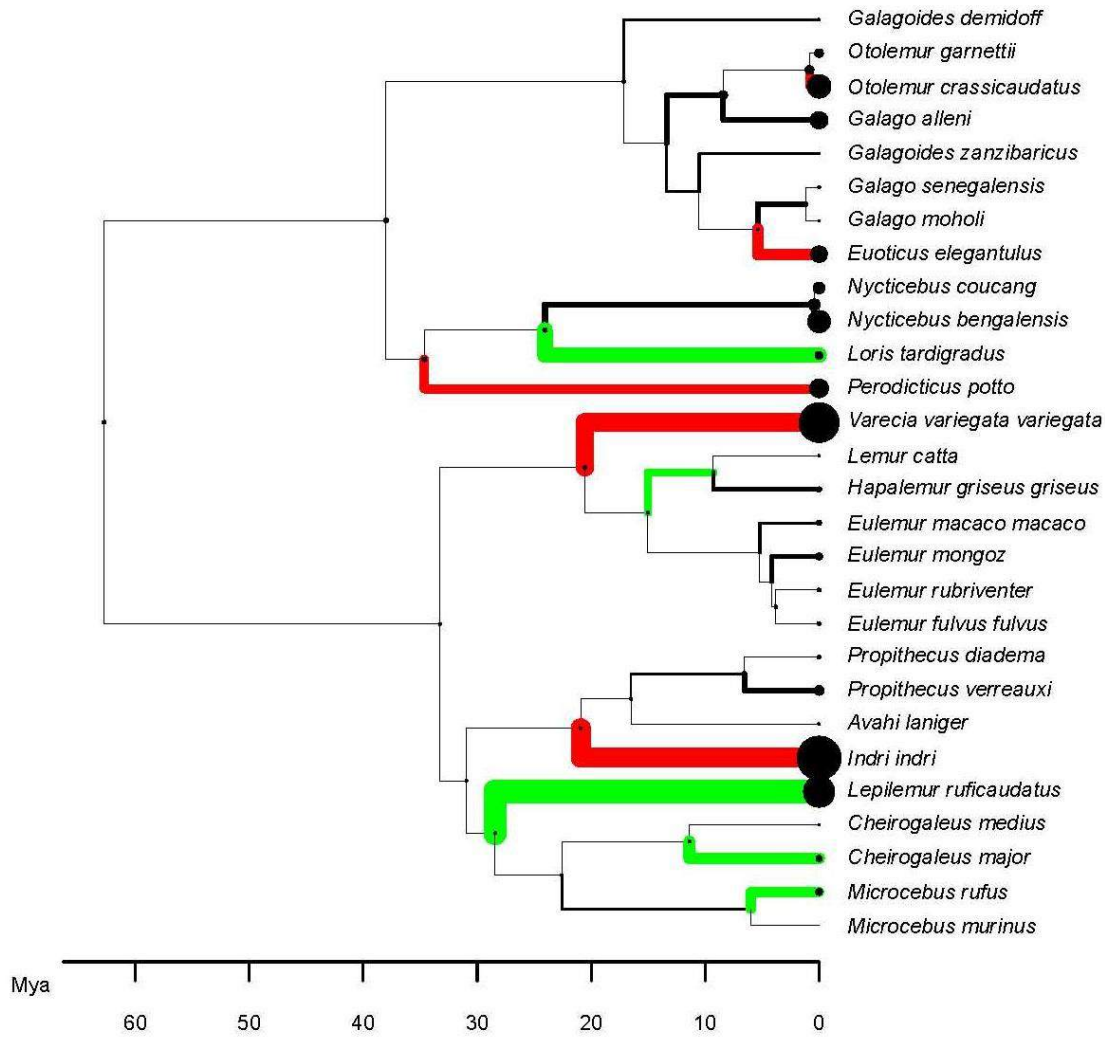

Figure 1: Evo-map of intra-species allometric scaling, in comparison to inter-species allometric scaling, for the Goswami model vault module for PC2. As with Figure 54.

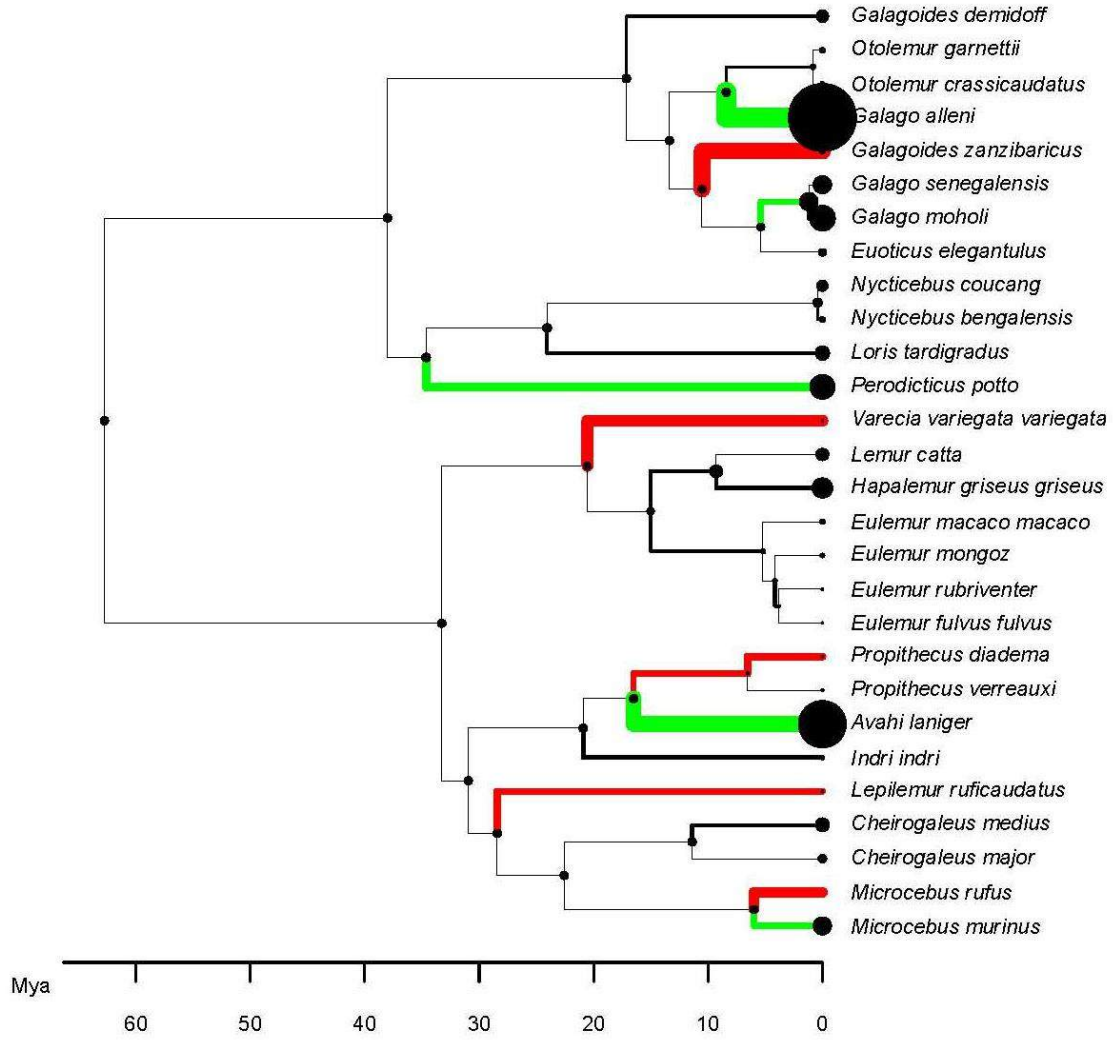

Figure 65: Evo-map of intra-species allometric scaling, in comparison to inter-species allometric scaling, for the Goswami model base module for PC3. As with Figure 54.

5.5. Discussion

5.5.1. Intra-species allometry

The static allometric pattern, observed across adult strepsirhine taxa at a within-species level, found smaller specimens to be more pedomorphic in appearance, with reduced prognathism in the face and a higher, more globular vault, in relation to larger specimens. This relationship between shape and size has been recorded in a wide range of placental mammals (Cardini & Polly, 2013), including some primate species, with both baboons (Frost *et al.,* 2003; Singleton, 2002) and red colobus monkeys (Cardini & Elton, 2009a) following the same pattern. However, guenons (Elton *et al.,* 2010), humans (Cardini & Polly, 2013), and capuchin monkeys did not, with the pattern actually reversed in capuchins, with larger craniums associated with more orthognathic faces and relatively expanded vaults (Cáceres *et al.,* 2014).

In addition to the wider mammalian trend seen for the whole cranium, further across species trends are also discernible at a modular level. These include straighter zygomatic arches with longer zygomaticotemporal sutures with increased size for the 2* face module (Table 41; Figure 30). This was not mirrored in the Goswami zygomatic module, where the principal axis of allometric shape change associated with size repeatedly showed a narrower cranial base and an increased distance between the meeting point of the presphenoid-basisphenoid and the basioccipital synchondrosis, in the midline (Table 46; Figure 35). While different aspects of allometric shape change in the zygomatic are found in these modules, both sets of traits are in line with the wider primate trend of longer, narrower crania with increased size (Cardini & Polly, 2013). For the vault modules in both the 2* and Goswami models, species correspond to the wider trend of a proportionally less globular vault with increased size (Table 42, 47; Figure 31, 36) (Cardini & Elton, 2009a; Frost *et al.,* 2003; Singleton, 2002).

The oral module showed a strong across species pattern, with the anterior end of the dental row placed more laterally and the posterior end more medially, a more lateral placement of the greater palatine foramen and a more posteriorly positioned posterior tip of the nasal spine as size increased (Table 45; Figure 34). Moreover, allometrically scaled morphological changes were more similar within family groups than between them; this was particularly true for the Lemuridae and the Lorisidae. Unfortunately, it has been notoriously difficult to determine the extent to which such patterns are the result of

phylogenetic relationships or shared diet, as the two variables are inter-related (Muchlinski & Perry, 2011). Even for the Lorisidae, where *L. tardigradus* have a 100% faunivorous diet and *N. coucang* a diet that is largely gummivorous and less than 12% faunivorous (Nekaris & Bearder, 2011; Wiens, 2002), the problem remains, as it could be the faunivorous element of *N. coucang*'s diet that drives these allometric similarities.

In contrast to the other modules, few of the traits related to the orbit consistently scaled across species (Table 44; Figure 33). Only the zygomatic foramen and the infraorbital foramen showed an across species trend, with the first being more anteriorly positioned and the latter more posteriorly positioned with increased size, a pattern that could possibly be linked with the positive allometric scaling of the length of the face (Table 41; Figure 30).

The link between size and shape is thought to have developed to maintain functionality in response to variation in size (Cardini & Polly, 2013; Emerson & Bramble, 1993), as size is proposed to be the more plastic of the two variables (Breuker *et al.,* 2006; Debat *et al.,* 2009; Marroig & Cheverud, 2010). Another suggestion as to why this particular pattern has arisen is linked to the differences in heterochrony; that is, the rate and period of growth in different areas of the skull (Klingenberg, 1998). The brain and the eyes, and so by conjecture the vault, cranial base and orbit, reach full size early on in development, in contrast to the face and oral cavity, which are slower to reach maturity (Marroig & Cheverud, 2004). Subsequently, the faster growing modules should not be exposed to the effects of growth hormone to the same extent as the slower growing modules. As a result, the traits associated with the face and oral modules are predicted to be more positively allometric compared to those related to the vault, cranial base or orbit, as is seen here and in the wider mammalian trend (Cardini & Polly, 2013; Marroig & Cheverud, 2004). In this sense, the influence of ontogenetic allometry can be seen in the pattern of both static and evolutionary allometry (Klingenberg, 1998; Klingenberg & Zimmermann, 1992).

It has been argued that, to break away from this mammalian-wide, allometric pattern, strong selective pressure would be required, such as the need to exploit a specialised diet (Baab *et al.,* 2014; Dumont, 1997; Muchlinski & Perry, 2011; Ravosa & Daniel, 2010; Ravosa *et al.,* 2010; Vinyard *et al.,* 2003). Amongst the extant Strepsirhini, the species with the most specialised diet include *H. griseus,* which feeds predominantly on bamboo and grasses (Gould *et al.,* 2011); *E. elegantulus, G. moholi*, *O. crassicaudatus* and *Nycticebus* sp.

all of which include a large proportion of gum in their diet, obtained using either a gouging or a scraping technique (Nekaris *et al.,* 2010; Ravosa *et al.,* 2010; Wiens, 2002); the nectar feeders *E. mongoz*, *V. variegata* and again *Nycticebus* sp. (Nekaris *et al.,* 2010; Sussman, 1991; Sussman & Raven, 1978; Wiens, 2002) and the faunivorous *Loris* (Nekaris, 2005, 2014; Nekaris & Bearder, 2011). For the whole cranium, none of these species differ greatly from other species in their allometric patterns (Table 40). *E. elegantulus* and *G. moholi* do show a less globular vault, but not a more prognathic face, with increased size; however, this is not unusual within the wider Galagidae family (Table 40).

The morphology of the 2* and Goswami face modules, as well as the Goswami oral module, are also expected to be influenced by dietary shifts. Here, the direction of shape change for each module was, again, largely consistent across species, but whether that shape change was shown to have a significant relationship with size was not (Table 41, 43, 45), suggesting that shape change has occurred both along allometric pathways, or the 'line of least resistance' (Marroig & Cheverud, 2005), and along non-allometric pathways. One exception to this trend is *E. mongoz*, for which the principal axis of shape change includes a less vertical upper face for both the whole cranium and the 2* face modules. This was significantly correlated with size for both modules (Table 40, 41), fitting with previous findings of a proportionally longer and narrower face for *E. mongoz* as size increases; this is thought to been selected for in order to better collect nectar from plants, without damaging them (Muchlinski & Perry, 2011).

Finally, orbit size, if not shape, has previously been linked to both activity pattern and diet (Kirk, 2006; Martin, 1990), both of which are very varied across strepsirhine species (Gould *et al.,* 2011; Nekaris & Bearder, 2011). It is possible that selection pressures linked to these variables have resulted in multiple species breaking away from primitive allometric scaling patterns, in a variety of directions, thereby explaining the relative lack of shared allometrically scaled traits across species for the orbit module (Table 44). Considered in a wider context, this may indicate that the general primate reliance on vision (Cartmill, 1992; Sussman, 1991), as opposed to olfaction, is true even for the mainly nocturnal strepsirhines (Gould *et al.,* 2011; Nekaris & Bearder, 2011)

5.5.2. Inter-species allometry

The trend seen at an intra-species level (i.e., a more prognathic face and less globular vault as size increases) was also seen at an inter-species level (Table 57; Figures 46-53). However, while the vault was seen to be allometrically scaled for PC1, it is only in PC4 that both traits covary and are significantly related to size. These results conflict with those of Baab *et al*., (2014) who identified the same direction of shape change for strepsirhine primates, but did not find this axis of change to be significantly correlated with size. The inconsistency in these results could have arisen for several reasons, the most likely being the difference in the samples used; Baab *et al*. (2014) focused only on lemuriforms, 39% of which were subfossil species. Two of these subfossil species (*Megaladapis* and *Hadropithecus*), although both relatively large in size, lie at opposing ends of the scale for PC1, which may have contributed to the non-significant relationship between PC1 and size for the inter-species sample. Specifically, it is *Hadropithecus* which appears to go against the general mammalian allometric trend (Cardini & Polly, 2013), with a pedomorphic morphology at large sizes, as also seen for the Cebidae (Cáceres *et al.,* 2014). There is some suggestion that this breakaway from the wider allometric pattern could be the result of selection for traits associated with hard object feeding in *Hadropithecus*, but this dietary reconstruction is contentious (Baab *et al.,* 2014; Dumont *et al.,* 2011). The addition of subfossil taxa, together with the exclusion of the Lorisidae and the Galagidae, could, explain the contrasting results. However, there are additional factors; while similar landmarks were used across both studies, Baab *et al*. (2014) used fewer of them (39 in comparison to 60), which is likely to have introduced a degree of difference in the results obtained. Finally, the sample sizes used by Baab *et al*. (2014) were relatively small (ranging from N=1-21, in comparison to N=22-175 here). Small sample sizes are often unavoidable, especially where fossil taxa are concerned. However, generating mean shapes from such small samples carries a high risk of inaccurate estimates, with a possible 494% percentage error for intraspecies samples of N=5, which could, in turn, account for up to 33% of inter-species shape distances (see Chapter 3).

At a modular level there is, again, a reflection of the results recorded for intra-species allometry (Table 57). The 2* face module still has a significant relationship between the length of the zygomaticotemporal suture and size (Figure 47), as does the Goswami zygomatic module (Figure 51). In addition, the allometric trend for the zygomatic module continues to represent a narrowing of the cranial base and an increase in cranial length, as

implied by the positively allometric relationship between size and the distance between the meeting of the presphenoid-basisphenoid and the basioccipital synchondrosis. Likewise, the 2* vault module continues to reflect the trend seen at an intra-species level, with increased size resulting in a less globular cranium (Figure 48). For the Goswami vault module, this pattern is less obvious, but the vault is less rounded as size increases (Figure 52). The oral module is once again consistent, showing a more laterally placed anterior end of the dentition and a more medially placed posterior end, together with a more laterally placed greater palatine foremen and a more posteriorly placed posterior tip of the nasal spine (Figure 50). Finally, the infraorbital and zygomatic foramens follow the same the same allometric trend as observed at the intraspecies level for the orbit module (Figure 49).

There is little difference between the results obtained using whole cranium size and those using the size of the corresponding module (Table 57), despite the difference seen between species and modules in size-versus-size modularity (Table 58). This suggests that shape-versus-size is an overriding pattern regardless of the influence of size-versus-size allometry.

While, the same basic overall trends are present at both the intra- and inter-specific level, there are many more significantly allometric relationships between size and shape at the intra-species level that are masked at the inter-species level. For example, with the exception of the facial foramen, the orbit module has relatively consistent allometric trends across species (Table 44), with traits such as the position of the nasolacrimal foramen, and the length, position and orientation of the zygomaticomaxillary and frontozygomatic sutures all having a significant allometric relationship with size, but with these relationships varying in their direction depending upon the species in question. At the inter-species level, this variation between species was masked, with an increase in size significantly associated with a more posterior placement of the nasolacrimal duct, a more vertically orientated zygomaticomaxillary suture and a more horizontally frontotemporal suture (Table 57). However, this was only true when the species average method was used; when the resampling approach was used instead, none of the relationships between the PCs for the orbit module and size were significant (Table 57). Again this may be the result of the strong reliance, and therefore strong selection pressure, on visions for primates, even nocturnal ones (Cartmill, 1992; Sussman, 1991).

5.5.3. Size-versus-size allometry

Previously, strepsirhine species had been shown to deviate from the wider primate trend of positive size-versus-size allometry in the face and palate, showing a relationship between overall size and the size of the vault and the orbit instead (unfortunately, the authors do not specify the direction of this relationship) (Fleagle *et al.,* 2012). Comparable results are found here at an inter-species level, with neither of the face modules deviating significantly from isometry, while the Goswami orbit and vault modules both show significant negative allometry (Table 58), which is in line with the wider primate trend (Schultz, 1940) and, possibly, with the results previously found for strepsirhines (Fleagle *et al.,* 2012). It has been suggested that in previous investigations of allometry in primates, the lack of allometry in strepsirhine facial traits has been masked by the robust nature of the relationship in anthropoid primates, and that these differences between the radiations are evidence of a period of cranial reorganisation during the origin of anthropoids (Fleagle *et al.,* 2012). The oral module, which includes two landmarks from the palate (the greater palatine foramen and the posterior tip of the nasal spine), but which is predominantly concerned with dentition, also shows positive allometry, while the base module is negatively allometric (Table 58).

Differences exist between the allometric patterns found at the inter- and intra-species level. Specifically, strong trends for positive facial allometry, in both the 2*(Table 49) and the Goswami face modules (Table 51) and in the zygomatic module (Table 54), as well as weaker trends for positive allometry in the orbit (Table 52) and base modules (Table 56), are found at an intra-species level, all of which are in contrast to the inter-species pattern (Table 58). There are also some similarities across the two levels; for example, the 2* and Goswami vault modules are negatively allometric both within (Table 50, 55) and across species (Table 58).

The Goswami orbit module is particularly interesting with regard to intra-species size-versus-size allometry. *M. rufus*, *G. moholi*, *G. zanzibaricus* and *P. potto* all have orbits that scale with positive allometry (Table 52), which is the reverse of the allometric pattern recorded at the inter-species level for strepsirhines (Table 58) and for all primates (Schultz, 1940). In addition, only *E. mongoz* shows negative allometry in the orbit at the intra-species level, while all other species examined did not significantly differ from isometry. All four of the species that show positive size allometry for the orbit are nocturnal, while *E. mongoz* is

diurnal; this may be significant, as nocturnal primates have relatively larger eyes than diurnal primates (Kirk, 2006; Martin, 1990; Ross, 1995). Furthermore, M*. rufus, G. moholi, G. zanzibaricus* and *P. potto* all have diets high in fauna, while the *E. mongoz* diet is largely nectivorous (Gould *et al.,* 2011; Nekaris & Bearder, 2011; Sussman & Raven, 1978). Again, faunivorous species have been shown to have relatively larger orbits compared to their non-faunivorous counterparts (Kirk, 2006). It is perhaps selection for morphological features associated with a nocturnal activity pattern and a faunivorous diet that have led to selection away from the primate trend of negative allometry in the orbit in the Strepsirhini (Fleagle *et al.,* 2012; Martin, 1990).

Alternatively, positive allometry in the orbit may represent the primitive primate condition, with diurnal lemurs and non-faunivorous species moving toward isometry or negative allometry in the orbit as a result of derived diets and activity patterns; this would indicate a cranial reorganisation during the origin of the anthropoids, as suggested by Fleagle and colleagues (2012). However, *L. tardigradus*, which is both nocturnal and 100% faunivorous (Nekaris & Bearder, 2011) (whereas *G. moholi* and *P. potto* have diets estimated to be 52% and 40% faunivorous, respectively (Nekaris & Bearder, 2011)), does not have an allometric relationship between orbit and overall cranial size. It is possible that selection for orbital frontation in *L. tardigradus* has negated the need for positive allometric scaling, as a negative correlation has been found between orbital frontation and orbit size in other primate taxa (Lieberman, 2000).

The particular use of landmarks and their ability to validly capture the size of the orbit should also be considered when interpreting these results. Orbital landmarks included the nasolacrimal foramen and the optical foramen, to approximate of the anterior-posterior size of the orbit, and the frontozygomatic and zygomaticomaxillary sutures, with the anterior landmarks of both being taken at the orbital rim. However, the supraorbital notch, which would also have been collected at the orbital rim and which would have helped to indicate the height of the orbit, was discarded as a landmark before analyses, as it was not easily detectable in many of the strepsirhine species. In addition, there is scope for the remaining landmarks (namely nasion, the zygomatic foramen and the infraorbital foramen) which are included in the orbit module following Goswami (2006a), to instead be deemed to be part of the face, which scales with positive allometry in other primate radiations and at an intra-species level for strepsirhines. Finally, where negative allometry has been found

for the orbit modules, different methods have been used, specifically measuring the volume of the orbit (Schultz, 1940), linear measurements (Jungers *et al.,* 2002; Ross, 1995), or GMM methods but with a different landmark composition (Baab *et al.,* 2014).

For strepsirhines, maxillary molar area scales with negative allometry or isometry relative to body mass, but with positive allometry relative to the length of the cranial base (Vinyard & Hanna, 2005). Furthermore, lemuriforms and lorisiforms both follow a similar pattern for dental allometry. The allometric scaling of tooth size in anthropoid primates has been shown to differentiate between dietary niches, with frugivores repeatedly found to have relatively smaller molars compared to folivores and insectivores (Strait, 1993; Ungar, 1998). For strepsirhines there is remarkably little difference in allometric scaling in relation to diet, although frugivorous lemuriforms are reported to have relatively smaller molars than their folivourous counterparts (Vinyard & Hanna, 2005). This is supported by the evo-map for the Goswami oral module which shows that it is extant lemuriforms that have shifted towards positive allometry, while the lorisiforms are moving towards a more negatively allometric pattern (Figure 42).

However, here rather than a measure of tooth area, the oral module instead gives an indication of the length of the dental row, from the septum P3 to the end of the third molar. As such, it is perhaps unsurprising that, as with the face, this distance shows a trend for positive allometry at both the intra-and inter-species level. This could also be seen to be in line with the finding that postcanine tooth area correlates positively with cranium length in strepsirhines. However, this issue is confused by the fact that here, in contrast to previous results, those species with positive allometry in the oral module are more likely to have a mainly frugivorous diet; in fact, *L. tardigradus,* the most faunivorous of all species examined is the only species for which negative allometry is present in the oral module. The difference in methodologies appears the most parsimonious reason for this confusion in the results. Folivores are thought to have a relatively large premolar and molar occlusal surface area, as their diet requires a more chewing; measuring only the length of the tooth row does not take surface area into account. The greater positive allometry seen here in frugivores may instead be a factor of the positive allometry of the face module, as the larger strepsirhine taxa, particularly the lemurids *Eulemur* and *Varecia*, are the main frugivores of the group (Britt, 2000; Gould *et al.,* 2011). Strepsirhine morphology has been linked to diet before (Viguier, 2004), but, due to a strong correlation between phylogenetic

relationships and diet, in addition to the relatively limited number of clear dietary shifts in the evolutionary history of the strepsirhines, it can be difficult to untangle the two variables (Baab *et al.,* 2014; Viguier, 2004). At an intra-species level, the only other module to indicate a phylogenetic based pattern is the Goswami base module, where negative allometry is restricted to species of *Otolemur* and positive allometry is concentrated within the Lorisidae, with the exception of *L. tardigradus* (Table 48).

5.5.4. Species average verses resampling method

Throughout the analyses, the resampling method is more conservative than the species average method for shape-versus-size allometry (Table 57). It is less likely to result in significant relationships between size and shape, and where a significant relationship was found, a smaller percentage of the change in shape is estimated to have been caused by variation in size. This resulted in the resampling approach only finding significant relationships between size and shape at an inter-species level for those module and traits that show a particularly consistent pattern in their allometric relationships at an intra-species level; namely those traits associated with allometric changes in the whole cranium and in the 2* face and vault modules. The difference in the results generated by the two methods are most likely caused by the inclusion of intra-species variation in inter-species calculations when the resampling method is used, but not when the species average method is applied.

Notably, the species average and resampling methods produced almost identical results for the analysis of size-versus-size allometry (Table 58). In an investigation into the effect of sample size on estimates of size and shape parameters in geometric morphometrics, estimates of mean centroid size generated from small sample sizes were much more accurate than estimates of mean shape generated from small sample sizes for both guenons and strepsirhines. This was thought to be due to the low level of size variation found within-species in comparison to levels of within-species shape variation (Cardini & Elton, 2007; see also Chapter 3). It therefore follows that not including intra-species variation (i.e., using the species average method) should make little difference for calculations based only on size. However, analyses which focus on shape would be expected to vary in their outcomes, depending on whether or not intra-species variation is taken into account.

5.5.5. Percentage of shape change caused by variation in size

The percentage of the total variation in shape caused by variation in size has been calculated as at least 20% for OWM at the subspecies level (Elton *et al.,* 2010); at an intraspecies level, it has been recorded at 20-40% for NWMs, rising to 93% across genera (Marroig & Cheverud, 2005), although a total of only 16% has also been recorded across Cebidae genera, but in that instance only two genera were included in the study (Cáceres *et al.,* 2014); in contrast, Marroig and Cheverud (2005) looked at 16 living genera and 15 of their ancestral nodes (Marroig & Cheverud, 2005). For OWM, size was responsible for 35-40% of total shape variation within papionin genera (Frost *et al.,* 2003) and from 35-98% across them, with the percentage appearing to increase in line with the genetic distance (Frost *et al.,* 2003; Profant, 1995; Singleton, 2002). Previously, only 3% of the principal axis of shape change (0.1% of total shape change) across families (an increase in prognathism and a decrease in the globularity of the vault, in larger specimens) was found to be the result of variation in size for lemurs. However, for PC2, 69% of shape change (10.7% of total shape change), a change in the angle of the neurocranium and the size of the orbit, was attributed to variation in size (Baab *et al.,* 2014).

For the strepsirhine species investigated here, the amount of within-species shape variation for the whole cranium accounted for by size ranged from 2-19% (for *G. senegalensis* and *L. tardigradus,* respectively; Appendix 4). This is a lesser degree of within-species shape variation attributed to size than in NWMs (Marroig & Cheverud, 2005) or in subspecies of OWM (Elton *et al.,* 2010), but here the percentage is calculated using only the first 13 PCs and so is a minimum rather than a total estimation. Moreover, the percentage of shape change remaining unexplained by PC1-13 is highest for *G. senegalensis* (49%) and lowest for *L. tardigradus* (14%). PC 1-25 were used for the OWM calculation, so again while not a complete estimate, it is likely to have accounted for a greater proportion of the total shape variance attributed to size (Elton *et al.,* 2010), while for NWM total shape variation was considered (Marroig & Cheverud, 2005).

Across all species, genera and families of stepsirrhines tested, size accounted for 29% of shape change in the whole cranium (again, based on PCs 1-13) for the species average approach and 25% for the resampling approach (Table 57, Appendix 5). This is considerably lower than the 35-98% calculated for other primate radiations (Frost *et al.,* 2003; Marroig & Cheverud, 2005; Profant, 1995; Singleton, 2002). Again, this could be attributed to the

calculation for strepsirhines using only the first 13 PCs rather than the full contingent, but this only leaves 8% of the total shape variation unexplained. When the percentage of shape change accounted for by size is examined for individual PCs, specifically those significantly correlated with size, the results are in line, or even higher than, those previously found for strepsirhine taxa (Baab *et al.,* 2004): 24% and 20% for PC1 for the species average and resampling model, respectively, and 4% and 3% for PC4 (Appendix 5). Baab *et al.,* (2014) found 0.1% for PC1 and 10.7% for PC2, although PCs do not correspond to the same shape change across the studies. Thus, strepsirhine morphology may be influenced by size to a lesser degree than that of anthropoids (Frost *et al.,* 2003; Marroig & Cheverud, 2005; Profant, 1995; Singleton, 2002).

At an intra-species level, the percentage of shape change accounted for by different 2* or Goswami modules was again relatively low (from 1.1-25%). It showed no specific pattern within or between-species (Tables 40-48; Appendix 4).

At an inter-species level, the resampling approach consistently produced a lower estimate for the percentage of shape change attributed to size, in comparison to the species average approach (Table 57; Appendix 5). This is in line with the more conservative R^2 values also returned for the resampling approach (Appendix 3). At a modular level, there was little difference between the results based on the size of the whole cranium and that based on module size. The 2* face and vault modules were similar in the amount of shape change attributed to size (21-27%, depending on the approach and size variable used), with the face variable always being fractionally higher (0.3-2.1%). Within the Goswami model, the shape of the face, oral and base modules were the least affected by size (9-13%), and the zygomatic and vault modules the most affected (15-31%; Table 57; Appendix 5).

With relatively low proportions of shape change in strepsirhines being the result of changes in size, there remains a large amount of residual shape variation to be explained, especially within the Goswami face, oral and base modules, suggesting that shape change has occurred along both allometric and non-allometric pathways (Table 57; Appendix 5). One of the possible courses for shape change, at least with the face and oral module, is diet. Here, with the exception of *E. mongoz*, species with specialised diets were not seen to clearly deviate from the principal axis of shape change (Table 40-48), but diet has been shown to

account for a significant proportion of shape change in lemurs (Baab *et al.,* 2014; Viguier, 2004).

5.5.6. Inter-species differences in allometric scaling

A strongly conserved allometric pattern has been reported for NWM (Cáceres *et al.,* 2014; Marroig & Cheverud, 2005), and for species of guenon (Cardini & Elton, 2008). For papionins, the situation is more contentious, with either *Cercocebus* and *Lophocebus* shown to share a similar slope and elevation that is significantly different from that shared by the larger bodied papionins (Singleton, 2002), or *Cercocebus* and *Lophocebus* differ in their slope, as do *Mandrillus* and *Papio* (Collard & O'Higgins, 2001).

For the cranium as a whole, strepsirhine taxa also appear to be relatively conserved in their allometric scaling patterns (Tables 59; Figure 54), suggesting that, at least to a certain extent, larger specimens are scaled up versions of smaller specimens following a common scaling pattern, at both within- and between- species levels. In general, significant differences are more likely to occur between species from different families or at least different genera. This suggests that changes in ontogenetic allometry may have occurred at this deeper family level. This is turn would lead to changes in static allometry, upon which natural selection could act, resulting in evolutionary change in those few species (*G. senegalensis, E. mongoz* and *O. garnettii*) which have been forced to move away from the common allometric scaling pattern by ecological factors.

Where significant differences in scaling were found between species, they were largely concentrated on specific taxa, particularly *G. senegalensis, O. garnettii* and *E. mongoz*. These species are not closely related, nor do they share any obvious dietary or habitat preferences (Gould *et al.,* 2011; Nekaris & Bearder, 2011), as such, a range of factors may result in the differences in allometric scaling for these species. *E. mongoz* is highly nectivorous, a diet that has been associated with a proportionally longer and narrower cranium as size increases (Dumont, 1997; Gould *et al.,* 2011; Muchlinski & Perry, 2011); The diet of *O. garnetti* is less clearly understood, but it is possible that they are gum feeders or at least have retained morphology associated with gummivory (Nash 1986; Ravosa *et al.,* 2010), this could have caused them to break away from the common strepsirhine allometric scaling pattern (this result is concordant with previous findings for *Otolemur*; Ravosa *et al.,* 2010; Vinyard *et al.,* 2003); finally, *G. senegalensis* is found in

sympatry with other Galagidae species, this has been linked to size divergence due to selection for niche exploration (Charles-Dominique, 1977; Nash, 1986; Nash *et al.,* 1989; Ravosa *et al.,* 2010), if competition is sufficiently strong it may have forced *G. senegalensis* to diverge away from the common allometric scaling pattern.

G. senegalensis is significantly different to *G. moholi*, its closest relative. An evo-map of PC1 for the whole cranium (Figure 54) indicates that there is very little change in slope value between-species, as indicated by the almost uniform size of the nodal and tip value markers. In addition, where there is an increase or decrease away from the inter-species slope value, as indicated by green and red branches, respectively, this predominantly occurs along terminal branches. This suggests a shared primitive allometric scaling pattern, with selection for slight increases or decreases in the allometric scaling of some extant species. Similar results can be seen for PCs 2-5, (Appendix 6, 7).

For the 2* face module (Tables 60; Figure 55), *G. senegalensis* and *O. garnettii* are, again, significantly different from other species in their allometric scaling; this is particularly pronounced when they are compared to species within the Lemuridae, where differences are seen for several axes of shape change (PCs 1-4). In addition, *G. zanzibaricus* repeatedly scales differently from the Lemuridae for PC1. Evo-mapping shows that, for PC1 of the 2* face module, *G. senegalensis* and, particularly, *G. zanzibaricus* have lower allometric slopes than the inter-species trend, while the Lemuridae have higher allometric slopes than the inter-species trend. At the inter-species level, PC1 correlates positively with size and represents a number of traits that indicate increased prognathism. Therefore, in morphological terms, the Lemuridae should respond with a greater increase in prognathism, per increase in unit size, than either of the galagos (Figure 55). The face module for the Goswami model again shows *G. zanzibaricus* and, in this instance, *G. alleni* to scale significantly differently to other species, including other galagoids. The evo-map reveals that this reflects a more positive allometric trajectory than the inter-species trend (Figure 58).

In the 2* vault module, the evo-map for PC1 (Figure 56) shows a divergence between the lemuriforms and the lorisiforms, with the lemurs showing a trend for a lower scalar, and the lorises and galagos a trend for a higher one. The lorisiforms would therefore respond more sensitively to a change in size, with either a more globular vault as size decreased or a

less globular vault at size increased. Also, for the 2* vault module, *V. variegata* consistently scales differently to other species for PC4. The evo-map of PC 4 (Figure 57) shows *V. variegata* to be more positively allometric than the other strepsirhine taxa; this would result in its becoming proportionally less globular compared to other taxa as size increases. *V. variegata* has previously been singled out as potentially differing from the general primate scaling pattern, due to its high level of nectar feeder. However, nectar feeding has been correlated with positive allometry in the length of the face, palate and dentition, rather than linked to traits in the vault (Muchlinski & Perry, 2011). The present results suggest that the derived scaling patterns seen in this species extend beyond the face. *G. alleni* also shows a similar increase in slope, but this is not reflected in the ANCOVA results (Table 62; Appendix 6).

The Goswami vault module, which represents a smaller proportion of the neurocranium than the 2* vault module (Table 28; Figure 19, 22), only goes part way to mirroring these results. The evo-map of PC1 shows that the lorisiforms have tendency towards more negative allometry, which in this case would, again, result in greater sensitivity between change in size and the roundness of the vault. It also highlights many shifts towards greater positive or negative allometry along terminal branches (Figure 63). In addition, ANCOVA analysis shows that any significant differences in slope between species are concentrated in comparisons with *G. senegalensis*.

Between-species differences in scaling of the orbit module are largely associated with *Otolemur*, especially for PC3 (Table 60). However, the extent of the difference in *Otolemur's* allometric scaling is reduced once phylogenetic history is taken into account, as shown by the evo-map for that PC (Figure 60). The reverse of this pattern is true for *A. laniger* and *I. indri*; both have a more negative slope value for PC1 when evolutionary history is taken into account (Figure 59), but it is not significantly different from the slope of any other taxa when it is not (Table 63). A more positive scalar for *Otolemur* for PC3 would result in a proportionally larger increase in traits that are possibly associated with a larger orbit per increase in unit of size, while a more negative scalar for *A. laniger* and *I. indri* for PC1 would mean a proportionally smaller increase in traits possible associated with facial prognathism per increase in unit of size.

Analysis of the oral module shows a relatively conserved scaling pattern across species (Table 64; Appendix 6). It is interesting that there is relatively little variation in scaling in the oral module, given that this is where variation in dietary adaptation might be expected to act. This may be due to the strong correlation between diet and size in primates (Leonard & Robertson, 1994; Sailer *et al.,* 1988). Between-species differences are associated with only *I. indri, O. garnettii*, and *E. mongoz*. For *I. indri*, differences were only found in relation to PC1, which predominantly represents a change in the position of the greater palatine foramen and the posterior tip of the nasal spine. *E. mongoz* showed a difference in scaling for PCs 2 and 4, which represent changes in the length and the curvature of the dental row, potentially corroborating previous research that concluded that increases in positive allometry in the length of both the palate and dental row in *E. mongoz* were possible adaptations for non-destructive nectar feeding (Muchlinski & Perry, 2011). *O. garnettii* showed scaling differences for PCs 1, 2 and 4. In contrast to *I. indri*, the difference in scaling for *O. garnettii* and *E. mongoz* was less dramatic, once evolutionary relationships had been taken into account.

As a module, the zygomatic is conserved in its scaling across species; the principal differences found between species are for PCs 3 and 4, which are both associated with changes in the width of the cranium (Table 65). These differences are predominantly linked to *Microcebus* and, for *M. rufus,* at least, are minimised once evolutionary history has been taken into account (Figure 62).

The difference between species' allometric scaling for the base module were also very limited, and is primarily associated with *E. fulvus* and PCs 2 and 3, which represent changes in the size of the external auditory meatus, the shape of the foramen magnum and the width of the cranial base (Appendix 3). However, once ancestral relationships had been taken into account, the allometric scaling of *E. fulvus* differed very little from the inter-species pattern (Figure 65; Appendix 7).

Both the zygomatic and base module are highly integrated within the cranium. They relate to both the face and the neurocranium and, in addition, the base is the point of contact between the crania and postcrania (Lieberman *et al.,* 2000), such high levels of integration, together with the need to maintain functionality, may result in the robust conservation in allometric scaling that is found (with the exception of PC3), both within- and between-

species, for the zygomatic and base modules (Table 65, 67; Figure 62, 63; Appendix 6, 7). In addition, the cranial base is one of the first areas of the cranium to reach full size, and so is less likely to be influenced by extrinsic environmental factors and more likely to be representative of genetic relationships (Goswami, 2006a; Lieberman, 2011; Lieberman *et al.,* 2000).

5.6. Conclusion

Overall, the allometric patterns seen within the Strepsirhini are consistent within and between species, and in line with a suggested wider mammalian trend of a more pedomorphic morphology in smaller specimens, shown as a more orthognathic face and more globular vault, in contrast to a more prognathic face with a flatter narrower vault in larger specimens. Size-versus-size allometry is similarly constrained within and between taxa, suggesting larger specimens are, at least to a certain extent, scaled up version of their smaller counterparts following a common allometric pattern.

In contrast to other primate taxa, a relatively small proportion of shape change is the result of change in size, leaving scope for further research in to the causes of the residual variation, with possible factors, including diet, climate and phylogenetic relationships. Allometric scaling is also relatively conserved across strepsirhine species, but with lemuriforms shown to respond more sharply to size differences for traits in the face, while the lorisiforms respond more sharply for traits in the vault. Otherwise, increases or decreases in the allometric slope are usually shown to occur along terminal branches

Where species deviate from the wider allometric pattern or scale, it can potentially be explained as selection for specialised morphology linked to diet (e.g., *E. mongoz* and *O. garnettii*) or to niche exploration (e.g., *G. senegalensis*). Such similarities in both allometric relationships and scaling patterns, are likely to result in homoplastic traits, where species, which are only distantly related, share similar traits, due to parallel responses to changes in size (Marroig & Cheverud, 2005).

Finally, the use of a new resampling approach for analysis at the inter-species level was found to produce more conservative results than the more generally used species average approach, but only for calculations involving species shape and not those involving size.

This is attributed to the greater amount of within-species variation, seen in shape, in comparison to size (Cardini & Elton, 2007; see Chapter 3).

– Chapter 6 –

Phylogenetic signal and mode of evolution in the strepsirhine cranium

6.1 Abstract

An increasingly well resolved picture of strepsirhine phylogenetic relationships enables the investigation of a number of key questions surrounding their morphological evolution, including, to what extent are morphological and molecular distance correlated with one another, which model of evolution best describes the phenotypic pattern present in crown groups species, which traits are homoplastic and where and when in the tree have homoplasies occurred and, finally, which traits represent homologies. In turn, the answers to these questions should help to identify the selective pressures and evolutionary constraints that have resulted in the morphology of the extant Strepsirhini.

The sample contained 28 species, each with a sample size of N>20. Species mean shapes (Principal Components) were calculated for both the full landmark composition and individual cranial modules. A Bayesian approach was used to estimate and compare the fit of seven different models of evolution (Brownian motion, Pagel's λ, kappa, delta, early burst, Ornstein-Uhlenbeck and Independent Evolution). Independent Evolution was overwhelmingly the best supported evolutionary model, as determined by AICc. Phylogenetic signal was robust for all cranial modules (as determined by Pagel's λ and Blomberg's *K*) with evidence that signal is strongly linked to size.

Evo-maps were created, mapping trait values back across the strepsirhine phylogenetic tree, with ancestral node values estimated according to the Independent Evolution model. Clear morphological shifts are shown at the infra-order and family level, with the morphology of the cranial base showing the clearest division between family groups. At shallower taxonomic depths, incidences of parallel evolution and reversals are revealed. Homoplasies are most commonly found between the lorisiforms and the cheirogaleids and are often linked to the influence of allometric scaling. The results are discussed with regard to their implications for assessing the phylogenetic relationships of fossil taxa.

6.2. Introduction

The combination of a well resolved phylogenetic tree and data from the extant tip species allows for the investigation into a number of key areas of evolutionary morphology, including which mathematical model of evolution best explains the data. Well-supported evolutionary models can be used to estimate an ancestral state, which, in turn, enables the examination of patterns of homology and homoplasy among species, and of the rates and timings of phenotypic change, this provides an insight into the selective pressures and evolutionary pathways that have resulted in tip species' phenotypes.

Evolutionary trees can also be used to quantitatively estimate the strength of phylogenetic signal within species data. Phylogenetic signal is the extent to which species trait values are statistically related to their phylogeny; it is said to be high when closely related species resemble one another more than distantly related species resemble one another and low when they do not. Morphological traits or regions identified as having a strong phylogenetic signal can subsequently be targeted when attempting to determine the phylogenetic relationships of fossil species, for which genetic data are unavailable (Lockwood *et al.,* 2002).

6.2.1. Models of evolution and ancestral trait reconstruction

Methods of ancestral trait reconstruction make several critical assumptions: first, that evidence of the patterns of evolutionary change undergone by ancestral species is preserved within the morphological variation of extant species; second, that the proposed phylogenetic relationships of species are accurately known; and finally, that the model of evolution used to assign the rate of evolutionary change along branch lengths is accurate (Pagel, 1999; Smaers & Vinicius, 2009).

When investigating the evolution of continuous, as opposed to discrete, traits, the model of evolution most commonly applied is Brownian motion (BM; Pagel, 1999). This is a random walk model, which mimics genetic drift; traits evolve with a mean change of zero and with an unknown and constant variance (σ^2), over each unit of 'time' (*dt*), where time can be measured chronologically or by genetic distance (Pagel, 1999). Each trait change is considered to occur independently from any previous evolution, and has no influence on the direction of future evolution. The change in a trait for any particular species, from the root of a tree to the tip, can therefore be given as $t\sigma^2$, where *t* is the total branch length

(i.e., time) between the two points (Pagel, 1999). Species that are closely related will 'share' branches for a large proportion of their evolutionary history, signifying that they share a large amount of their evolutionary history (Pagel, 1999). Under BM, closely related species are therefore expected to have similar trait values, while those species that diverged at an earlier date, and so share less of their evolutionary history, are expected be more divergent in their trait values (Pagel, 1999).

BM has received some criticism for not being a realistic model of evolution. Under the model, ancestral traits will always fall within the range observed in the tip data. Because of this, it is not possible to detect directional changes, such as Cope's Law, which states that species have a tendency to increase in size over evolutionary time (Hone & Benton, 2005; Pagel, 1999). In addition, the consistent rate of evolution assumed by BM ignores the influence of selection on the pace of change (Felsenstein, 1988; Price, 1997; Smaers & Vinicius, 2009). Attempts have been made to address this problem, through the scaling of branch lengths in line with different tempos of evolution (Pagel, 1999).

Different tempos of evolution previously described, include: direct gradualism, where trait evolution is smooth and occurs at constant rate along branches (this is akin to BM); scaled gradualism, where the relationship between branch length and trait evolution is non-linear (if trait change is shown to occur proportionately more in longer branches, it is implied that recent evolutionary changes have contributed more variation than earlier changes, but if shape change is shown to occur proportionately more in shorter branches, it is implied that earlier events have contributed more to trait variation than more recent events) (Pagel, 1999); and punctuated equilibria, where traits evolve in fits and starts in response to selection pressures or the exploitation of new niches (Gould & Eldredge, 1993). In some instances, punctuated equilibria might be in line with scaled gradualism, but, in others, the amount of trait evolution could be seen as independent of branch lengths (Gould and Eldredge, 1993).

A number of methods have been suggested as a way of transforming phylogenetic trees, through the rescaling of branch lengths, so that they comply with these different evolutionary tempos, they include: Pagal's λ, delta, kappa (Pagel, 1999), the early-burst model (Harmon *et al*., 2010), the Ornstein-Uhlenbeck model (Uhlenbeck & Ornstein, 1930) and the Independent evolution model (Felsenstein, 1998; Smaers & Vinicius, 2009).

6.2.1.1. Pagel's λ

Under Brownian motion, values for Pagel's λ are 0>1. When the tree is scaled to λ=1, branch lengths are directly proportional to the amount of trait change predicted under the BM model. When λ=0, all branch lengths are equal, with no shared evolutionary history implied, so that the tree effectively becomes a star phylogeny (Figure 66). The transformation is achieved by multiplying the off-diagonals of the variance-covariance matrix, based on the tree topology and branch lengths, by values between 0 and 1 (Pagel, 1999).

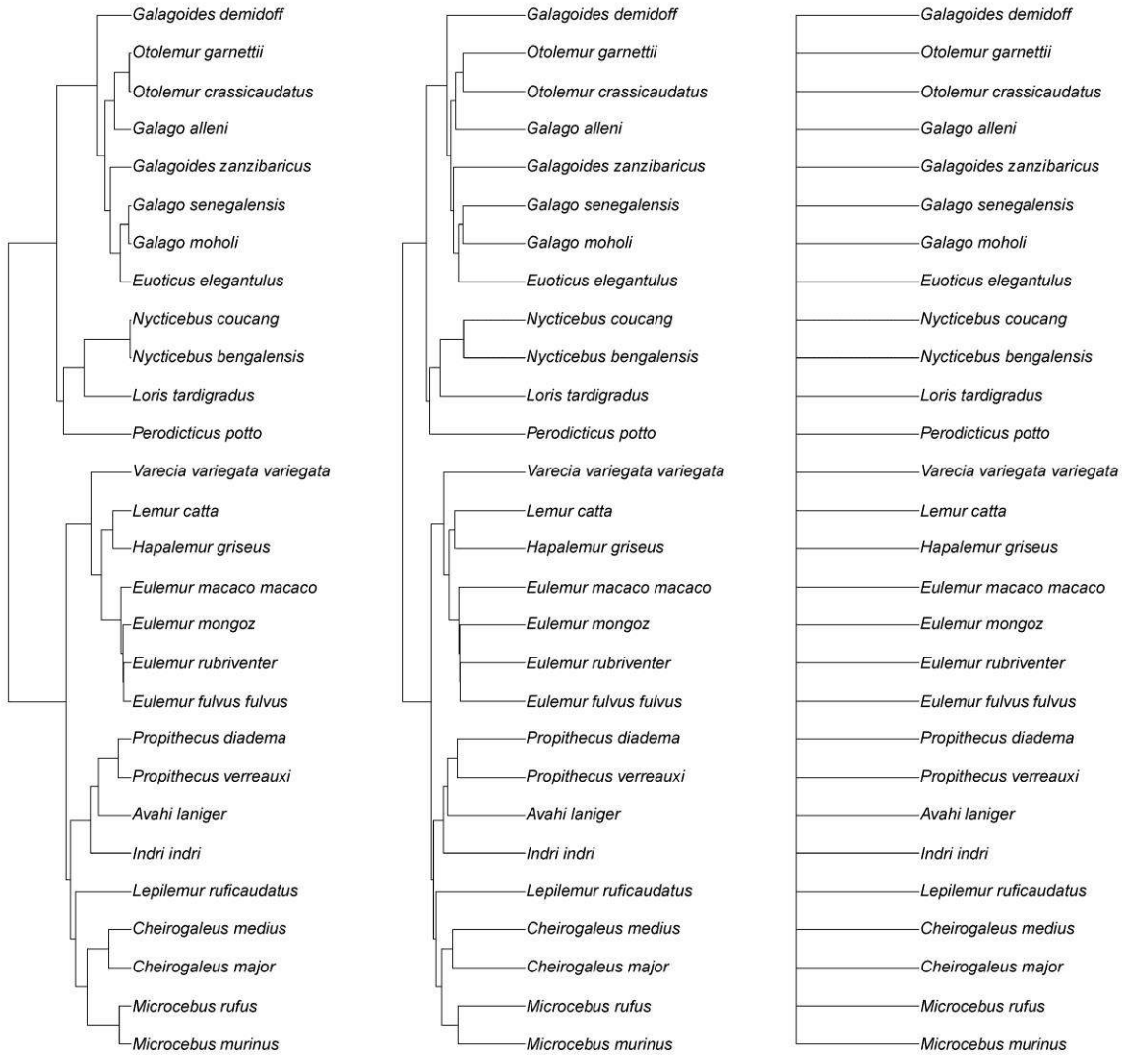

Figure 66: Strepsirhine phylogenetic tree transformed according to λ values of, from left to right, 1, 0.5 and 0.

6.2.1.2. Delta

Delta (which is very similar to Blomberg *et al.*'s (2003) acceleration-deceleration (ACDC) model), scales both the shared branch lengths between related species and the total branch lengths from the root to the tip of the tree to mimic either accelerating or decelerating evolutionary rates, thereby mimicking scaled gradualism (Pagel, 1999). Where early evolution has been comparatively fast, delta is less than one (branch lengths will become increasingly shorter towards the tips); where early evolution has been comparatively slow, delta is greater than one (branch lengths will become increasingly longer towards the tips). Where delta is 0, the model matches that described under BM (Harmon *et al.*, 2009; Pagel, 1999; Figure 67).

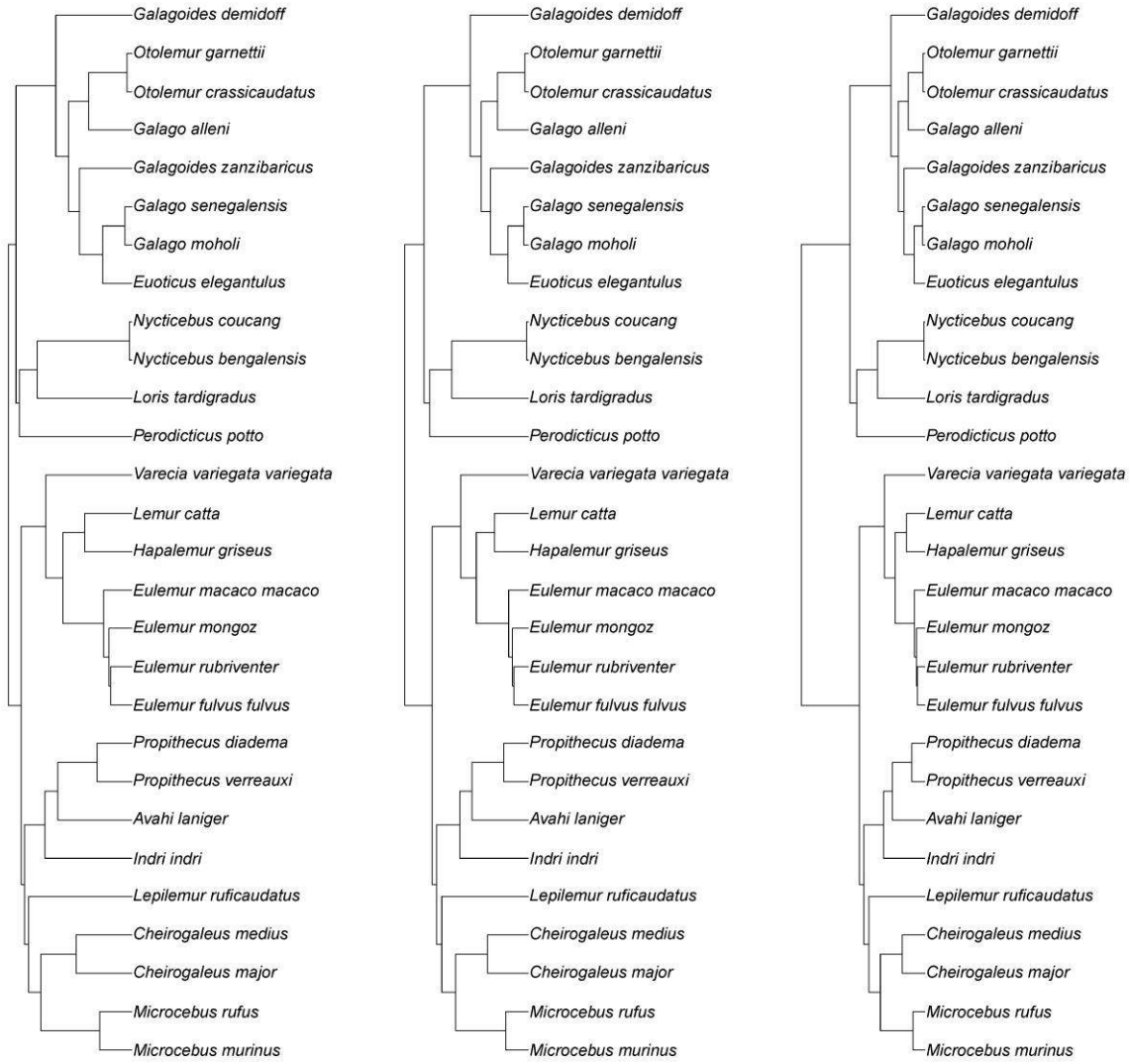

Figure 67: Strepsirhine phylogenetic tree transformed according to delta values of, from left to right, 3, 1.5 and 0.

6.2.1.3. Kappa

Kappa is another tree transformation method, where all branch lengths are multiplied by power kappa. When kappa=0, all branch lengths are equal, giving a punctuated model of evolution. Evolutionary change is therefore associated with speciation, with rates of change fastest immediately after an episode of speciation and slowing over time. When kappa is 1 the model matches that described under BM (Pagel, 1999; Figure 68).

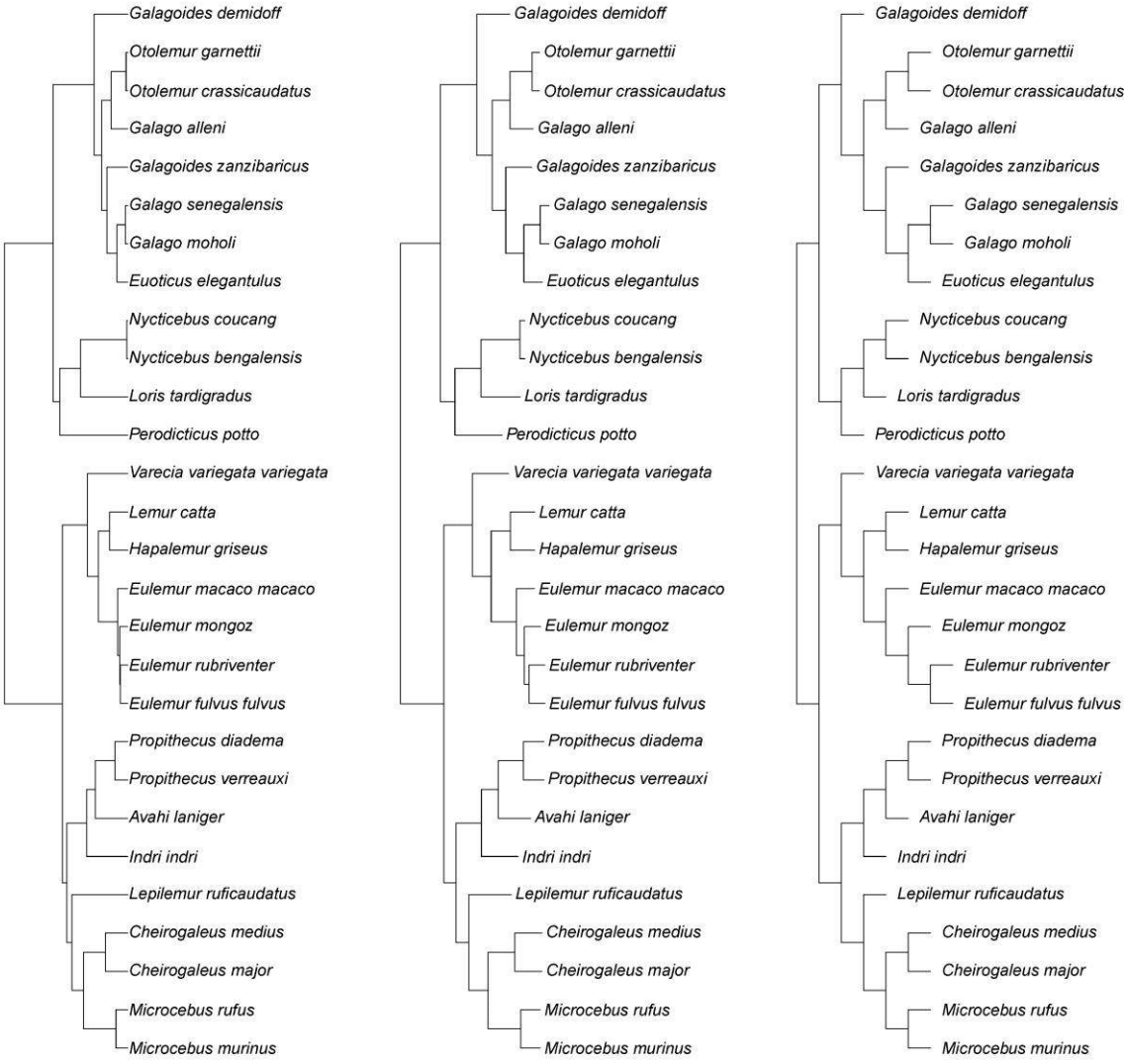

Figure 68: Strepsirhine phylogenetic tree transformed according to kappa values of, from left to right, 1, 0.5 and 0.

6.2.1.4. Early-Burst model (EB)

The Early-Burst (EB) model is based on the idea that when taxa first enter a new ecological niche, there should be an initial period of rapid morphological evolution (Harmon *et al.*, 2010). The rate of evolution is then expected to decrease over time, either because species have become relatively well adapted to the niche, or due to increasing constraint on evolutionary change as niches are filled and the level of inter-species competition rises (Harmon *et al.*, 2010). Where the rate of change parameter '*a*' is equal to 0, the model is equates to BM; as *a* becomes increasingly negative, the more closely the tree resembles the EB model i.e.,, the more rate decreases through time. Finally, when *a*>0, rate increases over time (Harmon *et al.*, 2010; Figure 69).

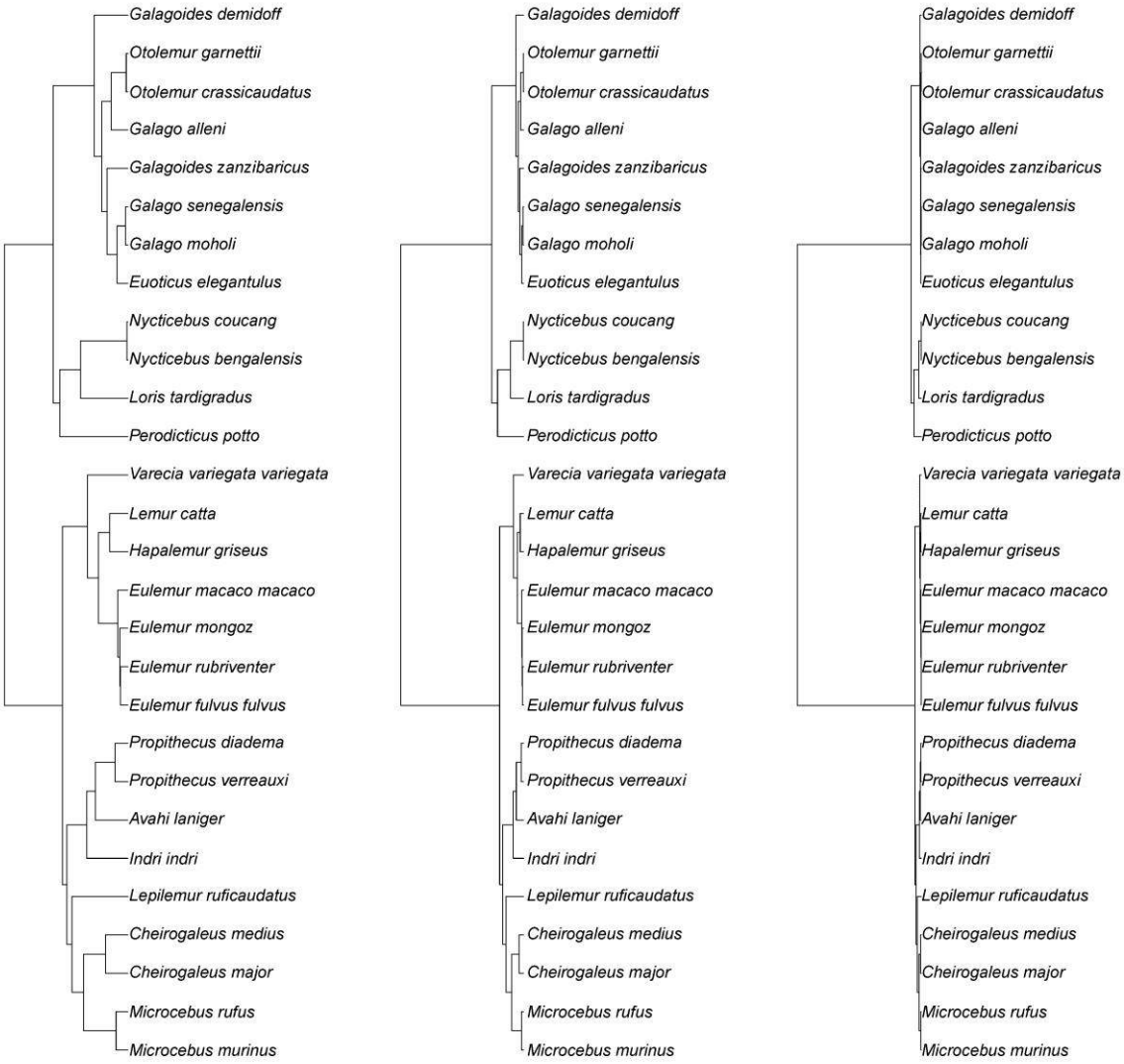

Figure 69: Strepsirhine phylogenetic tree transformed according to a values of, from left to right, 0, -0.05 and -0.1.

Tree transformation techniques go some way to addressing the problems associated with BM by attempting to gauge the tempo of evolution across the entire tree. However, they are still subject to many of the limitations of the BM model. For instance, due to stabilising selection, trait variance is expected, in most instances, to remain bounded, but under BM, it is expected to increase, unbound, over time (Butler *et al.,* 2004). In addition, under natural selection, species can encounter different selective pressures and would be expected to develop variations in phenotype as a result. However, under BM all lineages are expected to share the same mean phenotype, with no selection for a particular direction of change implied (Butler *et al.,* 2004).

6.2.1.5. The Ornstein-Uhlenbeck (OU) evolutionary model

Unlike BM, the Ornstein-Uhlenbeck (OU) evolutionary model (Uhlenbeck & Ornstein, 1930) attempts to incorporate the effect of selection on the direction of change into the model. Under the OU model, trait change within evolutionary space (which, for the purposes of this study is morphospace) is determined by random walk, but traits are tied to selective optimum values. Traits that stray too far from the optimum will be pulled back, with a force (α) proportional to the distance that they have wandered (Blomberg *et al*., 2003; Felsenstein, 1988). The higher the value of α, the stronger the selection implied and, the stronger the selection, the more rapidly the species will approach the optimum and the tighter the species distribution around that optimum will be (Blomberg *et al.*, 2003). The 'pull' towards the optimum in the OU model has been described as a way of modelling stabilising selection (Blomberg *et al.*, 2003). Very strong stabilising selection can result in the loss of any detectable phylogenetic signal, which would be the equivalent of a star phylogeny (Blomberg *et al.*, 2003); at the other end of the scale, when $\alpha = 0$, the model matches that described under BM (Harmon *et al.*, 2009).

Further development of the OU model means that it is capable of modelling more complex evolutionary scenarios. For example, each branch of the tree can be given its own specific phenotypic optimum (Butler *et al.,* 2004; Hansen, 1997), or selective optima can be allowed to vary over time (Hansen *et al.,* 2008), based on predetermined biological information or evolutionary hypotheses (Butler *et al.,* 2004). Unlike the BM model, the OU model has the ability to distinguish between stabilising selection and low levels of genetic drift. For instance, if stasis has occurred in a phylogeny, but closely related species do not vary too greatly in their traits, then the BM model would be a good fit (Butler *et al.,* 2004). However,

if closely related species are experiencing stabilising selection, but under different optima, then their traits will vary widely, and BM would be a poor fit. In the latter situation, the OU model would be able to distinguish between the underlying courses of either low levels of drift or strong stabilising selection for different optimum traits (Butler *et al.,* 2004).

One consequence of the OU method is that evolutionary history is gradually forgotten; species trait values vary around the selective peak to which they are being continually pulled, with recent variations having a much greater impact than historical ones and with historical influence gradually eroded (Felsenstein, 1988). In this way, comparisons between closely related species are given greater weight than those between distantly related species. However, it is generally accepted that morphology can contain information relating to ancient evolution and, under the OU model, details of these ancient evolutionary changes are lost (Felsenstein, 1988; Smaers & Vinicius, 2009).

6.2.1.6. Independent Evolution (IE) evolutionary model:

The Independent Evolution (IE) model of evolution is explained fully in the Methods Chapter. Briefly, the IE model assumes that evolutionary change is linked to an adaptive peak (Felsenstein, 1988), in a similar way to the OU model, but in this case the 'peak' can move over time. The IE model can collapse into either the BM or OU model, where it is appropriate for the data (Smaers & Vinicius, 2009).

The fit of the above evolutionary models and tree transformations can be tested and compared using Bayesian analyses and the Akaike Information Criterion (AIC). These methods are outlined below:

6.2.1.7. The Bayesian approach

The Bayesian approach derives the posterior probability of a tree as a function of the likelihood of the data given that tree, with the assumption that phylogenetic relationships are accurately known (Garamszegi & Gonzalez-Voyer, 2014). The posterior probability is calculated using the Markov Chain Monte Carlo (MCMC) process; this involves the evaluation of multiple different phylogenetic hypotheses (Garamszegi & Gonzalez-Voyer, 2014). These are obtained by altering either the topology of the tree, the parameters of sequence evolution or branch lengths (for the present study they are obtained only through the alteration of branch lengths). The remaining structure of the tree is assumed to

be an accurate portrayal of reality (Garamszegi & Gonzalez-Voyer, 2014). These alterations are given 'priors', which are specific to the model being tested, to specify the limits to which the tree (in this case, branch lengths) can be changed (Currie & Meade, 2014).

Each hypothetical tree in the chain is assessed on how well it fits the data; if a tree offers an improvement on the previous likelihood score, then it is accepted. If not, the previous 'best fit' tree is retained and the new tree is only accepted with a probability score. The probability score is dependent on how much poorer the likelihood score of the new tree is compared to the best fit tree (Currie & Meade, 2014). Ideally, the chain would be allowed to run until all possible trees had been evaluated, but, depending on the size of the tree, this is both time and computationally expensive. Instead, a predetermined number of iterations is used (here 1,000,000 iterations are run). The likelihood score is expected to be low for the initial trees in the chain and to climb as the chain converges on the posterior distribution. Because of this, the trees in the early, 'pre-convergence' section of the chain are discarded. Each model's likelihood score can then be used in further analyses, such as the Akaike Information Criterion (AIC), to compare the fit of the different models to the data (Currie & Meade, 2014).

6.2.1.8. Akaike Information Criterion (AIC)

The AIC is a method for gauging which of a set of models best describes the data (O'Meara, 2015). Models are judged on both their fit to the data (in terms of Kullback –Liebler distance) and the number of parameters that they use (O'Meara, 2015). Increasing the number of parameters will usually improve the fit of a model, but it also reduces the confidence that can be placed in its results (Butler *et al.*, 2004). Under the second order information criterion (AICc), models are also judged more harshly when sample sizes are small (O'Meara, 2015). AICc can be calculated as:

$$AICc = -2 (\ln (\text{likelihood})) = 2K * (n / n – K – 1)$$

Where likelihood is the probability of the data for a given model, K is the number of free parameters in that model and n is the number of species (O'Meara, 2015). AICc scores are usually ranked and rescaled to make them meaningful and easier to interpret (Burnham & Anderson, 2004). This transformation is calculated as:

$$\Delta_i = AICc_i - AICc_{min}$$

Where $AICc_{min}$ is the score for the best fitting model. The best model therefore has a score of Δ=0, while all other models have a score that is representative of the amount information lost, should that model be used instead of the best fit model, making it simple to rank the models, with the best fit model having the lowest score (Burnham & Anderson, 2004). The outcome of AIC analyses has been shown to be unaffected by sample size (number of species), except when tree size is very small. When N≤10 BM was found to be consistently selected over all other models (Harmon *et al.*, 2010).

6.2.1.9. Comparing evolutionary models

The AIC has previously been used to compare the fit of BM, OU (with one stationary peak, based on average trait values) and EB models, for size and shape traits, for 49 different animal clades, including amphibians, fish, insects, squamates, birds and mammals (including primates) (Harmon *et al.*, 2010). The OU model was found to be the best supported model overall and the EB the least. However, when examined individually, there were significant differences between clades. Most notably, the BM model was found to be the best supported for all mammalian trees, including primates (Harmon *et al.*, 2010). Furthermore, even though the sample taxa contained several recognised 'classic' adaptive radiations, including Galapagos finches and African lake cichlids, very few clades where shown to follow the EB pattern, which is predicted to mirror that of adaptive radiations. Harmon *et al.* (2010) suggest that because, within these radiations, sister species are often found to be morphologically divergent, their adaptive zones may not be full and, as a result, there is nothing to constrain and slow down the rate of evolutionary change. Alternatively, as the EB model was so weakly supported, across such a broad sample of taxa, perhaps it is, in fact, a rarely occurring evolutionary pattern (Harmon *et al.*, 2010).

A closer examination of the BM and OU models again found the OU model to be the best supported, but this was dependent on how the adaptive peaks of the OU model were selected (Butler *et al.,* 2004). Different OU models were assessed for the analysis, they included: OU(1), for which a single optimum peak was described for all species, as in the Harmon *et al.* (2010) study above; OU(3), for which three different optimum peaks were described, based on large, immediate and small species size; OU(4) had an additional fourth optimum associated with unknown ancestral branches; and finally, OU(LP), for

which optima were determined by a linear parsimony reconstruction. Only the OU(LP) model was found to be a better fit than the BM model, suggesting that the specification of the selective optima for internal branches has a crucial impact on performance of the OU model (Butler *et al.,* 2004).

The OU model has been adapted further, so that, as well as different selective regimes being able to have different optimum trait values, constraints on the rate of evolution (σ^2) and the strength of the pull towards the optima (α) can also be relaxed (Beaulieu *et al.,* 2012). When a variety of models were tested, which included a single BM model, a multiple rate BM model with a separate rate assigned to each character state, and five different OU models for which constraints were increasingly relaxed, ranging from an OU model with a single optimum for all species and constant σ^2 and α values (OU1), to an OU model with separate optima, σ^2 and α values estimated for each species (OU_{mva}). The OU_{mva} was found to be the best fit for the data (genome size evolution in monocots) as calculated by the AIC, while the BM models were the worst. This indicates that genome size in different species of monocots were under different selective regimes, subject to different rates and strengths of selection (Beaulieu *et al.,* 2012).

While it seems that these more 'realistic' models of evolution are edging ever closer to providing models that 'fit' the data, it is crucial to remember that a better fit does not necessarily mean that the model accurately depicts the original pattern of evolutionary activity (Blomberg *et al.*, 2003). Inferring underlying evolutionary process from the support shown for different evolutionary models is not a straightforward process. Even a single rate BM model has been shown to be consistent with neutral genetic drift, a drift/mutation balance or selection towards a moving optimum (Hansen & Martins, 1996). So, while parameter estimates can be helpful for investigating specific predictions, it is more difficult to reach conclusions relating to evolutionary processes having identified model parameters or the best model (Beaulieu *et al.*, 2012).

6.2.2. Phylogenetic signal

Previous attempts to identify phylogenetic signal within morphological traits have tended to use one of three key methods. First, morphological data has been used as the basis from which to construct phylogenies using methods of parsimony analysis; these phylogenies are then compared to those built using molecular data (Bjarnason *et al.,* 2011; 2015; Cole III *et*

al., 2002; Couette *et al.,* 2005; Gilbert, 2011; Lockwood *et al.,* 2004; Lycett & Collard, 2005; Viguier, 2002). It should be noted that phylogenetic relationships and genetic relationships are in essence the same thing; as such, when morphology-based and molecular-based phylogenies differ in their representations of species relationships, molecular-based phylogenies will always be considered the more accurate (Collard & Wood, 1999). Second, the extent of the correlation between molecular distance matrices and morphological based distance matrices has been examined (Cardini & Elton, 2008a; Harvati & Weaver, 2006; Horovitz *et al.,* 1998; Smith, 2009)**.** The third method sees the wide use of Pagel's λ estimation to assess the degree to which closely related species resemble each other more than distantly related species, as would be expected under BM (Cooper *et al.*, 2010; Kamilar & Cooper, 2013; Losos, 2008; Pagel, 1999)**.**

6.2.2.1. Pagel's λ

Pagel's λ has become an established method for measuring the strength of phylogenetic signal in traits (Cooper *et al.,* 2010; Kamilar & Cooper, 2013; Losos, 2008). Maximum Likelihood (ML) or Bayesian approaches can be used to assess which of the λ transformed trees provides the most probable explanation of the observed data (Pagel, 1999). A λ value close to or equal to 1 signifies that species that are closely related show greater similarity to one another than to distantly related species; that is, the data fits the BM model. A λ value close to or equal to 0 signifies that trait values are randomly distributed across a phylogeny or that distantly related species show greater similarity in a trait than closely related species, possibly due to convergent evolution (Kamilar & Cooper, 2013). Intermediate values of λ indicate that, while there is some phylogenetic signal present, the trait has also evolved following processes other than BM (Kamilar & Cooper, 2013). It is theoretically possible for λ to be greater than one, in which case closely related species would be found to be even more similar in their trait values than predicted by the BM model; however, the bounds of λ are restricted to 0-1 because it is not possible for covariance's to be greater than variances in a phylogenetic variance-covariance matrix (Kamilar & Cooper, 2013).

6.2.2.2. Blomberg's ' K'

An alternative approach to Pagel's λ, for the quantification of phylogenetic signal, is Blomberg's '*K*' which, unlike λ, can generate a phylogenetic score that is greater than one (Blomberg *et al.*, 2003). The *K* statistic is an estimate of the amount of phylogenetic signal

in an observed trait, given a specific phylogeny, relative to the amount expected for the same trait under BM over the same phylogeny (Blomberg *et al.,* 2003). *K* is calculated as the ratio of the mean squared error of the tip data, using the phylogenetically correct mean (MSE_0), divided by the mean squared error taken from the variance-covariance matrix based on the phylogenetic tree (MSE) (Blomberg *et al.,* 2003). To make *K* scores comparable between trees, MSE_0/MSE is scaled by the value expected under a BM model (Blomberg *et al.,* 2003). Therefore *K* can be calculated as:

$$K = \frac{\text{observed } MSE_0}{\text{observed MSE}} \Big/ \frac{\text{expected } MSE_0}{\text{expected MSE}}$$

As such, a *K* value of less than one indicates that closely related species show less similarity in a trait than would be expected under BM, while a *K* of one implies that closely related species show exactly the amount of phylogenetic signal as would be expected under a BM model of evolution, and a *K* value greater than one implies that closely related species show even greater similarity to one another for the trait in question than would be predicted under a BM model (Blomberg *et al.,* 2003).

K scores of less than one could indicate evolutionary pathways that do not correlate with the phylogenetic tree, such as convergent evolution, resulting in homoplasies. However, measurement error in species mean value (i.e., tip values) or errors in the phylogeny have been shown to affect the estimation of phylogenetic signal, usually diminishing the score (Blomberg *et al.*, 2003; Ives *et al.,* 2007).

Further analyses can be conducted to test if the value of *K* is significantly different from zero (i.e., no phylogenetic signal). This is done using a randomisation test, where trait values are arbitrarily reassigned across the tips of the phylogeny numerous times, calculating the *K* value each time. The number of times that the *K* value for the randomisation tests is greater than that for the observed data, divided by the total number of randomisations used, gives the *p* value and, therefore, determines whether the null hypotheses of no phylogenetic signal can be rejected (Blomberg *et al.*, 2003; Kamilar & Cooper, 2013).

There has been a tendency to interpret the strength of phylogenetic signal, as measured by Pagel's λ or Blomberg's *k,* as an indication of the underlying evolutionary processes or rate of evolution (Revell *et al.,* 2008). High phylogenetic signal is often seen to represent instances of gradual change over time in line with genetic drift (BM), especially when both λ and *K* are equal to one (Symonds & Blomberg, 2014), or evolutionary conservativism, especially when *K* values are greater than one. Evolutionary conservativism could be the result of stabilising selection, pleiotropy, functional constraints, or limited genetic variation (Kamilar & Cooper, 2013; Revell *et al.*, 2008). Low phylogenetic signal has been attributed to traits being highly evolutionarily liable (Kamilar & Cooper, 2013; Symonds & Blomberg, 2014). It should be noted that there are no agreed upon 'cut-off' points at which λ or *K* values are said to represent a particular evolutionary process; for example, λ is considered to be high enough to represent phylogenetic conservativism at >1 (Losos, 2008), =1 (Cooper *et al.*, 2010) and ≤1 (Kamilar & Cooper, 2013; Weins *et al.*, 2010).

However, modelling the relationship between phylogenetic signal, evolutionary process and rate, for a wide scope of evolutionary situations has revealed that such extrapolations may be invalid (Revell *et al.*, 2008). Under constant rate genetic drift (i.e., BM), there is no relationship between the rate of evolution and the strength of phylogenetic signal as measured by λ and, as such, low phylogenetic signal should not necessarily be interpreted as a sign of a high rate of evolution. Furthermore, no direct link was found between the underlying evolutionary process and the strength of signal (Revell *et al.*, 2008). Different processes (i.e., genetic drift or neutral evolution, stabilizing selection, variable selection and time dependent models) produce very similar scores, depending on the conditions specified (Revell *et al.*, 2008). Therefore, when investigating evolutionary processes, it is instead recommended to compare the fit of alternative models to the tree and data at hand (Revell *et al.*, 2008).

There are additional factors to consider when measuring phylogenetic signal in this way; specifically that the strength of the signal may vary across taxonomic levels. For example, a signal that is strong at generic or family level may be weaker or absent at a species level. Moreover, signal strength may be both taxa- and trait-specific (Kamilar & Cooper, 2013). Finally, measures of phylogenetic signal do not account for within-species variation. As a result, information about traits that are phylogenetically conserved across species, but vary within them, would go undetected without additional analyses (Kamilar & Cooper, 2013).

One example of this is body mass, which has been found to be conserved across primates, but to vary within species as a result of climate and environmental conditions (Cardini & Elton, 2007, 2009a; Cardini *et al.,* 2007; Kamilar *et al.,* 2012)

6.2.2.3. Homoplasy

Homoplasy refers to features shared among organisms for reasons other than inheritance from their last common ancestor (LCA) (Lockwood & Fleagle, 1999). It is generally viewed as the opposite of homology, which describes traits shared by organisms whose LCA possessed the same trait (Hall, 2007). Homoplasy can be the result of three different types of evolutionary process: convergence, parallelism and reversal (Hall, 2007). Convergence refers to similarity arising through independent evolution via different developmental pathways (Hall, 2007). Parallelism occurs when closely related organisms share the same feature, arrived at via the same developmental pathway, but when that feature is not continually present in all members of the lineage and, specifically, not in their LCA (Hall, 2007). Finally, reversal refers to a character found in a descendent and their ancestors, with the exception of their immediate ancestor (Lockwood & Fleagle, 1999).

There is some argument, however, over the classification of parallelism (and, to some extent, reversal) as homoplasy, as an element of common descent is still implied (Scotland, 2011). The characters in question might therefore be reflective of a deeper homology of shared genetic pathways/networks (Hall, 2012). For this school of thought, convergence is the only true form of phenotypic homoplasy (Scotland, 2011). Even so, in terms of recreating phylogenies, it is parallelism rather than convergence that is likely to be the major source of misleading information, especially when the taxa are closely related (Lockwood & Fleagle, 1999).

Phenotypes are often the expression of a compromise between the intrinsic and extrinsic (environmental) factors that the organism experiences (Lockwood & Fleagle, 1999) and homoplasies can arise for both extrinsic and intrinsic reasons; intrinsic factors may be thought of as the 'constraints' that dictate the way in which an organism can respond to environmental change. It has been argued that certain regions or modules of the cranium may be more susceptible to homoplasy than others. Specifically, those modules that form early on in development have a stronger genetic basis (i.e., are more heritable)

and are thought to be less homoplastic than later-developing traits (Lieberman, 2000). However, the validity of this argument has been questioned by those who argue that the traits most liable to homoplasy are more likely to be taxon-specific (Collard & Wood, 2001; Lockwood & Fleagle, 1999).

While identifying homologies is crucial for the accurate inference of phylogenies from phenotypic traits, homoplasies are usually considered to be noise, which may muffle or even obscure any true phylogenetic signal. However, they are also a key tool for identifying adaptations and for testing associated hypotheses relating to selection pressures and evolutionary pathways (Hall, 2007).

6.2.2.4. Where has phylogenetic signal been found?

In comparison to other types of traits, morphology has been shown to contain a relatively strong phytogenic signal (Blomberg *et al.*, 2003). In a very broad cross-species review, including reptiles, birds and mammals, significant (P<0.05) phylogenetic signal was found to be almost ubiquitous (92% of cases) for samples that included over 20 species, with a stronger phylogenetic signal found for morphological traits than for life history, physiology and behavioural traits, which, respectively showed incrementally smaller signal values (Blomberg *et al.*, 2003). It has been suggested that behavioural traits may show the weakest phylogenetic signal, as they are both the most evolutionarily liable and the most difficult to accurately record (Blomberg *et al.*, 2003). Morphological traits have also been shown to contain the strongest phylogenetic signal for primate-only data sets (Kamilar & Cooper, 2013). However, in both analyses, the morphological traits investigated were largely measures of size, such as body mass, brain size, testes size and body length, rather than aspects of shape (Blomberg *et al.*, 2003; Kamilar & Cooper, 2013).

The results of molecular- and morphology-based phylogenies have not always been congruent. When the phylogenetic tree of the great apes were initially resolved (Ruvolo, 1997), it was in disagreement with the majority of the existing morphology-based phylogenies (Andrews & Martin, 1987; Collard & Wood, 1999; Groves, 1986; Schwartz, 1983). Similar revelations were found in relation to baboons and mandrills (Disotell *et al.,* 1992; Pilbeam & Gould, 1974; Singleton, 2002) and NWM (Bjarnason *et al.*, 2011; Horovitz *et al.*, 1998). This incongruence has been attributed to widespread homoplasies within the

morphological data (Collard & O'Higgins, 2001), as well as problems with the particular methods of analysis used (Bjarnason *et al.*, 2011; Cardini & Elton, 2008a).
One specific reason proposed to explain the failure of morphological data to accurately recreate phylogenetic relationships is the plasticity of traits caused by the application of strain, specifically as a result of mastication (Collard & Wood, 2007). Strain can lead to a remodelling of the bone, through periosteal growth and the inhibition of resorption as protection against deformation, which could mask phylogenetic signal or even result in apparent homoplasies (Lieberman *et al.,* 2003). As such, those areas of morphology that are not subject to strain, or to only low levels of strain, would be predicted to be less variable within species, and therefore have stronger phylogenetic signal and be a better source of data for the cladistic reconstruction of phylogenies (Collard & Wood, 2007).

However, no support for this 'homoiology hypothesis'(Collard & Wood, 2007) was found when it was tested in both hominoids and papionins. Traits from four defined regions of the cranium (palate and upper dentition, mandible and lower dentition, face, and cranial vault and base) were all found to be poor indicators of phylogenetic relationships, with trees based on traits from regions unaffected by strain (the face and cranial vault and base) no more successful at accurately recreating evolutionary trees than traits from regions expected to be subjected to strain (the palate and upper dentition and the mandible and lower dentition) (Collard & Wood, 2001). Further research has shown that, while traits associated with the masticatory system do show greater variation, both within and across primate species, for papionins (Lycett & Collard, 2005), *H. sapiens* (von Cramon-Taubadel, 2009) and hominoids (Collard & Wood, 2007), respectively, this variation does not render those morphological areas any more or less successful at recreating accurate phylogenetic trees. It could therefore be argued that within-taxon variability cannot be used to judge the phylogenetic efficacy of morphological traits (von Cramon-Taubadel, 2009).

An alternative explanation, or possibly a contributing factor, for the lack of congruence between morphological and molecular data, in terms of phylogenetic relationships, may be the methods employed to investigate them. For example, papionin cranial morphology was found to produce phylogenies in line with the molecular data, once allometric scaling had been controlled for (Gilbert *et al.,* 2009; Gilbert & Rossie, 2007). Moreover, with the exception of von Cramon-Taubadel's (2009) intra-species research, the studies outlined above all used linear measurements which were subsequently coded into discrete

character states (Collard & Wood, 2001, 2007; Lycett & Collard, 2005) and it has been argued that this approach could lead to the loss of important shape data (Cardini & Elton, 2008a; Lockwood *et al.*, 2004).

Von Cramon-Taubadel (2009) used a Geometric morphometric (GMM) approach (see Methods Chapter) to quantify the shape of the human cranium, and compared morphological and molecular distances using matrix correlations. There was still no evidence that areas subjected to greater masticatory strain had weaker correlations between morphological and molecular distances than areas subject to a lesser degree of strain (von Cramon-Taubadel, 2009).

However, other similar studies have questioned this conclusion. For example, opposing findings relating to the correlation between morphological and molecular distance matrices for the *H. sapiens* face have been explained in terms of the definition of the 'face' module and whether or not it incorporates the upper jaw. No significant correlation was recorded when both the upper face and the upper jaw were included within the module (Harvati & Weaver, 2006), while a significant correlation was found when only the morphology of the upper face, and not the upper jaw, was included within the module (Smith, 2009). The influence of strain increasing variation and masking phylogenetic signal in masticatory regions has been invoked to explain this difference (Smith, 2009).

There has been a spate of additional studies, using GMM methods, aimed at identifying areas of the skull that contain a strong phylogenetic signal. Cardini and Elton (2008a) divide the guenon cranium into functional and development modules, as determined by a cranium-versus-mandible structural division, the mode of ossification (chondrocranium or dermatocranium) and the main contributing factor of epigenetic influence (brain growth, mastication or the teeth). The resulting functional and developmental modules comprised: the skull, cranium, mandible, chondrocranium, dermatocranium, face, cranial vault, oral, zygomatic, the horizontal ramus and the vertical ramus. Of these 11 modules only the chondrocranium, or cranial base, was found to have a strong phylogenetic signal, in both male and female specimens (Cardini & Elton, 2008a), as measured using morphological and molecular distance matrices. Evidence of a strong phylogenetic signal within the cranial base has also been recorded at an inter-species level for papionins, based on the ability to reconstruct phylogenetic relationships from allometrically controlled morphological data

(Gilbert, 2011), and within human populations, again using morphological and molecular distance matrices (Smith, 2009).

Several reasons have been put forward for to explain the relatively strong signal in the cranial base. It is early to develop with respect to other areas of the cranium, it develops from cartilaginous precursors, which are thought to be largely genetically determined and it plays a crucial role supporting the brain and connecting the cranial and postcranial skeleton. These factors could work to protect the cranial base from the influence of epigenetic factors, while also constraining its ability to respond to environmental selection pressures and thus maintaining a strong phylogenetic signal (Lieberman *et al.,* 2000). The cranial base may be further constrained, due to the role that it plays in supporting and integrating other elements of the skull, including the orbit, nasal and oral cavity (Lieberman *et al.*, 2000). However, Goswami (2006a) argues that the cranial base as defined by the Goswami model base module, which also corresponds to the base module described for the guenons (Cardini & Elton, 2008a), includes only the more posterior elements of the cranial base, and not the mid-base, which is assigned to the zygomatic module. As such, the base module cannot be said to have such a significant, integrating role in the cranium (Goswami, 2006a; Lieberman *et al.*, 2000).

Having been identified as having strong correlation between its morphological and molecular distance matrices, the cranial base was subsequently used in an attempt to reconstruct the guenon evolutionary tree. Although cranial base morphology was successful in identifying the two main guenon clades (arboreal and terrestrial), it was unable to match molecular topologies at shallower taxonomic levels (Cardini & Elton, 2008a). It has been suggested that within the two main guenon adaptive zones (arboreal and terrestrial), stabilising selection, similar to that described by the OU model of evolution (Felsenstein, 1988), may be at play. If species' adaptive peaks are similar within the clade, trait values will wander back and forth, but will be pulled back towards the same peak, resulting in lineage trait values repeatedly crossing one another and erasing any phylogenetic signal (Cardini & Elton, 2008a).

The morphology of the temporal bone has also been shown to be indicative of genetic distance, at both an inter-species level across the Hominoidea (Lockwood *et al.*, 2002), and at an intra-species level within *H. sapiens* (Harvati & Weaver, 2006a; Smith, 2009). The

temporal bone, like the cranial base, is early to develop and forms through endochondral ossification, and is relatively free from muscular strain, which may allow it to evolve neutrally and, as a result, reflect phylogenetic relationships more accurately than other areas of the cranium (Lieberman *et al.*, 2000).

For *H. sapiens,* the entire cranium was found to have a stronger phylogenetic signal than any of its composite, smaller modules (Smith, 2009). A range of different selective forces would be expected to act on cranial morphology, due to it being comprised of different functional areas responsible for respiration, mastication, vision, olfaction and vocalisation (Young, 2005). It has been proposed that the mosaic combination of these forces and traits could lead to a stronger phylogenetic signal recorded for the whole cranium than for separate cranial modules (Young, 2005).

This is in contrast to the results found for the guenons, where only the cranial base was found to have strong phylogenetic signal and the cranium as a whole was not. This reversal of pattern in the guenons has been explained by the potential homoplasy-inducing impact of allometry on the whole cranium, as major shape differences were linked to inter-species differences in size (Cardini & Elton, 2008a). The cranial base, being one of the first elements of the skull to reach full size, may be less susceptible to these allometric changes and therefore retain a stronger phylogenetic signal (Cardini & Elton, 2008a).

Research on catarrhine primates found that morphological distances were significantly correlated with molecular distances for both the cranium and the mandible when *H. sapiens* were excluded from the analysis, but only the cranium showed significant correlation when *H. sapiens* were included. This Indicates that the strength of phylogenetic signal in cranial modules can vary depending upon the taxa being studied (von Cramon-Taubadel & Lycett, 2014).

It is interesting to note that the cranial regions that contain a clear phylogenetic signal are not necessarily all strongly (or all weakly) integrated modules. For example, Goswami and Polly (2010a) find both the braincase and the anterior oral-nasal region to be strongly integrated modules for Japanese macaques (*Macaca fuscata fuscata*), but, while the brain case did reflect genetic distance, the anterior-oral nasal module (i.e., the lower face and upper jaw) did not.

6.2.2.5. Phylogenetic signal in stepsirrhines

Malagasy strepsirhines show strong phylogenetic signal, as determined by Pagel's λ (λ=1), with regard to body mass, at both a family and genus level (Kamilar *et al.*, 2012). This has been interpreted as evidence of rapid early evolution in body mass, as species initially diversified into different ecological niches, followed by a long period of conservative evolution within genera (Kamilar *et al.*, 2012). Similar results have been recorded across primates (Kappeler & Heymann, 1996) and for mammals in general (Smith *et al.,* 2004).

There has been some success in reconstructing accurate phylogenetic relationships for stepsirrhines using morphological data. Evolutionary relationships based on both soft and hard tissue phylogenies are congruent with molecular phylogenies for primates at an intra-ordinal level (Shoshani *et al.,* 1996). However, the Lemuroidea clade had the second lowest support on the tree, with a bootstrap value of 45, and only 50% of the strepsirhine synapomorphies identified were hard tissue traits (Shoshani *et al.,* 1996). In contrast, bootstrap support for the Lorisidae clade was 100, but only data from the Lorisidae, not the Galagidae, were included in the analysis. Further research has shown that a combination of molecular and craniodental data can produce a tree contingent with some molecular topologies for Lorisidae (Masters *et al.*, 2007).

Within strepsirhines, labyrinth morphology (the inner ear) has been shown to correlate significantly with molecular distances, based on neutral molecular markers, and was found to be a better phylogenetic marker than the whole cranium, the cranial base, face or vault (Lebrun *et al.*, 2010). This led researchers to conclude that evolutionary change in inner ear morphology could be explained with a BM model of evolution. Labyrinth morphology was also shown not to be simply a reflection of locomotor behaviour, as the Malagasy lemuriforms are diverse in their locomotor behaviour yet all species share very similar labyrinth morphology (Lebrun *et al.*, 2010). However, when haplorhine primates were included in the analyses the findings were reversed and distances in cranial morphology, rather than labyrinth morphology, were found to correlate better with molecular distances (Lebrun *et al.*, 2010). This could possibly be attributed to convergent evolution of labyrinth morphology between strepsirhines and haplorhines, masking phylogenetic signal (Lebrun *et al.*, 2010).

Strepsirhine craniodental characters have been found to decrease in their level of phylogenetic signal at shallower phylogenetic depths, with strong signal recorded at the family level, but becoming weaker at the genus and species level (Masters *et al.*, 2007). This is similar to results found for guenons, where data pertaining to the shape of the basicranium was only able to distinguish between the deepest clades of the phylogenetic tree (Cardini & Elton, 2008a).

Further evidence of the inability to detect phylogenetic signal below the family level comes from the intra-family and largely intra-genera analysis of *Lemur catta* and *Eulemur* cranial data*,* including sub-species of *E.* fulvus (Viguier, 2002). Morphological distance was found to be independent of molecular distance, but was closely correlated with eco-geographical factors, suggesting that convergent evolution due to similar environmental pressures has resulted in high levels of homoplasy in closely related species (Viguier, 2002). This mirrors the results found for NWM, where, again, cranial morphology was found to reflect environmental factors rather than phylogenetic relationships, specifically the level of folivory or gummivory in the diet, for the Atelinae (Cole III *et al.*, 2002) and Callithrichinae (Couette *et al.*, 2005), respectively.

Finally, the morphology of cheirogaleids has been found to closely resemble that of the lorisiforms, especially in the nasal region, the cranial base and the apparently derived organisation of their intra-cranial blood supply (Cartmill, 1975; Charles-Dominique, 1970). This has led to some confusion surrounding their phylogenetic relationships (Charles-Dominique, 1970), but the clarification of strepsirhine phylogenies through molecular analysis has confirmed this resemblance to be a homoplasy (Yoder, 1997), most likely resulting from allometric constraints (Lebrun *et al.*, 2010). An alternative explanation is that both sets of taxa have retained the primitive primate form, which would require subsequent incidences of parallel evolution in all remaining strepsirhine and haplorhine species for the trait, and therefore seems the least parsimonious of the two explanations (Matsui *et al.,* 2009; Yoder, 1994).

6.2.3. Investigating models of evolution, phylogenetic signal and evolutionary processes

Previous research has shown that a wide range of factors can influence the ability to detect phylogenetic signal in morphological data. These include the morphological region or module studied (Cardini & Elton, 2008a; Lockwood *et al.*, 2004), the taxa examined (von

Cramon-Taubadel & Lycett, 2014), the taxonomic level investigated (Cardini & Elton, 2008a; Lebrun *et al.*, 2010; Masters *et al.*, 2007) and the method of analysis used (Collard & Wood, 2007; Gilbert, 2011; Lockwood *et al.*, 2004)**.**

Criticisms have been made of attempts to model evolution using a BM approach, which ignores the influence of selection (Blomberg *et al.*, 2003; Felsenstein, 1988; Hansen *et al.*, 2008; Smaers & Vinicius, 2009). Here, multiple models of evolution are examined, including tree transformation models, such as Pagel's λ, kappa, delta (Pagel, 1999), and the early-burst model (Harmon *et al.*, 2010), all of which assume a BM model of evolution, as well as the OU (Blomberg *et al.*, 2003; Felsenstein, 1988; Hansen, 1997; Hansen *et al.*, 2008) and IE models (Smaers & Vinicius, 2009) which do not assume BM, with an aim to establish both which model best explains the evolutionary change in morphological data. Pagel's' λ and Blomberg's *K* are also calculated to quantify the strength of phylogenetic signal in different cranial modules (Pagel, 1999; Blomberg *et al.*, 2003).

Attempts to reconstruct phylogenetic relationships using morphological characteristics have sometimes been unsuccessful, possibly fir methodological reasons (Cole III *et al.*, 2002; Collard & Wood, 1999, 2007; Couette *et al.*, 2005; Viguier, 2002; although see Gilbert & Rossie, 2007; Lockwood *et al.*, 2004). However, valuable insights, into which areas of morphology represent homologous traits and which are homoplasies, can be gained by reversing the process of analysis; here morphological data is mapped back over the molecular based phylogeny to investigate when and where changes have occurred.

The combination of knowing which areas of cranial morphology, if any, contain strong phylogenetic signal and which are subject to homoplasy, and how this varies across species and taxonomic levels, should be very informative in terms of being able to identify phylogenetic signal in morphology, including the extrapolation of this information to fossil taxa, for which molecular data is not available (von Cramon-Taubadel, 2014), and for understanding the evolutionary pressures and pathways that have resulted in this pattern in extant taxa.

6.2.4. Aims

To assess the strength of phylogenetic signal present in the strepsirhine cranium and how the strength of this signal varies across cranial modules.

To explore which statistical model of evolution best explains the data, with regard to the morphology of the strepsirhine cranium, and to use this to identify both homologies and homoplasies present in strepsirhine morphology.

6.3. Materials and methods

6.3.1. Sample

The sample consisted of 1560 strepsirhine crania, from 28 species across 15 genera and 6 families (Table 68). Species were selected on the basis that they had sample sizes of N>20, as analysis of the effect of sample size on GMM studies found that shape parameters, especially the estimation of mean shape (as calculated here) can become increasingly inaccurate as sample size is reduced (see Chapter 3). Any measurement error in the data would likely work to obscure or reduce measurements of phylogenetic signal (Blomberg *et al.*, 2003).

Sixty craniodental 3D homologous landmarks were recorded for each specimen and analysis was conducted both on the full landmark composition (see Methods Chapter), as well as on separate cranial modules as described by the 2* and Goswami modularity hypotheses, which divide the cranium into face and vault modules and face, orbit, oral, zygomatic, vault and base modules respectively (See Chapter 4 Table 28 for modules landmark compositions).

Sample size (i.e., number of species) for inter-species analysis, has been shown to have an impact on the likelihood of a significant phylogenetic signal being detected, with a decrease in sample size making it less likely to be detected (Blomberg *et al.*, 2003). Pagel's λ has been shown to have good power for N≥30 (Freckleton *et al.,* 2002). Here N=28, which may make it harder to detect phylogenetic signal; λ values will therefore be interpreted with this in mind.

Table 68: Species and sample sizes included in analyses

Family	Genus	Species	Sample size
Cheirogaleidae	*Cheirogaleus*	*major*	25
		medius	29
	Microcebus	*murinus*	72
		rufus	29
Galagidae	*Euoticus*	*elegantulus*	34
	Galago	*alleni*	24
		moholi	73
		senegalensis	175
	Galagoides	*demidoff*	59
		zanzibaricus	25
	Otolemur	*crassicaudatus*	101
	Otolemur	*garnettii*	95
Indriidae	*Avahi*	*laniger*	23
	Indri	*indri*	39
	Propithecus	*diadema*	28
		verreauxi	43
Lemuridae	*Eulemur*	*fulvus*	175
		macaco	55
		mongoz	57
		rubriventer	27
	Hapalemur	*griseus*	27
	Lemur	*catta*	34
	Varecia	*variegata*	39
Lepilemuridae	*Lepilemur*	*ruficaudatus*	25
Lorisidae	*Loris*	*tardigradus*	27
	Nycticebus	*bengalensis*	22
		coucang	69
	Perodicticus	*potto*	129

6.3.2. Analysis

The full landmark composition for all specimens was subjected to Generalised Procrustes Analysis (GPA) and species average shapes were calculated based on the resulting Procrustes residuals and centroid sizes (CS). Species average shapes were then used in Principal Component Analysis (PCA) at an inter-species level (see Methods Chapter for details of GPA, CS and (PCA); this process was repeated for all cranial modules.

The resultant PC scores were used as species tip values, with PCs 1-3 investigated at each stage of the analyses, as scree plots showed that they described between 71-91% of shape variation for each of the modules. Individual results for each module were: whole cranium - 72%, 2* face module - 74%, 2* vault module - 71%, Goswami face module - 79%, Goswami orbit module - 79%, Goswami oral module 91%, Goswami zygomatic module -81%, Goswami vault module - 79% and Goswami base module - 80%.

The phylogenetic tree for the sample species, used in all subsequent analyses, is the composite tree, taken from the 10K trees website (Figure 70). This tree is generated through a Bayesian phylogenetic analysis of the available genetic data, taken from GenBank, encompassing eleven mitochondrial and six autosomal genes, and represents the best available estimation of the species' evolutionary relationships (Arnold *et al.,* 2010). However, the possibility of errors in the tree topology or branch lengths cannot be ruled out; either could work to obscure phylogenetic signal.

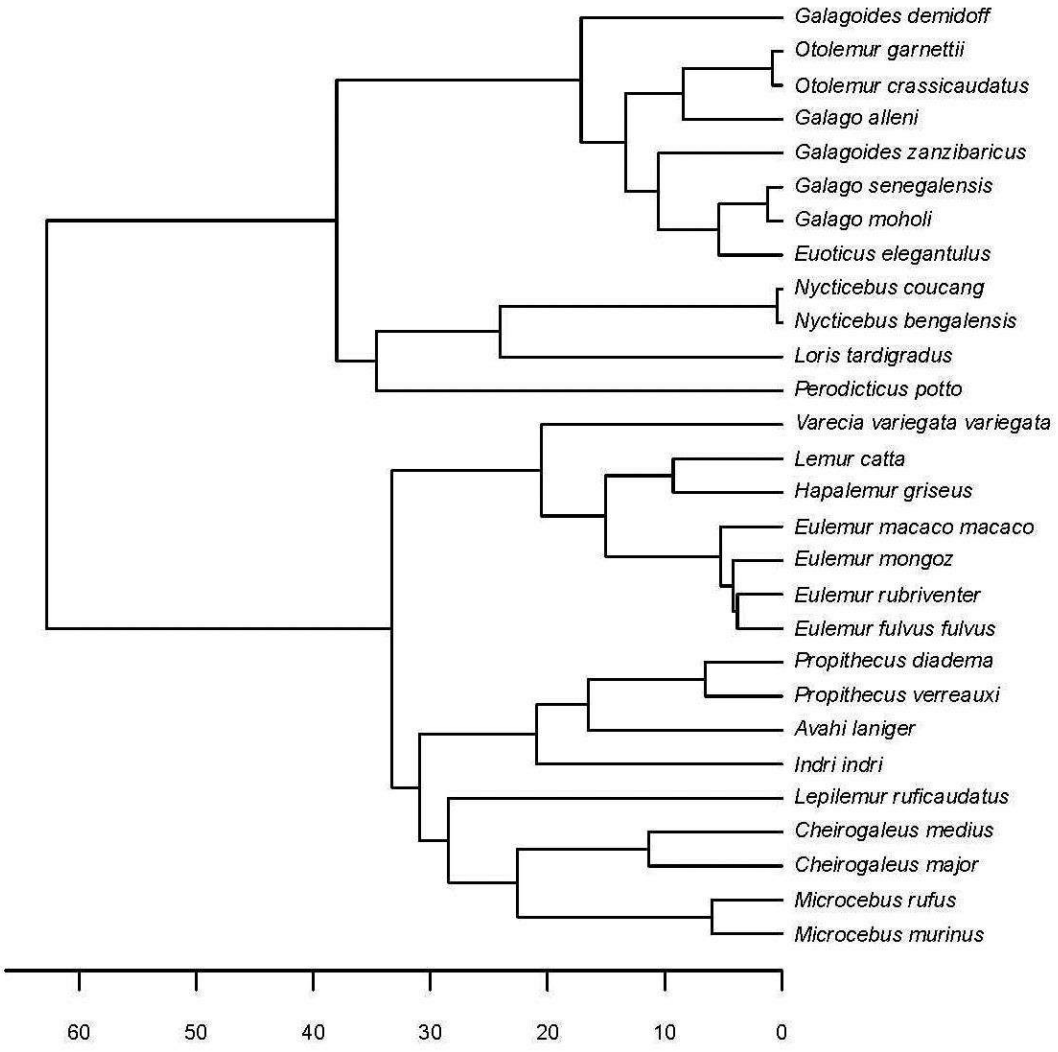

Figure 70: Composite phylogenetic tree of sample species (Arnold *et al.*, 2010).

6.3.2.1. Phylogenetic signal and evolutionary models

The strepsirhine phylogenetic tree was rescaled according to the following evolutionary models using the *R* package Geiger, which provides a function, corresponding to the model of evolution specified, which can be reiterated over many parameter values for transformation (Harmon *et al.*, 2009):

Brownian Motion (BM): the correlation structure among traits is assumed to be proportional to the amount of shared ancestry between species pairs (Harmon *et al.*, 2009), trait change along branches is determined by random walk, drawn from a normal distribution, with a mean of 0 (Symonds & Blomberg, 2014). Rate parameters are a minimum of 0 and maximum of infinity (Harmon *et al.*, 2009).

Pagel's λ: a tree transformation model, where all internal branch lengths are multiplied by λ. Bounds for λ are a minimum of 0 and maximum of 1 and trait change along branches is determined by BM (Harmon *et al.*, 2009; Pagel, 1999).

Delta: a tree transformation model, where the relative contributions of early versus late evolution are fitted to the covariance of species trait values. All node depths are raised to power delta, and bounds for delta are given as a minimum of 1 and a maximum of 3. Trait change along branches is determined by BM (Harmon *et al.*, 2009; Pagel, 1999).

Kappa: a tree transformation model, based on punctuated speciation, where all branch lengths are raised to the power kappa and bounds are given as a minimum of 0 and a maximum of 1. Trait change along branches is determined by BM (Harmon *et al.*, 2009; Pagel, 1999).

Early-burst (EB): a tree transformation model, where the rate of evolution either increases or decreases exponentially over time, calculated as r[t]=r[O]*exp(a*t), where r[0] is the initial rate, a is the rate of change and t is time. Bounds are set to a minimum of log($10^{\wedge}$-5)/depth of the tree and a maximum of -0.000001. Trait change along branches is determined by BM (Harmon *et al.*, 2009; 2010).

Ornstein-Uhlenbeck (OU): Trait change is determined by random walk, but around a selective peak, to which it is constrained by a strength proportional to α. Bounds for α are set to a minimum of 0 and a maximum of 150 (Butler *et al.*, 2004; Felsenstein, 1988; Harmon *et al.*, 2009). It should be noted that there can be computational difficulties when α is very small or very large (Butler *et al.*, 2004). When α equals or is close to 0 (i.e., BM) the optima become increasingly hard to identify. As a result, the likelihood profile in the corresponding direction becomes flat and the reliability of the parameters cannot be estimated; the use of the OU model is therefore not possible. At the other end of the continuum, as the strength of selection (α) increases, the influence of selection anywhere other than the terminal branches becomes increasingly weak and, as a result, estimates of selective optimum for the ancestral branches become increasingly less reliable (Butler *et al.,* 2004).

Independent Evolution (IE): Follows the Adaptive Peak (AP) model of evolution, which assumes that evolutionary change is linked to an adaptive peak that can move over time. The model allows both the 'peak' value and the rate of evolutionary change to be different for each internal branch, but can collapse into either the BM or OU model, where it is appropriate for the data (See Methods Chapter for full details of the IE and AP models)(Smaers & Vinicius, 2009).

Each rescaled tree was subjected to 'anc.Bayes' analysis from the *R* (ver. 3.2) (Team, 2015) package Phytools (Revell, 2012), which samples the posterior distribution for the trait values at the internal nodes of the tree. In each case, 1,000,000 iterations were used and values for the first 2000 (pre-convergence) trees were discarded. For the remaining iterations, the mean of the internal node values were recorded, as were the mean log likelihood values. The mean Log likelihood for each of the models was subsequently used in an AICc calculation to determine which of the models offered the best fit for the data.

In addition, the strength of the phylogenetic signal (i.e., the extent to which the data matches what would be expected under a BM model of evolution) was measured for PCs 1-3 for each cranial module using Blomberg's '*K*' (Blomberg *et al.*, 2003). Randomisation tests were also conducted to test if '*K*' was significantly different from zero for PCs 1-3 for each module. In each instance, 10,000 randomisations were used, as results were found to be

constant from this number of repeats (Kamilar & Cooper, 2013; Klingenberg & Gidaszewski, 2010). These analyses were again carried out in *R* (Ver 3.2) (Team, 2015) using the Phytools package (Revell, 2012).

6.3.2.2. Evo-maps

Plots were created for each PC (1-3), for the whole cranium and for each cranial module, using the *R* (Ver 3.2; Team, 2015) package 'Phytools' (Revell, 2012); mapping the PC values of extant species back across the phylogenetic tree (Arnold *et al.*, 2010), with ancestral node values estimated according to the IE model of evolution (Smaers & Vinicius, 2009). The IE model was used, as this was overwhelmingly found to be the best supported model of evolution for the data. Change in trait values is shown by graduated colour change along branch lengths, moving from the red to the blue end of the colour spectrum as trait values move from low to high. Colour graduation is scaled according to the maximum and minimum trait values of each particular PC. Shared trait values also share the same colour; as such instances of homology or homoplasy are easily identified, while the extent of colour change along the length of a branch indicates the amount, and therefore rate, of change that has occurred.

6.4. Results

6.4.1. Principal component (PC) shape change

The shape variation accounted for by PCs 1-3 for the whole cranium and for all of the cranial modules described by the 2* and Goswami modularity hypotheses are described below (Tables 69-77). The shape change in both positive and negative directions for each PC is also outlined with wire frame diagrams (Figures 71-79). Wire frames have been designed to ensure that all of the principal aspects of shape change can be visualised.

Table 69: Descriptions of shape change along the PC axis from negative to positive, for PCs 1-3, for the whole cranium, based on species averages at an inter-species level; the most significant change for each PC is shown in bold. The percentage of shape variation explained by each PC is also indicated.

Module	PC	Shape change described by PC axis, from negative to positive	% shape variance explained by PC
Whole cranium	1	**More globular vault.** An increase in the relative distance from lambda to inion, relatively larger and more anteriorly positioned external auditory meatus, relatively shorter palate, relatively shorter and more horizontally oriented zygomaticotemporal suture, relatively shorter tooth row, but with more medial/distal variation.	38.43
	2	**Relatively shorter snout and palate.** More globular vault, relatively larger and more distally placed external auditory meatus, more anteriorly placed meeting of the superior temporal crest and the coronal suture, relatively shorter and more distally curved tooth row, the posterior end of the zygomaticotemporal suture is more inferiorly positioned.	21.12
	3	**Shorter snout and superiorly/inferiorly deeper face.** More globular vault, with an increase in the relative distance from lambda to inion, more posteriorly positioned external auditory meatus, relatively longer tooth row achieved through a more posterior end of dentition.	12.77

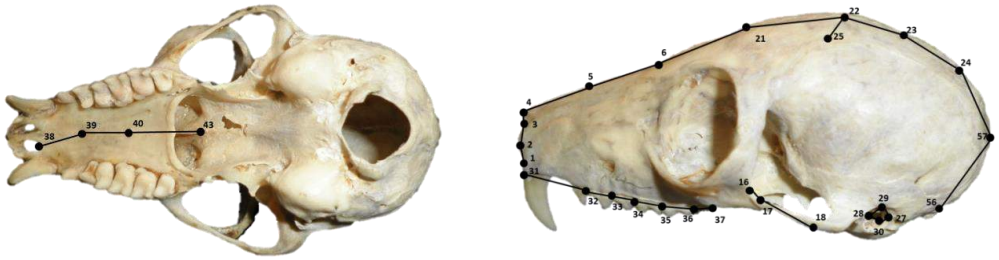

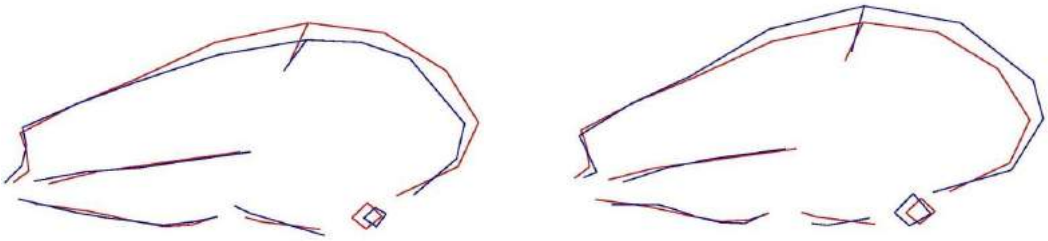

PC1 – negative shape change **PC1 – positive shape change**

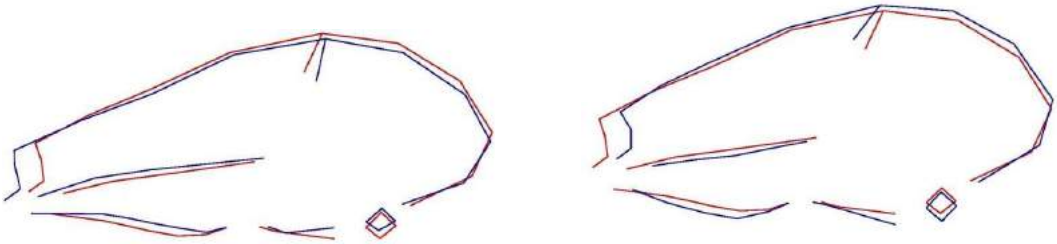

PC2 – negative shape change **PC2 – positive shape change**

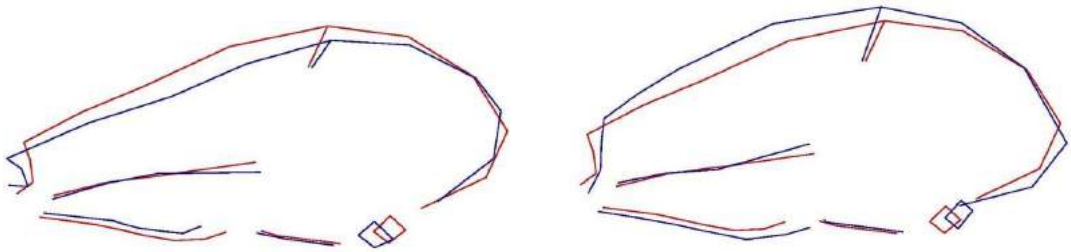

PC3 – negative shape change **PC3 – positive shape change**

Figure 71: Shape change for whole cranium for PCs 1-3, where red represents the inter-species average shape and blue the direction of shape change described by the PC. The figures on the left represent a change towards the negative end of the PC axis and the figures on the right a change towards the positive end, where the change is scaled as 0.1 units of the Procrustes distance. The wire frame is also shown, with landmarks, in relation to an *E. fulvus* cranium, for clarity.

Table 70: Descriptions of shape change along the PC axis from negative to positive, for PCs 1-3, for the 2* model face module, based on species averages at an inter-species level; the most significant change for each PC is shown in bold. The percentage of shape variation explained by each PC is also indicated.

Module	PC	Shape change described by PC axis, from negative to positive	% shape variance explained by PC
2* face	1	**Relatively shorter snout, relatively longer tooth row, more vertically orientated zygomaticomaxillary suture.** Relatively longer zygomaticotemporal suture, relatively shorter and more superiorly positioned frontotemporal suture, with a more superiorly positioned anterior end and a more inferiorly positioned posterior end.	34.45
	2	**More anteriorly, laterally and inferiorly positioned zygomaticomaxillary suture**. Relatively longer zygomaticotemporal suture with a more laterally positioned anterior end, more posteriorly positioned piriform aperture, relatively longer distance between rhinion and midway point between rhinion and nasion, more superiorly positioned frontotemporal suture.	28.16
	3	**Relatively longer distance between rhinion and midway point between rhinion and nasion.** More superiorly positioned nasospinale, more inferiorly positioned and vertically orientated zygomaticomaxillary suture, relatively longer zygomaticotemporal suture with a more inferiorly positioned posterior end, more superiorly positioned frontotemporal suture.	11.53

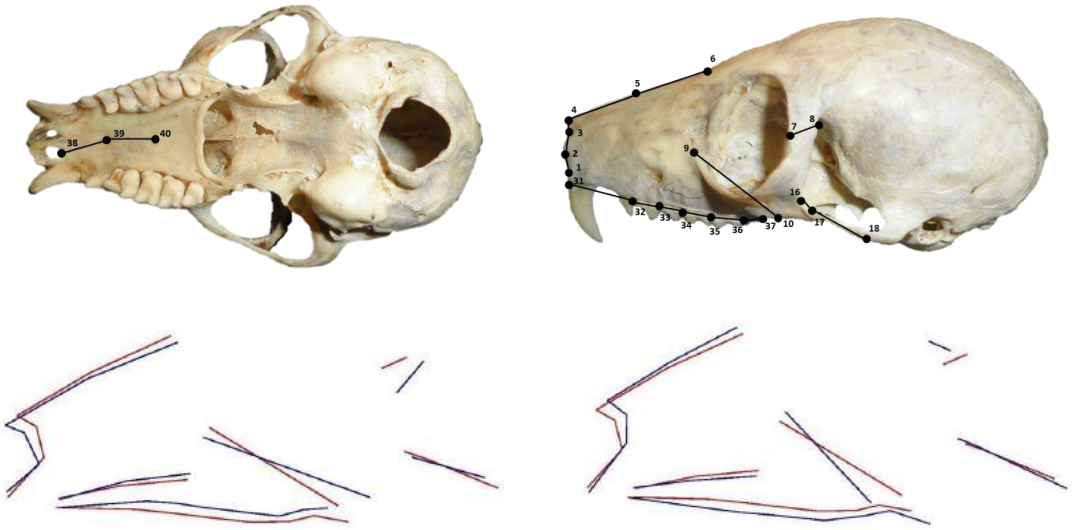

PC1 – negative shape change **PC1 – positive shape change**

Figure 72: Shape change for the 2*model face module for PCs 1-3, where red represents the inter-species average shape and blue the direction of shape change described by the PC. The figures on the left represent a change towards the negative end of the PC axis and the figures on the right a change towards the positive end, where the change is scaled as 0.1 units of the Procrustes distance. For PC2 the wire frame is also shown from the superior view in order to best illustrate the principal direction of shape change. The wire frame is also shown, with landmarks, in relation to an *E. fulvus* cranium, for clarity.

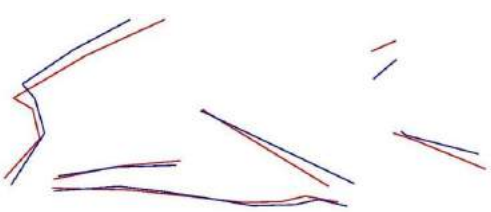

PC2 – negative shape change

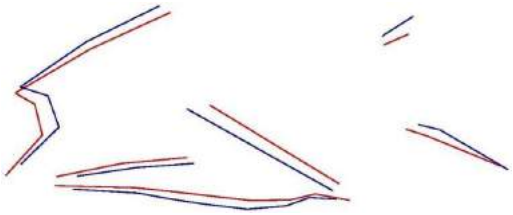

PC2 – positive shape change

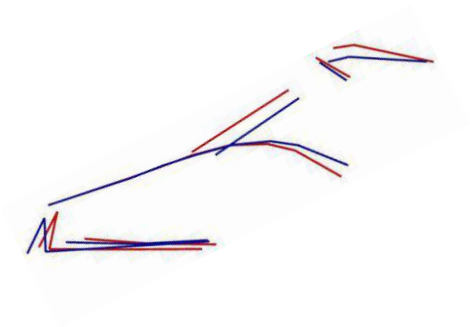

PC2 – negative shape change, superior view

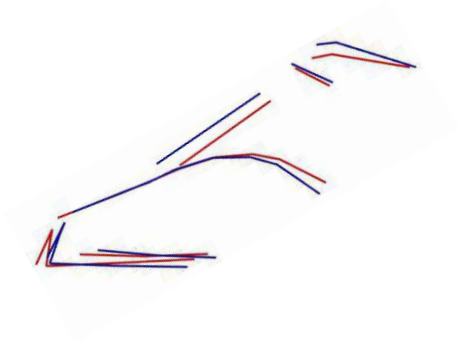

PC2 – positive shape change, superior view

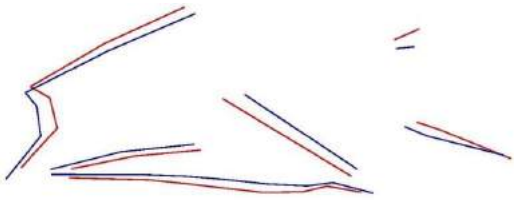

PC3 – negative shape change

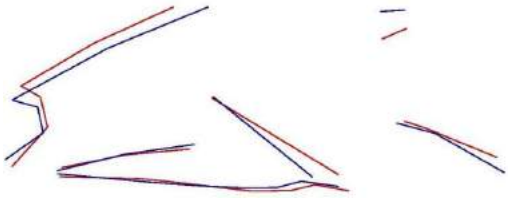

PC3 – positive shape change

Figure 72 (Cont.)

Table 71: Descriptions of shape change along the PC axis from negative to positive, for PCs 1-3, for the 2* model vault module, based on species averages at an inter-species level; the most significant change for each PC is shown in bold. The percentage of shape variation explained by each PC is also indicated.

Module	PC	Shape change described by PC axis, from negative to positive	% shape variance explained by PC
2* vault	1	**Less globular vault.** Greater distance between lambda and inion, smaller and more posteriorly positioned external auditory meatus, more anteriorly and inferiorly positioned meeting point of sphenoid, zygomatic and parietal bone, more anteriorly and superiorly positioned meeting point of zygomatic, frontal and parietal bones, more distally positioned asterion, greater basicranium flexion.	38.21
	2	**More posteriorly positioned inion, relatively larger and more posteriorly positioned external auditory meatus.** More distally positioned meeting of the superior temporal crest and the coronal suture more anteriorly and inferiorly positioned meeting point of zygomatic, frontal and parietal bones.	19.26
	3	**More globular anterior vault.** More medially and posteriorly positioned meeting of the superior temporal crest and the coronal suture, more anteriorly and inferiorly positioned meeting point of sphenoid, zygomatic and parietal bone, more anteriorly and superiorly positioned meeting point of zygomatic, frontal and parietal bones.	13.49

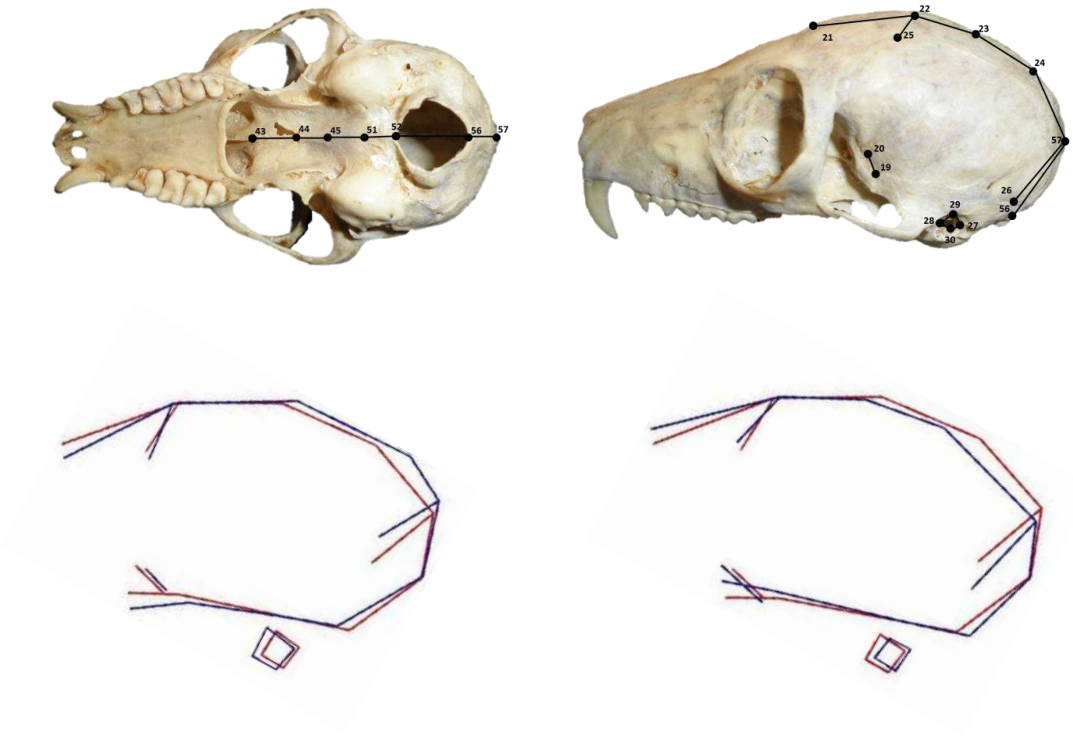

PC1 – negative shape change **PC1 – positive shape change**

Figure 73: Shape change for the 2*model vault module for PCs 1-3. As with Figure 72.

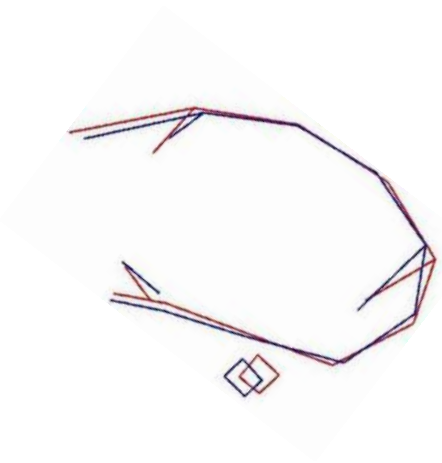

PC2 – negative shape change

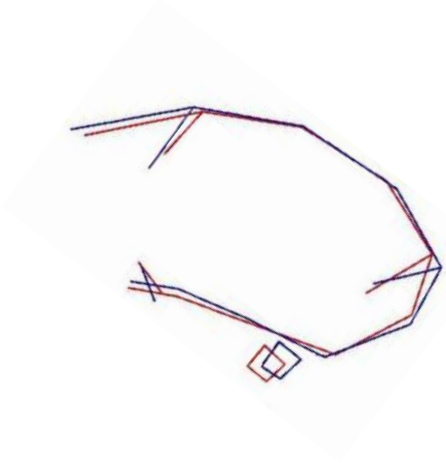

PC2 – positive shape change

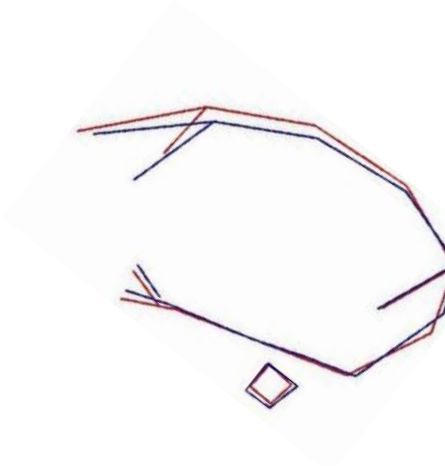

PC3 – negative shape change

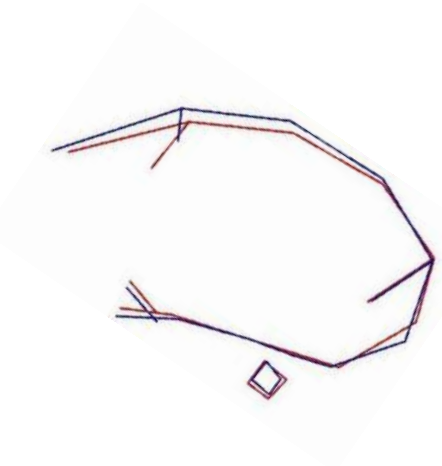

PC3 – positive shape change

Figure 73 (Cont.)

Table 72: Descriptions of shape change along the PC axis from negative to positive, for PCs 1-3, for the Goswami model face module, based on species averages at an inter-species level; the most significant change for each PC is shown in bold. The percentage of shape variation explained by each PC is also indicated.

Module	PC	Shape change described by PC axis, from negative to positive	% shape variance explained by PC
Goswami face	1	**Superiorly/inferiorly compressed snout.** Relatively longer distance between rhinion and midpoint between the rhinion and nasion, more anteriorly positioned incisive foramen.	43.06
	2	**Relatively shorter distance between rhinion and midpoint between the rhinion and nasion and a flatter nasal region.** More posteriorly placed rhinion, more posteriorly and inferiorly positioned nasospinale, more anteriorly positioned incisive foramen.	30.20
	3	**Relatively shorter distance between rhinion and midpoint between the rhinion and nasion.** More posteriorly and superiorly placed rhinion, more inferiorly positioned incisive foramen.	5.86

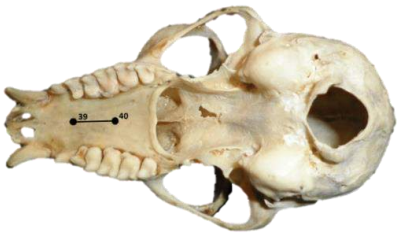

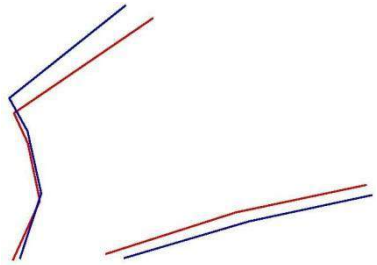

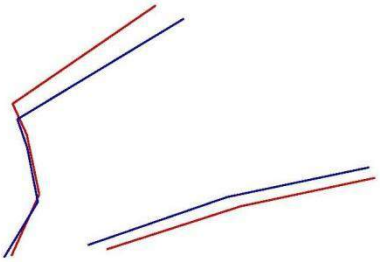

PC1 – negative shape change

PC1 – positive shape change

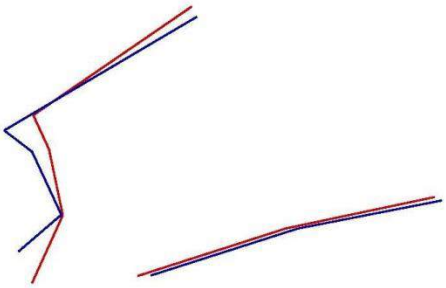

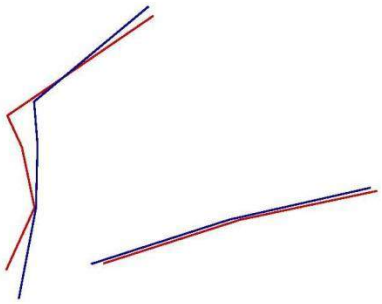

PC2 – negative shape change

PC2 – positive shape change

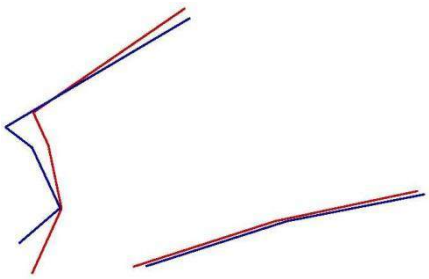

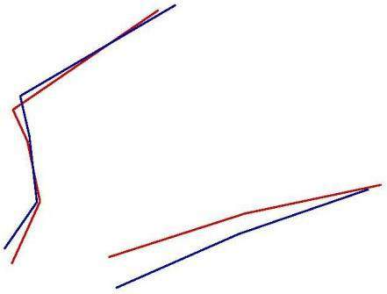

PC3 – negative shape change

PC3 – positive shape change

Figure 74: Shape change for the Goswami model face module for PCs 1-3. As with Figure 72.

Table 73: Descriptions of shape change along the PC axis from negative to positive, for PCs 1-3, for the Goswami model orbit module, based on species averages at an inter-species level; the most significant change for each PC is shown in bold. The percentage of shape variation explained by each PC is also indicated.

Module	PC	Shape change described by PC axis, from negative to positive	% of total shape variance explained by PC
Goswami orbit	1	**More inferiorly positioned anterior-most point of the frontotemporal suture.** More anteriorly placed infraorbital foramen, more anteriorly and superiorly positioned nasolacrimal foramen, relatively longer frontotemporal suture with a more inferiorly positioned anterior most point, more horizontally orientated zygomaticomaxillary suture.	41.45
	2	**More posteriorly positioned nasolacrimal foramen, more inferiorly positioned zygomaticomaxillary suture.** More posteriorly positioned infraorbital suture, more anteriorly positioned zygomatic suture, more anteriorly positioned nasion, more posteriorly positioned optical foramen.	27.26
	3	**More posteriorly positioned and vertically orientated frontotemporal suture.** More anteriorly positioned nasion, more anteriorly positioned nasolacrimal foramen, more inferiorly positioned infraorbital foramen, more posteriorly positioned zygomatic foramen, more superiorly positioned zygomaticomaxillary suture.	10.44

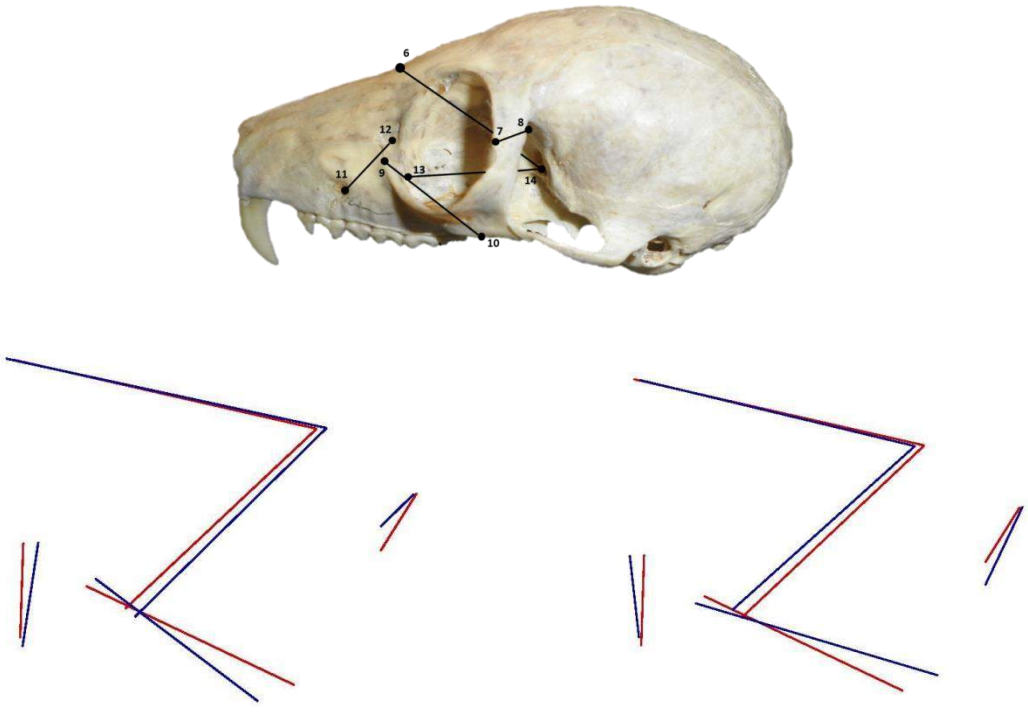

Figure 75: Shape change for the Goswami model orbit module for PCs 1-3. As with Figure 72.

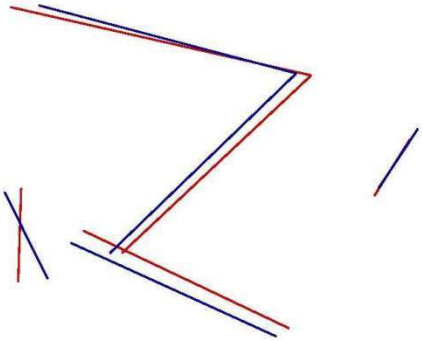

PC2 – negative shape change

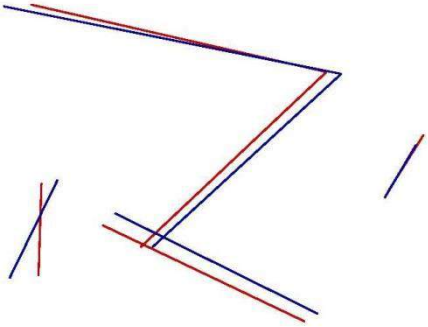

PC2 – positive shape change

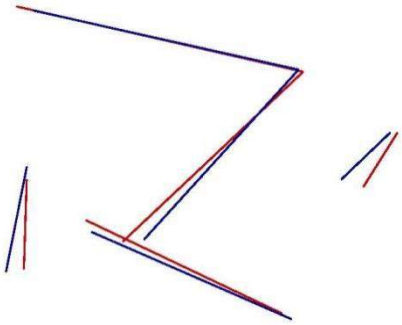

PC3 – negative shape change

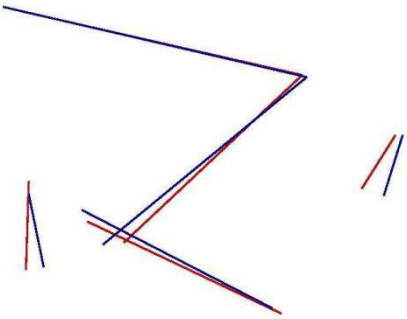

PC3 – positive shape change

Figure 75 (Cont.)

Table 74: Descriptions of shape change along the PC axis from negative to positive, for PCs 1-3, for the Goswami model oral module, based on species averages at an inter-species level; the most significant change for each PC is shown in bold. The percentage of shape variation explained by each PC is also indicated.

Module	PC	Shape change described by PC axis, from negative to positive	% shape variance explained by PC
Goswami oral	1	**More medially positioned 2nd molar septum and 3rd molar septum, more posteriorly positioned end of dentition, more anteriorly and laterally positioned greater palatine foramen.** More anteriorly positioned mesial P3 septum, more posteriorly and laterally positioned tip of posterior nasal spine.	41.51
	2	**More anteriorly positioned mesial P3 septum, more posteriorly positioned end of dentition more anteriorly and laterally positioned tip of posterior nasal spine.** More anteriorly positioned mesial P4 septum, more posteriorly positioned 3rd molar septum, more posteriorly positioned greater molar foramen.	36.21
	3	**More laterally positioned 3rd molar septum and end of dentition.** More medially positioned mesial P3 septum, more anteriorly and medially positioned greater palatine foramen, more anteriorly and medially positioned tip of posterior nasal spine.	13.69

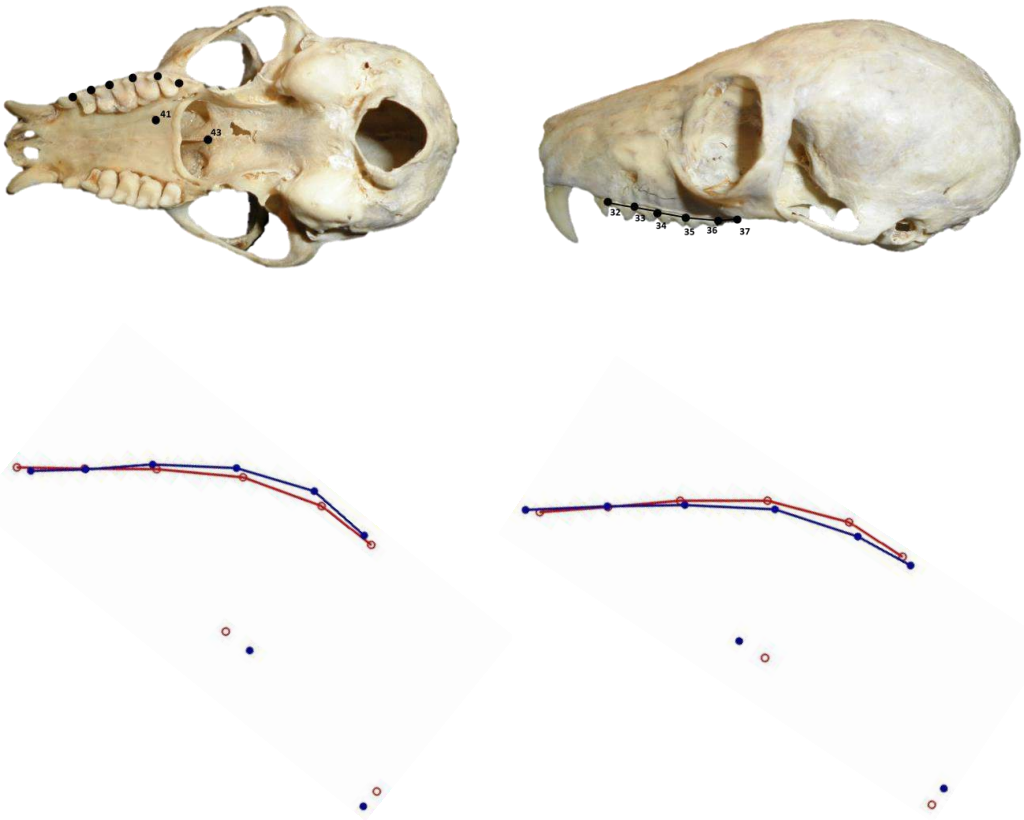

PC1 – negative shape change

PC1 – positive shape change

PC2 – negative shape change

PC2 – positive shape change

Figure 76: Shape change for the Goswami model oral module for PCs 1-3. As with Figure 72. For this module, the wireframe shows an inferior view, with individual landmarks marked so that the greater palatine foreman and tip of the nasal spine, where a large proportion of shape change is concentrated.

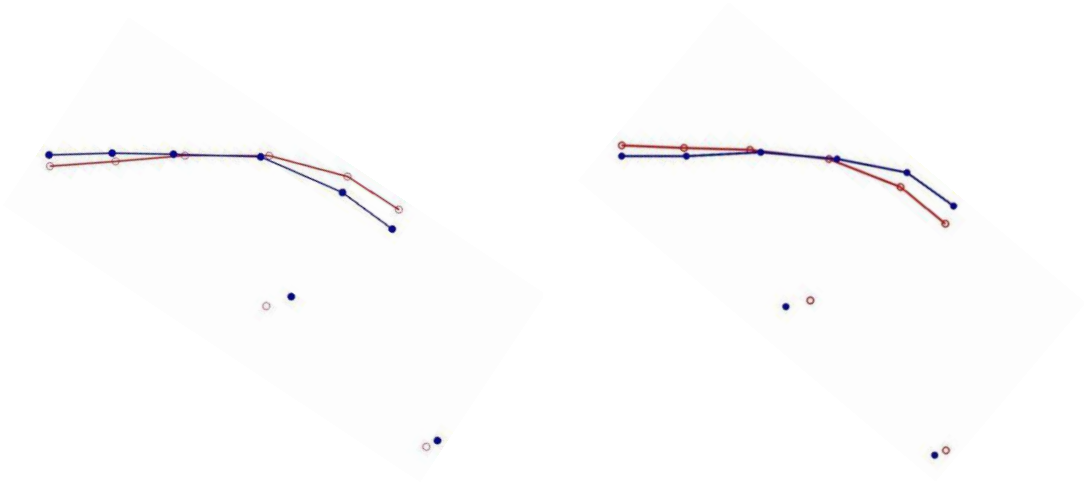

PC3 – negative shape change **PC3 – positive shape change**

Figure 76 (Cont.)

Table 75: Descriptions of shape change along the PC axis from negative to positive, for PCs 1-3, for the Goswami model zygomatic module, based on species averages at an inter-species level; the most significant change for each PC is shown in bold. The percentage of shape variation explained by each PC is also indicated.

Module	PC	Shape change described by PC axis, from negative to positive	% shape variance explained by PC
Goswami zygomatic	1	**More anteriorly positioned tip of postglenoid fossa and mandibular fossa.** Relatively shorter distance between meeting point of presphenoid-basisphenoid and basisphenoid-basioccipital in the midline, more medially positioned petrous apex, relatively shorter and more distally orientated zygomaticotemporal suture.	58.08
	2	**More anteriorly positioned foramen lavelli and petrous apex.** More anteriorly positioned presphenoid-basisphenoid and basioccipital synchondrosis in the midline, more laterally positioned tip of postglenoid fossa.	14.38
	3	**More medially positioned posterior-most point on curvature of anterior margin of zygomatic process.** Relatively longer distance between meeting point of presphenoid-basisphenoid and basioccipital synchondrosis in the midline, more laterally positioned petrous apex and foramen lavelli, more latterly orientated zygomaticotemporal suture.	8.37

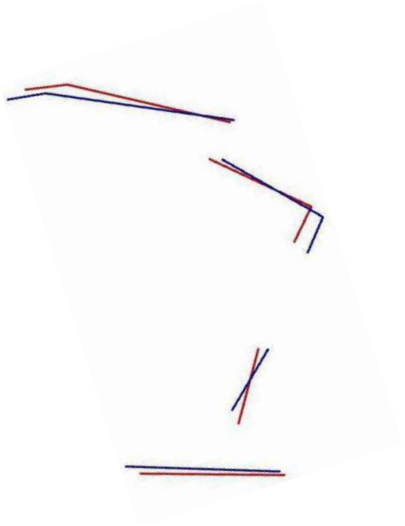

PC1 – negative shape change

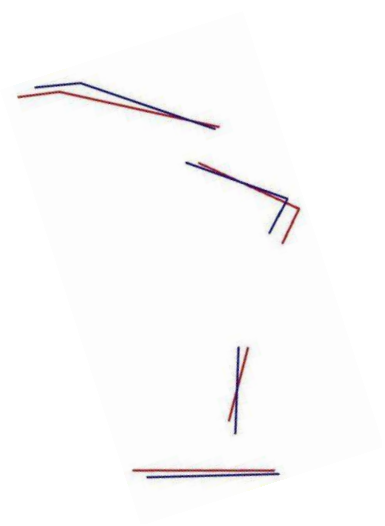

PC1 – positive shape change

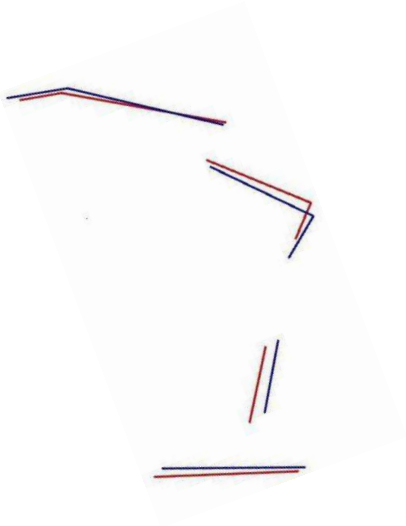

PC2 – negative shape change

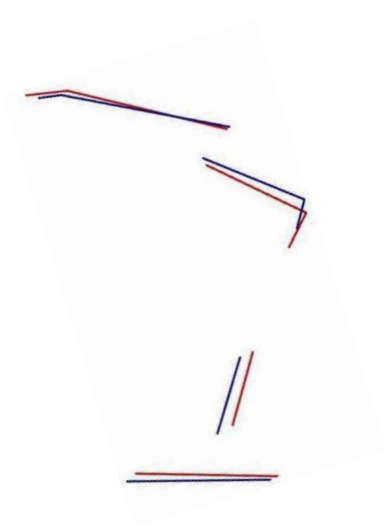

PC2 – positive shape change

Figure 771: Shape change for the Goswami model zygomatic module for PCs 1-3. As with Figure 72. For this module, the wireframe shows an inferior view.

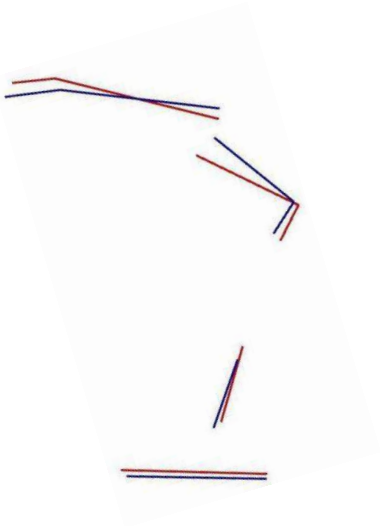

PC3 – negative shape change

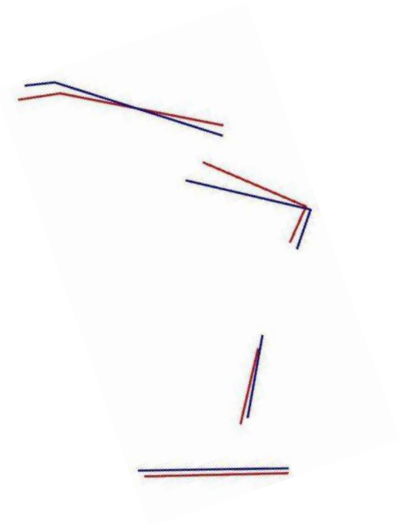

PC3 – positive shape change

Figure 77 (Cont.)

Table 76: Descriptions of shape change along the PC axis from negative to positive, for PCs 1-3, for the Goswami model vault module, based on species averages at an inter-species level; the most significant change for each PC is shown in bold. The percentage of shape variation explained by each PC is also indicated.

Module	PC	Shape change described by PC axis, from negative to positive	% shape variance explained by PC
Goswami vault	1	**Relatively shorter distance between lambda and inion, more anteriorly and superiorly positioned asterion**. More anteriorly placed bregma, more superiorly positioned meeting point of sphenoid, zygomatic and parietal bone, more superiorly positioned meeting point of zygomatic, frontal and parietal bones.	47.86
	2	**More medially and posteriorly positioned meeting of the superior temporal crest and the coronal suture.** More inferiorly and anteriorly positioned midpoint between nasion and bregma,, more anteriorly positioned meeting point of zygomatic, frontal and parietal bones.	19.73
	3	**More inferiorly positioned lambda and inion, more superiorly positioned asterion.** More superiorly positioned bregma, more posteriorly positioned meeting point of crest and suture on the frontal bone, more posteriorly and inferiorly positioned meeting point of sphenoid, zygomatic and parietal bone, more inferiorly positioned meeting point of zygomatic, frontal and parietal bones.	11.07

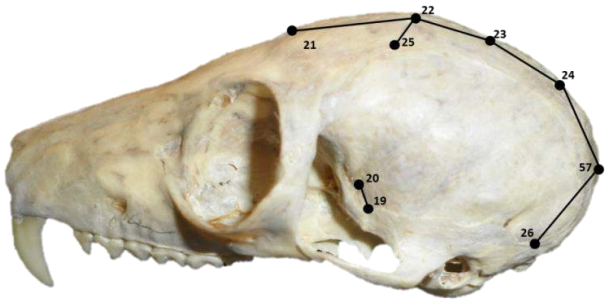

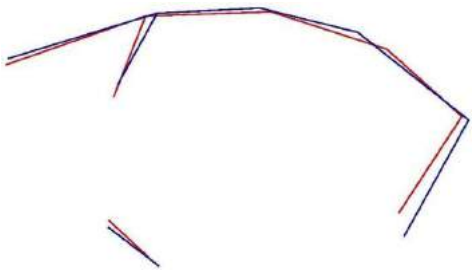

PC1 – negative shape change

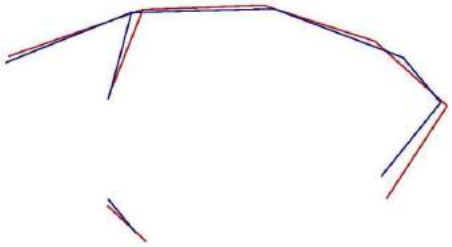

PC1 – positive shape change

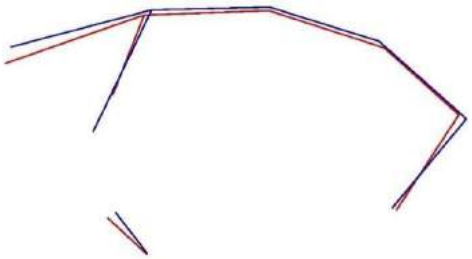

PC2– negative shape change

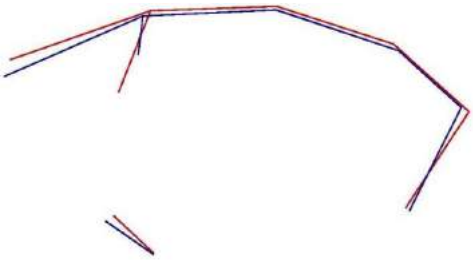

PC2 – positive shape change

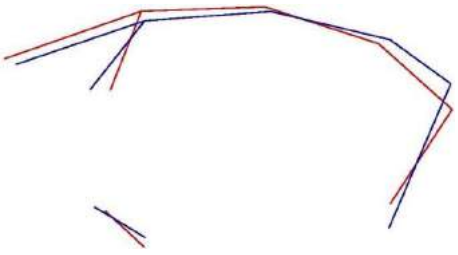

PC3 – negative shape change

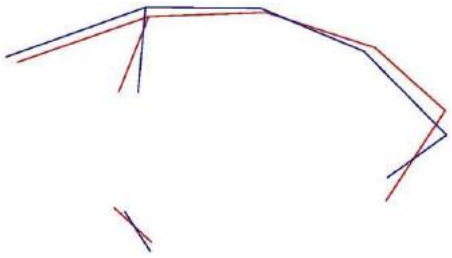

PC3 – positive shape change

Figure 78: Shape change for the Goswami model vault module for PCs 1-3. As with Figure 72.

Table 77: Descriptions of shape change along the PC axis from negative to positive, for PCs 1-3, for the Goswami model base module, based on species averages at an inter-species level; the most significant change for each PC is shown in bold. The percentage of shape variation explained by each PC is also indicated.

Module	PC	Shape change described by PC axis, from negative to positive	% shape variance explained by PC
Goswami base	1	**More posteriorly and medially positioned posterior-most point of occipital condyle.** Relatively shorter distance between basion and opisthion, more medially positioned hypoglossal canal.	48.16
	2	**Relatively longer distance between basion and opisthion, relatively larger external auditory meatus.** More anteriorly positioned basion, more posteriorly positioned opisthion, more anteriorly positioned anterior-most point of the occipital condyle, more laterally and posteriorly positioned posterior-most point of the occipital condyle.	19.52
	3	**More medially positioned hypoglossal canal, more laterally positioned external auditory meatus.** Relatively shorter distance between midline of foramen magnum (basion to opisthion), and the anterior-most point of the occipital canal, possibly indicating a narrowing of the foramen magnum.	12.28

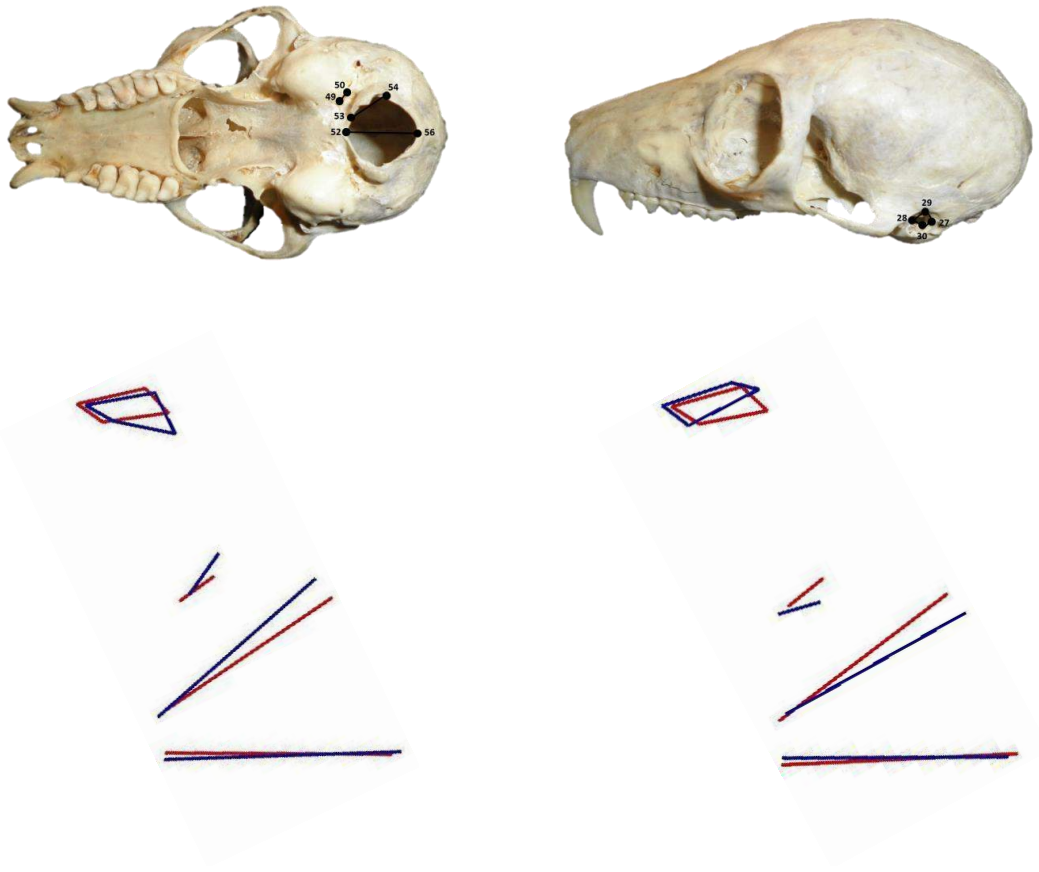

PC1 – negative shape change **PC1 – positive shape change**

Figure 79: Shape change for the Goswami model base module for PCs 1-3. As with Figure 72. For this module, the wireframe shows an inferior view.

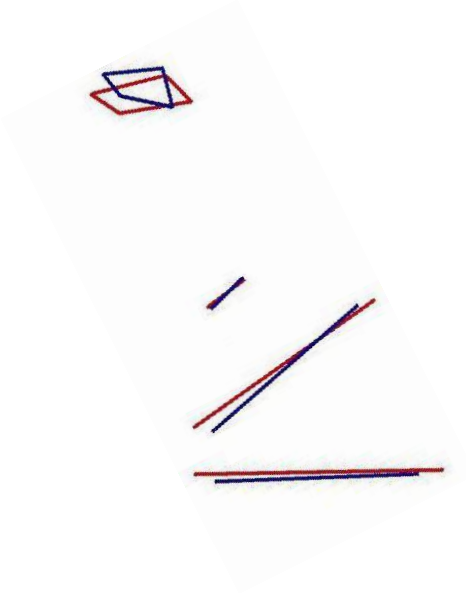

PC2 – negative shape change

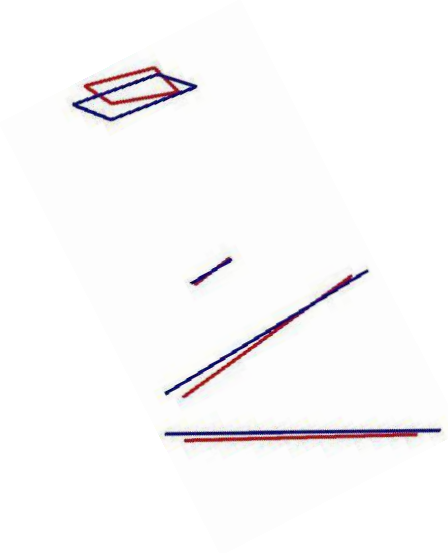

PC2 – positive shape change

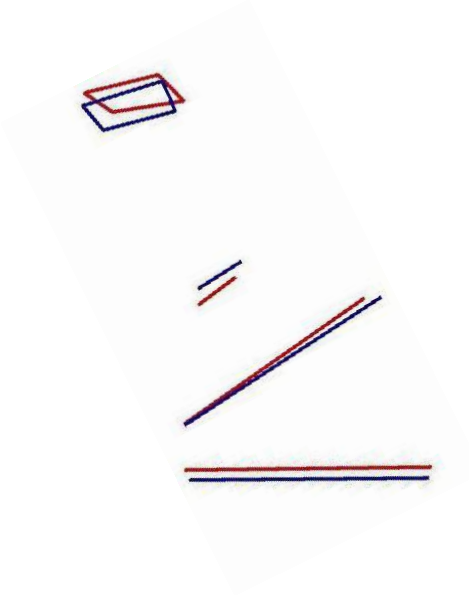

PC3 – negative shape change

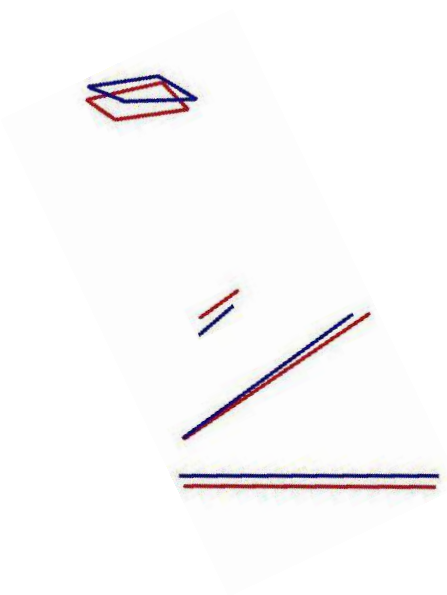

PC3 – positive shape change

Figure 79 (Cont.)

6.4.2. Evolutionary models and phylogenetic signal

A number of different evolutionary models were examined to determine how well they each described the data. Results, including the model parameters, log likelihood scores and AICc scores, for PCs 1-3 for the whole cranium and each cranial module outlined by the 2* and Goswami modularity hypotheses are recorded below (Tables 78-86). Results are not shown for the OU model of evolution as, for the majority of the modules, it was not possible to identify the optimum trait values; this occurs when α equals or is close to 0 (i.e., BM). As a result, the likelihood profile becomes flat and the reliability of the parameters cannot be estimated (Butler *et al.*, 2004).

The IE model was found overwhelmingly to be the best fit for all of the different cranial modules. The only exceptions were PC1 for the whole cranium, for which Pagel's λ was found to be the best fit and PC2 for the Goswami face module, for which the BM model was found to be the best fit. Model parameter scores also indicate that a great proportion of shape change has occurred in line with a BM model of evolution.

Table 78: The fit of evolutionary models, for PCs 1-3 for the whole cranium, showing the model parameter, log likelihood, AICc score and the ΔAICc score for each of the models tested. The model found to best describe the data is underlined.

PC	Model	Model parameter	Log likelihood	AICc	ΔAICc
PC1	BM	-	137.94	-273.73	2.50
	lambda	0.989	140.37	-276.23	0.00
	delta	1.665	139.56	-274.61	1.62
	kappa	0.825	137.38	-270.26	5.97
	EB	0.000	138.37	-272.24	4.00
	IE	-	131.74	-258.98	17.25
PC2	BM	-	152.11	-302.06	205.21
	lambda	1.000	150.52	-296.54	210.72
	delta	1.219	151.47	-298.44	208.83
	kappa	1.000	151.21	-297.91	209.35
	EB	-0.016	149.69	-294.89	212.38
	IE	-	255.88	-507.27	0.00
PC3	BM	-	163.07	-323.98	102.38
	lambda	0.988	166.03	-327.55	98.80
	delta	1.070	164.10	-323.69	102.67
	kappa	0.426	166.26	-328.02	98.34
	EB	-0.007	163.49	-322.47	103.89
	IE	-	215.43	-426.36	0.00

Table 79: The fit of evolutionary models, for PCs 1-3 for the 2* model face module, showing the model parameter, log likelihood, AICc score and the ΔAICc score for each of the models tested. The model found to best describe the data is underlined.

PC	Model	Model parameter	Log likelihood	AICc	ΔAICc
PC1	BM	-	138.41	-274.65	102.74
	lambda	0.999	139.56	-274.61	102.78
	delta	0.674	138.38	-272.26	105.13
	kappa	0.964	139.43	-274.35	103.04
	EB	-0.031	140.08	-275.67	101.72
	IE	-	190.94	-377.39	0.00
PC2	BM	-	127.29	-252.43	189.55
	lambda	1.000	127.28	-250.06	191.92
	delta	1.432	127.63	-250.76	191.22
	kappa	1.000	126.97	-249.44	192.53
	EB	0.000	127.09	-249.69	192.29
	IE	-	223.24	-441.98	0.00
PC3	BM	-	158.07	-313.97	194.38
	lambda	1.000	156.70	-308.91	199.44
	delta	0.805	157.19	-309.88	198.47
	kappa	0.838	156.01	-307.52	200.83
	EB	-0.034	157.78	-311.06	197.29
	IE	-	256.42	-508.35	0.00

Table 80: The fit of evolutionary models, for PCs 1-3 for the 2* vault model module, showing the model parameter, log likelihood, AICc score and the ΔAICc score for each of the models tested. The model found to best describe the data is underlined.

PC	Model	Model parameter	Log likelihood	AICc	ΔAICc
PC1	BM	-	136.06	-269.95	177.31
	lambda	0.997	136.52	-268.54	178.73
	delta	1.057	136.25	-268.01	179.26
	kappa	1.000	136.79	-269.08	178.18
	EB	0.000	136.74	-268.99	178.28
	IE	-	225.88	-447.26	0.00
PC2	BM	-	142.88	-283.61	217.35
	lambda	0.973	151.20	-297.90	203.06
	delta	1.457	143.64	-282.79	218.17
	kappa	0.462	146.06	-287.62	213.34
	EB	0.000	142.99	-281.47	219.49
	IE	-	252.73	-500.96	0.00
PC3	BM	-	149.25	-296.34	170.40
	lambda	0.966	152.39	-300.28	166.46
	delta	2.388	150.98	-297.46	169.28
	kappa	0.399	150.47	-296.44	170.29
	EB	0.000	148.78	-293.06	173.67
	IE	-	235.62	-466.74	0.00

Table 81: The fit of evolutionary models, for PCs 1-3 for the Goswami model face module, showing the model parameter, log likelihood, AICc score and the ΔAICc score for each of the models tested. The model found to best describe the data is underlined.

PC	Model	Model parameter	Log likelihood	AICc	ΔAICc
PC1	BM	-	122.32	-242.47	122.75
	lambda	1.000	121.09	-237.67	127.55
	delta	0.952	121.72	-238.95	126.27
	kappa	1.000	124.23	-243.96	121.26
	EB	-0.029	123.55	-242.60	122.62
	IE	-	184.86	-365.22	0.00
PC2	BM	-	136.85	-271.54	0.00
	lambda	1.000	136.39	-268.27	3.26
	delta	0.735	136.04	-267.58	3.95
	kappa	1.000	136.67	-268.85	2.69
	EB	-0.027	136.99	-269.49	2.05
	IE	-	120.09	-235.68	35.86
PC3	BM	-	165.44	-328.72	179.13
	lambda	0.981	168.18	-331.86	175.99
	delta	2.080	166.76	-329.02	178.83
	kappa	0.646	163.87	-323.24	184.61
	EB	0.000	164.95	-325.40	182.45
	IE	-	256.17	-507.85	0.00

Table 82: The fit of evolutionary models, for PCs 1-3 for the Goswami model orbit module, showing the model parameter, log likelihood, AICc score and the ΔAICc score for each of the models tested. The model found to best describe the data is underlined.

PC	Model	Model parameter	Log likelihood	AICc	ΔAICc
PC1	BM	-	133.35	-264.54	205.31
	lambda	0.992	134.34	-264.17	205.68
	delta	0.723	133.09	-261.67	208.18
	kappa	0.903	133.00	-261.51	208.34
	EB	-0.016	133.43	-262.37	207.48
	IE	-	237.17	-469.85	0.00
PC2	BM	-	120.97	-239.79	174.61
	lambda	0.993	120.45	-236.40	177.99
	delta	1.330	121.49	-238.47	175.93
	kappa	0.798	119.83	-235.16	179.24
	EB	-0.004	120.14	-235.78	178.62
	IE	-	209.45	-414.40	0.00
PC3	BM	-	132.05	-261.95	174.07
	lambda	0.978	136.09	-267.68	168.34
	delta	3.000	135.84	-267.17	168.84
	kappa	0.383	133.63	-262.75	173.26
	EB	0.000	131.08	-257.65	178.36
	IE	-	220.26	-436.01	0.00

Table 83: The fit of evolutionary models, for PCs 1-3 for the Goswami model oral module, showing the model parameter, log likelihood, AICc score and the ΔAICc score for each of the models tested. The model found to best describe the data is underlined.

PC	Model	Model parameter	Log likelihood	AICc	ΔAICc
PC1	BM	-	118.75	-235.35	153.52
	lambda	0.982	123.60	-242.71	146.16
	delta	2.246	120.47	-236.44	152.43
	kappa	0.661	119.69	-234.89	153.98
	EB	0.000	119.14	-233.78	155.09
	IE	-	196.68	-388.87	0.00
PC2	BM	-	103.70	-205.24	214.62
	lambda	0.951	112.49	-220.48	199.39
	delta	3.000	111.32	-218.14	201.72
	kappa	0.241	110.31	-216.12	203.74
	EB	0.000	104.97	-205.45	214.42
	IE	-	212.18	-419.86	0.00
PC3	BM	-	135.46	-268.77	129.03
	lambda	0.991	135.78	-267.06	130.74
	delta	3.000	141.28	-278.07	119.73
	kappa	0.769	135.19	-265.88	131.91
	EB	0.000	134.39	-264.27	133.52
	IE	-	201.15	-397.80	0.00

Table 84: The fit of evolutionary models, for PCs 1-3 for the Goswami model zygomatic module, showing the model parameter, log likelihood, AICc score and the ΔAICc score for each of the models tested. The model found to best describe the data is underlined.

PC	Model	Model parameter	Log likelihood	AICc	ΔAICc
PC1	BM	-	118.66	-235.16	165.90
	lambda	1.000	118.42	-232.33	168.73
	delta	0.943	119.35	-234.20	166.86
	kappa	1.000	119.05	-233.61	167.45
	EB	-0.008	117.89	-231.28	169.78
	IE	-	202.78	-401.06	0.00
PC2	BM	-	136.12	-270.09	160.52
	lambda	1.000	135.56	-266.63	163.98
	delta	1.854	135.94	-267.39	163.22
	kappa	0.989	135.21	-265.92	164.68
	EB	0.000	135.64	-266.79	163.82
	IE	-	217.55	-430.61	0.00
PC3	BM	-	164.95	-327.74	240.04
	lambda	0.996	165.87	-327.24	240.55
	delta	0.647	166.95	-329.41	238.37
	kappa	0.836	164.19	-323.89	243.89
	EB	-0.023	165.26	-326.03	241.76
	IE	-	286.14	-567.78	0.00

Table 85: The fit of evolutionary models, for PCs 1-3 for the Goswami model vault module, showing the model parameter, log likelihood, AICc score and the ΔAICc score for each of the models tested. The model found to best describe the data is underlined.

PC	Model	Model parameter	Log likelihood	AICc	ΔAICc
PC1	BM	-	121.12	-240.09	189.19
	lambda	0.982	124.18	-243.85	185.42
	delta	2.062	124.10	-243.69	185.58
	kappa	0.808	120.93	-237.36	191.91
	EB	0.000	121.75	-238.99	190.28
	IE	-	216.89	-429.27	0.00
PC2	BM	-	122.90	-243.64	190.91
	lambda	0.864	129.85	-255.21	179.34
	delta	3.000	129.17	-253.85	180.70
	kappa	0.557	123.32	-242.14	192.41
	EB	0.000	121.27	-238.04	196.51
	IE	-	219.53	-434.55	0.00
PC3	BM	-	137.82	-273.48	231.29
	lambda	0.938	151.72	-298.94	205.83
	delta	3.000	146.86	-289.22	215.55
	kappa	0.175	149.94	-295.38	209.39
	EB	0.000	138.04	-271.58	233.19
	IE	-	254.64	-504.77	0.00

Table 86: The fit of evolutionary models, for PCs 1-3 for the Goswami model base module, showing the model parameter, log likelihood, AICc score and the ΔAICc score for each of the models tested. The model found to best describe the data is underlined.

PC	Model	Model parameter	Log likelihood	AICc	ΔAICc
PC1	BM	-	142.58	-283.01	139.58
	lambda	0.992	143.15	-281.79	140.79
	delta	0.284	146.87	-289.24	133.35
	kappa	0.843	142.83	-281.15	141.44
	EB	-0.038	146.43	-288.35	134.24
	IE	-	213.54	-422.59	0.00
PC2	BM	-	132.21	-262.26	224.92
	lambda	0.951	144.53	-284.55	202.63
	delta	3.000	137.43	-270.37	216.81
	kappa	0.461	138.14	-271.78	215.40
	EB	0.000	131.79	-259.09	228.09
	IE	-	245.84	-487.18	0.00
PC3	BM	-	133.64	-265.13	179.29
	lambda	0.997	135.25	-266.00	178.41
	delta	3.000	139.08	-273.65	170.76
	kappa	0.882	134.00	-263.51	180.91
	EB	0.000	134.94	-265.38	179.04
	IE	-	224.46	-444.42	0.00

Blomberg's *K* was calculated for PCs 1-3 for the whole cranium and all cranial modules (Table 87). PC1 had the highest *K* value for all modules, with the exception of the Goswami face module, and all had a score greater than 1, with the exception of the Goswami oral module. This indicates that closely related species were even more similar to each other than would be expected under a BM model of evolution. Scores for PCs 2 and 3 were more variable across modules. All PCs (1-3) for all modules contained a significant phylogenetic signal, as determined by randomisation tests.

Table 87: Blomberg's *K* and significance results for PCs 1-3 for all cranial modules.

Model	Module	PC	*K*	p value
Whole cranium		1	1.14	0.0001
		2	1.10	0.0001
		3	1.09	0.0001
2*	face	1	1.83	0.0001
		2	0.99	0.0001
		3	1.24	0.0001
	vault	1	1.35	0.0001
		2	0.98	0.0001
		3	0.77	0.0001
Goswami	face	1	1.07	0.0001
		2	1.28	0.0001
		3	0.66	0.0001
	orbit	1	2.35	0.0001
		2	1.05	0.0001
		3	0.60	0.0001
	oral	1	0.81	0.0001
		2	0.41	0.0010
		3	0.50	0.0002
	zygomatic	1	1.58	0.0001
		2	0.75	0.0001
		3	1.41	0.0001
	vault	1	1.02	0.0001
		2	0.42	0.0010
		3	0.46	0.0004
	base	1	2.64	0.0001
		2	0.68	0.0001
		3	0.49	0.0004

6.4.3. Evo-maps

Plots of trait values, for PCs 1-3, for the whole cranium and all cranial modules from the 2* and Goswami modularity hypotheses are shown below (Figures 80-88). Plots use the composite phylogenetic tree for the study species taken from the 10K trees website (Arnold *et al.*, 2010) and ancestral node values are estimated according to the IE model of evolution (Smaers & Vinicius, 2009), as this was the model that best described the data. Standard phylogenies show trait change across the tree with colour graduation changing from red to blue as traits change from low to high values.

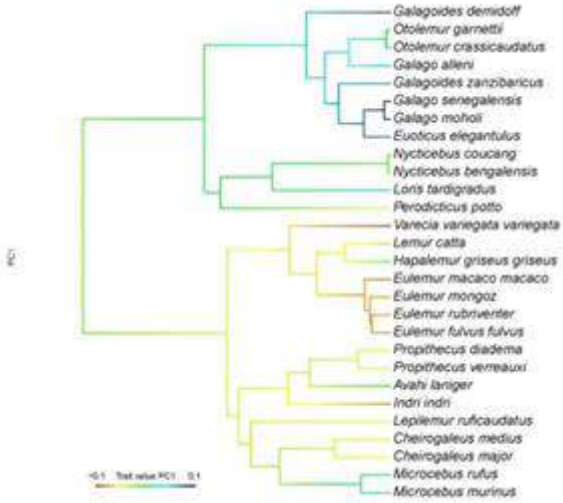

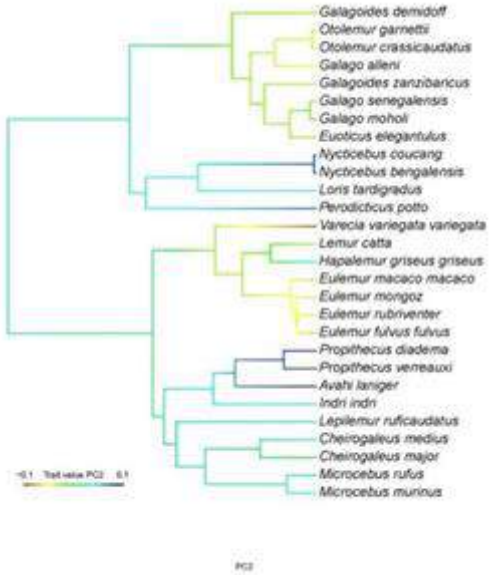

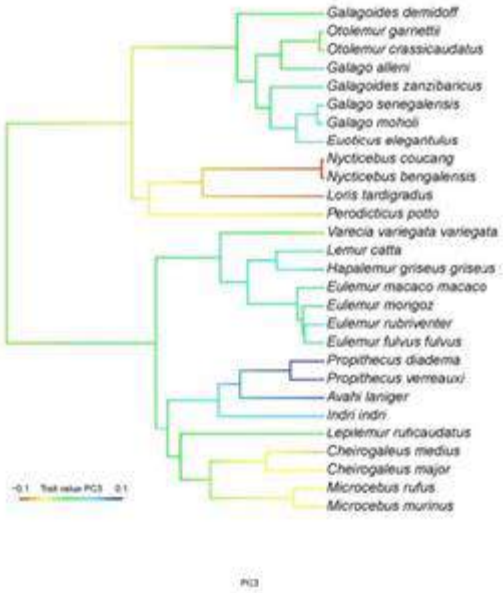

Figure 80: Ancestral character estimations for PC1, PC2, and PC3, for the whole cranium, with ancestral node values calculated following the IE method. In standard phylogenies, red indicates low PC values and blue high PC values, and the amount of colour change along a branch is indicative of the rate of change for that branch.

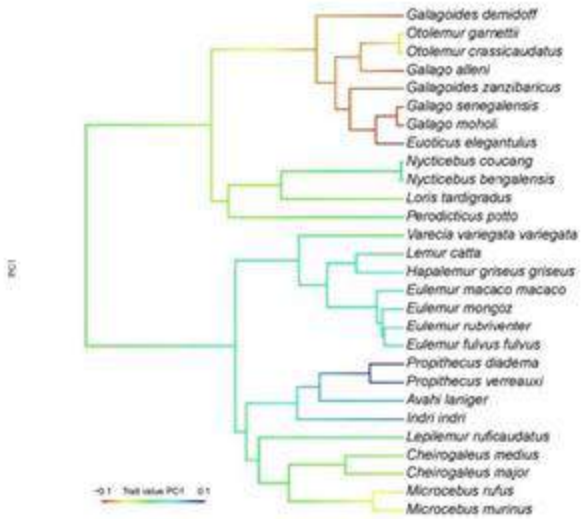

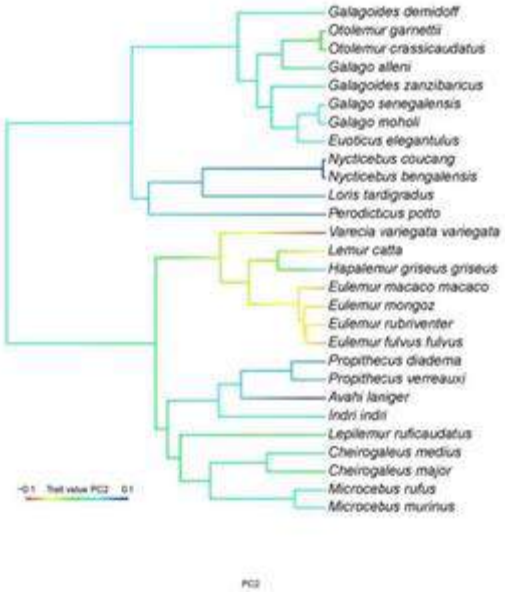

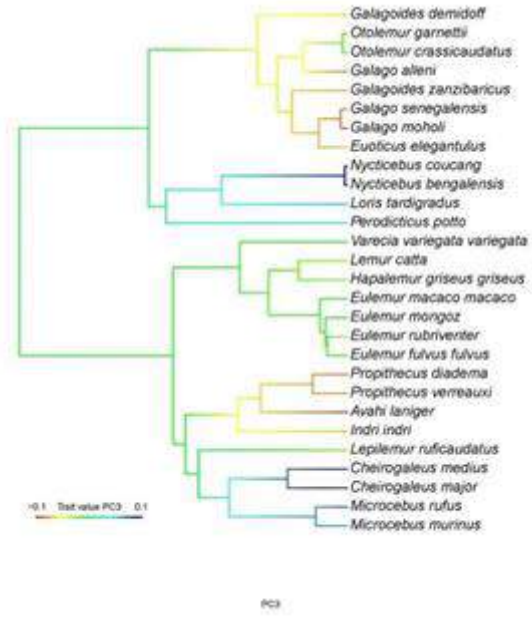

Figure 81: Ancestral character estimations for PC1, PC2, and PC3, for 2* model face module. As with Figure 80.

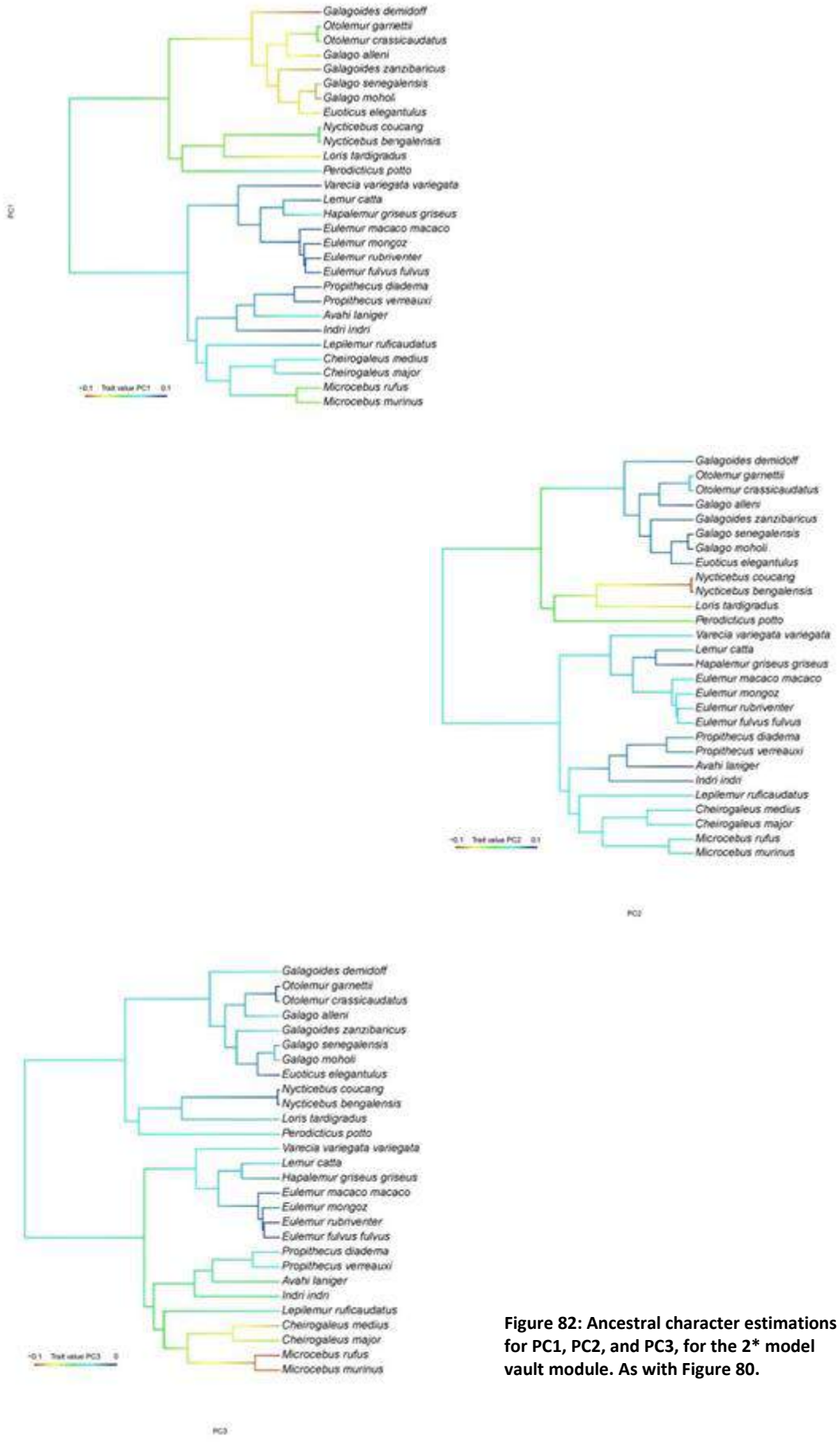

Figure 82: Ancestral character estimations for PC1, PC2, and PC3, for the 2* model vault module. As with Figure 80.

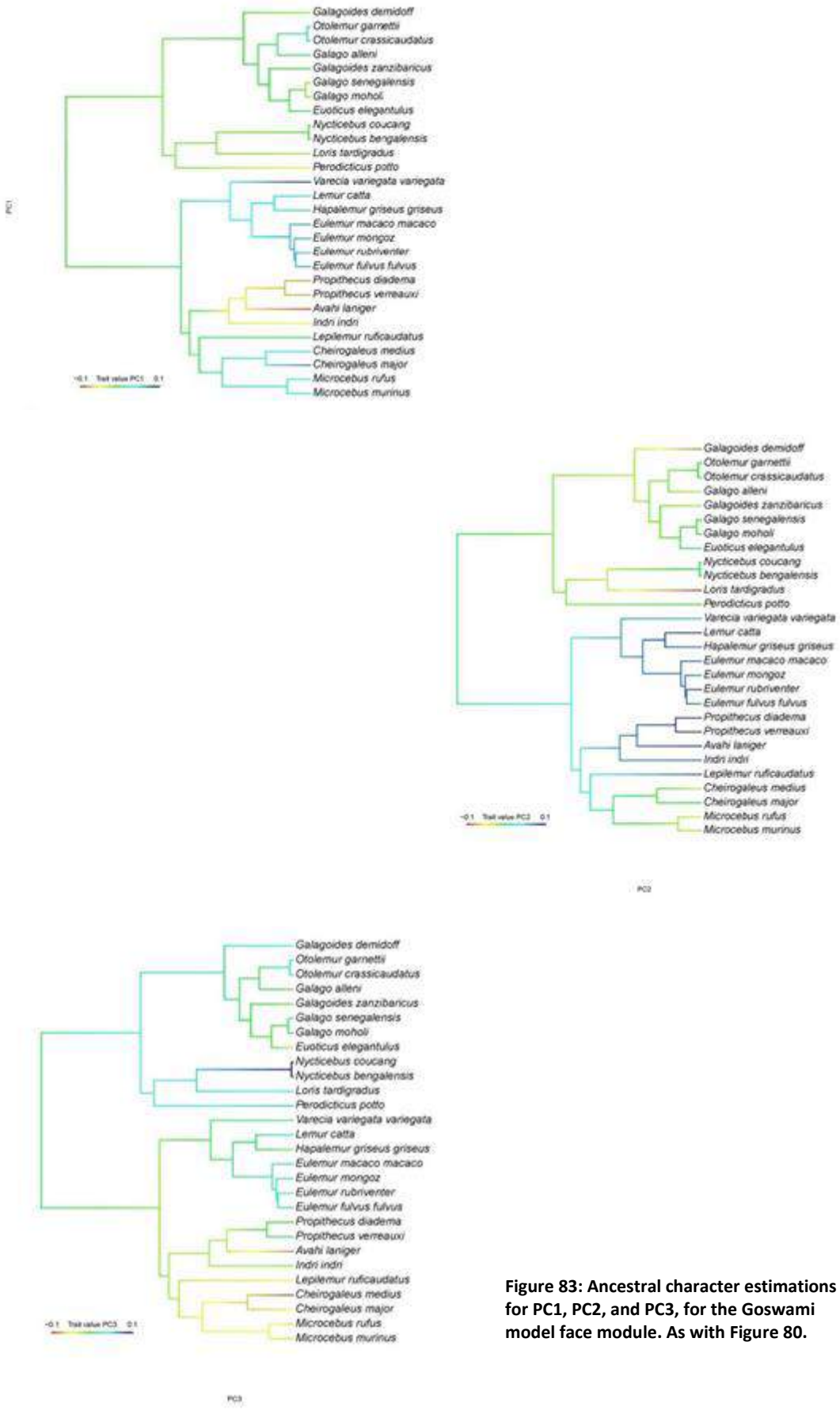

Figure 83: Ancestral character estimations for PC1, PC2, and PC3, for the Goswami model face module. As with Figure 80.

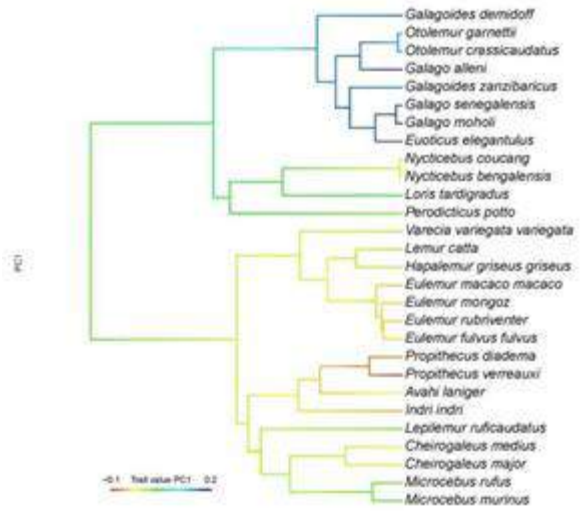

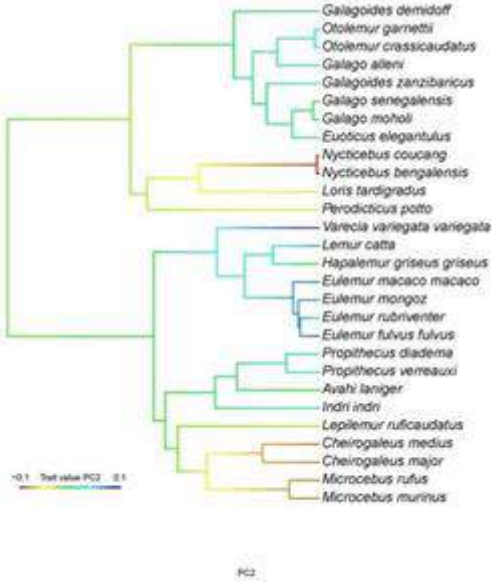

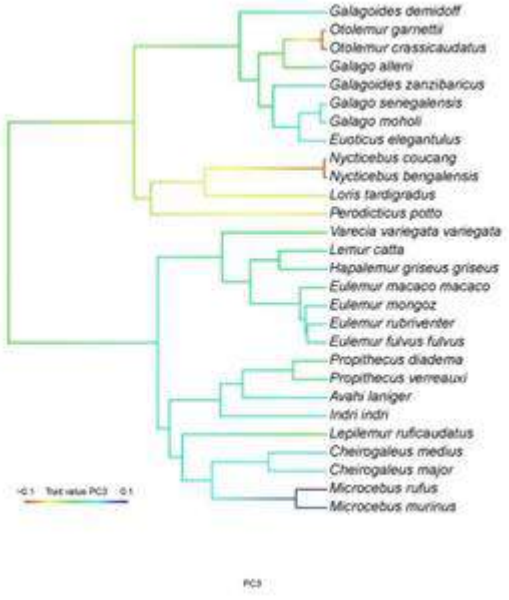

Figure 84: Ancestral character estimations for PC1, PC2, and PC3, for the Goswami model orbit module. As with Figure 80.

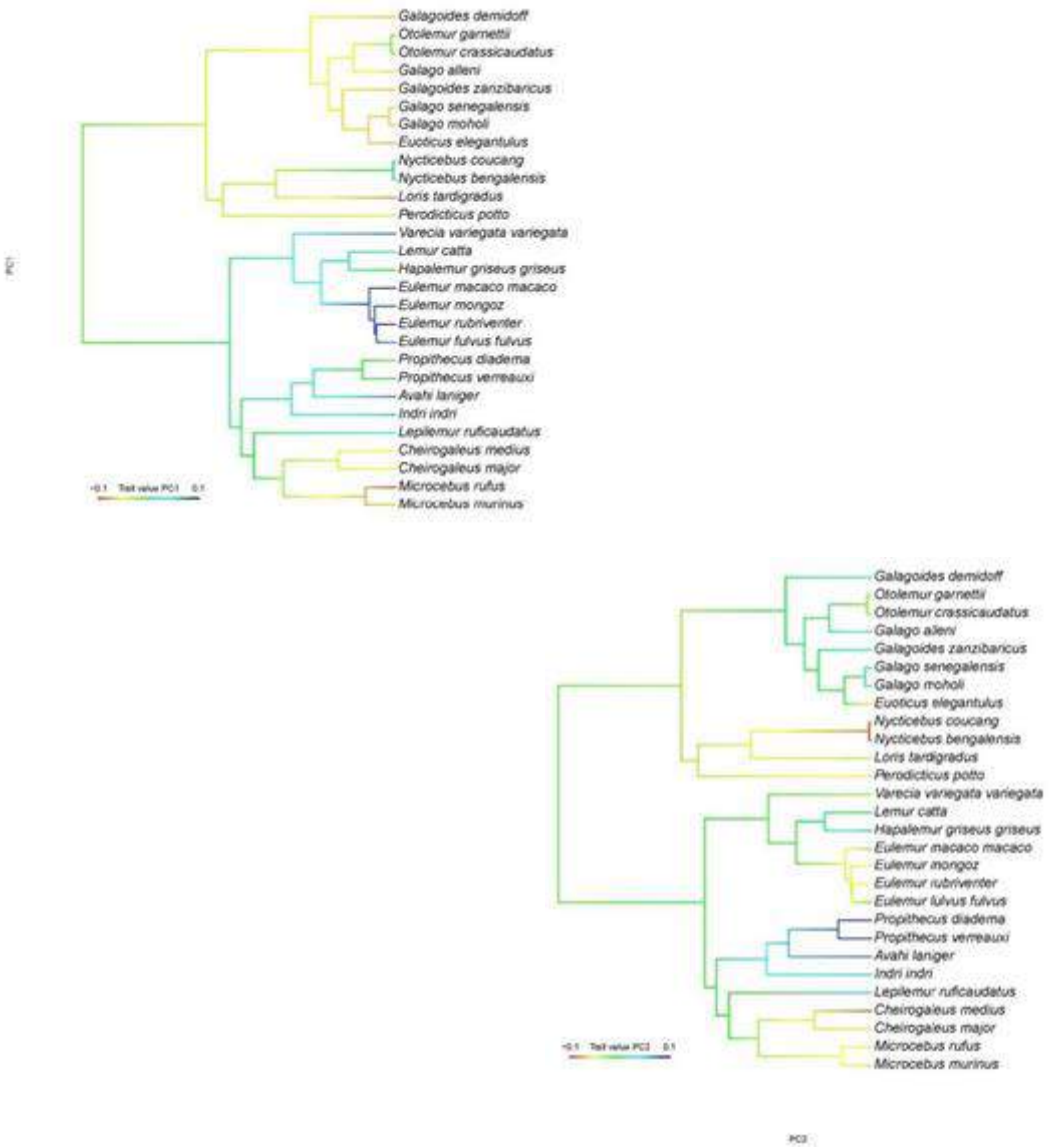

Figure 85: Ancestral character estimations for PC1, PC2, and PC3, for the Goswami model oral module. As with Figure 80.

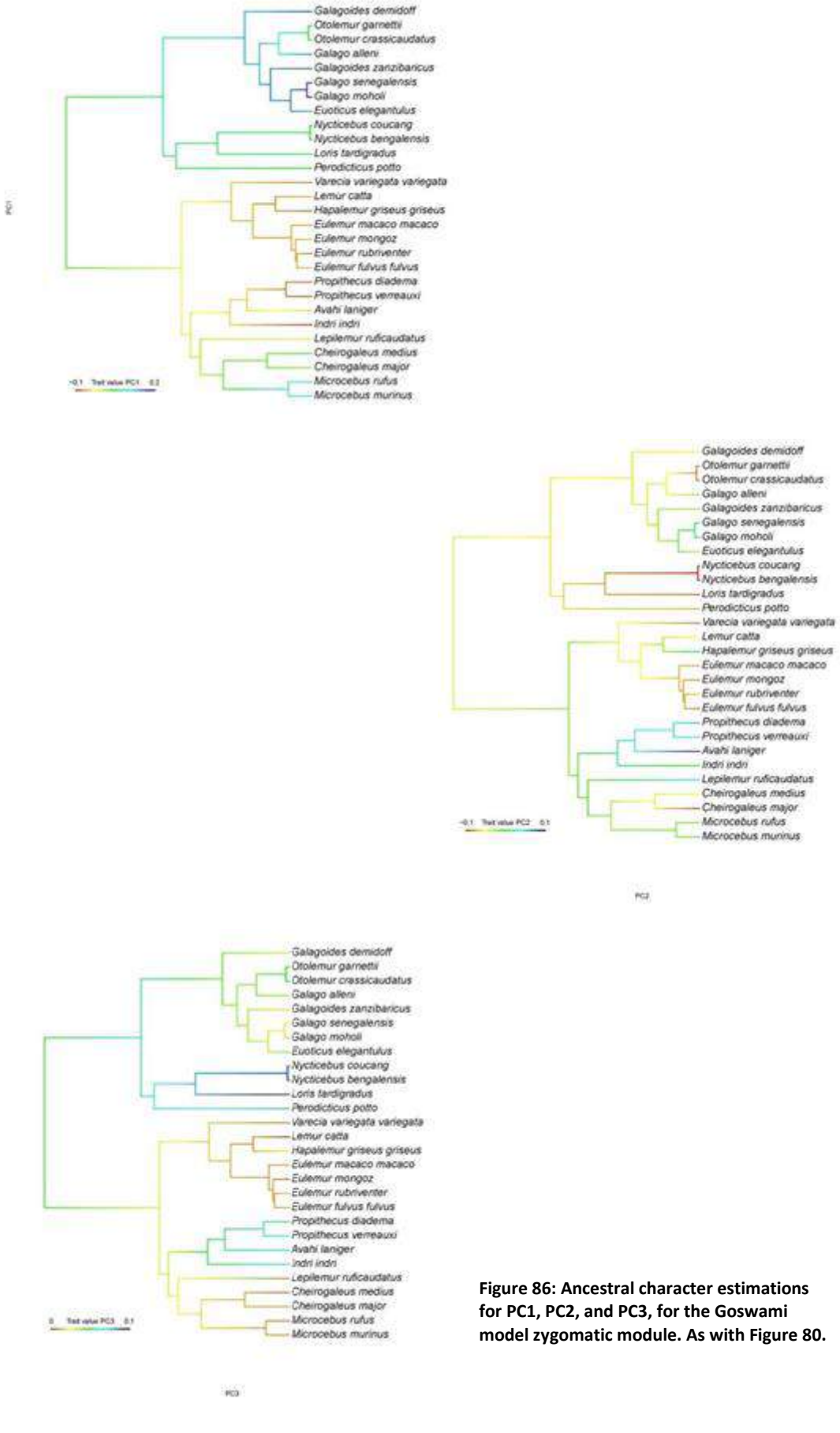

Figure 86: Ancestral character estimations for PC1, PC2, and PC3, for the Goswami model zygomatic module. As with Figure 80.

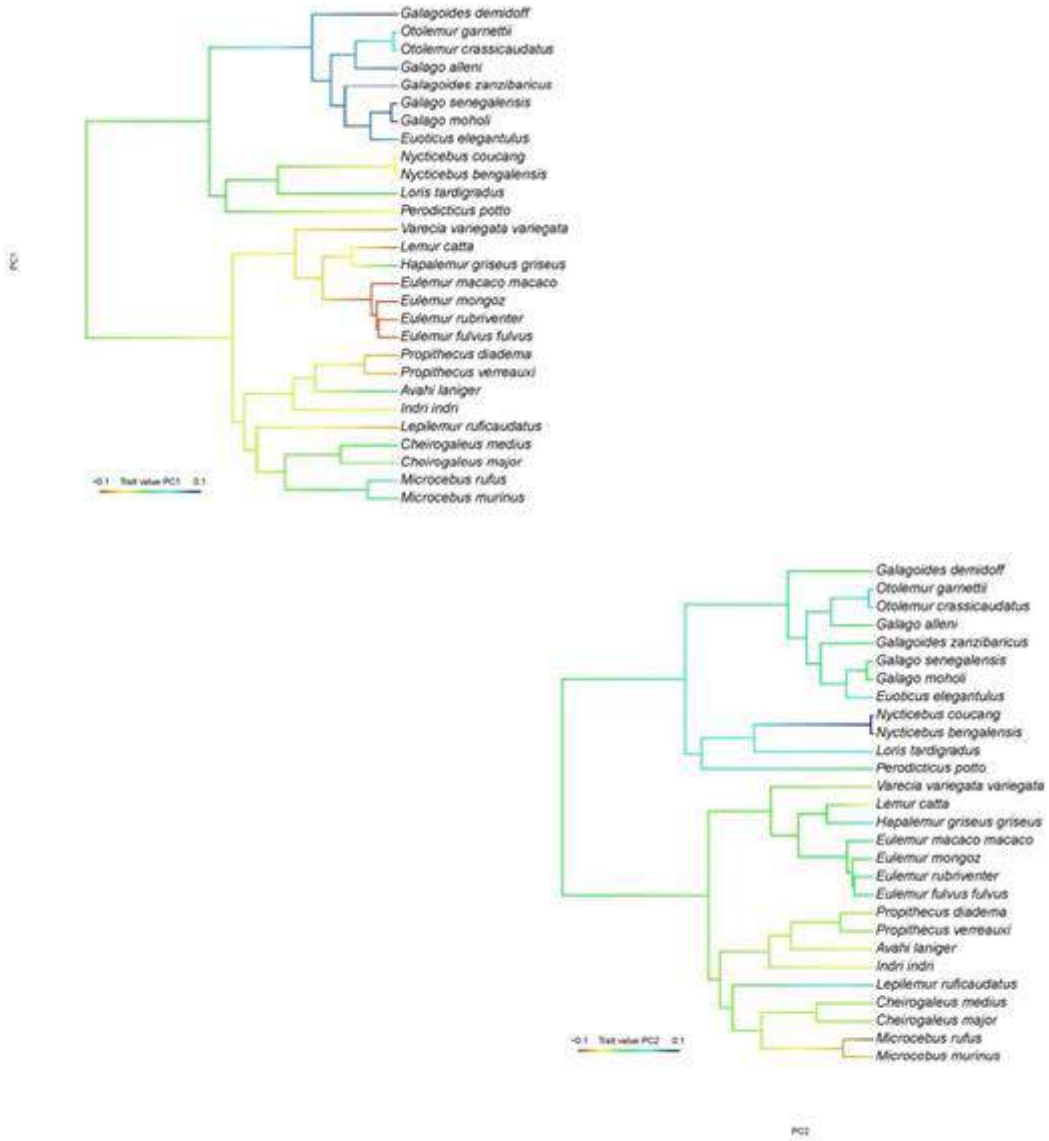

Figure 87: Ancestral character estimations for PC1, PC2, and PC3, for the Goswami model vault module. As with Figure 80.

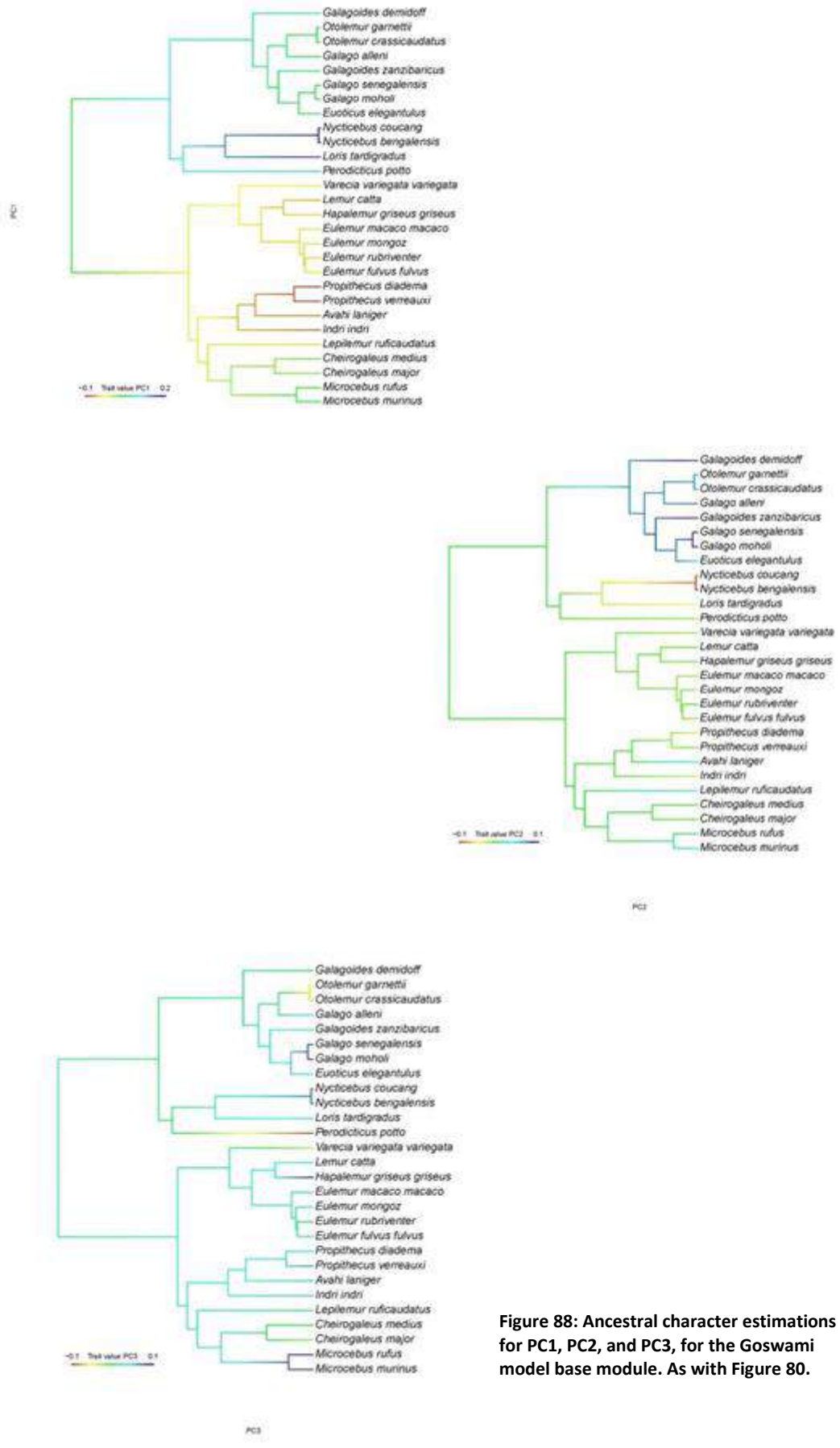

Figure 88: Ancestral character estimations for PC1, PC2, and PC3, for the Goswami model base module. As with Figure 80.

6.5. Discussion

6.5.1. Models of evolution

The IE model of evolution (Smaers & Vinicius, 2009) provided the best description of evolutionary morphological change within strepsirhines. It was the most strongly supported model for all cranial modules and for all PCs tested, with the exception of PC1 for the whole cranium and PC2 for the Goswami face module (Table 78-86). The success of the IE model is most likely because of its flexibility; it can collapse into both an OU and BM model where it is appropriate for the data, but also allows for a different rate of change and different optima on each branch (Smaers & Vinicius, 2009).

Unlike the vast majority of modules, evolutionary shape change for PC1 for the whole cranium was best described by Pagel's λ and not the IE model, which was actually the most weakly supported model in this instance. The EB model parameter for this PC was 0, indicating that it was equal to BM, in line with low support for the EB model, delta was greater than one, indicating that later evolution occurred at a faster rate than early evolution. This is again supported by a kappa of 0.83, which suggests a model closer to a BM than to punctuated evolution following speciation (Table 78). These findings, however, go against the principal of the IE model, which should collapse into the BM model of evolution, where appropriate; as such, the IE and BM models would be expected to be equally well supported. Improvements to the IE model may therefore be needed. However, the ΔAICc score for the IE model for PC1 for the whole cranium is only 17.25, which is remarkably small; when the IE model is the most strongly supported, ΔAICc scores for the other models are repeatedly found to be 100-200 (Tables 78-86). The ΔAICc is representative of the amount of information lost should another model be used rather than the best fitting model (Burnham & Anderson, 2004); as such, should the IE model be used rather than the BM model for PC1 for the whole cranium, very little information relating to trait evolution would be lost. As would be expected, the ΔAICc scores for the other evolutionary models, which all follow a BM model of trait change, are also very low, ranging from 1.62-5.97 (Table 78).

The only other occasion where the IE model was not found to be the best fit for the data was for PC2 for the Goswami face module. The shape change represented by PC2 for the face module describes a move to an anterior/posteriorly flatter nasal region. Here, instead, BM was the best fit model, and IE was again found to be the worst. Both λ and kappa are

also at their boundaries of 1, while the delta and EB models both have parameter values close to 0 (Table 81), all of which supports a BM model of trait change. As with PC1 for the whole cranium, the ΔAICc scores for the remaining models are very low, less than 4 for all of the tree transformations which follow a BM model of trait evolution and only 35.86 for the IE model.

Previous research found BM to be the best fit for all mammalian trees, including strepsirhines (Harmon *et al.*, 2010). However, that study tested only the BM, OU and EB models and not the IE model. Even so, in light of the results found here, the OU model would be predicted to be the best fit, due to its closer similarity to the IE model. However, further research found that the OU model would only be selected over the BM model, when the OU model conditions were very flexible; specifically, when optima were separately assigned to each branch and not when a single optimum peak was designated for the whole tree or for each clade (Beaulieu *et al.*, 2012; Butler *et al.,* 2004). When modelled in this way, OU more closely resembles the IE model, suggesting that other models may only be favoured over the BM model if they offer a high degree of flexibility in terms of adaptive peaks.

Adaptive peaks are thought to be a more realistic model of evolution then genetic drift, which, by definition, does not imply any selective forces (Smaers & Vinicius, 2009). For example, *Pan* has an average brain size of 378g and *Homo sapiens* of 1334g (Kaplan *et al.,* 2003); following a BM model, the last common ancestor (LCA) of *Pan* and *Homo* would be predicted to have a brain size of 856g, higher than extant chimps (chimpanzees would therefore have decreased in brain size since there LCA with humans, which is un-parsimonious; Smaers & Vinicius, 2009); the IE model, however, allows for different rates of evolution on different branches, representing the different selection pressures experienced by each species (in this instance increased pressure for encephalisation in Hominids - an adaptive peak - due to changes in their environment, diet and/or social structure; Leigh, 2004) and estimates the brain size of the LCA of *Pan and Homo* to be, a more parsimonious, 444g (Smaers & Vinicius, 2009).

Malagasy lemurs are thought to be an adaptive radiation (Martin, 1990). An adaptive radiation would also be expected to find in favour of an EB model of evolution, with species initially evolving rapidly to fill their new niches. However, EB is not the best fit for any

module, and the model parameter is often found to be close to or equal to 1, at which point the model is closer to BM than EB (Harmon *et al.*, 2010). This is in line with the lack of support of the EB model found across the animal kingdom including for other primates and well known adaptive radiations, such as Galapagos finches and African lake cichlids, indicating that the EB pattern may in fact occur very rarely (Harmon *et al.*, 2010).

6.5.2. Phylogenetic signal

6.5.2.1. The strength of phylogenetic signal

Measurements of λ are high for all modules, ranging from 0.86-1 (Table 78-86). This implies that change has occurred in line with BM, as such the distance between species trait values should be proportional to the distance from their last common ancestor. However, it is also possible that, as Pagel's λ has an upper bound of 1, shape change was even more closely aligned to phylogeny than BM would predict (Kamilar & Cooper, 2013). Blomberg's *K* scores indicate that this is the case, especially for PC1 for each module (Table 87). With the exception of the Goswami oral module, PC1 for each module has a *K* value of greater than 1, meaning that closely related species are even more similar in their principal axis of shape change than would be predicted under a BM model. Such a strong phylogenetic signal has previously been interpreted as evolutionary conservativism or stabilising selection (Kamilar & Cooper, 2013).

The results for the Strepsirhini show phylogenetic signal to be consistently high and significant for all modules and for the entire cranium (Tables 78-86). These results are therefore in contrast to both the guenons, where phylogenetic signal was only found in the cranial base (Cardini & Elton, 2008a), and, to lesser extent, to *H. sapiens,* for which the cranial base, temporal bone and upper face were all found to have significant phylogenetic signal, but the strongest signal was found for the entire cranium (Smith, 2009). This inconsistency may be for a number of reasons; first, simply that there is variation in the strength of phylogenetic signal between both traits and species, second, that the investigations are concerned with different levels of taxonomy (intra-species, tribe, and suborder), and phylogenetic signal has been found to be weaker at shallower taxonomic levels (Masters *et al.*, 2007), although this does not explain the strong signal found for human populations (Smith, 2009), and finally, different approaches are used to measure signal strength; Cardini & Elton (2008a) and Smith (2009) compare the molecular and

morphological distance matrices, while Pagel's λ and Blomberg's *K* are used for strepsirhines (Blomberg *et al.*, 2003; Pagel, 1999).

While phylogenetic signal is shown to be high and significant for all cranial modules, the Goswami oral and vault modules have the lowest scores, both in terms of λ and *K* values, especially for PC2 (Table 83, 85 and 87). It has previously been suggested that the high levels of muscular strain inflicted on the oral region are likely to cause epigenetic remodelling, although empirical support for this idea has been lacking (Collard & Wood, 2007; von Cramon-Taubadel, 2009). In this case, the weaker signal, in the Goswami oral module at least, may imply convergence due to dietary adaptations.

Lemuriforms have previously been upheld as a classic adaptive radiation, with a species explosion thought to have occurred once they reached the Island of Madagascar (Martin, 1990). However, results again contradict predictions for an adaptive radiation, which, due to strong selective pressure, should result in optimised traits, which in turn should produce a weak phylogenetic signal, as opposed to the strong signal found in strepsirhine morphology (O'Neill & Dobson, 2008). The fact that the analysis included the lorisiforms, in addition to the lemuriforms, may go some way to explaining this. Furthermore, strepsirhines have been found to possess limited inter-species cranial diversity, in comparison to other primate groups (Fleagle *et al.,* 2010). Therefore, lemuriforms, while diverse in their behaviour and socioecology, do not show a corresponding high level of diversity in their cranial morphology.

6.5.2.2. The influence of size on phylogenetic signal

Size, as represented by body mass, has previously been found to have a phylogenetic signal equal to BM for strepsirhine primates (Kamilar *et al.*, 2012), with further high phylogenetic signal in linear measurements of morphology generally linked to their high correlation with body size (Kamilar & Cooper, 2013). In this research GMM and Procrustes analysis are used to control for isometric scaling, but this does not remove elements of allometric scaling (O'Higgins, 2000).

Size, through the influence of allometric scaling, does appear to have a significant impact on the strength of phylogenetic signal, whether measured as λ or Blomberg's *K*. PC1 for the whole cranium represents a change from a flatter to a more globular vault and this

direction of shape change has previously been linked to size, with smaller specimens having a more pedomorphic, globular cranium in stepsirrhines (see Chapter 5), the order Primates (Collard & O'Higgins, 2001; Frost *et al.,* 2002) and mammals as a whole (Cardini & Polly, 2013). As such, the strong phylogenetic signal for PC1 for the whole cranium (λ = 0.99, *K*= 1.14, p= 0.0001; Table 78, 87) is likely to be the result of allometric shape variation. This could also be the case for PC2 and PC3 for the whole cranium, as the shorter snout and a superiorly/inferiorly deeper face, which they represent, respectively, have also been shown to be significantly related to size in the Strepsirhini at an inter-species level (See Chapter 5) and, for both PCs, trait change was again shown to be close to the BM model (PC2 - λ = 1.0, *K*= 1.10, p= 0.0001; PC3 - λ = 0.99, *K*= 1.09, p= 0.0001; Table 78, 87). Moreover, as many of the λ are equal to one and the *K* values are greater than one, these findings could be interpreted as the result of stabilising selection on species size, which has previously been proposed for strepsirhines (Kamilar *et al.,* 2012).

It is possible that much of the phylogenetic signal documented in the other cranial modules (face and vault following the 2* model, and face, oral, orbit, zygomatic, vault and base following the Goswami model) is also partly the result of allometric scaling. Some of the principal components of shape change that have a strong phylogenetic signal have previously been found to be significantly related to size (See Chapter 5). However, the results are not directly comparable due to methodological differences; specifically, PCs are calculated from all species data for the allometry analyses, while they are calculated from species averages for the phylogenetic signal analyses. In addition, phylogenetic covariation is controlled for in the analyses of allometry.

While size appears to contribute to the strength of the phylogenetic signal in strepsirhine primates, it has been shown to mask it in other taxa. For papionins, it was only after size and allometric scaling had been controlled for that it was possible to recreate accurate phylogenetic trees from cranial morphology (Collard & O'Higgins, 2001; Gilbert & Rossie, 2007), while for guenons, phylogenetic signal associated with module size was found to be very weak. The difference in results may be linked to both the focus on different species and different taxonomic levels, and on the use of different methodologies (Cardini & Elton, 2008a; Gilbert & Rossie, 2007).

6.5.2.3. Interpreting phylogenetic signal

A strong phylogenetic signal does not necessarily mean that it will be possible to recreate an accurate phylogenetic tree from the morphological data. The basicranium was found to have a strong phylogenetic signal for the guenon clade; however, morphological data from the basicranium was unable to recreate the guenon molecular phylogenetic tree, other than distinguishing between the arboreal and terrestrial clades (Cardini & Elton, 2008a). Similarly, while strong phylogenetic signal was found in strepsirhine labyrinth morphology, phylogenetic trees generated from morphological data were not fully congruent with molecular phylogenetic relationships (Lebrun *et al.*, 2010). Moreover, results for strepsirhines show that λ often reaches its upper boundary of 1 and *K* is often greater than 1; such strong signal has previously been interpreted as evidence of evolutionary conservatism (Kamilar & Cooper, 2013; Revell *et al.*, 2008). If traits are subject to evolutionary conservativism around similar optima, then shape change along each branch will wander back and forth around that same adaptive peak, erasing the ability to identify phylogenetic relationships, but phylogenetic signal, in terms of λ or *K,* will remain high (Cardini & Elton, 2008a).

Although it is tempting to read a strong phylogenetic signal as an indication that changes in traits have occurred in line with BM (Symonds & Blomberg, 2014) or as evidence of evolutionary conservatism (Kamilar & Cooper, 2013; Revell *et al.*, 2008), and to view a lack of phylogenetic signal as the result of highly liable evolutionary traits (Kamilar & Cooper, 2013; Symonds & Blomberg, 2014), such interpretations must be made with caution. Investigative modelling has found there to be no relationship between the rate of evolutionary change and either the strength of phylogenetic signal or the underlying evolutionary process (Revell *et al.*, 2008).

6.5.3. Evo-maps

The principal direction of shape change for the whole cranium is shown to represent a divide between the lemuriform and lorisiform clades (Figure 80). The lorisiforms, especially the galagos, have higher trait values, that is, a more globular cranium, while the lemuriforms, especially *V. variegata, Eulemur* and *I. Indri,* have flatter vaults. Within the lemurs, *Microbus*, *A. laniger* and *H. griseus* all show a reversal towards a more globular vault; this is most likely linked with a decrease in size; a more globular vault has previously been identified as an outcome of allometric scaling as size decreases (see Chapter 5) and

these are the smallest of the lemuriform taxa. Similarly, *Otolemur*, the largest of the Galagidae, show a reverse in the opposite direction, towards a less globular vault, as does *P. potto*, the largest of the Lorisidae.

6.5.3.1. Identifying homologies

The evo-map indicates some clear phenotypic shifts at both the infraorder and family level, while at genus and species level, greater variation, reversals and homoplasies result in reduced congruence between phylogenetic relationships and morphology (Figures 80- 88). This echoes previous results for guenons, where, despite the morphological data containing a strong phylogenetic signal, it was not possible to use it to recreate accurate phylogenetic trees (Cardini & Elton, 2008a). Furthermore, it was towards the tips of the trees that the inaccuracies were found (Cardini & Elton, 2008a).

Only the morphology of the strepsirhine cranial base (PC1) appears to clearly separate between taxa at the family level (Figure 88). PC1 represents a shape change from a more laterally to a more medially positioned occipital condyle and hypoglossal canal, as well as a small decrease in the distance from the basion to the opisthion, when travelling from negative to positive along the axis of change (Table 77; Figure79). Taken together, this suggests a decrease in the relative size, particularly a medial-lateral narrowing, of the foramen magnum. The Indriidae have the largest foramen magnum, it then decreases in size sequentially for the Lemuridae, Lepilemuridae, Cheirogalidae, Galagidae and finally Lorisidae. The only potential cause of confusing homoplasy for this shape change comes from *Microcebus murinus,* which has a trait value similar to that of the Galagidae. The axis of shape change represented by PC1 for the cranial base does not appear to be affected by allometry; this inference is based on the fact that there are no apparent reversals of morphology in those species derived in size. Moreover, there are no clear homoplasies between species that are not closely related but are similar in size, as has previously been seen between the Lorisidae and the Cheirogaleidae, as well as *H. griseus* and *A. laniger*. The morphology is also not clearly aligned to diet, activity pattern or mode of locomotion (Gould *et al.*, 2011; Nekaris & Bearder, 2011). The cranial base has been identified as a potential region of strong phylogenetic signal, due to its early development, its endochondral mode of ossification and its role in supporting the brain and integrating the crania and postcrania (Cardini & Elton, 2008a; Goswami, 2006a; Lieberman *et al.*, 2000).

6.5.3.2. Identifying homoplasies

It has been predicted that areas of the skull subject to large amounts of muscular strain, due to mastication, should, as a result, undergo a large amount of epigenetic remodelling, and therefore only carry a weak phylogenetic signal or be subject to homoplasies (Collard & Wood, 2007). Evo-maps for the 2* face and Goswami face and oral modules show no clear pattern with regard to phylogeny (Figure 81, 83 and 85); however, neither do they show any evidence of homoplasies or particularly derived morphologies for *H. griseus,* which has a unique bamboo diet (Mittermeier *et al.*, 2008), or *E. elegantulus* and *Nycticebus,* which rely largely on gum (Charles-Dominique, 1977; Nash, 1986; Nash *et al.,* 1989; Wiens, 2002). Morphological differences linked to diet have previously been recorded for *E. elegantulus,* but these differences were located in the mandible, and not the cranium (Ravosa *et al.,* 2010; Vinyard *et al.,* 2003). Contrasting results are found for the highly faunivorous *L. tardigradus* and *G. demidoff* (Charles-Dominique, 1977; Nekaris, 2014; Nekaris & Bearder, 2011); both species are similarly derived for PC2 of the Goswami face module (Figure 83). Their shared phenotype is represented by a relatively greater distance between the rhinion and the midpoint between the rhinion and the nasion, as well as more angled or pointed rhinion and piriform aperture in comparison to the other strepsirhine taxa (Table 72; Figure 74). The species' shared diet seems the most likely cause of this homoplasy. The other possible cause is allometric scaling, as both species are small; 137g and 60g for *L. tardigradus* and *G. demidoff,* respectively (Charles-Dominique, 1977; Nekaris & Bearder, 2011). However, there are other taxa of a similar size, such as *G. zanzibaricus,* which has an average body mass of 149g (Nekaris & Bearder, 2011), which do not share the morphology.

The most persistent offenders in terms of homoplasy are the Cheirogaleidae and the lorisiforms (with the cheirogaleids sharing similarities with either the Lorisidae or the Galagidae or with both families), with convergent or parallel evolution evident in the 2* face module and for all Goswami modules (Figure 81, 83-87), with the exception of the cranial base; while *M. murinus* is shown to be morphologically similar to the Galagidae, the remaining Cheirogalidae are not (Figure 88). The particular morphologies that the two groups are shown to share are associated with a more anterior (or more pointed) rhinion, a shorter tooth row and a more globular anterior vault, but less globular posterior vault, with an inferiorly positioned inion. The morphological similarities between the Cheirogaleidae and the lorisiforms have been noted previously, and were attributed to either a close

phylogenetic relationship, the retention of the primate primitive condition in both lineages, or convergent evolution (Cartmill, 1975; Charles-Dominique, 1977).

It is now known from molecular analyses that the Cheirogaleidae are not closely related to the lorisiforms (Yoder, 1994, 1997). However, for some of the homoplastic traits shared between the taxa, their trait values are close to that of their LCA, according to the ancestral trait values estimated using the IE model of evolution. These primitive traits include: Goswami model face module PC 2, orbit module PC1, zygomatic PC1 and vault PC1 (Figures 83 -86); however, the remaining homoplastic traits (2* face module PC3, Goswami model orbit PC2, oral PC1 and PC2, and vault PC3 (Figures 81, 84, 85 and 87) are estimated to be derived in relation to their LCA. Therefore, while some of these shared traits may be the retention of primitive characteristics, it is not an adequate explanation for all of them.

The derived traits found in both lineages are linked with a shortening of the face and the roundness of the vault (Tables 70, 72, 73, 74, and 76; Figures 72, 74, 75, 76 and 78). This particular shape change has previously been linked with size, specifically small species, in strepsirhines (See Chapter 5), other primate taxa (Collard & O'Higgins, 2001; Frost *et al.*, 2003; Singleton, 2002) and mammals as a whole (Cardini & Polly, 2013). It therefore seems likely that these shared traits are homoplasies that result from allometric constraints. The Cheirogaleidae and lorisiforms overlap one another in terms of size, weighing from 31-600g and 55g-2.1kg, respectively, and both groups are smaller than the majority of the remaining strepsirhine species (1-6.7kg). The exceptions are *H. griseus* (700g) *Lepilemur sp.* (600-800g) and *A. laniger* (1kg) (Gould *et al.*, 2011; Mittermeier *et al.*, 2008), none of which share these derived traits.

Only minimal change is apparent in PC2 for the whole cranium at the infra-order level, after which clear divisions are noticeable between families (Figure 80). However, there does appear to be evidence of convergent evolution between the Lorisidae and Indriidae, as both show a move toward higher PC values, signifying a shift towards a shorter snout and palate (the same shape change and homoplasy can be seen for PC2 for the 2* face module). The Indriidae and Lorisidae do not share any obvious ecological characteristics, such as diet or mode of locomotion, which may indicate that different selective pressures may have led to this convergent evolution (Gould *et al.*, 2011; Nekaris & Bearder, 2011). For the Lorisidae, this change could be linked to their high level of orbital convergence

(Ross, 1995), which in turn may be linked to their highly faunivorous diet, especially for *Loris tardigradus* (Nekaris & Rasmussen, 2003); orbital convergence has been linked to improved visual acuity for predation (Cartmill, 1992). As well as the possibility that a long snout could obstruct their line of sight for predation and the manipulation of objects in their forelimbs (Cartmill, 1992), it could also be an indication of reduced reliance on olfaction and an increased reliance on vision (Cartmill, 19992). For the Indriidae the shortened snout could be associated with their vertical clinging and leaping mode of locomotion (Mittermeier *et al.,* 2008), with a long snout simply being in the way if the cranium is held close to the tree trunk. Another possibility is that it is linked to the production of their unique song (Mittermeier *et al.,* 2006). Although the Indriidae and Lorisidae are very similar for PC2 of the whole cranium, PC3 identifies the key difference between their morphologies; while both families have relatively short snouts in relation to other strepsirhine species, the snouts of lorises are the shallowest (i.e., the most inferiorly/superiorly compressed) of the Strepsirhini, while the snouts of the Indriidae are the deepest, again this could be linked to their line of sight (Cartmill, 1992) and acoustic abilities (Mittermeier *et al.,* 2006), respectively.

A further incidence of homoplasy is seen between the Galagidae and the Indriidae for the 2* model face module (PC3; Figure 81). Both groups have a relatively short distance between the rhinion and the midway point between the rhinion and the nasion, a more vertical nasal area, a more anteriorly positioned incisive foramen and a relatively longer tooth row (Table 70; Figure 72). Despite their derived similarities in these traits, the two families share very little behaviour or social ecology that could explain this convergent evolution. They are different in their diet, method of locomotion, social structure and geographic location, as well as their activity pattern and size, with the exception of the small nocturnal *A. laniger* (Gould *et al.*, 2011; Mittermeier *et al.*, 2008; Müller & Thalmann, 2000; Nekaris & Bearder, 2011). It therefore seems that, in this instance, either different or possibly hidden selective pressures have resulted in a similar phenotypic outcome, or it is the result of genetic drift. Alternatively it could be the retention of a primitive morphology, however, this explanation is lacking in support, as the adapiformes (*Adapis* and *Leptadapis*), which are believed to be ancestral to extant strepsirhines and therefore be representative of primitive strepsirhine morphology (Bennett & Goswami, 2012; Fleagle, 2013), have a snout that is elongated in comparison to extant strepsirhines (or falls within

the average strepsirhine morphology once allometry is controlled for), rather than being shortened (Bennett & Goswami, 2012).

One other interesting incidence of homoplasy occurs between *Otolemur* and *Nycticebus,* which are similar in the shape of the orbit, as represented by PC3 for the Goswami orbit module (Figure 84). This is largely associated with the position and orientation of the frontotemporal suture, as well as a more posterior positioning of the nasolacrimal duct and the nasion, and a more anterior positioning of the zygomatic foramen (Table 73; Figure 75). Both genera are nocturnal and share a similar size range (~700g-1.4kg) (Nekaris & Bearder, 2011) and this axis of change has previously been shown to have a significant correlation with the size of the whole cranium, and of the orbit itself, for strepsirhine primates (see Chapter 5).

6.5.3.3. Derived species

Through evo-mapping, as well as identifying homologies and homoplasies, it is also possible to pinpoint species that are particularly derived, both within their own family groups and within the strepsirhine taxa as a whole. *Varecia variegata* is derived both for the whole cranium (PC1 and PC2; Figure 80) and the 2* module face module (PC2; Figure 81). Specifically, it is shown to be the most extreme species in terms of having the longest snout and the least globular vault (Table 69; Figure 71). Both of these characteristics have been associated with increased size in the strepsirhines (See Chapter 5) and *V. variegata* is the largest of the Lemuridae; in fact, at 3-4.5kg, it is between 70-400% larger than the other members (Gould *et al.*, 2011).

This allometric scaling pattern does not extend to the Indriidae, which, although generally larger than the Lemuridae (Gould *et al.*, 2011), have flatter faces. Indriids, namely *Propithecus,* are, however, derived for the Goswami model's oral module (PC3; Figure 85). As with the length of the snout, they again go against the general allometric scaling pattern for strepsirhines; these large species (2.8-6kg) are at the extreme negative of the axis of shape change for PC3, with a more medially positioned 3rd molar septum and end of dentition (Table 74; Figure 76). Previous research has shown this axis of change to be significantly related to size for strepsirhines, but with larger species found to have a more laterally placed 3rd molar septum and end of dentition. Even within the Indriidae, this pattern is reversed, with the smallest species, *A. laniger,* having the most laterally placed

end of dentition. It is possible that this move away from the general lemuriform pattern is associated with the family's shortened faces and/or with their derived dental formula of 2.1.2.3, as opposed to 2.1.3.3 (Godfrey, 2005; Gould *et al.*, 2011).

The final species found to be noticeably derived is *P. potto,* for PC3 for the Goswami base module (Figure 88), with an extreme phenotype of a more medially positioned external auditory meatus and a more laterally positioned hypoglossal canal (Table 77; Figure 79). However, in this case there appears to be no direct link with size or evident explanation for the morphological change.

6.5.3.4. Intra-genera trait change

In contrast to the derived species discussed above, the various species *Eulemur* are indistinguishable from one another through the evo-mapping of their trait values. This is true for all PCs for all modules (Figure 80-88), with the exception of PC2 for the Goswami oral module and, even then, differences were only minimal (Figure 85). This may, in part, be linked to the geographic distribution of *Eulemur,* which has resulted in hybrid zones between *E. fulvus* and *E. mongoz* and *E. macaca* (Goodman & Schütz, 2000; Pastorini *et al.,* 2009; Zaramody & Pastorini, 2001). It also falls in line with the findings that *Eulemur* phenotype was correlated with geographic and ecological conditions, rather than phylogeny (Viguier, 2002); as such, any significant morphological variation is likely to be found within species, rather than between them. It also mirrors the weaker phylogenetic signal found in morphological traits for both the Lorisidae (Masters *et al.*, 2007) and the guenons at shallow taxonomic levels (Cardini & Elton, 2008a).

6.6. Conclusion

From the range of evolutionary models and tree transformation methods tested (BM, Pagel's λ, kappa, delta, EB, OU and IE), the IE model of evolution was overwhelmingly the most strongly supported. However, the high values for λ suggest, that in most cases, the IE model is collapsing into something very close to BM. When measured in terms of Pagel's λ or Blomberg's *K*, phylogenetic signal is found to be strong throughout all cranial modules. Previous research has linked a strong phylogenetic signal to the effect of allometric scaling on morphological traits (Kamilar & Cooper, 2013; Kamilar *et al.*, 2012) and indeed the major axies of shape change seen in the strepsirhine cranium have previously been identified as being significantly correlated with size (see Chapter 5). However, evo-mapping

reveals that, at both genus and species level, it is often allometric scaling that is the cause of parallel evolution and reversals, while the clearest phenotype shifts are at the infraorder and familiy level.

Identifying the phylogentic position of fossil taxa based on their morphology therefore remains prone to error. However, assuming that an estimated date is avaliable for the fossil species, the IE model of evolution is the best method for the reconstruction of ancestral states for stresirrhine species. Evo-mapping suggests that it may be possible to predict which infra-order of the Strepsirhini fossil taxa should be placed in and that the morphology of the cranial base may offer the best estimate to which family a species belongs. Finally, knowledge of which factors are likely to result in homoplasies, and the phenotypes that have resulted from them, can help to alert researchers to possible homoplasies during the interpretation of results.

This analysis highlights avenues for further work; firstly the phylogentic relationships of fossil strepsrhine species, sparse though they are (Godfrey *et al.,* 2010; Seiffert *et al.,* 2003; 2005; 2010; Tavaré *et al.,* 2002), could be explored using the IE method with ,where possible, an enphasis on the cranial base; secondly, further work could be undertaken on the IE model, to investigate why it does not fully collapse into BM where appropriate; finally, the EB model could be explored further, using only data from the Lemuriformes (with the addition of further lemur taxa) which is thought to be an adaptive radiation (Martin, 1990) and excluding data pertaining to the Lorisiformes. If the EB model remains poorly supported, then either the pramators of the EB model or our understanding of the Lemuridae radiation need to be reconsidered.

– Chapter 7 –

Conclusions

7.1. Summary

This study investigated the evolution of cranial shape variation in the strepsirhine cranium, specifically how modularity, allometry and phylogeny have worked to shape the evolutionary pathways that have resulted in the morphology of the extant Strepsirhini. Strepsirhines had previously been relatively ignored in this area, in comparison to other primate species (Ackermann, 2005; Ackermann & Cheverud, 2000, 2004; Cáceres *et al.,* 2014; Cardini & Elton 2008a, 2008b, 2009a, 2009b; Cheverud, 1982, 1989; Collard & O'Higgins, 2001; Elton *et al.,* 2010; Frost *et al.,* 2003; Hallgrímsson *et al.,* 2004; Marroig & Cheverud, 2001; Singleton, 2002; Perez *et al.,* 2011), despite the availability of a numerous and broad sample (see Methods Chapter). What research has been done suggests that there may be important morphological differences between strepsirhines and their haplorhine sister clade (Baab *et al.,* 2014; Esteve-Altava *et al.*, 2015; Fleagle *et al.,* 2012; Shoshani *et al.,* 1996).

Advancements in both methods of data collection (Bookstein, 1997; Cooke & Terhune, 2015; Mitteroecker & Gunz, 2009) and analysis (Dryden, 2013; Harmon *et al.,* 2009, Klingenberg, 2011; Smaers & Vinicius, 2009), as well as a well-resolved phylogenetic tree for the taxa (Arnold *et al.,* 2010; Finstermeier *et al.*, 2013; Horvath *et al.*, 2008; Masters *et al.*, 2007; Matsui *et al.*, 2009; Perelman *et al.*, 2011; Roos *et al.*, 2004; Springer *et al.*, 2012; Steiper & Seiffert, 2012; Yoder & Yang, 2004), mean that it is possible to explore a range of previously unanswered questions, laid out in the aims of the study (see Chapter 1). Each aim is outlined again below, followed by a summary of the corresponding results and their interpretation.

To investigate the effect of reduced sample size in geometric morphometric studies of size and shape, across a broad range of strepsirhine taxa.

A 3D geometric morphometric (GMM) approach is now commonly used for comparative studies of morphological variation (Cardini & Elton, 2008a; Cardini *et al.*, 2007; Couette *et al.,* 2005; Fabre *et al.,* 2014; Fleagle *et al.,*2010; Goswami & Polly, 2010b; Lockwood *et al.,* 2004; Rohlf, 1998; Viguier, 2002; Viðarsdóttir *et al.,* 2002; Wood *et al.*, 2007). Unlike the

use of discrete character states or linear measurements, it has the benefit of maintaining the full geometry of landmarks, and enables landmarks to be treated as part of an integrated structure, rather than as independent of one another (Cooke & Terhune, 2015; O'Higgins, 2000). However, sample size in GMM studies is often small, usually as a result of availability (especially for fossil species) and logistic restrictions. For example, in a review of studies, 50% had an average sample size of N<30 and, in most cases, at least one species was represented by N<10 (Cardini & Elton, 2007).

Small sample size had previously been shown to have a significant effect on GMM shape parameters, but less of a negative impact on size parameters. However, that investigation was limited to guenons (Cardini & Elton, 2007). To ensure that appropriate sample sizes could be selected, and that the effect of sample size could be incorporated into the interpretation of the results, it was therefore important to understand how GMM shape and size parameters were affected by reduced sample size across the range of strepsirhine taxa used in this study. Moreover, if the same pattern was found to be true for strepsirhines, as well as guenons, then it might be possible to extrapolate the results to primates as a whole.

The effect of reduced sample sizes was tested for *Eulemur fulvus, Galago senegalensis, Microcebus murinus, Nycticebus coucang, Otolemur crassicaudatus* and *Perodicticus potto*. The impact was constant across all taxa and mirrored that found for guenons (Cardini & Elton, 2007). Estimates of mean size, the standard deviation of size and total shape variance all remained reasonably accurate at small sample sizes (N=5). The accuracy of size parameters at small sample sizes was attributed to a small coefficient of variation in size within species. In contrast, estimates of mean shape and the variance of mean shape became increasingly inaccurate as sample size was reduced. This is particularly a problem when comparing variation between populations of the same species. At the inter-species level, the error introduced by reduced sample sizes is likely to be less detrimental, but was still found to account for up to 30.8% of interspecies shape distances in the species tested here. In addition, the angle between allometric trajectories, and the amount of shape variation that is attributed to the influence of size, were both dramatically overestimated at small sample sizes, for both within-species (between males and females) and between-species comparisons.

These results were used to select the sample for all subsequent analysis, with a decision taken to only use species with a sample size of N>20, which provides a good level of accuracy for the size and shape parameters required. Furthermore, the repeated pattern of results across a broad range of strepsirhine taxa and in guenons (Cardini & Elton, 2007) suggests that this pattern might be true for all primates and, as such, the differing impact of small sample sizes on GMM parameters should be taken into account when interpreting other GMM studies relating to primates.

To assess modularity in the strepsirhine cranium, gaining an understanding of how this is structured and how it influences the evolutionary pathways available for strepsirhine morphological evolution.

The strepsirhine cranium is found to have low levels of overall integration and high levels of modularity at both the intra-species and inter-species level. The cranium was shown to be best divided into two modules, the face and neurocranium, and, within those, into a further six modules, the face, orbit, oral, zygomatic, vault and base, with the strongest support found for the six-module model of modularity proposed by Goswami (2006a).

The pattern of within-module correlation is different for strepsirhines, compared to other primate species; they were shown to have equal levels of within-module correlation for the face and neurocranium modules, while NWM, OWM and apes all had greater within-module correlation in the face compared to the neurocranium (Ackermann, 2005; Ackermann & Cheverud, 2000; Marroig & Cheverud, 2001). This difference could be explained by the general lack of sexual dimorphism in strepsirhines (Godfrey *et al.,* 1993; Jenkins & Albrecht, 1991; Kappeler, 1990, 1991; Thorén *et al.,* 2006), with the implication that high within-module correlation in the face of anthropoids is the result of sexual selection (Marroig & Cheverud, 2001). An alternative explanation is that the relative lack of encephalisation in strepsirhines in comparison to other primates (Isler *et al.*, 2008; Jerison, 1973; Kirk, 2013; Preuss, 2009) implies that they have not experienced the same pressure to reduce the level of correlation within the vault module that haplorrhines have undergone to accommodate their expanding brains (Cheverud, 1996).

Previous work on primates has suggested that high levels of within-module correlation may work to constrain evolutionary change, in order to maintain functional and developmental units (Goswami *et al*., 2014). It has also been suggested that modularity can limit the

evolutionary pathways that cranial morphology can follow (Goswami *et al*., 2014). Both of these factors, combined with the consistent pattern of modularity found for strepsirhines, could be expected to result in high levels of homoplasy within the strepsirhine cranium. Where there is selection for morphological change, it might be expected to follow a narrow trajectory, possibly showing extreme forms at either end (Goswami *et al*., 2014). Potential evidence of this is shown in the divergent morphology of the Lemuridae, especially *Varecia variegata*, which is extreme in terms of its extended snout and superiorly-inferiorly compressed neurocranium.

To understand the allometric patterns present in the strepsirhine cranium and how these vary both across cranial modules and across species.

Overall, at both the intra- and inter- species level, strepsirhines followed the general mammalian allometric pattern (Cardini & Elton, 2009a; Cardini & Polly, 2013, Elton *et al.,* 2010; Frost *et al.,* 2003, Singleton *et al.,* 2002), with smaller taxa having a more pedomorphic appearance, achieved through reduced facial prognathism and a higher, more globular vault. This allometric pattern has been linked to differences in heterochrony in the different regions of the cranium, with the slower growing modules (the face and oral cavity) exposed to the influence of growth hormones to a greater extent than the faster growing modules (the orbit, vault and cranial base) and are, therefore, more likely to be positively allometric (Klingenberg, 1998; Klingenberg & Zimmermann, 1992).

The oral and the orbit modules particularly stand out in terms of their relationship with size. The oral module was found to follow a generally consistent pattern across species, contrary to what might be predicted; given that adaptations for diet could cause the morphology of the oral module to break away from the common allometric pattern (Collard & Wood, 2007; Lieberman *et al.,* 2003). However, morphological similarilty within the oral module was even tighter within family groups; this could be attributed to the close relationship between phylogeny and diet (Viguier, 2002). The orbit module showed the least consistency of all modules in its allometric pattern across species. Orbit size has been shown to be significantly related to both diet and activity pattern (Kirk, 2006; Martin, 1990; Ross, 1995). The wide range of both of these variables across strepsrrhines (Gould *et al.,* 2011; Nekaris & Bearder, 2011) may have resulted in multiple species breaking away from the common allometric pattern in multiple directions.

Allometric scaling is relatively conserved across species, but there is a difference between the lemuriform and lorisiform clades. Facial traits respond more sensitively to size in the Lemuriformes (i.e., the amount of shape change per unit size is greater in the face than in the neurocranium), while in the Lorisiformes, traits in the neurocranium respond more sensitively to changes in size than those in the face.

In terms of size-versus-size allometry, strepsirhines scale with isometry in both of the face modules tested (2* and Goswami) at the inter-species level. This is in contrast to the wider primate trend of positive allometry in the face and palate (Fleagle *et al.,* 2012). The orbit and vault modules, however, do correspond to the general primate pattern of negative allometry at the inter-species level.

To test a re-sampling method that incorporates intra-species variation into inter-species analysis and to compare it with a method that uses species average data.
A new resampling approach was tested and the results compared to those generated using the more traditional approach of using species average scores. The resampling approach takes one specimen at random from each species to create a temporary dataset; the parameter in question is then calculated for this data set. This process is repeated numerous times (1000) and the average of all of the calculated parameters is then taken, rather than calculating the parameter using the species average score. In this way, intra-species variation could be incorporated into inter-species analyses.

For shape-versus-size allometry analyses, the resampling method was less likely to return a significant relationship between size and shape, and estimates of the estimated percentages of shape variation caused by variation in size were smaller than those produced by the species average method. Consequently, the resampling approach only found significant relationships between size and shape at the inter-species level for those modules that had also shown a consistent allometric relationship at the intra-species level. The species average approach, in contrast, found significant inter-species relationships between size and shape even for modules that did not show a consistent pattern at the intra-species level.

The same was not true for size-versus-size allometry, for which the species average and resampling method produced near identical results. This difference is likely to be caused by higher levels of within-species variation in shape than size (Cardini & Elton, 2007; Chapter 3).

The validity of using the species average method thus appears to rest on the extent of within species variation for the variables under analysis.

To assess the strength of phylogenetic signal present in the strepsirhine cranium and how the strength of this signal varies across cranial modules.

The whole cranium and all cranial modules where shown to have strong phylogenetic signal as measured by both Pagel's λ (Pagel, 1999) and Blomberg's *K* (Blomberg *et al.,* 2003). Such high scores could indicate that evolutionary trait change has occurred in line with Brownian Motion (BM), or that traits are subject to evolutionary conservativism or stabilising selection (Kamilar & Cooper, 2013; Pagel, 1999). Furthermore, it is likely that size (and therefore allometric scaling) has contributed substantially to the strength of phylogenetic signal within strepsirhines, as the majority of traits for which a strong phylogenetic signal was detected are significantly correlated with size.

To explore which statistical model of evolution best explains the data, with regard to the morphology of the strepsirhine cranium, and use this to identify both homologies and homoplasies present in strepsirhine morphology.

The variable rate Independent Evolution (IE) model of trait evolution (Smaers & Vinicius, 2009) was by far the most strongly supported across all cranial modules (compared to BM, Pagel's λ, delta, kappa, early burst and OU; Felsenstein, 1988; Harmon *et al.,* 2010; Pagel, 1999). The IE model's success is attributed to its flexibility; it allows for a different rate of change along each branch of the evolutionary tree, as well as different optimum trait values for each branch. As such, it is also able to collapse into either a BM or OU model where the data demands it (Smaers & Vinicius, 2009).

Through the reconstruction of ancestral states, as determined by the IE model, it was possible to identify both homologous and homoplastic traits in the strepsirhine cranium. The cranial base was the only cranial region found to be homologous at the family level; this is specifically linked to the relative size of the foramen magnum. *Loris tardigradus* and *Galagoides demidoff* were homoplastic in terms of their facial traits, particularly the length of their snout and shape of their piriform aperture; this was attributed to convergent adaptation to their shared, highly faunivorous, diet (Charles-Dominique, 1977; Nekaris, 2014; Nekaris & Bearder, 2011). The Cheirogaleidae share many traits with the lorisiforms; these are identified as either retained primitive primate traits (symplesiomorphies) or as

homoplasies, which are most likely the product of similar patterns of allometric scaling due to the species' shared, relatively small, size (Gould *et al.*, 2011; Mittermeier *et al.*, 2008). The Indridae also share homoplastic traits with the Lorisiformes; specifically a relatively shorter snout in comparison to the other strepsirhine species. Finally, *Nycticebus* and *Otolemur* share morphological traits relating to the orbit; this is attributed to convergent evolution as a result of their similar body size, possibly in combination with their shared nocturnal activity pattern (Nekaris & Bearder, 2011). Overall, the level of homoplasy within the strepsirhine cranium is likely to cause significant problems if attempting to reconstruct their evolutionary relationships based on their morphological data.

7.2. Evolutionary patterns in the strepsirhine cranium

The conserved patterns of both modularity and allometry across strepsirhine taxa suggest that pathways of morphological evolution within the suborder are relatively constrained. This is further supported by the strength of phylogenetic signal throughout the cranium, which can be indicative of evolutionary conservativism (Kamilar & Cooper, 2013). Moreover, much of the shape change, both within and across species, can be attributed to change in size. Taken together, this may suggest that species have previously been exposed to selection pressure for change in size, but that size is now subject to stabilising selection for extant species. Where species have diverged from the common strepsirhine pattern, either in modularity, allometry or the strength of phylogenetic signal, it is most parsimoniously attributed to selection for traits associated with a specialised diet or a change in activity pattern (Fleagle *et al.,* 2010).

7.2.1. Extrapolation of the results to other primate taxa

With the exception of *Allocebus, Daubentonia* and *Phaner*, all strepsirhine genera have been included in this analysis, with each genus generally represented by several species (Nekaris & Bearder, 2011; Gould *et al.,* 2011). This, in addition to the fact that most of the evolutionary trends uncovered were consistent across species, suggests that the same trends can be attributed to all extant strepsirhine taxa.

However, the application of the general strepsirhine evolutionary trends to fossil taxa may not be valid, as previous research has indicated that subfossil lemurs may flout these trends, specifically with regard to allometry (Baab *et al.,* 2014). Moreover, attempting to identify the position of fossil species within the phylogenetic history of the Strepsirhini

should be done with caution. The reconstruction of ancestral states revealed incidences of both convergent evolution and reversals in cranial morphology across the clade, as would be predicted by their conserved patterns of modularity, allometry and phylogenetic signal.

Strepsirhine taxa are found to differ from their haplorhine sister clade in terms of both modularity (Ackermann, 2005; Ackermann & Cheverud, 2000; Esteve-Altava *et al.*, 2015; Marroig & Cheverud, 2001) and size-versus-size allometry (Baab *et al.,* 2014; Fleagle *et al.,* 2012). There are also differences between the two clades with regard to the strength of phylogenetic signal (Cardini & Elton, 2008a; Shoshani *et al.,* 1996; Smith, 2009); however, this may in part be due to methodological disparities. The differences between the clades point towards a reorganisation of the cranium associated with the diversification of haplorhines (Fleagle *et al.,* 2012). This highlights the importance of studying strepsirhine taxa separately, as well as alongside, haplorhine taxa, to ensure that trends within the suborder are not masked by the, possibly more robust, trends of the haplorhine primates (Fleagle *et al.,* 2012).

7.3. Contributions of this study

This study has resulted in a substantial new dataset, containing GMM cranial data for a wide range of strepsirhine taxa. In addition, the reliability of GMM methods have been tested, both in terms of the effect of using small sample sizes and of using species average scores. Finally, GMM methods have been applied to larger samples and a broader range of strepsirhine species than have previously been studied. This has identified both similarities and differences with patterns of morphological variation in other taxa and increased our understanding of the role of modularity, allometry and phylogenetic relationships in the evolution of the strepsirhine cranium.

– References –

Ackermann, R. R. (2005). Ontogenetic integration of the hominoid face. *Journal of Human Evolution, 48*(2), 175-197.

Ackermann, R. R., & Cheverud, J. M. (2000). Phenotypic covariance structure in tamarins (genus *Saguinus*): a comparison of variation patterns using matrix correlation and common principal component analysis. *American Journal of Physical Anthropology, 111*(4), 489-501.

Ackermann, R. R., & Cheverud, J. M. (2004). Morphological integration in primate evolution. In M. Pigliucci & K. Preston (Eds.), *Phenotypic integration: studying the ecology and evolution of complex phenotypes* (pp. 302-319). New York: Oxford University Press.

Aiello, L. C., & Wheeler, P. (1995). The expensive-tissue hypothesis: the brain and the digestive system in human and primate evolution. *Current Anthropology*, 36(2), 199-221.

Ali, J. R., & Huber, M. (2010). Mammalian biodiversity on Madagascar controlled by ocean currents. *Nature, 463*(7281), 653-656.

Andrews, P., & Martin, L. (1987). Cladistic relationships of extant and fossil hominoids. *Journal of Human Evolution, 16*(1), 101-118.

Angielczyk, K. D., & Sheets, H. D. (2007). Investigation of simulated tectonic deformation in fossils using geometric morphometrics. *Journal Information, 33*(1), 125-148.

Arnason, U., Adegoke, J. A., Bodin, K., Born, E. W., Esa, Y. B., Gullberg, A., Janke, A. (2002). Mammalian mitogenomic relationships and the root of the eutherian tree. *Proceedings of the National Academy of Sciences USA, 99*(12), 8151-8156.

Arnold, C., Matthews, L. J., & Nunn, C. L. (2010). The 10kTrees website: a new online resource for primate phylogeny. *Evolutionary Anthropology: Issues, News, and Reviews, 19*(3), 114-118.

Baab, K., Rohlf, F. J., Jungers, W., & Perry, J. M. G. (2014). Phylogenetic, ecological, and allometric correlates of cranial shape in Malagasy lemuriforms. *Evolution, 68*(5), 1450-1468.

Barton, R. A. (1998). Visual specialization and brain evolution in primates. *Proceedings of the Royal Society of London B: Biological Sciences, 265*(1409), 1933-1937.

Beard, K. C. (1998). East of Eden: Asia as an important center of taxonomic origination in mammalian evolution. *Bulletin of the Carnegie Museum of Natural History, 34*, 5-39.

Bearder, S. K. (1999). Physical and social diversity among nocturnal primates: a new view based on long term research. *Primates, 40*(1), 267-282.

Bearder, S. K., Ambrose, L., Harcourt, C., Honess, P., Perkin, A., Pimley, E., Svoboda, N. (2003). Species-typical patterns of infant contact, sleeping site use and social cohesion among nocturnal primates in Africa. *Folia Primatologica, 74*(5-6), 337-354.

Beaulieu, J. M., Jhwueng, D.-C., Boettiger, C., & O'Meara, B. C. (2012). Modeling stabilizing selection: expanding the Ornstein–Uhlenbeck model of adaptive evolution. *Evolution, 66*(8), 2369-2383.

Beck, R. A., Burbank, D. W., Sercombe, W. J., Riley, G. W., Barndt, J. K., Berry, J. R., Metje, J. (1995). Stratigraphic evidence for an early collision between northwest India and Asia. *Nature, 373*(6509), 55-58.

Bennett, C. V., & Goswami, A. (2012). Morphometric analysis of cranial shape in fossil and recent Euprimates. *Anatomy Research International,* Article ID 478903.

Bjarnason, A., Chamberlain, A. T., & Lockwood, C. A. (2011). A methodological investigation of hominoid craniodental morphology and phylogenetics. *Journal of Human Evolution, 60*(1), 47-57.

Bjarnason, A., Soligo, C., & Elton, S. (2015). Phylogeny, ecology, and morphological evolution in the atelid cranium. *International Journal of Primatology, 36,* 513-529.

Blomberg, S. P., Garland, T., & Ives, A. R. (2003). Testing for phylogenetic signal in comparative data: behavioral traits are more labile. *Evolution, 57*(4), 717-745.

Blomberg, S. P., Lefevre, J. G., Wells, J. A., & Waterhouse, M. (2012). Independent contrasts and PGLS regression estimators are equivalent. *Systematic Biology, 61*(3), 382-391.

Bookstein, F. L. (1997). *Morphometric tools for landmark data: geometry and biology.* Cambridge: Cambridge University Press.

Breuker, C. J., Patterson, J. S., & Klingenberg, C. P. (2006). A single basis for developmental buffering of *Drosophila* wing shape. *PLoS One, 1*(1), e7.

Britt, A. (2000). Diet and feeding behaviour of the black-and-white ruffed lemur (*Varecia variegata variegata*) in the Betampona Reserve, eastern Madagascar. *Folia Primatologica, 71*(3), 133-141.

Burnham, K.P., & Anderson, D.R. (2004). Multimodel inference - understanding AIC and BIC in model slection. *Sociological Methods & Research, 33*(2), 261-304.

Butler, M., King, A., & Aaron, A. (2001). Phylogentic comparative analysis; a modeling approach for adaptive evolution. *The American Naturalist, 164*(6), 683-695.

Cáceres, N., Meloro, C., Carotenuto, F., Passaro, F., Sponchiado, J., Melo, G. L., & Raia, P. (2014). Ecogeographical variation in skull shape of capuchin monkeys. *Journal of Biogeography, 41*(3), 501-512.

Cardini, A., & Elton, S. (2007). Sample size and sampling error in geometric morphometric studies of size and shape. *Zoomorphology, 126*(2), 121-134.

Cardini, A., & Elton, S. (2008a). Does the skull carry a phylogenetic signal? Evolution and modularity in the guenons. *Biological Journal of the Linnean Society, 93*(4), 813-834.

Cardini, A., & Elton, S. (2008b). Variation in guenon skulls (I): species divergence, ecological and genetic differences. *Journal of Human Evolution, 54*(5), 615-637.

Cardini, A., & Elton, S. (2009a). Geographical and taxonomic influences on cranial variation in red colobus monkeys (Primates, Colobinae): introducing a new approach to 'morph' monkeys. *Global Ecology and Biogeography, 18*(2), 248-263.

Cardini, A., & Elton, S. (2009b). The radiation of red colobus monkeys (Primates, Colobinae): morphological evolution in a clade of endangered African primates. *Zoological Journal of the Linnean Society, 157*(1), 197-224.

Cardini, A., Jansson, A. U., & Elton, S. (2007). A geometric morphometric approach to the study of ecogeographical and clinal variation in vervet monkeys. *Journal of Biogeography, 34*(10), 1663-1678.

Cardini, A., & Polly, P. D. (2013). Larger mammals have longer faces because of size-related constraints on skull form. *Nature Communications, 4* Article ID 2458.

Cartmill, M. (1974). Rethinking primate origins. *Science, 184*(4135), 436-443.

Cartmill, M. (1975). Strepsirhine basicranial structures and the affinities of the Cheirogaleidae. In W. P. Luckett & F. Szalay (Eds.), *Phylogeny of the primates: A multidisciplinary approach* (pp. 313-354). New York: Plenum Press.

Cartmill, M. (1992). New views on primate origins. *Evolutionary Anthropology: Issues, News, and Reviews, 1*(3), 105-111.

Champy, C. (1924). *Sexualité et hormones.* Paris: Doin.

Charles-Dominique, P. (1970). Evolution of lorises and lemurs. *Nature, 227*, 257-260.

Charles-Dominique, P. (1977). *Ecology and behaviour of nocturnal primates: prosimians of equatorial West Africa.* New York: Columbia University Press.

Chatterjee, H. J., Ho, S. Y., Barnes, I. & Groves, C. (2009). Estimating the phylogeny and divergence times of primates using a supermatrix approach. *BMC Evolutionary Biology, 9*(1), 259.

Cheverud, J. M. (1982). Phenotypic, genetic, and environmental morphological integration in the cranium. *Evolution*, *36*(3), 499-516.

Cheverud, J. M. (1989). A comparative analysis of morphological variation patterns in the papionins. *Evolution*, *43,* 1737-1747.

Cheverud, J. M. (1995). Morphological integration in the saddle-back tamarin (*Saguinus fuscicollis*) cranium. *The American Naturalist, 145*(1), 63-89.

Cheverud, J. (1996a). Quantitative genetic analysis of cranial morphology in the cotton-top (*Saguinus oedipus*) and saddle-back (*S. fuscicollis*) tamarins. *Journal of Evolutionary Biology, 9*(1), 5-42.

Cheverud, J. M. (1996b). Developmental integration and the evolution of pleiotropy. *American Zoologist, 36*(1), 44-50.

Cheverud, J. M., Ehrich, T. H., Vaughn, T. T., Koreishi, S. F., Linsey, R. B., & Pletscher, L. S. (2004). Pleiotropic effects on mandibular morphology II: differential epistasis and genetic variation in morphological integration. *Journal of Experimental Zoology Part B: Molecular and Developmental Evolution, 302*(5), 424-435.

Cheverud, J. M., Wagner, G. P., & Dow, M. M. (1989). Methods for the comparative analysis of variation patterns. *Systematic Biology, 38*(3), 201-213.

Churchill, M., Clementz, M. T., & Kohno, N. (2015). Cope's rule and the evolution of body size in Pinnipedimorpha (Mammalia: Carnivora). *Evolution, 69*(1), 201-215.

Clutton-Brock, T. H., & Harvey, P. H. (1980). Primates, brains and ecology. *Journal of Zoology, 190*(3), 309-323.

Cobb, S., & O'Higgins, P. (2004). Hominins do not share a common postnatal facial ontogenetic shape trajectory. *Journal of Experimental Zoology Part B: Molecular and Developmental Evolution, 302*(3), 302-321.

Cole III, T. M., Lele, S., & Richtsmeier, J. T. (2002). A parametric bootstrap approach to the detection of phylogenetic signals in landmark data. In N. Macleod & P. Forey (Eds.), *Morphology, shape and phylogeny* (pp. 194-219). New York: Taylor & Francis.

Collard, M., & O'Higgins, P. (2001). Ontogeny and homoplasy in the papionin monkey face. *Evolution and Development, 3*(5), 322-331.

Collard, M., & Wood, B. (1999). How reliable are human phylogenetic hypotheses? *Proceedings of the National Academy of Science USAs, 97*(9), 5003-5006.

Collard, M., & Wood, B. (2001). Homoplasy and the early hominid masticatory system: inferences from analyses of extant hominoids and papionins. *Journal of Human Evolution, 41*(3), 167-194.

Collard, M., & Wood, B. (2007). Hominin homoiology: an assessment of the impact of phenotypic plasticity on phylogenetic analyses of humans and their fossil relatives. *Journal of Human Evolution, 52*(5), 573-584

Colquhoun, I. C. (1998). Cathemeral behavior of *Eulemur macaco macaco* at Ambato Massif, Madagascar. *Folia Primatologica, 69*(Suppl. 1), 22-34.

Cooke, S. B., & Terhune, C. E. (2015). Form, function, and geometric morphometrics. *The Anatomical Record, 298*(1), 5-28.

Cooper, N., Jetz, W., & Freckleton, R. P. (2010). Phylogenetic comparative approaches for studying niche conservatism. *Journal of Evolutionary Biology, 23*(12), 2529-2539.

Cope, E. (1896). *Primary factors of organic evolution*. Chicago: Open Court Publishing.

Couette, S., Escarguel, G., & Montuire, S. (2005). Constructing, bootstrapping, and comparing morphometric and phylogenetic trees: a case study of New World monkeys (Platyrrhini, Primates). *Journal of Mammalogy, 86*(4), 773-781.

Crawley, M. J. (2005). *Statistics: an introduction using R.* Chichester: John Wiley & Sons.

Crowley, B. E., Godfrey, L. R., & Irwin, M. T. (2011). A glance to the past: subfossils, stable isotopes, seed dispersal, and lemur species loss in southern Madagascar. *American Journal of Primatology, 73*(1), 25-37.

Currie, T. E., & Meade, A. (2014). Keeping yourself updated: Bayesian approaches in phylogenetic comparative methods with a focus on markov chain models of discrete character evolution. In L. Z. Garamszegi (Ed.), *Modern phylogenetic comparative methods and their application in evolutionary biology: concepts and practice* (pp. 263-286). Berlin: Springer.

Curtis, D., & Zaramody, A. (1999). Social structure and seasonal variation in the behaviour of *Eulemur mongoz*. *Folia Primatologica, 70*(2), 79-96.

Curtis, D., Zaramody, A., & Martin, R. D. (1999). Cathemerality in the mongoose lemur, *Eulemur mongoz*. *American Journal of Primatology, 47*(4), 279-298.

de Oliveira, F. B., Porto, A., & Marroig, G. (2009). Covariance structure in the skull of Catarrhini: a case of pattern stasis and magnitude evolution. *Journal of Human Evolution, 56*(4), 417-430.

Debat, V., Debelle, A., & Dworkin, I. (2009). Plasticity, canalization, and developmental stability of the *Drosophila* wing: joint effects of mutations and developmental temperature. *Evolution, 63*(11), 2864-2876.

DelPero, M., Masters, J., Zuccon, D., Cervella, P., Crovella, S., & Ardito, G. (2000). Mitochondrial sequences as indicators of genetic classification in bush babies. *International Journal of Primatology, 21*(5), 889-904.

DelPero, M., Pozzi, L., & Masters, J. C. (2006). A composite molecular phylogeny of living lemuroid primates. *Folia Primatologica, 77*(6), 434-445.

Disotell, T. R., Honeycutt, R. L., & Ruvolo, M. (1992). Mitochondrial DNA phylogeny of the Old World monkey tribe Papionini. *Molecular Biology and Evolution, 9*(1), 1-13.

Drake, A. G., & Klingenberg, C. P. (2010). Large-scale diversification of skull shape in domestic dogs: disparity and modularity. *The American Naturalist, 175*(3), 289-301.

Dryden, I. (2013). Statistical shape analysis. 'Shapes' package. from http://www.maths.nottingham.ac.uk/~ild/shapes

Dryden, I., & Mardia, K. (1993). Multivariate shape analysis. *Sankhyā: The Indian Journal of Statistics, Series A*, 460-480.

Dubois, E. (1897). Sur le rapport du poids de l'encéphale avec la grandeur du corps chez les mammifères. *Bulletins de la Societe d'Anthropologie de Paris, 8*(1), 337-376.

Dumont, E. R. (1997). Cranial shape in fruit, nectar, and exudate feeders: implications for interpreting the fossil record. *American Journal of Physical Anthropology, 102*(2), 187-202.

Dumont, E. R., Ryan, T. M., & Godfrey, L. R. (2011). The *Hadropithecus* conundrum reconsidered, with implications for interpreting diet in fossil hominins. *Proceedings of the Royal Society B-Biological Sciences, 278*(1725), 3654-3661

Dunbar, R. I. (1992). Neocortex size as a constraint on group size in primates. *Journal of Human Evolution, 22*(6), 469-493.

Dunbar, R. I. (2002). The social brain hypothesis. In J. T. Cacioppo, G. G. Berntson, R. Adolphs, C. S. Carter, R. J. Davidson, M. K. McClintock, B. S. McEwen, M. J. Meaney, D. L. Schacter, E. M. Sternberg, S. S. Suomi, & S. E. Taylor (Eds.), *Foundations in social neuroscience* (Vol. 5, pp. 69-87): Massachusetts Institute of Technology.

Dunbar, R. I., & Shultz, S. (2007a). Evolution in the social brain. *Science, 317*(5843), 1344-1347.

Dunbar, R. I., & Shultz, S. (2007b). Understanding primate brain evolution. *Philosophical Transactions of the Royal Society of London B: Biological Sciences, 362*(1480), 649-658.

Elton, S., Dunn, J., & Cardini, A. (2010). Size variation facilitates population divergence but does not explain it all: an example study from a widespread African monkey. *Biological Journal of the Linnean Society, 101*(4), 823-843.

Emerson, S. B., & Bramble, D. M. (1993). Scaling, allometry and skull design. In J. Hanken (Ed), *The skull, volume 3*: *Functional and evolutionary mechanisms* (pp 384-421). Chicago: University of Chicago Press.

Escoufier, Y. (1973). Le traitement des variables vectorielles. *Biometrics*, 751-760.

Esteve-Altava, B., Boughner, J. C., Diogo, R., Villmoare, B. A., & Rasskin-Gutman, D. (2015). Anatomical network analysis shows decoupling of modular lability and complexity in the evolution of the primate skull. *PLoS One,* e0127653

Fabre, A. C., Goswami, A., Peigné, S., & Cornette, R. (2014). Morphological integration in the forelimb of musteloid carnivorans. *Journal of Anatomy, 225*(1), 19-30.

Faria, J.C., Grosjean, P., Jelihovschi, E. (2013). Tinn-R - GUI/Editor for R language and environment statistical computing. URL http://sourceforge.net/projects/tinn-r.

Feistner, A., & Sterling, E. (1995). Body mass and sexual dimorphism in the aye-aye *Daubentonia madagascariensis*. *Dodo-Journal of the Wildlife Preservation Trusts*(31), 73-76.

Felsenstein, J. (1985). Phylogenies and the comparative method. *The American Naturalist, 125*(1), 1-15.

Felsenstein, J. (1988). Phylogenies and quantitative characters. *Annual Review of Ecology and Systematics*, *19,* 445-471.

Fernandez-Duque, E. (2011). Aotinae: social monogamy in the only nocturnal anthropoid. In C. J. Campbell, A. Fuentes, K. C. MacKinnon, S. Bearder, & R. Stumpf (Eds.), *Primates in Perspective.* New York: Oxford University Press.

Field, A. (2003). *Discovering statistics using SPSS for Windows*. London: Sage Publications

Fietz, J., & Ganzhorn, J. U. (1999). Feeding ecology of the hibernating primate *Cheirogaleus medius*: how does it get so fat? *Oecologia, 121*(2), 157-164.

Finstermeier, K., Zinner, D., Brameier, M., Meyer, M., Kreuz, E., Hofreiter, M., & Roos, C. (2013). A mitogenomic phylogeny of living primates. *PLoS One, 8*(7), e69504.

Fleagle, J. G. (1985). Size and adaptation in primates. In W. Jungers (Ed.), *Size and Scaling in primate biology* (pp. 1-19). New York: Plenum Press.

Fleagle, J. G. (2013). *Primate adaptation and evolution: 3rd Edn.* San Diego: Academic Press.

Fleagle, J. G., Gilbert, C. C., & Baden, A. L. (2010). Primate cranial diversity. *American Journal of Physical Anthropology, 142*(4), 565-578.

Fleagle, J. G., Gilbert, C. C., & Baden, A. L. (2012). *Primate cranial diversity: comparisons among the major primate radiations contradict larger and more general trends.* Paper presented at the American Journal of Physical Anthropology.

Freckleton, R. P., Harvey, P. H., & Pagel, M. (2002). Phylogenetic analysis and comparative data: a test and review of evidence. *American Nauralist, 160*(6), 712-726.

Frost, S. R., Marcus, L. F., Bookstein, F. L., Reddy, D. P., & Delson, E. (2003). Cranial allometry, phylogeography, and systematics of large-bodied papionins (Primates: Cercopithecinae) inferred from geometric morphometric analysis of landmark data. *The Anatomical Record Part A: Discoveries in Molecular, Cellular, and Evolutionary Biology, 275*(2), 1048-1072.

Fruciano, C., Franchini, P., & Meyer, A. (2013). Resampling-based approaches to study variation in morphological modularity. *PLoS One, 8*(7), e69376.

Ganzhorn, J., Goodman, S., Ramanamanjato, J., Ralison, J., Rakotondravony, D., & Rakotosamimanana, B. (2000). Effects of fragmentation and assessing minimum viable populations of lemurs in Madagascar. *Isolated Vertebrate Communities in the Tropics, 46*, 265-272.

Garamszegi, L. Z., & Gonzalez-Voyer, A. (2014). Working with the tree of life in comparative studies: how to build and tailor phylogenies tp interspecific datasets. In L. Z. Garamszegi (Ed.), *Modern phylogenetic comparative methods and their application in evolutionary biology: concepts and practice* (pp. 19-48). Berlin: Springer.

Gayon, J. (2000). History of the concept of allometry. *American Zoologist, 40*(5), 748-758.

Genty, E., & Roeder, J.-J. (2006). Can lemurs learn to deceive? A study in the black lemur (*Eulemur macaco*). *Journal of Experimental Psychology: Animal Behavior Processes, 32*(2), 196-200.

Gilbert, C. (2011). Phylogenetic analysis of the African papionin basicranium using 3-D geometric morphometrics: the need for improved methods to account for allometric effects. *American Journal of Physical Anthropology, 144*(1), 60-71.

Gilbert, C. C., Frost, S. R., & Strait, D. S. (2009). Allometry, sexual dimorphism, and phylogeny: a cladistic analysis of extant African papionins using craniodental data. *Journal of Human Evolution, 57*(3), 298-320.

Gilbert, C. C., & Rossie, J. B. (2007). Congruence of molecules and morphology using a narrow allometric approach. *Proceedings of the National Academy of Sciences USA, 104*(29), 11910-11914.

Gilbert, S. F. (2014). *Developmental biology* (10th ed.). Sunderland, MA: Sinauer Associates

Godfrey, L. (2005). General anatomy. In S. Wolfe-Coote (Ed.), *The laboratory primate* (pp. 29-45). London: Academic Press.

Godfrey, L., & Jungers, W. L. (2002). Quaternary fossil lemurs. In W. C. Hartwig (Ed.), *The primate fossil record* (pp. 97-121). Cambridge: Cambridge University Press.

Godfrey, L., & Jungers, W. L. (2003). Subfossil lemurs. In S. M. Goodman & J. P. Benstead (Eds.), *The Natural History of Madagascar* (pp. 1248-1252). Chicago: University of Chicago Press.

Godfrey, L. R., & Jungers, W. L. (2003). The extinct sloth lemurs of Madagascar. *Evolutionary Anthropology, 12*(6), 252-263.

Godfrey, L. R., Jungers, W. L., & Burney, D. A. (2010). Subfossil lemurs of Madagascar. In L. Werdelin & W. J. Sanders (Eds.), *Cenozoic mammals of Africa* (pp. 351-367). Berkeley: The University of California Press.

Godfrey, L. R., Lyon, S. K., & Sutherland, M. R. (1993). Sexual dimorphism in large-bodied primates: the case of the subfossil lemurs. *American Journal of Physical Anthropology, 90*(3), 315-334.

Godfrey, L. R., Semprebon, G. M., Jungers, W. L., Sutherland, M. R., Simons, E. L., & Solounias, N. (2004). Dental use wear in extinct lemurs: evidence of diet and niche differentiation. *Journal of Human Evolution, 47*(3), 145-169.

Godinot, M. (2006). Lemuriform origins as viewed from the fossil record. *Folia Primatologica, 77*(6), 446-464.

Goldizen, A. W. (2003). Social monogamy and its variations in callitrichids: do these relate to the costs of infant care? In U. H. Reichard & C. Boesch (Eds.), *Monogamy: Mating strategies and partnerships in birds, humans and other mammals* (pp. 232-247). Cambridge: Cambridge University Press.

González-José, R., Van der Molen, S., González-Pérez, E., & Hernandez, M. (2004). Patterns of phenotypic covariation and correlation in modern humans as viewed from morphological integration. *American Journal of Physical Anthropology, 123*(1), 69-77.

Goodman, S., & Schütz, H. (2000). The lemurs of the northeastern slopes of the Réserve Spéciale de Manongarivo. *Lemur News, 5*, 30-33.

Goswami, A. (2006a). Cranial modularity shifts during mammalian evolution. *The American Naturalist, 168*(2), 270-280.

Goswami, A. (2006b). Morphological integration in the carnivoran skull. *Evolution, 60*(1), 169-183.

Goswami, A., Polly, P. D. (2010a). Methods for studying morphological integration, modularity and covariance evolution. In J. Alroy & G. Hunt (Eds.), *The Paleontological Society Papers* (Vol. 16, pp. 213-243).

Goswami, A., & Polly, P. D. (2010b). The influence of modularity on cranial morphological disparity in Carnivora and Primates (Mammalia). *PLoS One, 5*(3), e9517.

Goswami, A., Smaers, J., Soligo, C., & Polly, P. (2014). The macroevolutionary consequences of phenotypic integration: from development to deep time. *Philosophical Transactions of the Royal Society B: Biological Sciences, 369*(1649), ID 20130254.

Gould, L., Sauther, M., & Cameron, A. (2011). Lemuriformes. In C. J. Campbell, A. Fuentes, K. C. MacKinnon, S. K. Bearder, & R. M. Stumpf (Eds.), *Primates in Perspective* (Vol. 2, pp. 55-79). New York: Oxford University Press.

Gould, S. J. (1966). Allometry and size in ontogeny and phylogeny. *Biological Review, 41*(4), 587-640.

Gould, S. J. (1971). Geometric similarity in allometric growth: a contribution to the problem of scaling in the evolution of size. *American Naturalist*, *105*, 113-136.

Gould, S. J. (1974). Allometry in primates, with emphasis on scaling and the evolution of the brain. *Contributions to Primatology, 5*, 244-292.

Gould, S. J., & Eldredge, N. (1993). Punctuated equilibrium comes of age. *Nature, 366*(6452), 223-227.

Grafen, A. (1989). The phylogenetic regression. *Philosophical Transactions of the Royal Society of London. Series B, Biological Sciences*, *326*, 119-157.

Grassi, C. (2001). The behavioral ecology of *Hapalemur griseus griseus*: the influences of microhabitat and population density on this small-bodied prosimian folivore (Madagascar). Ph.D. Dissertation, University of Texas, Austin.

Greaves, W. (1985). The mammalian postorbital bar as a torsion-resisting helical strut. *Journal of Zoology, 207*(1), 125-136.

Greaves, W. S. (1991). A relationship between premolar loss and jaw elongation in selenodont artiodactyls. *Zoological Journal of the Linnean Society, 101*(2), 121-129.

Groves, C. P. (1986). Systematics of the great apes. In D. R. Swindeler & J. Erwin (Eds.), *Comparative primate biology* (pp. 186-217). New York: Alan R. Liss.

Groves, C. (1998). Systematics of tarsiers and lorises. *Primates, 39*(1), 13-27.

Groves, C. P. (2000). The genus *Cheirogaleus*: unrecognized biodiversity in dwarf lemurs. *International Journal of Primatology, 21*(6), 943-962.

Groves, C. P. (2005). Order Primates. In D. E. Wilson & D. M. Reeder (Eds.), *Mammal species of the world: a taxonomic and geographic reference* (Vol. 3rd, pp. 111-184). Baltimore: The John Hopkins University Press.

Groves, C. P., & Eaglen, R. H. (1988). Systematics of the Lemuridae (Primates, Strepsirhini). *Journal of Human Evolution, 17*(5), 513-538.

Gunz, P., & Mitteroecker, P. (2013). Semilandmarks: a method for quantifying curves and surfaces. *Hystrix, the Italian Journal of Mammalogy, 24*(1), 103-109.

Gunz, P., Mitteroecker, P., Neubauer, S., Weber, G. W., & Bookstein, F. L. (2009). Principles for the virtual reconstruction of hominin crania. *Journal of Human Evolution, 57*(1), 48-62.

Haber, A. (2011). A comparative analysis of integration indices. *Evolutionary Biology, 38*(4), 476-488.

Hall, B. K. (2005). *Bones and cartilage: developmental and evolutionary skeletal biology*. London: Academic Press.

Hall, B. K. (2007). Homoplasy and homology: dichotomy or continuum? *Journal of Human Evolution, 52*(5), 473-479.

Hallgrímsson, B., Jamniczky, H., Young, N. M., Rolian, C., Parsons, T. E., Boughner, J. C., & Marcucio, R. S. (2009). Deciphering the palimpsest: studying the relationship between morphological integration and phenotypic covariation. *Evolutionary Biology, 36*(4), 355-376.

Hallgrímsson, B., Willmore, K., Dorval, C., & Cooper, D. M. (2004). Craniofacial variability and modularity in macaques and mice. *Journal of Experimental Zoology Part B: Molecular and Developmental Evolution, 302*(3), 207-225.

Hansen, T. F. (1997). Stabilizing selection and the comparative analysis of adaptation. *Evolution, 51*(5), 1341-1351.

Hansen, T. F., & Martins, E. P. (1996). Translating between microevolutionary process and macroevolutionary patterns: the correlation structure of interspecific data. *Evolution*, 1404-1417.

Hansen, T. F., Pienaar, J., & Orzack, S. H. (2008). A comparative method for studying adaptation to a randomly evolving environment. *Evolution, 62*(8), 1965-1977.

Harmon, L. , Losos, J. B., Jonathan Davies, T., Gillespie, R. G., Gittleman, J. L., Bryan Jennings, W., Mooers, A. Ø. (2010). Early bursts of body size and shape evolution are rare in comparative data. *Evolution, 64*(8), 2385-2396.

Harmon, L., Weir, J., Brock, C., Glor, R., Challenger, W., & Hunt, G. (2009). geiger: analysis of evolutionary diversification. *R package version 2.*

Harper, G. J., Steininger, M. K., Tucker, C. J., Juhn, D., & Hawkins, F. (2007). Fifty years of deforestation and forest fragmentation in Madagascar. *Environmental Conservation, 34*(04), 325-333.

Harvati, K., & Weaver, T. D. (2006a). Human cranial anatomy and the differential preservation of population history and climate signatures. *The Anatomical Record Part A: Discoveries in Molecular, Cellular, and Evolutionary Biology, 288*(12), 1225-1233.

Harvati, K., & Weaver, T. D. (2006b). Reliability of cranial morphology in reconstructing Neanderthal phylogeny. In K. Harvati & T. Harrison (Eds.), *Neanderthals revisited: new approaches and perspectives* (pp. 239-254). Netherlands: Springer

Heesy, C. P. (2005). Function of the mammalian postorbital bar. *Journal of Morphology, 264*(3), 363-380.

Hone, D. W., & Benton, M. J. (2005). The evolution of large size: how does Cope's Rule work? *Trends in Ecology & Evolution, 20*(1), 4-6.

Horovitz, I., Zardoya, R., & Meyer, A. (1998). Platyrrhine systematics: a simultaneous analysis of molecular and morphological data. *American Journal of Physical Anthropology, 106*(3), 261-281.

Horvath, J. E., Weisrock, D. W., Embry, S. L., Fiorentino, I., Balhoff, J. P., Kappeler, P., Yoder, A. D. (2008). Development and application of a phylogenomic toolkit: resolving the evolutionary history of Madagascar's lemurs. *Genome Research, 18*(3), 489-499.

Huxley, J. S. (1924). Constant differential growth-ratios and their significance. *Nature, 114*(2877), 895-896.

Huxley, J. S., & Teissier, G. (1936). Terminology of relative growth. *Nature, 137*(3471), 780-781.

Ishak, B., Warter, S., Dutrillaux, B., & Rumpler, Y. (1988). Phylogenetic relation between Lepilemuridae and other lemuriform families. *American Journal of Primatology, 15*(3), 275-280.

Isler, K., Kirk, E. C., Miller, J. M., Albrecht, G. A., Gelvin, B. R., & Martin, R. D. (2008). Endocranial volumes of primate species: scaling analyses using a comprehensive and reliable data set. *Journal of Human Evolution, 55*(6), 967-978.

Ives, A. R., Midford, P. E., & Garland, T. (2007). Within-species variation and measurement error in phylogenetic comparative methods. *Systematic Biology, 56*(2), 252-270.

IUCN. (2015). The IUCN Red List of Threatened Species. Version 2015.1. Retrieved 09/07/2015, 2015, from http://www.iucnredlist.org/

Jacobs, L. L. (1981). Miocene lorisid primates from the Pakistan Siwaliks. *Nature, 289*, 585-587

Jameson, N. M., Hou, Z.-C., Sterner, K. N., Weckle, A., Goodman, M., Steiper, M. E., & Wildman, D. E. (2011). Genomic data reject the hypothesis of a prosimian primate clade. *Journal of Human Evolution, 61*(3), 295-305.

Jenkins, P. D., & Albrecht, G. H. (1991). Sexual dimorphism and sex ratios in Madagascan prosimians. *American Journal of Primatology, 24*(1), 1-14.

Jenkins, R. K., Keane, A., Rakotoarivelo, A. R., Rakotomboavonjy, V., Randrianandrianina, F. H., Razafimanahaka, H. J., Jones, J. P. (2011). Analysis of patterns of bushmeat consumption reveals extensive exploitation of protected species in eastern Madagascar. *PLoS One, 6*(12), e27570.

Jerison, H. (1973). *Evolution of the brain and intelligence.* New York: Accademic Press

Jolly, A. (2004). *Lords and lemurs: mad scientists, kings with spears, and the survival of diversity in Madagascar.* USA: Houghton Mifflin Harcourt.

Jones, J. P., Andriamarovololona, M. M., & Hockley, N. (2008). The importance of taboos and social norms to conservation in Madagascar. *Conservation Biology, 22*(4), 976-986.

Jungers, W. L., Godfrey, L. R., Simons, E. L., Wunderlich, R. E., Richmond, B. G., & Chatrath, P. S. (2002). Ecomorphology and behavior of giant extinct lemurs from Madagascar. In J. M. Plavcan, R. F. Kay, W. L. Jungers, & C. P. van Schaik (Eds.), *Reconstructing behavior in the primate fossil record* (pp. 371-411). New York: Springer.

Kamilar, J. M., & Cooper, N. (2013). Phylogenetic signal in primate behaviour, ecology and life history . *Philosophical Transactions of the Royal Society B: Biological Sciences, 368* (1618), 20120341.

Kamilar, J. M., Muldoon, K. M., Lehman, S. M., & Herrera, J. P. (2012). Testing Bergmann's rule and the resource seasonality hypothesis in Malagasy primates using GIS-based climate data. *American Journal of Physical Anthropology, 147*(3), 401-408.

Kaplan, H., Mueller, T., Gangestad, S., & Lancaster, J.B. (2003). Neural capital and life span evolution among primates and humans. In C. E. Finch, J. M. Robine & Y. Christen (Eds.), *Brain and Longevity* (pp.69-98). Berlin: Springer.

Kappeler, P. M. (1990). The evolution of sexual size dimorphism in prosimian primates. *American Journal of Primatology, 21*(3), 201-214.

Kappeler, P. M. (1991). Patterns of sexual dimorphism in body weight among prosimian primates. *Folia Primatologica, 57*(3), 132-146.

Kappeler, P. M. (2000). Lemur origins: rafting by groups of hibernators? *Folia Primatologica, 71*(6), 422-425.

Kappeler, P. M., & Erkert, H. G. (2003). On the move around the clock: correlates and determinants of cathemeral activity in wild redfronted lemurs (*Eulemur fulvus rufus*). *Behavioral Ecology and Sociobiology, 54*(4), 359-369.

Kappeler, P. M., & Heymann, E. W. (1996). Nonconvergence in the evolution of primate life history and socio-ecology. *Biological Journal of the Linnean Society, 59*(3), 297-326.

Karanth, K. P., Delefosse, T., Rakotosamimanana, B., Parsons, T. J., & Yoder, A. D. (2005). Ancient DNA from giant extinct lemurs confirms single origin of Malagasy primates. *Proceedings of the National Academy of Sciences of the United States of America, 102*(14), 5090-5095.

Kendall, D. G. (1984). Shape manifolds, procrustean metrics, and complex projective spaces. *Bulletin of the London Mathematical Society, 16*(2), 81-121.

Kay, R. F., Ross, C., & Williams, B. A. (1997). Anthropoid origins. *Science, 275*(5301), 797-804.

Kirk, E. C. (2006). Effects of activity pattern on eye size and orbital aperture size in primates. *Journal of Human Evolution, 51*(2), 159-170.

Kirk, E. C. (2013). Characteristics of crown primates. *Nature Education Knowledge, 4*(8), 3.

Klingenberg, C. P. (1996). Individual variation of ontogenies: a longitudinal study of growth and timing. *Evolution*, 2412-2428.

Klingenberg, C. P. (1998). Heterochrony and allometry: the analysis of evolutionary change in ontogeny. *Biological Reviews of the Cambridge Philosophical Society, 73*(01), 79-123.

Klingenberg, C. P. (2008). Novelty and “homology-free” morphometrics: what’s in a name? *Evolutionary Biology, 35*(3), 186-190.

Klingenberg, C. P. (2009). Morphometric integration and modularity in configurations of landmarks: tools for evaluating a priori hypotheses. *Evolution and Development, 11*(4), 405-421.

Klingenberg, C. P. (2014). MorphoJ: an integrated software package for geometric morphometrics. *Molecular Ecology Resources, 11*(2), 353-357.

Klingenberg, C. P. (2013). Cranial integration and modularity: insights into evolution and development from morphometric data. *Hystrix, the Italian Journal of Mammalogy, 24*(1), 43-58.

Klingenberg, C. P., & Gidaszewski, N. A. (2010). Testing and quantifying phylogenetic signals and homoplasy in morphometric data. *Systematic Biology, 59*(3), 245-261.

Klingenberg, C. P., Leamy, L. J., & Cheverud, J. M. (2004). Integration and modularity of quantitative trait locus effects on geometric shape in the mouse mandible. *Genetics, 166*(4), 1909-1921.

Klingenberg, C. P., & Zimmermann, M. (1992). Static, ontogenetic, and evolutionary allometry: a multivariate comparison in nine species of water striders. *American Naturalist*, 601-620.

Krause, D. W., & Maas, M. C. (1990). The biogeographic origins of late Paleocene-early Eocene mammalian immigrants to the Western Interior of North America. *Geological Society of America Special Paper, 243*, 71-105.

Kress, W. J. (1993). Coevolution of plants and animals - pollination of flowers by primates in madagascar. *Current Science, 65*(3), 253-257.

Kress, W. J., Schatz, G. E., Andrianifahanana, M., & Morland, H. S. (1994). Pollination of *Ravenala madagascariensis* (strelitziaceae) by lemurs in Madagascar - evidence for an archaic coevolutionary system. *American Journal of Botany, 81*(5), 542-551.

Kuratani, S. (2005). Craniofacial development and the evolution of the vertebrates: the old problems on a new background. *Zoological science, 22*(1), 1-19.

Lapicque, L. (1898). Sur la relation du poids de l'encéphale aux poids du corps. *Comptes rendus des séances de la Société de biologie et de ses filiales, 5*(10), 62-63.

Lawing, A. M., & Polly, P. D. (2010). Geometric morphometrics: recent applications to the study of evolution and development. *Journal of Zoology, 280*(1), 1-7.

Lebrun, R., De León, M. P., Tafforeau, P., & Zollikofer, C. (2010). Deep evolutionary roots of strepsirrhine primate labyrinthine morphology. *Journal of Anatomy, 216*(3), 368-380.

Leakey, M. G., Spoor, F., Dean, M. C., Feibel, C. S., Antón, S. C., Kiarie, C., & Leakey, L. N. (2012). New fossils from Koobi Fora in northern Kenya confirm taxonomic diversity in early *Homo*. *Nature, 488*(7410), 201-204.

Leamy, L., & Atchley, W. (1984). Static and evolutionary allometry of osteometric traits in selected lines of rats. *Evolution*, *38*, 47-54.

Leonard, W. R., & Robertson, M. L. (1994). Evolutionary perspectives on human-nutrition - the influence of brain and body-size on diet and metabolism. *American Journal of Human Biology, 6*(1), 77-88

Leigh, S. R. (2004). Brain growth, life history and cognition in primate and human evolution. *American Journal of Primatology, 62*, 139-164.

Lieberman, D. E. (2000). Ontogeny, homology and phylogeny in the hominid craniofacial skeleton: the problem of the browridge. In P. O'Higgins & M. Cohn (Eds.), *Development, growth and evolution* (pp. 85-122). London: Academic Press.

Lieberman, D. E. (2011). *The evolution of the human head*. USA: Harvard University Press.

Lieberman, D. E., Pearson, O. M., Polk, J. D., Demes, B., & Crompton, A. (2003). Optimization of bone growth and remodeling in response to loading in tapered mammalian limbs. *Journal of Experimental Biology, 206*(18), 3125-3138.

Lieberman, D. E., Ross, C. F., & Ravosa, M. J. (2000). The primate cranial base: ontogeny, function, and integration. *American Journal of Physical Anthropology, 113*(s 31), 117-169.

Lockwood, C. A., & Fleagle, J. G. (1999). The recognition and evaluation of homoplasy in primate and human evolution. *American Journal of Physical Anthropology, 110*(S29), 189-232.

Lockwood, C. A., Kimbel, W. H., & Lynch, J. M. (2004). Morphometrics and hominoid phylogeny: support for a chimpanzee–human clade and differentiation among great ape subspecies. *Proceedings of the National Academy of Sciences of the United States of America, 101*(13), 4356-4360.

Lockwood, C. A., Lynch, J. M., & Kimbel, W. H. (2002). Quantifying temporal bone morphology of great apes and humans: an approach using geometric morphometrics. *Journal of Anatomy, 201*(6), 447-464.

Losos, J. B. (2008). Phylogenetic niche conservatism, phylogenetic signal and the relationship between phylogenetic relatedness and ecological similarity among species. *Ecology Letters, 11*(10), 995-1003.

Lovatt, F. M., & Hoelzel, A. (2011). The impact of population bottlenecks on fluctuating asymmetry and morphological variance in two separate populations of reindeer on the island of South Georgia. *Biological Journal of the Linnean Society, 102*(4), 798-811.

Lycett, S. J., & Collard, M. (2005). Do homoiologies impede phylogenetic analyses of the fossil hominids? An assessment based on extant papionin craniodental morphology. *Journal of Human Evolution, 49*(5), 618-642.

MacLean, E. L., Barrickman, N. L., Johnson, E. M., & Wall, C. E. (2009). Sociality, ecology, and relative brain size in lemurs. *Journal of Human Evolution, 56*(5), 471-478.

Maddison, W. P. (1991). Squared-change parsimony reconstructions of ancestral states for continuous-valued characters on a phylogenetic tree. *Systematic Zoology, 40*(3), 304-314.

Makedonska, J. (2014). New insights into the phenotypic covariance structure of the anthropoid cranium. *Journal of Anatomy, 225*(6), 634-658.

Makedonska, J., Wright, B. W., & Strait, D. S. (2012). The effect of dietary adaption on cranial morphological integration in capuchins (Order Primates, Genus *Cebus*). *PLoS One, 7*(10), e40398.

Manspeizer, W. (1994). The breakup of Pangea and its impact on climate: consequences of Variscan-Alleghanide orogenic collapse. *Geological Society of America Special Papers, 288*, 169-186.

Marivaux, L., Chaimanee, Y., Tafforeau, P., & Jaeger, J. J. (2006). New strepsirrhine primate from the late Eocene of peninsular Thailand (Krabi Basin). *American Journal of Physical Anthropology, 130*(4), 425-434.

Marivaux, L., Welcomme, J.-L., Antoine, P.-O., Métais, G., Baloch, I. M., Benammi, M., Jaeger, J.-J. (2001). A fossil lemur from the Oligocene of Pakistan. *Science, 294*(5542), 587-591.

Marroig, G., & Cheverud, J. M. (2001). A comparison of phenotypic variation and covariation patterns and the role of phylogeny, ecology, and ontogeny during cranial evolution of New World monkeys. *Evolution, 55*(12), 2576-2600.

Marroig, G., & Cheverud, J. M. (2004). Cranial evolution in sakis (*Pithecia*, Platyrrhini) I: interspecific differentiation and allometric patterns. *American Journal of Physical Anthropology, 125*(3), 266-278.

Marroig, G., & Cheverud, J. M. (2005). Size as a line of least evolutionary resistance: diet and adaptive morphological radiation in New World monkeys. *Evolution, 59*(5), 1128-1142.

Marroig, G., & Cheverud, J. M. (2010). Size as a line of least resistance II: direct selection on size or correlated response due to constraints? *Evolution, 64*(5), 1470-1488.

Marroig, G., Vivo, M., & Cheverud, J. (2004). Cranial evolution in sakis (*Pithecia*, Platyrrhini) II: evolutionary processes and morphological integration. *Journal of Evolutionary Biology, 17*(1), 144-155.

Martin, R. D. (1980). Sexual dimorphism and the evolution of higher primates. *Nature, 287*, 273-275.

Martin, R. D. (1984). Body size, brain size and feeding strategies. In D. J. Chivers, B. Wood, & A. Bilsborough (Eds.), *Food acquisition and processing in primates* (pp. 73-103). New York: Plenum Press.

Martin, R. D. (1990). *Primate origins and evolution: a phylogenetic reconstruction*. London: Chapman and Hall.

Martin, R. D. (1993). Primate origins: plugging the gaps. *Nature, 363*, 223-234.

Martin, R. D. (2003). Palaeontology: Combing the primate record. *Nature, 422*(6930), 388-391.

Martin, R. D., Soligo, C., & Tavaré, S. (2007). Primate origins: implications of a Cretaceous ancestry. *Folia Primatologica, 78*(5-6), 277-296.

Martins, E. P., & Hansen, T. F. (1997). Phylogenies and the comparative method: a general approach to incorporating phylogenetic information into the analysis of interspecific data. *The American Naturalist, 149*(4), 646-667

Masters, J., & Lubinsky, D. (1988). Morphological clues to genetic species: multivariate analysis of greater galago sibling species. *American Journal of Physical Anthropology, 75*(1), 37-52.

Masters, J. C., Boniotto, M., Crovella, S., Roos, C., Pozzi, L., & DelPero, M. (2007). Phylogenetic relationships among the Lorisoidea as indicated by craniodental morphology and mitochondrial sequence data. *American journal of primatology, 69*(1), 6-15.

Matsui, A., Rakotondraparany, F., Munechika, I., Hasegawa, M., & Horai, S. (2009). Molecular phylogeny and evolution of prosimians based on complete sequences of mitochondrial DNAs. *Gene, 441*(1), 53-66.

McCarthy, R. C., & Lieberman, D. E. (2001). Posterior maxillary (PM) plane and anterior cranial architecture in primates. *The Anatomical Record, 264*(3), 247-260.

Miller, E. R., Gunnell, G. F., & Martin, R. D. (2005). Deep time and the search for anthropoid origins. *American Journal of Physical Anthropology, 128*(S41), 60-95.

Milton, K. (1981). Distribution patterns of tropical plant foods as an evolutionary stimulus to primate mental development. *American Anthropologist, 83*(3), 534-548.

Mittermeier, R. A., Ganzhorn, J. U., Konstant, W. R., Glander, K., Tattersall, I., Groves, C. P., Mayor, M. I. (2008). Lemur diversity in Madagascar. *International Journal of Primatology, 29*(6), 1607-1656.

Mittermeier, R. A., Louis, E. E., Richardson, M., Schwitzer, C., Langrand, O., Rylands, A. B., Mackinnon, J. (2006). *Lemurs of Madagascar*: USA: Conservation International.

Mitteroecker, P. (2009). The developmental basis of variational modularity: insights from quantitative genetics, morphometrics, and developmental biology. *Evolutionary Biology, 36*(4), 377-385.

Mitteroecker, P., & Bookstein, F. (2008). The evolutionary role of modularity and integration in the hominoid cranium. *Evolution, 62*(4), 943-958.

Mitteroecker, P., & Gunz, P. (2009). Advances in geometric morphometrics. *Evolutionary Biology, 36*(2), 235-247.

Mitteroecker, P., Gunz, P., Bernhard, M., Schaefer, K., & Bookstein, F. L. (2004). Comparison of cranial ontogenetic trajectories among great apes and humans. *Journal of Human Evolution, 46*(6), 679-698.

Montagnon, D., Ravaoarimanana, B., Rakotosamimanana, B., & Rumpler, Y. (2001). Ancient DNA from *Megaladapis edwardsi* (Malagasy subfossil): preliminary results using partial cytochrome b sequence. *Folia Primatologica, 72*(1), 30-32.

Moore, W. J. (1981). *The Mammalian skull*. Cambridge: Cambridge University Press.

Muchlinski, M. N., & Perry, J. M. G. (2011). Anatomical correlates to nectar feeding among the strepsirrhines of Madagascar: implications for interpreting the fossil record. *Anatomy Research International, 2011*, 378431-378431.

Müller, A. E. (1999). Aspects of social life in the fat-tailed dwarf lemur (*Cheirogaleus medius*): inferences from body weights and trapping data. *American Journal of Primatology, 49*(3), 265-280.

Müller, A. E., & Thalmann, U. R. S. (2000). Origin and evolution of primate social organisation: a reconstruction. *Biological Reviews of the Cambridge Philosophical Society, 75*(03), 405-435.

Murphy, W. J., Eizirik, E., O'Brien, S. J., Madsen, O., Scally, M., Douady, C. J., de Jong, W. W. (2001). Resolution of the early placental mammal radiation using Bayesian phylogenetics. *Science, 294*(5550), 2348-2351.

Nagelkerke, N. J. (1991). A note on a general definition of the coefficient of determination. *Biometrika, 78*(3), 691-692.

Nakamichi, M., & Koyama, N. (1997). Social relationships among ring-tailed lemurs (*Lemur catta*) in two free-ranging troops at Berenty Reserve, Madagascar. *International Journal of Primatology, 18*(1), 73-93.

Nash, L. T. (1986). Dietary, behavioral, and morphological aspects of gummivory in primates. *American Journal of Physical Anthropology, 29*(S7), 113-137.

Nash, L. T., Bearder, S. K., & Olson, T. R. (1989). Synopsis of Galago species characteristics. *International Journal of Primatology, 10*(1), 57-80.

Nekaris, K. (2003). Spacing system of the Mysore slender loris (*Loris lydekkerianus lydekkerianus*). *American Journal of Physical Anthropology, 121*(1), 86-96.

Nekaris, K. (2005). Foraging behaviour of the slender loris (*Loris lydekkerianus lydekkerianus*): implications for theories of primate origins. *Journal of Human Evolution, 49*(3), 289-300.

Nekaris, K. (2014). Extreme primates: ecology and evolution of Asian lorises. *Evolutionary Anthropology: Issues, News, and Reviews, 23*(5), 177-187.

Nekaris, K., & Bearder, S. K. (2011). The lorisiform primtes of Asia and mainland Africa. In C. J. Campbell, A. Fuentes, K. C. MacKinnon, S. K. Bearder, & R. M. Stumpf (Eds.), *Primates in Perspective* (Vol. 2). New York: Oxford University Press.

Nekaris, K., & Jaffe, S. (2007). Unexpected diversity of slow lorises (*Nycticebus* sp.) within the Javan pet trade: implications for slow loris taxonomy. *Contributions to Zoology, 76*(3), 187-196.

Nekaris, K., Moore, R. S., Rode, E. J., & Fry, B. G. (2013). Mad, bad and dangerous to know: the biochemistry, ecology and evolution of slow loris venom. *Journal of Venom and Animal Toxins including Tropical Diseases, 19*(1), 21-31.

Nekaris, K., & Rasmussen, D. T. (2003). Diet and feeding behavior of Mysore slender lorises. *International Journal of Primatology, 24*(1), 33-46.

Nekaris, K., Starr, C. R., Collins, R. L., & Wilson, A. (2010). Comparative ecology of exudate feeding by lorises (*Nycticebus, Loris*) and pottos (*Perodicticus, Arctocebus*). In L. T. Nash & A. M. Burrows (Eds.), *The evolution of exudativory in primates* (pp. 155-168). New York: Springer.

Newell, N. D. (1949). Phyletic size increase, an important trend illustrated by fossil invertebrates. *Evolution*, 103-124.

Ni, X., Wang, Y., Hu, Y., & Li, C. (2004). A euprimate skull from the early Eocene of China. *Nature, 427*(6969), 65-68.

O'Higgins, P. (2000). The study of morphological variation in the hominid fossil record: biology, landmarks and geometry. *Journal of Anatomy, 197*(01), 103-120.

O'Mara, M. T., Gordon, A. D., Catlett, K. K., Terranova, C. J., & Schwartz, G. T. (2012). Growth and the development of sexual size dimorphism in lorises and galagos. *American Journal of Physical Anthropology, 147*(1), 11-20

O'Meara, B. C. O. (2015). Model selection using the akaike information criterion (AIC). from http://www.brianomeara.info/tutorials/aic

O'Neill, M. C., & Dobson, S. D. (2008). The degree and pattern of phylogenetic signal in primate long-bone structure. *Journal of Human Evolution, 54*(3), 309-322.

Olson, E. C., & Miller, R. L. (1951). A mathematical model applied to a study of the evolution of species. *Evolution, 5*(4), 325-338.

Orlando, L., Calvignac, S., Schnebelen, C., Douady, C. J., Godfrey, L. R., & Hänni, C. (2008). DNA from extinct giant lemurs links archaeolemurids to extant indriids. *BMC Evolutionary Biology, 8*(1), 121.

Pagel, M. (1992). A method for the analysis of comparative data. *Journal of Theoretical Biology, 156*(4), 431-442.

Pagel, M. (1999). Inferring the historical patterns of biological evolution. *Nature, 401*(6756), 877-884.

Parsons, T. E., Schmidt, E. J., Boughner, J. C., Jamniczky, H. A., Marcucio, R. S., & Hallgrímsson, B. (2011). Epigenetic integration of the developing brain and face. *Developmental Dynamics, 240*(10), 2233-2244.

Pastorini, J., Forstner, M. R., & Martin, R. D. (2002). Phylogenetic relationships among Lemuridae (Primates): evidence from mtDNA. *Journal of Human Evolution, 43*(4), 463-478.

Pastorini, J., Zaramody, A., Curtis, D. J., Nievergelt, C. M., & Mundy, N. I. (2009). Genetic analysis of hybridization and introgression between wild mongoose and brown lemurs. *BMC Evolutionary Biology, 9*(1), 32.

Pavlicev, M., Cheverud, J. M., & Wagner, G. P. (2009). Measuring morphological integration using eigenvalue variance. *Evolutionary Biology, 36*(1), 157-170.

Pavlicev, M., Kenney-Hunt, J. P., Norgard, E. A., Roseman, C. C., Wolf, J. B., & Cheverud, J. M. (2008). Genetic variation in pleiotropy: differential epistasis as a source of variation in the allometric relationship between long bone lengths and body weight. *Evolution, 62*(1), 199-213.

Perelman, P., Johnson, W. E., Roos, C., Seuánez, H. N., Horvath, J. E., Moreira, M., . . . Rumpler, Y. (2011). A molecular phylogeny of living primates. *PLoS Genet, 7*(3), e1001342.

Perez, V. R., Godfrey, L. R., Nowak-Kemp, M., Burney, D. A., Ratsimbazafy, J., & Vasey, N. (2005). Evidence of early butchery of giant lemurs in Madagascar. *Journal of Human Evolution, 49*(6), 722-742.

Perez, S. I., Klaczko, J., Rocatti, G., dos-Reis, S. F., & Dos Reis, S. F. (2011). Patterns of cranial shape diversification during the phylogenetic branching process of New World monkeys (Primates: Platyrrhini). *Journal of Evolutionary Biology, 24*(8), 1826-1835.

Perkin, A., Bearder, S., Honess, P., & Butynski, T. M. (2008). *Galagoides rondoensis*. *The IUCN Red List of Threatened Species*. Version 2015.2. Retrieved 09/07/2015, 2015, from www.iucnredlist.org

Petter, J. J., Albignac, R., & Rumpler, Y. (1977). Lemurine mammals (Primates, prosimians). *Faune Madagascar, 44*, 1-513.

Pézard, A. (1918). Le conditionnement physiologique des caractères sexuels secondaires chez les oiseaux. *Bulletin Biologique de la France et de la Belgique* , *52*, 1-176.

Pilbeam, D., & Gould, S. J. (1974). Size and scaling in human evolution. *Science, 186*(4167), 892-901.

Polly, P. D. (2001). On morphological clocks and paleophylogeography: towards a timescale for *Sorex* hybrid zones. *Genetica, 112*, 339-357.

Polly, P. D. (2005). Development and phenotypic correlations: the evolution of tooth shape in *Sorex araneus*. *Evolution and Development, 7*(1), 29-41.

Porter, L. M. (2001). Social organization, reproduction and rearing strategies of *Callimico goeldii*: new clues from the wild. *Folia Primatologica, 72*(2), 69-79.

Porto, A., de Oliveira, F. B., Shirai, L. T., De Conto, V., & Marroig, G. (2009). The evolution of modularity in the mammalian skull I: morphological integration patterns and magnitudes. *Evolutionary Biology, 36*(1), 118-135

Poux, C., Madsen, O., Marquard, E., Vieites, D. R., de Jong, W. W., & Vences, M. (2005). Asynchronous colonization of Madagascar by the four endemic clades of primates,

tenrecs, carnivores, and rodents as inferred from nuclear genes. *Systematic Biology, 54*(5), 719-730.

Pozzi, L., Hodgson, J. A., Burrell, A. S., Sterner, K. N., Raaum, R. L., & Disotell, T. R. (2014). Primate phylogenetic relationships and divergence dates inferred from complete mitochondrial genomes. *Molecular Phylogenetics and Evolution, 75*(0), 165-183.

Premkumar, S. (2011). *Textbook of craniofacial growth.* New Deli: Jaypee Brothers Medical Publishers Ltd.

Preuss, T. M. (2009). Primate brain evolution. In J. H. Kaas (Ed.), *Evolutionary neuroscience* (pp. 793-825). Oxford: Academic Press.

Price, T. (1997). Correlated evolution and independent contrasts. *Philosophical Transactions of the Royal Society of London B: Biological Sciences, 352*(1352), 519-529.

Profant, L. (1995). Historical allometric inputs to interspecific patterns of craniofacial diversity in the cercopithecine tribe Papionini. *American Journal of Physical Anthropology, 20*, 175.

Quinn, A., & Wilson, D. E. (2004). *Daubentonia madagascariensis*. *Mammalian Species*, *170*, 1-6.

Rabinowitz, P. D., Coffin, M. F., & Falvey, D. (1983). The separation of Madagascar and Africa. *Science, 220*(4592), 67-69.

Radespiel, U. (2000). Sociality in the gray mouse lemur (*Microcebus murinus*) in northwestern Madagascar. *American Journal of Primatology, 51*(1), 21-40.

Radespiel, U., Cepok, S., Zietemann, V., & Zimmermann, E. (1998). Sex-specific usage patterns of sleeping sites in grey mouse lemurs (*Microcebus murinus*) in northwestern Madagascar. *American Journal of Primatology, 46*(1), 77-84.

Ramsier, M. A., & Dominy, N. J. (2012). Receiver bias and the acoustic ecology of aye-ayes (*Daubentonia madagascariensis*). *Communicative and Integrative Biology, 5*(6), 637-640.

Rasmussen, D. T., & Izard, M. K. (1988). Scaling of growth and life history traits relative to body size, brain size, and metabolic rate in lorises and galagos (Lorisidae, Primates). *American Journal of Physical Anthropology, 75*(3), 357-367.

Rasmussen, T., & Nekaris, K. (1998). Evolutionary history of lorisiform primates. *Folia Primatologica, 69*(Suppl. 1), 250-285.

Rasoloharijaona, S., Randrianambinina, B., Braune, P., & Zimmermann, E. (2006). Loud calling, spacing, and cohesiveness in a nocturnal primate, the Milne Edwards'

sportive lemur (*Lepilemur edwardsi*). *American Journal of Physical Anthropology, 129*(4), 591-600.

Rasoloharijaona, S., Randrianambinina, B., & Zimmermann, E. (2008). Sleeping site ecology in a rain-forest dwelling nocturnal lemur (*Lepilemur mustelinus*): Implications for sociality and conservation. *American Journal of Primatology, 70*(3), 247-253.

Rasolooarison, R., Goodman, S., & Ganzhorn, J. (2000). Taxonomic revision of mouse lemurs (*Microcebus*) in the western portions of Madagascar. *International Journal of Primatology, 21*(6), 963-1019.

Ravosa, M. J. (1992). Allometry and heterochrony in extant and extinct Malagasy primates. *Journal of Human Evolution, 23*(2), 197-217.

Ravosa, M. J. (1998). Cranial allometry and geographic variation in slow lorises (*Nycticebus*). *American Journal of Primatology, 45*(3), 225-243.

Ravosa, M. J. (2007). Cranial ontogeny, diet, and ecogeographic variation in African lorises. *American journal of primatology, 69*(1), 59-73.

Ravosa, M. J., & Daniel, A. N. (2010). Ontogeny and phyletic size change in living and fossil lemurs. *American Journal of Primatology, 72*(2), 161-172.

Ravosa, M. J., Daniel, A. N., & Costley, D. B. (2010). Allometry and evolution in the galago skull. *Folia Primatologica, 81*(4), 177-196.

Ravosa, M. J., Noble, V. E., Hylander, W. L., Johnson, K. R., & Kowalski, E. M. (2000). Masticatory stress, orbital orientation and the evolution of the primate postorbital bar. *Journal of Human Evolution, 38*(5), 667-693.

Rehg, J., & Leigh, S. (1999). Estimating sexual dimorphism and size differences in the fossil record: a test of methods. *American Journal of Physical Anthropology, 110*(1), 95-104.

Rensch, B. (1948). Historical changes correlated with evolutionary changes in body size. *Evolution, 2*, 218-290.

Revell, L. J. (2012). phytools: an R package for phylogenetic comparative biology (and other things). *Methods in Ecology and Evolution, 3*(2), 217-223.

Revell, L. J., Harmon, L. J., & Collar, D. C. (2008). Phylogenetic signal, evolutionary process, and rate. *Systematic Biology, 57*(4), 591-601.

Rohlf, F. J. (1998). On applications of geometric morphometrics to studies of ontogeny and phylogeny. *Systematic Biology*, 147-158.

Rohlf, F. J. (1999). Shape statistics: procrustes superimpositions and tangent spaces. *Journal of Classification, 16*(2), 197-233.

Rohlf, F. J. (2003). Bias and error in estimates of mean shape in geometric morphometrics. *Journal of Human Evolution, 44*(6), 665-683.

Rohlf, F. J., & Marcus, L. F. (1993). A revolution morphometrics. *Trends in Ecology & Evolution, 8*(4), 129-132.

Rögl, F. (1997). Palaeogeographic considerations for Mediterranean and Paratethys seaways (Oligocene to Miocene). *Annalen des Naturhistorischen Museums in Wien. Serie A für Mineralogie und Petrographie, Geologie und Paläontologie, Anthropologie und Prähistorie*, 279-310.

Roos, C., Schmitz, J., & Zischler, H. (2004). Primate jumping genes elucidate strepsirrhine phylogeny. *Proceedings of the National Academy of Sciences of the United States of America, 101*(29), 10650-10654.

Ross, C. (1995). Allometric and functional influences on primate orbit orientation and the origins of the Anthropoidea. *Journal of Human Evolution, 29*(3), 201-227.

Ross, C. (1996). Adaptive explanation for the origins of the Anthropoidea (Primates). *American Journal of Primatology, 40*(3), 205-230.

Ross, C. (2000). Into the light: the origin of Anthropoidea. *Annual Review of Anthropology*, 147-194.

Ross, C. (2013). Complexity, modularity, and integration in the human head: the evolution of the human head. *Journal of Human Evolution, 64*(1), 56-67.

Ross, C., & Ravosa, M. J. (1993). Basicranial flexion, relative brain size, and facial kyphosis in nonhuman primates. *American Journal of Physical Anthropology, 91*(3), 305-324.

Ruvolo, M. (1997). Molecular phylogeny of the hominoids: inferences from multiple independent DNA sequence data sets. *Molecular Biology and Evolution, 14*(3), 248-265.

Sacher, G. A. (1982). The role of brain maturation in the evolution of the primates. In E. Armstrong & D. Falk (Eds.), *Primate Brain Evolution* (pp. 97-112). New York: Plenum Press.

Sailer, L. D., Gaulin, S. J., Boster, J. S., & Kurland, J. A. (1988). Measuring the relationship between dietary quality and body size in primates. *Primates, 26*(1), 14-27.

Sanderson, M. J., Boss, D., Chen, D., Cranston, K. A., & Wehe, A. (2008). The PhyLoTA Browser: processing GenBank for molecular phylogenetics research. *Systematic Biology, 57*(3), 335-346.

Schluter, D. (1996). Adaptive radiation along genetic lines of least resistance. *Evolution*, 1766-1774

Schultz, A. H. (1940).The size of the orbit and of the eye in primates. *American Journal of Physical Anthropology, 26*, 389-408

Schwab, D. (2000). A preliminary study of spatial distribution and mating system of pygmy mouse lemurs(*Microcebus cf. myoxinus*). *American Journal of Primatology, 51*(1), 41-60.

Schwartz, J. H. (1983). The evolutionary relationships of man and orang-utans. *Nature, 308*(5959), 501-505.

Schwitzer, C., Mittermeier, R., Davies, N., Johnson, S., Ratsimbazafy, J., Razafindramanana, J., Rajaobelina, S. (2013). *Lemurs of Madagascar: a strategy for their conservation 2013–2016*. IUCN SSC Primate Specialist Group, Bristol Conservation and Scienec Foundation, and Conservation International, pp. 185.

Schwitzer, C., Mittermeier, R., Rylands, A., Taylor, L., Chiozza, F., Williamson, E., Clark, F. (2014). *Primates in peril: The world's 25 most endangered primates 2012–2014.* IUCN SSC Primate Specialist Group (PSG), International Primatological Society (IPS), Conservation International (CI), and Bristol Zoological Society, pp. 87.

Schwitzer, N., Kaumanns, W., Seitz, P. C., & Schwitzer, C. (2007). Cathemeral activity patterns of the blue-eyed black lemur *Eulemur macaco flavifrons* in intact and degraded forest fragments. *Endangered Species Research, 3*(2), 239-247.

Scotland, R.W. (2011). What id parallelism? *Evolution & development, 13*(2), 214-227.

Seiffert, E. R. (2006). Revised age estimates for the later Paleogene mammal faunas of Egypt and Oman. *Proceedings of the National Academy of Sciences of the United States of America, 103*(13), 5000-5005.

Seiffert, E. R. (2007). Evolution and extinction of Afro-Arabian primates near the Eocene-Oligocene boundary. *Folia Primatologica, 78*(5-6), 314-327.

Seiffert, E. R. (2012). Early primate evolution in Afro-Arabia. *Evolutionary Anthropology: Issues, News, and Reviews, 21*(6), 239-253.

Seiffert, E. R., Simons, E. L., & Attia, Y. (2003). Fossil evidence for an ancient divergence of lorises and galagos. *Nature, 422*(6930), 421-424.

Seiffert, E. R., Simons, E. L., Boyer, D. M., Perry, J. M., Ryan, T. M., & Sallam, H. M. (2010). A fossil primate of uncertain affinities from the earliest late Eocene of Egypt. *Proceedings of the National Academy of Sciences, 107*(21), 9712-9717.

Seiffert, E. R., Simons, E. L., Ryan, T. M., & Attia, Y. (2005). Additional remains of *Wadilemur elegans*, a primitive stem galagid from the late Eocene of Egypt. *Proceedings of the National Academy of Sciences USA, 102*(32), 11396-11401.

Shoshani, J., Groves, C. P., Simons, E. L., & Gunnell, G. F. (1996). Primate phylogeny: morphological vs molecular results. *Molecular Phylogenetics and Evolution, 5*(1), 102-154.

Singh, N., Harvati, K., Hublin, J.-J., & Klingenberg, C. P. (2012). Morphological evolution through integration: A quantitative study of cranial integration in *Homo, Pan, Gorilla* and, *Pongo*. *Journal of Human Evolution, 62*(1), 155-164.

Singleton, M. (2002). Patterns of cranial shape variation in the Papionini (Primates: Cercopithecinae). *Journal of Human Evolution, 42*(5), 547-578.

Slice, D. E., Bookstein, F. L., Marcus, l. F., and Rholf, F. J. (1996). Appendix I - a glossary for geometric morphometrics. In L. F. Marcus, Corti, M., Loy, A., Naylor, G. J. P. and Slice, D. E. (Ed.), *Advances in Morphometrics*. New York: Plenum Press.

Smaers, J. B., Dechmann, D. K., Goswami, A., Soligo, C., & Safi, K. (2012). Comparative analyses of evolutionary rates reveal different pathways to encephalization in bats, carnivorans, and primates. *Proceedings of the National Academy of Sciences USA, 109*(44), 18006-18011.

Smaers, J. B., Steele, J., Case, C. R., & Amunts, K. (2013). Laterality and the evolution of the prefronto-cerebellar system in anthropoids. *Annals of the New York Academy of Sciences, 1288*(1), 59-69.

Smaers, J. B., & Vinicius, L. (2009). Inferring macro-evolutionary patterns using an adaptive peak model of evolution. *Evolutionary Ecology Research, 11*(7), 991-1015.

Smith, A.S, Brown, J.H., Haskell, J.P., Lyons S.K., Alroy, J., Charnov, E.L., Willig, M.R. (2004). Similarity of mammalian body size across the taxonomic hierarchy and across space and time. *The American Naturalist, 163*(5), 672-691.

Smith, H. F. (2009). Which cranial regions reflect molecular distances reliably in humans? Evidence from three-dimensional morphology. *American Journal of Human Biology, 21*(1), 36-47.

Smith, R. J. (1994). Degrees of freedom in interspecific allometry: an adjustment for the effects of phylogenetic constraint. *American Journal of Physical Anthropology, 93*(1), 95-107.

Soligo, C. (2006). Correlates of body mass evolution in primates. *American Journal of Physical Anthropology, 130*(3), 283-293

Soligo, C. (2007). Invading Europe: did climate or geography trigger early Eocene primate dispersals? *Folia Primatologica, 78*(5-6), 297-313.

Soligo, C., & Müller, A. E. (1999). Nails and claws in primate evolution. *Journal of Human Evolution, 36*(1), 97-114.

Springer, M. S., Meredith, R. W., Gatesy, J., Emerling, C. A., Park, J., Rabosky, D. L., Janečka, J. E. (2012). Macroevolutionary dynamics and historical biogeography of primate diversification inferred from a species supermatrix. *PLoS One, 7,* e49521.

Springer, M. S., Meredith, R. W., Janecka, J. E., & Murphy, W. J. (2011). The historical biogeography of Mammalia. *Philosophical Transactions of the Royal Society of London B: Biological Sciences, 366*(1577), 2478-2502.

Starr, C., & Nekaris, K. (2013). Obligate exudativory characterizes the diet of the pygmy slow loris *Nycticebus pygmaeus*. *American Journal of Primatology, 75*(10), 1054-1061.

Steiper, M. E., & Seiffert, E. R. (2012). Evidence for a convergent slowdown in primate molecular rates and its implications for the timing of early primate evolution. *Proceedings of the National Academy of Sciences USA, 109*(16), 6006-6011.

Sterling, E. J. (1994). Aye-ayes: specialists on structurally defended resources. *Folia Primatologica, 62*(1-3), 142-154.

Stock, D. W. (2001). The genetic basis of modularity in the development and evolution of the vertebrate dentition. *Philosophical Transactions of the Royal Society of London. Series B: Biological Sciences, 356*(1414), 1633-1653.

Storey, M., Mahoney, J. J., Saunders, A. D., Duncan, R. A., Kelley, S. P., & Coffin, M. F. (1995). Timing of hot spot—related volcanism and the breakup of Madagascar and India. *Science, 267*(5199), 852-855.

Strait, S. G. (1993). Differences in occlusal morphology and molar size in frugivores and faunivores. *Journal of Human Evolution, 25*(6), 471-484.

Streicher, U. (2005). *Aspects of ecology and conservation of the pygmy loris* Nycticebus pygmaeus i*n Vietnam.* Ph.D. Dissertation, Ludwig-Maximilians-Universität München.

Strier, K.B. (2007) *Primate Behavioural Ecology (3rd Ed.)*. Boston: Pearson Education.

Sussman, R. W. (1991). Primate origins and the evolution of angiosperms. *American Journal of Primatology, 23*(4), 209-223.

Sussman, R. W., & Raven, P. H. (1978). Pollination by lemurs and marsupials - archaic coevolutionary system. *Science, 200*(4343), 731-736.

Symonds, M. R. E., & Blomberg, S. P. (2014). A primer on phylogenetic generalised least squares. In L. Z. Garamszegi (Ed.), *Modern Phylogenetic Comparative Methods and Their Application in Evolutionary Biology* (pp. 105-130). Berlin: Springer.

Tan, C. L. (1999). Group composition, home range size, and diet of three sympatric bamboo lemur species (genus *Hapalemur*) in Ranomafana National Park, Madagascar. *International Journal of Primatology, 20*(4), 547-566.

Tan, C. L., & Drake, J. H. (2001). Evidence of tree gouging and exudate eating in pygmy slow lorises (*Nycticebus pygmaeus*). *Folia Primatologica, 72*(1), 37-39.

Tattersall, I. (2007). Origin of the Malagasy strepsirhine primates. In L. Gould & M. Sauther (Eds.), *Lemurs: Ecology and Adaptation* (pp. 3-17). New York: Springer .

Tavaré, S., Marshall, C. R., Will, O., Soligo, C., & Martin, R. D. (2002). Using the fossil record to estimate the age of the last common ancestor of extant primates. *Nature, 416*(6882), 726-729.

Team, R. C. (2015). *R: A Language and Environment for Statistical Computing*. R Foundation for Statistical Computing, Vienna, Austria.

Thorén, S., Lindenfors, P., & Kappeler, P. M. (2006). Phylogenetic analyses of dimorphism in primates: evidence for stronger selection on canine size than on body size. *American Journal of Physical Anthropology, 130*(1), 50-59.

Thorn, J. S., Nijman, V., Smith, D., & Nekaris, K. (2009). Ecological niche modelling as a technique for assessing threats and setting conservation priorities for Asian slow lorises (Primates: *Nycticebus)*. *Diversity and Distributions, 15*(2), 289-298.

Tosi, A. J., Detwiler, K. M., & Disotell, T. R. (2005). X-chromosomal window into the evolutionary history of the guenons (Primates: Cercopithecini). *Molecular Phylogenetics and Evolution, 36*(1), 58-66.

Uhlenbeck, G. E., & Ornstein, L. S. (1930). On the theory of the Brownian motion. *Physical Review, 36*(5), 823.

Ungar, P. (1998). Dental allometry, morphology, and wear as evidence for diet in fossil primates. *Evolutionary Anthropology: Issues, News and REviews 6*(6), 205-217.

Viðarsdóttir, U. S., O'Higgins, P., & Stringer, C. (2002). A geometric morphometric study of regional differences in the ontogeny of the modern human facial skeleton. *Journal of Anatomy, 201*(3), 211-229.

Viguier, B. (2002). Is the morphological disparity of lemur skulls (Primates) controlled by phylogeny and/or environmental constraints? *Biological Journal of the Linnean Society, 76*(4), 577-590.

Viguier, B. (2004). Functional adaptations in the craniofacial morphology of Malagasy primates: shape variations associated with gummivory in the family Cheirogaleidae. *Annals of Anatomy-Anatomischer Anzeiger, 186*(5), 495-501.

Villmoare, B. A., Dunmore, C., Kilpatrick, S., Oertelt, N., Depew, M. J., & Fish, J. L. (2014). Craniofacial modularity, character analysis, and the evolution of the premaxilla in early African hominins. *Journal of Human Evolution, 77*, 143-154.

Vinyard, C. J., & Hanna, J. (2005). Molar scaling in strepsirrhine primates. *Journal of Human Evolution, 49*(2), 241-269.

Vinyard, C. J., Wall, C. E., Williams, S. H., & Hylander, W. L. (2003). Comparative functional analysis of skull morphology of tree-gouging primates. *American Journal of Physical Anthropology, 120*(2), 153-170.

von Cramon-Taubadel, N. (2009). Revisiting the homoiology hypothesis: the impact of phenotypic plasticity on the reconstruction of human population history from craniometric data. *Journal of Human Evolution, 57*(2), 179-190.

von Cramon-Taubadel, N. (2014). The microevolution of modern human cranial variation: implications for hominin and primate evolution. *Annals of Human Biology, 41*(4), 323-335.

von Cramon-Taubadel, N., & Lycett, S. J. (2014). A comparison of catarrhine genetic distances with pelvic and cranial morphology: implications for determining hominin phylogeny. *Journal of Human Evolution, 77*, 179-186.

Wagner, G. P., Pavlicev, M., & Cheverud, J. M. (2007). The road to modularity. *Nature Reviews Genetics, 8*(12), 921-931.

Wagner, G. P., & Zhang, J. (2011). The pleiotropic structure of the genotype–phenotype map: the evolvability of complex organisms. *Nature Reviews Genetics, 12*(3), 204-213.

White, T., & Searle, J. (2008). Mandible asymmetry and genetic diversity in island populations of the common shrew, *Sorex araneus*. *Journal of Evolutionary Biology, 21*(2), 636-641.

Wiens, F. (2002). *Behavior and ecology of wild slow lorises* (Nycticebus coucang)*: Social organization, infant care system, and diet.* Ph.D. Dissertation, Bayreuth University.

Wiens, F., & Zitzmann, A. (2003). Social dependence of infant slow lorises to learn diet. *International Journal of Primatology, 24*(5), 1007-1021.

Wiens, F., Zitzmann, A., & Hussein, N. A. (2006). Fast food for slow lorises: is low metabolism related to secondary compounds in high-energy plant diet? *Journal Information, 87*(4), 790-798.

Wiens, J. J., Ackerly, D. D., Allen, A. P., Anacker, B. L., Buckley, L. B., Cornell, H. V., Stephens, P. R. (2010). Niche conservatism as an emerging principle in ecology and conservation biology. *Ecology Letters, 13*(10), 1310-1324.

Wilkinson, R. D., Steiper, M. E., Soligo, C., Martin, R. D., Yang, Z., & Tavaré, S. (2010). Dating primate divergences through an integrated analysis of palaeontological and molecular data. *Systematic Biology*, *60*(1), 16-31

Williams, B. A. (2007). Comparing levels of homoplasy in the primate skeleton. *Journal of Human Evolution, 52*(5), 480-489.

Williams, M. F. (2002). Primate encephalization and intelligence. *Medical Hypotheses, 58*(4), 284-290.

Wilmet, L., Schwitzer, C., Devillers, P., Beudels-Jamar, R. C., & Vermeulen, C. (2014). Speciation in Malagasy lemurs: a review of the cryptic diversity in genus *Lepilemur*. *Biotechnologie, Agronomie, Société et Environnement, 18*(4), 577-588.

Wilson, D. E., & Reeder, D. M. (2005). *Mammal species of the world: a taxonomic and geographic reference*. USA: John Hopkins University Press.

Wood, A. R., Zelditch, M. L., Rountrey, A. N., Eiting, T. P., Sheets, H. D., & Gingerich, P. D. (2007). Multivariate stasis in the dental morphology of the Paleocene-Eocene condylarth *Ectocion*. *Journal Information, 33*(2), 248-260.

Wood, B., & Collard, M. (1999). The changing face of genus *Homo*. *Evolutionary Anthropology: Issues, News, and Reviews, 8*(6), 195-207.

Wright, P.C. (1994). Thebehaviour and ecology pf the owl monkey. *Aotus: The owl monkey*, 97-112.

Wright, P. C., & Martin, L. B. (1995). Predation, pollination and torpor in two nocturnal prosimians: *Cheirogaleus major* and *Microcebus rufus* in the rain forest of Madagascar. In L. Alterman, G. Doyle, & M. K. Izard (Eds.), *Creatures of the dark* (pp. 45-60). New York: Plenum Press.

Wyner, Y., DeSalle, R., & Absher, R. (2000). Phylogeny and character behavior in the family Lemuridae. *Molecular Phylogenetics and Evolution, 15*(1), 124-134.

Yamashita, N., Tan, C. L., Vinyard, C. J., & Williams, C. (2010). Semi-quantitative tests of cyanide in foods and excreta of three *Hapalemur* species in Madagascar. *American Journal of Primatology, 72*(1), 56-61.

Yoder, A. D. (1994). Relative position of the Cheirogaleidae in strepsirhine phylogeny: a comparison of morphological and molecular methods and results. *American Journal of Physical Anthropology, 94*(1), 25-46.

Yoder, A. D. (1997). Back to the future: a synthesis of strepsirrhine systematics. *Evolutionary Anthropology: Issues, News, and Reviews, 6*(1), 11-22.

Yoder, A. D., & Irwin, J. A. (1999). Phylogeny of the Lemuridae: effects of character and taxon sampling on resolution of species relationships within *Eulemur*. *Cladistics, 15*(3), 351-361.

Yoder, A. D., & Yang, Z. (2004). Divergence dates for Malagasy lemurs estimated from multiple gene loci: geological and evolutionary context. *Molecular Ecology, 13*(4), 757-773.

Young, N. M. (2005). Estimating hominoid phylogeny from morphological data: character choice, phylogenetic signal and postcranial data. *Interpreting the Past.* Brill Academic, Boston, 1-13.

Zaramody, A., & Pastorini, J. (2001). Indications for hybridisation between red-fronted lemurs (*Eulemur fulvus rufus*) and mongoose lemurs (*E. mongoz*) in Northwest Madagascar. *Lemur News, 6*, 28-31.

Zelditch, M. L., Swiderski, D. L., & Sheets, H. D. (2012). *Geometric morphometrics for biologists: a primer.* USA: Academic Press.

– Appendices –

– Appendix 1 –

Sample size testing

The accuracy of mean size (centroid size (CS)) and standard deviation (SD) of size at reduced sample size

Galago senegalensis mean size (CS) and SD of size for observed, bootstrap and random subsamples

G. senegalensis	Sample size	Mean of CS	Percentile		SD of CS	Percentile	
			2.5th	97.5th		2.5th	97.5th
Observed	175	103.18	_	_	3.80	_	_
Bootstrap	175	103.17	102.59	103.74	3.79	3.39	4.21
Subsamples	170	103.17	102.63	103.77	3.76	3.32	4.24
	165	103.19	102.59	103.76	3.80	3.34	4.24
	160	103.18	102.65	103.78	3.78	3.33	4.28
	155	103.17	102.60	103.73	3.78	3.32	4.26
	150	103.18	102.60	103.78	3.77	3.32	4.22
	145	103.18	102.59	103.82	3.78	3.32	4.25
	140	103.19	102.58	103.81	3.77	3.30	4.25
	135	103.19	102.59	103.84	3.77	3.28	4.25
	130	103.18	102.55	103.86	3.77	3.25	4.32
	125	103.19	102.54	103.83	3.78	3.31	4.31
	120	103.17	102.50	103.87	3.79	3.27	4.31
	115	103.19	102.51	103.89	3.77	3.27	4.36
	110	103.17	102.41	103.85	3.76	3.25	4.37
	105	103.18	102.46	103.94	3.78	3.23	4.34
	100	103.16	102.44	103.95	3.79	3.21	4.36
	95	103.16	102.43	103.91	3.77	3.18	4.38
	90	103.18	102.41	103.95	3.77	3.17	4.39
	85	103.17	102.36	104.01	3.78	3.19	4.40
	80	103.17	102.35	104.04	3.77	3.12	4.46
	75	103.20	102.34	104.02	3.79	3.15	4.47
	70	103.20	102.32	104.08	3.78	3.10	4.52
	65	103.16	102.30	104.07	3.80	3.11	4.52
	60	103.20	102.27	104.19	3.78	3.07	4.54
	55	103.17	102.20	104.21	3.76	3.03	4.54
	50	103.20	102.14	104.25	3.77	2.90	4.69
	45	103.19	102.12	104.34	3.79	2.98	4.73
	40	103.18	102.07	104.32	3.76	2.88	4.76
	35	103.16	101.93	104.45	3.75	2.85	4.78
	30	103.15	101.75	104.60	3.74	2.75	4.81
	25	103.18	101.78	104.74	3.71	2.64	5.00
	20	103.21	101.59	104.93	3.72	2.62	5.20
	15	103.18	101.15	104.96	3.73	2.38	5.34
	10	103.16	101.03	105.51	3.69	1.99	5.78
	5	103.15	100.00	106.61	3.47	1.31	6.58

Microcebus murinus mean size (CS) and SD of size for observed, bootstrap and random subsamples

M. murinus	Sample size	Mean CS	Percentile		SD of CS	Percentile	
			2.5th	97.5th		2.5th	97.5th
Observed	72	76.40	_	_	2.88	_	_
Bootstrap	72	76.41	75.76	77.06	2.85	2.44	3.27
Subsamples	70	76.40	75.75	77.05	2.86	2.45	3.30
	65	76.39	75.69	77.09	2.85	2.41	3.30
	60	76.39	75.62	77.13	2.85	2.42	3.27
	55	76.40	75.63	77.17	2.85	2.37	3.35
	50	76.39	75.57	77.18	2.87	2.37	3.34
	45	76.44	75.60	77.28	2.83	2.29	3.34
	40	76.41	75.54	77.34	2.85	2.28	3.39
	35	76.42	75.50	77.36	2.84	2.25	3.45
	30	76.39	75.42	77.40	2.84	2.23	3.50
	25	76.37	75.22	77.56	2.85	2.14	3.56
	20	76.40	75.15	77.70	2.84	2.09	3.67
	15	76.38	74.88	77.77	2.84	1.98	3.78
	10	76.36	74.58	78.04	2.79	1.67	4.06
	5	76.38	73.66	78.93	2.68	1.07	4.46

Nycticebus coucang mean size (CS) and SD of size for observed, bootstrap and random subsamples

N. coucang	Sample size	Mean CS	Percentile		SD of CS	Percentile	
			2.5th	97.5th		2.5th	97.5th
Observed	69	146.04	_	_	7.76	_	_
Bootstrap	69	146.04	144.25	147.90	7.68	6.35	9.02
Subsamples	65	146.05	144.13	147.94	7.67	6.29	9.08
	60	146.03	144.07	148.05	7.66	6.28	9.04
	55	146.10	144.12	148.23	7.69	6.21	9.25
	50	146.03	143.98	148.09	7.63	6.18	9.19
	45	146.05	143.89	148.25	7.61	6.05	9.21
	40	146.08	143.63	148.51	7.64	5.95	9.41
	35	145.99	143.67	148.58	7.61	5.72	9.47
	30	146.12	143.33	148.95	7.61	5.48	9.67
	25	146.15	143.26	149.19	7.58	5.41	9.75
	20	145.94	142.70	149.32	7.54	5.19	10.33
	15	146.03	142.42	150.11	7.59	4.84	10.65
	10	146.21	141.41	150.72	7.48	4.11	11.46
	5	146.01	139.69	153.08	7.04	2.57	12.92

Otolemur crassicaudatus mean size (CS) and SD of size for observed, bootstrap and random subsamples

O. crassicaudatus	**Sample size**	**Mean CS**	**Percentile**		**SD of CS**	**Percentile**	
			2.5th	**97.5th**		**2.5th**	**97.5th**
Observed	101	166.90	_	_	10.05	_	_
Bootstrap	101	166.91	164.94	168.83	9.98	8.81	11.13
Subsamples	100	166.90	164.87	168.77	9.96	8.78	11.13
	95	166.89	164.74	168.93	10.00	8.75	11.23
	90	166.89	164.78	168.89	9.96	8.69	11.20
	85	166.86	164.77	169.09	9.97	8.80	11.18
	80	166.91	164.82	168.99	9.96	8.69	11.25
	75	166.82	164.55	169.05	9.96	8.55	11.33
	70	166.94	164.53	169.17	9.98	8.59	11.45
	65	166.87	164.41	169.30	9.95	8.47	11.49
	60	166.94	164.47	169.39	9.96	8.34	11.46
	55	166.92	164.32	169.71	9.95	8.33	11.56
	50	166.93	164.14	169.71	9.96	8.30	11.65
	45	166.89	164.26	169.76	9.97	8.30	11.68
	40	166.91	163.91	169.91	9.94	8.11	11.75
	35	166.94	163.61	170.34	9.99	7.99	11.90
	30	166.81	163.14	170.33	9.88	7.67	12.01
	25	166.90	162.75	170.63	9.91	7.41	12.32
	20	166.88	162.44	171.09	9.88	7.12	12.58
	15	166.82	161.71	171.62	9.80	6.63	12.79
	10	166.87	160.68	172.90	9.77	5.72	14.03
	5	166.85	158.10	176.01	9.62	3.42	16.17

Perodicticus potto mean size (CS) and SD of size for bootstrap and random subsamples

P. potto	Sample size	Mean CS	Percentile		SD of CS	Percentile	
			2.5th	97.5th		2.5th	97.5th
Observed	129	156.24	_	_	7.35	_	_
Bootstrap	129	156.22	155.00	157.47	7.32	6.43	8.28
Subsamples	125	156.25	155.04	157.54	7.29	6.38	8.24
	120	156.26	154.93	157.54	7.32	6.42	8.35
	115	156.23	154.86	157.56	7.32	6.39	8.33
	110	156.22	154.88	157.61	7.32	6.38	8.32
	105	156.24	154.82	157.75	7.30	6.30	8.28
	100	156.26	154.76	157.72	7.31	6.29	8.41
	95	156.19	154.76	157.66	7.29	6.21	8.37
	90	156.24	154.75	157.73	7.31	6.26	8.55
	85	156.25	154.81	157.82	7.29	6.22	8.48
	80	156.25	154.53	157.80	7.28	6.17	8.44
	75	156.20	154.65	157.73	7.32	6.23	8.57
	70	156.21	154.48	157.85	7.33	6.15	8.58
	65	156.22	154.39	158.01	7.26	5.97	8.68
	60	156.21	154.26	158.03	7.27	6.04	8.56
	55	156.26	154.52	158.14	7.31	6.05	8.80
	50	156.28	154.33	158.14	7.30	5.93	8.79
	45	156.24	154.00	158.39	7.26	5.74	9.04
	40	156.21	153.88	158.32	7.28	5.71	9.09
	35	156.17	153.66	158.55	7.34	5.64	9.23
	30	156.25	153.76	158.72	7.25	5.52	9.28
	25	156.24	153.54	159.26	7.18	5.24	9.48
	20	156.22	153.16	159.31	7.17	5.02	9.79
	15	156.26	152.54	160.00	7.16	4.84	10.01
	10	156.30	151.47	160.50	7.13	3.91	10.85
	5	156.24	149.70	162.50	6.95	2.71	12.66

The accuracy of mean shape and mean shape variance at reduced sample size

Mean Procrustes Distances (PRDs) from the subsample mean shapes to the observed mean shape and the variance in mean shape for *Galago senegalensis.*

G. senegalensis	Sample size	Mean PRD	95th percentile	Mean shape variance
Observed	175	–	–	–
Bootstrap	175	0.003601	0.004380	0.003602
Subsamples	170	0.003640	0.004438	0.003668
	165	0.003702	0.004513	0.003729
	160	0.003782	0.004582	0.003790
	155	0.003840	0.004732	0.003856
	150	0.003919	0.004773	0.003940
	145	0.003933	0.004802	0.003968
	140	0.004032	0.004880	0.004055
	135	0.004117	0.005027	0.004113
	130	0.004159	0.005032	0.004201
	125	0.004242	0.005195	0.004276
	120	0.004375	0.005272	0.004355
	115	0.004412	0.005345	0.004475
	110	0.004536	0.005519	0.004598
	105	0.004614	0.005581	0.004693
	100	0.004731	0.005679	0.004766
	95	0.004876	0.005957	0.004887
	90	0.005037	0.006079	0.005061
	85	0.005177	0.006284	0.005196
	80	0.005328	0.006428	0.005361
	75	0.005492	0.006732	0.005516
	70	0.005673	0.006870	0.005756
	65	0.005886	0.007234	0.005917
	60	0.006151	0.007495	0.006188
	55	0.006451	0.007897	0.006451
	50	0.006681	0.008057	0.006768
	45	0.007104	0.008646	0.007143
	40	0.007565	0.009247	0.007536
	35	0.007999	0.009691	0.008059
	30	0.008687	0.010473	0.008787
	25	0.009533	0.011544	0.009609
	20	0.010620	0.012968	0.010653
	15	0.012258	0.014985	0.012448
	10	0.014967	0.018500	0.015109
	5	0.021125	0.026197	0.021211

Mean Procrustes Distances (PRDs) from the subsample mean shapes to the observed mean shape and the variance in mean shape for *Microcebus murinus.*

M. murinus	Sample size	Mean PRD	95th percentile	Mean shape variance
Observed	72	–	–	–
Bootstrap	72	0.006516	0.008127	0.006955
Subsamples	70	0.006965	0.008550	0.007031
	65	0.007206	0.008900	0.007285
	60	0.007557	0.009374	0.007536
	55	0.007849	0.009833	0.007964
	50	0.008256	0.010272	0.008284
	45	0.008665	0.010754	0.008784
	40	0.009189	0.011365	0.009324
	35	0.009784	0.012122	0.009890
	30	0.010669	0.013189	0.010730
	25	0.011582	0.014434	0.011762
	20	0.012905	0.016030	0.013126
	15	0.015038	0.018451	0.015114
	10	0.018602	0.023357	0.018428
	5	0.025939	0.032279	0.026125

Mean Procrustes Distances (PRDs) from the subsample mean shapes to the observed mean shape and the variance in mean shape for *Nycticebus coucang.*

N. coucang	Sample size	Mean PRD	95th percentile	Mean shape variance
Observed	69	–	–	–
Bootstrap	69	0.007117	0.008959	0.007133
Subsamples	65	0.007293	0.009210	0.007445
	60	0.007619	0.009711	0.007682
	55	0.007980	0.010059	0.007986
	50	0.008338	0.010438	0.008490
	45	0.008792	0.011162	0.008912
	40	0.009268	0.011692	0.009471
	35	0.010131	0.012703	0.010064
	30	0.010787	0.013667	0.010863
	25	0.011765	0.014981	0.011829
	20	0.013270	0.017014	0.013383
	15	0.015125	0.019356	0.015446
	10	0.018768	0.023974	0.018927
	5	0.026190	0.033348	0.026569

Mean Procrustes Distances (PRDs) from the subsample mean shapes to the observed mean shape and the variance in mean shape for *Otolemur crassicaudatus.*

O. crassicaudatus	**Sample size**	**Mean PRD**	**95th percentile**	**Mean shape variance**
Observed	101	–	–	–
Bootstrap	101	0.005209	0.006651	0.005199
Subsamples	100	0.005205	0.006687	0.005235
	95	0.005323	0.006764	0.005403
	90	0.005462	0.006901	0.005570
	85	0.005612	0.007162	0.005709
	80	0.005834	0.007367	0.005906
	75	0.005985	0.007596	0.006103
	70	0.006223	0.008030	0.006313
	65	0.006490	0.008313	0.006523
	60	0.006739	0.008446	0.006789
	55	0.006984	0.008819	0.007120
	50	0.007350	0.009240	0.007417
	45	0.007788	0.009965	0.007813
	40	0.008316	0.010831	0.008321
	35	0.008836	0.011194	0.008914
	30	0.009492	0.012270	0.009633
	25	0.010441	0.013129	0.010442
	20	0.011632	0.014892	0.011819
	15	0.013504	0.017120	0.013565
	10	0.017010	0.021248	0.016691
	5	0.023140	0.029288	0.0233736

Mean Procrustes Distances (PRDs) from the subsample mean shapes to the observed mean shape and the variance in mean shape for *Perodicticus potto.*

P. potto	Sample size	Mean PRD	95th percentile	Mean shape variance
Observed	129	–	–	–
Bootstrap	129	0.005522	0.006877	0.005559
Subsamples	125	0.005611	0.006968	0.005620
	120	0.005711	0.007065	0.005805
	115	0.005816	0.007130	0.005869
	110	0.005969	0.007378	0.006021
	105	0.006126	0.007611	0.006142
	100	0.006287	0.007840	0.006334
	95	0.006406	0.007993	0.006500
	90	0.006643	0.008189	0.006669
	85	0.006814	0.008409	0.006828
	80	0.007014	0.008727	0.007065
	75	0.007228	0.008925	0.007272
	70	0.007484	0.009158	0.007582
	65	0.007719	0.009669	0.007802
	60	0.008093	0.009983	0.008137
	55	0.008521	0.010640	0.008476
	50	0.008937	0.011193	0.008970
	45	0.009389	0.011920	0.009360
	40	0.009822	0.012202	0.010011
	35	0.010546	0.013287	0.010728
	30	0.011419	0.014105	0.011605
	25	0.012501	0.015724	0.012571
	20	0.013976	0.017429	0.014074
	15	0.016186	0.019892	0.016260
	10	0.019965	0.025416	0.020096
	5	0.027946	0.034863	0.027965

The accuracy of total shape variance at reduced sample size

Galago senegalensis total shape variation: observed, bootstrap and random subsamples

G. senegalensis	Sample size	Mean total shape variation	2.5th percentile	97.5th percentile
Observed	175	0.002298	–	–
Bootstrap	175	0.002283	0.002173	0.002401
Subsamples	170	0.002284	0.002167	0.002407
	165	0.002284	0.002167	0.002407
	160	0.002283	0.002165	0.002403
	155	0.002283	0.002168	0.002408
	150	0.002284	0.002162	0.002418
	145	0.002285	0.002171	0.002410
	140	0.002287	0.002169	0.002414
	135	0.002285	0.002164	0.002410
	130	0.002291	0.002174	0.002426
	125	0.002282	0.002161	0.002424
	120	0.002287	0.002152	0.002415
	115	0.002287	0.002150	0.002439
	110	0.002282	0.002140	0.002428
	105	0.002286	0.002152	0.002429
	100	0.002286	0.002136	0.002434
	95	0.002283	0.002141	0.002452
	90	0.002286	0.002137	0.002444
	85	0.002285	0.002134	0.002454
	80	0.002288	0.002130	0.002448
	75	0.002285	0.002124	0.002462
	70	0.002285	0.002111	0.002476
	65	0.002290	0.002128	0.002476
	60	0.002284	0.002106	0.002473
	55	0.002279	0.002103	0.002479
	50	0.002282	0.002097	0.002495
	45	0.002282	0.002068	0.002518
	40	0.002282	0.002039	0.002545
	35	0.002284	0.002031	0.002549
	30	0.002281	0.002023	0.002580
	25	0.002279	0.002006	0.002603
	20	0.002289	0.001978	0.002670
	15	0.002278	0.001926	0.002715
	10	0.002289	0.001859	0.002837
	5	0.002282	0.001684	0.003074

Microcebus murinus total shape variation: observed, bootstrap and random subsamples

M. murinus	**Sample size**	**Mean total shape variation**	**2.5th percentile**	**97.5th percentile**
Observed	72	0.003479	–	–
Bootstrap	72	0.003440	0.003193	0.003716
Subsamples	70	0.003428	0.003165	0.003710
	65	0.003432	0.003170	0.003731
	60	0.003435	0.003166	0.003714
	55	0.003433	0.003149	0.003733
	50	0.003436	0.003157	0.003787
	45	0.003435	0.003115	0.003792
	40	0.003428	0.003099	0.003804
	35	0.003431	0.003071	0.003808
	30	0.003427	0.003062	0.003857
	25	0.003435	0.003007	0.003901
	20	0.003430	0.002949	0.003955
	15	0.003424	0.002900	0.004043
	10	0.003421	0.002732	0.004267
	5	0.003451	0.002506	0.004800

Nycticebus coucang total shape variation: observed, bootstrap and random subsamples

N. coucang	**Sample size**	**Mean total shape variation**	**2.5th percentile**	**97.5th percentile**
Observed	69	0.00358	–	–
Bootstrap	69	0.00353	0.00328	0.00382
Subsample	65	0.00353	0.00325	0.00381
	60	0.00353	0.00325	0.00384
	55	0.00353	0.00322	0.00385
	50	0.00354	0.00322	0.00387
	45	0.00353	0.00322	0.00385
	40	0.00354	0.00319	0.00393
	35	0.00354	0.00319	0.00392
	30	0.00353	0.00312	0.00395
	25	0.00353	0.00312	0.00398
	20	0.00353	0.00304	0.00407
	15	0.00355	0.00298	0.00418
	10	0.00352	0.00285	0.00427
	5	0.00352	0.00257	0.00473

Otolemur crassicaudatus total shape variation: observed, bootstrap and random subsamples

O. crassicaudatus	**Sample size**	**Mean total shape variation**	**2.5th percentile**	**97.5th percentile**
Observed	101	0.002784	–	–
Bootstrap	101	0.002755	0.002587	0.002931
Subsamples	100	0.002758	0.002586	0.002926
	95	0.002757	0.002566	0.002952
	90	0.002755	0.002567	0.002942
	85	0.002754	0.002555	0.002962
	80	0.002755	0.002560	0.002968
	75	0.002755	0.002556	0.002964
	70	0.002755	0.002550	0.002982
	65	0.002754	0.002542	0.002982
	60	0.002752	0.002522	0.002990
	55	0.002757	0.002516	0.003016
	50	0.002761	0.002524	0.003022
	45	0.002755	0.002499	0.003037
	40	0.002747	0.002478	0.003041
	35	0.002758	0.002458	0.003075
	30	0.002761	0.002445	0.003142
	25	0.002750	0.002394	0.003139
	20	0.002761	0.002327	0.003204
	15	0.002764	0.002309	0.003270
	10	0.002767	0.002204	0.003402
	5	0.002746	0.001986	0.003660

Perodicticus potto total shape variation: observed, bootstrap and random subsamples

P. potto	**Sample size**	**Mean total shape variation**	**2.5th percentile**	**97.5th percentile**
Observed	129	0.003991	–	–
Bootstrap	129	0.003965	0.003742	0.004198
Subsamples	125	0.003959	0.003724	0.004187
	120	0.003963	0.003749	0.004177
	115	0.003962	0.003736	0.004187
	110	0.003957	0.003742	0.004203
	105	0.003964	0.003720	0.004204
	100	0.003965	0.003737	0.004198
	95	0.003960	0.003731	0.004221
	90	0.003962	0.003708	0.004234
	85	0.003955	0.003688	0.004213
	80	0.003960	0.003695	0.004237
	75	0.003962	0.003684	0.004268
	70	0.003966	0.003680	0.004243
	65	0.003967	0.003691	0.004270
	60	0.003944	0.003647	0.004268
	55	0.003968	0.003650	0.004293
	50	0.003960	0.003616	0.004332
	45	0.003967	0.003604	0.004336
	40	0.003957	0.003569	0.004371
	35	0.003956	0.003571	0.004374
	30	0.003956	0.003502	0.004417
	25	0.003949	0.003465	0.004487
	20	0.003954	0.003456	0.004563
	15	0.003951	0.003274	0.004612
	10	0.003960	0.003208	0.004774
	5	0.003992	0.002889	0.005219

The variation in angles of allometric trajectory, at an intra-species level (males verses females), at reduced sample size

Variation in angles (degrees) between static allometric vectors for males and females, for *Galago senegalensis.*

***G. senegalensis* within species (male vs female)**				
N		**Vector angle**		
Group		**Mean**	**Percentile**	
Males	**Females**		**2.5th**	**97.5th**
Observed				
97	75	12.11	–	–
Bootstrap samples				
97	75	16.83	13.68	20.77
Random subsamples				
75	75	17.27	14.00	21.42
70	70	17.62	14.22	21.76
65	65	17.96	14.44	22.38
60	60	18.52	14.68	23.69
55	55	18.89	15.03	23.87
50	50	19.45	15.25	24.44
45	45	20.02	15.78	25.58
40	40	21.10	16.70	27.17
35	35	21.98	17.19	28.98
30	30	23.23	17.93	30.55
25	25	25.15	19.42	33.03
20	20	27.31	20.42	36.88
15	15	31.00	22.74	41.87
10	10	37.63	26.86	52.64
5	5	52.80	35.11	74.78

Variation in angles (degrees) between static allometric vectors for males and females, for *Otolemur crassicaudatus.*

***O. crassicaudatus* within species (male vs female)**				
N		**Vector angle**		
Group		**Mean**	**Percentile**	
Males	**Females**		**2.5th**	**97.5th**
Observed				
46	35	14.87	–	–
Bootstrap samples				
46	35	18.16	13.28	24.08
Random subsamples				
35	35	18.68	13.93	25.61
30	30	19.24	14.03	26.06
25	25	20.12	14.02	28.54
20	20	21.19	14.73	29.69
15	15	23.86	15.84	33.75
10	10	28.00	17.68	43.72
5	5	41.37	23.09	69.19

Variation in angles (degrees) between static allometric vectors for males and females, for *Perodicticus potto.*

***P. potto* within species (male vs female)**				
N		**Vector angle**		
Group		**Mean**	**Percentile**	
Males	**Females**		**2.5th**	**97.5th**
Observed				
59	38	15.41	_	_
Bootstrap samples				
59	38	21.34	17.56	26.15
Random subsamples				
38	38	22.44	18.12	28.20
35	35	22.89	18.38	28.97
30	30	23.95	19.28	30.82
25	25	25.13	19.71	32.08
20	20	27.42	21.21	35.87
15	15	30.45	23.05	42.02
10	10	36.09	26.61	49.51
5	5	50.64	34.06	74.52

The variation in angles of allometric trajectory, at an inter-species level, at reduced sample size

Variation in angles (degrees) between static allometric vectors for *Microcebus murinus* and *Galago senegalensis*

Inter-species: *M. murinus, G. senegalensis*				
N		**Vector angle**		
Group		**Mean**	**Percentile**	
M. murinus	***G. senegalensis***		**2.5th**	**97.5th**
Observed				
72	175	27.64	_	_
Bootstrap samples				
72	175	29.55	26.12	33.55
Random subsamples				
70	70	30.27	26.63	34.35
65	65	30.43	26.41	34.84
60	60	30.75	26.57	35.53
55	55	31.26	27.09	35.94
50	50	31.48	27.16	36.79
45	45	31.82	27.19	37.09
40	40	32.30	27.26	38.38
35	35	33.12	27.76	39.25
30	30	33.62	28.26	40.35
25	25	34.84	28.94	41.68
20	20	36.66	29.80	44.52
15	15	39.15	31.86	49.16
10	10	44.32	34.33	56.42
5	5	56.97	41.29	77.00

Variation in angles (degrees) between static allometric vectors for *Microcebus murinus* and *Nycticebus coucang*

Inter-species: *M. murinus, N. coucang*				
N		**Vector angle**		
Group		**Mean**	**Percentile**	
M. murinus	***N. coucang***		**2.5th**	**97.5th**
Observed				
72	69	18.82	–	–
Bootstrap samples				
72	69	22.40	18.24	27.07
Random subsamples				
65	65	22.76	18.20	27.78
60	60	22.85	18.79	27.93
55	55	23.35	19.26	28.59
50	50	23.63	19.46	28.75
45	45	24.21	19.47	29.47
40	40	24.81	19.60	30.82
35	35	25.67	20.30	31.99
30	30	26.72	20.94	34.10
25	25	28.02	21.80	35.50
20	20	29.98	23.30	38.05
15	15	33.35	25.53	43.61
10	10	38.87	27.87	53.00
5	5	52.28	35.82	72.24

Variation in angles (degrees) between static allometric vectors for *Microcebus murinus* and *Otolemur crassicaudatus*

Inter-species: *M. murinus, O. crassicaudatus*				
N		**Vector angle**		
Group		**Mean**	**Percentile**	
M. murinus	***O. crassicaudatus***		**2.5th**	**97.5th**
Observed				
72	101	16.55	–	–
Bootstrap samples				
72	101	19.65	16.37	23.70
Random subsamples				
70	70	19.78	16.45	23.97
65	65	20.18	16.42	24.57
60	60	20.44	16.45	25.05
55	55	20.84	16.95	25.37
50	50	21.14	16.98	26.44
45	45	21.68	17.55	26.97
40	40	22.20	17.74	27.77
35	35	22.85	18.10	28.85
30	30	23.84	18.66	30.66
25	25	25.11	19.39	32.52
20	20	27.04	20.41	35.51
15	15	30.06	22.29	39.66
10	10	35.03	25.25	48.40
5	5	48.46	32.33	69.23

Variation in angles (degrees) between static allometric vectors for *Microcebus murinus* and *Perodicticus potto*

Inter-species: *M. murinus, P. potto*				
N		**Vector angle**		
Group		**Mean**	**Percentile**	
M. murinus	***P. potto***		**2.5th**	**97.5th**
Observed				
72	129	17.43	–	–
Bootstrap samples				
72	129	20.86	17.57	24.49
Random subsamples				
70	70	21.73	18.32	25.69
65	65	22.11	18.38	26.78
60	60	22.32	18.63	26.98
55	55	22.83	18.61	28.39
50	50	23.25	19.09	28.33
45	45	23.92	19.36	30.04
40	40	24.64	19.73	30.54
35	35	25.58	20.65	31.89
30	30	26.60	21.22	34.02
25	25	27.84	22.04	35.16
20	20	30.39	23.51	38.95
15	15	33.58	25.46	44.14
10	10	39.26	28.56	52.78
5	5	53.64	37.22	74.46

Variation in angles (degrees) between static allometric vectors for *Nycticebus coucang* and *Galago senegalensis*

Inter-species: *N. coucang, G. senegalensis*				
N		**Vector angle**		
Group		**Mean**	**Percentile**	
N. coucang	***G. senegalensis***		**2.5th**	**97.5th**
Observed				
69	175	21.33	–	–
Bootstrap samples				
69	175	23.29	20.92	25.87
Random subsamples				
65	65	24.43	21.49	27.94
60	60	24.62	21.38	28.32
55	55	24.93	21.58	28.58
50	50	25.30	21.77	29.18
45	45	25.79	22.09	30.24
40	40	26.17	22.38	30.21
35	35	26.97	22.84	31.76
30	30	27.77	23.65	32.97
25	25	28.87	24.21	34.62
20	20	30.50	25.18	37.64
15	15	33.56	27.01	41.98
10	10	38.36	29.55	51.45
5	5	51.46	36.50	72.37

Variation in angles (degrees) between static allometric vectors for *Nycticebus coucang* and *Otolemur crassicaudatus*

Inter-species: *N. coucang, O. crassicaudatus*				
N		**Vector angle**		
Group		**Mean**	**Percentile**	
N. coucang	***O. crassicaudatus***		**2.5th**	**97.5th**
Observed				
69	101	14.32	–	–
Bootstrap samples				
69	101	16.90	13.78	20.93
Random subsamples				
65	65	17.31	13.98	22.06
60	60	17.73	13.91	22.12
55	55	17.98	14.25	22.57
50	50	18.26	14.38	22.64
45	45	18.65	14.61	23.74
40	40	19.14	15.03	24.29
35	35	19.79	15.31	24.85
30	30	20.52	16.16	26.04
25	25	21.84	16.49	27.89
20	20	23.30	17.49	30.68
15	15	26.38	19.58	36.20
10	10	30.57	21.28	42.68
5	5	43.29	27.78	66.70

Variation in angles (degrees) between static allometric vectors for *Nycticebus coucang* and *Perodicticus potto*

Inter-species: *N. coucang, P. potto*				
N		**Vector angle**		
Group		**Mean**	**Percentile**	
N. coucang	***P. potto***		**2.5th**	**97.5th**
Observed				
69	129	13.15	–	–
Bootstrap samples				
69	129	16.61	13.83	20.16
Random subsamples				
65	65	17.90	14.71	21.89
60	60	18.33	14.67	22.75
55	55	18.78	15.16	23.35
50	50	19.27	15.41	24.25
45	45	19.69	15.69	24.99
40	40	20.34	15.85	25.62
35	35	21.34	16.41	27.74
30	30	22.23	17.12	29.22
25	25	24.01	18.08	32.12
20	20	25.93	19.27	34.40
15	15	28.95	21.50	38.78
10	10	35.00	24.50	48.66
5	5	49.89	32.57	73.11

Variation in angles (degrees) between static allometric vectors for *Otolemur crassicaudatus* and *Galago senegalensis*

Inter-species: *O. crassicaudatus, G. senegalensis*				
N		**Vector angle**		
Group		**Mean**	**Percentile**	
O. crassicaudatus	***G. senegalensis***		**2.5th**	**97.5th**
Observed				
101	175	22.52	–	–
Bootstrap samples				
101	175	23.61	21.80	25.78
Random subsamples				
100	100	24.06	22.04	26.56
95	95	24.15	22.04	26.80
90	90	24.27	21.88	26.92
85	85	24.34	22.08	26.86
80	80	24.49	21.97	27.72
75	75	24.53	22.21	27.28
70	70	24.65	22.17	27.61
65	65	24.81	22.27	28.11
60	60	25.01	22.39	28.33
55	55	25.29	22.60	28.73
50	50	25.53	22.77	28.97
45	45	25.89	22.69	29.91
40	40	26.37	22.87	30.47
35	35	26.76	23.47	30.97
30	30	27.42	23.85	32.48
25	25	28.40	24.22	33.72
20	20	29.87	25.21	35.86
15	15	31.99	26.70	39.41
10	10	36.36	28.75	46.77
5	5	47.61	34.04	67.65

Variation in angles (degrees) between static allometric vectors for *Otolemur crassicaudatus* and *Galago senegalensis*

Inter-species: *O. crassicaudatus, P. potto*				
N		**Vector angle**		
Group		**Mean**	**Percentile**	
O. crassicaudatus	***P. potto***		**2.5th**	**97.5th**
Observed				
101	129	14.05	–	–
Bootstrap samples				
101	129	16.16	13.55	19.55
Random subsamples				
100	100	16.68	13.85	20.22
95	95	16.65	13.81	19.95
90	90	16.94	13.91	20.93
85	85	16.90	13.78	21.02
80	80	17.28	14.07	21.31
75	75	17.53	14.17	21.56
70	70	17.70	14.15	22.04
65	65	17.89	14.32	22.61
60	60	18.29	14.52	23.24
55	55	18.50	14.43	23.36
50	50	18.96	14.87	24.20
45	45	19.22	14.72	25.49
40	40	19.91	15.13	25.62
35	35	20.69	15.75	27.23
30	30	21.56	16.01	28.26
25	25	22.95	16.72	30.31
20	20	24.53	17.32	32.78
15	15	27.41	19.74	37.44
10	10	32.61	22.06	46.95
5	5	45.56	28.31	69.52

Variation in angles (degrees) between static allometric vectors for *Perodicticus potto* and *Galago senegalensis*

Inter-species: *P. potto, G. senegalensis*				
N		**Vector angle**		
Group		**Mean**	**Percentile**	
P. potto	***G. senegalensis***		**2.5th**	**97.5th**
Observed				
129	175	22.69	–	–
Bootstrap samples				
129	175	24.22	21.60	26.97
Random subsamples				
125	125	24.41	21.58	27.54
120	120	24.48	21.74	27.66
115	115	24.57	21.64	27.95
110	110	24.60	21.71	27.63
105	105	24.72	21.60	28.15
100	100	24.97	21.91	28.39
95	95	25.03	21.73	28.34
90	90	25.04	21.78	28.55
85	85	25.15	21.71	28.66
80	80	25.42	21.93	29.42
75	75	25.54	21.71	29.54
70	70	25.85	22.03	29.97
65	65	25.97	22.16	30.32
60	60	26.20	22.26	30.41
55	55	26.50	22.38	30.92
50	50	27.02	22.87	31.73
45	45	27.32	22.72	32.38
40	40	27.87	23.02	33.23
35	35	28.54	23.40	34.12
30	30	29.43	23.85	35.76
25	25	30.77	24.67	37.58
20	20	32.49	26.19	40.12
15	15	35.24	27.57	44.44
10	10	40.35	30.45	52.24
5	5	53.06	37.50	73.33

The accuracy of estimations, of the Percentage of shape variation explained by size, at reduced sample size

Mean percentage of shape variation explained by size for *Galago senegalensis*: observed, bootstrap and random subsamples

G. senegalensis	**Sample size**	**% shape variance caused by size**	**2.5th percentile**	**97.5th percentile**
Observed	175	4.85	–	–
Bootstrap	175	5.42	4.07	6.98
Subsamples	170	5.46	4.03	7.22
	165	5.45	4.00	7.23
	160	5.47	4.00	7.44
	155	5.51	4.03	7.18
	150	5.54	4.04	7.32
	145	5.59	4.10	7.45
	140	5.56	3.95	7.29
	135	5.55	3.94	7.46
	130	5.62	3.95	7.50
	125	5.68	3.96	7.77
	120	5.71	4.00	7.84
	115	5.79	4.02	7.86
	110	5.80	3.93	7.98
	105	5.89	4.01	8.29
	100	5.88	4.08	8.05
	95	5.91	4.02	8.01
	90	5.99	4.16	8.39
	85	6.06	4.06	8.73
	80	6.19	4.16	8.77
	75	6.26	3.99	9.05
	70	6.37	4.13	8.96
	65	6.43	4.25	9.39
	60	6.61	4.14	9.72
	55	6.66	4.21	10.03
	50	6.98	4.28	10.60
	45	7.17	4.46	10.98
	40	7.49	4.43	11.38
	35	7.87	4.72	12.26
	30	8.32	5.03	12.71
	25	8.99	5.26	13.72
	20	10.11	6.28	15.78
	15	11.84	7.15	18.93
	10	15.86	9.91	24.43
	5	28.86	18.13	42.61

Mean percentage of shape variation explained by size for *M. murinus*: observed, bootstrap and random subsamples

M. murinus	**Sample size**	**% shape variance caused by size**	**2.5th percentile**	**97.5th percentile**
Observed	72	5.23	–	–
Bootstrap	72	6.66	4.53	9.22
Subsamples	70	6.63	4.35	9.16
	65	6.72	4.49	9.53
	60	6.84	4.48	9.80
	55	6.95	4.55	10.06
	50	7.18	4.61	10.21
	45	7.40	4.77	10.94
	40	7.70	4.68	11.43
	35	7.96	4.88	11.88
	30	8.48	5.21	12.85
	25	9.18	5.51	13.97
	20	10.33	5.95	16.22
	15	12.16	7.16	19.46
	10	15.89	9.49	25.47
	5	29.46	18.62	46.15

Mean percentage of shape variation explained by size for *Nycticebus coucang*: observed, bootstrap and random subsamples

N. coucang	**Sample size**	**% shape variance caused by size**	**2.5th percentile**	**97.5th percentile**
Observed	69	3.57	–	–
Bootstrap	69	5.18	3.13	8.27
Subsamples	65	5.29	3.24	8.85
	60	5.26	3.23	8.52
	55	5.55	3.39	9.30
	50	5.74	3.32	9.51
	45	5.98	3.51	10.61
	40	6.36	3.56	11.16
	35	6.66	3.75	11.64
	30	7.27	4.21	12.27
	25	8.10	4.49	14.33
	20	9.06	4.88	16.10
	15	11.15	6.03	19.71
	10	15.15	8.77	24.98
	5	29.18	16.84	49.13

Mean percentage of shape variation explained by size for *Otolemur crassicaudatus*: observed, bootstrap and random subsamples

O. crassicaudatus	**Sample size**	**% shape variance caused by size**	**2.5th percentile**	**97.5th percentile**
Observed	101	8.20	–	–
Bootstrap	101	9.18	7.19	11.35
Subsamples	100	9.23	7.15	11.66
	95	9.32	7.21	11.84
	90	9.33	7.06	11.80
	85	9.41	7.05	12.04
	80	9.44	7.21	12.09
	75	9.57	7.30	12.47
	70	9.58	7.03	12.40
	65	9.67	6.97	12.74
	60	9.94	7.14	13.15
	55	10.00	7.12	13.50
	50	10.23	7.22	13.82
	45	10.48	7.27	14.34
	40	10.73	7.28	14.70
	35	11.18	7.40	15.75
	30	11.58	7.54	16.28
	25	12.33	7.67	18.09
	20	13.42	8.51	19.90
	15	15.24	9.17	23.54
	10	18.90	11.59	28.44
	5	32.41	19.37	49.95

Mean percentage of shape variation explained by size for *Perodicticus potto*: observed, bootstrap and random subsamples

P. potto	Sample size	% shape variance caused by size	2.5th percentile	97.5th percentile
Observed	129	4.55	–	–
Bootstrap	129	5.33	3.82	7.21
Subsamples	125	5.29	3.72	7.07
	120	5.40	4.02	7.27
	115	5.39	3.91	7.42
	110	5.49	3.92	7.46
	105	5.52	3.93	7.63
	100	5.59	3.91	7.88
	95	5.64	3.98	7.95
	90	5.73	4.00	8.11
	85	5.71	3.91	7.96
	80	5.80	3.88	8.24
	75	5.92	4.04	8.47
	70	6.04	3.98	8.65
	65	6.08	3.99	8.64
	60	6.25	4.03	9.14
	55	6.48	4.28	9.51
	50	6.67	4.21	10.09
	45	6.80	4.31	9.95
	40	7.02	4.34	10.34
	35	7.52	4.56	11.97
	30	7.99	4.77	12.31
	25	8.77	5.29	13.66
	20	9.83	5.85	15.80
	15	11.65	6.37	18.78
	10	15.42	8.86	24.88
	5	29.14	17.08	44.72

– Appendix 2 –

Allometry regression results – Intra-species

The results of intra-species major axis regressions of shape (PCs) against size (both the whole cranium ln CS and the corresponding module ln CS), for each species, for the full landmark configuration and for the 2* and Goswami models of modularity. Where the relationship was shown to be significant (p<0.003) results are underlined and shown in red.

Whole cranium against ln CS of whole cranium

Cheirogaleus major

PC	Slope	Slope lower CI	Slope higher CI	Intercept	Intercept lower CI	Intercept higher CI	p value	r squared
PC1	-0.4451	-0.6037	-0.3282	2.1631	1.4938	2.8324	0.0001	0.4855
PC2	-0.3938	-0.5858	-0.2647	1.9134	1.1330	2.6937	0.1122	0.1060
PC3	0.3501	0.2305	0.5320	-1.7014	-2.4340	-0.9688	0.7719	0.0037
PC4	-0.3389	-0.5148	-0.2230	1.6466	0.9377	2.3555	0.7645	0.0040
PC5	0.3295	0.2267	0.4788	-1.6009	-2.2136	-0.9882	0.0202	0.2129
PC6	0.3028	0.1994	0.4598	-1.4715	-2.1043	-0.8387	0.7072	0.0062
PC7	0.2847	0.1873	0.4328	-1.3836	-1.9802	-0.7870	0.8949	0.0008
PC8	-0.2718	-0.4131	-0.1788	1.3208	0.7515	1.8901	0.8489	0.0016
PC9	0.2558	0.1684	0.3884	-1.2429	-1.7775	-0.7082	0.7227	0.0056
PC10	-0.2484	-0.3752	-0.1645	1.2072	0.6952	1.7192	0.3815	0.0335
PC11	-0.2399	-0.3637	-0.1582	1.1657	0.6663	1.6651	0.5772	0.0137
PC12	-0.2261	-0.3436	-0.1488	1.0986	0.6253	1.5720	0.8175	0.0024
PC13	-0.2155	-0.3277	-0.1418	1.0474	0.5956	1.4992	0.9669	0.0001

Cheirogaleus medius

PC	Slope	Slope lower CI	Slope higher CI	Intercept	Intercept lower CI	Intercept higher CI	p value	r squared
PC1	0.3524	0.2515	0.4939	-1.6176	-2.1742	-1.0611	0.0068	0.2411
PC2	0.3404	0.2419	0.4789	-1.5624	-2.1063	-1.0185	0.0097	0.2229
PC3	-0.3306	-0.4844	-0.2256	1.5172	0.9232	2.1112	0.4972	0.0172
PC4	0.2814	0.1916	0.4133	-1.2919	-1.8007	-0.7830	0.7080	0.0053
PC5	0.2751	0.1873	0.4041	-1.2629	-1.7606	-0.7653	0.7321	0.0044
PC6	-0.2576	-0.3782	-0.1755	1.1824	0.7170	1.6478	0.6740	0.0067
PC7	0.2368	0.1637	0.3425	-1.0870	-1.4974	-0.6767	0.1219	0.0863
PC8	-0.2141	-0.3141	-0.1459	0.9825	0.5965	1.3685	0.5997	0.0103
PC9	-0.2135	-0.3113	-0.1464	0.9798	0.6013	1.3584	0.2815	0.0428
PC10	0.2057	0.1399	0.3024	-0.9443	-1.3172	-0.5714	0.9815	0.0000
PC11	-0.1968	-0.2889	-0.1340	0.9031	0.5476	1.2586	0.6766	0.0065
PC12	0.1899	0.1292	0.2791	-0.8717	-1.2159	-0.5275	0.9051	0.0005
PC13	-0.1785	-0.2600	-0.1225	0.8192	0.5037	1.1347	0.2482	0.0491

Microcebus murinus

PC	Slope	Slope lower CI	Slope higher CI	Intercept	Intercept lower CI	Intercept higher CI	p value	r squared
PC1	-0.5024	-0.6145	-0.4107	2.1779	1.7361	2.6198	0.0000	0.2757
PC2	0.4254	0.3446	0.5251	-1.8442	-2.2353	-1.4531	0.0001	0.2086
PC3	-0.4029	-0.5102	-0.3181	1.7467	1.3303	2.1630	0.9902	0.0000
PC4	-0.3509	-0.4444	-0.2771	1.5215	1.1588	1.8841	0.8637	0.0004
PC5	0.3381	0.2684	0.4259	-1.4656	-1.8071	-1.1242	0.0736	0.0450
PC6	0.3246	0.2563	0.4110	-1.4071	-1.7425	-1.0717	0.8597	0.0004
PC7	-0.3058	-0.3872	-0.2416	1.3258	1.0102	1.6414	0.6593	0.0028
PC8	-0.3036	-0.3839	-0.2401	1.3163	1.0046	1.6279	0.3284	0.0136
PC9	-0.2904	-0.3671	-0.2298	1.2590	0.9613	1.5567	0.2877	0.0161
PC10	0.2650	0.2097	0.3350	-1.1489	-1.4205	-0.8772	0.2857	0.0163
PC11	0.2573	0.2032	0.3259	-1.1156	-1.3815	-0.8497	0.8683	0.0004
PC12	0.2485	0.1965	0.3142	-1.0772	-1.3325	-0.8219	0.3625	0.0119
PC13	0.2426	0.1917	0.3070	-1.0517	-1.3015	-0.8019	0.4799	0.0072

Microcebus rufus

PC	Slope	Slope lower CI	Slope higher CI	Intercept	Intercept lower CI	Intercept higher CI	p value	r squared
PC1	-0.4035	-0.5728	-0.2842	1.7585	1.1296	2.3873	0.0218	0.1800
PC2	-0.3741	-0.4737	-0.2955	1.6305	1.2421	2.0189	0.0000	0.6361
PC3	-0.3012	-0.4416	-0.2055	1.3128	0.7983	1.8272	0.5229	0.0153
PC4	0.2701	0.1846	0.3952	-1.1772	-1.6361	-0.7183	0.4061	0.0257
PC5	0.2489	0.1702	0.3638	-1.0845	-1.5063	-0.6627	0.3675	0.0302
PC6	0.2353	0.1604	0.3453	-1.0256	-1.4286	-0.6226	0.6040	0.0101
PC7	-0.2261	-0.3324	-0.1538	0.9856	0.5963	1.3748	0.9812	0.0000
PC8	-0.2144	-0.3147	-0.1460	0.9343	0.5667	1.3019	0.6577	0.0074
PC9	0.2042	0.1390	0.3002	-0.8901	-1.2415	-0.5387	0.8926	0.0007
PC10	0.2000	0.1363	0.2934	-0.8715	-1.2138	-0.5292	0.5927	0.0107
PC11	0.1935	0.1318	0.2841	-0.8435	-1.1752	-0.5117	0.6447	0.0080
PC12	0.1857	0.1264	0.2728	-0.8095	-1.1285	-0.4904	0.7387	0.0042
PC13	-0.1749	-0.2571	-0.1190	0.7622	0.4614	1.0631	0.8703	0.0010

Galago alleni

PC	Slope	Slope lower CI	Slope higher CI	Intercept	Intercept lower CI	Intercept higher CI	p value	r squared
PC1	0.5273	0.3622	0.7676	-2.5094	-3.4738	-1.5449	0.0141	0.2444
PC2	-0.4452	-0.6292	-0.3150	2.1185	1.3707	2.8663	0.0018	0.3627
PC3	0.3912	0.2550	0.6003	-1.8618	-2.6836	-1.0399	0.7869	0.0034
PC4	0.3623	0.2362	0.5558	-1.7243	-2.4849	-0.9636	0.7478	0.0048
PC5	0.3353	0.2241	0.5017	-1.5956	-2.2564	-0.9348	0.0932	0.1228
PC6	0.3002	0.2004	0.4497	-1.4287	-2.0219	-0.8355	0.0999	0.1182
PC7	-0.2894	-0.4425	-0.1893	1.3772	0.7746	1.9797	0.4993	0.0210
PC8	-0.2625	-0.4030	-0.1710	1.2492	0.6970	1.8013	0.8954	0.0008
PC9	0.2376	0.1548	0.3645	-1.1305	-1.6294	-0.6317	0.7666	0.0041
PC10	-0.2262	-0.3468	-0.1475	1.0764	0.6020	1.5507	0.7007	0.0068
PC11	0.2145	0.1408	0.3268	-1.0206	-1.4632	-0.5780	0.3599	0.0382
PC12	-0.2131	-0.3269	-0.1389	1.0139	0.5664	1.4614	0.7796	0.0036
PC13	-0.1979	-0.3038	-0.1289	0.9417	0.5255	1.3578	0.8734	0.0012

Galago demidoff

PC	Slope	Slope lower CI	Slope higher CI	Intercept	Intercept lower CI	Intercept higher CI	p value	r squared
PC1	0.5637	0.4580	0.6937	-2.4978	-3.0200	-1.9757	0.0000	0.3789
PC2	-0.3940	-0.5100	-0.3044	1.7458	1.2903	2.2014	0.1729	0.0323
PC3	0.3675	0.2831	0.4770	-1.6285	-2.0581	-1.1989	0.4326	0.0108
PC4	-0.3273	-0.4240	-0.2526	1.4502	1.0705	1.8298	0.2231	0.0259
PC5	-0.3138	-0.4073	-0.2418	1.3905	1.0238	1.7572	0.4158	0.0117
PC6	-0.2903	-0.3774	-0.2234	1.2866	0.9454	1.6278	0.8521	0.0006
PC7	0.2791	0.2159	0.3607	-1.2366	-1.5573	-0.9159	0.1103	0.0441
PC8	0.2655	0.2045	0.3448	-1.1766	-1.4875	-0.8657	0.5102	0.0076
PC9	-0.2581	-0.3336	-0.1996	1.1435	0.8465	1.4405	0.1231	0.0412
PC10	-0.2390	-0.3105	-0.1840	1.0592	0.7789	1.3394	0.5899	0.0051
PC11	0.2297	0.1772	0.2978	-1.0179	-1.2850	-0.7508	0.2714	0.0212
PC12	0.2215	0.1708	0.2871	-0.9813	-1.2389	-0.7238	0.2717	0.0212
PC13	-0.2154	-0.2800	-0.1657	0.9544	0.7013	1.2076	0.9764	0.0000

Galago elegantulus

PC	Slope	Slope lower CI	Slope higher CI	Intercept	Intercept lower CI	Intercept higher CI	p value	r squared
PC1	0.7986	0.5613	1.1362	-3.7704	-5.1278	-2.4130	0.9015	0.0005
PC2	-0.6176	-0.8315	-0.4587	2.9160	2.0360	3.7961	0.0008	0.2975
PC3	-0.5700	-0.8072	-0.4024	2.6911	1.7354	3.6468	0.3498	0.0274
PC4	0.4880	0.3448	0.6907	-2.3042	-3.1209	-1.4875	0.3185	0.0311
PC5	0.4498	0.3161	0.6399	-2.1236	-2.8881	-1.3591	0.8955	0.0005
PC6	0.4334	0.3063	0.6132	-2.0461	-2.7706	-1.3217	0.3020	0.0332
PC7	0.3872	0.2722	0.5507	-1.8279	-2.4856	-1.1702	0.8195	0.0017
PC8	0.3615	0.2541	0.5142	-1.7067	-2.3208	-1.0925	0.8354	0.0014
PC9	-0.3514	-0.4992	-0.2474	1.6593	1.0648	2.2537	0.5701	0.0102
PC10	-0.3383	-0.4746	-0.2412	1.5974	1.0463	2.1486	0.1009	0.0819
PC11	0.3276	0.2311	0.4644	-1.5468	-2.0977	-0.9960	0.4042	0.0218
PC12	0.2946	0.2071	0.4190	-1.3909	-1.8911	-0.8908	0.7604	0.0029
PC13	0.2922	0.2054	0.4158	-1.3797	-1.8765	-0.8829	0.9718	0.0000

Galago moholi

PC	Slope	Slope lower CI	Slope higher CI	Intercept	Intercept lower CI	Intercept higher CI	p value	r squared
PC1	0.5610	0.4727	0.6657	-2.5512	-2.9901	-2.1124	0.0000	0.4716
PC2	-0.4531	-0.5684	-0.3612	2.0607	1.5897	2.5317	0.0268	0.0672
PC3	-0.3492	-0.4414	-0.2762	1.5879	1.2123	1.9634	0.7880	0.0010
PC4	-0.3264	-0.4124	-0.2584	1.4846	1.1345	1.8347	0.4808	0.0070
PC5	0.3201	0.2532	0.4046	-1.4555	-1.8000	-1.1111	0.9761	0.0000
PC6	-0.3000	-0.3793	-0.2373	1.3643	1.0415	1.6871	0.8722	0.0004
PC7	-0.2915	-0.3685	-0.2305	1.3255	1.0118	1.6392	0.9789	0.0000
PC8	0.2754	0.2183	0.3474	-1.2523	-1.5459	-0.9586	0.2530	0.0184
PC9	0.2542	0.2020	0.3200	-1.1562	-1.4247	-0.8877	0.1020	0.0372
PC10	0.2433	0.1925	0.3076	-1.1067	-1.3685	-0.8448	0.9114	0.0002
PC11	0.2282	0.1805	0.2885	-1.0379	-1.2834	-0.7924	0.8063	0.0009
PC12	-0.2211	-0.2790	-0.1753	1.0056	0.7698	1.2414	0.2589	0.0179
PC13	0.2185	0.1728	0.2762	-0.9935	-1.2287	-0.7584	0.9879	0.0000

Galago senegalensis

PC	Slope	Slope lower CI	Slope higher CI	Intercept	Intercept lower CI	Intercept higher CI	p value	r squared
PC1	-0.4069	-0.4605	-0.3594	1.8861	1.6517	2.1205	0.0000	0.3142
PC2	-0.3536	-0.4061	-0.3079	1.6392	1.4114	1.8670	0.0000	0.1424
PC3	-0.2854	-0.3310	-0.2460	1.3229	1.1257	1.5200	0.1198	0.0139
PC4	-0.2687	-0.3117	-0.2317	1.2457	1.0602	1.4313	0.1067	0.0150
PC5	0.2608	0.2246	0.3028	-1.2089	-1.3902	-1.0275	0.7920	0.0004
PC6	-0.2448	-0.2824	-0.2122	1.1348	0.9720	1.2976	0.0001	0.0864
PC7	0.2358	0.2031	0.2737	-1.0930	-1.2565	-0.9294	0.3215	0.0057
PC8	0.2215	0.1909	0.2571	-1.0270	-1.1807	-0.8734	0.2841	0.0066
PC9	0.2110	0.1818	0.2451	-0.9784	-1.1251	-0.8316	0.6957	0.0009
PC10	0.2060	0.1775	0.2390	-0.9549	-1.0974	-0.8124	0.1633	0.0112
PC11	-0.2003	-0.2323	-0.1727	0.9286	0.7905	1.0668	0.0807	0.0175
PC12	0.1912	0.1651	0.2216	-0.8866	-1.0176	-0.7556	0.0211	0.0304
PC13	0.1868	0.1609	0.2169	-0.8660	-0.9960	-0.7361	0.8279	0.0003

Galago zanzibaricus

PC	Slope	Slope lower CI	Slope higher CI	Intercept	Intercept lower CI	Intercept higher CI	p value	r squared
PC1	0.6421	0.4325	0.9533	-2.9450	-4.1393	-1.7507	0.0955	0.1161
PC2	-0.5958	-0.8807	-0.4030	2.7325	1.6369	3.8281	0.0696	0.1360
PC3	-0.4987	-0.7356	-0.3381	2.2873	1.3756	3.1989	0.0592	0.1462
PC4	-0.4454	-0.6421	-0.3089	2.0427	1.2786	2.8069	0.0113	0.2480
PC5	-0.3925	-0.5962	-0.2584	1.8002	1.0254	2.5750	0.7496	0.0045
PC6	-0.3721	-0.5656	-0.2448	1.7065	0.9706	2.4423	0.8972	0.0007
PC7	0.3637	0.2402	0.5507	-1.6679	-2.3800	-0.9558	0.4960	0.0204
PC8	-0.3359	-0.5091	-0.2216	1.5406	0.8813	2.2000	0.5510	0.0157
PC9	-0.3168	-0.4817	-0.2084	1.4530	0.8262	2.0798	0.9752	0.0000
PC10	-0.3076	-0.4573	-0.2070	1.4110	0.8370	1.9850	0.1044	0.1105
PC11	-0.2885	-0.4361	-0.1908	1.3231	0.7607	1.8855	0.4165	0.0289
PC12	0.2737	0.1804	0.4154	-1.2555	-1.7945	-0.7165	0.6411	0.0096
PC13	-0.2435	-0.3682	-0.1610	1.1166	0.6415	1.5918	0.4340	0.0268

Otolemur crassicaudatus

PC	Slope	Slope lower CI	Slope higher CI	Intercept	Intercept lower CI	Intercept higher CI	p value	r squared
PC1	-0.3149	-0.3774	-0.2627	1.6107	1.3172	1.9042	0.0000	0.1651
PC2	0.2832	0.2324	0.3452	-1.4489	-1.7375	-1.1602	0.6395	0.0022
PC3	-0.2665	-0.3014	-0.2356	1.3632	1.1948	1.5316	0.0000	0.6163
PC4	-0.2038	-0.2483	-0.1672	1.0424	0.8351	1.2497	0.4522	0.0057
PC5	0.1983	0.1627	0.2417	-1.0145	-1.2167	-0.8122	0.7715	0.0009
PC6	0.1807	0.1483	0.2202	-0.9245	-1.1082	-0.7408	0.3880	0.0075
PC7	0.1716	0.1408	0.2091	-0.8777	-1.0523	-0.7030	0.4982	0.0046
PC8	0.1416	0.1163	0.1726	-0.7246	-0.8685	-0.5806	0.4023	0.0071
PC9	-0.1379	-0.1679	-0.1133	0.7055	0.5658	0.8452	0.2358	0.0142
PC10	0.1338	0.1097	0.1631	-0.6843	-0.8207	-0.5478	0.8693	0.0003
PC11	0.1258	0.1032	0.1534	-0.6438	-0.7722	-0.5154	0.8797	0.0002
PC12	0.1245	0.1023	0.1516	-0.6371	-0.7632	-0.5110	0.2273	0.0147
PC13	-0.1173	-0.1430	-0.0962	0.6002	0.4805	0.7199	0.8859	0.0002

Otolemur garnettii

PC	Slope	Slope lower CI	Slope higher CI	Intercept	Intercept lower CI	Intercept higher CI	p value	r squared
PC1	-0.3472	-0.4093	-0.2945	1.7522	1.4625	2.0418	0.0000	0.3558
PC2	0.2875	0.2367	0.3493	-1.4509	-1.7350	-1.1668	0.0022	0.0961
PC3	-0.2816	-0.3374	-0.2350	1.4209	1.1624	1.6794	0.0000	0.2194
PC4	-0.2001	-0.2454	-0.1631	1.0096	0.8017	1.2174	0.8117	0.0006
PC5	-0.1925	-0.2362	-0.1570	0.9716	0.7718	1.1714	0.6222	0.0026
PC6	0.1842	0.1502	0.2260	-0.9298	-1.1210	-0.7385	0.6502	0.0022
PC7	-0.1682	-0.2063	-0.1371	0.8487	0.6741	1.0234	0.6710	0.0019
PC8	0.1635	0.1333	0.2006	-0.8250	-0.9948	-0.6552	0.7361	0.0012
PC9	-0.1539	-0.1882	-0.1259	0.7768	0.6198	0.9338	0.0632	0.0366
PC10	-0.1524	-0.1869	-0.1242	0.7688	0.6107	0.9269	0.6043	0.0029
PC11	-0.1467	-0.1798	-0.1197	0.7403	0.5886	0.8920	0.3290	0.0102
PC12	0.1373	0.1125	0.1676	-0.6929	-0.8320	-0.5539	0.0292	0.0501
PC13	-0.1296	-0.1589	-0.1057	0.6540	0.5198	0.7881	0.3933	0.0078

Avahi laniger

PC	Slope	Slope lower CI	Slope higher CI	Intercept	Intercept lower CI	Intercept higher CI	p value	r squared
PC1	0.7580	0.4890	1.1750	-3.7012	-5.3762	-2.0262	0.7337	0.0056
PC2	0.7111	0.4623	1.0939	-3.4723	-5.0143	-1.9303	0.3456	0.0424
PC3	-0.6647	-1.0123	-0.4365	3.2458	1.8399	4.6516	0.1665	0.0891
PC4	-0.5696	-0.8524	-0.3806	2.7814	1.6295	3.9332	0.0526	0.1673
PC5	-0.5491	-0.8519	-0.3539	2.6810	1.4652	3.8967	0.8588	0.0015
PC6	-0.4938	-0.7640	-0.3192	2.4111	1.3250	3.4972	0.5799	0.0148
PC7	-0.4659	-0.7196	-0.3016	2.2749	1.2544	3.2953	0.4892	0.0231
PC8	0.3998	0.2591	0.6171	-1.9523	-2.8265	-1.0782	0.4568	0.0266
PC9	0.3877	0.2501	0.6010	-1.8931	-2.7498	-1.0363	0.7349	0.0056
PC10	-0.3761	-0.5834	-0.2424	1.8362	1.0038	2.6686	0.8348	0.0021
PC11	-0.3594	-0.5540	-0.2332	1.7550	0.9718	2.5382	0.4067	0.0330
PC12	-0.3329	-0.5147	-0.2153	1.6253	0.8942	2.3565	0.5470	0.0175
PC13	0.3285	0.2118	0.5096	-1.6039	-2.3310	-0.8768	0.8281	0.0023

Indri indri

PC	Slope	Slope lower CI	Slope higher CI	Intercept	Intercept lower CI	Intercept higher CI	p value	r squared
PC1	-0.6415	-0.8887	-0.4631	3.5206	2.3525	4.6886	0.5878	0.0080
PC2	0.5349	0.4007	0.7140	-2.9357	-3.7954	-2.0760	0.0022	0.2272
PC3	-0.4936	-0.6842	-0.3562	2.7092	1.8090	3.6093	0.6656	0.0051
PC4	-0.4558	-0.6237	-0.3330	2.5013	1.7037	3.2990	0.0743	0.0836
PC5	-0.4347	-0.5924	-0.3190	2.3859	1.6358	3.1360	0.0398	0.1093
PC6	0.3973	0.2894	0.5454	-2.1802	-2.8827	-1.4777	0.1189	0.0645
PC7	-0.3852	-0.5317	-0.2790	2.1137	1.4201	2.8073	0.2945	0.0297
PC8	0.3728	0.2688	0.5170	-2.0458	-2.7270	-1.3647	0.8458	0.0010
PC9	0.3526	0.2543	0.4887	-1.9349	-2.5781	-1.2916	0.7022	0.0040
PC10	0.3184	0.2306	0.4397	-1.7476	-2.3215	-1.1736	0.3088	0.0280
PC11	-0.3034	-0.4200	-0.2191	1.6648	1.1134	2.2163	0.5200	0.0113
PC12	0.2898	0.2095	0.4007	-1.5904	-2.1150	-1.0657	0.4006	0.0192
PC13	0.2779	0.2012	0.3839	-1.5253	-2.0268	-1.0238	0.3277	0.0259

Propithecus diadema

PC	Slope	Slope lower CI	Slope higher CI	Intercept	Intercept lower CI	Intercept higher CI	p value	r squared
PC1	-0.5474	-0.8107	-0.3696	2.9390	1.7548	4.1233	0.8690	0.0011
PC2	-0.4497	-0.6047	-0.3344	2.4146	1.6888	3.1404	0.0001	0.4441
PC3	0.4191	0.2837	0.6192	-2.2502	-3.1510	-1.3494	0.5495	0.0139
PC4	0.3652	0.2478	0.5381	-1.9608	-2.7402	-1.1814	0.3969	0.0277
PC5	-0.3364	-0.4968	-0.2278	1.8062	1.0838	2.5286	0.5246	0.0157
PC6	-0.3228	-0.4702	-0.2216	1.7331	1.0657	2.4004	0.1260	0.0877
PC7	-0.2973	-0.4387	-0.2014	1.5960	0.9588	2.2333	0.4816	0.0192
PC8	0.2889	0.1952	0.4275	-1.5512	-2.1750	-0.9275	0.7164	0.0052
PC9	-0.2755	-0.4005	-0.1896	1.4794	0.9130	2.0458	0.1046	0.0981
PC10	0.2535	0.1717	0.3743	-1.3610	-1.9050	-0.8170	0.5077	0.0171
PC11	0.2380	0.1652	0.3429	-1.2780	-1.7552	-0.8007	0.0481	0.1420
PC12	-0.2306	-0.3408	-0.1560	1.2382	0.7422	1.7343	0.5708	0.0125
PC13	0.2274	0.1535	0.3369	-1.2210	-1.7133	-0.7288	0.9576	0.0001

Propithecus verreauxi

PC	Slope	Slope lower CI	Slope higher CI	Intercept	Intercept lower CI	Intercept higher CI	p value	r squared
PC1	0.5535	0.4196	0.7302	-2.9300	-3.7519	-2.1081	0.0021	0.2090
PC2	0.4695	0.3445	0.6398	-2.4852	-3.2668	-1.7037	0.6239	0.0059
PC3	-0.4659	-0.6163	-0.3521	2.4659	1.7668	3.1651	0.0033	0.1920
PC4	0.3873	0.2885	0.5200	-2.0502	-2.6630	-1.4373	0.0369	0.1019
PC5	0.3432	0.2517	0.4679	-1.8164	-2.3888	-1.2441	0.7662	0.0022
PC6	0.3314	0.2437	0.4507	-1.7541	-2.3020	-1.2062	0.3744	0.0193
PC7	0.3071	0.2260	0.4174	-1.6258	-2.1324	-1.1192	0.3202	0.0241
PC8	-0.3052	-0.4155	-0.2241	1.6152	1.1086	2.1218	0.4985	0.0112
PC9	0.2800	0.2068	0.3790	-1.4819	-1.9375	-1.0263	0.1503	0.0498
PC10	0.2697	0.1991	0.3652	-1.4273	-1.8671	-0.9876	0.1675	0.0459
PC11	0.2558	0.1886	0.3469	-1.3538	-1.7729	-0.9348	0.2164	0.0370
PC12	0.2542	0.1864	0.3467	-1.3454	-1.7698	-0.9211	0.9283	0.0002
PC13	-0.2379	-0.3234	-0.1749	1.2590	0.8661	1.6519	0.3515	0.0212

Eulemur fulvus

PC	Slope	Slope lower CI	Slope higher CI	Intercept	Intercept lower CI	Intercept higher CI	p value	r squared
PC1	-0.4757	-0.5471	-0.4136	2.5359	2.1801	2.8917	0.0000	0.1260
PC2	-0.4074	-0.4689	-0.3540	2.1717	1.8654	2.4779	0.0000	0.1169
PC3	-0.3517	-0.4060	-0.3046	1.8748	1.6046	2.1450	0.0002	0.0775
PC4	0.3244	0.2799	0.3761	-1.7294	-1.9858	-1.4731	0.0389	0.0244
PC5	0.3003	0.2595	0.3476	-1.6010	-1.8358	-1.3662	0.0049	0.0449
PC6	0.2761	0.2385	0.3196	-1.4718	-1.6880	-1.2555	0.0068	0.0415
PC7	-0.2617	-0.3039	-0.2254	1.3953	1.1859	1.6046	0.8825	0.0001
PC8	-0.2499	-0.2896	-0.2157	1.3323	1.1355	1.5291	0.0194	0.0312
PC9	0.2373	0.2044	0.2756	-1.2652	-1.4549	-1.0755	0.5477	0.0021
PC10	0.2293	0.1976	0.2660	-1.2223	-1.4047	-1.0398	0.1733	0.0107
PC11	-0.2180	-0.2531	-0.1878	1.1621	0.9880	1.3362	0.4146	0.0039
PC12	0.2070	0.1782	0.2403	-1.1033	-1.2688	-0.9377	0.8580	0.0002
PC13	-0.1987	-0.2305	-0.1714	1.0595	0.9020	1.2169	0.0664	0.0194

Eulemur macaco

PC	Slope	Slope lower CI	Slope higher CI	Intercept	Intercept lower CI	Intercept higher CI	p value	r squared
PC1	-0.6244	-0.8119	-0.4802	3.3421	2.4543	4.2298	0.0502	0.0705
PC2	-0.4889	-0.6303	-0.3791	2.6168	1.9445	3.2891	0.0067	0.1305
PC3	-0.4727	-0.6190	-0.3610	2.5303	1.8395	3.2210	0.3260	0.0182
PC4	-0.4582	-0.6010	-0.3492	2.4524	1.7785	3.1263	0.5973	0.0053
PC5	0.4494	0.3466	0.5826	-2.4055	-3.0372	-1.7738	0.0247	0.0916
PC6	-0.3771	-0.4939	-0.2880	2.0187	1.4675	2.5698	0.3292	0.0180
PC7	0.3572	0.2795	0.4564	-1.9118	-2.3855	-1.4381	0.0008	0.1913
PC8	-0.3488	-0.4527	-0.2687	1.8670	1.3746	2.3593	0.0321	0.0837
PC9	0.3209	0.2445	0.4212	-1.7179	-2.1907	-1.2451	0.7364	0.0022
PC10	0.3032	0.2310	0.3981	-1.6232	-2.0704	-1.1760	0.9438	0.0001
PC11	0.2840	0.2165	0.3726	-1.5201	-1.9380	-1.1023	0.6230	0.0046
PC12	0.2709	0.2074	0.3540	-1.4503	-1.8428	-1.0578	0.1717	0.0350
PC13	-0.2621	-0.3435	-0.2000	1.4029	1.0190	1.7869	0.4038	0.0132

Eulemur mongoz

PC	Slope	Slope lower CI	Slope higher CI	Intercept	Intercept lower CI	Intercept higher CI	p value	r squared
PC1	-0.4216	-0.5150	-0.3451	2.2274	1.7787	2.6761	0.0000	0.4444
PC2	0.3351	0.2567	0.4375	-1.7707	-2.2483	-1.2930	0.6526	0.0037
PC3	0.3159	0.2423	0.4118	-1.6690	-2.1168	-1.2213	0.3673	0.0148
PC4	0.2683	0.2069	0.3480	-1.4174	-1.7902	-1.0447	0.0842	0.0532
PC5	0.2589	0.1993	0.3363	-1.3678	-1.7299	-1.0058	0.1318	0.0408
PC6	0.2298	0.1775	0.2975	-1.2140	-1.5309	-0.8970	0.0525	0.0666
PC7	-0.2161	-0.2813	-0.1660	1.1418	0.8373	1.4462	0.2275	0.0264
PC8	-0.2045	-0.2668	-0.1567	1.0802	0.7892	1.3712	0.5589	0.0062
PC9	0.1962	0.1503	0.2563	-1.0368	-1.3168	-0.7569	0.7517	0.0018
PC10	0.1840	0.1410	0.2401	-0.9719	-1.2339	-0.7100	0.5757	0.0057
PC11	-0.1749	-0.2273	-0.1345	0.9239	0.6789	1.1690	0.1544	0.0365
PC12	0.1644	0.1259	0.2146	-0.8686	-1.1028	-0.6344	0.6192	0.0045
PC13	-0.1595	-0.2081	-0.1223	0.8427	0.6160	1.0693	0.4683	0.0096

Eulemur rubriventer

PC	Slope	Slope lower CI	Slope higher CI	Intercept	Intercept lower CI	Intercept higher CI	p value	r squared
PC1	0.8717	0.5872	1.2940	-4.6353	-6.5145	-2.7561	0.3770	0.0313
PC2	0.7859	0.5756	1.0730	-4.1790	-5.5015	-2.8566	0.0003	0.4098
PC3	-0.5421	-0.8093	-0.3631	2.8826	1.6962	4.0691	0.8405	0.0017
PC4	-0.5304	-0.7872	-0.3574	2.8206	1.6776	3.9635	0.3707	0.0322
PC5	0.5027	0.3373	0.7492	-2.6732	-3.7682	-1.5781	0.6025	0.0110
PC6	-0.4364	-0.6504	-0.2928	2.3207	1.3700	3.2714	0.6031	0.0110
PC7	-0.4141	-0.6116	-0.2804	2.2020	1.3215	3.0826	0.2276	0.0577
PC8	0.3914	0.2622	0.5841	-2.0811	-2.9369	-1.2253	0.7741	0.0034
PC9	0.3591	0.2416	0.5337	-1.9095	-2.6860	-1.1330	0.4278	0.0253
PC10	-0.3445	-0.5055	-0.2348	1.8321	1.1123	2.5518	0.1275	0.0904
PC11	-0.3217	-0.4783	-0.2164	1.7106	1.0141	2.4072	0.4518	0.0228
PC12	0.3064	0.2055	0.4570	-1.6295	-2.2981	-0.9608	0.6653	0.0076
PC13	0.2784	0.1865	0.4156	-1.4803	-2.0894	-0.8712	0.8142	0.0023

Hapalemur griseus

PC	Slope	Slope lower CI	Slope higher CI	Intercept	Intercept lower CI	Intercept higher CI	p value	r squared
PC1	0.5545	0.4209	0.7306	-2.7938	-3.5740	-2.0135	0.0000	0.5403
PC2	-0.4217	-0.6257	-0.2842	2.1245	1.2641	2.9849	0.3615	0.0334
PC3	0.3615	0.2442	0.5352	-1.8215	-2.5547	-1.0883	0.2872	0.0452
PC4	-0.3173	-0.4596	-0.2190	1.5985	0.9923	2.2047	0.0440	0.1525
PC5	0.3098	0.2076	0.4622	-1.5607	-2.2023	-0.9192	0.7444	0.0043
PC6	-0.2783	-0.4155	-0.1864	1.4021	0.8247	1.9795	0.9004	0.0006
PC7	0.2735	0.1850	0.4042	-1.3778	-1.9300	-0.8255	0.2470	0.0532
PC8	0.2553	0.1711	0.3809	-1.2863	-1.8146	-0.7579	0.7088	0.0057
PC9	-0.2503	-0.3699	-0.1694	1.2613	0.7564	1.7662	0.2357	0.0558
PC10	0.2297	0.1540	0.3428	-1.1575	-1.6332	-0.6818	0.7304	0.0048
PC11	-0.2237	-0.3338	-0.1500	1.1273	0.6640	1.5905	0.7302	0.0048
PC12	-0.2215	-0.3303	-0.1485	1.1160	0.6579	1.5741	0.6788	0.0070
PC13	-0.2078	-0.3103	-0.1391	1.0470	0.6157	1.4783	0.9851	0.0000

Lemur catta

PC	Slope	Slope lower CI	Slope higher CI	Intercept	Intercept lower CI	Intercept higher CI	p value	r squared
PC1	-0.5051	-0.6817	-0.3743	2.6555	1.8474	3.4636	0.0011	0.2858
PC2	-0.4583	-0.6437	-0.3264	2.4097	1.5755	3.2439	0.1149	0.0759
PC3	0.3214	0.2339	0.4417	-1.6900	-2.2361	-1.1439	0.0090	0.1947
PC4	0.3119	0.2193	0.4437	-1.6399	-2.2300	-1.0497	0.8399	0.0013
PC5	-0.2752	-0.3861	-0.1962	1.4469	0.9478	1.9461	0.1002	0.0822
PC6	-0.2494	-0.3533	-0.1760	1.3110	0.8447	1.7772	0.3753	0.0246
PC7	-0.2286	-0.3220	-0.1623	1.2020	0.7822	1.6219	0.1660	0.0591
PC8	0.2271	0.1597	0.3231	-1.1942	-1.6238	-0.7646	0.8065	0.0019
PC9	0.2154	0.1515	0.3064	-1.1325	-1.5397	-0.7252	0.7649	0.0028
PC10	0.2083	0.1464	0.2964	-1.0954	-1.4897	-0.7010	0.8882	0.0006
PC11	0.1983	0.1395	0.2819	-1.0427	-1.4170	-0.6684	0.6572	0.0062
PC12	-0.1899	-0.2697	-0.1337	0.9983	0.6409	1.3557	0.5464	0.0115
PC13	0.1838	0.1292	0.2615	-0.9665	-1.3142	-0.6188	0.8136	0.0018

Varecia variegata

PC	Slope	Slope lower CI	Slope higher CI	Intercept	Intercept lower CI	Intercept higher CI	p value	r squared
PC1	0.5288	0.3867	0.7232	-2.8967	-3.8181	-1.9753	0.0662	0.0883
PC2	-0.3967	-0.4752	-0.3313	2.1732	1.7791	2.5673	0.0000	0.7036
PC3	0.3568	0.2580	0.4934	-1.9543	-2.5990	-1.3097	0.3965	0.0195
PC4	-0.3186	-0.4418	-0.2297	1.7450	1.1641	2.3258	0.8145	0.0015
PC5	-0.2879	-0.3989	-0.2077	1.5769	1.0532	2.1005	0.6294	0.0064
PC6	-0.2700	-0.3746	-0.1947	1.4792	0.9865	1.9718	0.8989	0.0004
PC7	-0.2549	-0.3531	-0.1840	1.3961	0.9328	1.8595	0.5989	0.0076
PC8	-0.2240	-0.3107	-0.1616	1.2272	0.8189	1.6355	0.7619	0.0025
PC9	0.2193	0.1583	0.3037	-1.2010	-1.5995	-0.8026	0.5796	0.0084
PC10	-0.2009	-0.2779	-0.1453	1.1006	0.7374	1.4638	0.4064	0.0187
PC11	0.1901	0.1373	0.2631	-1.0412	-1.3857	-0.6967	0.4815	0.0135
PC12	-0.1813	-0.2515	-0.1307	0.9931	0.6623	1.3238	0.9032	0.0004
PC13	0.1774	0.1280	0.2458	-0.9714	-1.2941	-0.6488	0.6359	0.0061

Lepilemur ruficaudatus

PC	Slope	Slope lower CI	Slope higher CI	Intercept	Intercept lower CI	Intercept higher CI	p value	r squared
PC1	0.4685	0.3648	0.6016	-2.3034	-2.8855	-1.7213	0.0000	0.6568
PC2	-0.3875	-0.5832	-0.2575	1.9055	1.1046	2.7064	0.2789	0.0508
PC3	-0.3514	-0.5317	-0.2323	1.7280	0.9919	2.4641	0.4521	0.0248
PC4	0.2938	0.1936	0.4459	-1.4447	-2.0649	-0.8246	0.6379	0.0098
PC5	0.2750	0.1813	0.4171	-1.3520	-1.9318	-0.7721	0.6081	0.0116
PC6	-0.2435	-0.3701	-0.1602	1.1973	0.6813	1.7133	0.8341	0.0019
PC7	-0.2412	-0.3663	-0.1588	1.1859	0.6758	1.6959	0.7162	0.0059
PC8	-0.2366	-0.3592	-0.1558	1.1632	0.6631	1.6633	0.6998	0.0066
PC9	0.2078	0.1369	0.3154	-1.0216	-1.4607	-0.5826	0.6782	0.0076
PC10	0.2057	0.1354	0.3125	-1.0114	-1.4469	-0.5759	0.7757	0.0036
PC11	0.1986	0.1318	0.2991	-0.9763	-1.3877	-0.5648	0.3053	0.0456
PC12	-0.1901	-0.2876	-0.1256	0.9345	0.5360	1.3329	0.4706	0.0229
PC13	0.1827	0.1208	0.2761	-0.8982	-1.2799	-0.5164	0.4147	0.0291

Loris tardigradus

PC	Slope	Slope lower CI	Slope higher CI	Intercept	Intercept lower CI	Intercept higher CI	p value	r squared
PC1	-0.3163	-0.3816	-0.2622	1.5143	1.2284	1.8001	0.0000	0.7901
PC2	0.2634	0.1779	0.3901	-1.2612	-1.7692	-0.7531	0.2918	0.0443
PC3	-0.1868	-0.2787	-0.1252	0.8941	0.5263	1.2618	0.7528	0.0040
PC4	-0.1835	-0.2740	-0.1229	0.8786	0.5167	1.2405	0.8758	0.0010
PC5	-0.1640	-0.2443	-0.1101	0.7852	0.4640	1.1065	0.5495	0.0145
PC6	-0.1608	-0.2401	-0.1077	0.7699	0.4527	1.0870	0.8898	0.0008
PC7	-0.1396	-0.2073	-0.0939	0.6681	0.3966	0.9397	0.4089	0.0274
PC8	0.1347	0.0905	0.2004	-0.6447	-0.9080	-0.3814	0.5045	0.0180
PC9	0.1235	0.0828	0.1842	-0.5913	-0.8340	-0.3485	0.6660	0.0076
PC10	0.1190	0.0798	0.1776	-0.5698	-0.8042	-0.3355	0.7555	0.0039
PC11	0.1079	0.0726	0.1604	-0.5165	-0.7268	-0.3062	0.4384	0.0242
PC12	0.0992	0.0664	0.1481	-0.4747	-0.6703	-0.2791	0.9366	0.0003
PC13	-0.0951	-0.1412	-0.0641	0.4554	0.2705	0.6402	0.3881	0.0299

Nycticebus bengalensis

PC	Slope	Slope lower CI	Slope higher CI	Intercept	Intercept lower CI	Intercept higher CI	p value	r squared
PC1	0.5899	0.3776	0.9215	-2.9955	-4.3766	-1.6145	0.4994	0.0231
PC2	0.5215	0.3338	0.8148	-2.6484	-3.8699	-1.4268	0.5078	0.0222
PC3	-0.4658	-0.7197	-0.3015	2.3657	1.3038	3.4276	0.2208	0.0740
PC4	-0.4402	-0.6845	-0.2831	2.2357	1.2166	3.2548	0.3434	0.0450
PC5	0.4212	0.2865	0.6191	-2.1388	-2.9835	-1.2942	0.0108	0.2832
PC6	-0.4038	-0.6307	-0.2586	2.0509	1.1060	2.9957	0.4860	0.0246
PC7	-0.3547	-0.5564	-0.2261	1.8011	0.9624	2.6398	0.7989	0.0033
PC8	-0.3335	-0.5171	-0.2151	1.6935	0.9265	2.4604	0.2830	0.0574
PC9	-0.3237	-0.5002	-0.2095	1.6438	0.9057	2.3820	0.2230	0.0733
PC10	-0.3162	-0.4803	-0.2082	1.6057	0.9148	2.2967	0.0761	0.1490
PC11	0.2934	0.1917	0.4490	-1.4899	-2.1431	-0.8367	0.1197	0.1167
PC12	-0.2881	-0.4521	-0.1837	1.4633	0.7817	2.1448	0.8110	0.0029
PC13	-0.2740	-0.4293	-0.1748	1.3912	0.7449	2.0375	0.6909	0.0081

Nycticebus coucang

PC	Slope	Slope lower CI	Slope higher CI	Intercept	Intercept lower CI	Intercept higher CI	p value	r squared
PC1	-0.4087	-0.5167	-0.3233	2.0365	1.5548	2.5182	0.0437	0.0593
PC2	-0.3507	-0.4465	-0.2755	1.7476	1.3216	2.1736	0.8151	0.0008
PC3	0.2807	0.2265	0.3479	-1.3987	-1.7013	-1.0961	0.0001	0.2129
PC4	-0.2732	-0.3473	-0.2149	1.3611	1.0311	1.6912	0.3821	0.0114
PC5	-0.2618	-0.3301	-0.2076	1.3043	0.9990	1.6096	0.0193	0.0790
PC6	0.2378	0.1868	0.3027	-1.1849	-1.4736	-0.8963	0.6987	0.0023
PC7	0.2284	0.1815	0.2875	-1.1382	-1.4025	-0.8739	0.0107	0.0933
PC8	0.2188	0.1723	0.2777	-1.0899	-1.3524	-0.8275	0.1960	0.0248
PC9	-0.2126	-0.2705	-0.1670	1.0591	0.8013	1.3169	0.6233	0.0036
PC10	-0.1997	-0.2531	-0.1575	0.9949	0.7567	1.2331	0.1171	0.0363
PC11	0.1846	0.1451	0.2348	-0.9196	-1.1433	-0.6960	0.5387	0.0057
PC12	0.1781	0.1400	0.2267	-0.8875	-1.1035	-0.6715	0.6047	0.0040
PC13	0.1725	0.1357	0.2194	-0.8595	-1.0681	-0.6509	0.4190	0.0098

Perodicticus potto

PC	Slope	Slope lower CI	Slope higher CI	Intercept	Intercept lower CI	Intercept higher CI	p value	r squared
PC1	0.4622	0.3963	0.5391	-2.3343	-2.6948	-1.9739	0.0000	0.2268
PC2	-0.3460	-0.4119	-0.2906	1.7472	1.4411	2.0534	0.4617	0.0043
PC3	0.3287	0.2771	0.3900	-1.6602	-1.9453	-1.3751	0.0175	0.0436
PC4	-0.3136	-0.3696	-0.2662	1.5840	1.3229	1.8451	0.0001	0.1191
PC5	-0.2868	-0.3400	-0.2419	1.4486	1.2008	1.6963	0.0097	0.0515
PC6	0.2689	0.2264	0.3193	-1.3578	-1.5926	-1.1231	0.0467	0.0308
PC7	0.2576	0.2164	0.3067	-1.3011	-1.5292	-1.0730	0.5339	0.0031
PC8	0.2411	0.2028	0.2868	-1.2178	-1.4299	-1.0056	0.1556	0.0158
PC9	-0.2287	-0.2713	-0.1928	1.1550	0.9570	1.3531	0.0139	0.0467
PC10	0.2223	0.1867	0.2647	-1.1225	-1.3196	-0.9255	0.7482	0.0008
PC11	-0.2138	-0.2546	-0.1795	1.0798	0.8902	1.2694	0.9313	0.0001
PC12	-0.2097	-0.2497	-0.1761	1.0588	0.8729	1.2448	0.9042	0.0001
PC13	0.2008	0.1690	0.2385	-1.0140	-1.1896	-0.8385	0.0579	0.0280

2* model face module against ln CS whole cranium

Cheirogaleus major

PC	Slope	Slope lower CI	Slope higher CI	Intercept	Intercept lower CI	Intercept higher CI	p value	r squared
PC1	-0.5560	-0.8316	-0.3718	2.7018	1.5846	3.8190	0.1677	0.0811
PC2	-0.5290	-0.7702	-0.3633	2.5705	1.5818	3.5593	0.0231	0.2050
PC3	0.4837	0.3320	0.7047	-2.3502	-3.2559	-1.4446	0.0242	0.2020
PC4	0.4481	0.2947	0.6813	-2.1774	-3.1166	-1.2382	0.9438	0.0002
PC5	-0.4244	-0.6406	-0.2812	2.0625	1.1892	2.9357	0.3591	0.0367
PC6	0.3973	0.2618	0.6030	-1.9308	-2.7596	-1.1019	0.6398	0.0097
PC7	-0.3518	-0.5246	-0.2359	1.7093	1.0079	2.4107	0.1336	0.0951
PC8	-0.3459	-0.5241	-0.2283	1.6808	0.9621	2.3995	0.5293	0.0174
PC9	-0.3103	-0.4710	-0.2044	1.5076	0.8597	2.1555	0.6790	0.0076
PC10	0.3049	0.2006	0.4635	-1.4818	-2.1206	-0.8431	0.8552	0.0015
PC11	-0.2783	-0.4232	-0.1831	1.3526	0.7692	1.9360	0.9361	0.0003
PC12	0.2598	0.1736	0.3888	-1.2625	-1.7855	-0.7395	0.1768	0.0779
PC13	-0.2426	-0.3621	-0.1625	1.1788	0.6937	1.6639	0.1454	0.0899

Cheirogaleus medius

PC	Slope	Slope lower CI	Slope higher CI	Intercept	Intercept lower CI	Intercept higher CI	p value	r squared
PC1	-0.5272	-0.7384	-0.3765	2.4201	1.5894	3.2508	0.0064	0.2445
PC2	-0.4824	-0.7021	-0.3314	2.2140	1.3631	3.0649	0.2304	0.0528
PC3	0.4367	0.3025	0.6304	-2.0045	-2.7571	-1.2519	0.1017	0.0961
PC4	0.4330	0.2952	0.6351	-1.9875	-2.7675	-1.2076	0.5623	0.0126
PC5	0.3658	0.2494	0.5365	-1.6791	-2.3381	-1.0202	0.5631	0.0125
PC6	-0.3361	-0.4939	-0.2287	1.5427	0.9339	2.1514	0.8371	0.0016
PC7	0.3221	0.2193	0.4732	-1.4784	-2.0612	-0.8957	0.7509	0.0038
PC8	-0.3099	-0.4507	-0.2131	1.4226	0.8772	1.9680	0.2106	0.0574
PC9	0.2727	0.1885	0.3945	-1.2517	-1.7245	-0.7789	0.1245	0.0852
PC10	0.2510	0.1720	0.3664	-1.1522	-1.5985	-0.7058	0.3119	0.0378
PC11	0.2436	0.1659	0.3577	-1.1182	-1.5584	-0.6781	0.6791	0.0064
PC12	-0.2164	-0.3180	-0.1472	0.9931	0.6012	1.3850	0.8397	0.0015
PC13	0.2133	0.1462	0.3112	-0.9792	-1.3577	-0.6006	0.2889	0.0415

Microcebus murinus

PC	Slope	Slope lower CI	Slope higher CI	Intercept	Intercept lower CI	Intercept higher CI	p value	r squared
PC1	-0.6600	-0.8355	-0.5213	2.8611	2.1800	3.5422	0.6511	0.0029
PC2	-0.5839	-0.7387	-0.4616	2.5315	1.9307	3.1323	0.4329	0.0088
PC3	-0.5476	-0.6935	-0.4325	2.3742	1.8083	2.9401	0.8777	0.0003
PC4	-0.5259	-0.6467	-0.4277	2.2800	1.8053	2.7547	0.0000	0.2373
PC5	-0.4650	-0.5887	-0.3673	2.0161	1.5362	2.4959	0.6391	0.0032
PC6	-0.4385	-0.5550	-0.3465	1.9011	1.4490	2.3532	0.5525	0.0051
PC7	-0.4112	-0.5189	-0.3259	1.7829	1.3647	2.2011	0.1343	0.0317
PC8	0.3903	0.3082	0.4942	-1.6920	-2.0953	-1.2888	0.8398	0.0006
PC9	-0.3787	-0.4794	-0.2992	1.6419	1.2511	2.0327	0.6394	0.0032
PC10	0.3473	0.2747	0.4392	-1.5058	-1.8623	-1.1494	0.3229	0.0140
PC11	-0.3286	-0.4157	-0.2598	1.4247	1.0867	1.7627	0.4169	0.0094
PC12	0.3188	0.2518	0.4036	-1.3819	-1.7110	-1.0528	0.7160	0.0019
PC13	-0.3131	-0.3924	-0.2498	1.3573	1.0480	1.6666	0.0122	0.0864

Microcebus rufus

PC	Slope	Slope lower CI	Slope higher CI	Intercept	Intercept lower CI	Intercept higher CI	p value	r squared
PC1	0.5601	0.3830	0.8189	-2.4408	-3.3908	-1.4909	0.3779	0.0289
PC2	-0.4627	-0.6801	-0.3148	2.0164	1.2201	2.8127	0.9513	0.0001
PC3	0.3932	0.2675	0.5779	-1.7134	-2.3901	-1.0368	0.9580	0.0001
PC4	0.3512	0.2392	0.5156	-1.5305	-2.1330	-0.9280	0.6802	0.0064
PC5	-0.3276	-0.4810	-0.2231	1.4275	0.8654	1.9897	0.6971	0.0057
PC6	-0.3050	-0.4421	-0.2104	1.3293	0.8245	1.8341	0.1497	0.0753
PC7	-0.2801	-0.3851	-0.2038	1.2207	0.8256	1.6159	0.0012	0.3281
PC8	0.2718	0.1890	0.3910	-1.1846	-1.6248	-0.7444	0.0724	0.1146
PC9	0.2647	0.1805	0.3881	-1.1535	-1.6059	-0.7012	0.5414	0.0140
PC10	0.2474	0.1690	0.3623	-1.0782	-1.4995	-0.6569	0.4527	0.0210
PC11	-0.2279	-0.3342	-0.1554	0.9931	0.6032	1.3830	0.5726	0.0119
PC12	0.2229	0.1524	0.3259	-0.9713	-1.3493	-0.5933	0.3783	0.0289
PC13	0.1997	0.1388	0.2875	-0.8704	-1.1945	-0.5463	0.0775	0.1110

Galago alleni

PC	Slope	Slope lower CI	Slope higher CI	Intercept	Intercept lower CI	Intercept higher CI	p value	r squared
PC1	-0.6732	-1.0300	-0.4400	3.2037	1.7996	4.6078	0.5360	0.0176
PC2	0.5708	0.3729	0.8738	-2.7165	-3.9084	-1.5246	0.5626	0.0155
PC3	0.5357	0.3766	0.7619	-2.5492	-3.4661	-1.6323	0.0029	0.3383
PC4	0.4779	0.3149	0.7252	-2.2742	-3.2505	-1.2980	0.2589	0.0575
PC5	-0.4181	-0.6250	-0.2797	1.9899	1.1682	2.8116	0.0863	0.1279
PC6	0.3603	0.2440	0.5320	-1.7146	-2.4001	-1.0292	0.0372	0.1828
PC7	-0.3221	-0.4910	-0.2113	1.5327	0.8670	2.1984	0.3805	0.0351
PC8	0.3014	0.1963	0.4628	-1.4342	-2.0683	-0.8001	0.9429	0.0002
PC9	0.2951	0.1925	0.4525	-1.4046	-2.0233	-0.7859	0.6854	0.0076
PC10	0.2875	0.1879	0.4398	-1.3680	-1.9676	-0.7684	0.5366	0.0176
PC11	-0.2667	-0.4056	-0.1753	1.2690	0.7211	1.8170	0.3112	0.0466
PC12	0.2348	0.1540	0.3580	-1.1174	-1.6029	-0.6318	0.3861	0.0343
PC13	-0.2231	-0.3423	-0.1454	1.0619	0.5933	1.5304	0.7659	0.0041

Galago demidoff

PC	Slope	Slope lower CI	Slope higher CI	Intercept	Intercept lower CI	Intercept higher CI	p value	r squared
PC1	-0.8107	-1.0376	-0.6334	3.5926	2.6970	4.4882	0.0081	0.1167
PC2	-0.5918	-0.7687	-0.4556	2.6225	1.9287	3.3164	0.5864	0.0052
PC3	-0.5188	-0.6730	-0.4000	2.2991	1.6941	2.9042	0.3446	0.0157
PC4	0.5051	0.3890	0.6558	-2.2381	-2.8293	-1.6469	0.4938	0.0083
PC5	0.4769	0.3703	0.6142	-2.1134	-2.6538	-1.5729	0.0422	0.0704
PC6	0.4328	0.3340	0.5608	-1.9178	-2.4202	-1.4154	0.2345	0.0247
PC7	-0.4082	-0.5306	-0.3141	1.8089	1.3291	2.2888	0.9865	0.0000
PC8	-0.3620	-0.4700	-0.2788	1.6041	1.1807	2.0276	0.4634	0.0095
PC9	-0.3381	-0.4388	-0.2605	1.4983	1.1033	1.8933	0.4063	0.0121
PC10	-0.3297	-0.4284	-0.2538	1.4611	1.0741	1.8482	0.7006	0.0026
PC11	0.2997	0.2315	0.3881	-1.3282	-1.6752	-0.9812	0.1892	0.0301
PC12	-0.2940	-0.3816	-0.2265	1.3029	0.9593	1.6465	0.4197	0.0115
PC13	0.2780	0.2142	0.3609	-1.2320	-1.5573	-0.9068	0.4645	0.0094

Galago elegantulus

PC	Slope	Slope lower CI	Slope higher CI	Intercept	Intercept lower CI	Intercept higher CI	p value	r squared
PC1	-1.3138	-1.8680	-0.9240	6.2031	3.9746	8.4315	0.7004	0.0047
PC2	1.0204	0.7345	1.4176	-4.8179	-6.4304	-3.2053	0.0318	0.1361
PC3	0.7986	0.5661	1.1267	-3.7707	-5.0942	-2.4471	0.2045	0.0498
PC4	-0.7189	-1.0228	-0.5053	3.3942	2.1723	4.6160	0.8936	0.0006
PC5	0.6305	0.4438	0.8957	-2.9770	-4.0437	-1.9102	0.5771	0.0098
PC6	-0.5854	-0.8328	-0.4115	2.7641	1.7694	3.7588	0.8381	0.0013
PC7	0.5543	0.3897	0.7883	-2.6171	-3.5581	-1.6760	0.7648	0.0028
PC8	0.4890	0.3457	0.6917	-2.3089	-3.1257	-1.4920	0.2915	0.0347
PC9	-0.4659	-0.6627	-0.3275	2.1996	1.4081	2.9911	0.8283	0.0015
PC10	-0.4506	-0.6373	-0.3185	2.1274	1.3747	2.8800	0.2914	0.0347
PC11	0.3689	0.2618	0.5198	-1.7417	-2.3507	-1.1326	0.1739	0.0570
PC12	-0.3597	-0.5088	-0.2543	1.6982	1.0973	2.2991	0.2930	0.0345
PC13	0.3487	0.2508	0.4849	-1.6465	-2.1992	-1.0938	0.0354	0.1311

Galago moholi

PC	Slope	Slope lower CI	Slope higher CI	Intercept	Intercept lower CI	Intercept higher CI	p value	r squared
PC1	-0.7572	-0.9553	-0.6001	3.4435	2.6358	4.2512	0.2618	0.0177
PC2	0.5185	0.4187	0.6421	-2.3580	-2.8662	-1.8499	0.0003	0.1707
PC3	-0.4845	-0.6124	-0.3832	2.2032	1.6819	2.7245	0.8687	0.0004
PC4	0.4703	0.3747	0.5902	-2.1386	-2.6288	-1.6485	0.0336	0.0620
PC5	-0.4494	-0.5630	-0.3588	2.0439	1.5794	2.5083	0.0168	0.0779
PC6	-0.3825	-0.4835	-0.3026	1.7395	1.3280	2.1509	0.7918	0.0010
PC7	0.3556	0.2813	0.4495	-1.6170	-1.9996	-1.2345	0.8189	0.0007
PC8	0.3463	0.2739	0.4378	-1.5748	-1.9474	-1.2022	0.8527	0.0005
PC9	-0.3108	-0.3922	-0.2463	1.4135	1.0817	1.7453	0.2855	0.0160
PC10	-0.2910	-0.3664	-0.2312	1.3236	1.0160	1.6312	0.1096	0.0357
PC11	-0.2837	-0.3586	-0.2244	1.2900	0.9848	1.5952	0.8419	0.0006
PC12	-0.2794	-0.3502	-0.2229	1.2708	0.9813	1.5603	0.0204	0.0734
PC13	0.2617	0.2084	0.3287	-1.1903	-1.4638	-0.9168	0.0413	0.0573

Galago senegalensis

PC	Slope	Slope lower CI	Slope higher CI	Intercept	Intercept lower CI	Intercept higher CI	p value	r squared
PC1	-0.5590	-0.6480	-0.4822	2.5913	2.2068	2.9758	0.0479	0.0224
PC2	0.4614	0.4072	0.5229	-2.1391	-2.4074	-1.8708	0.0000	0.3014
PC3	-0.4292	-0.4942	-0.3727	1.9895	1.7078	2.2712	0.0000	0.1097
PC4	0.4040	0.3485	0.4684	-1.8730	-2.1507	-1.5952	0.0443	0.0232
PC5	-0.3435	-0.3985	-0.2961	1.5926	1.3553	1.8298	0.1113	0.0146
PC6	-0.3357	-0.3897	-0.2891	1.5561	1.3230	1.7892	0.4397	0.0035
PC7	-0.3276	-0.3770	-0.2847	1.5189	1.3049	1.7329	0.0000	0.1189
PC8	0.3094	0.2665	0.3592	-1.4343	-1.6491	-1.2195	0.3949	0.0042
PC9	-0.3065	-0.3559	-0.2640	1.4211	1.2082	1.6340	0.4449	0.0034
PC10	-0.2794	-0.3244	-0.2406	1.2952	1.1008	1.4896	0.9875	0.0000
PC11	0.2556	0.2202	0.2968	-1.1851	-1.3627	-1.0075	0.4659	0.0031
PC12	0.2519	0.2170	0.2924	-1.1678	-1.3423	-0.9932	0.2522	0.0076
PC13	-0.2420	-0.2810	-0.2085	1.1219	0.9539	1.2900	0.4455	0.0034

Galago zanzibaricus

PC	Slope	Slope lower CI	Slope higher CI	Intercept	Intercept lower CI	Intercept higher CI	p value	r squared
PC1	1.0332	0.6833	1.5622	-4.7387	-6.7543	-2.7231	0.4264	0.0277
PC2	-0.7441	-1.0934	-0.5063	3.4125	2.0662	4.7589	0.0450	0.1635
PC3	-0.5633	-0.8543	-0.3714	2.5834	1.4758	3.6910	0.6008	0.0121
PC4	0.5403	0.3575	0.8166	-2.4781	-3.5308	-1.4253	0.4068	0.0301
PC5	-0.4955	-0.7259	-0.3383	2.2728	1.3840	3.1616	0.0356	0.1782
PC6	0.4598	0.3062	0.6905	-2.1088	-2.9901	-1.2275	0.2321	0.0615
PC7	0.4207	0.2822	0.6272	-1.9294	-2.7206	-1.1382	0.1313	0.0962
PC8	0.3966	0.2615	0.6016	-1.8191	-2.5992	-1.0389	0.6098	0.0115
PC9	0.3692	0.2472	0.5514	-1.6932	-2.3907	-0.9956	0.1503	0.0878
PC10	-0.3481	-0.5214	-0.2324	1.5965	0.9337	2.2593	0.1894	0.0737
PC11	0.3203	0.2146	0.4780	-1.4691	-2.0731	-0.8650	0.1419	0.0914
PC12	0.3170	0.2095	0.4797	-1.4539	-2.0736	-0.8342	0.4633	0.0236
PC13	0.2873	0.1894	0.4360	-1.3177	-1.8833	-0.7522	0.6323	0.0101

Otolemur crassicaudatus

PC	Slope	Slope lower CI	Slope higher CI	Intercept	Intercept lower CI	Intercept higher CI	p value	r squared
PC1	0.4424	0.3631	0.5389	-2.2629	-2.7126	-1.8132	0.3942	0.0073
PC2	-0.3474	-0.4060	-0.2973	1.7772	1.4990	2.0554	0.0000	0.3841
PC3	-0.3172	-0.3847	-0.2615	1.6225	1.3071	1.9378	0.0242	0.0503
PC4	-0.2792	-0.3316	-0.2351	1.4284	1.1815	1.6753	0.0000	0.2487
PC5	-0.2396	-0.2908	-0.1974	1.2256	0.9866	1.4647	0.0358	0.0438
PC6	-0.2121	-0.2584	-0.1741	1.0849	0.8694	1.3005	0.3817	0.0077
PC7	0.2025	0.1662	0.2468	-1.0360	-1.2422	-0.8299	0.5104	0.0044
PC8	-0.1824	-0.2223	-0.1496	0.9328	0.7468	1.1189	0.9113	0.0001
PC9	-0.1775	-0.2163	-0.1456	0.9078	0.7267	1.0888	0.9764	0.0000
PC10	-0.1724	-0.2101	-0.1414	0.8818	0.7059	1.0576	0.8228	0.0005
PC11	0.1680	0.1380	0.2047	-0.8596	-1.0302	-0.6889	0.3384	0.0093
PC12	-0.1583	-0.1929	-0.1300	0.8100	0.6492	0.9709	0.3441	0.0090
PC13	-0.1530	-0.1865	-0.1255	0.7826	0.6266	0.9387	0.8012	0.0006

Otolemur garnettii

PC	Slope	Slope lower CI	Slope higher CI	Intercept	Intercept lower CI	Intercept higher CI	p value	r squared
PC1	-0.4938	-0.5719	-0.4263	2.4918	2.1245	2.8592	0.0000	0.4875
PC2	0.3911	0.3218	0.4753	-1.9736	-2.3610	-1.5862	0.0029	0.0914
PC3	0.3319	0.2714	0.4061	-1.6751	-2.0150	-1.3352	0.0979	0.0292
PC4	0.2786	0.2274	0.3415	-1.4061	-1.6940	-1.1182	0.3038	0.0114
PC5	-0.2644	-0.3244	-0.2155	1.3342	1.0595	1.6090	0.9550	0.0000
PC6	-0.2515	-0.3083	-0.2052	1.2691	1.0088	1.5295	0.3860	0.0081
PC7	-0.2385	-0.2926	-0.1944	1.2036	0.9560	1.4513	0.6984	0.0016
PC8	0.2206	0.1803	0.2698	-1.1131	-1.3388	-0.8874	0.0922	0.0302
PC9	-0.2055	-0.2506	-0.1686	1.0372	0.8301	1.2442	0.0164	0.0603
PC10	0.1890	0.1542	0.2317	-0.9539	-1.1493	-0.7584	0.3368	0.0099
PC11	0.1831	0.1493	0.2246	-0.9242	-1.1140	-0.7343	0.4971	0.0050
PC12	-0.1652	-0.2027	-0.1346	0.8336	0.6620	1.0053	0.8737	0.0003
PC13	-0.1598	-0.1952	-0.1308	0.8064	0.6440	0.9689	0.0433	0.0432

Avahi laniger

PC	Slope	Slope lower CI	Slope higher CI	Intercept	Intercept lower CI	Intercept higher CI	p value	r squared
PC1	-1.1766	-1.8227	-0.7595	5.7450	3.1494	8.3406	0.6688	0.0089
PC2	1.0100	0.6518	1.5648	-4.9314	-7.1605	-2.7023	0.6854	0.0080
PC3	0.8380	0.5407	1.2989	-4.0917	-5.9428	-2.2406	0.7203	0.0062
PC4	-0.7737	-1.1339	-0.5279	3.7779	2.2983	5.2574	0.0139	0.2553
PC5	0.6599	0.4259	1.0224	-3.2221	-4.6785	-1.7657	0.6846	0.0080
PC6	-0.5227	-0.7950	-0.3437	2.5523	1.4506	3.6540	0.1519	0.0953
PC7	-0.5085	-0.7879	-0.3282	2.4830	1.3607	3.6053	0.6847	0.0080
PC8	0.4875	0.3173	0.7490	-2.3804	-3.4343	-1.3266	0.3134	0.0484
PC9	-0.4253	-0.6600	-0.2741	2.0768	1.1345	3.0190	0.9198	0.0005
PC10	0.4004	0.2600	0.6167	-1.9552	-2.8262	-1.0842	0.3828	0.0365
PC11	-0.3829	-0.5940	-0.2467	1.8694	1.0215	2.7173	0.8803	0.0011
PC12	-0.3681	-0.5699	-0.2378	1.7976	0.9868	2.6084	0.6167	0.0121
PC13	0.3556	0.2292	0.5519	-1.7365	-2.5243	-0.9487	0.9023	0.0007

Indri indri

PC	Slope	Slope lower CI	Slope higher CI	Intercept	Intercept lower CI	Intercept higher CI	p value	r squared
PC1	-0.9955	-1.3691	-0.7238	5.4632	3.6923	7.2340	0.1579	0.0532
PC2	0.8115	0.5861	1.1234	-4.4533	-5.9277	-2.9790	0.5018	0.0123
PC3	-0.7373	-1.0172	-0.5344	4.0462	2.7212	5.3712	0.2639	0.0336
PC4	-0.6520	-0.9026	-0.4709	3.5780	2.3933	4.7627	0.5072	0.0120
PC5	-0.6138	-0.8295	-0.4542	3.3685	2.3385	4.3985	0.0124	0.1574
PC6	0.5570	0.4021	0.7717	-3.0570	-4.0715	-2.0426	0.5956	0.0077
PC7	-0.5241	-0.7207	-0.3811	2.8763	1.9444	3.8083	0.1548	0.0539
PC8	-0.4850	-0.6723	-0.3498	2.6615	1.7767	3.5463	0.7031	0.0040
PC9	-0.4397	-0.6089	-0.3175	2.4131	1.6135	3.2127	0.5347	0.0105
PC10	-0.3970	-0.5506	-0.2863	2.1788	1.4535	2.9041	0.8251	0.0013
PC11	0.3902	0.2859	0.5324	-2.1412	-2.8177	-1.4648	0.0492	0.1006
PC12	0.3847	0.2774	0.5336	-2.1115	-2.8146	-1.4083	0.8776	0.0006
PC13	-0.3369	-0.4672	-0.2429	1.8488	1.2331	2.4644	0.8837	0.0006

Propithecus diadema

PC	Slope	Slope lower CI	Slope higher CI	Intercept	Intercept lower CI	Intercept higher CI	p value	r squared
PC1	-0.7239	-1.0722	-0.4888	3.8870	2.3207	5.4532	0.8741	0.0010
PC2	-0.6419	-0.9184	-0.4486	3.4464	2.1851	4.7078	0.0264	0.1758
PC3	-0.5179	-0.7671	-0.3497	2.7809	1.6603	3.9016	0.8844	0.0008
PC4	-0.5113	-0.7539	-0.3467	2.7451	1.6519	3.8383	0.4291	0.0242
PC5	-0.4703	-0.6966	-0.3175	2.5250	1.5071	3.5429	0.9562	0.0001
PC6	-0.4095	-0.5982	-0.2804	2.1989	1.3457	3.0522	0.1628	0.0735
PC7	-0.4059	-0.5958	-0.2766	2.1797	1.3228	3.0366	0.2575	0.0490
PC8	0.3605	0.2434	0.5339	-1.9357	-2.7158	-1.1557	0.8799	0.0009
PC9	-0.3134	-0.4629	-0.2121	1.6826	1.0094	2.3559	0.5357	0.0149
PC10	-0.2931	-0.4241	-0.2025	1.5735	0.9784	2.1686	0.0711	0.1199
PC11	0.2700	0.1829	0.3986	-1.4496	-2.0287	-0.8705	0.4967	0.0180
PC12	-0.2635	-0.3890	-0.1785	1.4147	0.8495	1.9800	0.4998	0.0177
PC13	-0.2335	-0.3432	-0.1589	1.2540	0.7593	1.7487	0.2940	0.0423

Propithecus verreauxi

PC	Slope	Slope lower CI	Slope higher CI	Intercept	Intercept lower CI	Intercept higher CI	p value	r squared
PC1	0.7301	0.5471	0.9744	-3.8648	-4.9958	-2.7339	0.0137	0.1393
PC2	0.6688	0.5049	0.8860	-3.5401	-4.5487	-2.5314	0.0041	0.1839
PC3	-0.5585	-0.7585	-0.4112	2.9563	2.0373	3.8753	0.2781	0.0286
PC4	-0.5464	-0.7449	-0.4008	2.8923	1.9817	3.8028	0.6952	0.0038
PC5	-0.4519	-0.6130	-0.3331	2.3919	1.6511	3.1326	0.2230	0.0360
PC6	0.4457	0.3338	0.5950	-2.3591	-3.0505	-1.6678	0.0147	0.1368
PC7	-0.4090	-0.5549	-0.3015	2.1650	1.4945	2.8356	0.2242	0.0358
PC8	0.3722	0.2760	0.5020	-1.9703	-2.5684	-1.3722	0.0781	0.0738
PC9	0.3596	0.2639	0.4901	-1.9035	-2.5021	-1.3048	0.6324	0.0056
PC10	0.3421	0.2509	0.4665	-1.8108	-2.3815	-1.2401	0.8040	0.0015
PC11	-0.3269	-0.4457	-0.2398	1.7303	1.1853	2.2753	0.7336	0.0029
PC12	-0.3075	-0.4195	-0.2255	1.6279	1.1145	2.1414	0.9782	0.0000
PC13	-0.3012	-0.4098	-0.2213	1.5941	1.0952	2.0930	0.4262	0.0155

Eulemur fulvus

PC	Slope	Slope lower CI	Slope higher CI	Intercept	Intercept lower CI	Intercept higher CI	p value	r squared
PC1	-0.6858	-0.7950	-0.5916	3.6560	3.1138	4.1982	0.0436	0.0233
PC2	0.4540	0.3911	0.5270	-2.4202	-2.7823	-2.0581	0.3085	0.0060
PC3	-0.4420	-0.5130	-0.3808	2.3561	2.0037	2.7086	0.2910	0.0064
PC4	-0.4201	-0.4864	-0.3629	2.2395	1.9103	2.5687	0.0074	0.0407
PC5	-0.3834	-0.4440	-0.3311	2.0441	1.7431	2.3451	0.0106	0.0371
PC6	0.3568	0.3079	0.4134	-1.9020	-2.1832	-1.6207	0.0240	0.0291
PC7	0.3296	0.2839	0.3828	-1.7571	-2.0207	-1.4935	0.7747	0.0005
PC8	0.3246	0.2799	0.3764	-1.7301	-1.9874	-1.4728	0.0766	0.0180
PC9	-0.3083	-0.3566	-0.2666	1.6435	1.4035	1.8834	0.0021	0.0535
PC10	-0.2906	-0.3369	-0.2507	1.5491	1.3193	1.7789	0.0458	0.0229
PC11	-0.2622	-0.3041	-0.2261	1.3978	1.1897	1.6059	0.0962	0.0159
PC12	-0.2618	-0.3039	-0.2255	1.3955	1.1864	1.6047	0.4905	0.0028
PC13	-0.2535	-0.2943	-0.2184	1.3516	1.1494	1.5538	0.2950	0.0063

Eulemur macaco

PC	Slope	Slope lower CI	Slope higher CI	Intercept	Intercept lower CI	Intercept higher CI	p value	r squared
PC1	0.7922	0.6075	1.0331	-4.2404	-5.3795	-3.1013	0.1032	0.0493
PC2	0.6032	0.4600	0.7909	-3.2287	-4.1144	-2.3430	0.4963	0.0088
PC3	0.5862	0.4666	0.7365	-3.1379	-3.8601	-2.4156	0.0000	0.3020
PC4	0.5409	0.4220	0.6934	-2.8955	-3.6219	-2.1691	0.0017	0.1709
PC5	-0.5019	-0.6576	-0.3831	2.6865	1.9519	3.4211	0.3733	0.0150
PC6	0.4731	0.3606	0.6206	-2.5322	-3.2280	-1.8364	0.5974	0.0053
PC7	-0.4459	-0.5853	-0.3396	2.3867	1.7291	3.0443	0.9750	0.0000
PC8	-0.4131	-0.5422	-0.3147	2.2113	1.6024	2.8202	0.7976	0.0013
PC9	0.3870	0.2954	0.5070	-2.0714	-2.6379	-1.5050	0.3729	0.0150
PC10	0.3768	0.2870	0.4946	-2.0169	-2.5725	-1.4612	0.9418	0.0001
PC11	-0.3504	-0.4581	-0.2680	1.8756	1.3668	2.3844	0.2022	0.0305
PC12	0.3239	0.2467	0.4252	-1.7337	-2.2113	-1.2560	0.9802	0.0000
PC13	0.3140	0.2402	0.4105	-1.6806	-2.1364	-1.2249	0.1973	0.0312

Eulemur mongoz

PC	Slope	Slope lower CI	Slope higher CI	Intercept	Intercept lower CI	Intercept higher CI	p value	r squared
PC1	0.6320	0.5011	0.7969	-3.3387	-4.1201	-2.5574	0.0001	0.2501
PC2	0.5095	0.3909	0.6642	-2.6919	-3.4139	-1.9699	0.3651	0.0149
PC3	0.3500	0.2680	0.4570	-1.8491	-2.3484	-1.3498	0.7721	0.0015
PC4	-0.3436	-0.4480	-0.2636	1.8154	1.3283	2.3025	0.3760	0.0143
PC5	-0.3191	-0.3985	-0.2555	1.6857	1.3080	2.0635	0.0000	0.3123
PC6	0.2829	0.2171	0.3686	-1.4948	-1.8949	-1.0946	0.3117	0.0186
PC7	-0.2675	-0.3487	-0.2052	1.4131	1.0338	1.7923	0.3834	0.0138
PC8	0.2623	0.2010	0.3425	-1.3860	-1.7600	-1.0121	0.6607	0.0035
PC9	-0.2455	-0.3201	-0.1882	1.2968	0.9485	1.6452	0.4148	0.0121
PC10	0.2326	0.1781	0.3038	-1.2287	-1.5608	-0.8966	0.9815	0.0000
PC11	0.2137	0.1637	0.2788	-1.1288	-1.4328	-0.8248	0.5412	0.0068
PC12	0.2032	0.1564	0.2639	-1.0735	-1.3573	-0.7896	0.1225	0.0428
PC13	0.2016	0.1547	0.2628	-1.0651	-1.3508	-0.7794	0.3655	0.0149

Eulemur rubriventer

PC	Slope	Slope lower CI	Slope higher CI	Intercept	Intercept lower CI	Intercept higher CI	p value	r squared
PC1	1.5185	1.0263	2.2467	-8.0749	-11.3197	-4.8300	0.2707	0.0483
PC2	0.7830	0.5672	1.0808	-4.1636	-5.5293	-2.7979	0.0008	0.3659
PC3	-0.6988	-1.0327	-0.4729	3.7160	2.2274	5.2047	0.2426	0.0542
PC4	-0.6143	-0.9076	-0.4157	3.2664	1.9584	4.5744	0.2394	0.0549
PC5	0.5725	0.3835	0.8547	-3.0443	-4.2971	-1.7914	0.8315	0.0018
PC6	-0.5226	-0.7635	-0.3577	2.7789	1.6997	3.8581	0.0893	0.1111
PC7	0.4933	0.3304	0.7365	-2.6232	-3.7028	-1.5437	0.8321	0.0018
PC8	-0.4624	-0.6876	-0.3110	2.4589	1.4574	3.4604	0.4571	0.0223
PC9	0.3972	0.2666	0.5919	-2.1123	-2.9775	-1.2471	0.5991	0.0112
PC10	0.3922	0.2631	0.5845	-2.0853	-2.9399	-1.2308	0.6139	0.0103
PC11	-0.3567	-0.5303	-0.2399	1.8966	1.1244	2.6688	0.4496	0.0231
PC12	0.3443	0.2306	0.5142	-1.8311	-2.5852	-1.0769	0.9340	0.0003
PC13	0.3084	0.2072	0.4589	-1.6397	-2.3089	-0.9705	0.5008	0.0183

Hapalemur griseus

PC	Slope	Slope lower CI	Slope higher CI	Intercept	Intercept lower CI	Intercept higher CI	p value	r squared
PC1	0.7155	0.4939	1.0367	-3.6051	-4.9726	-2.2375	0.0444	0.1519
PC2	-0.6053	-0.9028	-0.4059	3.0498	1.7978	4.3019	0.6825	0.0068
PC3	0.5376	0.3663	0.7890	-2.7085	-3.7734	-1.6436	0.1306	0.0890
PC4	-0.4624	-0.6737	-0.3173	2.3296	1.4319	3.2273	0.0705	0.1249
PC5	-0.4334	-0.6386	-0.2941	2.1835	1.3158	3.0513	0.1846	0.0693
PC6	0.3561	0.2413	0.5256	-1.7942	-2.5107	-1.0777	0.2170	0.0603
PC7	-0.3485	-0.4963	-0.2447	1.7556	1.1217	2.3895	0.0110	0.2318
PC8	0.3223	0.2159	0.4810	-1.6236	-2.2916	-0.9557	0.7989	0.0026
PC9	-0.3131	-0.4589	-0.2136	1.5773	0.9593	2.1953	0.1172	0.0953
PC10	0.2954	0.1981	0.4405	-1.4883	-2.0989	-0.8776	0.6592	0.0079
PC11	-0.2721	-0.4059	-0.1824	1.3709	0.8079	1.9339	0.6975	0.0061
PC12	0.2409	0.1613	0.3597	-1.2135	-1.7134	-0.7136	0.9983	0.0000
PC13	-0.2385	-0.3561	-0.1597	1.2014	0.7065	1.6963	0.9485	0.0002

Lemur catta

PC	Slope	Slope lower CI	Slope higher CI	Intercept	Intercept lower CI	Intercept higher CI	p value	r squared
PC1	-0.5173	-0.7146	-0.3744	2.7195	1.8253	3.6138	0.0167	0.1662
PC2	0.4277	0.3098	0.5905	-2.2488	-2.9867	-1.5108	0.0155	0.1695
PC3	-0.4108	-0.5840	-0.2890	2.1600	1.3845	2.9354	0.6595	0.0061
PC4	-0.3918	-0.5538	-0.2773	2.0601	1.3332	2.7870	0.2573	0.0399
PC5	0.3492	0.2471	0.4934	-1.8357	-2.4831	-1.1882	0.2521	0.0408
PC6	0.3323	0.2341	0.4716	-1.7469	-2.3714	-1.1225	0.4941	0.0147
PC7	-0.2907	-0.4130	-0.2047	1.5285	0.9808	2.0761	0.5726	0.0101
PC8	0.2865	0.2015	0.4074	-1.5063	-2.0478	-0.9647	0.7452	0.0033
PC9	0.2586	0.1819	0.3676	-1.3593	-1.8476	-0.8710	0.6899	0.0050
PC10	0.2354	0.1657	0.3345	-1.2377	-1.6815	-0.7938	0.6074	0.0083
PC11	0.2339	0.1645	0.3326	-1.2296	-1.6716	-0.7877	0.7256	0.0039
PC12	-0.2231	-0.3085	-0.1613	1.1728	0.7857	1.5598	0.0191	0.1600
PC13	0.2192	0.1545	0.3111	-1.1526	-1.5642	-0.7410	0.4677	0.0166

Varecia variegata

PC	Slope	Slope lower CI	Slope higher CI	Intercept	Intercept lower CI	Intercept higher CI	p value	r squared
PC1	-0.6894	-0.9553	-0.4975	3.7759	2.5220	5.0298	0.6311	0.0063
PC2	-0.4971	-0.6216	-0.3976	2.7230	2.1096	3.3364	0.0000	0.5427
PC3	-0.4825	-0.6693	-0.3478	2.6428	1.7625	3.5232	0.9419	0.0001
PC4	-0.4069	-0.5560	-0.2978	2.2288	1.5216	2.9359	0.0592	0.0929
PC5	0.3373	0.2437	0.4669	-1.8478	-2.4590	-1.2366	0.4722	0.0141
PC6	0.3278	0.2373	0.4528	-1.7955	-2.3858	-1.2052	0.3269	0.0260
PC7	-0.3042	-0.4210	-0.2197	1.6660	1.1147	2.2174	0.4867	0.0132
PC8	0.2665	0.1952	0.3637	-1.4597	-1.9211	-0.9982	0.0506	0.0994
PC9	0.2578	0.1859	0.3574	-1.4119	-1.8815	-0.9423	0.7401	0.0030
PC10	0.2445	0.1763	0.3391	-1.3392	-1.7852	-0.8931	0.9207	0.0003
PC11	-0.2307	-0.3200	-0.1664	1.2639	0.8431	1.6846	0.8186	0.0014
PC12	-0.2040	-0.2830	-0.1471	1.1177	0.7455	1.4898	0.8397	0.0011
PC13	0.1960	0.1415	0.2715	-1.0735	-1.4295	-0.7176	0.5584	0.0093

Lepilemur ruficaudatus

PC	Slope	Slope lower CI	Slope higher CI	Intercept	Intercept lower CI	Intercept higher CI	p value	r squared
PC1	0.5781	0.4322	0.7732	-2.8424	-3.6806	-2.0042	0.0000	0.5327
PC2	0.4873	0.3242	0.7327	-2.3962	-3.4007	-1.3917	0.2561	0.0557
PC3	-0.4145	-0.6283	-0.2735	2.0382	1.1659	2.9106	0.5517	0.0156
PC4	-0.3898	-0.5925	-0.2564	1.9164	1.0900	2.7428	0.8991	0.0007
PC5	-0.3424	-0.5129	-0.2286	1.6835	0.9844	2.3825	0.1902	0.0734
PC6	-0.3003	-0.4565	-0.1975	1.4764	0.8396	2.1131	0.9372	0.0003
PC7	0.2921	0.1924	0.4437	-1.4364	-2.0542	-0.8185	0.7186	0.0058
PC8	-0.2882	-0.4379	-0.1897	1.4171	0.8068	2.0274	0.7816	0.0034
PC9	-0.2792	-0.4208	-0.1853	1.3730	0.7941	1.9519	0.3102	0.0447
PC10	-0.2484	-0.3751	-0.1646	1.2216	0.7041	1.7390	0.3657	0.0357
PC11	0.2423	0.1594	0.3683	-1.1912	-1.7048	-0.6777	0.8637	0.0013
PC12	0.2338	0.1538	0.3554	-1.1495	-1.6453	-0.6536	0.9712	0.0001
PC13	0.2202	0.1452	0.3339	-1.0825	-1.5464	-0.6185	0.5895	0.0128

Loris tardigradus

PC	Slope	Slope lower CI	Slope higher CI	Intercept	Intercept lower CI	Intercept higher CI	p value	r squared
PC1	0.3763	0.2707	0.5231	-1.8014	-2.4057	-1.1971	0.0015	0.3372
PC2	0.3396	0.2394	0.4818	-1.6259	-2.2064	-1.0454	0.0080	0.2493
PC3	0.3063	0.2135	0.4395	-1.4663	-2.0074	-0.9252	0.0200	0.1980
PC4	-0.2689	-0.3993	-0.1811	1.2874	0.7650	1.8098	0.3837	0.0305
PC5	-0.2073	-0.3095	-0.1388	0.9922	0.5836	1.4009	0.8592	0.0013
PC6	-0.2057	-0.3042	-0.1391	0.9847	0.5893	1.3800	0.2591	0.0506
PC7	0.1899	0.1273	0.2832	-0.9089	-1.2822	-0.5356	0.6856	0.0067
PC8	0.1561	0.1047	0.2329	-0.7474	-1.0545	-0.4403	0.7003	0.0060
PC9	0.1481	0.0992	0.2212	-0.7092	-1.0014	-0.4169	0.9473	0.0002
PC10	0.1366	0.0918	0.2035	-0.6541	-0.9216	-0.3866	0.5395	0.0152
PC11	-0.1215	-0.1811	-0.0815	0.5817	0.3433	0.8200	0.5966	0.0114
PC12	0.1196	0.0807	0.1774	-0.5728	-0.8043	-0.3412	0.3349	0.0372
PC13	0.1163	0.0781	0.1731	-0.5567	-0.7843	-0.3291	0.5324	0.0158

Nycticebus bengalensis

PC	Slope	Slope lower CI	Slope higher CI	Intercept	Intercept lower CI	Intercept higher CI	p value	r squared
PC1	0.7737	0.4996	1.1983	-3.9293	-5.7036	-2.1551	0.2601	0.0629
PC2	-0.6757	-1.0256	-0.4452	3.4315	1.9575	4.9055	0.0729	0.1520
PC3	0.5762	0.3670	0.9045	-2.9260	-4.2907	-1.5612	0.9564	0.0002
PC4	0.5207	0.3320	0.8165	-2.6443	-3.8745	-1.4140	0.7513	0.0051
PC5	-0.4579	-0.7171	-0.2923	2.3251	1.2464	3.4039	0.6461	0.0108
PC6	0.4419	0.2874	0.6794	-2.2440	-3.2396	-1.2485	0.1618	0.0955
PC7	-0.4019	-0.6298	-0.2565	2.0412	1.0932	2.9892	0.6801	0.0087
PC8	0.3545	0.2297	0.5470	-1.8003	-2.6061	-0.9946	0.2040	0.0794
PC9	-0.3358	-0.5139	-0.2194	1.7053	0.9577	2.4529	0.1198	0.1166
PC10	0.3237	0.2081	0.5036	-1.6441	-2.3943	-0.8939	0.3537	0.0431
PC11	0.3012	0.1928	0.4708	-1.5298	-2.2358	-0.8239	0.5165	0.0213
PC12	0.2711	0.1825	0.4028	-1.3769	-1.9364	-0.8174	0.0203	0.2410
PC13	-0.2669	-0.4146	-0.1718	1.3555	0.7389	1.9720	0.3225	0.0489

Nycticebus coucang

PC	Slope	Slope lower CI	Slope higher CI	Intercept	Intercept lower CI	Intercept higher CI	p value	r squared
PC1	-0.5745	-0.7307	-0.4517	2.8626	2.1675	3.5576	0.4451	0.0087
PC2	0.4053	0.3188	0.5154	-2.0196	-2.5093	-1.5298	0.3852	0.0113
PC3	0.3797	0.2983	0.4835	-1.8920	-2.3535	-1.4306	0.9666	0.0000
PC4	-0.3412	-0.4302	-0.2706	1.7001	1.3025	2.0976	0.0180	0.0807
PC5	0.3074	0.2447	0.3861	-1.5316	-1.8839	-1.1793	0.0052	0.1106
PC6	0.2794	0.2199	0.3551	-1.3923	-1.7290	-1.0556	0.2928	0.0165
PC7	0.2757	0.2176	0.3493	-1.3738	-1.7020	-1.0455	0.0990	0.0401
PC8	0.2523	0.1982	0.3211	-1.2569	-1.5630	-0.9508	0.6630	0.0029
PC9	0.2359	0.1902	0.2925	-1.1753	-1.4301	-0.9206	0.0001	0.2102
PC10	0.2302	0.1813	0.2924	-1.1472	-1.4238	-0.8705	0.2218	0.0222
PC11	0.2207	0.1739	0.2802	-1.0997	-1.3645	-0.8349	0.1917	0.0253
PC12	-0.2157	-0.2740	-0.1697	1.0745	0.8146	1.3343	0.2898	0.0167
PC13	-0.2044	-0.2600	-0.1607	1.0186	0.7712	1.2661	0.4694	0.0078

Perodicticus potto

PC	Slope	Slope lower CI	Slope higher CI	Intercept	Intercept lower CI	Intercept higher CI	p value	r squared
PC1	-0.5714	-0.6797	-0.4803	2.8857	2.3820	3.3893	0.2147	0.0121
PC2	-0.4892	-0.5760	-0.4155	2.4707	2.0653	2.8762	0.0000	0.1267
PC3	0.4345	0.3649	0.5174	-2.1945	-2.5797	-1.8093	0.7207	0.0010
PC4	0.4148	0.3488	0.4934	-2.0951	-2.4601	-1.7301	0.1582	0.0156
PC5	0.3806	0.3196	0.4532	-1.9221	-2.2597	-1.5846	0.9496	0.0000
PC6	0.3449	0.2950	0.4032	-1.7418	-2.0150	-1.4687	0.0000	0.2023
PC7	-0.3304	-0.3934	-0.2774	1.6684	1.3754	1.9614	0.9672	0.0000
PC8	-0.3222	-0.3837	-0.2706	1.6273	1.3418	1.9129	0.6723	0.0014
PC9	0.3199	0.2690	0.3804	-1.6155	-1.8969	-1.3340	0.1581	0.0156
PC10	0.2934	0.2468	0.3486	-1.4815	-1.7386	-1.2245	0.0794	0.0240
PC11	0.2762	0.2342	0.3257	-1.3948	-1.6257	-1.1639	0.0001	0.1114
PC12	0.2686	0.2257	0.3197	-1.3566	-1.5941	-1.1190	0.4076	0.0054
PC13	0.2599	0.2188	0.3088	-1.3128	-1.5399	-1.0856	0.0533	0.0291

2* model face module against ln CS of face

Cheirogaleus major

PC	Slope	Slope lower CI	Slope higher CI	Intercept	Intercept lower CI	Intercept higher CI	p value	r squared
PC1	-0.4916	-0.7410	-0.3262	2.0483	1.1841	2.9125	0.3169	0.0435
PC2	-0.4677	-0.6823	-0.3206	1.9488	1.1953	2.7023	0.0264	0.1967
PC3	0.4276	0.2945	0.6210	-1.7818	-2.4621	-1.1014	0.0191	0.2165
PC4	0.3962	0.2608	0.6019	-1.6508	-2.3614	-0.9401	0.7588	0.0042
PC5	-0.3753	-0.5676	-0.2481	1.5636	0.8978	2.2294	0.4432	0.0258
PC6	0.3513	0.2313	0.5337	-1.4638	-2.0939	-0.8337	0.7547	0.0043
PC7	-0.3110	-0.4659	-0.2076	1.2959	0.7578	1.8339	0.1895	0.0736
PC8	-0.3058	-0.4644	-0.2014	1.2743	0.7263	1.8223	0.7060	0.0063
PC9	-0.2743	-0.4160	-0.1809	1.1430	0.6530	1.6329	0.5944	0.0125
PC10	0.2696	0.1777	0.4092	-1.1234	-1.6059	-0.6409	0.6536	0.0089
PC11	-0.2461	-0.3742	-0.1619	1.0254	0.5832	1.4677	0.9182	0.0005
PC12	0.2297	0.1551	0.3403	-0.9571	-1.3429	-0.5713	0.0804	0.1269
PC13	-0.2145	-0.3196	-0.1439	0.8937	0.5277	1.2596	0.1258	0.0989

Cheirogaleus medius

PC	Slope	Slope lower CI	Slope higher CI	Intercept	Intercept lower CI	Intercept higher CI	p value	r squared
PC1	-0.5401	-0.7526	-0.3876	2.0894	1.3834	2.7954	0.0040	0.2679
PC2	-0.4941	-0.7183	-0.3399	1.9115	1.1796	2.6433	0.2000	0.0601
PC3	0.4474	0.3088	0.6481	-1.7306	-2.3869	-1.0742	0.1432	0.0777
PC4	0.4436	0.3020	0.6515	-1.7159	-2.3919	-1.0400	0.7124	0.0051
PC5	0.3747	0.2558	0.5489	-1.4497	-2.0166	-0.8828	0.4698	0.0195
PC6	-0.3443	-0.5058	-0.2344	1.3319	0.8068	1.8569	0.7614	0.0035
PC7	0.3300	0.2245	0.4849	-1.2764	-1.7802	-0.7727	0.8453	0.0014
PC8	-0.3175	-0.4622	-0.2181	1.2282	0.7560	1.7003	0.2319	0.0525
PC9	0.2793	0.1941	0.4020	-1.0806	-1.4829	-0.6784	0.0764	0.1117
PC10	0.2571	0.1762	0.3754	-0.9947	-1.3801	-0.6094	0.3122	0.0378
PC11	0.2496	0.1699	0.3666	-0.9654	-1.3460	-0.5848	0.7593	0.0035
PC12	-0.2216	-0.3254	-0.1510	0.8574	0.5199	1.1949	0.6705	0.0068
PC13	0.2185	0.1496	0.3191	-0.8454	-1.1732	-0.5175	0.3260	0.0357

Microcebus murinus

PC	Slope	Slope lower CI	Slope higher CI	Intercept	Intercept lower CI	Intercept higher CI	p value	r squared
PC1	0.5918	0.4679	0.7485	-2.1287	-2.6334	-1.6240	0.3822	0.0109
PC2	-0.5236	-0.6620	-0.4142	1.8834	1.4377	2.3291	0.3094	0.0148
PC3	-0.4911	-0.6216	-0.3880	1.7664	1.3461	2.1867	0.5985	0.0040
PC4	-0.4716	-0.5783	-0.3846	1.6964	1.3479	2.0448	0.0000	0.2576
PC5	0.4170	0.3298	0.5273	-1.5000	-1.8553	-1.1447	0.3444	0.0128
PC6	-0.3932	-0.4977	-0.3107	1.4144	1.0781	1.7508	0.5546	0.0050
PC7	-0.3688	-0.4647	-0.2927	1.3265	1.0170	1.6359	0.0823	0.0425
PC8	-0.3500	-0.4428	-0.2767	1.2589	0.9601	1.5576	0.4259	0.0091
PC9	-0.3396	-0.4297	-0.2684	1.2216	0.9316	1.5116	0.4461	0.0083
PC10	0.3115	0.2462	0.3940	-1.1204	-1.3862	-0.8545	0.4185	0.0094
PC11	-0.2947	-0.3727	-0.2330	1.0600	0.8089	1.3111	0.3508	0.0124
PC12	0.2858	0.2257	0.3620	-1.0281	-1.2732	-0.7831	0.8505	0.0005
PC13	-0.2808	-0.3525	-0.2236	1.0099	0.7782	1.2415	0.0209	0.0739

Microcebus rufus

PC	Slope	Slope lower CI	Slope higher CI	Intercept	Intercept lower CI	Intercept higher CI	p value	r squared
PC1	0.4499	0.3106	0.6519	-1.6434	-2.2669	-1.0200	0.1434	0.0776
PC2	0.3717	0.2534	0.5453	-1.3577	-1.8911	-0.8243	0.5924	0.0108
PC3	0.3159	0.2149	0.4642	-1.1537	-1.6090	-0.6983	0.8416	0.0015
PC4	0.2821	0.1923	0.4139	-1.0305	-1.4352	-0.6258	0.5832	0.0113
PC5	-0.2632	-0.3867	-0.1791	0.9612	0.5819	1.3405	0.8213	0.0019
PC6	-0.2450	-0.3526	-0.1703	0.8950	0.5620	1.2280	0.0749	0.1128
PC7	-0.2250	-0.3119	-0.1624	0.8219	0.5488	1.0951	0.0025	0.2919
PC8	0.2184	0.1517	0.3143	-0.7976	-1.0945	-0.5007	0.0761	0.1119
PC9	0.2126	0.1450	0.3118	-0.7767	-1.0812	-0.4721	0.5338	0.0145
PC10	0.1988	0.1353	0.2921	-0.7260	-1.0124	-0.4395	0.8227	0.0019
PC11	-0.1831	-0.2688	-0.1247	0.6687	0.4053	0.9321	0.7027	0.0055
PC12	0.1791	0.1224	0.2619	-0.6540	-0.9087	-0.3993	0.3891	0.0276
PC13	0.1604	0.1109	0.2321	-0.5860	-0.8073	-0.3648	0.1218	0.0864

Galago alleni

PC	Slope	Slope lower CI	Slope higher CI	Intercept	Intercept lower CI	Intercept higher CI	p value	r squared
PC1	-0.5756	-0.8829	-0.3753	2.3616	1.3203	3.4029	0.7236	0.0058
PC2	0.4881	0.3242	0.7348	-2.0025	-2.8448	-1.1602	0.1423	0.0952
PC3	0.4580	0.3146	0.6668	-1.8791	-2.6016	-1.1566	0.0142	0.2440
PC4	0.4086	0.2682	0.6225	-1.6764	-2.4032	-0.9497	0.3556	0.0389
PC5	-0.3575	-0.5305	-0.2410	1.4668	0.8729	2.0608	0.0515	0.1616
PC6	0.3081	0.2083	0.4558	-1.2640	-1.7717	-0.7562	0.0422	0.1746
PC7	-0.2754	-0.4211	-0.1801	1.1298	0.6355	1.6242	0.4994	0.0210
PC8	0.2577	0.1679	0.3956	-1.0572	-1.5245	-0.5899	0.8826	0.0010
PC9	0.2524	0.1646	0.3869	-1.0354	-1.4913	-0.5795	0.6679	0.0085
PC10	0.2458	0.1606	0.3761	-1.0084	-1.4506	-0.5663	0.5439	0.0170
PC11	-0.2280	-0.3448	-0.1508	0.9355	0.5375	1.3335	0.1971	0.0744
PC12	0.2008	0.1313	0.3070	-0.8237	-1.1841	-0.4632	0.5030	0.0206
PC13	0.1908	0.1243	0.2930	-0.7827	-1.1289	-0.4366	0.9718	0.0001

Galago demidoff

PC	Slope	Slope lower CI	Slope higher CI	Intercept	Intercept lower CI	Intercept higher CI	p value	r squared
PC1	-0.7050	-0.8974	-0.5538	2.6407	1.9970	3.2843	0.0020	0.1556
PC2	-0.5146	-0.6665	-0.3973	1.9276	1.4234	2.4318	0.2077	0.0277
PC3	-0.4512	-0.5848	-0.3481	1.6899	1.2464	2.1334	0.2704	0.0213
PC4	0.4392	0.3385	0.5699	-1.6451	-2.0785	-1.2116	0.3826	0.0134
PC5	0.4147	0.3230	0.5325	-1.5534	-1.9459	-1.1609	0.0191	0.0926
PC6	0.3763	0.2899	0.4885	-1.4097	-1.7817	-1.0376	0.4482	0.0101
PC7	0.3550	0.2731	0.4613	-1.3296	-1.6822	-0.9771	0.8218	0.0009
PC8	-0.3148	-0.4091	-0.2422	1.1791	0.8664	1.4918	0.8513	0.0006
PC9	-0.2940	-0.3807	-0.2270	1.1013	0.8134	1.3892	0.2003	0.0286
PC10	0.2867	0.2206	0.3727	-1.0740	-1.3589	-0.7891	0.9814	0.0000
PC11	0.2606	0.2014	0.3374	-0.9763	-1.2310	-0.7215	0.1727	0.0324
PC12	-0.2557	-0.3322	-0.1968	0.9577	0.7041	1.2112	0.6440	0.0038
PC13	0.2418	0.1860	0.3142	-0.9056	-1.1456	-0.6656	0.7445	0.0019

Galago elegantulus

PC	Slope	Slope lower CI	Slope higher CI	Intercept	Intercept lower CI	Intercept higher CI	p value	r squared
PC1	1.3108	0.9221	1.8632	-5.2981	-7.2002	-3.3961	0.6613	0.0061
PC2	1.0181	0.7324	1.4151	-4.1150	-5.4949	-2.7351	0.0341	0.1328
PC3	0.7968	0.5643	1.1251	-3.2206	-4.3540	-2.0872	0.2287	0.0450
PC4	0.7172	0.5046	1.0194	-2.8990	-3.9394	-1.8586	0.6421	0.0068
PC5	0.6291	0.4433	0.8927	-2.5427	-3.4511	-1.6343	0.4801	0.0157
PC6	0.5841	0.4107	0.8307	-2.3609	-3.2098	-1.5120	0.7587	0.0030
PC7	0.5530	0.3889	0.7864	-2.2353	-3.0387	-1.4319	0.7277	0.0038
PC8	0.4879	0.3443	0.6914	-1.9720	-2.6737	-1.2704	0.3848	0.0237
PC9	-0.4648	-0.6613	-0.3267	1.8787	1.2023	2.5552	0.9294	0.0002
PC10	-0.4495	-0.6385	-0.3165	1.8170	1.1662	2.4678	0.5633	0.0105
PC11	0.3680	0.2594	0.5221	-1.4876	-2.0186	-0.9566	0.4573	0.0174
PC12	-0.3588	-0.5097	-0.2526	1.4505	0.9308	1.9701	0.5707	0.0102
PC13	0.3479	0.2488	0.4864	-1.4063	-1.8865	-0.9261	0.0675	0.1007

Galago moholi

PC	Slope	Slope lower CI	Slope higher CI	Intercept	Intercept lower CI	Intercept higher CI	p value	r squared
PC1	-0.6035	-0.7567	-0.4813	2.3314	1.7995	2.8633	0.0231	0.0706
PC2	0.4132	0.3327	0.5133	-1.5965	-1.9455	-1.2475	0.0008	0.1467
PC3	-0.3861	-0.4879	-0.3055	1.4916	1.1393	1.8440	0.6099	0.0037
PC4	0.3748	0.2996	0.4689	-1.4480	-1.7750	-1.1209	0.0103	0.0891
PC5	-0.3582	-0.4508	-0.2846	1.3838	1.0628	1.7048	0.0936	0.0391
PC6	-0.3048	-0.3851	-0.2413	1.1777	0.8999	1.4555	0.4904	0.0067
PC7	0.2834	0.2242	0.3582	-1.0948	-1.3537	-0.8359	0.7249	0.0018
PC8	0.2760	0.2184	0.3488	-1.0662	-1.3182	-0.8143	0.6464	0.0030
PC9	-0.2477	-0.3122	-0.1966	0.9570	0.7336	1.1805	0.1673	0.0267
PC10	-0.2320	-0.2923	-0.1841	0.8961	0.6869	1.1053	0.1635	0.0272
PC11	-0.2261	-0.2858	-0.1788	0.8734	0.6667	1.0800	0.8633	0.0004
PC12	-0.2227	-0.2791	-0.1777	0.8604	0.6646	1.0562	0.0190	0.0750
PC13	0.2086	0.1665	0.2614	-0.8059	-0.9893	-0.6225	0.0191	0.0750

Galago senegalensis

PC	Slope	Slope lower CI	Slope higher CI	Intercept	Intercept lower CI	Intercept higher CI	p value	r squared
PC1	-0.5513	-0.6392	-0.4755	2.1818	1.8578	2.5057	0.0542	0.0213
PC2	0.4551	0.4022	0.5150	-1.8010	-2.0242	-1.5778	0.0000	0.3179
PC3	-0.4233	-0.4870	-0.3680	1.6750	1.4396	1.9105	0.0000	0.1227
PC4	0.3985	0.3450	0.4604	-1.5769	-1.8053	-1.3486	0.0004	0.0691
PC5	-0.3388	-0.3932	-0.2920	1.3408	1.1407	1.5410	0.1677	0.0110
PC6	-0.3311	-0.3844	-0.2852	1.3102	1.1140	1.5064	0.3842	0.0044
PC7	-0.3232	-0.3731	-0.2799	1.2788	1.0944	1.4632	0.0002	0.0769
PC8	0.3052	0.2629	0.3542	-1.2076	-1.3883	-1.0270	0.3076	0.0060
PC9	-0.3024	-0.3509	-0.2605	1.1965	1.0177	1.3752	0.2133	0.0089
PC10	-0.2756	-0.3200	-0.2373	1.0905	0.9269	1.2541	0.6388	0.0013
PC11	0.2521	0.2172	0.2928	-0.9978	-1.1474	-0.8482	0.5978	0.0016
PC12	0.2485	0.2141	0.2883	-0.9832	-1.1300	-0.8364	0.1970	0.0096
PC13	-0.2387	-0.2772	-0.2056	0.9446	0.8029	1.0864	0.7877	0.0004

Galago zanzibaricus

PC	Slope	Slope lower CI	Slope higher CI	Intercept	Intercept lower CI	Intercept higher CI	p value	r squared
PC1	0.9466	0.6375	1.4054	-3.6916	-5.1890	-2.1943	0.0959	0.1159
PC2	-0.6817	-0.9954	-0.4668	2.6585	1.6276	3.6894	0.0285	0.1920
PC3	-0.5160	-0.7772	-0.3427	2.0126	1.1652	2.8599	0.2957	0.0474
PC4	0.4950	0.3291	0.7446	-1.9305	-2.7408	-1.1203	0.2664	0.0534
PC5	-0.4540	-0.6623	-0.3112	1.7706	1.0860	2.4552	0.0264	0.1966
PC6	0.4212	0.2795	0.6348	-1.6429	-2.3357	-0.9500	0.3129	0.0442
PC7	0.3854	0.2550	0.5824	-1.5031	-2.1415	-0.8647	0.4025	0.0307
PC8	0.3634	0.2390	0.5525	-1.4171	-2.0285	-0.8058	0.9798	0.0000
PC9	0.3382	0.2243	0.5101	-1.3191	-1.8765	-0.7616	0.3365	0.0402
PC10	-0.3189	-0.4769	-0.2133	1.2437	0.7296	1.7579	0.1663	0.0816
PC11	0.2935	0.1968	0.4375	-1.1445	-1.6139	-0.6751	0.1319	0.0959
PC12	0.2904	0.1919	0.4395	-1.1326	-1.6155	-0.6498	0.4665	0.0233
PC13	0.2632	0.1734	0.3996	-1.0266	-1.4677	-0.5855	0.6717	0.0079

Otolemur crassicaudatus

PC	Slope	Slope lower CI	Slope higher CI	Intercept	Intercept lower CI	Intercept higher CI	p value	r squared
PC1	0.4146	0.3401	0.5055	-1.8382	-2.2048	-1.4716	0.8459	0.0004
PC2	-0.3256	-0.3781	-0.2805	1.4437	1.2273	1.6601	0.0000	0.4352
PC3	-0.2973	-0.3610	-0.2448	1.3179	1.0604	1.5755	0.0438	0.0404
PC4	-0.2617	-0.3097	-0.2212	1.1603	0.9642	1.3564	0.0000	0.2817
PC5	-0.2246	-0.2735	-0.1844	0.9956	0.7980	1.1932	0.3122	0.0103
PC6	-0.1988	-0.2423	-0.1631	0.8813	0.7056	1.0570	0.8122	0.0006
PC7	0.1898	0.1557	0.2314	-0.8416	-1.0094	-0.6738	0.7124	0.0014
PC8	0.1709	0.1402	0.2084	-0.7578	-0.9089	-0.6066	0.8825	0.0002
PC9	0.1663	0.1364	0.2028	-0.7374	-0.8845	-0.5903	0.9868	0.0000
PC10	-0.1616	-0.1970	-0.1325	0.7163	0.5734	0.8591	0.8196	0.0005
PC11	0.1575	0.1292	0.1919	-0.6982	-0.8372	-0.5593	0.5004	0.0046
PC12	-0.1484	-0.1808	-0.1219	0.6580	0.5275	0.7885	0.2982	0.0109
PC13	-0.1434	-0.1748	-0.1176	0.6358	0.5090	0.7625	0.8525	0.0004

Otolemur garnettii

PC	Slope	Slope lower CI	Slope higher CI	Intercept	Intercept lower CI	Intercept higher CI	p value	r squared
PC1	-0.4812	-0.5621	-0.4119	2.0970	1.7698	2.4243	0.0000	0.4257
PC2	0.3811	0.3141	0.4623	-1.6609	-1.9838	-1.3379	0.0011	0.1085
PC3	0.3235	0.2648	0.3952	-1.4097	-1.6939	-1.1255	0.0472	0.0417
PC4	0.2715	0.2215	0.3329	-1.1833	-1.4261	-0.9406	0.3931	0.0079
PC5	-0.2576	-0.3161	-0.2100	1.1228	0.8916	1.3541	0.8671	0.0003
PC6	-0.2451	-0.3007	-0.1998	1.0681	0.8481	1.2880	0.8418	0.0004
PC7	-0.2324	-0.2849	-0.1896	1.0129	0.8053	1.2206	0.3546	0.0092
PC8	0.2149	0.1764	0.2619	-0.9367	-1.1231	-0.7504	0.0116	0.0666
PC9	-0.2003	-0.2448	-0.1639	0.8729	0.6965	1.0492	0.0587	0.0379
PC10	0.1842	0.1501	0.2260	-0.8027	-0.9680	-0.6375	0.7822	0.0008
PC11	0.1785	0.1455	0.2188	-0.7778	-0.9375	-0.6180	0.4992	0.0049
PC12	-0.1610	-0.1975	-0.1312	0.7015	0.5572	0.8459	0.6663	0.0020
PC13	-0.1557	-0.1898	-0.1278	0.6787	0.5435	0.8139	0.0132	0.0642

Avahi laniger

PC	Slope	Slope lower CI	Slope higher CI	Intercept	Intercept lower CI	Intercept higher CI	p value	r squared
PC1	-1.3748	-2.1084	-0.8964	5.7346	3.2066	8.2627	0.2752	0.0564
PC2	1.1801	0.7613	1.8293	-4.9225	-7.1503	-2.6948	0.7348	0.0056
PC3	0.9791	0.6340	1.5122	-4.0843	-5.9161	-2.2526	0.4860	0.0234
PC4	-0.9040	-1.3491	-0.6058	3.7711	2.2207	5.3214	0.0441	0.1793
PC5	0.7710	0.4974	1.1952	-3.2163	-4.6717	-1.7609	0.7297	0.0058
PC6	-0.6108	-0.9341	-0.3993	2.5477	1.4323	3.6630	0.2244	0.0694
PC7	0.5942	0.3829	0.9221	-2.4785	-3.6032	-1.3538	0.9457	0.0002
PC8	0.5696	0.3715	0.8735	-2.3761	-3.4232	-1.3290	0.2723	0.0571
PC9	-0.4970	-0.7708	-0.3204	2.0730	1.1335	3.0125	0.8144	0.0027
PC10	0.4679	0.3049	0.7179	-1.9516	-2.8131	-1.0901	0.2864	0.0539
PC11	-0.4473	-0.6926	-0.2889	1.8660	1.0240	2.7080	0.6279	0.0114
PC12	0.4302	0.2772	0.6676	-1.7943	-2.6087	-0.9800	0.9949	0.0000
PC13	0.4155	0.2683	0.6435	-1.7334	-2.5159	-0.9509	0.6413	0.0105

Indri indri

PC	Slope	Slope lower CI	Slope higher CI	Intercept	Intercept lower CI	Intercept higher CI	p value	r squared
PC1	-0.8994	-1.2281	-0.6586	4.2993	2.9381	5.6605	0.0541	0.0966
PC2	0.7331	0.5313	1.0116	-3.5046	-4.6527	-2.3565	0.2689	0.0329
PC3	0.6661	0.4802	0.9240	-3.1842	-4.2450	-2.1235	0.9910	0.0000
PC4	-0.5890	-0.8141	-0.4262	2.8157	1.8883	3.7431	0.3626	0.0224
PC5	-0.5545	-0.7359	-0.4179	2.6509	1.8907	3.4111	0.0009	0.2589
PC6	0.5033	0.3633	0.6972	-2.4058	-3.2039	-1.6076	0.5851	0.0081
PC7	-0.4735	-0.6554	-0.3421	2.2635	1.5147	3.0124	0.4786	0.0137
PC8	0.4381	0.3170	0.6056	-2.0945	-2.7843	-1.4046	0.3631	0.0224
PC9	-0.3973	-0.5504	-0.2867	1.8990	1.2688	2.5292	0.6016	0.0074
PC10	-0.3587	-0.4972	-0.2587	1.7146	1.1445	2.2847	0.7057	0.0039
PC11	0.3525	0.2555	0.4863	-1.6851	-2.2369	-1.1333	0.2630	0.0337
PC12	0.3476	0.2506	0.4822	-1.6617	-2.2151	-1.1082	0.9333	0.0002
PC13	0.3044	0.2194	0.4222	-1.4549	-1.9395	-0.9703	0.9681	0.0000

Propithecus diadema

PC	Slope	Slope lower CI	Slope higher CI	Intercept	Intercept lower CI	Intercept higher CI	p value	r squared
PC1	0.8193	0.5531	1.2136	-3.8000	-5.3319	-2.2681	0.9713	0.0001
PC2	-0.7264	-1.0574	-0.4990	3.3693	2.0741	4.6645	0.1192	0.0908
PC3	0.5861	0.3957	0.8683	-2.7187	-3.8147	-1.6227	0.9999	0.0000
PC4	-0.5786	-0.8500	-0.3939	2.6837	1.6259	3.7415	0.2834	0.0441
PC5	-0.5322	-0.7883	-0.3593	2.4685	1.4733	3.4636	0.9876	0.0000
PC6	-0.4635	-0.6735	-0.3189	2.1497	1.3275	2.9720	0.1015	0.0998
PC7	-0.4594	-0.6752	-0.3126	2.1309	1.2899	2.9719	0.2979	0.0416
PC8	0.4080	0.2754	0.6044	-1.8924	-2.6553	-1.1296	0.9513	0.0001
PC9	-0.3547	-0.5250	-0.2396	1.6450	0.9831	2.3069	0.7512	0.0039
PC10	-0.3316	-0.4736	-0.2323	1.5383	0.9786	2.0979	0.0221	0.1856
PC11	0.3055	0.2087	0.4472	-1.4172	-1.9703	-0.8641	0.1983	0.0628
PC12	-0.2982	-0.4393	-0.2024	1.3831	0.8335	1.9327	0.3911	0.0284
PC13	-0.2643	-0.3881	-0.1800	1.2259	0.7433	1.7086	0.2706	0.0465

Propithecus verreauxi

PC	Slope	Slope lower CI	Slope higher CI	Intercept	Intercept lower CI	Intercept higher CI	p value	r squared
PC1	0.6028	0.4564	0.7962	-2.7654	-3.5449	-1.9860	0.0025	0.2015
PC2	0.5522	0.4269	0.7143	-2.5330	-3.1924	-1.8737	0.0001	0.3189
PC3	-0.4611	-0.6276	-0.3388	2.1153	1.4528	2.7778	0.4471	0.0142
PC4	-0.4511	-0.6152	-0.3308	2.0695	1.4172	2.7218	0.8007	0.0016
PC5	-0.3731	-0.5068	-0.2746	1.7115	1.1788	2.2441	0.2972	0.0265
PC6	0.3680	0.2755	0.4915	-1.6880	-2.1837	-1.1924	0.0160	0.1335
PC7	-0.3377	-0.4595	-0.2482	1.5492	1.0645	2.0338	0.4127	0.0164
PC8	0.3073	0.2270	0.4160	-1.4098	-1.8434	-0.9762	0.1524	0.0493
PC9	0.2969	0.2178	0.4047	-1.3620	-1.7908	-0.9332	0.6973	0.0037
PC10	0.2824	0.2072	0.3849	-1.2957	-1.7033	-0.8880	0.6492	0.0051
PC11	-0.2699	-0.3678	-0.1980	1.2381	0.8485	1.6276	0.6499	0.0051
PC12	0.2539	0.1863	0.3462	-1.1648	-1.5317	-0.7980	0.7245	0.0031
PC13	-0.2487	-0.3385	-0.1827	1.1406	0.7833	1.4980	0.4577	0.0135

Eulemur fulvus

PC	Slope	Slope lower CI	Slope higher CI	Intercept	Intercept lower CI	Intercept higher CI	p value	r squared
PC1	-0.6028	-0.6980	-0.5206	2.8138	2.3997	3.2279	0.0094	0.0384
PC2	0.3990	0.3438	0.4632	-1.8627	-2.1413	-1.5841	0.2822	0.0067
PC3	-0.3885	-0.4511	-0.3346	1.8134	1.5414	2.0854	0.6919	0.0009
PC4	-0.3693	-0.4272	-0.3191	1.7236	1.4713	1.9759	0.0034	0.0484
PC5	-0.3370	-0.3903	-0.2910	1.5732	1.3415	1.8049	0.0108	0.0370
PC6	0.3136	0.2707	0.3634	-1.4638	-1.6802	-1.2475	0.0218	0.0300
PC7	-0.2897	-0.3364	-0.2495	1.3523	1.1494	1.5553	0.8158	0.0003
PC8	0.2853	0.2461	0.3307	-1.3316	-1.5291	-1.1341	0.0442	0.0232
PC9	-0.2710	-0.3129	-0.2347	1.2649	1.0825	1.4473	0.0002	0.0768
PC10	-0.2554	-0.2965	-0.2200	1.1923	1.0137	1.3708	0.4238	0.0037
PC11	-0.2305	-0.2672	-0.1988	1.0758	0.9160	1.2355	0.0561	0.0209
PC12	-0.2301	-0.2668	-0.1984	1.0740	0.9145	1.2336	0.0635	0.0198
PC13	-0.2229	-0.2587	-0.1920	1.0402	0.8846	1.1958	0.2910	0.0064

Eulemur macaco

PC	Slope	Slope lower CI	Slope higher CI	Intercept	Intercept lower CI	Intercept higher CI	p value	r squared
PC1	0.7724	0.5893	1.0123	-3.6228	-4.6149	-2.6306	0.4263	0.0120
PC2	0.5881	0.4482	0.7716	-2.7584	-3.5168	-2.0001	0.6344	0.0043
PC3	0.5716	0.4514	0.7238	-2.6808	-3.3197	-2.0419	0.0001	0.2518
PC4	0.5274	0.4117	0.6756	-2.4737	-3.0926	-1.8549	0.0015	0.1756
PC5	-0.4893	-0.6381	-0.3753	2.2952	1.6789	2.9116	0.1007	0.0500
PC6	0.4612	0.3521	0.6043	-2.1634	-2.7548	-1.5720	0.3649	0.0155
PC7	0.4347	0.3316	0.5699	-2.0390	-2.5980	-1.4801	0.4652	0.0101
PC8	-0.4028	-0.5288	-0.3068	1.8892	1.3688	2.4097	0.9185	0.0002
PC9	0.3773	0.2883	0.4939	-1.7697	-2.2519	-1.2875	0.2787	0.0221
PC10	0.3674	0.2810	0.4803	-1.7231	-2.1907	-1.2555	0.2056	0.0301
PC11	-0.3416	-0.4458	-0.2618	1.6024	1.1708	2.0341	0.1237	0.0441
PC12	-0.3158	-0.4144	-0.2406	1.4811	1.0737	1.8886	0.6913	0.0030
PC13	0.3061	0.2358	0.3975	-1.4358	-1.8151	-1.0566	0.0352	0.0810

Eulemur mongoz

PC	Slope	Slope lower CI	Slope higher CI	Intercept	Intercept lower CI	Intercept higher CI	p value	r squared
PC1	0.5294	0.4223	0.6637	-2.4408	-2.9972	-1.8843	0.0000	0.2883
PC2	0.4269	0.3283	0.5551	-1.9679	-2.4908	-1.4450	0.1728	0.0335
PC3	-0.2932	-0.3829	-0.2245	1.3518	0.9866	1.7169	0.8033	0.0011
PC4	-0.2879	-0.3751	-0.2209	1.3271	0.9715	1.6827	0.3307	0.0172
PC5	-0.2673	-0.3355	-0.2130	1.2323	0.9500	1.5147	0.0000	0.2811
PC6	0.2370	0.1817	0.3091	-1.0927	-1.3864	-0.7990	0.4354	0.0111
PC7	-0.2241	-0.2921	-0.1719	1.0330	0.7558	1.3102	0.3798	0.0141
PC8	0.2198	0.1683	0.2870	-1.0133	-1.2870	-0.7395	0.8130	0.0010
PC9	-0.2056	-0.2685	-0.1575	0.9480	0.6921	1.2040	0.7202	0.0024
PC10	-0.1948	-0.2545	-0.1492	0.8982	0.6556	1.1409	0.8408	0.0007
PC11	0.1790	0.1372	0.2336	-0.8252	-1.0474	-0.6030	0.5289	0.0072
PC12	0.1702	0.1315	0.2204	-0.7847	-0.9898	-0.5797	0.0543	0.0657
PC13	0.1689	0.1296	0.2201	-0.7787	-0.9872	-0.5701	0.3172	0.0182

Eulemur rubriventer

PC	Slope	Slope lower CI	Slope higher CI	Intercept	Intercept lower CI	Intercept higher CI	p value	r squared
PC1	1.5357	1.0312	2.2870	-7.1369	-10.0552	-4.2186	0.5485	0.0146
PC2	0.7918	0.5826	1.0762	-3.6800	-4.8271	-2.5328	0.0002	0.4273
PC3	-0.7067	-1.0424	-0.4791	3.2844	1.9753	4.5935	0.2040	0.0637
PC4	-0.6212	-0.9128	-0.4228	2.8870	1.7482	4.0257	0.1449	0.0831
PC5	0.5790	0.3883	0.8633	-2.6907	-3.7946	-1.5867	0.6577	0.0080
PC6	-0.5285	-0.7678	-0.3638	2.4561	1.5172	3.3950	0.0556	0.1388
PC7	0.4989	0.3344	0.7442	-2.3185	-3.2707	-1.3664	0.7000	0.0060
PC8	-0.4676	-0.6980	-0.3133	2.1733	1.2793	3.0672	0.7897	0.0029
PC9	0.4017	0.2691	0.5997	-1.8669	-2.6353	-1.0985	0.8386	0.0017
PC10	0.3966	0.2657	0.5919	-1.8431	-2.6010	-1.0852	0.7729	0.0034
PC11	-0.3607	-0.5359	-0.2428	1.6763	0.9952	2.3574	0.4127	0.0270
PC12	0.3482	0.2334	0.5194	-1.6184	-2.2830	-0.9538	0.6990	0.0061
PC13	0.3118	0.2094	0.4644	-1.4492	-2.0420	-0.8565	0.5546	0.0141

Hapalemur griseus

PC	Slope	Slope lower CI	Slope higher CI	Intercept	Intercept lower CI	Intercept higher CI	p value	r squared
PC1	0.6992	0.4793	1.0198	-3.0197	-4.1870	-1.8523	0.0775	0.1194
PC2	-0.5915	-0.8815	-0.3969	2.5546	1.5080	3.6013	0.6051	0.0109
PC3	0.5253	0.3571	0.7726	-2.2687	-3.1661	-1.3714	0.1580	0.0781
PC4	-0.4518	-0.6624	-0.3081	1.9513	1.1861	2.7165	0.1201	0.0939
PC5	-0.4235	-0.6203	-0.2891	1.8290	1.1137	2.5443	0.1104	0.0987
PC6	0.3480	0.2355	0.5141	-1.5029	-2.1044	-0.9013	0.2348	0.0560
PC7	-0.3405	-0.4824	-0.2403	1.4706	0.9478	1.9933	0.0072	0.2553
PC8	0.3149	0.2112	0.4694	-1.3600	-1.9176	-0.8024	0.6288	0.0095
PC9	-0.3059	-0.4474	-0.2092	1.3212	0.8067	1.8356	0.0965	0.1066
PC10	0.2886	0.1933	0.4310	-1.2466	-1.7601	-0.7331	0.9692	0.0001
PC11	-0.2659	-0.3965	-0.1783	1.1483	0.6771	1.6195	0.6614	0.0078
PC12	0.2354	0.1579	0.3508	-1.0165	-1.4331	-0.5999	0.6149	0.0103
PC13	-0.2330	-0.3476	-0.1562	1.0063	0.5931	1.4196	0.6932	0.0063

Lemur catta

PC	Slope	Slope lower CI	Slope higher CI	Intercept	Intercept lower CI	Intercept higher CI	p value	r squared
PC1	-0.4326	-0.5953	-0.3144	1.9745	1.3333	2.6157	0.0107	0.1869
PC2	0.3577	0.2641	0.4845	-1.6327	-2.1356	-1.1298	0.0017	0.2684
PC3	-0.3436	-0.4862	-0.2429	1.5682	1.0129	2.1235	0.3022	0.0332
PC4	-0.3277	-0.4643	-0.2313	1.4957	0.9641	2.0274	0.3636	0.0259
PC5	0.2920	0.2071	0.4118	-1.3328	-1.8001	-0.8655	0.1941	0.0521
PC6	0.2779	0.1956	0.3948	-1.2683	-1.7229	-0.8138	0.5766	0.0098
PC7	-0.2432	-0.3459	-0.1709	1.1097	0.7105	1.5089	0.7902	0.0022
PC8	0.2396	0.1687	0.3404	-1.0936	-1.4854	-0.7018	0.5705	0.0102
PC9	0.2162	0.1520	0.3076	-0.9869	-1.3418	-0.6320	0.7625	0.0029
PC10	0.1969	0.1385	0.2800	-0.8986	-1.2216	-0.5756	0.7379	0.0035
PC11	0.1956	0.1375	0.2782	-0.8928	-1.2138	-0.5717	0.7559	0.0031
PC12	-0.1866	-0.2597	-0.1340	0.8515	0.5646	1.1384	0.0406	0.1245
PC13	0.1834	0.1289	0.2608	-0.8368	-1.1378	-0.5358	0.7815	0.0024

Varecia variegata

PC	Slope	Slope lower CI	Slope higher CI	Intercept	Intercept lower CI	Intercept higher CI	p value	r squared
PC1	-0.6299	-0.8733	-0.4544	3.0389	2.0283	4.0494	0.7156	0.0036
PC2	-0.4543	-0.5631	-0.3665	2.1915	1.7172	2.6658	0.0000	0.5779
PC3	0.4409	0.3179	0.6116	-2.1270	-2.8355	-1.4184	0.9828	0.0000
PC4	-0.3718	-0.5087	-0.2718	1.7937	1.2222	2.3653	0.0715	0.0851
PC5	0.3083	0.2231	0.4260	-1.4871	-1.9765	-0.9978	0.3431	0.0243
PC6	0.2995	0.2165	0.4144	-1.4450	-1.9222	-0.9678	0.4243	0.0173
PC7	-0.2779	-0.3845	-0.2009	1.3408	0.8980	1.7837	0.4269	0.0171
PC8	0.2435	0.1782	0.3328	-1.1748	-1.5476	-0.8019	0.0601	0.0923
PC9	0.2355	0.1699	0.3266	-1.1363	-1.5142	-0.7583	0.7341	0.0032
PC10	0.2234	0.1611	0.3099	-1.0778	-1.4367	-0.7188	0.9084	0.0004
PC11	-0.2109	-0.2920	-0.1523	1.0172	0.6801	1.3543	0.5357	0.0105
PC12	-0.1865	-0.2586	-0.1344	0.8995	0.5999	1.1991	0.9271	0.0002
PC13	0.1791	0.1292	0.2483	-0.8640	-1.1512	-0.5767	0.6968	0.0041

Lepilemur ruficaudatus

PC	Slope	Slope lower CI	Slope higher CI	Intercept	Intercept lower CI	Intercept higher CI	p value	r squared
PC1	0.4378	0.3402	0.5634	-1.8417	-2.3113	-1.3721	0.0000	0.6507
PC2	0.3691	0.2444	0.5574	-1.5526	-2.2111	-0.8940	0.3819	0.0334
PC3	-0.3139	-0.4750	-0.2075	1.3206	0.7578	1.8835	0.4575	0.0242
PC4	-0.2952	-0.4487	-0.1942	1.2417	0.7061	1.7773	0.9084	0.0006
PC5	-0.2593	-0.3915	-0.1717	1.0908	0.6284	1.5532	0.3740	0.0345
PC6	0.2274	0.1496	0.3457	-0.9566	-1.3691	-0.5441	0.8862	0.0009
PC7	0.2212	0.1455	0.3363	-0.9307	-1.3320	-0.5294	0.8777	0.0011
PC8	-0.2183	-0.3318	-0.1436	0.9182	0.5221	1.3143	0.9257	0.0004
PC9	-0.2115	-0.3192	-0.1401	0.8896	0.5128	1.2665	0.3638	0.0360
PC10	-0.1881	-0.2843	-0.1245	0.7915	0.4552	1.1278	0.4052	0.0303
PC11	0.1835	0.1207	0.2789	-0.7718	-1.1048	-0.4389	0.9544	0.0001
PC12	-0.1770	-0.2692	-0.1164	0.7448	0.4235	1.0661	0.9634	0.0001
PC13	0.1667	0.1098	0.2532	-0.7014	-1.0031	-0.3997	0.7144	0.0059

Loris tardigradus

PC	Slope	Slope lower CI	Slope higher CI	Intercept	Intercept lower CI	Intercept higher CI	p value	r squared
PC1	0.3577	0.2503	0.5113	-1.4562	-1.9876	-0.9248	0.0146	0.2159
PC2	0.3229	0.2320	0.4495	-1.3143	-1.7573	-0.8714	0.0017	0.3313
PC3	0.2912	0.2057	0.4122	-1.1853	-1.6058	-0.7648	0.0067	0.2591
PC4	-0.2557	-0.3798	-0.1721	1.0407	0.6178	1.4637	0.4050	0.0279
PC5	-0.1970	-0.2943	-0.1320	0.8021	0.4715	1.1327	0.9280	0.0003
PC6	-0.1955	-0.2896	-0.1321	0.7960	0.4752	1.1167	0.2931	0.0441
PC7	0.1805	0.1213	0.2686	-0.7347	-1.0348	-0.4346	0.5040	0.0181
PC8	0.1484	0.0995	0.2213	-0.6042	-0.8523	-0.3561	0.6671	0.0075
PC9	0.1408	0.0943	0.2103	-0.5733	-0.8096	-0.3369	0.9699	0.0001
PC10	0.1299	0.0871	0.1937	-0.5288	-0.7459	-0.3116	0.6725	0.0073
PC11	-0.1155	-0.1719	-0.0776	0.4702	0.2781	0.6623	0.5086	0.0177
PC12	0.1137	0.0766	0.1689	-0.4630	-0.6509	-0.2751	0.3826	0.0306
PC13	0.1106	0.0742	0.1648	-0.4500	-0.6346	-0.2654	0.6181	0.0101

Nycticebus bengalensis

PC	Slope	Slope lower CI	Slope higher CI	Intercept	Intercept lower CI	Intercept higher CI	p value	r squared
PC1	0.8024	0.5205	1.2372	-3.4777	-5.0309	-1.9245	0.1928	0.0833
PC2	-0.7008	-1.0651	-0.4611	3.0371	1.7281	4.3461	0.0790	0.1462
PC3	-0.5975	-0.9380	-0.3806	2.5897	1.3818	3.7976	0.9527	0.0002
PC4	0.5400	0.3444	0.8468	-2.3403	-3.4292	-1.2514	0.7528	0.0051
PC5	-0.4748	-0.7451	-0.3026	2.0579	1.0991	3.0167	0.8291	0.0024
PC6	0.4583	0.2972	0.7067	-1.9861	-2.8736	-1.0986	0.1955	0.0823
PC7	-0.4169	-0.6489	-0.2678	1.8066	0.9808	2.6324	0.3741	0.0397
PC8	0.3677	0.2386	0.5665	-1.5934	-2.3038	-0.8830	0.1844	0.0864
PC9	-0.3483	-0.5312	-0.2283	1.5093	0.8529	2.1657	0.0982	0.1307
PC10	0.3358	0.2151	0.5242	-1.4551	-2.1250	-0.7853	0.4724	0.0261
PC11	0.3124	0.1997	0.4887	-1.3540	-1.9802	-0.7278	0.5625	0.0170
PC12	0.2812	0.1852	0.4269	-1.2186	-1.7424	-0.6949	0.0739	0.1510
PC13	-0.2768	-0.4293	-0.1785	1.1997	0.6560	1.7433	0.2877	0.0563

Nycticebus coucang

PC	Slope	Slope lower CI	Slope higher CI	Intercept	Intercept lower CI	Intercept higher CI	p value	r squared
PC1	-0.5361	-0.6824	-0.4211	2.2708	1.7174	2.8242	0.7507	0.0015
PC2	0.3782	0.2977	0.4805	-1.6021	-1.9893	-1.2149	0.2740	0.0178
PC3	0.3543	0.2784	0.4509	-1.5009	-1.8663	-1.1355	0.6248	0.0036
PC4	-0.3184	-0.4016	-0.2524	1.3486	1.0325	1.6647	0.0213	0.0766
PC5	0.2868	0.2288	0.3596	-1.2150	-1.4921	-0.9378	0.0029	0.1252
PC6	0.2607	0.2052	0.3313	-1.1045	-1.3717	-0.8372	0.3023	0.0159
PC7	0.2573	0.2031	0.3259	-1.0898	-1.3499	-0.8296	0.0906	0.0421
PC8	0.2354	0.1850	0.2996	-0.9971	-1.2399	-0.7543	0.6282	0.0035
PC9	0.2201	0.1777	0.2727	-0.9324	-1.1335	-0.7312	0.0001	0.2171
PC10	0.2148	0.1695	0.2722	-0.9100	-1.1276	-0.6924	0.1044	0.0389
PC11	0.2059	0.1622	0.2615	-0.8724	-1.0828	-0.6620	0.2236	0.0220
PC12	-0.2012	-0.2557	-0.1583	0.8524	0.6460	1.0588	0.3300	0.0142
PC13	-0.1908	-0.2427	-0.1499	0.8080	0.6116	1.0045	0.5280	0.0060

Perodicticus potto

PC	Slope	Slope lower CI	Slope higher CI	Intercept	Intercept lower CI	Intercept higher CI	p value	r squared
PC1	-0.4898	-0.5833	-0.4113	2.1045	1.7350	2.4741	0.8903	0.0002
PC2	-0.4194	-0.4953	-0.3551	1.8019	1.5008	2.1031	0.0004	0.0944
PC3	0.3725	0.3129	0.4435	-1.6005	-1.8812	-1.3198	0.5722	0.0025
PC4	0.3556	0.2993	0.4226	-1.5280	-1.7931	-1.2629	0.0799	0.0240
PC5	0.3263	0.2740	0.3886	-1.4018	-1.6480	-1.1557	0.8862	0.0002
PC6	0.2957	0.2530	0.3456	-1.2703	-1.4694	-1.0713	0.0000	0.2037
PC7	-0.2832	-0.3372	-0.2379	1.2168	1.0033	1.4303	0.6384	0.0017
PC8	-0.2762	-0.3290	-0.2320	1.1868	0.9784	1.3953	0.9288	0.0001
PC9	0.2742	0.2312	0.3253	-1.1782	-1.3805	-0.9759	0.0168	0.0442
PC10	0.2515	0.2116	0.2989	-1.0805	-1.2681	-0.8929	0.0921	0.0222
PC11	0.2368	0.2013	0.2785	-1.0173	-1.1830	-0.8515	0.0000	0.1394
PC12	-0.2303	-0.2742	-0.1934	0.9894	0.8157	1.1630	0.6608	0.0015
PC13	0.2228	0.1879	0.2643	-0.9574	-1.1215	-0.7934	0.0126	0.0481

2* model vault module against ln CS whole cranium

Cheirogaleus major

PC	Slope	Slope lower CI	Slope higher CI	Intercept	Intercept lower CI	Intercept higher CI	p value	r squared
PC1	0.7674	0.5181	1.1367	-3.7291	-5.2322	-2.2259	0.0806	0.1268
PC2	-0.6821	-1.0152	-0.4583	3.3146	1.9613	4.6679	0.1155	0.1042
PC3	0.5630	0.3957	0.8012	-2.7359	-3.7213	-1.7506	0.0044	0.3030
PC4	-0.5102	-0.7758	-0.3356	2.4794	1.4099	3.5490	0.9759	0.0000
PC5	0.4901	0.3345	0.7182	-2.3817	-3.3141	-1.4493	0.0366	0.1764
PC6	0.4547	0.2993	0.6907	-2.2095	-3.1606	-1.2584	0.7554	0.0043
PC7	0.3829	0.2521	0.5814	-1.8605	-2.6606	-1.0603	0.7116	0.0061
PC8	0.3745	0.2469	0.5680	-1.8197	-2.6001	-1.0392	0.6097	0.0115
PC9	-0.3474	-0.5158	-0.2340	1.6882	1.0035	2.3730	0.0959	0.1159
PC10	-0.3436	-0.5222	-0.2260	1.6694	0.9496	2.3893	0.8898	0.0009
PC11	0.3296	0.2172	0.5001	-1.6015	-2.2890	-0.9141	0.6373	0.0098
PC12	-0.2981	-0.4531	-0.1961	1.4486	0.8243	2.0729	0.8366	0.0019
PC13	-0.2859	-0.4326	-0.1889	1.3893	0.7972	1.9815	0.4608	0.0239

Cheirogaleus medius

PC	Slope	Slope lower CI	Slope higher CI	Intercept	Intercept lower CI	Intercept higher CI	p value	r squared
PC1	-0.6024	-0.8852	-0.4100	2.7651	1.6743	3.8560	0.8128	0.0021
PC2	-0.5559	-0.8065	-0.3831	2.5514	1.5796	3.5232	0.1661	0.0698
PC3	-0.4943	-0.6702	-0.3646	2.2689	1.5676	2.9702	0.0003	0.3873
PC4	-0.4499	-0.6519	-0.3104	2.0649	1.2811	2.8487	0.1471	0.0762
PC5	0.4080	0.2782	0.5984	-1.8728	-2.6077	-1.1380	0.5599	0.0127
PC6	-0.3781	-0.5513	-0.2593	1.7354	1.0650	2.4057	0.2788	0.0433
PC7	0.3575	0.2432	0.5255	-1.6411	-2.2891	-0.9931	0.9172	0.0004
PC8	0.3221	0.2221	0.4672	-1.4787	-2.0413	-0.9160	0.1602	0.0717
PC9	0.3052	0.2077	0.4484	-1.4007	-1.9533	-0.8481	0.8135	0.0021
PC10	0.2809	0.1911	0.4128	-1.2892	-1.7981	-0.7803	0.8795	0.0009
PC11	0.2715	0.1851	0.3981	-1.2460	-1.7350	-0.7571	0.5595	0.0128
PC12	0.2532	0.1722	0.3721	-1.1621	-1.6208	-0.7033	0.8988	0.0006
PC13	0.2416	0.1644	0.3551	-1.1089	-1.5466	-0.6712	0.8782	0.0009

Microcebus murinus

PC	Slope	Slope lower CI	Slope higher CI	Intercept	Intercept lower CI	Intercept higher CI	p value	r squared
PC1	-0.8078	-1.0133	-0.6440	3.5021	2.7015	4.3027	0.0157	0.0805
PC2	-0.6861	-0.8520	-0.5526	2.9746	2.3255	3.6238	0.0005	0.1620
PC3	0.5969	0.4717	0.7554	-2.5879	-3.2027	-1.9730	0.4906	0.0068
PC4	0.5537	0.4438	0.6906	-2.4002	-2.9352	-1.8652	0.0022	0.1258
PC5	0.5326	0.4206	0.6743	-2.3088	-2.8586	-1.7590	0.6905	0.0023
PC6	-0.5024	-0.6357	-0.3970	2.1780	1.6605	2.6955	0.4949	0.0067
PC7	0.4716	0.3726	0.5969	-2.0445	-2.5306	-1.5584	0.5417	0.0053
PC8	0.4310	0.3416	0.5440	-1.8687	-2.3075	-1.4299	0.1471	0.0298
PC9	-0.4038	-0.5093	-0.3202	1.7508	1.3410	2.1606	0.1096	0.0362
PC10	0.3916	0.3094	0.4957	-1.6977	-2.1016	-1.2938	0.5963	0.0040
PC11	0.3791	0.2994	0.4801	-1.6436	-2.0355	-1.2518	0.9615	0.0000
PC12	-0.3524	-0.4449	-0.2791	1.5277	1.1683	1.8871	0.1734	0.0263
PC13	0.3364	0.2667	0.4243	-1.4583	-1.7998	-1.1169	0.1144	0.0352

Microcebus rufus

PC	Slope	Slope lower CI	Slope higher CI	Intercept	Intercept lower CI	Intercept higher CI	p value	r squared
PC1	-0.6174	-0.8946	-0.4261	2.6909	1.6699	3.7119	0.1453	0.0769
PC2	0.4902	0.3855	0.6232	-2.1362	-2.6540	-1.6184	0.0000	0.6232
PC3	-0.4228	-0.6205	-0.2881	1.8426	1.1181	2.5670	0.6270	0.0089
PC4	0.3951	0.2727	0.5726	-1.7220	-2.3757	-1.0683	0.1477	0.0760
PC5	0.3715	0.2528	0.5460	-1.6192	-2.2583	-0.9801	0.8615	0.0011
PC6	-0.3553	-0.5213	-0.2422	1.5484	0.9401	2.1567	0.5974	0.0105
PC7	0.3257	0.2229	0.4758	-1.4193	-1.9703	-0.8682	0.3421	0.0335
PC8	0.3187	0.2171	0.4678	-1.3889	-1.9352	-0.8426	0.6420	0.0081
PC9	0.2860	0.1946	0.4204	-1.2464	-1.7387	-0.7542	0.9877	0.0000
PC10	-0.2776	-0.4068	-0.1894	1.2097	0.7360	1.6835	0.5021	0.0169
PC11	0.2698	0.1837	0.3962	-1.1759	-1.6390	-0.7128	0.6983	0.0057
PC12	-0.2582	-0.3794	-0.1757	1.1252	0.6813	1.5691	0.8053	0.0023
PC13	0.2333	0.1591	0.3421	-1.0167	-1.4155	-0.6180	0.5440	0.0138

Galago alleni

PC	Slope	Slope lower CI	Slope higher CI	Intercept	Intercept lower CI	Intercept higher CI	p value	r squared
PC1	0.8977	0.6037	1.3348	-4.2721	-6.0118	-2.5325	0.0597	0.1519
PC2	0.6266	0.4096	0.9587	-2.9820	-4.2886	-1.6754	0.5306	0.0181
PC3	0.5472	0.3737	0.8014	-2.6043	-3.6221	-1.5865	0.0212	0.2188
PC4	-0.4693	-0.7090	-0.3106	2.2333	1.2852	3.1814	0.1855	0.0783
PC5	-0.4405	-0.6749	-0.2875	2.0964	1.1745	3.0183	0.6251	0.0110
PC6	-0.4077	-0.6148	-0.2703	1.9401	1.1204	2.7597	0.1615	0.0871
PC7	0.3850	0.2517	0.5891	-1.8324	-2.6352	-1.0295	0.5297	0.0182
PC8	-0.3642	-0.5539	-0.2395	1.7334	0.9853	2.4815	0.3072	0.0473
PC9	0.3368	0.2230	0.5086	-1.6027	-2.2821	-0.9232	0.1785	0.0807
PC10	0.3136	0.2052	0.4790	-1.4922	-2.1436	-0.8407	0.4592	0.0252
PC11	0.2859	0.1904	0.4293	-1.3607	-1.9291	-0.7923	0.1179	0.1074
PC12	-0.2707	-0.4134	-0.1773	1.2882	0.7263	1.8500	0.4422	0.0271
PC13	0.2630	0.1722	0.4019	-1.2518	-1.7985	-0.7051	0.4659	0.0244

Galago demidoff

PC	Slope	Slope lower CI	Slope higher CI	Intercept	Intercept lower CI	Intercept higher CI	p value	r squared
PC1	0.6676	0.5553	0.8026	-2.9585	-3.5064	-2.4106	0.0000	0.5124
PC2	-0.5135	-0.6674	-0.3951	2.2755	1.6721	2.8788	0.8332	0.0008
PC3	0.4912	0.3779	0.6385	-2.1768	-2.7542	-1.5994	0.9982	0.0000
PC4	0.4631	0.3563	0.6019	-2.0521	-2.5964	-1.5079	0.8900	0.0003
PC5	0.4382	0.3377	0.5686	-1.9418	-2.4534	-1.4303	0.3789	0.0136
PC6	0.4079	0.3139	0.5301	-1.8075	-2.2865	-1.3285	0.7460	0.0019
PC7	0.3909	0.3008	0.5079	-1.7321	-2.1909	-1.2733	0.6971	0.0027
PC8	-0.3864	-0.5005	-0.2983	1.7123	1.2641	2.1604	0.2188	0.0264
PC9	-0.3626	-0.4712	-0.2790	1.6069	1.1810	2.0328	0.7656	0.0016
PC10	0.3447	0.2652	0.4480	-1.5273	-1.9324	-1.1222	0.9326	0.0001
PC11	-0.3313	-0.4303	-0.2551	1.4681	1.0797	1.8565	0.5891	0.0051
PC12	0.3224	0.2487	0.4180	-1.4286	-1.8038	-1.0534	0.2890	0.0197
PC13	0.3043	0.2341	0.3954	-1.3484	-1.7058	-0.9910	0.7845	0.0013

Galago elegantulus

PC	Slope	Slope lower CI	Slope higher CI	Intercept	Intercept lower CI	Intercept higher CI	p value	r squared
PC1	-1.0268	-1.4440	-0.7301	4.8479	3.1627	6.5332	0.1362	0.0681
PC2	-0.8369	-1.1519	-0.6080	3.9513	2.6673	5.2353	0.0110	0.1856
PC3	-0.6842	-0.9620	-0.4867	3.2306	2.1086	4.3526	0.1313	0.0697
PC4	0.6066	0.4264	0.8630	-2.8643	-3.8950	-1.8336	0.8353	0.0014
PC5	0.5627	0.3966	0.7983	-2.6568	-3.6051	-1.7085	0.4564	0.0175
PC6	0.5282	0.3714	0.7510	-2.4937	-3.3898	-1.5976	0.7181	0.0041
PC7	0.5035	0.3591	0.7058	-2.3772	-3.1956	-1.5587	0.0926	0.0859
PC8	-0.4752	-0.6741	-0.3350	2.2437	1.4431	3.0444	0.4496	0.0180
PC9	-0.4198	-0.5952	-0.2961	1.9820	1.2759	2.6881	0.4110	0.0212
PC10	-0.4039	-0.5607	-0.2909	1.9069	1.2699	2.5439	0.0297	0.1393
PC11	0.4022	0.2845	0.5687	-1.8990	-2.5699	-1.2280	0.2746	0.0372
PC12	-0.3867	-0.5489	-0.2723	1.8256	1.1726	2.4786	0.5166	0.0133
PC13	0.3741	0.2631	0.5319	-1.7664	-2.4009	-1.1318	0.6950	0.0049

Galago moholi

PC	Slope	Slope lower CI	Slope higher CI	Intercept	Intercept lower CI	Intercept higher CI	p value	r squared
PC1	-0.7128	-0.8561	-0.5935	3.2416	2.6445	3.8388	0.0000	0.3940
PC2	0.6528	0.5183	0.8222	-2.9687	-3.6597	-2.2778	0.1257	0.0327
PC3	-0.5740	-0.7241	-0.4550	2.6105	1.9985	3.2225	0.2495	0.0186
PC4	0.4985	0.3944	0.6300	-2.2671	-2.8029	-1.7313	0.6628	0.0027
PC5	-0.4441	-0.5614	-0.3513	2.0195	1.5418	2.4973	0.8185	0.0007
PC6	-0.4143	-0.5226	-0.3284	1.8841	1.4426	2.3256	0.2401	0.0194
PC7	0.3923	0.3105	0.4957	-1.7841	-2.2052	-1.3631	0.5279	0.0056
PC8	0.3708	0.2934	0.4686	-1.6862	-2.0848	-1.2876	0.6928	0.0022
PC9	0.3577	0.2829	0.4522	-1.6266	-2.0114	-1.2417	0.8414	0.0006
PC10	0.3504	0.2772	0.4430	-1.5937	-1.9708	-1.2167	0.8327	0.0006
PC11	0.3389	0.2681	0.4284	-1.5412	-1.9056	-1.1768	0.7392	0.0016
PC12	0.3324	0.2629	0.4202	-1.5115	-1.8692	-1.1538	0.8962	0.0002
PC13	-0.3101	-0.3919	-0.2454	1.4103	1.0772	1.7434	0.5966	0.0040

Galago senegalensis

PC	Slope	Slope lower CI	Slope higher CI	Intercept	Intercept lower CI	Intercept higher CI	p value	r squared
PC1	-0.5991	-0.6782	-0.5292	2.7773	2.4317	3.1228	0.0000	0.3127
PC2	0.5436	0.4682	0.6313	-2.5202	-2.8984	-2.1421	0.8275	0.0003
PC3	-0.4459	-0.5147	-0.3863	2.0672	1.7694	2.3649	0.0002	0.0787
PC4	-0.4266	-0.4954	-0.3673	1.9775	1.6808	2.2743	0.9880	0.0000
PC5	0.4132	0.3566	0.4788	-1.9157	-2.1989	-1.6324	0.0235	0.0293
PC6	-0.3901	-0.4529	-0.3361	1.8086	1.5377	2.0796	0.4378	0.0035
PC7	0.3369	0.2901	0.3912	-1.5617	-1.7961	-1.3274	0.9828	0.0000
PC8	-0.3200	-0.3709	-0.2761	1.4835	1.2637	1.7033	0.0355	0.0253
PC9	-0.3119	-0.3621	-0.2686	1.4458	1.2289	1.6627	0.7305	0.0007
PC10	0.2951	0.2543	0.3425	-1.3681	-1.5725	-1.1636	0.2260	0.0085
PC11	0.2885	0.2488	0.3346	-1.3376	-1.5366	-1.1385	0.0866	0.0169
PC12	-0.2812	-0.3252	-0.2431	1.3035	1.1134	1.4937	0.0017	0.0552
PC13	0.2697	0.2324	0.3130	-1.2503	-1.4370	-1.0635	0.1972	0.0096

Galago zanzibaricus

PC	Slope	Slope lower CI	Slope higher CI	Intercept	Intercept lower CI	Intercept higher CI	p value	r squared
PC1	-0.9330	-1.3151	-0.6620	4.2794	2.7816	5.7771	0.0022	0.3417
PC2	-0.8877	-1.3496	-0.5839	4.0715	2.3154	5.8276	0.9382	0.0003
PC3	-0.6976	-1.0139	-0.4799	3.1994	1.9748	4.4241	0.0204	0.2126
PC4	-0.6281	-0.9547	-0.4133	2.8809	1.6394	4.1225	0.8373	0.0019
PC5	0.5911	0.3904	0.8950	-2.7110	-3.8683	-1.5537	0.4927	0.0207
PC6	0.5481	0.3644	0.8244	-2.5139	-3.5688	-1.4590	0.2650	0.0537
PC7	0.5051	0.3329	0.7666	-2.3168	-3.3114	-1.3221	0.6434	0.0095
PC8	-0.4576	-0.6903	-0.3033	2.0987	1.2111	2.9863	0.3457	0.0387
PC9	-0.4352	-0.6615	-0.2863	1.9960	1.1354	2.8566	0.8849	0.0009
PC10	-0.3949	-0.5925	-0.2631	1.8110	1.0555	2.5664	0.2192	0.0649
PC11	-0.3601	-0.5462	-0.2375	1.6518	0.9439	2.3597	0.5891	0.0129
PC12	-0.3496	-0.5295	-0.2308	1.6035	0.9185	2.2885	0.5091	0.0192
PC13	0.3417	0.2275	0.5133	-1.5673	-2.2226	-0.9120	0.2360	0.0605

Otolemur crassicaudatus

PC	Slope	Slope lower CI	Slope higher CI	Intercept	Intercept lower CI	Intercept higher CI	p value	r squared
PC1	0.5994	0.4958	0.7247	-3.0664	-3.6519	-2.4808	0.0035	0.0831
PC2	0.5029	0.4140	0.6107	-2.5724	-3.0756	-2.0693	0.0498	0.0383
PC3	0.3377	0.2874	0.3969	-1.7277	-2.0077	-1.4477	0.0000	0.3397
PC4	-0.2768	-0.3374	-0.2270	1.4159	1.1336	1.6981	0.7704	0.0009
PC5	-0.2615	-0.3183	-0.2148	1.3377	1.0728	1.6025	0.2281	0.0146
PC6	0.2477	0.2032	0.3019	-1.2670	-1.5196	-1.0143	0.8868	0.0002
PC7	0.2360	0.1950	0.2857	-1.2075	-1.4395	-0.9754	0.0068	0.0716
PC8	0.2271	0.1877	0.2746	-1.1615	-1.3839	-0.9392	0.0045	0.0786
PC9	0.2215	0.1818	0.2699	-1.1332	-1.3587	-0.9078	0.4708	0.0053
PC10	0.2120	0.1739	0.2583	-1.0843	-1.3003	-0.8683	0.6234	0.0024
PC11	0.2033	0.1668	0.2478	-1.0400	-1.2474	-0.8326	0.9525	0.0000
PC12	-0.1979	-0.2412	-0.1624	1.0123	0.8107	1.2139	0.5879	0.0030
PC13	0.1859	0.1525	0.2266	-0.9510	-1.1407	-0.7613	0.9338	0.0001

Otolemur garnettii

PC	Slope	Slope lower CI	Slope higher CI	Intercept	Intercept lower CI	Intercept higher CI	p value	r squared
PC1	0.6720	0.5513	0.8191	-3.3910	-4.0669	-2.7151	0.0140	0.0632
PC2	-0.4050	-0.4934	-0.3324	2.0438	1.6376	2.4499	0.0102	0.0688
PC3	-0.3738	-0.4438	-0.3148	1.8862	1.5606	2.2119	0.0000	0.2973
PC4	0.2960	0.2415	0.3629	-1.4938	-1.8001	-1.1874	0.3837	0.0082
PC5	-0.2868	-0.3516	-0.2339	1.4472	1.1500	1.7443	0.4558	0.0060
PC6	-0.2511	-0.3080	-0.2048	1.2673	1.0069	1.5278	0.5326	0.0042
PC7	-0.2491	-0.3056	-0.2030	1.2570	0.9981	1.5159	0.9414	0.0001
PC8	-0.2370	-0.2884	-0.1948	1.1961	0.9599	1.4322	0.0052	0.0810
PC9	-0.2319	-0.2842	-0.1892	1.1702	0.9306	1.4098	0.3041	0.0114
PC10	0.2189	0.1788	0.2681	-1.1048	-1.3303	-0.8793	0.2013	0.0175
PC11	0.2015	0.1645	0.2468	-1.0167	-1.2245	-0.8090	0.2277	0.0156
PC12	-0.1978	-0.2416	-0.1619	0.9981	0.7968	1.1993	0.0476	0.0415
PC13	0.1911	0.1559	0.2343	-0.9645	-1.1622	-0.7668	0.3617	0.0090

Avahi laniger

PC	Slope	Slope lower CI	Slope higher CI	Intercept	Intercept lower CI	Intercept higher CI	p value	r squared
PC1	1.2365	0.8021	1.9063	-6.0378	-8.7337	-3.3419	0.4142	0.0320
PC2	-0.9989	-1.5492	-0.6441	4.8773	2.6674	7.0872	0.7965	0.0032
PC3	0.8125	0.5350	1.2337	-3.9670	-5.6729	-2.2612	0.1370	0.1022
PC4	0.7397	0.4775	1.1458	-3.6118	-5.2432	-1.9803	0.6609	0.0093
PC5	0.7200	0.4747	1.0919	-3.5154	-5.0221	-2.0088	0.1255	0.1081
PC6	0.6782	0.4370	1.0525	-3.3114	-4.8141	-1.8086	0.9731	0.0001
PC7	-0.6191	-0.9578	-0.4001	3.0228	1.6612	4.3845	0.5805	0.0148
PC8	0.5692	0.3668	0.8834	-2.7795	-4.0409	-1.5181	0.9703	0.0001
PC9	0.5353	0.3453	0.8299	-2.6137	-3.7969	-1.4306	0.7462	0.0051
PC10	-0.5195	-0.7959	-0.3391	2.5366	1.4214	3.6518	0.2538	0.0615
PC11	-0.4798	-0.7408	-0.3107	2.3427	1.2927	3.3928	0.4756	0.0245
PC12	-0.4589	-0.6921	-0.3042	2.2405	1.2935	3.1876	0.0877	0.1325
PC13	-0.4064	-0.6084	-0.2715	1.9845	1.1621	2.8069	0.0535	0.1661

Indri indri

PC	Slope	Slope lower CI	Slope higher CI	Intercept	Intercept lower CI	Intercept higher CI	p value	r squared
PC1	1.0584	0.7640	1.4663	-5.8086	-7.7357	-3.8815	0.5874	0.0080
PC2	0.7957	0.5795	1.0926	-4.3671	-5.7750	-2.9592	0.1221	0.0634
PC3	0.6604	0.4782	0.9120	-3.6244	-4.8146	-2.4342	0.3071	0.0282
PC4	0.6332	0.4573	0.8768	-3.4753	-4.6262	-2.3243	0.5156	0.0115
PC5	0.5889	0.4301	0.8062	-3.2319	-4.2640	-2.1999	0.0790	0.0810
PC6	0.5477	0.3949	0.7598	-3.0059	-4.0072	-2.0046	0.9822	0.0000
PC7	-0.5099	-0.6765	-0.3843	2.7983	1.9966	3.5999	0.0009	0.2603
PC8	-0.5023	-0.6965	-0.3622	2.7565	1.8391	3.6739	0.7980	0.0018
PC9	0.4633	0.3354	0.6398	-2.5424	-3.3776	-1.7072	0.3127	0.0275
PC10	0.4281	0.3130	0.5854	-2.3492	-3.0966	-1.6019	0.0668	0.0879
PC11	-0.4032	-0.5592	-0.2907	2.2127	1.4759	2.9495	0.8780	0.0006
PC12	0.3939	0.2840	0.5464	-2.1618	-2.8819	-1.4417	0.9518	0.0001
PC13	-0.3679	-0.5102	-0.2653	2.0190	1.3468	2.6912	0.8397	0.0011

Propithecus diadema

PC	Slope	Slope lower CI	Slope higher CI	Intercept	Intercept lower CI	Intercept higher CI	p value	r squared
PC1	-0.8884	-1.3153	-0.6000	4.7700	2.8494	6.6906	0.7993	0.0025
PC2	-0.6496	-0.9087	-0.4643	3.4878	2.2946	4.6810	0.0038	0.2799
PC3	0.5599	0.3810	0.8229	-3.0064	-4.1928	-1.8200	0.2966	0.0418
PC4	-0.4672	-0.6693	-0.3262	2.5088	1.5877	3.4299	0.0289	0.1706
PC5	0.4561	0.3087	0.6739	-2.4489	-3.4294	-1.4684	0.5535	0.0137
PC6	0.4387	0.2962	0.6499	-2.3556	-3.3052	-1.4059	0.9991	0.0000
PC7	0.4001	0.2706	0.5916	-2.1481	-3.0100	-1.2863	0.6204	0.0096
PC8	-0.3759	-0.5522	-0.2558	2.0182	1.2225	2.8139	0.2866	0.0435
PC9	0.3626	0.2452	0.5362	-1.9471	-2.7283	-1.1659	0.6204	0.0096
PC10	0.3101	0.2147	0.4478	-1.6648	-2.2906	-1.0390	0.0589	0.1305
PC11	0.3012	0.2034	0.4462	-1.6175	-2.2695	-0.9654	0.9525	0.0001
PC12	0.2909	0.1974	0.4289	-1.5621	-2.1837	-0.9405	0.4145	0.0258
PC13	-0.2844	-0.4211	-0.1920	1.5268	0.9117	2.1420	0.8545	0.0013

Propithecus verreauxi

PC	Slope	Slope lower CI	Slope higher CI	Intercept	Intercept lower CI	Intercept higher CI	p value	r squared
PC1	-0.9048	-1.2203	-0.6708	4.7892	3.3350	6.2434	0.0793	0.0732
PC2	-0.7628	-1.0366	-0.5614	4.0379	2.7803	5.2955	0.3115	0.0250
PC3	0.6210	0.4616	0.8355	-3.2872	-4.2768	-2.2976	0.0520	0.0890
PC4	0.5265	0.3872	0.7159	-2.7869	-3.6569	-1.9169	0.3600	0.0205
PC5	-0.4998	-0.6802	-0.3672	2.6453	1.8170	3.4737	0.4426	0.0145
PC6	0.4868	0.3570	0.6640	-2.5770	-3.3896	-1.7644	0.8824	0.0005
PC7	-0.4358	-0.5919	-0.3208	2.3067	1.5891	3.0243	0.2903	0.0272
PC8	0.4135	0.3053	0.5601	-2.1889	-2.8633	-1.5144	0.1688	0.0457
PC9	-0.4024	-0.5415	-0.2990	2.1300	1.4881	2.7719	0.0546	0.0872
PC10	-0.3690	-0.5026	-0.2710	1.9534	1.3403	2.5666	0.5318	0.0096
PC11	-0.3361	-0.4526	-0.2497	1.7793	1.2423	2.3163	0.0588	0.0844
PC12	-0.3254	-0.4426	-0.2393	1.7226	1.1847	2.2606	0.3676	0.0198
PC13	-0.3111	-0.4243	-0.2281	1.6468	1.1275	2.1661	0.8836	0.0005

Eulemur fulvus

PC	Slope	Slope lower CI	Slope higher CI	Intercept	Intercept lower CI	Intercept higher CI	p value	r squared
PC1	-0.8487	-0.9745	-0.7391	4.5240	3.8964	5.1516	0.0000	0.1454
PC2	-0.7930	-0.9199	-0.6835	4.2271	3.5970	4.8571	0.1249	0.0136
PC3	0.5923	0.5101	0.6878	-3.1574	-3.6311	-2.6837	0.7446	0.0006
PC4	0.4978	0.4334	0.5717	-2.6534	-3.0219	-2.2849	0.0000	0.1437
PC5	0.4633	0.3993	0.5375	-2.4695	-2.8380	-2.1011	0.1571	0.0115
PC6	-0.4431	-0.5145	-0.3817	2.3622	2.0082	2.7161	0.4711	0.0030
PC7	0.4013	0.3462	0.4652	-2.1393	-2.4567	-1.8220	0.0454	0.0230
PC8	0.3515	0.3034	0.4072	-1.8737	-2.1505	-1.5969	0.0198	0.0310
PC9	0.3465	0.2985	0.4021	-1.8469	-2.1230	-1.5707	0.2581	0.0074
PC10	-0.3278	-0.3806	-0.2823	1.7473	1.4853	2.0092	0.5437	0.0021
PC11	0.3187	0.2744	0.3700	-1.6987	-1.9536	-1.4439	0.6747	0.0010
PC12	-0.3006	-0.3490	-0.2589	1.6024	1.3622	1.8426	0.5371	0.0022
PC13	0.2783	0.2397	0.3232	-1.4837	-1.7064	-1.2611	0.8933	0.0001

Eulemur macaco

PC	Slope	Slope lower CI	Slope higher CI	Intercept	Intercept lower CI	Intercept higher CI	p value	r squared
PC1	-1.2006	-1.5627	-0.9225	6.4268	4.7133	8.1403	0.0633	0.0636
PC2	-0.9071	-1.1849	-0.6944	4.8553	3.5424	6.1683	0.1611	0.0367
PC3	-0.8330	-1.0808	-0.6420	4.4588	3.2843	5.6333	0.0299	0.0859
PC4	0.7114	0.5479	0.9237	-3.8081	-4.8140	-2.8021	0.0355	0.0807
PC5	0.6781	0.5166	0.8900	-3.6296	-4.6290	-2.6302	0.7977	0.0013
PC6	-0.6212	-0.8120	-0.4752	3.3251	2.4236	4.2265	0.1927	0.0318
PC7	-0.5671	-0.7435	-0.4325	3.0356	2.2033	3.8680	0.4764	0.0096
PC8	0.5171	0.3946	0.6775	-2.7677	-3.5249	-2.0105	0.3905	0.0139
PC9	-0.4949	-0.6475	-0.3783	2.6492	1.9284	3.3699	0.2497	0.0249
PC10	-0.4521	-0.5875	-0.3479	2.4201	1.7789	3.0614	0.0430	0.0750
PC11	0.4321	0.3292	0.5671	-2.3129	-2.9496	-1.6761	0.7761	0.0015
PC12	0.4138	0.3158	0.5423	-2.2152	-2.8215	-1.6090	0.4011	0.0133
PC13	0.3963	0.3022	0.5197	-2.1213	-2.7033	-1.5393	0.5027	0.0085

Eulemur mongoz

PC	Slope	Slope lower CI	Slope higher CI	Intercept	Intercept lower CI	Intercept higher CI	p value	r squared
PC1	0.6774	0.5247	0.8746	-3.5790	-4.5032	-2.6549	0.0259	0.0870
PC2	0.5018	0.3901	0.6454	-2.6510	-3.3255	-1.9764	0.0104	0.1135
PC3	-0.4730	-0.6169	-0.3627	2.4991	1.8276	3.1706	0.4283	0.0114
PC4	0.4013	0.3073	0.5241	-2.1201	-2.6930	-1.5472	0.9053	0.0003
PC5	-0.3660	-0.4720	-0.2838	1.9338	1.4366	2.4309	0.0196	0.0951
PC6	0.3506	0.2703	0.4547	-1.8521	-2.3394	-1.3649	0.0862	0.0526
PC7	0.3390	0.2596	0.4427	-1.7911	-2.2749	-1.3073	0.8139	0.0010
PC8	-0.2989	-0.3897	-0.2292	1.5789	1.1549	2.0029	0.4052	0.0126
PC9	-0.2809	-0.3658	-0.2156	1.4838	1.0870	1.8806	0.2845	0.0208
PC10	0.2575	0.1973	0.3360	-1.3603	-1.7265	-0.9941	0.5162	0.0077
PC11	-0.2515	-0.3281	-0.1928	1.3287	0.9714	1.6860	0.4595	0.0100
PC12	-0.2378	-0.3105	-0.1822	1.2566	0.9175	1.5957	0.6860	0.0030
PC13	-0.2331	-0.3026	-0.1795	1.2313	0.9060	1.5566	0.1157	0.0444

Eulemur rubriventer

PC	Slope	Slope lower CI	Slope higher CI	Intercept	Intercept lower CI	Intercept higher CI	p value	r squared
PC1	-1.3247	-1.8402	-0.9536	7.0443	4.6870	9.4015	0.0014	0.3400
PC2	-1.0528	-1.5661	-0.7078	5.5986	3.3166	7.8807	0.4726	0.0208
PC3	0.9325	0.6372	1.3646	-4.9588	-6.8928	-3.0248	0.1017	0.1035
PC4	-0.8787	-1.3089	-0.5899	4.6724	2.7607	6.5841	0.5651	0.0134
PC5	-0.8665	-1.2920	-0.5812	4.6078	2.7178	6.4977	0.6483	0.0085
PC6	-0.7378	-1.0922	-0.4984	3.9233	2.3445	5.5021	0.2849	0.0456
PC7	0.5738	0.3845	0.8563	-3.0512	-4.3056	-1.7968	0.7555	0.0039
PC8	-0.5204	-0.7746	-0.3497	2.7675	1.6377	3.8974	0.5075	0.0178
PC9	0.5084	0.3406	0.7591	-2.7037	-3.8164	-1.5909	0.8398	0.0017
PC10	0.4674	0.3131	0.6976	-2.4852	-3.5074	-1.4630	0.7902	0.0029
PC11	-0.4331	-0.6468	-0.2900	2.3031	1.3546	3.2516	0.9244	0.0004
PC12	0.4092	0.2746	0.6098	-2.1759	-3.0673	-1.2845	0.6037	0.0109
PC13	0.3774	0.2535	0.5617	-2.0067	-2.8261	-1.1873	0.5131	0.0173

Hapalemur griseus

PC	Slope	Slope lower CI	Slope higher CI	Intercept	Intercept lower CI	Intercept higher CI	p value	r squared
PC1	-0.7625	-1.0797	-0.5385	3.8418	2.4784	5.2053	0.0069	0.2577
PC2	-0.5165	-0.7456	-0.3578	2.6021	1.6251	3.5792	0.0330	0.1692
PC3	0.4765	0.3215	0.7060	-2.4006	-3.3693	-1.4318	0.3151	0.0404
PC4	-0.4558	-0.6623	-0.3136	2.2963	1.4179	3.1747	0.0567	0.1377
PC5	-0.4228	-0.6313	-0.2832	2.1302	1.2532	3.0073	0.8734	0.0010
PC6	-0.3920	-0.5841	-0.2631	1.9750	1.1661	2.7840	0.5956	0.0114
PC7	-0.3802	-0.5677	-0.2547	1.9158	1.1271	2.7045	0.8669	0.0011
PC8	-0.3703	-0.5465	-0.2509	1.8655	1.1207	2.6102	0.2150	0.0608
PC9	-0.3326	-0.4959	-0.2231	1.6758	0.9884	2.3631	0.6469	0.0085
PC10	0.3130	0.2102	0.4661	-1.5769	-2.2216	-0.9322	0.5423	0.0150
PC11	0.3028	0.2028	0.4521	-1.5256	-2.1538	-0.8973	0.8989	0.0007
PC12	0.2881	0.1935	0.4290	-1.4518	-2.0450	-0.8586	0.5283	0.0161
PC13	-0.2612	-0.3884	-0.1757	1.3162	0.7803	1.8521	0.4495	0.0231

Lemur catta

PC	Slope	Slope lower CI	Slope higher CI	Intercept	Intercept lower CI	Intercept higher CI	p value	r squared
PC1	-0.8377	-1.1344	-0.6185	4.4039	3.0479	5.7600	0.0017	0.2688
PC2	-0.5820	-0.8203	-0.4130	3.0601	1.9892	4.1309	0.1790	0.0557
PC3	0.5521	0.3914	0.7789	-2.9028	-3.9215	-1.8841	0.2023	0.0503
PC4	0.4925	0.3463	0.7005	-2.5894	-3.5207	-1.6582	0.7715	0.0027
PC5	-0.4374	-0.6043	-0.3166	2.2996	1.5433	3.0559	0.0168	0.1659
PC6	0.3890	0.2733	0.5535	-2.0449	-2.7813	-1.3085	0.9842	0.0000
PC7	-0.3712	-0.5209	-0.2646	1.9517	1.2780	2.6255	0.1029	0.0810
PC8	-0.3513	-0.4999	-0.2469	1.8470	1.1820	2.5120	0.9200	0.0003
PC9	-0.3199	-0.4547	-0.2251	1.6821	1.0785	2.2857	0.6374	0.0070
PC10	-0.2997	-0.4241	-0.2117	1.5755	1.0172	2.1338	0.3150	0.0315
PC11	-0.2746	-0.3893	-0.1938	1.4439	0.9299	1.9579	0.3932	0.0229
PC12	-0.2561	-0.3644	-0.1800	1.3465	0.8616	1.8313	0.9479	0.0001
PC13	-0.2471	-0.3505	-0.1741	1.2989	0.8353	1.7625	0.4543	0.0176

Varecia variegata

PC	Slope	Slope lower CI	Slope higher CI	Intercept	Intercept lower CI	Intercept higher CI	p value	r squared
PC1	0.9006	0.6548	1.2387	-4.9331	-6.5325	-3.3337	0.1595	0.0528
PC2	-0.6575	-0.8881	-0.4868	3.6014	2.5021	4.7006	0.0115	0.1605
PC3	-0.6182	-0.8476	-0.4510	3.3865	2.3002	4.4727	0.0966	0.0728
PC4	-0.4823	-0.6689	-0.3478	2.6420	1.7625	3.5215	0.8244	0.0013
PC5	0.4443	0.3203	0.6163	-2.4338	-3.2443	-1.6232	0.8885	0.0005
PC6	-0.4105	-0.5662	-0.2976	2.2483	1.5124	2.9842	0.2566	0.0346
PC7	-0.3758	-0.5196	-0.2719	2.0587	1.3801	2.7373	0.3793	0.0210
PC8	-0.3699	-0.4986	-0.2744	2.0261	1.4120	2.6403	0.0087	0.1720
PC9	0.3376	0.2472	0.4610	-1.8493	-2.4348	-1.2638	0.0540	0.0967
PC10	0.3227	0.2343	0.4443	-1.7675	-2.3426	-1.1924	0.1895	0.0461
PC11	-0.2896	-0.3985	-0.2104	1.5861	1.0708	2.1015	0.1772	0.0487
PC12	-0.2781	-0.3849	-0.2010	1.5235	1.0199	2.0271	0.4522	0.0154
PC13	0.2610	0.1899	0.3587	-1.4296	-1.8917	-0.9674	0.1388	0.0582

Lepilemur ruficaudatus

PC	Slope	Slope lower CI	Slope higher CI	Intercept	Intercept lower CI	Intercept higher CI	p value	r squared
PC1	-0.6285	-0.8959	-0.4409	3.0901	1.9713	4.2089	0.0050	0.2955
PC2	-0.5422	-0.8148	-0.3608	2.6658	1.5497	3.7819	0.2459	0.0581
PC3	-0.4887	-0.7422	-0.3219	2.4031	1.3697	3.4364	0.7047	0.0064
PC4	0.4270	0.2867	0.6361	-2.0996	-2.9585	-1.2407	0.1222	0.1007
PC5	-0.3802	-0.5762	-0.2509	1.8695	1.0697	2.6693	0.5421	0.0164
PC6	0.3654	0.2408	0.5543	-1.7964	-2.5671	-1.0257	0.6192	0.0109
PC7	0.3456	0.2279	0.5241	-1.6995	-2.4277	-0.9713	0.5811	0.0134
PC8	0.3247	0.2166	0.4869	-1.5966	-2.2611	-0.9320	0.2046	0.0690
PC9	0.3124	0.2056	0.4746	-1.5359	-2.1972	-0.8746	0.7680	0.0039
PC10	-0.2987	-0.4502	-0.1982	1.4687	0.8491	2.0883	0.3158	0.0437
PC11	-0.2838	-0.4256	-0.1893	1.3955	0.8145	1.9765	0.2061	0.0686
PC12	0.2698	0.1779	0.4093	-1.3268	-1.8955	-0.7580	0.5959	0.0124
PC13	0.2339	0.1540	0.3553	-1.1501	-1.6451	-0.6551	0.7458	0.0047

Loris tardigradus

PC	Slope	Slope lower CI	Slope higher CI	Intercept	Intercept lower CI	Intercept higher CI	p value	r squared
PC1	-0.4317	-0.5333	-0.3495	2.0668	1.6266	2.5069	0.0000	0.7328
PC2	0.3445	0.2314	0.5130	-1.6493	-2.3239	-0.9747	0.5434	0.0150
PC3	-0.3127	-0.4581	-0.2134	1.4968	0.9110	2.0827	0.1122	0.0978
PC4	-0.2374	-0.3544	-0.1590	1.1365	0.6685	1.6045	0.8439	0.0016
PC5	0.2259	0.1514	0.3371	-1.0816	-1.5261	-0.6370	0.7177	0.0053
PC6	0.2164	0.1449	0.3230	-1.0359	-1.4623	-0.6094	0.8290	0.0019
PC7	0.1991	0.1335	0.2969	-0.9531	-1.3445	-0.5617	0.6754	0.0071
PC8	-0.1868	-0.2790	-0.1251	0.8944	0.5258	1.2629	0.9914	0.0000
PC9	-0.1779	-0.2644	-0.1197	0.8518	0.5054	1.1983	0.4214	0.0260
PC10	0.1488	0.0996	0.2221	-0.7121	-1.0054	-0.4188	0.8685	0.0011
PC11	0.1363	0.0913	0.2034	-0.6526	-0.9210	-0.3842	0.7511	0.0041
PC12	0.1257	0.0848	0.1865	-0.6020	-0.8455	-0.3584	0.3443	0.0358
PC13	0.1172	0.0785	0.1750	-0.5612	-0.7923	-0.3301	0.8420	0.0016

Nycticebus bengalensis

PC	Slope	Slope lower CI	Slope higher CI	Intercept	Intercept lower CI	Intercept higher CI	p value	r squared
PC1	-0.9820	-1.5163	-0.6360	4.9871	2.7518	7.2224	0.2122	0.0767
PC2	-0.8999	-1.4056	-0.5761	4.5700	2.4638	6.6763	0.4937	0.0237
PC3	0.8002	0.5250	1.2198	-4.0639	-5.8283	-2.2995	0.0943	0.1337
PC4	0.7687	0.4914	1.2026	-3.9039	-5.7099	-2.0978	0.5708	0.0163
PC5	0.6916	0.4606	1.0386	-3.5123	-4.9801	-2.0445	0.0383	0.1974
PC6	-0.6231	-0.9767	-0.3976	3.1645	1.6940	4.6350	0.7004	0.0076
PC7	-0.5659	-0.8883	-0.3605	2.8741	1.5338	4.2143	0.9144	0.0006
PC8	0.5300	0.3584	0.7837	-2.6915	-3.7714	-1.6116	0.0153	0.2601
PC9	0.5097	0.3254	0.7983	-2.5883	-3.7893	-1.3874	0.6489	0.0106
PC10	0.4585	0.2965	0.7089	-2.3284	-3.3756	-1.2812	0.2328	0.0704
PC11	-0.4211	-0.6598	-0.2687	2.1383	1.1452	3.1315	0.6828	0.0085
PC12	0.3625	0.2336	0.5627	-1.8410	-2.6768	-1.0052	0.3041	0.0527
PC13	0.3564	0.2292	0.5541	-1.8098	-2.6349	-0.9847	0.3450	0.0447

Nycticebus coucang

PC	Slope	Slope lower CI	Slope higher CI	Intercept	Intercept lower CI	Intercept higher CI	p value	r squared
PC1	0.6897	0.5431	0.8758	-3.4365	-4.2654	-2.6075	0.2276	0.0217
PC2	-0.5421	-0.6843	-0.4294	2.7010	2.0661	3.3358	0.0269	0.0710
PC3	0.5055	0.4007	0.6376	-2.5185	-3.1088	-1.9283	0.0214	0.0765
PC4	-0.4588	-0.5841	-0.3604	2.2861	1.7287	2.8436	0.8902	0.0003
PC5	0.4220	0.3315	0.5372	-2.1026	-2.6151	-1.5902	0.7741	0.0012
PC6	-0.3720	-0.4701	-0.2943	1.8535	1.4155	2.2915	0.0407	0.0610
PC7	0.3573	0.2808	0.4547	-1.7804	-2.2136	-1.3473	0.5730	0.0048
PC8	0.3297	0.2606	0.4172	-1.6428	-2.0329	-1.2527	0.0597	0.0519
PC9	0.3157	0.2485	0.4011	-1.5729	-1.9533	-1.1926	0.2854	0.0170
PC10	0.2819	0.2214	0.3588	-1.4045	-1.7468	-1.0621	0.7934	0.0010
PC11	-0.2683	-0.3403	-0.2116	1.3370	1.0165	1.6575	0.1316	0.0336
PC12	-0.2604	-0.3303	-0.2053	1.2973	0.9858	1.6087	0.1482	0.0309
PC13	0.2505	0.1992	0.3151	-1.2482	-1.5371	-0.9593	0.0084	0.0992

Perodicticus potto

PC	Slope	Slope lower CI	Slope higher CI	Intercept	Intercept lower CI	Intercept higher CI	p value	r squared
PC1	0.6987	0.5908	0.8263	-3.5285	-4.1234	-2.9337	0.0013	0.0784
PC2	0.6465	0.5437	0.7688	-3.2652	-3.8336	-2.6968	0.1379	0.0172
PC3	-0.5498	-0.6470	-0.4672	2.7765	2.3224	3.2307	0.0000	0.1322
PC4	-0.4565	-0.5396	-0.3861	2.3053	1.9178	2.6927	0.0009	0.0839
PC5	0.4210	0.3538	0.5010	-2.1262	-2.4980	-1.7545	0.2877	0.0089
PC6	-0.4039	-0.4792	-0.3404	2.0396	1.6891	2.3901	0.0193	0.0423
PC7	0.3883	0.3262	0.4623	-1.9610	-2.3047	-1.6173	0.4954	0.0037
PC8	-0.3683	-0.4382	-0.3096	1.8601	1.5351	2.1851	0.2550	0.0102
PC9	0.3459	0.2916	0.4105	-1.7471	-2.0473	-1.4468	0.0196	0.0422
PC10	-0.3255	-0.3876	-0.2733	1.6437	1.3552	1.9323	0.7502	0.0008
PC11	0.2978	0.2502	0.3546	-1.5042	-1.7678	-1.2405	0.4975	0.0036
PC12	-0.2855	-0.3383	-0.2409	1.4417	1.1955	1.6878	0.0078	0.0544
PC13	-0.2700	-0.3212	-0.2270	1.3636	1.1257	1.6014	0.1906	0.0135

2* model vault module against ln CS of vault

Cheirogaleus major

PC	Slope	Slope lower CI	Slope higher CI	Intercept	Intercept lower CI	Intercept higher CI	p value	r squared
PC1	1.0415	0.6946	1.5618	-4.2278	-5.9881	-2.4676	0.2065	0.0684
PC2	-0.9257	-1.3854	-0.6186	3.7579	2.2015	5.3143	0.1759	0.0782
PC3	0.7641	0.5303	1.1010	-3.1019	-4.2602	-1.9436	0.0108	0.2506
PC4	0.6925	0.4559	1.0517	-2.8110	-4.0204	-1.6017	0.7277	0.0054
PC5	0.6652	0.4444	0.9956	-2.7003	-3.8190	-1.5815	0.1778	0.0775
PC6	-0.6171	-0.9260	-0.4112	2.5050	1.4602	3.5498	0.2183	0.0651
PC7	0.5196	0.3421	0.7894	-2.1093	-3.0173	-1.2014	0.7560	0.0043
PC8	0.5082	0.3346	0.7720	-2.0630	-2.9509	-1.1752	0.7445	0.0047
PC9	-0.4715	-0.6921	-0.3212	1.9141	1.1613	2.6668	0.0414	0.1687
PC10	0.4663	0.3073	0.7075	-1.8927	-2.7052	-1.0802	0.6391	0.0097
PC11	0.4473	0.2943	0.6799	-1.8158	-2.5984	-1.0331	0.8466	0.0017
PC12	-0.4046	-0.6128	-0.2671	1.6423	0.9406	2.3441	0.5142	0.0187
PC13	-0.3880	-0.5899	-0.2552	1.5752	0.8959	2.2544	0.9050	0.0006

Cheirogaleus medius

PC	Slope	Slope lower CI	Slope higher CI	Intercept	Intercept lower CI	Intercept higher CI	p value	r squared
PC1	-0.6486	-0.9511	-0.4423	2.4875	1.5116	3.4635	0.5546	0.0131
PC2	-0.5984	-0.8688	-0.4122	2.2952	1.4197	3.1708	0.1751	0.0670
PC3	-0.5322	-0.7358	-0.3849	2.0411	1.3683	2.7139	0.0020	0.3033
PC4	-0.4843	-0.7107	-0.3301	1.8576	1.1276	2.5876	0.6095	0.0098
PC5	0.4393	0.3000	0.6432	-1.6848	-2.3431	-1.0265	0.4518	0.0211
PC6	-0.4070	-0.5894	-0.2811	1.5611	0.9698	2.1525	0.1373	0.0799
PC7	-0.3849	-0.5657	-0.2619	1.4763	0.8938	2.0589	0.8353	0.0016
PC8	0.3468	0.2420	0.4971	-1.3302	-1.8194	-0.8411	0.0518	0.1330
PC9	0.3286	0.2236	0.4828	-1.2601	-1.7572	-0.7630	0.8137	0.0021
PC10	-0.3024	-0.4445	-0.2057	1.1597	0.7018	1.6176	0.9170	0.0004
PC11	0.2923	0.1994	0.4284	-1.1209	-1.5602	-0.6817	0.5218	0.0154
PC12	-0.2726	-0.4007	-0.1854	1.0454	0.6325	1.4582	0.9644	0.0001
PC13	-0.2601	-0.3823	-0.1769	0.9975	0.6036	1.3915	0.9801	0.0000

Microcebus murinus

PC	Slope	Slope lower CI	Slope higher CI	Intercept	Intercept lower CI	Intercept higher CI	p value	r squared
PC1	-1.0804	-1.3643	-0.8555	3.9347	3.0081	4.8614	0.1932	0.0241
PC2	-0.9176	-1.1492	-0.7328	3.3421	2.5838	4.1004	0.0088	0.0941
PC3	-0.7983	-1.0108	-0.6305	2.9076	2.2150	3.6002	0.7424	0.0016
PC4	0.7404	0.5911	0.9275	-2.6967	-3.3095	-2.0840	0.0098	0.0916
PC5	0.7122	0.5624	0.9020	-2.5940	-3.2124	-1.9756	0.9349	0.0001
PC6	0.6719	0.5307	0.8506	-2.4470	-3.0297	-1.8644	0.6874	0.0023
PC7	0.6307	0.4993	0.7967	-2.2970	-2.8386	-1.7554	0.2162	0.0218
PC8	0.5765	0.4553	0.7299	-2.0996	-2.5997	-1.5994	0.7368	0.0016
PC9	-0.5401	-0.6793	-0.4294	1.9671	1.5120	2.4221	0.0410	0.0583
PC10	-0.5237	-0.6632	-0.4136	1.9074	1.4528	2.3621	0.8775	0.0003
PC11	-0.5070	-0.6420	-0.4005	1.8467	1.4068	2.2865	0.7227	0.0018
PC12	-0.4713	-0.5941	-0.3739	1.7164	1.3154	2.1175	0.0948	0.0394
PC13	0.4499	0.3591	0.5636	-1.6385	-2.0110	-1.2660	0.0102	0.0906

Microcebus rufus

PC	Slope	Slope lower CI	Slope higher CI	Intercept	Intercept lower CI	Intercept higher CI	p value	r squared
PC1	-0.9499	-1.3934	-0.6476	3.4641	2.1039	4.8242	0.5807	0.0114
PC2	0.7541	0.6114	0.9301	-2.7500	-3.3311	-2.1688	0.0000	0.7136
PC3	-0.6504	-0.9562	-0.4425	2.3720	1.4353	3.3087	0.9848	0.0000
PC4	0.6079	0.4160	0.8883	-2.2167	-3.0781	-1.3554	0.3551	0.0318
PC5	0.5716	0.3888	0.8402	-2.0844	-2.9075	-1.2613	0.9745	0.0000
PC6	0.5466	0.3718	0.8035	-1.9933	-2.7804	-1.2062	0.9493	0.0002
PC7	0.5010	0.3444	0.7289	-1.8270	-2.5282	-1.1259	0.2181	0.0556
PC8	0.4903	0.3340	0.7198	-1.7880	-2.4916	-1.0844	0.6633	0.0071
PC9	-0.4400	-0.6468	-0.2993	1.6045	0.9709	2.2382	0.9865	0.0000
PC10	-0.4271	-0.6271	-0.2908	1.5573	0.9441	2.1705	0.6934	0.0058
PC11	0.4151	0.2835	0.6077	-1.5138	-2.1049	-0.9226	0.4414	0.0221
PC12	0.3972	0.2702	0.5839	-1.4485	-2.0205	-0.8765	0.9619	0.0001
PC13	0.3589	0.2448	0.5262	-1.3089	-1.8221	-0.7957	0.5384	0.0142

Galago alleni

PC	Slope	Slope lower CI	Slope higher CI	Intercept	Intercept lower CI	Intercept higher CI	p value	r squared
PC1	1.3376	0.9122	1.9614	-5.3576	-7.4587	-3.2565	0.0231	0.2134
PC2	-0.9337	-1.4329	-0.6084	3.7397	2.0884	5.3910	0.8072	0.0028
PC3	0.8154	0.5517	1.2051	-3.2660	-4.5744	-1.9575	0.0394	0.1791
PC4	-0.6993	-1.0596	-0.4614	2.8007	1.6027	3.9987	0.2323	0.0642
PC5	-0.6564	-1.0079	-0.4275	2.6290	1.4667	3.7914	0.9479	0.0002
PC6	-0.6074	-0.9054	-0.4075	2.4330	1.4359	3.4300	0.0705	0.1410
PC7	0.5737	0.3799	0.8664	-2.2979	-3.2722	-1.3237	0.1787	0.0806
PC8	-0.5427	-0.8283	-0.3556	2.1738	1.2270	3.1205	0.4198	0.0298
PC9	0.5018	0.3273	0.7693	-2.0099	-2.8950	-1.1247	0.6770	0.0080
PC10	0.4672	0.3065	0.7121	-1.8713	-2.6837	-1.0589	0.3746	0.0360
PC11	0.4260	0.2796	0.6491	-1.7064	-2.4463	-0.9665	0.3591	0.0383
PC12	-0.4033	-0.6176	-0.2634	1.6155	0.9062	2.3247	0.5817	0.0140
PC13	0.3919	0.2565	0.5989	-1.5698	-2.2555	-0.8841	0.4691	0.0241

Galago demidoff

PC	Slope	Slope lower CI	Slope higher CI	Intercept	Intercept lower CI	Intercept higher CI	p value	r squared
PC1	0.8246	0.6465	1.0517	-3.0845	-3.8423	-2.3267	0.0033	0.1421
PC2	0.6342	0.4884	0.8236	-2.3724	-2.9995	-1.7453	0.5330	0.0069
PC3	0.6067	0.4668	0.7885	-2.2695	-2.8711	-1.6679	0.7952	0.0012
PC4	0.5720	0.4401	0.7433	-2.1395	-2.7065	-1.5725	0.7448	0.0019
PC5	0.5412	0.4174	0.7018	-2.0245	-2.5564	-1.4926	0.2990	0.0189
PC6	0.5038	0.3879	0.6543	-1.8844	-2.3829	-1.3860	0.5725	0.0056
PC7	-0.4828	-0.6273	-0.3715	1.8059	1.3275	2.2842	0.6948	0.0027
PC8	-0.4772	-0.6153	-0.3702	1.7852	1.3268	2.2436	0.0556	0.0628
PC9	0.4479	0.3446	0.5822	-1.6753	-2.1197	-1.2309	0.9990	0.0000
PC10	0.4257	0.3276	0.5532	-1.5923	-2.0142	-1.1704	0.7255	0.0022
PC11	-0.4092	-0.5304	-0.3157	1.5306	1.1289	1.9323	0.2724	0.0211
PC12	0.3982	0.3064	0.5174	-1.4894	-1.8840	-1.0948	0.7118	0.0024
PC13	0.3758	0.2892	0.4884	-1.4058	-1.7783	-1.0333	0.7183	0.0023

Galago elegantulus

PC	Slope	Slope lower CI	Slope higher CI	Intercept	Intercept lower CI	Intercept higher CI	p value	r squared
PC1	1.1123	0.7817	1.5827	-4.4605	-6.0667	-2.8543	0.9749	0.0000
PC2	-0.9066	-1.2611	-0.6517	3.6355	2.4135	4.8575	0.0372	0.1287
PC3	-0.7412	-1.0378	-0.5294	2.9724	1.9531	3.9917	0.0794	0.0931
PC4	0.6572	0.4652	0.9284	-2.6354	-3.5640	-1.7067	0.2425	0.0424
PC5	0.6096	0.4305	0.8632	-2.4445	-3.3121	-1.5768	0.3404	0.0284
PC6	0.5721	0.4030	0.8124	-2.2944	-3.1153	-1.4735	0.5239	0.0128
PC7	0.5454	0.3901	0.7625	-2.1872	-2.9339	-1.4406	0.0666	0.1013
PC8	-0.5148	-0.7321	-0.3620	2.0644	1.3224	2.8064	0.7355	0.0036
PC9	-0.4547	-0.6431	-0.3215	1.8236	1.1787	2.4685	0.2851	0.0356
PC10	-0.4375	-0.6179	-0.3098	1.7545	1.1367	2.3723	0.2350	0.0438
PC11	0.4357	0.3084	0.6156	-1.7472	-2.3632	-1.1312	0.2477	0.0415
PC12	-0.4189	-0.5954	-0.2947	1.6797	1.0767	2.2827	0.6574	0.0062
PC13	0.4053	0.2858	0.5747	-1.6252	-2.2046	-1.0458	0.4279	0.0198

Galago moholi

PC	Slope	Slope lower CI	Slope higher CI	Intercept	Intercept lower CI	Intercept higher CI	p value	r squared
PC1	-0.9678	-1.2073	-0.7759	3.7536	2.9170	4.5901	0.0036	0.1130
PC2	0.8864	0.7013	1.1202	-3.4376	-4.2499	-2.6252	0.6534	0.0029
PC3	-0.7794	-0.9842	-0.6172	3.0227	2.3112	3.7343	0.3875	0.0105
PC4	0.6769	0.5360	0.8548	-2.6251	-3.2435	-2.0068	0.4173	0.0093
PC5	-0.6030	-0.7588	-0.4791	2.3385	1.7962	2.8808	0.0912	0.0397
PC6	-0.5625	-0.7071	-0.4475	2.1816	1.6783	2.6850	0.0587	0.0494
PC7	0.5327	0.4213	0.6734	-2.0659	-2.5548	-1.5770	0.9469	0.0001
PC8	0.5034	0.3994	0.6346	-1.9525	-2.4086	-1.4964	0.1775	0.0255
PC9	0.4856	0.3846	0.6132	-1.8834	-2.3269	-1.4400	0.3941	0.0103
PC10	-0.4758	-0.6015	-0.3764	1.8454	1.4089	2.2819	0.7851	0.0011
PC11	0.4601	0.3640	0.5817	-1.7846	-2.2068	-1.3623	0.8662	0.0004
PC12	0.4513	0.3573	0.5701	-1.7502	-2.1629	-1.3375	0.4742	0.0072
PC13	-0.4211	-0.5323	-0.3331	1.6330	1.2466	2.0194	0.9169	0.0002

Galago senegalensis

PC	Slope	Slope lower CI	Slope higher CI	Intercept	Intercept lower CI	Intercept higher CI	p value	r squared
PC1	-0.6210	-0.7108	-0.5426	2.4493	2.1176	2.7810	0.0000	0.1858
PC2	-0.5635	-0.6534	-0.4860	2.2226	1.8926	2.5526	0.0554	0.0210
PC3	-0.4622	-0.5344	-0.3998	1.8231	1.5575	2.0886	0.0013	0.0580
PC4	-0.4422	-0.5134	-0.3809	1.7440	1.4827	2.0053	0.4716	0.0030
PC5	0.4284	0.3696	0.4965	-1.6895	-1.9398	-1.4391	0.0360	0.0252
PC6	-0.4044	-0.4696	-0.3483	1.5951	1.3557	1.8344	0.9237	0.0001
PC7	0.3492	0.3008	0.4055	-1.3773	-1.5839	-1.1708	0.6205	0.0014
PC8	-0.3317	-0.3843	-0.2864	1.3083	1.1152	1.5014	0.0168	0.0326
PC9	-0.3233	-0.3754	-0.2784	1.2750	1.0837	1.4664	0.8485	0.0002
PC10	0.3059	0.2641	0.3543	-1.2065	-1.3844	-1.0287	0.0125	0.0355
PC11	0.2991	0.2579	0.3469	-1.1796	-1.3551	-1.0041	0.0817	0.0174
PC12	-0.2915	-0.3371	-0.2520	1.1496	0.9818	1.3174	0.0020	0.0539
PC13	0.2796	0.2411	0.3242	-1.1026	-1.2664	-0.9388	0.0638	0.0197

Galago zanzibaricus

PC	Slope	Slope lower CI	Slope higher CI	Intercept	Intercept lower CI	Intercept higher CI	p value	r squared
PC1	-0.8894	-1.3193	-0.5995	3.4423	2.0492	4.8353	0.0900	0.1199
PC2	0.8462	0.5594	1.2800	-3.2751	-4.6698	-1.8803	0.4472	0.0253
PC3	-0.6649	-0.9105	-0.4856	2.5736	1.7512	3.3959	0.0002	0.4513
PC4	-0.5987	-0.9102	-0.3938	2.3174	1.3181	3.3167	0.8968	0.0007
PC5	0.5634	0.3708	0.8560	-2.1807	-3.1196	-1.2418	0.7694	0.0038
PC6	0.5224	0.3459	0.7891	-2.0221	-2.8800	-1.1643	0.3856	0.0329
PC7	0.4815	0.3171	0.7312	-1.8636	-2.6650	-1.0621	0.7116	0.0061
PC8	-0.4362	-0.6630	-0.2869	1.6882	0.9602	2.4161	0.9010	0.0007
PC9	0.4148	0.2734	0.6293	-1.6055	-2.2943	-0.9168	0.6153	0.0112
PC10	-0.3764	-0.5683	-0.2492	1.4567	0.8392	2.0743	0.3763	0.0342
PC11	-0.3433	-0.5215	-0.2260	1.3287	0.7568	1.9006	0.7538	0.0044
PC12	-0.3332	-0.5064	-0.2193	1.2898	0.7343	1.8454	0.7958	0.0030
PC13	0.3257	0.2161	0.4910	-1.2607	-1.7929	-0.7285	0.3238	0.0423

Otolemur crassicaudatus

PC	Slope	Slope lower CI	Slope higher CI	Intercept	Intercept lower CI	Intercept higher CI	p value	r squared
PC1	0.7979	0.6616	0.9623	-3.4426	-4.0914	-2.7938	0.0008	0.1070
PC2	0.6694	0.5494	0.8155	-2.8881	-3.4623	-2.3139	0.4298	0.0063
PC3	0.4496	0.3835	0.5271	-1.9397	-2.2495	-1.6299	0.0000	0.3586
PC4	-0.3684	-0.4491	-0.3023	1.5896	1.2728	1.9063	0.6673	0.0019
PC5	-0.3481	-0.4234	-0.2861	1.5018	1.2055	1.7981	0.1421	0.0216
PC6	-0.3297	-0.4019	-0.2704	1.4224	1.1387	1.7061	0.9876	0.0000
PC7	0.3142	0.2590	0.3812	-1.3556	-1.6194	-1.0919	0.0275	0.0481
PC8	0.3022	0.2488	0.3671	-1.3041	-1.5594	-1.0488	0.0559	0.0364
PC9	0.2949	0.2419	0.3594	-1.2723	-1.5259	-1.0187	0.7350	0.0012
PC10	0.2822	0.2319	0.3433	-1.2174	-1.4579	-0.9768	0.1748	0.0185
PC11	0.2706	0.2220	0.3299	-1.1676	-1.4004	-0.9348	0.7899	0.0007
PC12	-0.2634	-0.3210	-0.2161	1.1365	0.9102	1.3628	0.5702	0.0033
PC13	0.2475	0.2031	0.3015	-1.0677	-1.2801	-0.8552	0.5008	0.0046

Otolemur garnettii

PC	Slope	Slope lower CI	Slope higher CI	Intercept	Intercept lower CI	Intercept higher CI	p value	r squared
PC1	0.7545	0.6195	0.9187	-3.2241	-3.8634	-2.5847	0.0082	0.0727
PC2	-0.4547	-0.5575	-0.3709	1.9432	1.5442	2.3421	0.4508	0.0061
PC3	-0.4197	-0.4950	-0.3558	1.7934	1.4960	2.0908	0.0000	0.3514
PC4	0.3323	0.2713	0.4071	-1.4202	-1.7106	-1.1299	0.2406	0.0148
PC5	-0.3220	-0.3950	-0.2625	1.3759	1.0927	1.6591	0.7417	0.0012
PC6	-0.2820	-0.3456	-0.2300	1.2049	0.9579	1.4520	0.3600	0.0090
PC7	-0.2797	-0.3431	-0.2280	1.1951	0.9492	1.4411	0.7164	0.0014
PC8	-0.2661	-0.3235	-0.2189	1.1372	0.9137	1.3607	0.0033	0.0890
PC9	-0.2604	-0.3192	-0.2124	1.1126	0.8844	1.3407	0.3755	0.0085
PC10	0.2458	0.2006	0.3012	-1.0504	-1.2653	-0.8355	0.2687	0.0131
PC11	0.2262	0.1846	0.2772	-0.9667	-1.1646	-0.7688	0.3010	0.0115
PC12	-0.2221	-0.2717	-0.1815	0.9489	0.7561	1.1418	0.1174	0.0262
PC13	0.2146	0.1751	0.2630	-0.9170	-1.1050	-0.7291	0.3421	0.0097

Avahi laniger

PC	Slope	Slope lower CI	Slope higher CI	Intercept	Intercept lower CI	Intercept higher CI	p value	r squared
PC1	1.0739	0.7000	1.6474	-4.5098	-6.4993	-2.5204	0.2806	0.0552
PC2	0.8675	0.5601	1.3435	-3.6431	-5.2883	-1.9978	0.6530	0.0098
PC3	0.7056	0.4729	1.0528	-2.9631	-4.1809	-1.7454	0.0436	0.1800
PC4	-0.6424	-0.9966	-0.4141	2.6978	1.4745	3.9211	0.8503	0.0017
PC5	0.6252	0.4059	0.9632	-2.6258	-3.7963	-1.4554	0.3903	0.0353
PC6	0.5889	0.3796	0.9137	-2.4734	-3.5949	-1.3519	0.8467	0.0018
PC7	-0.5376	-0.8245	-0.3506	2.2579	1.2627	3.2531	0.2737	0.0567
PC8	0.4944	0.3199	0.7639	-2.0761	-3.0086	-1.1437	0.5135	0.0206
PC9	0.4649	0.3007	0.7186	-1.9523	-2.8298	-1.0748	0.5297	0.0191
PC10	-0.4511	-0.6942	-0.2932	1.8947	1.0526	2.7367	0.3538	0.0411
PC11	-0.4167	-0.6460	-0.2688	1.7499	0.9577	2.5421	0.7494	0.0050
PC12	-0.3985	-0.6058	-0.2621	1.6735	0.9519	2.3952	0.1475	0.0972
PC13	-0.3530	-0.5359	-0.2324	1.4823	0.8450	2.1196	0.1365	0.1025

Indri indri

PC	Slope	Slope lower CI	Slope higher CI	Intercept	Intercept lower CI	Intercept higher CI	p value	r squared
PC1	1.3039	0.9617	1.7680	-6.1377	-8.0354	-4.2401	0.0196	0.1386
PC2	0.9803	0.7072	1.3590	-4.6145	-6.1487	-3.0803	0.7071	0.0039
PC3	0.8136	0.5866	1.1286	-3.8298	-5.1055	-2.5541	0.9600	0.0001
PC4	-0.7801	-1.0812	-0.5629	3.6722	2.4524	4.8920	0.6481	0.0057
PC5	0.7255	0.5239	1.0048	-3.4151	-4.5469	-2.2832	0.5418	0.0101
PC6	-0.6748	-0.9358	-0.4866	3.1762	2.1190	4.2335	0.8174	0.0015
PC7	-0.6282	-0.8517	-0.4633	2.9568	2.0428	3.8709	0.0195	0.1388
PC8	0.6188	0.4463	0.8579	-2.9127	-3.8816	-1.9439	0.7431	0.0029
PC9	0.5707	0.4149	0.7852	-2.6865	-3.5581	-1.8149	0.1650	0.0514
PC10	0.5274	0.3819	0.7282	-2.4824	-3.2972	-1.6675	0.3010	0.0289
PC11	0.4967	0.3584	0.6885	-2.3381	-3.1150	-1.5611	0.6731	0.0049
PC12	0.4853	0.3512	0.6706	-2.2843	-3.0360	-1.5326	0.3447	0.0242
PC13	0.4532	0.3271	0.6281	-2.1334	-2.8418	-1.4251	0.6272	0.0064

Propithecus diadema

PC	Slope	Slope lower CI	Slope higher CI	Intercept	Intercept lower CI	Intercept higher CI	p value	r squared
PC1	0.9013	0.6176	1.3152	-4.2149	-5.8463	-2.5835	0.1493	0.0783
PC2	-0.6590	-0.9080	-0.4783	3.0819	2.0771	4.0868	0.0010	0.3459
PC3	0.5680	0.3850	0.8381	-2.6566	-3.7160	-1.5971	0.4576	0.0214
PC4	-0.4740	-0.6714	-0.3347	2.2169	1.4296	3.0041	0.0110	0.2240
PC5	0.4627	0.3128	0.6844	-2.1639	-3.0330	-1.2949	0.6572	0.0077
PC6	-0.4451	-0.6576	-0.3012	2.0815	1.2482	2.9147	0.5494	0.0140
PC7	0.4059	0.2747	0.5997	-1.8982	-2.6581	-1.1382	0.5527	0.0137
PC8	-0.3813	-0.5629	-0.2583	1.7833	1.0709	2.4958	0.4951	0.0181
PC9	0.3679	0.2484	0.5448	-1.7205	-2.4137	-1.0273	0.8577	0.0013
PC10	0.3146	0.2130	0.4645	-1.4711	-2.0591	-0.8831	0.5084	0.0170
PC11	-0.3056	-0.4527	-0.2063	1.4292	0.8530	2.0054	0.9720	0.0000
PC12	0.2951	0.2006	0.4342	-1.3803	-1.9267	-0.8340	0.3334	0.0360
PC13	0.2885	0.1948	0.4273	-1.3491	-1.8930	-0.8053	0.9530	0.0001

Propithecus verreauxi

PC	Slope	Slope lower CI	Slope higher CI	Intercept	Intercept lower CI	Intercept higher CI	p value	r squared
PC1	-1.1758	-1.5995	-0.8644	5.3753	3.6949	7.0558	0.3964	0.0176
PC2	-0.9914	-1.3397	-0.7336	4.5321	3.1466	5.9176	0.1115	0.0606
PC3	0.8071	0.5917	1.1008	-3.6895	-4.8532	-2.5258	0.9744	0.0000
PC4	0.6842	0.5019	0.9329	-3.1280	-4.1132	-2.1428	0.7331	0.0029
PC5	0.6495	0.4766	0.8851	-2.9691	-3.9030	-2.0351	0.6395	0.0054
PC6	-0.6327	-0.8615	-0.4647	2.8924	1.9852	3.7996	0.5009	0.0111
PC7	-0.5663	-0.7710	-0.4160	2.5890	1.7776	3.4003	0.4699	0.0128
PC8	0.5374	0.3961	0.7292	-2.4568	-3.2181	-1.6954	0.2322	0.0346
PC9	-0.5230	-0.7043	-0.3883	2.3907	1.6685	3.1128	0.0613	0.0828
PC10	-0.4796	-0.6532	-0.3521	2.1925	1.5043	2.8807	0.5310	0.0096
PC11	-0.4369	-0.5913	-0.3228	1.9971	1.3833	2.6109	0.1477	0.0504
PC12	0.4229	0.3101	0.5769	-1.9335	-2.5432	-1.3237	0.9114	0.0003
PC13	-0.4043	-0.5513	-0.2965	1.8483	1.2658	2.4308	0.7907	0.0017

Eulemur fulvus

PC	Slope	Slope lower CI	Slope higher CI	Intercept	Intercept lower CI	Intercept higher CI	p value	r squared
PC1	-1.0086	-1.1706	-0.8689	4.5505	3.8698	5.2312	0.2915	0.0064
PC2	-0.9424	-1.0906	-0.8143	4.2518	3.6285	4.8752	0.0046	0.0456
PC3	0.7039	0.6066	0.8167	-3.1759	-3.6499	-2.7019	0.1703	0.0108
PC4	0.5915	0.5142	0.6805	-2.6690	-3.0442	-2.2938	0.0000	0.1225
PC5	-0.5505	-0.6393	-0.4741	2.4840	2.1113	2.8567	0.7486	0.0006
PC6	-0.5266	-0.6115	-0.4535	2.3760	2.0197	2.7323	0.5912	0.0017
PC7	0.4769	0.4112	0.5532	-2.1519	-2.4724	-1.8314	0.1072	0.0149
PC8	-0.4177	-0.4851	-0.3597	1.8847	1.6018	2.1675	0.9860	0.0000
PC9	0.4117	0.3548	0.4778	-1.8577	-2.1353	-1.5801	0.2181	0.0088
PC10	-0.3895	-0.4522	-0.3355	1.7575	1.4941	2.0209	0.4887	0.0028
PC11	-0.3787	-0.4395	-0.3263	1.7087	1.4535	1.9639	0.2022	0.0094
PC12	-0.3572	-0.4148	-0.3076	1.6117	1.3700	1.8535	0.6960	0.0009
PC13	0.3308	0.2850	0.3839	-1.4924	-1.7155	-1.2694	0.2386	0.0080

Eulemur macaco

PC	Slope	Slope lower CI	Slope higher CI	Intercept	Intercept lower CI	Intercept higher CI	p value	r squared
PC1	-1.1613	-1.5232	-0.8854	5.2565	3.8131	6.6998	0.5511	0.0067
PC2	-0.8774	-1.1516	-0.6684	3.9711	2.8774	5.0649	0.8397	0.0008
PC3	-0.8057	-1.0566	-0.6144	3.6468	2.6460	4.6477	0.5192	0.0079
PC4	0.6881	0.5396	0.8776	-3.1146	-3.8796	-2.3496	0.0005	0.2052
PC5	0.6559	0.5022	0.8565	-2.9686	-3.7705	-2.1668	0.1488	0.0389
PC6	0.6008	0.4580	0.7883	-2.7196	-3.4673	-1.9719	0.6341	0.0043
PC7	-0.5485	-0.7177	-0.4193	2.4828	1.8075	3.1582	0.2455	0.0254
PC8	0.5001	0.3837	0.6519	-2.2637	-2.8709	-1.6565	0.0930	0.0523
PC9	-0.4787	-0.6277	-0.3651	2.1668	1.5725	2.7611	0.4909	0.0090
PC10	-0.4373	-0.5741	-0.3331	1.9794	1.4341	2.5248	0.9659	0.0000
PC11	0.4179	0.3187	0.5480	-1.8917	-2.4107	-1.3727	0.5057	0.0084
PC12	0.4003	0.3050	0.5253	-1.8118	-2.3105	-1.3132	0.7301	0.0023
PC13	0.3833	0.2925	0.5024	-1.7350	-2.2100	-1.2600	0.4169	0.0125

Eulemur mongoz

PC	Slope	Slope lower CI	Slope higher CI	Intercept	Intercept lower CI	Intercept higher CI	p value	r squared
PC1	0.7948	0.6158	1.0257	-3.5563	-4.4734	-2.6392	0.0238	0.0894
PC2	0.5887	0.4537	0.7639	-2.6341	-3.3282	-1.9401	0.0967	0.0494
PC3	-0.5550	-0.7235	-0.4257	2.4833	1.8170	3.1495	0.3754	0.0143
PC4	0.4708	0.3609	0.6142	-2.1066	-2.6734	-1.5399	0.4817	0.0090
PC5	-0.4294	-0.5548	-0.3324	1.9215	1.4238	2.4192	0.0315	0.0813
PC6	0.4113	0.3188	0.5307	-1.8404	-2.3145	-1.3663	0.0222	0.0915
PC7	-0.3977	-0.5191	-0.3047	1.7798	1.3001	2.2594	0.5810	0.0056
PC8	-0.3506	-0.4524	-0.2717	1.5689	1.1645	1.9733	0.0231	0.0904
PC9	-0.3295	-0.4289	-0.2531	1.4744	1.0812	1.8676	0.2304	0.0260
PC10	0.3021	0.2318	0.3937	-1.3517	-1.7140	-0.9893	0.3465	0.0161
PC11	-0.2951	-0.3848	-0.2263	1.3203	0.9656	1.6750	0.4207	0.0118
PC12	-0.2790	-0.3644	-0.2136	1.2486	0.9112	1.5860	0.9429	0.0001
PC13	-0.2734	-0.3562	-0.2099	1.2235	0.8959	1.5510	0.3111	0.0186

Eulemur rubriventer

PC	Slope	Slope lower CI	Slope higher CI	Intercept	Intercept lower CI	Intercept higher CI	p value	r squared
PC1	-1.3821	-2.0465	-0.9334	6.2344	3.7240	8.7448	0.2913	0.0444
PC2	-1.0985	-1.6405	-0.7356	4.9549	2.9140	6.9959	0.9548	0.0001
PC3	0.9729	0.6765	1.3992	-4.3887	-6.0186	-2.7588	0.0242	0.1871
PC4	0.9168	0.6139	1.3690	-4.1352	-5.8382	-2.4323	0.9080	0.0005
PC5	-0.9041	-1.3311	-0.6140	4.0780	2.4606	5.6954	0.1730	0.0730
PC6	-0.7698	-1.1353	-0.5219	3.4722	2.0888	4.8557	0.2015	0.0644
PC7	-0.5987	-0.8927	-0.4015	2.7004	1.5926	3.8082	0.6533	0.0082
PC8	-0.5430	-0.7855	-0.3754	2.4494	1.5245	3.3742	0.0389	0.1597
PC9	0.5305	0.3566	0.7892	-2.3928	-3.3684	-1.4172	0.4790	0.0202
PC10	0.4876	0.3275	0.7260	-2.1995	-3.0984	-1.3006	0.5340	0.0157
PC11	0.4519	0.3027	0.6746	-2.0383	-2.8770	-1.1997	0.8104	0.0023
PC12	0.4269	0.2859	0.6375	-1.9258	-2.7189	-1.1326	0.9272	0.0003
PC13	0.3937	0.2638	0.5877	-1.7760	-2.5067	-1.0453	0.8110	0.0023

Hapalemur griseus

PC	Slope	Slope lower CI	Slope higher CI	Intercept	Intercept lower CI	Intercept higher CI	p value	r squared
PC1	-1.1128	-1.6420	-0.7541	4.8117	2.8919	6.7314	0.2109	0.0619
PC2	-0.7537	-1.1024	-0.5153	3.2591	1.9898	4.5283	0.0972	0.1061
PC3	0.6953	0.4697	1.0294	-3.0066	-4.2167	-1.7965	0.2862	0.0454
PC4	-0.6651	-0.9514	-0.4650	2.8760	1.8242	3.9277	0.0157	0.2118
PC5	0.6170	0.4154	0.9166	-2.6680	-3.7517	-1.5843	0.4069	0.0277
PC6	-0.5721	-0.8500	-0.3850	2.4736	1.4683	3.4789	0.4162	0.0266
PC7	0.5549	0.3721	0.8276	-2.3994	-3.3844	-1.4145	0.6807	0.0069
PC8	-0.5403	-0.7939	-0.3678	2.3364	1.4151	3.2577	0.1432	0.0837
PC9	-0.4854	-0.7236	-0.3256	2.0988	1.2382	2.9594	0.6357	0.0091
PC10	0.4567	0.3072	0.6791	-1.9750	-2.7791	-1.1709	0.4495	0.0231
PC11	0.4419	0.2960	0.6598	-1.9107	-2.6974	-1.1241	0.8688	0.0011
PC12	0.4205	0.2825	0.6259	-1.8183	-2.5609	-1.0757	0.5157	0.0171
PC13	-0.3812	-0.5595	-0.2598	1.6485	1.0005	2.2965	0.1297	0.0894

Lemur catta

PC	Slope	Slope lower CI	Slope higher CI	Intercept	Intercept lower CI	Intercept higher CI	p value	r squared
PC1	-1.1261	-1.5785	-0.8033	5.0613	3.3192	6.8034	0.0917	0.0863
PC2	-0.7825	-1.1099	-0.5516	3.5168	2.2622	4.7715	0.4431	0.0185
PC3	0.7422	0.5345	1.0307	-3.3361	-4.4513	-2.2208	0.0305	0.1381
PC4	0.6621	0.4660	0.9408	-2.9760	-4.0431	-1.9088	0.6068	0.0084
PC5	-0.5880	-0.8143	-0.4246	2.6429	1.7670	3.5187	0.0222	0.1530
PC6	0.5229	0.3675	0.7440	-2.3502	-3.1964	-1.5040	0.9264	0.0003
PC7	-0.4991	-0.7027	-0.3544	2.2431	1.4603	3.0258	0.1595	0.0609
PC8	0.4723	0.3322	0.6714	-2.1227	-2.8849	-1.3604	0.6732	0.0056
PC9	-0.4301	-0.6093	-0.3036	1.9332	1.2461	2.6203	0.3643	0.0258
PC10	-0.4029	-0.5695	-0.2850	1.8107	1.1714	2.4500	0.2652	0.0386
PC11	-0.3692	-0.5250	-0.2597	1.6594	1.0632	2.2557	0.7098	0.0044
PC12	-0.3443	-0.4876	-0.2431	1.5475	0.9979	2.0970	0.3495	0.0274
PC13	-0.3321	-0.4719	-0.2338	1.4928	0.9575	2.0280	0.6002	0.0087

Varecia variegata

PC	Slope	Slope lower CI	Slope higher CI	Intercept	Intercept lower CI	Intercept higher CI	p value	r squared
PC1	1.2557	0.9445	1.6694	-5.7781	-7.4461	-4.1100	0.0012	0.2489
PC2	-0.9167	-1.2456	-0.6747	4.2183	2.9047	5.5319	0.0265	0.1261
PC3	-0.8620	-1.1712	-0.6344	3.9665	2.7315	5.2016	0.0264	0.1263
PC4	-0.6725	-0.9327	-0.4849	3.0946	2.0641	4.1250	0.8673	0.0008
PC5	-0.6195	-0.8562	-0.4482	2.8506	1.9119	3.7893	0.3582	0.0229
PC6	-0.5723	-0.7935	-0.4128	2.6335	1.7575	3.5095	0.7460	0.0029
PC7	-0.5240	-0.7267	-0.3778	2.4113	1.6085	3.2141	0.8322	0.0012
PC8	-0.5157	-0.7019	-0.3789	2.3732	1.6300	3.1164	0.0337	0.1163
PC9	0.4707	0.3394	0.6529	-2.1661	-2.8873	-1.4448	0.8592	0.0009
PC10	0.4499	0.3246	0.6236	-2.0702	-2.7583	-1.3822	0.6803	0.0046
PC11	0.4037	0.2911	0.5600	-1.8578	-2.4767	-1.2389	0.9757	0.0000
PC12	-0.3878	-0.5372	-0.2799	1.7844	1.1926	2.3763	0.5736	0.0086
PC13	0.3639	0.2637	0.5021	-1.6745	-2.2228	-1.1261	0.2638	0.0336

Lepilemur ruficaudatus

PC	Slope	Slope lower CI	Slope higher CI	Intercept	Intercept lower CI	Intercept higher CI	p value	r squared
PC1	-0.9547	-1.3710	-0.6649	4.0021	2.5220	5.4823	0.0085	0.2649
PC2	-0.8237	-1.2420	-0.5462	3.4526	1.9942	4.9110	0.3310	0.0411
PC3	-0.7425	-1.1207	-0.4919	3.1124	1.7944	4.4303	0.3614	0.0363
PC4	0.6487	0.4290	0.9810	-2.7193	-3.8763	-1.5624	0.4305	0.0272
PC5	-0.5776	-0.8760	-0.3809	2.4213	1.3836	3.4590	0.5883	0.0129
PC6	0.5550	0.3653	0.8433	-2.3267	-3.3285	-1.3248	0.7754	0.0036
PC7	0.5251	0.3455	0.7980	-2.2011	-3.1497	-1.2525	0.8333	0.0020
PC8	0.4933	0.3301	0.7372	-2.0678	-2.9212	-1.2145	0.1580	0.0847
PC9	0.4746	0.3125	0.7207	-1.9893	-2.8450	-1.1336	0.7211	0.0056
PC10	0.4538	0.2986	0.6897	-1.9022	-2.7221	-1.0823	0.8497	0.0016
PC11	-0.4312	-0.6400	-0.2905	1.8074	1.0748	2.5400	0.0940	0.1171
PC12	-0.4099	-0.6232	-0.2697	1.7184	0.9774	2.4593	0.8906	0.0008
PC13	-0.3554	-0.5391	-0.2342	1.4896	0.8505	2.1287	0.6230	0.0107

Loris tardigradus

PC	Slope	Slope lower CI	Slope higher CI	Intercept	Intercept lower CI	Intercept higher CI	p value	r squared
PC1	-0.5102	-0.6419	-0.4056	2.0768	1.5957	2.5579	0.0000	0.6839
PC2	0.4072	0.2733	0.6067	-1.6573	-2.3362	-0.9783	0.5923	0.0116
PC3	-0.3695	-0.5376	-0.2540	1.5041	0.9267	2.0815	0.0623	0.1322
PC4	0.2806	0.1880	0.4188	-1.1420	-1.6120	-0.6719	0.8056	0.0025
PC5	0.2670	0.1790	0.3983	-1.0868	-1.5334	-0.6403	0.7024	0.0059
PC6	-0.2557	-0.3819	-0.1712	1.0409	0.6119	1.4698	0.9965	0.0000
PC7	-0.2353	-0.3514	-0.1576	0.9578	0.5631	1.3524	0.9592	0.0001
PC8	-0.2208	-0.3297	-0.1479	0.8987	0.5283	1.2690	0.9446	0.0002
PC9	-0.2103	-0.3114	-0.1420	0.8560	0.5112	1.2007	0.2888	0.0449
PC10	0.1758	0.1178	0.2623	-0.7156	-1.0098	-0.4213	0.7465	0.0043
PC11	-0.1611	-0.2406	-0.1079	0.6557	0.3855	0.9260	0.9757	0.0000
PC12	0.1486	0.1001	0.2207	-0.6049	-0.8504	-0.3593	0.3894	0.0298
PC13	0.1386	0.0928	0.2069	-0.5639	-0.7963	-0.3315	0.9483	0.0002

Nycticebus bengalensis

PC	Slope	Slope lower CI	Slope higher CI	Intercept	Intercept lower CI	Intercept higher CI	p value	r squared
PC1	-0.9367	-1.4691	-0.5973	4.0770	2.1795	5.9745	0.7669	0.0045
PC2	-0.8584	-1.3421	-0.5490	3.7360	2.0101	5.4619	0.5387	0.0192
PC3	0.7633	0.5008	1.1635	-3.3223	-4.7647	-1.8798	0.0943	0.1336
PC4	-0.7333	-1.1510	-0.4671	3.1914	1.7032	4.6797	0.9143	0.0006
PC5	0.6597	0.4516	0.9636	-2.8713	-3.9856	-1.7571	0.0074	0.3079
PC6	0.5944	0.3786	0.9331	-2.5870	-3.7937	-1.3802	0.9969	0.0000
PC7	0.5398	0.3441	0.8468	-2.3496	-3.4436	-1.2555	0.7928	0.0035
PC8	0.5055	0.3357	0.7614	-2.2003	-3.1268	-1.2738	0.0457	0.1851
PC9	0.4862	0.3098	0.7630	-2.1160	-3.1023	-1.1297	0.8652	0.0015
PC10	0.4373	0.2866	0.6673	-1.9035	-2.7319	-1.0751	0.1000	0.1295
PC11	-0.4016	-0.6284	-0.2567	1.7481	0.9391	2.5571	0.5784	0.0157
PC12	0.3458	0.2225	0.5373	-1.5050	-2.1901	-0.8199	0.3288	0.0477
PC13	0.3399	0.2179	0.5302	-1.4795	-2.1592	-0.7999	0.4396	0.0302

Nycticebus coucang

PC	Slope	Slope lower CI	Slope higher CI	Intercept	Intercept lower CI	Intercept higher CI	p value	r squared
PC1	0.7336	0.5798	0.9281	-3.1364	-3.8810	-2.3918	0.0586	0.0524
PC2	-0.5766	-0.7262	-0.4578	2.4651	1.8912	3.0390	0.0130	0.0886
PC3	0.5376	0.4265	0.6777	-2.2986	-2.8357	-1.7615	0.0170	0.0821
PC4	-0.4880	-0.6208	-0.3836	2.0865	1.5794	2.5936	0.4984	0.0069
PC5	0.4488	0.3525	0.5714	-1.9190	-2.3870	-1.4510	0.9709	0.0000
PC6	-0.3956	-0.5009	-0.3125	1.6916	1.2890	2.0943	0.0722	0.0474
PC7	0.3801	0.2989	0.4833	-1.6249	-2.0193	-1.2306	0.4199	0.0097
PC8	0.3507	0.2757	0.4460	-1.4993	-1.8635	-1.1352	0.4578	0.0083
PC9	0.3358	0.2640	0.4270	-1.4356	-1.7841	-1.0870	0.4404	0.0089
PC10	0.2998	0.2355	0.3817	-1.2818	-1.5944	-0.9693	0.8914	0.0003
PC11	-0.2854	-0.3616	-0.2253	1.2202	0.9289	1.5116	0.0924	0.0417
PC12	-0.2769	-0.3512	-0.2183	1.1840	0.8998	1.4682	0.1465	0.0312
PC13	0.2664	0.2109	0.3367	-1.1392	-1.4081	-0.8703	0.0375	0.0630

Perodicticus potto

PC	Slope	Slope lower CI	Slope higher CI	Intercept	Intercept lower CI	Intercept higher CI	p value	r squared
PC1	0.7966	0.6748	0.9404	-3.4495	-4.0246	-2.8744	0.0003	0.0988
PC2	0.7372	0.6214	0.8745	-3.1920	-3.7400	-2.6441	0.0166	0.0444
PC3	-0.6269	-0.7407	-0.5305	2.7143	2.2594	3.1693	0.0006	0.0890
PC4	-0.5205	-0.6181	-0.4383	2.2536	1.8643	2.6429	0.0417	0.0322
PC5	0.4800	0.4039	0.5706	-2.0786	-2.4397	-1.7176	0.0969	0.0215
PC6	-0.4605	-0.5476	-0.3872	1.9939	1.6466	2.3412	0.1514	0.0161
PC7	0.4427	0.3721	0.5268	-1.9171	-2.2519	-1.5822	0.2496	0.0104
PC8	-0.4200	-0.4988	-0.3536	1.8184	1.5040	2.1329	0.0489	0.0302
PC9	0.3944	0.3316	0.4692	-1.7079	-2.0059	-1.4099	0.2017	0.0128
PC10	-0.3711	-0.4419	-0.3116	1.6069	1.3248	1.8890	0.7692	0.0007
PC11	0.3396	0.2854	0.4040	-1.4705	-1.7273	-1.2136	0.2439	0.0107
PC12	-0.3255	-0.3865	-0.2741	1.4094	1.1659	1.6529	0.0428	0.0319
PC13	-0.3079	-0.3665	-0.2586	1.3330	1.0995	1.5665	0.4247	0.0050

Goswami model face module against ln CS whole cranium

Cheirogaleus major

PC	Slope	Slope lower CI	Slope higher CI	Intercept	Intercept lower CI	Intercept higher CI	p value	r squared
PC1	-0.7462	-1.1336	-0.4911	3.6258	2.0648	5.1869	0.7674	0.0039
PC2	0.6439	0.4268	0.9715	-3.1289	-4.4525	-1.8053	0.3481	0.0384
PC3	-0.5057	-0.7655	-0.3341	2.4573	1.4089	3.5057	0.4812	0.0218
PC4	0.4331	0.2849	0.6582	-2.1044	-3.0113	-1.1974	0.8375	0.0019
PC5	-0.4087	-0.6141	-0.2720	1.9861	1.1549	2.8174	0.2432	0.0587
PC6	-0.3671	-0.5461	-0.2468	1.7840	1.0568	2.5113	0.1104	0.1070
PC7	0.3492	0.2321	0.5253	-1.6968	-2.4093	-0.9844	0.2695	0.0527
PC8	-0.3235	-0.4845	-0.2160	1.5720	0.9194	2.2246	0.1888	0.0738
PC9	-0.2888	-0.4341	-0.1922	1.4035	0.8158	1.9913	0.2479	0.0576
PC10	-0.2528	-0.3822	-0.1672	1.2285	0.7063	1.7508	0.4172	0.0288
PC11	0.2413	0.1587	0.3669	-1.1725	-1.6783	-0.6667	0.9737	0.0000
PC12	0.1906	0.1254	0.2896	-0.9262	-1.3251	-0.5272	0.7968	0.0029
PC13	0.1726	0.1156	0.2578	-0.8387	-1.1844	-0.4931	0.1519	0.0872

Cheirogaleus medius

PC	Slope	Slope lower CI	Slope higher CI	Intercept	Intercept lower CI	Intercept higher CI	p value	r squared
PC1	0.5425	0.3806	0.7733	-2.4901	-3.3914	-1.5889	0.0315	0.1600
PC2	-0.5005	-0.7349	-0.3408	2.2972	1.3925	3.2018	0.6987	0.0056
PC3	0.4547	0.3093	0.6683	-2.0870	-2.9110	-1.2630	0.9064	0.0005
PC4	0.4331	0.3118	0.6016	-1.9878	-2.6529	-1.3227	0.0030	0.2822
PC5	-0.3631	-0.5317	-0.2480	1.6668	1.0156	2.3179	0.4489	0.0214
PC6	-0.3459	-0.5075	-0.2357	1.5875	0.9635	2.2115	0.6166	0.0094
PC7	0.3009	0.2050	0.4416	-1.3810	-1.9241	-0.8379	0.6383	0.0083
PC8	-0.2755	-0.4049	-0.1875	1.2647	0.7657	1.7636	0.8181	0.0020
PC9	0.2453	0.1675	0.3593	-1.1260	-1.5661	-0.6859	0.4602	0.0204
PC10	-0.2277	-0.3229	-0.1605	1.0450	0.6724	1.4176	0.0199	0.1849
PC11	0.2119	0.1445	0.3109	-0.9727	-1.3546	-0.5908	0.5800	0.0115
PC12	-0.2006	-0.2914	-0.1381	0.9207	0.5687	1.2726	0.1898	0.0628
PC13	-0.1610	-0.2366	-0.1096	0.7391	0.4476	1.0306	0.7882	0.0027

Microcebus murinus

PC	Slope	Slope lower CI	Slope higher CI	Intercept	Intercept lower CI	Intercept higher CI	p value	r squared
PC1	0.9023	0.7201	1.1306	-3.9118	-4.8017	-3.0218	0.0108	0.0892
PC2	0.7738	0.6111	0.9800	-3.3548	-4.1545	-2.5552	0.8844	0.0003
PC3	-0.6885	-0.8683	-0.5459	2.9847	2.2858	3.6835	0.1135	0.0354
PC4	-0.5796	-0.7321	-0.4588	2.5125	1.9199	3.1052	0.2240	0.0211
PC5	0.5255	0.4187	0.6596	-2.2783	-2.8006	-1.7561	0.0196	0.0754
PC6	0.5119	0.4058	0.6458	-2.2192	-2.7394	-1.6991	0.1251	0.0333
PC7	-0.4458	-0.5644	-0.3521	1.9327	1.4725	2.3928	0.6791	0.0025
PC8	0.4405	0.3479	0.5577	-1.9095	-2.3644	-1.4547	0.7296	0.0017
PC9	0.4162	0.3289	0.5267	-1.8042	-2.2330	-1.3755	0.5077	0.0063
PC10	-0.3719	-0.4710	-0.2937	1.6125	1.2281	1.9968	0.9300	0.0001
PC11	0.3590	0.2835	0.4547	-1.5565	-1.9276	-1.1855	0.9329	0.0001
PC12	0.3329	0.2649	0.4182	-1.4430	-1.7752	-1.1108	0.0275	0.0675
PC13	-0.3210	-0.4065	-0.2535	1.3916	1.0600	1.7232	0.8190	0.0008

Microcebus rufus

PC	Slope	Slope lower CI	Slope higher CI	Intercept	Intercept lower CI	Intercept higher CI	p value	r squared
PC1	0.5106	0.3609	0.7224	-2.2250	-3.0129	-1.4372	0.0161	0.1962
PC2	0.4975	0.3434	0.7207	-2.1680	-2.9902	-1.3457	0.1434	0.0776
PC3	-0.4625	-0.6679	-0.3203	2.0157	1.2581	2.7733	0.1051	0.0943
PC4	-0.4503	-0.6503	-0.3119	1.9626	1.2251	2.7001	0.1045	0.0946
PC5	0.4029	0.2759	0.5884	-1.7559	-2.4370	-1.0747	0.3298	0.0352
PC6	0.3349	0.2303	0.4870	-1.4594	-2.0188	-0.9000	0.2088	0.0579
PC7	0.3239	0.2221	0.4725	-1.4117	-1.9574	-0.8660	0.2870	0.0419
PC8	0.3127	0.2132	0.4587	-1.3627	-1.8977	-0.8277	0.5752	0.0118
PC9	0.2469	0.1704	0.3576	-1.0760	-1.4839	-0.6680	0.1411	0.0784
PC10	-0.2286	-0.3356	-0.1558	0.9965	0.6044	1.3885	0.6509	0.0077
PC11	-0.2120	-0.3116	-0.1443	0.9241	0.5595	1.2888	0.8287	0.0018
PC12	-0.1834	-0.2689	-0.1251	0.7994	0.4860	1.1128	0.5325	0.0146
PC13	-0.1697	-0.2461	-0.1169	0.7394	0.4578	1.0210	0.1650	0.0701

Galago alleni

PC	Slope	Slope lower CI	Slope higher CI	Intercept	Intercept lower CI	Intercept higher CI	p value	r squared
PC1	0.7067	0.5097	0.9797	-3.3630	-4.4812	-2.2447	0.0005	0.4345
PC2	-0.5892	-0.9018	-0.3849	2.8038	1.5740	4.0337	0.5557	0.0160
PC3	-0.5401	-0.8293	-0.3517	2.5701	1.4337	3.7066	0.9669	0.0001
PC4	0.4975	0.3256	0.7601	-2.3677	-3.4016	-1.3338	0.4628	0.0248
PC5	-0.4594	-0.7028	-0.3002	2.1860	1.2280	3.1440	0.5355	0.0177
PC6	0.4004	0.2613	0.6134	-1.9053	-2.7432	-1.0674	0.6268	0.0109
PC7	-0.3761	-0.5726	-0.2470	1.7897	1.0147	2.5646	0.3424	0.0410
PC8	-0.3140	-0.4766	-0.2068	1.4942	0.8521	2.1362	0.2669	0.0557
PC9	-0.3055	-0.4688	-0.1990	1.4536	0.8115	2.0957	0.8317	0.0021
PC10	0.2796	0.1822	0.4291	-1.3308	-1.9181	-0.7434	0.7771	0.0037
PC11	0.2688	0.1752	0.4123	-1.2790	-1.8432	-0.7148	0.7479	0.0048
PC12	-0.2043	-0.3122	-0.1338	0.9724	0.5479	1.3970	0.4590	0.0252
PC13	-0.1819	-0.2781	-0.1190	0.8657	0.4870	1.2445	0.4969	0.0212

Galago demidoff

PC	Slope	Slope lower CI	Slope higher CI	Intercept	Intercept lower CI	Intercept higher CI	p value	r squared
PC1	-0.8925	-1.1530	-0.6908	3.9549	2.9309	4.9790	0.0988	0.0471
PC2	-0.7353	-0.9551	-0.5661	3.2584	2.3963	4.1204	0.5902	0.0051
PC3	-0.6587	-0.8537	-0.5082	2.9188	2.1534	3.6842	0.2558	0.0226
PC4	-0.5620	-0.7297	-0.4329	2.4905	1.8328	3.1482	0.4833	0.0087
PC5	-0.5358	-0.6961	-0.4125	2.3744	1.7460	3.0027	0.6130	0.0045
PC6	-0.4922	-0.6379	-0.3798	2.1813	1.6093	2.7532	0.2540	0.0228
PC7	-0.4140	-0.5308	-0.3229	1.8347	1.3740	2.2954	0.0128	0.1038
PC8	0.4026	0.3104	0.5222	-1.7841	-2.2535	-1.3147	0.3374	0.0162
PC9	0.3758	0.2902	0.4865	-1.6651	-2.1000	-1.2302	0.1863	0.0304
PC10	-0.3576	-0.4648	-0.2751	1.5847	1.1644	2.0050	0.9120	0.0002
PC11	-0.3408	-0.4419	-0.2628	1.5101	1.1132	1.9070	0.3087	0.0182
PC12	0.3061	0.2355	0.3979	-1.3564	-1.7161	-0.9966	0.9781	0.0000
PC13	0.2980	0.2322	0.3824	-1.3205	-1.6532	-0.9878	0.0159	0.0977

Galago elegantulus

PC	Slope	Slope lower CI	Slope higher CI	Intercept	Intercept lower CI	Intercept higher CI	p value	r squared
PC1	-0.9956	-1.3836	-0.7163	4.7006	3.1252	6.2759	0.0334	0.1338
PC2	0.8585	0.6062	1.2157	-4.0533	-5.4922	-2.6145	0.3424	0.0282
PC3	0.7803	0.5486	1.1098	-3.6841	-5.0090	-2.3592	0.7725	0.0026
PC4	0.7381	0.5194	1.0488	-3.4848	-4.7348	-2.2348	0.6213	0.0077
PC5	0.6259	0.4400	0.8903	-2.9550	-4.0182	-1.8919	0.8093	0.0018
PC6	-0.5927	-0.8423	-0.4170	2.7983	1.7943	3.8024	0.6340	0.0072
PC7	-0.5211	-0.7406	-0.3667	2.4605	1.5780	3.3431	0.6193	0.0078
PC8	-0.4563	-0.6491	-0.3207	2.1542	1.3789	2.9296	0.8642	0.0009
PC9	0.4132	0.2908	0.5871	-1.9507	-2.6502	-1.2512	0.6073	0.0083
PC10	0.3547	0.2494	0.5045	-1.6748	-2.2771	-1.0725	0.7747	0.0026
PC11	-0.3150	-0.4483	-0.2214	1.4874	0.9519	2.0230	0.9391	0.0002
PC12	-0.3066	-0.4243	-0.2215	1.4474	0.9685	1.9264	0.0209	0.1557
PC13	-0.2885	-0.4106	-0.2028	1.3624	0.8719	1.8529	0.9132	0.0004

Galago moholi

PC	Slope	Slope lower CI	Slope higher CI	Intercept	Intercept lower CI	Intercept higher CI	p value	r squared
PC1	0.7666	0.6064	0.9691	-3.4862	-4.3110	-2.6614	0.8403	0.0006
PC2	0.6507	0.5147	0.8226	-2.9592	-3.6593	-2.2591	0.8423	0.0006
PC3	0.6309	0.4991	0.7977	-2.8694	-3.5483	-2.1904	0.9082	0.0002
PC4	-0.5964	-0.7524	-0.4727	2.7123	2.0763	3.3484	0.2562	0.0181
PC5	0.5330	0.4218	0.6735	-2.4238	-2.9962	-1.8514	0.5880	0.0042
PC6	-0.5030	-0.6337	-0.3992	2.2873	1.7540	2.8206	0.1484	0.0292
PC7	-0.4711	-0.5912	-0.3753	2.1423	1.6513	2.6333	0.0337	0.0619
PC8	-0.4449	-0.5615	-0.3525	2.0233	1.5480	2.4985	0.3082	0.0146
PC9	0.4026	0.3186	0.5087	-1.8308	-2.2632	-1.3985	0.5907	0.0041
PC10	-0.3970	-0.5020	-0.3140	1.8056	1.3783	2.2329	0.9869	0.0000
PC11	0.3636	0.2881	0.4590	-1.6536	-2.0422	-1.2650	0.3198	0.0139
PC12	-0.3384	-0.4248	-0.2696	1.5390	1.1859	1.8920	0.0361	0.0604
PC13	0.3049	0.2416	0.3847	-1.3865	-1.7120	-1.0610	0.2905	0.0157

Galago senegalensis

PC	Slope	Slope lower CI	Slope higher CI	Intercept	Intercept lower CI	Intercept higher CI	p value	r squared
PC1	-0.6472	-0.7510	-0.5577	3.0002	2.5522	3.4481	0.1844	0.0102
PC2	0.5821	0.5014	0.6758	-2.6985	-3.1028	-2.2941	0.4648	0.0031
PC3	-0.5583	-0.6444	-0.4836	2.5880	2.2153	2.9608	0.0002	0.0788
PC4	0.4906	0.4225	0.5696	-2.2744	-2.6154	-1.9334	0.5626	0.0019
PC5	0.4522	0.3906	0.5234	-2.0961	-2.4040	-1.7882	0.0066	0.0419
PC6	-0.4226	-0.4903	-0.3643	1.9593	1.6672	2.2514	0.1300	0.0132
PC7	-0.4009	-0.4629	-0.3471	1.8583	1.5900	2.1266	0.0003	0.0745
PC8	0.3732	0.3216	0.4330	-1.7301	-1.9882	-1.4719	0.1586	0.0115
PC9	0.3615	0.3118	0.4192	-1.6759	-1.9247	-1.4271	0.0535	0.0214
PC10	-0.3312	-0.3842	-0.2855	1.5354	1.3067	1.7642	0.1122	0.0145
PC11	0.3270	0.2817	0.3797	-1.5161	-1.7434	-1.2887	0.6149	0.0015
PC12	0.2945	0.2536	0.3420	-1.3654	-1.5703	-1.1605	0.7998	0.0004
PC13	-0.2907	-0.3376	-0.2504	1.3478	1.1456	1.5500	0.7159	0.0008

Galago zanzibaricus

PC	Slope	Slope lower CI	Slope higher CI	Intercept	Intercept lower CI	Intercept higher CI	p value	r squared
PC1	0.8451	0.5615	1.2718	-3.8758	-5.5046	-2.2471	0.2781	0.0509
PC2	-0.7135	-1.0800	-0.4713	3.2722	1.8762	4.6682	0.4801	0.0219
PC3	0.6683	0.4406	1.0137	-3.0650	-4.3793	-1.7507	0.6046	0.0118
PC4	0.6027	0.4136	0.8783	-2.7643	-3.8299	-1.6986	0.0245	0.2013
PC5	-0.5981	-0.8795	-0.4068	2.7431	1.6591	3.8272	0.0471	0.1607
PC6	-0.4699	-0.6973	-0.3167	2.1552	1.2824	3.0281	0.0920	0.1185
PC7	0.4335	0.2880	0.6524	-1.9880	-2.8237	-1.1524	0.2802	0.0505
PC8	0.3900	0.2583	0.5888	-1.7887	-2.5466	-1.0307	0.3709	0.0349
PC9	0.3184	0.2098	0.4833	-1.4605	-2.0878	-0.8332	0.6599	0.0086
PC10	-0.3049	-0.4634	-0.2006	1.3985	0.7959	2.0010	0.8226	0.0022
PC11	-0.2832	-0.4233	-0.1895	1.2989	0.7626	1.8352	0.1603	0.0839
PC12	0.2627	0.1742	0.3962	-1.2048	-1.7140	-0.6957	0.3355	0.0404
PC13	0.2201	0.1452	0.3337	-1.0095	-1.4419	-0.5770	0.5799	0.0135

Otolemur crassicaudatus

PC	Slope	Slope lower CI	Slope higher CI	Intercept	Intercept lower CI	Intercept higher CI	p value	r squared
PC1	0.4149	0.3403	0.5058	-2.1225	-2.5458	-1.6991	0.9986	0.0000
PC2	0.3580	0.2937	0.4363	-1.8313	-2.1960	-1.4666	0.5955	0.0029
PC3	0.3186	0.2630	0.3859	-1.6297	-1.9440	-1.3153	0.0105	0.0644
PC4	0.2971	0.2480	0.3559	-1.5198	-1.7957	-1.2439	0.0000	0.1715
PC5	-0.2682	-0.3260	-0.2206	1.3720	1.1023	1.6417	0.0909	0.0286
PC6	-0.2404	-0.2927	-0.1975	1.2300	0.9864	1.4736	0.2377	0.0141
PC7	0.2166	0.1787	0.2626	-1.1081	-1.3229	-0.8933	0.0181	0.0552
PC8	0.2058	0.1691	0.2506	-1.0530	-1.2615	-0.8446	0.2210	0.0151
PC9	0.1884	0.1551	0.2288	-0.9639	-1.1524	-0.7753	0.0506	0.0381
PC10	-0.1836	-0.2232	-0.1510	0.9392	0.7545	1.1239	0.0976	0.0275
PC11	0.1766	0.1453	0.2145	-0.9033	-1.0803	-0.7262	0.0638	0.0343
PC12	-0.1647	-0.2008	-0.1351	0.8427	0.6748	1.0106	0.6747	0.0018
PC13	0.1498	0.1230	0.1825	-0.7665	-0.9186	-0.6143	0.3461	0.0090

Otolemur garnettii

PC	Slope	Slope lower CI	Slope higher CI	Intercept	Intercept lower CI	Intercept higher CI	p value	r squared
PC1	-0.4242	-0.5126	-0.3510	2.1407	1.7329	2.5485	0.0001	0.1444
PC2	-0.4031	-0.4943	-0.3287	2.0341	1.6161	2.4521	0.5270	0.0043
PC3	-0.3483	-0.4223	-0.2873	1.7577	1.4170	2.0984	0.0008	0.1141
PC4	-0.3234	-0.3951	-0.2648	1.6321	1.3034	1.9608	0.0427	0.0434
PC5	-0.2756	-0.3356	-0.2262	1.3905	1.1145	1.6666	0.0092	0.0706
PC6	0.2633	0.2157	0.3214	-1.3287	-1.5952	-1.0622	0.0271	0.0514
PC7	0.2420	0.1975	0.2964	-1.2210	-1.4707	-0.9714	0.2489	0.0143
PC8	-0.2368	-0.2903	-0.1931	1.1949	0.9497	1.4401	0.4223	0.0069
PC9	-0.2000	-0.2453	-0.1630	1.0092	0.8014	1.2169	0.8437	0.0004
PC10	-0.1887	-0.2310	-0.1542	0.9524	0.7587	1.1461	0.1269	0.0249
PC11	-0.1809	-0.2205	-0.1484	0.9127	0.7308	1.0947	0.0141	0.0631
PC12	0.1731	0.1411	0.2124	-0.8735	-1.0533	-0.6936	0.8334	0.0005
PC13	-0.1600	-0.1963	-0.1304	0.8074	0.6411	0.9737	0.8994	0.0002

Avahi laniger

PC	Slope	Slope lower CI	Slope higher CI	Intercept	Intercept lower CI	Intercept higher CI	p value	r squared
PC1	-1.0971	-1.6940	-0.7105	5.3567	2.9555	7.7578	0.4764	0.0244
PC2	-0.9972	-1.5459	-0.6433	4.8693	2.6658	7.0728	0.7323	0.0057
PC3	0.9474	0.6113	1.4682	-4.6258	-6.7177	-2.5338	0.7050	0.0070
PC4	0.7396	0.4854	1.1270	-3.6114	-5.1777	-2.0451	0.1727	0.0867
PC5	0.7066	0.4621	1.0806	-3.4503	-4.9605	-1.9401	0.2230	0.0698
PC6	-0.6287	-0.9757	-0.4051	3.0700	1.6769	4.4631	0.9445	0.0002
PC7	-0.5728	-0.8846	-0.3709	2.7971	1.5429	4.0512	0.4819	0.0238
PC8	-0.4772	-0.7270	-0.3132	2.3299	1.3194	3.3403	0.1726	0.0867
PC9	-0.4550	-0.7044	-0.2939	2.2216	1.2193	3.2239	0.6220	0.0118
PC10	-0.4370	-0.6564	-0.2909	2.1338	1.2413	3.0262	0.0672	0.1507
PC11	0.3935	0.2537	0.6101	-1.9212	-2.7912	-1.0511	0.7688	0.0042
PC12	-0.3553	-0.5474	-0.2306	1.7349	0.9615	2.5084	0.3925	0.0350
PC13	-0.2968	-0.4587	-0.1920	1.4491	0.7982	2.1001	0.5168	0.0203

Indri indri

PC	Slope	Slope lower CI	Slope higher CI	Intercept	Intercept lower CI	Intercept higher CI	p value	r squared
PC1	-1.6426	-2.2703	-1.1884	9.0145	6.0456	11.9834	0.3621	0.0225
PC2	1.3297	0.9601	1.8416	-7.2975	-9.7163	-4.8787	0.5461	0.0099
PC3	-1.0082	-1.3934	-0.7295	5.5329	3.7111	7.3548	0.3578	0.0229
PC4	0.7784	0.5670	1.0685	-4.2718	-5.6481	-2.8955	0.1186	0.0645
PC5	-0.6140	-0.8494	-0.4438	3.3695	2.2563	4.4827	0.4380	0.0163
PC6	0.6014	0.4379	0.8261	-3.3007	-4.3661	-2.2353	0.1291	0.0612
PC7	0.5291	0.3814	0.7339	-2.9038	-3.8711	-1.9365	0.9929	0.0000
PC8	-0.5021	-0.6958	-0.3623	2.7556	1.8404	3.6707	0.6394	0.0060
PC9	0.4537	0.3277	0.6283	-2.4901	-3.3151	-1.6651	0.5285	0.0108
PC10	0.4132	0.2980	0.5731	-2.2678	-3.0228	-1.5129	0.8236	0.0014
PC11	-0.3953	-0.5454	-0.2865	2.1693	1.4589	2.8798	0.2646	0.0335
PC12	-0.3575	-0.4954	-0.2580	1.9622	1.3106	2.6137	0.6301	0.0063
PC13	0.3099	0.2243	0.4282	-1.7010	-2.2605	-1.1416	0.3347	0.0252

Propithecus diadema

PC	Slope	Slope lower CI	Slope higher CI	Intercept	Intercept lower CI	Intercept higher CI	p value	r squared
PC1	1.1968	0.8136	1.7605	-6.4259	-8.9683	-3.8835	0.3279	0.0368
PC2	0.9164	0.6215	1.3510	-4.9202	-6.8788	-2.9616	0.4218	0.0250
PC3	-0.6641	-0.9695	-0.4549	3.5657	2.1839	4.9474	0.1555	0.0761
PC4	0.6166	0.4271	0.8901	-3.3106	-4.5537	-2.0676	0.0568	0.1326
PC5	-0.4770	-0.7063	-0.3222	2.5614	1.5300	3.5928	0.8083	0.0023
PC6	-0.4435	-0.6491	-0.3030	2.3811	1.4519	3.3103	0.1978	0.0629
PC7	-0.3881	-0.5700	-0.2643	2.0840	1.2632	2.9049	0.2765	0.0454
PC8	-0.3693	-0.5404	-0.2524	1.9828	1.2095	2.7562	0.1940	0.0640
PC9	0.3451	0.2339	0.5092	-1.8531	-2.5922	-1.1140	0.4596	0.0212
PC10	0.3073	0.2114	0.4465	-1.6498	-2.2808	-1.0187	0.1015	0.0998
PC11	-0.2671	-0.3956	-0.1803	1.4339	0.8559	2.0119	0.9271	0.0003
PC12	0.2443	0.1652	0.3612	-1.3117	-1.8379	-0.7855	0.6174	0.0097
PC13	-0.2038	-0.2987	-0.1391	1.0942	0.6657	1.5227	0.2240	0.0563

Propithecus verreauxi

PC	Slope	Slope lower CI	Slope higher CI	Intercept	Intercept lower CI	Intercept higher CI	p value	r squared
PC1	-1.0929	-1.4335	-0.8333	5.7852	4.1967	7.3737	0.0008	0.2421
PC2	-0.8925	-1.2028	-0.6623	4.7243	3.2938	6.1547	0.0690	0.0784
PC3	0.7281	0.5392	0.9832	-3.8540	-5.0290	-2.6790	0.0970	0.0657
PC4	0.6242	0.4583	0.8503	-3.3042	-4.3417	-2.2667	0.5455	0.0090
PC5	-0.5971	-0.8135	-0.4383	3.1608	2.1677	4.1538	0.5722	0.0078
PC6	0.5362	0.3935	0.7307	-2.8383	-3.7309	-1.9456	0.6294	0.0057
PC7	-0.5227	-0.7128	-0.3832	2.7667	1.8943	3.6391	0.8778	0.0006
PC8	0.4734	0.3521	0.6363	-2.5056	-3.2577	-1.7535	0.0451	0.0943
PC9	-0.4049	-0.5500	-0.2981	2.1433	1.4766	2.8100	0.2883	0.0275
PC10	-0.3746	-0.5093	-0.2755	1.9829	1.3642	2.6016	0.3498	0.0214
PC11	0.3096	0.2274	0.4216	-1.6388	-2.1527	-1.1249	0.4934	0.0115
PC12	-0.2714	-0.3695	-0.1994	1.4368	0.9864	1.8871	0.4755	0.0125
PC13	-0.2479	-0.3367	-0.1825	1.3121	0.9038	1.7204	0.2945	0.0268

Eulemur fulvus

PC	Slope	Slope lower CI	Slope higher CI	Intercept	Intercept lower CI	Intercept higher CI	p value	r squared
PC1	0.7200	0.6200	0.8361	-3.8383	-4.4143	-3.2623	0.9708	0.0000
PC2	-0.6306	-0.7319	-0.5433	3.3614	2.8586	3.8643	0.2961	0.0063
PC3	0.5646	0.4870	0.6544	-3.0095	-3.4557	-2.5633	0.0410	0.0239
PC4	-0.5077	-0.5893	-0.4373	2.7064	2.3012	3.1115	0.3558	0.0049
PC5	0.4652	0.4007	0.5400	-2.4797	-2.8511	-2.1083	0.4060	0.0040
PC6	0.4301	0.3725	0.4966	-2.2927	-2.6237	-1.9617	0.0003	0.0745
PC7	-0.3812	-0.4426	-0.3284	2.0323	1.7277	2.3369	0.4834	0.0028
PC8	-0.3474	-0.4032	-0.2994	1.8521	1.5755	2.1288	0.2066	0.0092
PC9	-0.2928	-0.3400	-0.2522	1.5611	1.3270	1.7951	0.5619	0.0019
PC10	0.2825	0.2433	0.3280	-1.5060	-1.7318	-1.2801	0.6039	0.0016
PC11	0.2689	0.2317	0.3121	-1.4334	-1.6478	-1.2189	0.3037	0.0061
PC12	-0.2424	-0.2813	-0.2088	1.2920	1.0986	1.4854	0.3477	0.0051
PC13	-0.2317	-0.2690	-0.1995	1.2351	1.0499	1.4204	0.7000	0.0009

Eulemur macaco

PC	Slope	Slope lower CI	Slope higher CI	Intercept	Intercept lower CI	Intercept higher CI	p value	r squared
PC1	0.9926	0.7562	1.3030	-5.3133	-6.7769	-3.8497	0.8818	0.0004
PC2	-0.8514	-1.1045	-0.6563	4.5574	3.3578	5.7571	0.0286	0.0872
PC3	0.7839	0.5975	1.0286	-4.1962	-5.3502	-3.0423	0.6564	0.0038
PC4	0.6746	0.5188	0.8773	-3.6112	-4.5708	-2.6517	0.0511	0.0699
PC5	0.6050	0.4647	0.7878	-3.2385	-4.1034	-2.3737	0.0702	0.0605
PC6	0.5523	0.4221	0.7226	-2.9563	-3.7607	-2.1520	0.2495	0.0249
PC7	0.4498	0.3429	0.5901	-2.4078	-3.0694	-1.7462	0.5975	0.0053
PC8	0.4227	0.3270	0.5464	-2.2628	-2.8499	-1.6757	0.0120	0.1132
PC9	-0.4039	-0.5276	-0.3092	2.1618	1.5772	2.7463	0.1615	0.0366
PC10	-0.3688	-0.4841	-0.2810	1.9743	1.4308	2.5178	0.7630	0.0017
PC11	-0.3092	-0.4047	-0.2362	1.6551	1.2042	2.1060	0.2775	0.0222
PC12	-0.2865	-0.3754	-0.2186	1.5335	1.1138	1.9533	0.4085	0.0129
PC13	0.2635	0.2009	0.3457	-1.4105	-1.7981	-1.0229	0.6034	0.0051

Eulemur mongoz

PC	Slope	Slope lower CI	Slope higher CI	Intercept	Intercept lower CI	Intercept higher CI	p value	r squared
PC1	0.6504	0.5013	0.8439	-3.4364	-4.3413	-2.5315	0.0924	0.0506
PC2	-0.5728	-0.7440	-0.4409	3.0261	2.2253	3.8269	0.1298	0.0412
PC3	-0.4644	-0.6003	-0.3592	2.4534	1.8164	3.0904	0.0367	0.0770
PC4	-0.4358	-0.5605	-0.3388	2.3023	1.7165	2.8881	0.0104	0.1136
PC5	0.3897	0.2992	0.5074	-2.0587	-2.6087	-1.5087	0.2633	0.0227
PC6	0.3495	0.2686	0.4549	-1.8465	-2.3387	-1.3543	0.2206	0.0272
PC7	-0.3011	-0.3932	-0.2305	1.5908	1.1610	2.0206	0.8759	0.0004
PC8	0.2896	0.2227	0.3766	-1.5300	-1.9364	-1.1235	0.1722	0.0336
PC9	-0.2613	-0.3406	-0.2004	1.3804	1.0101	1.7508	0.3730	0.0145
PC10	-0.2440	-0.3183	-0.1871	1.2893	0.9429	1.6358	0.4296	0.0114
PC11	-0.2323	-0.3016	-0.1790	1.2274	0.9034	1.5514	0.1092	0.0460
PC12	0.1983	0.1520	0.2587	-1.0476	-1.3293	-0.7658	0.4739	0.0094
PC13	0.1870	0.1432	0.2442	-0.9881	-1.2549	-0.7213	0.7543	0.0018

Eulemur rubriventer

PC	Slope	Slope lower CI	Slope higher CI	Intercept	Intercept lower CI	Intercept higher CI	p value	r squared
PC1	0.9510	0.6374	1.4189	-5.0569	-7.1350	-2.9789	0.7312	0.0048
PC2	-0.8579	-1.2139	-0.6063	4.5620	2.9463	6.1777	0.0065	0.2607
PC3	-0.6914	-1.0297	-0.4642	3.6764	2.1727	5.1801	0.5565	0.0140
PC4	-0.6107	-0.9065	-0.4114	3.2475	1.9311	4.5639	0.3752	0.0316
PC5	-0.5922	-0.8841	-0.3968	3.1493	1.8536	4.4450	0.8074	0.0024
PC6	0.5641	0.3838	0.8290	-2.9994	-4.1834	-1.8155	0.1483	0.0817
PC7	0.4828	0.3259	0.7152	-2.5674	-3.6025	-1.5323	0.3050	0.0420
PC8	-0.4491	-0.6685	-0.3017	2.3880	1.4128	3.3632	0.5156	0.0171
PC9	0.3958	0.2656	0.5897	-2.1045	-2.9661	-1.2429	0.5846	0.0121
PC10	-0.3759	-0.5613	-0.2517	1.9988	1.1757	2.8219	0.8973	0.0007
PC11	0.3224	0.2189	0.4749	-1.7145	-2.3953	-1.0336	0.1804	0.0706
PC12	-0.3185	-0.4724	-0.2148	1.6937	1.0087	2.3787	0.3430	0.0360
PC13	0.2537	0.1702	0.3781	-1.3490	-1.9019	-0.7961	0.6223	0.0099

Hapalemur griseus

PC	Slope	Slope lower CI	Slope higher CI	Intercept	Intercept lower CI	Intercept higher CI	p value	r squared
PC1	-0.7464	-1.0981	-0.5073	3.7606	2.2721	5.2491	0.1619	0.0767
PC2	0.7081	0.4747	1.0561	-3.5675	-5.0323	-2.1027	0.6882	0.0065
PC3	0.5803	0.3961	0.8501	-2.9236	-4.0674	-1.7799	0.1118	0.0980
PC4	-0.4956	-0.7384	-0.3326	2.4968	1.4743	3.5193	0.5909	0.0117
PC5	0.4508	0.3095	0.6564	-2.2711	-3.1450	-1.3973	0.0674	0.1276
PC6	-0.3897	-0.5619	-0.2702	1.9634	1.2285	2.6983	0.0302	0.1744
PC7	-0.3365	-0.5020	-0.2255	1.6952	0.9985	2.3919	0.7352	0.0047
PC8	-0.3234	-0.4679	-0.2234	1.6292	1.0132	2.2451	0.0404	0.1576
PC9	-0.2828	-0.4223	-0.1893	1.4247	0.8378	2.0116	0.9943	0.0000
PC10	-0.2633	-0.3841	-0.1805	1.3265	0.8136	1.8394	0.0780	0.1190
PC11	0.2196	0.1471	0.3280	-1.1066	-1.5624	-0.6507	0.9726	0.0000
PC12	0.1927	0.1300	0.2856	-0.9707	-1.3630	-0.5785	0.3305	0.0379
PC13	-0.1774	-0.2649	-0.1188	0.8936	0.5256	1.2616	0.9046	0.0006

Lemur catta

PC	Slope	Slope lower CI	Slope higher CI	Intercept	Intercept lower CI	Intercept higher CI	p value	r squared
PC1	0.7085	0.4992	1.0055	-3.7247	-5.0558	-2.3935	0.4884	0.0151
PC2	0.5924	0.4395	0.7985	-3.1145	-4.0582	-2.1709	0.0010	0.2921
PC3	-0.5149	-0.7256	-0.3653	2.7068	1.7599	3.6538	0.1770	0.0562
PC4	0.4356	0.3064	0.6191	-2.2899	-3.1119	-1.4679	0.6535	0.0064
PC5	0.3952	0.2793	0.5593	-2.0779	-2.8139	-1.3418	0.3082	0.0324
PC6	0.3502	0.2462	0.4981	-1.8410	-2.5033	-1.1788	0.7944	0.0022
PC7	0.3023	0.2126	0.4299	-1.5893	-2.1608	-1.0179	0.7594	0.0030
PC8	0.2767	0.1945	0.3936	-1.4546	-1.9779	-0.9313	0.8082	0.0019
PC9	-0.2658	-0.3775	-0.1872	1.3977	0.8973	1.8980	0.5440	0.0116
PC10	-0.2309	-0.3263	-0.1634	1.2140	0.7857	1.6423	0.2555	0.0402
PC11	0.2187	0.1542	0.3102	-1.1498	-1.5601	-0.7396	0.4473	0.0182
PC12	-0.1874	-0.2646	-0.1328	0.9854	0.6388	1.3320	0.2243	0.0458
PC13	-0.1795	-0.2549	-0.1264	0.9439	0.6061	1.2817	0.5315	0.0123

Varecia variegata

PC	Slope	Slope lower CI	Slope higher CI	Intercept	Intercept lower CI	Intercept higher CI	p value	r squared
PC1	0.6687	0.4896	0.9133	-3.6627	-4.8232	-2.5022	0.0558	0.0954
PC2	0.5349	0.3977	0.7194	-2.9299	-3.8110	-2.0489	0.0063	0.1851
PC3	-0.4276	-0.5836	-0.3133	2.3422	1.6018	3.0827	0.0505	0.0995
PC4	-0.3802	-0.5265	-0.2746	2.0825	1.3925	2.7725	0.5286	0.0108
PC5	0.3353	0.2439	0.4608	-1.8364	-2.4304	-1.2425	0.1416	0.0575
PC6	-0.3125	-0.4247	-0.2300	1.7119	1.1784	2.2454	0.0274	0.1248
PC7	0.2573	0.1856	0.3568	-1.4095	-1.8783	-0.9408	0.7233	0.0034
PC8	-0.2554	-0.3536	-0.1845	1.3990	0.9360	1.8621	0.4903	0.0129
PC9	-0.2254	-0.3116	-0.1631	1.2347	0.8278	1.6416	0.3745	0.0214
PC10	-0.1895	-0.2627	-0.1367	1.0381	0.6930	1.3832	0.6953	0.0042
PC11	-0.1779	-0.2465	-0.1284	0.9743	0.6507	1.2978	0.6354	0.0061
PC12	-0.1682	-0.2295	-0.1232	0.9211	0.6299	1.2123	0.0506	0.0994
PC13	0.1649	0.1190	0.2285	-0.9031	-1.2030	-0.6032	0.6293	0.0064

Lepilemur ruficaudatus

PC	Slope	Slope lower CI	Slope higher CI	Intercept	Intercept lower CI	Intercept higher CI	p value	r squared
PC1	0.8156	0.5514	1.2063	-4.0100	-5.6200	-2.3999	0.0723	0.1337
PC2	-0.6493	-0.9651	-0.4369	3.1927	1.8941	4.4912	0.1035	0.1111
PC3	-0.5444	-0.7990	-0.3709	2.6766	1.6243	3.7290	0.0410	0.1693
PC4	-0.4638	-0.7044	-0.3054	2.2806	1.2997	3.2616	0.7148	0.0059
PC5	0.4060	0.2676	0.6159	-1.9962	-2.8526	-1.1397	0.6208	0.0108
PC6	0.3836	0.2556	0.5757	-1.8863	-2.6732	-1.0993	0.2202	0.0646
PC7	-0.3334	-0.4909	-0.2265	1.6395	0.9894	2.2895	0.0513	0.1552
PC8	-0.2829	-0.4290	-0.1865	1.3908	0.7947	1.9869	0.5882	0.0129
PC9	0.2546	0.1675	0.3871	-1.2519	-1.7918	-0.7121	0.8902	0.0008
PC10	0.2344	0.1546	0.3553	-1.1525	-1.6457	-0.6592	0.5494	0.0158
PC11	-0.2047	-0.3111	-0.1347	1.0066	0.5731	1.4401	0.7841	0.0033
PC12	0.1894	0.1275	0.2813	-0.9313	-1.3093	-0.5533	0.0977	0.1147
PC13	0.1828	0.1206	0.2771	-0.8987	-1.2834	-0.5140	0.5562	0.0153

Loris tardigradus

PC	Slope	Slope lower CI	Slope higher CI	Intercept	Intercept lower CI	Intercept higher CI	p value	r squared
PC1	0.4469	0.3042	0.6566	-2.1394	-2.9834	-1.2954	0.1438	0.0835
PC2	0.3208	0.2170	0.4741	-1.5357	-2.1512	-0.9201	0.2446	0.0537
PC3	-0.2431	-0.3617	-0.1634	1.1637	0.6888	1.6387	0.4889	0.0194
PC4	0.1834	0.1269	0.2651	-0.8780	-1.2088	-0.5472	0.0363	0.1638
PC5	0.1724	0.1190	0.2499	-0.8255	-1.1391	-0.5119	0.0460	0.1499
PC6	-0.1550	-0.2270	-0.1058	0.7420	0.4518	1.0322	0.1098	0.0991
PC7	-0.1322	-0.1953	-0.0894	0.6327	0.3791	0.8864	0.2446	0.0537
PC8	0.1232	0.0826	0.1838	-0.5896	-0.8321	-0.3472	0.7306	0.0048
PC9	-0.1175	-0.1704	-0.0811	0.5626	0.3488	0.7765	0.0468	0.1490
PC10	0.1093	0.0732	0.1633	-0.5234	-0.7390	-0.3077	0.9249	0.0004
PC11	-0.1015	-0.1482	-0.0695	0.4859	0.2974	0.6744	0.0858	0.1135
PC12	0.0901	0.0608	0.1337	-0.4315	-0.6062	-0.2569	0.3479	0.0353
PC13	0.0761	0.0511	0.1134	-0.3643	-0.5136	-0.2150	0.5977	0.0113

Nycticebus bengalensis

PC	Slope	Slope lower CI	Slope higher CI	Intercept	Intercept lower CI	Intercept higher CI	p value	r squared
PC1	0.7855	0.5117	1.2059	-3.9892	-5.7520	-2.2264	0.1462	0.1026
PC2	0.6757	0.4343	1.0513	-3.4315	-4.9982	-1.8649	0.3600	0.0420
PC3	-0.6332	-0.9822	-0.4082	3.2156	1.7579	4.6733	0.2910	0.0556
PC4	-0.5726	-0.8336	-0.3933	2.9079	1.7897	4.0260	0.0060	0.3204
PC5	-0.4780	-0.7317	-0.3123	2.4277	1.3628	3.4926	0.1215	0.1156
PC6	0.4180	0.2699	0.6473	-2.1228	-3.0811	-1.1644	0.2590	0.0632
PC7	-0.3898	-0.6116	-0.2484	1.9796	1.0574	2.9018	0.8234	0.0025
PC8	0.3501	0.2236	0.5483	-1.7780	-2.6027	-0.9534	0.6365	0.0114
PC9	-0.2946	-0.4619	-0.1879	1.4962	0.8004	2.1919	0.7302	0.0061
PC10	-0.2697	-0.4231	-0.1719	1.3696	0.7319	2.0074	0.7905	0.0036
PC11	-0.2494	-0.3890	-0.1599	1.2664	0.6846	1.8483	0.4425	0.0298
PC12	0.2285	0.1455	0.3586	-1.1602	-1.7013	-0.6190	0.9743	0.0001
PC13	0.1996	0.1311	0.3039	-1.0135	-1.4523	-0.5747	0.0881	0.1385

Nycticebus coucang

PC	Slope	Slope lower CI	Slope higher CI	Intercept	Intercept lower CI	Intercept higher CI	p value	r squared
PC1	-0.5711	-0.7271	-0.4486	2.8456	2.1517	3.5396	0.9780	0.0000
PC2	-0.4731	-0.5980	-0.3743	2.3573	1.7999	2.9146	0.0425	0.0600
PC3	-0.4202	-0.5315	-0.3321	2.0934	1.5966	2.5903	0.0575	0.0528
PC4	-0.3692	-0.4678	-0.2913	1.8394	1.3996	2.2792	0.1051	0.0387
PC5	0.3389	0.2686	0.4277	-1.6887	-2.0850	-1.2924	0.0238	0.0740
PC6	0.3312	0.2606	0.4209	-1.6502	-2.0496	-1.2508	0.3148	0.0151
PC7	0.2853	0.2243	0.3630	-1.4216	-1.7672	-1.0761	0.5088	0.0065
PC8	0.2755	0.2172	0.3494	-1.3726	-1.7018	-1.0434	0.1364	0.0328
PC9	-0.2665	-0.3387	-0.2097	1.3279	1.0066	1.6491	0.3001	0.0160
PC10	0.2461	0.1953	0.3101	-1.2261	-1.5120	-0.9402	0.0145	0.0860
PC11	0.2280	0.1791	0.2902	-1.1360	-1.4125	-0.8594	0.6361	0.0034
PC12	0.2073	0.1629	0.2639	-1.0331	-1.2848	-0.7814	0.7085	0.0021
PC13	-0.2006	-0.2550	-0.1578	0.9994	0.7572	1.2416	0.3601	0.0125

Perodicticus potto

PC	Slope	Slope lower CI	Slope higher CI	Intercept	Intercept lower CI	Intercept higher CI	p value	r squared
PC1	0.5996	0.5036	0.7139	-3.0281	-3.5590	-2.4972	0.5311	0.0031
PC2	-0.5598	-0.6651	-0.4711	2.8270	2.3372	3.3168	0.0646	0.0266
PC3	-0.4922	-0.5830	-0.4155	2.4856	2.0627	2.9084	0.0046	0.0614
PC4	-0.4666	-0.5554	-0.3920	2.3565	1.9439	2.7690	0.3855	0.0059
PC5	-0.4193	-0.4993	-0.3521	2.1175	1.7460	2.4891	0.6474	0.0017
PC6	0.3699	0.3106	0.4406	-1.8683	-2.1964	-1.5402	0.9550	0.0000
PC7	-0.3530	-0.4200	-0.2967	1.7827	1.4712	2.0943	0.2701	0.0096
PC8	-0.3238	-0.3856	-0.2719	1.6352	1.3481	1.9224	0.8426	0.0003
PC9	0.3095	0.2600	0.3684	-1.5632	-1.8370	-1.2895	0.3987	0.0056
PC10	0.2969	0.2493	0.3536	-1.4995	-1.7628	-1.2363	0.7892	0.0006
PC11	0.2677	0.2263	0.3168	-1.3521	-1.5806	-1.1237	0.0018	0.0745
PC12	-0.2552	-0.3037	-0.2144	1.2888	1.0634	1.5143	0.3204	0.0078
PC13	0.2342	0.1967	0.2788	-1.1826	-1.3902	-0.9751	0.6756	0.0014

Goswami model face module against ln CS of face

Cheirogaleus major

PC	Slope	Slope lower CI	Slope higher CI	Intercept	Intercept lower CI	Intercept higher CI	p value	r squared
PC1	0.6944	0.4571	1.0548	-2.2579	-3.2300	-1.2858	0.7580	0.0042
PC2	0.5992	0.3965	0.9054	-1.9485	-2.7761	-1.1209	0.4019	0.0307
PC3	-0.4706	-0.7119	-0.3110	1.5303	0.8783	2.1822	0.4511	0.0249
PC4	0.4030	0.2685	0.6049	-1.3105	-1.8575	-0.7634	0.2238	0.0636
PC5	-0.3803	-0.5666	-0.2553	1.2368	0.7306	1.7431	0.1240	0.0998
PC6	-0.3416	-0.5156	-0.2264	1.1110	0.6408	1.5812	0.3534	0.0375
PC7	0.3249	0.2140	0.4934	-1.0567	-1.5110	-0.6024	0.6891	0.0071
PC8	-0.3010	-0.4403	-0.2058	0.9789	0.5977	1.3601	0.0318	0.1851
PC9	-0.2688	-0.4074	-0.1773	0.8740	0.4999	1.2482	0.5544	0.0154
PC10	-0.2353	-0.3576	-0.1548	0.7651	0.4352	1.0949	0.8694	0.0012
PC11	0.2245	0.1477	0.3413	-0.7302	-1.0450	-0.4154	0.8542	0.0015
PC12	-0.1774	-0.2696	-0.1167	0.5768	0.3281	0.8254	0.8703	0.0012
PC13	0.1606	0.1077	0.2396	-0.5223	-0.7368	-0.3078	0.1368	0.0936

Cheirogaleus medius

PC	Slope	Slope lower CI	Slope higher CI	Intercept	Intercept lower CI	Intercept higher CI	p value	r squared
PC1	0.4951	0.3404	0.7201	-1.4586	-2.0181	-0.8991	0.2125	0.0570
PC2	-0.4567	-0.6712	-0.3108	1.3456	0.8145	1.8767	0.8332	0.0017
PC3	0.4150	0.2836	0.6071	-1.2225	-1.6991	-0.7460	0.4030	0.0260
PC4	0.3952	0.2847	0.5486	-1.1644	-1.5532	-0.7756	0.0029	0.2851
PC5	-0.3314	-0.4869	-0.2256	0.9763	0.5912	1.3614	0.7846	0.0028
PC6	-0.3156	-0.4638	-0.2148	0.9299	0.5629	1.2969	0.8294	0.0018
PC7	0.2746	0.1877	0.4016	-0.8089	-1.1242	-0.4937	0.3982	0.0266
PC8	0.2515	0.1711	0.3695	-0.7408	-1.0331	-0.4485	0.8178	0.0020
PC9	0.2239	0.1527	0.3283	-0.6596	-0.9183	-0.4008	0.5496	0.0134
PC10	-0.2078	-0.2907	-0.1485	0.6121	0.4027	0.8216	0.0058	0.2495
PC11	0.1934	0.1329	0.2814	-0.5698	-0.7886	-0.3510	0.2211	0.0549
PC12	-0.1830	-0.2659	-0.1260	0.5393	0.3331	0.7455	0.1886	0.0631
PC13	-0.1470	-0.2152	-0.1004	0.4329	0.2638	0.6021	0.4440	0.0219

Microcebus murinus

PC	Slope	Slope lower CI	Slope higher CI	Intercept	Intercept lower CI	Intercept higher CI	p value	r squared
PC1	0.6790	0.5362	0.8599	-1.7933	-2.2209	-1.3657	0.9004	0.0002
PC2	-0.5823	-0.7373	-0.4600	1.5380	1.1717	1.9043	0.6761	0.0025
PC3	-0.5181	-0.6517	-0.4118	1.3683	1.0514	1.6851	0.0439	0.0567
PC4	-0.4361	-0.5496	-0.3461	1.1518	0.8830	1.4207	0.0843	0.0420
PC5	0.3955	0.3128	0.5000	-1.0445	-1.2918	-0.7971	0.3328	0.0134
PC6	0.3852	0.3055	0.4857	-1.0174	-1.2553	-0.7794	0.1012	0.0379
PC7	0.3355	0.2650	0.4248	-0.8860	-1.0971	-0.6749	0.7279	0.0017
PC8	0.3315	0.2617	0.4198	-0.8754	-1.0841	-0.6667	0.9254	0.0001
PC9	0.3132	0.2484	0.3948	-0.8271	-1.0205	-0.6338	0.0973	0.0388
PC10	-0.2799	-0.3544	-0.2210	0.7392	0.5630	0.9154	0.8850	0.0003
PC11	0.2702	0.2135	0.3420	-0.7136	-0.8833	-0.5438	0.5624	0.0048
PC12	0.2505	0.1990	0.3153	-0.6615	-0.8152	-0.5078	0.0573	0.0507
PC13	-0.2416	-0.3058	-0.1908	0.6380	0.4860	0.7899	0.6783	0.0025

Microcebus rufus

PC	Slope	Slope lower CI	Slope higher CI	Intercept	Intercept lower CI	Intercept higher CI	p value	r squared
PC1	0.3789	0.2638	0.5443	-1.0383	-1.4228	-0.6538	0.0642	0.1212
PC2	0.3692	0.2696	0.5056	-1.0117	-1.3351	-0.6882	0.0008	0.3450
PC3	-0.3433	-0.4987	-0.2363	0.9406	0.5808	1.3004	0.1897	0.0628
PC4	-0.3342	-0.4902	-0.2279	0.9158	0.5563	1.2754	0.5578	0.0129
PC5	0.2990	0.2040	0.4384	-0.8194	-1.1407	-0.4980	0.5318	0.0146
PC6	0.2485	0.1693	0.3649	-0.6810	-0.9493	-0.4127	0.6903	0.0060
PC7	0.2404	0.1640	0.3525	-0.6587	-0.9171	-0.4004	0.5334	0.0145
PC8	0.2321	0.1581	0.3406	-0.6359	-0.8861	-0.3857	0.6356	0.0084
PC9	0.1832	0.1257	0.2670	-0.5021	-0.6958	-0.3084	0.2614	0.0465
PC10	-0.1697	-0.2481	-0.1161	0.4650	0.2840	0.6460	0.3725	0.0296
PC11	0.1574	0.1071	0.2312	-0.4312	-0.6014	-0.2610	0.7984	0.0025
PC12	-0.1361	-0.1995	-0.0929	0.3730	0.2270	0.5191	0.4902	0.0178
PC13	-0.1259	-0.1837	-0.0863	0.3450	0.2115	0.4785	0.2933	0.0408

Galago alleni

PC	Slope	Slope lower CI	Slope higher CI	Intercept	Intercept lower CI	Intercept higher CI	p value	r squared
PC1	0.5163	0.3553	0.7501	-1.6091	-2.2244	-0.9937	0.0124	0.2522
PC2	-0.4304	-0.6301	-0.2940	1.3415	0.8176	1.8654	0.0207	0.2202
PC3	-0.3946	-0.6054	-0.2572	1.2297	0.6869	1.7725	0.7683	0.0040
PC4	-0.3635	-0.5580	-0.2368	1.1328	0.6321	1.6336	0.8731	0.0012
PC5	-0.3356	-0.5131	-0.2195	1.0459	0.5881	1.5037	0.5026	0.0207
PC6	0.2925	0.1919	0.4457	-0.9116	-1.3073	-0.5160	0.3672	0.0371
PC7	-0.2747	-0.4195	-0.1799	0.8563	0.4828	1.2298	0.4391	0.0274
PC8	-0.2294	-0.3449	-0.1525	0.7149	0.4150	1.0148	0.1311	0.1006
PC9	-0.2232	-0.3425	-0.1454	0.6955	0.3882	1.0028	0.8306	0.0021
PC10	0.2043	0.1331	0.3135	-0.6367	-0.9180	-0.3555	0.8087	0.0027
PC11	-0.1963	-0.3014	-0.1279	0.6120	0.3415	0.8824	0.8529	0.0016
PC12	-0.1493	-0.2278	-0.0978	0.4653	0.2628	0.6678	0.4058	0.0316
PC13	-0.1329	-0.2034	-0.0868	0.4142	0.2325	0.5959	0.5525	0.0163

Galago demidoff

PC	Slope	Slope lower CI	Slope higher CI	Intercept	Intercept lower CI	Intercept higher CI	p value	r squared
PC1	-0.6269	-0.7816	-0.5028	1.7588	1.3676	2.1501	0.0000	0.2969
PC2	-0.5165	-0.6696	-0.3984	1.4491	1.0685	1.8296	0.2806	0.0204
PC3	-0.4627	-0.6008	-0.3562	1.2981	0.9548	1.6413	0.5407	0.0066
PC4	-0.3948	-0.5099	-0.3057	1.1076	0.8210	1.3941	0.0916	0.0491
PC5	0.3764	0.2896	0.4891	-1.0559	-1.3358	-0.7760	0.7407	0.0019
PC6	0.3457	0.2660	0.4494	-0.9701	-1.2274	-0.7127	0.8652	0.0005
PC7	-0.2908	-0.3739	-0.2262	0.8159	0.6088	1.0231	0.0259	0.0840
PC8	0.2828	0.2187	0.3656	-0.7934	-0.9996	-0.5873	0.1235	0.0411
PC9	0.2639	0.2036	0.3421	-0.7405	-0.9348	-0.5462	0.2636	0.0219
PC10	0.2512	0.1934	0.3262	-0.7048	-0.8911	-0.5184	0.5249	0.0071
PC11	-0.2394	-0.3106	-0.1845	0.6716	0.4945	0.8486	0.3894	0.0130
PC12	0.2150	0.1654	0.2794	-0.6032	-0.7633	-0.4432	0.9618	0.0000
PC13	0.2093	0.1621	0.2702	-0.5872	-0.7390	-0.4355	0.0841	0.0514

Galago elegantulus

PC	Slope	Slope lower CI	Slope higher CI	Intercept	Intercept lower CI	Intercept higher CI	p value	r squared
PC1	-0.7134	-0.9818	-0.5184	2.1775	1.4703	2.8848	0.0107	0.1867
PC2	0.6152	0.4329	0.8742	-1.8777	-2.5513	-1.2042	0.6161	0.0079
PC3	-0.5591	-0.7929	-0.3943	1.7067	1.0983	2.3151	0.4225	0.0202
PC4	0.5289	0.3742	0.7475	-1.6143	-2.1842	-1.0445	0.2606	0.0394
PC5	-0.4485	-0.6374	-0.3156	1.3689	0.8777	1.8602	0.6364	0.0071
PC6	-0.4247	-0.6021	-0.2996	1.2963	0.8347	1.7580	0.4003	0.0222
PC7	-0.3734	-0.5239	-0.2662	1.1399	0.7466	1.5331	0.1000	0.0823
PC8	-0.3270	-0.4645	-0.2301	0.9980	0.6403	1.3556	0.5819	0.0096
PC9	-0.2961	-0.4213	-0.2081	0.9037	0.5783	1.2291	0.9159	0.0004
PC10	0.2542	0.1791	0.3607	-0.7759	-1.0531	-0.4986	0.4813	0.0156
PC11	0.2258	0.1588	0.3209	-0.6891	-0.9366	-0.4415	0.6859	0.0052
PC12	-0.2197	-0.3096	-0.1559	0.6705	0.4358	0.9052	0.1802	0.0554
PC13	-0.2068	-0.2942	-0.1453	0.6311	0.4039	0.8583	0.8879	0.0006

Galago moholi

PC	Slope	Slope lower CI	Slope higher CI	Intercept	Intercept lower CI	Intercept higher CI	p value	r squared
PC1	-0.6102	-0.7689	-0.4842	1.7332	1.3288	2.1377	0.1566	0.0281
PC2	0.5179	0.4097	0.6548	-1.4712	-1.8194	-1.1230	0.8764	0.0003
PC3	-0.5022	-0.6349	-0.3972	1.4265	1.0889	1.7642	0.9070	0.0002
PC4	-0.4747	-0.5995	-0.3759	1.3485	1.0307	1.6662	0.4269	0.0089
PC5	0.4242	0.3363	0.5351	-1.2050	-1.4873	-0.9227	0.2287	0.0203
PC6	-0.4003	-0.5029	-0.3186	1.1372	0.8754	1.3990	0.0481	0.0539
PC7	-0.3749	-0.4724	-0.2976	1.0651	0.8168	1.3133	0.1426	0.0300
PC8	-0.3541	-0.4469	-0.2806	1.0059	0.7696	1.2421	0.2953	0.0154
PC9	0.3204	0.2541	0.4040	-0.9102	-1.1231	-0.6973	0.1977	0.0233
PC10	0.3160	0.2500	0.3995	-0.8977	-1.1101	-0.6853	0.7878	0.0010
PC11	0.2894	0.2299	0.3643	-0.8221	-1.0129	-0.6313	0.0966	0.0384
PC12	-0.2693	-0.3381	-0.2146	0.7651	0.5897	0.9405	0.0342	0.0616
PC13	0.2427	0.1933	0.3046	-0.6893	-0.8474	-0.5312	0.0356	0.0607

Galago senegalensis

PC	Slope	Slope lower CI	Slope higher CI	Intercept	Intercept lower CI	Intercept higher CI	p value	r squared
PC1	-0.6124	-0.7111	-0.5274	1.7969	1.5274	2.0663	0.5768	0.0018
PC2	0.5508	0.4751	0.6387	-1.6162	-1.8563	-1.3761	0.0599	0.0203
PC3	-0.5283	-0.6109	-0.4568	1.5500	1.3239	1.7762	0.0018	0.0549
PC4	0.4643	0.4003	0.5384	-1.3622	-1.5648	-1.1596	0.0756	0.0181
PC5	0.4279	0.3708	0.4937	-1.2554	-1.4356	-1.0752	0.0001	0.0851
PC6	-0.4000	-0.4644	-0.3444	1.1735	0.9974	1.3496	0.8880	0.0001
PC7	-0.3793	-0.4385	-0.3282	1.1130	0.9512	1.2748	0.0009	0.0618
PC8	0.3532	0.3047	0.4093	-1.0362	-1.1896	-0.8828	0.0307	0.0267
PC9	0.3421	0.2949	0.3969	-1.0038	-1.1535	-0.8541	0.1367	0.0128
PC10	-0.3134	-0.3637	-0.2701	0.9196	0.7824	1.0569	0.1671	0.0110
PC11	0.3095	0.2665	0.3593	-0.9080	-1.0442	-0.7719	0.5296	0.0023
PC12	-0.2787	-0.3236	-0.2400	0.8178	0.6951	0.9404	0.5684	0.0019
PC13	0.2751	0.2370	0.3193	-0.8072	-0.9280	-0.6865	0.2697	0.0070

Galago zanzibaricus

PC	Slope	Slope lower CI	Slope higher CI	Intercept	Intercept lower CI	Intercept higher CI	p value	r squared
PC1	-0.8059	-1.2145	-0.5348	2.3650	1.3677	3.3623	0.3118	0.0444
PC2	-0.6804	-1.0341	-0.4477	1.9966	1.1361	2.8572	0.8355	0.0019
PC3	0.6373	0.4203	0.9664	-1.8702	-2.6715	-1.0690	0.5768	0.0137
PC4	0.5748	0.3816	0.8658	-1.6867	-2.3973	-0.9762	0.3009	0.0464
PC5	-0.5704	-0.8192	-0.3972	1.6738	1.0546	2.2931	0.0085	0.2645
PC6	-0.4482	-0.6716	-0.2991	1.3151	0.7685	1.8617	0.1958	0.0717
PC7	-0.4134	-0.6273	-0.2724	1.2131	0.6923	1.7338	0.6378	0.0098
PC8	-0.3719	-0.5655	-0.2446	1.0914	0.6206	1.5622	0.9652	0.0001
PC9	0.3037	0.2018	0.4571	-0.8912	-1.2658	-0.5166	0.2796	0.0506
PC10	0.2908	0.1935	0.4369	-0.8533	-1.2105	-0.4962	0.2435	0.0586
PC11	-0.2701	-0.4059	-0.1797	0.7926	0.4607	1.1244	0.2460	0.0580
PC12	0.2505	0.1648	0.3809	-0.7352	-1.0523	-0.4181	0.9220	0.0004
PC13	0.2099	0.1399	0.3149	-0.6159	-0.8727	-0.3592	0.2149	0.0660

Otolemur crassicaudatus

PC	Slope	Slope lower CI	Slope higher CI	Intercept	Intercept lower CI	Intercept higher CI	p value	r squared
PC1	-0.3880	-0.4725	-0.3186	1.3531	1.0848	1.6214	0.2738	0.0121
PC2	-0.3348	-0.4081	-0.2746	1.1675	0.9346	1.4003	0.9231	0.0001
PC3	0.2979	0.2457	0.3613	-1.0389	-1.2405	-0.8373	0.0197	0.0537
PC4	0.2778	0.2304	0.3351	-0.9689	-1.1515	-0.7863	0.0008	0.1072
PC5	-0.2508	-0.3048	-0.2064	0.8747	0.7030	1.0463	0.0729	0.0321
PC6	-0.2249	-0.2735	-0.1849	0.7841	0.6295	0.9387	0.1288	0.0232
PC7	0.2026	0.1672	0.2454	-0.7064	-0.8429	-0.5700	0.0116	0.0626
PC8	0.1925	0.1582	0.2343	-0.6713	-0.8040	-0.5386	0.1812	0.0180
PC9	0.1762	0.1448	0.2144	-0.6145	-0.7359	-0.4931	0.1708	0.0189
PC10	-0.1717	-0.2088	-0.1412	0.5988	0.4807	0.7168	0.1252	0.0236
PC11	0.1651	0.1359	0.2007	-0.5758	-0.6889	-0.4628	0.0748	0.0317
PC12	-0.1541	-0.1876	-0.1265	0.5372	0.4306	0.6439	0.3264	0.0097
PC13	0.1401	0.1151	0.1706	-0.4886	-0.5855	-0.3917	0.2890	0.0114

Otolemur garnettii

PC	Slope	Slope lower CI	Slope higher CI	Intercept	Intercept lower CI	Intercept higher CI	p value	r squared
PC1	-0.3511	-0.4262	-0.2893	1.1959	0.9627	1.4292	0.0015	0.1035
PC2	-0.3336	-0.4093	-0.2719	1.1364	0.9023	1.3704	0.8828	0.0002
PC3	-0.2883	-0.3489	-0.2382	0.9819	0.7934	1.1705	0.0003	0.1310
PC4	-0.2677	-0.3274	-0.2189	0.9118	0.7268	1.0967	0.0923	0.0302
PC5	-0.2281	-0.2781	-0.1871	0.7768	0.6217	0.9319	0.0163	0.0605
PC6	0.2179	0.1787	0.2658	-0.7423	-0.8906	-0.5940	0.0173	0.0595
PC7	0.2003	0.1636	0.2452	-0.6821	-0.8213	-0.5430	0.1775	0.0195
PC8	-0.1960	-0.2399	-0.1601	0.6675	0.5315	0.8036	0.1605	0.0211
PC9	-0.1655	-0.2030	-0.1350	0.5638	0.4479	0.6797	0.5615	0.0036
PC10	-0.1562	-0.1909	-0.1278	0.5321	0.4246	0.6396	0.0600	0.0375
PC11	-0.1497	-0.1826	-0.1227	0.5099	0.4079	0.6119	0.0199	0.0569
PC12	-0.1433	-0.1758	-0.1168	0.4880	0.3875	0.5885	0.9997	0.0000
PC13	-0.1324	-0.1625	-0.1080	0.4511	0.3582	0.5439	0.7355	0.0012

Avahi laniger

PC	Slope	Slope lower CI	Slope higher CI	Intercept	Intercept lower CI	Intercept higher CI	p value	r squared
PC1	0.8643	0.5569	1.3413	-2.7098	-3.9398	-1.4799	0.9690	0.0001
PC2	-0.7856	-1.2097	-0.5103	2.4633	1.3667	3.5599	0.3734	0.0379
PC3	0.7464	0.4813	1.1575	-2.3401	-3.4003	-1.2799	0.7866	0.0036
PC4	0.5827	0.3769	0.9009	-1.8269	-2.6485	-1.0054	0.5369	0.0184
PC5	0.5567	0.3654	0.8482	-1.7454	-2.5026	-0.9883	0.1729	0.0866
PC6	-0.4953	-0.7510	-0.3267	1.5531	0.8879	2.2183	0.1231	0.1094
PC7	-0.4513	-0.7004	-0.2908	1.4150	0.7728	2.0572	0.9701	0.0001
PC8	-0.3759	-0.5828	-0.2425	1.1786	0.6449	1.7123	0.7557	0.0047
PC9	0.3584	0.2310	0.5563	-1.1239	-1.6339	-0.6138	0.9420	0.0003
PC10	-0.3443	-0.5230	-0.2266	1.0794	0.6147	1.5442	0.1414	0.1001
PC11	0.3100	0.2001	0.4801	-0.9719	-1.4109	-0.5328	0.6621	0.0093
PC12	-0.2799	-0.4238	-0.1849	0.8777	0.5032	1.2522	0.1115	0.1161
PC13	0.2338	0.1507	0.3628	-0.7331	-1.0658	-0.4004	0.9232	0.0005

Indri indri

PC	Slope	Slope lower CI	Slope higher CI	Intercept	Intercept lower CI	Intercept higher CI	p value	r squared
PC1	0.9984	0.7214	1.3816	-3.7936	-5.0481	-2.5391	0.4597	0.0149
PC2	0.8082	0.5993	1.0900	-3.0710	-4.0033	-2.1387	0.0092	0.1696
PC3	-0.6128	-0.8275	-0.4538	2.3284	1.6184	3.0384	0.0110	0.1623
PC4	0.4731	0.3411	0.6562	-1.7977	-2.3965	-1.1990	0.8801	0.0006
PC5	-0.3732	-0.5151	-0.2704	1.4180	0.9529	1.8830	0.2840	0.0309
PC6	0.3656	0.2679	0.4989	-1.3890	-1.8281	-0.9500	0.0500	0.0999
PC7	0.3216	0.2330	0.4439	-1.2220	-1.6226	-0.8214	0.2774	0.0318
PC8	-0.3052	-0.4227	-0.2204	1.1596	0.7752	1.5441	0.5490	0.0098
PC9	0.2758	0.2028	0.3751	-1.0479	-1.3753	-0.7205	0.0304	0.1205
PC10	-0.2512	-0.3479	-0.1813	0.9544	0.6379	1.2709	0.5586	0.0093
PC11	-0.2403	-0.3313	-0.1743	0.9129	0.6146	1.2113	0.2365	0.0377
PC12	-0.2173	-0.3014	-0.1567	0.8257	0.5507	1.1007	0.8603	0.0008
PC13	0.1884	0.1359	0.2611	-0.7158	-0.9536	-0.4781	0.6343	0.0062

Propithecus diadema

PC	Slope	Slope lower CI	Slope higher CI	Intercept	Intercept lower CI	Intercept higher CI	p value	r squared
PC1	1.2000	0.8121	1.7730	-4.3837	-6.1390	-2.6284	0.5539	0.0136
PC2	-0.9188	-1.3601	-0.6207	3.3565	2.0057	4.7074	0.7609	0.0036
PC3	-0.6658	-0.9640	-0.4599	2.4325	1.5116	3.3534	0.0732	0.1183
PC4	0.6182	0.4273	0.8945	-2.2585	-3.1120	-1.4050	0.0693	0.1213
PC5	0.4783	0.3231	0.7081	-1.7474	-2.4507	-1.0440	0.7759	0.0032
PC6	0.4446	0.3002	0.6586	-1.6243	-2.2791	-0.9696	0.9098	0.0005
PC7	-0.3892	-0.5730	-0.2643	1.4217	0.8578	1.9856	0.3616	0.0321
PC8	-0.3703	-0.5454	-0.2514	1.3527	0.8155	1.8898	0.3786	0.0299
PC9	-0.3460	-0.5126	-0.2336	1.2642	0.7545	1.7738	0.9608	0.0001
PC10	0.3081	0.2099	0.4522	-1.1255	-1.5681	-0.6829	0.2600	0.0485
PC11	-0.2678	-0.3964	-0.1809	0.9782	0.5845	1.3719	0.7649	0.0035
PC12	0.2449	0.1654	0.3628	-0.8948	-1.2556	-0.5341	0.9628	0.0001
PC13	-0.2043	-0.2990	-0.1396	0.7465	0.4554	1.0375	0.1925	0.0644

Propithecus verreauxi

PC	Slope	Slope lower CI	Slope higher CI	Intercept	Intercept lower CI	Intercept higher CI	p value	r squared
PC1	-0.6160	-0.8026	-0.4728	2.2577	1.6531	2.8623	0.0003	0.2795
PC2	-0.5030	-0.6636	-0.3813	1.8437	1.3263	2.3610	0.0021	0.2088
PC3	0.4104	0.3014	0.5586	-1.5040	-1.9755	-1.0326	0.4696	0.0128
PC4	-0.3518	-0.4764	-0.2598	1.2895	0.8923	1.6866	0.1629	0.0469
PC5	0.3365	0.2475	0.4576	-1.2335	-1.6186	-0.8484	0.3569	0.0207
PC6	0.3022	0.2218	0.4118	-1.1076	-1.4561	-0.7592	0.6303	0.0057
PC7	0.2946	0.2167	0.4004	-1.0797	-1.4164	-0.7430	0.3296	0.0232
PC8	0.2668	0.1967	0.3618	-0.9778	-1.2803	-0.6753	0.2081	0.0384
PC9	-0.2282	-0.3105	-0.1677	0.8364	0.5748	1.0981	0.4086	0.0167
PC10	-0.2111	-0.2880	-0.1548	0.7738	0.5297	1.0180	0.9219	0.0002
PC11	0.1745	0.1282	0.2374	-0.6396	-0.8397	-0.4394	0.4135	0.0164
PC12	-0.1530	-0.2059	-0.1136	0.5607	0.3915	0.7299	0.0576	0.0852
PC13	-0.1397	-0.1906	-0.1024	0.5121	0.3505	0.6736	0.9612	0.0001

Eulemur fulvus

PC	Slope	Slope lower CI	Slope higher CI	Intercept	Intercept lower CI	Intercept higher CI	p value	r squared
PC1	-0.5426	-0.6300	-0.4674	2.0228	1.7196	2.3261	0.5318	0.0023
PC2	-0.4752	-0.5516	-0.4094	1.7715	1.5063	2.0368	0.3604	0.0048
PC3	0.4255	0.3667	0.4936	-1.5861	-1.8226	-1.3495	0.1439	0.0123
PC4	-0.3826	-0.4440	-0.3297	1.4263	1.2132	1.6394	0.2122	0.0090
PC5	0.3506	0.3027	0.4060	-1.3069	-1.4994	-1.1143	0.0120	0.0359
PC6	0.3241	0.2796	0.3757	-1.2083	-1.3874	-1.0292	0.0376	0.0248
PC7	-0.2873	-0.3333	-0.2477	1.0710	0.9114	1.2307	0.1235	0.0137
PC8	-0.2618	-0.3035	-0.2259	0.9761	0.8313	1.1209	0.0448	0.0231
PC9	0.2207	0.1900	0.2563	-0.8227	-0.9462	-0.6992	0.9629	0.0000
PC10	-0.2129	-0.2472	-0.1833	0.7937	0.6745	0.9128	0.8824	0.0001
PC11	0.2026	0.1746	0.2352	-0.7554	-0.8683	-0.6425	0.2458	0.0078
PC12	-0.1827	-0.2118	-0.1575	0.6809	0.5798	0.7820	0.0540	0.0213
PC13	-0.1746	-0.2028	-0.1504	0.6509	0.5532	0.7486	0.8024	0.0004

Eulemur macaco

PC	Slope	Slope lower CI	Slope higher CI	Intercept	Intercept lower CI	Intercept higher CI	p value	r squared
PC1	-0.6692	-0.8732	-0.5129	2.5008	1.8274	3.1742	0.1199	0.0450
PC2	-0.5740	-0.7266	-0.4535	2.1451	1.6347	2.6554	0.0001	0.2544
PC3	-0.5285	-0.6933	-0.4029	1.9751	1.4324	2.5177	0.5829	0.0057
PC4	0.4548	0.3507	0.5899	-1.6997	-2.1467	-1.2527	0.0268	0.0891
PC5	0.4079	0.3129	0.5317	-1.5243	-1.9332	-1.1154	0.0937	0.0521
PC6	0.3724	0.2843	0.4877	-1.3915	-1.7716	-1.0113	0.3424	0.0170
PC7	0.3033	0.2310	0.3981	-1.1333	-1.4454	-0.8212	0.8173	0.0010
PC8	0.2850	0.2223	0.3654	-1.0650	-1.3324	-0.7976	0.0018	0.1698
PC9	-0.2723	-0.3574	-0.2074	1.0175	0.7373	1.2977	0.8037	0.0012
PC10	0.2487	0.1895	0.3262	-0.9293	-1.1847	-0.6738	0.6242	0.0046
PC11	-0.2085	-0.2734	-0.1590	0.7790	0.5652	0.9928	0.5183	0.0079
PC12	-0.1932	-0.2530	-0.1475	0.7218	0.5246	0.9190	0.3421	0.0170
PC13	0.1777	0.1354	0.2331	-0.6639	-0.8464	-0.4813	0.6472	0.0040

Eulemur mongoz

PC	Slope	Slope lower CI	Slope higher CI	Intercept	Intercept lower CI	Intercept higher CI	p value	r squared
PC1	0.3850	0.2984	0.4967	-1.4049	-1.7669	-1.0428	0.0223	0.0913
PC2	-0.3390	-0.4370	-0.2630	1.2371	0.9194	1.5549	0.0181	0.0974
PC3	-0.2749	-0.3567	-0.2118	1.0030	0.7385	1.2675	0.1002	0.0484
PC4	-0.2579	-0.3314	-0.2007	0.9412	0.7026	1.1799	0.0081	0.1207
PC5	0.2306	0.1776	0.2995	-0.8417	-1.0641	-0.6192	0.1164	0.0442
PC6	0.2069	0.1584	0.2702	-0.7549	-0.9590	-0.5508	0.9175	0.0002
PC7	0.1782	0.1366	0.2326	-0.6503	-0.8257	-0.4750	0.5715	0.0059
PC8	0.1714	0.1320	0.2226	-0.6255	-0.7908	-0.4602	0.1163	0.0442
PC9	-0.1546	-0.2009	-0.1190	0.5643	0.4149	0.7138	0.1332	0.0405
PC10	-0.1444	-0.1881	-0.1109	0.5271	0.3863	0.6679	0.2483	0.0242
PC11	-0.1375	-0.1784	-0.1060	0.5018	0.3697	0.6339	0.0896	0.0515
PC12	0.1174	0.0899	0.1532	-0.4283	-0.5439	-0.3126	0.7322	0.0021
PC13	-0.1107	-0.1445	-0.0848	0.4040	0.2949	0.5130	0.6691	0.0033

Eulemur rubriventer

PC	Slope	Slope lower CI	Slope higher CI	Intercept	Intercept lower CI	Intercept higher CI	p value	r squared
PC1	0.8600	0.5790	1.2773	-3.1572	-4.4390	-1.8754	0.3986	0.0287
PC2	-0.7758	-1.1369	-0.5294	2.8482	1.7330	3.9633	0.1146	0.0966
PC3	-0.6252	-0.9332	-0.4189	2.2953	1.3510	3.2395	0.7987	0.0026
PC4	-0.5523	-0.8229	-0.3706	2.0275	1.1973	2.8577	0.5885	0.0119
PC5	-0.5356	-0.7950	-0.3608	1.9662	1.1692	2.7632	0.3746	0.0317
PC6	0.5101	0.3528	0.7376	-1.8726	-2.5790	-1.1662	0.0378	0.1614
PC7	0.4366	0.2936	0.6493	-1.6029	-2.2558	-0.9500	0.4572	0.0223
PC8	-0.4061	-0.6046	-0.2728	1.4909	0.8817	2.1001	0.5294	0.0160
PC9	0.3579	0.2403	0.5331	-1.3139	-1.8515	-0.7763	0.5664	0.0133
PC10	0.3399	0.2277	0.5075	-1.2479	-1.7617	-0.7341	0.8789	0.0009
PC11	0.2916	0.1993	0.4265	-1.0704	-1.4874	-0.6534	0.0980	0.1057
PC12	0.2880	0.1930	0.4298	-1.0574	-1.4920	-0.6228	0.7417	0.0044
PC13	0.2294	0.1569	0.3354	-0.8422	-1.1697	-0.5147	0.0930	0.1087

Hapalemur griseus

PC	Slope	Slope lower CI	Slope higher CI	Intercept	Intercept lower CI	Intercept higher CI	p value	r squared
PC1	-0.5007	-0.7439	-0.3370	1.6931	1.0049	2.3814	0.4142	0.0268
PC2	0.4750	0.3210	0.7028	-1.6062	-2.2521	-0.9603	0.2739	0.0477
PC3	0.3892	0.2636	0.5747	-1.3163	-1.8424	-0.7902	0.2218	0.0591
PC4	-0.3324	-0.4963	-0.2226	1.1241	0.6611	1.5872	0.8813	0.0009
PC5	0.3024	0.2114	0.4324	-1.0225	-1.3963	-0.6487	0.0154	0.2128
PC6	-0.2614	-0.3719	-0.1837	0.8840	0.5656	1.2023	0.0102	0.2360
PC7	-0.2257	-0.3355	-0.1518	0.7632	0.4526	1.0739	0.4351	0.0246
PC8	-0.2169	-0.3161	-0.1488	0.7335	0.4505	1.0165	0.0724	0.1234
PC9	0.1897	0.1270	0.2833	-0.6415	-0.9057	-0.3772	0.9332	0.0003
PC10	-0.1766	-0.2605	-0.1197	0.5972	0.3591	0.8354	0.2046	0.0636
PC11	0.1473	0.0988	0.2197	-0.4982	-0.7027	-0.2937	0.6571	0.0080
PC12	0.1292	0.0870	0.1921	-0.4371	-0.6149	-0.2593	0.4281	0.0253
PC13	0.1190	0.0797	0.1777	-0.4023	-0.5681	-0.2365	0.9996	0.0000

Lemur catta

PC	Slope	Slope lower CI	Slope higher CI	Intercept	Intercept lower CI	Intercept higher CI	p value	r squared
PC1	0.5768	0.4078	0.8158	-2.0904	-2.8301	-1.3508	0.2898	0.0349
PC2	0.4823	0.3543	0.6566	-1.7480	-2.2960	-1.2000	0.0031	0.2423
PC3	-0.4192	-0.5887	-0.2984	1.5192	0.9931	2.0453	0.1159	0.0755
PC4	-0.3546	-0.5017	-0.2506	1.2852	0.8300	1.7404	0.3041	0.0330
PC5	0.3218	0.2264	0.4573	-1.1662	-1.5847	-0.7477	0.6301	0.0073
PC6	0.2851	0.2006	0.4052	-1.0333	-1.4041	-0.6624	0.6372	0.0070
PC7	0.2461	0.1732	0.3496	-0.8920	-1.2117	-0.5723	0.5797	0.0097
PC8	0.2252	0.1584	0.3202	-0.8164	-1.1097	-0.5231	0.6920	0.0050
PC9	-0.2164	-0.3060	-0.1531	0.7844	0.5073	1.0616	0.2724	0.0375
PC10	-0.1880	-0.2669	-0.1324	0.6813	0.4377	0.9250	0.5049	0.0140
PC11	0.1781	0.1254	0.2528	-0.6453	-0.8763	-0.4144	0.5218	0.0129
PC12	-0.1526	-0.2158	-0.1079	0.5530	0.3574	0.7487	0.2871	0.0353
PC13	-0.1462	-0.2079	-0.1027	0.5298	0.3391	0.7205	0.8473	0.0012

Varecia variegata

PC	Slope	Slope lower CI	Slope higher CI	Intercept	Intercept lower CI	Intercept higher CI	p value	r squared
PC1	0.4589	0.3428	0.6141	-1.7963	-2.3274	-1.2651	0.0031	0.2124
PC2	0.3671	0.2692	0.5005	-1.4369	-1.8897	-0.9841	0.0437	0.1054
PC3	-0.2934	-0.4012	-0.2146	1.1487	0.7832	1.5141	0.0662	0.0883
PC4	-0.2609	-0.3579	-0.1902	1.0213	0.6929	1.3498	0.1080	0.0683
PC5	0.2301	0.1660	0.3189	-0.9006	-1.1999	-0.6013	0.6618	0.0052
PC6	-0.2145	-0.2913	-0.1579	0.8395	0.5783	1.1008	0.0255	0.1277
PC7	-0.1766	-0.2449	-0.1273	0.6913	0.4610	0.9215	0.8988	0.0004
PC8	-0.1753	-0.2429	-0.1265	0.6861	0.4582	0.9140	0.6342	0.0062
PC9	-0.1547	-0.2144	-0.1116	0.6055	0.4043	0.8067	0.6444	0.0058
PC10	-0.1300	-0.1794	-0.0943	0.5091	0.3426	0.6756	0.2456	0.0363
PC11	-0.1221	-0.1691	-0.0881	0.4778	0.3191	0.6365	0.6195	0.0067
PC12	-0.1154	-0.1572	-0.0847	0.4517	0.3099	0.5936	0.0375	0.1118
PC13	0.1131	0.0816	0.1569	-0.4429	-0.5904	-0.2954	0.8226	0.0014

Lepilemur ruficaudatus

PC	Slope	Slope lower CI	Slope higher CI	Intercept	Intercept lower CI	Intercept higher CI	p value	r squared
PC1	0.4968	0.3418	0.7221	-1.6154	-2.2338	-0.9970	0.0202	0.2130
PC2	-0.3956	-0.5919	-0.2643	1.2861	0.7533	1.8190	0.1748	0.0785
PC3	-0.3316	-0.4917	-0.2237	1.0783	0.6424	1.5141	0.0861	0.1227
PC4	-0.2826	-0.4259	-0.1875	0.9187	0.5310	1.3065	0.3155	0.0438
PC5	-0.2473	-0.3760	-0.1627	0.8041	0.4571	1.1512	0.9674	0.0001
PC6	0.2337	0.1562	0.3496	-0.7599	-1.0744	-0.4453	0.1707	0.0800
PC7	-0.2031	-0.3001	-0.1375	0.6604	0.3961	0.9248	0.0658	0.1396
PC8	0.1723	0.1135	0.2616	-0.5603	-0.8012	-0.3193	0.6838	0.0073
PC9	-0.1551	-0.2356	-0.1021	0.5043	0.2873	0.7214	0.7151	0.0059
PC10	0.1428	0.0939	0.2171	-0.4643	-0.6646	-0.2639	0.9621	0.0001
PC11	0.1247	0.0820	0.1896	-0.4055	-0.5804	-0.2306	0.8808	0.0010
PC12	0.1154	0.0778	0.1711	-0.3752	-0.5269	-0.2234	0.0876	0.1216
PC13	0.1113	0.0738	0.1679	-0.3620	-0.5151	-0.2090	0.3341	0.0406

Loris tardigradus

PC	Slope	Slope lower CI	Slope higher CI	Intercept	Intercept lower CI	Intercept higher CI	p value	r squared
PC1	-0.4439	-0.6598	-0.2987	1.4106	0.8363	1.9849	0.4298	0.0251
PC2	0.3187	0.2161	0.4698	-1.0125	-1.4159	-0.6091	0.1950	0.0662
PC3	-0.2415	-0.3593	-0.1623	0.7673	0.4540	1.0806	0.4845	0.0197
PC4	0.1822	0.1262	0.2630	-0.5789	-0.7964	-0.3614	0.0327	0.1698
PC5	0.1713	0.1176	0.2494	-0.5443	-0.7539	-0.3347	0.0672	0.1277
PC6	-0.1540	-0.2222	-0.1067	0.4892	0.3055	0.6729	0.0323	0.1705
PC7	-0.1313	-0.1950	-0.0884	0.4172	0.2476	0.5868	0.4039	0.0280
PC8	0.1224	0.0820	0.1826	-0.3888	-0.5488	-0.2287	0.7783	0.0032
PC9	-0.1168	-0.1698	-0.0803	0.3710	0.2286	0.5133	0.0607	0.1337
PC10	-0.1086	-0.1621	-0.0727	0.3451	0.2029	0.4873	0.8602	0.0013
PC11	-0.1008	-0.1465	-0.0694	0.3204	0.1978	0.4430	0.0564	0.1380
PC12	0.0895	0.0603	0.1329	-0.2845	-0.3999	-0.1691	0.3731	0.0319
PC13	0.0756	0.0506	0.1129	-0.2402	-0.3392	-0.1412	0.8499	0.0015

Nycticebus bengalensis

PC	Slope	Slope lower CI	Slope higher CI	Intercept	Intercept lower CI	Intercept higher CI	p value	r squared
PC1	0.8300	0.5595	1.2313	-2.7539	-3.8685	-1.6393	0.0186	0.2471
PC2	0.7140	0.4575	1.1141	-2.3689	-3.4583	-1.2795	0.4558	0.0281
PC3	-0.6690	-1.0306	-0.4343	2.2199	1.2306	3.2091	0.1817	0.0874
PC4	-0.6050	-0.8952	-0.4089	2.0074	1.2006	2.8142	0.0159	0.2576
PC5	-0.5051	-0.7785	-0.3277	1.6759	0.9281	2.4238	0.1881	0.0850
PC6	0.4417	0.2814	0.6931	-1.4654	-2.1484	-0.7825	0.8463	0.0019
PC7	-0.4119	-0.6430	-0.2638	1.3666	0.7373	1.9958	0.4760	0.0257
PC8	0.3699	0.2367	0.5781	-1.2275	-1.7937	-0.6612	0.5110	0.0219
PC9	-0.3113	-0.4774	-0.2030	1.0329	0.5776	1.4881	0.1369	0.1072
PC10	-0.2850	-0.4472	-0.1816	0.9455	0.5049	1.3862	0.8488	0.0019
PC11	-0.2635	-0.4131	-0.1681	0.8743	0.4677	1.2809	0.7304	0.0061
PC12	-0.2414	-0.3789	-0.1538	0.8009	0.4273	1.1745	0.9764	0.0000
PC13	0.2109	0.1358	0.3274	-0.6997	-1.0176	-0.3817	0.3121	0.0510

Nycticebus coucang

PC	Slope	Slope lower CI	Slope higher CI	Intercept	Intercept lower CI	Intercept higher CI	p value	r squared
PC1	-0.4588	-0.5837	-0.3607	1.4734	1.1153	1.8316	0.4930	0.0070
PC2	-0.3801	-0.4763	-0.3033	1.2206	0.9428	1.4983	0.0024	0.1298
PC3	-0.3376	-0.4258	-0.2676	1.0839	0.8299	1.3380	0.0211	0.0768
PC4	-0.2966	-0.3759	-0.2341	0.9524	0.7247	1.1802	0.1036	0.0390
PC5	0.2723	0.2163	0.3427	-0.8744	-1.0773	-0.6714	0.0101	0.0947
PC6	0.2661	0.2093	0.3382	-0.8544	-1.0614	-0.6475	0.3332	0.0140
PC7	-0.2292	-0.2918	-0.1801	0.7361	0.5567	0.9155	0.6970	0.0023
PC8	0.2213	0.1740	0.2816	-0.7107	-0.8835	-0.5379	0.5182	0.0063
PC9	-0.2141	-0.2722	-0.1684	0.6875	0.5209	0.8542	0.3576	0.0126
PC10	0.1977	0.1559	0.2507	-0.6349	-0.7871	-0.4827	0.1278	0.0343
PC11	0.1832	0.1442	0.2327	-0.5882	-0.7304	-0.4460	0.2784	0.0175
PC12	0.1666	0.1309	0.2120	-0.5349	-0.6652	-0.4046	0.6480	0.0031
PC13	-0.1612	-0.2049	-0.1267	0.5175	0.3919	0.6430	0.4028	0.0105

Perodicticus potto

PC	Slope	Slope lower CI	Slope higher CI	Intercept	Intercept lower CI	Intercept higher CI	p value	r squared
PC1	0.4577	0.3843	0.5451	-1.5219	-1.7893	-1.2546	0.9043	0.0001
PC2	-0.4273	-0.5088	-0.3588	1.4209	1.1714	1.6703	0.6924	0.0012
PC3	-0.3757	-0.4456	-0.3168	1.2493	1.0350	1.4635	0.0137	0.0469
PC4	-0.3562	-0.4240	-0.2992	1.1844	0.9768	1.3919	0.4399	0.0047
PC5	0.3201	0.2689	0.3810	-1.0643	-1.2508	-0.8778	0.4266	0.0050
PC6	0.2824	0.2372	0.3362	-0.9390	-1.1037	-0.7743	0.5451	0.0029
PC7	0.2695	0.2263	0.3209	-0.8960	-1.0534	-0.7386	0.9440	0.0000
PC8	-0.2472	-0.2942	-0.2077	0.8219	0.6780	0.9658	0.3722	0.0063
PC9	0.2363	0.1985	0.2813	-0.7857	-0.9235	-0.6479	0.5320	0.0031
PC10	-0.2267	-0.2699	-0.1903	0.7537	0.6213	0.8861	0.8932	0.0001
PC11	0.2044	0.1728	0.2418	-0.6796	-0.7944	-0.5648	0.0017	0.0748
PC12	-0.1948	-0.2319	-0.1637	0.6478	0.5343	0.7613	0.4122	0.0053
PC13	0.1788	0.1501	0.2129	-0.5944	-0.6987	-0.4901	0.6678	0.0015

Goswami model orbit module against ln CS whole cranium

Cheirogaleus major

PC	Slope	Slope lower CI	Slope higher CI	Intercept	Intercept lower CI	Intercept higher CI	p value	r squared
PC1	0.8192	0.5487	1.2230	-3.9807	-5.6190	-2.3425	0.1455	0.0898
PC2	0.7099	0.4669	1.0793	-3.4496	-4.9377	-1.9616	0.9582	0.0001
PC3	-0.6716	-0.9918	-0.4548	3.2637	1.9588	4.5685	0.0644	0.1409
PC4	-0.6531	-0.9918	-0.4301	3.1737	1.8089	4.5384	0.7064	0.0063
PC5	0.5174	0.3465	0.7725	-2.5141	-3.5491	-1.4791	0.1469	0.0893
PC6	0.4798	0.3166	0.7272	-2.3315	-3.3292	-1.3338	0.5480	0.0159
PC7	-0.4094	-0.6133	-0.2733	1.9896	1.1635	2.8156	0.1893	0.0737
PC8	0.3730	0.2474	0.5624	-1.8126	-2.5778	-1.0474	0.3242	0.0423
PC9	0.3422	0.2251	0.5202	-1.6627	-2.3798	-0.9456	0.9192	0.0005
PC10	0.2713	0.1784	0.4124	-1.3181	-1.8867	-0.7495	0.9791	0.0000
PC11	-0.2659	-0.3986	-0.1774	1.2920	0.7545	1.8294	0.2009	0.0701
PC12	-0.2240	-0.3323	-0.1511	1.0887	0.6483	1.5290	0.0888	0.1208
PC13	-0.1892	-0.2877	-0.1245	0.9196	0.5229	1.3163	0.9923	0.0000

Cheirogaleus medius

PC	Slope	Slope lower CI	Slope higher CI	Intercept	Intercept lower CI	Intercept higher CI	p value	r squared
PC1	0.8767	0.6021	1.2767	-4.0242	-5.5727	-2.4758	0.2402	0.0507
PC2	-0.7274	-1.0597	-0.4993	3.3388	2.0526	4.6250	0.2511	0.0485
PC3	-0.7128	-1.0462	-0.4856	3.2718	1.9851	4.5586	0.6392	0.0083
PC4	0.5964	0.4059	0.8765	-2.7377	-3.8179	-1.6574	0.8370	0.0016
PC5	0.5452	0.3933	0.7558	-2.5026	-3.3345	-1.6707	0.0025	0.2915
PC6	-0.4814	-0.6863	-0.3377	2.2096	1.4095	3.0097	0.0320	0.1593
PC7	-0.4066	-0.5951	-0.2778	1.8663	1.1382	2.5944	0.4226	0.0240
PC8	-0.3928	-0.5774	-0.2672	1.8029	1.0909	2.5148	0.9588	0.0001
PC9	-0.2923	-0.4241	-0.2015	1.3417	0.8308	1.8527	0.1651	0.0701
PC10	-0.2539	-0.3715	-0.1735	1.1652	0.7108	1.6196	0.4134	0.0249
PC11	-0.2275	-0.3333	-0.1552	1.0441	0.6354	1.4528	0.4927	0.0176
PC12	-0.2169	-0.3186	-0.1476	0.9954	0.6029	1.3878	0.7766	0.0030
PC13	-0.1755	-0.2579	-0.1194	0.8056	0.4877	1.1235	0.8320	0.0017

Microcebus murinus

PC	Slope	Slope lower CI	Slope higher CI	Intercept	Intercept lower CI	Intercept higher CI	p value	r squared
PC1	0.9958	0.7873	1.2595	-4.3170	-5.3406	-3.2935	0.3842	0.0108
PC2	0.8260	0.6538	1.0436	-3.5811	-4.4261	-2.7360	0.2340	0.0202
PC3	-0.7808	-0.9888	-0.6166	3.3850	2.5782	4.1918	0.8609	0.0004
PC4	-0.6401	-0.8106	-0.5055	2.7750	2.1136	3.4365	0.8861	0.0003
PC5	0.5603	0.4451	0.7052	-2.4289	-2.9928	-1.8650	0.0547	0.0517
PC6	0.5383	0.4256	0.6808	-2.3336	-2.8867	-1.7805	0.3722	0.0114
PC7	0.4814	0.3803	0.6096	-2.0872	-2.5843	-1.5901	0.7120	0.0020
PC8	0.4558	0.3604	0.5765	-1.9761	-2.4444	-1.5077	0.3676	0.0116
PC9	0.4219	0.3337	0.5334	-1.8290	-2.2620	-1.3961	0.3195	0.0142
PC10	0.3806	0.3006	0.4819	-1.6500	-2.0431	-1.2570	0.7378	0.0016
PC11	-0.3764	-0.4760	-0.2976	1.6316	1.2448	2.0183	0.3736	0.0113
PC12	0.3357	0.2658	0.4240	-1.4554	-1.7985	-1.1124	0.2070	0.0226
PC13	-0.3243	-0.4088	-0.2573	1.4060	1.0776	1.7344	0.0917	0.0401

Microcebus rufus

PC	Slope	Slope lower CI	Slope higher CI	Intercept	Intercept lower CI	Intercept higher CI	p value	r squared
PC1	-0.7214	-1.0573	-0.4922	3.1439	1.9124	4.3753	0.5093	0.0163
PC2	-0.6780	-0.9966	-0.4612	2.9547	1.7879	4.1215	0.9402	0.0002
PC3	0.5694	0.3874	0.8368	-2.4814	-3.4608	-1.5019	0.8630	0.0011
PC4	0.4847	0.3323	0.7071	-2.1125	-2.9295	-1.2954	0.2927	0.0409
PC5	0.4342	0.2958	0.6374	-1.8924	-2.6369	-1.1478	0.6568	0.0074
PC6	0.3856	0.2623	0.5668	-1.6804	-2.3441	-1.0168	0.9688	0.0001
PC7	0.3399	0.2393	0.4829	-1.4814	-2.0122	-0.9505	0.0233	0.1765
PC8	-0.2942	-0.4247	-0.2038	1.2821	0.8006	1.7635	0.1023	0.0958
PC9	-0.2829	-0.4142	-0.1932	1.2328	0.7512	1.7144	0.4477	0.0215
PC10	0.2306	0.1575	0.3375	-1.0049	-1.3971	-0.6127	0.4284	0.0234
PC11	-0.2112	-0.3105	-0.1437	0.9206	0.5571	1.2842	0.9598	0.0001
PC12	0.1810	0.1232	0.2659	-0.7887	-1.0998	-0.4775	0.8153	0.0021
PC13	-0.1607	-0.2322	-0.1111	0.7001	0.4363	0.9640	0.1154	0.0892

Galago alleni

PC	Slope	Slope lower CI	Slope higher CI	Intercept	Intercept lower CI	Intercept higher CI	p value	r squared
PC1	-1.2241	-1.8776	-0.7980	5.8252	3.2564	8.3941	0.7325	0.0054
PC2	0.8104	0.5337	1.2306	-3.8565	-5.5149	-2.1981	0.2736	0.0542
PC3	0.6492	0.4553	0.9259	-3.0897	-4.2095	-1.9699	0.0034	0.3282
PC4	0.6106	0.4023	0.9268	-2.9059	-4.1541	-1.6577	0.2640	0.0564
PC5	-0.5481	-0.8397	-0.3578	2.6084	1.4617	3.7551	0.6178	0.0115
PC6	-0.4636	-0.7112	-0.3021	2.2060	1.2326	3.1793	0.7602	0.0043
PC7	0.3875	0.2586	0.5809	-1.8443	-2.6114	-1.0772	0.1045	0.1153
PC8	0.3572	0.2351	0.5428	-1.7000	-2.4324	-0.9676	0.2894	0.0508
PC9	-0.3088	-0.4736	-0.2013	1.4695	0.8217	2.1173	0.7162	0.0061
PC10	0.2768	0.1869	0.4101	-1.3174	-1.8485	-0.7863	0.0462	0.1687
PC11	-0.2286	-0.3508	-0.1490	1.0881	0.6077	1.5684	0.7886	0.0033
PC12	0.1897	0.1249	0.2881	-0.9026	-1.2912	-0.5141	0.2829	0.0522
PC13	0.1536	0.1001	0.2356	-0.7309	-1.0534	-0.4084	0.7651	0.0041

Galago demidoff

PC	Slope	Slope lower CI	Slope higher CI	Intercept	Intercept lower CI	Intercept higher CI	p value	r squared
PC1	-1.2404	-1.5978	-0.9629	5.4964	4.0895	6.9033	0.0449	0.0687
PC2	1.0814	0.8323	1.4051	-4.7920	-6.0613	-3.5227	0.6883	0.0028
PC3	-0.8600	-1.1126	-0.6647	3.8109	2.8185	4.8032	0.1484	0.0363
PC4	-0.6504	-0.8450	-0.5006	2.8820	2.1188	3.6452	0.6652	0.0033
PC5	-0.5689	-0.7389	-0.4380	2.5210	1.8544	3.1877	0.5556	0.0061
PC6	0.5072	0.3907	0.6585	-2.2477	-2.8409	-1.6545	0.4518	0.0100
PC7	-0.4355	-0.5660	-0.3351	1.9301	1.4184	2.4417	0.7944	0.0012
PC8	-0.4126	-0.5361	-0.3176	1.8285	1.3443	2.3127	0.6616	0.0034
PC9	-0.3669	-0.4768	-0.2822	1.6257	1.1945	2.0568	0.9316	0.0001
PC10	-0.3491	-0.4500	-0.2707	1.5468	1.1495	1.9440	0.0560	0.0626
PC11	0.3360	0.2590	0.4358	-1.4888	-1.8804	-1.0972	0.3309	0.0166
PC12	0.2628	0.2027	0.3408	-1.1646	-1.4705	-0.8587	0.2937	0.0193
PC13	-0.2528	-0.3285	-0.1945	1.1200	0.8229	1.4171	0.9815	0.0000

Galago elegantulus

PC	Slope	Slope lower CI	Slope higher CI	Intercept	Intercept lower CI	Intercept higher CI	p value	r squared
PC1	2.4072	1.6924	3.4239	-11.3655	-15.4533	-7.2777	0.7833	0.0024
PC2	-1.7827	-2.4790	-1.2820	8.4171	5.5911	11.2431	0.0357	0.1307
PC3	1.2315	0.8676	1.7480	-5.8146	-7.8931	-3.7361	0.4970	0.0145
PC4	-0.8929	-1.2689	-0.6283	4.2157	2.7033	5.7280	0.6261	0.0075
PC5	-0.8533	-1.2142	-0.5997	4.0290	2.5782	5.4799	0.9801	0.0000
PC6	0.7977	0.5631	1.1301	-3.7665	-5.1051	-2.4278	0.3641	0.0258
PC7	0.6394	0.4567	0.8950	-3.0187	-4.0534	-1.9840	0.0779	0.0939
PC8	0.5203	0.3701	0.7315	-2.4568	-3.3100	-1.6037	0.1304	0.0700
PC9	-0.4869	-0.6882	-0.3445	2.2991	1.4877	3.1105	0.2597	0.0395
PC10	-0.4135	-0.5878	-0.2909	1.9524	1.2516	2.6533	0.6550	0.0063
PC11	0.3890	0.2738	0.5525	-1.8366	-2.4944	-1.1787	0.5649	0.0105
PC12	0.3350	0.2357	0.4762	-1.5818	-2.1497	-1.0140	0.6603	0.0061
PC13	0.2865	0.2061	0.3983	-1.3526	-1.8064	-0.8989	0.0347	0.1320

Galago moholi

PC	Slope	Slope lower CI	Slope higher CI	Intercept	Intercept lower CI	Intercept higher CI	p value	r squared
PC1	-1.3103	-1.6565	-1.0365	5.9589	4.5491	7.3688	0.8602	0.0004
PC2	0.8761	0.6986	1.0987	-3.9842	-4.8939	-3.0745	0.0246	0.0691
PC3	0.6838	0.5454	0.8573	-3.1095	-3.8188	-2.4003	0.0227	0.0710
PC4	-0.6131	-0.7732	-0.4861	2.7882	2.1354	3.4410	0.2193	0.0212
PC5	0.5212	0.4123	0.6589	-2.3703	-2.9312	-1.8093	0.9932	0.0000
PC6	-0.4932	-0.6225	-0.3908	2.2430	1.7160	2.7700	0.3136	0.0143
PC7	-0.4419	-0.5584	-0.3497	2.0095	1.5348	2.4842	0.6181	0.0035
PC8	-0.4026	-0.5010	-0.3235	1.8309	1.4272	2.2345	0.0016	0.1318
PC9	0.3683	0.2914	0.4655	-1.6748	-2.0707	-1.2790	0.6774	0.0025
PC10	-0.3481	-0.4380	-0.2766	1.5830	1.2160	1.9500	0.0894	0.0401
PC11	0.3087	0.2446	0.3897	-1.4039	-1.7340	-1.0739	0.3313	0.0133
PC12	-0.2825	-0.3570	-0.2235	1.2846	0.9809	1.5883	0.7127	0.0019
PC13	0.2579	0.2043	0.3257	-1.1729	-1.4490	-0.8969	0.3734	0.0112

Galago senegalensis

PC	Slope	Slope lower CI	Slope higher CI	Intercept	Intercept lower CI	Intercept higher CI	p value	r squared
PC1	-1.0289	-1.1895	-0.8900	4.7699	4.0757	5.4641	0.0011	0.0595
PC2	-0.7916	-0.9117	-0.6874	3.6699	3.1500	4.1897	0.0000	0.1091
PC3	0.6339	0.5460	0.7358	-2.9384	-3.3784	-2.4985	0.3744	0.0046
PC4	0.5875	0.5065	0.6814	-2.7235	-3.1290	-2.3181	0.0960	0.0159
PC5	-0.5365	-0.6176	-0.4660	2.4870	2.1356	2.8384	0.0000	0.1135
PC6	-0.5207	-0.6030	-0.4495	2.4137	2.0579	2.7695	0.0127	0.0353
PC7	-0.4272	-0.4945	-0.3690	1.9802	1.6895	2.2710	0.0060	0.0428
PC8	0.4016	0.3459	0.4664	-1.8618	-2.1412	-1.5825	0.8565	0.0002
PC9	-0.3620	-0.4190	-0.3128	1.6783	1.4319	1.9246	0.0056	0.0435
PC10	0.3526	0.3037	0.4094	-1.6346	-1.8797	-1.3896	0.5714	0.0019
PC11	-0.3014	-0.3490	-0.2603	1.3971	1.1916	1.6027	0.0091	0.0387
PC12	-0.2780	-0.3227	-0.2395	1.2887	1.0958	1.4817	0.3655	0.0047
PC13	-0.2350	-0.2729	-0.2024	1.0893	0.9259	1.2528	0.7781	0.0005

Galago zanzibaricus

PC	Slope	Slope lower CI	Slope higher CI	Intercept	Intercept lower CI	Intercept higher CI	p value	r squared
PC1	-2.0085	-3.0178	-1.3368	9.2118	5.3568	13.0669	0.2428	0.0588
PC2	-1.0375	-1.5611	-0.6895	4.7584	2.7594	6.7574	0.2752	0.0515
PC3	0.7369	0.4867	1.1157	-3.3798	-4.8222	-1.9373	0.4884	0.0211
PC4	0.6580	0.4421	0.9794	-3.0179	-4.2500	-1.7859	0.1153	0.1043
PC5	-0.5792	-0.8778	-0.3821	2.6564	1.5197	3.7931	0.5476	0.0159
PC6	0.5197	0.3439	0.7855	-2.3837	-3.3965	-1.3710	0.4083	0.0299
PC7	-0.4976	-0.6897	-0.3590	2.2821	1.5236	3.0407	0.0006	0.4062
PC8	0.4350	0.2865	0.6603	-1.9950	-2.8522	-1.1378	0.6748	0.0078
PC9	0.3786	0.2492	0.5754	-1.7366	-2.4847	-0.9885	0.8051	0.0027
PC10	-0.3389	-0.5096	-0.2253	1.5542	0.9023	2.2061	0.2611	0.0546
PC11	0.2748	0.1827	0.4136	-1.2606	-1.7901	-0.7311	0.2743	0.0517
PC12	0.2555	0.1681	0.3885	-1.1720	-1.6774	-0.6667	0.8853	0.0009
PC13	0.2335	0.1555	0.3506	-1.0708	-1.5182	-0.6235	0.2295	0.0621

Otolemur crassicaudatus

PC	Slope	Slope lower CI	Slope higher CI	Intercept	Intercept lower CI	Intercept higher CI	p value	r squared
PC1	0.7058	0.5792	0.8599	-3.6104	-4.3285	-2.8923	0.4634	0.0054
PC2	0.4791	0.4080	0.5626	-2.4507	-2.8462	-2.0552	0.0000	0.3452
PC3	0.4502	0.3741	0.5416	-2.3028	-2.7313	-1.8743	0.0002	0.1296
PC4	0.3543	0.2933	0.4281	-1.8127	-2.1574	-1.4680	0.0022	0.0910
PC5	-0.3381	-0.4105	-0.2785	1.7295	1.3918	2.0671	0.0402	0.0418
PC6	0.3028	0.2491	0.3680	-1.5489	-1.8529	-1.2448	0.0778	0.0311
PC7	-0.2797	-0.3410	-0.2295	1.4311	1.1458	1.7164	0.7869	0.0007
PC8	0.2489	0.2042	0.3034	-1.2733	-1.5272	-1.0194	0.8736	0.0003
PC9	-0.2384	-0.2904	-0.1957	1.2195	0.9773	1.4616	0.3498	0.0088
PC10	-0.2254	-0.2747	-0.1850	1.1530	0.9236	1.3825	0.5090	0.0044
PC11	-0.2121	-0.2586	-0.1740	1.0851	0.8688	1.3014	0.7684	0.0009
PC12	-0.1939	-0.2364	-0.1591	0.9919	0.7941	1.1898	0.9649	0.0000
PC13	-0.1787	-0.2178	-0.1466	0.9142	0.7319	1.0964	0.7834	0.0008

Otolemur garnettii

PC	Slope	Slope lower CI	Slope higher CI	Intercept	Intercept lower CI	Intercept higher CI	p value	r squared
PC1	-0.7921	-0.9538	-0.6578	3.9970	3.2502	4.7439	0.0000	0.1768
PC2	-0.5356	-0.6399	-0.4483	2.7029	2.2194	3.1864	0.0000	0.2456
PC3	-0.4306	-0.5283	-0.3510	2.1730	1.7255	2.6204	0.8720	0.0003
PC4	-0.3927	-0.4805	-0.3208	1.9815	1.5785	2.3845	0.1280	0.0247
PC5	-0.3355	-0.4050	-0.2779	1.6931	1.3725	2.0137	0.0001	0.1544
PC6	-0.3094	-0.3791	-0.2525	1.5612	1.2416	1.8807	0.2892	0.0121
PC7	-0.2941	-0.3607	-0.2399	1.4842	1.1794	1.7890	0.4759	0.0055
PC8	0.2642	0.2158	0.3235	-1.3332	-1.6052	-1.0613	0.1821	0.0191
PC9	-0.2479	-0.3040	-0.2022	1.2511	0.9941	1.5080	0.4849	0.0053
PC10	0.2328	0.1906	0.2844	-1.1750	-1.4117	-0.9383	0.0434	0.0432
PC11	0.2037	0.1661	0.2497	-1.0278	-1.2387	-0.8170	0.3938	0.0078
PC12	0.1769	0.1442	0.2171	-0.8929	-1.0768	-0.7090	0.8686	0.0003
PC13	0.1732	0.1412	0.2125	-0.8739	-1.0539	-0.6939	0.9190	0.0001

Avahi laniger

PC	Slope	Slope lower CI	Slope higher CI	Intercept	Intercept lower CI	Intercept higher CI	p value	r squared
PC1	2.2266	1.4395	3.4443	-10.8722	-15.7670	-5.9774	0.5670	0.0159
PC2	-1.8795	-2.9123	-1.2130	9.1772	5.0282	13.3262	0.6921	0.0076
PC3	1.3835	0.9237	2.0724	-6.7556	-9.5602	-3.9509	0.0560	0.1631
PC4	1.1047	0.7266	1.6796	-5.3940	-7.7206	-3.0673	0.1488	0.0966
PC5	0.9677	0.6245	1.4994	-4.7250	-6.8610	-2.5890	0.6893	0.0078
PC6	0.7599	0.4942	1.1685	-3.7105	-5.3568	-2.0642	0.3359	0.0441
PC7	-0.6845	-1.0622	-0.4410	3.3420	1.8253	4.8587	0.9868	0.0000
PC8	-0.6241	-0.9638	-0.4041	3.0474	1.6810	4.4138	0.4816	0.0239
PC9	-0.4579	-0.7031	-0.2982	2.2359	1.2474	3.2244	0.3003	0.0510
PC10	-0.4221	-0.6422	-0.2774	2.0608	1.1700	2.9516	0.1577	0.0928
PC11	0.3973	0.2593	0.6088	-1.9400	-2.7932	-1.0868	0.2566	0.0608
PC12	0.3386	0.2189	0.5237	-1.6535	-2.3976	-0.9093	0.5589	0.0165
PC13	0.2924	0.1933	0.4423	-1.4276	-2.0356	-0.8196	0.1065	0.1193

Indri indri

PC	Slope	Slope lower CI	Slope higher CI	Intercept	Intercept lower CI	Intercept higher CI	p value	r squared
PC1	-1.8501	-2.5380	-1.3486	10.1532	6.8893	13.4171	0.1070	0.0687
PC2	1.3537	0.9858	1.8588	-7.4291	-9.8248	-5.0335	0.1236	0.0629
PC3	-1.0902	-1.5120	-0.7861	5.9832	3.9911	7.9753	0.8472	0.0010
PC4	-0.8461	-1.1699	-0.6119	4.6434	3.1121	6.1746	0.3906	0.0200
PC5	0.7500	0.5453	1.0317	-4.1163	-5.4512	-2.7813	0.1621	0.0521
PC6	0.6736	0.4864	0.9329	-3.6968	-4.9223	-2.4713	0.5512	0.0097
PC7	-0.5525	-0.7429	-0.4110	3.0323	2.1216	3.9431	0.0060	0.1870
PC8	-0.5071	-0.7024	-0.3662	2.7833	1.8607	3.7058	0.5467	0.0099
PC9	-0.4711	-0.6535	-0.3397	2.5855	1.7244	3.4466	0.9013	0.0004
PC10	-0.4052	-0.5616	-0.2923	2.2235	1.4846	2.9624	0.6745	0.0048
PC11	0.3766	0.2728	0.5199	-2.0669	-2.7448	-1.3890	0.2868	0.0306
PC12	0.3608	0.2601	0.5003	-1.9800	-2.6391	-1.3208	0.8321	0.0012
PC13	-0.3403	-0.4719	-0.2454	1.8676	1.2461	2.4891	0.7937	0.0019

Propithecus diadema

PC	Slope	Slope lower CI	Slope higher CI	Intercept	Intercept lower CI	Intercept higher CI	p value	r squared
PC1	-1.2096	-1.7862	-0.8192	6.4950	3.8989	9.0911	0.5089	0.0170
PC2	-0.9196	-1.3619	-0.6209	4.9376	2.9484	6.9268	0.8524	0.0014
PC3	-0.8312	-1.2167	-0.5679	4.4631	2.7210	6.2053	0.1994	0.0625
PC4	-0.6940	-1.0280	-0.4685	3.7261	2.2239	5.2282	0.9963	0.0000
PC5	0.6638	0.4482	0.9832	-3.5643	-5.0005	-2.1282	0.8692	0.0011
PC6	0.5018	0.3389	0.7430	-2.6943	-3.7791	-1.6095	0.7966	0.0026
PC7	0.4264	0.2879	0.6315	-2.2893	-3.2119	-1.3668	0.8838	0.0008
PC8	-0.3417	-0.5060	-0.2307	1.8346	1.0953	2.5738	0.8744	0.0010
PC9	-0.3068	-0.4528	-0.2079	1.6474	0.9899	2.3049	0.4746	0.0198
PC10	0.2890	0.1981	0.4216	-1.5519	-2.1518	-0.9520	0.1434	0.0805
PC11	0.2611	0.1924	0.3544	-1.4020	-1.8369	-0.9671	0.0003	0.4079
PC12	-0.2358	-0.3405	-0.1634	1.2663	0.7907	1.7419	0.0572	0.1321
PC13	-0.2266	-0.3347	-0.1534	1.2167	0.7299	1.7036	0.5332	0.0151

Propithecus verreauxi

PC	Slope	Slope lower CI	Slope higher CI	Intercept	Intercept lower CI	Intercept higher CI	p value	r squared
PC1	1.2954	0.9526	1.7617	-6.8571	-8.9987	-4.7155	0.3716	0.0195
PC2	-0.9698	-1.2947	-0.7264	5.1335	3.6293	6.6376	0.0146	0.1370
PC3	0.8687	0.6541	1.1539	-4.5984	-5.9213	-3.2755	0.0063	0.1681
PC4	0.7499	0.5498	1.0228	-3.9696	-5.2215	-2.7176	0.9292	0.0002
PC5	-0.6104	-0.8324	-0.4476	3.2311	2.2127	4.2496	0.8149	0.0014
PC6	-0.5787	-0.7888	-0.4245	3.0631	2.0989	4.0273	0.6864	0.0040
PC7	0.5293	0.3880	0.7219	-2.8015	-3.6850	-1.9179	0.9256	0.0002
PC8	-0.4404	-0.5928	-0.3272	2.3313	1.6282	3.0343	0.0566	0.0858
PC9	-0.4056	-0.5532	-0.2974	2.1471	1.4700	2.8242	0.9026	0.0004
PC10	-0.3784	-0.5149	-0.2780	2.0028	1.3758	2.6298	0.4358	0.0149
PC11	0.3368	0.2508	0.4521	-1.7827	-2.3154	-1.2499	0.0367	0.1021
PC12	0.2954	0.2178	0.4005	-1.5635	-2.0470	-1.0801	0.2051	0.0389
PC13	0.2705	0.1984	0.3688	-1.4317	-1.8829	-0.9806	0.7757	0.0020

Eulemur fulvus

PC	Slope	Slope lower CI	Slope higher CI	Intercept	Intercept lower CI	Intercept higher CI	p value	r squared
PC1	-0.9938	-1.1526	-0.8569	5.2976	4.5093	6.0860	0.0875	0.0168
PC2	-0.8296	-0.9634	-0.7145	4.4225	3.7591	5.0860	0.7280	0.0007
PC3	-0.6415	-0.7443	-0.5528	3.4194	2.9091	3.9298	0.1679	0.0110
PC4	-0.6292	-0.7306	-0.5418	3.3540	2.8507	3.8574	0.9928	0.0000
PC5	0.5638	0.4857	0.6545	-3.0056	-3.4553	-2.5559	0.3136	0.0059
PC6	-0.5485	-0.6356	-0.4733	2.9239	2.4915	3.3563	0.0246	0.0289
PC7	0.4630	0.3989	0.5374	-2.4682	-2.8376	-2.0989	0.3121	0.0059
PC8	-0.4478	-0.5197	-0.3859	2.3872	2.0305	2.7438	0.2128	0.0090
PC9	0.4251	0.3661	0.4935	-2.2661	-2.6056	-1.9265	0.4560	0.0032
PC10	0.4198	0.3618	0.4870	-2.2377	-2.5714	-1.9039	0.1470	0.0121
PC11	-0.3915	-0.4542	-0.3374	2.0869	1.7755	2.3982	0.1562	0.0116
PC12	0.3689	0.3184	0.4274	-1.9664	-2.2568	-1.6759	0.0192	0.0313
PC13	-0.3321	-0.3856	-0.2860	1.7702	1.5048	2.0357	0.6043	0.0016

Eulemur macaco

PC	Slope	Slope lower CI	Slope higher CI	Intercept	Intercept lower CI	Intercept higher CI	p value	r squared
PC1	1.0650	0.8233	1.3775	-5.7005	-7.1836	-4.2174	0.0142	0.1083
PC2	-1.0303	-1.3495	-0.7866	5.5149	4.0083	7.0215	0.3448	0.0169
PC3	0.9481	0.7232	1.2430	-5.0751	-6.4665	-3.6836	0.4726	0.0098
PC4	0.8360	0.6472	1.0799	-4.4750	-5.6331	-3.3170	0.0103	0.1178
PC5	0.7954	0.6062	1.0436	-4.2574	-5.4283	-3.0865	0.6624	0.0036
PC6	-0.6589	-0.8613	-0.5041	3.5271	2.5709	4.4833	0.1926	0.0318
PC7	0.6525	0.4989	0.8535	-3.4929	-4.4422	-2.5437	0.2294	0.0271
PC8	-0.5388	-0.7039	-0.4124	2.8841	2.1038	3.6644	0.1665	0.0358
PC9	0.5224	0.3983	0.6850	-2.7961	-3.5634	-2.0288	0.5152	0.0080
PC10	0.4556	0.3497	0.5935	-2.4387	-3.0912	-1.7863	0.0786	0.0572
PC11	0.4321	0.3324	0.5617	-2.3127	-2.9264	-1.6990	0.0472	0.0723
PC12	0.4046	0.3093	0.5292	-2.1657	-2.7542	-1.5773	0.2262	0.0275
PC13	0.3574	0.2723	0.4692	-1.9131	-2.4401	-1.3862	0.8640	0.0006

Eulemur mongoz

PC	Slope	Slope lower CI	Slope higher CI	Intercept	Intercept lower CI	Intercept higher CI	p value	r squared
PC1	-0.8815	-1.1525	-0.6742	4.6567	3.3931	5.9204	0.4377	0.0112
PC2	-0.6327	-0.8168	-0.4900	3.3434	2.4801	4.2068	0.0153	0.1040
PC3	-0.5484	-0.7175	-0.4192	2.8980	2.1096	3.6863	0.5738	0.0059
PC4	0.5062	0.3867	0.6626	-2.6745	-3.4035	-1.9456	0.7234	0.0023
PC5	0.4935	0.3806	0.6398	-2.6076	-3.2927	-1.9226	0.0444	0.0727
PC6	0.4098	0.3132	0.5363	-2.1651	-2.7546	-1.5755	0.6259	0.0044
PC7	-0.3900	-0.5081	-0.2994	2.0606	1.5093	2.6120	0.1470	0.0386
PC8	-0.3670	-0.4800	-0.2806	1.9387	1.4119	2.4655	0.4909	0.0088
PC9	-0.3317	-0.4289	-0.2566	1.7527	1.2974	2.2081	0.0219	0.0935
PC10	0.2871	0.2203	0.3742	-1.5177	-1.9244	-1.1111	0.1680	0.0349
PC11	-0.2762	-0.3617	-0.2110	1.4594	1.0613	1.8575	0.8219	0.0009
PC12	0.2641	0.2019	0.3454	-1.3953	-1.7744	-1.0161	0.4999	0.0085
PC13	0.2303	0.1776	0.2987	-1.2164	-1.5363	-0.8965	0.0466	0.0713

Eulemur rubriventer

PC	Slope	Slope lower CI	Slope higher CI	Intercept	Intercept lower CI	Intercept higher CI	p value	r squared
PC1	-1.4760	-2.0496	-1.0630	7.8491	5.2257	10.4725	0.0014	0.3416
PC2	-1.2337	-1.8407	-0.8269	6.5605	3.8650	9.2560	0.7240	0.0051
PC3	1.0446	0.6996	1.5598	-5.5549	-7.8423	-3.2675	0.8969	0.0007
PC4	0.8065	0.5488	1.1852	-4.2885	-5.9807	-2.5964	0.1465	0.0824
PC5	0.6772	0.4541	1.0101	-3.6013	-5.0797	-2.1228	0.6857	0.0067
PC6	0.6210	0.4175	0.9236	-3.3022	-4.6479	-1.9565	0.4679	0.0213
PC7	-0.5848	-0.8630	-0.3963	3.1100	1.8691	4.3509	0.2115	0.0617
PC8	0.5463	0.3705	0.8054	-2.9048	-4.0612	-1.7485	0.1957	0.0660
PC9	0.4606	0.3085	0.6879	-2.4496	-3.4586	-1.4406	0.9751	0.0000
PC10	-0.4242	-0.6314	-0.2850	2.2558	1.3349	3.1767	0.5063	0.0179
PC11	0.3975	0.2662	0.5934	-2.1137	-2.9837	-1.2438	0.8407	0.0016
PC12	-0.3447	-0.5117	-0.2322	1.8328	1.0897	2.5759	0.3781	0.0312
PC13	0.3215	0.2159	0.4789	-1.7098	-2.4093	-1.0103	0.5626	0.0136

Hapalemur griseus

PC	Slope	Slope lower CI	Slope higher CI	Intercept	Intercept lower CI	Intercept higher CI	p value	r squared
PC1	1.3138	0.8941	1.9305	-6.6194	-9.2304	-4.0084	0.1447	0.0831
PC2	-0.7200	-1.0614	-0.4884	3.6275	2.1839	5.0710	0.1934	0.0667
PC3	0.6489	0.4389	0.9594	-3.2695	-4.5808	-1.9582	0.2525	0.0520
PC4	0.5496	0.3680	0.8208	-2.7691	-3.9097	-1.6285	0.9372	0.0003
PC5	-0.5379	-0.8024	-0.3606	2.7101	1.5969	3.8233	0.7077	0.0057
PC6	-0.4286	-0.5876	-0.3127	2.1595	1.4669	2.8521	0.0005	0.3938
PC7	-0.4012	-0.5868	-0.2742	2.0211	1.2336	2.8087	0.0986	0.1053
PC8	0.3439	0.2364	0.5003	-1.7328	-2.3977	-1.0679	0.0622	0.1323
PC9	-0.3318	-0.4955	-0.2222	1.6718	0.9832	2.3605	0.9492	0.0002
PC10	-0.3061	-0.4571	-0.2050	1.5424	0.9075	2.1774	0.8565	0.0013
PC11	-0.3018	-0.4498	-0.2025	1.5205	0.8975	2.1435	0.6092	0.0106
PC12	-0.2335	-0.3481	-0.1567	1.1766	0.6943	1.6588	0.6189	0.0100
PC13	-0.2043	-0.3037	-0.1375	1.0294	0.6107	1.4482	0.4319	0.0249

Lemur catta

PC	Slope	Slope lower CI	Slope higher CI	Intercept	Intercept lower CI	Intercept higher CI	p value	r squared
PC1	-0.8385	-1.1866	-0.5925	4.4083	2.8464	5.9702	0.3115	0.0320
PC2	-0.8023	-1.1366	-0.5663	4.2178	2.7185	5.7171	0.3658	0.0256
PC3	-0.5743	-0.8169	-0.4037	3.0194	1.9332	4.1056	0.7999	0.0020
PC4	0.5142	0.3617	0.7311	-2.7035	-3.6747	-1.7323	0.6943	0.0049
PC5	-0.4477	-0.6368	-0.3148	2.3539	1.5075	3.2004	0.7605	0.0029
PC6	-0.4075	-0.5567	-0.2982	2.1422	1.4625	2.8218	0.0047	0.2238
PC7	0.3658	0.2571	0.5205	-1.9233	-2.6156	-1.2311	0.8504	0.0011
PC8	-0.3335	-0.4738	-0.2347	1.7533	1.1247	2.3820	0.6014	0.0086
PC9	0.3252	0.2288	0.4624	-1.7100	-2.3243	-1.0956	0.7007	0.0047
PC10	0.3085	0.2168	0.4389	-1.6218	-2.2058	-1.0378	0.9998	0.0000
PC11	0.2859	0.2009	0.4068	-1.5032	-2.0444	-0.9620	0.9094	0.0004
PC12	0.2557	0.1801	0.3628	-1.3441	-1.8244	-0.8638	0.4836	0.0155
PC13	0.2195	0.1548	0.3113	-1.1542	-1.5657	-0.7426	0.4298	0.0196

Varecia variegata

PC	Slope	Slope lower CI	Slope higher CI	Intercept	Intercept lower CI	Intercept higher CI	p value	r squared
PC1	-1.0482	-1.4530	-0.7562	5.7415	3.8332	7.6499	0.6857	0.0045
PC2	-0.9125	-1.1893	-0.7002	4.9983	3.6587	6.3379	0.0001	0.3527
PC3	0.7168	0.5253	0.9780	-3.9260	-5.1658	-2.6863	0.0481	0.1015
PC4	0.6229	0.4514	0.8595	-3.4119	-4.5296	-2.2942	0.2689	0.0329
PC5	0.4864	0.3511	0.6738	-2.6641	-3.5479	-1.7803	0.5828	0.0082
PC6	0.4307	0.3111	0.5962	-2.3591	-3.1401	-1.5781	0.5005	0.0124
PC7	-0.4100	-0.5679	-0.2959	2.2455	1.5006	2.9904	0.5794	0.0084
PC8	-0.3399	-0.4713	-0.2452	1.8619	1.2427	2.4812	0.7238	0.0034
PC9	0.2935	0.2134	0.4035	-1.6074	-2.1282	-1.0866	0.1538	0.0542
PC10	-0.2817	-0.3892	-0.2038	1.5428	1.0351	2.0504	0.3441	0.0242
PC11	-0.2723	-0.3741	-0.1983	1.4917	1.0103	1.9732	0.1288	0.0612
PC12	-0.2605	-0.3606	-0.1882	1.4269	0.9549	1.8990	0.4766	0.0138
PC13	-0.2329	-0.3202	-0.1695	1.2760	0.8630	1.6890	0.1471	0.0560

Lepilemur ruficaudatus

PC	Slope	Slope lower CI	Slope higher CI	Intercept	Intercept lower CI	Intercept higher CI	p value	r squared
PC1	-0.7782	-1.1831	-0.5118	3.8261	2.1758	5.4765	0.9414	0.0002
PC2	-0.6817	-1.0244	-0.4537	3.3519	1.9486	4.7552	0.2457	0.0581
PC3	0.6500	0.4293	0.9843	-3.1961	-4.5606	-1.8315	0.4950	0.0205
PC4	-0.5726	-0.8252	-0.3973	2.8152	1.7632	3.8673	0.0110	0.2495
PC5	-0.4546	-0.6910	-0.2991	2.2351	1.2715	3.1987	0.8668	0.0012
PC6	-0.4078	-0.6159	-0.2701	2.0052	1.1550	2.8555	0.3790	0.0338
PC7	0.3937	0.2597	0.5968	-1.9357	-2.7645	-1.1069	0.5605	0.0149
PC8	0.3528	0.2321	0.5362	-1.7345	-2.4822	-0.9869	0.8485	0.0016
PC9	0.2719	0.1841	0.4015	-1.3367	-1.8712	-0.8022	0.0645	0.1409
PC10	-0.2502	-0.3800	-0.1647	1.2302	0.7009	1.7595	0.7345	0.0051
PC11	-0.2344	-0.3561	-0.1544	1.1527	0.6569	1.6486	0.7188	0.0057
PC12	-0.2100	-0.3184	-0.1386	1.0327	0.5907	1.4747	0.5507	0.0157
PC13	-0.1716	-0.2588	-0.1137	0.8435	0.4868	1.2002	0.3436	0.0391

Loris tardigradus

PC	Slope	Slope lower CI	Slope higher CI	Intercept	Intercept lower CI	Intercept higher CI	p value	r squared
PC1	-0.6015	-0.8759	-0.4131	2.8795	1.7712	3.9878	0.0674	0.1275
PC2	0.5709	0.3836	0.8496	-2.7331	-3.8489	-1.6172	0.4992	0.0185
PC3	0.3939	0.2648	0.5859	-1.8858	-2.6548	-1.1169	0.4702	0.0211
PC4	0.3226	0.2221	0.4687	-1.5446	-2.1349	-0.9542	0.0548	0.1397
PC5	0.2959	0.2120	0.4130	-1.4166	-1.8978	-0.9353	0.0021	0.3202
PC6	0.2425	0.1624	0.3621	-1.1607	-1.6391	-0.6824	0.9915	0.0000
PC7	-0.2022	-0.3004	-0.1361	0.9678	0.5743	1.3614	0.4195	0.0262
PC8	-0.1665	-0.2377	-0.1167	0.7973	0.5077	1.0869	0.0129	0.2230
PC9	-0.1459	-0.2176	-0.0978	0.6983	0.4113	0.9853	0.7100	0.0056
PC10	-0.1087	-0.1622	-0.0728	0.5203	0.3061	0.7344	0.8027	0.0025
PC11	-0.1021	-0.1523	-0.0685	0.4889	0.2881	0.6897	0.6789	0.0070
PC12	-0.0961	-0.1430	-0.0646	0.4600	0.2723	0.6477	0.4842	0.0198
PC13	-0.0844	-0.1260	-0.0565	0.4040	0.2377	0.5702	0.8047	0.0025

Nycticebus bengalensis

PC	Slope	Slope lower CI	Slope higher CI	Intercept	Intercept lower CI	Intercept higher CI	p value	r squared
PC1	1.3435	0.8721	2.0697	-6.8230	-9.8640	-3.7820	0.1827	0.0870
PC2	1.2033	0.7707	1.8788	-6.1109	-8.9246	-3.2971	0.4771	0.0256
PC3	0.7048	0.4500	1.1038	-3.5790	-5.2391	-1.9190	0.6387	0.0112
PC4	-0.6243	-0.9624	-0.4050	3.1704	1.7549	4.5858	0.1910	0.0839
PC5	-0.5611	-0.8537	-0.3688	2.8493	1.6181	4.0806	0.0841	0.1418
PC6	-0.5430	-0.8473	-0.3479	2.7574	1.4892	4.0255	0.4577	0.0279
PC7	-0.4857	-0.7619	-0.3097	2.4666	1.3183	3.6150	0.7842	0.0038
PC8	-0.4699	-0.7363	-0.2999	2.3864	1.2784	3.4943	0.6691	0.0093
PC9	0.4053	0.2582	0.6362	-2.0582	-3.0181	-1.0983	0.9298	0.0004
PC10	-0.3761	-0.5879	-0.2406	1.9101	1.0283	2.7920	0.5258	0.0204
PC11	-0.3284	-0.5111	-0.2110	1.6677	0.9055	2.4298	0.3721	0.0400
PC12	0.2617	0.1685	0.4064	-1.3289	-1.9329	-0.7250	0.3136	0.0507
PC13	0.2376	0.1519	0.3715	-1.2065	-1.7642	-0.6488	0.5526	0.0179

Nycticebus coucang

PC	Slope	Slope lower CI	Slope higher CI	Intercept	Intercept lower CI	Intercept higher CI	p value	r squared
PC1	-1.0920	-1.3881	-0.8590	5.4407	4.1222	6.7592	0.3583	0.0126
PC2	0.6390	0.5021	0.8132	-3.1839	-3.9590	-2.4087	0.6348	0.0034
PC3	-0.5409	-0.6877	-0.4254	2.6949	2.0415	3.3483	0.3777	0.0116
PC4	0.4506	0.3543	0.5732	-2.2453	-2.7908	-1.6999	0.4755	0.0076
PC5	0.4264	0.3396	0.5353	-2.1244	-2.6118	-1.6370	0.0044	0.1148
PC6	-0.4061	-0.5170	-0.3190	2.0235	1.5301	2.5168	0.8678	0.0004
PC7	-0.3674	-0.4678	-0.2886	1.8308	1.3843	2.2773	0.9939	0.0000
PC8	-0.3348	-0.4263	-0.2630	1.6684	1.2616	2.0751	0.8293	0.0007
PC9	0.2994	0.2353	0.3811	-1.4919	-1.8552	-1.1287	0.6375	0.0033
PC10	-0.2550	-0.3197	-0.2033	1.2703	0.9804	1.5603	0.0030	0.1242
PC11	-0.2445	-0.3087	-0.1936	1.2183	0.9315	1.5050	0.0300	0.0684
PC12	-0.2385	-0.3030	-0.1877	1.1882	0.9011	1.4753	0.2670	0.0184
PC13	-0.2145	-0.2730	-0.1686	1.0689	0.8088	1.3291	0.5948	0.0042

Perodicticus potto

PC	Slope	Slope lower CI	Slope higher CI	Intercept	Intercept lower CI	Intercept higher CI	p value	r squared
PC1	-1.1720	-1.3942	-0.9852	5.9188	4.8860	6.9516	0.2054	0.0126
PC2	0.9077	0.7708	1.0689	-4.5840	-5.3370	-3.8310	0.0000	0.1250
PC3	-0.7238	-0.8608	-0.6087	3.6556	3.0188	4.2923	0.1515	0.0161
PC4	0.6673	0.5668	0.7856	-3.3701	-3.9225	-2.8177	0.0000	0.1287
PC5	0.5817	0.4930	0.6864	-2.9377	-3.4261	-2.4494	0.0002	0.1040
PC6	0.5240	0.4407	0.6231	-2.6464	-3.1070	-2.1857	0.1360	0.0174
PC7	0.4953	0.4160	0.5898	-2.5016	-2.9404	-2.0628	0.6078	0.0021
PC8	-0.4639	-0.5525	-0.3896	2.3430	1.9316	2.7544	0.8913	0.0001
PC9	-0.4166	-0.4958	-0.3500	2.1038	1.7356	2.4720	0.3580	0.0067
PC10	0.4083	0.3429	0.4863	-2.0622	-2.4243	-1.7001	0.8463	0.0003
PC11	0.3770	0.3169	0.4485	-1.9040	-2.2362	-1.5719	0.1939	0.0133
PC12	-0.3210	-0.3818	-0.2699	1.6212	1.3386	1.9038	0.1708	0.0147
PC13	-0.3043	-0.3610	-0.2564	1.5366	1.2724	1.8007	0.0201	0.0418

Goswami model orbit module against ln CS of orbit

Cheirogaleus major

PC	Slope	Slope lower CI	Slope higher CI	Intercept	Intercept lower CI	Intercept higher CI	p value	r squared
PC1	0.6982	0.4716	1.0335	-2.3244	-3.2600	-1.3888	0.0772	0.1295
PC2	0.6050	0.3999	0.9153	-2.0143	-2.8725	-1.1560	0.4533	0.0247
PC3	-0.5724	-0.8571	-0.3822	1.9057	1.1150	2.6964	0.1849	0.0751
PC4	-0.5566	-0.8463	-0.3661	1.8531	1.0536	2.6527	0.9702	0.0001
PC5	0.4409	0.2936	0.6623	-1.4680	-2.0819	-0.8541	0.2362	0.0604
PC6	0.4089	0.2690	0.6215	-1.3614	-1.9484	-0.7744	0.8631	0.0013
PC7	-0.3489	-0.5046	-0.2413	1.1617	0.7234	1.6000	0.0140	0.2353
PC8	0.3179	0.2095	0.4823	-1.0584	-1.5126	-0.6042	0.6239	0.0106
PC9	-0.2916	-0.4427	-0.1921	0.9709	0.5537	1.3881	0.6728	0.0079
PC10	-0.2312	-0.3502	-0.1526	0.7697	0.4407	1.0986	0.5139	0.0188
PC11	-0.2266	-0.3378	-0.1520	0.7544	0.4451	1.0637	0.1299	0.0969
PC12	-0.1909	-0.2862	-0.1274	0.6357	0.3712	0.9002	0.2017	0.0699
PC13	-0.1613	-0.2452	-0.1061	0.5370	0.3054	0.7685	0.8749	0.0011

Cheirogaleus medius

PC	Slope	Slope lower CI	Slope higher CI	Intercept	Intercept lower CI	Intercept higher CI	p value	r squared
PC1	0.9949	0.6899	1.4349	-3.0253	-4.1581	-1.8924	0.0929	0.1010
PC2	-0.8255	-1.2022	-0.5668	2.5100	1.5438	3.4763	0.2440	0.0499
PC3	-0.8089	-1.1832	-0.5530	2.4596	1.5013	3.4180	0.3971	0.0267
PC4	-0.6768	-0.9936	-0.4611	2.0581	1.2483	2.8678	0.6548	0.0075
PC5	0.6187	0.4363	0.8774	-1.8814	-2.5521	-1.2107	0.0198	0.1852
PC6	-0.5463	-0.7769	-0.3841	1.6611	1.0638	2.2583	0.0257	0.1710
PC7	-0.4614	-0.6781	-0.3140	1.4030	0.8494	1.9567	0.8326	0.0017
PC8	-0.4457	-0.6552	-0.3032	1.3553	0.8201	1.8905	0.9319	0.0003
PC9	-0.3317	-0.4844	-0.2272	1.0087	0.6175	1.3999	0.3262	0.0357
PC10	-0.2881	-0.4217	-0.1968	0.8760	0.5341	1.2179	0.4304	0.0232
PC11	-0.2581	-0.3788	-0.1759	0.7849	0.4765	1.0933	0.6008	0.0103
PC12	0.2461	0.1674	0.3617	-0.7483	-1.0437	-0.4529	0.8835	0.0008
PC13	0.1992	0.1355	0.2928	-0.6056	-0.8448	-0.3665	0.9346	0.0003

Microcebus murinus

PC	Slope	Slope lower CI	Slope higher CI	Intercept	Intercept lower CI	Intercept higher CI	p value	r squared
PC1	0.9882	0.7805	1.2513	-2.8025	-3.4701	-2.1348	0.7426	0.0016
PC2	0.8198	0.6509	1.0325	-2.3247	-2.8658	-1.7836	0.0681	0.0468
PC3	0.7749	0.6140	0.9779	-2.1974	-2.7134	-1.6815	0.1453	0.0301
PC4	0.6352	0.5028	0.8026	-1.8014	-2.2267	-1.3762	0.2389	0.0198
PC5	0.5560	0.4418	0.6997	-1.5768	-1.9425	-1.2111	0.0502	0.0537
PC6	-0.5342	-0.6764	-0.4219	1.5149	1.1539	1.8759	0.8011	0.0009
PC7	0.4778	0.3785	0.6032	-1.3549	-1.6737	-1.0362	0.1715	0.0265
PC8	0.4524	0.3572	0.5728	-1.2828	-1.5886	-0.9770	0.8639	0.0004
PC9	-0.4187	-0.5294	-0.3311	1.1873	0.9062	1.4685	0.3300	0.0136
PC10	-0.3777	-0.4781	-0.2984	1.0711	0.8163	1.3260	0.5879	0.0042
PC11	-0.3735	-0.4727	-0.2951	1.0592	0.8074	1.3110	0.5306	0.0056
PC12	0.3332	0.2635	0.4213	-0.9448	-1.1687	-0.7209	0.3592	0.0120
PC13	-0.3218	-0.4049	-0.2558	0.9127	0.7012	1.1242	0.0462	0.0556

Microcebus rufus

PC	Slope	Slope lower CI	Slope higher CI	Intercept	Intercept lower CI	Intercept higher CI	p value	r squared
PC1	-0.5783	-0.8464	-0.3951	1.6619	1.0131	2.3107	0.4280	0.0234
PC2	-0.5435	-0.7988	-0.3698	1.5619	0.9451	2.1788	0.8837	0.0008
PC3	-0.4564	-0.6707	-0.3106	1.3117	0.7941	1.8293	0.7989	0.0024
PC4	0.3886	0.2680	0.5635	-1.1167	-1.5415	-0.6918	0.1579	0.0725
PC5	0.3481	0.2392	0.5066	-1.0003	-1.3848	-0.6158	0.2283	0.0533
PC6	-0.3091	-0.4544	-0.2103	0.8883	0.5374	1.2393	0.9893	0.0000
PC7	0.2725	0.1907	0.3893	-0.7831	-1.0685	-0.4977	0.0387	0.1489
PC8	-0.2358	-0.3437	-0.1618	0.6777	0.4162	0.9392	0.2639	0.0460
PC9	-0.2268	-0.3324	-0.1547	0.6517	0.3962	0.9072	0.5264	0.0150
PC10	0.1848	0.1267	0.2697	-0.5312	-0.7367	-0.3257	0.2921	0.0410
PC11	0.1693	0.1156	0.2481	-0.4867	-0.6772	-0.2961	0.4875	0.0180
PC12	-0.1451	-0.2133	-0.0987	0.4169	0.2522	0.5816	0.9406	0.0002
PC13	-0.1288	-0.1859	-0.0892	0.3701	0.2311	0.5091	0.1007	0.0967

Galago alleni

PC	Slope	Slope lower CI	Slope higher CI	Intercept	Intercept lower CI	Intercept higher CI	p value	r squared
PC1	-1.1492	-1.7641	-0.7487	3.8555	2.1518	5.5591	0.8529	0.0016
PC2	0.7608	0.4960	1.1670	-2.5524	-3.6781	-1.4268	0.7306	0.0055
PC3	0.6096	0.4245	0.8752	-2.0449	-2.8010	-1.2889	0.0055	0.3010
PC4	0.5733	0.3738	0.8792	-1.9233	-2.7711	-1.0755	0.7102	0.0064
PC5	-0.5146	-0.7876	-0.3362	1.7264	0.9692	2.4836	0.5515	0.0164
PC6	0.4352	0.2836	0.6679	-1.4601	-2.1049	-0.8152	0.8130	0.0026
PC7	0.3639	0.2462	0.5378	-1.2207	-1.7100	-0.7313	0.0399	0.1782
PC8	0.3354	0.2212	0.5085	-1.1252	-1.6072	-0.6431	0.2427	0.0615
PC9	-0.2899	-0.4448	-0.1889	0.9726	0.5433	1.4019	0.7744	0.0038
PC10	0.2599	0.1783	0.3788	-0.8719	-1.2082	-0.5356	0.0153	0.2391
PC11	0.2147	0.1398	0.3296	-0.7201	-1.0386	-0.4017	0.9347	0.0003
PC12	0.1781	0.1167	0.2717	-0.5974	-0.8574	-0.3374	0.4047	0.0318
PC13	0.1442	0.0939	0.2214	-0.4837	-0.6977	-0.2698	0.9866	0.0000

Galago demidoff

PC	Slope	Slope lower CI	Slope higher CI	Intercept	Intercept lower CI	Intercept higher CI	p value	r squared
PC1	-1.1445	-1.4846	-0.8824	3.4247	2.5235	4.3258	0.3382	0.0161
PC2	0.9979	0.7677	1.2970	-2.9858	-3.7777	-2.1938	0.8908	0.0003
PC3	-0.7936	-1.0283	-0.6124	2.3745	1.7521	2.9968	0.2439	0.0237
PC4	-0.6001	-0.7744	-0.4651	1.7957	1.3329	2.2586	0.0711	0.0560
PC5	-0.5250	-0.6818	-0.4042	1.5708	1.1553	1.9862	0.5593	0.0060
PC6	0.4680	0.3605	0.6076	-1.4005	-1.7703	-1.0307	0.4655	0.0094
PC7	0.4019	0.3097	0.5216	-1.2026	-1.5198	-0.8854	0.4222	0.0113
PC8	-0.3808	-0.4947	-0.2931	1.1393	0.8377	1.4409	0.6329	0.0040
PC9	-0.3385	-0.4381	-0.2616	1.0129	0.7487	1.2771	0.1686	0.0330
PC10	-0.3221	-0.4131	-0.2511	0.9638	0.7214	1.2062	0.0141	0.1010
PC11	0.3100	0.2392	0.4018	-0.9276	-1.1708	-0.6844	0.2494	0.0232
PC12	-0.2425	-0.3148	-0.1868	0.7256	0.5341	0.9171	0.4476	0.0102
PC13	-0.2332	-0.3031	-0.1795	0.6979	0.5128	0.8829	0.7947	0.0012

Galago elegantulus

PC	Slope	Slope lower CI	Slope higher CI	Intercept	Intercept lower CI	Intercept higher CI	p value	r squared
PC1	2.5055	1.7614	3.5639	-8.3652	-11.3747	-5.3558	0.8024	0.0020
PC2	-1.8555	-2.6219	-1.3131	6.1951	4.0102	8.3800	0.2520	0.0408
PC3	1.2818	0.9204	1.7851	-4.2797	-5.7232	-2.8361	0.0423	0.1227
PC4	0.9293	0.6544	1.3197	-3.1028	-4.2135	-1.9922	0.5383	0.0119
PC5	-0.8882	-1.2635	-0.6243	2.9654	1.8984	4.0325	0.8280	0.0015
PC6	0.8303	0.5835	1.1815	-2.7722	-3.7705	-1.7739	0.9965	0.0000
PC7	-0.6655	-0.9464	-0.4679	2.2218	1.4229	3.0207	0.7572	0.0030
PC8	0.5416	0.3835	0.7649	-1.8083	-2.4451	-1.1714	0.2366	0.0435
PC9	-0.5068	-0.7177	-0.3579	1.6922	1.0915	2.2928	0.3404	0.0284
PC10	-0.4304	-0.6122	-0.3026	1.4370	0.9202	1.9538	0.7719	0.0027
PC11	0.4049	0.2852	0.5746	-1.3517	-1.8349	-0.8686	0.4931	0.0148
PC12	0.3487	0.2451	0.4962	-1.1643	-1.5835	-0.7450	0.9604	0.0001
PC13	0.2982	0.2141	0.4153	-0.9956	-1.3316	-0.6596	0.0431	0.1217

Galago moholi

PC	Slope	Slope lower CI	Slope higher CI	Intercept	Intercept lower CI	Intercept higher CI	p value	r squared
PC1	-1.0516	-1.3274	-0.8332	3.3181	2.5382	4.0979	0.3208	0.0139
PC2	0.7031	0.5598	0.8832	-2.2185	-2.7288	-1.7082	0.0449	0.0554
PC3	0.5488	0.4363	0.6902	-1.7315	-2.1320	-1.3309	0.0724	0.0447
PC4	-0.4921	-0.6218	-0.3894	1.5525	1.1859	1.9192	0.5799	0.0043
PC5	0.4183	0.3309	0.5288	-1.3198	-1.6322	-1.0074	0.9875	0.0000
PC6	-0.3958	-0.5000	-0.3134	1.2489	0.9544	1.5435	0.4726	0.0073
PC7	0.3546	0.2807	0.4481	-1.1189	-1.3830	-0.8548	0.5371	0.0054
PC8	-0.3231	-0.4034	-0.2588	1.0195	0.7914	1.2475	0.0048	0.1065
PC9	0.2956	0.2340	0.3733	-0.9326	-1.1524	-0.7128	0.4362	0.0086
PC10	-0.2794	-0.3492	-0.2235	0.8814	0.6832	1.0797	0.0074	0.0968
PC11	0.2478	0.1970	0.3116	-0.7817	-0.9625	-0.6010	0.0693	0.0457
PC12	-0.2267	-0.2866	-0.1793	0.7153	0.5460	0.8846	0.9078	0.0002
PC13	0.2070	0.1643	0.2609	-0.6531	-0.8055	-0.5007	0.1571	0.0280

Galago senegalensis

PC	Slope	Slope lower CI	Slope higher CI	Intercept	Intercept lower CI	Intercept higher CI	p value	r squared
PC1	-0.9704	-1.1219	-0.8394	3.1407	2.6836	3.5978	0.0011	0.0597
PC2	-0.7466	-0.8614	-0.6471	2.4164	2.0696	2.7632	0.0001	0.0855
PC3	0.5978	0.5150	0.6940	-1.9348	-2.2246	-1.6449	0.4259	0.0037
PC4	0.5541	0.4776	0.6428	-1.7933	-2.0607	-1.5259	0.1367	0.0128
PC5	-0.5060	-0.5857	-0.4371	1.6375	1.3971	1.8780	0.0059	0.0429
PC6	0.4911	0.4229	0.5703	-1.5893	-1.8278	-1.3508	0.9118	0.0001
PC7	-0.4029	-0.4620	-0.3513	1.3039	1.1247	1.4831	0.0000	0.1611
PC8	-0.3788	-0.4397	-0.3263	1.2259	1.0424	1.4095	0.3679	0.0047
PC9	-0.3414	-0.3963	-0.2942	1.1051	0.9399	1.2702	0.2323	0.0082
PC10	-0.3326	-0.3862	-0.2864	1.0763	0.9148	1.2378	0.8276	0.0003
PC11	-0.2842	-0.3289	-0.2457	0.9199	0.7853	1.0546	0.0033	0.0488
PC12	-0.2622	-0.3044	-0.2258	0.8486	0.7214	0.9757	0.4306	0.0036
PC13	-0.2216	-0.2574	-0.1909	0.7173	0.6096	0.8249	0.7849	0.0004

Galago zanzibaricus

PC	Slope	Slope lower CI	Slope higher CI	Intercept	Intercept lower CI	Intercept higher CI	p value	r squared
PC1	-1.4966	-2.2236	-1.0072	4.7030	2.7915	6.6144	0.1013	0.1124
PC2	-0.7730	-1.1599	-0.5152	2.4293	1.4163	3.4424	0.2164	0.0656
PC3	0.5491	0.3642	0.8278	-1.7255	-2.4541	-0.9968	0.3264	0.0419
PC4	0.4903	0.3257	0.7380	-1.5408	-2.1887	-0.8928	0.2840	0.0497
PC5	0.4316	0.2839	0.6559	-1.3562	-1.9408	-0.7715	0.8537	0.0015
PC6	0.3873	0.2557	0.5866	-1.2170	-1.7370	-0.6969	0.5120	0.0189
PC7	-0.3708	-0.5232	-0.2627	1.1651	0.7558	1.5744	0.0024	0.3369
PC8	0.3241	0.2160	0.4862	-1.0185	-1.4432	-0.5939	0.2145	0.0662
PC9	0.2821	0.1857	0.4287	-0.8866	-1.2685	-0.5047	0.7876	0.0032
PC10	-0.2525	-0.3772	-0.1690	0.7935	0.4663	1.1206	0.1536	0.0865
PC11	0.2048	0.1357	0.3090	-0.6436	-0.9158	-0.3713	0.3474	0.0385
PC12	0.1904	0.1256	0.2888	-0.5984	-0.8549	-0.3419	0.5913	0.0127
PC13	0.1740	0.1159	0.2611	-0.5467	-0.7750	-0.3185	0.2245	0.0634

Otolemur crassicaudatus

PC	Slope	Slope lower CI	Slope higher CI	Intercept	Intercept lower CI	Intercept higher CI	p value	r squared
PC1	0.6830	0.5632	0.8283	-2.4742	-2.9545	-1.9939	0.0206	0.0530
PC2	0.4636	0.3956	0.5434	-1.6795	-1.9473	-1.4117	0.0000	0.3609
PC3	0.4357	0.3610	0.5257	-1.5781	-1.8765	-1.2798	0.0011	0.1018
PC4	0.3429	0.2829	0.4157	-1.2422	-1.4829	-1.0016	0.0164	0.0568
PC5	-0.3272	-0.3974	-0.2694	1.1852	0.9534	1.4170	0.0487	0.0387
PC6	0.2930	0.2406	0.3568	-1.0614	-1.2719	-0.8510	0.2770	0.0119
PC7	0.2707	0.2221	0.3301	-0.9807	-1.1763	-0.7851	0.9084	0.0001
PC8	-0.2409	-0.2936	-0.1976	0.8726	0.6987	1.0465	0.6644	0.0019
PC9	-0.2307	-0.2807	-0.1896	0.8357	0.6707	1.0008	0.1607	0.0198
PC10	-0.2181	-0.2653	-0.1793	0.7902	0.6344	0.9460	0.1330	0.0227
PC11	-0.2053	-0.2503	-0.1684	0.7436	0.5953	0.8919	0.8462	0.0004
PC12	-0.1877	-0.2288	-0.1539	0.6798	0.5442	0.8154	0.8997	0.0002
PC13	0.1730	0.1419	0.2108	-0.6265	-0.7515	-0.5015	0.9535	0.0000

Otolemur garnettii

PC	Slope	Slope lower CI	Slope higher CI	Intercept	Intercept lower CI	Intercept higher CI	p value	r squared
PC1	-0.8426	-1.0255	-0.6923	2.9921	2.4005	3.5838	0.0060	0.0782
PC2	-0.5698	-0.6802	-0.4773	2.0233	1.6629	2.3838	0.0000	0.2519
PC3	-0.4581	-0.5617	-0.3735	1.6267	1.2925	1.9608	0.4888	0.0052
PC4	-0.4177	-0.5124	-0.3405	1.4833	1.1782	1.7884	0.6422	0.0023
PC5	-0.3569	-0.4310	-0.2956	1.2674	1.0269	1.5080	0.0001	0.1510
PC6	-0.3291	-0.4036	-0.2683	1.1687	0.9283	1.4090	0.5900	0.0031
PC7	-0.3129	-0.3839	-0.2550	1.1111	0.8822	1.3399	0.9063	0.0001
PC8	0.2810	0.2303	0.3429	-0.9980	-1.1980	-0.7980	0.0246	0.0532
PC9	-0.2637	-0.3229	-0.2154	0.9365	0.7456	1.1275	0.1682	0.0203
PC10	0.2477	0.2034	0.3017	-0.8796	-1.0542	-0.7050	0.0089	0.0713
PC11	0.2167	0.1768	0.2656	-0.7694	-0.9271	-0.6118	0.3307	0.0102
PC12	-0.1882	-0.2309	-0.1534	0.6684	0.5308	0.8060	0.7556	0.0010
PC13	0.1842	0.1502	0.2260	-0.6542	-0.7889	-0.5195	0.9934	0.0000

Avahi laniger

PC	Slope	Slope lower CI	Slope higher CI	Intercept	Intercept lower CI	Intercept higher CI	p value	r squared
PC1	2.3465	1.5940	3.4542	-8.0199	-11.1991	-4.8406	0.0185	0.2370
PC2	1.9806	1.2807	3.0632	-6.7696	-9.8161	-3.7231	0.5564	0.0167
PC3	1.4580	0.9557	2.2244	-4.9832	-7.1516	-2.8149	0.1888	0.0807
PC4	-1.1641	-1.8036	-0.7514	3.9789	2.1806	5.7771	0.6798	0.0083
PC5	1.0198	0.6591	1.5778	-3.4854	-5.0555	-1.9153	0.5810	0.0147
PC6	0.8008	0.5233	1.2255	-2.7371	-3.9371	-1.5370	0.2342	0.0667
PC7	0.7213	0.4657	1.1171	-2.4652	-3.5785	-1.3520	0.6511	0.0099
PC8	-0.6577	-1.0207	-0.4238	2.2479	1.2279	3.2680	0.9387	0.0003
PC9	-0.4826	-0.7387	-0.3152	1.6493	0.9255	2.3731	0.2402	0.0650
PC10	-0.4448	-0.6889	-0.2872	1.5201	0.8336	2.2066	0.6528	0.0098
PC11	0.4187	0.2699	0.6495	-1.4310	-2.0798	-0.7823	0.8300	0.0022
PC12	0.3569	0.2328	0.5470	-1.2197	-1.7567	-0.6827	0.2647	0.0589
PC13	0.3081	0.1996	0.4756	-1.0531	-1.5249	-0.5813	0.4670	0.0255

Indri indri

PC	Slope	Slope lower CI	Slope higher CI	Intercept	Intercept lower CI	Intercept higher CI	p value	r squared
PC1	-1.8297	-2.4553	-1.3635	7.1454	5.0132	9.2775	0.0046	0.1976
PC2	1.3388	0.9680	1.8516	-5.2283	-6.9536	-3.5030	0.4068	0.0187
PC3	-1.0782	-1.4785	-0.7863	4.2107	2.8590	5.5624	0.1001	0.0714
PC4	0.8368	0.6033	1.1607	-3.2678	-4.3563	-2.1793	0.9525	0.0001
PC5	0.7418	0.5403	1.0184	-2.8968	-3.8305	-1.9632	0.1204	0.0640
PC6	0.6662	0.4807	0.9232	-2.6017	-3.4656	-1.7377	0.6326	0.0062
PC7	-0.5465	-0.7440	-0.4014	2.1340	1.4650	2.8030	0.0353	0.1143
PC8	-0.5016	-0.6954	-0.3617	1.9587	1.3071	2.6104	0.7550	0.0027
PC9	-0.4659	-0.6453	-0.3364	1.8196	1.2164	2.4228	0.5510	0.0097
PC10	-0.4007	-0.5549	-0.2893	1.5648	1.0463	2.0833	0.5336	0.0106
PC11	0.3725	0.2697	0.5144	-1.4546	-1.9324	-0.9768	0.3120	0.0276
PC12	0.3568	0.2579	0.4936	-1.3934	-1.8536	-0.9332	0.4271	0.0171
PC13	-0.3366	-0.4646	-0.2438	1.3143	0.8831	1.7455	0.2915	0.0300

Propithecus diadema

PC	Slope	Slope lower CI	Slope higher CI	Intercept	Intercept lower CI	Intercept higher CI	p value	r squared
PC1	1.1061	0.7474	1.6370	-4.2108	-5.9044	-2.5172	0.7260	0.0048
PC2	0.8409	0.5684	1.2439	-3.2011	-4.4870	-1.9152	0.6651	0.0073
PC3	-0.7601	-1.1056	-0.5226	2.8935	1.7837	4.0033	0.1108	0.0949
PC4	0.6346	0.4299	0.9366	-2.4157	-3.3802	-1.4511	0.4834	0.0191
PC5	-0.6070	-0.8984	-0.4101	2.3108	1.3812	3.2404	0.7355	0.0045
PC6	-0.4588	-0.6794	-0.3099	1.7467	1.0433	2.4502	0.8136	0.0022
PC7	0.3899	0.2652	0.5731	-1.4842	-2.0702	-0.8982	0.3013	0.0410
PC8	-0.3124	-0.4627	-0.2110	1.1894	0.7101	1.6687	0.8696	0.0011
PC9	0.2806	0.1894	0.4155	-1.0680	-1.4984	-0.6377	0.8658	0.0011
PC10	0.2643	0.1820	0.3838	-1.0061	-1.3902	-0.6221	0.0948	0.1036
PC11	0.2388	0.1736	0.3285	-0.9089	-1.2038	-0.6141	0.0009	0.3526
PC12	-0.2157	-0.3167	-0.1469	0.8210	0.4977	1.1442	0.2720	0.0462
PC13	-0.2072	-0.3062	-0.1402	0.7888	0.4729	1.1048	0.5641	0.0130

Propithecus verreauxi

PC	Slope	Slope lower CI	Slope higher CI	Intercept	Intercept lower CI	Intercept higher CI	p value	r squared
PC1	1.1172	0.8191	1.5237	-4.1709	-5.4865	-2.8553	0.9494	0.0001
PC2	-0.8363	-1.1143	-0.6277	3.1225	2.2141	4.0308	0.0105	0.1494
PC3	0.7492	0.5755	0.9753	-2.7970	-3.5434	-2.0506	0.0002	0.2843
PC4	0.6467	0.4745	0.8813	-2.4145	-3.1740	-1.6550	0.6325	0.0056
PC5	-0.5264	-0.7177	-0.3861	1.9653	1.3463	2.5844	0.7290	0.0030
PC6	-0.4990	-0.6796	-0.3665	1.8632	1.2786	2.4477	0.5069	0.0108
PC7	0.4564	0.3352	0.6215	-1.7040	-2.2384	-1.1695	0.4969	0.0113
PC8	-0.3798	-0.5129	-0.2813	1.4180	0.9856	1.8504	0.0978	0.0654
PC9	-0.3498	-0.4770	-0.2565	1.3060	0.8944	1.7176	0.7982	0.0016
PC10	-0.3263	-0.4447	-0.2394	1.2182	0.8350	1.6014	0.6326	0.0056
PC11	0.2904	0.2172	0.3884	-1.0843	-1.4040	-0.7647	0.0192	0.1266
PC12	0.2547	0.1877	0.3457	-0.9510	-1.2460	-0.6560	0.2433	0.0330
PC13	-0.2333	-0.3180	-0.1711	0.8709	0.5965	1.1452	0.7512	0.0025

Eulemur fulvus

PC	Slope	Slope lower CI	Slope higher CI	Intercept	Intercept lower CI	Intercept higher CI	p value	r squared
PC1	-0.9538	-1.1071	-0.8217	3.5630	3.0299	4.0962	0.3109	0.0059
PC2	-0.7962	-0.9246	-0.6857	2.9745	2.5281	3.4209	0.9905	0.0000
PC3	-0.6156	-0.7127	-0.5318	2.2998	1.9618	2.6378	0.0071	0.0411
PC4	-0.6039	-0.7010	-0.5202	2.2558	1.9180	2.5937	0.4036	0.0040
PC5	-0.5411	-0.6282	-0.4661	2.0215	1.7188	2.3242	0.3849	0.0044
PC6	-0.5264	-0.6106	-0.4538	1.9665	1.6738	2.2593	0.0948	0.0160
PC7	0.4444	0.3830	0.5156	-1.6601	-1.9078	-1.4124	0.1583	0.0115
PC8	-0.4298	-0.4987	-0.3704	1.6056	1.3660	1.8452	0.1622	0.0113
PC9	0.4080	0.3515	0.4735	-1.5241	-1.7520	-1.2961	0.2718	0.0070
PC10	0.4029	0.3472	0.4675	-1.5050	-1.7297	-1.2803	0.1782	0.0105
PC11	-0.3757	-0.4357	-0.3240	1.4036	1.1950	1.6122	0.0672	0.0192
PC12	0.3540	0.3055	0.4103	-1.3225	-1.5183	-1.1268	0.0288	0.0273
PC13	0.3187	0.2745	0.3701	-1.1906	-1.3693	-1.0119	0.9323	0.0000

Eulemur macaco

PC	Slope	Slope lower CI	Slope higher CI	Intercept	Intercept lower CI	Intercept higher CI	p value	r squared
PC1	1.0088	0.7709	1.3202	-3.7980	-4.8320	-2.7639	0.2634	0.0235
PC2	-0.9760	-1.2786	-0.7450	3.6743	2.6698	4.6789	0.3671	0.0154
PC3	0.8982	0.6874	1.1736	-3.3813	-4.2965	-2.4661	0.1714	0.0350
PC4	0.7920	0.6112	1.0263	-2.9815	-3.7629	-2.2001	0.0219	0.0952
PC5	-0.7535	-0.9891	-0.5739	2.8365	2.0550	3.6180	0.9682	0.0000
PC6	-0.6242	-0.8183	-0.4761	2.3499	1.7058	2.9941	0.4620	0.0103
PC7	0.6182	0.4754	0.8038	-2.3272	-2.9453	-1.7090	0.0499	0.0706
PC8	-0.5104	-0.6597	-0.3949	1.9215	1.4232	2.4199	0.0117	0.1140
PC9	0.4948	0.3791	0.6460	-1.8629	-2.3653	-1.3605	0.1340	0.0419
PC10	0.4316	0.3288	0.5665	-1.6248	-2.0723	-1.1774	0.8158	0.0010
PC11	0.4093	0.3128	0.5356	-1.5408	-1.9603	-1.1214	0.2615	0.0237
PC12	0.3833	0.2920	0.5031	-1.4429	-1.8404	-1.0454	0.8966	0.0003
PC13	0.3386	0.2579	0.4445	-1.2746	-1.6258	-0.9234	0.9984	0.0000

Eulemur mongoz

PC	Slope	Slope lower CI	Slope higher CI	Intercept	Intercept lower CI	Intercept higher CI	p value	r squared
PC1	1.0716	0.8192	1.4019	-3.9645	-5.0424	-2.8866	0.5445	0.0068
PC2	-0.7692	-0.9855	-0.6003	2.8457	2.1333	3.5580	0.0024	0.1580
PC3	-0.6668	-0.8717	-0.5100	2.4665	1.7976	3.1354	0.4226	0.0119
PC4	0.6154	0.4701	0.8056	-2.2763	-2.8968	-1.6558	0.7440	0.0020
PC5	0.5999	0.4620	0.7790	-2.2194	-2.8056	-1.6332	0.0627	0.0627
PC6	0.4982	0.3806	0.6523	-1.8426	-2.3452	-1.3400	0.8098	0.0011
PC7	-0.4742	-0.6203	-0.3624	1.7538	1.2767	2.2308	0.5571	0.0064
PC8	0.4462	0.3408	0.5842	-1.6508	-2.1010	-1.2005	0.8702	0.0005
PC9	-0.4033	-0.5233	-0.3108	1.4917	1.0988	1.8847	0.0521	0.0681
PC10	0.3491	0.2673	0.4560	-1.2918	-1.6409	-0.9427	0.3204	0.0183
PC11	0.3358	0.2572	0.4386	-1.2424	-1.5780	-0.9068	0.2990	0.0200
PC12	0.3211	0.2455	0.4200	-1.1875	-1.5103	-0.8646	0.5267	0.0075
PC13	0.2800	0.2146	0.3653	-1.0352	-1.3139	-0.7565	0.2260	0.0270

Eulemur rubriventer

PC	Slope	Slope lower CI	Slope higher CI	Intercept	Intercept lower CI	Intercept higher CI	p value	r squared
PC1	-1.4482	-1.9693	-1.0651	5.4365	3.7393	7.1337	0.0002	0.4256
PC2	-1.2105	-1.8041	-0.8122	4.5440	2.6820	6.4059	0.6105	0.0105
PC3	-1.0249	-1.5300	-0.6866	3.8475	2.2643	5.4306	0.8168	0.0022
PC4	0.7913	0.5340	1.1726	-2.9703	-4.1689	-1.7718	0.3146	0.0404
PC5	-0.6645	-0.9923	-0.4450	2.4943	1.4670	3.5216	0.9216	0.0004
PC6	0.6093	0.4111	0.9030	-2.2872	-3.2105	-1.3639	0.3197	0.0396
PC7	-0.5738	-0.8510	-0.3869	2.1541	1.2831	3.0251	0.3400	0.0365
PC8	0.5360	0.3630	0.7913	-2.0120	-2.8158	-1.2081	0.2211	0.0593
PC9	0.4520	0.3048	0.6703	-1.6966	-2.3827	-1.0106	0.3401	0.0365
PC10	-0.4162	-0.6206	-0.2792	1.5624	0.9215	2.2033	0.6486	0.0084
PC11	0.3900	0.2616	0.5814	-1.4640	-2.0643	-0.8637	0.6361	0.0091
PC12	0.3382	0.2266	0.5047	-1.2695	-1.7915	-0.7474	0.7739	0.0034
PC13	-0.3155	-0.4709	-0.2113	1.1842	0.6970	1.6715	0.8081	0.0024

Hapalemur griseus

PC	Slope	Slope lower CI	Slope higher CI	Intercept	Intercept lower CI	Intercept higher CI	p value	r squared
PC1	-1.5861	-2.3663	-1.0631	5.5719	3.2826	7.8613	0.7191	0.0053
PC2	-0.8692	-1.2817	-0.5894	3.0535	1.8372	4.2697	0.1989	0.0651
PC3	-0.7834	-1.1699	-0.5246	2.7521	1.6184	3.8859	0.9882	0.0000
PC4	-0.6635	-0.9902	-0.4446	2.3309	1.3725	3.2894	0.7615	0.0038
PC5	0.6494	0.4353	0.9686	-2.2812	-3.2181	-1.3444	0.6978	0.0061
PC6	-0.5174	-0.6922	-0.3868	1.8178	1.2813	2.3543	0.0001	0.4867
PC7	-0.4843	-0.7043	-0.3330	1.7013	1.0491	2.3536	0.0605	0.1339
PC8	0.4152	0.2804	0.6148	-1.4586	-2.0462	-0.8710	0.2948	0.0438
PC9	-0.4006	-0.5982	-0.2683	1.4073	0.8278	1.9868	0.8942	0.0007
PC10	-0.3696	-0.5519	-0.2475	1.2983	0.7635	1.8332	0.9517	0.0001
PC11	-0.3643	-0.5395	-0.2460	1.2799	0.7643	1.7954	0.2945	0.0439
PC12	-0.2819	-0.4208	-0.1889	0.9904	0.5831	1.3977	0.7767	0.0033
PC13	-0.2467	-0.3658	-0.1663	0.8665	0.5160	1.2171	0.3459	0.0356

Lemur catta

PC	Slope	Slope lower CI	Slope higher CI	Intercept	Intercept lower CI	Intercept higher CI	p value	r squared
PC1	-0.8778	-1.2482	-0.6173	3.2163	2.0602	4.3723	0.7278	0.0038
PC2	-0.8398	-1.1852	-0.5951	3.0773	1.9961	4.1585	0.2125	0.0481
PC3	-0.6012	-0.8551	-0.4227	2.2029	1.4106	2.9952	0.7692	0.0027
PC4	0.5383	0.3813	0.7600	-1.9725	-2.6665	-1.2785	0.2258	0.0455
PC5	-0.4687	-0.6665	-0.3296	1.7174	1.1000	2.3348	0.7363	0.0036
PC6	-0.4265	-0.5840	-0.3115	1.5629	1.0636	2.0622	0.0060	0.2131
PC7	0.3830	0.2692	0.5449	-1.4033	-1.9085	-0.8980	0.9071	0.0004
PC8	-0.3491	-0.4962	-0.2456	1.2792	0.8200	1.7384	0.6499	0.0065
PC9	0.3405	0.2407	0.4816	-1.2476	-1.6891	-0.8061	0.2924	0.0346
PC10	0.3229	0.2276	0.4583	-1.1833	-1.6060	-0.7605	0.4767	0.0159
PC11	0.2993	0.2106	0.4253	-1.0967	-1.4901	-0.7034	0.6098	0.0082
PC12	0.2676	0.1889	0.3792	-0.9806	-1.3294	-0.6319	0.3714	0.0250
PC13	0.2298	0.1616	0.3267	-0.8421	-1.1446	-0.5395	0.6969	0.0048

Varecia variegata

PC	Slope	Slope lower CI	Slope higher CI	Intercept	Intercept lower CI	Intercept higher CI	p value	r squared
PC1	1.1424	0.8363	1.5605	-4.4074	-5.8045	-3.0104	0.0567	0.0947
PC2	-0.9945	-1.2996	-0.7611	3.8369	2.7981	4.8757	0.0001	0.3395
PC3	0.7812	0.5681	1.0741	-3.0138	-3.9899	-2.0377	0.1511	0.0549
PC4	0.6789	0.4957	0.9297	-2.6191	-3.4563	-1.7819	0.0825	0.0793
PC5	0.5301	0.3827	0.7342	-2.0451	-2.7231	-1.3670	0.5543	0.0095
PC6	0.4694	0.3402	0.6477	-1.8109	-2.4043	-1.2175	0.2721	0.0325
PC7	0.4468	0.3221	0.6198	-1.7237	-2.2980	-1.1495	0.9528	0.0001
PC8	0.3705	0.2672	0.5138	-1.4293	-1.9051	-0.9535	0.8047	0.0017
PC9	0.3198	0.2307	0.4433	-1.2339	-1.6440	-0.8238	0.6823	0.0046
PC10	-0.3070	-0.4234	-0.2226	1.1843	0.7969	1.5717	0.2492	0.0357
PC11	-0.2968	-0.4095	-0.2151	1.1451	0.7702	1.5201	0.2606	0.0341
PC12	-0.2839	-0.3927	-0.2053	1.0954	0.7337	1.4571	0.4231	0.0174
PC13	-0.2539	-0.3512	-0.1835	0.9795	0.6559	1.3031	0.4361	0.0165

Lepilemur ruficaudatus

PC	Slope	Slope lower CI	Slope higher CI	Intercept	Intercept lower CI	Intercept higher CI	p value	r squared
PC1	0.8427	0.5547	1.2800	-2.8310	-4.0495	-1.6125	0.7458	0.0047
PC2	-0.7382	-1.1139	-0.4893	2.4801	1.4307	3.5295	0.3501	0.0381
PC3	0.7039	0.4658	1.0637	-2.3648	-3.3694	-1.3602	0.4046	0.0304
PC4	-0.6200	-0.9023	-0.4261	2.0831	1.2831	2.8830	0.0221	0.2075
PC5	-0.4923	-0.7467	-0.3245	1.6538	0.9446	2.3630	0.6012	0.0121
PC6	-0.4416	-0.6695	-0.2913	1.4837	0.8483	2.1192	0.5671	0.0145
PC7	0.4263	0.2812	0.6464	-1.4323	-2.0458	-0.8187	0.5721	0.0141
PC8	0.3820	0.2520	0.5792	-1.2834	-1.8333	-0.7336	0.5754	0.0138
PC9	0.2944	0.1999	0.4336	-0.9891	-1.3817	-0.5964	0.0529	0.1534
PC10	-0.2709	-0.4110	-0.1786	0.9102	0.5198	1.3007	0.6145	0.0112
PC11	-0.2539	-0.3841	-0.1678	0.8529	0.4896	1.2163	0.4513	0.0249
PC12	-0.2274	-0.3458	-0.1496	0.7641	0.4345	1.0938	0.9454	0.0002
PC13	-0.1858	-0.2808	-0.1229	0.6242	0.3589	0.8894	0.4090	0.0298

Loris tardigradus

PC	Slope	Slope lower CI	Slope higher CI	Intercept	Intercept lower CI	Intercept higher CI	p value	r squared
PC1	-0.5756	-0.8498	-0.3900	1.9061	1.1442	2.6681	0.2183	0.0600
PC2	0.5464	0.3690	0.8089	-1.8092	-2.5383	-1.0802	0.2886	0.0449
PC3	0.3770	0.2550	0.5574	-1.2484	-1.7494	-0.7473	0.2506	0.0524
PC4	0.3088	0.2168	0.4398	-1.0225	-1.3920	-0.6529	0.0111	0.2313
PC5	0.2832	0.2017	0.3977	-0.9377	-1.2625	-0.6130	0.0035	0.2943
PC6	0.2320	0.1556	0.3461	-0.7684	-1.0841	-0.4526	0.6776	0.0070
PC7	-0.1935	-0.2864	-0.1307	0.6407	0.3827	0.8986	0.2805	0.0464
PC8	-0.1594	-0.2311	-0.1099	0.5278	0.3270	0.7286	0.0470	0.1486
PC9	-0.1396	-0.2084	-0.0935	0.4623	0.2717	0.6528	0.8723	0.0011
PC10	-0.1040	-0.1553	-0.0697	0.3444	0.2025	0.4863	0.8527	0.0014
PC11	-0.0977	-0.1457	-0.0656	0.3236	0.1909	0.4564	0.6021	0.0110
PC12	-0.0920	-0.1369	-0.0618	0.3045	0.1800	0.4290	0.5133	0.0173
PC13	-0.0808	-0.1206	-0.0541	0.2674	0.1571	0.3777	0.9826	0.0000

Nycticebus bengalensis

PC	Slope	Slope lower CI	Slope higher CI	Intercept	Intercept lower CI	Intercept higher CI	p value	r squared
PC1	1.6014	1.0322	2.4845	-5.6685	-8.2390	-3.0980	0.2939	0.0549
PC2	1.4342	0.9234	2.2276	-5.0768	-7.3851	-2.7686	0.3175	0.0499
PC3	-0.8400	-1.3187	-0.5351	2.9734	1.5865	4.3603	0.9537	0.0002
PC4	-0.7441	-1.1578	-0.4782	2.6339	1.4311	3.8367	0.3627	0.0416
PC5	-0.6688	-1.0182	-0.4392	2.3672	1.3425	3.3919	0.0877	0.1389
PC6	-0.6472	-0.9925	-0.4220	2.2908	1.2811	3.3005	0.1370	0.1071
PC7	0.5789	0.3698	0.9064	-2.0493	-2.9991	-1.0994	0.6186	0.0126
PC8	-0.5601	-0.8710	-0.3602	1.9826	1.0785	2.8866	0.3467	0.0444
PC9	0.4831	0.3082	0.7570	-1.7099	-2.5043	-0.9156	0.6890	0.0082
PC10	-0.4483	-0.7011	-0.2867	1.5869	0.8535	2.3204	0.5489	0.0182
PC11	-0.3914	-0.6090	-0.2516	1.3855	0.7529	2.0181	0.3609	0.0419
PC12	0.3119	0.2033	0.4784	-1.1041	-1.5910	-0.6171	0.1391	0.1061
PC13	-0.2832	-0.4438	-0.1807	1.0023	0.5367	1.4680	0.6899	0.0081

Nycticebus coucang

PC	Slope	Slope lower CI	Slope higher CI	Intercept	Intercept lower CI	Intercept higher CI	p value	r squared
PC1	-1.1240	-1.4244	-0.8870	3.8962	2.9647	4.8278	0.1040	0.0390
PC2	0.6578	0.5169	0.8371	-2.2801	-2.8351	-1.7250	0.6162	0.0038
PC3	-0.5568	-0.7055	-0.4394	1.9299	1.4686	2.3912	0.1013	0.0396
PC4	0.4639	0.3644	0.5906	-1.6080	-2.0001	-1.2158	0.9993	0.0000
PC5	0.4389	0.3478	0.5539	-1.5213	-1.8786	-1.1641	0.0246	0.0731
PC6	-0.4180	-0.5320	-0.3285	1.4491	1.0962	1.8019	0.6432	0.0032
PC7	0.3782	0.2972	0.4814	-1.3111	-1.6304	-0.9918	0.6602	0.0029
PC8	-0.3447	-0.4388	-0.2707	1.1948	0.9034	1.4862	0.9175	0.0002
PC9	0.3082	0.2423	0.3921	-1.0684	-1.3282	-0.8086	0.5188	0.0062
PC10	-0.2625	-0.3299	-0.2088	0.9097	0.6997	1.1198	0.0069	0.1040
PC11	-0.2517	-0.3170	-0.1998	0.8724	0.6693	1.0756	0.0132	0.0883
PC12	-0.2455	-0.3120	-0.1931	0.8509	0.6449	1.0569	0.3240	0.0145
PC13	0.2208	0.1735	0.2812	-0.7655	-0.9522	-0.5788	0.9772	0.0000

Perodicticus potto

PC	Slope	Slope lower CI	Slope higher CI	Intercept	Intercept lower CI	Intercept higher CI	p value	r squared
PC1	-1.0701	-1.2744	-0.8986	3.7155	3.0630	4.3680	0.8633	0.0002
PC2	0.8288	0.7049	0.9744	-2.8776	-3.3456	-2.4096	0.0000	0.1425
PC3	-0.6609	-0.7869	-0.5551	2.2948	1.8923	2.6972	0.5428	0.0029
PC4	0.6093	0.5187	0.7157	-2.1156	-2.4576	-1.7735	0.0000	0.1525
PC5	0.5311	0.4489	0.6284	-1.8442	-2.1559	-1.5325	0.0019	0.0737
PC6	0.4785	0.4022	0.5693	-1.6613	-1.9514	-1.3711	0.2371	0.0110
PC7	0.4523	0.3799	0.5384	-1.5704	-1.8456	-1.2951	0.4797	0.0039
PC8	-0.4236	-0.5044	-0.3558	1.4708	1.2128	1.7288	0.5963	0.0022
PC9	-0.3804	-0.4518	-0.3202	1.3206	1.0923	1.5490	0.0470	0.0307
PC10	-0.3728	-0.4439	-0.3132	1.2945	1.0676	1.5215	0.4905	0.0038
PC11	0.3442	0.2894	0.4095	-1.1953	-1.4038	-0.9868	0.1904	0.0135
PC12	-0.2931	-0.3485	-0.2466	1.0177	0.8408	1.1946	0.1063	0.0204
PC13	-0.2778	-0.3297	-0.2341	0.9646	0.7985	1.1307	0.0259	0.0385

Goswami model oral module against ln CS whole cranium

Cheirogaleus major

PC	Slope	Slope lower CI	Slope higher CI	Intercept	Intercept lower CI	Intercept higher CI	p value	r squared
PC1	1.5247	1.0079	2.3065	-7.4087	-10.5641	-4.2534	0.4482	0.0252
PC2	0.9955	0.6629	1.4950	-4.8374	-6.8593	-2.8155	0.2333	0.0612
PC3	0.5982	0.4011	0.8921	-2.9069	-4.0999	-1.7139	0.1341	0.0949
PC4	0.3801	0.2504	0.5770	-1.8468	-2.6405	-1.0532	0.6780	0.0076
PC5	0.3572	0.2428	0.5255	-1.7355	-2.4225	-1.0486	0.0491	0.1580
PC6	0.2782	0.1835	0.4215	-1.3516	-1.9299	-0.7733	0.5444	0.0162
PC7	-0.2550	-0.3846	-0.1690	1.2390	0.7153	1.7626	0.3376	0.0400
PC8	-0.2334	-0.3509	-0.1553	1.1342	0.6589	1.6095	0.2535	0.0563
PC9	0.1936	0.1275	0.2939	-0.9406	-1.3450	-0.5362	0.7030	0.0064
PC10	-0.1561	-0.2370	-0.1028	0.7585	0.4325	1.0844	0.6835	0.0074
PC11	-0.1394	-0.2119	-0.0917	0.6775	0.3854	0.9696	0.8704	0.0012
PC12	-0.1173	-0.1784	-0.0772	0.5702	0.3244	0.8160	0.8497	0.0016
PC13	-0.1139	-0.1731	-0.0750	0.5537	0.3151	0.7922	0.8053	0.0027

Cheirogaleus medius

PC	Slope	Slope lower CI	Slope higher CI	Intercept	Intercept lower CI	Intercept higher CI	p value	r squared
PC1	-1.3585	-1.9877	-0.9285	6.2357	3.8046	8.6669	0.4093	0.0254
PC2	-0.8719	-1.2625	-0.6021	4.0020	2.4862	5.5177	0.1368	0.0801
PC3	-0.5444	-0.7961	-0.3723	2.4990	1.5265	3.4715	0.3779	0.0289
PC4	-0.4149	-0.6089	-0.2827	1.9045	1.1559	2.6531	0.6193	0.0093
PC5	0.2905	0.1999	0.4222	-1.3333	-1.8435	-0.8231	0.1963	0.0611
PC6	0.2463	0.1715	0.3539	-1.1307	-1.5493	-0.7120	0.0645	0.1210
PC7	-0.2183	-0.3209	-0.1485	1.0021	0.6065	1.3978	0.9211	0.0004
PC8	-0.1880	-0.2759	-0.1281	0.8627	0.5234	1.2020	0.6396	0.0082
PC9	0.1800	0.1263	0.2565	-0.8261	-1.1251	-0.5271	0.0316	0.1599
PC10	-0.1646	-0.2404	-0.1128	0.7557	0.4627	1.0486	0.3210	0.0365
PC11	0.1404	0.0957	0.2060	-0.6443	-0.8975	-0.3911	0.6057	0.0100
PC12	0.1194	0.0813	0.1754	-0.5480	-0.7641	-0.3320	0.7513	0.0038
PC13	0.0919	0.0625	0.1351	-0.4218	-0.5883	-0.2553	0.8901	0.0007

Microcebus murinus

PC	Slope	Slope lower CI	Slope higher CI	Intercept	Intercept lower CI	Intercept higher CI	p value	r squared
PC1	-1.7602	-2.2285	-1.3904	7.6311	5.8142	9.4480	0.6729	0.0026
PC2	1.2514	1.0124	1.5468	-5.4251	-6.5836	-4.2666	0.0001	0.1977
PC3	0.7604	0.6033	0.9584	-3.2965	-4.0663	-2.5268	0.0897	0.0406
PC4	0.7364	0.5843	0.9282	-3.1927	-3.9382	-2.4471	0.0903	0.0404
PC5	-0.4624	-0.5852	-0.3653	2.0045	1.5276	2.4813	0.5836	0.0043
PC6	-0.3780	-0.4775	-0.2992	1.6387	1.2522	2.0252	0.2209	0.0213
PC7	-0.3345	-0.4235	-0.2642	1.4502	1.1049	1.7956	0.6990	0.0021
PC8	0.3106	0.2453	0.3932	-1.3465	-1.6671	-1.0259	0.6727	0.0026
PC9	0.2566	0.2027	0.3248	-1.1123	-1.3772	-0.8475	0.6933	0.0022
PC10	-0.2257	-0.2858	-0.1782	0.9783	0.7451	1.2115	0.8899	0.0003
PC11	-0.2081	-0.2634	-0.1644	0.9021	0.6874	1.1167	0.6144	0.0036
PC12	-0.1861	-0.2354	-0.1471	0.8068	0.6153	0.9982	0.4229	0.0092
PC13	-0.1716	-0.2173	-0.1355	0.7441	0.5667	0.9214	0.8745	0.0004

Microcebus rufus

PC	Slope	Slope lower CI	Slope higher CI	Intercept	Intercept lower CI	Intercept higher CI	p value	r squared
PC1	-1.4508	-2.1300	-0.9881	6.3226	3.8339	8.8113	0.6742	0.0066
PC2	-0.4798	-0.6945	-0.3314	2.0908	1.2996	2.8821	0.1326	0.0818
PC3	-0.4223	-0.6132	-0.2909	1.8405	1.1381	2.5429	0.1778	0.0662
PC4	0.4036	0.2826	0.5764	-1.7590	-2.3991	-1.1189	0.0373	0.1508
PC5	0.3300	0.2273	0.4791	-1.4383	-1.9871	-0.8895	0.1765	0.0666
PC6	0.2104	0.1464	0.3022	-0.9167	-1.2562	-0.5772	0.0649	0.1206
PC7	0.1962	0.1336	0.2882	-0.8550	-1.1919	-0.5180	0.7385	0.0042
PC8	-0.1939	-0.2850	-0.1320	0.8452	0.5119	1.1786	0.7933	0.0026
PC9	-0.1883	-0.2768	-0.1281	0.8205	0.4965	1.1446	0.9819	0.0000
PC10	0.1500	0.1022	0.2201	-0.6536	-0.9107	-0.3966	0.6377	0.0083
PC11	-0.1384	-0.1965	-0.0975	0.6031	0.3875	0.8188	0.0217	0.1801
PC12	0.1223	0.0832	0.1797	-0.5328	-0.7431	-0.3225	0.8528	0.0013
PC13	-0.0880	-0.1286	-0.0602	0.3833	0.2342	0.5325	0.3769	0.0290

Galago alleni

PC	Slope	Slope lower CI	Slope higher CI	Intercept	Intercept lower CI	Intercept higher CI	p value	r squared
PC1	-1.3414	-2.0464	-0.8793	6.3836	3.6063	9.1609	0.4037	0.0319
PC2	-0.8726	-1.2991	-0.5861	4.1524	2.4558	5.8490	0.0652	0.1462
PC3	0.4819	0.3162	0.7344	-2.2931	-3.2884	-1.2978	0.3714	0.0365
PC4	-0.3748	-0.5751	-0.2443	1.7838	0.9967	2.5710	0.7671	0.0041
PC5	0.3616	0.2357	0.5545	-1.7206	-2.4792	-0.9619	0.7268	0.0057
PC6	-0.3047	-0.4673	-0.1987	1.4500	0.8107	2.0893	0.7197	0.0060
PC7	0.2583	0.1798	0.3711	-1.2291	-1.6843	-0.7738	0.0058	0.2982
PC8	0.2309	0.1517	0.3515	-1.0988	-1.5742	-0.6235	0.3317	0.0429
PC9	-0.2090	-0.3192	-0.1369	0.9947	0.5608	1.4287	0.4449	0.0268
PC10	0.1602	0.1045	0.2458	-0.7626	-1.0989	-0.4263	0.7334	0.0054
PC11	-0.1470	-0.2248	-0.0962	0.6996	0.3936	1.0057	0.4954	0.0214
PC12	0.1188	0.0774	0.1824	-0.5654	-0.8153	-0.3154	0.9047	0.0007
PC13	-0.1037	-0.1587	-0.0677	0.4933	0.2767	0.7098	0.5751	0.0145

Galago demidoff

PC	Slope	Slope lower CI	Slope higher CI	Intercept	Intercept lower CI	Intercept higher CI	p value	r squared
PC1	-1.5150	-1.9639	-1.1687	6.7134	4.9513	8.4756	0.2759	0.0208
PC2	0.8581	0.6615	1.1131	-3.8025	-4.8032	-2.8018	0.3456	0.0156
PC3	0.7556	0.5864	0.9736	-3.3483	-4.2063	-2.4903	0.0483	0.0667
PC4	0.5935	0.4567	0.7714	-2.6301	-3.3274	-1.9328	0.8174	0.0009
PC5	-0.4124	-0.5290	-0.3214	1.8273	1.3674	2.2872	0.0148	0.0997
PC6	-0.3420	-0.4433	-0.2638	1.5154	1.1178	1.9131	0.2680	0.0215
PC7	0.3060	0.2354	0.3977	-1.3558	-1.7153	-0.9964	0.8253	0.0009
PC8	0.2960	0.2279	0.3844	-1.3116	-1.6585	-0.9648	0.5578	0.0061
PC9	0.2475	0.1906	0.3215	-1.0969	-1.3870	-0.8068	0.5650	0.0058
PC10	0.2299	0.1769	0.2986	-1.0185	-1.2882	-0.7489	0.6527	0.0036
PC11	-0.1990	-0.2585	-0.1531	0.8817	0.6482	1.1152	0.6617	0.0034
PC12	0.1716	0.1322	0.2228	-0.7605	-0.9614	-0.5595	0.5157	0.0075
PC13	-0.1642	-0.2134	-0.1264	0.7278	0.5352	0.9205	0.6254	0.0042

Galago elegantulus

PC	Slope	Slope lower CI	Slope higher CI	Intercept	Intercept lower CI	Intercept higher CI	p value	r squared
PC1	2.4550	1.7290	3.4857	-11.5911	-15.7382	-7.4439	0.5243	0.0128
PC2	1.3693	0.9637	1.9455	-6.4650	-8.7828	-4.1472	0.5984	0.0088
PC3	0.9218	0.6478	1.3116	-4.3521	-5.9192	-2.7849	0.9657	0.0001
PC4	-0.7210	-1.0184	-0.5104	3.4040	2.2047	4.6034	0.2412	0.0427
PC5	-0.5895	-0.8383	-0.4146	2.7834	1.7832	3.7837	0.7190	0.0041
PC6	0.4377	0.3077	0.6227	-2.0668	-2.8105	-1.3231	0.8358	0.0014
PC7	0.3647	0.2567	0.5181	-1.7219	-2.3391	-1.1047	0.5905	0.0091
PC8	0.3388	0.2477	0.4634	-1.5995	-2.1087	-1.0902	0.0053	0.2183
PC9	-0.2985	-0.4240	-0.2101	1.4093	0.9045	1.9142	0.5659	0.0104
PC10	0.2922	0.2063	0.4139	-1.3798	-1.8699	-0.8897	0.3525	0.0271
PC11	0.2664	0.1876	0.3782	-1.2578	-1.7078	-0.8078	0.5223	0.0129
PC12	0.2498	0.1764	0.3537	-1.1795	-1.5981	-0.7609	0.3386	0.0286
PC13	0.2362	0.1673	0.3334	-1.1152	-1.5073	-0.7231	0.2205	0.0465

Galago moholi

PC	Slope	Slope lower CI	Slope higher CI	Intercept	Intercept lower CI	Intercept higher CI	p value	r squared
PC1	-1.6533	-2.0902	-1.3078	7.5190	5.7400	9.2981	0.8687	0.0004
PC2	-1.1101	-1.4032	-0.8782	5.0483	3.8545	6.2422	0.7495	0.0014
PC3	0.7366	0.5929	0.9152	-3.3499	-4.0828	-2.6171	0.0009	0.1454
PC4	0.5807	0.4593	0.7341	-2.6407	-3.2655	-2.0158	0.8831	0.0003
PC5	0.4155	0.3294	0.5242	-1.8897	-2.3329	-1.4466	0.2562	0.0181
PC6	0.4030	0.3209	0.5062	-1.8329	-2.2545	-1.4113	0.0452	0.0553
PC7	-0.3538	-0.4461	-0.2806	1.6089	1.2327	1.9852	0.1938	0.0237
PC8	-0.2890	-0.3646	-0.2290	1.3141	1.0059	1.6223	0.2626	0.0176
PC9	-0.2690	-0.3391	-0.2134	1.2235	0.9377	1.5092	0.1730	0.0260
PC10	0.2483	0.1968	0.3134	-1.1294	-1.3946	-0.8642	0.2901	0.0157
PC11	0.2184	0.1730	0.2758	-0.9933	-1.2272	-0.7594	0.4064	0.0097
PC12	0.2013	0.1607	0.2521	-0.9155	-1.1233	-0.7077	0.0155	0.0797
PC13	-0.1729	-0.2183	-0.1369	0.7863	0.6013	0.9713	0.3702	0.0113

Galago senegalensis

PC	Slope	Slope lower CI	Slope higher CI	Intercept	Intercept lower CI	Intercept higher CI	p value	r squared
PC1	1.5126	1.3026	1.7565	-7.0123	-8.0645	-5.9601	0.8287	0.0003
PC2	-1.0231	-1.1859	-0.8826	4.7429	4.0399	5.4459	0.0385	0.0245
PC3	-0.7558	-0.8688	-0.6575	3.5038	3.0140	3.9937	0.0000	0.1321
PC4	-0.5977	-0.6931	-0.5154	2.7708	2.3591	3.1825	0.0641	0.0197
PC5	0.4277	0.3683	0.4966	-1.9826	-2.2802	-1.6851	0.9888	0.0000
PC6	0.4029	0.3493	0.4646	-1.8676	-2.1347	-1.6005	0.0000	0.0918
PC7	0.3344	0.2880	0.3883	-1.5502	-1.7828	-1.3176	0.8290	0.0003
PC8	0.3108	0.2676	0.3609	-1.4407	-1.6569	-1.2245	0.8060	0.0003
PC9	0.2730	0.2351	0.3170	-1.2657	-1.4556	-1.0758	0.8380	0.0002
PC10	0.2582	0.2225	0.2995	-1.1968	-1.3752	-1.0184	0.1250	0.0135
PC11	0.2451	0.2115	0.2840	-1.1362	-1.3043	-0.9681	0.0264	0.0282
PC12	-0.2235	-0.2595	-0.1926	1.0363	0.8811	1.1916	0.4290	0.0036
PC13	0.1889	0.1628	0.2193	-0.8759	-1.0070	-0.7447	0.3461	0.0051

Galago zanzibaricus

PC	Slope	Slope lower CI	Slope higher CI	Intercept	Intercept lower CI	Intercept higher CI	p value	r squared
PC1	1.6602	1.1215	2.4575	-7.6144	-10.6782	-4.5506	0.0768	0.1299
PC2	1.1521	0.7611	1.7439	-5.2839	-7.5378	-3.0300	0.4777	0.0222
PC3	0.7461	0.4911	1.1333	-3.4218	-4.8945	-1.9490	0.7520	0.0044
PC4	0.6185	0.4072	0.9393	-2.8366	-4.0567	-1.6164	0.7230	0.0056
PC5	0.4522	0.2974	0.6875	-2.0740	-2.9687	-1.1794	0.9958	0.0000
PC6	0.4074	0.2703	0.6142	-1.8687	-2.6572	-1.0801	0.3202	0.0430
PC7	-0.3627	-0.5475	-0.2403	1.6635	0.9590	2.3680	0.3632	0.0361
PC8	-0.3433	-0.5212	-0.2261	1.5744	0.8976	2.2512	0.6913	0.0070
PC9	0.2802	0.1857	0.4226	-1.2850	-1.8282	-0.7417	0.3414	0.0394
PC10	-0.2656	-0.3918	-0.1801	1.2183	0.7327	1.7039	0.0592	0.1463
PC11	0.2125	0.1400	0.3227	-0.9748	-1.3939	-0.5557	0.6969	0.0067
PC12	-0.1935	-0.2884	-0.1298	0.8875	0.5239	1.2511	0.1276	0.0980
PC13	0.1654	0.1088	0.2514	-0.7585	-1.0855	-0.4314	0.9106	0.0006

Otolemur crassicaudatus

PC	Slope	Slope lower CI	Slope higher CI	Intercept	Intercept lower CI	Intercept higher CI	p value	r squared
PC1	-1.0733	-1.3020	-0.8848	5.4908	4.4237	6.5579	0.0239	0.0505
PC2	-0.6147	-0.7241	-0.5219	3.1446	2.6273	3.6618	0.0000	0.3199
PC3	-0.4417	-0.5385	-0.3623	2.2595	1.8088	2.7101	0.9326	0.0001
PC4	0.3077	0.2553	0.3709	-1.5741	-1.8699	-1.2783	0.0006	0.1122
PC5	0.2295	0.1886	0.2794	-1.1742	-1.4064	-0.9419	0.2041	0.0162
PC6	0.2164	0.1780	0.2632	-1.1073	-1.3253	-0.8892	0.1131	0.0252
PC7	-0.1905	-0.2322	-0.1563	0.9746	0.7804	1.1687	0.6209	0.0025
PC8	0.1840	0.1512	0.2239	-0.9413	-1.1274	-0.7552	0.1847	0.0177
PC9	0.1604	0.1317	0.1952	-0.8203	-0.9829	-0.6578	0.2599	0.0128
PC10	-0.1390	-0.1693	-0.1140	0.7109	0.5694	0.8523	0.5215	0.0042
PC11	-0.1255	-0.1530	-0.1030	0.6422	0.5142	0.7702	0.6558	0.0020
PC12	-0.1245	-0.1517	-0.1022	0.6370	0.5101	0.7638	0.5652	0.0034
PC13	0.1105	0.0907	0.1347	-0.5653	-0.6778	-0.4528	0.5079	0.0044

Otolemur garnettii

PC	Slope	Slope lower CI	Slope higher CI	Intercept	Intercept lower CI	Intercept higher CI	p value	r squared
PC1	-1.3329	-1.6205	-1.0963	6.7262	5.4034	8.0489	0.0035	0.0881
PC2	-0.7218	-0.8535	-0.6104	3.6423	3.0288	4.2559	0.0000	0.3309
PC3	-0.4239	-0.5198	-0.3457	2.1392	1.6998	2.5786	0.4859	0.0052
PC4	0.3955	0.3230	0.4843	-1.9960	-2.4030	-1.5889	0.1794	0.0193
PC5	0.3163	0.2594	0.3856	-1.5962	-1.9147	-1.2777	0.0156	0.0612
PC6	0.2819	0.2303	0.3451	-1.4226	-1.7124	-1.1328	0.1556	0.0216
PC7	0.2342	0.1909	0.2874	-1.1820	-1.4254	-0.9387	0.8593	0.0003
PC8	-0.1960	-0.2397	-0.1603	0.9892	0.7887	1.1897	0.0875	0.0311
PC9	-0.1841	-0.2252	-0.1505	0.9290	0.7403	1.1177	0.1096	0.0273
PC10	0.1627	0.1328	0.1995	-0.8213	-0.9897	-0.6528	0.3993	0.0076
PC11	-0.1312	-0.1609	-0.1069	0.6619	0.5258	0.7980	0.5796	0.0033
PC12	0.1241	0.1012	0.1523	-0.6264	-0.7553	-0.4976	0.6538	0.0022
PC13	-0.1130	-0.1386	-0.0921	0.5703	0.4529	0.6876	0.7084	0.0015

Avahi laniger

PC	Slope	Slope lower CI	Slope higher CI	Intercept	Intercept lower CI	Intercept higher CI	p value	r squared
PC1	-2.2902	-3.5342	-1.4841	11.1827	6.1776	16.1878	0.4507	0.0274
PC2	1.0115	0.6541	1.5643	-4.9390	-7.1612	-2.7169	0.5509	0.0172
PC3	-0.6318	-0.9792	-0.4076	3.0849	1.6894	4.4804	0.7155	0.0065
PC4	0.6085	0.4062	0.9117	-2.9714	-4.2055	-1.7372	0.0566	0.1623
PC5	0.4349	0.2810	0.6731	-2.1237	-3.0809	-1.1665	0.5957	0.0136
PC6	-0.4002	-0.6189	-0.2588	1.9541	1.0751	2.8332	0.5471	0.0175
PC7	0.3167	0.2048	0.4895	-1.5461	-2.2412	-0.8511	0.5329	0.0188
PC8	0.2916	0.1880	0.4524	-1.4238	-2.0693	-0.7783	0.8388	0.0020
PC9	-0.2641	-0.4043	-0.1725	1.2894	0.7234	1.8555	0.2434	0.0642
PC10	0.2069	0.1347	0.3179	-1.0104	-1.4576	-0.5632	0.3108	0.0489
PC11	-0.1982	-0.3067	-0.1281	0.9678	0.5315	1.4040	0.5981	0.0135
PC12	0.1651	0.1094	0.2492	-0.8061	-1.1474	-0.4647	0.0920	0.1292
PC13	0.1437	0.0935	0.2209	-0.7018	-1.0129	-0.3907	0.3254	0.0461

Indri indri

PC	Slope	Slope lower CI	Slope higher CI	Intercept	Intercept lower CI	Intercept higher CI	p value	r squared
PC1	-2.0181	-2.7589	-1.4762	11.0756	7.5557	14.5955	0.0638	0.0898
PC2	1.0973	0.7910	1.5220	-6.0218	-8.0277	-4.0159	0.9574	0.0001
PC3	0.7670	0.5606	1.0495	-4.2095	-5.5513	-2.8676	0.0730	0.0843
PC4	-0.6144	-0.8506	-0.4438	3.3717	2.2554	4.4880	0.5032	0.0122
PC5	-0.4582	-0.6327	-0.3318	2.5144	1.6886	3.3403	0.3102	0.0278
PC6	-0.4055	-0.5551	-0.2963	2.2256	1.5155	2.9358	0.0763	0.0825
PC7	0.3728	0.2692	0.5164	-2.0461	-2.7246	-1.3676	0.5667	0.0089
PC8	0.3605	0.2600	0.5000	-1.9786	-2.6373	-1.3199	0.8419	0.0011
PC9	-0.3124	-0.4315	-0.2261	1.7142	1.1507	2.2777	0.3242	0.0263
PC10	-0.2185	-0.3028	-0.1577	1.1990	0.8008	1.5972	0.6393	0.0060
PC11	0.1937	0.1413	0.2656	-1.0631	-1.4041	-0.7221	0.0964	0.0729
PC12	-0.1728	-0.2395	-0.1247	0.9484	0.6336	1.2633	0.6138	0.0070
PC13	-0.1705	-0.2356	-0.1233	0.9356	0.6275	1.2437	0.3623	0.0225

Propithecus diadema

PC	Slope	Slope lower CI	Slope higher CI	Intercept	Intercept lower CI	Intercept higher CI	p value	r squared
PC1	1.3493	0.9548	1.9067	-7.2447	-9.8003	-4.6892	0.0090	0.2344
PC2	0.8594	0.5830	1.2667	-4.6142	-6.4497	-2.7787	0.4088	0.0264
PC3	0.5674	0.3831	0.8403	-3.0465	-4.2740	-1.8189	0.8725	0.0010
PC4	-0.4538	-0.6672	-0.3086	2.4365	1.4737	3.3993	0.3120	0.0393
PC5	-0.3271	-0.4771	-0.2242	1.7561	1.0773	2.4350	0.1433	0.0805
PC6	0.3062	0.2084	0.4500	-1.6441	-2.2928	-0.9954	0.2952	0.0421
PC7	0.2815	0.1904	0.4161	-1.5114	-2.1172	-0.9055	0.5913	0.0112
PC8	0.2194	0.1481	0.3251	-1.1783	-1.6533	-0.7033	0.9509	0.0001
PC9	0.1840	0.1243	0.2725	-0.9882	-1.3860	-0.5903	0.7913	0.0027
PC10	0.1510	0.1019	0.2236	-0.8106	-1.1372	-0.4839	0.8855	0.0008
PC11	-0.1272	-0.1868	-0.0866	0.6829	0.4139	0.9518	0.2753	0.0456
PC12	-0.1159	-0.1715	-0.0783	0.6224	0.3721	0.8727	0.7204	0.0050
PC13	0.1076	0.0726	0.1593	-0.5776	-0.8104	-0.3449	0.8780	0.0009

Propithecus verreauxi

PC	Slope	Slope lower CI	Slope higher CI	Intercept	Intercept lower CI	Intercept higher CI	p value	r squared
PC1	1.2527	0.9215	1.7029	-6.6309	-8.6991	-4.5627	0.3410	0.0221
PC2	-1.0219	-1.3725	-0.7608	5.4090	3.7899	7.0280	0.0395	0.0994
PC3	-0.6057	-0.8219	-0.4464	3.2061	2.2122	4.2001	0.2372	0.0339
PC4	0.4637	0.3473	0.6191	-2.4544	-3.1737	-1.7352	0.0146	0.1368
PC5	0.3878	0.2844	0.5290	-2.0529	-2.7003	-1.4055	0.9122	0.0003
PC6	0.3218	0.2368	0.4374	-1.7035	-2.2344	-1.1726	0.3252	0.0236
PC7	-0.3186	-0.4341	-0.2339	1.6867	1.1569	2.2164	0.5560	0.0085
PC8	0.2781	0.2054	0.3766	-1.4721	-1.9253	-1.0189	0.1606	0.0474
PC9	0.2444	0.1795	0.3329	-1.2939	-1.6999	-0.8880	0.5108	0.0106
PC10	0.2097	0.1540	0.2855	-1.1098	-1.4578	-0.7617	0.4974	0.0113
PC11	0.2005	0.1470	0.2735	-1.0613	-1.3960	-0.7267	0.8925	0.0005
PC12	0.1715	0.1258	0.2337	-0.9079	-1.1935	-0.6223	0.6415	0.0053
PC13	0.1583	0.1161	0.2159	-0.8379	-1.1020	-0.5738	0.8018	0.0016

Eulemur fulvus

PC	Slope	Slope lower CI	Slope higher CI	Intercept	Intercept lower CI	Intercept higher CI	p value	r squared
PC1	-2.2293	-2.5842	-1.9232	11.8841	10.1222	13.6459	0.0403	0.0241
PC2	-1.2938	-1.5005	-1.1156	6.8971	5.8713	7.9230	0.0792	0.0177
PC3	-0.5468	-0.6348	-0.4710	2.9148	2.4780	3.3516	0.4789	0.0029
PC4	-0.4217	-0.4870	-0.3651	2.2479	1.9231	2.5726	0.0003	0.0733
PC5	0.3782	0.3257	0.4392	-2.0161	-2.3187	-1.7136	0.8730	0.0001
PC6	0.3280	0.2827	0.3805	-1.7483	-2.0089	-1.4878	0.1218	0.0138
PC7	0.3169	0.2731	0.3678	-1.6894	-1.9417	-1.4370	0.2055	0.0092
PC8	-0.2792	-0.3242	-0.2404	1.4883	1.2649	1.7116	0.9077	0.0001
PC9	0.2371	0.2043	0.2753	-1.2641	-1.4534	-1.0749	0.3481	0.0051
PC10	-0.1885	-0.2189	-0.1623	1.0047	0.8539	1.1554	0.9380	0.0000
PC11	-0.1781	-0.2068	-0.1535	0.9496	0.8075	1.0917	0.3260	0.0056
PC12	0.1626	0.1402	0.1886	-0.8668	-0.9959	-0.7378	0.0966	0.0159
PC13	-0.1595	-0.1852	-0.1374	0.8504	0.7228	0.9779	0.7105	0.0008

Eulemur macaco

PC	Slope	Slope lower CI	Slope higher CI	Intercept	Intercept lower CI	Intercept higher CI	p value	r squared
PC1	-2.2603	-2.9289	-1.7443	12.0988	8.9282	15.2694	0.0218	0.0953
PC2	1.4342	1.1045	1.8624	-7.6770	-9.7055	-5.6485	0.0361	0.0802
PC3	-0.6968	-0.9129	-0.5318	3.7297	2.7099	4.7495	0.3709	0.0151
PC4	-0.5823	-0.7610	-0.4455	3.1169	2.2726	3.9613	0.1827	0.0333
PC5	-0.4775	-0.6258	-0.3644	2.5561	1.8564	3.2558	0.4101	0.0128
PC6	-0.4213	-0.5511	-0.3220	2.2549	1.6417	2.8682	0.2422	0.0257
PC7	0.3952	0.3011	0.5187	-2.1155	-2.6980	-1.5329	0.8098	0.0011
PC8	0.3428	0.2632	0.4466	-1.8351	-2.3261	-1.3441	0.0793	0.0570
PC9	0.3002	0.2292	0.3931	-1.6069	-2.0456	-1.1683	0.3253	0.0183
PC10	-0.2805	-0.3661	-0.2150	1.5016	1.0972	1.9060	0.1223	0.0445
PC11	0.2379	0.1812	0.3123	-1.2735	-1.6243	-0.9226	0.9645	0.0000
PC12	-0.2248	-0.2936	-0.1722	1.2035	0.8786	1.5284	0.1431	0.0400
PC13	0.1934	0.1474	0.2539	-1.0354	-1.3205	-0.7502	0.8221	0.0010

Eulemur mongoz

PC	Slope	Slope lower CI	Slope higher CI	Intercept	Intercept lower CI	Intercept higher CI	p value	r squared
PC1	-1.6300	-2.1180	-1.2544	8.6117	6.3303	10.8932	0.1408	0.0390
PC2	0.9673	0.7424	1.2601	-5.1102	-6.4779	-3.7426	0.3029	0.0193
PC3	-0.5160	-0.6470	-0.4115	2.7260	2.1037	3.3483	0.0000	0.2865
PC4	-0.4068	-0.5313	-0.3114	2.1490	1.5682	2.7298	0.9742	0.0000
PC5	-0.2870	-0.3749	-0.2198	1.5164	1.1067	1.9261	0.8724	0.0005
PC6	0.2728	0.2092	0.3557	-1.4413	-1.8284	-1.0542	0.4123	0.0123
PC7	0.2218	0.1700	0.2893	-1.1716	-1.4869	-0.8563	0.4996	0.0083
PC8	-0.1966	-0.2565	-0.1506	1.0385	0.7586	1.3183	0.5790	0.0056
PC9	0.1683	0.1288	0.2197	-0.8890	-1.1291	-0.6488	0.8486	0.0007
PC10	-0.1582	-0.2058	-0.1217	0.8360	0.6139	1.0581	0.1731	0.0335
PC11	-0.1411	-0.1841	-0.1081	0.7454	0.5446	0.9463	0.5559	0.0063
PC12	-0.1236	-0.1592	-0.0960	0.6533	0.4863	0.8202	0.0136	0.1056
PC13	0.1093	0.0840	0.1423	-0.5776	-0.7317	-0.4236	0.2268	0.0265

Eulemur rubriventer

PC	Slope	Slope lower CI	Slope higher CI	Intercept	Intercept lower CI	Intercept higher CI	p value	r squared
PC1	-4.1700	-6.1625	-2.8218	22.1749	13.2924	31.0573	0.2418	0.0544
PC2	-1.0642	-1.5443	-0.7333	5.6588	3.5023	7.8153	0.0508	0.1441
PC3	0.6549	0.4385	0.9779	-3.4823	-4.9163	-2.0483	0.9034	0.0006
PC4	0.5310	0.3610	0.7813	-2.8239	-3.9415	-1.7064	0.1612	0.0770
PC5	0.4725	0.3175	0.7033	-2.5127	-3.5385	-1.4869	0.5080	0.0177
PC6	0.3890	0.2605	0.5809	-2.0685	-2.9206	-1.2165	0.9762	0.0000
PC7	0.3289	0.2202	0.4912	-1.7489	-2.4693	-1.0285	0.9933	0.0000
PC8	0.2998	0.2058	0.4366	-1.5940	-2.2075	-0.9805	0.0682	0.1269
PC9	-0.2700	-0.4007	-0.1819	1.4356	0.8538	2.0175	0.3729	0.0319
PC10	0.2067	0.1387	0.3079	-1.0991	-1.5489	-0.6494	0.5686	0.0132
PC11	0.1806	0.1210	0.2697	-0.9606	-1.3560	-0.5653	0.8381	0.0017
PC12	0.1598	0.1071	0.2383	-0.8496	-1.1983	-0.5009	0.6724	0.0073
PC13	0.1478	0.0999	0.2188	-0.7861	-1.1023	-0.4699	0.2806	0.0464

Hapalemur griseus

PC	Slope	Slope lower CI	Slope higher CI	Intercept	Intercept lower CI	Intercept higher CI	p value	r squared
PC1	1.3998	0.9504	2.0617	-7.0526	-9.8524	-4.2528	0.1783	0.0713
PC2	0.6711	0.4606	0.9778	-3.3811	-4.6843	-2.0780	0.0710	0.1246
PC3	0.4049	0.2725	0.6016	-2.0400	-2.8690	-1.2109	0.4152	0.0267
PC4	0.3556	0.2386	0.5299	-1.7914	-2.5253	-1.0575	0.6055	0.0108
PC5	0.2877	0.1952	0.4239	-1.4494	-2.0254	-0.8733	0.1852	0.0691
PC6	-0.2491	-0.3719	-0.1669	1.2551	0.7385	1.7718	0.8494	0.0015
PC7	-0.2278	-0.3381	-0.1535	1.1479	0.6829	1.6130	0.3664	0.0327
PC8	-0.2108	-0.3125	-0.1422	1.0622	0.6334	1.4910	0.3206	0.0395
PC9	-0.1984	-0.2938	-0.1340	0.9996	0.5970	1.4021	0.2916	0.0444
PC10	-0.1662	-0.2480	-0.1114	0.8373	0.4932	1.1814	0.7298	0.0049
PC11	0.1388	0.0929	0.2073	-0.6993	-0.9873	-0.4112	0.9750	0.0000
PC12	0.1212	0.0836	0.1756	-0.6105	-0.8423	-0.3788	0.0454	0.1507
PC13	0.1126	0.0769	0.1650	-0.5675	-0.7894	-0.3455	0.1105	0.0987

Lemur catta

PC	Slope	Slope lower CI	Slope higher CI	Intercept	Intercept lower CI	Intercept higher CI	p value	r squared
PC1	-1.2521	-1.7409	-0.9005	6.5826	4.3731	8.7921	0.0353	0.1312
PC2	1.0451	0.7349	1.4862	-5.4945	-7.4695	-3.5195	0.7324	0.0037
PC3	-0.5297	-0.7377	-0.3804	2.7851	1.8460	3.7243	0.0418	0.1232
PC4	-0.4743	-0.6749	-0.3334	2.4936	1.5958	3.3914	0.9040	0.0005
PC5	-0.3326	-0.4722	-0.2342	1.7485	1.1228	2.3742	0.5279	0.0126
PC6	-0.2937	-0.4178	-0.2065	1.5442	0.9885	2.0999	0.8352	0.0014
PC7	0.2651	0.1880	0.3740	-1.3938	-1.8828	-0.9048	0.1998	0.0508
PC8	0.2294	0.1615	0.3259	-1.2063	-1.6384	-0.7742	0.5608	0.0107
PC9	0.2039	0.1491	0.2789	-1.0723	-1.4134	-0.7311	0.0052	0.2196
PC10	0.1553	0.1110	0.2172	-0.8163	-1.0956	-0.5370	0.0725	0.0973
PC11	-0.1445	-0.2054	-0.1017	0.7599	0.4873	1.0326	0.6283	0.0074
PC12	-0.1273	-0.1806	-0.0897	0.6692	0.4304	0.9080	0.4513	0.0178
PC13	-0.1084	-0.1531	-0.0768	0.5699	0.3692	0.7705	0.2322	0.0443

Varecia variegate

PC	Slope	Slope lower CI	Slope higher CI	Intercept	Intercept lower CI	Intercept higher CI	p value	r squared
PC1	1.9436	1.4013	2.6959	-10.6463	-14.1921	-7.1005	0.8965	0.0005
PC2	-0.9501	-1.3139	-0.6870	5.2040	3.4870	6.9209	0.4017	0.0191
PC3	-0.5023	-0.6918	-0.3647	2.7511	1.8553	3.6470	0.1974	0.0445
PC4	0.4413	0.3267	0.5961	-2.4170	-3.1549	-1.6791	0.0116	0.1601
PC5	0.3532	0.2552	0.4888	-1.9344	-2.5742	-1.2946	0.4692	0.0142
PC6	0.2916	0.2114	0.4023	-1.5974	-2.1204	-1.0744	0.2616	0.0339
PC7	-0.2736	-0.3652	-0.2050	1.4989	1.0602	1.9376	0.0021	0.2281
PC8	-0.2013	-0.2760	-0.1467	1.1024	0.7482	1.4565	0.1035	0.0701
PC9	0.1574	0.1144	0.2167	-0.8624	-1.1424	-0.5824	0.1702	0.0502
PC10	-0.1553	-0.2153	-0.1120	0.8507	0.5679	1.1336	0.7075	0.0039
PC11	0.1416	0.1021	0.1964	-0.7756	-1.0340	-0.5173	0.9574	0.0001
PC12	0.1221	0.0884	0.1688	-0.6690	-0.8894	-0.4487	0.3629	0.0224
PC13	-0.1022	-0.1417	-0.0737	0.5599	0.3737	0.7461	0.7303	0.0033

Lepilemur ruficaudatus

PC	Slope	Slope lower CI	Slope higher CI	Intercept	Intercept lower CI	Intercept higher CI	p value	r squared
PC1	1.1022	0.7255	1.6743	-5.4191	-7.7517	-3.0864	0.7551	0.0043
PC2	-0.7476	-1.1188	-0.4995	3.6756	2.1531	5.1980	0.1763	0.0780
PC3	0.6518	0.4355	0.9756	-3.2047	-4.5326	-1.8768	0.1783	0.0773
PC4	0.3989	0.2649	0.6007	-1.9615	-2.7869	-1.1360	0.2911	0.0483
PC5	-0.3552	-0.5397	-0.2338	1.7467	0.9947	2.4986	0.7601	0.0041
PC6	-0.3173	-0.4795	-0.2099	1.5599	0.8970	2.2228	0.4118	0.0295
PC7	-0.2236	-0.3398	-0.1472	1.0995	0.6259	1.5730	0.7875	0.0032
PC8	0.2130	0.1406	0.3228	-1.0474	-1.4953	-0.5995	0.5318	0.0172
PC9	0.1930	0.1270	0.2934	-0.9490	-1.3583	-0.5397	0.9380	0.0003
PC10	0.1699	0.1131	0.2551	-0.8352	-1.1842	-0.4862	0.2316	0.0616
PC11	-0.1281	-0.1908	-0.0860	0.6297	0.3722	0.8873	0.1215	0.1010
PC12	-0.1172	-0.1778	-0.0772	0.5761	0.3287	0.8235	0.6505	0.0091
PC13	-0.1112	-0.1691	-0.0732	0.5469	0.3111	0.7827	0.8823	0.0010

Loris tardigradus

PC	Slope	Slope lower CI	Slope higher CI	Intercept	Intercept lower CI	Intercept higher CI	p value	r squared
PC1	0.7001	0.4743	1.0333	-3.3513	-4.6899	-2.0127	0.2162	0.0605
PC2	-0.5498	-0.7681	-0.3936	2.6322	1.7355	3.5289	0.0023	0.3165
PC3	-0.2687	-0.3988	-0.1810	1.2861	0.7646	1.8076	0.3734	0.0318
PC4	0.2180	0.1471	0.3231	-1.0438	-1.4653	-0.6223	0.3181	0.0399
PC5	0.2003	0.1425	0.2815	-0.9589	-1.2916	-0.6262	0.0037	0.2909
PC6	-0.1448	-0.2161	-0.0970	0.6931	0.4077	0.9785	0.8254	0.0020
PC7	-0.1266	-0.1880	-0.0852	0.6059	0.3599	0.8520	0.3958	0.0290
PC8	0.0979	0.0656	0.1462	-0.4688	-0.6619	-0.2757	0.8845	0.0009
PC9	0.0786	0.0527	0.1172	-0.3761	-0.5306	-0.2216	0.6882	0.0065
PC10	-0.0732	-0.1091	-0.0491	0.3506	0.2070	0.4942	0.5852	0.0121
PC11	-0.0659	-0.0978	-0.0444	0.3154	0.1876	0.4431	0.3628	0.0332
PC12	0.0559	0.0377	0.0829	-0.2676	-0.3757	-0.1594	0.3341	0.0374
PC13	-0.0442	-0.0661	-0.0296	0.2118	0.1245	0.2991	0.9364	0.0003

Nycticebus bengalensis

PC	Slope	Slope lower CI	Slope higher CI	Intercept	Intercept lower CI	Intercept higher CI	p value	r squared
PC1	1.1204	0.7412	1.6935	-5.6897	-8.1079	-3.2714	0.0568	0.1697
PC2	0.9335	0.6092	1.4304	-4.7405	-6.8258	-2.6551	0.1305	0.1106
PC3	0.7211	0.4640	1.1209	-3.6622	-5.3302	-1.9942	0.3350	0.0465
PC4	-0.5743	-0.8980	-0.3673	2.9167	1.5692	4.2643	0.5408	0.0190
PC5	0.4485	0.2873	0.7001	-2.2775	-3.3259	-1.2292	0.4716	0.0262
PC6	-0.3203	-0.5001	-0.2052	1.6268	0.8779	2.3756	0.4722	0.0261
PC7	0.3168	0.2024	0.4957	-1.6086	-2.3533	-0.8639	0.5872	0.0150
PC8	0.2783	0.1834	0.4224	-1.4135	-2.0203	-0.8068	0.0717	0.1532
PC9	0.2462	0.1570	0.3862	-1.2504	-1.8323	-0.6685	0.7630	0.0046
PC10	0.2177	0.1457	0.3253	-1.1053	-1.5614	-0.6493	0.0286	0.2176
PC11	0.1662	0.1064	0.2596	-0.8439	-1.2331	-0.4547	0.5063	0.0224
PC12	0.1484	0.0946	0.2329	-0.7538	-1.1051	-0.4025	0.8579	0.0016
PC13	0.1260	0.0804	0.1972	-0.6396	-0.9362	-0.3431	0.6286	0.0119

Nycticebus coucang

PC	Slope	Slope lower CI	Slope higher CI	Intercept	Intercept lower CI	Intercept higher CI	p value	r squared
PC1	1.0317	0.8173	1.3024	-5.1405	-6.3490	-3.9319	0.0273	0.0706
PC2	0.8389	0.6626	1.0621	-4.1798	-5.1751	-3.1844	0.0752	0.0465
PC3	-0.4338	-0.5502	-0.3420	2.1614	1.6427	2.6801	0.1443	0.0315
PC4	0.3448	0.2718	0.4375	-1.7182	-2.1312	-1.3052	0.1648	0.0286
PC5	0.2966	0.2333	0.3771	-1.4780	-1.8362	-1.1197	0.3701	0.0120
PC6	-0.2693	-0.3426	-0.2117	1.3418	1.0155	1.6681	0.5329	0.0058
PC7	0.2340	0.1838	0.2979	-1.1658	-1.4501	-0.8816	0.8257	0.0007
PC8	0.2234	0.1760	0.2836	-1.1131	-1.3813	-0.8449	0.2043	0.0239
PC9	0.1969	0.1549	0.2504	-0.9812	-1.2190	-0.7433	0.3747	0.0118
PC10	-0.1701	-0.2165	-0.1336	0.8474	0.6409	1.0540	0.7648	0.0013
PC11	-0.1509	-0.1899	-0.1198	0.7517	0.5771	0.9263	0.0109	0.0928
PC12	-0.1438	-0.1830	-0.1129	0.7164	0.5418	0.8910	0.8085	0.0009
PC13	-0.1315	-0.1666	-0.1037	0.6550	0.4983	0.8116	0.1070	0.0383

Perodicticus potto

PC	Slope	Slope lower CI	Slope higher CI	Intercept	Intercept lower CI	Intercept higher CI	p value	r squared
PC1	1.2983	1.0928	1.5424	-6.5566	-7.6922	-5.4211	0.0614	0.0273
PC2	-1.0094	-1.2019	-0.8478	5.0979	4.2037	5.9921	0.5985	0.0022
PC3	0.6315	0.5303	0.7521	-3.1893	-3.7494	-2.6293	0.9734	0.0000
PC4	-0.4460	-0.5310	-0.3746	2.2523	1.8575	2.6472	0.5125	0.0034
PC5	0.4191	0.3530	0.4976	-2.1166	-2.4816	-1.7517	0.0313	0.0360
PC6	-0.3686	-0.4379	-0.3102	1.8615	1.5390	2.1839	0.0642	0.0267
PC7	0.3197	0.2687	0.3804	-1.6147	-1.8969	-1.3326	0.2636	0.0098
PC8	-0.3000	-0.3527	-0.2552	1.5151	1.2687	1.7615	0.0000	0.1421
PC9	-0.2748	-0.3258	-0.2318	1.3879	1.1504	1.6253	0.0102	0.0509
PC10	-0.2430	-0.2890	-0.2044	1.2274	1.0137	1.4410	0.1367	0.0174
PC11	-0.2198	-0.2617	-0.1846	1.1100	0.9155	1.3045	0.4778	0.0040
PC12	-0.2057	-0.2450	-0.1727	1.0389	0.8565	1.2213	0.8991	0.0001
PC13	-0.1983	-0.2361	-0.1665	1.0014	0.8256	1.1772	0.8482	0.0003

Goswami model oral module against ln CS of oral

Cheirogaleus major

PC	Slope	Slope lower CI	Slope higher CI	Intercept	Intercept lower CI	Intercept higher CI	p value	r squared
PC1	1.2881	0.8775	1.8909	-3.8542	-5.3706	-2.3379	0.0416	0.1684
PC2	-0.8411	-1.2766	-0.5541	2.5166	1.4353	3.5978	0.6637	0.0084
PC3	0.5054	0.3401	0.7510	-1.5122	-2.1272	-0.8973	0.1025	0.1117
PC4	0.3211	0.2112	0.4881	-0.9608	-1.3751	-0.5464	0.8806	0.0010
PC5	0.3018	0.2014	0.4520	-0.9029	-1.2778	-0.5279	0.1900	0.0735
PC6	0.2350	0.1547	0.3569	-0.7032	-1.0058	-0.4005	0.7386	0.0049
PC7	-0.2154	-0.3273	-0.1418	0.6445	0.3669	0.9222	0.7837	0.0033
PC8	-0.1972	-0.2998	-0.1297	0.5900	0.3354	0.8446	0.9922	0.0000
PC9	0.1635	0.1084	0.2467	-0.4893	-0.6962	-0.2824	0.3394	0.0397
PC10	0.1319	0.0871	0.1997	-0.3946	-0.5631	-0.2261	0.4952	0.0205
PC11	0.1178	0.0777	0.1787	-0.3525	-0.5037	-0.2013	0.6120	0.0114
PC12	0.0991	0.0653	0.1506	-0.2967	-0.4244	-0.1689	0.7850	0.0033
PC13	-0.0963	-0.1464	-0.0633	0.2880	0.1638	0.4123	0.9812	0.0000

Cheirogaleus medius

PC	Slope	Slope lower CI	Slope higher CI	Intercept	Intercept lower CI	Intercept higher CI	p value	r squared
PC1	-0.9251	-1.3261	-0.6453	2.4509	1.5485	3.3532	0.0531	0.1316
PC2	-0.5937	-0.8261	-0.4267	1.5729	1.0435	2.1023	0.0035	0.2743
PC3	-0.3707	-0.5406	-0.2542	0.9822	0.6026	1.3618	0.2798	0.0431
PC4	-0.2825	-0.4103	-0.1945	0.7485	0.4625	1.0346	0.1834	0.0646
PC5	0.1978	0.1350	0.2898	-0.5240	-0.7292	-0.3188	0.4892	0.0179
PC6	0.1677	0.1147	0.2452	-0.4444	-0.6173	-0.2715	0.3690	0.0300
PC7	0.1487	0.1013	0.2182	-0.3939	-0.5489	-0.2389	0.6444	0.0080
PC8	0.1280	0.0871	0.1880	-0.3391	-0.4728	-0.2054	0.7212	0.0048
PC9	0.1226	0.0842	0.1785	-0.3247	-0.4497	-0.1997	0.2426	0.0502
PC10	-0.1121	-0.1648	-0.0763	0.2970	0.1797	0.4143	0.8513	0.0013
PC11	0.0956	0.0650	0.1405	-0.2532	-0.3533	-0.1532	0.8946	0.0007
PC12	-0.0813	-0.1195	-0.0553	0.2154	0.1303	0.3005	0.8630	0.0011
PC13	0.0626	0.0426	0.0919	-0.1658	-0.2312	-0.1004	0.7944	0.0026

Microcebus murinus

PC	Slope	Slope lower CI	Slope higher CI	Intercept	Intercept lower CI	Intercept higher CI	p value	r squared
PC1	-1.0535	-1.3328	-0.8327	2.4481	1.8667	3.0296	0.4386	0.0086
PC2	0.7490	0.6346	0.8839	-1.7404	-2.0303	-1.4506	0.0000	0.5124
PC3	0.4551	0.3595	0.5761	-1.0576	-1.3093	-0.8058	0.5930	0.0041
PC4	0.4408	0.3481	0.5581	-1.0242	-1.2683	-0.7801	0.7165	0.0019
PC5	-0.2767	-0.3504	-0.2186	0.6431	0.4898	0.7963	0.7074	0.0020
PC6	-0.2262	-0.2860	-0.1789	0.5257	0.4012	0.6502	0.3241	0.0139
PC7	0.2002	0.1583	0.2531	-0.4652	-0.5754	-0.3550	0.3260	0.0138
PC8	0.1859	0.1469	0.2353	-0.4320	-0.5348	-0.3292	0.5421	0.0053
PC9	-0.1536	-0.1945	-0.1213	0.3569	0.2717	0.4420	0.9625	0.0000
PC10	-0.1351	-0.1710	-0.1066	0.3138	0.2390	0.3887	0.9298	0.0001
PC11	-0.1245	-0.1577	-0.0983	0.2894	0.2204	0.3584	0.8778	0.0003
PC12	0.1114	0.0880	0.1410	-0.2588	-0.3205	-0.1971	0.7305	0.0017
PC13	-0.1027	-0.1299	-0.0812	0.2387	0.1821	0.2953	0.3573	0.0121

Microcebus rufus

PC	Slope	Slope lower CI	Slope higher CI	Intercept	Intercept lower CI	Intercept higher CI	p value	r squared
PC1	-1.0090	-1.4651	-0.6950	2.4469	1.5124	3.3815	0.1784	0.0660
PC2	-0.3337	-0.4796	-0.2322	0.8092	0.5090	1.1094	0.0671	0.1188
PC3	-0.2937	-0.4280	-0.2016	0.7123	0.4376	0.9870	0.2554	0.0476
PC4	0.2807	0.1991	0.3958	-0.6808	-0.9194	-0.4421	0.0118	0.2128
PC5	0.2295	0.1577	0.3341	-0.5566	-0.7708	-0.3425	0.2320	0.0525
PC6	0.1463	0.1004	0.2131	-0.3548	-0.4915	-0.2180	0.2501	0.0487
PC7	-0.1365	-0.2006	-0.0928	0.3309	0.2001	0.4616	0.8989	0.0006
PC8	-0.1349	-0.1963	-0.0927	0.3271	0.2014	0.4529	0.2255	0.0539
PC9	0.1309	0.0894	0.1918	-0.3176	-0.4418	-0.1933	0.4668	0.0198
PC10	0.1043	0.0711	0.1529	-0.2530	-0.3522	-0.1537	0.5393	0.0141
PC11	-0.0963	-0.1398	-0.0663	0.2334	0.1442	0.3226	0.1810	0.0653
PC12	-0.0850	-0.1247	-0.0580	0.2062	0.1253	0.2871	0.5403	0.0140
PC13	-0.0612	-0.0898	-0.0417	0.1484	0.0899	0.2068	0.7162	0.0050

Galago alleni

PC	Slope	Slope lower CI	Slope higher CI	Intercept	Intercept lower CI	Intercept higher CI	p value	r squared
PC1	-1.0874	-1.6275	-0.7266	3.0548	1.7890	4.3206	0.0940	0.1222
PC2	-0.7073	-1.0857	-0.4608	1.9870	1.1091	2.8650	0.8315	0.0021
PC3	0.3906	0.2545	0.5996	-1.0973	-1.5823	-0.6124	0.8483	0.0017
PC4	0.3039	0.1981	0.4662	-0.8536	-1.2304	-0.4768	0.7664	0.0041
PC5	0.2931	0.1919	0.4476	-0.8234	-1.1826	-0.4641	0.4453	0.0267
PC6	-0.2470	-0.3571	-0.1709	0.6939	0.4323	0.9555	0.0088	0.2733
PC7	0.2094	0.1414	0.3100	-0.5881	-0.8250	-0.3513	0.0445	0.1712
PC8	0.1872	0.1226	0.2858	-0.5258	-0.7552	-0.2965	0.4390	0.0275
PC9	-0.1694	-0.2601	-0.1104	0.4760	0.2656	0.6864	0.8696	0.0013
PC10	-0.1299	-0.1985	-0.0850	0.3649	0.2054	0.5245	0.4797	0.0230
PC11	-0.1192	-0.1827	-0.0778	0.3348	0.1874	0.4822	0.6582	0.0091
PC12	0.0963	0.0630	0.1473	-0.2705	-0.3891	-0.1520	0.5242	0.0187
PC13	0.0840	0.0551	0.1282	-0.2361	-0.3388	-0.1333	0.4009	0.0323

Galago demidoff

PC	Slope	Slope lower CI	Slope higher CI	Intercept	Intercept lower CI	Intercept higher CI	p value	r squared
PC1	-1.4156	-1.8362	-1.0913	3.4304	2.5276	4.3333	0.3412	0.0159
PC2	0.8018	0.6177	1.0408	-1.9430	-2.4558	-1.4302	0.4414	0.0104
PC3	0.7060	0.5432	0.9177	-1.7109	-2.1648	-1.2570	0.9981	0.0000
PC4	0.5546	0.4280	0.7186	-1.3439	-1.6962	-0.9917	0.2412	0.0240
PC5	-0.3853	-0.5008	-0.2964	0.9337	0.6861	1.1814	0.8702	0.0005
PC6	-0.3195	-0.4142	-0.2465	0.7744	0.5712	0.9775	0.2642	0.0218
PC7	0.2859	0.2200	0.3716	-0.6928	-0.8765	-0.5091	0.8286	0.0008
PC8	-0.2766	-0.3593	-0.2129	0.6702	0.4927	0.8477	0.6491	0.0037
PC9	-0.2313	-0.3000	-0.1783	0.5605	0.4131	0.7079	0.3252	0.0170
PC10	-0.2148	-0.2787	-0.1655	0.5205	0.3832	0.6577	0.3989	0.0125
PC11	0.1859	0.1430	0.2417	-0.4505	-0.5701	-0.3310	0.9332	0.0001
PC12	0.1603	0.1234	0.2083	-0.3886	-0.4915	-0.2857	0.6707	0.0032
PC13	-0.1535	-0.1985	-0.1186	0.3719	0.2751	0.4687	0.1446	0.0370

Galago elegantulus

PC	Slope	Slope lower CI	Slope higher CI	Intercept	Intercept lower CI	Intercept higher CI	p value	r squared
PC1	-2.1140	-2.9982	-1.4906	5.7079	3.6723	7.7435	0.4317	0.0194
PC2	1.1791	0.8421	1.6511	-3.1836	-4.2759	-2.0913	0.0806	0.0923
PC3	0.7938	0.5688	1.1077	-2.1431	-2.8707	-1.4156	0.0537	0.1115
PC4	-0.6208	-0.8790	-0.4385	1.6763	1.0816	2.2710	0.3317	0.0295
PC5	-0.5077	-0.7201	-0.3579	1.3707	0.8815	1.8598	0.4478	0.0181
PC6	0.3770	0.2695	0.5273	-1.0178	-1.3658	-0.6698	0.0707	0.0985
PC7	0.3141	0.2230	0.4423	-0.8479	-1.1440	-0.5519	0.1615	0.0603
PC8	0.2917	0.2062	0.4127	-0.7877	-1.0664	-0.5089	0.2936	0.0344
PC9	0.2570	0.1808	0.3654	-0.6940	-0.9432	-0.4448	0.6585	0.0062
PC10	0.2517	0.1770	0.3579	-0.6795	-0.9238	-0.4352	0.7481	0.0033
PC11	-0.2294	-0.3222	-0.1633	0.6194	0.4049	0.8339	0.1158	0.0755
PC12	0.2151	0.1538	0.3010	-0.5808	-0.7796	-0.3820	0.0735	0.0967
PC13	0.2034	0.1448	0.2857	-0.5492	-0.7395	-0.3589	0.1197	0.0740

Galago moholi

PC	Slope	Slope lower CI	Slope higher CI	Intercept	Intercept lower CI	Intercept higher CI	p value	r squared
PC1	-1.1593	-1.4634	-0.9184	2.9395	2.2484	3.6306	0.3246	0.0137
PC2	-0.7784	-0.9800	-0.6182	1.9736	1.5148	2.4324	0.1102	0.0355
PC3	0.5165	0.4134	0.6453	-1.3096	-1.6036	-1.0156	0.0062	0.1007
PC4	-0.4072	-0.5146	-0.3221	1.0323	0.7882	1.2765	0.7325	0.0017
PC5	0.2914	0.2327	0.3648	-0.7388	-0.9062	-0.5714	0.0131	0.0835
PC6	0.2826	0.2239	0.3566	-0.7165	-0.8849	-0.5482	0.2954	0.0154
PC7	-0.2481	-0.3126	-0.1969	0.6290	0.4822	0.7758	0.1584	0.0278
PC8	-0.2026	-0.2543	-0.1614	0.5137	0.3959	0.6316	0.0356	0.0607
PC9	-0.1886	-0.2385	-0.1492	0.4783	0.3652	0.5915	0.7518	0.0014
PC10	0.1741	0.1379	0.2199	-0.4415	-0.5455	-0.3376	0.3725	0.0112
PC11	0.1531	0.1211	0.1936	-0.3883	-0.4802	-0.2964	0.8488	0.0005
PC12	0.1412	0.1120	0.1779	-0.3579	-0.4415	-0.2743	0.1745	0.0258
PC13	-0.1212	-0.1529	-0.0961	0.3074	0.2353	0.3795	0.2498	0.0186

Galago senegalensis

PC	Slope	Slope lower CI	Slope higher CI	Intercept	Intercept lower CI	Intercept higher CI	p value	r squared
PC1	1.3719	1.1816	1.5929	-3.5682	-4.1031	-3.0332	0.5345	0.0022
PC2	-0.9279	-1.0547	-0.8165	2.4134	2.1036	2.7232	0.0000	0.2686
PC3	-0.6855	-0.7902	-0.5947	1.7829	1.5286	2.0372	0.0000	0.0970
PC4	0.5421	0.4669	0.6294	-1.4099	-1.6213	-1.1985	0.5467	0.0021
PC5	-0.3879	-0.4504	-0.3340	1.0088	0.8574	1.1603	0.8610	0.0002
PC6	0.3654	0.3155	0.4232	-0.9503	-1.0905	-0.8101	0.0145	0.0341
PC7	0.3033	0.2612	0.3522	-0.7888	-0.9071	-0.6705	0.6460	0.0012
PC8	-0.2819	-0.3268	-0.2431	0.7331	0.6242	0.8420	0.0552	0.0211
PC9	-0.2476	-0.2874	-0.2134	0.6440	0.5478	0.7402	0.1932	0.0098
PC10	0.2342	0.2018	0.2717	-0.6090	-0.6998	-0.5181	0.1458	0.0122
PC11	0.2223	0.1916	0.2580	-0.5782	-0.6645	-0.4918	0.1800	0.0104
PC12	-0.2028	-0.2354	-0.1746	0.5273	0.4483	0.6063	0.4609	0.0031
PC13	-0.1714	-0.1990	-0.1476	0.4457	0.3788	0.5126	0.8186	0.0003

Galago zanzibaricus

PC	Slope	Slope lower CI	Slope higher CI	Intercept	Intercept lower CI	Intercept higher CI	p value	r squared
PC1	-1.5341	-2.3296	-1.0103	3.9772	2.2668	5.6875	0.7046	0.0064
PC2	1.0646	0.7316	1.5492	-2.7599	-3.8199	-1.6999	0.0222	0.2074
PC3	0.6894	0.4536	1.0478	-1.7873	-2.5576	-1.0169	0.8374	0.0019
PC4	-0.5715	-0.8550	-0.3820	1.4816	0.8685	2.0947	0.1712	0.0798
PC5	0.4179	0.2756	0.6335	-1.0833	-1.5473	-0.6193	0.5689	0.0143
PC6	0.3765	0.2477	0.5724	-0.9760	-1.3970	-0.5551	0.9127	0.0005
PC7	-0.3352	-0.5016	-0.2240	0.8689	0.5090	1.2287	0.1756	0.0783
PC8	-0.3172	-0.4818	-0.2088	0.8223	0.4685	1.1762	0.7346	0.0051
PC9	0.2589	0.1713	0.3913	-0.6712	-0.9564	-0.3860	0.4102	0.0297
PC10	0.2455	0.1615	0.3732	-0.6364	-0.9109	-0.3619	0.9357	0.0003
PC11	0.1964	0.1297	0.2975	-0.5092	-0.7268	-0.2916	0.5110	0.0190
PC12	-0.1788	-0.2682	-0.1192	0.4635	0.2704	0.6566	0.2093	0.0676
PC13	-0.1528	-0.2308	-0.1012	0.3962	0.2281	0.5642	0.3842	0.0331

Otolemur crassicaudatus

PC	Slope	Slope lower CI	Slope higher CI	Intercept	Intercept lower CI	Intercept higher CI	p value	r squared
PC1	-1.0692	-1.2992	-0.8798	3.3503	2.6930	4.0076	0.0700	0.0328
PC2	-0.6123	-0.7096	-0.5283	1.9187	1.6346	2.2028	0.0000	0.4489
PC3	-0.4400	-0.5362	-0.3610	1.3786	1.1039	1.6533	0.6284	0.0024
PC4	0.3065	0.2528	0.3715	-0.9604	-1.1465	-0.7744	0.0162	0.0570
PC5	0.2286	0.1884	0.2774	-0.7164	-0.8559	-0.5770	0.0279	0.0479
PC6	0.2156	0.1774	0.2621	-0.6756	-0.8084	-0.5428	0.0870	0.0293
PC7	-0.1898	-0.2313	-0.1557	0.5946	0.4761	0.7132	0.6634	0.0019
PC8	0.1833	0.1504	0.2234	-0.5744	-0.6887	-0.4600	0.5364	0.0039
PC9	0.1597	0.1311	0.1947	-0.5005	-0.6002	-0.4008	0.5689	0.0033
PC10	0.1384	0.1136	0.1687	-0.4337	-0.5202	-0.3473	0.7236	0.0013
PC11	-0.1250	-0.1522	-0.1027	0.3919	0.3143	0.4694	0.2187	0.0152
PC12	-0.1240	-0.1512	-0.1018	0.3886	0.3112	0.4661	0.6015	0.0028
PC13	0.1101	0.0903	0.1341	-0.3449	-0.4136	-0.2762	0.5557	0.0035

Otolemur garnettii

PC	Slope	Slope lower CI	Slope higher CI	Intercept	Intercept lower CI	Intercept higher CI	p value	r squared
PC1	-1.5335	-1.8553	-1.2676	4.6995	3.7988	5.6002	0.0003	0.1340
PC2	-0.8304	-0.9851	-0.7001	2.5448	2.1081	2.9816	0.0000	0.3056
PC3	-0.4877	-0.5981	-0.3977	1.4946	1.1875	1.8018	0.5192	0.0045
PC4	0.4551	0.3712	0.5579	-1.3946	-1.6806	-1.1085	0.3810	0.0083
PC5	0.3639	0.2967	0.4463	-1.1152	-1.3446	-0.8859	0.5947	0.0031
PC6	-0.3243	-0.3979	-0.2644	0.9940	0.7893	1.1987	0.9415	0.0001
PC7	-0.2695	-0.3306	-0.2197	0.8259	0.6558	0.9960	0.9516	0.0000
PC8	-0.2255	-0.2754	-0.1847	0.6912	0.5520	0.8303	0.0396	0.0448
PC9	-0.2118	-0.2582	-0.1737	0.6491	0.5196	0.7786	0.0150	0.0620
PC10	0.1872	0.1527	0.2296	-0.5738	-0.6916	-0.4560	0.4159	0.0071
PC11	-0.1509	-0.1851	-0.1230	0.4624	0.3672	0.5577	0.8025	0.0007
PC12	0.1428	0.1164	0.1752	-0.4377	-0.5276	-0.3477	0.5601	0.0037
PC13	-0.1300	-0.1595	-0.1060	0.3984	0.3164	0.4805	0.7769	0.0009

Avahi laniger

PC	Slope	Slope lower CI	Slope higher CI	Intercept	Intercept lower CI	Intercept higher CI	p value	r squared
PC1	1.6437	1.1222	2.4074	-4.9520	-6.8883	-3.0157	0.0134	0.2579
PC2	0.7260	0.4680	1.1263	-2.1871	-3.1790	-1.1953	0.8467	0.0018
PC3	-0.4534	-0.6940	-0.2963	1.3661	0.7668	1.9654	0.2372	0.0658
PC4	0.4367	0.2921	0.6531	-1.3158	-1.8597	-0.7718	0.0502	0.1704
PC5	0.3122	0.2016	0.4834	-0.9404	-1.3651	-0.5158	0.6464	0.0102
PC6	-0.2872	-0.4455	-0.1852	0.8653	0.4730	1.2577	0.8249	0.0024
PC7	-0.2273	-0.3523	-0.1466	0.6847	0.3747	0.9946	0.7372	0.0055
PC8	0.2093	0.1350	0.3244	-0.6305	-0.9159	-0.3451	0.7382	0.0054
PC9	-0.1895	-0.2922	-0.1229	0.5710	0.3160	0.8260	0.4157	0.0318
PC10	0.1485	0.0968	0.2279	-0.4474	-0.6449	-0.2499	0.2851	0.0542
PC11	-0.1423	-0.2204	-0.0918	0.4286	0.2349	0.6222	0.6724	0.0087
PC12	0.1185	0.0777	0.1807	-0.3569	-0.5122	-0.2017	0.1850	0.0821
PC13	0.1032	0.0678	0.1570	-0.3108	-0.4452	-0.1764	0.1593	0.0920

Indri indri

PC	Slope	Slope lower CI	Slope higher CI	Intercept	Intercept lower CI	Intercept higher CI	p value	r squared
PC1	-1.3880	-1.7813	-1.0815	5.0765	3.7966	6.3564	0.0000	0.4272
PC2	-0.7546	-1.0461	-0.5444	2.7601	1.8425	3.6776	0.6914	0.0043
PC3	-0.5275	-0.7314	-0.3805	1.9294	1.2876	2.5711	0.7307	0.0032
PC4	-0.4225	-0.5819	-0.3068	1.5454	1.0422	2.0486	0.1962	0.0447
PC5	-0.3151	-0.4345	-0.2285	1.1525	0.7758	1.5291	0.2363	0.0377
PC6	-0.2789	-0.3851	-0.2020	1.0201	0.6852	1.3550	0.2996	0.0290
PC7	0.2564	0.1852	0.3551	-0.9378	-1.2487	-0.6270	0.5425	0.0101
PC8	0.2480	0.1788	0.3438	-0.9069	-1.2087	-0.6050	0.7899	0.0019
PC9	-0.2148	-0.2980	-0.1549	0.7857	0.5240	1.0474	0.8805	0.0006
PC10	0.1503	0.1084	0.2083	-0.5496	-0.7324	-0.3667	0.7598	0.0026
PC11	0.1332	0.0962	0.1846	-0.4873	-0.6490	-0.3256	0.5943	0.0077
PC12	0.1189	0.0859	0.1644	-0.4347	-0.5782	-0.2912	0.4193	0.0177
PC13	-0.1172	-0.1622	-0.0847	0.4288	0.2872	0.5705	0.4346	0.0166

Propithecus diadema

PC	Slope	Slope lower CI	Slope higher CI	Intercept	Intercept lower CI	Intercept higher CI	p value	r squared
PC1	1.3794	0.9634	1.9751	-4.8675	-6.6527	-3.0822	0.0280	0.1724
PC2	0.8785	0.6135	1.2581	-3.1001	-4.2374	-1.9628	0.0282	0.1720
PC3	0.5801	0.3980	0.8453	-2.0468	-2.8360	-1.2577	0.1311	0.0855
PC4	-0.4639	-0.6861	-0.3137	1.6370	0.9799	2.2941	0.6344	0.0088
PC5	-0.3344	-0.4883	-0.2290	1.1799	0.7222	1.6375	0.1599	0.0745
PC6	0.3130	0.2113	0.4637	-1.1046	-1.5499	-0.6592	0.9824	0.0000
PC7	0.2878	0.1951	0.4244	-1.0154	-1.4200	-0.6108	0.4379	0.0233
PC8	-0.2243	-0.3308	-0.1521	0.7916	0.4764	1.1069	0.4280	0.0243
PC9	0.1882	0.1275	0.2776	-0.6639	-0.9287	-0.3992	0.4526	0.0219
PC10	0.1543	0.1048	0.2272	-0.5446	-0.7605	-0.3287	0.3566	0.0328
PC11	-0.1300	-0.1888	-0.0895	0.4588	0.2836	0.6340	0.0958	0.1031
PC12	-0.1185	-0.1755	-0.0800	0.4182	0.2496	0.5867	0.9758	0.0000
PC13	0.1100	0.0743	0.1628	-0.3881	-0.5443	-0.2318	0.7942	0.0027

Propithecus verreauxi

PC	Slope	Slope lower CI	Slope higher CI	Intercept	Intercept lower CI	Intercept higher CI	p value	r squared
PC1	1.1903	0.8745	1.6203	-4.1446	-5.4432	-2.8460	0.4609	0.0133
PC2	-0.9710	-1.2803	-0.7364	3.3808	2.4339	4.3278	0.0019	0.2115
PC3	-0.5755	-0.7850	-0.4220	2.0040	1.3718	2.6361	0.9948	0.0000
PC4	0.4406	0.3235	0.6000	-1.5341	-2.0156	-1.0527	0.5173	0.0103
PC5	-0.3685	-0.5023	-0.2704	1.2832	0.8794	1.6869	0.6511	0.0050
PC6	0.3058	0.2242	0.4171	-1.0648	-1.4006	-0.7289	0.9687	0.0000
PC7	0.3028	0.2220	0.4130	-1.0542	-1.3867	-0.7217	0.9065	0.0003
PC8	0.2643	0.1955	0.3572	-0.9201	-1.2017	-0.6385	0.1176	0.0587
PC9	0.2323	0.1706	0.3163	-0.8088	-1.0625	-0.5550	0.5094	0.0107
PC10	-0.1992	-0.2717	-0.1461	0.6937	0.4749	0.9124	0.8950	0.0004
PC11	0.1905	0.1397	0.2598	-0.6634	-0.8724	-0.4544	0.7480	0.0025
PC12	-0.1630	-0.2223	-0.1195	0.5675	0.3885	0.7465	0.9884	0.0000
PC13	-0.1504	-0.2046	-0.1106	0.5237	0.3600	0.6874	0.3902	0.0181

Eulemur fulvus

PC	Slope	Slope lower CI	Slope higher CI	Intercept	Intercept lower CI	Intercept higher CI	p value	r squared
PC1	1.4542	1.2533	1.6874	-4.9908	-5.7360	-4.2457	0.1737	0.0107
PC2	-0.8440	-0.9477	-0.7516	2.8965	2.5601	3.2330	0.0000	0.4011
PC3	0.3567	0.3076	0.4136	-1.2241	-1.4060	-1.0422	0.0643	0.0196
PC4	-0.2751	-0.3189	-0.2373	0.9440	0.8040	1.0840	0.0417	0.0237
PC5	-0.2467	-0.2865	-0.2124	0.8467	0.7196	0.9738	0.9517	0.0000
PC6	0.2139	0.1842	0.2484	-0.7342	-0.8444	-0.6240	0.9370	0.0000
PC7	-0.2067	-0.2400	-0.1780	0.7095	0.6030	0.8159	0.8078	0.0003
PC8	-0.1821	-0.2115	-0.1568	0.6250	0.5312	0.7188	0.7642	0.0005
PC9	-0.1547	-0.1796	-0.1332	0.5309	0.4512	0.6106	0.8017	0.0004
PC10	0.1229	0.1059	0.1427	-0.4219	-0.4852	-0.3587	0.5378	0.0022
PC11	-0.1162	-0.1348	-0.1001	0.3988	0.3392	0.4584	0.2350	0.0081
PC12	0.1061	0.0914	0.1231	-0.3640	-0.4184	-0.3096	0.2225	0.0086
PC13	-0.1041	-0.1208	-0.0896	0.3571	0.3035	0.4107	0.9115	0.0001

Eulemur macaco

PC	Slope	Slope lower CI	Slope higher CI	Intercept	Intercept lower CI	Intercept higher CI	p value	r squared
PC1	-1.3474	-1.7383	-1.0444	4.6981	3.4880	5.9081	0.0077	0.1263
PC2	0.8549	0.6906	1.0584	-2.9810	-3.6224	-2.3397	0.0000	0.3904
PC3	0.4154	0.3165	0.5452	-1.4483	-1.8471	-1.0495	0.7869	0.0014
PC4	-0.3471	-0.4538	-0.2655	1.2103	0.8821	1.5386	0.1960	0.0313
PC5	-0.2847	-0.3732	-0.2171	0.9926	0.7204	1.2647	0.4671	0.0100
PC6	0.2511	0.1914	0.3295	-0.8756	-1.1165	-0.6347	0.6686	0.0035
PC7	0.2356	0.1796	0.3090	-0.8215	-1.0471	-0.5958	0.5579	0.0065
PC8	0.2044	0.1558	0.2681	-0.7126	-0.9086	-0.5166	0.6556	0.0038
PC9	0.1790	0.1366	0.2345	-0.6240	-0.7948	-0.4531	0.4100	0.0128
PC10	-0.1672	-0.2195	-0.1274	0.5831	0.4224	0.7437	0.9118	0.0002
PC11	-0.1418	-0.1858	-0.1082	0.4945	0.3592	0.6298	0.3973	0.0136
PC12	-0.1340	-0.1752	-0.1025	0.4673	0.3405	0.5941	0.2017	0.0306
PC13	-0.1153	-0.1514	-0.0878	0.4020	0.2913	0.5128	0.8545	0.0006

Eulemur mongoz

PC	Slope	Slope lower CI	Slope higher CI	Intercept	Intercept lower CI	Intercept higher CI	p value	r squared
PC1	1.2263	0.9389	1.6016	-4.1470	-5.2681	-3.0260	0.9266	0.0002
PC2	-0.7277	-0.9425	-0.5618	2.4609	1.8170	3.1047	0.0591	0.0633
PC3	-0.3882	-0.4819	-0.3126	1.3127	1.0264	1.5991	0.0000	0.3488
PC4	-0.3060	-0.3995	-0.2344	1.0349	0.7555	1.3143	0.7099	0.0025
PC5	-0.2159	-0.2815	-0.1656	0.7302	0.5342	0.9262	0.3762	0.0143
PC6	0.2052	0.1572	0.2679	-0.6941	-0.8814	-0.5068	0.6519	0.0037
PC7	0.1668	0.1278	0.2178	-0.5642	-0.7164	-0.4120	0.6110	0.0047
PC8	-0.1479	-0.1930	-0.1133	0.5001	0.3653	0.6348	0.5611	0.0062
PC9	-0.1266	-0.1653	-0.0969	0.4281	0.3124	0.5438	0.9359	0.0001
PC10	-0.1190	-0.1552	-0.0913	0.4026	0.2945	0.5107	0.3972	0.0131
PC11	-0.1061	-0.1384	-0.0814	0.3590	0.2626	0.4554	0.3981	0.0130
PC12	-0.0930	-0.1199	-0.0722	0.3146	0.2338	0.3954	0.0179	0.0977
PC13	0.0823	0.0632	0.1070	-0.2782	-0.3523	-0.2040	0.2183	0.0274

Eulemur rubriventer

PC	Slope	Slope lower CI	Slope higher CI	Intercept	Intercept lower CI	Intercept higher CI	p value	r squared
PC1	-3.4283	-5.0482	-2.3283	12.0046	7.2423	16.7670	0.1742	0.0726
PC2	-0.8749	-1.2622	-0.6064	3.0635	1.9153	4.2116	0.0314	0.1722
PC3	-0.5384	-0.8037	-0.3607	1.8852	1.1096	2.6608	0.8061	0.0025
PC4	0.4366	0.2942	0.6479	-1.5288	-2.1482	-0.9093	0.3678	0.0326
PC5	0.3885	0.2601	0.5802	-1.3603	-1.9207	-0.7999	0.9949	0.0000
PC6	-0.3198	-0.4770	-0.2144	1.1198	0.6602	1.5795	0.6763	0.0071
PC7	0.2704	0.1811	0.4038	-0.9468	-1.3368	-0.5568	0.9789	0.0000
PC8	0.2464	0.1703	0.3567	-0.8629	-1.1893	-0.5365	0.0408	0.1569
PC9	0.2220	0.1487	0.3314	-0.7772	-1.0971	-0.4573	0.8417	0.0016
PC10	-0.1699	-0.2528	-0.1142	0.5950	0.3525	0.8375	0.4713	0.0210
PC11	0.1485	0.0995	0.2217	-0.5200	-0.7341	-0.3060	0.8585	0.0013
PC12	-0.1314	-0.1962	-0.0880	0.4599	0.2705	0.6494	0.9956	0.0000
PC13	0.1215	0.0814	0.1814	-0.4256	-0.6006	-0.2505	0.7736	0.0034

Hapalemur griseus

PC	Slope	Slope lower CI	Slope higher CI	Intercept	Intercept lower CI	Intercept higher CI	p value	r squared
PC1	1.1653	0.8039	1.6892	-3.6600	-5.0506	-2.2695	0.0462	0.1497
PC2	0.5587	0.3867	0.8072	-1.7547	-2.4152	-1.0942	0.0353	0.1654
PC3	0.3371	0.2258	0.5032	-1.0587	-1.4945	-0.6228	0.8356	0.0018
PC4	-0.2960	-0.4420	-0.1982	0.9297	0.5468	1.3126	0.8831	0.0009
PC5	0.2395	0.1618	0.3544	-0.7522	-1.0547	-0.4496	0.2777	0.0470
PC6	-0.2074	-0.3094	-0.1390	0.6514	0.3838	0.9189	0.7023	0.0059
PC7	-0.1897	-0.2833	-0.1270	0.5957	0.3503	0.8412	0.9467	0.0002
PC8	-0.1755	-0.2617	-0.1177	0.5512	0.3250	0.7775	0.6630	0.0077
PC9	-0.1652	-0.2466	-0.1106	0.5187	0.3050	0.7325	0.9448	0.0002
PC10	0.1384	0.0927	0.2065	-0.4345	-0.6132	-0.2558	0.7589	0.0038
PC11	-0.1155	-0.1718	-0.0777	0.3629	0.2150	0.5108	0.4644	0.0216
PC12	0.1009	0.0700	0.1453	-0.3168	-0.4351	-0.1986	0.0275	0.1797
PC13	0.0938	0.0631	0.1394	-0.2945	-0.4143	-0.1747	0.4300	0.0251

Lemur catta

PC	Slope	Slope lower CI	Slope higher CI	Intercept	Intercept lower CI	Intercept higher CI	p value	r squared
PC1	-0.9648	-1.2752	-0.7300	3.2067	2.3004	4.1130	0.0001	0.3842
PC2	0.8053	0.5662	1.1454	-2.6766	-3.6394	-1.7138	0.7647	0.0028
PC3	-0.4082	-0.5671	-0.2938	1.3568	0.9024	1.8111	0.0321	0.1356
PC4	0.3655	0.2569	0.5199	-1.2148	-1.6520	-0.7775	0.8293	0.0015
PC5	-0.2563	-0.3602	-0.1824	0.8518	0.5562	1.1473	0.1250	0.0720
PC6	-0.2263	-0.3220	-0.1591	0.7523	0.4814	1.0231	0.8836	0.0007
PC7	0.2043	0.1439	0.2900	-0.6790	-0.9219	-0.4361	0.5122	0.0135
PC8	0.1768	0.1243	0.2516	-0.5876	-0.7993	-0.3760	0.9144	0.0004
PC9	0.1572	0.1121	0.2204	-0.5223	-0.7025	-0.3422	0.0975	0.0835
PC10	0.1196	0.0841	0.1702	-0.3977	-0.5408	-0.2545	0.8227	0.0016
PC11	-0.1114	-0.1583	-0.0784	0.3702	0.2374	0.5030	0.6175	0.0079
PC12	-0.0981	-0.1386	-0.0694	0.3260	0.2111	0.4409	0.2464	0.0417
PC13	-0.0835	-0.1185	-0.0589	0.2776	0.1785	0.3767	0.4639	0.0169

Varecia variegata

PC	Slope	Slope lower CI	Slope higher CI	Intercept	Intercept lower CI	Intercept higher CI	p value	r squared
PC1	1.6120	1.1658	2.2290	-5.8230	-7.7437	-3.9022	0.3921	0.0199
PC2	-0.7880	-1.0556	-0.5882	2.8463	2.0021	3.6905	0.0036	0.2074
PC3	-0.4166	-0.5724	-0.3032	1.5047	1.0184	1.9910	0.1356	0.0592
PC4	0.3660	0.2646	0.5061	-1.3220	-1.7582	-0.8857	0.4039	0.0189
PC5	0.2929	0.2112	0.4063	-1.0580	-1.4105	-0.7055	0.9869	0.0000
PC6	0.2419	0.1745	0.3353	-0.8737	-1.1643	-0.5831	0.7299	0.0033
PC7	-0.2270	-0.3070	-0.1678	0.8198	0.5683	1.0713	0.0141	0.1523
PC8	-0.1669	-0.2310	-0.1206	0.6029	0.4035	0.8024	0.4672	0.0144
PC9	0.1306	0.0942	0.1811	-0.4717	-0.6287	-0.3147	0.8105	0.0016
PC10	-0.1288	-0.1779	-0.0933	0.4653	0.3124	0.6182	0.3103	0.0278
PC11	0.1174	0.0847	0.1629	-0.4242	-0.5656	-0.2829	0.9921	0.0000
PC12	0.1013	0.0732	0.1402	-0.3659	-0.4870	-0.2449	0.4639	0.0146
PC13	-0.0848	-0.1174	-0.0612	0.3062	0.2048	0.4076	0.5041	0.0121

Lepilemur ruficaudatus

PC	Slope	Slope lower CI	Slope higher CI	Intercept	Intercept lower CI	Intercept higher CI	p value	r squared
PC1	-1.0074	-1.5174	-0.6689	3.0002	1.7363	4.2640	0.2992	0.0468
PC2	-0.6833	-1.0265	-0.4548	2.0349	1.1834	2.8865	0.2403	0.0594
PC3	0.5958	0.3935	0.9019	-1.7742	-2.5314	-1.0171	0.4821	0.0217
PC4	0.3646	0.2426	0.5482	-1.0859	-1.5411	-0.6308	0.2532	0.0564
PC5	0.3247	0.2137	0.4935	-0.9670	-1.3838	-0.5502	0.8251	0.0022
PC6	-0.2900	-0.4362	-0.1928	0.8636	0.5010	1.2262	0.2679	0.0531
PC7	0.2044	0.1345	0.3106	-0.6087	-0.8711	-0.3463	0.8364	0.0019
PC8	-0.1947	-0.2960	-0.1281	0.5799	0.3298	0.8299	0.8647	0.0013
PC9	0.1764	0.1161	0.2682	-0.5254	-0.7520	-0.2988	0.9077	0.0006
PC10	0.1553	0.1028	0.2346	-0.4624	-0.6588	-0.2660	0.3997	0.0310
PC11	-0.1171	-0.1727	-0.0793	0.3486	0.2095	0.4878	0.0607	0.1447
PC12	0.1071	0.0704	0.1628	-0.3190	-0.4566	-0.1813	0.9952	0.0000
PC13	-0.1017	-0.1546	-0.0669	0.3028	0.1721	0.4334	0.9924	0.0000

Loris tardigradus

PC	Slope	Slope lower CI	Slope higher CI	Intercept	Intercept lower CI	Intercept higher CI	p value	r squared
PC1	0.8174	0.5539	1.2062	-2.2875	-3.2013	-1.3738	0.2128	0.0614
PC2	-0.6420	-0.8509	-0.4844	1.7967	1.2834	2.3099	0.0000	0.5197
PC3	-0.3137	-0.4668	-0.2108	0.8779	0.5193	1.2365	0.4987	0.0185
PC4	0.2546	0.1705	0.3802	-0.7125	-1.0063	-0.4187	0.9929	0.0000
PC5	0.2339	0.1645	0.3326	-0.6545	-0.8899	-0.4191	0.0097	0.2388
PC6	0.1690	0.1133	0.2523	-0.4731	-0.6678	-0.2784	0.7622	0.0037
PC7	-0.1478	-0.2203	-0.0991	0.4136	0.2438	0.5833	0.6324	0.0093
PC8	-0.1143	-0.1708	-0.0766	0.3200	0.1880	0.4520	0.9894	0.0000
PC9	0.0917	0.0615	0.1368	-0.2567	-0.3621	-0.1513	0.6471	0.0085
PC10	-0.0855	-0.1273	-0.0574	0.2393	0.1413	0.3372	0.5507	0.0144
PC11	-0.0769	-0.1147	-0.0516	0.2153	0.1269	0.3037	0.6521	0.0083
PC12	0.0653	0.0438	0.0972	-0.1826	-0.2573	-0.1079	0.5321	0.0158
PC13	0.0517	0.0346	0.0771	-0.1446	-0.2041	-0.0850	0.8585	0.0013

Nycticebus bengalensis

PC	Slope	Slope lower CI	Slope higher CI	Intercept	Intercept lower CI	Intercept higher CI	p value	r squared
PC1	0.8578	0.6217	1.1835	-2.6153	-3.4718	-1.7588	0.0002	0.5072
PC2	0.7147	0.4559	1.1205	-2.1790	-3.1924	-1.1656	0.7277	0.0062
PC3	-0.5521	-0.8576	-0.3555	1.6833	0.9178	2.4489	0.3189	0.0497
PC4	-0.4397	-0.6864	-0.2817	1.3407	0.7236	1.9578	0.4682	0.0266
PC5	-0.3434	-0.5390	-0.2187	1.0469	0.5585	1.5353	0.9773	0.0000
PC6	0.2453	0.1563	0.3848	-0.7478	-1.0961	-0.3994	0.8043	0.0031
PC7	-0.2425	-0.3807	-0.1545	0.7394	0.3944	1.0844	0.9941	0.0000
PC8	0.2131	0.1421	0.3196	-0.6497	-0.9204	-0.3791	0.0355	0.2028
PC9	0.1885	0.1205	0.2950	-0.5748	-0.8408	-0.3088	0.5752	0.0160
PC10	0.1666	0.1074	0.2586	-0.5081	-0.7386	-0.2776	0.2959	0.0545
PC11	0.1272	0.0811	0.1997	-0.3879	-0.5688	-0.2070	0.9316	0.0004
PC12	0.1136	0.0724	0.1784	-0.3465	-0.5081	-0.1848	0.9534	0.0002
PC13	-0.0964	-0.1512	-0.0615	0.2940	0.1573	0.4307	0.7280	0.0062

Nycticebus coucang

PC	Slope	Slope lower CI	Slope higher CI	Intercept	Intercept lower CI	Intercept higher CI	p value	r squared
PC1	0.6952	0.5611	0.8615	-2.0270	-2.4652	-1.5888	0.0001	0.2149
PC2	0.5653	0.4500	0.7102	-1.6482	-2.0277	-1.2686	0.0056	0.1091
PC3	-0.2923	-0.3702	-0.2308	0.8523	0.6491	1.0555	0.0799	0.0451
PC4	0.2324	0.1829	0.2952	-0.6775	-0.8413	-0.5137	0.2679	0.0183
PC5	0.1999	0.1571	0.2543	-0.5828	-0.7246	-0.4410	0.5335	0.0058
PC6	-0.1815	-0.2310	-0.1425	0.5291	0.4000	0.6582	0.8762	0.0004
PC7	0.1577	0.1239	0.2007	-0.4597	-0.5718	-0.3477	0.6713	0.0027
PC8	0.1505	0.1182	0.1917	-0.4389	-0.5460	-0.3318	0.9259	0.0001
PC9	-0.1327	-0.1689	-0.1042	0.3869	0.2925	0.4813	0.8966	0.0003
PC10	0.1146	0.0900	0.1459	-0.3342	-0.4157	-0.2526	0.9001	0.0002
PC11	-0.1017	-0.1283	-0.0806	0.2964	0.2268	0.3660	0.0235	0.0742
PC12	-0.0969	-0.1233	-0.0761	0.2825	0.2136	0.3514	0.7975	0.0010
PC13	-0.0886	-0.1124	-0.0698	0.2583	0.1962	0.3204	0.1662	0.0284

Perodicticus potto

PC	Slope	Slope lower CI	Slope higher CI	Intercept	Intercept lower CI	Intercept higher CI	p value	r squared
PC1	0.8161	0.7007	0.9504	-2.4178	-2.7879	-2.0477	0.0000	0.2407
PC2	-0.6345	-0.7554	-0.5329	1.8798	1.5501	2.2096	0.5387	0.0030
PC3	-0.3969	-0.4726	-0.3334	1.1761	0.9696	1.3825	0.6316	0.0018
PC4	-0.2803	-0.3338	-0.2354	0.8306	0.6847	0.9764	0.6626	0.0015
PC5	0.2634	0.2221	0.3125	-0.7805	-0.9146	-0.6465	0.0165	0.0444
PC6	-0.2317	-0.2756	-0.1947	0.6864	0.5665	0.8063	0.2142	0.0121
PC7	0.2010	0.1688	0.2393	-0.5954	-0.7000	-0.4909	0.6785	0.0014
PC8	-0.1886	-0.2228	-0.1596	0.5587	0.4649	0.6525	0.0007	0.0873
PC9	-0.1727	-0.2054	-0.1453	0.5118	0.4226	0.6010	0.1509	0.0162
PC10	-0.1528	-0.1818	-0.1284	0.4526	0.3735	0.5317	0.2446	0.0106
PC11	-0.1382	-0.1644	-0.1161	0.4093	0.3376	0.4810	0.3767	0.0062
PC12	0.1293	0.1086	0.1539	-0.3831	-0.4502	-0.3160	0.3863	0.0059
PC13	-0.1246	-0.1484	-0.1047	0.3693	0.3044	0.4341	0.9144	0.0001

Goswami model zygomatic module against ln CS whole cranium

Cheirogaleus major

PC	Slope	Slope lower CI	Slope higher CI	Intercept	Intercept lower CI	Intercept higher CI	p value	r squared
PC1	0.9270	0.6233	1.3787	-4.5045	-6.3400	-2.6689	0.1093	0.1076
PC2	0.8070	0.5331	1.2217	-3.9215	-5.5948	-2.2481	0.4841	0.0215
PC3	0.6960	0.4812	1.0067	-3.3819	-4.6587	-2.1051	0.0143	0.2340
PC4	-0.6855	-1.0188	-0.4613	3.3313	1.9768	4.6857	0.1026	0.1116
PC5	-0.5650	-0.8588	-0.3716	2.7453	1.5615	3.9291	0.8937	0.0008
PC6	-0.5502	-0.8340	-0.3630	2.6738	1.5292	3.8183	0.5567	0.0152
PC7	0.4955	0.3259	0.7534	-2.4080	-3.4468	-1.3693	0.9778	0.0000
PC8	0.4052	0.2728	0.6018	-1.9690	-2.7684	-1.1695	0.0988	0.1140
PC9	-0.3519	-0.5333	-0.2322	1.7099	0.9782	2.4417	0.5485	0.0159
PC10	0.3112	0.2048	0.4731	-1.5123	-2.1643	-0.8604	0.8590	0.0014
PC11	-0.2830	-0.4303	-0.1862	1.3752	0.7821	1.9683	0.9208	0.0004
PC12	-0.2442	-0.3676	-0.1623	1.1868	0.6878	1.6859	0.2832	0.0499
PC13	-0.2309	-0.3459	-0.1541	1.1218	0.6558	1.5878	0.1922	0.0728

Cheirogaleus medius

PC	Slope	Slope lower CI	Slope higher CI	Intercept	Intercept lower CI	Intercept higher CI	p value	r squared
PC1	-0.7471	-1.0883	-0.5129	3.4293	2.1085	4.7500	0.2490	0.0489
PC2	0.6572	0.4615	0.9358	-3.0165	-4.1049	-1.9281	0.0287	0.1652
PC3	-0.6470	-0.9487	-0.4412	2.9696	1.8049	4.1343	0.5457	0.0137
PC4	-0.5625	-0.8104	-0.3904	2.5819	1.6180	3.5459	0.0844	0.1063
PC5	0.4833	0.3303	0.7072	-2.2186	-3.0837	-1.3535	0.4124	0.0250
PC6	0.4526	0.3082	0.6646	-2.0774	-2.8953	-1.2595	0.6870	0.0061
PC7	0.4139	0.2816	0.6085	-1.8999	-2.6502	-1.1496	0.9710	0.0001
PC8	-0.3418	-0.4988	-0.2343	1.5690	0.9618	2.1763	0.3012	0.0395
PC9	-0.3235	-0.4642	-0.2255	1.4850	0.9370	2.0330	0.0579	0.1268
PC10	0.2915	0.1983	0.4284	-1.3379	-1.8660	-0.8097	0.8866	0.0008
PC11	0.2869	0.1952	0.4215	-1.3168	-1.8362	-0.7973	0.8106	0.0022
PC12	0.2642	0.1808	0.3861	-1.2127	-1.6838	-0.7415	0.3522	0.0321
PC13	-0.2283	-0.3356	-0.1553	1.0479	0.6342	1.4616	0.8901	0.0007

Microcebus murinus

PC	Slope	Slope lower CI	Slope higher CI	Intercept	Intercept lower CI	Intercept higher CI	p value	r squared
PC1	1.1714	0.9358	1.4664	-5.0786	-6.2288	-3.9283	0.0076	0.0974
PC2	-1.0463	-1.3247	-0.8264	4.5361	3.4558	5.6164	0.7073	0.0020
PC3	-1.0143	-1.2838	-0.8014	4.3974	3.3517	5.4431	0.5543	0.0050
PC4	0.8173	0.6454	1.0350	-3.5432	-4.3878	-2.6985	0.9168	0.0002
PC5	0.8081	0.6383	1.0232	-3.5035	-4.3380	-2.6691	0.7165	0.0019
PC6	0.7204	0.5704	0.9098	-3.1230	-3.8589	-2.3871	0.2036	0.0230
PC7	-0.6609	-0.8366	-0.5221	2.8651	2.1833	3.5468	0.6119	0.0037
PC8	-0.6366	-0.8039	-0.5041	2.7597	2.1099	3.4096	0.1908	0.0243
PC9	-0.6060	-0.7671	-0.4788	2.6272	2.0023	3.2522	0.5832	0.0043
PC10	-0.5775	-0.7307	-0.4564	2.5036	1.9091	3.0982	0.4666	0.0076
PC11	0.5252	0.4176	0.6606	-2.2771	-2.8037	-1.7505	0.0400	0.0589
PC12	-0.5051	-0.6394	-0.3990	2.1897	1.6688	2.7107	0.5978	0.0040
PC13	0.4382	0.3506	0.5476	-1.8995	-2.3267	-1.4724	0.0044	0.1104

Microcebus rufus

PC	Slope	Slope lower CI	Slope higher CI	Intercept	Intercept lower CI	Intercept higher CI	p value	r squared
PC1	0.7463	0.5092	1.0939	-3.2525	-4.5268	-1.9782	0.5162	0.0158
PC2	-0.6741	-0.9531	-0.4767	2.9376	1.8995	3.9757	0.0152	0.1993
PC3	-0.5614	-0.8209	-0.3840	2.4468	1.4946	3.3990	0.3778	0.0289
PC4	-0.5057	-0.7432	-0.3441	2.2040	1.3341	3.0739	0.8581	0.0012
PC5	-0.4627	-0.6802	-0.3148	2.0166	1.2203	2.8130	0.9266	0.0003
PC6	0.4325	0.2943	0.6358	-1.8851	-2.6294	-1.1407	0.9219	0.0004
PC7	-0.4310	-0.6262	-0.2966	1.8783	1.1600	2.5965	0.1917	0.0623
PC8	0.3576	0.2490	0.5135	-1.5583	-2.1348	-0.9818	0.0628	0.1224
PC9	-0.3354	-0.4908	-0.2292	1.4619	0.8917	2.0320	0.4157	0.0247
PC10	0.3133	0.2142	0.4584	-1.3655	-1.8977	-0.8333	0.4030	0.0260
PC11	-0.2698	-0.3961	-0.1838	1.1758	0.7133	1.6384	0.6502	0.0077
PC12	0.2454	0.1713	0.3516	-1.0695	-1.4625	-0.6765	0.0505	0.1343
PC13	0.2148	0.1463	0.3154	-0.9360	-1.3045	-0.5676	0.6788	0.0065

Galago alleni

PC	Slope	Slope lower CI	Slope higher CI	Intercept	Intercept lower CI	Intercept higher CI	p value	r squared
PC1	1.0048	0.6545	1.5426	-4.7818	-6.8950	-2.6686	0.8722	0.0012
PC2	0.7024	0.4625	1.0666	-3.3425	-4.7801	-1.9049	0.2750	0.0539
PC3	0.5937	0.4034	0.8736	-2.8252	-3.9440	-1.7064	0.0294	0.1979
PC4	0.5785	0.3840	0.8715	-2.7529	-3.9131	-1.5927	0.1506	0.0916
PC5	0.5445	0.3548	0.8358	-2.5913	-3.7359	-1.4466	0.8332	0.0021
PC6	0.4856	0.3179	0.7417	-2.3109	-3.3193	-1.3025	0.4502	0.0262
PC7	0.4159	0.2723	0.6351	-1.9792	-2.8424	-1.1160	0.4418	0.0271
PC8	0.3705	0.2414	0.5688	-1.7633	-2.5424	-0.9842	0.8572	0.0015
PC9	-0.3609	-0.5385	-0.2419	1.7177	1.0121	2.4233	0.0751	0.1369
PC10	0.3258	0.2143	0.4954	-1.5503	-2.2193	-0.8814	0.3044	0.0479
PC11	0.2929	0.1913	0.4486	-1.3941	-2.0062	-0.7819	0.5841	0.0138
PC12	-0.2327	-0.3520	-0.1538	1.1072	0.6356	1.5788	0.2046	0.0721
PC13	-0.2050	-0.3120	-0.1347	0.9757	0.5538	1.3976	0.3275	0.0436

Galago demidoff

PC	Slope	Slope lower CI	Slope higher CI	Intercept	Intercept lower CI	Intercept higher CI	p value	r squared
PC1	-1.1935	-1.5400	-0.9250	5.2888	3.9260	6.6516	0.0705	0.0563
PC2	0.9741	0.7501	1.2651	-4.3167	-5.4580	-3.1754	0.5452	0.0065
PC3	0.8713	0.6705	1.1321	-3.8608	-4.8835	-2.8382	0.6918	0.0028
PC4	-0.7150	-0.9287	-0.5504	3.1683	2.3300	4.0066	0.5968	0.0049
PC5	0.6733	0.5182	0.8749	-2.9837	-3.7741	-2.1932	0.7082	0.0025
PC6	-0.6075	-0.7894	-0.4675	2.6918	1.9786	3.4051	0.7327	0.0021
PC7	0.5812	0.4472	0.7554	-2.5755	-3.2586	-1.8924	0.9346	0.0001
PC8	0.5332	0.4115	0.6908	-2.3627	-2.9815	-1.7439	0.2303	0.0251
PC9	0.4819	0.3729	0.6228	-2.1355	-2.6892	-1.5818	0.1088	0.0445
PC10	0.4641	0.3604	0.5977	-2.0566	-2.5825	-1.5307	0.0419	0.0706
PC11	0.3987	0.3069	0.5180	-1.7667	-2.2344	-1.2990	0.6380	0.0039
PC12	0.3929	0.3023	0.5108	-1.7413	-2.2032	-1.2794	0.9822	0.0000
PC13	0.3556	0.2736	0.4622	-1.5758	-1.9937	-1.1579	0.8799	0.0004

Galago elegantulus

PC	Slope	Slope lower CI	Slope higher CI	Intercept	Intercept lower CI	Intercept higher CI	p value	r squared
PC1	-1.2567	-1.7877	-0.8834	5.9334	3.7987	8.0682	0.8152	0.0017
PC2	-1.0798	-1.4932	-0.7808	5.0982	3.4163	6.7801	0.0188	0.1606
PC3	-0.9841	-1.3979	-0.6928	4.6465	2.9819	6.3112	0.5698	0.0102
PC4	0.8399	0.5903	1.1951	-3.9656	-5.3936	-2.5376	0.9756	0.0000
PC5	0.7813	0.5491	1.1117	-3.6891	-5.0173	-2.3609	0.9147	0.0004
PC6	0.7154	0.5064	1.0106	-3.3777	-4.5680	-2.1874	0.2435	0.0423
PC7	-0.6781	-0.9641	-0.4769	3.2015	2.0514	4.3517	0.6988	0.0047
PC8	0.6237	0.4400	0.8843	-2.9450	-3.9941	-1.8959	0.4089	0.0214
PC9	-0.5215	-0.7355	-0.3697	2.4620	1.5983	3.3258	0.1995	0.0509
PC10	-0.4753	-0.6541	-0.3454	2.2443	1.5156	2.9729	0.0106	0.1870
PC11	-0.4440	-0.6312	-0.3123	2.0962	1.3431	2.8492	0.6992	0.0047
PC12	-0.3897	-0.5520	-0.2752	1.8401	1.1865	2.4936	0.3515	0.0272
PC13	0.3608	0.2538	0.5128	-1.7034	-2.3148	-1.0920	0.6512	0.0065

Galago moholi

PC	Slope	Slope lower CI	Slope higher CI	Intercept	Intercept lower CI	Intercept higher CI	p value	r squared
PC1	-1.0918	-1.3551	-0.8798	4.9654	3.8846	6.0463	0.0006	0.1540
PC2	-0.9744	-1.2318	-0.7708	4.4314	3.3831	5.4797	0.8154	0.0008
PC3	0.8330	0.6597	1.0518	-3.7882	-4.6798	-2.8966	0.3808	0.0108
PC4	0.6335	0.5041	0.7961	-2.8810	-3.5451	-2.2168	0.0546	0.0511
PC5	-0.5997	-0.7575	-0.4748	2.7275	2.0847	3.3703	0.4445	0.0083
PC6	0.5763	0.4566	0.7275	-2.6211	-3.2370	-2.0051	0.3198	0.0139
PC7	0.5506	0.4359	0.6954	-2.5040	-3.0941	-1.9139	0.4416	0.0084
PC8	0.5107	0.4055	0.6432	-2.3224	-2.8629	-1.7818	0.1265	0.0326
PC9	-0.4748	-0.6000	-0.3758	2.1593	1.6494	2.6693	0.5847	0.0042
PC10	0.4494	0.3565	0.5666	-2.0438	-2.5217	-1.5659	0.1925	0.0238
PC11	-0.3944	-0.4981	-0.3124	1.7939	1.3716	2.2161	0.3809	0.0108
PC12	-0.3615	-0.4568	-0.2860	1.6438	1.2555	2.0322	0.6169	0.0035
PC13	-0.3370	-0.4254	-0.2669	1.5325	1.1720	1.8930	0.3552	0.0120

Galago senegalensis

PC	Slope	Slope lower CI	Slope higher CI	Intercept	Intercept lower CI	Intercept higher CI	p value	r squared
PC1	-0.8247	-0.9568	-0.7109	3.8232	3.2534	4.3931	0.1255	0.0135
PC2	-0.6562	-0.7611	-0.5657	3.0419	2.5889	3.4949	0.1037	0.0152
PC3	0.6237	0.5381	0.7229	-2.8914	-3.3197	-2.4631	0.0342	0.0257
PC4	0.5650	0.4867	0.6560	-2.6192	-3.0117	-2.2268	0.4702	0.0030
PC5	-0.5520	-0.6408	-0.4754	2.5588	2.1753	2.9423	0.4978	0.0027
PC6	-0.4864	-0.5643	-0.4192	2.2547	1.9182	2.5912	0.1648	0.0111
PC7	-0.4770	-0.5538	-0.4108	2.2113	1.8798	2.5428	0.5521	0.0020
PC8	-0.4522	-0.5249	-0.3896	2.0962	1.7826	2.4099	0.3144	0.0059
PC9	0.4204	0.3629	0.4871	-1.9491	-2.2368	-1.6613	0.0178	0.0320
PC10	-0.3993	-0.4626	-0.3446	1.8511	1.5776	2.1245	0.0203	0.0307
PC11	-0.3784	-0.4391	-0.3261	1.7543	1.4925	2.0162	0.1722	0.0107
PC12	0.3547	0.3056	0.4118	-1.6444	-1.8907	-1.3981	0.4026	0.0041
PC13	0.3341	0.2877	0.3880	-1.5488	-1.7812	-1.3164	0.8569	0.0002

Galago zanzibaricus

PC	Slope	Slope lower CI	Slope higher CI	Intercept	Intercept lower CI	Intercept higher CI	p value	r squared
PC1	1.3476	0.8898	2.0408	-6.1807	-8.8203	-3.5411	0.5024	0.0198
PC2	1.0966	0.7214	1.6669	-5.0294	-7.1977	-2.8611	0.8740	0.0011
PC3	0.8881	0.6081	1.2971	-4.0733	-5.6535	-2.4931	0.0288	0.1912
PC4	0.8157	0.5464	1.2176	-3.7410	-5.2803	-2.2017	0.1448	0.0901
PC5	0.7370	0.4915	1.1053	-3.3803	-4.7880	-1.9726	0.2080	0.0680
PC6	0.7134	0.4692	1.0846	-3.2720	-4.6832	-1.8607	0.9436	0.0002
PC7	-0.5976	-0.8685	-0.4112	2.7410	1.6922	3.7898	0.0202	0.2132
PC8	0.5419	0.3584	0.8192	-2.4852	-3.5420	-1.4285	0.4214	0.0283
PC9	0.4726	0.3120	0.7158	-2.1674	-3.0935	-1.2413	0.5128	0.0189
PC10	-0.4228	-0.6368	-0.2808	1.9393	1.1228	2.7558	0.2964	0.0473
PC11	-0.3941	-0.5915	-0.2626	1.8077	1.0534	2.5620	0.2213	0.0643
PC12	0.3316	0.2206	0.4986	-1.5210	-2.1588	-0.8832	0.2585	0.0551
PC13	0.3181	0.2093	0.4836	-1.4590	-2.0880	-0.8299	0.8917	0.0008

Otolemur crassicaudatus

PC	Slope	Slope lower CI	Slope higher CI	Intercept	Intercept lower CI	Intercept higher CI	p value	r squared
PC1	-0.5590	-0.6724	-0.4647	2.8595	2.3283	3.3906	0.0002	0.1325
PC2	0.4141	0.3501	0.4898	-2.1183	-2.4757	-1.7609	0.0000	0.2843
PC3	0.3713	0.3046	0.4525	-1.8992	-2.2776	-1.5209	0.6296	0.0024
PC4	-0.3566	-0.4340	-0.2930	1.8241	1.4636	2.1847	0.1816	0.0180
PC5	-0.3342	-0.4066	-0.2748	1.7099	1.3728	2.0470	0.1310	0.0229
PC6	0.3145	0.2600	0.3806	-1.6091	-1.9175	-1.3007	0.0052	0.0763
PC7	0.2953	0.2422	0.3600	-1.5106	-1.8119	-1.2094	0.8391	0.0004
PC8	-0.2850	-0.3461	-0.2347	1.4581	1.1731	1.7430	0.0447	0.0401
PC9	-0.2664	-0.3245	-0.2187	1.3626	1.0919	1.6332	0.3665	0.0082
PC10	-0.2446	-0.2980	-0.2008	1.2513	1.0026	1.5000	0.4009	0.0071
PC11	0.2300	0.1887	0.2803	-1.1764	-1.4107	-0.9422	0.5644	0.0034
PC12	0.2121	0.1752	0.2567	-1.0850	-1.2934	-0.8766	0.0064	0.0727
PC13	-0.1887	-0.2299	-0.1549	0.9655	0.7736	1.1574	0.4192	0.0066

Otolemur garnettii

PC	Slope	Slope lower CI	Slope higher CI	Intercept	Intercept lower CI	Intercept higher CI	p value	r squared
PC1	0.5194	0.4410	0.6117	-2.6211	-3.0517	-2.1905	0.0000	0.3635
PC2	0.4579	0.3733	0.5617	-2.3106	-2.7860	-1.8351	0.6928	0.0017
PC3	-0.4276	-0.5242	-0.3489	2.1580	1.7155	2.6006	0.3757	0.0084
PC4	-0.3788	-0.4644	-0.3089	1.9115	1.5191	2.3039	0.4449	0.0063
PC5	-0.3589	-0.4379	-0.2941	1.8110	1.4481	2.1740	0.0248	0.0530
PC6	-0.3126	-0.3790	-0.2578	1.5773	1.2714	1.8831	0.0008	0.1134
PC7	-0.3081	-0.3777	-0.2513	1.5548	1.2357	1.8738	0.4256	0.0068
PC8	-0.2915	-0.3571	-0.2379	1.4708	1.1700	1.7717	0.2606	0.0136
PC9	-0.2594	-0.3144	-0.2141	1.3091	1.0561	1.5621	0.0006	0.1194
PC10	0.2410	0.1970	0.2949	-1.2164	-1.4633	-0.9695	0.1015	0.0286
PC11	0.2244	0.1831	0.2752	-1.1326	-1.3651	-0.9001	0.4419	0.0064
PC12	0.2149	0.1752	0.2637	-1.0846	-1.3079	-0.8614	0.7670	0.0009
PC13	0.2026	0.1652	0.2485	-1.0225	-1.2327	-0.8122	0.5882	0.0032

Avahi laniger

PC	Slope	Slope lower CI	Slope higher CI	Intercept	Intercept lower CI	Intercept higher CI	p value	r squared
PC1	1.5391	0.9989	2.3713	-7.5150	-10.8656	-4.1643	0.3942	0.0348
PC2	1.1874	0.7660	1.8407	-5.7979	-8.4219	-3.1739	0.7363	0.0055
PC3	-1.0078	-1.5517	-0.6546	4.9210	2.7306	7.1114	0.3726	0.0380
PC4	-0.9834	-1.5161	-0.6379	4.8017	2.6575	6.9460	0.4155	0.0318
PC5	0.8610	0.5559	1.3335	-4.2040	-6.1023	-2.3056	0.6505	0.0100
PC6	-0.8176	-1.2441	-0.5373	3.9920	2.2662	5.7177	0.1581	0.0926
PC7	-0.7484	-1.1464	-0.4886	3.6542	2.0481	5.2602	0.2515	0.0621
PC8	0.6949	0.4534	1.0651	-3.3932	-4.8866	-1.8998	0.2622	0.0595
PC9	0.6165	0.4075	0.9327	-3.0104	-4.2925	-1.7282	0.1066	0.1192
PC10	-0.5126	-0.7924	-0.3316	2.5029	1.3780	3.6279	0.5283	0.0192
PC11	-0.4777	-0.7305	-0.3124	2.3327	1.3120	3.3534	0.2210	0.0704
PC12	0.4056	0.2672	0.6157	-1.9804	-2.8313	-1.1295	0.1341	0.1036
PC13	0.3740	0.2414	0.5793	-1.8260	-2.6510	-1.0010	0.6684	0.0089

Indri indri

PC	Slope	Slope lower CI	Slope higher CI	Intercept	Intercept lower CI	Intercept higher CI	p value	r squared
PC1	1.2036	0.8686	1.6679	-6.6054	-8.7988	-4.4121	0.6297	0.0063
PC2	-1.0363	-1.4299	-0.7511	5.6875	3.8246	7.5504	0.2672	0.0332
PC3	-0.9045	-1.2382	-0.6607	4.9640	3.3794	6.5486	0.0778	0.0816
PC4	-0.7624	-1.0467	-0.5553	4.1842	2.8358	5.5326	0.1198	0.0641
PC5	-0.7324	-1.0158	-0.5282	4.0197	2.6817	5.3577	0.8153	0.0015
PC6	-0.6802	-0.9270	-0.4991	3.7329	2.5588	4.9070	0.0406	0.1085
PC7	0.6439	0.4674	0.8869	-3.5336	-4.6846	-2.3825	0.2014	0.0437
PC8	0.5962	0.4346	0.8178	-3.2719	-4.3232	-2.2205	0.1048	0.0695
PC9	-0.5334	-0.7364	-0.3863	2.9271	1.9664	3.8879	0.2990	0.0291
PC10	0.5047	0.3640	0.6998	-2.7698	-3.6915	-1.8482	0.7784	0.0022
PC11	0.4519	0.3316	0.6160	-2.4803	-3.2609	-1.6997	0.0417	0.1074
PC12	0.4044	0.2926	0.5590	-2.2196	-2.9504	-1.4888	0.3558	0.0231
PC13	-0.4002	-0.5444	-0.2942	2.1962	1.5094	2.8830	0.0317	0.1187

Propithecus diadema

PC	Slope	Slope lower CI	Slope higher CI	Intercept	Intercept lower CI	Intercept higher CI	p value	r squared
PC1	0.8400	0.5688	1.2404	-4.5101	-6.3131	-2.7070	0.5131	0.0166
PC2	-0.7074	-1.0188	-0.4912	3.7984	2.3821	5.2147	0.0460	0.1446
PC3	0.6165	0.4183	0.9086	-3.3101	-4.6267	-1.9935	0.4071	0.0266
PC4	0.5597	0.4165	0.7521	-3.0052	-3.9061	-2.1042	0.0001	0.4470
PC5	-0.5103	-0.7523	-0.3462	2.7402	1.6498	3.8306	0.4146	0.0258
PC6	-0.4609	-0.6806	-0.3122	2.4749	1.4857	3.4641	0.5075	0.0171
PC7	-0.4190	-0.6186	-0.2838	2.2498	1.3508	3.1488	0.5018	0.0175
PC8	-0.4030	-0.5962	-0.2724	2.1640	1.2946	3.0334	0.6760	0.0068
PC9	-0.3476	-0.5121	-0.2360	1.8666	1.1252	2.6079	0.3833	0.0294
PC10	0.3099	0.2095	0.4585	-1.6641	-2.3328	-0.9954	0.6834	0.0065
PC11	0.3081	0.2086	0.4548	-1.6541	-2.3151	-0.9931	0.5030	0.0174
PC12	0.2872	0.1945	0.4242	-1.5421	-2.1588	-0.9254	0.5225	0.0159
PC13	0.2434	0.1644	0.3606	-1.3071	-1.8339	-0.7803	0.9001	0.0006

Propithecus verreauxi

PC	Slope	Slope lower CI	Slope higher CI	Intercept	Intercept lower CI	Intercept higher CI	p value	r squared
PC1	-0.8305	-1.1300	-0.6104	4.3962	3.0210	5.7714	0.4130	0.0164
PC2	0.7418	0.5489	1.0025	-3.9266	-5.1272	-2.7260	0.1125	0.0603
PC3	-0.6624	-0.9031	-0.4858	3.5062	2.4018	4.6106	0.7410	0.0027
PC4	-0.6176	-0.8424	-0.4528	3.2692	2.2382	4.3003	0.9348	0.0002
PC5	0.5798	0.4310	0.7799	-3.0689	-3.9923	-2.1455	0.0507	0.0899
PC6	-0.5376	-0.7328	-0.3944	2.8457	1.9502	3.7412	0.6635	0.0047
PC7	0.5217	0.3826	0.7114	-2.7614	-3.6319	-1.8910	0.8278	0.0012
PC8	-0.4631	-0.6316	-0.3396	2.4512	1.6784	3.2241	0.8528	0.0008
PC9	-0.3962	-0.5345	-0.2936	2.0971	1.4596	2.7346	0.0839	0.0711
PC10	-0.3803	-0.5159	-0.2802	2.0128	1.3890	2.6366	0.2334	0.0344
PC11	0.3482	0.2553	0.4749	-1.8433	-2.4244	-1.2621	0.8437	0.0010
PC12	-0.3139	-0.4264	-0.2311	1.6617	1.1448	2.1786	0.2894	0.0273
PC13	0.2962	0.2204	0.3982	-1.5680	-2.0385	-1.0974	0.0445	0.0948

Eulemur fulvus

PC	Slope	Slope lower CI	Slope higher CI	Intercept	Intercept lower CI	Intercept higher CI	p value	r squared
PC1	1.0967	0.9444	1.2735	-5.8460	-6.7233	-4.9688	0.8304	0.0003
PC2	0.9248	0.7970	1.0732	-4.9301	-5.6664	-4.1938	0.1937	0.0097
PC3	0.7498	0.6463	0.8699	-3.9970	-4.5930	-3.4010	0.1380	0.0127
PC4	-0.6614	-0.7676	-0.5700	3.5260	2.9993	4.0526	0.2008	0.0094
PC5	0.5861	0.5051	0.6801	-3.1245	-3.5909	-2.6582	0.1706	0.0108
PC6	0.5599	0.4824	0.6498	-2.9846	-3.4308	-2.5384	0.2518	0.0076
PC7	0.5026	0.4334	0.5828	-2.6790	-3.0774	-2.2806	0.0762	0.0181
PC8	-0.4643	-0.5344	-0.4033	2.4750	2.1255	2.8245	0.0000	0.1147
PC9	-0.4310	-0.4984	-0.3726	2.2974	1.9620	2.6328	0.0020	0.0536
PC10	0.3999	0.3444	0.4642	-2.1317	-2.4510	-1.8123	0.4332	0.0036
PC11	-0.3876	-0.4483	-0.3352	2.0664	1.7651	2.3678	0.0017	0.0558
PC12	0.3430	0.2956	0.3981	-1.8285	-2.1017	-1.5552	0.2229	0.0086
PC13	0.3257	0.2805	0.3782	-1.7362	-1.9967	-1.4756	0.9495	0.0000

Eulemur macaco

PC	Slope	Slope lower CI	Slope higher CI	Intercept	Intercept lower CI	Intercept higher CI	p value	r squared
PC1	1.3777	1.0498	1.8080	-7.3744	-9.4039	-5.3449	0.7295	0.0023
PC2	-1.0849	-1.4215	-0.8280	5.8072	4.2188	7.3956	0.3820	0.0145
PC3	0.9197	0.7120	1.1879	-4.9228	-6.1966	-3.6490	0.0102	0.1180
PC4	-0.8443	-1.1009	-0.6475	4.5193	3.3060	5.7327	0.0992	0.0505
PC5	-0.8147	-1.0691	-0.6207	4.3607	3.1606	5.5608	0.7338	0.0022
PC6	-0.6933	-0.9061	-0.5305	3.7112	2.7059	4.7165	0.1814	0.0334
PC7	0.6386	0.4879	0.8358	-3.4184	-4.3494	-2.4873	0.2723	0.0227
PC8	0.5786	0.4444	0.7533	-3.0971	-3.9237	-2.2704	0.0679	0.0615
PC9	0.5581	0.4251	0.7326	-2.9872	-3.8101	-2.1644	0.8641	0.0006
PC10	0.5193	0.3988	0.6761	-2.7796	-3.5217	-2.0375	0.0691	0.0610
PC11	-0.4506	-0.5909	-0.3436	2.4122	1.7503	3.0741	0.5116	0.0082
PC12	-0.4140	-0.5420	-0.3163	2.2161	1.6121	2.8201	0.2872	0.0213
PC13	-0.3707	-0.4865	-0.2824	1.9841	1.4379	2.5303	0.7660	0.0017

Eulemur mongoz

PC	Slope	Slope lower CI	Slope higher CI	Intercept	Intercept lower CI	Intercept higher CI	p value	r squared
PC1	-0.8020	-1.0127	-0.6352	4.2373	3.2398	5.2348	0.0001	0.2412
PC2	0.6811	0.5266	0.8809	-3.5985	-4.5345	-2.6625	0.0411	0.0737
PC3	-0.5190	-0.6779	-0.3974	2.7422	2.0012	3.4831	0.8961	0.0003
PC4	-0.4637	-0.6021	-0.3571	2.4499	1.8028	3.0970	0.1138	0.0448
PC5	0.4232	0.3256	0.5501	-2.2360	-2.8292	-1.6427	0.1570	0.0361
PC6	0.3927	0.3008	0.5127	-2.0749	-2.6347	-1.5152	0.6527	0.0037
PC7	0.3617	0.2810	0.4655	-1.9109	-2.3984	-1.4235	0.0121	0.1091
PC8	-0.3246	-0.4228	-0.2492	1.7150	1.2565	2.1734	0.2751	0.0216
PC9	0.3067	0.2351	0.4000	-1.6202	-2.0557	-1.1846	0.4527	0.0103
PC10	-0.2776	-0.3625	-0.2126	1.4665	1.0705	1.8626	0.7792	0.0014
PC11	-0.2686	-0.3502	-0.2060	1.4189	1.0379	1.7999	0.4012	0.0128
PC12	0.2587	0.1986	0.3369	-1.3665	-1.7319	-1.0011	0.2809	0.0211
PC13	-0.2337	-0.3049	-0.1791	1.2347	0.9025	1.5670	0.4980	0.0084

Eulemur rubriventer

PC	Slope	Slope lower CI	Slope higher CI	Intercept	Intercept lower CI	Intercept higher CI	p value	r squared
PC1	1.7642	1.2283	2.5338	-9.3814	-12.8526	-5.9102	0.0218	0.1931
PC2	1.2456	0.8345	1.8591	-6.6236	-9.3478	-3.8994	0.7847	0.0030
PC3	1.0732	0.7259	1.5868	-5.7071	-7.9961	-3.4180	0.2532	0.0519
PC4	1.0236	0.6895	1.5196	-5.4434	-7.6505	-3.2362	0.3795	0.0310
PC5	-0.9252	-1.3336	-0.6418	4.9197	3.0804	6.7591	0.0293	0.1762
PC6	-0.7883	-1.1758	-0.5286	4.1921	2.4712	5.9131	0.6823	0.0068
PC7	0.7348	0.4924	1.0965	-3.9072	-5.5136	-2.3008	0.7602	0.0038
PC8	-0.6039	-0.8925	-0.4086	3.2111	1.9245	4.4978	0.2444	0.0538
PC9	0.5179	0.3473	0.7724	-2.7540	-3.8844	-1.6236	0.6748	0.0072
PC10	-0.4829	-0.7102	-0.3284	2.5681	1.5529	3.5832	0.1555	0.0790
PC11	0.4316	0.2894	0.6435	-2.2950	-3.2365	-1.3534	0.6566	0.0080
PC12	0.3827	0.2573	0.5694	-2.0353	-2.8654	-1.2053	0.4839	0.0198
PC13	0.3321	0.2232	0.4942	-1.7661	-2.4868	-1.0453	0.5004	0.0184

Hapalemur griseus

PC	Slope	Slope lower CI	Slope higher CI	Intercept	Intercept lower CI	Intercept higher CI	p value	r squared
PC1	0.8848	0.5934	1.3193	-4.4581	-6.2869	-2.6292	0.6513	0.0083
PC2	0.7284	0.4891	1.0848	-3.6698	-5.1707	-2.1689	0.5522	0.0143
PC3	-0.6976	-1.0352	-0.4701	3.5150	2.0914	4.9385	0.3619	0.0334
PC4	-0.6650	-0.9772	-0.4526	3.3506	2.0287	4.6725	0.1456	0.0828
PC5	-0.6137	-0.9007	-0.4182	3.0920	1.8765	4.3076	0.1301	0.0892
PC6	0.4867	0.3405	0.6956	-2.4521	-3.3466	-1.5576	0.0146	0.2158
PC7	0.4165	0.2820	0.6153	-2.0987	-2.9385	-1.2589	0.2330	0.0564
PC8	-0.3689	-0.5457	-0.2494	1.8586	1.1121	2.6051	0.2660	0.0492
PC9	-0.3447	-0.5063	-0.2347	1.7369	1.0526	2.4212	0.1394	0.0853
PC10	0.3192	0.2144	0.4754	-1.6083	-2.2659	-0.9508	0.5424	0.0150
PC11	-0.2973	-0.4429	-0.1995	1.4979	0.8847	2.1111	0.5816	0.0123
PC12	0.2536	0.1702	0.3777	-1.2776	-1.8004	-0.7547	0.5700	0.0131
PC13	-0.2246	-0.3349	-0.1506	1.1315	0.6671	1.5959	0.6739	0.0072

Lemur catta

PC	Slope	Slope lower CI	Slope higher CI	Intercept	Intercept lower CI	Intercept higher CI	p value	r squared
PC1	0.9834	0.6915	1.3984	-5.1702	-7.0286	-3.3118	0.7334	0.0037
PC2	-0.7741	-1.1014	-0.5440	4.0696	2.6043	5.5348	0.9115	0.0004
PC3	0.6401	0.4639	0.8832	-3.3651	-4.4674	-2.2629	0.0145	0.1726
PC4	0.5874	0.4129	0.8355	-3.0881	-4.1991	-1.9770	0.8110	0.0018
PC5	0.5163	0.3671	0.7261	-2.7143	-3.6582	-1.7704	0.1378	0.0675
PC6	0.4913	0.3458	0.6982	-2.5831	-3.5096	-1.6567	0.6128	0.0081
PC7	-0.4071	-0.5782	-0.2866	2.1402	1.3738	2.9066	0.5523	0.0111
PC8	-0.3967	-0.5612	-0.2805	2.0859	1.3477	2.8241	0.2947	0.0342
PC9	0.3374	0.2377	0.4790	-1.7739	-2.4083	-1.1394	0.5129	0.0135
PC10	-0.2930	-0.4165	-0.2061	1.5402	0.9870	2.0935	0.6837	0.0053
PC11	-0.2693	-0.3832	-0.1893	1.4159	0.9061	1.9257	0.9301	0.0002
PC12	-0.2514	-0.3544	-0.1784	1.3218	0.8592	1.7844	0.1805	0.0553
PC13	0.2340	0.1645	0.3328	-1.2300	-1.6725	-0.7875	0.7979	0.0021

Varecia variegata

PC	Slope	Slope lower CI	Slope higher CI	Intercept	Intercept lower CI	Intercept higher CI	p value	r squared
PC1	-1.0938	-1.5146	-0.7898	5.9911	4.0059	7.9762	0.5320	0.0106
PC2	-0.8466	-1.1592	-0.6183	4.6374	3.1559	6.1189	0.0804	0.0803
PC3	0.7275	0.5245	1.0091	-3.9847	-5.3120	-2.6574	0.9416	0.0001
PC4	0.6885	0.5000	0.9480	-3.7714	-4.9984	-2.5444	0.1890	0.0462
PC5	0.5645	0.4070	0.7829	-3.0920	-4.1216	-2.0624	0.8585	0.0009
PC6	-0.4641	-0.6433	-0.3349	2.5423	1.6975	3.3871	0.6719	0.0049
PC7	-0.4258	-0.5884	-0.3082	2.3324	1.5649	3.0999	0.3432	0.0243
PC8	0.3802	0.2785	0.5192	-2.0827	-2.7420	-1.4233	0.0538	0.0968
PC9	-0.3595	-0.4957	-0.2608	1.9693	1.3259	2.6128	0.2345	0.0380
PC10	-0.3200	-0.4439	-0.2307	1.7531	1.1692	2.3369	0.9010	0.0004
PC11	0.2959	0.2136	0.4099	-1.6210	-2.1586	-1.0834	0.5695	0.0088
PC12	0.2542	0.1835	0.3521	-1.3921	-1.8539	-0.9303	0.5789	0.0084
PC13	-0.2383	-0.3278	-0.1732	1.3051	0.8814	1.7287	0.1690	0.0505

Lepilemur ruficaudatus

PC	Slope	Slope lower CI	Slope higher CI	Intercept	Intercept lower CI	Intercept higher CI	p value	r squared
PC1	0.6838	0.4504	1.0381	-3.3620	-4.8068	-1.9172	0.6789	0.0076
PC2	0.6672	0.4501	0.9890	-3.2803	-4.6053	-1.9552	0.0854	0.1232
PC3	-0.5817	-0.8779	-0.3855	2.8602	1.6496	4.0708	0.3552	0.0373
PC4	-0.5383	-0.7920	-0.3659	2.6468	1.5991	3.6944	0.0491	0.1580
PC5	-0.4816	-0.7322	-0.3168	2.3680	1.3465	3.3894	0.9598	0.0001
PC6	0.4564	0.3017	0.6904	-2.2441	-3.1999	-1.2883	0.4480	0.0253
PC7	-0.3975	-0.5987	-0.2639	1.9543	1.1313	2.7774	0.2985	0.0469
PC8	-0.3614	-0.5394	-0.2421	1.7769	1.0462	2.5076	0.1423	0.0912
PC9	-0.3585	-0.5408	-0.2376	1.7626	1.0172	2.5080	0.3444	0.0389
PC10	-0.3254	-0.4937	-0.2145	1.6001	0.9137	2.2864	0.6139	0.0112
PC11	0.2921	0.1929	0.4425	-1.4364	-2.0502	-0.8226	0.5139	0.0188
PC12	0.2682	0.1770	0.4064	-1.3187	-1.8828	-0.7546	0.5395	0.0166
PC13	0.2329	0.1538	0.3525	-1.1449	-1.6335	-0.6564	0.4834	0.0216

Loris tardigradus

PC	Slope	Slope lower CI	Slope higher CI	Intercept	Intercept lower CI	Intercept higher CI	p value	r squared
PC1	0.4809	0.3276	0.7060	-2.3023	-3.2084	-1.3963	0.1330	0.0880
PC2	-0.4283	-0.6396	-0.2868	2.0502	1.2052	2.8951	0.9846	0.0000
PC3	0.3398	0.2275	0.5073	-1.6265	-2.2965	-0.9565	0.8801	0.0009
PC4	-0.3280	-0.4616	-0.2331	1.5704	1.0232	2.1176	0.0041	0.2849
PC5	0.3168	0.2175	0.4613	-1.5165	-2.1003	-0.9327	0.0678	0.1272
PC6	-0.2634	-0.3807	-0.1822	1.2608	0.7854	1.7363	0.0370	0.1627
PC7	0.2487	0.1679	0.3686	-1.1907	-1.6714	-0.7101	0.3145	0.0404
PC8	0.2245	0.1506	0.3347	-1.0747	-1.5156	-0.6338	0.6363	0.0091
PC9	0.1853	0.1266	0.2711	-0.8869	-1.2330	-0.5408	0.1022	0.1032
PC10	0.1624	0.1088	0.2426	-0.7776	-1.0980	-0.4572	0.9387	0.0002
PC11	-0.1509	-0.2250	-0.1012	0.7222	0.4257	1.0187	0.6650	0.0076
PC12	0.1344	0.0903	0.1999	-0.6433	-0.9056	-0.3810	0.4688	0.0212
PC13	0.1223	0.0822	0.1819	-0.5854	-0.8243	-0.3464	0.4951	0.0188

Nycticebus bengalensis

PC	Slope	Slope lower CI	Slope higher CI	Intercept	Intercept lower CI	Intercept higher CI	p value	r squared
PC1	-1.3303	-2.0272	-0.8729	6.7555	3.8244	9.6867	0.0928	0.1348
PC2	0.9619	0.6154	1.5036	-4.8850	-7.1404	-2.6295	0.5279	0.0202
PC3	0.8770	0.5587	1.3768	-4.4538	-6.5313	-2.3763	0.9876	0.0000
PC4	0.7051	0.4498	1.1052	-3.5806	-5.2447	-1.9164	0.7076	0.0072
PC5	-0.6491	-1.0071	-0.4184	3.2966	1.8017	4.7915	0.2939	0.0549
PC6	0.5513	0.3607	0.8425	-2.7995	-4.0229	-1.5761	0.1107	0.1223
PC7	-0.4980	-0.7811	-0.3175	2.5289	1.3516	3.7062	0.7802	0.0040
PC8	0.4719	0.3014	0.7388	-2.3965	-3.5069	-1.2861	0.6100	0.0132
PC9	-0.3877	-0.6005	-0.2503	1.9688	1.0795	2.8582	0.2632	0.0622
PC10	-0.3330	-0.5206	-0.2130	1.6910	0.9097	2.4722	0.5413	0.0189
PC11	-0.3175	-0.4898	-0.2057	1.6121	0.8908	2.3335	0.2027	0.0798
PC12	0.2984	0.1973	0.4513	-1.5152	-2.1603	-0.8701	0.0591	0.1669
PC13	0.2804	0.1808	0.4349	-1.4240	-2.0694	-0.7785	0.2900	0.0558

Nycticebus coucang

PC	Slope	Slope lower CI	Slope higher CI	Intercept	Intercept lower CI	Intercept higher CI	p value	r squared
PC1	0.6883	0.5440	0.8710	-3.4297	-4.2445	-2.6149	0.0623	0.0509
PC2	-0.5625	-0.7162	-0.4418	2.8029	2.1193	3.4864	0.9566	0.0000
PC3	0.5081	0.4001	0.6452	-2.5314	-3.1420	-1.9208	0.2280	0.0216
PC4	0.4778	0.3759	0.6073	-2.3808	-2.9573	-1.8043	0.3327	0.0140
PC5	0.4556	0.3595	0.5774	-2.2701	-2.8131	-1.7271	0.1085	0.0380
PC6	0.4351	0.3421	0.5532	-2.1677	-2.6937	-1.6416	0.4185	0.0098
PC7	0.4332	0.3425	0.5478	-2.1582	-2.6698	-1.6466	0.0522	0.0551
PC8	-0.3621	-0.4597	-0.2851	1.8039	1.3690	2.2389	0.2161	0.0227
PC9	0.3544	0.2802	0.4482	-1.7657	-2.1844	-1.3469	0.0541	0.0542
PC10	-0.3253	-0.4123	-0.2566	1.6206	1.2328	2.0084	0.1127	0.0371
PC11	0.3044	0.2391	0.3876	-1.5169	-1.8868	-1.1470	0.8834	0.0003
PC12	0.2791	0.2192	0.3553	-1.3905	-1.7294	-1.0516	0.7733	0.0012
PC13	0.2605	0.2047	0.3314	-1.2978	-1.6136	-0.9820	0.5889	0.0044

Perodicticus potto

PC	Slope	Slope lower CI	Slope higher CI	Intercept	Intercept lower CI	Intercept higher CI	p value	r squared
PC1	-0.7385	-0.8795	-0.6202	3.7298	3.0751	4.3846	0.7546	0.0008
PC2	-0.6111	-0.7243	-0.5156	3.0862	2.5591	3.6133	0.0081	0.0539
PC3	-0.5714	-0.6767	-0.4825	2.8858	2.3953	3.3762	0.0040	0.0633
PC4	-0.5519	-0.6550	-0.4650	2.7872	2.3075	3.2669	0.0240	0.0395
PC5	-0.4664	-0.5543	-0.3925	2.3555	1.9469	2.7642	0.0789	0.0241
PC6	0.4447	0.3756	0.5265	-2.2457	-2.6270	-1.8645	0.0034	0.0654
PC7	-0.4084	-0.4863	-0.3429	2.0624	1.7003	2.4246	0.8957	0.0001
PC8	-0.3755	-0.4467	-0.3157	1.8964	1.5655	2.2273	0.2045	0.0126
PC9	-0.3481	-0.4141	-0.2926	1.7580	1.4510	2.0650	0.2297	0.0113
PC10	-0.3294	-0.3922	-0.2767	1.6635	1.3718	1.9553	0.5616	0.0027
PC11	0.3121	0.2622	0.3717	-1.5764	-1.8530	-1.2998	0.6434	0.0017
PC12	0.3094	0.2603	0.3677	-1.5625	-1.8336	-1.2914	0.0822	0.0236
PC13	0.2796	0.2348	0.3329	-1.4120	-1.6597	-1.1643	0.5819	0.0024

Goswami model zygomatic module against ln CS of zygomatic

Cheirogaleus major

PC	Slope	Slope lower CI	Slope higher CI	Intercept	Intercept lower CI	Intercept higher CI	p value	r squared
PC1	0.5963	0.4088	0.8696	-1.9621	-2.7204	-1.2037	0.0260	0.1976
PC2	-0.5191	-0.7892	-0.3414	1.7081	0.9710	2.4452	0.9749	0.0000
PC3	0.4477	0.3026	0.6623	-1.4731	-2.0652	-0.8810	0.0740	0.1322
PC4	-0.4410	-0.6638	-0.2930	1.4510	0.8407	2.0614	0.2831	0.0499
PC5	-0.3634	-0.5522	-0.2391	1.1958	0.6804	1.7112	0.8109	0.0025
PC6	0.3539	0.2328	0.5381	-1.1646	-1.6671	-0.6622	0.9156	0.0005
PC7	0.3188	0.2098	0.4844	-1.0489	-1.5009	-0.5969	0.7979	0.0029
PC8	0.2606	0.1767	0.3844	-0.8576	-1.1994	-0.5159	0.0583	0.1472
PC9	-0.2263	-0.3440	-0.1489	0.7448	0.4237	1.0659	0.8386	0.0018
PC10	0.2002	0.1321	0.3034	-0.6587	-0.9407	-0.3768	0.5453	0.0161
PC11	-0.1820	-0.2768	-0.1197	0.5990	0.3405	0.8575	0.9898	0.0000
PC12	-0.1571	-0.2355	-0.1048	0.5170	0.3018	0.7321	0.2010	0.0701
PC13	-0.1485	-0.2201	-0.1002	0.4886	0.2914	0.6859	0.0835	0.1246

Cheirogaleus medius

PC	Slope	Slope lower CI	Slope higher CI	Intercept	Intercept lower CI	Intercept higher CI	p value	r squared
PC1	-0.6334	-0.9106	-0.4407	1.9219	1.2088	2.6349	0.0686	0.1176
PC2	0.5572	0.3876	0.8010	-1.6905	-2.3177	-1.0633	0.0684	0.1177
PC3	-0.5485	-0.8052	-0.3737	1.6642	1.0094	2.3190	0.6472	0.0079
PC4	-0.4769	-0.6658	-0.3417	1.4470	0.9552	1.9388	0.0048	0.2595
PC5	0.4098	0.2798	0.6003	-1.2434	-1.7297	-0.7570	0.4733	0.0192
PC6	0.3837	0.2621	0.5618	-1.1642	-1.6191	-0.7094	0.4449	0.0218
PC7	0.3510	0.2388	0.5157	-1.0648	-1.4850	-0.6445	0.8283	0.0018
PC8	-0.2898	-0.4245	-0.1979	0.8793	0.5354	1.2232	0.4671	0.0198
PC9	-0.2743	-0.4011	-0.1876	0.8322	0.5082	1.1562	0.3806	0.0286
PC10	0.2471	0.1682	0.3631	-0.7498	-1.0456	-0.4540	0.8030	0.0023
PC11	0.2432	0.1655	0.3575	-0.7379	-1.0294	-0.4465	0.9034	0.0006
PC12	0.2240	0.1550	0.3237	-0.6796	-0.9355	-0.4237	0.1110	0.0914
PC13	-0.1936	-0.2836	-0.1321	0.5873	0.3574	0.8171	0.4862	0.0181

Microcebus murinus

PC	Slope	Slope lower CI	Slope higher CI	Intercept	Intercept lower CI	Intercept higher CI	p value	r squared
PC1	0.7947	0.6415	0.9844	-2.1674	-2.6352	-1.6997	0.0002	0.1809
PC2	0.7098	0.5616	0.8971	-1.9359	-2.3936	-1.4782	0.2733	0.0171
PC3	-0.6881	-0.8656	-0.5470	1.8767	1.4421	2.3114	0.0439	0.0568
PC4	-0.5544	-0.7011	-0.4384	1.5122	1.1538	1.8705	0.3530	0.0123
PC5	0.5482	0.4341	0.6924	-1.4953	-1.8476	-1.1429	0.1989	0.0235
PC6	0.4887	0.3865	0.6179	-1.3329	-1.6485	-1.0172	0.3297	0.0136
PC7	0.4483	0.3541	0.5677	-1.2228	-1.5142	-0.9313	0.8129	0.0008
PC8	-0.4318	-0.5464	-0.3413	1.1778	0.8979	1.4577	0.4837	0.0070
PC9	-0.4111	-0.5184	-0.3260	1.1213	0.8588	1.3837	0.1067	0.0367
PC10	-0.3918	-0.4959	-0.3095	1.0685	0.8143	1.3228	0.5756	0.0045
PC11	0.3563	0.2828	0.4490	-0.9718	-1.1985	-0.7452	0.0794	0.0433
PC12	0.3427	0.2706	0.4339	-0.9345	-1.1573	-0.7118	0.7833	0.0011
PC13	0.2972	0.2370	0.3727	-0.8107	-0.9958	-0.6256	0.0141	0.0830

Microcebus rufus

PC	Slope	Slope lower CI	Slope higher CI	Intercept	Intercept lower CI	Intercept higher CI	p value	r squared
PC1	0.6315	0.4313	0.9246	-1.7391	-2.4187	-1.0596	0.4459	0.0217
PC2	-0.5703	-0.7880	-0.4128	1.5707	1.0538	2.0877	0.0019	0.3059
PC3	-0.4750	-0.6970	-0.3238	1.3083	0.7940	1.8226	0.6051	0.0100
PC4	-0.4279	-0.6272	-0.2919	1.1785	0.7165	1.6404	0.5206	0.0154
PC5	-0.3915	-0.5740	-0.2671	1.0783	0.6554	1.5012	0.5355	0.0144
PC6	-0.3660	-0.5373	-0.2493	1.0080	0.6111	1.4048	0.6657	0.0070
PC7	-0.3647	-0.5305	-0.2507	1.0043	0.6189	1.3897	0.2151	0.0563
PC8	0.3025	0.2092	0.4375	-0.8332	-1.1476	-0.5188	0.1193	0.0875
PC9	0.2838	0.1931	0.4172	-0.7817	-1.0904	-0.4729	0.8956	0.0006
PC10	0.2651	0.1823	0.3855	-0.7301	-1.0100	-0.4502	0.2065	0.0584
PC11	-0.2283	-0.3352	-0.1555	0.6287	0.3811	0.8763	0.6798	0.0064
PC12	0.2076	0.1445	0.2983	-0.5719	-0.7837	-0.3600	0.0649	0.1206
PC13	0.1817	0.1239	0.2666	-0.5005	-0.6972	-0.3038	0.5971	0.0105

Galago alleni

PC	Slope	Slope lower CI	Slope higher CI	Intercept	Intercept lower CI	Intercept higher CI	p value	r squared
PC1	0.8097	0.5331	1.2297	-2.5339	-3.6242	-1.4436	0.2770	0.0535
PC2	0.5660	0.3700	0.8657	-1.7712	-2.5470	-0.9954	0.5196	0.0191
PC3	0.4784	0.3264	0.7012	-1.4971	-2.0837	-0.9105	0.0225	0.2151
PC4	0.4661	0.3184	0.6823	-1.4588	-2.0283	-0.8892	0.0206	0.2206
PC5	0.4388	0.2858	0.6735	-1.3731	-1.9799	-0.7663	0.8524	0.0016
PC6	0.3913	0.2555	0.5992	-1.2246	-1.7625	-0.6866	0.5894	0.0135
PC7	0.3351	0.2185	0.5140	-1.0488	-1.5113	-0.5863	0.7239	0.0058
PC8	-0.2986	-0.4585	-0.1944	0.9344	0.5211	1.3476	0.9984	0.0000
PC9	-0.2908	-0.4437	-0.1906	0.9102	0.5141	1.3064	0.4054	0.0317
PC10	0.2625	0.1714	0.4020	-0.8215	-1.1825	-0.4606	0.5924	0.0132
PC11	0.2360	0.1549	0.3597	-0.7387	-1.0592	-0.4182	0.3633	0.0377
PC12	-0.1875	-0.2851	-0.1233	0.5867	0.3333	0.8401	0.3127	0.0463
PC13	-0.1652	-0.2490	-0.1096	0.5170	0.2988	0.7353	0.1565	0.0891

Galago demidoff

PC	Slope	Slope lower CI	Slope higher CI	Intercept	Intercept lower CI	Intercept higher CI	p value	r squared
PC1	-0.8850	-1.1496	-0.6812	2.4539	1.8043	3.1035	0.6134	0.0045
PC2	0.7223	0.5560	0.9383	-2.0028	-2.5329	-1.4727	0.5983	0.0049
PC3	0.6460	0.4984	0.8374	-1.7913	-2.2616	-1.3211	0.2730	0.0210
PC4	-0.5301	-0.6887	-0.4081	1.4700	1.0807	1.8593	0.6358	0.0040
PC5	0.4992	0.3843	0.6486	-1.3843	-1.7509	-1.0178	0.6339	0.0040
PC6	0.4504	0.3468	0.5850	-1.2489	-1.5792	-0.9187	0.5402	0.0066
PC7	0.4309	0.3316	0.5602	-1.1950	-1.5120	-0.8779	0.9625	0.0000
PC8	0.3953	0.3043	0.5135	-1.0962	-1.3864	-0.8061	0.5960	0.0050
PC9	0.3573	0.2768	0.4613	-0.9908	-1.2467	-0.7350	0.0802	0.0527
PC10	0.3441	0.2712	0.4366	-0.9542	-1.1835	-0.7249	0.0008	0.1796
PC11	-0.2956	-0.3842	-0.2274	0.8197	0.6022	1.0372	0.9027	0.0003
PC12	0.2914	0.2256	0.3764	-0.8079	-1.0170	-0.5988	0.0953	0.0480
PC13	0.2637	0.2029	0.3426	-0.7311	-0.9249	-0.5374	0.6991	0.0026

Galago elegantulus

PC	Slope	Slope lower CI	Slope higher CI	Intercept	Intercept lower CI	Intercept higher CI	p value	r squared
PC1	-0.9252	-1.3164	-0.6503	2.8705	1.8370	3.9040	0.8906	0.0006
PC2	-0.7950	-1.0778	-0.5864	2.4664	1.7041	3.2288	0.0019	0.2634
PC3	-0.7246	-1.0201	-0.5146	2.2479	1.4636	3.0322	0.1575	0.0615
PC4	-0.6184	-0.8782	-0.4354	1.9185	1.2316	2.6054	0.5458	0.0115
PC5	0.5753	0.4045	0.8181	-1.7847	-2.4264	-1.1430	0.7483	0.0033
PC6	-0.5267	-0.7480	-0.3709	1.6341	1.0489	2.2192	0.5473	0.0114
PC7	-0.4992	-0.7090	-0.3515	1.5488	0.9942	2.1035	0.5522	0.0112
PC8	0.4592	0.3227	0.6534	-1.4247	-1.9379	-0.9116	0.9847	0.0000
PC9	-0.3839	-0.5427	-0.2716	1.1911	0.7704	1.6118	0.2696	0.0379
PC10	-0.3500	-0.4947	-0.2475	1.0857	0.7022	1.4692	0.2690	0.0380
PC11	-0.3269	-0.4627	-0.2309	1.0141	0.6545	1.3737	0.3220	0.0307
PC12	-0.2869	-0.4070	-0.2023	0.8902	0.5727	1.2077	0.4347	0.0192
PC13	0.2656	0.1873	0.3768	-0.8241	-1.1181	-0.5301	0.4410	0.0187

Galago moholi

PC	Slope	Slope lower CI	Slope higher CI	Intercept	Intercept lower CI	Intercept higher CI	p value	r squared
PC1	-0.8331	-1.0530	-0.6591	2.4312	1.8563	3.0061	0.7139	0.0019
PC2	-0.7435	-0.9399	-0.5882	2.1697	1.6564	2.6830	0.7857	0.0010
PC3	0.6356	0.5083	0.7948	-1.8548	-2.2729	-1.4366	0.0089	0.0926
PC4	0.4834	0.3878	0.6025	-1.4106	-1.7239	-1.0973	0.0028	0.1193
PC5	-0.4576	-0.5750	-0.3642	1.3354	1.0277	1.6432	0.0522	0.0521
PC6	0.4398	0.3479	0.5559	-1.2833	-1.5869	-0.9797	0.7774	0.0011
PC7	0.4201	0.3325	0.5308	-1.2260	-1.5154	-0.9366	0.5362	0.0054
PC8	0.3896	0.3090	0.4913	-1.1371	-1.4031	-0.8711	0.1972	0.0233
PC9	-0.3623	-0.4580	-0.2866	1.0573	0.8070	1.3075	0.9352	0.0001
PC10	0.3429	0.2714	0.4333	-1.0007	-1.2370	-0.7644	0.5732	0.0045
PC11	-0.3010	-0.3785	-0.2393	0.8783	0.6752	1.0814	0.0697	0.0456
PC12	-0.2758	-0.3486	-0.2182	0.8049	0.6144	0.9953	0.7968	0.0009
PC13	-0.2571	-0.3234	-0.2044	0.7503	0.5767	0.9239	0.0729	0.0446

Galago senegalensis

PC	Slope	Slope lower CI	Slope higher CI	Intercept	Intercept lower CI	Intercept higher CI	p value	r squared
PC1	0.5769	0.4968	0.6698	-1.7384	-1.9990	-1.4777	0.5334	0.0022
PC2	-0.4590	-0.5310	-0.3967	1.3831	1.1807	1.5855	0.0030	0.0499
PC3	0.4363	0.3763	0.5058	-1.3147	-1.5099	-1.1195	0.0542	0.0212
PC4	0.3952	0.3412	0.4578	-1.1909	-1.3668	-1.0151	0.0171	0.0325
PC5	-0.3861	-0.4475	-0.3331	1.1634	0.9910	1.3358	0.0349	0.0255
PC6	-0.3402	-0.3947	-0.2932	1.0252	0.8722	1.1781	0.1487	0.0120
PC7	-0.3337	-0.3874	-0.2874	1.0055	0.8548	1.1561	0.4156	0.0038
PC8	-0.3163	-0.3669	-0.2726	0.9531	0.8110	1.0952	0.1264	0.0135
PC9	0.2941	0.2545	0.3398	-0.8862	-1.0148	-0.7576	0.0007	0.0647
PC10	-0.2793	-0.3242	-0.2406	0.8416	0.7157	0.9676	0.2921	0.0064
PC11	-0.2647	-0.3073	-0.2280	0.7977	0.6780	0.9173	0.5688	0.0019
PC12	0.2481	0.2138	0.2880	-0.7477	-0.8596	-0.6358	0.3209	0.0057
PC13	0.2337	0.2013	0.2713	-0.7042	-0.8099	-0.5986	0.5879	0.0017

Galago zanzibaricus

PC	Slope	Slope lower CI	Slope higher CI	Intercept	Intercept lower CI	Intercept higher CI	p value	r squared
PC1	0.7771	0.5271	1.1456	-2.2824	-3.1911	-1.3738	0.0569	0.1487
PC2	-0.6323	-0.9614	-0.4159	1.8573	1.0559	2.6586	0.9537	0.0001
PC3	0.5121	0.3384	0.7749	-1.5042	-2.1454	-0.8630	0.4591	0.0241
PC4	0.4703	0.3204	0.6904	-1.3815	-1.9250	-0.8380	0.0415	0.1686
PC5	0.4250	0.2854	0.6329	-1.2483	-1.7588	-0.7378	0.1203	0.1017
PC6	-0.4114	-0.6254	-0.2706	1.2083	0.6870	1.7295	0.9149	0.0005
PC7	-0.3446	-0.5152	-0.2305	1.0122	0.5940	1.4304	0.1624	0.0831
PC8	0.3125	0.2081	0.4692	-0.9178	-1.3013	-0.5342	0.2305	0.0619
PC9	0.2725	0.1804	0.4116	-0.8004	-1.1400	-0.4608	0.3850	0.0330
PC10	-0.2438	-0.3706	-0.1604	0.7162	0.4073	1.0250	0.8890	0.0009
PC11	-0.2273	-0.3454	-0.1496	0.6676	0.3799	0.9552	0.7991	0.0029
PC12	0.1912	0.1278	0.2861	-0.5617	-0.7941	-0.3293	0.1701	0.0802
PC13	0.1834	0.1207	0.2787	-0.5388	-0.7709	-0.3067	0.7818	0.0034

Otolemur crassicaudatus

PC	Slope	Slope lower CI	Slope higher CI	Intercept	Intercept lower CI	Intercept higher CI	p value	r squared
PC1	-0.4354	-0.5290	-0.3584	1.5348	1.2341	1.8355	0.0589	0.0356
PC2	0.3226	0.2749	0.3786	-1.1370	-1.3199	-0.9541	0.0000	0.3499
PC3	0.2892	0.2372	0.3526	-1.0194	-1.2228	-0.8160	0.8674	0.0003
PC4	-0.2778	-0.3375	-0.2286	0.9791	0.7870	1.1712	0.0689	0.0330
PC5	-0.2604	-0.3158	-0.2147	0.9178	0.7395	1.0960	0.0214	0.0523
PC6	0.2450	0.2028	0.2961	-0.8637	-1.0282	-0.6991	0.0026	0.0881
PC7	0.2300	0.1891	0.2798	-0.8108	-0.9707	-0.6509	0.1296	0.0231
PC8	-0.2220	-0.2690	-0.1833	0.7826	0.6315	0.9337	0.0112	0.0632
PC9	-0.2075	-0.2527	-0.1704	0.7314	0.5863	0.8764	0.2774	0.0119
PC10	-0.1906	-0.2322	-0.1564	0.6716	0.5379	0.8054	0.5699	0.0033
PC11	0.1791	0.1470	0.2184	-0.6314	-0.7573	-0.5055	0.7428	0.0011
PC12	0.1652	0.1364	0.2002	-0.5824	-0.6948	-0.4699	0.0109	0.0637
PC13	-0.1470	-0.1792	-0.1206	0.5182	0.4150	0.6215	0.5701	0.0033

Otolemur garnettii

PC	Slope	Slope lower CI	Slope higher CI	Intercept	Intercept lower CI	Intercept higher CI	p value	r squared
PC1	0.3562	0.3033	0.4182	-1.2279	-1.4259	-1.0299	0.0000	0.3871
PC2	0.3140	0.2559	0.3852	-1.0825	-1.3053	-0.8596	0.7195	0.0014
PC3	-0.2932	-0.3596	-0.2391	1.0110	0.8031	1.2188	0.5357	0.0041
PC4	-0.2597	-0.3182	-0.2120	0.8955	0.7123	1.0787	0.2622	0.0135
PC5	-0.2461	-0.3007	-0.2014	0.8484	0.6771	1.0197	0.0544	0.0392
PC6	-0.2143	-0.2592	-0.1773	0.7389	0.5977	0.8802	0.0002	0.1390
PC7	-0.2113	-0.2591	-0.1722	0.7284	0.5785	0.8783	0.6552	0.0022
PC8	-0.1999	-0.2451	-0.1630	0.6891	0.5474	0.8307	0.5512	0.0038
PC9	-0.1779	-0.2167	-0.1460	0.6133	0.4914	0.7352	0.0097	0.0698
PC10	0.1653	0.1354	0.2018	-0.5699	-0.6844	-0.4553	0.0332	0.0478
PC11	0.1539	0.1256	0.1886	-0.5306	-0.6394	-0.4218	0.3376	0.0099
PC12	0.1474	0.1201	0.1808	-0.5081	-0.6128	-0.4035	0.8299	0.0005
PC13	0.1389	0.1132	0.1705	-0.4790	-0.5777	-0.3803	0.9153	0.0001

Avahi laniger

PC	Slope	Slope lower CI	Slope higher CI	Intercept	Intercept lower CI	Intercept higher CI	p value	r squared
PC1	1.1010	0.7158	1.6936	-3.6581	-5.2828	-2.0334	0.3454	0.0425
PC2	0.8494	0.5482	1.3161	-2.8223	-4.0981	-1.5465	0.6839	0.0081
PC3	-0.7210	-1.1003	-0.4724	2.3954	1.3521	3.4387	0.1933	0.0792
PC4	0.7035	0.4567	1.0835	-2.3374	-3.3789	-1.2959	0.3843	0.0362
PC5	-0.6159	-0.9556	-0.3969	2.0464	1.1181	2.9747	0.8800	0.0011
PC6	-0.5848	-0.8974	-0.3812	1.9432	1.0855	2.8009	0.2846	0.0543
PC7	-0.5354	-0.8131	-0.3525	1.7788	1.0133	2.5442	0.1392	0.1011
PC8	0.4971	0.3251	0.7602	-1.6517	-2.3747	-0.9287	0.2229	0.0699
PC9	0.4410	0.2948	0.6599	-1.4654	-2.0720	-0.8588	0.0519	0.1682
PC10	-0.3667	-0.5659	-0.2376	1.2184	0.6729	1.7638	0.4530	0.0271
PC11	-0.3418	-0.5232	-0.2232	1.1355	0.6371	1.6339	0.2410	0.0648
PC12	0.2901	0.1892	0.4449	-0.9640	-1.3888	-0.5393	0.2697	0.0577
PC13	0.2675	0.1724	0.4152	-0.8889	-1.2923	-0.4854	0.9660	0.0001

Indri indri

PC	Slope	Slope lower CI	Slope higher CI	Intercept	Intercept lower CI	Intercept higher CI	p value	r squared
PC1	0.9832	0.7089	1.3637	-3.8372	-5.1150	-2.5593	0.8725	0.0007
PC2	-0.8466	-1.1528	-0.6218	3.3039	2.2677	4.3402	0.0359	0.1136
PC3	-0.7389	-1.0231	-0.5336	2.8837	1.9285	3.8388	0.5184	0.0114
PC4	-0.6228	-0.8638	-0.4491	2.4307	1.6214	3.2399	0.8285	0.0013
PC5	0.5983	0.4316	0.8296	-2.3351	-3.1118	-1.5584	0.7399	0.0030
PC6	-0.5557	-0.7658	-0.4032	2.1685	1.4608	2.8762	0.2213	0.0401
PC7	0.5260	0.3800	0.7280	-2.0527	-2.7319	-1.3735	0.4806	0.0135
PC8	0.4870	0.3551	0.6680	-1.9007	-2.5114	-1.2900	0.1044	0.0697
PC9	-0.4357	-0.5985	-0.3172	1.7004	1.1514	2.2494	0.1301	0.0608
PC10	-0.4123	-0.5679	-0.2993	1.6090	1.0850	2.1331	0.1996	0.0441
PC11	0.3692	0.2701	0.5046	-1.4408	-1.8985	-0.9832	0.0620	0.0910
PC12	0.3304	0.2382	0.4583	-1.2894	-1.7189	-0.8600	0.8895	0.0005
PC13	-0.3269	-0.4440	-0.2407	1.2758	0.8792	1.6724	0.0246	0.1292

Propithecus diadema

PC	Slope	Slope lower CI	Slope higher CI	Intercept	Intercept lower CI	Intercept higher CI	p value	r squared
PC1	0.6530	0.4412	0.9664	-2.5085	-3.5175	-1.4995	0.7278	0.0047
PC2	-0.5499	-0.7773	-0.3890	2.1127	1.3667	2.8586	0.0093	0.2330
PC3	-0.4792	-0.7099	-0.3235	1.8411	1.0988	2.5834	0.9606	0.0001
PC4	0.4351	0.3136	0.6035	-1.6715	-2.2284	-1.1146	0.0018	0.3170
PC5	-0.3967	-0.5866	-0.2683	1.5241	0.9125	2.1357	0.6208	0.0096
PC6	0.3583	0.2420	0.5304	-1.3765	-1.9307	-0.8224	0.7726	0.0033
PC7	-0.3257	-0.4762	-0.2228	1.2514	0.7644	1.7383	0.1783	0.0686
PC8	0.3133	0.2115	0.4640	-1.2036	-1.6888	-0.7185	0.8981	0.0006
PC9	-0.2702	-0.3964	-0.1842	1.0382	0.6306	1.4458	0.2440	0.0518
PC10	0.2409	0.1633	0.3555	-0.9256	-1.2950	-0.5562	0.4685	0.0204
PC11	0.2395	0.1617	0.3547	-0.9200	-1.2908	-0.5492	0.8737	0.0010
PC12	0.2233	0.1512	0.3296	-0.8577	-1.2004	-0.5150	0.4983	0.0178
PC13	0.1892	0.1278	0.2802	-0.7270	-1.0199	-0.4341	0.8453	0.0015

Propithecus verreauxi

PC	Slope	Slope lower CI	Slope higher CI	Intercept	Intercept lower CI	Intercept higher CI	p value	r squared
PC1	0.7110	0.5216	0.9693	-2.6783	-3.5217	-1.8348	0.7159	0.0033
PC2	0.6351	0.4687	0.8604	-2.3922	-3.1300	-1.6544	0.1774	0.0439
PC3	0.5671	0.4167	0.7717	-2.1361	-2.8048	-1.4673	0.4358	0.0149
PC4	-0.5288	-0.7197	-0.3885	1.9917	1.3677	2.6157	0.4585	0.0135
PC5	0.4964	0.3663	0.6726	-1.8696	-2.4465	-1.2928	0.1813	0.0432
PC6	-0.4603	-0.6276	-0.3375	1.7337	1.1873	2.2801	0.7896	0.0018
PC7	-0.4466	-0.6056	-0.3294	1.6823	1.1620	2.2027	0.2066	0.0386
PC8	0.3965	0.2908	0.5405	-1.4934	-1.9638	-1.0229	0.7486	0.0025
PC9	-0.3392	-0.4552	-0.2527	1.2776	0.8961	1.6590	0.0349	0.1040
PC10	-0.3255	-0.4396	-0.2411	1.2262	0.8524	1.6001	0.0964	0.0660
PC11	-0.2981	-0.4066	-0.2186	1.1230	0.7689	1.4770	0.8481	0.0009
PC12	-0.2688	-0.3647	-0.1981	1.0123	0.6984	1.3263	0.2393	0.0336
PC13	0.2536	0.1870	0.3439	-0.9552	-1.2507	-0.6598	0.2076	0.0384

Eulemur fulvus

PC	Slope	Slope lower CI	Slope higher CI	Intercept	Intercept lower CI	Intercept higher CI	p value	r squared
PC1	0.8943	0.7701	1.0386	-3.2693	-3.7600	-2.7786	0.9787	0.0000
PC2	0.7542	0.6520	0.8725	-2.7571	-3.1602	-2.3540	0.0026	0.0512
PC3	0.6115	0.5267	0.7099	-2.2353	-2.5703	-1.9003	0.4785	0.0029
PC4	-0.5394	-0.6256	-0.4651	1.9719	1.6784	2.2653	0.0842	0.0171
PC5	0.4780	0.4120	0.5546	-1.7473	-2.0081	-1.4865	0.1642	0.0112
PC6	0.4566	0.3943	0.5287	-1.6691	-1.9146	-1.4236	0.0085	0.0394
PC7	-0.4098	-0.4759	-0.3529	1.4982	1.2734	1.7231	0.8631	0.0002
PC8	-0.3786	-0.4338	-0.3305	1.3841	1.1953	1.5729	0.0000	0.1739
PC9	-0.3515	-0.4073	-0.3033	1.2848	1.0947	1.4749	0.0270	0.0280
PC10	0.3261	0.2811	0.3783	-1.1921	-1.3698	-1.0145	0.1178	0.0141
PC11	-0.3161	-0.3667	-0.2725	1.1556	0.9835	1.3277	0.1028	0.0153
PC12	0.2797	0.2409	0.3248	-1.0225	-1.1760	-0.8691	0.8824	0.0001
PC13	-0.2656	-0.3082	-0.2289	0.9709	0.8258	1.1160	0.2198	0.0087

Eulemur macaco

PC	Slope	Slope lower CI	Slope higher CI	Intercept	Intercept lower CI	Intercept higher CI	p value	r squared
PC1	-1.0291	-1.3494	-0.7848	3.7815	2.7440	4.8190	0.5012	0.0086
PC2	0.8104	0.6175	1.0635	-2.9779	-3.7974	-2.1583	0.7248	0.0024
PC3	0.6870	0.5327	0.8858	-2.5244	-3.1732	-1.8755	0.0069	0.1299
PC4	-0.6306	-0.8227	-0.4834	2.3175	1.6941	2.9408	0.1115	0.0471
PC5	-0.6085	-0.7985	-0.4637	2.2361	1.6210	2.8512	0.6686	0.0035
PC6	-0.5179	-0.6797	-0.3946	1.9031	1.3790	2.4271	0.7914	0.0013
PC7	0.4770	0.3649	0.6235	-1.7529	-2.2280	-1.2778	0.1885	0.0324
PC8	0.4322	0.3320	0.5626	-1.5881	-2.0119	-1.1644	0.0663	0.0622
PC9	0.4169	0.3181	0.5463	-1.5318	-1.9513	-1.1124	0.4164	0.0125
PC10	0.3879	0.3009	0.5001	-1.4253	-1.7914	-1.0593	0.0066	0.1312
PC11	-0.3366	-0.4417	-0.2565	1.2370	0.8966	1.5773	0.6890	0.0030
PC12	0.3092	0.2356	0.4060	-1.1364	-1.4495	-0.8233	0.9420	0.0001
PC13	-0.2769	-0.3628	-0.2113	1.0174	0.7391	1.2957	0.3810	0.0145

Eulemur mongoz

PC	Slope	Slope lower CI	Slope higher CI	Intercept	Intercept lower CI	Intercept higher CI	p value	r squared
PC1	-0.7770	-1.0059	-0.6002	2.7982	2.0674	3.5290	0.0530	0.0664
PC2	0.6598	0.5174	0.8415	-2.3763	-2.9600	-1.7927	0.0012	0.1741
PC3	-0.5028	-0.6565	-0.3851	1.8109	1.3221	2.2996	0.6896	0.0029
PC4	-0.4492	-0.5836	-0.3458	1.6178	1.1894	2.0463	0.1353	0.0401
PC5	0.4100	0.3169	0.5304	-1.4766	-1.8611	-1.0920	0.0446	0.0713
PC6	0.3805	0.2913	0.4969	-1.3702	-1.7405	-0.9999	0.9077	0.0002
PC7	0.3504	0.2723	0.4509	-1.2619	-1.5836	-0.9403	0.0115	0.1106
PC8	-0.3145	-0.4097	-0.2414	1.1325	0.8294	1.4356	0.2997	0.0195
PC9	0.2971	0.2277	0.3877	-1.0699	-1.3581	-0.7817	0.5396	0.0069
PC10	-0.2689	-0.3509	-0.2061	0.9685	0.7075	1.2294	0.5559	0.0063
PC11	-0.2602	-0.3397	-0.1993	0.9370	0.6841	1.1900	0.7006	0.0027
PC12	0.2506	0.1920	0.3270	-0.9024	-1.1457	-0.6592	0.5837	0.0055
PC13	-0.2264	-0.2933	-0.1748	0.8154	0.6019	1.0289	0.0631	0.0614

Eulemur rubriventer

PC	Slope	Slope lower CI	Slope higher CI	Intercept	Intercept lower CI	Intercept higher CI	p value	r squared
PC1	1.0727	0.7355	1.5644	-3.9540	-5.4818	-2.4261	0.0765	0.1202
PC2	-0.7573	-1.1263	-0.5092	2.7916	1.6542	3.9291	0.4623	0.0218
PC3	0.6525	0.4375	0.9733	-2.4053	-3.3930	-1.4177	0.6881	0.0066
PC4	-0.6224	-0.9293	-0.4168	2.2942	1.3494	3.2390	0.8912	0.0008
PC5	-0.5625	-0.8238	-0.3841	2.0735	1.2630	2.8840	0.1086	0.0997
PC6	-0.4793	-0.7150	-0.3213	1.7669	1.0412	2.4925	0.7001	0.0060
PC7	0.4467	0.3157	0.6322	-1.6468	-2.2300	-1.0635	0.0065	0.2607
PC8	-0.3672	-0.5453	-0.2472	1.3534	0.8039	1.9029	0.3996	0.0285
PC9	0.3149	0.2119	0.4679	-1.1607	-1.6326	-0.6889	0.4197	0.0262
PC10	-0.2936	-0.4312	-0.1999	1.0824	0.6560	1.5087	0.1380	0.0858
PC11	-0.2624	-0.3918	-0.1758	0.9673	0.5691	1.3655	0.8529	0.0014
PC12	0.2327	0.1559	0.3475	-0.8578	-1.2111	-0.5046	0.8844	0.0009
PC13	0.2019	0.1354	0.3012	-0.7443	-1.0500	-0.4387	0.6856	0.0067

Hapalemur griseus

PC	Slope	Slope lower CI	Slope higher CI	Intercept	Intercept lower CI	Intercept higher CI	p value	r squared
PC1	0.8594	0.5761	1.2819	-2.9840	-4.2095	-1.7584	0.6965	0.0062
PC2	0.7074	0.4757	1.0519	-2.4563	-3.4568	-1.4559	0.4544	0.0226
PC3	-0.6776	-1.0115	-0.4539	2.3527	1.3844	3.3210	0.8200	0.0021
PC4	-0.6459	-0.9454	-0.4413	2.2427	1.3672	3.1181	0.1041	0.1022
PC5	-0.5960	-0.8841	-0.4018	2.0696	1.2322	2.9070	0.3469	0.0355
PC6	0.4727	0.3396	0.6579	-1.6413	-2.1939	-1.0887	0.0017	0.3321
PC7	0.4046	0.2724	0.6009	-1.4047	-1.9751	-0.8344	0.3986	0.0287
PC8	-0.3583	-0.5325	-0.2410	1.2440	0.7379	1.7502	0.4346	0.0246
PC9	-0.3348	-0.4931	-0.2274	1.1626	0.7012	1.6240	0.1762	0.0719
PC10	0.3100	0.2081	0.4619	-1.0765	-1.5173	-0.6357	0.5846	0.0121
PC11	-0.2887	-0.4287	-0.1945	1.0026	0.5958	1.4094	0.3874	0.0300
PC12	0.2463	0.1653	0.3670	-0.8551	-1.2055	-0.5048	0.6018	0.0111
PC13	-0.2181	-0.3257	-0.1461	0.7574	0.4455	1.0693	0.8859	0.0008

Lemur catta

PC	Slope	Slope lower CI	Slope higher CI	Intercept	Intercept lower CI	Intercept higher CI	p value	r squared
PC1	-0.8087	-1.1402	-0.5735	2.9051	1.8870	3.9231	0.1891	0.0533
PC2	0.6365	0.4489	0.9026	-2.2866	-3.1017	-1.4716	0.4182	0.0206
PC3	0.5263	0.3804	0.7282	-1.8908	-2.5157	-1.2660	0.0199	0.1581
PC4	0.4830	0.3394	0.6873	-1.7352	-2.3601	-1.1102	0.9812	0.0000
PC5	0.4245	0.2991	0.6027	-1.5251	-2.0706	-0.9797	0.5059	0.0140
PC6	-0.4040	-0.5749	-0.2839	1.4514	0.9287	1.9742	0.9996	0.0000
PC7	-0.3348	-0.4762	-0.2353	1.2026	0.7698	1.6354	0.8246	0.0016
PC8	-0.3263	-0.4595	-0.2316	1.1720	0.7626	1.5814	0.1648	0.0594
PC9	0.2775	0.1957	0.3933	-0.9967	-1.3518	-0.6417	0.4029	0.0220
PC10	-0.2409	-0.3419	-0.1698	0.8655	0.5562	1.1747	0.4765	0.0160
PC11	-0.2215	-0.3150	-0.1557	0.7956	0.5093	1.0818	0.7986	0.0021
PC12	-0.2067	-0.2901	-0.1473	0.7427	0.4863	0.9991	0.1030	0.0809
PC13	-0.1924	-0.2738	-0.1352	0.6911	0.4422	0.9401	0.9680	0.0001

Varecia variegata

PC	Slope	Slope lower CI	Slope higher CI	Intercept	Intercept lower CI	Intercept higher CI	p value	r squared
PC1	-1.0496	-1.4550	-0.7571	3.9714	2.6508	5.2920	0.7108	0.0038
PC2	-0.8124	-1.1221	-0.5882	3.0741	2.0637	4.0845	0.3205	0.0267
PC3	-0.6981	-0.9678	-0.5035	2.6414	1.7627	3.5201	0.7376	0.0031
PC4	0.6607	0.4771	0.9150	-2.5000	-3.3285	-1.6714	0.5367	0.0104
PC5	-0.5417	-0.7512	-0.3906	2.0496	1.3672	2.7321	0.8388	0.0011
PC6	0.4454	0.3230	0.6142	-1.6853	-2.2362	-1.1343	0.2403	0.0371
PC7	-0.4086	-0.5616	-0.2973	1.5461	1.0459	2.0463	0.1431	0.0571
PC8	0.3649	0.2678	0.4971	-1.3806	-1.8145	-0.9466	0.0393	0.1099
PC9	-0.3450	-0.4768	-0.2496	1.3055	0.8756	1.7353	0.3537	0.0233
PC10	-0.3071	-0.4239	-0.2225	1.1621	0.7809	1.5433	0.2870	0.0306
PC11	0.2840	0.2052	0.3929	-1.0745	-1.4297	-0.7194	0.4448	0.0159
PC12	0.2439	0.1758	0.3382	-0.9228	-1.2301	-0.6155	0.8514	0.0010
PC13	-0.2286	-0.3169	-0.1650	0.8651	0.5776	1.1526	0.6674	0.0050

Lepilemur ruficaudatus

PC	Slope	Slope lower CI	Slope higher CI	Intercept	Intercept lower CI	Intercept higher CI	p value	r squared
PC1	0.6901	0.4548	1.0470	-2.3004	-3.2877	-1.3132	0.6251	0.0106
PC2	0.6733	0.4454	1.0179	-2.2445	-3.1990	-1.2900	0.4207	0.0284
PC3	-0.5871	-0.8875	-0.3883	1.9571	1.1249	2.7893	0.4194	0.0286
PC4	-0.5433	-0.7954	-0.3711	1.8110	1.1037	2.5183	0.0343	0.1805
PC5	-0.4861	-0.7389	-0.3198	1.6203	0.9216	2.3190	0.8796	0.0010
PC6	0.4606	0.3040	0.6979	-1.5355	-2.1922	-0.8789	0.5291	0.0175
PC7	-0.4012	-0.6014	-0.2676	1.3372	0.7809	1.8936	0.2016	0.0699
PC8	-0.3647	-0.5471	-0.2431	1.2158	0.7091	1.7226	0.2130	0.0666
PC9	-0.3618	-0.5477	-0.2390	1.2060	0.6913	1.7208	0.4861	0.0213
PC10	-0.3284	-0.4955	-0.2177	1.0948	0.6318	1.5578	0.3429	0.0392
PC11	0.2948	0.1951	0.4455	-0.9829	-1.4003	-0.5655	0.3993	0.0311
PC12	-0.2707	-0.4108	-0.1783	0.9023	0.5148	1.2898	0.6515	0.0090
PC13	0.2350	0.1561	0.3537	-0.7834	-1.1128	-0.4540	0.2815	0.0502

Loris tardigradus

PC	Slope	Slope lower CI	Slope higher CI	Intercept	Intercept lower CI	Intercept higher CI	p value	r squared
PC1	0.3606	0.2449	0.5309	-1.1321	-1.5819	-0.6824	0.1726	0.0731
PC2	-0.3211	-0.4795	-0.2150	1.0081	0.5921	1.4242	0.9194	0.0004
PC3	-0.2547	-0.3803	-0.1706	0.7998	0.4698	1.1298	0.8869	0.0008
PC4	-0.2459	-0.3451	-0.1753	0.7722	0.5052	1.0392	0.0033	0.2973
PC5	0.2375	0.1637	0.3446	-0.7457	-1.0301	-0.4613	0.0496	0.1455
PC6	-0.1975	-0.2853	-0.1367	0.6200	0.3863	0.8537	0.0353	0.1653
PC7	0.1865	0.1255	0.2770	-0.5855	-0.8237	-0.3473	0.4040	0.0280
PC8	0.1683	0.1131	0.2505	-0.5285	-0.7446	-0.3123	0.5031	0.0181
PC9	0.1389	0.0949	0.2033	-0.4361	-0.6067	-0.2656	0.1050	0.1017
PC10	0.1218	0.0816	0.1818	-0.3824	-0.5401	-0.2246	0.9072	0.0006
PC11	-0.1131	-0.1686	-0.0759	0.3551	0.2093	0.5010	0.6180	0.0101
PC12	0.1007	0.0677	0.1498	-0.3163	-0.4455	-0.1872	0.4683	0.0212
PC13	0.0917	0.0617	0.1363	-0.2878	-0.4052	-0.1704	0.4496	0.0231

Nycticebus bengalensis

PC	Slope	Slope lower CI	Slope higher CI	Intercept	Intercept lower CI	Intercept higher CI	p value	r squared
PC1	-0.9951	-1.5126	-0.6547	3.5032	1.9930	5.0134	0.0792	0.1460
PC2	-0.7196	-1.1296	-0.4584	2.5332	1.3514	3.7149	0.9703	0.0001
PC3	0.6561	0.4191	1.0271	-2.3096	-3.3799	-1.2393	0.6106	0.0132
PC4	0.5274	0.3360	0.8279	-1.8567	-2.7226	-0.9909	0.8978	0.0008
PC5	-0.4856	-0.7463	-0.3160	1.7095	0.9519	2.4671	0.1571	0.0975
PC6	0.4124	0.2685	0.6333	-1.4517	-2.0938	-0.8097	0.1492	0.1012
PC7	-0.3725	-0.5848	-0.2373	1.3114	0.6996	1.9232	0.9959	0.0000
PC8	0.3530	0.2249	0.5542	-1.2427	-1.8225	-0.6630	0.9631	0.0001
PC9	-0.2900	-0.4427	-0.1900	1.0210	0.5762	1.4658	0.1023	0.1279
PC10	-0.2491	-0.3907	-0.1588	0.8769	0.4687	1.2851	0.7697	0.0044
PC11	-0.2375	-0.3624	-0.1556	0.8360	0.4720	1.2000	0.1011	0.1287
PC12	0.2232	0.1454	0.3425	-0.7857	-1.1327	-0.4388	0.1432	0.1040
PC13	0.2098	0.1343	0.3277	-0.7384	-1.0790	-0.3978	0.5065	0.0224

Nycticebus coucang

PC	Slope	Slope lower CI	Slope higher CI	Intercept	Intercept lower CI	Intercept higher CI	p value	r squared
PC1	0.5726	0.4534	0.7233	-1.9551	-2.4160	-1.4943	0.0331	0.0660
PC2	0.4680	0.3676	0.5958	-1.5978	-1.9876	-1.2081	0.9932	0.0000
PC3	0.4227	0.3321	0.5379	-1.4431	-1.7945	-1.0916	0.6526	0.0030
PC4	0.3975	0.3138	0.5036	-1.3572	-1.6813	-1.0331	0.0937	0.0414
PC5	0.3790	0.3005	0.4781	-1.2941	-1.5973	-0.9909	0.0207	0.0773
PC6	0.3619	0.2849	0.4597	-1.2357	-1.5342	-0.9372	0.2537	0.0194
PC7	0.3603	0.2845	0.4563	-1.2303	-1.5237	-0.9370	0.0818	0.0445
PC8	-0.3012	-0.3821	-0.2374	1.0284	0.7813	1.2755	0.1577	0.0296
PC9	0.2948	0.2323	0.3742	-1.0065	-1.2489	-0.7642	0.1908	0.0254
PC10	-0.2706	-0.3433	-0.2133	0.9238	0.7019	1.1458	0.1569	0.0297
PC11	0.2533	0.1991	0.3221	-0.8647	-1.0748	-0.6547	0.4529	0.0084
PC12	0.2322	0.1825	0.2954	-0.7927	-0.9855	-0.5999	0.5352	0.0058
PC13	-0.2167	-0.2758	-0.1702	0.7398	0.5595	0.9201	0.7531	0.0015

Perodicticus potto

PC	Slope	Slope lower CI	Slope higher CI	Intercept	Intercept lower CI	Intercept higher CI	p value	r squared
PC1	-0.5068	-0.6022	-0.4264	1.8010	1.4885	2.1136	0.0793	0.0241
PC2	-0.4193	-0.4959	-0.3546	1.4902	1.2390	1.7414	0.0013	0.0790
PC3	-0.3921	-0.4662	-0.3298	1.3935	1.1510	1.6359	0.1242	0.0185
PC4	-0.3787	-0.4493	-0.3192	1.3459	1.1145	1.5772	0.0191	0.0425
PC5	-0.3200	-0.3810	-0.2688	1.1374	0.9380	1.3369	0.5180	0.0033
PC6	0.3051	0.2572	0.3619	-1.0844	-1.2706	-0.8982	0.0165	0.0444
PC7	-0.2802	-0.3335	-0.2354	0.9959	0.8215	1.1703	0.3804	0.0061
PC8	-0.2577	-0.3066	-0.2165	0.9157	0.7556	1.0759	0.2938	0.0087
PC9	-0.2388	-0.2843	-0.2007	0.8489	0.7002	0.9976	0.4005	0.0056
PC10	-0.2260	-0.2691	-0.1899	0.8033	0.6625	0.9441	0.4569	0.0044
PC11	0.2142	0.1801	0.2547	-0.7612	-0.8939	-0.6285	0.1713	0.0147
PC12	0.2123	0.1789	0.2520	-0.7545	-0.8844	-0.6245	0.0258	0.0385
PC13	0.1918	0.1612	0.2282	-0.6818	-0.8009	-0.5627	0.2335	0.0112

Goswami model vault module against ln CS whole cranium

Cheirogaleus major

PC	Slope	Slope lower CI	Slope higher CI	Intercept	Intercept lower CI	Intercept higher CI	p value	r squared
PC1	0.9900	0.6765	1.4487	-4.8107	-6.6869	-2.9345	0.0331	0.1826
PC2	0.7352	0.5161	1.0473	-3.5725	-4.8632	-2.2817	0.0047	0.2985
PC3	-0.6318	-0.9540	-0.4184	3.0700	1.7686	4.3714	0.3750	0.0344
PC4	-0.5473	-0.8319	-0.3601	2.6597	1.5133	3.8061	0.8449	0.0017
PC5	-0.4962	-0.7508	-0.3280	2.4113	1.3838	3.4388	0.4569	0.0243
PC6	0.3620	0.2383	0.5500	-1.7592	-2.5164	-1.0020	0.7513	0.0045
PC7	-0.3275	-0.4808	-0.2230	1.5912	0.9648	2.2177	0.0424	0.1672
PC8	0.3098	0.2043	0.4700	-1.5056	-2.1513	-0.8599	0.6092	0.0115
PC9	-0.2882	-0.4379	-0.1896	1.4002	0.7971	2.0034	0.7945	0.0030
PC10	-0.2632	-0.4001	-0.1731	1.2789	0.7274	1.8305	0.9188	0.0005
PC11	0.2263	0.1492	0.3434	-1.0998	-1.5718	-0.6279	0.6267	0.0105
PC12	0.2102	0.1391	0.3178	-1.0216	-1.4557	-0.5875	0.4103	0.0297
PC13	0.1695	0.1120	0.2566	-0.8236	-1.1750	-0.4722	0.4835	0.0216

Cheirogaleus medius

PC	Slope	Slope lower CI	Slope higher CI	Intercept	Intercept lower CI	Intercept higher CI	p value	r squared
PC1	-0.8310	-1.1893	-0.5806	3.8144	2.4172	5.2115	0.0458	0.1397
PC2	0.6711	0.4569	0.9859	-3.0805	-4.2948	-1.8662	0.7529	0.0037
PC3	0.4900	0.3376	0.7112	-2.2492	-3.1067	-1.3918	0.1715	0.0681
PC4	-0.4228	-0.6212	-0.2878	1.9407	1.1754	2.7061	0.7857	0.0028
PC5	-0.4159	-0.6113	-0.2830	1.9092	1.1557	2.6627	0.8536	0.0013
PC6	-0.3690	-0.5420	-0.2512	1.6938	1.0263	2.3612	0.7360	0.0043
PC7	0.3446	0.2351	0.5051	-1.5816	-2.2013	-0.9619	0.5193	0.0155
PC8	0.3037	0.2070	0.4457	-1.3941	-1.9422	-0.8460	0.6248	0.0090
PC9	-0.2756	-0.4030	-0.1885	1.2650	0.7725	1.7575	0.3836	0.0282
PC10	-0.2355	-0.3439	-0.1613	1.0809	0.6618	1.5001	0.3251	0.0359
PC11	0.1672	0.1140	0.2451	-0.7673	-1.0683	-0.4663	0.5486	0.0135
PC12	0.1567	0.1066	0.2303	-0.7191	-1.0030	-0.4352	0.8841	0.0008
PC13	0.1431	0.0980	0.2089	-0.6568	-0.9112	-0.4024	0.3115	0.0379

Microcebus murinus

PC	Slope	Slope lower CI	Slope higher CI	Intercept	Intercept lower CI	Intercept higher CI	p value	r squared
PC1	1.0912	0.8770	1.3579	-4.7309	-5.7733	-3.6884	0.0009	0.1457
PC2	1.0182	0.8060	1.2862	-4.4142	-5.4550	-3.3733	0.2169	0.0217
PC3	0.6908	0.5462	0.8737	-2.9949	-3.7047	-2.2850	0.3702	0.0115
PC4	0.6409	0.5070	0.8101	-2.7784	-3.4355	-2.1214	0.2886	0.0161
PC5	0.5202	0.4111	0.6582	-2.2552	-2.7908	-1.7195	0.4703	0.0075
PC6	-0.5181	-0.6561	-0.4091	2.2462	1.7108	2.7815	0.8555	0.0005
PC7	-0.4699	-0.5941	-0.3716	2.0371	1.5548	2.5194	0.3264	0.0138
PC8	-0.4288	-0.5424	-0.3389	1.8588	1.4178	2.2997	0.4103	0.0097
PC9	0.3789	0.2996	0.4792	-1.6427	-2.0320	-1.2534	0.3621	0.0119
PC10	0.3509	0.2773	0.4442	-1.5214	-1.8833	-1.1596	0.5700	0.0046
PC11	0.3041	0.2401	0.3851	-1.3182	-1.6325	-1.0040	0.8809	0.0003
PC12	-0.2746	-0.3476	-0.2169	1.1903	0.9068	1.4739	0.7206	0.0018
PC13	0.2406	0.1901	0.3047	-1.0432	-1.2917	-0.7948	0.7127	0.0019

Microcebus rufus

PC	Slope	Slope lower CI	Slope higher CI	Intercept	Intercept lower CI	Intercept higher CI	p value	r squared
PC1	0.7628	0.5286	1.1008	-3.3246	-4.5716	-2.0776	0.0984	0.0979
PC2	0.6711	0.4831	0.9322	-2.9247	-3.9034	-1.9460	0.0030	0.2820
PC3	-0.4888	-0.7129	-0.3352	2.1303	1.3071	2.9535	0.2829	0.0426
PC4	-0.4347	-0.6372	-0.2965	1.8943	1.1520	2.6367	0.5209	0.0154
PC5	0.4148	0.2877	0.5981	-1.8078	-2.4842	-1.1313	0.0908	0.1023
PC6	-0.3473	-0.5086	-0.2371	1.5134	0.9217	2.1051	0.4646	0.0200
PC7	-0.3042	-0.4466	-0.2072	1.3258	0.8041	1.8476	0.6614	0.0072
PC8	-0.2828	-0.4144	-0.1929	1.2323	0.7495	1.7151	0.5156	0.0158
PC9	0.2619	0.1782	0.3849	-1.1413	-1.5919	-0.6908	0.8784	0.0009
PC10	-0.2060	-0.3028	-0.1401	0.8976	0.5431	1.2521	0.9640	0.0001
PC11	0.1751	0.1234	0.2484	-0.7631	-1.0354	-0.4908	0.0204	0.1836
PC12	0.1651	0.1126	0.2421	-0.7194	-1.0017	-0.4371	0.5601	0.0127
PC13	0.1492	0.1023	0.2177	-0.6503	-0.9019	-0.3987	0.2969	0.0402

Galago alleni

PC	Slope	Slope lower CI	Slope higher CI	Intercept	Intercept lower CI	Intercept higher CI	p value	r squared
PC1	0.8838	0.5827	1.3405	-4.2060	-6.0091	-2.4029	0.2485	0.0600
PC2	-0.6254	-0.9553	-0.4095	2.9763	1.6775	4.2750	0.4508	0.0261
PC3	-0.5197	-0.7863	-0.3435	2.4733	1.4195	3.5270	0.2064	0.0715
PC4	-0.4744	-0.7230	-0.3112	2.2575	1.2776	3.2375	0.3723	0.0363
PC5	-0.3681	-0.5650	-0.2398	1.7519	0.9780	2.5257	0.8298	0.0021
PC6	0.3459	0.2342	0.5109	-1.6462	-2.3048	-0.9877	0.0379	0.1815
PC7	-0.3150	-0.4783	-0.2075	1.4991	0.8546	2.1436	0.2719	0.0546
PC8	0.2702	0.1799	0.4059	-1.2859	-1.8239	-0.7480	0.1225	0.1049
PC9	-0.2370	-0.3625	-0.1550	1.1281	0.6343	1.6218	0.5074	0.0202
PC10	-0.2272	-0.3341	-0.1545	1.0810	0.6536	1.5084	0.0282	0.2006
PC11	0.1854	0.1208	0.2845	-0.8824	-1.2719	-0.4929	0.7877	0.0034
PC12	0.1826	0.1190	0.2802	-0.8690	-1.2527	-0.4854	0.7879	0.0034
PC13	-0.1289	-0.1968	-0.0844	0.6133	0.3459	0.8808	0.4401	0.0273

Galago demidoff

PC	Slope	Slope lower CI	Slope higher CI	Intercept	Intercept lower CI	Intercept higher CI	p value	r squared
PC1	0.7328	0.5837	0.9201	-3.2473	-3.9927	-2.5019	0.0001	0.2511
PC2	0.6584	0.5080	0.8534	-2.9177	-3.6830	-2.1524	0.2597	0.0222
PC3	-0.5440	-0.7049	-0.4198	2.4104	1.7787	3.0422	0.2453	0.0236
PC4	0.5054	0.3889	0.6567	-2.2395	-2.8328	-1.6462	0.7086	0.0025
PC5	0.4388	0.3385	0.5688	-1.9445	-2.4548	-1.4342	0.2730	0.0210
PC6	-0.4047	-0.5255	-0.3116	1.7932	1.3192	2.2671	0.5254	0.0071
PC7	0.3760	0.2906	0.4865	-1.6661	-2.1002	-1.2321	0.1538	0.0354
PC8	-0.3446	-0.4449	-0.2669	1.5271	1.1327	1.9216	0.0833	0.0517
PC9	-0.3276	-0.4258	-0.2521	1.4519	1.0670	1.8368	0.7984	0.0012
PC10	0.2926	0.2251	0.3803	-1.2966	-1.6405	-0.9528	0.8821	0.0004
PC11	-0.2625	-0.3410	-0.2020	1.1631	0.8550	1.4712	0.6848	0.0029
PC12	-0.2404	-0.3120	-0.1853	1.0654	0.7845	1.3463	0.4090	0.0120
PC13	0.2223	0.1716	0.2881	-0.9853	-1.2434	-0.7271	0.2414	0.0240

Galago elegantulus

PC	Slope	Slope lower CI	Slope higher CI	Intercept	Intercept lower CI	Intercept higher CI	p value	r squared
PC1	1.2681	0.9028	1.7814	-5.9876	-8.0618	-3.9134	0.1183	0.0745
PC2	-1.0507	-1.4466	-0.7631	4.9607	3.3471	6.5744	0.0114	0.1840
PC3	-0.7547	-1.0726	-0.5310	3.5633	2.2847	4.8419	0.6364	0.0071
PC4	0.6638	0.4686	0.9404	-3.1341	-4.2479	-2.0203	0.3622	0.0260
PC5	0.5892	0.4151	0.8362	-2.7817	-3.7758	-1.7877	0.4881	0.0151
PC6	0.5608	0.3983	0.7895	-2.6477	-3.5711	-1.7243	0.1555	0.0620
PC7	-0.4447	-0.6326	-0.3126	2.0995	1.3439	2.8551	0.8469	0.0012
PC8	-0.4259	-0.6057	-0.2995	2.0111	1.2883	2.7339	0.7258	0.0039
PC9	-0.3590	-0.5061	-0.2546	1.6950	1.1012	2.2887	0.1871	0.0537
PC10	-0.3090	-0.4376	-0.2182	1.4590	0.9412	1.9769	0.3387	0.0286
PC11	-0.2945	-0.4166	-0.2082	1.3905	0.8985	1.8824	0.2920	0.0346
PC12	0.2699	0.1897	0.3840	-1.2742	-1.7330	-0.8154	0.9412	0.0002
PC13	0.2254	0.1584	0.3207	-1.0642	-1.4474	-0.6810	0.9447	0.0002

Galago moholi

PC	Slope	Slope lower CI	Slope higher CI	Intercept	Intercept lower CI	Intercept higher CI	p value	r squared
PC1	0.9288	0.7606	1.1342	-4.2240	-5.0734	-3.3745	0.0000	0.2779
PC2	-0.6110	-0.7709	-0.4842	2.7786	2.1267	3.4304	0.2672	0.0173
PC3	-0.5700	-0.7185	-0.4521	2.5921	1.9863	3.1978	0.1828	0.0249
PC4	0.5301	0.4196	0.6696	-2.4107	-2.9792	-1.8422	0.4813	0.0070
PC5	0.5029	0.3980	0.6355	-2.2873	-2.8272	-1.7473	0.5589	0.0048
PC6	-0.4248	-0.5369	-0.3360	1.9317	1.4748	2.3886	0.7711	0.0012
PC7	-0.3765	-0.4760	-0.2979	1.7125	1.3074	2.1175	0.7898	0.0010
PC8	-0.3499	-0.4414	-0.2773	1.5911	1.2178	1.9644	0.2684	0.0172
PC9	-0.3431	-0.4337	-0.2714	1.5604	1.1913	1.9295	0.8064	0.0009
PC10	0.2947	0.2342	0.3708	-1.3402	-1.6509	-1.0294	0.0909	0.0397
PC11	-0.2693	-0.3399	-0.2134	1.2247	0.9370	1.5125	0.3106	0.0145
PC12	-0.2483	-0.3131	-0.1970	1.1293	0.8652	1.3934	0.1948	0.0236
PC13	0.2138	0.1694	0.2697	-0.9722	-1.2003	-0.7441	0.2687	0.0172

Galago senegalensis

PC	Slope	Slope lower CI	Slope higher CI	Intercept	Intercept lower CI	Intercept higher CI	p value	r squared
PC1	0.8025	0.7049	0.9137	-3.7203	-4.2044	-3.2362	0.0000	0.2482
PC2	-0.5876	-0.6817	-0.5065	2.7241	2.3179	3.1304	0.1401	0.0125
PC3	0.4931	0.4256	0.5714	-2.2860	-2.6239	-1.9482	0.0213	0.0303
PC4	-0.4381	-0.5087	-0.3773	2.0309	1.7261	2.3357	0.8925	0.0001
PC5	0.4173	0.3595	0.4843	-1.9345	-2.2238	-1.6452	0.2686	0.0071
PC6	0.4086	0.3521	0.4742	-1.8942	-2.1773	-1.6112	0.2206	0.0087
PC7	-0.3872	-0.4486	-0.3341	1.7948	1.5295	2.0601	0.0223	0.0298
PC8	-0.3458	-0.3999	-0.2990	1.6030	1.3690	1.8370	0.0020	0.0539
PC9	0.3323	0.2862	0.3858	-1.5405	-1.7712	-1.3098	0.3861	0.0043
PC10	0.2910	0.2510	0.3373	-1.3489	-1.5489	-1.1488	0.0430	0.0235
PC11	-0.2575	-0.2989	-0.2219	1.1938	1.0154	1.3723	0.2521	0.0076
PC12	0.2521	0.2171	0.2928	-1.1687	-1.3441	-0.9934	0.8114	0.0003
PC13	-0.2313	-0.2685	-0.1992	1.0721	0.9112	1.2329	0.7811	0.0004

Galago zanzibaricus

PC	Slope	Slope lower CI	Slope higher CI	Intercept	Intercept lower CI	Intercept higher CI	p value	r squared
PC1	1.1042	0.7647	1.5943	-5.0643	-6.9668	-3.1618	0.0126	0.2416
PC2	0.8152	0.5382	1.2348	-3.7388	-5.3363	-2.1412	0.5137	0.0188
PC3	0.6711	0.4415	1.0203	-3.0781	-4.4056	-1.7506	0.9207	0.0004
PC4	0.5978	0.3964	0.9016	-2.7419	-3.9006	-1.5832	0.3364	0.0402
PC5	-0.5643	-0.8570	-0.3716	2.5882	1.4751	3.7013	0.7138	0.0060
PC6	0.5024	0.3491	0.7232	-2.3043	-3.1623	-1.4464	0.0100	0.2550
PC7	0.3931	0.2586	0.5977	-1.8031	-2.5808	-1.0254	0.9535	0.0002
PC8	0.3244	0.2153	0.4887	-1.4878	-2.1147	-0.8610	0.3027	0.0461
PC9	-0.2968	-0.4500	-0.1958	1.3614	0.7785	1.9444	0.5640	0.0147
PC10	0.2650	0.1744	0.4026	-1.2154	-1.7387	-0.6922	0.7638	0.0040
PC11	-0.2266	-0.3339	-0.1538	1.0392	0.6261	1.4522	0.0549	0.1510
PC12	-0.2107	-0.3202	-0.1387	0.9665	0.5503	1.3827	0.7843	0.0033
PC13	-0.1815	-0.2756	-0.1195	0.8322	0.4743	1.1901	0.7121	0.0060

Otolemur crassicaudatus

PC	Slope	Slope lower CI	Slope higher CI	Intercept	Intercept lower CI	Intercept higher CI	p value	r squared
PC1	0.9182	0.7595	1.1102	-4.6974	-5.5944	-3.8004	0.0034	0.0833
PC2	0.7148	0.5883	0.8686	-3.6568	-4.3741	-2.9395	0.0701	0.0328
PC3	-0.3964	-0.4744	-0.3312	2.0276	1.6612	2.3939	0.0000	0.1792
PC4	-0.3713	-0.4518	-0.3052	1.8995	1.5243	2.2746	0.1651	0.0194
PC5	0.3204	0.2632	0.3901	-1.6393	-1.9637	-1.3148	0.2200	0.0152
PC6	-0.2925	-0.3560	-0.2403	1.4963	1.2004	1.7923	0.1988	0.0166
PC7	0.2750	0.2256	0.3353	-1.4070	-1.6876	-1.1264	0.8717	0.0003
PC8	-0.2625	-0.3199	-0.2153	1.3427	1.0751	1.6103	0.7140	0.0014
PC9	-0.2446	-0.2963	-0.2019	1.2511	1.0096	1.4925	0.0110	0.0635
PC10	0.1966	0.1618	0.2388	-1.0056	-1.2025	-0.8088	0.0548	0.0368
PC11	0.1842	0.1513	0.2243	-0.9424	-1.1293	-0.7555	0.2860	0.0115
PC12	-0.1663	-0.2028	-0.1365	0.8510	0.6813	1.0206	0.8253	0.0005
PC13	-0.1547	-0.1878	-0.1274	0.7913	0.6369	0.9457	0.0373	0.0431

Otolemur garnettii

PC	Slope	Slope lower CI	Slope higher CI	Intercept	Intercept lower CI	Intercept higher CI	p value	r squared
PC1	1.0060	0.8233	1.2293	-5.0766	-6.1010	-4.0523	0.0522	0.0399
PC2	0.5225	0.4319	0.6322	-2.6367	-3.1421	-2.1312	0.0003	0.1335
PC3	-0.4058	-0.4928	-0.3341	2.0478	1.6473	2.4483	0.0020	0.0981
PC4	0.3611	0.2944	0.4429	-1.8221	-2.1969	-1.4472	0.6638	0.0020
PC5	-0.3262	-0.3999	-0.2661	1.6462	1.3086	1.9837	0.3764	0.0084
PC6	0.3027	0.2467	0.3714	-1.5277	-1.8423	-1.2131	0.9285	0.0001
PC7	-0.2640	-0.3229	-0.2157	1.3320	1.0615	1.6025	0.1067	0.0277
PC8	0.2408	0.1963	0.2955	-1.2153	-1.4656	-0.9650	0.9347	0.0001
PC9	-0.2243	-0.2733	-0.1841	1.1317	0.9067	1.3568	0.0110	0.0675
PC10	-0.2001	-0.2450	-0.1634	1.0096	0.8035	1.2157	0.2013	0.0175
PC11	-0.1843	-0.2261	-0.1502	0.9298	0.7384	1.1213	0.9749	0.0000
PC12	-0.1676	-0.2051	-0.1370	0.8459	0.6743	1.0176	0.0990	0.0290
PC13	-0.1382	-0.1678	-0.1138	0.6973	0.5608	0.8338	0.0022	0.0966

Avahi laniger

PC	Slope	Slope lower CI	Slope higher CI	Intercept	Intercept lower CI	Intercept higher CI	p value	r squared
PC1	1.2805	0.8323	1.9700	-6.2522	-9.0300	-3.4743	0.3510	0.0415
PC2	1.0028	0.6591	1.5258	-4.8965	-7.0126	-2.7805	0.1566	0.0932
PC3	0.8519	0.5554	1.3068	-4.1597	-5.9943	-2.3251	0.2791	0.0555
PC4	-0.7470	-1.1542	-0.4835	3.6476	2.0101	5.2851	0.5044	0.0215
PC5	-0.6791	-1.0534	-0.4378	3.3159	1.8130	4.8187	0.8170	0.0026
PC6	0.6142	0.4009	0.9410	-2.9991	-4.3176	-1.6807	0.2534	0.0616
PC7	-0.4512	-0.6813	-0.2988	2.2030	1.2691	3.1369	0.0945	0.1274
PC8	-0.4029	-0.6251	-0.2597	1.9672	1.0750	2.8595	0.8760	0.0012
PC9	0.3803	0.2455	0.5890	-1.8569	-2.6953	-1.0184	0.6490	0.0101
PC10	-0.3295	-0.5074	-0.2139	1.6087	0.8921	2.3253	0.3818	0.0366
PC11	-0.2791	-0.4322	-0.1803	1.3630	0.7479	1.9781	0.6309	0.0112
PC12	-0.2758	-0.4258	-0.1787	1.3469	0.7437	1.9500	0.4594	0.0263
PC13	-0.2444	-0.3793	-0.1575	1.1934	0.6519	1.7350	0.9445	0.0002

Indri indri

PC	Slope	Slope lower CI	Slope higher CI	Intercept	Intercept lower CI	Intercept higher CI	p value	r squared
PC1	-1.2852	-1.7673	-0.9346	7.0533	4.7683	9.3383	0.1538	0.0542
PC2	-1.0226	-1.4087	-0.7422	5.6119	3.7829	7.4409	0.2065	0.0428
PC3	0.8123	0.5974	1.1045	-4.4580	-5.8495	-3.0666	0.0293	0.1220
PC4	-0.7162	-0.9602	-0.5342	3.9306	2.7617	5.0995	0.0040	0.2030
PC5	-0.6298	-0.8727	-0.4545	3.4566	2.3091	4.6042	0.6187	0.0068
PC6	0.5429	0.3928	0.7503	-2.9796	-3.9604	-1.9987	0.3535	0.0233
PC7	0.4718	0.3401	0.6545	-2.5894	-3.4519	-1.7269	0.9560	0.0001
PC8	-0.3916	-0.5427	-0.2826	2.1493	1.4356	2.8631	0.6351	0.0062
PC9	0.3372	0.2438	0.4663	-1.8504	-2.4610	-1.2398	0.4060	0.0187
PC10	-0.3243	-0.4441	-0.2368	1.7797	1.2107	2.3486	0.0830	0.0790
PC11	0.3069	0.2213	0.4257	-1.6844	-2.2454	-1.1234	0.9090	0.0004
PC12	-0.2786	-0.3862	-0.2010	1.5289	1.0207	2.0371	0.6965	0.0042
PC13	-0.2627	-0.3644	-0.1894	1.4416	0.9614	1.9218	0.9772	0.0000

Propithecus diadema

PC	Slope	Slope lower CI	Slope higher CI	Intercept	Intercept lower CI	Intercept higher CI	p value	r squared
PC1	-1.2513	-1.8513	-0.8458	6.7188	4.0191	9.4186	0.6816	0.0066
PC2	-0.9121	-1.3077	-0.6362	4.8976	3.0948	6.7003	0.0312	0.1663
PC3	0.6301	0.4280	0.9277	-3.3832	-4.7247	-2.0416	0.3590	0.0324
PC4	-0.5782	-0.8111	-0.4122	3.1044	2.0334	4.1754	0.0048	0.2676
PC5	0.5018	0.3415	0.7373	-2.6942	-3.7567	-1.6316	0.2900	0.0429
PC6	-0.4644	-0.6802	-0.3171	2.4935	1.5186	3.4683	0.2113	0.0594
PC7	0.4069	0.2749	0.6024	-2.1850	-3.0642	-1.3057	0.7595	0.0037
PC8	-0.2950	-0.4367	-0.1993	1.5840	0.9467	2.2213	0.7481	0.0040
PC9	0.2806	0.1897	0.4152	-1.5067	-2.1121	-0.9013	0.6783	0.0067
PC10	-0.2332	-0.3450	-0.1576	1.2522	0.7491	1.7553	0.6767	0.0068
PC11	0.2211	0.1496	0.3267	-1.1871	-1.6624	-0.7118	0.5522	0.0138
PC12	0.2011	0.1358	0.2978	-1.0799	-1.5149	-0.6449	0.8411	0.0016
PC13	-0.1629	-0.2392	-0.1110	0.8749	0.5307	1.2192	0.2655	0.0474

Propithecus verreauxi

PC	Slope	Slope lower CI	Slope higher CI	Intercept	Intercept lower CI	Intercept higher CI	p value	r squared
PC1	-1.2564	-1.7016	-0.9277	6.6503	4.6019	8.6987	0.1657	0.0463
PC2	1.0478	0.7690	1.4277	-5.5462	-7.2895	-3.8030	0.5955	0.0069
PC3	0.8768	0.6484	1.1855	-4.6409	-6.0623	-3.2196	0.1226	0.0571
PC4	0.7235	0.5400	0.9692	-3.8295	-4.9655	-2.6934	0.0258	0.1154
PC5	0.6261	0.4592	0.8536	-3.3141	-4.3578	-2.2704	0.7243	0.0031
PC6	-0.5439	-0.7348	-0.4026	2.8788	1.9995	3.7581	0.1065	0.0623
PC7	-0.4391	-0.5988	-0.3220	2.3242	1.5915	3.0569	0.8417	0.0010
PC8	0.3983	0.2951	0.5375	-2.1083	-2.7499	-1.4667	0.0886	0.0691
PC9	0.3533	0.2590	0.4819	-1.8702	-2.4601	-1.2804	0.9341	0.0002
PC10	-0.3252	-0.4371	-0.2419	1.7212	1.2046	2.2379	0.0451	0.0944
PC11	0.2733	0.2007	0.3720	-1.4465	-1.8998	-0.9931	0.4724	0.0127
PC12	0.2317	0.1699	0.3160	-1.2263	-1.6130	-0.8397	0.8682	0.0007
PC13	-0.2092	-0.2839	-0.1541	1.1071	0.7635	1.4507	0.2512	0.0320

Eulemur fulvus

PC	Slope	Slope lower CI	Slope higher CI	Intercept	Intercept lower CI	Intercept higher CI	p value	r squared
PC1	1.2174	1.0623	1.3951	-6.4895	-7.3766	-5.6025	0.0000	0.1703
PC2	-0.8746	-1.0149	-0.7537	4.6622	3.9660	5.3585	0.1934	0.0098
PC3	-0.6890	-0.7996	-0.5937	3.6728	3.1240	4.2216	0.2196	0.0087
PC4	-0.6689	-0.7748	-0.5775	3.5658	3.0399	4.0917	0.0143	0.0342
PC5	-0.5206	-0.6045	-0.4483	2.7751	2.3586	3.1915	0.9794	0.0000
PC6	-0.4776	-0.5543	-0.4115	2.5460	2.1655	2.9266	0.2374	0.0081
PC7	0.4435	0.3828	0.5139	-2.3644	-2.7138	-2.0150	0.0207	0.0305
PC8	-0.4347	-0.5046	-0.3745	2.3175	1.9706	2.6644	0.3399	0.0053
PC9	-0.3885	-0.4511	-0.3345	2.0708	1.7601	2.3815	0.7982	0.0004
PC10	0.3577	0.3084	0.4149	-1.9070	-2.1908	-1.6232	0.0904	0.0165
PC11	-0.3300	-0.3823	-0.2849	1.7593	1.4997	2.0189	0.0155	0.0334
PC12	-0.3106	-0.3606	-0.2674	1.6555	1.4071	1.9040	0.8179	0.0003
PC13	0.2221	0.1913	0.2579	-1.1842	-1.3617	-1.0066	0.5605	0.0020

Eulemur macaco

PC	Slope	Slope lower CI	Slope higher CI	Intercept	Intercept lower CI	Intercept higher CI	p value	r squared
PC1	1.7484	1.3473	2.2689	-9.3589	-11.8256	-6.8923	0.0309	0.0849
PC2	1.1559	0.8829	1.5132	-6.1870	-7.8739	-4.5001	0.2945	0.0207
PC3	-1.0133	-1.3176	-0.7793	5.4242	3.9836	6.8647	0.0495	0.0708
PC4	-0.8679	-1.1392	-0.6612	4.6456	3.3662	5.9250	0.8287	0.0009
PC5	-0.7820	-1.0210	-0.5989	4.1856	3.0557	5.3156	0.1437	0.0399
PC6	-0.6770	-0.8886	-0.5158	3.6238	2.6258	4.6218	0.8322	0.0009
PC7	-0.6110	-0.8011	-0.4661	3.2708	2.3742	4.1675	0.4687	0.0100
PC8	0.4923	0.3822	0.6341	-2.6351	-3.3094	-1.9608	0.0054	0.1373
PC9	0.4589	0.3506	0.6006	-2.4562	-3.1253	-1.7871	0.2748	0.0225
PC10	0.4188	0.3207	0.5468	-2.2415	-2.8467	-1.6363	0.1454	0.0396
PC11	0.3246	0.2473	0.4262	-1.7377	-2.2165	-1.2590	0.9285	0.0002
PC12	-0.2983	-0.3910	-0.2276	1.5967	1.1593	2.0341	0.4382	0.0114
PC13	-0.2611	-0.3428	-0.1989	1.3977	1.0127	1.7827	0.8561	0.0006

Eulemur mongoz

PC	Slope	Slope lower CI	Slope higher CI	Intercept	Intercept lower CI	Intercept higher CI	p value	r squared
PC1	-0.8026	-1.0439	-0.6170	4.2402	3.1125	5.3678	0.1857	0.0316
PC2	0.6475	0.5012	0.8365	-3.4209	-4.3065	-2.5353	0.0305	0.0823
PC3	-0.5883	-0.7683	-0.4504	3.1080	2.2681	3.9479	0.9117	0.0002
PC4	-0.5174	-0.6696	-0.3999	2.7337	2.0211	3.4462	0.0472	0.0697
PC5	-0.4012	-0.5231	-0.3077	2.1194	1.5503	2.6885	0.4037	0.0127
PC6	-0.3703	-0.4835	-0.2836	1.9564	1.4283	2.4845	0.7152	0.0024
PC7	0.3617	0.2770	0.4724	-1.9110	-2.4273	-1.3947	0.8542	0.0006
PC8	0.3313	0.2538	0.4323	-1.7501	-2.2216	-1.2786	0.5601	0.0062
PC9	-0.2965	-0.3865	-0.2275	1.5666	1.1464	1.9867	0.3632	0.0151
PC10	-0.2615	-0.3414	-0.2003	1.3817	1.0089	1.7545	0.6745	0.0032
PC11	0.2523	0.1932	0.3294	-1.3329	-1.6928	-0.9729	0.7818	0.0014
PC12	-0.2002	-0.2568	-0.1561	1.0578	0.7917	1.3240	0.0052	0.1333
PC13	0.1664	0.1275	0.2171	-0.8792	-1.1159	-0.6425	0.5199	0.0076

Eulemur rubriventer

PC	Slope	Slope lower CI	Slope higher CI	Intercept	Intercept lower CI	Intercept higher CI	p value	r squared
PC1	1.7750	1.2612	2.4980	-9.4388	-12.7273	-6.1502	0.0042	0.2846
PC2	-1.3700	-2.0436	-0.9184	7.2852	4.2936	10.2769	0.6973	0.0062
PC3	-1.1661	-1.7415	-0.7808	6.2010	3.6467	8.7553	0.9928	0.0000
PC4	-1.0909	-1.5643	-0.7607	5.8010	3.6644	7.9377	0.0192	0.2005
PC5	0.8544	0.5725	1.2750	-4.5434	-6.4113	-2.6755	0.7589	0.0038
PC6	-0.6356	-0.9492	-0.4256	3.3798	1.9877	4.7720	0.9662	0.0001
PC7	0.6097	0.4083	0.9102	-3.2419	-4.5765	-1.9074	0.8590	0.0013
PC8	-0.5253	-0.7844	-0.3518	2.7935	1.6432	3.9438	0.8993	0.0007
PC9	-0.4683	-0.6957	-0.3152	2.4902	1.4786	3.5019	0.4100	0.0273
PC10	0.4205	0.2817	0.6279	-2.2363	-3.1568	-1.3158	0.8509	0.0014
PC11	0.3214	0.2153	0.4799	-1.7092	-2.4127	-1.0058	0.8363	0.0017
PC12	-0.2376	-0.3520	-0.1604	1.2637	0.7544	1.7731	0.3021	0.0425
PC13	-0.1843	-0.2717	-0.1250	0.9799	0.5898	1.3700	0.1963	0.0659

Hapalemur griseus

PC	Slope	Slope lower CI	Slope higher CI	Intercept	Intercept lower CI	Intercept higher CI	p value	r squared
PC1	-1.1118	-1.5654	-0.7897	5.6018	3.6473	7.5562	0.0043	0.2826
PC2	0.6008	0.4103	0.8796	-3.0269	-4.2092	-1.8447	0.1062	0.1010
PC3	-0.5910	-0.8671	-0.4028	2.9776	1.8076	4.1475	0.1280	0.0902
PC4	-0.4610	-0.6845	-0.3105	2.3228	1.3807	3.2650	0.3835	0.0305
PC5	0.4164	0.2828	0.6132	-2.0981	-2.9305	-1.2657	0.1750	0.0723
PC6	-0.3964	-0.5919	-0.2654	1.9971	1.1745	2.8197	0.9369	0.0003
PC7	0.3678	0.2504	0.5401	-1.8529	-2.5826	-1.1233	0.1373	0.0862
PC8	0.3125	0.2130	0.4585	-1.5745	-2.1930	-0.9561	0.1268	0.0907
PC9	-0.2820	-0.4211	-0.1889	1.4209	0.8358	2.0060	0.8831	0.0009
PC10	0.2447	0.1651	0.3626	-1.2327	-1.7302	-0.7352	0.3164	0.0401
PC11	-0.1958	-0.2922	-0.1311	0.9863	0.5804	1.3922	0.8287	0.0019
PC12	0.1632	0.1093	0.2437	-0.8223	-1.1610	-0.4836	0.9451	0.0002
PC13	-0.1492	-0.2226	-0.1000	0.7519	0.4430	1.0608	0.7093	0.0057

Lemur catta

PC	Slope	Slope lower CI	Slope higher CI	Intercept	Intercept lower CI	Intercept higher CI	p value	r squared
PC1	1.1412	0.8432	1.5445	-5.9998	-7.8433	-4.1562	0.0016	0.2719
PC2	0.7987	0.5665	1.1260	-4.1991	-5.6698	-2.7284	0.1857	0.0541
PC3	0.7150	0.5122	0.9980	-3.7588	-5.0360	-2.4817	0.0556	0.1098
PC4	-0.5300	-0.7481	-0.3755	2.7864	1.8069	3.7659	0.2174	0.0471
PC5	0.4782	0.3380	0.6764	-2.5139	-3.4033	-1.6244	0.2916	0.0347
PC6	0.4218	0.2966	0.5998	-2.2176	-3.0147	-1.4206	0.7270	0.0039
PC7	0.3446	0.2432	0.4883	-1.8118	-2.4561	-1.1676	0.3713	0.0251
PC8	-0.2835	-0.4033	-0.1993	1.4905	0.9543	2.0267	0.8005	0.0020
PC9	0.2546	0.1794	0.3615	-1.3387	-1.8175	-0.8599	0.5132	0.0135
PC10	-0.2473	-0.3369	-0.1815	1.3002	0.8918	1.7086	0.0033	0.2393
PC11	-0.1969	-0.2801	-0.1385	1.0353	0.6630	1.4076	0.7616	0.0029
PC12	-0.1720	-0.2437	-0.1214	0.9041	0.5827	1.2256	0.3702	0.0252
PC13	0.1450	0.1019	0.2064	-0.7625	-1.0371	-0.4880	0.8973	0.0005

Varecia variegata

PC	Slope	Slope lower CI	Slope higher CI	Intercept	Intercept lower CI	Intercept higher CI	p value	r squared
PC1	-1.2506	-1.7347	-0.9017	6.8503	4.5687	9.1318	0.9018	0.0004
PC2	-0.7820	-1.0846	-0.5638	4.2835	2.8571	5.7100	0.8706	0.0007
PC3	-0.6588	-0.9096	-0.4772	3.6088	2.4245	4.7932	0.2960	0.0295
PC4	0.5591	0.4031	0.7756	-3.0625	-4.0827	-2.0423	0.9809	0.0000
PC5	-0.5067	-0.7017	-0.3659	2.7755	1.8556	3.6954	0.5412	0.0102
PC6	-0.4048	-0.5571	-0.2941	2.2171	1.4966	2.9376	0.1787	0.0483
PC7	-0.3649	-0.5050	-0.2636	1.9986	1.3374	2.6597	0.4766	0.0138
PC8	-0.3185	-0.4398	-0.2307	1.7446	1.1718	2.3175	0.3038	0.0285
PC9	-0.2986	-0.4062	-0.2194	1.6353	1.1236	2.1471	0.0325	0.1177
PC10	-0.2431	-0.3371	-0.1753	1.3315	0.8881	1.7749	0.8590	0.0009
PC11	0.2279	0.1646	0.3156	-1.2482	-1.6619	-0.8346	0.5371	0.0104
PC12	-0.2122	-0.2942	-0.1531	1.1623	0.7759	1.5488	0.6995	0.0041
PC13	0.1878	0.1374	0.2566	-1.0284	-1.3551	-0.7017	0.0629	0.0904

Lepilemur ruficaudatus

PC	Slope	Slope lower CI	Slope higher CI	Intercept	Intercept lower CI	Intercept higher CI	p value	r squared
PC1	0.8716	0.6022	1.2613	-4.2853	-5.9056	-2.6650	0.0148	0.2317
PC2	0.6871	0.4525	1.0433	-3.3784	-4.8308	-1.9259	0.6956	0.0068
PC3	0.5167	0.3399	0.7853	-2.5403	-3.6354	-1.4453	0.8522	0.0015
PC4	0.4757	0.3152	0.7179	-2.3389	-3.3288	-1.3489	0.3553	0.0373
PC5	-0.4292	-0.6494	-0.2837	2.1105	1.2113	3.0096	0.4537	0.0246
PC6	-0.3755	-0.5634	-0.2503	1.8462	1.0763	2.6161	0.2168	0.0655
PC7	0.3561	0.2344	0.5411	-1.7511	-2.5053	-0.9969	0.7866	0.0033
PC8	-0.3050	-0.4638	-0.2006	1.4998	0.8528	2.1467	0.9809	0.0000
PC9	0.2212	0.1455	0.3363	-1.0876	-1.5566	-0.6187	0.8723	0.0011
PC10	0.2033	0.1337	0.3091	-0.9996	-1.4307	-0.5685	0.9025	0.0007
PC11	0.1708	0.1124	0.2597	-0.8399	-1.2021	-0.4776	0.9376	0.0003
PC12	-0.1561	-0.2369	-0.1028	0.7674	0.4376	1.0972	0.6825	0.0074
PC13	0.1284	0.0870	0.1896	-0.6315	-0.8836	-0.3794	0.0616	0.1437

Loris tardigradus

PC	Slope	Slope lower CI	Slope higher CI	Intercept	Intercept lower CI	Intercept higher CI	p value	r squared
PC1	-0.4863	-0.7173	-0.3297	2.3282	1.4001	3.2562	0.2018	0.0643
PC2	-0.4647	-0.6366	-0.3393	2.2247	1.5128	2.9367	0.0004	0.3968
PC3	-0.3973	-0.5797	-0.2723	1.9018	1.1658	2.6379	0.0796	0.1178
PC4	-0.2799	-0.4167	-0.1880	1.3398	0.7920	1.8875	0.5330	0.0157
PC5	0.2543	0.1722	0.3756	-1.2174	-1.7046	-0.7303	0.2306	0.0570
PC6	0.2444	0.1657	0.3606	-1.1702	-1.6370	-0.7033	0.2080	0.0626
PC7	-0.1780	-0.2652	-0.1195	0.8523	0.5033	1.2012	0.5709	0.0130
PC8	0.1510	0.1029	0.2217	-0.7229	-1.0076	-0.4383	0.1353	0.0870
PC9	-0.1194	-0.1777	-0.0802	0.5714	0.3378	0.8050	0.5313	0.0159
PC10	0.1121	0.0751	0.1673	-0.5366	-0.7573	-0.3160	0.7387	0.0045
PC11	-0.1025	-0.1530	-0.0687	0.4907	0.2889	0.6925	0.7515	0.0041
PC12	0.0831	0.0563	0.1227	-0.3981	-0.5571	-0.2391	0.2162	0.0605
PC13	-0.0658	-0.0983	-0.0441	0.3150	0.1852	0.4448	0.9576	0.0001

Nycticebus bengalensis

PC	Slope	Slope lower CI	Slope higher CI	Intercept	Intercept lower CI	Intercept higher CI	p value	r squared
PC1	1.3731	0.8937	2.1096	-6.9730	-10.0604	-3.8855	0.1539	0.0990
PC2	1.3306	0.8476	2.0887	-6.7571	-9.9087	-3.6055	0.9513	0.0002
PC3	-0.9979	-1.5562	-0.6398	5.0675	2.7405	7.3944	0.4339	0.0309
PC4	0.9257	0.5905	1.4512	-4.7011	-6.8867	-2.5156	0.7184	0.0066
PC5	0.7668	0.4962	1.1849	-3.8941	-5.6429	-2.1453	0.2238	0.0730
PC6	0.6277	0.3999	0.9853	-3.1878	-4.6742	-1.7014	0.9048	0.0007
PC7	0.5440	0.3492	0.8475	-2.7626	-4.0280	-1.4973	0.3992	0.0358
PC8	-0.4730	-0.7413	-0.3018	2.4020	1.2859	3.5181	0.6983	0.0077
PC9	-0.4321	-0.6486	-0.2879	2.1945	1.2786	3.1104	0.0372	0.1994
PC10	0.3506	0.2234	0.5500	-1.7802	-2.6095	-0.9509	0.8200	0.0026
PC11	0.3055	0.1946	0.4795	-1.5513	-2.2747	-0.8279	0.9215	0.0005
PC12	0.2284	0.1523	0.3424	-1.1597	-1.6425	-0.6769	0.0352	0.2033
PC13	-0.1966	-0.3030	-0.1276	0.9986	0.5532	1.4439	0.1856	0.0859

Nycticebus coucang

PC	Slope	Slope lower CI	Slope higher CI	Intercept	Intercept lower CI	Intercept higher CI	p value	r squared
PC1	0.6883	0.5440	0.8710	-3.4297	-4.2445	-2.6149	0.0623	0.0509
PC2	-0.5625	-0.7162	-0.4418	2.8029	2.1193	3.4864	0.9566	0.0000
PC3	0.5081	0.4001	0.6452	-2.5314	-3.1420	-1.9208	0.2280	0.0216
PC4	0.4778	0.3759	0.6073	-2.3808	-2.9573	-1.8043	0.3327	0.0140
PC5	0.4556	0.3595	0.5774	-2.2701	-2.8131	-1.7271	0.1085	0.0380
PC6	0.4351	0.3421	0.5532	-2.1677	-2.6937	-1.6416	0.4185	0.0098
PC7	0.4332	0.3425	0.5478	-2.1582	-2.6698	-1.6466	0.0522	0.0551
PC8	-0.3621	-0.4597	-0.2851	1.8039	1.3690	2.2389	0.2161	0.0227
PC9	0.3544	0.2802	0.4482	-1.7657	-2.1844	-1.3469	0.0541	0.0542
PC10	-0.3253	-0.4123	-0.2566	1.6206	1.2328	2.0084	0.1127	0.0371
PC11	0.3044	0.2391	0.3876	-1.5169	-1.8868	-1.1470	0.8834	0.0003
PC12	0.2791	0.2192	0.3553	-1.3905	-1.7294	-1.0516	0.7733	0.0012
PC13	0.2605	0.2047	0.3314	-1.2978	-1.6136	-0.9820	0.5889	0.0044

Perodicticus potto

PC	Slope	Slope lower CI	Slope higher CI	Intercept	Intercept lower CI	Intercept higher CI	p value	r squared
PC1	1.0721	0.9030	1.2729	-5.4146	-6.3487	-4.4806	0.0336	0.0351
PC2	-0.7352	-0.8741	-0.6184	3.7129	3.0671	4.3588	0.1212	0.0188
PC3	-0.6558	-0.7807	-0.5508	3.3118	2.7312	3.8924	0.5156	0.0033
PC4	0.5896	0.5003	0.6948	-2.9775	-3.4687	-2.4864	0.0001	0.1176
PC5	0.5463	0.4589	0.6503	-2.7590	-3.2423	-2.2757	0.4297	0.0049
PC6	0.4887	0.4132	0.5779	-2.4679	-2.8839	-2.0519	0.0013	0.0786
PC7	0.4145	0.3483	0.4934	-2.0934	-2.4599	-1.7270	0.3749	0.0062
PC8	-0.3634	-0.4328	-0.3052	1.8353	1.5131	2.1575	0.8389	0.0003
PC9	-0.3473	-0.4133	-0.2918	1.7538	1.4468	2.0608	0.3714	0.0063
PC10	-0.2961	-0.3526	-0.2487	1.4955	1.2331	1.7579	0.6620	0.0015
PC11	-0.2688	-0.3199	-0.2258	1.3573	1.1198	1.5948	0.3340	0.0074
PC12	-0.2523	-0.3002	-0.2120	1.2742	1.0514	1.4969	0.2887	0.0089
PC13	-0.2040	-0.2426	-0.1716	1.0304	0.8508	1.2099	0.1576	0.0157

Goswami model vault module against ln CS of vault

Cheirogaleus major

PC	Slope	Slope lower CI	Slope higher CI	Intercept	Intercept lower CI	Intercept higher CI	p value	r squared
PC1	1.3861	0.9388	2.0466	-4.9045	-6.8645	-2.9445	0.0636	0.1418
PC2	1.0294	0.6810	1.5560	-3.6421	-5.1903	-2.0940	0.4152	0.0291
PC3	-0.8846	-1.3446	-0.5820	3.1299	1.7806	4.4791	0.8614	0.0014
PC4	0.7664	0.5059	1.1608	-2.7116	-3.8702	-1.5529	0.5129	0.0188
PC5	-0.6948	-1.0558	-0.4572	2.4583	1.3991	3.5175	0.8163	0.0024
PC6	0.5069	0.3334	0.7707	-1.7935	-2.5672	-1.0199	0.9757	0.0000
PC7	-0.4585	-0.6396	-0.3287	1.6223	1.0721	2.1724	0.0010	0.3820
PC8	0.4338	0.2870	0.6558	-1.5350	-2.1875	-0.8824	0.4177	0.0288
PC9	0.4035	0.2670	0.6097	-1.4276	-2.0340	-0.8211	0.4071	0.0301
PC10	-0.3685	-0.5520	-0.2460	1.3039	0.7626	1.8452	0.1889	0.0738
PC11	0.3169	0.2085	0.4818	-1.1213	-1.6048	-0.6377	0.9105	0.0006
PC12	0.2944	0.1976	0.4384	-1.0415	-1.4675	-0.6156	0.1215	0.1010
PC13	0.2373	0.1561	0.3608	-0.8397	-1.2017	-0.4776	0.8985	0.0007

Cheirogaleus medius

PC	Slope	Slope lower CI	Slope higher CI	Intercept	Intercept lower CI	Intercept higher CI	p value	r squared
PC1	-0.8229	-1.1802	-0.5737	2.7253	1.7209	3.7298	0.0555	0.1292
PC2	0.6645	0.4561	0.9681	-2.2010	-3.0490	-1.3530	0.2520	0.0483
PC3	0.4852	0.3304	0.7125	-1.6071	-2.2400	-0.9742	0.6952	0.0058
PC4	0.4187	0.2916	0.6011	-1.3867	-1.8994	-0.8739	0.0615	0.1235
PC5	-0.4119	-0.6053	-0.2802	1.3641	0.8255	1.9026	0.8835	0.0008
PC6	-0.3654	-0.5370	-0.2486	1.2102	0.7326	1.6878	0.8325	0.0017
PC7	0.3412	0.2324	0.5010	-1.1301	-1.5750	-0.6851	0.6848	0.0062
PC8	-0.3007	-0.4419	-0.2047	0.9961	0.6030	1.3891	0.8238	0.0019
PC9	-0.2729	-0.4009	-0.1858	0.9038	0.5475	1.2602	0.7665	0.0033
PC10	-0.2332	-0.3377	-0.1610	0.7723	0.4797	1.0650	0.1380	0.0796
PC11	0.1655	0.1130	0.2425	-0.5483	-0.7628	-0.3337	0.4808	0.0186
PC12	0.1551	0.1057	0.2277	-0.5138	-0.7160	-0.3116	0.6605	0.0073
PC13	0.1417	0.0978	0.2053	-0.4693	-0.6473	-0.2912	0.1449	0.0770

Microcebus murinus

PC	Slope	Slope lower CI	Slope higher CI	Intercept	Intercept lower CI	Intercept higher CI	p value	r squared
PC1	-1.2833	-1.6246	-1.0137	3.9929	3.0426	4.9433	0.6350	0.0032
PC2	1.1974	0.9559	1.5000	-3.7257	-4.5722	-2.8792	0.0097	0.0917
PC3	0.8124	0.6484	1.0179	-2.5277	-3.1026	-1.9528	0.0106	0.0898
PC4	-0.7537	-0.9543	-0.5952	2.3451	1.7864	2.9037	0.7534	0.0014
PC5	0.6117	0.4834	0.7741	-1.9034	-2.3556	-1.4512	0.4877	0.0069
PC6	-0.6093	-0.7714	-0.4813	1.8958	1.4445	2.3472	0.6606	0.0028
PC7	-0.5526	-0.6998	-0.4364	1.7194	1.3095	2.1293	0.9882	0.0000
PC8	0.5042	0.3982	0.6385	-1.5688	-1.9428	-1.1948	0.9354	0.0001
PC9	0.4456	0.3551	0.5592	-1.3865	-1.7040	-1.0689	0.0181	0.0772
PC10	0.4127	0.3268	0.5212	-1.2841	-1.5866	-0.9817	0.1949	0.0239
PC11	0.3576	0.2829	0.4521	-1.1126	-1.3759	-0.8493	0.3085	0.0148
PC12	-0.3229	-0.4087	-0.2551	1.0047	0.7657	1.2436	0.5617	0.0048
PC13	-0.2830	-0.3579	-0.2238	0.8805	0.6719	1.0891	0.3484	0.0126

Microcebus rufus

PC	Slope	Slope lower CI	Slope higher CI	Intercept	Intercept lower CI	Intercept higher CI	p value	r squared
PC1	-1.0376	-1.5235	-0.7067	3.2560	1.9743	4.5377	0.6758	0.0066
PC2	0.9128	0.6775	1.2299	-2.8644	-3.7311	-1.9976	0.0002	0.4128
PC3	-0.6649	-0.9767	-0.4526	2.0864	1.2640	2.9087	0.7476	0.0039
PC4	-0.5913	-0.8622	-0.4054	1.8553	1.1385	2.5720	0.2800	0.0431
PC5	0.5642	0.3928	0.8104	-1.7705	-2.4257	-1.1152	0.0637	0.1217
PC6	-0.4724	-0.6910	-0.3229	1.4822	0.9046	2.0598	0.4009	0.0263
PC7	-0.4138	-0.6015	-0.2847	1.2985	0.8013	1.7956	0.1998	0.0601
PC8	0.3846	0.2617	0.5652	-1.2068	-1.6831	-0.7306	0.8446	0.0014
PC9	-0.3562	-0.5184	-0.2448	1.1178	0.6885	1.5471	0.2231	0.0545
PC10	0.2801	0.1906	0.4117	-0.8791	-1.2259	-0.5322	0.8221	0.0019
PC11	0.2382	0.1638	0.3462	-0.7474	-1.0336	-0.4611	0.2022	0.0595
PC12	-0.2245	-0.3300	-0.1528	0.7046	0.4265	0.9827	0.8647	0.0011
PC13	0.2030	0.1400	0.2943	-0.6369	-0.8790	-0.3948	0.1554	0.0733

Galago alleni

PC	Slope	Slope lower CI	Slope higher CI	Intercept	Intercept lower CI	Intercept higher CI	p value	r squared
PC1	-1.6862	-2.5727	-1.1052	5.9694	3.3717	8.5671	0.4075	0.0314
PC2	-1.1932	-1.8313	-0.7774	4.2241	2.3584	6.0898	0.8261	0.0022
PC3	-0.9915	-1.4625	-0.6722	3.5102	2.1114	4.9090	0.0344	0.1878
PC4	-0.9050	-1.3849	-0.5914	3.2040	1.7994	4.6086	0.5431	0.0170
PC5	-0.7023	-1.0718	-0.4602	2.4864	1.4038	3.5689	0.4153	0.0304
PC6	-0.6600	-1.0134	-0.4298	2.3364	1.3034	3.3695	0.9638	0.0001
PC7	-0.6010	-0.9104	-0.3967	2.1276	1.2183	3.0369	0.2266	0.0657
PC8	0.5155	0.3365	0.7898	-1.8251	-2.6274	-1.0227	0.6190	0.0114
PC9	-0.4522	-0.6710	-0.3048	1.6010	0.9529	2.2491	0.0513	0.1618
PC10	-0.4334	-0.6408	-0.2931	1.5342	0.9185	2.1499	0.0410	0.1764
PC11	-0.3538	-0.5416	-0.2311	1.2524	0.7026	1.8021	0.5766	0.0144
PC12	0.3484	0.2276	0.5333	-1.2334	-1.7744	-0.6923	0.5582	0.0158
PC13	0.2459	0.1610	0.3755	-0.8705	-1.2502	-0.4908	0.4436	0.0269

Galago demidoff

PC	Slope	Slope lower CI	Slope higher CI	Intercept	Intercept lower CI	Intercept higher CI	p value	r squared
PC1	-0.8753	-1.1377	-0.6734	2.8830	2.1183	3.6478	0.9585	0.0000
PC2	0.7865	0.6064	1.0200	-2.5904	-3.2716	-1.9093	0.3200	0.0173
PC3	-0.6497	-0.8445	-0.4999	2.1401	1.5724	2.7077	0.9919	0.0000
PC4	-0.6037	-0.7810	-0.4666	1.9883	1.4705	2.5060	0.1482	0.0363
PC5	0.5241	0.4054	0.6777	-1.7264	-2.1749	-1.2778	0.1262	0.0405
PC6	-0.4834	-0.6275	-0.3723	1.5921	1.1717	2.0124	0.4697	0.0092
PC7	-0.4491	-0.5837	-0.3456	1.4792	1.0871	1.8714	0.8002	0.0011
PC8	-0.4116	-0.5256	-0.3224	1.3558	1.0210	1.6906	0.0044	0.1334
PC9	-0.3914	-0.5077	-0.3017	1.2890	0.9497	1.6284	0.3572	0.0149
PC10	-0.3495	-0.4523	-0.2701	1.1512	0.8510	1.4514	0.1645	0.0336
PC11	-0.3135	-0.4068	-0.2416	1.0326	0.7606	1.3047	0.3771	0.0137
PC12	-0.2872	-0.3731	-0.2211	0.9459	0.6955	1.1962	0.6153	0.0045
PC13	-0.2656	-0.3449	-0.2045	0.8747	0.6435	1.1060	0.5261	0.0071

Galago elegantulus

PC	Slope	Slope lower CI	Slope higher CI	Intercept	Intercept lower CI	Intercept higher CI	p value	r squared
PC1	-1.2209	-1.7052	-0.8742	4.3355	2.8600	5.8110	0.0593	0.1068
PC2	-1.0115	-1.4165	-0.7223	3.5920	2.3593	4.8246	0.0814	0.0919
PC3	-0.7266	-1.0338	-0.5107	2.5801	1.6511	3.5091	0.9188	0.0003
PC4	0.6391	0.4494	0.9088	-2.2694	-3.0851	-1.4536	0.7334	0.0037
PC5	0.5672	0.4042	0.7961	-2.0142	-2.7101	-1.3183	0.1063	0.0794
PC6	0.5399	0.3885	0.7504	-1.9172	-2.5598	-1.2745	0.0336	0.1335
PC7	0.4281	0.3010	0.6088	-1.5202	-2.0667	-0.9738	0.7348	0.0036
PC8	-0.4101	-0.5817	-0.2891	1.4562	0.9367	1.9757	0.4427	0.0185
PC9	-0.3456	-0.4882	-0.2447	1.2273	0.7949	1.6597	0.2401	0.0429
PC10	-0.2975	-0.4231	-0.2092	1.0565	0.6766	1.4363	0.7499	0.0032
PC11	-0.2835	-0.3983	-0.2018	1.0068	0.6580	1.3556	0.1183	0.0745
PC12	0.2598	0.1841	0.3667	-0.9226	-1.2468	-0.5984	0.2145	0.0477
PC13	-0.2170	-0.3085	-0.1526	0.7706	0.4938	1.0474	0.6922	0.0050

Galago moholi

PC	Slope	Slope lower CI	Slope higher CI	Intercept	Intercept lower CI	Intercept higher CI	p value	r squared
PC1	1.2106	0.9581	1.5297	-4.1222	-5.0953	-3.1490	0.5579	0.0049
PC2	0.7964	0.6310	1.0051	-2.7116	-3.3486	-2.0746	0.3093	0.0146
PC3	0.7429	0.5885	0.9379	-2.5296	-3.1245	-1.9348	0.3442	0.0126
PC4	0.6909	0.5535	0.8625	-2.3526	-2.8786	-1.8265	0.0047	0.1072
PC5	-0.6556	-0.8252	-0.5208	2.2321	1.7138	2.7505	0.1027	0.0371
PC6	-0.5537	-0.6999	-0.4379	1.8852	1.4391	2.3312	0.9083	0.0002
PC7	0.4908	0.3884	0.6202	-1.6712	-2.0659	-1.2765	0.6041	0.0038
PC8	-0.4560	-0.5757	-0.3612	1.5527	1.1877	1.9178	0.3368	0.0130
PC9	-0.4472	-0.5619	-0.3559	1.5228	1.1720	1.8735	0.0507	0.0527
PC10	0.3841	0.3044	0.4847	-1.3079	-1.6148	-1.0010	0.2740	0.0168
PC11	-0.3510	-0.4437	-0.2777	1.1952	0.9126	1.4778	0.7308	0.0017
PC12	-0.3237	-0.4083	-0.2566	1.1021	0.8438	1.3605	0.2472	0.0188
PC13	0.2786	0.2213	0.3509	-0.9488	-1.1694	-0.7281	0.1164	0.0344

Galago senegalensis

PC	Slope	Slope lower CI	Slope higher CI	Intercept	Intercept lower CI	Intercept higher CI	p value	r squared
PC1	0.7545	0.6518	0.8734	-2.6219	-3.0071	-2.2367	0.0067	0.0418
PC2	-0.5525	-0.6402	-0.4767	1.9198	1.6357	2.2039	0.0278	0.0277
PC3	0.4636	0.4001	0.5372	-1.6111	-1.8492	-1.3730	0.0210	0.0304
PC4	-0.4119	-0.4770	-0.3557	1.4313	1.2204	1.6421	0.0113	0.0365
PC5	-0.3923	-0.4556	-0.3379	1.3634	1.1588	1.5680	0.8735	0.0001
PC6	0.3842	0.3311	0.4458	-1.3350	-1.5343	-1.1356	0.1863	0.0101
PC7	-0.3640	-0.4216	-0.3143	1.2649	1.0784	1.4513	0.0131	0.0350
PC8	-0.3251	-0.3765	-0.2807	1.1297	0.9631	1.2963	0.0139	0.0345
PC9	-0.3124	-0.3626	-0.2692	1.0857	0.9233	1.2481	0.2904	0.0065
PC10	0.2736	0.2366	0.3163	-0.9506	-1.0891	-0.8122	0.0013	0.0585
PC11	-0.2421	-0.2810	-0.2086	0.8414	0.7157	0.9670	0.1990	0.0095
PC12	-0.2370	-0.2752	-0.2041	0.8237	0.7001	0.9472	0.6838	0.0010
PC13	-0.2174	-0.2525	-0.1872	0.7555	0.6422	0.8689	0.8482	0.0002

Galago zanzibaricus

PC	Slope	Slope lower CI	Slope higher CI	Intercept	Intercept lower CI	Intercept higher CI	p value	r squared
PC1	-1.2073	-1.8352	-0.7942	4.1213	2.3444	5.8981	0.8744	0.0011
PC2	0.8913	0.6069	1.3090	-3.0426	-4.2409	-1.8442	0.0430	0.1663
PC3	0.7338	0.4842	1.1120	-2.5049	-3.5766	-1.4333	0.5414	0.0164
PC4	0.6536	0.4409	0.9692	-2.2313	-3.1331	-1.3296	0.0866	0.1223
PC5	-0.6170	-0.9178	-0.4148	2.1062	1.2476	2.9649	0.1106	0.1069
PC6	0.5493	0.3676	0.8210	-1.8752	-2.6493	-1.1012	0.1587	0.0845
PC7	-0.4298	-0.6533	-0.2828	1.4673	0.8349	2.0997	0.8400	0.0018
PC8	0.3547	0.2348	0.5357	-1.2108	-1.7243	-0.6973	0.3819	0.0334
PC9	-0.3246	-0.4889	-0.2154	1.1079	0.6411	1.5748	0.3043	0.0458
PC10	0.2897	0.1924	0.4364	-0.9891	-1.4056	-0.5726	0.2982	0.0469
PC11	-0.2477	-0.3709	-0.1655	0.8457	0.4951	1.1962	0.1802	0.0767
PC12	-0.2304	-0.3495	-0.1519	0.7865	0.4492	1.1239	0.6136	0.0113
PC13	-0.1984	-0.3014	-0.1306	0.6773	0.3857	0.9688	0.7570	0.0042

Otolemur crassicaudatus

PC	Slope	Slope lower CI	Slope higher CI	Intercept	Intercept lower CI	Intercept higher CI	p value	r squared
PC1	1.1791	0.9919	1.4018	-4.5087	-5.2924	-3.7250	0.0000	0.2404
PC2	0.9179	0.7545	1.1168	-3.5099	-4.2027	-2.8172	0.1510	0.0207
PC3	-0.5090	-0.6103	-0.4245	1.9462	1.5909	2.3014	0.0000	0.1624
PC4	-0.4768	-0.5804	-0.3917	1.8232	1.4623	2.1841	0.2263	0.0147
PC5	0.4115	0.3378	0.5012	-1.5734	-1.8858	-1.2611	0.3417	0.0091
PC6	-0.3756	-0.4578	-0.3082	1.4362	1.1500	1.7224	0.6618	0.0019
PC7	0.3532	0.2905	0.4294	-1.3505	-1.6162	-1.0848	0.0997	0.0271
PC8	-0.3371	-0.4108	-0.2765	1.2888	1.0320	1.5456	0.6699	0.0018
PC9	-0.3140	-0.3820	-0.2582	1.2008	0.9642	1.4375	0.1245	0.0237
PC10	0.2524	0.2072	0.3076	-0.9652	-1.1573	-0.7732	0.4951	0.0047
PC11	0.2366	0.1941	0.2884	-0.9046	-1.0849	-0.7242	0.8013	0.0006
PC12	-0.2136	-0.2604	-0.1752	0.8168	0.6539	0.9797	0.9721	0.0000
PC13	-0.1986	-0.2415	-0.1634	0.7595	0.6100	0.9091	0.1078	0.0259

Otolemur garnettii

PC	Slope	Slope lower CI	Slope higher CI	Intercept	Intercept lower CI	Intercept higher CI	p value	r squared
PC1	0.9875	0.8136	1.1986	-3.7433	-4.4731	-3.0136	0.0014	0.1040
PC2	0.5129	0.4198	0.6266	-1.9442	-2.3361	-1.5523	0.0466	0.0419
PC3	-0.3984	-0.4765	-0.3330	1.5100	1.2379	1.7820	0.0000	0.2346
PC4	0.3544	0.2894	0.4341	-1.3435	-1.6179	-1.0692	0.2062	0.0171
PC5	-0.3202	-0.3927	-0.2611	1.2138	0.9643	1.4633	0.5388	0.0041
PC6	0.2972	0.2427	0.3639	-1.1265	-1.3562	-0.8967	0.1785	0.0194
PC7	-0.2591	-0.3169	-0.2119	0.9822	0.7830	1.1813	0.0899	0.0306
PC8	0.2364	0.1927	0.2900	-0.8961	-1.0806	-0.7117	0.7293	0.0013
PC9	-0.2202	-0.2687	-0.1804	0.8345	0.6670	1.0020	0.0290	0.0503
PC10	-0.1964	-0.2404	-0.1604	0.7445	0.5928	0.8961	0.1509	0.0221
PC11	-0.1809	-0.2219	-0.1475	0.6856	0.5446	0.8266	0.5951	0.0030
PC12	-0.1646	-0.2017	-0.1343	0.6238	0.4961	0.7515	0.2964	0.0117
PC13	-0.1356	-0.1655	-0.1112	0.5142	0.4112	0.6171	0.0219	0.0552

Avahi laniger

PC	Slope	Slope lower CI	Slope higher CI	Intercept	Intercept lower CI	Intercept higher CI	p value	r squared
PC1	0.9437	0.6585	1.3526	-3.5058	-4.7952	-2.2164	0.0033	0.3433
PC2	0.7391	0.4794	1.1394	-2.7457	-3.9717	-1.5196	0.4140	0.0320
PC3	0.6279	0.4060	0.9710	-2.3325	-3.3821	-1.2830	0.5520	0.0171
PC4	-0.5506	-0.8387	-0.3614	2.0454	1.1587	2.9320	0.1699	0.0877
PC5	0.5005	0.3225	0.7767	-1.8593	-2.7030	-1.0157	0.9145	0.0006
PC6	-0.4527	-0.7026	-0.2917	1.6817	0.9184	2.4450	0.9915	0.0000
PC7	-0.3325	-0.5075	-0.2179	1.2353	0.6973	1.7733	0.1933	0.0792
PC8	-0.2969	-0.4590	-0.1921	1.1031	0.6074	1.5988	0.5214	0.0199
PC9	0.2803	0.1808	0.4346	-1.0412	-1.5128	-0.5696	0.7712	0.0041
PC10	-0.2428	-0.3765	-0.1566	0.9021	0.4937	1.3105	0.7446	0.0052
PC11	-0.2057	-0.3191	-0.1326	0.7643	0.4178	1.1107	0.8190	0.0025
PC12	-0.2033	-0.3128	-0.1321	0.7552	0.4196	1.0909	0.3546	0.0409
PC13	-0.1801	-0.2796	-0.1161	0.6692	0.3655	0.9729	0.9449	0.0002

Indri indri

PC	Slope	Slope lower CI	Slope higher CI	Intercept	Intercept lower CI	Intercept higher CI	p value	r squared
PC1	-1.3376	-1.7812	-1.0044	5.6061	3.9781	7.2342	0.0015	0.2400
PC2	1.0642	0.7673	1.4761	-4.4605	-5.9459	-2.9750	0.8800	0.0006
PC3	-0.8454	-1.1727	-0.6095	3.5434	2.3631	4.7236	0.9430	0.0001
PC4	-0.7454	-1.0193	-0.5451	3.1241	2.1302	4.1180	0.0668	0.0879
PC5	0.6555	0.4726	0.9092	-2.7474	-3.6625	-1.8323	0.9180	0.0003
PC6	0.5650	0.4079	0.7827	-2.3682	-3.1536	-1.5829	0.5658	0.0090
PC7	-0.4910	-0.6810	-0.3541	2.0581	1.3729	2.7433	0.8424	0.0011
PC8	-0.4076	-0.5534	-0.3002	1.7083	1.1778	2.2389	0.0236	0.1309
PC9	-0.3509	-0.4863	-0.2532	1.4708	0.9821	1.9594	0.6578	0.0054
PC10	-0.3375	-0.4625	-0.2463	1.4145	0.9614	1.8677	0.0912	0.0752
PC11	-0.3194	-0.4430	-0.2303	1.3388	0.8932	1.7844	0.8065	0.0016
PC12	-0.2899	-0.4022	-0.2090	1.2152	0.8104	1.6200	0.9775	0.0000
PC13	-0.2734	-0.3773	-0.1981	1.1458	0.7702	1.5214	0.2774	0.0318

Propithecus diadema

PC	Slope	Slope lower CI	Slope higher CI	Intercept	Intercept lower CI	Intercept higher CI	p value	r squared
PC1	-1.1907	-1.6259	-0.8720	4.9612	3.3906	6.5319	0.0004	0.3833
PC2	-0.8679	-1.2672	-0.5945	3.6164	2.2148	5.0181	0.1562	0.0758
PC3	0.5996	0.4090	0.8789	-2.4982	-3.4773	-1.5190	0.2300	0.0549
PC4	-0.5502	-0.7978	-0.3794	2.2923	1.4206	3.1640	0.0842	0.1103
PC5	0.4775	0.3236	0.7044	-1.9894	-2.7827	-1.1961	0.4535	0.0218
PC6	0.4419	0.2983	0.6546	-1.8412	-2.5835	-1.0989	0.9610	0.0001
PC7	0.3872	0.2615	0.5735	-1.6134	-2.2635	-0.9633	0.8602	0.0012
PC8	-0.2807	-0.4158	-0.1895	1.1696	0.6981	1.6411	0.9296	0.0003
PC9	0.2670	0.1811	0.3937	-1.1126	-1.5557	-0.6695	0.4282	0.0243
PC10	-0.2219	-0.3245	-0.1518	0.9246	0.5648	1.2845	0.1798	0.0681
PC11	0.2104	0.1426	0.3104	-0.8766	-1.2262	-0.5270	0.4568	0.0215
PC12	0.1914	0.1295	0.2828	-0.7974	-1.1167	-0.4782	0.5491	0.0140
PC13	-0.1551	-0.2282	-0.1054	0.6461	0.3901	0.9020	0.3434	0.0346

Propithecus verreauxi

PC	Slope	Slope lower CI	Slope higher CI	Intercept	Intercept lower CI	Intercept higher CI	p value	r squared
PC1	1.6318	1.2122	2.1968	-6.6405	-8.6439	-4.6371	0.0577	0.0851
PC2	1.3609	0.9979	1.8560	-5.5380	-7.2840	-3.7921	0.8419	0.0010
PC3	-1.1388	-1.5512	-0.8360	4.6341	3.1788	6.0894	0.5522	0.0087
PC4	0.9397	0.6908	1.2783	-3.8238	-5.0192	-2.6284	0.3959	0.0176
PC5	0.8132	0.5992	1.1037	-3.3092	-4.3358	-2.2826	0.2463	0.0326
PC6	-0.7064	-0.9505	-0.5250	2.8745	2.0088	3.7403	0.0531	0.0882
PC7	-0.5703	-0.7775	-0.4183	2.3208	1.5899	3.0516	0.7187	0.0032
PC8	0.5173	0.3811	0.7022	-2.1052	-2.7584	-1.4520	0.2492	0.0322
PC9	0.4589	0.3366	0.6257	-1.8674	-2.4557	-1.2791	0.7529	0.0024
PC10	-0.4224	-0.5747	-0.3104	1.7187	1.1810	2.2564	0.4168	0.0161
PC11	0.3549	0.2602	0.4841	-1.4443	-1.8999	-0.9888	0.9735	0.0000
PC12	-0.3009	-0.4103	-0.2207	1.2245	0.8386	1.6104	0.7917	0.0017
PC13	-0.2717	-0.3661	-0.2016	1.1055	0.7707	1.4402	0.0690	0.0784

Eulemur fulvus

PC	Slope	Slope lower CI	Slope higher CI	Intercept	Intercept lower CI	Intercept higher CI	p value	r squared
PC1	-1.3227	-1.5327	-1.1415	5.3357	4.5466	6.1249	0.0247	0.0288
PC2	-0.9503	-1.1028	-0.8188	3.8333	3.2605	4.4061	0.2187	0.0087
PC3	-0.7486	-0.8668	-0.6465	3.0198	2.5755	3.4641	0.0090	0.0388
PC4	-0.7268	-0.8387	-0.6298	2.9318	2.5106	3.3530	0.0001	0.0835
PC5	-0.5656	-0.6563	-0.4875	2.2817	1.9412	2.6221	0.1617	0.0113
PC6	-0.5189	-0.6017	-0.4475	2.0934	1.7823	2.4044	0.0644	0.0196
PC7	0.4819	0.4151	0.5594	-1.9440	-2.2351	-1.6530	0.3579	0.0049
PC8	0.4724	0.4068	0.5485	-1.9055	-2.1913	-1.6196	0.6933	0.0009
PC9	-0.4221	-0.4901	-0.3635	1.7026	1.4472	1.9581	0.8148	0.0003
PC10	0.3887	0.3355	0.4503	-1.5679	-1.7994	-1.3365	0.0170	0.0325
PC11	-0.3586	-0.4163	-0.3089	1.4465	1.2298	1.6632	0.4270	0.0037
PC12	0.3374	0.2907	0.3917	-1.3612	-1.5648	-1.1576	0.2842	0.0066
PC13	0.2414	0.2079	0.2802	-0.9736	-1.1196	-0.8276	0.5834	0.0017

Eulemur macaco

PC	Slope	Slope lower CI	Slope higher CI	Intercept	Intercept lower CI	Intercept higher CI	p value	r squared
PC1	-1.5750	-2.0579	-1.2053	6.3647	4.6418	8.0876	0.1727	0.0348
PC2	1.0412	0.7952	1.3632	-4.2076	-5.3553	-3.0600	0.3025	0.0200
PC3	-0.9128	-1.1698	-0.7123	3.6888	2.7643	4.6133	0.0016	0.1726
PC4	-0.7818	-1.0183	-0.6002	3.1593	2.3143	4.0043	0.0772	0.0577
PC5	-0.7044	-0.9247	-0.5366	2.8465	2.0622	3.6308	0.9628	0.0000
PC6	-0.6098	-0.7998	-0.4650	2.4644	1.7878	3.1410	0.5381	0.0072
PC7	0.5504	0.4194	0.7223	-2.2244	-2.8364	-1.6123	0.7040	0.0027
PC8	0.4434	0.3399	0.5785	-1.7921	-2.2742	-1.3099	0.1140	0.0465
PC9	0.4133	0.3163	0.5402	-1.6704	-2.1230	-1.2178	0.1853	0.0329
PC10	-0.3772	-0.4949	-0.2875	1.5244	1.1052	1.9436	0.6467	0.0040
PC11	0.2924	0.2228	0.3839	-1.1818	-1.5073	-0.8563	0.8390	0.0008
PC12	-0.2687	-0.3519	-0.2052	1.0858	0.7893	1.3823	0.3319	0.0178
PC13	-0.2352	-0.3086	-0.1793	0.9505	0.6892	1.2118	0.6285	0.0044

Eulemur mongoz

PC	Slope	Slope lower CI	Slope higher CI	Intercept	Intercept lower CI	Intercept higher CI	p value	r squared
PC1	-0.8747	-1.1235	-0.6809	3.4935	2.6095	4.3776	0.0074	0.1232
PC2	0.7057	0.5441	0.9152	-2.8185	-3.5598	-2.0773	0.0848	0.0530
PC3	0.6411	0.4917	0.8359	-2.5607	-3.2483	-1.8731	0.3997	0.0129
PC4	-0.5639	-0.7252	-0.4384	2.2523	1.6795	2.8252	0.0101	0.1143
PC5	-0.4372	-0.5699	-0.3354	1.7462	1.2778	2.2146	0.3637	0.0150
PC6	-0.4036	-0.5254	-0.3100	1.6119	1.1818	2.0421	0.2398	0.0250
PC7	-0.3942	-0.5138	-0.3024	1.5745	1.1523	1.9967	0.3540	0.0156
PC8	0.3610	0.2767	0.4710	-1.4419	-1.8299	-1.0540	0.4830	0.0090
PC9	-0.3231	-0.4189	-0.2493	1.2907	0.9520	1.6294	0.0732	0.0572
PC10	-0.2850	-0.3713	-0.2188	1.1384	0.8339	1.4429	0.2903	0.0203
PC11	0.2749	0.2105	0.3590	-1.0982	-1.3948	-0.8015	0.8011	0.0012
PC12	-0.2182	-0.2797	-0.1703	0.8716	0.6530	1.0901	0.0042	0.1393
PC13	0.1814	0.1389	0.2368	-0.7244	-0.9200	-0.5288	0.7595	0.0017

Eulemur rubriventer

PC	Slope	Slope lower CI	Slope higher CI	Intercept	Intercept lower CI	Intercept higher CI	p value	r squared
PC1	-1.5575	-2.3165	-1.0472	6.2859	3.7243	8.8475	0.4676	0.0213
PC2	1.2021	0.8067	1.7913	-4.8517	-6.8387	-2.8647	0.5937	0.0115
PC3	-1.0232	-1.4949	-0.7003	4.1296	2.5260	5.7332	0.0889	0.1114
PC4	-0.9572	-1.3956	-0.6565	3.8633	2.3718	5.3548	0.0746	0.1216
PC5	-0.7497	-1.1193	-0.5022	3.0257	1.7803	4.2711	0.8424	0.0016
PC6	0.5577	0.3736	0.8326	-2.2509	-3.1773	-1.3244	0.8387	0.0017
PC7	0.5349	0.3584	0.7984	-2.1590	-3.0470	-1.2711	0.7793	0.0032
PC8	0.4609	0.3111	0.6829	-1.8603	-2.6105	-1.1102	0.3068	0.0417
PC9	-0.4109	-0.6031	-0.2800	1.6584	1.0064	2.3104	0.1306	0.0890
PC10	0.3690	0.2496	0.5456	-1.4893	-2.0867	-0.8919	0.2537	0.0518
PC11	0.2820	0.1890	0.4208	-1.1383	-1.6059	-0.6706	0.7159	0.0054
PC12	-0.2085	-0.3112	-0.1397	0.8416	0.4955	1.1876	0.7665	0.0036
PC13	-0.1617	-0.2397	-0.1091	0.6526	0.3890	0.9161	0.3261	0.0386

Hapalemur griseus

PC	Slope	Slope lower CI	Slope higher CI	Intercept	Intercept lower CI	Intercept higher CI	p value	r squared
PC1	-1.5620	-2.3243	-1.0497	6.0475	3.5799	8.5150	0.4949	0.0188
PC2	0.8440	0.5733	1.2425	-3.2678	-4.5633	-1.9722	0.1708	0.0737
PC3	-0.8302	-1.2200	-0.5650	3.2145	1.9464	4.4825	0.1452	0.0829
PC4	-0.6477	-0.9588	-0.4375	2.5076	1.4985	3.5168	0.2849	0.0456
PC5	0.5850	0.3932	0.8705	-2.2650	-3.1892	-1.3408	0.4948	0.0188
PC6	-0.5569	-0.8193	-0.3785	2.1560	1.3027	3.0093	0.1615	0.0769
PC7	0.5167	0.3566	0.7486	-2.0004	-2.7593	-1.2414	0.0446	0.1517
PC8	0.4390	0.3018	0.6388	-1.6998	-2.3522	-1.0474	0.0627	0.1318
PC9	-0.3962	-0.5903	-0.2659	1.5340	0.9060	2.1619	0.5787	0.0125
PC10	0.3437	0.2345	0.5038	-1.3308	-1.8520	-0.8095	0.1160	0.0959
PC11	0.2750	0.1847	0.4095	-1.0647	-1.5000	-0.6294	0.5427	0.0150
PC12	0.2293	0.1535	0.3424	-0.8877	-1.2532	-0.5222	0.8923	0.0007
PC13	0.2097	0.1413	0.3111	-0.8117	-1.1404	-0.4830	0.3593	0.0337

Lemur catta

PC	Slope	Slope lower CI	Slope higher CI	Intercept	Intercept lower CI	Intercept higher CI	p value	r squared
PC1	1.4607	1.0266	2.0785	-5.8435	-7.9477	-3.7394	0.9428	0.0002
PC2	1.0223	0.7280	1.4356	-4.0898	-5.5053	-2.6743	0.1140	0.0762
PC3	0.9151	0.6761	1.2388	-3.6610	-4.7866	-2.5353	0.0016	0.2710
PC4	-0.6784	-0.9642	-0.4773	2.7139	1.7398	3.6879	0.6479	0.0066
PC5	0.6120	0.4321	0.8669	-2.4484	-3.3181	-1.5787	0.3522	0.0271
PC6	-0.5399	-0.7680	-0.3795	2.1599	1.3827	2.9370	0.8180	0.0017
PC7	0.4411	0.3122	0.6234	-1.7647	-2.3872	-1.1421	0.2551	0.0403
PC8	-0.3629	-0.5163	-0.2550	1.4517	0.9290	1.9744	0.9323	0.0002
PC9	0.3259	0.2296	0.4627	-1.3038	-1.7702	-0.8374	0.5155	0.0133
PC10	-0.3166	-0.4431	-0.2262	1.2664	0.8325	1.7003	0.0765	0.0948
PC11	0.2521	0.1779	0.3571	-1.0083	-1.3669	-0.6498	0.3701	0.0252
PC12	-0.2201	-0.3075	-0.1576	0.8806	0.5806	1.1805	0.0612	0.1053
PC13	0.1857	0.1311	0.2628	-0.7427	-1.0061	-0.4792	0.3294	0.0297

Varecia variegata

PC	Slope	Slope lower CI	Slope higher CI	Intercept	Intercept lower CI	Intercept higher CI	p value	r squared
PC1	-1.7147	-2.3136	-1.2709	7.0392	4.8988	9.1795	0.0098	0.1668
PC2	-1.0722	-1.4537	-0.7909	4.4016	3.0411	5.7621	0.0194	0.1391
PC3	-0.9033	-1.2199	-0.6689	3.7083	2.5772	4.8395	0.0112	0.1616
PC4	-0.7666	-1.0618	-0.5534	3.1470	2.1034	4.1906	0.5643	0.0091
PC5	-0.6948	-0.9615	-0.5020	2.8521	1.9088	3.7953	0.4680	0.0143
PC6	-0.5550	-0.7675	-0.4013	2.2783	1.5267	3.0298	0.3989	0.0193
PC7	-0.5003	-0.6932	-0.3610	2.0537	1.3717	2.7357	0.6322	0.0063
PC8	0.4367	0.3149	0.6055	-1.7928	-2.3893	-1.1963	0.7672	0.0024
PC9	-0.4093	-0.5632	-0.2976	1.6804	1.1352	2.2256	0.1650	0.0514
PC10	0.3333	0.2409	0.4612	-1.3682	-1.8205	-0.9159	0.4531	0.0153
PC11	0.3125	0.2258	0.4323	-1.2827	-1.7064	-0.8589	0.4344	0.0166
PC12	0.2909	0.2098	0.4035	-1.1944	-1.5920	-0.7968	0.8262	0.0013
PC13	0.2574	0.1859	0.3564	-1.0568	-1.4068	-0.7067	0.5219	0.0112

Lepilemur ruficaudatus

PC	Slope	Slope lower CI	Slope higher CI	Intercept	Intercept lower CI	Intercept higher CI	p value	r squared
PC1	1.5207	1.0132	2.2824	-5.5670	-7.8903	-3.2438	0.2222	0.0641
PC2	1.1989	0.8145	1.7646	-4.3889	-6.1281	-2.6497	0.0506	0.1561
PC3	0.9015	0.5939	1.3684	-3.3002	-4.7181	-1.8823	0.6700	0.0080
PC4	-0.8300	-1.2610	-0.5463	3.0384	1.7300	4.3469	0.7804	0.0034
PC5	-0.7489	-1.1342	-0.4945	2.7418	1.5708	3.9128	0.5032	0.0197
PC6	-0.6551	-0.9943	-0.4317	2.3984	1.3686	3.4283	0.6488	0.0092
PC7	0.6214	0.4116	0.9381	-2.2749	-3.2387	-1.3110	0.3689	0.0352
PC8	-0.5322	-0.8028	-0.3528	1.9484	1.1246	2.7721	0.3416	0.0394
PC9	0.3860	0.2582	0.5768	-1.4130	-1.9962	-0.8298	0.1587	0.0845
PC10	0.3547	0.2336	0.5386	-1.2986	-1.8569	-0.7404	0.6937	0.0069
PC11	0.2980	0.1969	0.4512	-1.0911	-1.5567	-0.6255	0.4861	0.0213
PC12	-0.2723	-0.4120	-0.1800	0.9969	0.5722	1.4216	0.4527	0.0247
PC13	0.2241	0.1524	0.3295	-0.8204	-1.1446	-0.4962	0.0470	0.1608

Loris tardigradus

PC	Slope	Slope lower CI	Slope higher CI	Intercept	Intercept lower CI	Intercept higher CI	p value	r squared
PC1	-0.7827	-1.1548	-0.5304	2.7846	1.6735	3.8957	0.2098	0.0622
PC2	-0.7479	-1.0739	-0.5208	2.6609	1.6766	3.6451	0.0215	0.1940
PC3	-0.6393	-0.9251	-0.4418	2.2747	1.4147	3.1346	0.0400	0.1581
PC4	-0.4504	-0.6673	-0.3040	1.6024	0.9558	2.2490	0.3114	0.0410
PC5	0.4093	0.2761	0.6066	-1.4561	-2.0442	-0.8680	0.3223	0.0392
PC6	0.3934	0.2657	0.5824	-1.3996	-1.9630	-0.8361	0.2858	0.0454
PC7	-0.2865	-0.4261	-0.1927	1.0193	0.6040	1.4347	0.4610	0.0219
PC8	0.2430	0.1673	0.3530	-0.8647	-1.1952	-0.5341	0.0552	0.1392
PC9	-0.1921	-0.2852	-0.1294	0.6834	0.4061	0.9608	0.3893	0.0298
PC10	0.1804	0.1210	0.2689	-0.6418	-0.9049	-0.3787	0.6123	0.0104
PC11	-0.1650	-0.2463	-0.1105	0.5869	0.3451	0.8287	0.9042	0.0006
PC12	0.1338	0.0920	0.1946	-0.4761	-0.6587	-0.2935	0.0611	0.1333
PC13	-0.1059	-0.1581	-0.0709	0.3767	0.2215	0.5319	0.9736	0.0000

Nycticebus bengalensis

PC	Slope	Slope lower CI	Slope higher CI	Intercept	Intercept lower CI	Intercept higher CI	p value	r squared
PC1	-1.3596	-2.1121	-0.8752	5.1549	2.8099	7.4998	0.3224	0.0490
PC2	-1.3175	-1.9947	-0.8702	4.9953	2.8632	7.1273	0.0626	0.1628
PC3	-0.9880	-1.5132	-0.6452	3.7462	2.1006	5.3919	0.1258	0.1132
PC4	-0.9166	-1.4382	-0.5842	3.4754	1.8562	5.0946	0.8271	0.0024
PC5	0.7593	0.4978	1.1581	-2.8788	-4.1307	-1.6269	0.0981	0.1309
PC6	-0.6215	-0.9738	-0.3967	2.3566	1.2624	3.4508	0.6705	0.0092
PC7	0.5387	0.3490	0.8313	-2.0423	-2.9567	-1.1279	0.2060	0.0787
PC8	-0.4683	-0.7342	-0.2987	1.7757	0.9500	2.6014	0.7248	0.0063
PC9	-0.4279	-0.6674	-0.2743	1.6223	0.8771	2.3676	0.4386	0.0303
PC10	0.3471	0.2211	0.5449	-1.3161	-1.9300	-0.7022	0.9805	0.0000
PC11	0.3025	0.1934	0.4731	-1.1468	-1.6772	-0.6164	0.5621	0.0171
PC12	0.2261	0.1528	0.3347	-0.8573	-1.2022	-0.5124	0.0162	0.2562
PC13	-0.1947	-0.3027	-0.1252	0.7382	0.4018	1.0747	0.3411	0.0454

Nycticebus coucang

PC	Slope	Slope lower CI	Slope higher CI	Intercept	Intercept lower CI	Intercept higher CI	p value	r squared
PC1	0.7311	0.5763	0.9276	-2.7231	-3.3775	-2.0687	0.1613	0.0291
PC2	0.5975	0.4693	0.7607	-2.2254	-2.7680	-1.6828	0.8488	0.0005
PC3	0.5396	0.4249	0.6854	-2.0099	-2.4950	-1.5247	0.2417	0.0204
PC4	0.5075	0.3994	0.6450	-1.8903	-2.3478	-1.4329	0.3082	0.0155
PC5	0.4839	0.3838	0.6101	-1.8024	-2.2239	-1.3809	0.0180	0.0807
PC6	0.4621	0.3633	0.5878	-1.7211	-2.1393	-1.3029	0.4837	0.0073
PC7	0.4601	0.3644	0.5809	-1.7136	-2.1170	-1.3102	0.0301	0.0683
PC8	-0.3846	-0.4891	-0.3023	1.4323	1.0844	1.7802	0.4659	0.0080
PC9	0.3764	0.2975	0.4763	-1.4019	-1.7350	-1.0688	0.0622	0.0510
PC10	-0.3455	-0.4391	-0.2718	1.2867	0.9752	1.5983	0.3275	0.0143
PC11	-0.3234	-0.4114	-0.2542	1.2044	0.9114	1.4973	0.5504	0.0053
PC12	-0.2964	-0.3771	-0.2330	1.1040	0.8356	1.3725	0.5214	0.0062
PC13	-0.2767	-0.3521	-0.2174	1.0304	0.7794	1.2814	0.6677	0.0028

Perodicticus potto

PC	Slope	Slope lower CI	Slope higher CI	Intercept	Intercept lower CI	Intercept higher CI	p value	r squared
PC1	1.1867	1.0080	1.3971	-4.4927	-5.2292	-3.7561	0.0000	0.1284
PC2	-0.8138	-0.9689	-0.6835	3.0807	2.5403	3.6211	0.5937	0.0022
PC3	0.7258	0.6103	0.8632	-2.7478	-3.2265	-2.2692	0.1539	0.0159
PC4	0.6526	0.5536	0.7693	-2.4705	-2.8790	-2.0621	0.0001	0.1138
PC5	-0.6047	-0.7193	-0.5083	2.2892	1.8897	2.6887	0.2066	0.0125
PC6	0.5409	0.4542	0.6441	-2.0477	-2.4071	-1.6882	0.7189	0.0010
PC7	0.4588	0.3861	0.5452	-1.7370	-2.0382	-1.4358	0.0728	0.0251
PC8	-0.4022	-0.4790	-0.3378	1.5228	1.2554	1.7902	0.9800	0.0000
PC9	0.3844	0.3228	0.4577	-1.4552	-1.7105	-1.1999	0.6396	0.0017
PC10	-0.3278	-0.3886	-0.2764	1.2408	1.0284	1.4533	0.0112	0.0496
PC11	-0.2975	-0.3543	-0.2498	1.1262	0.9284	1.3240	0.9467	0.0000
PC12	0.2793	0.2345	0.3325	-1.0572	-1.2426	-0.8717	0.5942	0.0022
PC13	-0.2258	-0.2674	-0.1907	0.8549	0.7097	1.0001	0.0036	0.0649

Goswami model base module against ln CS whole cranium

Cheirogaleus major

PC	Slope	Slope lower CI	Slope higher CI	Intercept	Intercept lower CI	Intercept higher CI	p value	r squared
PC1	1.0054	0.6629	1.5248	-4.8854	-6.9797	-2.7911	0.5950	0.0125
PC2	0.9166	0.6121	1.3724	-4.4539	-6.3013	-2.6064	0.1841	0.0754
PC3	0.7493	0.4929	1.1392	-3.6412	-5.2118	-2.0705	0.9581	0.0001
PC4	0.6927	0.4673	1.0268	-3.3660	-4.7253	-2.0066	0.0849	0.1235
PC5	0.6299	0.4186	0.9478	-3.0608	-4.3467	-1.7749	0.2755	0.0515
PC6	0.5847	0.4025	0.8493	-2.8412	-3.9268	-1.7556	0.0194	0.2154
PC7	-0.5540	-0.8422	-0.3644	2.6920	1.5309	3.8531	0.9400	0.0003
PC8	-0.4866	-0.7313	-0.3238	2.3645	1.3742	3.3548	0.2487	0.0574
PC9	-0.4649	-0.6933	-0.3118	2.2593	1.3322	3.1863	0.1336	0.0951
PC10	-0.3990	-0.6022	-0.2643	1.9387	1.1176	2.7597	0.3631	0.0361
PC11	-0.3715	-0.5645	-0.2445	1.8052	1.0276	2.5828	0.7967	0.0029
PC12	-0.3341	-0.5065	-0.2203	1.6233	0.9278	2.3188	0.5791	0.0136
PC13	-0.3198	-0.4808	-0.2127	1.5541	0.9027	2.2056	0.2560	0.0557

Cheirogaleus medius

PC	Slope	Slope lower CI	Slope higher CI	Intercept	Intercept lower CI	Intercept higher CI	p value	r squared
PC1	-0.9074	-1.2644	-0.6512	4.1650	2.7575	5.5725	0.0041	0.2677
PC2	-0.7238	-1.0578	-0.4953	3.3225	2.0313	4.6136	0.3559	0.0316
PC3	0.6445	0.4473	0.9288	-2.9585	-4.0635	-1.8534	0.0857	0.1054
PC4	-0.5703	-0.8374	-0.3884	2.6178	1.5874	3.6483	0.6767	0.0065
PC5	0.5251	0.3576	0.7713	-2.4104	-3.3600	-1.4609	0.7170	0.0049
PC6	-0.4672	-0.6865	-0.3180	2.1446	1.2986	2.9905	0.8052	0.0023
PC7	0.4364	0.2973	0.6408	-2.0032	-2.7917	-1.2148	0.6729	0.0067
PC8	0.4052	0.2765	0.5940	-1.8601	-2.5889	-1.1312	0.5207	0.0154
PC9	0.3742	0.2568	0.5452	-1.7175	-2.3793	-1.0557	0.2537	0.0480
PC10	0.3694	0.2524	0.5405	-1.6955	-2.3566	-1.0344	0.4122	0.0250
PC11	-0.3276	-0.4733	-0.2267	1.5037	0.9377	2.0697	0.1107	0.0915
PC12	-0.2946	-0.4301	-0.2018	1.3522	0.8283	1.8762	0.3150	0.0374
PC13	0.2631	0.1799	0.3847	-1.2075	-1.6775	-0.7374	0.3823	0.0284

Microcebus murinus

PC	Slope	Slope lower CI	Slope higher CI	Intercept	Intercept lower CI	Intercept higher CI	p value	r squared
PC1	-1.1513	-1.4572	-0.9097	4.9914	3.8046	6.1781	0.5427	0.0053
PC2	-1.0067	-1.2442	-0.8145	4.3643	3.4330	5.2956	0.0001	0.1987
PC3	0.7945	0.6402	0.9860	-3.4443	-4.1939	-2.6948	0.0004	0.1668
PC4	-0.7170	-0.8988	-0.5719	3.1083	2.3997	3.8168	0.0126	0.0857
PC5	-0.7035	-0.8871	-0.5580	3.0500	2.3366	3.7634	0.1035	0.0374
PC6	0.6255	0.4941	0.7919	-2.7119	-3.3573	-2.0665	0.6272	0.0034
PC7	-0.5814	-0.7362	-0.4592	2.5206	1.9200	3.1211	0.7811	0.0011
PC8	-0.5513	-0.6978	-0.4355	2.3899	1.8212	2.9586	0.6145	0.0036
PC9	-0.5278	-0.6684	-0.4168	2.2882	1.7428	2.8335	0.8353	0.0006
PC10	0.4987	0.3940	0.6314	-2.1622	-2.6768	-1.6476	0.6227	0.0035
PC11	0.4672	0.3700	0.5901	-2.0257	-2.5027	-1.5486	0.1940	0.0240
PC12	0.4532	0.3598	0.5709	-1.9648	-2.4224	-1.5071	0.0728	0.0453
PC13	0.4250	0.3358	0.5380	-1.8426	-2.2810	-1.4042	0.5997	0.0040

Microcebus rufus

PC	Slope	Slope lower CI	Slope higher CI	Intercept	Intercept lower CI	Intercept higher CI	p value	r squared
PC1	0.7603	0.5501	1.0509	-3.3136	-4.4051	-2.2222	0.0019	0.3044
PC2	-0.6281	-0.9016	-0.4375	2.7372	1.7259	3.7486	0.0603	0.1246
PC3	0.5678	0.3863	0.8346	-2.4746	-3.4517	-1.4974	0.9402	0.0002
PC4	-0.5100	-0.7376	-0.3527	2.2227	1.3839	3.0615	0.1206	0.0869
PC5	-0.4963	-0.7242	-0.3401	2.1628	1.3257	3.0000	0.3017	0.0394
PC6	0.4227	0.2880	0.6204	-1.8421	-2.5665	-1.1177	0.6355	0.0084
PC7	0.4072	0.2777	0.5971	-1.7746	-2.4706	-1.0785	0.5474	0.0136
PC8	-0.3718	-0.5459	-0.2533	1.6205	0.9827	2.2583	0.6697	0.0068
PC9	0.3164	0.2153	0.4648	-1.3788	-1.9225	-0.8350	0.7809	0.0029
PC10	0.3022	0.2076	0.4398	-1.3170	-1.8230	-0.8110	0.2276	0.0534
PC11	0.2897	0.1974	0.4253	-1.2626	-1.7593	-0.7659	0.6507	0.0077
PC12	-0.2623	-0.3853	-0.1785	1.1430	0.6925	1.5935	0.7430	0.0040
PC13	0.2607	0.1784	0.3809	-1.1360	-1.5772	-0.6947	0.3489	0.0326

Galago alleni

PC	Slope	Slope lower CI	Slope higher CI	Intercept	Intercept lower CI	Intercept higher CI	p value	r squared
PC1	-1.4628	-2.2450	-0.9531	6.9611	3.8866	10.0355	0.8221	0.0023
PC2	0.8669	0.5826	1.2897	-4.1252	-5.8078	-2.4427	0.0623	0.1492
PC3	0.7807	0.5125	1.1891	-3.7151	-5.3250	-2.1052	0.3511	0.0396
PC4	-0.7208	-1.0810	-0.4807	3.4304	2.0017	4.8591	0.1085	0.1128
PC5	-0.5877	-0.9012	-0.3833	2.7970	1.5647	4.0293	0.6920	0.0073
PC6	-0.4989	-0.7466	-0.3333	2.3741	1.3907	3.3574	0.0936	0.1225
PC7	-0.4778	-0.7236	-0.3156	2.2740	1.3031	3.2448	0.2194	0.0677
PC8	0.4474	0.2917	0.6862	-2.1292	-3.0678	-1.1905	0.7187	0.0060
PC9	0.4058	0.2667	0.6176	-1.9313	-2.7663	-1.0963	0.3257	0.0439
PC10	-0.3809	-0.5848	-0.2481	1.8126	1.0114	2.6137	0.8906	0.0009
PC11	-0.3466	-0.5270	-0.2279	1.6492	0.9374	2.3611	0.3077	0.0472
PC12	-0.3365	-0.5161	-0.2194	1.6013	0.8953	2.3073	0.7204	0.0059
PC13	0.2964	0.1933	0.4546	-1.4107	-2.0326	-0.7888	0.7146	0.0062

Galago demidoff

PC	Slope	Slope lower CI	Slope higher CI	Intercept	Intercept lower CI	Intercept higher CI	p value	r squared
PC1	-1.1102	-1.4426	-0.8544	4.9198	3.6166	6.2229	0.6924	0.0028
PC2	1.0316	0.7994	1.3313	-4.5714	-5.7501	-3.3928	0.0734	0.0551
PC3	0.8570	0.6597	1.1133	-3.7977	-4.8027	-2.7927	0.6064	0.0047
PC4	0.7170	0.5539	0.9281	-3.1774	-4.0064	-2.3483	0.1730	0.0323
PC5	0.6267	0.4860	0.8081	-2.7771	-3.4907	-2.0636	0.0580	0.0616
PC6	0.5872	0.4523	0.7623	-2.6020	-3.2890	-1.9150	0.4694	0.0092
PC7	-0.5538	-0.7085	-0.4328	2.4539	1.8430	3.0649	0.0075	0.1190
PC8	0.5024	0.3881	0.6503	-2.2262	-2.8071	-1.6452	0.1755	0.0320
PC9	0.4706	0.3625	0.6111	-2.0855	-2.6363	-1.5347	0.4874	0.0085
PC10	0.4574	0.3526	0.5933	-2.0269	-2.5603	-1.4936	0.3391	0.0160
PC11	-0.4378	-0.5679	-0.3375	1.9401	1.4296	2.4505	0.3391	0.0160
PC12	-0.4136	-0.5373	-0.3184	1.8328	1.3476	2.3180	0.6355	0.0040
PC13	-0.3845	-0.4990	-0.2963	1.7040	1.2548	2.1531	0.3993	0.0125

Galago elegantulus

PC	Slope	Slope lower CI	Slope higher CI	Intercept	Intercept lower CI	Intercept higher CI	p value	r squared
PC1	-1.4442	-2.0541	-1.0153	6.8186	4.3661	9.2711	0.7869	0.0023
PC2	1.0339	0.7356	1.4531	-4.8816	-6.5755	-3.1877	0.1264	0.0715
PC3	0.9901	0.6988	1.4027	-4.6746	-6.3365	-3.0126	0.3696	0.0252
PC4	0.9091	0.6494	1.2727	-4.2924	-5.7640	-2.8208	0.0786	0.0935
PC5	-0.7414	-1.0527	-0.5222	3.5007	2.2483	4.7532	0.5222	0.0129
PC6	0.6870	0.4833	0.9765	-3.2437	-4.4079	-2.0795	0.6493	0.0065
PC7	-0.6396	-0.8903	-0.4595	3.0200	2.0030	4.0371	0.0399	0.1253
PC8	0.6228	0.4437	0.8742	-2.9404	-3.9568	-1.9240	0.1084	0.0786
PC9	0.5699	0.4037	0.8044	-2.6906	-3.6366	-1.7446	0.2194	0.0467
PC10	0.5449	0.3838	0.7736	-2.5727	-3.4930	-1.6524	0.5196	0.0131
PC11	0.5165	0.3647	0.7317	-2.4389	-3.3054	-1.5724	0.3577	0.0265
PC12	0.5059	0.3557	0.7194	-2.3885	-3.2470	-1.5300	0.7335	0.0037
PC13	0.4572	0.3230	0.6474	-2.1589	-2.9247	-1.3930	0.3316	0.0295

Galago moholi

PC	Slope	Slope lower CI	Slope higher CI	Intercept	Intercept lower CI	Intercept higher CI	p value	r squared
PC1	1.3482	1.0678	1.7023	-6.1313	-7.5744	-4.6883	0.3796	0.0109
PC2	1.0811	0.8611	1.3572	-4.9165	-6.0445	-3.7884	0.0368	0.0600
PC3	0.9384	0.7464	1.1798	-4.2675	-5.2532	-3.2818	0.0643	0.0474
PC4	0.8309	0.6645	1.0391	-3.7789	-4.6309	-2.9269	0.0090	0.0923
PC5	0.7862	0.6219	0.9939	-3.5753	-4.4213	-2.7293	0.9048	0.0002
PC6	-0.7032	-0.8846	-0.5590	3.1979	2.4575	3.9382	0.0787	0.0429
PC7	0.6375	0.5054	0.8041	-2.8991	-3.5783	-2.2200	0.2302	0.0202
PC8	0.5979	0.4730	0.7558	-2.7192	-3.3623	-2.0762	0.7446	0.0015
PC9	0.5637	0.4464	0.7120	-2.5638	-3.1678	-1.9597	0.4324	0.0087
PC10	0.5250	0.4153	0.6637	-2.3876	-2.9523	-1.8230	0.7595	0.0013
PC11	-0.4722	-0.5967	-0.3737	2.1476	1.6406	2.6546	0.5594	0.0048
PC12	0.4643	0.3680	0.5857	-2.1114	-2.6063	-1.6165	0.2448	0.0190
PC13	-0.4255	-0.5374	-0.3369	1.9349	1.4791	2.3908	0.4299	0.0088

Galago senegalensis

PC	Slope	Slope lower CI	Slope higher CI	Intercept	Intercept lower CI	Intercept higher CI	p value	r squared
PC1	1.1347	0.9840	1.3084	-5.2600	-6.0121	-4.5079	0.0000	0.0922
PC2	1.0426	0.8987	1.2096	-4.8332	-5.5540	-4.1125	0.1390	0.0126
PC3	-0.8650	-1.0036	-0.7455	4.0100	3.4118	4.6082	0.1521	0.0118
PC4	0.7454	0.6427	0.8644	-3.4553	-3.9692	-2.9414	0.0779	0.0179
PC5	-0.6478	-0.7520	-0.5581	3.0032	2.5537	3.4527	0.3375	0.0053
PC6	-0.5999	-0.6965	-0.5166	2.7808	2.3639	3.1978	0.5643	0.0019
PC7	-0.5702	-0.6614	-0.4916	2.6435	2.2498	3.0371	0.1015	0.0154
PC8	-0.5260	-0.6070	-0.4558	2.4385	2.0880	2.7889	0.0001	0.0828
PC9	-0.5059	-0.5874	-0.4357	2.3452	1.9935	2.6970	0.6647	0.0011
PC10	-0.4852	-0.5633	-0.4179	2.2494	1.9124	2.5865	0.4617	0.0031
PC11	-0.4655	-0.5405	-0.4009	2.1581	1.8344	2.4817	0.6057	0.0015
PC12	0.4326	0.3727	0.5020	-2.0052	-2.3051	-1.7054	0.2567	0.0074
PC13	0.4254	0.3673	0.4927	-1.9721	-2.2627	-1.6814	0.0125	0.0355

Galago zanzibaricus

PC	Slope	Slope lower CI	Slope higher CI	Intercept	Intercept lower CI	Intercept higher CI	p value	r squared
PC1	-1.2095	-1.8341	-0.7976	5.5471	3.1701	7.9241	0.5849	0.0132
PC2	1.0710	0.7072	1.6221	-4.9122	-7.0105	-2.8140	0.5057	0.0195
PC3	0.9975	0.6621	1.5028	-4.5749	-6.5028	-2.6470	0.3052	0.0456
PC4	-0.8917	-1.3401	-0.5933	4.0897	2.3773	5.8022	0.2472	0.0578
PC5	-0.7868	-1.1896	-0.5204	3.6087	2.0739	5.1435	0.4251	0.0279
PC6	-0.7450	-1.1222	-0.4946	3.4170	1.9780	4.8561	0.2989	0.0468
PC7	0.6847	0.4505	1.0408	-3.1405	-4.4943	-1.7867	0.8656	0.0013
PC8	0.6291	0.4138	0.9564	-2.8855	-4.1299	-1.6411	0.9189	0.0005
PC9	0.5814	0.3948	0.8561	-2.6665	-3.7243	-1.6087	0.0521	0.1543
PC10	0.5138	0.3518	0.7503	-2.3564	-3.2703	-1.4426	0.0286	0.1917
PC11	-0.4269	-0.6397	-0.2848	1.9578	1.1439	2.7716	0.1970	0.0713
PC12	0.4086	0.2687	0.6212	-1.8738	-2.6821	-1.0656	0.9487	0.0002
PC13	-0.3866	-0.5856	-0.2553	1.7733	1.0159	2.5308	0.5043	0.0196

Otolemur crassicaudatus

PC	Slope	Slope lower CI	Slope higher CI	Intercept	Intercept lower CI	Intercept higher CI	p value	r squared
PC1	0.6757	0.5546	0.8233	-3.4567	-4.1441	-2.7692	0.4488	0.0058
PC2	0.5830	0.4855	0.7000	-2.9822	-3.5308	-2.4336	0.0001	0.1493
PC3	0.4806	0.3945	0.5855	-2.4586	-2.9471	-1.9700	0.3916	0.0074
PC4	0.4468	0.3685	0.5418	-2.2857	-2.7290	-1.8425	0.0186	0.0547
PC5	0.4188	0.3436	0.5106	-2.1426	-2.5697	-1.7154	0.7664	0.0009
PC6	0.3891	0.3202	0.4728	-1.9903	-2.3806	-1.5999	0.0686	0.0331
PC7	0.3647	0.3008	0.4420	-1.8655	-2.2267	-1.5044	0.0155	0.0578
PC8	0.3556	0.2928	0.4319	-1.8190	-2.1750	-1.4631	0.0528	0.0374
PC9	-0.3206	-0.3900	-0.2636	1.6401	1.3166	1.9636	0.1388	0.0220
PC10	-0.3006	-0.3662	-0.2467	1.5377	1.2321	1.8433	0.4085	0.0069
PC11	-0.2826	-0.3446	-0.2318	1.4459	1.1575	1.7342	0.9319	0.0001
PC12	-0.2672	-0.3245	-0.2200	1.3668	1.0996	1.6339	0.0464	0.0395
PC13	0.2501	0.2052	0.3047	-1.2792	-1.5338	-1.0245	0.5619	0.0034

Otolemur garnettii

PC	Slope	Slope lower CI	Slope higher CI	Intercept	Intercept lower CI	Intercept higher CI	p value	r squared
PC1	0.8212	0.6695	1.0073	-4.1441	-4.9965	-3.2916	0.6443	0.0023
PC2	-0.6423	-0.7625	-0.5411	3.2415	2.6827	3.8002	0.0000	0.2993
PC3	-0.6172	-0.7497	-0.5082	3.1148	2.5055	3.7241	0.0020	0.0978
PC4	0.5010	0.4088	0.6141	-2.5284	-3.0467	-2.0101	0.3553	0.0092
PC5	0.4512	0.3688	0.5521	-2.2770	-2.7397	-1.8144	0.1139	0.0267
PC6	-0.4389	-0.5363	-0.3592	2.2148	1.7677	2.6619	0.0543	0.0393
PC7	0.4044	0.3296	0.4962	-2.0409	-2.4612	-1.6206	0.9188	0.0001
PC8	0.3681	0.3001	0.4516	-1.8577	-2.2398	-1.4755	0.6595	0.0021
PC9	-0.3453	-0.4225	-0.2822	1.7424	1.3884	2.0963	0.1110	0.0271
PC10	0.3291	0.2691	0.4026	-1.6610	-1.9979	-1.3240	0.0949	0.0297
PC11	0.2900	0.2364	0.3558	-1.4635	-1.7647	-1.1623	0.7203	0.0014
PC12	0.2864	0.2334	0.3513	-1.4450	-1.7426	-1.1475	0.8516	0.0004
PC13	-0.2722	-0.3339	-0.2219	1.3736	1.0912	1.6561	0.5931	0.0031

Avahi laniger

PC	Slope	Slope lower CI	Slope higher CI	Intercept	Intercept lower CI	Intercept higher CI	p value	r squared
PC1	-2.4597	-3.8143	-1.5862	12.0103	6.5704	17.4502	0.7765	0.0039
PC2	-1.7202	-2.6696	-1.1084	8.3992	4.5877	12.2108	0.9566	0.0001
PC3	1.4709	0.9514	2.2739	-7.1818	-10.4108	-3.9529	0.5358	0.0185
PC4	-1.1146	-1.7102	-0.7265	5.4425	3.0406	7.8444	0.2843	0.0544
PC5	-1.0808	-1.6745	-0.6976	5.2773	2.8924	7.6623	0.6782	0.0084
PC6	-0.8812	-1.3674	-0.5679	4.3027	2.3508	6.2546	0.8958	0.0008
PC7	-0.8245	-1.2654	-0.5372	4.0258	2.2480	5.8036	0.2898	0.0532
PC8	-0.8090	-1.2458	-0.5253	3.9501	2.1912	5.7089	0.3773	0.0373
PC9	-0.7329	-1.1066	-0.4854	3.5786	2.0620	5.0951	0.0937	0.1280
PC10	-0.5969	-0.9189	-0.3877	2.9144	1.6174	4.2114	0.3707	0.0383
PC11	-0.5550	-0.8317	-0.3704	2.7100	1.5836	3.8364	0.0576	0.1611
PC12	0.4806	0.3118	0.7408	-2.3467	-3.3941	-1.2993	0.4086	0.0327
PC13	-0.4449	-0.6898	-0.2869	2.1722	1.1887	3.1557	0.7568	0.0047

Indri indri

PC	Slope	Slope lower CI	Slope higher CI	Intercept	Intercept lower CI	Intercept higher CI	p value	r squared
PC1	-1.1083	-1.5321	-0.8017	6.0823	4.0778	8.0868	0.3762	0.0212
PC2	-1.0399	-1.4372	-0.7525	5.7073	3.8286	7.5860	0.3519	0.0235
PC3	-0.9967	-1.3806	-0.7195	5.4699	3.6556	7.2841	0.5751	0.0086
PC4	-0.9555	-1.3255	-0.6889	5.2441	3.4972	6.9910	0.9840	0.0000
PC5	-0.8373	-1.1612	-0.6038	4.5954	3.0658	6.1250	0.8083	0.0016
PC6	0.7377	0.5318	1.0233	-4.0486	-5.3971	-2.7001	0.9274	0.0002
PC7	-0.6793	-0.9039	-0.5105	3.7282	2.6488	4.8076	0.0014	0.2446
PC8	-0.6700	-0.9187	-0.4886	3.6770	2.4968	4.8571	0.0995	0.0716
PC9	-0.6071	-0.8419	-0.4378	3.3318	2.2230	4.4406	0.7922	0.0019
PC10	0.5612	0.4047	0.7782	-3.0798	-4.1047	-2.0548	0.7898	0.0019
PC11	0.5526	0.3990	0.7653	-3.0326	-4.0379	-2.0272	0.5538	0.0096
PC12	-0.4987	-0.6902	-0.3603	2.7368	1.8316	3.6420	0.4705	0.0142
PC13	0.4651	0.3365	0.6428	-2.5523	-3.3929	-1.7116	0.3634	0.0224

Propithecus diadema

PC	Slope	Slope lower CI	Slope higher CI	Intercept	Intercept lower CI	Intercept higher CI	p value	r squared
PC1	-0.9621	-1.4022	-0.6601	5.1658	3.1734	7.1583	0.1330	0.0847
PC2	0.8424	0.6052	1.1728	-4.5234	-6.0473	-2.9995	0.0025	0.3017
PC3	0.7467	0.5196	1.0732	-4.0094	-5.4956	-2.5232	0.0385	0.1546
PC4	-0.7173	-1.0492	-0.4903	3.8512	2.3507	5.3516	0.1869	0.0660
PC5	-0.6276	-0.9295	-0.4238	3.3698	2.0121	4.7276	0.8635	0.0012
PC6	0.5599	0.3780	0.8293	-3.0061	-4.2177	-1.7945	0.9068	0.0005
PC7	0.5351	0.3613	0.7927	-2.8734	-4.0317	-1.7150	0.9603	0.0001
PC8	-0.4495	-0.6643	-0.3042	2.4137	1.4469	3.3806	0.5681	0.0127
PC9	0.4043	0.2730	0.5989	-2.1710	-3.0459	-1.2962	0.8824	0.0009
PC10	0.3913	0.2664	0.5748	-2.1009	-2.9290	-1.2729	0.2831	0.0442
PC11	0.3415	0.2313	0.5043	-1.8337	-2.5668	-1.1006	0.5137	0.0166
PC12	-0.3281	-0.4818	-0.2234	1.7614	1.0676	2.4553	0.2774	0.0452
PC13	-0.2991	-0.4430	-0.2020	1.6061	0.9588	2.2534	0.9011	0.0006

Propithecus verreauxi

PC	Slope	Slope lower CI	Slope higher CI	Intercept	Intercept lower CI	Intercept higher CI	p value	r squared
PC1	-0.9881	-1.3477	-0.7245	5.2304	3.5810	6.8799	0.8993	0.0004
PC2	0.8629	0.6338	1.1748	-4.5677	-5.9996	-3.1358	0.4809	0.0122
PC3	-0.7525	-1.0236	-0.5532	3.9832	2.7380	5.2283	0.3942	0.0178
PC4	-0.6946	-0.9388	-0.5140	3.6768	2.5525	4.8011	0.1130	0.0601
PC5	0.6643	0.4957	0.8904	-3.5164	-4.5611	-2.4717	0.0277	0.1128
PC6	-0.6210	-0.8440	-0.4569	3.2869	2.2622	4.3116	0.3304	0.0231
PC7	0.5791	0.4248	0.7896	-3.0655	-4.0309	-2.1001	0.7257	0.0030
PC8	0.5528	0.4094	0.7464	-2.9263	-3.8182	-2.0343	0.0960	0.0661
PC9	0.5268	0.3878	0.7158	-2.7887	-3.6570	-1.9205	0.3052	0.0256
PC10	0.4750	0.3486	0.6472	-2.5142	-3.3045	-1.7238	0.6021	0.0067
PC11	0.4361	0.3204	0.5935	-2.3082	-3.0310	-1.5855	0.4430	0.0144
PC12	-0.3949	-0.5385	-0.2896	2.0903	1.4317	2.7490	0.7698	0.0021
PC13	-0.3764	-0.5134	-0.2760	1.9924	1.3640	2.6209	0.9487	0.0001

Eulemur fulvus

PC	Slope	Slope lower CI	Slope higher CI	Intercept	Intercept lower CI	Intercept higher CI	p value	r squared
PC1	-0.8639	-1.0025	-0.7444	4.6052	3.9173	5.2931	0.2055	0.0092
PC2	-0.7971	-0.9219	-0.6891	4.2489	3.6283	4.8696	0.0023	0.0526
PC3	0.6603	0.5689	0.7665	-3.5202	-4.0471	-2.9932	0.3536	0.0050
PC4	-0.6042	-0.6998	-0.5216	3.2208	2.7458	3.6957	0.0140	0.0344
PC5	0.5759	0.4959	0.6687	-3.0698	-3.5303	-2.6094	0.6702	0.0011
PC6	-0.5279	-0.6115	-0.4557	2.8139	2.3987	3.2291	0.0158	0.0332
PC7	0.4966	0.4280	0.5763	-2.6474	-3.0427	-2.2521	0.1841	0.0102
PC8	-0.4576	-0.5313	-0.3942	2.4395	2.0742	2.8049	0.4067	0.0040
PC9	-0.4562	-0.5294	-0.3931	2.4317	2.0683	2.7951	0.2263	0.0084
PC10	-0.4463	-0.5182	-0.3843	2.3789	2.0221	2.7357	0.6688	0.0011
PC11	-0.4298	-0.4984	-0.3707	2.2913	1.9510	2.6316	0.0570	0.0208
PC12	0.4008	0.3454	0.4652	-2.1367	-2.4560	-1.8174	0.2199	0.0087
PC13	-0.3782	-0.4392	-0.3257	2.0162	1.7137	2.3188	0.8990	0.0001

Eulemur macaco

PC	Slope	Slope lower CI	Slope higher CI	Intercept	Intercept lower CI	Intercept higher CI	p value	r squared
PC1	-1.1712	-1.5318	-0.8954	6.2690	4.5659	7.9720	0.2241	0.0278
PC2	1.0926	0.8330	1.4333	-5.8486	-7.4553	-4.2419	0.5794	0.0058
PC3	-0.9403	-1.2023	-0.7353	5.0332	3.7833	6.2831	0.0010	0.1876
PC4	0.9065	0.6906	1.1901	-4.8525	-6.1894	-3.5156	0.9571	0.0001
PC5	-0.7658	-1.0046	-0.5838	4.0993	2.9729	5.2257	0.5967	0.0053
PC6	-0.6629	-0.8692	-0.5056	3.5486	2.5754	4.5218	0.4842	0.0093
PC7	-0.6246	-0.8173	-0.4774	3.3436	2.4338	4.2534	0.2526	0.0246
PC8	0.5773	0.4401	0.7573	-3.0903	-3.9393	-2.2413	0.5864	0.0056
PC9	-0.5490	-0.7195	-0.4188	2.9386	2.1337	3.7434	0.4299	0.0118
PC10	0.5256	0.4012	0.6885	-2.8134	-3.5824	-2.0443	0.3624	0.0157
PC11	0.4942	0.3782	0.6458	-2.6454	-3.3615	-1.9292	0.1747	0.0345
PC12	0.4737	0.3611	0.6216	-2.5358	-3.2330	-1.8385	0.6442	0.0041
PC13	0.4361	0.3327	0.5716	-2.3342	-2.9737	-1.6948	0.4393	0.0113

Eulemur mongoz

PC	Slope	Slope lower CI	Slope higher CI	Intercept	Intercept lower CI	Intercept higher CI	p value	r squared
PC1	0.7228	0.5534	0.9440	-3.8185	-4.8504	-2.7866	0.9349	0.0001
PC2	0.6786	0.5231	0.8803	-3.5852	-4.5289	-2.6415	0.0903	0.0513
PC3	0.6165	0.4864	0.7815	-3.2573	-4.0367	-2.4779	0.0003	0.2160
PC4	0.5164	0.3958	0.6738	-2.7285	-3.4628	-1.9942	0.5006	0.0083
PC5	-0.4531	-0.5908	-0.3475	2.3939	1.7511	3.0366	0.3992	0.0130
PC6	-0.4390	-0.5699	-0.3381	2.3191	1.7067	2.9314	0.1115	0.0454
PC7	0.3704	0.2836	0.4838	-1.9571	-2.4860	-1.4282	0.9607	0.0000
PC8	-0.3575	-0.4653	-0.2746	1.8887	1.3850	2.3925	0.2312	0.0260
PC9	0.3475	0.2682	0.4504	-1.8362	-2.3174	-1.3549	0.0680	0.0593
PC10	-0.3154	-0.4103	-0.2424	1.6661	1.2227	2.1096	0.1966	0.0301
PC11	-0.2834	-0.3683	-0.2181	1.4972	1.1005	1.8939	0.1430	0.0386
PC12	-0.2654	-0.3449	-0.2042	1.4022	1.0305	1.7738	0.1472	0.0378
PC13	-0.2576	-0.3363	-0.1974	1.3612	0.9943	1.7281	0.5905	0.0053

Eulemur rubriventer

PC	Slope	Slope lower CI	Slope higher CI	Intercept	Intercept lower CI	Intercept higher CI	p value	r squared
PC1	1.2292	0.8323	1.8155	-6.5366	-9.1509	-3.9222	0.2295	0.0572
PC2	1.2177	0.8208	1.8065	-6.4752	-9.0960	-3.8545	0.3529	0.0346
PC3	1.1168	0.7604	1.6403	-5.9389	-8.2783	-3.5994	0.1390	0.0855
PC4	-0.9790	-1.4609	-0.6561	5.2061	3.0663	7.3460	0.7441	0.0043
PC5	-0.8485	-1.2425	-0.5794	4.5119	2.7486	6.2751	0.1083	0.0999
PC6	0.8257	0.5529	1.2331	-4.3908	-6.1993	-2.5823	0.9493	0.0002
PC7	-0.7101	-1.0580	-0.4766	3.7760	2.2301	5.3219	0.5841	0.0122
PC8	0.6752	0.4559	0.9999	-3.5903	-5.0369	-2.1437	0.2980	0.0432
PC9	0.6488	0.4345	0.9689	-3.4503	-4.8711	-2.0295	0.8984	0.0007
PC10	0.6096	0.4220	0.8805	-3.2417	-4.4608	-2.0226	0.0346	0.1665
PC11	0.5189	0.3475	0.7749	-2.7592	-3.8957	-1.6227	0.9543	0.0001
PC12	-0.4760	-0.7093	-0.3194	2.5311	1.4944	3.5679	0.5980	0.0113
PC13	0.4583	0.3069	0.6845	-2.4373	-3.4412	-1.4334	0.9670	0.0001

Hapalemur griseus

PC	Slope	Slope lower CI	Slope higher CI	Intercept	Intercept lower CI	Intercept higher CI	p value	r squared
PC1	-1.0483	-1.5493	-0.7093	5.2818	3.1656	7.3980	0.2435	0.0540
PC2	-0.8783	-1.2917	-0.5972	4.4254	2.6757	6.1751	0.1561	0.0788
PC3	0.7271	0.4906	1.0775	-3.6633	-5.1419	-2.1846	0.3179	0.0399
PC4	0.6959	0.4755	1.0184	-3.5062	-4.8740	-2.1383	0.1024	0.1031
PC5	-0.5935	-0.8765	-0.4018	2.9901	1.7943	4.1859	0.2283	0.0575
PC6	0.5512	0.3691	0.8231	-2.7769	-3.9208	-1.6330	0.9663	0.0001
PC7	0.5016	0.3367	0.7472	-2.5271	-3.5614	-1.4928	0.5742	0.0128
PC8	0.4553	0.3089	0.6711	-2.2939	-3.2066	-1.3812	0.1921	0.0671
PC9	-0.4195	-0.6225	-0.2827	2.1137	1.2575	2.9698	0.3638	0.0331
PC10	-0.4138	-0.6173	-0.2774	2.0849	1.2284	2.9413	0.7095	0.0056
PC11	0.3659	0.2465	0.5430	-1.8433	-2.5902	-1.0965	0.3678	0.0326
PC12	-0.3578	-0.5337	-0.2399	1.8030	1.0628	2.5432	0.6832	0.0068
PC13	0.3420	0.2292	0.5102	-1.7230	-2.4310	-1.0149	0.7306	0.0048

Lemur catta

PC	Slope	Slope lower CI	Slope higher CI	Intercept	Intercept lower CI	Intercept higher CI	p value	r squared
PC1	0.8592	0.6078	1.2147	-4.5174	-6.1130	-2.9218	0.2697	0.0379
PC2	0.7292	0.5134	1.0358	-3.8340	-5.2071	-2.4608	0.5576	0.0109
PC3	-0.6269	-0.8911	-0.4410	3.2958	2.1126	4.4790	0.6581	0.0062
PC4	-0.5709	-0.8074	-0.4037	3.0017	1.9404	4.0629	0.2817	0.0361
PC5	0.5565	0.3937	0.7866	-2.9255	-3.9584	-1.8927	0.2641	0.0388
PC6	0.4980	0.3605	0.6880	-2.6182	-3.4794	-1.7571	0.0168	0.1658
PC7	-0.4419	-0.6277	-0.3111	2.3234	1.4913	3.1555	0.5579	0.0108
PC8	-0.4210	-0.5987	-0.2960	2.2132	1.4175	3.0088	0.7465	0.0033
PC9	-0.3775	-0.5367	-0.2656	1.9848	1.2720	2.6976	0.6769	0.0055
PC10	0.3471	0.2458	0.4900	-1.8247	-2.4667	-1.1827	0.2267	0.0453
PC11	0.3129	0.2200	0.4451	-1.6453	-2.2371	-1.0534	0.7936	0.0022
PC12	0.3072	0.2159	0.4371	-1.6152	-2.1967	-1.0337	0.8889	0.0006
PC13	-0.2680	-0.3787	-0.1896	1.4090	0.9118	1.9062	0.2577	0.0398

Varecia variegata

PC	Slope	Slope lower CI	Slope higher CI	Intercept	Intercept lower CI	Intercept higher CI	p value	r squared
PC1	0.9792	0.7152	1.3407	-5.3636	-7.0769	-3.6504	0.0799	0.0806
PC2	0.7342	0.5294	1.0181	-4.0214	-5.3599	-2.6829	0.7998	0.0018
PC3	-0.6334	-0.8456	-0.4745	3.4697	2.4534	4.4859	0.0022	0.2269
PC4	0.5471	0.3957	0.7564	-2.9967	-3.9846	-2.0088	0.3830	0.0206
PC5	0.5267	0.3824	0.7255	-2.8852	-3.8248	-1.9456	0.1982	0.0443
PC6	0.4752	0.3441	0.6563	-2.6032	-3.4583	-1.7480	0.3121	0.0276
PC7	-0.4451	-0.6096	-0.3249	2.4379	1.6582	3.2175	0.0845	0.0783
PC8	-0.4123	-0.5706	-0.2980	2.2586	1.5121	3.0052	0.4488	0.0156
PC9	-0.3904	-0.5389	-0.2828	2.1384	1.4369	2.8398	0.2891	0.0303
PC10	0.3712	0.2677	0.5148	-2.0335	-2.7101	-1.3568	0.7745	0.0022
PC11	0.3568	0.2601	0.4896	-1.9545	-2.5832	-1.3258	0.1099	0.0676
PC12	0.3275	0.2361	0.4542	-1.7938	-2.3910	-1.1966	0.8363	0.0012
PC13	-0.3025	-0.4196	-0.2181	1.6569	1.1051	2.2087	0.8738	0.0007

Lepilemur ruficaudatus

PC	Slope	Slope lower CI	Slope higher CI	Intercept	Intercept lower CI	Intercept higher CI	p value	r squared
PC1	-0.8740	-1.3151	-0.5809	4.2975	2.4926	6.1024	0.2724	0.0521
PC2	-0.8565	-1.2841	-0.5713	4.2114	2.4590	5.9639	0.2029	0.0695
PC3	0.6720	0.4443	1.0164	-3.3041	-4.7108	-1.8974	0.4413	0.0260
PC4	0.6019	0.4144	0.8744	-2.9596	-4.0906	-1.8286	0.0195	0.2152
PC5	-0.5855	-0.8770	-0.3909	2.8787	1.6834	4.0739	0.1896	0.0736
PC6	-0.5137	-0.7803	-0.3382	2.5259	1.4391	3.6127	0.7321	0.0052
PC7	-0.4634	-0.7016	-0.3061	2.2786	1.3062	3.2510	0.4854	0.0214
PC8	0.4402	0.2942	0.6584	-2.1641	-3.0596	-1.2687	0.1708	0.0800
PC9	-0.4138	-0.6224	-0.2752	2.0348	1.1811	2.8885	0.2629	0.0542
PC10	0.3861	0.2551	0.5843	-1.8983	-2.7077	-1.0889	0.4694	0.0230
PC11	-0.3331	-0.5062	-0.2192	1.6378	0.9321	2.3435	0.8209	0.0023
PC12	0.3182	0.2094	0.4834	-1.5646	-2.2382	-0.8909	0.7699	0.0038
PC13	-0.2976	-0.4488	-0.1973	1.4631	0.8448	2.0815	0.3373	0.0401

Loris tardigradus

PC	Slope	Slope lower CI	Slope higher CI	Intercept	Intercept lower CI	Intercept higher CI	p value	r squared
PC1	-0.5590	-0.7456	-0.4191	2.6760	1.8943	3.4576	0.0000	0.4974
PC2	0.3839	0.2616	0.5635	-1.8379	-2.5609	-1.1149	0.1314	0.0887
PC3	-0.3085	-0.4524	-0.2104	1.4770	0.8975	2.0566	0.1214	0.0933
PC4	-0.2580	-0.3845	-0.1732	1.2353	0.7292	1.7415	0.5954	0.0114
PC5	-0.2433	-0.3633	-0.1629	1.1647	0.6847	1.6446	0.9410	0.0002
PC6	0.2273	0.1526	0.3386	-1.0881	-1.5336	-0.6425	0.5773	0.0126
PC7	0.2204	0.1497	0.3246	-1.0553	-1.4740	-0.6366	0.1725	0.0731
PC8	0.2035	0.1376	0.3010	-0.9742	-1.3654	-0.5829	0.2624	0.0500
PC9	0.1715	0.1148	0.2561	-0.8209	-1.1593	-0.4826	0.9624	0.0001
PC10	0.1686	0.1130	0.2515	-0.8071	-1.1387	-0.4755	0.6963	0.0062
PC11	0.1539	0.1033	0.2291	-0.7367	-1.0379	-0.4354	0.5380	0.0154
PC12	0.1433	0.0962	0.2135	-0.6862	-0.9672	-0.4053	0.5703	0.0131
PC13	-0.1326	-0.1972	-0.0892	0.6350	0.3763	0.8936	0.4511	0.0229

Nycticebus bengalensis

PC	Slope	Slope lower CI	Slope higher CI	Intercept	Intercept lower CI	Intercept higher CI	p value	r squared
PC1	1.1344	0.7367	1.7467	-5.7608	-8.3255	-3.1961	0.1773	0.0891
PC2	-1.0043	-1.5496	-0.6509	5.1003	2.8183	7.3824	0.2025	0.0799
PC3	0.9097	0.5812	1.4238	-4.6196	-6.7592	-2.4800	0.5986	0.0141
PC4	-0.8553	-1.3390	-0.5463	4.3434	2.3306	6.3562	0.6134	0.0130
PC5	-0.8111	-1.2499	-0.5264	4.1192	2.2820	5.9564	0.1861	0.0857
PC6	-0.7754	-1.1923	-0.5043	3.9378	2.1908	5.6848	0.1619	0.0954
PC7	-0.5840	-0.9081	-0.3755	2.9655	1.6133	4.3178	0.3470	0.0443
PC8	-0.5204	-0.8143	-0.3326	2.6427	1.4195	3.8659	0.5832	0.0153
PC9	-0.4798	-0.7443	-0.3092	2.4364	1.3317	3.5411	0.2931	0.0551
PC10	0.4352	0.2805	0.6754	-2.2102	-3.2131	-1.2074	0.2985	0.0539
PC11	0.4022	0.2562	0.6314	-2.0425	-2.9952	-1.0898	0.9601	0.0001
PC12	0.3829	0.2464	0.5951	-1.9445	-2.8301	-1.0589	0.3339	0.0467
PC13	-0.3345	-0.5247	-0.2132	1.6986	0.9077	2.4895	0.7928	0.0035

Nycticebus coucang

PC	Slope	Slope lower CI	Slope higher CI	Intercept	Intercept lower CI	Intercept higher CI	p value	r squared
PC1	0.8263	0.6652	1.0265	-4.1171	-5.0172	-3.2170	0.0001	0.1963
PC2	-0.7622	-0.9690	-0.5995	3.7976	2.8770	4.7182	0.3710	0.0120
PC3	0.5971	0.4718	0.7557	-2.9750	-3.6823	-2.2676	0.0663	0.0494
PC4	-0.5340	-0.6795	-0.4197	2.6607	2.0135	3.3079	0.5607	0.0051
PC5	0.4952	0.3892	0.6301	-2.4673	-3.0676	-1.8671	0.5670	0.0049
PC6	-0.4430	-0.5638	-0.3480	2.2072	1.6694	2.7449	0.7126	0.0020
PC7	0.3813	0.2996	0.4852	-1.8997	-2.3622	-1.4372	0.6365	0.0034
PC8	0.3737	0.2970	0.4703	-1.8621	-2.2940	-1.4302	0.0098	0.0954
PC9	-0.3475	-0.4411	-0.2737	1.7312	1.3140	2.1484	0.2091	0.0234
PC10	-0.3395	-0.4319	-0.2669	1.6917	1.2806	2.1029	0.4989	0.0069
PC11	-0.3233	-0.4113	-0.2541	1.6110	1.2193	2.0027	0.5282	0.0060
PC12	-0.2993	-0.3801	-0.2356	1.4911	1.1312	1.8510	0.2410	0.0205
PC13	-0.2798	-0.3554	-0.2202	1.3939	1.0570	1.7308	0.2754	0.0177

Perodicticus potto

PC	Slope	Slope lower CI	Slope higher CI	Intercept	Intercept lower CI	Intercept higher CI	p value	r squared
PC1	1.0855	0.9143	1.2889	-5.4823	-6.4282	-4.5363	0.0351	0.0345
PC2	-0.9256	-1.1022	-0.7773	4.6744	3.8540	5.4949	0.7128	0.0011
PC3	0.6733	0.5682	0.7978	-3.4003	-3.9802	-2.8204	0.0065	0.0569
PC4	-0.6206	-0.7385	-0.5215	3.1341	2.5863	3.6820	0.2809	0.0091
PC5	-0.6106	-0.7268	-0.5129	3.0836	2.5434	3.6238	0.4303	0.0049
PC6	0.5860	0.4977	0.6901	-2.9597	-3.4454	-2.4739	0.0000	0.1265
PC7	0.4741	0.3982	0.5644	-2.3942	-2.8138	-1.9747	0.4696	0.0041
PC8	-0.4615	-0.5472	-0.3892	2.3307	1.9317	2.7296	0.0110	0.0498
PC9	0.4447	0.3735	0.5295	-2.2459	-2.6397	-1.8521	0.5268	0.0032
PC10	-0.3950	-0.4704	-0.3317	1.9947	1.6444	2.3450	0.9779	0.0000
PC11	-0.3702	-0.4406	-0.3110	1.8695	1.5422	2.1967	0.3655	0.0065
PC12	-0.3456	-0.4115	-0.2903	1.7455	1.4393	2.0517	0.6107	0.0020
PC13	-0.3348	-0.3985	-0.2812	1.6908	1.3946	1.9869	0.4215	0.0051

Goswami model orbit module against ln CS of base

Cheirogaleus major

PC	Slope	Slope lower CI	Slope higher CI	Intercept	Intercept lower CI	Intercept higher CI	p value	r squared
PC1	1.0590	0.7232	1.5506	-3.2042	-4.4561	-1.9523	0.0347	0.1798
PC2	0.9654	0.6473	1.4400	-2.9212	-4.1206	-1.7217	0.1358	0.0941
PC3	0.7893	0.5238	1.1892	-2.3881	-3.3950	-1.3812	0.3093	0.0449
PC4	0.7296	0.4810	1.1067	-2.2076	-3.1543	-1.2609	0.6033	0.0119
PC5	0.6635	0.4374	1.0063	-2.0075	-2.8682	-1.1468	0.5972	0.0123
PC6	0.6159	0.4096	0.9260	-1.8635	-2.6447	-1.0822	0.2567	0.0555
PC7	0.5835	0.3851	0.8843	-1.7656	-2.5210	-1.0102	0.5413	0.0164
PC8	0.5125	0.3417	0.7687	-1.5508	-2.1969	-0.9047	0.2101	0.0674
PC9	0.4897	0.3223	0.7440	-1.4818	-2.1199	-0.8437	0.7733	0.0037
PC10	-0.4202	-0.6379	-0.2768	1.2715	0.7252	1.8178	0.6647	0.0083
PC11	0.3913	0.2575	0.5946	-1.1840	-1.6940	-0.6740	0.7895	0.0032
PC12	0.3519	0.2318	0.5341	-1.0647	-1.5220	-0.6074	0.6535	0.0089
PC13	-0.3369	-0.4974	-0.2282	1.0193	0.6120	1.4266	0.0632	0.1421

Cheirogaleus medius

PC	Slope	Slope lower CI	Slope higher CI	Intercept	Intercept lower CI	Intercept higher CI	p value	r squared
PC1	-0.7704	-1.0644	-0.5577	2.1967	1.4741	2.9192	0.0018	0.3065
PC2	-0.6146	-0.9035	-0.4181	1.7523	1.0601	2.4445	0.9672	0.0001
PC3	0.5473	0.3762	0.7961	-1.5603	-2.1592	-0.9614	0.2172	0.0558
PC4	0.4842	0.3305	0.7094	-1.3807	-1.9210	-0.8403	0.4835	0.0183
PC5	0.4459	0.3040	0.6541	-1.2713	-1.7706	-0.7720	0.5816	0.0114
PC6	-0.3967	-0.5819	-0.2705	1.1311	0.6869	1.5752	0.5755	0.0118
PC7	0.3706	0.2535	0.5416	-1.0565	-1.4673	-0.6457	0.3600	0.0311
PC8	0.3441	0.2382	0.4970	-0.9810	-1.3500	-0.6120	0.1072	0.0933
PC9	0.3177	0.2181	0.4629	-0.9058	-1.2549	-0.5567	0.2530	0.0481
PC10	0.3136	0.2139	0.4599	-0.8942	-1.2451	-0.5433	0.5532	0.0132
PC11	-0.2782	-0.4003	-0.1933	0.7931	0.4978	1.0883	0.0764	0.1117
PC12	-0.2501	-0.3646	-0.1716	0.7132	0.4380	0.9883	0.2645	0.0459
PC13	0.2234	0.1543	0.3234	-0.6368	-0.8780	-0.3957	0.1352	0.0808

Microcebus murinus

PC	Slope	Slope lower CI	Slope higher CI	Intercept	Intercept lower CI	Intercept higher CI	p value	r squared
PC1	-1.2212	-1.5403	-0.9683	3.2912	2.5204	4.0621	0.1159	0.0349
PC2	-1.0678	-1.3329	-0.8554	2.8777	2.2343	3.5212	0.0028	0.1204
PC3	0.8427	0.6655	1.0672	-2.2711	-2.8125	-1.7298	0.8498	0.0005
PC4	-0.7605	-0.9472	-0.6106	2.0495	1.5959	2.5031	0.0013	0.1382
PC5	0.7462	0.5893	0.9450	-2.0111	-2.4906	-1.5317	0.9311	0.0001
PC6	-0.6635	-0.8358	-0.5268	1.7882	1.3717	2.2047	0.0713	0.0457
PC7	0.6167	0.4875	0.7801	-1.6620	-2.0562	-1.2678	0.3980	0.0102
PC8	-0.5847	-0.7404	-0.4618	1.5758	1.2004	1.9513	0.7466	0.0015
PC9	0.5598	0.4423	0.7087	-1.5088	-1.8678	-1.1497	0.6092	0.0038
PC10	0.5290	0.4189	0.6680	-1.4257	-1.7614	-1.0900	0.1875	0.0247
PC11	0.4956	0.3914	0.6276	-1.3357	-1.6541	-1.0172	0.9743	0.0000
PC12	0.4807	0.3825	0.6041	-1.2955	-1.5941	-0.9970	0.0297	0.0658
PC13	-0.4508	-0.5705	-0.3563	1.2150	0.9263	1.5037	0.4913	0.0068

Microcebus rufus

PC	Slope	Slope lower CI	Slope higher CI	Intercept	Intercept lower CI	Intercept higher CI	p value	r squared
PC1	0.9579	0.6887	1.3323	-2.5755	-3.4408	-1.7102	0.0034	0.2763
PC2	0.7913	0.5396	1.1604	-2.1275	-2.9623	-1.2926	0.5577	0.0129
PC3	-0.7153	-1.0497	-0.4875	1.9233	1.1673	2.6793	0.6148	0.0095
PC4	-0.6425	-0.9126	-0.4524	1.7276	1.1089	2.3463	0.0227	0.1777
PC5	-0.6252	-0.9002	-0.4342	1.6810	1.0545	2.3076	0.0797	0.1094
PC6	0.5325	0.3627	0.7819	-1.4318	-1.9954	-0.8681	0.6768	0.0065
PC7	0.5130	0.3503	0.7511	-1.3792	-1.9181	-0.8403	0.4495	0.0213
PC8	0.4685	0.3206	0.6846	-1.2595	-1.7490	-0.7700	0.3543	0.0319
PC9	-0.3986	-0.5825	-0.2727	1.0716	0.6552	1.4881	0.3548	0.0318
PC10	0.3807	0.2591	0.5594	-1.0236	-1.4273	-0.6199	0.7884	0.0027
PC11	-0.3650	-0.5347	-0.2491	0.9813	0.5973	1.3654	0.4852	0.0182
PC12	-0.3304	-0.4829	-0.2261	0.8884	0.5432	1.2336	0.3530	0.0320
PC13	0.3284	0.2259	0.4773	-0.8829	-1.2209	-0.5449	0.1987	0.0604

Galago alleni

PC	Slope	Slope lower CI	Slope higher CI	Intercept	Intercept lower CI	Intercept higher CI	p value	r squared
PC1	1.2992	0.9586	1.7609	-3.8211	-5.0012	-2.6410	0.0001	0.5123
PC2	-0.7699	-1.1817	-0.5017	2.2645	1.2643	3.2647	0.8136	0.0026
PC3	-0.6934	-1.0595	-0.4538	2.0393	1.1485	2.9302	0.4658	0.0244
PC4	-0.6402	-0.9802	-0.4182	1.8830	1.0564	2.7097	0.5732	0.0147
PC5	-0.5220	-0.7933	-0.3435	1.5353	0.8739	2.1968	0.2888	0.0510
PC6	-0.4431	-0.6794	-0.2890	1.3032	0.7290	1.8774	0.6901	0.0074
PC7	-0.4244	-0.6262	-0.2876	1.2482	0.7503	1.7462	0.0352	0.1862
PC8	0.3974	0.2588	0.6101	-1.1688	-1.6854	-0.6521	0.8784	0.0011
PC9	0.3605	0.2352	0.5524	-1.0601	-1.5268	-0.5935	0.6528	0.0094
PC10	-0.3383	-0.5191	-0.2205	0.9950	0.5557	1.4343	0.7837	0.0035
PC11	-0.3078	-0.4703	-0.2015	0.9053	0.5100	1.3007	0.4612	0.0249
PC12	0.2989	0.1948	0.4585	-0.8790	-1.2669	-0.4911	0.7539	0.0046
PC13	0.2633	0.1715	0.4043	-0.7744	-1.1168	-0.4320	0.9224	0.0004

Galago demidoff

PC	Slope	Slope lower CI	Slope higher CI	Intercept	Intercept lower CI	Intercept higher CI	p value	r squared
PC1	1.1013	0.8563	1.4164	-2.9560	-3.7078	-2.2043	0.0290	0.0809
PC2	1.0234	0.7876	1.3297	-2.7467	-3.4744	-2.0191	0.6932	0.0028
PC3	0.8502	0.6542	1.1048	-2.2818	-2.8866	-1.6771	0.7355	0.0020
PC4	0.7113	0.5553	0.9111	-1.9091	-2.3866	-1.4316	0.0099	0.1112
PC5	0.6217	0.4784	0.8079	-1.6686	-2.1109	-1.2264	0.7401	0.0019
PC6	0.5825	0.4481	0.7571	-1.5634	-1.9782	-1.1487	0.9969	0.0000
PC7	-0.5493	-0.7009	-0.4306	1.4744	1.1116	1.8373	0.0036	0.1393
PC8	0.4984	0.3836	0.6474	-1.3376	-1.6917	-0.9835	0.6195	0.0044
PC9	0.4669	0.3597	0.6059	-1.2531	-1.5835	-0.9226	0.4132	0.0118
PC10	0.4538	0.3494	0.5892	-1.2179	-1.5397	-0.8960	0.5077	0.0077
PC11	-0.4343	-0.5641	-0.3344	1.1657	0.8574	1.4740	0.5511	0.0063
PC12	-0.4103	-0.5315	-0.3168	1.1012	0.8130	1.3895	0.2163	0.0267
PC13	-0.3815	-0.4949	-0.2940	1.0238	0.7541	1.2935	0.3711	0.0141

Galago elegantulus

PC	Slope	Slope lower CI	Slope higher CI	Intercept	Intercept lower CI	Intercept higher CI	p value	r squared
PC1	-0.9860	-1.3995	-0.6947	2.8964	1.8610	3.9317	0.4920	0.0149
PC2	0.7059	0.5053	0.9861	-2.0736	-2.7798	-1.3673	0.0608	0.1056
PC3	0.6760	0.4905	0.9317	-1.9856	-2.6338	-1.3375	0.0128	0.1785
PC4	0.6207	0.4380	0.8798	-1.8233	-2.4723	-1.1743	0.3905	0.0231
PC5	-0.5062	-0.7089	-0.3615	1.4870	0.9768	1.9972	0.0805	0.0924
PC6	0.4691	0.3297	0.6674	-1.3778	-1.8739	-0.8817	0.8827	0.0007
PC7	-0.4367	-0.5975	-0.3192	1.2828	0.8740	1.6916	0.0055	0.2171
PC8	0.4252	0.2989	0.6050	-1.2490	-1.6987	-0.7993	0.9004	0.0005
PC9	0.3891	0.2734	0.5536	-1.1429	-1.5545	-0.7313	0.9821	0.0000
PC10	-0.3720	-0.5261	-0.2631	1.0928	0.7064	1.4792	0.2810	0.0362
PC11	0.3527	0.2490	0.4995	-1.0360	-1.4038	-0.6681	0.3459	0.0278
PC12	-0.3454	-0.4910	-0.2430	1.0146	0.6501	1.3790	0.6813	0.0053
PC13	-0.3122	-0.4441	-0.2195	0.9170	0.5871	1.2469	0.7904	0.0022

Galago moholi

PC	Slope	Slope lower CI	Slope higher CI	Intercept	Intercept lower CI	Intercept higher CI	p value	r squared
PC1	1.1635	0.9479	1.4283	-3.2992	-3.9803	-2.6181	0.0000	0.2391
PC2	0.9330	0.7414	1.1741	-2.6455	-3.2590	-2.0319	0.0908	0.0398
PC3	-0.8098	-1.0234	-0.6409	2.2963	1.7539	2.8387	0.5949	0.0040
PC4	0.7171	0.5702	0.9020	-2.0334	-2.5039	-1.5628	0.0748	0.0440
PC5	0.6785	0.5373	0.8567	-1.9238	-2.3768	-1.4709	0.3887	0.0105
PC6	-0.6069	-0.7664	-0.4806	1.7207	1.3155	2.1260	0.4063	0.0097
PC7	0.5502	0.4418	0.6852	-1.5600	-1.9051	-1.2149	0.0020	0.1264
PC8	-0.5160	-0.6524	-0.4082	1.4632	1.1169	1.8095	0.9751	0.0000
PC9	0.4865	0.3849	0.6151	-1.3795	-1.7060	-1.0531	0.8405	0.0006
PC10	0.4531	0.3585	0.5727	-1.2848	-1.5885	-0.9810	0.6984	0.0021
PC11	-0.4076	-0.5150	-0.3225	1.1556	0.8826	1.4286	0.6172	0.0035
PC12	-0.4007	-0.5066	-0.3169	1.1361	0.8672	1.4050	0.9628	0.0000
PC13	0.3672	0.2906	0.4641	-1.0412	-1.2872	-0.7951	0.6325	0.0032

Galago senegalensis

PC	Slope	Slope lower CI	Slope higher CI	Intercept	Intercept lower CI	Intercept higher CI	p value	r squared
PC1	0.8428	0.7548	0.9410	-2.4283	-2.6967	-2.1600	0.0000	0.4579
PC2	-0.7744	-0.8992	-0.6669	2.2313	1.8964	2.5662	0.8749	0.0001
PC3	-0.6425	-0.7455	-0.5537	1.8512	1.5749	2.1276	0.1659	0.0111
PC4	0.5536	0.4768	0.6428	-1.5952	-1.8344	-1.3559	0.6258	0.0014
PC5	0.4812	0.4144	0.5587	-1.3864	-1.5944	-1.1785	0.6291	0.0014
PC6	0.4455	0.3838	0.5172	-1.2838	-1.4760	-1.0915	0.3642	0.0048
PC7	-0.4235	-0.4917	-0.3648	1.2204	1.0375	1.4033	0.4638	0.0031
PC8	-0.3907	-0.4530	-0.3370	1.1257	0.9585	1.2929	0.0577	0.0207
PC9	0.3758	0.3236	0.4363	-1.0827	-1.2451	-0.9203	0.5817	0.0018
PC10	0.3604	0.3104	0.4184	-1.0385	-1.1941	-0.8828	0.5248	0.0023
PC11	0.3458	0.2978	0.4014	-0.9963	-1.1456	-0.8469	0.4868	0.0028
PC12	0.3213	0.2767	0.3731	-0.9257	-1.0647	-0.7868	0.8716	0.0002
PC13	0.3160	0.2726	0.3663	-0.9104	-1.0455	-0.7753	0.0458	0.0229

Galago zanzibaricus

PC	Slope	Slope lower CI	Slope higher CI	Intercept	Intercept lower CI	Intercept higher CI	p value	r squared
PC1	0.9532	0.6270	1.4493	-2.6840	-3.8420	-1.5260	0.9860	0.0000
PC2	0.8441	0.5575	1.2782	-2.3768	-3.3917	-1.3620	0.4939	0.0206
PC3	-0.7862	-1.1937	-0.5178	2.2136	1.2617	3.1655	0.7004	0.0066
PC4	-0.7028	-1.0237	-0.4825	1.9789	1.2168	2.7409	0.0237	0.2032
PC5	-0.6201	-0.9428	-0.4079	1.7461	0.9929	2.4993	0.9212	0.0004
PC6	-0.5872	-0.8922	-0.3865	1.6534	0.9412	2.3656	0.7882	0.0032
PC7	-0.5397	-0.8167	-0.3566	1.5196	0.8716	2.1675	0.4673	0.0232
PC8	0.4959	0.3309	0.7430	-1.3962	-1.9764	-0.8159	0.1944	0.0721
PC9	0.4582	0.3102	0.6769	-1.2902	-1.8066	-0.7739	0.0659	0.1395
PC10	0.4049	0.2701	0.6071	-1.1402	-1.6147	-0.6656	0.2035	0.0693
PC11	-0.3364	-0.4982	-0.2272	0.9473	0.5657	1.3288	0.0788	0.1282
PC12	0.3220	0.2121	0.4889	-0.9067	-1.2965	-0.5169	0.6927	0.0069
PC13	0.3047	0.2004	0.4633	-0.8580	-1.2282	-0.4879	0.9347	0.0003

Otolemur crassicaudatus

PC	Slope	Slope lower CI	Slope higher CI	Intercept	Intercept lower CI	Intercept higher CI	p value	r squared
PC1	0.8350	0.6870	1.0149	-2.6701	-3.1944	-2.1458	0.0795	0.0307
PC2	0.7204	0.6111	0.8493	-2.3036	-2.6844	-1.9228	0.0000	0.3132
PC3	0.5939	0.4878	0.7231	-1.8991	-2.2754	-1.5228	0.2512	0.0133
PC4	-0.5522	-0.6731	-0.4530	1.7656	1.4136	2.1177	0.7700	0.0009
PC5	-0.5176	-0.6298	-0.4254	1.6550	1.3282	1.9819	0.1619	0.0197
PC6	0.4808	0.3956	0.5843	-1.5374	-1.8391	-1.2356	0.0750	0.0317
PC7	0.4507	0.3702	0.5486	-1.4410	-1.7263	-1.1558	0.2220	0.0150
PC8	0.4394	0.3607	0.5354	-1.4051	-1.6844	-1.1258	0.4089	0.0069
PC9	-0.3962	-0.4824	-0.3254	1.2669	1.0158	1.5180	0.2607	0.0128
PC10	-0.3715	-0.4527	-0.3048	1.1878	0.9514	1.4242	0.5197	0.0042
PC11	-0.3493	-0.4258	-0.2865	1.1169	0.8941	1.3396	0.8784	0.0002
PC12	-0.3302	-0.4017	-0.2714	1.0558	0.8473	1.2642	0.1599	0.0199
PC13	0.3090	0.2535	0.3767	-0.9881	-1.1851	-0.7911	0.7651	0.0009

Otolemur garnettii

PC	Slope	Slope lower CI	Slope higher CI	Intercept	Intercept lower CI	Intercept higher CI	p value	r squared
PC1	0.9736	0.7982	1.1876	-3.0648	-3.6777	-2.4519	0.0196	0.0572
PC2	-0.7615	-0.9254	-0.6267	2.3973	1.9271	2.8675	0.0027	0.0929
PC3	-0.7318	-0.8699	-0.6156	2.3036	1.9033	2.7039	0.0000	0.2879
PC4	0.5940	0.4845	0.7282	-1.8699	-2.2536	-1.4862	0.4021	0.0076
PC5	0.5350	0.4362	0.6561	-1.6840	-2.0301	-1.3379	0.5390	0.0041
PC6	-0.5203	-0.6369	-0.4251	1.6380	1.3046	1.9714	0.1405	0.0232
PC7	-0.4795	-0.5870	-0.3917	1.5094	1.2019	1.8169	0.1566	0.0215
PC8	-0.4364	-0.5350	-0.3560	1.3739	1.0922	1.6555	0.3591	0.0091
PC9	0.4094	0.3342	0.5015	-1.2886	-1.5520	-1.0252	0.2393	0.0149
PC10	0.3902	0.3192	0.4771	-1.2284	-1.4771	-0.9797	0.0743	0.0339
PC11	0.3438	0.2805	0.4214	-1.0824	-1.3042	-0.8605	0.3445	0.0096
PC12	-0.3395	-0.4164	-0.2768	1.0687	0.8488	1.2886	0.6735	0.0019
PC13	-0.3227	-0.3952	-0.2635	1.0159	0.8085	1.2233	0.2013	0.0175

Avahi laniger

PC	Slope	Slope lower CI	Slope higher CI	Intercept	Intercept lower CI	Intercept higher CI	p value	r squared
PC1	1.4809	1.0092	2.1729	-4.6052	-6.4150	-2.7954	0.0150	0.2503
PC2	-1.0356	-1.5778	-0.6797	3.2206	1.8239	4.6173	0.1714	0.0872
PC3	0.8855	0.5712	1.3729	-2.7538	-4.0007	-1.5068	0.7508	0.0049
PC4	-0.6711	-1.0403	-0.4328	2.0869	1.1420	3.0317	0.7457	0.0051
PC5	0.6507	0.4249	0.9964	-2.0235	-2.9124	-1.1346	0.2461	0.0635
PC6	0.5305	0.3421	0.8228	-1.6498	-2.3976	-0.9021	0.7989	0.0032
PC7	-0.4964	-0.7660	-0.3217	1.5436	0.8526	2.2347	0.4505	0.0274
PC8	0.4870	0.3143	0.7546	-1.5146	-2.1993	-0.8298	0.6836	0.0081
PC9	-0.4412	-0.6660	-0.2923	1.3722	0.7910	1.9533	0.0919	0.1293
PC10	-0.3593	-0.5510	-0.2344	1.1175	0.6251	1.6099	0.2699	0.0576
PC11	-0.3341	-0.5073	-0.2201	1.0391	0.5924	1.4858	0.1355	0.1029
PC12	0.2893	0.1869	0.4480	-0.8998	-1.3060	-0.4936	0.6366	0.0108
PC13	-0.2678	-0.4146	-0.1730	0.8329	0.4572	1.2087	0.6144	0.0123

Indri indri

PC	Slope	Slope lower CI	Slope higher CI	Intercept	Intercept lower CI	Intercept higher CI	p value	r squared
PC1	-1.1727	-1.6254	-0.8460	4.2409	2.8314	5.6503	0.6791	0.0047
PC2	1.1004	0.7938	1.5254	-3.9794	-5.3025	-2.6563	0.7067	0.0039
PC3	1.0546	0.7606	1.4622	-3.8139	-5.0826	-2.5452	0.7475	0.0028
PC4	-1.0111	-1.3368	-0.7647	3.6564	2.6219	4.6910	0.0006	0.2785
PC5	0.8860	0.6388	1.2289	-3.2041	-4.2712	-2.1371	0.8793	0.0006
PC6	0.7806	0.5661	1.0764	-2.8229	-3.7458	-1.9000	0.2415	0.0369
PC7	-0.7188	-0.9795	-0.5275	2.5995	1.7820	3.4170	0.0403	0.1088
PC8	-0.7089	-0.9692	-0.5186	2.5638	1.7489	3.3786	0.0640	0.0897
PC9	-0.6424	-0.8910	-0.4631	2.3231	1.5493	3.0969	0.9296	0.0002
PC10	0.5938	0.4283	0.8232	-2.1474	-2.8615	-1.4332	0.7268	0.0033
PC11	0.5847	0.4298	0.7954	-2.1145	-2.7757	-1.4532	0.0317	0.1187
PC12	-0.5277	-0.7269	-0.3830	1.9082	1.2863	2.5301	0.2056	0.0429
PC13	0.4921	0.3548	0.6826	-1.7796	-2.3724	-1.1868	0.9492	0.0001

Propithecus diadema

PC	Slope	Slope lower CI	Slope higher CI	Intercept	Intercept lower CI	Intercept higher CI	p value	r squared
PC1	0.8234	0.5559	1.2197	-2.9678	-4.1643	-1.7712	0.9652	0.0001
PC2	0.7210	0.5088	1.0217	-2.5987	-3.5229	-1.6744	0.0114	0.2218
PC3	0.6391	0.4515	0.9045	-2.3034	-3.1199	-1.4869	0.0104	0.2271
PC4	-0.6139	-0.8981	-0.4196	2.2125	1.3500	3.0750	0.1898	0.0652
PC5	0.5371	0.3638	0.7930	-1.9360	-2.7094	-1.1625	0.4949	0.0181
PC6	-0.4792	-0.7078	-0.3244	1.7270	1.0360	2.4180	0.5307	0.0153
PC7	-0.4580	-0.6777	-0.3095	1.6507	0.9872	2.3142	0.6909	0.0062
PC8	0.3847	0.2597	0.5699	-1.3867	-1.9458	-0.8276	0.9742	0.0000
PC9	0.3461	0.2339	0.5120	-1.2472	-1.7486	-0.7459	0.6895	0.0062
PC10	0.3349	0.2262	0.4958	-1.2070	-1.6929	-0.7211	0.7801	0.0031
PC11	-0.2923	-0.4328	-0.1974	1.0535	0.6291	1.4779	0.8373	0.0017
PC12	-0.2808	-0.4147	-0.1901	1.0119	0.6071	1.4168	0.5272	0.0156
PC13	-0.2560	-0.3785	-0.1732	0.9227	0.5526	1.2928	0.6041	0.0105

Propithecus verreauxi

PC	Slope	Slope lower CI	Slope higher CI	Intercept	Intercept lower CI	Intercept higher CI	p value	r squared
PC1	-0.8098	-1.0998	-0.5962	2.8147	1.9394	3.6899	0.2813	0.0282
PC2	-0.7072	-0.9638	-0.5189	2.4580	1.6847	3.2314	0.6432	0.0053
PC3	0.6167	0.4523	0.8407	-2.1435	-2.8185	-1.4685	0.7106	0.0034
PC4	-0.5692	-0.7714	-0.4201	1.9786	1.3680	2.5893	0.1827	0.0429
PC5	0.5444	0.4017	0.7378	-1.8923	-2.4765	-1.3080	0.1873	0.0420
PC6	-0.5089	-0.6872	-0.3768	1.7688	1.2294	2.3083	0.0984	0.0652
PC7	0.4746	0.3487	0.6460	-1.6497	-2.1665	-1.1328	0.4554	0.0137
PC8	0.4530	0.3382	0.6069	-1.5747	-2.0418	-1.1076	0.0256	0.1158
PC9	0.4317	0.3196	0.5832	-1.5007	-1.9588	-1.0426	0.1027	0.0636
PC10	-0.3892	-0.5309	-0.2854	1.3530	0.9262	1.7798	0.9611	0.0001
PC11	0.3574	0.2621	0.4872	-1.2421	-1.6334	-0.8509	0.7314	0.0029
PC12	-0.3236	-0.4414	-0.2373	1.1249	0.7701	1.4797	0.9366	0.0002
PC13	-0.3085	-0.4189	-0.2271	1.0722	0.7389	1.4055	0.2772	0.0287

Eulemur fulvus

PC	Slope	Slope lower CI	Slope higher CI	Intercept	Intercept lower CI	Intercept higher CI	p value	r squared
PC1	0.8864	0.7635	1.0290	-3.0142	-3.4656	-2.5628	0.3939	0.0042
PC2	-0.8178	-0.9495	-0.7044	2.7810	2.3642	3.1978	0.4886	0.0028
PC3	0.6775	0.5844	0.7855	-2.3040	-2.6460	-1.9621	0.0498	0.0221
PC4	-0.6199	-0.7197	-0.5339	2.1081	1.7921	2.4240	0.4827	0.0029
PC5	-0.5909	-0.6859	-0.5090	2.0093	1.7085	2.3101	0.3564	0.0049
PC6	-0.5416	-0.6272	-0.4677	1.8418	1.5705	2.1130	0.0106	0.0371
PC7	0.5096	0.4391	0.5913	-1.7328	-1.9915	-1.4741	0.1770	0.0105
PC8	-0.4695	-0.5450	-0.4045	1.5967	1.3578	1.8357	0.3268	0.0056
PC9	0.4680	0.4030	0.5435	-1.5916	-1.8305	-1.3527	0.8870	0.0001
PC10	-0.4579	-0.5313	-0.3946	1.5570	1.3245	1.7895	0.1851	0.0101
PC11	0.4410	0.3798	0.5121	-1.4997	-1.7246	-1.2748	0.6388	0.0013
PC12	-0.4113	-0.4775	-0.3542	1.3985	1.1890	1.6081	0.4393	0.0035
PC13	0.3881	0.3345	0.4502	-1.3197	-1.5165	-1.1229	0.1409	0.0125

Eulemur macaco

PC	Slope	Slope lower CI	Slope higher CI	Intercept	Intercept lower CI	Intercept higher CI	p value	r squared
PC1	-0.8951	-1.1658	-0.6873	3.0624	2.2437	3.8812	0.0752	0.0585
PC2	0.8351	0.6374	1.0942	-2.8571	-3.6387	-2.0755	0.3837	0.0143
PC3	-0.7187	-0.9229	-0.5597	2.4587	1.8374	3.0801	0.0026	0.1588
PC4	-0.6929	-0.9089	-0.5282	2.3705	1.7191	3.0219	0.5924	0.0054
PC5	-0.5853	-0.7679	-0.4461	2.0025	1.4520	2.5531	0.6227	0.0046
PC6	-0.5067	-0.6632	-0.3871	1.7335	1.2613	2.2058	0.2738	0.0226
PC7	-0.4774	-0.6258	-0.3642	1.6333	1.1857	2.0810	0.4508	0.0108
PC8	-0.4413	-0.5793	-0.3361	1.5096	1.0937	1.9256	0.9673	0.0000
PC9	0.4196	0.3197	0.5507	-1.4355	-1.8308	-1.0403	0.7767	0.0015
PC10	0.4017	0.3065	0.5264	-1.3743	-1.7505	-0.9982	0.4001	0.0134
PC11	0.3777	0.2920	0.4886	-1.2923	-1.6287	-0.9559	0.0145	0.1076
PC12	0.3621	0.2761	0.4748	-1.2387	-1.5787	-0.8988	0.5104	0.0082
PC13	-0.3333	-0.4365	-0.2545	1.1403	0.8290	1.4516	0.3269	0.0181

Eulemur mongoz

PC	Slope	Slope lower CI	Slope higher CI	Intercept	Intercept lower CI	Intercept higher CI	p value	r squared
PC1	0.7457	0.5803	0.9582	-2.5159	-3.1535	-1.8783	0.0081	0.1208
PC2	0.7001	0.5386	0.9101	-2.3622	-2.9890	-1.7354	0.1566	0.0362
PC3	0.6361	0.4968	0.8144	-2.1462	-2.6821	-1.6103	0.0033	0.1465
PC4	0.5328	0.4100	0.6924	-1.7977	-2.2741	-1.3214	0.1421	0.0388
PC5	-0.4675	-0.6104	-0.3580	1.5773	1.1515	2.0030	0.7042	0.0026
PC6	-0.4529	-0.5882	-0.3487	1.5280	1.1239	1.9321	0.1239	0.0425
PC7	-0.3822	-0.4992	-0.2926	1.2895	0.9410	1.6380	0.9238	0.0002
PC8	-0.3688	-0.4813	-0.2826	1.2444	0.9092	1.5796	0.5397	0.0069
PC9	0.3586	0.2769	0.4643	-1.2098	-1.5261	-0.8935	0.0571	0.0643
PC10	-0.3254	-0.4247	-0.2492	1.0978	0.8017	1.3939	0.6442	0.0039
PC11	-0.2924	-0.3801	-0.2249	0.9865	0.7247	1.2483	0.1574	0.0360
PC12	-0.2738	-0.3566	-0.2102	0.9239	0.6769	1.1708	0.2714	0.0219
PC13	-0.2658	-0.3466	-0.2038	0.8969	0.6559	1.1378	0.4161	0.0121

Eulemur rubriventer

PC	Slope	Slope lower CI	Slope higher CI	Intercept	Intercept lower CI	Intercept higher CI	p value	r squared
PC1	1.1137	0.7459	1.6628	-3.7690	-5.3208	-2.2172	0.8722	0.0011
PC2	1.1032	0.7483	1.6264	-3.7337	-5.2196	-2.2477	0.1938	0.0666
PC3	1.0118	0.7003	1.4619	-3.4244	-4.7133	-2.1355	0.0354	0.1651
PC4	-0.8870	-1.3217	-0.5952	3.0019	1.7724	4.2313	0.5940	0.0115
PC5	-0.7687	-1.1390	-0.5188	2.6016	1.5520	3.6512	0.3123	0.0408
PC6	0.7481	0.5061	1.1058	-2.5317	-3.5467	-1.5168	0.2484	0.0529
PC7	-0.6433	-0.9539	-0.4339	2.1773	1.2971	3.0574	0.3361	0.0371
PC8	-0.6117	-0.9091	-0.4116	2.0702	1.2283	2.9120	0.4263	0.0255
PC9	0.5879	0.3941	0.8769	-1.9895	-2.8065	-1.1725	0.6964	0.0062
PC10	0.5523	0.3773	0.8085	-1.8692	-2.5990	-1.1394	0.1049	0.1017
PC11	-0.4701	-0.6732	-0.3283	1.5910	1.0072	2.1747	0.0172	0.2067
PC12	0.4312	0.2908	0.6395	-1.4595	-2.0497	-0.8693	0.3411	0.0363
PC13	0.4153	0.2784	0.6193	-1.4053	-1.9822	-0.8285	0.6771	0.0070

Hapalemur griseus

PC	Slope	Slope lower CI	Slope higher CI	Intercept	Intercept lower CI	Intercept higher CI	p value	r squared
PC1	-1.2488	-1.8156	-0.8590	3.9694	2.4490	5.4898	0.0589	0.1355
PC2	1.0463	0.7007	1.5625	-3.3258	-4.6956	-1.9559	0.9214	0.0004
PC3	0.8661	0.5804	1.2926	-2.7530	-3.8851	-1.6210	0.7608	0.0038
PC4	0.8290	0.5677	1.2105	-2.6350	-3.6567	-1.6132	0.0851	0.1140
PC5	-0.7070	-1.0446	-0.4785	2.2471	1.3472	3.1470	0.2388	0.0551
PC6	-0.6566	-0.9682	-0.4452	2.0869	1.2557	2.9181	0.1982	0.0653
PC7	0.5975	0.4001	0.8923	-1.8992	-2.6815	-1.1169	0.9352	0.0003
PC8	0.5424	0.3647	0.8065	-1.7239	-2.4261	-1.0217	0.4557	0.0225
PC9	-0.4997	-0.7389	-0.3380	1.5885	0.9512	2.2257	0.2539	0.0517
PC10	-0.4929	-0.7337	-0.3312	1.5668	0.9271	2.2065	0.5066	0.0178
PC11	0.4358	0.2985	0.6362	-1.3853	-1.9221	-0.8485	0.0830	0.1154
PC12	0.4263	0.2864	0.6346	-1.3550	-1.9085	-0.8015	0.5188	0.0168
PC13	0.4074	0.2759	0.6015	-1.2948	-1.8124	-0.7773	0.2231	0.0588

Lemur catta

PC	Slope	Slope lower CI	Slope higher CI	Intercept	Intercept lower CI	Intercept higher CI	p value	r squared
PC1	0.9890	0.7072	1.3830	-3.3466	-4.4901	-2.2031	0.0688	0.0998
PC2	0.8394	0.6064	1.1618	-2.8403	-3.7803	-1.9004	0.0209	0.1557
PC3	0.7215	0.5074	1.0261	-2.4417	-3.3194	-1.5639	0.7353	0.0036
PC4	-0.6571	-0.9270	-0.4658	2.2237	1.4433	3.0042	0.2026	0.0502
PC5	0.6405	0.4607	0.8903	-2.1673	-2.8942	-1.4404	0.0342	0.1326
PC6	0.5732	0.4053	0.8106	-1.9397	-2.6254	-1.2540	0.2800	0.0364
PC7	0.5087	0.3576	0.7236	-1.7213	-2.3407	-1.1019	0.8227	0.0016
PC8	-0.4845	-0.6883	-0.3411	1.6396	1.0521	2.2271	0.5747	0.0099
PC9	0.4345	0.3054	0.6183	-1.4704	-1.9999	-0.9409	0.9867	0.0000
PC10	0.3995	0.2815	0.5669	-1.3518	-1.8347	-0.8688	0.4775	0.0159
PC11	0.3602	0.2538	0.5111	-1.2189	-1.6543	-0.7834	0.4765	0.0160
PC12	0.3536	0.2497	0.5007	-1.1966	-1.6212	-0.7720	0.3359	0.0290
PC13	-0.3085	-0.4388	-0.2169	1.0438	0.6683	1.4193	0.7890	0.0023

Varecia variegata

PC	Slope	Slope lower CI	Slope higher CI	Intercept	Intercept lower CI	Intercept higher CI	p value	r squared
PC1	1.1188	0.8087	1.5477	-3.9247	-5.2210	-2.6283	0.4295	0.0170
PC2	-0.8388	-1.1634	-0.6048	2.9425	1.9625	3.9225	0.8766	0.0007
PC3	-0.7237	-0.9834	-0.5327	2.5388	1.7482	3.3294	0.0264	0.1262
PC4	-0.6251	-0.8653	-0.4515	2.1927	1.4669	2.9186	0.4948	0.0127
PC5	0.6018	0.4342	0.8341	-2.1112	-2.8127	-1.4096	0.6657	0.0051
PC6	-0.5430	-0.7532	-0.3915	1.9048	1.2703	2.5393	0.9105	0.0003
PC7	-0.5085	-0.7010	-0.3689	1.7838	1.2012	2.3665	0.2298	0.0387
PC8	-0.4711	-0.6516	-0.3406	1.6527	1.1072	2.1982	0.4101	0.0184
PC9	-0.4460	-0.6177	-0.3221	1.5647	1.0461	2.0832	0.5363	0.0104
PC10	0.4242	0.3068	0.5864	-1.4879	-1.9783	-0.9975	0.3754	0.0213
PC11	0.4077	0.2939	0.5655	-1.4302	-1.9066	-0.9537	0.9627	0.0001
PC12	0.3742	0.2700	0.5185	-1.3125	-1.7484	-0.8766	0.6294	0.0064
PC13	0.3456	0.2494	0.4790	-1.2124	-1.6153	-0.8095	0.6625	0.0052

Lepilemur ruficaudatus

PC	Slope	Slope lower CI	Slope higher CI	Intercept	Intercept lower CI	Intercept higher CI	p value	r squared
PC1	0.8678	0.5711	1.3186	-2.7132	-3.8822	-1.5443	0.7987	0.0029
PC2	-0.8504	-1.2849	-0.5628	2.6589	1.5299	3.7879	0.3967	0.0314
PC3	0.6672	0.4391	1.0138	-2.0860	-2.9848	-1.1872	0.8038	0.0027
PC4	0.5976	0.4155	0.8596	-1.8685	-2.5629	-1.1742	0.0095	0.2580
PC5	-0.5813	-0.8341	-0.4051	1.8174	1.1466	2.4882	0.0080	0.2681
PC6	-0.5100	-0.7676	-0.3389	1.5947	0.9243	2.2651	0.2795	0.0506
PC7	0.4601	0.3027	0.6994	-1.4386	-2.0588	-0.8183	0.8597	0.0014
PC8	0.4370	0.2880	0.6632	-1.3663	-1.9530	-0.7797	0.6412	0.0096
PC9	-0.4109	-0.6198	-0.2724	1.2847	0.7415	1.8278	0.3403	0.0396
PC10	-0.3833	-0.5827	-0.2522	1.1985	0.6816	1.7154	0.8979	0.0007
PC11	-0.3307	-0.4918	-0.2224	1.0340	0.6127	1.4553	0.1085	0.1081
PC12	0.3159	0.2082	0.4794	-0.9878	-1.4118	-0.5638	0.6308	0.0102
PC13	-0.2955	-0.4448	-0.1962	0.9238	0.5351	1.3124	0.2873	0.0491

Loris tardigradus

PC	Slope	Slope lower CI	Slope higher CI	Intercept	Intercept lower CI	Intercept higher CI	p value	r squared
PC1	-0.5202	-0.6719	-0.4028	1.6294	1.2077	2.0512	0.0000	0.6057
PC2	0.3573	0.2436	0.5241	-1.1191	-1.5590	-0.6793	0.1249	0.0916
PC3	-0.2871	-0.4267	-0.1932	0.8994	0.5334	1.2654	0.4202	0.0262
PC4	-0.2401	-0.3585	-0.1609	0.7522	0.4422	1.0622	0.8353	0.0018
PC5	-0.2264	-0.3381	-0.1516	0.7092	0.4168	1.0016	0.9015	0.0006
PC6	0.2115	0.1416	0.3159	-0.6625	-0.9358	-0.3893	0.9153	0.0005
PC7	0.2051	0.1387	0.3033	-0.6426	-0.9006	-0.3845	0.2538	0.0518
PC8	0.1894	0.1286	0.2790	-0.5932	-0.8290	-0.3573	0.1807	0.0705
PC9	0.1596	0.1073	0.2373	-0.4999	-0.7038	-0.2960	0.4641	0.0216
PC10	0.1569	0.1052	0.2340	-0.4915	-0.6935	-0.2894	0.6916	0.0064
PC11	0.1432	0.0969	0.2117	-0.4486	-0.6286	-0.2685	0.2494	0.0527
PC12	0.1334	0.0896	0.1987	-0.4179	-0.5889	-0.2468	0.5446	0.0149
PC13	-0.1234	-0.1841	-0.0828	0.3866	0.2278	0.5455	0.6620	0.0078

Nycticebus bengalensis

PC	Slope	Slope lower CI	Slope higher CI	Intercept	Intercept lower CI	Intercept higher CI	p value	r squared
PC1	0.6853	0.4434	1.0591	-2.3610	-3.4218	-1.3003	0.2252	0.0726
PC2	-0.6067	-0.8305	-0.4433	2.0904	1.4233	2.7574	0.0001	0.5321
PC3	0.5495	0.3523	0.8572	-1.8933	-2.7632	-1.0235	0.4382	0.0303
PC4	-0.5167	-0.8111	-0.3292	1.7801	0.9497	2.6106	0.9363	0.0003
PC5	-0.4900	-0.7650	-0.3139	1.6882	0.9109	2.4655	0.4723	0.0261
PC6	-0.4684	-0.7309	-0.3002	1.6139	0.8719	2.3559	0.4500	0.0288
PC7	-0.3528	-0.5492	-0.2266	1.2154	0.6596	1.7712	0.3763	0.0393
PC8	-0.3144	-0.4930	-0.2005	1.0831	0.5791	1.5871	0.7477	0.0053
PC9	-0.2898	-0.4513	-0.1862	0.9986	0.5418	1.4553	0.3799	0.0388
PC10	0.2629	0.1682	0.4111	-0.9059	-1.3245	-0.4872	0.5417	0.0189
PC11	-0.2430	-0.3814	-0.1548	0.8371	0.4467	1.2276	0.9031	0.0008
PC12	0.2313	0.1474	0.3631	-0.7969	-1.1687	-0.4252	0.9336	0.0004
PC13	0.2021	0.1287	0.3172	-0.6962	-1.0209	-0.3714	0.9377	0.0003

Nycticebus coucang

PC	Slope	Slope lower CI	Slope higher CI	Intercept	Intercept lower CI	Intercept higher CI	p value	r squared
PC1	0.5777	0.4770	0.6997	-1.9212	-2.2917	-1.5507	0.0000	0.3749
PC2	-0.5329	-0.6647	-0.4273	1.7721	1.3772	2.1670	0.0005	0.1655
PC3	0.4175	0.3300	0.5281	-1.3882	-1.7178	-1.0587	0.0566	0.0532
PC4	-0.3734	-0.4727	-0.2949	1.2416	0.9458	1.5374	0.0763	0.0462
PC5	0.3462	0.2728	0.4394	-1.1514	-1.4285	-0.8743	0.1797	0.0267
PC6	-0.3097	-0.3943	-0.2433	1.0300	0.7787	1.2812	0.9460	0.0001
PC7	0.2666	0.2095	0.3392	-0.8865	-1.1022	-0.6708	0.5396	0.0056
PC8	0.2613	0.2060	0.3315	-0.8690	-1.0777	-0.6602	0.1528	0.0303
PC9	-0.2429	-0.3089	-0.1910	0.8078	0.6118	1.0039	0.3989	0.0106
PC10	-0.2374	-0.3016	-0.1868	0.7894	0.5985	0.9803	0.2810	0.0173
PC11	-0.2261	-0.2878	-0.1776	0.7517	0.5683	0.9351	0.9594	0.0000
PC12	-0.2092	-0.2658	-0.1647	0.6958	0.5277	0.8640	0.2633	0.0186
PC13	-0.1956	-0.2489	-0.1537	0.6504	0.4922	0.8087	0.5637	0.0050

Perodicticus potto

PC	Slope	Slope lower CI	Slope higher CI	Intercept	Intercept lower CI	Intercept higher CI	p value	r squared
PC1	0.7484	0.6556	0.8542	-2.4675	-2.7949	-2.1401	0.0000	0.4293
PC2	-0.6381	-0.7596	-0.5360	2.1039	1.7350	2.4728	0.4833	0.0039
PC3	0.4642	0.3900	0.5525	-1.5304	-1.7984	-1.2624	0.3747	0.0062
PC4	-0.4278	-0.5090	-0.3596	1.4106	1.1641	1.6572	0.2556	0.0102
PC5	-0.4209	-0.5011	-0.3536	1.3879	1.1445	1.6313	0.5165	0.0033
PC6	0.4040	0.3407	0.4791	-1.3321	-1.5605	-1.1037	0.0133	0.0473
PC7	0.3268	0.2750	0.3885	-1.0776	-1.2648	-0.8904	0.0947	0.0218
PC8	-0.3181	-0.3783	-0.2676	1.0490	0.8664	1.2316	0.1304	0.0179
PC9	-0.3066	-0.3651	-0.2575	1.0108	0.8334	1.1883	0.7218	0.0010
PC10	-0.2723	-0.3242	-0.2287	0.8978	0.7403	1.0552	0.5108	0.0034
PC11	-0.2552	-0.3039	-0.2143	0.8414	0.6938	0.9891	0.6146	0.0020
PC12	-0.2383	-0.2834	-0.2003	0.7856	0.6485	0.9228	0.2061	0.0126
PC13	-0.2308	-0.2746	-0.1940	0.7610	0.6280	0.8940	0.2635	0.0098

– Appendix 3 –

Allometry regression results – Inter-species

The results of inter-species major axis regressions of shape (PCs) against size (both the whole cranium ln CS and the corresponding module ln CS), for each species, for the full landmark configuration and for the 2* and Goswami models of modularity. Calculations are based on SPECIES AVERAGE results. Where the relationship was shown to be significant (p<0.003) results are underlined and shown in red.

Whole cranium against ln CS of whole cranium

PC	Mean slope	Mean slope lower CI	Mean slope higher CI	Mean intercept	Mean intercept lower CI	Mean intercept higher CI	Mean p value	Mean r squared	Mean r squared adjusted
PC1	-0.1200	0.4300	0.7100	0.5700	0.4300	0.7100	0.0000	0.7500	0.7400
PC2	-0.0200	-0.0740	0.3100	0.1200	-0.0740	0.3100	0.2900	0.0430	0.0061
PC3	-0.0230	-0.0510	0.2800	0.1100	-0.0510	0.2800	0.1500	0.0780	0.0420
PC4	0.0460	-0.3400	-0.1300	-0.2300	-0.3400	-0.1300	0.0001	0.4600	0.4400
PC5	-0.0035	-0.0960	0.1300	0.0170	-0.0960	0.1300	0.7500	0.0039	-0.0340
PC6	0.0006	-0.1000	0.1000	-0.0013	-0.1000	0.1000	0.9500	0.0001	-0.0380
PC7	0.0004	-0.0810	0.0730	-0.0041	-0.0810	0.0730	0.9500	0.0001	-0.0380
PC8	0.0040	-0.1000	0.0610	-0.0200	-0.1000	0.0610	0.6100	0.0100	-0.0280
PC9	-0.0060	-0.0200	0.0840	0.0320	-0.0200	0.0840	0.2500	0.0510	0.0150
PC10	0.0068	-0.0810	0.0130	-0.0340	-0.0810	0.0130	0.1500	0.0780	0.0430
PC11	-0.0056	-0.0500	0.1000	0.0270	-0.0500	0.1000	0.4600	0.0210	-0.0160
PC12	-0.0001	-0.0410	0.0430	0.0011	-0.0410	0.0430	0.9800	0.0000	-0.0380
PC13	0.0011	-0.0440	0.0360	-0.0041	-0.0440	0.0360	0.7700	0.0032	-0.0350

2* model face module against ln CS of whole cranium

PC	Mean slope	Mean slope lower CI	Mean slope higher CI	Mean intercept	Mean intercept lower CI	Mean intercept higher CI	Mean p value	Mean r squared	Mean r squared adjusted
PC1	0.1000	-0.6300	-0.3900	-0.5100	-0.6300	-0.3900	0.0000	0.7500	0.7400
PC2	-0.0023	-0.3000	0.3700	0.0370	-0.3000	0.3700	0.9400	0.0002	-0.0380
PC3	0.0200	-0.3000	0.1100	-0.0960	-0.3000	0.1100	0.3200	0.0380	0.0010
PC4	0.0640	-0.4500	-0.1900	-0.3200	-0.4500	-0.1900	0.0000	0.5100	0.4900
PC5	-0.0150	-0.1000	0.2400	0.0680	-0.1000	0.2400	0.3700	0.0310	-0.0064
PC6	-0.0250	-0.0089	0.2700	0.1300	-0.0089	0.2700	0.0730	0.1200	0.0840
PC7	0.0059	-0.1600	0.0940	-0.0340	-0.1600	0.0940	0.6300	0.0090	-0.0290
PC8	0.0067	-0.1400	0.0770	-0.0340	-0.1400	0.0770	0.5300	0.0150	-0.0220
PC9	-0.0074	-0.0370	0.1100	0.0370	-0.0370	0.1100	0.3200	0.0380	0.0010
PC10	-0.0048	-0.0340	0.0860	0.0260	-0.0340	0.0860	0.4200	0.0250	-0.0120
PC11	-0.0041	-0.0270	0.0690	0.0210	-0.0270	0.0690	0.3800	0.0290	-0.0079
PC12	0.0045	-0.1100	0.0630	-0.0240	-0.1100	0.0630	0.6000	0.0110	-0.0270
PC13	0.0024	-0.0570	0.0350	-0.0110	-0.0570	0.0350	0.6000	0.0100	-0.0280

2* model face module against ln CS of face

PC	Mean slope	Mean slope lower CI	Mean slope higher CI	Mean intercept	Mean intercept lower CI	Mean intercept higher CI	Mean p value	Mean r squared	Mean r squared adjusted
PC1	0.1000	-0.5300	-0.3300	-0.4300	-0.5300	-0.3300	0.0000	0.7600	0.7500
PC2	-0.0110	-0.2100	0.3500	0.0710	-0.2100	0.3500	0.7300	0.0046	-0.0340
PC3	0.0200	-0.2600	0.0950	-0.0810	-0.2600	0.0950	0.3100	0.0390	0.0025
PC4	0.0610	-0.3800	-0.1500	-0.2600	-0.3800	-0.1500	0.0000	0.4900	0.4700
PC5	-0.0140	-0.0890	0.2000	0.0540	-0.0890	0.2000	0.3900	0.0280	-0.0090
PC6	-0.0230	-0.0160	0.2200	0.1000	-0.0160	0.2200	0.0970	0.1000	0.0680
PC7	0.0072	-0.1400	0.0720	-0.0350	-0.1400	0.0720	0.5500	0.0140	-0.0240
PC8	0.0078	-0.1300	0.0600	-0.0330	-0.1300	0.0600	0.4600	0.0220	-0.0160
PC9	-0.0070	-0.0320	0.0930	0.0300	-0.0320	0.0930	0.3400	0.0350	-0.0020
PC10	-0.0044	-0.0300	0.0710	0.0210	-0.0300	0.0710	0.4600	0.0210	-0.0160
PC11	-0.0039	-0.0230	0.0580	0.0170	-0.0230	0.0580	0.4000	0.0270	-0.0100
PC12	0.0040	-0.0920	0.0550	-0.0190	-0.0920	0.0550	0.6300	0.0091	-0.0290
PC13	0.0022	-0.0480	0.0300	-0.0089	-0.0480	0.0300	0.6300	0.0093	-0.0290

2* model vault module against ln CS of whole cranium

PC	Mean slope	Mean slope lower CI	Mean slope higher CI	Mean intercept	Mean intercept lower CI	Mean intercept higher CI	Mean p value	Mean r squared	Mean r squared adjusted
PC1	0.1200	-0.7500	-0.4300	-0.5900	-0.7500	-0.4300	0.0000	0.7100	0.6900
PC2	-0.0069	-0.1800	0.2200	0.0190	-0.1800	0.2200	0.7200	0.0050	-0.0330
PC3	-0.0560	0.1000	0.4700	0.2800	0.1000	0.4700	0.0036	0.2800	0.2500
PC4	0.0300	-0.3200	0.0270	-0.1500	-0.3200	0.0270	0.0860	0.1100	0.0750
PC5	0.0072	-0.1800	0.1100	-0.0380	-0.1800	0.1100	0.6200	0.0098	-0.0280
PC6	0.0150	-0.1900	0.0380	-0.0750	-0.1900	0.0380	0.2000	0.0620	0.0260
PC7	0.0210	-0.2100	0.0070	-0.1000	-0.2100	0.0070	0.0520	0.1400	0.1000
PC8	0.0052	-0.0930	0.0400	-0.0270	-0.0930	0.0400	0.4300	0.0240	-0.0130
PC9	0.0028	-0.1000	0.0790	-0.0110	-0.1000	0.0790	0.7500	0.0038	-0.0350
PC10	0.0028	-0.1000	0.0790	-0.0110	-0.1000	0.0790	0.7500	0.0038	-0.0350
PC11	-0.0066	-0.0640	0.1200	0.0280	-0.0640	0.1200	0.4600	0.0210	-0.0170
PC12	0.0038	-0.0990	0.0540	-0.0230	-0.0990	0.0540	0.6100	0.0100	-0.0280
PC13	-0.0010	-0.0440	0.0540	0.0047	-0.0440	0.0540	0.8400	0.0015	-0.0370

2* model vault module against ln CS of vault

PC	Mean slope	Mean slope lower CI	Mean slope higher CI	Mean intercept	Mean intercept lower CI	Mean intercept higher CI	Mean p value	Mean r squared	Mean r squared adjusted
PC1	0.1300	-0.7200	-0.4000	-0.5600	-0.7200	-0.4000	0.0000	0.6800	0.6700
PC2	-0.0050	-0.1800	0.2000	0.0057	-0.1800	0.2000	0.8200	0.0020	-0.0360
PC3	-0.0650	0.1100	0.4500	0.2800	0.1100	0.4500	0.0022	0.3100	0.2800
PC4	0.0300	-0.2900	0.0460	-0.1200	-0.2900	0.0460	0.1300	0.0840	0.0490
PC5	0.0061	-0.1700	0.1100	-0.0280	-0.1700	0.1100	0.7000	0.0056	-0.0330
PC6	0.0200	-0.1900	0.0170	-0.0870	-0.1900	0.0170	0.1100	0.0960	0.0620
PC7	0.0270	-0.2100	-0.0051	-0.1100	-0.2100	-0.0051	0.0310	0.1700	0.1300
PC8	0.0071	-0.0930	0.0320	-0.0300	-0.0930	0.0320	0.3300	0.0370	-0.0004
PC9	0.0046	-0.1000	0.0690	-0.0170	-0.1000	0.0690	0.6400	0.0086	-0.0300
PC10	0.0046	-0.1000	0.0690	-0.0170	-0.1000	0.0690	0.6400	0.0086	-0.0300
PC11	0.0001	-0.0590	0.0540	-0.0025	-0.0590	0.0540	0.9900	0.0000	-0.0380
PC12	0.0017	-0.0870	0.0650	-0.0110	-0.0870	0.0650	0.8400	0.0016	-0.0370
PC13	-0.0004	-0.0440	0.0480	0.0017	-0.0440	0.0480	0.9400	0.0002	-0.0380

Goswami model face module against ln CS of whole cranium

PC	Slope	Slope (Higher CI)	Slope (Lower CI)	Intercept	Intercept (Higher CI)	Intercept (Lower CI)	p value	R squared	R Squared adjusted
PC1	0.0674	-0.6775	-0.0258	-0.3516	-0.6775	-0.0258	0.0401	0.1523	0.1197
PC2	-0.0476	-0.0393	0.5160	0.2383	-0.0393	0.5160	0.0847	0.1100	0.0758
PC3	-0.0056	-0.1673	0.2095	0.0211	-0.1673	0.2095	0.7600	0.0037	-0.0347
PC4	-0.0413	0.0533	0.3702	0.2117	0.0533	0.3702	0.0120	0.2189	0.1889
PC5	-0.0240	-0.0134	0.2336	0.1101	-0.0134	0.2336	0.0530	0.1365	0.1032
PC6	-0.0051	-0.1423	0.1930	0.0254	-0.1423	0.1930	0.7544	0.0038	-0.0345
PC7	-0.0118	-0.0688	0.1908	0.0610	-0.0688	0.1908	0.3489	0.0338	-0.0033
PC8	0.0021	-0.1136	0.0850	-0.0143	-0.1136	0.0850	0.8297	0.0018	-0.0366
PC9	-0.0092	-0.0523	0.1372	0.0425	-0.0523	0.1372	0.3225	0.0376	0.0006
PC10	0.0007	-0.0603	0.0524	-0.0040	-0.0603	0.0524	0.9028	0.0006	-0.0379
PC11	0.0115	-0.1023	-0.0099	-0.0561	-0.1023	-0.0099	0.0156	0.2048	0.1742
PC12	-0.0009	-0.0287	0.0378	0.0046	-0.0287	0.0378	0.7823	0.0030	-0.0354
PC13	0.0035	-0.0555	0.0195	-0.0180	-0.0555	0.0195	0.3510	0.0335	-0.0036

Goswami model face module against ln CS of face

PC	Slope	Slope (Higher CI)	Slope (Lower CI)	Intercept	Intercept (Higher CI)	Intercept (Lower CI)	p value	R squared	R Squared adjusted
PC1	0.0760	-0.4700	-0.0630	-0.2700	-0.4700	-0.0630	0.0130	0.2200	0.1900
PC2	-0.0270	-0.0950	0.2800	0.0910	-0.0950	0.2800	0.3100	0.0400	0.0035
PC3	-0.0036	-0.1200	0.1300	0.0053	-0.1200	0.1300	0.8400	0.0017	-0.0370
PC4	-0.0370	0.0240	0.2300	0.1300	0.0240	0.2300	0.0200	0.1900	0.1600
PC5	-0.0250	-0.0046	0.1500	0.0740	-0.0046	0.1500	0.0300	0.1700	0.1400
PC6	-0.0098	-0.0760	0.1400	0.0330	-0.0760	0.1400	0.5200	0.0160	-0.0210
PC7	-0.0084	-0.0550	0.1200	0.0300	-0.0550	0.1200	0.4800	0.0190	-0.0180
PC8	0.0039	-0.0810	0.0480	-0.0170	-0.0810	0.0480	0.6700	0.0069	-0.0310
PC9	-0.0100	-0.0300	0.0920	0.0310	-0.0300	0.0920	0.2300	0.0540	0.0170
PC10	0.0003	-0.0380	0.0350	-0.0015	-0.0380	0.0350	0.9600	0.0001	-0.0380
PC11	0.0110	-0.0660	-0.0056	-0.0360	-0.0660	-0.0056	0.0140	0.2100	0.1800
PC12	-0.0009	-0.0180	0.0250	0.0031	-0.0180	0.0250	0.7700	0.0034	-0.0350
PC13	0.0032	-0.0350	0.0130	-0.0110	-0.0350	0.0130	0.3800	0.0290	-0.0080

Goswami model orbit module against ln CS of whole cranium

PC	Slope	Slope (Higher CI)	Slope (Lower CI)	Intercept	Intercept (Higher CI)	Intercept (Lower CI)	p value	R squared	R Squared adjusted
PC1	0.0760	-0.6000	-0.1200	-0.3600	-0.6000	-0.1200	0.0025	0.3000	0.2700
PC2	0.0940	-0.8100	-0.1800	-0.4900	-0.8100	-0.1800	0.0047	0.2700	0.2400
PC3	0.1100	-0.7600	-0.2800	-0.5200	-0.7600	-0.2800	0.0001	0.4500	0.4300
PC4	-0.0300	-0.0640	0.3700	0.1500	-0.0640	0.3700	0.1600	0.0730	0.0370
PC5	-0.0008	-0.1900	0.2100	0.0078	-0.1900	0.2100	0.9700	0.0001	-0.0380
PC6	0.0100	-0.2000	0.1100	-0.0490	-0.2000	0.1100	0.4900	0.0190	-0.0190
PC7	-0.0200	-0.0500	0.2600	0.1000	-0.0500	0.2600	0.1900	0.0640	0.0280
PC8	-0.0029	-0.1100	0.1300	0.0099	-0.1100	0.1300	0.8100	0.0024	-0.0360
PC9	-0.0042	-0.0930	0.1400	0.0230	-0.0930	0.1400	0.7100	0.0053	-0.0330
PC10	0.0031	-0.0970	0.0670	-0.0150	-0.0970	0.0670	0.7100	0.0055	-0.0330
PC11	0.0051	-0.0940	0.0500	-0.0220	-0.0940	0.0500	0.4700	0.0200	-0.0180
PC12	0.0290	-0.2400	-0.0500	-0.1400	-0.2400	-0.0500	0.0034	0.2900	0.2600
PC13	-0.0016	-0.0440	0.0610	0.0082	-0.0440	0.0610	0.7500	0.0039	-0.0340

Goswami model orbit module against ln CS of orbit

PC	Slope	Slope (Higher CI)	Slope (Lower CI)	Intercept	Intercept (Higher CI)	Intercept (Lower CI)	p value	R squared	R Squared adjusted
PC1	0.0805	-0.4552	-0.0635	-0.2593	-0.4552	-0.0635	0.0055	0.2610	0.2325
PC2	0.1056	-0.6416	-0.1357	-0.3886	-0.6416	-0.1357	0.0052	0.2636	0.2352
PC3	0.1076	-0.5684	-0.1625	-0.3655	-0.5684	-0.1625	0.0006	0.3668	0.3424
PC4	-0.0271	-0.0751	0.2720	0.0984	-0.0751	0.2720	0.2623	0.0481	0.0115
PC5	0.0025	-0.1634	0.1545	-0.0044	-0.1634	0.1545	0.9095	0.0005	-0.0379
PC6	0.0082	-0.1503	0.0993	-0.0255	-0.1503	0.0993	0.6337	0.0089	-0.0293
PC7	-0.0178	-0.0550	0.1892	0.0671	-0.0550	0.1892	0.2962	0.0419	0.0050
PC8	-0.0065	-0.0746	0.1107	0.0181	-0.0746	0.1107	0.6158	0.0098	-0.0283
PC9	-0.0018	-0.0837	0.1004	0.0084	-0.0837	0.1004	0.8905	0.0007	-0.0377
PC10	0.0032	-0.0773	0.0555	-0.0109	-0.0773	0.0555	0.7355	0.0045	-0.0338
PC11	0.0057	-0.0742	0.0417	-0.0163	-0.0742	0.0417	0.4882	0.0187	-0.0191
PC12	0.0330	-0.1893	-0.0372	-0.1132	-0.1893	-0.0372	0.0036	0.2824	0.2548
PC13	-0.0034	-0.0297	0.0534	0.0118	-0.0297	0.0534	0.5627	0.0131	-0.0249

Goswami model oral module against ln CS of whole cranium

PC	Slope	Slope (Higher CI)	Slope (Lower CI)	Intercept	Intercept (Higher CI)	Intercept (Lower CI)	p value	R squared	R Squared adjusted
PC1	0.0774	-0.7964	0.0180	-0.3892	-0.7964	0.0180	0.0591	0.1303	0.0968
PC2	0.0153	-0.4571	0.3179	-0.0696	-0.4571	0.3179	0.6834	0.0065	-0.0317
PC3	-0.0710	0.1650	0.5259	0.3454	0.1650	0.5259	0.0004	0.3922	0.3689
PC4	0.0261	-0.2537	-0.0043	-0.1290	-0.2537	-0.0043	0.0388	0.1541	0.1216
PC5	0.0124	-0.1436	0.0204	-0.0616	-0.1436	0.0204	0.1312	0.0854	0.0503
PC6	-0.0162	-0.0016	0.1742	0.0863	-0.0016	0.1742	0.0676	0.1227	0.0890
PC7	0.0058	-0.0926	0.0394	-0.0266	-0.0926	0.0394	0.3719	0.0308	-0.0065
PC8	0.0041	-0.0569	0.0219	-0.0175	-0.0569	0.0219	0.2879	0.0433	0.0065
PC9	0.0041	-0.0534	0.0137	-0.0199	-0.0534	0.0137	0.2266	0.0557	0.0194
PC10	0.0034	-0.0351	0.0004	-0.0173	-0.0351	0.0004	0.0631	0.1267	0.0931
PC11	0.0032	-0.0470	0.0141	-0.0164	-0.0470	0.0141	0.2872	0.0434	0.0066
PC12	-0.0018	-0.0173	0.0361	0.0094	-0.0173	0.0361	0.5040	0.0174	-0.0204
PC13	-0.0007	-0.0103	0.0166	0.0032	-0.0103	0.0166	0.6216	0.0095	-0.0286

Goswami model oral module against ln CS of oral

PC	Slope	Slope (Higher CI)	Slope (Lower CI)	Intercept	Intercept (Higher CI)	Intercept (Lower CI)	p value	R squared	R Squared adjusted
PC1	0.0680	-0.4500	0.0330	-0.2100	-0.4500	0.0330	0.0770	0.1200	0.0810
PC2	0.0110	-0.2500	0.2000	-0.0270	-0.2500	0.2000	0.7400	0.0042	-0.0340
PC3	-0.0700	0.1100	0.3000	0.2000	0.1100	0.3000	0.0001	0.4600	0.4400
PC4	0.0230	-0.1400	0.0041	-0.0690	-0.1400	0.0041	0.0470	0.1400	0.1100
PC5	0.0120	-0.0810	0.0110	-0.0350	-0.0810	0.0110	0.1200	0.0910	0.0560
PC6	-0.0160	0.0024	0.1000	0.0530	0.0024	0.1000	0.0550	0.1300	0.1000
PC7	0.0049	-0.0500	0.0250	-0.0120	-0.0500	0.0250	0.4100	0.0260	-0.0120
PC8	0.0044	-0.0330	0.0130	-0.0100	-0.0330	0.0130	0.2200	0.0580	0.0210
PC9	0.0034	-0.0310	0.0130	-0.0092	-0.0310	0.0130	0.3300	0.0360	-0.0011
PC10	0.0026	-0.0180	0.0010	-0.0086	-0.0180	0.0010	0.0970	0.1000	0.0680
PC11	0.0032	-0.0270	0.0073	-0.0100	-0.0270	0.0073	0.2500	0.0500	0.0130
PC12	-0.0021	-0.0073	0.0210	0.0068	-0.0073	0.0210	0.3700	0.0310	-0.0064
PC13	-0.0006	-0.0056	0.0088	0.0016	-0.0056	0.0088	0.6300	0.0090	-0.0290

Goswami model zygomatic module against ln CS of whole cranium

PC	Slope	Slope (Higher CI)	Slope (Lower CI)	Intercept	Intercept (Higher CI)	Intercept (Lower CI)	p value	R squared	R Squared adjusted
PC1	-0.1800	0.6500	1.1000	0.8700	0.6500	1.1000	0.0000	0.7300	0.7200
PC2	0.0530	-0.5000	-0.0210	-0.2600	-0.5000	-0.0210	0.0300	0.1700	0.1400
PC3	0.0015	-0.1800	0.1900	0.0065	-0.1800	0.1900	0.9300	0.0003	-0.0380
PC4	-0.0380	0.0550	0.3300	0.1900	0.0550	0.3300	0.0086	0.2400	0.2100
PC5	0.0160	-0.2500	0.0710	-0.0870	-0.2500	0.0710	0.3100	0.0400	0.0034
PC6	0.0110	-0.1600	0.0490	-0.0570	-0.1600	0.0490	0.2900	0.0440	0.0069
PC7	-0.0130	-0.0160	0.1500	0.0690	-0.0160	0.1500	0.1300	0.0870	0.0520
PC8	0.0054	-0.1000	0.0450	-0.0290	-0.1000	0.0450	0.4600	0.0210	-0.0160
PC9	-0.0140	-0.0470	0.1800	0.0670	-0.0470	0.1800	0.2200	0.0570	0.0210
PC10	0.0045	-0.0810	0.0360	-0.0230	-0.0810	0.0360	0.4400	0.0240	-0.0140
PC11	-0.0120	-0.0320	0.1500	0.0600	-0.0320	0.1500	0.1700	0.0710	0.0350
PC12	-0.0044	-0.0660	0.1100	0.0200	-0.0660	0.1100	0.6000	0.0110	-0.0270
PC13	-0.0090	-0.0580	0.1500	0.0440	-0.0580	0.1500	0.3700	0.0310	-0.0064

Goswami model zygomatic module against ln CS of zygomatic

PC	Slope	Slope (Higher CI)	Slope (Lower CI)	Intercept	Intercept (Higher CI)	Intercept (Lower CI)	p value	R squared	R Squared adjusted
PC1	-0.1800	0.4500	0.7200	0.5800	0.4500	0.7200	0.0000	0.7800	0.7700
PC2	0.0440	-0.3100	0.0190	-0.1500	-0.3100	0.0190	0.0650	0.1300	0.0910
PC3	0.0110	-0.1500	0.1000	-0.0230	-0.1500	0.1000	0.5300	0.0150	-0.0230
PC4	-0.0410	0.0510	0.2300	0.1400	0.0510	0.2300	0.0033	0.2900	0.2600
PC5	0.0150	-0.1600	0.0490	-0.0580	-0.1600	0.0490	0.3300	0.0360	-0.0011
PC6	0.0099	-0.1100	0.0370	-0.0350	-0.1100	0.0370	0.3500	0.0340	-0.0029
PC7	-0.0120	-0.0120	0.1000	0.0460	-0.0120	0.1000	0.1400	0.0820	0.0460
PC8	0.0047	-0.0690	0.0320	-0.0180	-0.0690	0.0320	0.5100	0.0170	-0.0210
PC9	-0.0110	-0.0400	0.1200	0.0380	-0.0400	0.1200	0.2900	0.0420	0.0054
PC10	0.0062	-0.0600	0.0180	-0.0210	-0.0600	0.0180	0.2800	0.0450	0.0083
PC11	-0.0086	-0.0360	0.0910	0.0270	-0.0360	0.0910	0.3400	0.0360	-0.0014
PC12	-0.0042	-0.0450	0.0700	0.0130	-0.0450	0.0700	0.6100	0.0100	-0.0280
PC13	-0.0110	-0.0330	0.1100	0.0360	-0.0330	0.1100	0.2700	0.0470	0.0099

Goswami model vault module against ln CS of whole cranium

PC	Slope	Slope (Higher CI)	Slope (Lower CI)	Intercept	Intercept (Higher CI)	Intercept (Lower CI)	p value	R squared	R Squared adjusted
PC1	-0.1200	0.3800	0.8300	0.6100	0.3800	0.8300	0.0000	0.5500	0.5400
PC2	0.0500	-0.5300	0.0370	-0.2500	-0.5300	0.0370	0.0830	0.1100	0.0770
PC3	0.0170	-0.3200	0.1300	-0.0950	-0.3200	0.1300	0.4500	0.0220	-0.0160
PC4	0.0200	-0.2800	0.0960	-0.0930	-0.2800	0.0960	0.2800	0.0450	0.0080
PC5	-0.0075	-0.1100	0.2000	0.0430	-0.1100	0.2000	0.6300	0.0091	-0.0290
PC6	0.0170	-0.1700	0.0096	-0.0820	-0.1700	0.0096	0.0690	0.1200	0.0880
PC7	-0.0043	-0.1200	0.1500	0.0150	-0.1200	0.1500	0.7400	0.0043	-0.0340
PC8	0.0120	-0.1500	0.0220	-0.0620	-0.1500	0.0220	0.1500	0.0780	0.0430
PC9	0.0068	-0.0860	0.0220	-0.0320	-0.0860	0.0220	0.2100	0.0590	0.0230
PC10	-0.0067	-0.0460	0.1200	0.0350	-0.0460	0.1200	0.4000	0.0270	-0.0100
PC11	0.0023	-0.0660	0.0430	-0.0110	-0.0660	0.0430	0.6700	0.0069	-0.0310
PC12	0.0004	-0.0430	0.0370	-0.0029	-0.0430	0.0370	0.9200	0.0004	-0.0380
PC13	0.0033	-0.0560	0.0240	-0.0160	-0.0560	0.0240	0.4100	0.0260	-0.0110

Goswami model vault module against ln CS of vault

PC	Slope	Slope (Higher CI)	Slope (Lower CI)	Intercept	Intercept (Higher CI)	Intercept (Lower CI)	p value	R squared	R Squared adjusted
PC1	-0.1400	0.2900	0.7200	0.5000	0.2900	0.7200	0.0000	0.4900	0.4700
PC2	0.0610	-0.4800	0.0200	-0.2300	-0.4800	0.0200	0.0660	0.1200	0.0900
PC3	0.0280	-0.3000	0.0770	-0.1100	-0.3000	0.0770	0.2700	0.0470	0.0100
PC4	0.0190	-0.2400	0.1100	-0.0660	-0.2400	0.1100	0.3800	0.0300	-0.0075
PC5	-0.0088	-0.0970	0.1800	0.0390	-0.0970	0.1800	0.6200	0.0096	-0.0290
PC6	0.0210	-0.1500	0.0029	-0.0750	-0.1500	0.0029	0.0490	0.1400	0.1100
PC7	-0.0054	-0.1100	0.1300	0.0140	-0.1100	0.1300	0.7300	0.0048	-0.0330
PC8	0.0100	-0.1100	0.0350	-0.0400	-0.1100	0.0350	0.3100	0.0400	0.0030
PC9	0.0110	-0.0820	0.0064	-0.0380	-0.0820	0.0064	0.0800	0.1100	0.0790
PC10	-0.0038	-0.0540	0.0870	0.0170	-0.0540	0.0870	0.6800	0.0068	-0.0310
PC11	0.0039	-0.0600	0.0310	-0.0140	-0.0600	0.0310	0.5200	0.0160	-0.0220
PC12	0.0005	-0.0380	0.0320	-0.0030	-0.0380	0.0320	0.9100	0.0005	-0.0380
PC13	0.0029	-0.0440	0.0220	-0.0110	-0.0440	0.0220	0.5100	0.0170	-0.0210

Goswami model base module against ln CS of whole cranium

PC	Slope	Slope (Higher CI)	Slope (Lower CI)	Intercept	Intercept (Higher CI)	Intercept (Lower CI)	p value	R squared	R Squared adjusted
PC1	-0.0340	-0.0480	0.4200	0.1800	-0.0480	0.4200	0.1400	0.0830	0.0480
PC2	-0.0860	0.2200	0.6000	0.4100	0.2200	0.6000	0.0001	0.4500	0.4300
PC3	-0.0430	-0.0410	0.4800	0.2200	-0.0410	0.4800	0.0960	0.1000	0.0690
PC4	-0.0064	-0.0830	0.1400	0.0300	-0.0830	0.1400	0.5700	0.0130	-0.0250
PC5	0.0280	-0.2600	-0.0220	-0.1400	-0.2600	-0.0220	0.0200	0.1900	0.1600
PC6	0.0210	-0.2200	0.0073	-0.1100	-0.2200	0.0073	0.0700	0.1200	0.0870
PC7	0.0033	-0.0880	0.0510	-0.0180	-0.0880	0.0510	0.6300	0.0091	-0.0290
PC8	-0.0008	-0.0870	0.0970	0.0049	-0.0870	0.0970	0.9300	0.0003	-0.0380
PC9	-0.0084	-0.0190	0.1000	0.0420	-0.0190	0.1000	0.1700	0.0720	0.0360
PC10	-0.0081	-0.0060	0.0890	0.0410	-0.0060	0.0890	0.0930	0.1000	0.0700
PC11	-0.0041	-0.0350	0.0710	0.0180	-0.0350	0.0710	0.4400	0.0230	-0.0140
PC12	0.0077	-0.0870	0.0079	-0.0390	-0.0870	0.0079	0.1100	0.0970	0.0630
PC13	0.0038	-0.0440	0.0085	-0.0180	-0.0440	0.0085	0.1600	0.0750	0.0400

Goswami model base module against ln CS of base

PC	Slope	Slope (Higher CI)	Slope (Lower CI)	Intercept	Intercept (Higher CI)	Intercept (Lower CI)	p value	R squared	R Squared adjusted
PC1	-0.0310	-0.0710	0.3000	0.1100	-0.0710	0.3000	0.2600	0.0480	0.0110
PC2	-0.1200	0.2100	0.4900	0.3500	0.2100	0.4900	0.0000	0.5400	0.5200
PC3	-0.0320	-0.1100	0.3200	0.1100	-0.1100	0.3200	0.3200	0.0380	0.0013
PC4	-0.0068	-0.0680	0.1100	0.0200	-0.0680	0.1100	0.6200	0.0097	-0.0280
PC5	0.0340	-0.2000	-0.0160	-0.1100	-0.2000	-0.0160	0.0210	0.1900	0.1600
PC6	0.0130	-0.1300	0.0400	-0.0430	-0.1300	0.0400	0.3100	0.0390	0.0020
PC7	0.0041	-0.0680	0.0390	-0.0150	-0.0680	0.0390	0.6200	0.0095	-0.0290
PC8	0.0015	-0.0770	0.0690	-0.0039	-0.0770	0.0690	0.8900	0.0007	-0.0380
PC9	-0.0099	-0.0160	0.0780	0.0310	-0.0160	0.0780	0.1800	0.0680	0.0330
PC10	-0.0083	-0.0094	0.0650	0.0280	-0.0094	0.0650	0.1500	0.0760	0.0410
PC11	-0.0058	-0.0250	0.0570	0.0160	-0.0250	0.0570	0.3600	0.0320	-0.0056
PC12	0.0120	-0.0740	-0.0045	-0.0390	-0.0740	-0.0045	0.0320	0.1700	0.1300
PC13	0.0042	-0.0330	0.0080	-0.0120	-0.0330	0.0080	0.2000	0.0630	0.0270

The results of inter-species major axis regressions of shape (PCs) against size (both the whole cranium ln CS and the corresponding module ln CS), for each species, for the full landmark configuration and for the 2* and Goswami models of modularity. Calculations use the RESAMPLING METHOD. Where the relationship was shown to be significant (p<0.003) results are underlined and shown in red.

Whole cranium against ln CS of whole cranium

PC	Mean slope	Mean slope lower CI	Mean slope higher CI	Mean intercept	Mean intercept lower CI	Mean intercept higher CI	Mean p value	Mean r squared	Mean r squared adjusted
PC1	-0.1100	-0.1400	-0.0780	0.5400	0.5100	0.5700	0.0000	0.6200	0.6100
PC2	-0.0240	-0.0640	0.0170	0.1350	0.0950	0.1760	0.3190	0.0560	0.0200
PC3	-0.0200	-0.0540	0.0140	0.0990	0.0650	0.1330	0.3100	0.0620	0.0260
PC4	0.0495	0.0268	0.0722	-0.2485	-0.2711	-0.2258	0.0009	0.4130	0.3904
PC5	-0.0025	-0.0303	0.0253	0.0129	-0.0150	0.0407	0.6569	0.0145	-0.0234
PC6	-0.0007	-0.0216	0.0202	0.0063	-0.0146	0.0272	0.6276	0.0166	-0.0212
PC7	0.0021	-0.0163	0.0205	-0.0126	-0.0310	0.0058	0.6294	0.0176	-0.0202
PC8	0.0059	-0.0128	0.0247	-0.0284	-0.0472	-0.0097	0.5411	0.0254	-0.0121
PC9	-0.0059	-0.0205	0.0086	0.0319	0.0173	0.0464	0.4509	0.0406	0.0037
PC10	0.0065	-0.0072	0.0202	-0.0324	-0.0461	-0.0187	0.3946	0.0535	0.0171
PC11	-0.0041	-0.0186	0.0104	0.0196	0.0051	0.0341	0.5325	0.0284	-0.0089
PC12	0.0000	-0.0140	0.0130	0.0007	-0.0130	0.0140	0.5800	0.0230	-0.0150
PC13	0.0004	-0.0117	0.0126	-0.0007	-0.0129	0.0115	0.5594	0.0260	9.0000

2* model face module against ln CS of whole cranium

PC	Mean slope	Mean slope lower CI	Mean slope higher CI	Mean intercept	Mean intercept lower CI	Mean intercept higher CI	Mean p value	Mean r squared	Mean r squared adjusted
PC1	0.1100	0.1400	0.0780	-0.5400	-0.5100	-0.5700	0.0000	0.6400	0.6300
PC2	-0.0046	0.0659	-0.0751	0.048	0.1185	-0.0225	0.6924	0.0112	-0.0268
PC3	0.0167	0.064	-0.0306	-0.079	-0.0317	-0.1263	0.5067	0.032	-0.0052
PC4	0.0635	0.094	0.033	-0.3195	-0.289	-0.35	0.0025	0.3926	0.3693
PC5	-0.0084	0.026	-0.0428	0.0379	0.0723	0.0035	0.5521	0.0271	-0.0104
PC6	-0.017	0.013	-0.046	0.087	0.117	0.057	0.355	0.06	0.023
PC7	-0.0011	0.0219	-0.0241	0.0017	0.0247	-0.0213	0.6058	0.0197	-0.0180
PC8	0.0087	0.0328	-0.0154	-0.0418	-0.0177	-0.0658	0.4764	0.0381	0.0011
PC9	-0.00731	0.01357	-0.02819	0.03712	0.058	0.01625	0.47388	0.03745	0.00043
PC10	-0.0039	0.015	-0.0229	0.0217	0.0406	0.0027	0.512	0.0335	-0.0036
PC11	-0.0037	0.0141	-0.0216	0.0189	0.0368	0.0011	0.5211	0.0312	-0.006
PC12	-0.00028	0.01872	-0.01927	0.00089	0.01988	-0.0181	0.5817	0.02265	-0.01494
PC13	0.0025	0.0191	-0.0141	-0.012	0.0046	-0.0285	0.5502	0.0271	-0.0103

2* model face module against ln CS of face

PC	Mean slope	Mean slope lower CI	Mean slope higher CI	Mean intercept	Mean intercept lower CI	Mean intercept higher CI	Mean p value	Mean r squared	Mean r squared adjusted
PC1	0.1100	0.1400	0.0770	-0.4500	-0.4200	-0.4800	0.0000	0.6500	0.6400
PC2	-0.0140	0.0540	-0.0830	0.0870	0.1550	0.0180	0.6280	0.0170	-0.0200
PC3	0.0164	0.0625	-0.0296	-0.0663	-0.0203	-0.1123	0.5034	0.0327	-0.0045
PC4	0.0610	0.0911	0.0309	-0.2639	-0.2338	-0.2940	0.0028	0.3796	0.3557
PC5	-0.0075	0.0259	-0.0409	0.0283	0.0617	-0.0051	0.5500	0.0257	-0.0118
PC6	-0.0150	0.0140	-0.0440	0.0690	0.0980	0.0400	0.3750	0.0560	0.0190
PC7	0.0000	0.0230	-0.0230	-0.0039	0.0190	-0.0270	0.6000	0.0210	-0.0170
PC8	0.0110	0.0340	-0.0130	-0.0440	-0.0200	-0.0670	0.4250	0.0480	0.0110
PC9	-0.0069	0.0135	-0.0272	0.0300	0.0503	0.0096	0.4882	0.0360	-0.0010
PC10	-0.0042	0.0145	-0.0229	0.0198	0.0385	0.0011	0.5151	0.0341	-0.0031
PC11	-0.0034	0.0142	-0.0210	0.0154	0.0330	-0.0022	0.5239	0.0324	-0.0048
PC12	-0.0003	0.0181	-0.0188	0.0008	0.0192	-0.0177	0.5767	0.0238	-0.0138
PC13	0.0023	0.0185	-0.0140	-0.0093	0.0070	-0.0255	0.5328	0.0296	-0.0077

2* model vault module against ln CS of whole cranium

PC	Mean slope	Mean slope lower CI	Mean slope higher CI	Mean intercept	Mean intercept lower CI	Mean intercept higher CI	Mean p value	Mean r squared	Mean r squared adjusted
PC1	0.1200	0.1600	0.0780	-0.5700	-0.5300	-0.6100	0.0000	0.5700	0.5600
PC2	-0.0032	0.0445	-0.0510	0.0014	0.0492	-0.0463	0.6635	0.0140	-0.0240
PC3	-0.0590	-0.0170	-0.1010	0.3020	0.3440	0.2600	0.0250	0.2320	0.2020
PC4	0.0270	0.0700	-0.0170	-0.1320	-0.0890	-0.1750	0.3070	0.0670	0.0310
PC5	0.0060	0.0389	-0.0268	-0.0340	-0.0011	-0.0669	0.5814	0.0208	-0.0168
PC6	0.0150	0.0440	-0.0140	-0.0790	-0.0500	-0.1080	0.3650	0.0510	0.0140
PC7	0.0043	0.0283	-0.0196	-0.0220	0.0019	-0.0460	0.5279	0.0316	-0.0057
PC8	0.0186	0.0449	-0.0077	-0.0896	-0.0633	-0.1160	0.2629	0.0857	0.0506
PC9	0.0054	0.0266	-0.0157	-0.0276	-0.0065	-0.0487	0.5096	0.0340	-0.0031
PC10	0.0047	0.0244	-0.0150	-0.0213	-0.0016	-0.0411	0.5058	0.0348	-0.0023
PC11	-0.0009	0.0184	-0.0202	0.0020	0.0213	-0.0172	0.5713	0.0234	-0.0142
PC12	0.0018	0.0230	-0.0194	-0.0121	0.0091	-0.0332	0.5858	0.0221	-0.0156
PC13	-0.0022	0.0144	-0.0188	0.0107	0.0274	-0.0059	0.5471	0.0282	-0.0092

2* model vault module against ln CS of vault

PC	Mean slope	Mean slope lower CI	Mean slope higher CI	Mean intercept	Mean intercept lower CI	Mean intercept higher CI	Mean p value	Mean r squared	Mean r squared adjusted
PC1	0.1300	0.1700	0.0840	-0.5400	-0.4900	-0.5800	0.0000	0.5500	0.5300
PC2	0.0019	0.0563	-0.0525	-0.0224	0.032	-0.0767	0.6754	0.0123	-0.0257
PC3	-0.066	-0.02	-0.112	0.286	0.333	0.24	0.023	0.235	0.206
PC4	0.027	0.076	-0.023	-0.112	-0.063	-0.162	0.354	0.053	0.017
PC5	0.0059	0.0423	-0.0304	-0.029	0.0073	-0.0653	0.614	0.0179	-0.0198
PC6	0.021	0.053	-0.011	-0.091	-0.059	-0.123	0.265	0.071	0.035
PC7	0.0047	0.0313	-0.0218	-0.0205	0.006	-0.047	0.5189	0.033	-0.0042
PC8	0.0247	0.0533	-0.0039	-0.1012	-0.0726	-0.1299	0.1839	0.1149	0.0809
PC9	0.0068	0.0302	-0.0167	-0.0292	-0.0057	-0.0526	0.501	0.0342	-0.003
PC10	0.0068	0.0286	-0.015	-0.0269	-0.005	-0.0487	0.4811	0.0385	0.0015
PC11	-0.00023	0.02096	-0.02141	-0.00133	0.01986	-0.02251	0.56879	0.02388	-0.01366
PC12	-0.0014	0.0221	-0.0248	0.0025	0.0259	-0.0209	0.5918	0.0207	-0.017
PC13	-0.001	0.0172	-0.0193	0.0042	0.0225	-0.014	0.543	0.0271	-0.0103

Goswami model face module against ln CS of whole cranium

PC	Slope	Slope (Higher CI)	Slope (Lower CI)	Intercept	Intercept (Higher CI)	Intercept (Lower CI)	p value	R squared	R Squared adjusted
PC1	0.0690	0.1420	-0.0050	-0.3570	-0.2840	-0.4310	0.1190	0.1210	0.0870
PC2	-0.0624	0.0017	-0.1265	0.3111	0.3752	0.2470	0.1208	0.1337	0.1004
PC3	0.0005	0.0382	-0.0372	-0.0099	0.0278	-0.0476	0.5765	0.0246	-0.0129
PC4	-0.0250	0.0120	-0.0620	0.1310	0.1680	0.0950	0.2840	0.0830	0.0480
PC5	-0.0223	0.0085	-0.0531	0.1043	0.1351	0.0736	0.2426	0.0881	0.0530
PC6	-0.0007	0.0345	-0.0357	0.0038	0.0389	-0.0313	0.6621	0.0134	-0.0246
PC7	-0.0140	0.0200	-0.0470	0.0690	0.1030	0.0350	0.4430	0.0430	0.0060
PC8	0.0018	0.0260	-0.0224	-0.0112	0.0130	-0.0354	0.5626	0.0259	-0.0116
PC9	-0.0061	0.0163	-0.0285	0.0283	0.0507	0.0060	0.5230	0.0327	-0.0045
PC10	0.0004	0.0197	-0.0189	-0.0029	0.0165	-0.0221	0.5439	0.0296	-0.0078
PC11	0.0070	0.0250	-0.0110	-0.0340	-0.0160	-0.0520	0.4260	0.0510	0.0150
PC12	-0.0013	0.0156	-0.0183	0.0067	0.0237	-0.0102	0.5066	0.0338	-0.0033
PC13	0.0039	0.0197	-0.0118	-0.0203	-0.0046	-0.0361	0.4941	0.0393	0.0024

Goswami model face module against ln CS of face

PC	Slope	Slope (Higher CI)	Slope (Lower CI)	Intercept	Intercept (Higher CI)	Intercept (Lower CI)	p value	R squared	R Squared adjusted
PC1	0.0756	0.1430	0.0082	-0.2657	-0.1983	-0.3331	0.0679	0.1640	0.1319
PC2	-0.0370	0.0260	-0.1000	0.1240	0.1870	0.0620	0.3200	0.0620	0.0260
PC3	0.0012	0.0377	-0.0353	-0.0110	0.0255	-0.0475	0.5672	0.0254	-0.0121
PC4	-0.0210	0.0140	-0.0570	0.0770	0.1130	0.0420	0.3340	0.0690	0.0330
PC5	-0.0249	0.0043	-0.0541	0.0757	0.1049	0.0466	0.1936	0.1112	0.0771
PC6	-0.0062	0.0272	-0.0397	0.0211	0.0546	-0.0123	0.6218	0.0184	-0.0194
PC7	-0.0117	0.0204	-0.0437	0.0401	0.0722	0.0080	0.4646	0.0387	0.0018
PC8	0.0034	0.0268	-0.0200	-0.0133	0.0101	-0.0368	0.5516	0.0282	-0.0092
PC9	-0.0076	0.0142	-0.0294	0.0226	0.0444	0.0008	0.4857	0.0378	0.0008
PC10	0.0002	0.0187	-0.0184	-0.0011	0.0175	-0.0196	0.5290	0.0323	-0.0050
PC11	0.0069	0.0244	-0.0107	-0.0220	-0.0044	-0.0396	0.4282	0.0521	0.0156
PC12	-0.0018	0.0146	-0.0182	0.0059	0.0223	-0.0105	0.5050	0.0361	-0.0010
PC13	0.0035	0.0189	-0.0119	-0.0123	0.0031	-0.0277	0.5092	0.0354	-0.0017

Goswami model orbit module against ln CS of whole cranium

PC	Slope	Slope (Higher CI)	Slope (Lower CI)	Intercept	Intercept (Higher CI)	Intercept (Lower CI)	p value	R squared	R Squared adjusted
PC1	0.0785	0.1543	0.0027	-0.3725	-0.2967	-0.4483	0.1158	0.1519	0.1193
PC2	0.0960	0.1700	0.0220	-0.5030	-0.4290	-0.5770	0.0390	0.2060	0.1750
PC3	0.0973	0.1513	0.0434	-0.4799	-0.4259	-0.5338	0.0052	0.3261	0.3002
PC4	-0.0163	0.0325	-0.0650	0.0846	0.1334	0.0359	0.5108	0.0321	-0.0052
PC5	0.0140	0.0586	-0.0306	-0.0675	-0.0229	-0.1120	0.4982	0.0323	-0.0049
PC6	0.0140	0.0504	-0.0223	-0.0680	-0.0316	-0.1043	0.4554	0.0415	0.0046
PC7	-0.0099	0.0279	-0.0477	0.0528	0.0906	0.0150	0.5338	0.0310	-0.0063
PC8	-0.0075	0.0231	-0.0382	0.0329	0.0635	0.0023	0.4942	0.0369	-0.0002
PC9	-0.0050	0.0250	-0.0350	0.0274	0.0574	-0.0026	0.5659	0.0243	-0.0132
PC10	0.0034	0.0301	-0.0233	-0.0164	0.0103	-0.0431	0.5707	0.0252	-0.0123
PC11	0.0065	0.0306	-0.0176	-0.0286	-0.0045	-0.0527	0.5211	0.0325	-0.0047
PC12	0.0094	0.0324	-0.0135	-0.0466	-0.0236	-0.0695	0.4560	0.0433	0.0065
PC13	-0.0009	0.0195	-0.0213	0.0049	0.0252	-0.0155	0.5705	0.0271	-0.0103

Goswami model orbit module against ln CS of orbit

PC	Slope	Slope (Higher CI)	Slope (Lower CI)	Intercept	Intercept (Higher CI)	Intercept (Lower CI)	p value	R squared	R Squared adjusted
PC1	0.0786	0.1650	-0.0078	-0.2534	-0.1670	-0.3398	0.1588	0.1251	0.0915
PC2	0.1080	0.1910	0.0260	-0.3980	-0.3150	-0.4810	0.0380	0.2090	0.1790
PC3	0.1000	0.1620	0.0380	-0.3420	-0.2800	-0.4030	0.0110	0.2810	0.2540
PC4	-0.0152	0.0414	-0.0718	0.0568	0.1134	0.0002	0.5560	0.0256	-0.0119
PC5	0.0197	0.0697	-0.0303	-0.0660	-0.0160	-0.1160	0.4348	0.0439	0.0071
PC6	0.0128	0.0547	-0.0291	-0.0426	-0.0007	-0.0845	0.4967	0.0347	-0.0024
PC7	-0.0085	0.0344	-0.0514	0.0328	0.0757	-0.0101	0.5607	0.0261	-0.0114
PC8	-0.0110	0.0230	-0.0460	0.0350	0.0690	-0.0001	0.4800	0.0420	0.0048
PC9	-0.0038	0.0306	-0.0382	0.0157	0.0502	-0.0187	0.6004	0.0207	-0.0170
PC10	0.0030	0.0330	-0.0270	-0.0100	0.0200	-0.0410	0.5710	0.0230	-0.0150
PC11	0.0072	0.0351	-0.0206	-0.0214	0.0064	-0.0493	0.5134	0.0345	-0.0026
PC12	0.0106	0.0365	-0.0153	-0.0363	-0.0104	-0.0622	0.4498	0.0454	0.0087
PC13	-0.0024	0.0209	-0.0258	0.0086	0.0320	-0.0147	0.5427	0.0290	-0.0083

Goswami model oral module against ln CS of whole cranium

PC	Slope	Slope (Higher CI)	Slope (Lower CI)	Intercept	Intercept (Higher CI)	Intercept (Lower CI)	p value	R squared	R Squared adjusted
PC1	0.0810	0.1770	-0.0150	-0.4050	-0.3090	-0.5010	0.1980	0.1170	0.0830
PC2	-0.0310	0.0550	-0.1160	0.1570	0.2430	0.0710	0.4200	0.0600	0.0240
PC3	-0.0820	-0.0320	-0.1320	0.4010	0.4510	0.3510	0.0190	0.2940	0.2670
PC4	0.0247	0.0572	-0.0078	-0.1227	-0.0902	-0.1552	0.2294	0.0937	0.0588
PC5	0.0095	0.0357	-0.0168	-0.0474	-0.0212	-0.0736	0.4488	0.0481	0.0115
PC6	-0.0144	0.0081	-0.0370	0.0763	0.0988	0.0537	0.3026	0.0716	0.0359
PC7	0.0040	0.0216	-0.0137	-0.0182	-0.0006	-0.0359	0.5107	0.0374	0.0004
PC8	0.0018	0.0173	-0.0138	-0.0070	0.0086	-0.0225	0.5131	0.0320	-0.0052
PC9	0.0034	0.0186	-0.0119	-0.0161	-0.0008	-0.0314	0.4805	0.0412	0.0043
PC10	0.0035	0.0149	-0.0080	-0.0179	-0.0064	-0.0293	0.4689	0.0429	0.0061
PC11	0.0017	0.0128	-0.0094	-0.0086	0.0026	-0.0197	0.5180	0.0343	-0.0028
PC12	-0.0015	0.0091	-0.0120	0.0079	0.0184	-0.0026	0.5395	0.0303	-0.0070
PC13	-0.0008	0.0082	-0.0097	0.0036	0.0125	-0.0054	0.5039	0.0353	-0.0018

Goswami model oral module against ln CS of oral

PC	Slope	Slope (Higher CI)	Slope (Lower CI)	Intercept	Intercept (Higher CI)	Intercept (Lower CI)	p value	R squared	R Squared adjusted
PC1	0.0710	0.1560	-0.0150	-0.2170	-0.1320	-0.3020	0.2080	0.1140	0.0800
PC2	-0.0220	0.0550	-0.0990	0.0700	0.1470	-0.0070	0.4060	0.0640	0.0280
PC3	-0.0826	-0.0410	-0.1241	0.2416	0.2831	0.2000	0.0095	0.3740	0.3499
PC4	0.0225	0.0521	-0.0071	-0.0677	-0.0380	-0.0973	0.2293	0.0930	0.0581
PC5	0.0082	0.0312	-0.0147	-0.0253	-0.0023	-0.0482	0.4521	0.0477	0.0110
PC6	-0.0126	0.0079	-0.0330	0.0426	0.0630	0.0221	0.3148	0.0683	0.0325
PC7	0.0033	0.0189	-0.0122	-0.0084	0.0071	-0.0239	0.5059	0.0357	-0.0014
PC8	0.0014	0.0152	-0.0125	-0.0024	0.0114	-0.0163	0.5137	0.0340	-0.0031
PC9	0.0025	0.0159	-0.0109	-0.0072	0.0062	-0.0206	0.4832	0.0404	0.0035
PC10	0.0025	0.0127	-0.0077	-0.0082	0.0020	-0.0184	0.4813	0.0400	0.0030
PC11	0.0018	0.0117	-0.0080	-0.0057	0.0041	-0.0156	0.4978	0.0353	-0.0018
PC12	-0.0018	0.0074	-0.0109	0.0061	0.0153	-0.0030	0.5178	0.0336	-0.0036
PC13	-0.0003	0.0075	-0.0081	0.0009	0.0087	-0.0069	0.5247	0.0332	-0.0040

Goswami model zygomatic module against ln CS of whole cranium

PC	Slope	Slope (Higher CI)	Slope (Lower CI)	Intercept	Intercept (Higher CI)	Intercept (Lower CI)	p value	R squared	R Squared adjusted
PC1	-0.1800	-0.1300	-0.2300	0.8800	0.9300	0.8300	0.0000	0.6400	0.6300
PC2	0.0420	0.1070	-0.0220	-0.2110	-0.1470	-0.2760	0.2830	0.0730	0.0370
PC3	0.0094	0.0542	-0.0354	-0.0327	0.0121	-0.0775	0.5892	0.0211	-0.0165
PC4	-0.0444	-0.0041	-0.0846	0.2252	0.2655	0.1850	0.0993	0.1665	0.1344
PC5	-0.0223	0.0085	-0.0531	0.1043	0.1351	0.0736	0.2426	0.0881	0.053
PC6	0.0114	0.0444	-0.0216	-0.0574	-0.0245	-0.0904	0.4732	0.0402	0.0033
PC7	-0.0120	0.0180	-0.0430	0.0640	0.0950	0.0330	0.4230	0.0510	0.0150
PC8	0.0071	0.0349	-0.0206	-0.0370	-0.0093	-0.0648	0.4499	0.0485	0.0119
PC9	-0.0066	0.0215	-0.0346	0.0321	0.0601	0.0041	0.5271	0.0314	-0.0058
PC10	0.0041	0.0293	-0.0210	-0.0206	0.0046	-0.0457	0.4848	0.0399	0.0030
PC11	-0.0061	0.0179	-0.0300	0.0282	0.0521	0.0042	0.4906	0.0408	0.0039
PC12	-0.0040	0.0180	-0.0260	0.0170	0.0390	-0.0051	0.4900	0.0370	-0.0001
PC13	-0.0053	0.0187	-0.0293	0.0269	0.0509	0.0029	0.5195	0.0352	-0.0059

Goswami model face module against ln CS of zygomatic

PC	Slope	Slope (Higher CI)	Slope (Lower CI)	Intercept	Intercept (Higher CI)	Intercept (Lower CI)	p value	R squared	R Squared adjusted
PC1	-0.1800	-0.1300	-0.2300	0.5800	0.6300	0.5400	0.0000	0.6700	0.6600
PC2	0.0370	0.0990	-0.0250	-0.1260	-0.0640	-0.1880	0.3290	0.0640	0.0280
PC3	0.0181	0.0605	-0.0244	-0.0470	-0.0046	-0.0895	0.4341	0.0424	0.0056
PC4	-0.0460	-0.0070	-0.0850	0.1590	0.1980	0.1200	0.0730	0.1810	0.1500
PC5	0.0046	0.0469	-0.0377	-0.0211	0.0213	-0.0634	0.5769	0.0239	-0.0137
PC6	0.0092	0.0415	-0.0232	-0.0316	0.0007	-0.0639	0.4778	0.0382	0.0012
PC7	-0.0120	0.0180	-0.0430	0.0430	0.0740	0.0130	0.4210	0.0510	0.0150
PC8	0.0056	0.0330	-0.0218	-0.0202	0.0071	-0.0476	0.4627	0.0439	0.0071
PC9	-0.0044	0.0231	-0.0318	0.0144	0.0418	-0.0131	0.5352	0.0295	-0.0078
PC10	0.0061	0.0309	-0.0187	-0.0204	0.0044	-0.0452	0.4732	0.0420	0.0052
PC11	-0.0041	0.0197	-0.0280	0.0121	0.0360	-0.0117	0.4937	0.0402	0.0033
PC12	-0.0047	0.0168	-0.0261	0.0129	0.0344	-0.0086	0.4950	0.0372	0.0002
PC13	-0.0041	0.0195	-0.0277	0.0147	0.0383	-0.0089	0.5405	0.0307	-0.0105

Goswami model vault module against ln CS of whole cranium

PC	Slope	Slope (Higher CI)	Slope (Lower CI)	Intercept	Intercept (Higher CI)	Intercept (Lower CI)	p value	R squared	R Squared adjusted
PC1	-0.1210	-0.0629	-0.1791	0.5917	0.6498	0.5336	0.0021	0.3919	0.3685
PC2	0.0480	0.1170	-0.0200	-0.2420	-0.1740	-0.3100	0.2620	0.0850	0.0500
PC3	0.0226	0.0726	-0.0274	-0.1224	-0.0724	-0.1724	0.4180	0.0455	0.0088
PC4	0.0210	0.0660	-0.0230	-0.1020	-0.0570	-0.1470	0.4030	0.0500	0.0140
PC5	-0.0070	0.0313	-0.0454	0.0381	0.0764	-0.0003	0.5546	0.0256	-0.0119
PC6	0.0118	0.0410	-0.0175	-0.0589	-0.0297	-0.0881	0.4373	0.0465	0.0099
PC7	-0.0017	0.0272	-0.0306	0.0051	0.0340	-0.0238	0.5772	0.0236	-0.0139
PC8	0.0077	0.0317	-0.0164	-0.0402	-0.0161	-0.0642	0.4744	0.0401	0.0032
PC9	0.0059	0.0262	-0.0145	-0.0281	-0.0078	-0.0484	0.4827	0.0409	0.0040
PC10	0.0015	0.0217	-0.0187	-0.0063	0.0138	-0.0265	0.5434	0.0287	-0.0087
PC11	0.0039	0.0237	-0.0159	-0.0193	0.0005	-0.0391	0.5110	0.0352	-0.0019
PC12	0.0003	0.0163	-0.0157	-0.0024	0.0136	-0.0183	0.5198	0.0339	-0.0033
PC13	0.0030	0.0182	-0.0121	-0.0149	0.0002	-0.0301	0.5299	0.0305	-0.0068

Goswami model vault module against ln CS of vault

PC	Slope	Slope (Higher CI)	Slope (Lower CI)	Intercept	Intercept (Higher CI)	Intercept (Lower CI)	p value	R squared	R Squared adjusted
PC1	-0.1252	-0.0552	-0.1953	0.4569	0.5269	0.3869	0.0052	0.3236	0.2976
PC2	0.0480	0.1240	-0.0290	-0.1800	-0.1040	-0.2570	0.3040	0.0700	0.0340
PC3	0.0340	0.0890	-0.0200	-0.1370	-0.0830	-0.1920	0.2930	0.0730	0.0380
PC4	0.0190	0.0690	-0.0310	-0.0650	-0.0150	-0.1200	0.4800	0.0370	0.0000
PC5	-0.0098	0.0331	-0.0527	0.0392	0.0821	-0.0037	0.5568	0.0268	-0.0107
PC6	0.0170	0.0490	-0.0150	-0.0630	-0.0310	-0.0950	0.3780	0.0600	0.0230
PC7	-0.0015	0.0305	-0.0335	0.0025	0.0345	-0.0296	0.5631	0.0254	-0.0121
PC8	0.0051	0.0321	-0.0220	-0.0212	0.0059	-0.0482	0.5276	0.0313	-0.0059
PC9	0.0110	0.0330	-0.0120	-0.0380	-0.0160	-0.0610	0.3900	0.0570	0.0210
PC10	0.0047	0.0272	-0.0179	-0.0163	0.0063	-0.0388	0.5201	0.0325	-0.0048
PC11	0.0065	0.0282	-0.0152	-0.0241	-0.0024	-0.0457	0.4771	0.0386	0.0017
PC12	0.0002	0.0180	-0.0176	-0.0014	0.0164	-0.0191	0.5435	0.0295	-0.0078
PC13	0.0031	0.0201	-0.0139	-0.0114	0.0056	-0.0284	0.5219	0.0320	-0.0053

Goswami model base module against ln CS of whole cranium

PC	Slope	Slope (Higher CI)	Slope (Lower CI)	Intercept	Intercept (Higher CI)	Intercept (Lower CI)	p value	R squared	R Squared adjusted
PC1	-0.0370	0.0200	-0.0930	0.1950	0.2520	0.1380	0.2870	0.0710	0.0350
PC2	-0.0820	-0.0300	-0.1330	0.3920	0.4430	0.3400	0.0120	0.2750	0.2470
PC3	-0.0380	0.0260	-0.1020	0.1940	0.2580	0.1300	0.3340	0.0620	0.0260
PC4	-0.0052	0.0354	-0.0458	0.0237	0.0643	-0.0169	0.5595	0.0267	-0.0108
PC5	0.0352	0.0719	-0.0015	-0.1750	-0.1383	-0.2117	0.1490	0.1391	0.1060
PC6	0.0190	0.0520	-0.0140	-0.0970	-0.0630	-0.1300	0.3500	0.0690	0.0330
PC7	0.0023	0.0317	-0.0272	-0.0131	0.0164	-0.0425	0.5099	0.0337	-0.0035
PC8	-0.0039	0.0215	-0.0293	0.0198	0.0452	-0.0056	0.5400	0.0281	-0.0093
PC9	-0.0088	0.0155	-0.0330	0.0433	0.0676	0.0191	0.4533	0.0456	0.0089
PC10	-0.0082	0.0148	-0.0312	0.0422	0.0652	0.0193	0.4497	0.0455	0.0088
PC11	-0.0044	0.0190	-0.0279	0.0195	0.0430	-0.0039	0.4988	0.0364	-0.0006
PC12	0.0081	0.0294	-0.0133	-0.0409	-0.0195	-0.0622	0.4581	0.0457	0.0089
PC13	0.0026	0.0233	-0.0181	-0.0123	0.0084	-0.0330	0.5267	0.0334	-0.0038

Goswami model base module against ln CS of base

PC	Slope	Slope (Higher CI)	Slope (Lower CI)	Intercept	Intercept (Higher CI)	Intercept (Lower CI)	p value	R squared	R Squared adjusted
PC1	-0.0350	0.0330	-0.1030	0.1250	0.1920	0.0570	0.3700	0.0520	0.0160
PC2	-0.1107	-0.0538	-0.1675	0.3373	0.3942	0.2805	0.0035	0.3604	0.3358
PC3	-0.0150	0.0640	-0.0930	0.0530	0.1320	-0.0250	0.5860	0.0230	-0.0150
PC4	-0.0016	0.0470	-0.0501	0.0029	0.0515	-0.0456	0.5749	0.0245	-0.0130
PC5	0.0415	0.0853	-0.0024	-0.1327	-0.0888	-0.1765	0.1627	0.1393	0.1062
PC6	0.0190	0.0590	-0.0220	-0.0610	-0.0200	-0.1010	0.4060	0.0540	0.0170
PC7	0.0026	0.0380	-0.0327	-0.0104	0.0250	-0.0458	0.5133	0.0327	-0.0045
PC8	-0.0027	0.0275	-0.0330	0.0093	0.0395	-0.0210	0.5681	0.0245	-0.0130
PC9	-0.0110	0.0180	-0.0400	0.0340	0.0630	0.0050	0.4400	0.0490	0.0120
PC10	-0.0068	0.0210	-0.0347	0.0229	0.0507	-0.0050	0.4774	0.0411	0.0042
PC11	-0.0068	0.0214	-0.0349	0.0191	0.0472	-0.0091	0.4916	0.0356	-0.0015
PC12	0.0120	0.0380	-0.0130	-0.0390	-0.0140	-0.0650	0.4020	0.0580	0.0210
PC13	0.0023	0.0269	-0.0223	-0.0066	0.0180	-0.0312	0.5280	0.0323	-0.0049

– Appendix 4 –

Percentage of shape change attributed to size – Intra-species

The percentage of total shape variation explained by size for each Principal Component, for the full landmark configuration and for each module from the 2* and Goswami models of modularity for each species. Where unshaded rows are calculated using the log centroid size of the whole cranium and shaded rows are calculated using the log centroid size of the corresponding module. Underlined/red results are those for which there was shown to be a significant (p<0.003) interaction between shape and size.

PC	*Cheirogaleus major* % of shape variation explained by size								
		2* model		Goswami model					
	Whole cranium	Face	Vault	Face	Orbit	Oral	Zygo	Vault	Base
1	6.39	1.08	2.24	0.09	1.84	1.38	2.28	5.70	0.24
	-	0.58	1.21	0.10	2.60	9.18	4.19	4.42	3.46
2	1.09	2.46	1.46	0.69	0.00	1.42	0.35	5.13	1.20
	-	2.36	1.09	0.56	0.38	0.19	0.00	0.50	1.5
3	0.03	2.03	2.88	0.24	1.94	0.80	2.79	0.44	0.00
	-	2.17	2.39	0.28	1.04	0.94	1.58	0.02	0.48
4	0.03	0.00	0.00	0.02	0.08	0.03	1.29	0.02	1.13
	-	0.04	0.04	0.52	0.00	0.00	0.58	0.18	0.11
5	1.53	0.28	1.27	0.43	0.73	0.47	0.01	0.19	0.39
	-	0.20	0.56	0.73	0.49	0.22	0.02	0.02	0.09
6	0.04	0.07	0.03	0.63	0.11	0.03	0.11	0.02	1.40
	-	0.03	0.40	0.22	0.01	0.10	0.00	0.00	0.36
7	0.00	0.51	0.03	0.28	0.38	0.06	0.00	0.57	0.00
	-	0.39	0.02	0.04	0.12	0.10	0.20	1.30	0.1
8	0.01	0.09	0.05	0.34	0.18	0.07	0.46	0.04	0.26
	-	0.03	0.02	0.84	0.05	0.00	0.60	0.09	0.3
9	0.02	0.03	0.42	0.21	0.00	0.01	0.05	0.01	0.39
	-	0.05	0.61	0.06	0.03	0.30	0.01	0.08	0.02
10	0.14	0.01	0.00	0.08	0.00	0.00	0.00	0.00	0.11
	-	0.04	0.03	0.00	0.04	0.10	0.04	0.16	0.03
11	0.05	0.00	0.03	0.00	0.15	0.00	0.00	0.02	0.01
	-	0.00	0.01	0.00	0.21	0.10	0.00	0.00	0.01
12	0.01	0.23	0.01	0.00	0.19	0.00	0.07	0.04	0.03
	-	0.37	0.05	0.00	0.11	0.00	0.10	0.14	0.02
13	0.00	0.23	0.06	0.11	0.00	0.00	0.10	0.02	0.11
	-	0.25	0.00	0.12	0.00	0.00	0.16	0.00	0.28

PC	*Cheirogaleus medius* % of shape variation explained by size								
		2* model		Goswami model					
	Whole cranium	Face	Vault	Face	Orbit	Oral	Zygo	Vault	Base
1	2.64	3.51	0.03	2.84	1.16	1.37	0.91	4.13	5.79
	-	3.84	0.19	1.10	2.30	7.10	2.18	3.82	6.63
2	2.28	0.63	0.88	0.09	0.76	1.78	2.37	0.07	0.44
	-	0.72	0.84	0.03	0.78	6.10	1.69	0.93	0.00
3	0.17	0.95	3.85	0.01	0.12	0.25	0.19	0.70	1.15
	-	0.76	3.01	0.32	0.40	0.37	0.11	0.06	0.61
4	0.04	0.12	0.63	3.19	0.02	0.05	1.12	0.02	0.06
	-	0.05	0.08	3.23	0.08	0.33	2.73	0.95	0.16
5	0.03	0.09	0.09	0.17	2.57	0.15	0.19	0.01	0.04
	-	0.13	0.14	0.02	1.63	0.04	0.15	0.01	0.08
6	0.04	0.01	0.25	0.07	1.10	0.21	0.04	0.02	0.01
	-	0.02	0.46	0.01	1.18	0.05	0.15	0.01	0.07
7	0.43	0.02	0.00	0.05	0.12	0.00	0.00	0.08	0.03
	-	0.01	0.01	0.15	0.01	0.01	0.01	0.03	0.16
8	0.04	0.29	0.30	0.01	0.00	0.01	0.15	0.04	0.07
	-	0.26	0.56	0.01	0.00	0.00	0.08	0.01	0.40
9	0.17	0.33	0.01	0.07	0.18	0.15	0.44	0.09	0.18
	-	0.43	0.01	0.05	0.09	0.05	0.10	0.01	0.18
10	0.00	0.12	0.00	0.58	0.05	0.03	0.00	0.09	0.09
	-	0.12	0.00	0.78	0.04	0.00	0.01	0.19	0.05
11	0.02	0.02	0.04	0.03	0.03	0.01	0.01	0.02	0.26
	-	0.01	0.05	0.15	0.02	0.00	0.00	0.02	0.31
12	0.00	0.00	0.00	0.15	0.00	0.00	0.07	0.00	0.09
	-	0.02	0.00	0.15	0.00	0.00	0.21	0.01	0.10
13	0.14	0.10	0.00	0.00	0.00	0.00	0.00	0.03	0.05
	-	0.08	0.00	0.03	0.00	0.00	0.03	0.07	0.15

PC	*Microcebus murinus* % of shape variation explained by size								
		2* model		Goswami model					
	Whole cranium	Face	Vault	Face	Orbit	Oral	Zygo	Vault	Base
1	2.85	0.03	1.06	1.72	0.23	0.12	1.57	3.64	0.09
	-	0.13	0.32	0.00	0.03	0.40	2.92	0.08	0.62
2	1.55	-0.08	-1.54	0.00	0.29	4.66	0.03	0.47	2.71
	-	0.13	0.89	0.04	0.67	12.09	0.22	2.00	1.64
3	0.00	0.00	0.05	0.40	0.01	0.35	0.06	0.12	1.42
	-	0.03	0.01	0.64	0.39	0.04	0.69	0.90	0.00
4	0.00	1.74	-0.78	0.17	0.00	0.33	0.00	0.14	0.59
	-	1.89	0.57	0.33	0.17	0.02	0.10	0.01	0.96
5	0.21	-0.02	0.01	0.49	34.00	0.01	0.01	0.04	0.25
	-	0.07	0.00	0.09	0.36	0.01	0.18	0.04	0.00
6	0.00	0.03	0.03	0.21	0.07	0.05	0.15	0.00	0.02
	-	0.03	0.01	0.23	0.01	0.03	0.08	0.02	0.24
7	0.01	0.14	0.02	0.01	0.01	0.00	0.02	0.06	0.01
	-	0.19	0.10	0.01	0.13	0.02	0.00	0.00	0.05
8	0.05	0.00	0.11	0.01	0.05	0.00	0.12	0.04	0.01
	-	0.04	0.01	0.00	0.00	0.01	0.03	0.00	0.01
9	0.06	0.01	0.12	0.03	0.05	0.00	0.02	0.04	0.00
	-	0.03	0.19	0.16	0.05	0.00	0.16	0.23	0.01
10	0.05	0.04	0.01	0.00	0.00	0.00	0.03	0.01	0.01
	-	0.03	0.00	0.00	0.01	0.00	0.02	0.06	0.08
11	0.00	0.03	0.00	0.00	0.03	0.00	0.19	0.00	0.07
	-	0.04	0.01	0.01	0.02	0.00	0.14	0.03	0.00
12	0.03	0.01	0.07	0.18	0.05	0.00	0.01	0.00	0.12
	-	0.00	0.10	0.13	0.03	0.00	0.00	0.01	0.18
13	0.02	0.22	0.08	0.00	0.09	0.00	0.25	0.00	0.01
	-	0.19	0.21	0.01	0.12	0.01	0.19	0.02	0.02

PC	*Microcebus rufus* % of shape variation explained by size								
		2* model		Goswami model					
	Whole cranium	Face	Vault	Face	Orbit	Oral	Zygo	Vault	Base
1	2.61	0.53	1.35	2.97	0.36	0.46	0.31	2.63	5.89
	-	1.43	0.20	1.83	0.51	4.61	0.42	0.18	5.35
2	7.94	0.00	6.91	1.11	0.00	0.62	3.16	5.87	1.65
	-	0.14	7.91	4.95	0.02	0.91	4.86	8.59	0.17
3	0.12	0.00	0.07	1.17	0.02	0.39	0.32	0.47	0.00
	-	0.01	0.00	0.78	0.03	0.28	0.11	0.04	0.10
4	0.17	0.05	0.55	1.11	0.40	0.81	0.01	0.13	0.76
	-	0.08	0.23	0.15	0.71	1.15	0.14	0.38	1.55
5	0.17	0.04	0.01	0.33	0.06	0.24	0.00	0.81	0.33
	-	0.01	0.00	0.14	0.42	0.19	0.11	0.97	0.90
6	0.05	0.41	0.06	0.38	0.00	0.18	0.00	0.11	0.05
	-	0.62	0.00	0.04	0.00	0.07	0.05	0.15	0.04
7	0.00	1.51	0.16	0.25	0.86	0.01	0.40	0.03	0.08
	-	1.34	0.27	0.09	0.72	0.00	0.36	0.26	0.12
8	0.03	0.50	0.04	0.07	0.35	0.00	0.55	0.06	0.03
	-	0.48	0.03	0.05	0.17	0.07	0.39	0.01	0.15
9	0.00	0.06	0.00	0.28	0.07	0.00	0.10	0.00	0.01
	-	0.06	0.00	0.16	0.05	0.02	0.00	0.17	0.11
10	0.04	0.08	0.06	0.02	0.05	0.01	0.09	0.00	0.16
	-	0.01	0.02	0.09	0.09	0.01	0.20	0.00	0.01
11	0.03	0.04	0.02	0.00	0.00	0.11	0.02	0.26	0.02
	-	0.02	0.07	0.01	0.03	0.04	0.02	0.08	0.05
12	0.01	0.08	0.01	0.03	0.00	0.00	0.28	0.02	0.01
	-	0.08	0.00	0.03	0.00	0.01	0.25	0.00	0.07
13	0.00	0.26	0.03	0.12	0.10	0.01	0.01	0.04	0.07
	-	0.20	0.04	0.07	0.10	0.00	0.02	0.08	0.14

PC	*Galago alleni* % of shape variation explained by size								
		2* model		Goswami model					
	Whole cranium	Face	Vault	Face	Orbit	Oral	Zygo	Vault	Base
1	4.28	0.33	3.95	8.96	0.20	1.68	0.03	2.01	0.08
	-	0.11	5.55	5.20	0.06	6.44	1.51	1.05	18.35
2	4.53	0.21	0.49	0.23	0.87	3.26	0.74	0.44	1.88
	-	1.30	0.07	3.16	0.09	0.05	0.26	0.04	0.03
3	0.03	4.05	6.13	0.00	3.32	0.25	1.95	0.83	0.40
	-	2.92	5.02	0.05	3.05	0.01	2.12	2.18	0.25
4	0.04	0.55	2.27	0.25	0.51	0.02	0.86	0.35	0.98
	-	0.37	1.86	0.01	0.06	0.02	2.06	0.02	0.13
5	0.87	0.93	0.33	0.15	0.08	0.02	0.02	0.01	0.04
	-	1.18	0.01	0.02	0.12	0.10	0.01	0.18	0.29
6	0.67	0.99	2.27	0.07	0.02	0.02	0.17	0.93	0.51
	-	0.95	4.37	0.03	0.01	0.74	0.09	0.00	0.03
7	0.11	0.15	0.58	0.24	0.42	0.58	0.01	0.23	0.26
	-	0.09	2.58	0.16	0.65	0.33	0.03	0.28	0.71
8	0.00	0.00	1.56	0.23	0.16	0.07	0.01	0.33	0.20
	-	0.00	0.98	0.14	0.19	0.04	0.00	0.04	0.00
9	0.01	0.03	2.75	0.01	0.01	0.03	0.50	0.05	0.12
	-	0.03	0.27	0.01	0.01	0.00	0.12	0.39	0.03
10	0.02	0.06	0.88	0.01	0.32	0.00	0.14	0.44	0.00
	-	0.06	1.26	0.01	0.45	0.02	0.04	0.39	0.01
11	0.11	0.14	3.87	0.01	0.00	0.01	0.03	0.00	0.09
	-	0.22	1.38	0.00	0.00	0.01	0.09	0.02	0.05
12	0.01	0.08	1.00	0.04	0.02	0.00	0.11	0.00	0.01
	-	0.05	0.52	0.05	0.03	0.01	0.07	0.02	0.01
13	0.00	0.01	0.93	0.03	0.00	0.00	0.05	0.02	0.01
	-	0.00	0.92	0.02	0.00	0.01	0.10	0.02	0.00

PC	*Galago moholi* % of shape variation explained by size								
		2* model		Goswami model					
	Whole cranium	Face	Vault	Face	Orbit	Oral	Zygo	Vault	Base
1	6.79	0.32	5.06	0.01	0.02	0.02	3.04	7.80	0.22
	-	1.27	1.45	0.43	0.48	0.65	0.04	0.14	4.85
2	0.63	1.45	0.35	0.01	1.08	0.03	0.01	0.21	0.78
	-	1.24	0.03	0.00	0.86	0.77	0.02	0.18	0.52
3	0.01	0.00	0.16	0.00	0.67	1.38	0.12	0.26	0.04
	-	0.03	0.09	0.00	0.43	0.96	1.07	0.13	
4	0.03	0.43	0.02	0.17	0.16	0.00	0.34	0.06	0.71
	-	0.62	0.06	0.08	0.03	0.01	0.79	0.98	0.34
5	0.00	0.50	0.00	0.03	0.00	0.05	0.05	0.04	0.00
	-	0.25	0.20	0.15	0.00	0.25	0.31	0.31	0.07
6	0.00	0.00	0.08	0.19	0.07	0.16	0.08	0.01	0.24
	-	0.03	0.21	0.35	0.04	0.04	0.01	0.00	0.05
7	0.00	0.00	0.02	0.36	0.01	0.05	0.04	0.00	0.09
	-	0.01	0.00	0.18	0.02	0.06	0.03	0.02	0.57
8	0.06	0.00	0.01	0.07	0.43	0.03	0.14	0.07	0.01
	-	0.01	0.09	0.08	0.24	0.09	0.10	0.05	0.00
9	0.11	0.05	0.00	0.02	0.01	0.03	0.02	0.00	0.03
	-	0.08	0.03	0.10	0.09	0.00	0.00	0.20	0.00
10	0.00	0.10	0.00	0.00	0.10	0.02	0.08	0.11	0.00
	-	0.07	0.00	0.00	0.00	0.01	0.02	0.05	0.01
11	0.00	0.00	0.00	0.05	0.03	0.01	0.03	0.03	0.01
	-	0.00	0.00	0.13	0.04	0.00	0.12	0.00	0.01
12	0.04	0.18	0.00	0.18	0.00	0.06	0.01	0.05	0.05
	-	0.18	0.02	0.18	0.00	0.02	0.00	0.04	0.00
13	0.00	0.12	0.01	0.04	0.02	0.01	0.02	0.03	0.02
	-	0.16	0.00	0.15	0.04	0.01	0.08	0.05	0.01

PC	*Galago senegalensis* % of shape variation explained by size								
		2* model		Goswami model					
	Whole cranium	Face	Vault	Face	Orbit	Oral	Zygo	Vault	Base
1	1.37	0.27	3.45	0.14	1.55	0.01	0.22	6.25	1.55
	-	0.26	2.05	0.03	1.56	0.10	0.04	1.05	7.69
2	0.10	2.50	0.00	0.04	1.68	0.49	0.16	0.17	0.18
	-	2.64	0.19	0.23	1.32	5.40	0.51	0.37	0.00
3	0.07	0.79	0.48	0.83	0.05	1.45	0.24	0.29	0.12
	-	0.88	0.35	0.58	0.04	1.07	0.20	0.29	0.11
4	0.00	0.15	0.00	0.02	0.14	0.14	0.02	0.00	0.13
	-	0.44	0.02	0.15	0.11	0.01	0.25	0.27	0.01
5	0.34	0.07	0.15	0.29	0.80	0.00	0.02	0.05	0.03
	-	0.05	0.13	0.59	0.30	0.00	0.18	0.00	0.01
6	0.02	0.02	0.02	0.08	0.24	0.29	0.06	0.05	0.01
	-	0.02	0.00	0.00	0.00	0.11	0.07	0.06	0.02
7	0.02	0.50	0.00	0.40	0.19	0.00	0.01	0.17	0.07
	-	0.32	0.00	0.34	0.72	0.00	0.02	0.21	0.01
8	0.00	0.02	0.08	0.05	0.00	0.00	0.03	0.25	0.30
	-	0.02	0.10	0.13	0.02	0.04	0.07	0.16	0.07
9	0.03	0.01	0.00	0.09	0.14	0.00	0.13	0.02	0.00
	-	0.03	0.00	0.06	0.03	0.01	0.27	0.03	0.01
10	0.04	0.00	0.02	0.05	0.01	0.02	0.12	0.08	0.01
	-	0.00	0.10	0.04	0.00	0.02	0.02	0.19	0.01
11	0.07	0.01	0.04	0.01	0.09	0.03	0.04	0.02	0.00
	-	0.00	0.04	0.01	0.11	0.01	0.01	0.02	0.01
12	0.00	0.02	0.13	0.00	0.01	0.00	0.01	0.00	0.02
	-	0.02	0.13	0.01	0.01	0.00	0.02	0.00	0.00
13	0.00	0.01	0.02	0.00	0.00	0.00	0.00	0.00	0.08
	-	0.00	0.04	0.02	0.00	0.00	0.00	0.00	0.05

PC	*Galagoides demidoff* % of shape variation explained by size								
		2* model		Goswami model					
	Whole cranium	Face	Vault	Face	Orbit	Oral	Zygo	Vault	Base
1	5.77	2.13	6.73	0.96	1.91	1.02	1.22	5.11	0.05
	-	2.84	1.87	6.04	0.45	0.78	0.10	0.00	1.48
2	0.24	0.05	0.01	0.07	0.06	0.24	0.09	0.37	0.87
	-	0.27	0.05	0.28	0.01	0.16	0.07	0.29	0.04
3	0.07	0.12	0.00	0.25	0.49	0.81	0.03	0.27	0.05
	-	0.16	0.01	0.07	0.32	0.00	0.02	0.00	0.02
4	0.13	0.06	0.00	0.07	0.03	0.01	0.04	0.02	0.25
	-	0.09	0.01	0.40	0.43	0.18	0.03	0.35	0.85
5	0.06	0.44	0.08	0.03	0.04	0.36	0.02	0.15	0.36
	-	0.58	0.11	0.01	0.04	0.00	0.03	0.30	0.01
6	0.00	0.13	0.01	0.14	0.05	0.05	0.01	0.04	0.05
	-	0.05	0.03	0.00	0.04	0.05	0.04	0.06	0.00
7	0.16	0.00	0.01	0.45	0.00	0.00	0.00	0.19	0.54
	-	0.00	0.01	0.37	0.04	0.00	0.00	0.01	0.63
8	0.03	0.03	0.12	0.07	0.01	0.01	0.11	0.23	0.12
	-	0.00	0.28	0.17	0.01	0.01	0.02	0.60	0.02
9	0.13	0.04	0.01	0.11	0.00	0.01	0.16	0.00	0.03
	-	0.09	0.00	0.08	0.08	0.02	0.19	0.06	0.04
10	0.01	0.01	0.00	0.00	0.14	0.00	0.23	0.00	0.05
	-	0.00	0.01	0.02	0.22	0.01	0.59	0.11	0.02
11	0.05	0.07	0.02	0.05	0.03	0.00	0.01	0.01	0.05
	-	0.08	0.07	0.04	0.05	0.00	0.00	0.04	0.02
12	0.05	0.03	0.06	0.00	0.02	0.00	0.00	0.03	0.01
	-	0.01	0.01	0.00	0.01	0.00	0.11	0.01	0.07
13	0.00	0.02	0.00	0.22	0.00	0.00	0.00	0.04	0.03
	-	0.00	0.01	0.12	0.00	0.02	0.01	0.01	0.03

PC	*Galagoides zanzibaricus*% of shape variation explained by size								
		2* model		Goswami model					
	Whole cranium	Face	Vault	Face	Orbit	Oral	Zygo	Vault	Base
1	1.87	0.74	6.03	1.04	1.55	6.02	0.50	7.59	0.24
	-	3.08	2.11	0.91	1.56	0.30	3.73	0.03	0.00
2	1.89	2.25	0.00	0.32	1.68	0.49	0.02	0.32	0.28
	-	2.64	0.40	0.03	0.32	4.63	0.00	2.85	0.29
3	1.42	0.10	2.10	0.15	0.05	0.04	2.08	0.01	0.56
	-	0.37	4.45	0.18	0.04	0.02	0.26	0.19	0.08
4	1.92	0.22	0.01	2.09	0.14	0.04	0.83	0.37	0.57
	-	0.39	0.01	0.48	0.11	0.51	1.55	1.13	2.00
5	0.03	1.09	0.15	1.64	0.80	0.00	0.51	0.05	0.21
	-	1.20	0.03	2.70	0.30	0.05	0.76	0.88	0.00
6	0.00	0.32	0.33	0.75	0.24	0.12	0.00	1.66	0.32
	-	0.23	0.20	0.45	0.00	0.00	0.00	0.55	0.02
7	0.11	0.42	0.05	0.27	0.19	0.08	1.05	0.00	0.01
	-	0.13	0.03	0.05	0.72	0.17	0.41	0.01	0.13
8	0.07	0.05	0.16	0.15	0.00	0.01	0.11	0.13	0.00
	-	0.00	0.00	0.00	0.02	0.01	0.25	0.09	0.35
9	0.00	0.30	0.00	0.02	0.14	0.05	0.06	0.03	0.64
	-	0.14	0.04	0.15	0.03	0.04	0.10	0.10	0.58
10	0.41	0.22	0.20	0.01	0.01	0.17	0.12	0.01	0.63
	-	0.25	0.11	0.16	0.00	0.00	0.00	0.08	0.23
11	0.09	0.23	0.03	0.19	0.09	0.01	0.14	0.20	0.16
	-	0.24	0.01	0.13	0.11	0.01	0.01	0.10	0.29
12	0.03	0.06	0.05	0.08	0.01	0.06	0.08	0.00	0.00
	-	0.06	0.01	0.00	0.01	0.04	0.12	0.01	0.01
13	0.06	0.02	0.14	0.02	0.00	0.00	0.00	0.01	0.04
	-	0.02	0.10	0.09	0.00	0.02	0.00	0.00	0.00

PC	*Euoticus elegantulus* % of shape variation explained by size								
		2* model		Goswami model					
	Whole cranium	Face	Vault	Face	Orbit	Oral	Zygo	Vault	Base
1	0.01	0.12	1.30	2.66	0.10	0.73	0.03	4.64	0.05
	-	0.15	0.00	3.72	0.08	1.12	0.01	0.06	0.34
2	3.17	2.04	2.36	0.42	2.90	0.16	2.39	0.02	0.84
	-	1.99	1.63	0.12	0.90	1.65	3.92	0.02	1.24
3	0.25	0.46	0.59	0.03	0.15	0.00	0.13	0.12	0.27
	-	0.41	0.79	0.25	1.30	0.90	0.76	0.99	1.92
4	0.21	0.00	0.01	0.08	0.04	0.21	0.00	0.42	0.85
	-	0.05	0.28	0.43	0.07	0.15	0.10	0.10	0.21
5	0.00	0.06	0.10	0.01	0.00	0.01	0.00	0.05	0.08
	-	0.09	0.16	0.06	0.01	0.06	0.03	0.03	0.56
6	0.17	0.01	0.02	0.05	0.11	0.00	0.28	0.08	0.03
	-	0.01	0.06	0.16	0.00	0.18	0.07	0.01	0.00
7	0.01	0.01	0.39	0.04	0.27	0.01	0.03	0.03	0.56
	-	0.02	0.47	0.45	0.01	0.08	0.07	0.02	0.98
8	0.01	0.12	0.07	0.00	0.13	0.24	0.11	0.11	0.33
	-	0.08	0.01	0.04	0.08	0.04	0.00	0.08	0.00
9	0.04	0.00	0.07	0.03	0.07	0.01	0.02	0.01	0.17
	-	0.00	0.11	0.00	0.05	0.01	0.02	0.00	0.00
10	0.26	0.10	0.41	0.01	0.01	0.02	0.54	0.04	0.04
	-	0.03	0.13	0.04	0.00	0.00	0.11	0.01	0.12
11	0.07	0.11	0.11	0.00	0.01	0.01	0.01	0.02	0.08
	-	0.03	0.12	0.01	0.02	0.05	0.08	0.07	0.08
12	0.01	0.06	0.04	0.29	0.00	0.02	0.05	0.00	0.01
	-	0.02	0.02	0.10	0.00	0.06	0.04	0.00	0.02
13	0.00	0.23	0.01	0.00	0.08	0.02	0.01	0.01	0.07
	-	0.18	0.05	0.00	0.07	0.04	0.03	0.04	0.01

PC	*Otolemur crassicaudatus* % of shape variation explained by size								
	Whole cranium	2* model		Goswami model					
		Face	Vault	Face	Orbit	Oral	Zygo	Vault	Base
1	2.16	0.13	1.75	0.00	0.16	2.76	2.65	3.15	0.10
	-	0.01	2.26	0.21	1.52	1.79	0.71	9.08	0.52
2	0.02	4.21	0.57	0.04	4.58	5.73	3.12	0.75	1.86
	-	4.77	0.09	0.00	4.79	8.05	3.84	0.47	3.91
3	5.94	0.46	2.28	0.67	1.52	0.00	0.02	1.26	0.06
	-	0.37	2.40	0.56	1.19	0.02	0.00	1.14	0.11
4	0.03	1.76	0.00	1.56	0.66	0.50	0.15	0.12	0.40
	-	1.99	0.01	0.98	0.41	0.26	0.27	0.09	0.01
5	0.00	0.23	0.06	0.21	0.28	0.04	0.16	0.07	0.01
	-	0.05	0.09	0.24	0.26	0.12	0.37	0.04	0.13
6	0.03	0.03	0.00	0.08	0.16	0.06	0.48	0.06	0.18
	-	0.00	0.00	0.14	0.06	0.07	0.55	0.01	0.18
7	0.02	0.02	0.23	0.27	0.00	0.00	0.00	0.00	0.28
	-	0.01	0.16	0.30	0.00	0.00	0.13	0.09	0.07
8	0.02	0.00	0.24	0.07	0.00	0.03	0.21	0.00	0.17
	-	0.00	0.11	0.08	0.01	0.01	0.33	0.01	0.03
9	0.04	0.00	0.02	0.14	0.03	0.02	0.04	0.17	0.08
	-	0.00	0.00	0.07	0.06	0.00	0.05	0.06	0.05
10	0.00	0.00	0.01	0.10	0.01	0.00	0.03	0.06	0.02
	-	0.00	0.05	0.08	0.07	0.00	0.01	0.01	0.01
11	0.00	0.02	0.00	0.11	0.00	0.00	0.01	0.02	0.00
	-	0.01	0.00	0.10	0.00	0.01	0.00	0.00	0.00
12	0.03	0.02	0.01	0.01	0.00	0.00	0.21	0.00	0.10
	-	0.02	0.01	0.03	0.00	0.00	0.18	0.00	0.05
13	0.00	0.00	0.00	0.02	0.00	0.00	0.02	0.05	0.01
	-	0.00	0.01	0.03	0.00	0.00	0.01	0.03	0.00

PC	*Otolemur garnettii* % of shape variation explained by size								
		2* model		Goswami model					
	Whole cranium	Face	Vault	Face	Orbit	Oral	Zygo	Vault	Base
1	4.94	8.88	1.52	2.33	5.66	5.14	5.83	1.88	0.05
	-	7.75	1.74	1.67	2.51	7.83	6.21	4.90	1.12
2	0.32	1.04	0.62	0.06	3.60	5.67	0.02	1.69	3.59
	-	1.24	0.06	0.00	3.69	5.23	0.02	0.53	1.20
3	2.01	0.24	2.28	1.24	0.00	0.03	0.09	0.75	1.08
	-	0.34	2.70	1.42	0.05	0.03	0.04	1.80	3.19
4	0.00	0.07	0.04	0.41	0.19	0.10	0.05	0.01	0.07
	-	0.05	0.07	0.28	0.02	0.04	0.12	0.10	0.06
5	0.01	0.00	0.03	0.48	0.89	0.20	0.41	0.04	0.16
	-	0.00	0.01	0.41	0.87	0.01	0.30	0.02	0.02
6	0.01	0.04	0.01	0.32	0.06	0.06	0.66	0.00	0.22
	-	0.00	0.03	0.37	0.02	0.00	0.81	0.08	0.13
7	0.01	0.01	0.00	0.07	0.02	0.00	0.04	0.09	0.00
	-	0.04	0.00	0.10	0.00	0.00	0.01	0.10	0.10
8	0.00	0.11	0.25	0.03	0.07	0.04	0.07	0.00	0.01
	-	0.24	0.27	0.11	0.19	0.06	0.02	0.00	0.04
9	0.10	0.19	0.03	0.00	0.02	0.03	0.48	0.16	0.09
	-	0.12	0.02	0.01	0.06	0.07	0.28	0.12	0.05
10	0.01	0.03	0.05	0.08	0.12	0.01	0.10	0.03	0.09
	-	0.00	0.03	0.12	0.20	0.01	0.17	0.04	0.11
11	0.03	0.01	0.03	0.18	0.02	0.00	0.02	0.00	0.00
	-	0.01	0.03	0.17	0.02	0.00	0.03	0.00	0.02
12	0.11	0.00	0.09	0.00	0.00	0.00	0.00	0.04	0.00
	-	0.00	0.06	0.00	0.00	0.00	0.00	0.02	0.00
13	0.02	0.08	0.02	0.00	0.00	0.00	0.01	0.09	0.01
	-	0.12	0.02	0.00	0.00	0.00	0.00	0.05	0.04

PC	*Avahi laniger* % of shape variation explained by size								
		2* model		Goswami model					
	Whole cranium	Face	Vault	Face	Orbit	Oral	Zygo	Vault	Base
1	0.08	0.19	0.65	0.48	0.53	1.84	0.84	1.20	0.13
	-	1.24	1.13	0.00	7.89	17.33	1.03	9.91	8.44
2	0.53	0.13	0.04	0.09	0.18	0.23	0.08	1.65	0.00
	-	0.09	0.13	0.62	0.40	0.02	0.12	0.57	1.44
3	0.98	0.07	0.90	0.10	2.10	0.03	0.39	0.71	0.22
	-	0.26	1.58	0.05	1.04	0.34	0.82	0.22	0.06
4	1.35	2.42	0.07	0.78	0.79	0.77	0.31	0.21	0.38
	-	1.70	0.01	0.17	0.07	0.81	0.36	0.86	0.04
5	0.01	0.06	0.75	0.57	0.05	0.03	0.08	0.02	0.05
	-	0.04	0.24	0.71	0.09	0.02	0.01	0.00	0.41
6	0.09	0.41	0.00	0.00	0.17	0.04	0.63	0.41	0.00
	-	0.30	0.01	0.71	0.26	0.00	0.37	0.00	0.01
7	0.12	0.03	0.08	0.13	0.00	0.02	0.35	0.46	0.20
	-	0.00	0.29	0.00	0.03	0.01	0.58	0.28	0.10
8	0.11	0.18	0.00	0.32	0.06	0.00	0.29	0.00	0.14
	-	0.21	0.09	0.02	0.00	0.01	0.34	0.06	0.03
9	0.02	0.00	0.02	0.04	0.07	0.06	0.46	0.03	0.38
	-	0.01	0.07	0.00	0.09	0.03	0.65	0.01	0.39
10	0.01	0.09	0.22	0.47	0.11	0.03	0.05	0.07	0.08
	-	0.14	0.15	0.31	0.01	0.03	0.07	0.01	0.11
11	0.11	0.00	0.08	0.01	0.06	0.01	0.16	0.02	0.28
	-	0.03	0.02	0.02	0.00	0.00	0.15	0.00	0.18
12	0.05	0.03	0.37	0.07	0.01	0.05	0.17	0.04	0.04
	-	0.00	0.27	0.24	0.05	0.03	0.10	0.05	0.01
13	0.01	0.00	0.37	0.03	0.07	0.01	0.01	0.00	0.01
	-	0.02	0.23	0.00	0.01	0.02	0.00	0.00	0.01

PC	*Indri indri* % of shape variation explained by size								
		2* model		Goswami model					
	Whole cranium	Face	Vault	Face	Orbit	Oral	Zygo	Vault	Base
1	0.11	0.95	0.16	0.72	2.39	5.09	0.12	1.61	0.29
	-	1.72	2.69	0.48	6.89	24.20	0.01	7.14	0.06
2	2.12	0.15	0.70	0.21	1.17	0.00	0.48	0.81	0.28
	-	0.39	0.04	3.56	0.35	0.07	1.65	0.01	0.05
3	0.04	0.33	0.21	0.28	0.01	0.69	0.90	1.45	0.09
	-	0.00	0.00	1.96	0.86	0.03	0.13	0.00	0.03
4	0.57	0.09	0.08	0.46	0.15	0.06	0.50	1.88	0.00
	-	0.17	0.04	0.00	0.00	0.23	0.01	0.81	2.80
5	0.67	1.07	0.49	0.07	0.30	0.08	0.01	0.05	0.01
	-	1.75	0.06	0.14	0.37	0.11	0.02	0.00	0.00
6	0.33	0.04	0.00	0.26	0.04	0.19	0.68	0.12	0.00
	-	0.05	0.01	0.43	0.03	0.07	0.25	0.05	0.22
7	0.14	0.27	1.17	0.00	0.59	0.02	0.24	0.00	1.24
	-	0.07	0.63	0.11	0.36	0.02	0.08	0.00	0.55
8	0.00	0.02	0.01	0.02	0.03	0.00	0.33	0.02	0.35
	-	0.09	0.01	0.03	0.01	0.00	0.33	0.36	0.44
9	0.02	0.04	0.10	0.03	0.00	0.04	0.11	0.04	0.01
	-	0.03	0.19	0.29	0.02	0.00	0.23	0.01	0.00
10	0.09	0.00	0.28	0.00	0.01	0.00	0.01	0.15	0.01
	-	0.01	0.09	0.02	0.02	0.00	0.15	0.14	0.01
11	0.03	0.28	0.00	0.06	0.04	0.04	0.30	0.00	0.03
	-	0.09	0.01	0.07	0.04	0.00	0.25	0.00	0.40
12	0.05	0.00	0.00	0.01	0.00	0.00	0.05	0.01	0.04
	-	0.00	0.07	0.00	0.02	0.01	0.00	0.00	0.12
13	0.07	0.00	0.00	0.03	0.00	0.01	0.26	0.00	0.05
	-	0.00	0.02	0.01	0.04	0.01	0.28	0.04	0.00

PC	*Propithecus diadema* % of shape variation explained by size								
		2* model		Goswami model					
	Whole cranium	Face	Vault	Face	Orbit	Oral	Zygo	Vault	Base
1	0.02	0.02	0.06	1.22	0.50	12.07	0.35	0.25	1.61
	-	0.00	1.82	0.45	0.14	8.88	0.10	14.47	0.00
2	4.88	2.49	3.48	0.49	0.02	0.55	2.15	3.34	4.39
	-	1.28	4.30	0.07	0.13	3.59	3.46	1.52	3.22
3	0.13	0.01	0.39	0.78	0.88	0.01	0.03	0.31	1.77
	-	0.00	0.20	1.21	1.33	0.78	0.00	0.53	2.59
4	0.20	0.22	1.10	1.17	0.00	0.23	4.16	2.16	0.70
	-	0.40	1.44	1.07	0.19	0.05	2.95	0.89	0.69
5	0.10	0.00	0.08	0.01	0.01	0.24	0.20	0.26	0.01
	-	0.00	0.05	0.02	0.04	0.23	0.07	0.13	0.15
6	0.50	0.42	0.00	0.29	0.01	0.11	0.11	0.31	0.00
	-	0.57	0.08	0.00	0.01	0.00	0.02	0.00	0.10
7	0.09	0.28	0.05	0.16	0.00	0.03	0.09	0.01	0.00
	-	0.24	0.06	0.11	0.15	0.05	0.36	0.00	0.04
8	0.02	0.00	0.18	0.20	0.00	0.00	0.03	0.01	0.05
	-	0.00	0.08	0.09	0.00	0.03	0.00	0.00	0.00
9	0.40	0.05	0.04	0.06	0.04	0.00	0.11	0.01	0.00
	-	0.01	0.00	0.00	0.00	0.02	0.19	0.05	0.02
10	0.06	0.35	0.37	0.22	0.14	0.00	0.02	0.01	0.14
	-	0.55	0.05	0.11	0.18	0.02	0.06	0.09	0.01
11	0.44	0.04	0.00	0.00	0.56	0.02	0.05	0.02	0.04
	-	0.16	0.00	0.01	0.49	0.05	0.00	0.03	0.00
12	0.04	0.04	0.06	0.01	0.15	0.00	0.04	0.00	0.10
	-	0.07	0.09	0.00	0.05	0.00	0.04	0.01	0.03
13	0.00	0.08	0.00	0.05	0.02	0.00	0.00	0.03	0.00
	-	0.09	0.00	0.06	0.01	0.00	0.00	0.02	0.02

PC	*Propithecus verreauxi* % of shape variation explained by size								
		2* model		Goswami model					
	Whole cranium	Face	Vault	Face	Orbit	Oral	Zygo	Vault	Base
1	0.73	2.04	1.34	6.00	0.55	0.90	0.27	1.33	0.01
	-	2.96	0.32	6.92	0.00	0.54	0.05	2.44	0.45
2	0.06	2.26	0.32	1.29	2.18	2.68	0.79	0.01	0.15
	-	3.92	0.79	3.45	2.37	5.69	0.57	0.02	0.06
3	1.77	0.25	0.76	0.72	2.14	0.32	0.03	0.80	0.16
	-	0.12	0.00	0.14	3.62	0.00	0.16	0.12	0.03
4	0.65	0.03	0.13	0.07	0.00	0.76	0.00	1.09	0.47
	-	0.01	0.02	0.38	0.05	0.06	0.13	0.17	0.34
5	0.01	0.19	0.08	0.06	0.01	0.00	0.72	0.02	0.81
	-	0.14	0.03	0.15	0.02	0.02	0.34	0.23	0.30
6	0.09	0.75	0.00	0.03	0.02	0.06	0.03	0.33	0.14
	-	0.73	0.06	0.03	0.06	0.00	0.01	0.47	0.41
7	0.10	0.16	0.12	0.00	0.00	0.02	0.01	0.00	0.02
	-	0.08	0.05	0.13	0.05	0.00	0.25	0.00	0.07
8	0.04	0.28	0.17	0.44	0.28	0.09	0.00	0.20	0.33
	-	0.19	0.12	0.18	0.21	0.12	0.01	0.09	0.58
9	0.17	0.02	0.31	0.09	0.00	0.02	0.27	0.00	0.12
	-	0.01	0.30	0.06	0.00	0.02	0.39	0.01	0.29
10	0.14	0.00	0.03	0.06	0.04	0.01	0.12	0.18	0.02
	-	0.02	0.03	0.00	0.01	0.00	0.23	0.03	0.00
11	0.10	0.01	0.18	0.02	0.20	0.00	0.00	0.02	0.04
	-	0.01	0.11	0.03	0.24	0.00	0.00	0.00	0.01
12	0.00	0.00	0.05	0.02	0.06	0.00	0.06	0.00	0.01
	-	0.01	0.00	0.13	0.05	0.00	0.08	0.00	0.00
13	0.05	0.04	0.00	0.03	0.00	0.00	1.98	0.03	0.00
	-	0.03	0.00	0.00	0.00	0.01	0.80	0.06	0.07

PC	*Eulemur fulvus* % of shape variation explained by size								
		2* model		Goswami model					
	Whole cranium	Face	Vault	Face	Orbit	Oral	Zygo	Vault	Base
1	1.47	0.39	2.40	0.00	0.35	1.54	0.01	5.32	0.13
	-	0.64	0.11	0.04	0.12	0.68	0.00	0.90	0.06
2	1.00	0.04	0.20	0.09	0.01	0.38	0.15	0.16	0.62
	-	0.05	0.66	0.07	0.00	8.62	0.80	0.14	0.03
3	0.50	0.04	0.00	0.28	0.10	0.01	0.13	0.09	0.04
	-	0.01	0.09	0.14	0.36	0.08	0.03	0.39	0.18
4	0.13	0.26	0.82	0.05	0.00	0.17	0.08	0.32	0.23
	-	0.30	0.70	0.08	0.03	0.05	0.14	0.79	0.02
5	0.21	0.19	0.06	0.03	0.04	0.00	0.07	0.00	0.01
	-	0.19	0.00	0.28	0.03	0.00	0.07	0.06	0.03
6	0.16	0.13	0.01	0.50	0.18	0.02	0.04	0.04	0.17
	-	0.14	0.01	0.17	0.10	0.00	0.23	0.09	0.19
7	0.00	0.00	0.08	0.01	0.03	0.01	0.08	0.13	0.05
	-	0.00	0.06	0.07	0.05	0.00	0.00	0.02	0.05
8	0.10	0.07	0.09	0.04	0.04	0.00	0.45	0.02	0.02
	-	0.09	0.00	0.10	0.05	0.00	0.68	0.00	0.02
9	0.01	0.18	0.02	0.01	0.01	0.00	0.18	0.00	0.03
	-	0.26	0.02	0.00	0.03	0.00	0.09	0.00	0.00
10	0.03	0.07	0.01	0.00	0.05	0.00	0.01	0.04	0.00
	-	0.01	0.01	0.00	0.04	0.00	0.04	0.09	0.04
11	0.01	0.04	0.00	0.02	0.04	0.00	0.15	0.08	0.07
	-	0.05	0.02	0.02	0.06	0.00	0.04	0.01	0.00
12	0.00	0.01	0.00	0.01	0.09	0.01	0.02	0.00	0.03
	-	0.05	0.00	0.05	0.08	0.00	0.00	0.01	0.01
13	0.04	0.01	0.00	0.00	0.00	0.00	0.00	0.00	0.00
	-	0.01	0.01	0.00	0.00	0.00	0.02	0.00	0.03

PC	*Eulemur macaco* % of shape variation explained by size								
		2* model		Goswami model					
	Whole cranium	Face	Vault	Face	Orbit	Oral	Zygo	Vault	Base
1	0.91	0.75	1.25	0.01	1.77	5.37	0.05	2.99	0.44
	-	0.18	0.13	0.95	0.38	7.12	0.20	1.23	0.93
2	1.04	0.08	0.41	1.35	0.26	1.82	0.21	0.32	0.08
	-	0.04	0.01	3.93	0.24	8.86	0.03	0.31	0.20
3	0.14	2.51	0.81	0.05	0.13	0.01	1.21	0.84	1.93
	-	2.10	0.07	0.08	0.45	0.01	1.33	2.04	1.63
4	0.04	1.21	0.56	0.68	1.19	0.12	0.44	0.01	0.00
	-	1.24	1.42	0.87	0.96	0.12	0.41	0.50	0.05
5	0.62	0.09	0.01	0.47	0.03	0.03	0.02	0.28	0.04
	-	0.31	0.24	0.41	0.00	0.03	0.03	0.00	0.03
6	0.09	0.03	0.17	0.16	0.20	0.05	0.19	0.00	0.05
	-	0.08	0.02	0.11	0.06	0.01	0.01	0.04	0.12
7	0.81	0.00	0.04	0.02	0.17	0.00	0.11	0.04	0.11
	-	0.05	0.11	0.00	0.43	0.01	0.16	0.01	0.05
8	0.34	0.01	0.05	0.43	0.15	0.07	0.25	0.38	0.02
	-	0.00	0.19	0.65	0.48	0.00	0.25	0.13	0.00
9	0.01	0.05	0.08	0.13	0.03	0.02	0.00	0.05	0.04
	-	0.08	0.03	0.00	0.16	0.01	0.05	0.08	0.01
10	0.00	0.00	0.21	0.01	0.17	0.04	0.20	0.08	0.05
	-	0.10	0.00	0.01	0.00	0.00	0.43	0.01	0.04
11	0.01	0.09	0.00	0.05	0.19	0.00	0.02	0.00	0.10
	-	0.13	0.02	0.02	0.06	0.01	0.01	0.00	0.31
12	0.09	0.00	0.03	0.02	0.06	0.02	0.04	0.01	0.01
	-	0.01	0.01	0.03	0.00	0.02	0.00	0.02	0.02
13	0.03	0.07	0.02	0.01	0.00	0.00	0.00	0.00	0.03
	-	0.19	0.03	0.01	0.00	0.00	0.02	0.00	0.04

PC	*Eulemur mongoz* % of shape variation explained by size								
		2* model		Goswami model					
	Whole cranium	Face	Vault	Face	Orbit	Oral	Zygo	Vault	Base
1	6.76	5.37	1.65	1.07	0.29	2.36	5.63	0.79	0.00
	-	6.19	1.70	1.93	0.18	0.01	1.55	3.07	1.99
2	0.04	0.21	1.18	0.68	1.39	0.41	1.24	1.33	0.74
	-	0.47	0.51	1.60	2.12	1.35	2.93	0.86	0.52
3	0.13	0.01	0.11	0.83	0.06	1.73	0.00	0.00	2.59
	-	0.01	0.13	0.52	0.12	2.11	0.03	0.17	1.76
4	0.33	0.09	0.00	1.08	0.02	0.00	0.35	0.72	0.07
	-	0.11	0.06	1.15	0.02	0.01	0.31	1.18	0.33
5	0.23	1.71	0.53	0.17	0.59	0.00	0.23	0.08	0.08
	-	1.54	0.45	0.34	0.51	0.03	0.46	0.09	0.02
6	0.30	0.08	0.27	0.17	0.02	0.02	0.02	0.01	0.28
	-	0.05	0.43	0.00	0.01	0.01	0.00	0.13	0.26
7	0.11	0.05	0.00	0.00	0.19	0.01	0.52	0.00	0.00
	-	0.05	0.03	0.03	0.03	0.01	0.53	0.08	0.00
8	0.02	0.01	0.05	0.14	0.04	0.00	0.08	0.03	0.10
	-	0.00	0.33	0.19	0.00	0.01	0.07	0.04	0.03
9	0.01	0.04	0.07	0.05	0.34	0.00	0.04	0.05	0.23
	-	0.01	0.08	0.14	0.25	0.00	0.02	0.19	0.24
10	0.02	0.00	0.02	0.03	0.10	0.02	0.00	0.01	0.09
	-	0.00	0.04	0.07	0.05	0.01	0.02	0.05	0.01
11	0.10	0.02	0.03	0.12	0.00	0.00	0.03	0.00	0.10
	-	0.02	0.03	0.14	0.05	0.01	0.01	0.00	0.09
12	0.01	0.10	0.01	0.02	0.02	0.04	0.05	0.21	0.08
	-	0.12	0.00	0.00	0.02	0.03	0.01	0.22	0.05
13	0.02	0.03	0.10	0.00	0.13	0.01	0.02	0.01	0.01
	-	0.04	0.04	0.01	0.05	0.01	0.12	0.00	0.03

PC	*Eulemur rubriventer* % of shape variation explained by size								
		2* model		Goswami model					
	Whole cranium	Face	Vault	Face	Orbit	Oral	Zygo	Vault	Base
1	0.62	1.82	7.22	0.10	9.36	4.72	5.66	8.93	0.88
	-	0.55	0.94	0.60	11.66	6.30	3.52	0.67	0.02
2	6.64	3.66	0.28	4.41	0.10	0.81	0.04	0.12	0.52
	-	4.27	0.00	1.63	0.20	0.97	0.32	0.22	1.00
3	0.01	0.43	1.09	0.15	0.01	0.00	0.56	0.00	1.08
	-	0.51	1.97	0.03	0.03	0.01	0.07	1.51	2.09
4	0.24	0.34	0.13	0.27	0.67	0.11	0.31	2.38	0.04
	-	0.51	0.01	0.10	0.33	0.05	0.01	1.44	0.11
5	0.07	0.01	0.08	0.02	0.04	0.02	1.42	0.03	0.73
	-	0.04	0.66	0.26	0.00	0.00	0.80	0.01	0.30
6	0.05	0.49	0.30	0.60	0.10	0.00	0.04	0.00	0.00
	-	0.62	0.42	0.18	0.19	0.01	0.04	0.01	0.37
7	0.26	0.01	0.02	0.23	0.27	0.00	0.02	0.00	0.06
	-	0.02	0.03	0.12	0.16	0.00	1.33	0.01	0.19
8	0.01	0.08	0.06	0.08	0.25	0.06	0.18	0.00	0.20
	-	0.01	0.52	0.07	0.22	0.07	0.10	0.11	0.12
9	0.09	0.03	0.01	0.04	0.00	0.01	0.02	0.06	0.00
	-	0.00	0.06	0.05	0.10	0.00	0.07	0.19	0.03
10	0.28	0.03	0.01	0.00	0.04	0.00	0.17	0.00	0.63
	-	0.01	0.04	0.00	0.02	0.00	0.19	0.09	0.38
11	0.06	0.05	0.00	0.17	0.00	0.00	0.01	0.00	0.00
	-	0.06	0.01	0.25	0.02	0.00	0.00	0.01	0.57
12	0.02	0.00	0.02	0.08	0.05	0.00	0.03	0.02	0.03
	-	0.01	0.00	0.01	0.01	0.00	0.00	0.00	0.08
13	0.00	0.03	0.03	0.01	0.02	0.01	0.02	0.02	0.00
	-	0.02	0.00	0.16	0.00	0.00	0.01	0.01	0.02

PC	*Hapalemur griseus* % of shape variation explained by size								
		2* model		Goswami model					
	Whole cranium	Face	Vault	Face	Orbit	Oral	Zygo	Vault	Base
1	10.48	2.96	5.37	1.67	3.39	4.53	0.17	11.66	1.16
	-	2.33	1.29	0.59	0.22	9.50	0.13	0.78	2.91
2	0.37	0.09	1.62	0.13	0.82	1.82	0.20	1.22	1.19
	-	0.15	1.01	0.94	0.80	2.41	0.32	0.89	0.01
3	0.37	0.98	0.33	1.29	0.52	0.14	0.43	1.05	0.41
	-	0.86	0.37	0.78	0.00	0.01	0.03	0.97	0.04
4	0.97	1.02	1.02	0.11	0.00	0.04	0.97	0.22	0.98
	-	0.76	1.58	0.01	0.03	0.00	1.20	0.32	1.08
5	0.03	0.50	0.01	1.01	0.04	0.19	0.89	0.42	0.40
	-	0.71	0.18	1.69	0.04	0.13	0.35	0.11	0.38
6	0.00	0.29	0.06	1.04	1.71	0.00	1.36	0.00	0.00
	-	0.27	0.15	1.40	2.12	0.01	2.09	0.40	0.39
7	0.25	1.07	0.01	0.02	0.40	0.06	0.26	0.39	0.06
	-	1.18	0.04	0.11	0.51	0.00	0.13	0.68	0.00
8	0.02	0.01	0.30	0.64	0.37	0.06	0.18	0.30	0.27
	-	0.04	0.41	0.50	0.12	0.01	0.09	0.43	0.09
9	0.22	0.36	0.03	0.00	0.00	0.06	0.27	0.00	0.11
	-	0.40	0.04	0.00	0.00	0.00	0.23	0.03	0.18
10	0.02	0.03	0.05	0.32	0.00	0.00	0.04	0.08	0.02
	-	0.00	0.08	0.17	0.00	0.00	0.03	0.19	0.06
11	0.02	0.02	0.00	0.00	0.02	0.00	0.03	0.00	0.09
	-	0.02	0.00	0.02	0.09	0.01	0.07	0.02	0.30
12	0.02	0.00	0.05	0.06	0.01	0.07	0.02	0.00	0.02
	-	0.02	0.05	0.04	0.00	0.09	0.02	0.00	0.04
13	0.00	0.00	0.06	0.00	0.02	0.04	0.01	0.00	0.01
	-	0.01	0.22	0.00	0.04	0.01	0.00	0.03	0.13

PC	*Lemur catta* % of shape variation explained by size								
	Whole cranium	2* model		Goswami model					
		Face	Vault	Face	Orbit	Oral	Zygo	Vault	Base
1	5.15	2.44	6.27	0.36	0.73	5.68	0.10	9.84	0.73
	-	2.74	2.01	0.84	0.09	16.63	1.38	0.01	1.93
2	1.12	1.70	0.63	4.89	0.53	0.11	0.01	0.96	0.15
	-	2.69	0.21	4.05	1.00	0.09	0.33	1.35	2.16
3	1.42	0.06	0.51	0.71	0.02	0.95	1.89	1.56	0.06
	-	0.31	1.40	0.95	0.03	1.05	1.73	3.85	0.04
4	0.01	0.34	0.02	0.06	0.04	0.00	0.02	0.37	0.31
	-	0.22	0.07	0.30	0.39	0.01	0.00	0.05	0.43
5	0.44	0.28	1.05	0.24	0.02	0.04	0.48	0.22	0.31
	-	0.36	0.97	0.05	0.02	0.22	0.10	0.17	1.07
6	0.11	0.09	0.00	0.01	1.20	0.00	0.05	0.02	1.07
	-	0.06	0.00	0.04	1.14	0.00	0.00	0.01	0.24
7	0.22	0.05	0.37	0.01	0.00	0.10	0.05	0.08	0.06
	-	0.01	0.28	0.04	0.00	0.03	0.01	0.13	0.01
8	0.01	0.02	0.00	0.01	0.03	0.02	0.12	0.00	0.02
	-	0.05	0.02	0.02	0.02	0.00	0.25	0.00	0.05
9	0.01	0.02	0.02	0.04	0.02	0.25	0.04	0.02	0.02
	-	0.01	0.09	0.13	0.12	0.10	0.07	0.02	0.00
10	0.00	0.03	0.09	0.10	0.00	0.06	0.01	0.41	0.14
	-	0.01	0.12	0.04	0.05	0.00	0.04	0.16	0.05
11	0.02	0.01	0.06	0.04	0.00	0.00	0.00	0.00	0.01
	-	0.01	0.01	0.03	0.02	0.00	0.00	0.03	0.04
12	0.03	0.44	0.00	0.08	0.03	0.01	0.09	0.02	0.00
	-	0.34	0.06	0.06	0.05	0.02	0.14	0.09	0.07
13	0.00	0.04	0.04	0.02	0.03	0.01	0.00	0.00	0.07
	-	0.01	0.02	0.00	0.01	0.01	0.00	0.02	0.00

PC	*Varecia variegate* % of shape variation explained by size								
		2* model		Goswami model					
	Whole cranium	Face	Vault	Face	Orbit	Oral	Zygo	Vault	Base
1	1.72	0.14	1.22	2.55	0.12	0.03	0.29	0.02	1.82
	-	0.08	5.73	5.69	2.55	1.35	0.10	6.63	0.38
2	7.71	6.38	1.97	3.17	7.21	0.31	1.30	0.01	0.02
	-	6.79	1.55	1.81	6.94	3.36	0.43	2.16	0.01
3	0.17	0.00	0.79	1.09	1.28	0.20	0.00	0.33	2.15
	-	0.00	1.37	0.97	0.69	0.27	0.04	1.78	1.19
4	0.01	0.73	0.01	0.09	0.31	0.56	0.49	0.00	0.15
	-	0.67	0.01	0.59	0.75	0.07	0.11	0.07	0.09
5	0.04	0.08	0.00	0.39	0.05	0.03	0.01	0.07	0.29
	-	0.13	0.13	0.04	0.06	0.00	0.01	0.09	0.03
6	0.00	0.13	0.17	0.73	0.06	0.05	0.02	0.20	0.15
	-	0.09	0.01	0.75	0.15	0.00	0.18	0.08	0.00
7	0.03	0.06	0.08	0.01	0.03	0.31	0.10	0.05	0.37
	-	0.08	0.00	0.00	0.00	0.20	0.23	0.02	0.18
8	0.01	0.34	0.67	0.05	0.01	0.05	0.32	0.07	0.06
	-	0.31	0.45	0.02	0.00	0.01	0.36	0.01	0.07
9	0.03	0.01	0.31	0.07	0.11	0.02	0.11	0.27	0.11
	-	0.01	0.00	0.02	0.01	0.00	0.07	0.12	0.04
10	0.05	0.00	0.14	0.01	0.05	0.00	0.00	0.00	0.01
	-	0.00	0.01	0.08	0.07	0.01	0.07	0.02	0.07
11	0.03	0.00	0.12	0.01	0.11	0.00	0.02	0.01	0.20
	-	0.03	0.00	0.01	0.06	0.00	0.03	0.02	0.00
12	0.00	0.00	0.03	0.17	0.02	0.01	0.01	0.00	0.00
	-	0.00	0.02	0.19	0.03	0.00	0.00	0.00	0.02
13	0.01	0.02	0.11	0.01	0.07	0.00	0.06	0.08	0.00
	-	0.01	0.07	0.00	0.02	0.00	0.01	0.01	0.01

PC	*Lepilemur ruficaudatus* % of shape variation explained by size								
		2* model		Goswami model					
	Whole cranium	Face	Vault	Face	Orbit	Oral	Zygo	Vault	Base
1	11.53	9.71	5.00	3.69	0.01	0.19	0.12	7.16	0.94
	-	11.86	4.48	5.89	0.10	2.03	0.17	1.98	0.05
2	0.61	0.72	0.73	1.95	0.96	1.56	1.92	0.13	1.20
	-	0.43	0.52	1.38	0.63	1.18	0.44	3.00	0.54
3	0.25	0.15	0.07	2.08	0.25	1.17	0.44	0.02	0.28
	-	0.23	0.37	1.51	0.37	0.33	0.34	0.09	0.03
4	0.07	0.01	0.79	0.05	2.91	0.27	1.61	0.34	1.83
	-	0.00	0.21	0.39	2.42	0.32	1.83	0.03	2.20
5	0.07	0.47	0.10	0.07	0.01	0.02	0.00	0.18	0.95
	-	0.22	0.08	0.00	0.09	0.01	0.01	0.15	2.16
6	0.01	0.00	0.06	0.40	0.20	0.11	0.18	0.38	0.03
	-	0.00	0.02	0.49	0.09	0.19	0.13	0.05	0.31
7	0.03	0.03	0.07	0.72	0.08	0.01	0.26	0.02	0.11
	-	0.00	0.01	0.64	0.08	0.00	0.39	0.18	0.01
8	0.03	0.02	0.31	0.04	0.01	0.03	0.42	0.00	0.36
	-	0.00	0.38	0.02	0.06	0.00	0.31	0.15	0.04
9	0.03	0.19	0.02	0.00	0.37	0.00	0.18	0.00	0.22
	-	0.15	0.02	0.02	0.40	0.00	0.10	0.17	0.16
10	0.01	0.12	0.17	0.04	0.01	0.06	0.04	0.00	0.08
	-	0.10	0.01	0.00	0.02	0.03	0.15	0.01	0.00
11	0.14	0.00	0.24	0.01	0.01	0.06	0.06	0.00	0.01
	-	0.00	0.40	0.00	0.05	0.08	0.09	0.03	0.28
12	0.07	0.00	0.04	0.17	0.02	0.00	0.04	0.01	0.01
	-	0.00	0.00	0.18	0.00	0.00	0.02	0.02	0.02
13	0.08	0.03	0.01	0.02	0.04	0.00	0.04	0.10	0.08
	-	0.02	0.03	0.06	0.03	0.00	0.10	0.11	0.10

PC	*Loris tardigradus* % of shape variation explained by size								
		2* model		Goswami model					
	Whole cranium	Face	Vault	Face	Orbit	Oral	Zygo	Vault	Base
1	17.59	6.70	16.55	3.02	3.72	2.89	1.88	1.64	15.50
	-	4.29	15.45	0.91	1.75	2.94	1.56	1.59	18.88
2	0.68	4.03	0.22	1.00	0.49	9.34	0.00	9.25	1.30
	-	5.36	0.17	1.24	1.18	15.33	0.01	4.52	1.35
3	0.03	2.61	0.16	0.21	0.26	0.22	0.01	2.01	0.89
	-	3.41	1.57	0.21	0.66	0.13	0.01	2.69	0.25
4	0.01	0.31	0.01	1.00	1.17	0.19	2.83	0.13	0.08
	-	0.28	0.02	1.04	1.94	0.00	2.95	0.35	0.01
5	0.09	0.01	0.03	0.81	2.26	1.14	1.18	0.40	0.00
	-	0.00	0.04	0.69	2.08	0.94	1.35	0.27	0.00
6	0.00	0.30	0.01	0.43	0.00	0.00	1.04	0.40	0.06
	-	0.26	0.00	0.74	0.03	0.01	1.06	0.29	0.00
7	0.12	0.03	0.03	0.17	0.09	0.05	0.23	0.04	0.35
	-	0.09	0.00	0.09	0.15	0.01	0.16	0.07	0.25
8	0.07	0.02	0.00	0.01	0.50	0.00	0.04	0.21	0.21
	-	0.03	0.00	0.01	0.33	0.00	0.08	0.34	0.29
9	0.03	0.00	0.10	0.37	0.01	0.00	0.33	0.02	0.00
	-	0.00	0.17	0.33	0.00	0.01	0.32	0.05	0.06
10	0.01	0.04	0.00	0.00	0.00	0.01	0.00	0.01	0.02
	-	0.02	0.01	0.00	0.00	0.01	0.00	0.01	0.02
11	0.06	0.02	0.01	0.21	0.01	0.01	0.02	0.00	0.04
	-	0.04	0.00	0.26	0.01	0.00	0.02	0.00	0.12
12	0.00	0.07	0.07	0.05	0.01	0.01	0.04	0.05	0.03
	-	0.06	0.06	0.05	0.01	0.00	0.04	0.10	0.03
13	0.06	0.03	0.00	0.01	0.00	0.00	0.03	0.00	0.04
	-	0.02	0.00	0.00	0.00	0.00	0.03	0.00	0.01

PC	*Nycticebus bengalensis* % of shape variation explained by size								
		2* model		Goswami model					
	Whole cranium	Face	Vault	Face	Orbit	Oral	Zygo	Vault	Base
1	0.33	1.21	1.24	2.20	2.69	5.84	4.08	2.46	1.64
	-	1.60	0.07	5.30	1.70	17.44	4.42	1.22	1.34
2	0.25	2.23	0.32	0.67	0.64	2.64	0.32	0.00	1.15
	-	2.15	0.26	0.45	1.24	0.15	0.00	3.80	7.67
3	0.67	0.00	1.43	0.77	0.10	0.66	0.00	0.41	0.17
	-	0.00	1.43	1.22	0.00	0.71	0.17	1.48	0.36
4	0.36	0.04	0.16	3.65	0.56	0.17	0.06	0.08	0.14
	-	0.04	0.01	2.94	0.28	0.24	0.01	0.03	0.00
5	2.08	0.07	1.58	0.92	0.77	0.14	0.40	0.57	0.81
	-	0.02	2.46	0.68	0.75	0.00	0.70	1.01	0.25
6	0.17	0.60	0.05	0.38	0.14	0.07	0.64	0.00	0.82
	-	0.52	0.00	0.01	0.54	0.01	0.53	0.05	0.25
7	0.02	0.05	0.00	0.01	0.02	0.04	0.02	0.14	0.22
	-	0.21	0.02	0.14	0.05	0.00	0.00	0.31	0.19
8	0.26	0.32	1.22	0.05	0.04	0.33	0.05	0.02	0.06
	-	0.35	0.87	0.09	0.17	0.43	0.00	0.02	0.02
9	0.32	0.42	0.05	0.02	0.00	0.01	0.16	0.49	0.18
	-	0.47	0.01	0.32	0.02	0.03	0.33	0.07	0.13
10	0.62	0.15	0.25	0.01	0.05	0.28	0.04	0.00	0.15
	-	0.09	0.45	0.00	0.04	0.07	0.01	0.00	0.05
11	0.42	0.06	0.03	0.06	0.07	0.02	0.14	0.00	0.00
	-	0.05	0.05	0.01	0.08	0.00	0.22	0.02	0.00
12	0.01	0.57	0.12	0.00	0.06	0.00	0.25	0.14	0.10
	-	0.36	0.10	0.00	0.12	0.00	0.16	0.18	0.00
13	0.03	0.11	0.09	0.19	0.02	0.01	0.08	0.04	0.01
	-	0.13	0.06	0.07	0.01	0.00	0.03	0.02	0.00

PC	*Nycticebus coucang* % of shape variation explained by size								
		2* model		Goswami model					
	Whole cranium	Face	Vault	Face	Orbit	Oral	Zygo	Vault	Base
1	0.76	0.16	0.14	0.00	0.48	3.00	0.87	1.62	3.66
	-	0.03	0.33	0.13	1.47	9.13	1.12	0.92	6.99
2	0.01	0.10	0.72	0.78	0.04	1.21	0.00	0.00	0.19
	-	0.16	0.90	1.69	0.05	3.06	0.00	0.01	2.63
3	1.29	0.00	0.67	0.54	0.11	0.24	0.20	0.26	0.48
	-	0.03	0.72	0.79	0.37	0.34	0.03	0.24	0.52
4	0.07	0.53	0.00	0.31	0.05	0.14	0.12	0.11	0.04
	-	0.50	0.05	0.31	0.00	0.09	0.34	0.12	0.36
5	0.42	0.59	0.01	0.50	0.66	0.04	0.28	0.24	0.03
	-	0.66	0.00	0.63	0.42	0.02	0.58	0.52	0.18
6	0.01	0.07	0.29	0.10	0.00	0.02	0.07	0.05	0.01
	-	0.07	0.23	0.09	0.02	0.00	0.13	0.04	0.00
7	0.38	0.17	0.02	0.03	0.00	0.00	0.37	0.23	0.01
	-	0.18	0.04	0.01	0.01	0.01	0.30	0.29	0.02
8	0.09	0.01	0.19	0.15	0.00	0.05	0.11	0.07	0.36
	-	0.01	0.03	0.03	0.00	0.00	0.14	0.03	0.12
9	0.01	0.66	0.06	0.07	0.01	0.02	0.24	0.15	0.08
	-	0.68	0.03	0.05	0.02	0.00	0.11	0.14	0.04
10	0.11	0.07	0.00	0.30	0.26	0.00	0.14	0.09	0.02
	-	0.12	0.00	0.12	0.21	0.00	0.11	0.04	0.05
11	0.01	0.07	0.08	0.01	0.01	0.08	0.00	0.00	0.02
	-	0.06	0.10	0.05	0.17	0.07	0.03	0.01	0.00
12	0.01	0.04	0.07	0.01	0.03	0.00	0.00	0.00	0.05
	-	0.04	0.07	0.01	0.03	0.00	0.02	0.01	0.05
13	0.02	0.02	0.21	0.03	0.01	0.03	0.01	0.00	0.04
	-	0.01	0.14	0.02	0.00	0.02	0.00	0.00	0.01

PC	*Perodicticus potto* % of shape variation explained by size								
	Whole cranium	2* model		Goswami model					
		Face	Vault	Face	Orbit	Oral	Zygo	Vault	Base
1	2.73	0.14	1.06	0.05	0.33	1.10	0.01	1.05	0.71
	-	0.00	1.34	0.00	0.01	9.71	0.41	3.85	8.88
2	0.03	1.11	0.20	0.36	1.96	0.05	0.63	0.27	0.02
	-	0.83	0.52	0.02	2.23	0.07	0.92	0.03	0.06
3	0.27	0.01	1.11	0.64	0.16	0.00	0.64	0.04	0.45
	-	0.02	0.75	0.49	0.03	0.02	0.19	0.18	0.05
4	0.66	0.10	0.49	0.06	1.09	0.02	0.37	1.07	0.06
	-	0.15	0.19	0.04	1.29	0.01	0.40	1.03	0.07
5	0.24	0.00	0.04	0.01	0.67	0.15	0.16	0.04	0.03
	-	0.00	0.11	0.04	0.47	0.19	0.02	0.10	0.02
6	0.13	0.88	0.19	0.00	0.09	0.09	0.40	0.49	0.76
	-	0.89	0.07	0.02	0.06	0.04	0.27	0.01	0.28
7	0.01	0.00	0.02	0.05	0.01	0.02	0.00	0.03	0.02
	-	0.01	0.04	0.00	0.02	0.00	0.03	0.11	0.09
8	0.05	0.01	0.04	0.00	0.00	0.31	0.06	0.00	0.19
	-	0.00	0.11	0.03	0.01	0.19	0.04	0.00	0.07
9	0.14	0.06	0.14	0.02	0.02	0.09	0.04	0.02	0.01
	-	0.17	0.04	0.01	0.10	0.03	0.02	0.01	0.00
10	0.00	0.08	0.00	0.00	0.00	0.02	0.01	0.00	0.00
	-	0.07	0.00	0.00	0.01	0.02	0.01	0.11	0.01
11	0.00	0.31	0.01	0.23	0.04	0.00	0.00	0.01	0.02
	-	0.39	0.03	0.23	0.04	0.01	0.00	0.00	0.00
12	0.00	0.01	0.12	0.02	0.03	0.00	0.07	0.01	0.00
	-	0.00	0.07	0.01	0.04	0.01	0.11	0.00	0.03
13	0.06	0.07	0.03	0.00	0.07	0.00	0.01	0.02	0.01
	-	0.12	0.01	0.00	0.07	0.00	0.03	0.07	0.02

– Appendix 5 –

Percentage of shape change attributed to size – Inter-species

The percentage of total shape variation explained by size for each Principal Component, for the full landmark configuration and for each module from the 2* and Goswami models of modularity. Where unshaded rows are calculated using the ln CS size of the whole cranium and shaded rows are calculated using the log centroid size of the corresponding module. Calculations use the R^2 result from the interspecies regressions, of PCs against ln CS, based on SPECIES AVERAGE results. Underlined/red results are those for which there was shown to be a significant (p<0.003) interaction between shape and size.

PC	Inter-species % of shape variation explained by size								
		2* model		Goswami model					
	Whole cranium	Face	Vault	Face	Orbit	Oral	Zygo	Vault	Base
1	23.92	21.23	20.42	4.62	8.30	7.27	23.67	19.07	3.27
	-	21.51	19.56	6.68	7.22	6.70	25.29	16.99	1.89
2	0.67	- 0.00	- 0.09	2.10	6.62	0.15	3.01	2.96	7.05
	-	0.09	0.04	0.76	6.46	0.10	2.30	3.23	8.46
3	0.69	0.33	3.85	0.06	5.83	4.76	0.00	0.31	1.14
	-	0.34	4.27	0.03	4.75	5.58	0.20	0.66	0.43
4	3.50	3.94	- 0.96	2.38	0.50	0.66	2.20	0.37	0.11
	-	3.79	0.74	2.07	0.33	0.60	2.66	0.25	0.08
5	0.03	- 0.21	0.05	0.82	0.00	0.23	0.26	0.04	1.29
	-	0.19	0.03	1.02	0.00	0.24	0.23	0.04	1.29
6	0.00	0.60	0.29	0.02	0.10	0.20	0.26	0.39	0.46
	-	0.50	0.45	0.06	0.05	0.22	0.20	0.45	0.15
7	0.00	0.03	0.58	0.11	0.27	0.03	0.31	0.01	0.03
	-	0.05	0.70	0.06	0.17	0.02	0.30	0.01	0.03
8	0.03	0.05	0.06	0.00	0.01	0.02	0.06	0.14	0.00
	-	0.08	0.10	0.02	0.03	0.03	0.05	0.07	0.00
9	0.13	0.11	0.01	0.09	0.01	0.02	0.11	0.10	0.16
	-	0.10	0.02	0.13	0.00	0.01	0.08	0.19	0.15
10	0.17	0.06	0.01	0.00	0.01	0.03	0.04	0.02	0.15
	-	0.05	0.02	0.00	0.01	0.02	0.07	0.00	0.11
11	0.04	0.06	0.04	0.25	0.03	0.01	0.08	0.00	0.03
	-	0.06	0.00	0.26	0.03	0.01	0.04	0.01	0.04
12	0.00	0.02	0.01	0.00	0.26	0.00	0.01	0.00	0.07
	-	0.02	0.00	0.00	0.25	0.00	0.01	0.00	0.13
13	0.01	0.02	0.00	0.02	0.00	0.00	0.02	0.01	0.05
	-	0.02	0.00	0.02	0.01	0.00	0.03	0.01	0.04

The percentage of total shape variation explained by size for each Principal Component, for the full landmark configuration and for each module from the 2* and Goswami models of modularity. Where unshaded rows are calculated using the log centroid size of the whole cranium and shaded rows are calculated using the ln CS size of the corresponding module. Calculations use the R^2 result from the interspecies regressions, of PCs against ln CS, based on the results of the RESAMPLING method. Underlined results are those for which there was shown to be a significant (p<0.003) interaction between shape and size.

PC	Inter-species % of shape variation explained by size								
		2* model		Goswami model					
	Whole cranium	Face	Vault	Face	Orbit	Oral	Zygo	Vault	Base
1	19.77	18.12	16.40	3.68	4.21	6.53	20.75	13.59	2.80
	-	18.40	15.82	4.98	3.46	3.36	21.72	11.22	2.05
2	0.87	- 0.21	- 0.26	2.55	5.05	1.38	1.29	2.29	4.31
	-	0.32	0.23	1.18	5.12	1.48	1.13	1.88	5.65
3	0.55	0.28	3.19	0.38	4.23	3.57	0.28	0.64	0.71
	-	0.29	3.24	0.40	3.64	4.54	0.57	1.03	0.26
4	3.14	3.03	0.59	0.90	0.22	0.40	1.52	0.41	0.23
	-	2.93	0.46	0.75	0.18	0.40	1.66	0.30	0.21
5	0.10	- 0.18	0.10	0.53	0.21	0.13	0.56	0.12	0.95
	-	0.18	0.09	0.67	0.28	0.13	0.15	0.12	0.95
6	0.08	0.30	0.24	0.05	0.22	0.12	0.24	0.15	0.27
	-	0.28	0.33	0.07	0.18	0.11	0.23	0.19	0.21
7	0.06	0.07	0.13	0.15	0.13	0.03	0.18	0.06	0.11
	-	0.08	0.14	0.13	0.11	0.03	0.18	0.06	0.11
8	0.08	0.13	0.23	0.06	0.13	0.02	0.14	0.07	0.08
	-	0.17	0.31	0.07	0.14	0.02	0.12	0.05	0.07
9	0.10	0.11	0.08	0.08	0.06	0.01	0.06	0.07	0.10
	-	0.11	0.08	0.09	0.05	0.01	0.06	0.10	0.11
10	0.12	0.08	0.07	0.04	0.04	0.01	0.06	0.02	0.07
	-	0.08	0.07	0.04	0.04	0.01	0.06	0.02	0.06
11	0.06	0.07	0.04	0.06	0.05	0.01	0.05	0.02	0.04
	-	0.07	0.04	0.06	0.05	0.01	0.05	0.02	0.04
12	0.04	0.05	0.03	0.03	0.04	0.00	0.03	0.01	0.03
	-	0.05	0.03	0.03	0.04	0.00	0.03	0.01	0.04
13	0.04	0.05	0.03	0.03	0.02	0.00	0.02	0.01	0.02
	-	0.05	0.03	0.03	0.02	0.00	0.02	0.01	0.02

– Appendix 6 –

Inter-species differences in allometric scaling – ANCOVA results

ANCOVA results for all possible species pairs, calculated with the PC as the dependent variable, the log of centroid size as the covariate and species as the independent variable, for PCs 1-5 to relating the whole cranium and for the modules of the 2* and Goswami modularity models. Results are underlines/in red where significant differences were found between species (p<0.0001).

Whole cranium - PC1	*C. major*		*C. medius*		*M. murinus*		*M. rufus*		*G. alleni*		*G. demidoff*		*E. elegantulus*		*G. moholi*		*G. senegalensis*	
	F value	p value	F value	p value	F value	p value	F value	p value	F value	p value	F value	p value	F value	p value	F value	p value	F value	p value
C. major																		
C. medius	0.101	0.751																
M. murinus	2.980	0.088	5.682	0.019														
M. rufus	0.882	0.352	2.303	0.135	0.878	0.351												
G. alleni	6.838	0.012	11.960	0.001	1.496	0.224	4.358	0.042										
G. demidoff	4.214	0.043	8.128	0.005	0.014	0.907	1.394	0.241	1.719	0.194								
E. elegantulus	2.651	0.109	4.894	0.031	0.023	0.879	0.871	0.354	0.929	0.339	0.007	0.936						
G. moholi	4.203	0.043	8.180	0.005	0.000	0.988	1.217	0.273	2.263	0.136	0.023	0.879	0.039	0.844				
G. senegalensus	0.442	0.507	0.090	0.765	13.519	0.000	5.359	0.022	19.439	0.000	15.515	0.000	7.237	0.008	15.194	0.000		
G. zanzibaricus	0.028	0.867	0.260	0.612	1.737	0.191	0.492	0.486	6.149	0.017	2.749	0.101	2.235	0.141	2.642	0.107	0.564	0.453
O. crassicaudatus	0.008	0.930	0.352	0.554	7.626	0.006	1.973	0.163	13.300	0.000	9.305	0.003	4.125	0.044	9.021	0.003	2.003	0.158
O. garnettii	0.071	0.790	0.031	0.861	10.152	0.002	3.479	0.065	16.817	0.000	12.574	0.001	5.800	0.017	12.350	0.001	0.521	0.471
A. laniger	0.005	0.943	0.018	0.895	1.700	0.196	0.508	0.480	3.574	0.065	2.275	0.136	1.577	0.215	2.303	0.133	0.123	0.726
I. Indri	0.373	0.544	1.060	0.307	0.997	0.320	0.060	0.807	4.228	0.044	1.511	0.222	1.100	0.298	1.370	0.244	2.123	0.147
P. diadema	0.500	0.483	1.370	0.247	0.897	0.346	0.022	0.883	3.988	0.052	1.396	0.241	0.959	0.331	1.258	0.265	2.943	0.088
P. verreauxi	0.141	0.709	0.008	0.927	5.434	0.022	2.183	0.144	10.451	0.002	7.257	0.008	4.368	0.040	7.285	0.008	0.025	0.874
E. fulvus	0.280	0.597	1.164	0.282	4.199	0.042	0.573	0.450	8.820	0.003	4.933	0.027	2.269	0.134	4.563	0.034	4.583	0.033
E. macaco	0.346	0.558	1.018	0.316	1.298	0.257	0.095	0.758	4.531	0.037	1.813	0.181	1.178	0.281	1.656	0.201	2.416	0.122
E. mongoz	2.454	0.121	5.687	0.019	0.528	0.469	0.225	0.636	4.778	0.032	0.916	0.341	0.557	0.457	0.679	0.411	13.414	0.000
E. rubriventer	0.273	0.604	0.126	0.724	3.438	0.067	1.675	0.201	6.923	0.011	4.774	0.032	3.559	0.064	4.882	0.030	0.059	0.809
H. griseus	9.532	0.003	16.800	0.000	2.499	0.117	6.622	0.013	0.040	0.842	2.931	0.091	1.532	0.221	3.758	0.055	27.805	0.000
L. catta	0.168	0.684	0.006	0.936	6.858	0.010	2.966	0.090	14.355	0.000	9.812	0.002	5.824	0.019	9.841	0.002	0.048	0.826
V. variegata	5.006	0.029	10.030	0.002	0.062	0.804	1.898	0.173	1.613	0.209	0.023	0.881	0.001	0.980	0.101	0.751	17.759	0.000
L. ruficaudatus	1.339	0.253	3.062	0.086	0.290	0.592	0.109	0.743	2.830	0.099	0.528	0.470	0.381	0.540	0.402	0.528	6.352	0.013
L. tardigradus	0.910	0.345	2.536	0.117	1.240	0.268	0.000	0.993	4.120	0.048	1.765	0.188	0.781	0.381	1.587	0.211	10.887	0.001
N. bengalensis	0.015	0.903	0.015	0.905	2.320	0.131	0.819	0.370	5.538	0.023	3.337	0.072	2.416	0.126	3.350	0.070	0.117	0.733
N. coucang	0.464	0.497	1.432	0.234	2.039	0.156	0.119	0.731	5.339	0.023	2.601	0.109	1.257	0.265	2.401	0.124	5.214	0.023
P. potto	2.405	0.123	4.740	0.031	0.005	0.942	0.704	0.403	1.331	0.251	0.034	0.853	0.032	0.859	0.004	0.952	17.218	0.000

Whole cranium - PC1	*G. zanzibaricus*		*O. crassicaudatus*		*O. garnettii*		*A. laniger*		*I. indri*		*P. diadema*		*P. verreauxi*		*E. fulvus*		*E. macaco*	
	F value	p value	F value	p value	F value	p value	F value	p value	F value	p value	F value	p value	F value	p value	F value	p value	F value	p value
C. major																		
C. medius																		
M. murinus																		
M. rufus																		
G. alleni																		
G. demidoff																		
E. elegantulus																		
G. moholi																		
G. senegalensus																		
G. zanzibaricus																		
O. crassicaudatus	0.020	0.889																
O. garnettii	0.195	0.659	0.487	0.486														
A. laniger	0.037	0.848	0.026	0.872	0.005	0.942												
I. Indri	0.181	0.672	0.566	0.453	1.219	0.272	0.270	0.605										
P. diadema	0.270	0.606	0.899	0.345	1.771	0.186	0.326	0.571	0.008	0.927								
P. verreauxi	0.279	0.599	0.435	0.510	0.078	0.781	0.034	0.854	1.062	0.306	1.348	0.250						
E. fulvus	0.051	0.821	0.825	0.365	2.239	0.136	0.217	0.642	0.085	0.770	0.194	0.660	1.240	0.267				
E. macaco	0.138	0.711	0.597	0.441	1.315	0.253	0.257	0.613	0.002	0.964	0.020	0.889	1.062	0.305	0.071	0.790		
E. mongoz	1.354	0.248	6.823	0.010	10.129	0.002	1.282	0.261	0.438	0.510	0.335	0.564	5.057	0.027	2.661	0.104	0.591	0.444
E. rubriventer	0.464	0.499	0.559	0.456	0.273	0.602	0.112	0.740	1.082	0.302	1.216	0.275	0.076	0.784	1.046	0.308	1.021	0.315
H. griseus	8.305	0.006	19.949	0.000	24.733	0.000	4.727	0.035	5.933	0.018	5.791	0.020	14.299	0.000	13.265	0.000	6.416	0.013
L. catta	0.369	0.546	0.552	0.459	0.086	0.770	0.035	0.853	1.345	0.250	1.758	0.190	0.001	0.979	1.560	0.213	1.295	0.258
V. variegata	3.686	0.060	11.045	0.001	14.941	0.000	2.479	0.121	1.951	0.167	1.832	0.181	8.429	0.005	5.863	0.016	2.224	0.139
L. ruficaudatus	0.899	0.348	2.832	0.095	4.474	0.037	0.748	0.392	0.266	0.608	0.184	0.670	2.850	0.096	1.162	0.282	0.339	0.562
L. tardigradus	0.413	0.523	4.416	0.038	6.975	0.009	0.473	0.495	0.063	0.803	0.024	0.876	2.512	0.118	1.311	0.254	0.115	0.735
N. bengalensis	0.076	0.783	0.055	0.815	0.001	0.974	0.001	0.979	0.427	0.516	0.525	0.472	0.032	0.859	0.318	0.573	0.387	0.536
N. coucang	0.156	0.694	1.439	0.232	2.866	0.092	0.303	0.584	0.001	0.976	0.019	0.892	1.486	0.225	0.194	0.660	0.000	0.983
P. potto	1.162	0.283	10.201	0.002	12.407	0.001	1.334	0.250	0.720	0.397	0.668	0.415	4.636	0.033	5.803	0.017	1.057	0.305

Whole cranium - PC1	*E. mongoz*		*E. rubriventer*		*H. griseus*		*L. catta*		*V. variegata*		*L. ruficaudatus*		*L. tardigradus*		*N. bengalensis*		*N. coucang*	
	F value	p value	F value	p value	F value	p value	F value	p value	F value	p value	F value	p value	F value	p value	F value	p value	F value	p value
C. major																		
C. medius																		
M. murinus																		
M. rufus																		
G. alleni																		
G. demidoff																		
E. elegantulus																		
G. moholi																		
G. senegalensus																		
G. zanzibaricus																		
O. crassicaudatus																		
O. garnettii																		
A. laniger																		
I. Indri																		
P. diadema																		
P. verreauxi																		
E. fulvus																		
E. macaco																		
E. mongoz																		
E. rubriventer	3.303	0.073																
H. griseus	7.660	0.007	9.532	0.003														
L. catta	7.159	0.009	0.168	0.684	20.214	0.000												
V. variegata	1.415	0.237	5.467	0.023	2.870	0.095	12.287	0.001										
L. ruficaudatus	0.000	0.989	2.121	0.152	4.374	0.042	3.863	0.054	0.798	0.375								
L. tardigradus	0.334	0.565	1.474	0.230	6.752	0.012	3.418	0.070	2.225	0.141	0.110	0.742						
N. bengalensis	1.970	0.165	0.132	0.718	7.388	0.009	0.034	0.855	3.948	0.052	1.193	0.281	0.728	0.398				
N. coucang	0.972	0.326	1.106	0.296	8.121	0.005	1.879	0.174	3.106	0.081	0.419	0.519	0.223	0.638	0.442	0.508		
P. potto	0.445	0.506	2.517	0.115	2.290	0.132	5.812	0.017	0.095	0.758	0.199	0.656	1.535	0.217	1.704	0.194	2.382	0.124

Whole cranium - PC2	*C. major*		*C. medius*		*M. murinus*		*M. rufus*		*G. alleni*		*G. demidoff*		*E. elegantulus*		*G. moholi*		*G. senegalensis*	
	F value	p value	F value	p value	F value	p value	F value	p value	F value	p value	F value	p value	F value	p value	F value	p value	F value	p value
C. major																		
C. medius	0.014	0.905	0.014	0.905	0.014	0.905	0.014	0.905	0.014	0.905	0.014	0.905	0.014	0.905	0.014	0.905	0.014	0.905
M. murinus	0.059	0.809	0.158	0.692	0.059	0.809	0.059	0.809	0.059	0.809	0.059	0.809	0.059	0.809	0.059	0.809	0.059	0.809
M. rufus	1.260	0.267	2.018	0.161	1.108	0.295	1.260	0.267	1.260	0.267	1.260	0.267	1.260	0.267	1.260	0.267	1.260	0.267
G. alleni	0.000	0.983	0.008	0.930	0.064	0.801	1.173	0.284	0.000	0.983	0.000	0.983	0.000	0.983	0.000	0.983	0.000	0.983
G. demidoff	0.018	0.894	0.001	0.982	0.196	0.659	2.302	0.133	0.011	0.918	0.018	0.894	0.018	0.894	0.018	0.894	0.018	0.894
E. elegantulus	2.125	0.151	2.365	0.129	2.770	0.099	5.435	0.023	1.891	0.175	2.159	0.145	2.125	0.151	2.125	0.151	2.125	0.151
G. moholi	0.005	0.941	0.051	0.822	0.054	0.817	2.005	0.160	0.009	0.924	0.063	0.802	3.082	0.082	0.005	0.941	0.005	0.941
G. senegalensus	7.413	0.007	8.882	0.003	12.235	0.001	27.686	0.000	6.510	0.011	8.676	0.004	0.018	0.893	11.861	0.001	7.413	0.007
G. zanzibaricus	2.591	0.114	2.963	0.091	3.262	0.074	5.498	0.023	2.309	0.136	2.742	0.102	0.065	0.800	3.810	0.054	0.344	0.558
O. crassicaudatus	0.012	0.914	0.000	0.994	0.218	0.642	2.347	0.128	0.007	0.935	0.000	0.989	1.653	0.201	0.057	0.811	11.739	0.001
O. garnettii	6.144	0.015	7.621	0.007	10.611	0.001	21.556	0.000	5.353	0.022	7.691	0.006	0.000	0.995	10.689	0.001	0.073	0.788
A. laniger	1.001	0.322	1.074	0.305	1.324	0.253	2.997	0.090	0.879	0.354	0.933	0.337	0.079	0.780	1.448	0.232	0.139	0.710
I. Indri	2.192	0.144	3.044	0.086	2.160	0.145	0.334	0.565	2.067	0.156	3.431	0.067	6.158	0.016	3.280	0.073	22.816	0.000
P. diadema	4.090	0.049	4.901	0.031	5.852	0.017	8.990	0.004	3.627	0.063	4.919	0.029	0.212	0.647	6.726	0.011	1.210	0.273
P. verreauxi	0.199	0.657	0.383	0.538	0.061	0.806	0.476	0.493	0.199	0.657	0.429	0.514	3.116	0.082	0.237	0.628	12.178	0.001
E. fulvus	1.156	0.284	1.993	0.160	0.961	0.328	0.268	0.605	1.104	0.295	2.421	0.121	6.882	0.009	1.748	0.187	39.081	0.000
E. macaco	0.553	0.460	0.514	0.476	1.043	0.309	4.003	0.049	0.472	0.494	0.453	0.503	0.864	0.355	0.890	0.347	2.482	0.117
E. mongoz	3.141	0.080	4.967	0.029	3.167	0.078	0.165	0.686	2.898	0.093	5.592	0.020	9.553	0.003	5.052	0.026	55.821	0.000
E. rubriventer	0.238	0.628	0.202	0.655	0.389	0.534	1.713	0.196	0.199	0.657	0.150	0.699	0.703	0.405	0.340	0.561	1.579	0.210
H. griseus	0.077	0.783	0.207	0.651	0.000	0.989	0.945	0.336	0.080	0.778	0.201	0.655	3.225	0.078	0.061	0.806	11.937	0.001
L. catta	1.043	0.312	1.702	0.197	0.801	0.373	0.028	0.868	0.978	0.327	1.878	0.174	5.299	0.025	1.548	0.216	25.211	0.000
V. variegata	2.383	0.128	3.903	0.053	1.499	0.223	0.001	0.970	2.188	0.144	3.460	0.066	9.386	0.003	2.931	0.090	38.885	0.000
L. ruficaudatus	7.676	0.008	11.111	0.002	7.799	0.006	2.507	0.120	6.979	0.011	11.504	0.001	14.356	0.000	11.906	0.001	64.931	0.000
L. tardigradus	5.902	0.019	8.040	0.007	12.007	0.001	16.637	0.000	5.065	0.029	9.368	0.003	0.217	0.643	13.200	0.000	2.977	0.086
N. bengalensis	3.888	0.055	4.584	0.037	4.100	0.046	6.954	0.011	3.421	0.071	3.710	0.058	0.176	0.676	5.084	0.027	0.746	0.389
N. coucang	1.526	0.220	1.728	0.192	3.358	0.069	8.315	0.005	1.318	0.254	1.875	0.173	0.346	0.558	3.014	0.085	1.546	0.215
P. potto	1.027	0.313	1.108	0.294	2.733	0.100	7.720	0.006	0.885	0.348	1.266	0.262	0.567	0.453	2.144	0.145	2.896	0.090

Whole cranium - PC2	*G. zanzibaricus*		*O. crassicaudatus*		*O. garnettii*		*A. laniger*		*I. indri*		*P. diadema*		*P. verreauxi*		*E. fulvus*		*E. macaco*	
	F value	p value	F value	p value	F value	p value	F value	p value	F value	p value	F value	p value	F value	p value	F value	p value	F value	p value
C. major																		
C. medius	0.014	0.905	0.014	0.905	0.014	0.905	0.014	0.905	0.014	0.905	0.014	0.905	0.014	0.905	0.014	0.905	0.014	0.905
M. murinus	0.059	0.809	0.059	0.809	0.059	0.809	0.059	0.809	0.059	0.809	0.059	0.809	0.059	0.809	0.059	0.809	0.059	0.809
M. rufus	1.260	0.267	1.260	0.267	1.260	0.267	1.260	0.267	1.260	0.267	1.260	0.267	1.260	0.267	1.260	0.267	1.260	0.267
G. alleni	0.000	0.983	0.000	0.983	0.000	0.983	0.000	0.983	0.000	0.983	0.000	0.983	0.000	0.983	0.000	0.983	0.000	0.983
G. demidoff	0.018	0.894	0.018	0.894	0.018	0.894	0.018	0.894	0.018	0.894	0.018	0.894	0.018	0.894	0.018	0.894	0.018	0.894
E. elegantulus	2.125	0.151	2.125	0.151	2.125	0.151	2.125	0.151	2.125	0.151	2.125	0.151	2.125	0.151	2.125	0.151	2.125	0.151
G. moholi	0.005	0.941	0.005	0.941	0.005	0.941	0.005	0.941	0.005	0.941	0.005	0.941	0.005	0.941	0.005	0.941	0.005	0.941
G. senegalensus	7.413	0.007	7.413	0.007	7.413	0.007	7.413	0.007	7.413	0.007	7.413	0.007	7.413	0.007	7.413	0.007	7.413	0.007
G. zanzibaricus	2.591	0.114	2.591	0.114	2.591	0.114	2.591	0.114	2.591	0.114	2.591	0.114	2.591	0.114	2.591	0.114	2.591	0.114
O. crassicaudatus	2.043	0.155	0.012	0.914	0.012	0.914	0.012	0.914	0.012	0.914	0.012	0.914	0.012	0.914	0.012	0.914	0.012	0.914
O. garnettii	0.159	0.691	11.066	0.001	6.144	0.015	6.144	0.015	6.144	0.015	6.144	0.015	6.144	0.015	6.144	0.015	6.144	0.015
A. laniger	0.240	0.627	0.662	0.417	0.171	0.680	1.001	0.322	1.001	0.322	1.001	0.322	1.001	0.322	1.001	0.322	1.001	0.322
I. Indri	6.174	0.016	3.141	0.079	17.332	0.000	3.811	0.056	2.192	0.144	2.192	0.144	2.192	0.144	2.192	0.144	2.192	0.144
P. diadema	0.026	0.872	4.293	0.040	0.660	0.418	0.468	0.497	9.042	0.004	4.090	0.049	4.090	0.049	4.090	0.049	4.090	0.049
P. verreauxi	3.525	0.065	0.392	0.533	9.940	0.002	1.612	0.209	1.305	0.257	5.742	0.019	0.199	0.657	0.199	0.657	0.199	0.657
E. fulvus	7.565	0.007	4.299	0.039	38.103	0.000	3.654	0.057	1.423	0.234	14.507	0.000	0.251	0.617	1.156	0.284	1.156	0.284
E. macaco	1.371	0.245	0.396	0.530	2.354	0.127	0.255	0.615	5.030	0.027	2.471	0.120	1.433	0.234	4.258	0.040	0.553	0.460
E. mongoz	9.698	0.003	7.150	0.008	46.979	0.000	5.495	0.022	0.166	0.684	16.896	0.000	1.537	0.218	1.763	0.186	7.847	0.006
E. rubriventer	1.069	0.306	0.102	0.750	1.395	0.240	0.256	0.615	2.543	0.116	1.592	0.213	0.625	0.432	1.599	0.208	0.010	0.920
H. griseus	3.764	0.058	0.153	0.696	9.896	0.002	1.650	0.205	1.907	0.172	5.927	0.018	0.052	0.821	0.690	0.407	1.199	0.277
L. catta	5.517	0.022	1.860	0.175	20.057	0.000	2.923	0.093	0.540	0.465	9.020	0.004	0.306	0.582	0.075	0.784	3.571	0.062
V. variegata	10.016	0.002	3.014	0.085	32.712	0.000	5.681	0.020	0.557	0.458	15.725	0.000	0.703	0.404	0.292	0.589	6.373	0.013
L. ruficaudatus	13.473	0.001	10.314	0.002	49.298	0.000	9.184	0.004	0.495	0.485	19.977	0.000	5.166	0.026	7.800	0.006	14.622	0.000
L. tardigradus	0.014	0.905	15.174	0.000	1.646	0.202	0.487	0.489	13.051	0.001	0.006	0.936	9.410	0.003	49.196	0.000	3.707	0.058
N. bengalensis	0.017	0.897	2.519	0.115	0.402	0.528	0.461	0.501	7.383	0.009	0.001	0.972	4.569	0.037	8.911	0.003	2.068	0.155
N. coucang	0.719	0.399	2.664	0.105	1.732	0.190	0.031	0.860	8.130	0.005	1.712	0.194	3.357	0.070	14.960	0.000	0.235	0.629
P. potto	0.996	0.320	2.348	0.127	3.208	0.075	0.104	0.748	7.688	0.006	2.345	0.128	2.723	0.101	14.745	0.000	0.062	0.804

Whole cranium - PC2	*E. mongoz*		*E. rubriventer*		*H. griseus*		*L. catta*		*V. variegata*		*L. ruficaudatus*		*L. tardigradus*		*N. bengalensis*		*N. coucang*	
	F value	p value	F value	p value	F value	p value	F value	p value	F value	p value	F value	p value	F value	p value	F value	p value	F value	p value
C. major																		
C. medius	0.014	0.905	0.014	0.905	0.014	0.905	0.014	0.905	0.014	0.905	0.014	0.905	0.014	0.905	0.014	0.905	0.014	0.905
M. murinus	0.059	0.809	0.059	0.809	0.059	0.809	0.059	0.809	0.059	0.809	0.059	0.809	0.059	0.809	0.059	0.809	0.059	0.809
M. rufus	1.260	0.267	1.260	0.267	1.260	0.267	1.260	0.267	1.260	0.267	1.260	0.267	1.260	0.267	1.260	0.267	1.260	0.267
G. alleni	0.000	0.983	0.000	0.983	0.000	0.983	0.000	0.983	0.000	0.983	0.000	0.983	0.000	0.983	0.000	0.983	0.000	0.983
G. demidoff	0.018	0.894	0.018	0.894	0.018	0.894	0.018	0.894	0.018	0.894	0.018	0.894	0.018	0.894	0.018	0.894	0.018	0.894
E. elegantulus	2.125	0.151	2.125	0.151	2.125	0.151	2.125	0.151	2.125	0.151	2.125	0.151	2.125	0.151	2.125	0.151	2.125	0.151
G. moholi	0.005	0.941	0.005	0.941	0.005	0.941	0.005	0.941	0.005	0.941	0.005	0.941	0.005	0.941	0.005	0.941	0.005	0.941
G. senegalensus	7.413	0.007	7.413	0.007	7.413	0.007	7.413	0.007	7.413	0.007	7.413	0.007	7.413	0.007	7.413	0.007	7.413	0.007
G. zanzibaricus	2.591	0.114	2.591	0.114	2.591	0.114	2.591	0.114	2.591	0.114	2.591	0.114	2.591	0.114	2.591	0.114	2.591	0.114
O. crassicaudatus	0.012	0.914	0.012	0.914	0.012	0.914	0.012	0.914	0.012	0.914	0.012	0.914	0.012	0.914	0.012	0.914	0.012	0.914
O. garnettii	6.144	0.015	6.144	0.015	6.144	0.015	6.144	0.015	6.144	0.015	6.144	0.015	6.144	0.015	6.144	0.015	6.144	0.015
A. laniger	1.001	0.322	1.001	0.322	1.001	0.322	1.001	0.322	1.001	0.322	1.001	0.322	1.001	0.322	1.001	0.322	1.001	0.322
I. Indri	2.192	0.144	2.192	0.144	2.192	0.144	2.192	0.144	2.192	0.144	2.192	0.144	2.192	0.144	2.192	0.144	2.192	0.144
P. diadema	4.090	0.049	4.090	0.049	4.090	0.049	4.090	0.049	4.090	0.049	4.090	0.049	4.090	0.049	4.090	0.049	4.090	0.049
P. verreauxi	0.199	0.657	0.199	0.657	0.199	0.657	0.199	0.657	0.199	0.657	0.199	0.657	0.199	0.657	0.199	0.657	0.199	0.657
E. fulvus	1.156	0.284	1.156	0.284	1.156	0.284	1.156	0.284	1.156	0.284	1.156	0.284	1.156	0.284	1.156	0.284	1.156	0.284
E. macaco	0.553	0.460	0.553	0.460	0.553	0.460	0.553	0.460	0.553	0.460	0.553	0.460	0.553	0.460	0.553	0.460	0.553	0.460
E. mongoz	3.141	0.080	3.141	0.080	3.141	0.080	3.141	0.080	3.141	0.080	3.141	0.080	3.141	0.080	3.141	0.080	3.141	0.080
E. rubriventer	3.257	0.075	0.238	0.628	0.238	0.628	0.238	0.628	0.238	0.628	0.238	0.628	0.238	0.628	0.238	0.628	0.238	0.628
H. griseus	2.655	0.107	0.077	0.783	0.077	0.783	0.077	0.783	0.077	0.783	0.077	0.783	0.077	0.783	0.077	0.783	0.077	0.783
L. catta	0.404	0.527	1.043	0.312	0.715	0.401	1.043	0.312	1.043	0.312	1.043	0.312	1.043	0.312	1.043	0.312	1.043	0.312
V. variegata	0.312	0.578	3.344	0.072	1.789	0.186	0.032	0.859	2.383	0.128	2.383	0.128	2.383	0.128	2.383	0.128	2.383	0.128
L. ruficaudatus	2.709	0.104	7.354	0.009	7.655	0.008	3.365	0.072	4.813	0.032	7.676	0.008	7.676	0.008	7.676	0.008	7.676	0.008
L. tardigradus	43.628	0.000	1.733	0.194	9.253	0.004	16.634	0.000	30.055	0.000	33.224	0.000	5.902	0.019	5.902	0.019	5.902	0.019
N. bengalensis	11.934	0.001	1.781	0.189	5.635	0.022	7.082	0.010	14.348	0.000	17.171	0.000	0.001	0.978	3.888	0.055	3.888	0.055
N. coucang	19.246	0.000	0.179	0.673	2.808	0.097	7.558	0.007	12.236	0.001	22.797	0.000	4.254	0.042	1.107	0.296	1.526	0.220
P. potto	18.710	0.000	0.065	0.799	2.034	0.156	6.757	0.010	10.041	0.002	21.651	0.000	7.250	0.008	1.391	0.240	0.115	0.735

Whole cranium - PC3	*C. major*		*C. medius*		*M. murinus*		*M. rufus*		*G. alleni*		*G. demidoff*		*E. elegantulus*		*G. moholi*		*G. senegalensis*	
	F value	p value	F value	p value	F value	p value	F value	p value	F value	p value	F value	p value	F value	p value	F value	p value	F value	p value
C. major																		
C. medius	3.418	0.070																
M. murinus	0.108	0.743	5.309	0.023														
M. rufus	1.691	0.199	0.442	0.509	2.328	0.130												
G. alleni	0.025	0.874	4.314	0.043	0.310	0.579	2.287	0.137										
G. demidoff	0.231	0.632	3.586	0.062	0.062	0.804	1.382	0.243	0.478	0.491								
E. elegantulus	0.839	0.364	0.382	0.539	0.919	0.340	0.014	0.907	1.176	0.283	0.532	0.468						
G. moholi	0.417	0.520	4.536	0.036	0.150	0.699	1.650	0.202	0.813	0.370	0.010	0.922	0.599	0.441				
G. senegalensus	0.995	0.320	6.332	0.013	0.557	0.456	2.105	0.148	1.650	0.200	0.132	0.717	0.624	0.430	0.067	0.796		
G. zanzibaricus	0.168	0.684	1.292	0.261	0.079	0.779	0.424	0.518	0.325	0.572	0.011	0.915	0.201	0.656	0.003	0.953	0.006	0.938
O. crassicaudatus	0.948	0.332	4.199	0.043	0.742	0.390	1.255	0.265	1.483	0.226	0.239	0.626	0.333	0.565	0.174	0.677	0.068	0.795
O. garnettii	3.393	0.068	0.755	0.387	4.535	0.035	0.005	0.945	4.277	0.041	2.812	0.096	0.039	0.843	3.052	0.083	4.762	0.030
A. laniger	0.412	0.524	0.433	0.514	0.420	0.519	0.057	0.812	0.615	0.437	0.213	0.646	0.015	0.904	0.231	0.632	0.204	0.652
I. Indri	0.374	0.543	1.112	0.296	0.285	0.594	0.279	0.599	0.600	0.442	0.107	0.744	0.106	0.746	0.092	0.762	0.045	0.832
P. diadema	0.074	0.786	2.684	0.107	0.002	0.966	1.114	0.296	0.203	0.654	0.022	0.883	0.512	0.477	0.066	0.798	0.258	0.612
P. verreauxi	0.468	0.497	2.072	0.155	0.310	0.579	0.600	0.441	0.796	0.376	0.093	0.761	0.218	0.642	0.069	0.793	0.014	0.907
E. fulvus	1.074	0.301	3.726	0.055	0.854	0.356	1.027	0.312	1.594	0.208	0.322	0.571	0.268	0.605	0.243	0.622	0.147	0.701
E. macaco	6.848	0.011	0.425	0.516	9.401	0.003	1.898	0.172	8.286	0.005	6.961	0.010	1.409	0.238	8.561	0.004	11.162	0.001
E. mongoz	1.820	0.181	1.521	0.221	2.130	0.147	0.147	0.702	2.533	0.116	1.143	0.287	0.014	0.904	1.230	0.270	1.489	0.224
E. rubriventer	0.704	0.406	0.274	0.603	0.764	0.384	0.006	0.936	1.005	0.321	0.447	0.506	0.000	0.984	0.520	0.473	0.517	0.473
H. griseus	0.351	0.556	8.670	0.005	1.477	0.227	5.207	0.027	0.181	0.673	1.749	0.190	2.552	0.116	2.816	0.097	5.027	0.026
L. catta	0.116	0.735	4.660	0.035	0.002	0.969	1.974	0.165	0.332	0.567	0.041	0.840	0.790	0.377	0.121	0.729	0.453	0.502
V. variegata	0.110	0.741	8.808	0.004	0.825	0.366	4.969	0.029	0.015	0.902	1.155	0.285	2.165	0.146	1.878	0.173	3.922	0.049
L. ruficaudatus	0.001	0.972	5.267	0.026	0.124	0.726	2.564	0.116	0.059	0.809	0.292	0.591	1.150	0.288	0.563	0.455	1.262	0.263
L. tardigradus	3.228	0.079	0.312	0.579	5.798	0.018	0.086	0.771	4.176	0.047	3.509	0.065	0.108	0.744	4.419	0.038	7.895	0.005
N. bengalensis	1.981	0.167	0.021	0.885	2.561	0.113	0.143	0.707	2.717	0.107	1.705	0.195	0.172	0.680	2.222	0.139	2.440	0.120
N. coucang	3.900	0.051	0.241	0.625	5.578	0.020	0.149	0.700	4.847	0.030	3.627	0.059	0.167	0.684	4.155	0.043	6.470	0.012
P. potto	5.190	0.024	0.011	0.918	8.114	0.005	0.889	0.347	5.877	0.017	5.757	0.017	0.587	0.445	6.258	0.013	11.850	0.001

Whole cranium - PC3	*G. zanzibaricus*		*O. crassicaudatus*		*O. garnettii*		*A. laniger*		*I. indri*		*P. diadema*		*P. verreauxi*		*E. fulvus*		*E. macaco*	
	F value	p value	F value	p value	F value	p value	F value	p value	F value	p value	F value	p value	F value	p value	F value	p value	F value	p value
C. major																		
C. medius																		
M. murinus																		
M. rufus																		
G. alleni																		
G. demidoff																		
E. elegantulus																		
G. moholi																		
G. senegalensus																		
G. zanzibaricus																		
O. crassicaudatus	0.026	0.873																
O. garnettii	0.766	0.383	3.624	0.058														
A. laniger	0.072	0.790	0.087	0.768	0.126	0.724												
I. Indri	0.022	0.882	0.006	0.939	0.553	0.459	0.024	0.878										
P. diadema	0.037	0.848	0.313	0.577	2.161	0.144	0.222	0.640	0.145	0.705								
P. verreauxi	0.012	0.913	0.001	0.972	1.168	0.282	0.062	0.804	0.006	0.938	0.153	0.697						
E. fulvus	0.046	0.831	0.022	0.883	2.793	0.096	0.061	0.804	0.000	0.990	0.387	0.535	0.013	0.910				
E. macaco	3.142	0.080	8.043	0.005	2.818	0.095	1.421	0.237	2.803	0.098	5.695	0.019	4.710	0.033	7.097	0.008		
E. mongoz	0.292	0.590	0.869	0.353	0.437	0.510	0.005	0.941	0.134	0.715	1.010	0.318	0.354	0.554	0.597	0.441	4.154	0.044
E. rubriventer	0.188	0.666	0.274	0.602	0.020	0.889	0.016	0.898	0.098	0.755	0.443	0.509	0.197	0.659	0.221	0.639	1.094	0.299
H. griseus	1.046	0.312	4.376	0.038	9.362	0.003	1.441	0.236	1.582	0.213	0.930	0.339	2.339	0.131	4.344	0.038	14.729	0.000
L. catta	0.064	0.802	0.577	0.449	3.786	0.054	0.345	0.559	0.229	0.634	0.000	0.991	0.263	0.610	0.661	0.417	9.040	0.003
V. variegata	0.681	0.412	3.772	0.054	9.676	0.002	1.165	0.285	1.198	0.277	0.522	0.473	1.715	0.194	3.789	0.053	14.637	0.000
L. ruficaudatus	0.234	0.631	1.261	0.264	4.692	0.032	0.564	0.457	0.487	0.488	0.094	0.760	0.654	0.422	1.329	0.250	10.016	0.002
L. tardigradus	0.854	0.360	5.717	0.018	0.163	0.687	0.179	0.674	0.686	0.411	2.303	0.135	1.553	0.217	4.568	0.034	1.940	0.168
N. bengalensis	0.818	0.371	1.500	0.223	0.181	0.671	0.233	0.632	0.578	0.450	1.540	0.221	1.057	0.308	1.284	0.259	0.495	0.484
N. coucang	1.083	0.301	4.811	0.030	0.237	0.627	0.270	0.604	0.875	0.352	2.711	0.103	1.742	0.190	3.940	0.048	1.638	0.203
P. potto	1.668	0.198	10.302	0.002	2.014	0.157	0.655	0.420	1.678	0.197	3.853	0.051	2.982	0.086	9.184	0.003	0.373	0.542

Whole cranium - PC3	*E. mongoz*		*E. rubriventer*		*H. griseus*		*L. catta*		*V. variegata*		*L. ruficaudatus*		*L. tardigradus*		*N. bengalensis*		*N. coucang*	
	F value	p value	F value	p value	F value	p value	F value	p value	F value	p value	F value	p value	F value	p value	F value	p value	F value	p value
C. major																		
C. medius																		
M. murinus																		
M. rufus																		
G. alleni																		
G. demidoff																		
E. elegantulus																		
G. moholi																		
G. senegalensus																		
G. zanzibaricus																		
O. crassicaudatus																		
O. garnettii																		
A. laniger																		
I. Indri																		
P. diadema																		
P. verreauxi																		
E. fulvus																		
E. macaco																		
E. mongoz																		
E. rubriventer	0.018	0.895																
H. griseus	6.239	0.015	0.351	0.556														
L. catta	1.828	0.180	0.116	0.735	1.651	0.204												
V. variegata	5.820	0.018	1.794	0.185	0.178	0.675	0.906	0.345										
L. ruficaudatus	2.666	0.107	1.005	0.321	0.720	0.400	0.164	0.687	0.236	0.629								
L. tardigradus	0.978	0.326	0.064	0.801	9.898	0.003	4.744	0.034	10.997	0.002	5.391	0.025						
N. bengalensis	0.538	0.466	0.134	0.716	5.632	0.022	2.615	0.112	4.911	0.031	3.344	0.074	0.054	0.818				
N. coucang	1.060	0.305	0.105	0.746	10.169	0.002	4.740	0.032	10.619	0.002	5.567	0.020	0.016	0.899	0.033	0.857		
P. potto	3.123	0.079	0.386	0.535	10.987	0.001	6.365	0.013	12.622	0.000	6.691	0.011	1.073	0.302	0.048	0.827	0.673	0.413

Whole cranium - PC4	*C. major*		*C. medius*		*M. murinus*		*M. rufus*		*G. alleni*		*G. demidoff*		*E. elegantulus*		*G. moholi*		*G. senegalensis*	
	F value	p value	F value	p value	F value	p value	F value	p value	F value	p value	F value	p value	F value	p value	F value	p value	F value	p value
C. major																		
C. medius	7.682	0.008																
M. murinus	0.535	0.466	3.077	0.083														
M. rufus	0.036	0.850	9.146	0.004	0.976	0.326												
G. alleni	2.321	0.135	0.184	0.670	0.891	0.348	2.959	0.092										
G. demidoff	0.962	0.330	2.325	0.131	0.062	0.805	1.567	0.214	0.563	0.455								
E. elegantulus	3.494	0.067	0.181	0.672	2.536	0.114	4.338	0.042	0.387	0.536	2.000	0.161						
G. moholi	0.018	0.894	8.334	0.005	0.994	0.320	0.001	0.974	3.191	0.077	1.573	0.212	5.262	0.024				
G. senegalensus	0.838	0.361	6.191	0.014	0.004	0.948	1.715	0.192	1.820	0.179	0.166	0.684	4.833	0.029	1.658	0.199		
G. zanzibaricus	0.695	0.409	6.235	0.016	1.713	0.194	0.528	0.471	2.768	0.103	2.172	0.144	3.784	0.057	0.579	0.449	2.862	0.092
O. crassicaudatus	6.403	0.013	0.027	0.870	5.492	0.020	10.534	0.002	0.354	0.553	3.894	0.050	0.148	0.701	12.356	0.001	14.039	0.000
O. garnettii	6.619	0.011	0.011	0.918	4.606	0.033	10.574	0.001	0.183	0.670	3.203	0.076	0.345	0.558	11.609	0.001	11.018	0.001
A. laniger	2.358	0.132	0.084	0.773	0.742	0.391	2.617	0.112	0.005	0.945	0.509	0.478	0.248	0.621	2.502	0.117	1.359	0.245
I. Indri	8.140	0.006	0.238	0.627	3.751	0.055	9.250	0.003	0.587	0.447	3.085	0.082	0.009	0.926	8.488	0.004	6.635	0.011
P. diadema	2.418	0.126	0.325	0.571	0.802	0.373	3.101	0.084	0.006	0.936	0.481	0.490	0.529	0.470	3.178	0.078	1.630	0.203
P. verreauxi	2.596	0.112	0.194	0.661	1.143	0.287	3.555	0.064	0.000	0.984	0.724	0.397	0.463	0.498	3.873	0.052	2.322	0.129
E. fulvus	0.654	0.420	3.392	0.067	0.007	0.934	1.345	0.248	0.958	0.329	0.042	0.838	3.007	0.084	1.468	0.227	0.042	0.838
E. macaco	1.264	0.264	0.564	0.455	0.393	0.532	1.832	0.180	0.070	0.793	0.181	0.671	0.806	0.372	2.045	0.155	0.810	0.369
E. mongoz	13.176	0.001	1.411	0.238	11.090	0.001	18.992	0.000	1.872	0.175	8.926	0.003	0.063	0.802	21.002	0.000	25.209	0.000
E. rubriventer	3.370	0.073	11.584	0.001	4.295	0.041	2.780	0.101	5.569	0.022	5.103	0.027	6.166	0.016	2.653	0.107	6.927	0.009
H. griseus	1.243	0.271	1.330	0.254	0.168	0.683	1.741	0.193	0.244	0.624	0.038	0.846	1.176	0.283	1.744	0.190	0.391	0.532
L. catta	0.623	0.433	1.697	0.198	0.035	0.852	1.028	0.315	0.413	0.523	0.001	0.975	1.477	0.229	1.157	0.285	0.107	0.744
V. variegata	9.959	0.003	0.917	0.342	7.654	0.007	13.378	0.001	1.288	0.261	6.191	0.015	0.033	0.857	15.000	0.000	16.307	0.000
L. ruficaudatus	3.114	0.084	0.690	0.410	0.746	0.390	3.852	0.055	0.042	0.839	0.411	0.524	0.771	0.384	3.518	0.064	1.567	0.212
L. tardigradus	0.918	0.343	2.769	0.102	0.054	0.817	1.703	0.198	0.582	0.449	0.003	0.956	1.871	0.177	1.977	0.163	0.226	0.635
N. bengalensis	6.612	0.014	0.156	0.695	2.596	0.111	6.777	0.012	0.387	0.537	2.143	0.147	0.009	0.926	6.096	0.015	4.634	0.033
N. coucang	10.644	0.002	1.210	0.274	10.208	0.002	15.976	0.000	1.662	0.201	8.058	0.005	0.060	0.807	18.795	0.000	23.788	0.000
P. potto	5.803	0.017	0.105	0.746	5.423	0.021	9.462	0.002	0.471	0.494	3.917	0.049	0.060	0.807	11.298	0.001	13.025	0.000

Whole cranium - PC4	*G. zanzibaricus*		*O. crassicaudatus*		*O. garnettii*		*A. laniger*		*I. indri*		*P. diadema*		*P. verreauxi*		*E. fulvus*		*E. macaco*	
	F value	p value	F value	p value	F value	p value	F value	p value	F value	p value	F value	p value	F value	p value	F value	p value	F value	p value
C. major																		
C. medius																		
M. murinus																		
M. rufus																		
G. alleni																		
G. demidoff																		
E. elegantulus																		
G. moholi																		
G. senegalensus																		
G. zanzibaricus																		
O. crassicaudatus	6.632	0.011																
O. garnettii	7.044	0.009	0.182	0.670														
A. laniger	2.629	0.112	0.138	0.711	0.058	0.810												
I. Indri	7.048	0.010	0.114	0.736	0.357	0.551	0.380	0.540										
P. diadema	2.949	0.092	0.553	0.459	0.332	0.565	0.021	0.884	0.833	0.365								
P. verreauxi	3.328	0.073	0.430	0.513	0.205	0.652	0.003	0.955	0.623	0.432	0.012	0.913						
E. fulvus	1.987	0.160	10.598	0.001	7.632	0.006	0.695	0.406	3.758	0.054	0.837	0.361	1.306	0.254				
E. macaco	2.180	0.144	1.048	0.308	0.726	0.395	0.087	0.769	1.076	0.302	0.038	0.845	0.098	0.755	0.425	0.515		
E. mongoz	10.738	0.002	1.943	0.165	3.292	0.072	1.027	0.314	0.236	0.628	2.487	0.119	2.307	0.132	16.922	0.000	3.257	0.074
E. rubriventer	0.417	0.522	10.112	0.002	11.321	0.001	5.500	0.023	12.206	0.001	6.053	0.017	6.278	0.015	4.479	0.036	4.422	0.039
H. griseus	2.046	0.159	1.963	0.164	1.611	0.207	0.263	0.611	2.065	0.156	0.196	0.660	0.326	0.570	0.150	0.699	0.047	0.829
L. catta	1.462	0.232	3.181	0.077	2.639	0.107	0.375	0.543	2.349	0.130	0.364	0.549	0.569	0.453	0.022	0.882	0.156	0.694
V. variegata	8.298	0.005	1.021	0.314	1.866	0.174	0.757	0.388	0.146	0.704	1.734	0.193	1.581	0.212	10.291	0.002	2.319	0.131
L. ruficaudatus	3.378	0.073	1.005	0.318	0.694	0.407	0.072	0.790	1.398	0.242	0.015	0.903	0.061	0.806	0.754	0.386	0.011	0.918
L. tardigradus	1.811	0.185	8.449	0.004	6.531	0.012	0.472	0.495	3.307	0.074	0.533	0.469	0.871	0.354	0.045	0.832	0.236	0.629
N. bengalensis	5.194	0.028	0.064	0.800	0.220	0.640	0.274	0.603	0.000	0.983	0.565	0.456	0.415	0.522	2.506	0.115	0.738	0.393
N. coucang	9.296	0.003	1.948	0.165	3.171	0.077	0.878	0.351	0.204	0.652	2.185	0.143	2.100	0.150	17.022	0.000	3.031	0.084
P. potto	6.134	0.014	0.087	0.769	0.444	0.506	0.200	0.656	0.027	0.870	0.683	0.410	0.583	0.446	10.418	0.001	1.216	0.272

Whole cranium - PC4	*E. mongoz*		*E. rubriventer*		*H. griseus*		*L. catta*		*V. variegata*		*L. ruficaudatus*		*L. tardigradus*		*N. bengalensis*		*N. coucang*	
	F value	p value	F value	p value	F value	p value	F value	p value	F value	p value	F value	p value	F value	p value	F value	p value	F value	p value
C. major																		
C. medius																		
M. murinus																		
M. rufus																		
G. alleni																		
G. demidoff																		
E. elegantulus																		
G. moholi																		
G. senegalensus																		
G. zanzibaricus																		
O. crassicaudatus																		
O. garnettii																		
A. laniger																		
I. Indri																		
P. diadema																		
P. verreauxi																		
E. fulvus																		
E. macaco																		
E. mongoz																		
E. rubriventer	15.709	0.000																
H. griseus	5.248	0.025	1.243	0.271														
L. catta	6.817	0.011	0.623	0.433	0.035	0.852												
V. variegata	0.005	0.941	12.689	0.001	3.647	0.061	4.550	0.036										
L. ruficaudatus	3.884	0.052	7.357	0.009	0.145	0.705	0.311	0.579	2.680	0.107								
L. tardigradus	14.213	0.000	4.339	0.042	0.058	0.810	0.000	0.990	7.765	0.007	0.498	0.484						
N. bengalensis	0.179	0.674	9.664	0.003	1.406	0.242	1.523	0.223	0.112	0.739	0.975	0.329	1.968	0.168				
N. coucang	0.000	0.994	13.216	0.000	4.595	0.035	6.273	0.014	0.006	0.939	3.313	0.072	13.369	0.000	0.152	0.697		
P. potto	1.012	0.316	9.016	0.003	2.054	0.154	3.279	0.072	0.528	0.468	1.142	0.287	8.018	0.005	0.013	0.909	1.040	0.309

Whole cranium - PC2	*C. major*		*C. medius*		*M. murinus*		*M. rufus*		*G. alleni*		*G. demidoff*		*E. elegantulus*		*G. moholi*		*G. senegalensis*	
	F value	p value	F value	p value	F value	p value	F value	p value	F value	p value	F value	p value	F value	p value	F value	p value	F value	p value
C. major																		
C. medius	1.732	0.194																
M. murinus	3.341	0.071	0.177	0.675														
M. rufus	0.737	0.395	0.348	0.558	1.200	0.276												
G. alleni	0.291	0.592	0.252	0.618	0.839	0.362	0.008	0.929										
G. demidoff	0.631	0.429	4.964	0.029	8.999	0.003	3.278	0.074	1.671	0.200								
E. elegantulus	7.045	0.010	2.989	0.089	2.370	0.127	5.056	0.028	3.160	0.081	10.676	0.002						
G. moholi	0.147	0.702	1.069	0.304	2.574	0.111	0.255	0.615	0.085	0.771	1.950	0.165	6.119	0.015				
G. senegalensus	2.751	0.099	0.002	0.966	0.381	0.538	0.543	0.462	0.453	0.502	10.635	0.001	4.504	0.035	2.011	0.157		
G. zanzibaricus	0.466	0.498	3.042	0.087	4.997	0.028	2.001	0.163	1.036	0.314	0.004	0.949	7.801	0.007	1.104	0.296	4.867	0.029
O. crassicaudatus	0.172	0.679	3.704	0.057	8.005	0.005	2.176	0.143	0.992	0.321	0.278	0.599	8.379	0.004	1.121	0.291	11.991	0.001
O. garnettii	0.484	0.488	0.268	0.606	1.123	0.291	0.000	0.986	0.005	0.945	3.497	0.063	3.246	0.074	0.241	0.624	0.778	0.379
A. laniger	0.921	0.342	3.868	0.055	6.145	0.015	2.791	0.101	1.507	0.226	0.151	0.698	8.596	0.005	1.798	0.183	6.294	0.013
I. Indri	0.060	0.807	0.614	0.436	1.460	0.230	0.160	0.690	0.061	0.806	0.910	0.343	3.889	0.053	0.002	0.966	1.086	0.299
P. diadema	2.286	0.137	0.335	0.565	0.120	0.730	1.076	0.304	0.722	0.400	5.649	0.020	0.774	0.383	2.128	0.148	0.747	0.388
P. verreauxi	8.452	0.005	4.374	0.040	4.429	0.038	6.939	0.010	4.397	0.040	16.147	0.000	0.091	0.764	9.919	0.002	9.505	0.002
E. fulvus	3.505	0.063	0.932	0.335	0.637	0.426	2.284	0.132	1.505	0.221	11.128	0.001	0.358	0.550	4.534	0.034	3.118	0.078
E. macaco	5.940	0.017	2.902	0.092	2.957	0.088	4.659	0.034	3.197	0.078	12.321	0.001	0.032	0.858	7.255	0.008	6.738	0.010
E. mongoz	0.005	0.944	2.163	0.145	4.964	0.028	1.006	0.319	0.426	0.516	0.798	0.374	6.900	0.010	0.310	0.579	5.848	0.016
E. rubriventer	12.461	0.001	8.614	0.005	9.257	0.003	11.321	0.001	7.266	0.010	16.964	0.000	2.066	0.156	13.245	0.000	14.429	0.000
H. griseus	0.037	0.847	0.808	0.373	2.041	0.156	0.249	0.620	0.093	0.762	0.949	0.333	4.311	0.042	0.015	0.902	1.758	0.186
L. catta	11.481	0.001	7.913	0.007	10.208	0.002	11.243	0.001	6.810	0.012	23.720	0.000	1.016	0.317	17.200	0.000	22.659	0.000
V. variegata	0.455	0.503	2.817	0.098	6.130	0.015	1.955	0.167	1.042	0.312	0.032	0.859	5.712	0.020	1.625	0.205	9.190	0.003
L. ruficaudatus	1.340	0.253	0.028	0.867	0.022	0.882	0.391	0.535	0.282	0.598	4.291	0.042	1.518	0.223	1.143	0.288	0.086	0.770
L. tardigradus	6.073	0.017	2.425	0.126	2.494	0.118	4.966	0.030	2.572	0.115	17.575	0.000	0.133	0.717	9.239	0.003	9.912	0.002
N. bengalensis	3.740	0.060	1.573	0.216	1.483	0.227	2.655	0.110	1.749	0.193	6.993	0.010	0.001	0.981	4.040	0.047	3.193	0.076
N. coucang	0.483	0.489	0.082	0.775	0.517	0.473	0.017	0.895	0.028	0.867	2.990	0.086	2.018	0.159	0.339	0.561	0.239	0.625
P. potto	0.114	0.736	2.371	0.126	5.159	0.024	1.385	0.241	0.671	0.414	0.182	0.670	5.485	0.020	0.756	0.386	7.797	0.006

Whole cranium - PC2	*G. zanzibaricus*		*O. crassicaudatus*		*O. garnettii*		*A. laniger*		*I. indri*		*P. diadema*		*P. verreauxi*		*E. fulvus*		*E. macaco*	
	F value	p value	F value	p value	F value	p value	F value	p value	F value	p value	F value	p value	F value	p value	F value	p value	F value	p value
C. major																		
C. medius																		
M. murinus																		
M. rufus																		
G. alleni																		
G. demidoff																		
E. elegantulus																		
G. moholi																		
G. senegalensus																		
G. zanzibaricus																		
O. crassicaudatus	0.139	0.709																
O. garnettii	1.363	0.245	4.130	0.044														
A. laniger	0.074	0.787	0.452	0.503	1.925	0.168												
I. Indri	0.615	0.436	0.413	0.522	0.129	0.720	1.035	0.313										
P. diadema	3.225	0.079	4.737	0.031	0.988	0.322	3.814	0.057	1.198	0.278								
P. verreauxi	8.586	0.005	16.419	0.000	6.977	0.009	9.161	0.004	5.398	0.023	1.473	0.229						
E. fulvus	4.059	0.045	19.516	0.000	5.006	0.026	4.645	0.032	2.099	0.149	0.078	0.780	1.285	0.258				
E. macaco	6.396	0.014	12.920	0.000	5.405	0.021	6.934	0.010	4.051	0.047	1.003	0.320	0.009	0.925	0.919	0.339		
E. mongoz	0.389	0.534	0.284	0.595	1.365	0.245	0.810	0.371	0.109	0.742	3.099	0.082	12.109	0.001	9.378	0.002	9.187	0.003
E. rubriventer	12.082	0.001	14.496	0.000	8.145	0.005	12.424	0.001	8.414	0.005	4.031	0.050	1.280	0.262	3.217	0.074	1.177	0.281
H. griseus	0.541	0.466	0.448	0.504	0.236	0.628	0.923	0.342	0.003	0.957	1.399	0.242	6.347	0.014	3.103	0.080	4.773	0.032
L. catta	10.281	0.002	29.544	0.000	14.893	0.000	10.410	0.002	8.235	0.005	3.464	0.068	0.710	0.402	5.268	0.023	0.755	0.387
V. variegata	0.004	0.948	0.453	0.502	3.189	0.076	0.027	0.871	0.681	0.412	3.268	0.075	9.799	0.002	10.476	0.001	8.321	0.005
L. ruficaudatus	2.246	0.141	3.595	0.060	0.404	0.526	2.783	0.102	0.617	0.435	0.114	0.737	2.623	0.110	0.523	0.470	1.866	0.176
L. tardigradus	5.937	0.019	30.006	0.000	8.864	0.004	6.348	0.015	3.535	0.065	0.403	0.528	0.675	0.414	0.384	0.536	0.393	0.533
N. bengalensis	4.406	0.042	5.914	0.017	2.271	0.135	4.854	0.033	2.410	0.126	0.429	0.516	0.071	0.791	0.254	0.615	0.029	0.865
N. coucang	1.149	0.287	3.501	0.063	0.041	0.841	1.563	0.215	0.171	0.680	0.508	0.478	4.395	0.038	2.834	0.094	3.496	0.064
P. potto	0.090	0.764	0.000	0.991	2.926	0.089	0.298	0.586	0.287	0.593	3.207	0.075	11.243	0.001	14.925	0.000	9.356	0.003

Whole cranium - PC2	*E. mongoz*		*E. rubriventer*		*H. griseus*		*L. catta*		*V. variegata*		*L. ruficaudatus*		*L. tardigradus*		*N. bengalensis*		*N. coucang*	
	F value	p value	F value	p value	F value	p value	F value	p value	F value	p value	F value	p value	F value	p value	F value	p value	F value	p value
C. major																		
C. medius																		
M. murinus																		
M. rufus																		
G. alleni																		
G. demidoff																		
E. elegantulus																		
G. moholi																		
G. senegalensus																		
G. zanzibaricus																		
O. crassicaudatus																		
O. garnettii																		
A. laniger																		
I. Indri																		
P. diadema																		
P. verreauxi																		
E. fulvus																		
E. macaco																		
E. mongoz																		
E. rubriventer	12.629	0.001																
H. griseus	0.088	0.767	0.037	0.847														
L. catta	20.345	0.000	11.481	0.001	9.539	0.003												
V. variegata	0.790	0.376	8.734	0.004	0.689	0.410	14.359	0.000										
L. ruficaudatus	2.055	0.156	5.136	0.028	0.758	0.388	5.136	0.027	2.541	0.116								
L. tardigradus	14.958	0.000	2.751	0.103	4.608	0.037	3.353	0.072	10.388	0.002	1.209	0.277						
N. bengalensis	4.463	0.038	1.280	0.264	2.485	0.122	0.680	0.414	3.748	0.058	0.840	0.364	0.064	0.801				
N. coucang	1.295	0.257	5.436	0.022	0.274	0.602	9.389	0.003	2.598	0.110	0.160	0.690	4.410	0.038	1.383	0.243		
P. potto	0.198	0.657	9.805	0.002	0.310	0.578	20.929	0.000	0.333	0.564	2.437	0.121	19.160	0.000	4.080	0.045	2.610	0.108

2* model FACE PC1	*C. major*		*C. medius*		*M. murinus*		*M. rufus*		*G. alleni*		*G. demidoff*		*E. elegantulus*		*G. moholi*		*G. senegalensis*	
	F value	p value	F value	p value	F value	p value	F value	p value	F value	p value	F value	p value	F value	p value	F value	p value	F value	p value
C. major																		
C. medius	2.440	0.125																
M. murinus	4.048	0.047	0.565	0.454														
M. rufus	2.243	0.140	0.001	0.970	0.650	0.422												
G. alleni	8.454	0.006	3.388	0.072	0.790	0.376	2.911	0.094										
G. demidoff	0.863	0.356	0.214	0.645	1.707	0.194	0.295	0.588	4.199	0.044								
E. elegantulus	2.050	0.158	0.094	0.761	0.103	0.749	0.063	0.802	1.254	0.268	0.363	0.548						
G. moholi	0.288	0.593	1.277	0.261	4.332	0.039	1.674	0.199	8.527	0.004	0.376	0.541	1.251	0.266				
G. senegalensus	0.747	0.389	7.542	0.007	17.369	0.000	11.104	0.001	21.910	0.000	5.987	0.015	5.301	0.022	3.774	0.053		
G. zanzibaricus	5.423	0.024	14.121	0.000	14.421	0.000	12.331	0.001	19.545	0.000	9.276	0.003	10.599	0.002	9.527	0.003	5.472	0.020
O. crassicaudatus	1.198	0.276	0.429	0.513	3.421	0.066	0.710	0.401	7.052	0.009	0.008	0.927	0.580	0.448	0.530	0.467	11.139	0.001
O. garnettii	1.489	0.225	0.436	0.511	3.268	0.073	0.673	0.414	7.841	0.006	0.002	0.968	0.626	0.430	0.638	0.425	10.978	0.001
A. laniger	0.073	0.789	0.262	0.611	0.721	0.398	0.236	0.629	1.733	0.195	0.055	0.816	0.369	0.546	0.001	0.979	0.659	0.418
I. Indri	3.959	0.051	0.604	0.440	0.000	0.999	0.505	0.480	0.759	0.387	1.186	0.279	0.116	0.735	3.050	0.084	10.285	0.002
P. diadema	0.183	0.671	0.306	0.583	1.151	0.286	0.319	0.575	2.560	0.116	0.051	0.821	0.423	0.518	0.019	0.889	1.590	0.209
P. verreauxi	0.188	0.666	0.630	0.430	2.413	0.123	0.773	0.382	4.456	0.039	0.177	0.675	0.703	0.405	0.003	0.959	2.490	0.116
E. fulvus	5.973	0.015	0.859	0.355	0.003	0.953	1.229	0.269	1.036	0.310	3.016	0.084	0.153	0.696	7.486	0.007	31.705	0.000
E. macaco	8.492	0.005	2.861	0.095	0.618	0.433	2.726	0.103	0.020	0.887	3.989	0.048	1.076	0.302	7.839	0.006	19.799	0.000
E. mongoz	12.509	0.001	4.117	0.046	1.109	0.294	4.965	0.029	0.050	0.824	7.428	0.007	1.270	0.263	15.771	0.000	47.766	0.000
E. rubriventer	0.356	0.554	0.156	0.695	0.608	0.437	0.139	0.711	2.131	0.151	0.002	0.962	0.282	0.597	0.089	0.767	1.508	0.221
H. griseus	8.760	0.005	4.462	0.039	2.288	0.134	4.504	0.039	0.360	0.551	6.482	0.013	2.106	0.152	11.618	0.001	28.611	0.000
L. catta	5.943	0.018	0.979	0.327	0.001	0.974	0.917	0.342	1.031	0.315	2.068	0.154	0.170	0.681	5.531	0.021	20.082	0.000
V. variegata	11.093	0.001	4.185	0.045	1.149	0.286	4.284	0.043	0.000	0.990	6.135	0.015	1.459	0.231	12.454	0.001	33.559	0.000
L. ruficaudatus	12.990	0.001	5.484	0.023	1.279	0.261	4.889	0.032	0.002	0.964	6.542	0.012	1.797	0.186	13.625	0.000	35.360	0.000
L. tardigradus	0.418	0.521	0.442	0.509	2.890	0.092	0.665	0.419	4.285	0.044	0.076	0.784	0.497	0.484	0.127	0.722	7.085	0.008
N. bengalensis	2.975	0.092	0.778	0.382	0.061	0.805	0.590	0.446	0.147	0.703	1.099	0.298	0.264	0.610	2.463	0.120	7.172	0.008
N. coucang	2.333	0.130	0.043	0.836	1.514	0.221	0.078	0.780	5.032	0.027	0.158	0.691	0.210	0.648	1.539	0.217	13.132	0.000
P. potto	4.001	0.047	0.484	0.488	0.005	0.941	0.686	0.409	0.936	0.335	1.969	0.162	0.070	0.791	5.202	0.024	24.887	0.000

2* model FACE PC1	*G. zanzibaricus*		*O. crassicaudatus*		*O. garnettii*		*A. laniger*		*I. indri*		*P. diadema*		*P. verreauxi*		*E. fulvus*		*E. macaco*	
	F value	p value	F value	p value	F value	p value	F value	p value	F value	p value	F value	p value	F value	p value	F value	p value	F value	p value
C. major																		
C. medius																		
M. murinus																		
M. rufus																		
G. alleni																		
G. demidoff																		
E. elegantulus																		
G. moholi																		
G. senegalensus																		
G. zanzibaricus																		
O. crassicaudatus	12.930	0.000																
O. garnettii	15.215	0.000	0.006	0.938														
A. laniger	2.729	0.106	0.055	0.814	0.076	0.783												
I. Indri	14.824	0.000	1.907	0.170	2.067	0.153	0.764	0.386										
P. diadema	4.300	0.043	0.050	0.823	0.072	0.789	0.003	0.959	1.011	0.319								
P. verreauxi	5.692	0.020	0.227	0.635	0.284	0.595	0.000	0.999	1.715	0.194	0.006	0.938						
E. fulvus	19.324	0.000	7.915	0.005	6.601	0.011	0.973	0.325	0.002	0.966	1.723	0.191	4.130	0.043				
E. macaco	22.156	0.000	6.220	0.014	6.728	0.010	1.952	0.167	0.582	0.448	2.829	0.097	4.648	0.034	0.732	0.393		
E. mongoz	27.905	0.000	17.024	0.000	16.523	0.000	2.142	0.147	0.742	0.391	3.706	0.058	7.927	0.006	1.883	0.171	0.002	0.961
E. rubriventer	5.138	0.028	0.000	0.992	0.001	0.969	0.025	0.875	0.717	0.400	0.014	0.905	0.042	0.838	0.791	0.375	2.109	0.150
H. griseus	17.365	0.000	11.193	0.001	11.924	0.001	2.192	0.146	1.789	0.186	3.496	0.067	6.266	0.015	3.397	0.067	0.631	0.429
L. catta	18.960	0.000	4.096	0.045	4.264	0.041	0.898	0.348	0.001	0.975	1.358	0.249	2.751	0.101	0.000	0.985	0.780	0.380
V. variegata	24.596	0.000	11.526	0.001	12.136	0.001	2.111	0.152	0.927	0.339	3.402	0.070	6.491	0.013	1.666	0.198	0.022	0.883
L. ruficaudatus	26.516	0.000	12.371	0.001	13.506	0.000	2.221	0.143	1.155	0.287	3.501	0.067	6.660	0.012	1.858	0.174	0.046	0.830
L. tardigradus	6.219	0.016	0.113	0.737	0.153	0.696	0.008	0.928	1.486	0.227	0.003	0.959	0.038	0.846	7.735	0.006	4.792	0.032
N. bengalensis	9.982	0.003	1.648	0.202	1.860	0.175	0.736	0.396	0.069	0.794	0.901	0.347	1.376	0.245	0.062	0.804	0.097	0.756
N. coucang	15.560	0.000	0.478	0.490	0.391	0.533	0.208	0.649	1.026	0.313	0.271	0.604	0.739	0.392	2.974	0.086	4.337	0.039
P. potto	13.732	0.000	5.409	0.021	4.463	0.036	0.633	0.428	0.003	0.960	1.119	0.292	2.771	0.098	0.037	0.847	0.718	0.398

2* model FACE PC1	*E. mongoz*		*E. rubriventer*		*H. griseus*		*L. catta*		*V. variegata*		*L. ruficaudatus*		*L. tardigradus*		*N. bengalensis*		*N. coucang*	
	F value	p value	F value	p value	F value	p value	F value	p value	F value	p value	F value	p value	F value	p value	F value	p value	F value	p value
C. major																		
C. medius																		
M. murinus																		
M. rufus																		
G. alleni																		
G. demidoff																		
E. elegantulus																		
G. moholi																		
G. senegalensus																		
G. zanzibaricus																		
O. crassicaudatus																		
O. garnettii																		
A. laniger																		
I. Indri																		
P. diadema																		
P. verreauxi																		
E. fulvus																		
E. macaco																		
E. mongoz																		
E. rubriventer	2.346	0.130																
H. griseus	1.073	0.303	8.760	0.005														
L. catta	1.302	0.257	5.943	0.018	2.464	0.122												
V. variegata	0.068	0.795	2.459	0.122	0.537	0.467	1.431	0.236										
L. ruficaudatus	0.123	0.727	2.874	0.097	0.457	0.502	1.787	0.187	0.005	0.944								
L. tardigradus	12.679	0.001	0.008	0.931	6.335	0.015	3.009	0.088	7.849	0.007	7.643	0.008						
N. bengalensis	0.095	0.759	0.785	0.380	0.571	0.454	0.071	0.791	0.172	0.680	0.224	0.638	1.031	0.315				
N. coucang	9.604	0.002	0.076	0.783	8.050	0.006	2.047	0.156	7.596	0.007	8.574	0.004	0.716	0.400	1.079	0.302		
P. potto	1.872	0.173	0.498	0.481	2.818	0.095	0.012	0.913	1.545	0.216	1.664	0.199	4.966	0.027	0.076	0.783	1.852	0.175

2* model FACE PC2	*C. major*		*C. medius*		*M. murinus*		*M. rufus*		*G. alleni*		*G. demidoff*		*E. elegantulus*		*G. moholi*		*G. senegalensis*	
	F value	p value	F value	p value	F value	p value	F value	p value	F value	p value	F value	p value	F value	p value	F value	p value	F value	p value
C. major																		
C. medius	2.679	0.108																
M. murinus	1.486	0.226	0.235	0.629														
M. rufus	1.185	0.282	0.429	0.515	0.036	0.850												
G. alleni	1.005	0.321	0.242	0.625	0.007	0.936	0.005	0.943										
G. demidoff	3.760	0.056	0.074	0.786	0.764	0.384	1.104	0.296	0.609	0.437								
E. elegantulus	1.718	0.195	5.617	0.021	5.226	0.024	4.256	0.044	3.566	0.064	7.482	0.008						
G. moholi	0.448	0.505	1.240	0.268	0.510	0.476	0.266	0.607	0.237	0.627	2.620	0.108	3.769	0.055				
G. senegalensus	0.069	0.794	5.819	0.017	4.628	0.032	3.869	0.051	2.609	0.108	10.588	0.001	2.598	0.109	1.854	0.175		
G. zanzibaricus	0.532	0.470	0.043	0.837	0.005	0.944	0.025	0.875	0.010	0.920	0.166	0.684	2.150	0.148	0.211	0.647	1.644	0.201
O. crassicaudatus	0.309	0.579	0.819	0.367	0.429	0.514	0.194	0.660	0.151	0.698	2.223	0.138	2.672	0.105	0.001	0.982	2.156	0.143
O. garnettii	3.879	0.051	14.276	0.000	16.966	0.000	14.889	0.000	9.027	0.003	24.879	0.000	0.015	0.901	12.893	0.000	9.377	0.002
A. laniger	2.016	0.163	0.180	0.674	0.505	0.479	0.618	0.435	0.477	0.493	0.071	0.790	3.728	0.059	1.143	0.288	3.402	0.067
I. Indri	10.771	0.002	3.971	0.051	6.986	0.009	7.147	0.010	5.149	0.027	3.794	0.054	12.579	0.001	10.509	0.002	23.278	0.000
P. diadema	0.001	0.974	1.500	0.226	0.943	0.334	0.662	0.420	0.590	0.446	2.291	0.134	1.090	0.301	0.297	0.587	0.024	0.876
P. verreauxi	0.086	0.771	1.610	0.209	0.892	0.347	0.582	0.448	0.488	0.488	2.885	0.093	2.299	0.134	0.125	0.724	0.503	0.479
E. fulvus	0.993	0.320	1.067	0.303	0.321	0.571	0.106	0.745	0.110	0.740	2.832	0.094	5.655	0.018	0.108	0.743	4.513	0.034
E. macaco	2.042	0.157	9.416	0.003	7.096	0.009	6.924	0.010	5.587	0.021	11.532	0.001	0.210	0.648	4.668	0.033	2.121	0.147
E. mongoz	9.354	0.003	1.584	0.212	4.806	0.030	5.634	0.020	3.039	0.085	1.330	0.251	12.211	0.001	9.975	0.002	31.372	0.000
E. rubriventer	1.284	0.263	4.541	0.038	3.598	0.061	3.113	0.084	2.781	0.102	5.368	0.023	0.013	0.909	2.490	0.118	1.484	0.225
H. griseus	0.961	0.332	0.102	0.751	0.003	0.954	0.036	0.850	0.011	0.916	0.359	0.551	3.336	0.073	0.355	0.553	2.970	0.086
L. catta	0.151	0.699	1.840	0.180	0.959	0.330	0.630	0.431	0.514	0.476	3.293	0.073	2.694	0.106	0.106	0.746	0.783	0.377
V. variegata	6.521	0.013	0.438	0.510	1.715	0.193	2.377	0.128	1.403	0.241	0.153	0.696	9.531	0.003	4.453	0.037	14.993	0.000
L. ruficaudatus	8.288	0.006	1.704	0.198	4.310	0.041	4.644	0.036	2.808	0.101	1.454	0.231	10.102	0.002	8.136	0.005	23.587	0.000
L. tardigradus	4.406	0.041	14.324	0.000	19.101	0.000	15.244	0.000	8.685	0.005	26.287	0.000	0.002	0.962	15.312	0.000	14.001	0.000
N. bengalensis	2.189	0.146	6.472	0.014	5.214	0.025	4.631	0.037	4.038	0.051	7.451	0.008	0.002	0.963	3.809	0.054	2.594	0.109
N. coucang	0.001	0.976	2.726	0.102	2.144	0.145	1.518	0.221	1.046	0.309	5.450	0.021	2.009	0.160	0.638	0.426	0.165	0.685
P. potto	0.065	0.799	4.061	0.046	3.841	0.051	2.939	0.088	1.833	0.178	8.382	0.004	1.649	0.201	1.629	0.203	0.006	0.936

2* model FACE PC2	*G. zanzibaricus*		*O. crassicaudatus*		*O. garnettii*		*A. laniger*		*I. indri*		*P. diadema*		*P. verreauxi*		*E. fulvus*		*E. macaco*	
	F value	p value	F value	p value	F value	p value	F value	p value	F value	p value	F value	p value	F value	p value	F value	p value	F value	p value
C. major																		
C. medius																		
M. murinus																		
M. rufus																		
G. alleni																		
G. demidoff																		
E. elegantulus																		
G. moholi																		
G. senegalensus																		
G. zanzibaricus																		
O. crassicaudatus	0.148	0.701																
O. garnettii	4.752	0.031	15.520	0.000														
A. laniger	0.177	0.676	0.671	0.414	5.974	0.016												
I. Indri	2.299	0.135	7.636	0.007	30.257	0.000	0.830	0.366										
P. diadema	0.392	0.534	0.212	0.646	2.135	0.147	1.320	0.256	6.960	0.010								
P. verreauxi	0.338	0.563	0.111	0.740	6.411	0.012	1.322	0.255	9.508	0.003	0.065	0.800						
E. fulvus	0.147	0.701	0.119	0.730	27.777	0.000	1.063	0.304	12.600	0.000	0.645	0.423	0.476	0.491				
E. macaco	2.901	0.093	3.199	0.076	0.267	0.606	5.722	0.019	21.368	0.000	1.082	0.301	2.729	0.102	6.772	0.010		
E. mongoz	1.029	0.313	10.160	0.002	57.597	0.000	0.059	0.809	1.673	0.199	5.305	0.024	8.533	0.004	14.641	0.000	21.627	0.000
E. rubriventer	1.601	0.212	1.556	0.215	0.002	0.962	3.445	0.070	10.160	0.002	0.769	0.385	1.563	0.216	3.472	0.064	0.077	0.783
H. griseus	0.000	0.983	0.253	0.616	9.138	0.003	0.294	0.590	4.006	0.050	0.619	0.435	0.578	0.450	0.239	0.626	5.012	0.028
L. catta	0.325	0.571	0.095	0.758	8.492	0.004	1.431	0.237	10.618	0.002	0.100	0.754	0.003	0.953	0.484	0.487	3.610	0.061
V. variegata	0.389	0.535	3.329	0.070	30.182	0.000	0.007	0.931	3.054	0.085	3.506	0.066	4.641	0.034	4.869	0.028	17.065	0.000
L. ruficaudatus	0.945	0.336	6.447	0.012	36.772	0.000	0.119	0.732	0.846	0.361	4.614	0.037	7.094	0.010	10.593	0.001	19.927	0.000
L. tardigradus	3.793	0.057	17.422	0.000	0.168	0.683	5.269	0.026	26.899	0.000	2.173	0.147	7.023	0.010	36.870	0.000	0.610	0.437
N. bengalensis	2.117	0.153	2.333	0.129	0.033	0.856	4.445	0.041	12.754	0.001	1.233	0.273	2.451	0.123	5.231	0.023	0.305	0.582
N. coucang	0.666	0.417	0.726	0.396	8.252	0.005	1.692	0.197	12.896	0.001	0.003	0.954	0.093	0.761	2.006	0.158	2.081	0.152
P. potto	1.151	0.285	2.339	0.128	8.015	0.005	2.185	0.142	16.252	0.000	0.026	0.873	0.422	0.517	4.919	0.027	1.363	0.245

2* model FACE PC2	*E. mongoz*		*E. rubriventer*		*H. griseus*		*L. catta*		*V. variegata*		*L. ruficaudatus*		*L. tardigradus*		*N. bengalensis*		*N. coucang*	
	F value	p value	F value	p value	F value	p value	F value	p value	F value	p value	F value	p value	F value	p value	F value	p value	F value	p value
C. major																		
C. medius																		
M. murinus																		
M. rufus																		
G. alleni																		
G. demidoff																		
E. elegantulus																		
G. moholi																		
G. senegalensus																		
G. zanzibaricus																		
O. crassicaudatus																		
O. garnettii																		
A. laniger																		
I. Indri																		
P. diadema																		
P. verreauxi																		
E. fulvus																		
E. macaco																		
E. mongoz																		
E. rubriventer	8.643	0.004																
H. griseus	2.223	0.140	0.961	0.332														
L. catta	10.374	0.002	0.151	0.699	0.594	0.444												
V. variegata	0.561	0.456	7.502	0.008	0.851	0.360	5.615	0.021										
L. ruficaudatus	0.087	0.768	7.724	0.008	1.980	0.166	8.344	0.006	0.810	0.372								
L. tardigradus	60.750	0.000	0.033	0.857	8.137	0.006	9.423	0.003	32.126	0.000	32.400	0.000						
N. bengalensis	11.725	0.001	0.028	0.867	3.400	0.072	3.007	0.089	10.569	0.002	10.219	0.003	0.000	0.989				
N. coucang	16.874	0.000	1.194	0.277	1.221	0.272	0.166	0.685	7.750	0.006	11.791	0.001	9.878	0.002	1.961	0.165		
P. potto	26.485	0.000	0.889	0.347	2.134	0.146	0.643	0.424	11.045	0.001	16.952	0.000	10.907	0.001	1.549	0.215	0.192	0.662

2* model FACE PC3	*C. major*		*C. medius*		*M. murinus*		*M. rufus*		*G. alleni*		*G. demidoff*		*E. elegantulus*		*G. moholi*		*G. senegalensis*	
	F value	p value	F value	p value	F value	p value	F value	p value	F value	p value	F value	p value	F value	p value	F value	p value	F value	p value
C. major																		
C. medius	2.929	0.093																
M. murinus	0.061	0.806	4.409	0.038														
M. rufus	1.816	0.184	0.613	0.437	2.425	0.123												
G. alleni	0.179	0.674	4.212	0.046	0.642	0.425	3.244	0.078										
G. demidoff	1.348	0.249	0.957	0.331	1.568	0.213	0.048	0.826	2.652	0.107								
E. elegantulus	0.094	0.760	2.464	0.122	0.321	0.572	1.604	0.210	0.000	0.996	1.406	0.239						
G. moholi	4.254	0.042	0.160	0.690	5.669	0.019	0.453	0.502	6.637	0.012	0.799	0.373	3.366	0.069				
G. senegalensus	0.020	0.887	9.989	0.002	0.338	0.562	6.927	0.009	0.321	0.572	4.700	0.031	0.155	0.694	13.483	0.000		
G. zanzibaricus	1.261	0.267	0.366	0.548	1.233	0.270	0.000	0.995	2.247	0.141	0.026	0.873	1.199	0.278	0.207	0.651	2.770	0.098
O. crassicaudatus	0.066	0.798	5.783	0.018	0.000	0.983	3.572	0.061	0.756	0.386	2.343	0.128	0.358	0.550	8.723	0.004	0.531	0.467
O. garnettii	2.189	0.142	15.548	0.000	5.630	0.019	16.042	0.000	0.739	0.392	12.979	0.000	0.374	0.542	27.153	0.000	6.283	0.013
A. laniger	0.782	0.381	0.026	0.872	0.994	0.321	0.066	0.799	1.214	0.277	0.137	0.713	0.882	0.352	0.000	0.993	2.171	0.142
I. Indri	4.648	0.035	0.556	0.459	7.360	0.008	2.266	0.137	5.880	0.018	3.019	0.086	3.911	0.052	1.864	0.175	15.088	0.000
P. diadema	0.787	0.379	0.833	0.366	0.677	0.413	0.111	0.740	1.682	0.201	0.022	0.883	0.878	0.353	0.714	0.400	1.847	0.176
P. verreauxi	3.263	0.076	0.069	0.794	4.416	0.038	0.400	0.529	4.981	0.029	0.685	0.410	2.668	0.107	0.010	0.922	10.152	0.002
E. fulvus	3.211	0.075	0.457	0.500	4.544	0.034	0.140	0.709	5.364	0.022	0.398	0.529	2.790	0.096	0.142	0.707	12.907	0.000
E. macaco	2.940	0.090	0.047	0.829	3.584	0.061	0.364	0.548	4.484	0.038	0.599	0.441	2.584	0.112	0.016	0.901	7.552	0.006
E. mongoz	0.896	0.347	1.862	0.176	0.995	0.320	0.431	0.513	2.125	0.149	0.159	0.691	1.047	0.309	2.248	0.136	4.134	0.043
E. rubriventer	3.079	0.086	0.072	0.789	3.671	0.058	0.870	0.355	4.148	0.047	1.077	0.302	2.555	0.115	0.413	0.522	6.492	0.012
H. griseus	0.011	0.917	3.061	0.086	0.017	0.898	1.832	0.182	0.323	0.572	1.233	0.270	0.161	0.690	4.179	0.044	0.096	0.757
L. catta	0.299	0.587	2.946	0.091	0.153	0.697	1.378	0.245	1.177	0.283	0.769	0.383	0.540	0.465	3.906	0.051	1.174	0.280
V. variegata	0.072	0.789	5.891	0.018	0.434	0.511	4.499	0.038	0.080	0.778	3.193	0.077	0.036	0.850	8.916	0.003	0.067	0.797
L. ruficaudatus	0.363	0.550	2.245	0.140	0.253	0.616	0.932	0.339	1.197	0.280	0.509	0.477	0.564	0.456	3.050	0.084	1.475	0.226
L. tardigradus	0.542	0.465	2.382	0.129	0.558	0.457	0.959	0.332	1.562	0.218	0.506	0.479	0.707	0.404	3.881	0.052	3.353	0.069
N. bengalensis	0.019	0.892	1.400	0.243	0.000	0.991	0.691	0.410	0.215	0.646	0.479	0.491	0.128	0.722	1.701	0.195	0.089	0.766
N. coucang	2.632	0.108	0.740	0.392	3.471	0.065	0.009	0.923	4.636	0.034	0.123	0.727	2.279	0.134	0.449	0.504	9.920	0.002
P. potto	3.506	0.063	0.042	0.839	5.630	0.019	0.646	0.423	5.312	0.023	1.072	0.302	2.835	0.094	0.052	0.820	15.876	0.000

2* model FACE PC3	*G. zanzibaricus*		*O. crassicaudatus*		*O. garnettii*		*A. laniger*		*I. indri*		*P. diadema*		*P. verreauxi*		*E. fulvus*		*E. macaco*	
	F value	p value	F value	p value	F value	p value	F value	p value	F value	p value	F value	p value	F value	p value	F value	p value	F value	p value
C. major																		
C. medius																		
M. murinus																		
M. rufus																		
G. alleni																		
G. demidoff																		
E. elegantulus																		
G. moholi																		
G. senegalensus																		
G. zanzibaricus																		
O. crassicaudatus	1.295	0.257																
O. garnettii	6.187	0.014	10.283	0.002														
A. laniger	0.058	0.811	1.089	0.299	3.641	0.059												
I. Indri	1.387	0.244	9.517	0.002	18.322	0.000	0.391	0.534										
P. diadema	0.107	0.745	0.736	0.392	5.411	0.022	0.184	0.670	2.144	0.148								
P. verreauxi	0.221	0.640	5.985	0.016	18.360	0.000	0.001	0.973	1.183	0.280	0.672	0.415						
E. fulvus	0.045	0.833	9.759	0.002	32.659	0.000	0.021	0.885	2.880	0.091	0.307	0.580	0.161	0.689				
E. macaco	0.227	0.635	4.416	0.037	13.634	0.000	0.003	0.959	1.030	0.313	0.645	0.424	0.001	0.973	0.142	0.707		
E. mongoz	0.182	0.671	1.833	0.178	15.266	0.000	0.290	0.592	4.393	0.039	0.016	0.901	1.650	0.202	1.782	0.183	1.325	0.252
E. rubriventer	0.853	0.360	3.770	0.054	8.956	0.003	0.125	0.725	0.136	0.714	1.467	0.231	0.271	0.604	0.560	0.455	0.235	0.629
H. griseus	1.381	0.246	0.015	0.902	2.818	0.096	0.810	0.373	4.810	0.032	0.799	0.376	3.334	0.072	2.891	0.091	2.961	0.089
L. catta	0.847	0.361	0.225	0.636	7.573	0.007	0.612	0.437	5.139	0.027	0.345	0.559	3.029	0.086	2.722	0.101	2.523	0.116
V. variegata	2.659	0.108	0.554	0.458	2.436	0.121	1.447	0.234	8.042	0.006	1.849	0.179	6.704	0.011	7.201	0.008	5.511	0.021
L. ruficaudatus	0.588	0.447	0.364	0.548	7.622	0.007	0.450	0.506	4.187	0.045	0.203	0.654	2.322	0.132	2.103	0.149	1.985	0.163
L. tardigradus	0.409	0.526	1.156	0.284	15.515	0.000	0.374	0.544	4.633	0.035	0.116	0.735	2.534	0.116	3.657	0.057	1.995	0.162
N. bengalensis	0.673	0.417	0.000	0.999	1.370	0.244	0.479	0.493	2.499	0.119	0.355	0.554	1.447	0.234	1.075	0.301	1.430	0.236
N. coucang	0.003	0.955	5.993	0.015	24.450	0.000	0.066	0.798	3.043	0.084	0.176	0.676	0.413	0.522	0.116	0.734	0.354	0.553
P. potto	0.211	0.647	12.412	0.001	32.651	0.000	0.005	0.942	1.307	0.255	0.595	0.442	0.008	0.927	0.566	0.452	0.002	0.964

2* model FACE PC3	*E. mongoz*		*E. rubriventer*		*H. griseus*		*L. catta*		*V. variegata*		*L. ruficaudatus*		*L. tardigradus*		*N. bengalensis*		*N. coucang*	
	F value	p value	F value	p value	F value	p value	F value	p value	F value	p value	F value	p value	F value	p value	F value	p value	F value	p value
C. major																		
C. medius																		
M. murinus																		
M. rufus																		
G. alleni																		
G. demidoff																		
E. elegantulus																		
G. moholi																		
G. senegalensus																		
G. zanzibaricus																		
O. crassicaudatus																		
O. garnettii																		
A. laniger																		
I. Indri																		
P. diadema																		
P. verreauxi																		
E. fulvus																		
E. macaco																		
E. mongoz																		
E. rubriventer	1.618	0.207																
H. griseus	0.763	0.385	0.011	0.917														
L. catta	0.327	0.569	0.299	0.587	0.220	0.641												
V. variegata	2.591	0.111	5.279	0.025	0.184	0.670	1.160	0.285										
L. ruficaudatus	0.166	0.685	2.474	0.122	0.297	0.588	0.018	0.894	1.299	0.259								
L. tardigradus	0.133	0.716	2.051	0.158	0.452	0.505	0.089	0.767	2.028	0.159	0.018	0.893						
N. bengalensis	0.249	0.620	2.053	0.159	0.005	0.944	0.055	0.815	0.135	0.715	0.084	0.773	0.121	0.730				
N. coucang	0.840	0.361	0.905	0.344	2.487	0.118	2.029	0.157	6.202	0.014	1.466	0.229	1.911	0.170	0.926	0.339		
P. potto	3.134	0.078	0.160	0.690	3.251	0.073	3.540	0.062	7.609	0.006	2.827	0.095	5.219	0.024	1.234	0.268	0.836	0.362

2* model FACE PC4	*C. major*		*C. medius*		*M. murinus*		*M. rufus*		*G. alleni*		*G. demidoff*		*E. elegantulus*		*G. moholi*		*G. senegalensis*	
	F value	p value	F value	p value	F value	p value	F value	p value	F value	p value	F value	p value	F value	p value	F value	p value	F value	p value
C. major																		
C. medius	0.038	0.845																
M. murinus	0.461	0.499	0.758	0.386														
M. rufus	2.437	0.125	3.055	0.086	0.469	0.495												
G. alleni	0.244	0.624	0.427	0.516	0.014	0.908	0.505	0.481										
G. demidoff	0.251	0.618	0.082	0.776	1.838	0.178	5.514	0.021	1.027	0.314								
E. elegantulus	0.960	0.331	1.216	0.275	0.345	0.558	0.045	0.832	0.321	0.573	2.107	0.150						
G. moholi	0.018	0.895	0.135	0.714	0.599	0.440	3.210	0.076	0.263	0.609	0.636	0.427	1.325	0.252				
G. senegalensus	2.273	0.133	1.511	0.220	7.935	0.005	18.723	0.000	4.746	0.031	1.021	0.313	6.296	0.013	4.764	0.030		
G. zanzibaricus	3.317	0.075	2.888	0.095	5.676	0.019	8.683	0.005	3.716	0.060	3.098	0.082	4.149	0.046	5.665	0.019	3.267	0.072
O. crassicaudatus	0.648	0.422	0.281	0.597	4.178	0.043	12.170	0.001	2.164	0.144	0.039	0.844	3.593	0.060	1.759	0.187	1.353	0.246
O. garnettii	0.033	0.857	0.180	0.672	0.659	0.418	3.457	0.065	0.245	0.622	0.854	0.357	1.360	0.246	0.004	0.950	6.664	0.010
A. laniger	1.794	0.187	1.586	0.214	3.152	0.079	4.351	0.042	2.059	0.159	1.705	0.196	2.608	0.112	3.043	0.084	1.833	0.177
I. Indri	1.204	0.277	0.886	0.350	2.938	0.089	5.831	0.019	1.907	0.173	0.701	0.404	2.676	0.106	2.152	0.145	0.176	0.675
P. diadema	0.000	0.984	0.028	0.868	0.270	0.605	1.211	0.276	0.136	0.714	0.166	0.685	0.672	0.416	0.006	0.938	1.412	0.236
P. verreauxi	0.155	0.695	0.322	0.572	0.070	0.792	0.826	0.367	0.012	0.913	0.910	0.342	0.487	0.487	0.155	0.695	4.787	0.030
E. fulvus	0.694	0.406	1.197	0.275	0.010	0.921	1.211	0.272	0.007	0.934	3.222	0.074	0.683	0.410	0.957	0.329	14.737	0.000
E. macaco	1.105	0.296	1.527	0.220	0.035	0.852	0.286	0.594	0.098	0.756	2.540	0.114	0.257	0.613	1.013	0.316	7.854	0.006
E. mongoz	1.166	0.283	1.737	0.191	0.036	0.850	0.530	0.469	0.091	0.764	3.943	0.050	0.337	0.563	1.617	0.206	16.717	0.000
E. rubriventer	2.742	0.104	2.031	0.160	3.205	0.077	8.162	0.006	2.888	0.096	1.480	0.227	3.243	0.077	3.168	0.078	0.895	0.345
H. griseus	2.296	0.136	2.782	0.101	0.656	0.420	0.102	0.751	0.653	0.423	4.597	0.035	0.000	0.988	2.953	0.089	13.623	0.000
L. catta	0.231	0.633	0.485	0.489	0.135	0.714	1.734	0.193	0.034	0.854	1.285	0.260	0.704	0.405	0.183	0.669	6.728	0.010
V. variegata	1.754	0.190	2.294	0.135	0.430	0.513	0.001	0.980	0.424	0.517	4.461	0.037	0.035	0.852	2.587	0.111	15.389	0.000
L. ruficaudatus	1.418	0.240	1.890	0.175	0.055	0.815	0.350	0.557	0.117	0.734	3.427	0.068	0.226	0.637	1.494	0.225	12.626	0.000
L. tardigradus	0.006	0.940	0.006	0.941	0.778	0.380	2.072	0.156	0.226	0.637	0.159	0.692	0.788	0.378	0.074	0.787	3.207	0.075
N. bengalensis	0.582	0.450	0.772	0.384	0.037	0.848	0.059	0.809	0.069	0.795	1.243	0.268	0.086	0.770	0.556	0.458	3.932	0.049
N. coucang	0.132	0.717	0.015	0.901	1.853	0.176	6.235	0.014	0.929	0.338	0.056	0.813	2.129	0.148	0.448	0.504	2.385	0.124
P. potto	0.034	0.854	0.001	0.982	1.422	0.235	4.305	0.040	0.574	0.450	0.154	0.695	1.671	0.198	0.193	0.661	3.125	0.078

2* model FACE PC4	*G. zanzibaricus*		*O. crassicaudatus*		*O. garnettii*		*A. laniger*		*I. indri*		*P. diadema*		*P. verreauxi*		*E. fulvus*		*E. macaco*	
	F value	p value	F value	p value	F value	p value	F value	p value	F value	p value	F value	p value	F value	p value	F value	p value	F value	p value
C. major																		
C. medius																		
M. murinus																		
M. rufus																		
G. alleni																		
G. demidoff																		
E. elegantulus																		
G. moholi																		
G. senegalensus																		
G. zanzibaricus																		
O. crassicaudatus	4.376	0.039																
O. garnettii	6.147	0.015	2.784	0.097														
A. laniger	0.001	0.979	2.298	0.132	3.255	0.074												
I. Indri	0.679	0.413	0.858	0.356	2.441	0.121	0.425	0.517										
P. diadema	2.347	0.132	0.390	0.533	0.013	0.910	1.406	0.242	0.827	0.367								
P. verreauxi	4.052	0.048	2.082	0.151	0.144	0.705	2.256	0.138	1.903	0.172	0.086	0.770						
E. fulvus	9.586	0.002	9.468	0.002	1.225	0.269	5.152	0.024	4.828	0.029	0.380	0.538	0.080	0.777				
E. macaco	8.023	0.006	4.479	0.036	0.932	0.336	4.499	0.037	4.150	0.045	0.601	0.441	0.201	0.655	0.101	0.751		
E. mongoz	8.714	0.004	10.488	0.001	1.906	0.169	4.432	0.039	4.976	0.028	0.598	0.442	0.251	0.618	0.180	0.672	0.004	0.951
E. rubriventer	0.179	0.674	1.753	0.188	3.043	0.084	0.127	0.723	0.162	0.688	1.675	0.201	2.489	0.119	4.642	0.032	6.981	0.010
H. griseus	7.326	0.009	8.568	0.004	2.996	0.086	3.973	0.052	5.049	0.028	1.295	0.260	0.954	0.332	1.387	0.240	0.562	0.456
L. catta	5.595	0.022	3.094	0.081	0.158	0.692	2.874	0.096	2.636	0.109	0.106	0.746	0.002	0.961	0.173	0.678	0.435	0.511
V. variegata	7.506	0.008	9.590	0.002	2.882	0.092	3.979	0.051	4.928	0.029	0.993	0.323	0.725	0.397	1.079	0.300	0.224	0.637
L. ruficaudatus	7.442	0.009	7.448	0.007	1.483	0.226	3.691	0.061	4.442	0.039	0.641	0.427	0.253	0.617	0.190	0.663	0.001	0.977
L. tardigradus	1.984	0.165	0.811	0.369	0.160	0.690	1.027	0.316	0.770	0.384	0.005	0.942	0.226	0.636	2.156	0.144	0.804	0.373
N. bengalensis	3.711	0.061	2.083	0.152	0.493	0.484	2.260	0.140	2.036	0.159	0.339	0.563	0.124	0.726	0.088	0.767	0.009	0.926
N. coucang	4.202	0.043	0.354	0.553	0.690	0.407	2.223	0.140	1.173	0.281	0.088	0.767	0.805	0.371	3.638	0.058	2.390	0.125
P. potto	3.943	0.049	0.762	0.383	0.373	0.542	2.150	0.145	1.232	0.269	0.027	0.870	0.517	0.473	3.172	0.076	1.366	0.244

2* model FACE PC4	*E. mongoz*		*E. rubriventer*		*H. griseus*		*L. catta*		*V. variegata*		*L. ruficaudatus*		*L. tardigradus*		*N. bengalensis*		*N. coucang*	
	F value	p value	F value	p value	F value	p value	F value	p value	F value	p value	F value	p value	F value	p value	F value	p value	F value	p value
C. major																		
C. medius																		
M. murinus																		
M. rufus																		
G. alleni																		
G. demidoff																		
E. elegantulus																		
G. moholi																		
G. senegalensus																		
G. zanzibaricus																		
O. crassicaudatus																		
O. garnettii																		
A. laniger																		
I. Indri																		
P. diadema																		
P. verreauxi																		
E. fulvus																		
E. macaco																		
E. mongoz																		
E. rubriventer	5.844	0.018																
H. griseus	0.786	0.378	2.296	0.136														
L. catta	0.529	0.469	0.231	0.633	1.761	0.190												
V. variegata	0.438	0.510	5.619	0.021	0.065	0.799	1.274	0.263										
L. ruficaudatus	0.011	0.915	8.031	0.007	0.606	0.440	0.641	0.427	0.248	0.620								
L. tardigradus	1.861	0.176	0.905	0.346	1.601	0.212	0.263	0.610	1.921	0.171	0.984	0.326						
N. bengalensis	0.016	0.899	4.083	0.049	0.166	0.686	0.256	0.615	0.049	0.826	0.006	0.939	0.290	0.593				
N. coucang	4.489	0.036	2.028	0.158	4.913	0.029	1.141	0.288	4.980	0.028	3.577	0.062	0.078	0.780	1.139	0.289		
P. potto	3.364	0.068	1.553	0.215	3.386	0.068	0.617	0.433	3.802	0.053	2.164	0.143	0.015	0.903	0.666	0.416	0.045	0.832

2* model FACE PC5	*C. major*		*C. medius*		*M. murinus*		*M. rufus*		*G. alleni*		*G. demidoff*		*E. elegantulus*		*G. moholi*		*G. senegalensis*	
	F value	p value	F value	p value	F value	p value	F value	p value	F value	p value	F value	p value	F value	p value	F value	p value	F value	p value
C. major																		
C. medius	0.881	0.352																
M. murinus	1.713	0.194	0.014	0.905														
M. rufus	0.419	0.520	0.231	0.633	0.613	0.436												
G. alleni	0.061	0.806	1.498	0.227	2.689	0.104	0.954	0.333										
G. demidoff	2.157	0.146	0.069	0.794	0.032	0.859	0.935	0.336	3.329	0.072								
E. elegantulus	0.001	0.972	0.460	0.500	0.842	0.361	0.177	0.675	0.047	0.828	1.049	0.309						
G. moholi	1.504	0.223	0.018	0.893	0.001	0.975	0.580	0.448	2.297	0.133	0.019	0.890	0.755	0.387				
G. senegalensus	0.553	0.458	0.453	0.502	1.078	0.300	0.006	0.940	1.194	0.276	1.570	0.211	0.237	0.627	1.165	0.282		
G. zanzibaricus	4.471	0.040	1.270	0.265	1.460	0.230	3.150	0.082	6.600	0.014	1.255	0.266	2.454	0.123	1.127	0.291	3.973	0.048
O. crassicaudatus	4.172	0.043	0.549	0.460	0.674	0.413	3.023	0.085	5.699	0.019	0.363	0.548	1.957	0.164	0.615	0.434	6.084	0.014
O. garnettii	2.895	0.092	0.249	0.619	0.253	0.616	1.777	0.185	4.060	0.046	0.092	0.762	1.399	0.239	0.218	0.641	3.617	0.058
A. laniger	3.916	0.054	1.524	0.223	1.821	0.181	2.957	0.092	5.436	0.024	1.666	0.201	2.491	0.120	1.420	0.236	3.896	0.050
I. Indri	0.086	0.770	1.132	0.291	2.075	0.153	0.717	0.400	0.013	0.911	2.396	0.125	0.072	0.790	1.903	0.171	1.136	0.288
P. diadema	0.855	0.360	2.816	0.099	4.698	0.033	2.435	0.125	0.602	0.442	5.281	0.024	0.588	0.446	4.054	0.047	3.595	0.059
P. verreauxi	0.007	0.933	0.843	0.362	1.700	0.195	0.351	0.555	0.115	0.735	2.132	0.147	0.001	0.979	1.586	0.210	0.479	0.490
E. fulvus	1.645	0.201	0.055	0.814	0.029	0.865	0.833	0.363	2.337	0.128	0.000	0.996	0.811	0.369	0.021	0.886	1.887	0.170
E. macaco	0.017	0.897	0.469	0.495	0.926	0.338	0.150	0.700	0.110	0.741	1.157	0.284	0.005	0.943	0.889	0.348	0.207	0.650
E. mongoz	3.816	0.054	0.913	0.342	1.416	0.236	3.244	0.075	4.943	0.029	0.997	0.320	1.957	0.165	1.324	0.252	7.532	0.007
E. rubriventer	1.289	0.262	2.742	0.104	4.611	0.034	2.491	0.121	1.085	0.303	4.836	0.031	1.031	0.314	4.077	0.046	4.547	0.034
H. griseus	4.309	0.043	1.644	0.205	2.550	0.114	3.719	0.059	5.476	0.024	2.113	0.150	2.610	0.112	2.206	0.141	7.611	0.006
L. catta	0.834	0.365	4.307	0.042	7.683	0.007	3.971	0.051	0.438	0.511	9.087	0.003	0.461	0.499	6.739	0.011	5.209	0.024
V. variegata	0.173	0.679	0.221	0.640	0.580	0.448	0.011	0.916	0.409	0.525	0.795	0.375	0.081	0.777	0.580	0.448	0.007	0.931
L. ruficaudatus	1.972	0.167	0.069	0.794	0.039	0.845	0.879	0.353	3.226	0.079	0.001	0.980	0.919	0.342	0.023	0.879	1.564	0.213
L. tardigradus	0.200	0.656	2.372	0.130	5.921	0.017	2.074	0.156	0.037	0.848	6.715	0.011	0.125	0.725	5.745	0.018	4.463	0.036
N. bengalensis	0.265	0.609	1.630	0.208	2.399	0.125	1.201	0.279	0.121	0.730	2.956	0.090	0.179	0.674	1.931	0.168	1.264	0.262
N. coucang	3.479	0.065	0.125	0.725	0.067	0.797	1.679	0.198	5.443	0.022	0.001	0.971	1.505	0.223	0.043	0.836	2.610	0.107
P. potto	0.583	0.446	0.286	0.593	0.800	0.372	0.002	0.969	1.170	0.281	1.195	0.276	0.250	0.618	0.889	0.347	0.022	0.882

2* model FACE PC5	*G. zanzibaricus*		*O. crassicaudatus*		*O. garnettii*		*A. laniger*		*I. indri*		*P. diadema*		*P. verreauxi*		*E. fulvus*		*E. macaco*	
	F value	p value	F value	p value	F value	p value	F value	p value	F value	p value	F value	p value	F value	p value	F value	p value	F value	p value
C. major																		
C. medius																		
M. murinus																		
M. rufus																		
G. alleni																		
G. demidoff																		
E. elegantulus																		
G. moholi																		
G. senegalensus																		
G. zanzibaricus																		
O. crassicaudatus	0.569	0.452																
O. garnettii	0.724	0.397	0.118	0.732														
A. laniger	0.199	0.658	0.995	0.321	1.093	0.298												
I. Indri	3.603	0.062	4.365	0.039	3.249	0.074	3.268	0.076										
P. diadema	7.055	0.011	7.692	0.006	5.992	0.016	5.848	0.020	0.274	0.603								
P. verreauxi	3.946	0.051	4.804	0.030	3.280	0.072	3.551	0.064	0.150	0.700	1.073	0.304						
E. fulvus	0.757	0.385	0.545	0.461	0.133	0.715	0.997	0.319	2.132	0.146	3.946	0.048	1.920	0.167				
E. macaco	2.396	0.126	2.615	0.108	1.825	0.179	2.370	0.128	0.148	0.701	0.848	0.360	0.005	0.946	1.105	0.294		
E. mongoz	0.086	0.770	0.523	0.471	0.835	0.362	0.328	0.569	3.969	0.049	6.197	0.015	4.660	0.033	1.469	0.227	2.776	0.099
E. rubriventer	5.192	0.027	6.757	0.010	5.559	0.020	4.533	0.039	0.734	0.395	0.224	0.638	1.621	0.207	4.176	0.042	1.394	0.241
H. griseus	0.053	0.820	1.601	0.208	1.810	0.181	0.024	0.878	4.276	0.043	6.397	0.015	4.981	0.029	2.047	0.154	3.335	0.072
L. catta	12.139	0.001	16.180	0.000	11.631	0.001	8.956	0.004	0.111	0.740	0.181	0.672	1.108	0.296	7.215	0.008	0.774	0.382
V. variegata	1.877	0.176	2.603	0.109	1.620	0.205	1.836	0.181	0.420	0.519	1.404	0.241	0.150	0.700	0.909	0.341	0.066	0.798
L. ruficaudatus	1.226	0.274	0.292	0.590	0.067	0.796	1.553	0.219	2.023	0.160	4.627	0.036	1.924	0.170	0.001	0.978	1.009	0.318
L. tardigradus	5.966	0.018	20.368	0.000	13.073	0.000	4.437	0.041	0.001	0.978	0.410	0.525	0.391	0.534	9.525	0.002	0.308	0.580
N. bengalensis	7.525	0.009	3.838	0.052	2.895	0.092	6.428	0.015	0.021	0.885	0.163	0.688	0.311	0.579	1.645	0.201	0.251	0.618
N. coucang	1.827	0.180	0.562	0.454	0.124	0.726	2.331	0.130	3.458	0.066	7.775	0.006	3.378	0.069	0.002	0.967	1.666	0.199
P. potto	2.979	0.086	5.929	0.016	3.280	0.071	2.904	0.090	1.093	0.297	3.161	0.077	0.554	0.458	1.782	0.183	0.247	0.620

2* model FACE PC5	*E. mongoz*		*E. rubriventer*		*H. griseus*		*L. catta*		*V. variegata*		*L. ruficaudatus*		*L. tardigradus*		*N. bengalensis*		*N. coucang*	
	F value	p value	F value	p value	F value	p value	F value	p value	F value	p value	F value	p value	F value	p value	F value	p value	F value	p value
C. major																		
C. medius																		
M. murinus																		
M. rufus																		
G. alleni																		
G. demidoff																		
E. elegantulus																		
G. moholi																		
G. senegalensus																		
G. zanzibaricus																		
O. crassicaudatus																		
O. garnettii																		
A. laniger																		
I. Indri																		
P. diadema																		
P. verreauxi																		
E. fulvus																		
E. macaco																		
E. mongoz																		
E. rubriventer	5.189	0.025																
H. griseus	0.402	0.528	4.309	0.043														
L. catta	12.817	0.001	0.834	0.365	11.272	0.001												
V. variegata	2.788	0.098	1.769	0.188	2.930	0.092	1.872	0.176										
L. ruficaudatus	0.765	0.384	3.741	0.059	1.595	0.213	9.031	0.004	0.654	0.422								
L. tardigradus	14.117	0.000	0.912	0.344	8.161	0.006	0.251	0.618	1.093	0.300	5.344	0.025						
N. bengalensis	3.277	0.074	0.554	0.460	4.339	0.043	0.019	0.891	0.513	0.477	3.160	0.083	0.024	0.879				
N. coucang	1.570	0.213	6.530	0.012	3.046	0.084	15.642	0.000	1.292	0.258	0.000	0.997	13.093	0.000	4.568	0.035		
P. potto	6.823	0.010	3.795	0.053	6.003	0.015	5.137	0.025	0.031	0.860	1.135	0.288	5.129	0.025	1.122	0.291	2.152	0.144

2* model VAULT PC1	*C. major*		*C. medius*		*M. murinus*		*M. rufus*		*G. alleni*		*G. demidoff*		*E. elegantulus*		*G. moholi*		*G. senegalensis*	
	F value	p value	F value	p value	F value	p value	F value	p value	F value	p value	F value	p value	F value	p value	F value	p value	F value	p value
C. major																		
C. medius	1.052	0.310																
M. murinus	0.037	0.848	0.779	0.380														
M. rufus	0.190	0.665	2.744	0.103	0.428	0.514												
G. alleni	1.105	0.299	4.619	0.037	1.378	0.244	0.505	0.481										
G. demidoff	0.936	0.336	7.397	0.008	1.585	0.210	0.207	0.650	0.237	0.628								
E. elegantulus	1.400	0.242	5.811	0.019	1.964	0.164	0.716	0.401	0.010	0.920	0.421	0.518						
G. moholi	0.115	0.735	3.533	0.063	0.377	0.540	0.047	0.829	1.079	0.302	0.652	0.421	1.509	0.222				
G. senegalensus	0.615	0.434	0.863	0.354	0.316	0.574	2.588	0.109	5.224	0.023	7.747	0.006	7.325	0.007	2.626	0.106		
G. zanzibaricus	1.736	0.194	7.354	0.009	2.065	0.154	0.852	0.360	0.004	0.953	0.452	0.503	0.004	0.952	1.742	0.190	8.302	0.004
O. crassicaudatus	1.007	0.318	0.003	0.960	1.124	0.290	2.622	0.108	3.762	0.055	7.196	0.008	5.444	0.021	3.481	0.064	1.551	0.214
O. garnettii	2.079	0.152	0.044	0.835	1.951	0.164	5.167	0.025	7.373	0.008	13.492	0.000	9.993	0.002	6.488	0.012	3.066	0.081
A. laniger	2.218	0.144	0.586	0.448	1.970	0.164	4.211	0.046	5.871	0.020	9.512	0.003	7.072	0.010	5.882	0.017	3.435	0.065
I. Indri	0.011	0.919	1.401	0.241	0.090	0.765	0.116	0.735	0.977	0.327	0.695	0.407	1.260	0.266	0.043	0.836	0.876	0.350
P. diadema	0.028	0.869	1.335	0.253	0.006	0.940	0.549	0.462	2.197	0.145	2.216	0.140	2.670	0.108	0.427	0.515	0.567	0.452
P. verreauxi	0.000	0.998	1.038	0.312	0.042	0.837	0.172	0.680	0.928	0.339	0.857	0.357	1.297	0.258	0.107	0.744	0.685	0.409
E. fulvus	0.285	0.594	0.879	0.350	0.121	0.728	1.454	0.229	3.162	0.077	4.703	0.031	4.622	0.033	1.476	0.226	0.073	0.787
E. macaco	0.020	0.887	2.092	0.152	0.166	0.685	0.118	0.732	1.002	0.320	0.855	0.357	1.449	0.232	0.039	0.844	1.713	0.192
E. mongoz	0.192	0.662	0.865	0.355	0.052	0.820	1.132	0.290	2.757	0.101	3.991	0.048	3.836	0.053	1.187	0.278	0.148	0.701
E. rubriventer	0.007	0.934	0.924	0.341	0.065	0.799	0.080	0.779	0.675	0.415	0.497	0.483	0.890	0.350	0.032	0.858	0.646	0.423
H. griseus	0.317	0.576	0.274	0.603	0.102	0.750	1.236	0.271	3.204	0.080	3.382	0.070	3.557	0.064	1.203	0.275	0.000	0.984
L. catta	2.057	0.157	0.217	0.643	1.540	0.217	4.398	0.040	6.756	0.012	10.126	0.002	7.966	0.006	5.481	0.021	2.280	0.133
V. variegata	0.033	0.856	0.895	0.348	0.001	0.980	0.454	0.503	1.578	0.214	1.777	0.186	2.137	0.148	0.397	0.530	0.382	0.537
L. ruficaudatus	0.045	0.832	0.723	0.399	0.000	0.995	0.490	0.487	1.836	0.182	1.729	0.192	2.159	0.147	0.404	0.527	0.222	0.638
L. tardigradus	1.140	0.291	9.029	0.004	2.661	0.106	0.440	0.510	0.048	0.827	0.126	0.723	0.140	0.710	1.444	0.232	21.212	0.000
N. bengalensis	0.130	0.721	0.258	0.614	0.044	0.835	0.619	0.435	1.602	0.213	2.014	0.160	2.092	0.154	0.693	0.407	0.014	0.904
N. coucang	0.006	0.937	2.223	0.139	0.145	0.704	0.177	0.675	1.044	0.310	1.194	0.277	1.629	0.205	0.093	0.761	2.421	0.121
P. potto	0.014	0.907	3.066	0.082	0.216	0.643	0.196	0.658	1.258	0.264	1.341	0.248	1.967	0.163	0.085	0.771	3.166	0.076

2* model VAULT PC1	*G. zanzibaricus*		*O. crassicaudatus*		*O. garnettii*		*A. laniger*		*I. indri*		*P. diadema*		*P. verreauxi*		*E. fulvus*		*E. macaco*	
	F value	p value	F value	p value	F value	p value	F value	p value	F value	p value	F value	p value	F value	p value	F value	p value	F value	p value
C. major																		
C. medius																		
M. murinus																		
M. rufus																		
G. alleni																		
G. demidoff																		
E. elegantulus																		
G. moholi																		
G. senegalensus																		
G. zanzibaricus																		
O. crassicaudatus	5.830	0.017																
O. garnettii	11.751	0.001	0.032	0.858														
A. laniger	8.704	0.005	0.542	0.463	0.744	0.390												
I. Indri	1.500	0.225	1.280	0.260	2.524	0.115	2.801	0.100										
P. diadema	3.707	0.060	1.285	0.259	2.823	0.096	2.985	0.091	0.088	0.768								
P. verreauxi	1.398	0.241	1.247	0.266	2.280	0.133	2.176	0.145	0.009	0.924	0.025	0.876						
E. fulvus	4.976	0.027	1.806	0.180	3.147	0.077	2.787	0.097	0.445	0.505	0.218	0.641	0.341	0.560				
E. macaco	1.591	0.211	2.601	0.109	4.705	0.032	3.683	0.059	0.001	0.974	0.138	0.711	0.021	0.886	0.930	0.336		
E. mongoz	4.460	0.038	1.351	0.247	2.747	0.100	2.491	0.119	0.331	0.567	0.130	0.720	0.208	0.649	0.015	0.904	0.616	0.434
E. rubriventer	1.012	0.320	0.918	0.340	1.790	0.183	1.875	0.177	0.000	0.999	0.058	0.811	0.006	0.937	0.329	0.567	0.001	0.977
H. griseus	5.115	0.028	0.246	0.621	0.621	0.432	1.355	0.250	0.475	0.493	0.284	0.596	0.260	0.611	0.019	0.890	0.581	0.448
L. catta	10.467	0.002	0.165	0.686	0.167	0.683	0.166	0.685	2.528	0.116	2.751	0.103	1.897	0.173	1.967	0.162	3.410	0.068
V. variegata	2.451	0.123	1.084	0.300	2.141	0.146	2.167	0.146	0.089	0.766	0.003	0.957	0.035	0.853	0.143	0.705	0.152	0.698
L. ruficaudatus	2.920	0.094	0.643	0.424	1.425	0.235	1.924	0.172	0.108	0.744	0.008	0.927	0.039	0.843	0.073	0.788	0.147	0.703
L. tardigradus	0.123	0.727	16.703	0.000	31.182	0.000	8.736	0.005	0.986	0.325	2.981	0.090	1.255	0.267	13.143	0.000	1.642	0.204
N. bengalensis	2.410	0.128	0.318	0.574	0.696	0.406	0.991	0.325	0.228	0.635	0.093	0.762	0.133	0.717	0.000	0.987	0.328	0.569
N. coucang	1.713	0.194	4.270	0.040	7.186	0.008	3.615	0.061	0.001	0.974	0.091	0.764	0.007	0.933	1.339	0.248	0.008	0.930
P. potto	2.060	0.153	6.064	0.015	9.650	0.002	4.885	0.029	0.000	0.993	0.142	0.707	0.016	0.900	1.847	0.175	0.004	0.952

2* model VAULT PC1	*E. mongoz*		*E. rubriventer*		*H. griseus*		*L. catta*		*V. variegata*		*L. ruficaudatus*		*L. tardigradus*		*N. bengalensis*		*N. coucang*	
	F value	p value	F value	p value	F value	p value	F value	p value	F value	p value	F value	p value	F value	p value	F value	p value	F value	p value
C. major																		
C. medius																		
M. murinus																		
M. rufus																		
G. alleni																		
G. demidoff																		
E. elegantulus																		
G. moholi																		
G. senegalensus																		
G. zanzibaricus																		
O. crassicaudatus																		
O. garnettii																		
A. laniger																		
I. Indri																		
P. diadema																		
P. verreauxi																		
E. fulvus																		
E. macaco																		
E. mongoz																		
E. rubriventer	0.227	0.635																
H. griseus	0.042	0.838	0.317	0.576														
L. catta	1.959	0.165	2.057	0.157	0.953	0.333												
V. variegata	0.070	0.792	0.061	0.805	0.143	0.706	1.832	0.180										
L. ruficaudatus	0.037	0.847	0.073	0.789	0.135	0.715	1.652	0.204	0.001	0.975								
L. tardigradus	7.781	0.007	0.620	0.435	3.553	0.065	11.330	0.001	2.530	0.117	1.922	0.172						
N. bengalensis	0.006	0.940	0.152	0.698	0.007	0.932	0.749	0.391	0.055	0.816	0.038	0.846	2.099	0.154				
N. coucang	0.700	0.405	0.001	0.979	0.460	0.499	3.414	0.068	0.116	0.734	0.097	0.756	3.202	0.077	0.278	0.599		
P. potto	1.016	0.315	0.000	0.995	0.619	0.433	4.471	0.036	0.178	0.673	0.143	0.706	4.460	0.036	0.405	0.525	0.003	0.959

2* model VAULT PC2	*C. major*		*C. medius*		*M. murinus*		*M. rufus*		*G. alleni*		*G. demidoff*		*E. elegantulus*		*G. moholi*		*G. senegalensis*	
	F value	p value	F value	p value	F value	p value	F value	p value	F value	p value	F value	p value	F value	p value	F value	p value	F value	p value
C. major																		
C. medius	0.072	0.790																
M. murinus	0.278	0.599	1.018	0.316														
M. rufus	0.624	0.433	0.568	0.454	2.320	0.131												
G. alleni	0.641	0.427	1.472	0.231	0.188	0.666	2.067	0.157										
G. demidoff	0.206	0.651	0.981	0.325	0.043	0.837	2.441	0.122	0.460	0.500								
E. elegantulus	0.601	0.441	1.465	0.231	0.164	0.686	2.269	0.137	0.002	0.960	0.405	0.526						
G. moholi	0.520	0.473	1.762	0.187	0.007	0.933	3.398	0.068	0.216	0.643	0.118	0.732	0.167	0.684				
G. senegalensus	1.863	0.174	6.316	0.013	0.426	0.515	9.129	0.003	0.046	0.830	1.177	0.279	0.018	0.893	0.337	0.562		
G. zanzibaricus	0.015	0.902	0.204	0.653	0.179	0.673	0.914	0.344	0.573	0.453	0.105	0.747	0.514	0.476	0.369	0.545	1.553	0.214
O. crassicaudatus	0.455	0.501	0.312	0.577	2.995	0.085	0.247	0.620	2.574	0.111	2.753	0.099	2.980	0.087	3.856	0.051	18.305	0.000
O. garnettii	0.590	0.444	0.506	0.478	3.425	0.066	0.125	0.724	2.700	0.103	3.203	0.076	3.173	0.077	4.338	0.039	20.720	0.000
A. laniger	0.005	0.944	0.035	0.851	0.401	0.528	0.555	0.460	0.769	0.385	0.329	0.568	0.741	0.393	0.730	0.395	2.530	0.113
I. Indri	0.142	0.708	0.033	0.856	0.926	0.338	0.254	0.616	1.440	0.235	0.923	0.339	1.384	0.243	1.525	0.220	3.997	0.047
P. diadema	0.119	0.731	0.525	0.472	0.016	0.899	1.331	0.254	0.204	0.654	0.002	0.967	0.193	0.662	0.051	0.822	0.693	0.406
P. verreauxi	2.407	0.126	5.020	0.028	1.638	0.203	5.503	0.022	0.334	0.565	2.760	0.100	0.451	0.504	2.007	0.159	2.158	0.143
E. fulvus	0.082	0.775	0.537	0.464	0.083	0.774	1.751	0.187	0.328	0.568	0.009	0.922	0.352	0.553	0.139	0.710	1.717	0.191
E. macaco	0.019	0.891	0.008	0.931	0.577	0.449	0.493	0.485	0.753	0.388	0.422	0.517	0.831	0.365	0.821	0.367	3.514	0.062
E. mongoz	0.147	0.702	0.024	0.877	1.600	0.208	0.521	0.472	1.733	0.192	1.439	0.233	1.906	0.171	2.332	0.129	10.437	0.001
E. rubriventer	0.011	0.916	0.006	0.938	0.322	0.572	0.307	0.582	0.550	0.462	0.255	0.615	0.551	0.461	0.530	0.468	1.704	0.193
H. griseus	0.144	0.706	0.543	0.465	0.007	0.936	1.290	0.261	0.191	0.664	0.007	0.936	0.163	0.688	0.029	0.865	0.426	0.515
L. catta	1.045	0.311	2.476	0.121	0.634	0.428	3.215	0.078	0.042	0.839	1.124	0.292	0.077	0.783	0.695	0.406	0.585	0.445
V. variegata	0.796	0.376	0.794	0.376	2.989	0.087	0.003	0.953	2.419	0.125	3.064	0.083	2.741	0.102	4.134	0.044	12.116	0.001
L. ruficaudatus	1.295	0.261	2.841	0.098	0.627	0.430	3.305	0.075	0.061	0.806	1.266	0.264	0.096	0.758	0.801	0.373	0.551	0.459
L. tardigradus	2.936	0.093	8.353	0.006	3.217	0.076	7.274	0.009	0.428	0.516	5.234	0.025	0.658	0.421	3.778	0.055	8.537	0.004
N. bengalensis	0.882	0.353	2.020	0.162	0.447	0.505	2.597	0.114	0.023	0.881	0.881	0.351	0.045	0.833	0.528	0.469	0.336	0.563
N. coucang	0.277	0.600	1.296	0.258	0.006	0.939	2.783	0.099	0.267	0.606	0.027	0.870	0.255	0.615	0.034	0.854	1.170	0.280
P. potto	0.013	0.910	0.279	0.598	0.359	0.550	1.507	0.221	0.661	0.417	0.171	0.680	0.734	0.393	0.512	0.475	4.084	0.044

2* model VAULT PC2	*G. zanzibaricus*		*O. crassicaudatus*		*O. garnettii*		*A. laniger*		*I. indri*		*P. diadema*		*P. verreauxi*		*E. fulvus*		*E. macaco*	
	F value	p value	F value	p value	F value	p value	F value	p value	F value	p value	F value	p value	F value	p value	F value	p value	F value	p value
C. major																		
C. medius																		
M. murinus																		
M. rufus																		
G. alleni																		
G. demidoff																		
E. elegantulus																		
G. moholi																		
G. senegalensus																		
G. zanzibaricus																		
O. crassicaudatus	0.782	0.378																
O. garnettii	0.954	0.331	0.066	0.798														
A. laniger	0.041	0.840	0.383	0.537	0.521	0.472												
I. Indri	0.288	0.593	0.044	0.834	0.106	0.746	0.096	0.758										
P. diadema	0.064	0.801	1.875	0.173	2.147	0.145	0.181	0.673	0.546	0.463								
P. verreauxi	2.367	0.129	8.707	0.004	8.916	0.003	2.800	0.099	4.041	0.048	1.473	0.229						
E. fulvus	0.030	0.862	3.343	0.069	4.176	0.042	0.147	0.702	0.453	0.502	0.014	0.904	2.217	0.138				
E. macaco	0.068	0.795	0.355	0.552	0.535	0.466	0.006	0.941	0.043	0.836	0.285	0.595	3.006	0.086	0.351	0.554		
E. mongoz	0.325	0.570	0.240	0.625	0.484	0.488	0.097	0.757	0.005	0.946	0.893	0.347	6.265	0.014	1.254	0.264	0.052	0.819
E. rubriventer	0.044	0.835	0.169	0.682	0.244	0.622	0.003	0.959	0.036	0.851	0.150	0.700	1.924	0.170	0.135	0.714	0.000	0.993
H. griseus	0.085	0.772	1.431	0.234	1.615	0.206	0.209	0.650	0.597	0.443	0.001	0.976	1.290	0.260	0.017	0.895	0.259	0.612
L. catta	0.964	0.330	5.922	0.016	6.197	0.014	1.252	0.268	2.067	0.155	0.564	0.456	0.133	0.716	1.211	0.272	1.684	0.198
V. variegata	1.141	0.290	0.436	0.510	0.246	0.621	0.729	0.397	0.346	0.558	1.774	0.188	6.589	0.012	2.577	0.110	0.713	0.401
L. ruficaudatus	1.248	0.270	4.766	0.031	4.904	0.029	1.517	0.225	2.509	0.118	0.579	0.450	0.122	0.728	0.887	0.347	1.491	0.226
L. tardigradus	3.006	0.089	28.744	0.000	29.782	0.000	3.535	0.066	5.102	0.027	2.361	0.131	0.010	0.920	8.307	0.004	5.576	0.021
N. bengalensis	0.818	0.371	4.198	0.043	4.355	0.039	1.040	0.314	1.843	0.180	0.397	0.532	0.165	0.686	0.753	0.387	1.223	0.272
N. coucang	0.170	0.681	5.516	0.020	6.436	0.012	0.422	0.517	1.010	0.317	0.007	0.933	2.321	0.131	0.100	0.752	0.725	0.396
P. potto	0.001	0.982	2.442	0.119	3.210	0.075	0.043	0.835	0.295	0.588	0.145	0.704	3.517	0.062	0.158	0.692	0.138	0.710

2* model VAULT PC2	*E. mongoz*		*E. rubriventer*		*H. griseus*		*L. catta*		*V. variegata*		*L. ruficaudatus*		*L. tardigradus*		*N. bengalensis*		*N. coucang*	
	F value	p value	F value	p value	F value	p value	F value	p value	F value	p value	F value	p value	F value	p value	F value	p value	F value	p value
C. major																		
C. medius																		
M. murinus																		
M. rufus																		
G. alleni																		
G. demidoff																		
E. elegantulus																		
G. moholi																		
G. senegalensus																		
G. zanzibaricus																		
O. crassicaudatus																		
O. garnettii																		
A. laniger																		
I. Indri																		
P. diadema																		
P. verreauxi																		
E. fulvus																		
E. macaco																		
E. mongoz																		
E. rubriventer	0.030	0.864																
H. griseus	0.765	0.384	0.144	0.706														
L. catta	3.680	0.058	1.045	0.311	0.450	0.505												
V. variegata	0.797	0.374	0.406	0.526	1.596	0.211	4.130	0.046										
L. ruficaudatus	3.349	0.071	1.024	0.317	0.546	0.464	0.000	0.983	3.909	0.053								
L. tardigradus	15.610	0.000	2.186	0.146	1.680	0.201	0.279	0.599	10.333	0.002	0.205	0.653						
N. bengalensis	2.720	0.103	0.748	0.392	0.350	0.557	0.003	0.959	3.222	0.078	0.005	0.941	0.263	0.611				
N. coucang	2.500	0.116	0.321	0.572	0.001	0.974	0.984	0.324	3.885	0.051	0.868	0.354	7.141	0.009	0.642	0.425		
P. potto	0.748	0.388	0.053	0.819	0.124	0.725	2.046	0.155	2.235	0.137	1.558	0.214	12.701	0.000	1.334	0.250	0.569	0.451

2* model VAULT PC3	*C. major*		*C. medius*		*M. murinus*		*M. rufus*		*G. alleni*		*G. demidoff*		*E. elegantulus*		*G. moholi*		*G. senegalensis*	
	F value	p value	F value	p value	F value	p value	F value	p value	F value	p value	F value	p value	F value	p value	F value	p value	F value	p value
C. major																		
C. medius	1.527	0.222																
M. murinus	0.113	0.738	1.097	0.297														
M. rufus	1.701	0.198	7.787	0.007	2.931	0.090												
G. alleni	0.438	0.511	0.089	0.767	0.187	0.666	3.119	0.084										
G. demidoff	3.614	0.061	0.173	0.678	2.460	0.119	14.654	0.000	0.445	0.507								
E. elegantulus	2.457	0.123	0.344	0.560	2.018	0.158	8.182	0.006	0.500	0.482	0.152	0.697						
G. moholi	0.065	0.799	1.634	0.204	0.018	0.894	3.131	0.080	0.333	0.566	3.457	0.065	2.744	0.101				
G. senegalensus	1.388	0.240	0.791	0.375	0.663	0.416	11.629	0.001	0.009	0.924	2.393	0.123	2.338	0.128	1.090	0.298		
G. zanzibaricus	0.066	0.799	0.975	0.328	0.006	0.940	2.555	0.116	0.211	0.648	2.556	0.114	1.849	0.180	0.001	0.970	0.656	0.419
O. crassicaudatus	4.187	0.043	2.027	0.157	6.291	0.013	12.019	0.001	1.306	0.255	1.452	0.230	0.258	0.612	7.004	0.009	14.278	0.000
O. garnettii	1.388	0.241	0.065	0.799	1.675	0.197	6.089	0.015	0.170	0.681	0.005	0.943	0.108	0.743	2.033	0.156	2.261	0.134
A. laniger	2.269	0.139	0.105	0.747	1.488	0.226	9.064	0.004	0.279	0.600	0.001	0.975	0.078	0.782	2.195	0.142	1.445	0.231
I. Indri	7.191	0.009	3.415	0.069	7.180	0.009	16.253	0.000	2.820	0.098	3.635	0.060	1.178	0.282	9.041	0.003	11.630	0.001
P. diadema	1.009	0.320	0.016	0.901	0.686	0.409	5.656	0.021	0.034	0.854	0.278	0.599	0.406	0.526	1.050	0.308	0.334	0.564
P. verreauxi	0.266	0.608	0.280	0.599	0.087	0.769	2.711	0.104	0.020	0.887	0.885	0.349	0.850	0.359	0.179	0.673	0.040	0.842
E. fulvus	0.004	0.950	1.848	0.176	0.102	0.750	1.570	0.212	0.333	0.565	3.227	0.074	2.300	0.131	0.036	0.851	2.353	0.126
E. macaco	0.060	0.807	0.748	0.390	0.001	0.982	1.776	0.186	0.129	0.721	1.742	0.190	1.368	0.245	0.008	0.929	0.595	0.441
E. mongoz	1.338	0.251	0.004	0.951	1.311	0.254	6.606	0.012	0.102	0.751	0.102	0.750	0.264	0.609	1.750	0.188	1.222	0.270
E. rubriventer	0.383	0.539	2.521	0.118	0.965	0.328	0.066	0.798	1.074	0.305	5.018	0.028	3.267	0.076	0.947	0.333	4.028	0.046
H. griseus	0.043	0.837	1.320	0.256	0.294	0.589	0.437	0.512	0.436	0.512	2.869	0.094	1.935	0.170	0.233	0.630	2.024	0.156
L. catta	1.028	0.315	5.756	0.020	2.548	0.114	0.001	0.980	2.123	0.151	10.586	0.002	6.039	0.017	2.522	0.115	11.089	0.001
V. variegata	5.368	0.024	3.106	0.083	7.511	0.007	12.572	0.001	2.163	0.147	3.315	0.072	0.993	0.323	8.853	0.004	14.634	0.000
L. ruficaudatus	0.768	0.385	4.412	0.041	1.619	0.206	0.053	0.818	1.787	0.188	8.763	0.004	5.177	0.027	1.664	0.200	6.784	0.010
L. tardigradus	0.339	0.563	0.802	0.375	0.100	0.753	4.583	0.037	0.057	0.812	2.512	0.117	1.574	0.215	0.247	0.620	0.411	0.522
N. bengalensis	3.874	0.056	0.762	0.387	3.030	0.085	11.991	0.001	0.868	0.357	0.548	0.461	0.040	0.843	4.222	0.043	4.143	0.043
N. coucang	4.358	0.040	2.223	0.139	6.684	0.011	12.195	0.001	1.408	0.239	1.783	0.184	0.344	0.559	7.577	0.007	15.617	0.000
P. potto	6.062	0.015	3.597	0.060	9.112	0.003	16.128	0.000	2.116	0.148	2.776	0.097	0.646	0.423	9.969	0.002	21.308	0.000

2* model VAULT PC3	*G. zanzibaricus*		*O. crassicaudatus*		*O. garnettii*		*A. laniger*		*I. indri*		*P. diadema*		*P. verreauxi*		*E. fulvus*		*E. macaco*	
	F value	p value	F value	p value	F value	p value	F value	p value	F value	p value	F value	p value	F value	p value	F value	p value	F value	p value
C. major																		
C. medius																		
M. murinus																		
M. rufus																		
G. alleni																		
G. demidoff																		
E. elegantulus																		
G. moholi																		
G. senegalensus																		
G. zanzibaricus																		
O. crassicaudatus	3.645	0.059																
O. garnettii	1.013	0.316	2.660	0.105														
A. laniger	1.569	0.217	0.673	0.414	0.005	0.944												
I. Indri	6.232	0.015	0.420	0.518	2.097	0.150	2.121	0.151										
P. diadema	0.605	0.440	1.963	0.164	0.122	0.728	0.161	0.690	3.239	0.077								
P. verreauxi	0.096	0.757	2.754	0.099	0.518	0.473	0.522	0.473	3.884	0.052	0.149	0.700						
E. fulvus	0.030	0.864	16.131	0.000	5.377	0.021	1.738	0.189	7.078	0.008	1.212	0.272	0.295	0.588				
E. macaco	0.002	0.967	5.392	0.022	1.459	0.229	0.946	0.334	4.901	0.029	0.475	0.493	0.070	0.792	0.076	0.783		
E. mongoz	0.903	0.345	2.924	0.089	0.062	0.804	0.060	0.807	2.994	0.087	0.033	0.856	0.349	0.556	3.205	0.075	1.031	0.312
E. rubriventer	0.657	0.421	5.476	0.021	2.556	0.113	2.898	0.095	7.319	0.009	1.920	0.172	0.994	0.322	0.494	0.483	0.608	0.438
H. griseus	0.150	0.700	4.670	0.033	1.808	0.181	1.511	0.225	5.213	0.026	0.961	0.332	0.398	0.530	0.103	0.749	0.186	0.668
L. catta	1.600	0.211	13.346	0.000	6.749	0.011	5.620	0.021	12.465	0.001	4.311	0.042	2.278	0.136	1.757	0.186	1.680	0.198
V. variegata	4.784	0.033	0.608	0.437	2.997	0.086	1.619	0.208	0.000	0.993	2.930	0.092	3.717	0.058	10.597	0.001	5.494	0.021
L. ruficaudatus	1.254	0.269	8.042	0.005	3.853	0.052	5.166	0.028	11.052	0.002	3.247	0.078	1.583	0.213	0.820	0.366	0.981	0.325
L. tardigradus	0.102	0.750	10.442	0.002	2.216	0.139	1.090	0.302	6.588	0.013	0.405	0.527	0.007	0.934	0.775	0.380	0.081	0.777
N. bengalensis	2.989	0.091	0.102	0.750	0.287	0.593	0.291	0.592	0.911	0.344	0.793	0.378	1.309	0.257	3.156	0.077	1.906	0.172
N. coucang	3.815	0.054	0.029	0.865	2.805	0.096	0.799	0.374	0.294	0.589	2.119	0.149	2.903	0.091	15.442	0.000	5.424	0.022
P. potto	5.421	0.021	0.250	0.617	5.033	0.026	1.348	0.248	0.192	0.662	3.370	0.068	4.248	0.041	22.503	0.000	7.961	0.005

2* model VAULT PC3	*E. mongoz*		*E. rubriventer*		*H. griseus*		*L. catta*		*V. variegata*		*L. ruficaudatus*		*L. tardigradus*		*N. bengalensis*		*N. coucang*	
	F value	p value	F value	p value	F value	p value	F value	p value	F value	p value	F value	p value	F value	p value	F value	p value	F value	p value
C. major																		
C. medius																		
M. murinus																		
M. rufus																		
G. alleni																		
G. demidoff																		
E. elegantulus																		
G. moholi																		
G. senegalensus																		
G. zanzibaricus																		
O. crassicaudatus																		
O. garnettii																		
A. laniger																		
I. Indri																		
P. diadema																		
P. verreauxi																		
E. fulvus																		
E. macaco																		
E. mongoz																		
E. rubriventer	2.534	0.115																
H. griseus	1.562	0.215	0.043	0.837														
L. catta	6.412	0.013	1.028	0.315	0.358	0.552												
V. variegata	3.594	0.061	5.993	0.017	4.804	0.032	11.811	0.001										
L. ruficaudatus	4.014	0.049	0.005	0.947	0.182	0.671	0.029	0.866	8.614	0.005								
L. tardigradus	1.267	0.264	1.253	0.268	0.497	0.484	3.870	0.054	7.212	0.009	2.316	0.135						
N. bengalensis	0.567	0.454	4.107	0.049	2.404	0.128	7.598	0.008	0.702	0.406	7.105	0.011	2.484	0.122				
N. coucang	3.119	0.080	5.449	0.022	4.573	0.035	13.042	0.000	0.402	0.527	8.077	0.006	9.893	0.002	0.163	0.687		
P. potto	5.216	0.024	7.504	0.007	6.658	0.011	18.002	0.000	0.288	0.592	10.967	0.001	16.594	0.000	0.377	0.540	0.081	0.776

2* model VAULT PC4	*C. major*		*C. medius*		*M. murinus*		*M. rufus*		*G. alleni*		*G. demidoff*		*E. elegantulus*		*G. moholi*		*G. senegalensis*	
	F value	p value	F value	p value	F value	p value	F value	p value	F value	p value	F value	p value	F value	p value	F value	p value	F value	p value
C. major																		
C. medius	9.583	0.003																
M. murinus	2.032	0.157	4.565	0.035														
M. rufus	0.727	0.398	5.124	0.028	0.207	0.650												
G. alleni	0.876	0.354	12.477	0.001	5.790	0.018	2.833	0.099										
G. demidoff	1.284	0.261	5.302	0.024	0.074	0.786	0.042	0.839	4.344	0.040								
E. elegantulus	5.580	0.022	0.001	0.975	2.575	0.112	2.904	0.094	8.256	0.006	2.965	0.089						
G. moholi	2.978	0.088	4.269	0.041	0.051	0.822	0.473	0.493	7.397	0.008	0.252	0.617	2.365	0.127				
G. senegalensus	7.103	0.008	3.115	0.079	1.283	0.258	2.327	0.129	14.546	0.000	2.275	0.133	1.555	0.214	0.715	0.399		
G. zanzibaricus	0.589	0.447	6.812	0.012	0.398	0.530	0.022	0.883	2.645	0.111	0.134	0.716	3.623	0.062	0.800	0.373	2.916	0.089
O. crassicaudatus	0.709	0.401	18.082	0.000	1.587	0.210	0.202	0.654	4.758	0.031	0.764	0.384	8.336	0.005	2.505	0.115	14.751	0.000
O. garnettii	5.958	0.016	2.240	0.137	1.287	0.258	2.071	0.153	11.472	0.001	2.129	0.147	1.094	0.298	0.777	0.379	0.025	0.876
A. laniger	0.367	0.548	4.552	0.038	0.359	0.550	0.022	0.882	1.895	0.176	0.128	0.721	2.731	0.104	0.675	0.413	2.768	0.098
I. Indri	7.313	0.009	0.167	0.684	3.901	0.051	4.196	0.045	10.153	0.002	4.319	0.040	0.086	0.770	3.732	0.056	2.896	0.090
P. diadema	3.439	0.070	2.546	0.117	0.314	0.576	0.866	0.356	6.522	0.014	0.628	0.430	1.291	0.260	0.142	0.707	0.123	0.726
P. verreauxi	4.096	0.047	0.931	0.338	0.814	0.369	1.419	0.238	7.448	0.008	1.206	0.275	0.557	0.458	0.577	0.449	0.045	0.833
E. fulvus	1.398	0.238	6.972	0.009	0.117	0.733	0.039	0.844	5.172	0.024	0.001	0.974	3.542	0.061	0.332	0.565	4.493	0.035
E. macaco	3.367	0.070	1.593	0.211	0.498	0.482	0.998	0.321	6.920	0.010	0.876	0.351	0.917	0.341	0.273	0.603	0.015	0.903
E. mongoz	4.156	0.045	2.407	0.125	0.631	0.429	1.237	0.269	8.299	0.005	1.151	0.286	1.213	0.274	0.328	0.568	0.048	0.827
E. rubriventer	3.814	0.057	0.136	0.714	1.213	0.274	1.655	0.204	6.066	0.018	1.495	0.225	0.095	0.759	1.058	0.306	0.400	0.528
H. griseus	0.403	0.529	8.942	0.004	0.718	0.399	0.118	0.733	2.444	0.125	0.321	0.573	4.598	0.036	1.304	0.256	3.795	0.053
L. catta	2.551	0.116	1.378	0.245	0.339	0.562	0.714	0.401	5.241	0.026	0.612	0.436	0.815	0.370	0.175	0.676	0.036	0.850
V. variegata	3.188	0.079	33.849	0.000	16.134	0.000	8.311	0.005	0.177	0.675	12.859	0.001	18.975	0.000	19.696	0.000	43.641	0.000
L. ruficaudatus	0.667	0.418	6.295	0.015	0.305	0.582	0.008	0.928	2.738	0.105	0.088	0.767	3.361	0.072	0.650	0.422	2.428	0.121
L. tardigradus	4.998	0.030	0.519	0.474	2.301	0.133	2.306	0.135	7.881	0.007	3.028	0.086	0.257	0.614	1.766	0.187	1.200	0.275
N. bengalensis	3.052	0.088	1.353	0.251	0.412	0.523	0.892	0.350	5.482	0.024	0.680	0.412	0.751	0.390	0.254	0.615	0.006	0.940
N. coucang	8.079	0.006	0.008	0.927	4.548	0.035	4.398	0.039	12.342	0.001	5.620	0.019	0.009	0.926	3.748	0.055	4.238	0.041
P. potto	2.266	0.134	3.039	0.083	0.108	0.743	0.453	0.502	5.817	0.017	0.368	0.545	1.564	0.213	0.012	0.914	0.811	0.369

2* model VAULT PC4	*G. zanzibaricus*		*O. crassicaudatus*		*O. garnettii*		*A. laniger*		*I. indri*		*P. diadema*		*P. verreauxi*		*E. fulvus*		*E. macaco*	
	F value	p value	F value	p value	F value	p value	F value	p value	F value	p value	F value	p value	F value	p value	F value	p value	F value	p value
C. major																		
C. medius																		
M. murinus																		
M. rufus																		
G. alleni																		
G. demidoff																		
E. elegantulus																		
G. moholi																		
G. senegalensus																		
G. zanzibaricus																		
O. crassicaudatus	0.056	0.813																
O. garnettii	2.605	0.109	14.045	0.000														
A. laniger	0.001	0.978	0.031	0.861	2.345	0.128												
I. Indri	5.131	0.027	10.972	0.001	2.136	0.146	3.890	0.053										
P. diadema	1.406	0.242	3.905	0.050	0.166	0.684	0.953	0.334	2.296	0.135								
P. verreauxi	1.974	0.165	4.858	0.029	0.013	0.910	1.500	0.225	1.192	0.278	0.162	0.688						
E. fulvus	0.125	0.724	1.280	0.259	4.421	0.036	0.143	0.706	4.985	0.027	0.804	0.371	1.444	0.231				
E. macaco	1.353	0.248	4.716	0.031	0.040	0.841	1.149	0.287	1.706	0.195	0.025	0.875	0.052	0.820	1.304	0.255		
E. mongoz	1.671	0.200	7.811	0.006	0.101	0.751	1.418	0.238	2.210	0.141	0.023	0.881	0.085	0.771	2.088	0.150	0.001	0.972
E. rubriventer	2.260	0.139	4.567	0.035	0.256	0.614	1.580	0.215	0.352	0.555	0.492	0.486	0.123	0.726	1.634	0.203	0.277	0.600
H. griseus	0.044	0.835	0.000	0.987	3.410	0.067	0.017	0.896	6.338	0.014	2.212	0.143	2.738	0.103	0.295	0.588	1.887	0.174
L. catta	1.006	0.320	3.406	0.067	0.061	0.805	0.807	0.373	1.506	0.224	0.008	0.931	0.066	0.798	0.881	0.349	0.003	0.958
V. variegata	7.795	0.007	17.497	0.000	35.642	0.000	5.847	0.019	22.291	0.000	18.382	0.000	18.436	0.000	17.263	0.000	18.952	0.000
L. ruficaudatus	0.004	0.950	0.094	0.760	2.190	0.142	0.006	0.940	4.800	0.032	1.228	0.273	1.761	0.189	0.077	0.782	1.158	0.285
L. tardigradus	2.763	0.103	18.986	0.000	0.683	0.410	2.212	0.144	0.740	0.393	0.617	0.436	0.099	0.755	7.408	0.007	0.421	0.518
N. bengalensis	1.414	0.241	3.252	0.074	0.020	0.889	0.919	0.343	1.451	0.233	0.029	0.865	0.039	0.844	0.785	0.377	0.000	0.987
N. coucang	4.922	0.029	24.771	0.000	2.999	0.085	4.362	0.040	0.208	0.649	1.944	0.167	0.716	0.399	11.763	0.001	1.615	0.206
P. potto	0.631	0.428	4.411	0.037	0.886	0.348	0.642	0.424	2.491	0.116	0.051	0.822	0.326	0.569	0.969	0.326	0.172	0.679

2* model VAULT PC4	*E. mongoz*		*E. rubriventer*		*H. griseus*		*L. catta*		*V. variegata*		*L. ruficaudatus*		*L. tardigradus*		*N. bengalensis*		*N. coucang*	
	F value	p value	F value	p value	F value	p value	F value	p value	F value	p value	F value	p value	F value	p value	F value	p value	F value	p value
C. major																		
C. medius																		
M. murinus																		
M. rufus																		
G. alleni																		
G. demidoff																		
E. elegantulus																		
G. moholi																		
G. senegalensus																		
G. zanzibaricus																		
O. crassicaudatus																		
O. garnettii																		
A. laniger																		
I. Indri																		
P. diadema																		
P. verreauxi																		
E. fulvus																		
E. macaco																		
E. mongoz																		
E. rubriventer	0.366	0.547																
H. griseus	2.327	0.131	0.403	0.529														
L. catta	0.001	0.975	2.551	0.116	1.460	0.232												
V. variegata	25.531	0.000	13.685	0.000	7.237	0.009	14.423	0.000										
L. ruficaudatus	1.406	0.239	2.108	0.153	0.078	0.782	0.868	0.356	7.787	0.007								
L. tardigradus	0.833	0.364	0.012	0.914	3.575	0.064	0.349	0.557	27.601	0.000	2.394	0.128						
N. bengalensis	0.002	0.962	0.249	0.620	2.184	0.146	0.004	0.952	14.243	0.000	1.276	0.265	0.216	0.644				
N. coucang	2.837	0.095	0.078	0.781	5.847	0.018	1.338	0.250	36.553	0.000	4.307	0.041	0.695	0.407	0.937	0.336		
P. potto	0.251	0.617	0.574	0.450	0.921	0.339	0.091	0.763	18.737	0.000	0.497	0.482	2.344	0.128	0.106	0.745	5.200	0.024

2* model VAULT PC5	*C. major*		*C. medius*		*M. murinus*		*M. rufus*		*G. alleni*		*G. demidoff*		*E. elegantulus*		*G. moholi*		*G. senegalensis*	
	F value	p value	F value	p value	F value	p value	F value	p value	F value	p value	F value	p value	F value	p value	F value	p value	F value	p value
C. major																		
C. medius	1.250	0.269																
M. murinus	0.124	0.726	0.734	0.394														
M. rufus	0.384	0.538	0.198	0.658	0.103	0.749												
G. alleni	5.460	0.024	3.875	0.055	6.297	0.014	4.132	0.048										
G. demidoff	1.841	0.179	0.168	0.683	1.470	0.228	0.572	0.452	2.984	0.088								
E. elegantulus	5.011	0.029	2.866	0.096	5.039	0.027	3.306	0.074	0.258	0.613	1.758	0.188						
G. moholi	0.450	0.504	0.160	0.690	0.162	0.688	0.002	0.961	4.726	0.032	0.576	0.449	3.451	0.066				
G. senegalensus	1.088	0.298	0.069	0.793	0.677	0.412	0.084	0.772	6.596	0.011	0.583	0.446	4.583	0.033	0.068	0.794		
G. zanzibaricus	1.469	0.232	0.345	0.560	1.454	0.231	0.649	0.424	1.060	0.309	0.100	0.753	0.513	0.477	0.753	0.388	0.906	0.342
O. crassicaudatus	2.999	0.086	0.944	0.333	3.561	0.061	1.415	0.237	2.181	0.142	0.267	0.606	1.005	0.318	1.805	0.181	3.647	0.057
O. garnettii	6.154	0.015	3.521	0.063	7.776	0.006	3.767	0.055	1.363	0.245	1.769	0.186	0.314	0.576	4.679	0.032	10.524	0.001
A. laniger	0.395	0.533	0.115	0.737	0.135	0.714	0.004	0.952	3.364	0.074	0.413	0.522	2.691	0.107	0.000	0.986	0.038	0.847
I. Indri	6.442	0.014	3.900	0.053	6.084	0.015	4.362	0.041	0.178	0.674	2.364	0.128	0.020	0.889	4.260	0.041	5.463	0.020
P. diadema	1.673	0.202	0.040	0.843	0.996	0.321	0.378	0.541	3.486	0.068	0.049	0.825	2.424	0.125	0.303	0.583	0.210	0.647
P. verreauxi	0.623	0.433	0.069	0.793	0.254	0.616	0.027	0.870	4.110	0.047	0.359	0.551	3.013	0.087	0.014	0.906	0.007	0.934
E. fulvus	3.478	0.064	1.178	0.279	4.096	0.044	1.687	0.195	2.349	0.127	0.369	0.544	1.002	0.318	2.132	0.146	4.250	0.040
E. macaco	0.412	0.523	0.297	0.587	0.110	0.740	0.001	0.972	5.433	0.022	0.840	0.361	4.217	0.043	0.009	0.925	0.170	0.680
E. mongoz	8.334	0.005	6.879	0.010	11.788	0.001	6.290	0.014	0.138	0.711	4.794	0.031	0.077	0.782	8.194	0.005	17.924	0.000
E. rubriventer	0.143	0.707	0.267	0.607	0.012	0.914	0.022	0.884	3.401	0.071	0.591	0.444	2.747	0.103	0.036	0.851	0.167	0.684
H. griseus	0.052	0.821	0.727	0.398	0.010	0.919	0.147	0.703	4.842	0.033	1.246	0.268	4.219	0.045	0.188	0.666	0.567	0.452
L. catta	0.159	0.692	0.459	0.501	0.009	0.925	0.043	0.836	4.602	0.036	1.016	0.316	3.852	0.054	0.076	0.783	0.386	0.535
V. variegata	2.768	0.101	0.780	0.381	2.554	0.113	1.285	0.261	1.644	0.205	0.232	0.631	0.746	0.391	1.348	0.248	1.721	0.191
L. ruficaudatus	0.260	0.612	0.337	0.564	0.033	0.856	0.015	0.903	4.343	0.043	0.721	0.398	3.603	0.063	0.027	0.870	0.169	0.682
L. tardigradus	0.533	0.469	0.512	0.477	0.165	0.686	0.002	0.961	6.028	0.018	1.357	0.248	5.398	0.024	0.015	0.902	0.432	0.512
N. bengalensis	0.798	0.377	0.018	0.893	0.347	0.557	0.075	0.785	3.324	0.075	0.211	0.647	2.528	0.118	0.048	0.827	0.003	0.955
N. coucang	2.830	0.096	0.753	0.388	3.158	0.078	1.252	0.266	2.366	0.128	0.164	0.686	1.196	0.277	1.531	0.218	2.791	0.096
P. potto	1.345	0.248	0.075	0.784	1.340	0.248	0.370	0.544	3.066	0.082	0.020	0.889	1.872	0.173	0.455	0.501	0.641	0.424

2* model VAULT PC5	*G. zanzibaricus*		*O. crassicaudatus*		*O. garnettii*		*A. laniger*		*I. indri*		*P. diadema*		*P. verreauxi*		*E. fulvus*		*E. macaco*	
	F value	p value	F value	p value	F value	p value	F value	p value	F value	p value	F value	p value	F value	p value	F value	p value	F value	p value
C. major																		
C. medius																		
M. murinus																		
M. rufus																		
G. alleni																		
G. demidoff																		
E. elegantulus																		
G. moholi																		
G. senegalensus																		
G. zanzibaricus																		
O. crassicaudatus	0.000	0.989																
O. garnettii	0.292	0.590	1.143	0.286														
A. laniger	0.483	0.491	1.101	0.296	3.048	0.084												
I. Indri	0.778	0.381	1.395	0.240	0.570	0.452	3.605	0.063										
P. diadema	0.211	0.648	0.512	0.476	2.367	0.127	0.245	0.623	3.391	0.070								
P. verreauxi	0.528	0.470	1.101	0.296	3.228	0.075	0.008	0.928	3.922	0.051	0.185	0.669						
E. fulvus	0.004	0.948	0.010	0.919	1.001	0.318	1.343	0.248	1.382	0.241	0.654	0.420	1.312	0.253				
E. macaco	0.952	0.332	2.407	0.123	6.110	0.015	0.010	0.919	5.276	0.024	0.506	0.479	0.048	0.828	2.821	0.094		
E. mongoz	1.365	0.246	4.961	0.027	2.235	0.137	5.157	0.026	0.015	0.904	5.303	0.024	5.988	0.016	5.146	0.024	10.010	0.002
E. rubriventer	0.618	0.436	1.169	0.282	2.808	0.096	0.035	0.853	3.603	0.062	0.435	0.513	0.083	0.775	1.389	0.240	0.017	0.897
H. griseus	1.101	0.299	2.265	0.135	5.010	0.027	0.169	0.683	5.460	0.023	1.042	0.312	0.300	0.585	2.647	0.105	0.148	0.701
L. catta	0.949	0.334	2.409	0.123	5.606	0.019	0.063	0.802	4.892	0.030	0.681	0.413	0.143	0.706	2.882	0.091	0.042	0.838
V. variegata	0.003	0.958	0.004	0.949	0.387	0.535	0.984	0.325	1.130	0.291	0.495	0.484	1.008	0.319	0.000	0.998	1.795	0.184
L. ruficaudatus	0.753	0.390	1.468	0.228	3.710	0.057	0.030	0.863	4.809	0.032	0.589	0.446	0.082	0.776	1.721	0.191	0.009	0.925
L. tardigradus	1.124	0.294	5.557	0.020	14.776	0.000	0.015	0.903	7.011	0.010	0.847	0.362	0.072	0.789	6.753	0.010	0.000	0.993
N. bengalensis	0.343	0.561	0.716	0.399	2.378	0.126	0.036	0.850	3.505	0.066	0.099	0.755	0.012	0.912	0.876	0.351	0.107	0.745
N. coucang	0.004	0.950	0.024	0.878	1.438	0.232	0.951	0.332	1.662	0.200	0.389	0.534	0.950	0.332	0.067	0.796	2.090	0.151
P. potto	0.177	0.674	0.843	0.359	3.952	0.048	0.260	0.611	2.333	0.129	0.007	0.934	0.212	0.645	1.144	0.286	0.673	0.413

2* model VAULT PC5	*E. mongoz*		*E. rubriventer*		*H. griseus*		*L. catta*		*V. variegata*		*L. ruficaudatus*		*L. tardigradus*		*N. bengalensis*		*N. coucang*	
	F value	p value	F value	p value	F value	p value	F value	p value	F value	p value	F value	p value	F value	p value	F value	p value	F value	p value
C. major																		
C. medius																		
M. murinus																		
M. rufus																		
G. alleni																		
G. demidoff																		
E. elegantulus																		
G. moholi																		
G. senegalensus																		
G. zanzibaricus																		
O. crassicaudatus																		
O. garnettii																		
A. laniger																		
I. Indri																		
P. diadema																		
P. verreauxi																		
E. fulvus																		
E. macaco																		
E. mongoz																		
E. rubriventer	4.478	0.037																
H. griseus	7.285	0.008	0.052	0.821														
L. catta	8.372	0.005	0.159	0.692	0.029	0.865												
V. variegata	2.181	0.143	1.142	0.289	2.086	0.154	1.825	0.181										
L. ruficaudatus	5.991	0.017	0.002	0.963	0.072	0.789	0.008	0.930	1.484	0.228								
L. tardigradus	18.982	0.000	0.019	0.891	0.192	0.664	0.056	0.814	2.670	0.107	0.011	0.917						
N. bengalensis	4.551	0.036	0.140	0.710	0.423	0.519	0.213	0.647	0.733	0.395	0.169	0.683	0.158	0.693				
N. coucang	5.238	0.024	1.058	0.306	2.099	0.151	2.112	0.149	0.028	0.868	1.350	0.248	4.505	0.036	0.610	0.437		
P. potto	8.363	0.004	0.382	0.537	0.886	0.348	0.834	0.362	0.382	0.537	0.444	0.506	1.578	0.211	0.099	0.754	0.516	0.474

Goswami model FACE- PC1	*C. major*		*C.medius*		*M. murinus*		*M. rufus*		*G. alleni*		*G. denidoff*		*E. elegantulus*		*G. moholi*		*G.senegalensis*	
	F value	p value	F value	p value	F value	p value	F value	p value	F value	p value	F value	p value	F value	p value	F value	p value	F value	p value
C. major																		
C. medius	0.888	0.350																
M. murinus	0.164	0.687	0.284	0.596														
M. rufus	3.348	0.073	1.590	0.213	3.408	0.068												
G. alleni	6.969	0.011	5.851	0.019	7.834	0.006	1.615	0.210										
G. demidoff	0.398	0.530	3.211	0.077	2.097	0.150	10.222	0.002	14.983	0.000								
E. elegantulus	3.054	0.086	8.911	0.004	6.373	0.013	14.747	0.000	18.900	0.000	2.072	0.154						
G. moholi	0.518	0.474	0.047	0.829	0.144	0.705	2.389	0.125	6.962	0.010	3.393	0.068	8.609	0.004				
G. senegalensus	0.080	0.777	1.102	0.295	0.136	0.713	8.838	0.003	17.665	0.000	2.589	0.109	9.974	0.002	0.752	0.387		
G. zanzibaricus	1.438	0.237	0.487	0.489	0.826	0.366	0.032	0.859	1.069	0.307	2.868	0.094	6.674	0.012	0.567	0.453	2.022	0.157
O. crassicaudatus	0.039	0.844	1.048	0.308	0.187	0.666	7.987	0.005	14.650	0.000	2.101	0.149	7.630	0.007	0.822	0.366	0.011	0.915
O. garnettii	0.386	0.536	4.661	0.033	2.683	0.103	17.677	0.000	25.370	0.000	0.098	0.754	4.416	0.038	4.558	0.034	2.914	0.089
A. laniger	0.131	0.719	0.142	0.708	0.002	0.962	1.344	0.252	3.780	0.058	0.838	0.363	3.553	0.065	0.038	0.846	0.085	0.771
I. Indri	2.222	0.141	1.041	0.311	2.696	0.104	0.020	0.887	0.711	0.403	7.341	0.008	10.081	0.002	1.908	0.170	6.668	0.010
P. diadema	0.400	0.530	2.471	0.122	1.231	0.270	5.429	0.024	8.827	0.005	0.023	0.879	0.935	0.338	2.057	0.155	1.605	0.207
P. verreauxi	3.746	0.057	10.185	0.002	12.178	0.001	20.925	0.000	22.238	0.000	4.655	0.033	0.080	0.778	14.675	0.000	21.550	0.000
E. fulvus	0.030	0.863	1.429	0.233	0.829	0.363	7.878	0.006	12.223	0.001	0.533	0.466	3.790	0.053	1.637	0.202	0.633	0.427
E. macaco	2.486	0.119	9.255	0.003	6.431	0.012	19.376	0.000	25.251	0.000	1.276	0.261	0.387	0.535	8.920	0.003	9.236	0.003
E. mongoz	1.235	0.270	0.100	0.753	1.201	0.275	1.096	0.298	4.667	0.034	7.644	0.007	11.025	0.001	0.428	0.514	4.124	0.043
E. rubriventer	1.389	0.244	4.536	0.038	2.402	0.125	6.828	0.012	10.039	0.003	0.585	0.447	0.065	0.799	3.513	0.064	3.540	0.061
H. griseus	0.081	0.778	0.202	0.655	0.002	0.969	2.038	0.159	4.545	0.038	1.247	0.267	3.792	0.056	0.125	0.724	0.071	0.790
L. catta	0.176	0.677	0.342	0.561	0.000	0.999	3.322	0.073	7.869	0.007	1.812	0.182	6.239	0.015	0.137	0.712	0.125	0.724
V. variegata	1.913	0.172	0.343	0.560	1.563	0.214	0.629	0.431	4.161	0.046	7.697	0.007	12.899	0.001	0.766	0.383	4.659	0.032
L. ruficaudatus	1.296	0.261	0.152	0.698	0.993	0.322	0.732	0.396	3.767	0.059	5.647	0.020	9.935	0.003	0.426	0.515	3.289	0.071
L. tardigradus	0.319	0.575	2.481	0.121	2.246	0.137	8.230	0.006	10.628	0.002	0.007	0.934	1.357	0.249	3.471	0.066	3.466	0.064
N. bengalensis	3.152	0.083	9.375	0.004	4.157	0.044	10.867	0.002	14.885	0.000	1.546	0.218	0.033	0.856	5.919	0.017	6.422	0.012
N. coucang	0.770	0.383	5.128	0.026	3.672	0.057	15.970	0.000	21.511	0.000	0.055	0.815	2.130	0.148	5.556	0.020	4.824	0.029
P. potto	0.010	0.920	1.252	0.265	0.626	0.430	7.252	0.008	11.603	0.001	0.708	0.401	4.079	0.045	1.377	0.242	0.427	0.514

Goswami model FACE- PC1	*G. zanzibaricus*		*O. crassicaudatus*		*O. garnettii*		*A. laniger*		*I. indri*		*P. diadema*		*P. verreauxi*		*E. fulvus*		*E. macaco*	
	F value	p value	F value	p value	F value	p value	F value	p value	F value	p value	F value	p value	F value	p value	F value	p value	F value	p value
C. major																		
C. medius																		
M. murinus																		
M. rufus																		
G. alleni																		
G. demidoff																		
E. elegantulus																		
G. moholi																		
G. senegalensus																		
G. zanzibaricus																		
O. crassicaudatus	1.658	0.200																
O. garnettii	4.103	0.045	2.692	0.102														
A. laniger	0.613	0.438	0.090	0.765	1.034	0.311												
I. Indri	0.050	0.824	5.738	0.018	11.538	0.001	0.950	0.334										
P. diadema	2.568	0.115	1.141	0.288	0.156	0.694	0.785	0.380	3.803	0.056								
P. verreauxi	6.062	0.017	17.970	0.000	10.861	0.001	3.728	0.058	15.607	0.000	1.411	0.239						
E. fulvus	1.574	0.211	0.554	0.457	0.429	0.513	0.261	0.610	6.373	0.012	0.326	0.568	11.587	0.001				
E. macaco	6.767	0.011	7.673	0.006	3.239	0.074	3.154	0.080	12.750	0.001	0.412	0.523	1.159	0.284	3.336	0.069		
E. mongoz	0.140	0.709	4.564	0.034	14.041	0.000	0.278	0.599	0.967	0.328	3.068	0.084	24.697	0.000	6.986	0.009	14.599	0.000
E. rubriventer	4.274	0.044	2.569	0.111	1.282	0.260	1.915	0.173	4.564	0.037	0.308	0.581	0.183	0.670	1.107	0.294	0.028	0.868
H. griseus	0.536	0.468	0.093	0.761	1.692	0.196	0.003	0.953	1.668	0.201	0.693	0.409	6.801	0.011	0.513	0.475	4.091	0.047
L. catta	0.977	0.327	0.159	0.691	2.426	0.122	0.003	0.959	2.256	0.138	1.236	0.271	9.173	0.003	0.617	0.433	6.306	0.014
V. variegata	0.078	0.780	4.559	0.035	12.985	0.000	0.546	0.463	0.555	0.459	4.007	0.050	20.573	0.000	5.385	0.021	16.134	0.000
L. ruficaudatus	0.120	0.731	3.090	0.081	9.609	0.002	0.330	0.568	0.606	0.439	2.926	0.093	15.268	0.000	3.871	0.051	12.597	0.001
L. tardigradus	1.917	0.173	2.800	0.097	0.210	0.647	0.591	0.446	6.049	0.017	0.006	0.937	3.761	0.057	0.886	0.348	0.935	0.337
N. bengalensis	7.712	0.008	4.726	0.032	3.120	0.080	3.935	0.054	6.337	0.015	1.027	0.316	0.002	0.966	2.130	0.146	0.500	0.482
N. coucang	4.037	0.048	4.284	0.040	0.505	0.478	1.349	0.249	10.781	0.001	0.001	0.979	5.451	0.021	1.336	0.249	1.155	0.285
P. potto	1.464	0.228	0.338	0.562	0.678	0.411	0.205	0.651	5.758	0.018	0.406	0.525	11.746	0.001	0.025	0.875	3.763	0.054

Goswami model FACE- PC1	*E. mongoz*		*E. rubriventer*		*H. griseus*		*L. catta*		*V. variegata*		*L. ruficaudatus*		*L. tardigradus*		*N. bengalensis*		*N. coucang*	
	F value	p value	F value	p value	F value	p value	F value	p value	F value	p value	F value	p value	F value	p value	F value	p value	F value	p value
C. major																		
C. medius																		
M. murinus																		
M. rufus																		
G. alleni																		
G. demidoff																		
E. elegantulus																		
G. moholi																		
G. senegalensus																		
G. zanzibaricus																		
O. crassicaudatus																		
O. garnettii																		
A. laniger																		
I. Indri																		
P. diadema																		
P. verreauxi																		
E. fulvus																		
E. macaco																		
E. mongoz																		
E. rubriventer	4.067	0.047																
H. griseus	0.788	0.378	0.081	0.778														
L. catta	0.953	0.332	0.176	0.677	0.001	0.973												
V. variegata	0.081	0.777	5.538	0.022	1.011	0.319	1.505	0.224										
L. ruficaudatus	0.007	0.935	4.266	0.044	0.591	0.446	0.928	0.340	0.028	0.869								
L. tardigradus	8.609	0.004	0.330	0.568	1.051	0.310	1.572	0.215	6.988	0.010	4.573	0.038						
N. bengalensis	6.195	0.015	0.171	0.681	2.451	0.124	5.118	0.028	9.157	0.004	7.190	0.010	0.872	0.355				
N. coucang	13.659	0.000	0.533	0.467	2.231	0.139	3.186	0.077	12.650	0.001	9.372	0.003	0.018	0.894	1.600	0.209		
P. potto	5.968	0.016	1.227	0.270	0.367	0.545	0.470	0.494	4.826	0.029	3.396	0.067	1.080	0.300	2.316	0.130	1.668	0.198

Goswami model FACE- PC2	*C. major*		*C.medius*		*M. murinus*		*M. rufus*		*G. alleni*		*G. denidoff*		*E. elegantulus*		*G. moholi*		*G.senegalensis*	
	F value	p value	F value	p value	F value	p value	F value	p value	F value	p value	F value	p value	F value	p value	F value	p value	F value	p value
C. major																		
C. medius	2.555	0.116																
M. murinus	1.052	0.308	0.083	0.773														
M. rufus	1.490	0.228	0.266	0.608	0.012	0.911												
G. alleni	0.446	0.508	0.799	0.376	0.231	0.632	0.236	0.629										
G. demidoff	1.372	0.245	10.184	0.002	8.628	0.004	9.916	0.002	4.471	0.038								
E. elegantulus	0.675	0.415	0.535	0.467	0.105	0.747	0.095	0.759	0.021	0.885	4.661	0.034						
G. moholi	0.061	0.806	1.714	0.194	1.146	0.286	1.063	0.305	0.198	0.658	3.310	0.071	0.313	0.577				
G. senegalensus	1.872	0.173	0.104	0.748	0.003	0.954	0.044	0.834	0.465	0.496	15.057	0.000	0.208	0.649	2.033	0.155		
G. zanzibaricus	0.000	0.987	1.345	0.252	0.572	0.452	0.739	0.394	0.232	0.633	0.780	0.380	0.372	0.544	0.029	0.865	0.998	0.319
O. crassicaudatus	0.945	0.333	1.998	0.160	0.822	0.366	0.806	0.371	0.002	0.967	13.801	0.000	0.064	0.801	0.512	0.475	1.514	0.220
O. garnettii	1.319	0.253	1.261	0.264	0.403	0.526	0.326	0.569	0.038	0.845	15.236	0.000	0.001	0.976	0.901	0.344	0.792	0.374
A. laniger	0.030	0.864	1.909	0.173	0.995	0.321	1.209	0.277	0.463	0.500	0.519	0.473	0.667	0.418	0.146	0.704	1.771	0.185
I. Indri	1.446	0.234	8.125	0.006	7.014	0.009	7.614	0.008	3.800	0.056	0.117	0.734	4.173	0.045	3.188	0.077	12.583	0.000
P. diadema	1.602	0.212	0.206	0.652	0.444	0.507	0.562	0.457	0.815	0.371	6.300	0.014	0.705	0.405	1.873	0.174	0.719	0.397
P. verreauxi	5.364	0.024	1.141	0.289	2.104	0.150	3.027	0.086	3.383	0.071	23.702	0.000	2.619	0.110	6.959	0.010	3.510	0.062
E. fulvus	2.262	0.134	0.067	0.795	0.028	0.868	0.113	0.737	0.657	0.419	20.052	0.000	0.307	0.580	2.819	0.094	0.016	0.899
E. macaco	0.402	0.528	0.583	0.448	0.243	0.623	0.180	0.673	0.001	0.977	4.949	0.028	0.011	0.918	0.253	0.616	0.477	0.490
E. mongoz	0.354	0.553	1.968	0.164	1.109	0.294	1.067	0.305	0.067	0.797	8.610	0.004	0.174	0.678	0.138	0.711	2.259	0.134
E. rubriventer	4.196	0.046	1.213	0.276	1.027	0.313	1.961	0.167	2.411	0.127	8.634	0.004	2.293	0.135	2.982	0.087	1.557	0.214
H. griseus	0.334	0.566	8.840	0.004	3.889	0.052	6.554	0.013	2.410	0.127	0.964	0.329	2.943	0.092	0.858	0.357	7.062	0.009
L. catta	1.087	0.302	0.115	0.735	0.001	0.973	0.006	0.941	0.207	0.651	7.764	0.007	0.097	0.757	0.965	0.328	0.010	0.921
V. variegata	0.023	0.881	3.412	0.069	1.863	0.175	2.269	0.137	0.501	0.482	3.762	0.055	0.724	0.398	0.032	0.859	3.527	0.062
L. ruficaudatus	0.158	0.692	1.819	0.184	0.881	0.350	0.963	0.331	0.116	0.735	4.474	0.038	0.241	0.625	0.024	0.878	1.790	0.182
L. tardigradus	1.302	0.259	0.008	0.930	0.058	0.811	0.126	0.724	0.421	0.520	11.730	0.001	0.250	0.619	1.900	0.171	0.077	0.782
N. bengalensis	0.000	0.987	1.412	0.241	0.527	0.470	0.758	0.388	0.252	0.618	0.631	0.429	0.404	0.528	0.036	0.851	0.913	0.341
N. coucang	0.696	0.406	1.102	0.297	0.458	0.500	0.380	0.539	0.001	0.973	9.615	0.002	0.020	0.888	0.449	0.504	0.911	0.341
P. potto	1.567	0.213	0.069	0.792	0.009	0.924	0.056	0.814	0.424	0.516	14.800	0.000	0.194	0.660	2.041	0.155	0.002	0.961

Goswami model FACE- PC2	*G. zanzibaricus*		*O. crassicaudatus*		*O. garnettii*		*A. laniger*		*I. indri*		*P. diadema*		*P. verreauxi*		*E. fulvus*		*E. macaco*	
	F value	p value	F value	p value	F value	p value	F value	p value	F value	p value	F value	p value	F value	p value	F value	p value	F value	p value
C. major																		
C. medius																		
M. murinus																		
M. rufus																		
G. alleni																		
G. demidoff																		
E. elegantulus																		
G. moholi																		
G. senegalensus																		
G. zanzibaricus																		
O. crassicaudatus	0.448	0.504																
O. garnettii	0.635	0.427	0.190	0.663														
A. laniger	0.023	0.880	1.028	0.313	1.303	0.256												
I. Indri	0.864	0.356	11.271	0.001	12.162	0.001	0.630	0.431										
P. diadema	1.028	0.316	2.333	0.129	1.792	0.183	1.365	0.249	5.048	0.028								
P. verreauxi	2.832	0.097	12.222	0.001	9.635	0.002	3.899	0.053	16.723	0.000	0.028	0.867						
E. fulvus	1.157	0.283	2.714	0.101	1.508	0.221	2.045	0.154	15.452	0.000	0.683	0.410	4.030	0.046				
E. macaco	0.218	0.642	0.008	0.928	0.021	0.885	0.464	0.498	4.351	0.040	0.915	0.342	3.570	0.062	0.713	0.399		
E. mongoz	0.163	0.688	0.218	0.641	0.722	0.397	0.449	0.505	6.729	0.011	1.914	0.170	10.621	0.002	3.967	0.048	0.097	0.756
E. rubriventer	2.723	0.105	4.652	0.033	3.818	0.053	3.133	0.083	7.116	0.010	0.095	0.759	0.083	0.774	1.506	0.221	1.833	0.180
H. griseus	0.184	0.670	6.191	0.014	7.389	0.008	0.038	0.847	1.209	0.276	3.661	0.061	15.737	0.000	9.150	0.003	1.975	0.164
L. catta	0.584	0.448	0.722	0.397	0.333	0.565	0.964	0.331	6.150	0.016	0.412	0.524	1.995	0.162	0.041	0.841	0.191	0.663
V. variegata	0.008	0.928	1.513	0.221	2.297	0.132	0.104	0.749	3.405	0.069	2.352	0.130	10.845	0.001	5.034	0.026	0.537	0.466
L. ruficaudatus	0.073	0.788	0.346	0.557	0.750	0.388	0.232	0.633	3.691	0.059	1.403	0.242	6.778	0.011	2.571	0.110	0.141	0.708
L. tardigradus	0.657	0.421	2.394	0.124	1.414	0.237	1.057	0.309	7.822	0.007	0.223	0.639	1.611	0.209	0.042	0.839	0.516	0.475
N. bengalensis	0.001	0.979	0.457	0.500	0.631	0.429	0.015	0.903	0.714	0.402	0.956	0.333	2.587	0.113	1.044	0.308	0.217	0.643
N. coucang	0.342	0.560	0.016	0.900	0.052	0.821	0.746	0.390	7.792	0.006	1.461	0.230	7.291	0.008	1.559	0.213	0.000	0.995
P. potto	0.805	0.371	1.875	0.172	1.000	0.318	1.432	0.233	11.251	0.001	0.548	0.460	3.188	0.076	0.007	0.935	0.479	0.490

Goswami model FACE- PC2	*E. mongoz*		*E. rubriventer*		*H. griseus*		*L. catta*		*V. variegata*		*L. ruficaudatus*		*L. tardigradus*		*N. bengalensis*		*N. coucang*	
	F value	p value	F value	p value	F value	p value	F value	p value	F value	p value	F value	p value	F value	p value	F value	p value	F value	p value
C. major																		
C. medius																		
M. murinus																		
M. rufus																		
G. alleni																		
G. demidoff																		
E. elegantulus																		
G. moholi																		
G. senegalensus																		
G. zanzibaricus																		
O. crassicaudatus																		
O. garnettii																		
A. laniger																		
I. Indri																		
P. diadema																		
P. verreauxi																		
E. fulvus																		
E. macaco																		
E. mongoz																		
E. rubriventer	3.573	0.062																
H. griseus	3.067	0.084	0.334	0.566														
L. catta	0.898	0.346	1.087	0.302	4.104	0.047												
V. variegata	0.519	0.473	4.775	0.033	0.998	0.322	1.711	0.195										
L. ruficaudatus	0.039	0.844	3.224	0.079	1.644	0.206	0.758	0.388	0.149	0.701								
L. tardigradus	2.509	0.117	0.689	0.411	5.185	0.027	0.058	0.810	2.999	0.088	1.383	0.245						
N. bengalensis	0.171	0.680	2.864	0.098	0.150	0.701	0.565	0.456	0.015	0.903	0.085	0.773	0.593	0.445				
N. coucang	0.224	0.637	2.916	0.091	4.071	0.047	0.370	0.545	1.119	0.293	0.290	0.591	1.206	0.275	0.341	0.561		
P. potto	2.691	0.103	1.162	0.283	6.383	0.013	0.016	0.899	3.491	0.064	1.719	0.192	0.055	0.816	0.724	0.396	1.046	0.308

Goswami model FACE- PC3	*C. major*		*C.medius*		*M. murinus*		*M. rufus*		*G. alleni*		*G. denidoff*		*E. elegantulus*		*G. moholi*		*G.senegalensis*	
	F value	p value	F value	p value	F value	p value	F value	p value	F value	p value	F value	p value	F value	p value	F value	p value	F value	p value
C. major																		
C. medius	0.453	0.504																
M. murinus	0.831	0.364	0.140	0.709														
M. rufus	1.073	0.305	0.089	0.767	0.021	0.884												
G. alleni	0.785	0.380	0.030	0.863	0.045	0.832	0.012	0.913										
G. demidoff	0.529	0.469	2.341	0.130	4.661	0.033	4.690	0.033	3.010	0.087								
E. elegantulus	0.000	0.988	0.351	0.556	0.812	0.370	0.848	0.361	0.579	0.450	0.524	0.471						
G. moholi	0.006	0.938	0.764	0.384	1.928	0.167	1.936	0.167	1.195	0.277	0.806	0.371	0.008	0.927				
G. senegalensus	0.050	0.822	1.541	0.216	4.015	0.046	3.924	0.049	2.298	0.131	0.996	0.319	0.058	0.809	0.031	0.861		
G. zanzibaricus	0.846	0.362	0.064	0.801	0.004	0.953	0.001	0.972	0.014	0.906	1.781	0.186	0.535	0.468	0.823	0.367	1.342	0.248
O. crassicaudatus	0.012	0.914	0.683	0.410	2.427	0.121	2.232	0.138	1.177	0.280	2.098	0.149	0.007	0.932	0.077	0.782	0.354	0.552
O. garnettii	0.208	0.649	0.212	0.646	1.286	0.258	1.091	0.298	0.516	0.474	3.751	0.055	0.175	0.676	0.570	0.451	1.488	0.224
A. laniger	0.010	0.922	0.387	0.537	0.686	0.410	0.799	0.376	0.604	0.441	0.237	0.628	0.010	0.922	0.002	0.966	0.003	0.957
I. Indri	0.020	0.889	0.332	0.567	1.069	0.304	0.721	0.399	0.447	0.506	0.150	0.700	0.024	0.877	0.024	0.878	0.009	0.923
P. diadema	2.970	0.091	0.926	0.340	0.247	0.621	0.605	0.440	0.707	0.405	5.186	0.025	2.065	0.156	3.271	0.074	5.196	0.024
P. verreauxi	0.792	0.377	0.037	0.848	0.072	0.788	0.016	0.900	0.000	0.999	4.615	0.034	0.686	0.410	1.684	0.197	3.600	0.059
E. fulvus	0.216	0.643	0.050	0.823	0.740	0.391	0.434	0.511	0.174	0.677	3.473	0.064	0.211	0.647	0.665	0.416	1.690	0.194
E. macaco	0.817	0.369	2.863	0.095	4.666	0.033	5.272	0.024	3.663	0.059	0.033	0.856	0.760	0.386	1.092	0.298	1.329	0.250
E. mongoz	0.442	0.508	0.000	0.986	0.262	0.610	0.116	0.734	0.029	0.866	4.452	0.037	0.420	0.518	1.287	0.259	3.322	0.070
E. rubriventer	0.383	0.539	0.008	0.930	0.028	0.868	0.012	0.913	0.001	0.971	1.174	0.282	0.276	0.601	0.460	0.499	0.802	0.372
H. griseus	0.117	0.734	0.122	0.729	0.608	0.437	0.532	0.469	0.287	0.594	1.699	0.196	0.091	0.764	0.285	0.595	0.750	0.387
L. catta	5.622	0.021	2.432	0.124	1.043	0.309	2.095	0.153	2.002	0.163	12.350	0.001	4.251	0.043	8.009	0.006	13.804	0.000
V. variegata	0.005	0.944	0.549	0.461	1.575	0.212	1.614	0.209	0.943	0.336	1.268	0.263	0.002	0.962	0.039	0.844	0.204	0.652
L. ruficaudatus	0.994	0.324	2.964	0.091	5.605	0.020	5.486	0.023	3.575	0.065	0.225	0.637	0.961	0.331	1.781	0.185	2.719	0.101
L. tardigradus	1.847	0.180	0.237	0.628	0.002	0.967	0.027	0.870	0.073	0.788	8.047	0.006	1.377	0.245	3.461	0.066	7.523	0.007
N. bengalensis	1.279	0.264	2.255	0.140	1.908	0.171	3.293	0.076	3.113	0.085	0.114	0.737	0.777	0.382	0.821	0.367	0.907	0.342
N. coucang	0.280	0.598	0.158	0.692	0.986	0.322	0.901	0.345	0.435	0.511	3.659	0.058	0.222	0.639	0.652	0.421	1.589	0.209
P. potto	2.234	0.137	0.686	0.409	0.145	0.704	0.370	0.544	0.377	0.540	12.250	0.001	2.168	0.143	5.347	0.022	10.951	0.001

Goswami model FACE- PC3	*G. zanzibaricus*		*O. crassicaudatus*		*O. garnettii*		*A. laniger*		*I. indri*		*P. diadema*		*P. verreauxi*		*E. fulvus*		*E. macaco*	
	F value	p value	F value	p value	F value	p value	F value	p value	F value	p value	F value	p value	F value	p value	F value	p value	F value	p value
C. major																		
C. medius																		
M. murinus																		
M. rufus																		
G. alleni																		
G. demidoff																		
E. elegantulus																		
G. moholi																		
G. senegalensus																		
G. zanzibaricus																		
O. crassicaudatus	0.721	0.398																
O. garnettii	0.376	0.541	0.444	0.506														
A. laniger	0.653	0.423	0.042	0.838	0.232	0.631												
I. Indri	0.299	0.587	0.134	0.715	0.421	0.518	0.004	0.951										
P. diadema	0.409	0.525	3.494	0.064	2.557	0.112	2.077	0.156	1.076	0.304								
P. verreauxi	0.012	0.913	1.986	0.161	0.853	0.357	0.635	0.428	0.746	0.391	0.694	0.408						
E. fulvus	0.132	0.717	0.717	0.398	0.071	0.791	0.222	0.638	0.595	0.441	1.194	0.276	0.335	0.563				
E. macaco	2.381	0.127	2.384	0.125	3.997	0.047	0.393	0.533	0.223	0.638	6.319	0.014	4.946	0.029	3.302	0.071		
E. mongoz	0.043	0.835	1.757	0.187	0.545	0.462	0.378	0.540	0.688	0.409	0.801	0.373	0.055	0.816	0.187	0.666	4.302	0.040
E. rubriventer	0.017	0.897	0.375	0.541	0.154	0.696	0.339	0.563	0.194	0.661	0.451	0.505	0.001	0.971	0.047	0.829	1.562	0.215
H. griseus	0.269	0.606	0.174	0.678	0.000	0.983	0.129	0.721	0.162	0.689	1.655	0.204	0.401	0.529	0.035	0.853	2.078	0.153
L. catta	0.978	0.327	10.392	0.002	8.018	0.005	3.692	0.060	2.571	0.113	0.117	0.733	2.418	0.124	4.133	0.043	13.489	0.000
V. variegata	0.693	0.408	0.002	0.961	0.335	0.564	0.026	0.873	0.062	0.803	3.079	0.084	1.358	0.247	0.451	0.503	1.622	0.206
L. ruficaudatus	2.186	0.146	4.079	0.046	6.186	0.014	0.485	0.490	0.347	0.558	5.670	0.021	5.701	0.020	5.332	0.022	0.081	0.777
L. tardigradus	0.004	0.951	4.985	0.027	2.671	0.105	1.232	0.273	1.115	0.295	0.624	0.433	0.106	0.746	1.150	0.285	8.450	0.005
N. bengalensis	3.956	0.053	1.265	0.263	1.976	0.163	0.608	0.440	0.145	0.705	6.914	0.012	2.486	0.120	1.215	0.272	0.063	0.803
N. coucang	0.360	0.550	0.523	0.471	0.011	0.918	0.286	0.594	0.402	0.528	2.558	0.113	0.649	0.422	0.024	0.877	4.083	0.046
P. potto	0.081	0.777	8.715	0.003	5.309	0.022	1.708	0.193	2.926	0.089	0.156	0.693	0.677	0.412	3.397	0.066	11.054	0.001

Goswami model FACE- PC3	*E. mongoz*		*E. rubriventer*		*H. griseus*		*L. catta*		*V. variegata*		*L. ruficaudatus*		*L. tardigradus*		*N. bengalensis*		*N. coucang*	
	F value	p value	F value	p value	F value	p value	F value	p value	F value	p value	F value	p value	F value	p value	F value	p value	F value	p value
C. major																		
C. medius																		
M. murinus																		
M. rufus																		
G. alleni																		
G. demidoff																		
E. elegantulus																		
G. moholi																		
G. senegalensus																		
G. zanzibaricus																		
O. crassicaudatus																		
O. garnettii																		
A. laniger																		
I. Indri																		
P. diadema																		
P. verreauxi																		
E. fulvus																		
E. macaco																		
E. mongoz																		
E. rubriventer	0.005	0.944																
H. griseus	0.202	0.654	0.117	0.734														
L. catta	3.004	0.087	5.622	0.021	4.341	0.042												
V. variegata	0.978	0.325	0.340	0.562	0.139	0.711	8.059	0.006										
L. ruficaudatus	5.640	0.020	1.465	0.232	2.359	0.131	13.144	0.001	2.267	0.137								
L. tardigradus	0.411	0.523	0.043	0.836	1.089	0.302	2.642	0.110	3.247	0.076	9.190	0.004						
N. bengalensis	1.558	0.216	2.040	0.160	1.392	0.244	9.177	0.004	1.153	0.287	0.002	0.963	4.938	0.031				
N. coucang	0.335	0.564	0.132	0.717	0.008	0.927	7.644	0.007	0.415	0.521	5.849	0.018	2.183	0.143	2.372	0.127		
P. potto	1.838	0.177	0.164	0.686	2.246	0.136	1.116	0.292	5.279	0.023	15.320	0.000	0.360	0.549	3.848	0.052	4.042	0.046

Goswami model FACE- PC4	*C. major*		*C.medius*		*M. murinus*		*M. rufus*		*G. alleni*		*G. denidoff*		*E. elegantulus*		*G. moholi*		*G.senegalensis*	
	F value	p value	F value	p value	F value	p value	F value	p value	F value	p value	F value	p value	F value	p value	F value	p value	F value	p value
C. major																		
C. medius	0.084	0.773																
M. murinus	0.001	0.976	0.169	0.682														
M. rufus	0.251	0.618	0.055	0.815	0.549	0.461												
G. alleni	0.227	0.636	0.054	0.817	0.417	0.520	0.000	0.986										
G. demidoff	0.705	0.403	2.160	0.145	1.308	0.255	4.138	0.045	3.125	0.081								
E. elegantulus	0.523	0.473	0.307	0.582	0.860	0.356	0.161	0.690	0.131	0.719	3.781	0.055						
G. moholi	0.365	0.547	0.112	0.738	0.770	0.382	0.016	0.901	0.009	0.926	4.567	0.034	0.086	0.770				
G. senegalensus	1.174	0.280	0.674	0.413	2.594	0.109	0.435	0.510	0.283	0.595	10.369	0.001	0.000	0.986	0.238	0.626		
G. zanzibaricus	3.078	0.086	3.585	0.064	3.747	0.056	3.365	0.073	3.402	0.072	8.714	0.004	1.754	0.191	2.516	0.116	2.342	0.128
O. crassicaudatus	2.006	0.159	1.510	0.221	4.452	0.036	1.278	0.260	0.838	0.362	16.725	0.000	0.069	0.794	0.765	0.383	0.162	0.688
O. garnettii	1.651	0.201	1.241	0.267	3.935	0.049	1.069	0.303	0.690	0.408	13.987	0.000	0.069	0.794	0.706	0.402	0.184	0.668
A. laniger	0.155	0.695	0.051	0.822	0.267	0.606	0.008	0.929	0.006	0.941	1.557	0.216	0.031	0.860	0.000	0.985	0.069	0.793
I. Indri	1.283	0.262	2.834	0.097	2.568	0.112	4.539	0.037	3.516	0.066	0.628	0.430	4.097	0.047	5.677	0.019	12.140	0.001
P. diadema	0.067	0.798	0.340	0.562	0.091	0.763	0.646	0.425	0.577	0.451	0.176	0.676	0.955	0.333	0.840	0.362	2.067	0.152
P. verreauxi	0.332	0.567	0.097	0.756	0.764	0.384	0.007	0.931	0.003	0.954	4.981	0.028	0.115	0.735	0.002	0.963	0.351	0.554
E. fulvus	0.841	0.360	0.447	0.505	2.283	0.132	0.269	0.605	0.158	0.692	9.491	0.002	0.004	0.949	0.135	0.713	0.022	0.881
E. macaco	0.012	0.913	0.230	0.633	0.013	0.910	0.614	0.436	0.489	0.486	0.818	0.368	0.925	0.339	0.835	0.362	2.524	0.114
E. mongoz	0.915	0.342	0.621	0.433	2.539	0.114	0.464	0.498	0.286	0.595	9.949	0.002	0.005	0.943	0.298	0.586	0.013	0.911
E. rubriventer	0.001	0.981	0.058	0.811	0.003	0.960	0.174	0.678	0.183	0.671	0.521	0.473	0.425	0.517	0.216	0.643	0.631	0.428
H. griseus	0.025	0.875	0.296	0.589	0.038	0.846	0.741	0.393	0.582	0.449	0.689	0.409	1.032	0.314	1.029	0.313	3.160	0.077
L. catta	0.699	0.407	0.427	0.516	1.318	0.254	0.231	0.632	0.174	0.678	6.115	0.015	0.001	0.975	0.111	0.740	0.005	0.945
V. variegata	0.044	0.834	0.451	0.504	0.071	0.791	1.161	0.285	0.881	0.352	0.878	0.351	1.441	0.234	1.472	0.228	4.430	0.037
L. ruficaudatus	0.590	0.447	0.394	0.533	1.464	0.229	0.253	0.617	0.174	0.679	5.946	0.017	0.002	0.969	0.168	0.683	0.002	0.962
L. tardigradus	0.688	0.411	0.427	0.517	1.776	0.186	0.237	0.628	0.154	0.697	8.565	0.004	0.007	0.935	0.109	0.741	0.031	0.859
N. bengalensis	4.032	0.051	4.970	0.031	4.846	0.030	4.798	0.033	4.930	0.032	10.080	0.002	2.909	0.094	3.779	0.055	3.883	0.050
N. coucang	0.105	0.747	0.000	0.993	0.296	0.587	0.087	0.768	0.068	0.794	3.571	0.061	0.370	0.545	0.189	0.664	1.294	0.256
P. potto	0.060	0.806	0.021	0.886	0.197	0.658	0.249	0.619	0.176	0.675	3.720	0.055	0.593	0.442	0.423	0.516	2.200	0.139

Goswami model FACE- PC4	*G. zanzibaricus*		*O. crassicaudatus*		*O. garnettii*		*A. laniger*		*I. indri*		*P. diadema*		*P. verreauxi*		*E. fulvus*		*E. macaco*	
	F value	p value	F value	p value	F value	p value	F value	p value	F value	p value	F value	p value	F value	p value	F value	p value	F value	p value
C. major																		
C. medius																		
M. murinus																		
M. rufus																		
G. alleni																		
G. demidoff																		
E. elegantulus																		
G. moholi																		
G. senegalensus																		
G. zanzibaricus																		
O. crassicaudatus	2.585	0.110																
O. garnettii	1.866	0.175	0.004	0.949														
A. laniger	1.397	0.244	0.219	0.641	0.192	0.662												
I. Indri	6.975	0.011	15.979	0.000	13.508	0.000	1.885	0.175										
P. diadema	3.657	0.062	3.117	0.080	2.570	0.112	0.367	0.547	0.642	0.426								
P. verreauxi	2.887	0.094	1.127	0.290	0.985	0.323	0.002	0.965	5.535	0.021	0.784	0.379						
E. fulvus	1.960	0.163	0.367	0.545	0.394	0.531	0.031	0.861	10.742	0.001	1.547	0.215	0.213	0.645				
E. macaco	3.797	0.055	4.117	0.044	3.566	0.061	0.309	0.580	1.823	0.180	0.042	0.838	0.814	0.369	2.095	0.149		
E. mongoz	1.646	0.203	0.092	0.762	0.110	0.741	0.066	0.798	9.266	0.003	1.544	0.218	0.416	0.521	0.082	0.775	2.250	0.137
E. rubriventer	3.545	0.066	1.173	0.281	0.935	0.336	0.132	0.718	0.949	0.334	0.070	0.792	0.207	0.651	0.416	0.520	0.014	0.908
H. griseus	3.998	0.051	5.297	0.023	4.369	0.039	0.324	0.572	1.498	0.226	0.021	0.887	0.989	0.324	2.591	0.109	0.005	0.942
L. catta	2.492	0.120	0.169	0.682	0.161	0.689	0.033	0.856	6.096	0.016	1.259	0.267	0.162	0.688	0.002	0.966	1.358	0.247
V. variegata	5.314	0.025	7.910	0.006	6.537	0.012	0.462	0.499	1.983	0.163	0.020	0.888	1.522	0.221	3.871	0.050	0.014	0.907
L. ruficaudatus	1.395	0.244	0.074	0.786	0.080	0.778	0.040	0.843	5.537	0.022	1.035	0.314	0.215	0.644	0.026	0.872	1.383	0.243
L. tardigradus	2.573	0.115	0.443	0.507	0.404	0.526	0.022	0.882	7.473	0.008	1.255	0.268	0.172	0.680	0.001	0.975	1.662	0.201
N. bengalensis	0.300	0.587	4.522	0.036	3.295	0.072	2.152	0.150	7.614	0.008	4.567	0.038	4.208	0.045	3.136	0.078	4.852	0.031
N. coucang	3.093	0.082	2.866	0.092	2.551	0.112	0.064	0.801	4.783	0.031	0.426	0.516	0.171	0.680	1.107	0.294	0.363	0.548
P. potto	3.652	0.058	4.727	0.031	4.342	0.038	0.133	0.716	5.553	0.020	0.375	0.541	0.425	0.515	2.251	0.135	0.275	0.601

Goswami model FACE- PC4	*E. mongoz*		*E. rubriventer*		*H. griseus*		*L. catta*		*V. variegata*		*L. ruficaudatus*		*L. tardigradus*		*N. bengalensis*		*N. coucang*	
	F value	p value	F value	p value	F value	p value	F value	p value	F value	p value	F value	p value	F value	p value	F value	p value	F value	p value
C. major																		
C. medius																		
M. murinus																		
M. rufus																		
G. alleni																		
G. demidoff																		
E. elegantulus																		
G. moholi																		
G. senegalensus																		
G. zanzibaricus																		
O. crassicaudatus																		
O. garnettii																		
A. laniger																		
I. Indri																		
P. diadema																		
P. verreauxi																		
E. fulvus																		
E. macaco																		
E. mongoz																		
E. rubriventer	0.517	0.474																
H. griseus	2.597	0.111	0.025	0.875														
L. catta	0.020	0.888	0.699	0.407	1.583	0.213												
V. variegata	4.130	0.045	0.042	0.838	0.001	0.974	2.342	0.131										
L. ruficaudatus	0.001	0.972	0.398	0.531	1.428	0.238	0.007	0.932	2.250	0.139								
L. tardigradus	0.076	0.784	0.465	0.498	1.902	0.174	0.004	0.947	3.169	0.080	0.025	0.874						
N. bengalensis	2.696	0.105	4.880	0.032	4.921	0.032	3.990	0.051	6.535	0.013	2.243	0.142	3.935	0.053				
N. coucang	1.458	0.230	0.051	0.822	0.489	0.486	0.583	0.447	0.775	0.381	0.728	0.396	0.824	0.366	4.248	0.042		
P. potto	2.873	0.092	0.024	0.878	0.416	0.520	0.986	0.322	0.674	0.413	1.335	0.250	1.660	0.200	4.936	0.028	0.043	0.837

Goswami model FACE- PC5	*C. major*		*C.medius*		*M. murinus*		*M. rufus*		*G. alleni*		*G. denidoff*		*E. elegantulus*		*G. moholi*		*G.senegalensis*	
	F value	p value	F value	p value	F value	p value	F value	p value	F value	p value	F value	p value	F value	p value	F value	p value	F value	p value
C. major																		
C. medius	0.520	0.474																
M. murinus	0.001	0.972	0.666	0.417														
M. rufus	1.748	0.192	6.480	0.014	3.017	0.086												
G. alleni	0.310	0.580	2.234	0.141	0.498	0.482	0.698	0.408										
G. demidoff	1.001	0.320	3.716	0.057	2.337	0.129	0.003	0.956	0.354	0.554								
E. elegantulus	3.541	0.065	8.794	0.004	4.664	0.033	0.871	0.355	2.356	0.131	0.574	0.451						
G. moholi	0.000	0.990	0.697	0.406	0.001	0.976	2.794	0.098	0.454	0.502	2.109	0.149	4.524	0.036				
G. senegalensus	1.109	0.294	0.056	0.813	2.118	0.147	12.449	0.001	4.094	0.044	10.783	0.001	12.582	0.000	2.045	0.154		
G. zanzibaricus	0.000	0.989	0.302	0.585	0.000	0.990	1.031	0.315	0.203	0.655	0.600	0.441	2.319	0.134	0.000	0.996	0.601	0.439
O. crassicaudatus	0.762	0.385	0.000	0.984	1.512	0.221	12.432	0.001	3.553	0.062	9.850	0.002	12.391	0.001	1.464	0.228	0.165	0.685
O. garnettii	0.021	0.886	1.694	0.196	0.075	0.784	4.451	0.037	0.500	0.481	3.187	0.076	6.573	0.012	0.049	0.825	5.021	0.026
A. laniger	0.060	0.808	0.062	0.804	0.073	0.788	1.527	0.223	0.447	0.507	1.088	0.300	2.792	0.101	0.083	0.774	0.234	0.629
I. Indri	0.043	0.837	1.155	0.286	0.095	0.758	1.710	0.196	0.162	0.688	1.082	0.301	3.539	0.064	0.076	0.783	2.701	0.102
P. diadema	0.085	0.771	1.187	0.281	0.124	0.726	1.014	0.319	0.065	0.800	0.503	0.480	2.724	0.104	0.109	0.742	1.885	0.171
P. verreauxi	1.580	0.213	0.302	0.585	2.734	0.101	13.721	0.000	5.018	0.029	9.257	0.003	14.148	0.000	2.690	0.104	0.195	0.659
E. fulvus	0.811	0.369	4.519	0.035	2.138	0.145	0.664	0.416	0.071	0.791	0.509	0.476	2.363	0.126	1.801	0.181	13.595	0.000
E. macaco	0.694	0.407	3.285	0.074	1.290	0.258	0.233	0.631	0.100	0.753	0.133	0.716	1.446	0.232	1.175	0.280	7.083	0.008
E. mongoz	0.863	0.356	4.636	0.034	2.174	0.143	0.479	0.491	0.114	0.736	0.299	0.586	2.098	0.151	1.871	0.174	13.927	0.000
E. rubriventer	0.109	0.743	0.985	0.326	0.128	0.721	0.504	0.481	0.014	0.905	0.234	0.630	1.693	0.198	0.118	0.732	1.326	0.251
H. griseus	0.919	0.343	4.094	0.048	1.696	0.196	0.129	0.721	0.209	0.650	0.057	0.812	1.313	0.257	1.560	0.215	8.732	0.004
L. catta	0.010	0.919	0.765	0.385	0.033	0.855	1.720	0.195	0.213	0.647	1.243	0.268	3.243	0.076	0.023	0.879	2.266	0.134
V. variegata	1.941	0.169	7.398	0.008	3.512	0.064	0.003	0.958	0.750	0.390	0.000	0.984	1.080	0.302	3.202	0.076	14.727	0.000
L. ruficaudatus	0.621	0.435	3.501	0.067	1.235	0.269	0.454	0.503	0.055	0.816	0.241	0.625	2.018	0.161	1.113	0.294	8.091	0.005
L. tardigradus	0.094	0.761	1.624	0.208	0.277	0.600	1.883	0.176	0.101	0.752	1.333	0.252	3.516	0.066	0.224	0.637	5.710	0.018
N. bengalensis	1.255	0.269	3.132	0.083	1.510	0.222	0.167	0.685	0.688	0.412	0.120	0.730	0.025	0.874	1.500	0.224	4.456	0.036
N. coucang	0.937	0.336	4.810	0.031	2.052	0.154	0.440	0.509	0.128	0.721	0.260	0.611	2.134	0.147	1.798	0.182	11.974	0.001
P. potto	0.014	0.907	1.325	0.252	0.060	0.807	3.689	0.057	0.416	0.520	3.124	0.079	5.268	0.023	0.038	0.847	4.721	0.031

Goswami model FACE- PC5	*G. zanzibaricus*		*O. crassicaudatus*		*O. garnettii*		*A. laniger*		*I. indri*		*P. diadema*		*P. verreauxi*		*E. fulvus*		*E. macaco*	
	F value	p value	F value	p value	F value	p value	F value	p value	F value	p value	F value	p value	F value	p value	F value	p value	F value	p value
C. major																		
C. medius																		
M. murinus																		
M. rufus																		
G. alleni																		
G. demidoff																		
E. elegantulus																		
G. moholi																		
G. senegalensus																		
G. zanzibaricus																		
O. crassicaudatus	0.392	0.533																
O. garnettii	0.016	0.901	4.531	0.035														
A. laniger	0.038	0.847	0.096	0.757	0.230	0.632												
I. Indri	0.031	0.861	2.124	0.147	0.027	0.870	0.190	0.665										
P. diadema	0.064	0.802	1.510	0.222	0.069	0.793	0.222	0.640	0.012	0.913								
P. verreauxi	0.862	0.357	0.730	0.394	6.699	0.011	0.380	0.540	3.391	0.069	2.643	0.109						
E. fulvus	0.463	0.497	14.430	0.000	2.804	0.095	1.142	0.287	0.716	0.399	0.242	0.624	14.152	0.000				
E. macaco	0.436	0.511	6.427	0.012	1.517	0.220	0.868	0.355	0.566	0.454	0.266	0.607	7.665	0.007	0.022	0.883		
E. mongoz	0.485	0.488	14.714	0.000	3.262	0.073	1.025	0.315	0.799	0.374	0.305	0.582	13.890	0.000	0.023	0.881	0.003	0.959
E. rubriventer	0.086	0.770	1.071	0.303	0.092	0.762	0.220	0.641	0.030	0.862	0.008	0.930	1.884	0.175	0.079	0.779	0.108	0.743
H. griseus	0.556	0.460	8.217	0.005	2.286	0.133	0.940	0.337	0.816	0.370	0.430	0.515	9.289	0.003	0.114	0.736	0.018	0.894
L. catta	0.008	0.927	1.661	0.200	0.000	0.995	0.110	0.741	0.011	0.917	0.034	0.855	2.588	0.112	1.019	0.314	0.678	0.412
V. variegata	1.119	0.294	15.296	0.000	5.308	0.023	1.742	0.192	1.928	0.169	1.070	0.305	16.582	0.000	0.736	0.392	0.233	0.631
L. ruficaudatus	0.369	0.546	7.604	0.007	1.600	0.208	0.711	0.404	0.487	0.488	0.220	0.641	8.724	0.004	0.000	0.997	0.014	0.908
L. tardigradus	0.057	0.812	5.061	0.026	0.195	0.659	0.246	0.622	0.015	0.903	0.000	0.987	5.795	0.019	1.052	0.306	0.556	0.458
N. bengalensis	0.955	0.334	4.011	0.047	1.958	0.164	1.118	0.296	1.126	0.293	0.966	0.331	4.697	0.034	0.616	0.433	0.394	0.532
N. coucang	0.542	0.463	12.183	0.001	2.766	0.098	1.134	0.290	0.821	0.367	0.337	0.563	13.080	0.000	0.025	0.875	0.001	0.973
P. potto	0.011	0.918	4.142	0.043	0.001	0.979	0.189	0.664	0.028	0.868	0.059	0.808	5.649	0.019	2.908	0.089	1.360	0.245

Goswami model FACE- PC5	*E. mongoz*		*E. rubriventer*		*H. griseus*		*L. catta*		*V. variegata*		*L. ruficaudatus*		*L. tardigradus*		*N. bengalensis*		*N. coucang*	
	F value	p value	F value	p value	F value	p value	F value	p value	F value	p value	F value	p value	F value	p value	F value	p value	F value	p value
C. major																		
C. medius																		
M. murinus																		
M. rufus																		
G. alleni																		
G. demidoff																		
E. elegantulus																		
G. moholi																		
G. senegalensus																		
G. zanzibaricus																		
O. crassicaudatus																		
O. garnettii																		
A. laniger																		
I. Indri																		
P. diadema																		
P. verreauxi																		
E. fulvus																		
E. macaco																		
E. mongoz																		
E. rubriventer	0.109	0.743																
H. griseus	0.052	0.821	0.919	0.343														
L. catta	1.009	0.318	0.010	0.919	0.876	0.353												
V. variegata	0.534	0.467	0.512	0.477	0.122	0.728	2.012	0.161										
L. ruficaudatus	0.010	0.922	0.079	0.780	0.071	0.791	0.567	0.455	0.496	0.484								
L. tardigradus	1.103	0.297	0.009	0.924	0.808	0.373	0.055	0.816	2.352	0.130	0.458	0.502						
N. bengalensis	0.495	0.484	0.672	0.417	0.308	0.582	1.006	0.321	0.212	0.647	0.494	0.486	0.902	0.347				
N. coucang	0.001	0.981	0.125	0.725	0.043	0.836	1.029	0.313	0.467	0.496	0.013	0.908	1.026	0.314	0.534	0.467		
P. potto	3.113	0.079	0.075	0.784	1.945	0.165	0.000	0.983	4.467	0.036	1.376	0.243	0.195	0.659	1.580	0.211	2.545	0.112

Goswami model ORBIT- PC1	*C. major*		*C.medius*		*M. murinus*		*M. rufus*		*G. alleni*		*G. denidoff*		*E. elegantulus*		*G. moholi*		*G.senegalensis*	
	F value	p value	F value	p value	F value	p value	F value	p value	F value	p value	F value	p value	F value	p value	F value	p value	F value	p value
C. major																		
C. medius	0.567	0.455																
M. murinus	0.122	0.728	0.223	0.637														
M. rufus	0.011	0.918	0.828	0.367	0.263	0.609												
G. alleni	0.125	0.725	0.770	0.384	0.469	0.495	0.102	0.751										
G. demidoff	1.407	0.239	0.089	0.766	0.865	0.354	2.198	0.142	1.744	0.190								
E. elegantulus	1.256	0.267	2.374	0.129	2.151	0.146	1.291	0.261	0.424	0.518	3.902	0.051						
G. moholi	0.310	0.579	0.097	0.757	0.048	0.827	0.608	0.437	0.741	0.392	0.599	0.440	2.606	0.109				
G. senegalensus	2.165	0.143	0.141	0.708	1.418	0.235	3.872	0.050	2.960	0.087	0.000	0.990	5.887	0.016	1.086	0.298		
G. zanzibaricus	3.508	0.067	1.606	0.211	4.075	0.046	4.649	0.036	3.080	0.086	1.792	0.185	4.871	0.031	3.788	0.055	3.172	0.076
O. crassicaudatus	0.494	0.483	0.037	0.848	0.161	0.688	1.044	0.309	1.009	0.317	0.461	0.498	2.917	0.090	0.035	0.853	1.060	0.304
O. garnettii	0.876	0.351	2.663	0.105	2.290	0.132	1.079	0.301	0.112	0.738	6.354	0.013	0.385	0.536	3.740	0.055	12.983	0.000
A. laniger	5.124	0.029	2.982	0.091	5.532	0.021	5.939	0.019	4.049	0.050	3.212	0.077	6.103	0.017	5.083	0.027	4.859	0.029
I. Indri	4.480	0.038	2.149	0.148	4.655	0.033	5.670	0.020	3.973	0.051	2.224	0.139	5.993	0.017	4.311	0.040	3.527	0.062
P. diadema	0.373	0.544	0.001	0.978	0.165	0.685	0.579	0.450	0.586	0.448	0.095	0.758	1.884	0.175	0.066	0.798	0.168	0.682
P. verreauxi	1.020	0.316	0.073	0.787	0.687	0.409	1.549	0.217	1.277	0.263	0.000	0.982	2.993	0.088	0.473	0.493	0.000	0.985
E. fulvus	0.016	0.899	0.559	0.456	0.090	0.764	0.086	0.770	0.333	0.564	2.003	0.158	2.049	0.154	0.378	0.539	4.113	0.043
E. macaco	3.775	0.056	6.307	0.014	5.364	0.022	4.123	0.046	1.191	0.279	9.848	0.002	0.005	0.943	6.727	0.011	13.874	0.000
E. mongoz	0.047	0.828	1.070	0.304	0.401	0.527	0.017	0.896	0.068	0.796	2.603	0.109	1.302	0.257	0.823	0.366	4.233	0.041
E. rubriventer	0.161	0.690	0.030	0.864	0.027	0.871	0.229	0.634	0.305	0.583	0.162	0.688	1.333	0.253	0.001	0.971	0.219	0.640
H. griseus	0.111	0.741	0.021	0.885	0.028	0.868	0.182	0.671	0.258	0.614	0.159	0.692	1.083	0.302	0.002	0.968	0.285	0.594
L. catta	0.100	0.753	1.079	0.303	0.466	0.496	0.061	0.805	0.019	0.891	2.346	0.129	0.905	0.345	0.829	0.365	3.630	0.058
V. variegata	0.141	0.709	0.933	0.338	0.562	0.455	0.118	0.732	0.000	0.983	2.213	0.140	0.550	0.461	0.939	0.335	3.927	0.049
L. ruficaudatus	0.215	0.645	0.057	0.813	0.033	0.856	0.350	0.557	0.424	0.518	0.319	0.574	1.745	0.192	0.000	0.988	0.501	0.480
L. tardigradus	0.020	0.888	0.592	0.445	0.323	0.571	0.007	0.936	0.047	0.830	2.143	0.147	0.793	0.377	0.761	0.385	5.868	0.016
N. bengalensis	1.161	0.287	2.128	0.151	1.709	0.194	1.099	0.300	0.333	0.567	3.115	0.082	0.000	0.992	1.998	0.161	4.258	0.040
N. coucang	0.507	0.478	0.114	0.737	0.083	0.773	0.976	0.326	1.032	0.312	0.730	0.394	3.423	0.067	0.002	0.968	1.261	0.263
P. potto	0.239	0.626	1.309	0.254	0.957	0.329	0.263	0.609	0.001	0.982	3.646	0.058	0.616	0.434	1.807	0.180	8.400	0.004

Goswami model ORBIT- PC1	*G. zanzibaricus*		*O. crassicaudatus*		*O. garnettii*		*A. laniger*		*I. indri*		*P. diadema*		*P. verreauxi*		*E. fulvus*		*E. macaco*	
	F value	p value	F value	p value	F value	p value	F value	p value	F value	p value	F value	p value	F value	p value	F value	p value	F value	p value
C. major																		
C. medius																		
M. murinus																		
M. rufus																		
G. alleni																		
G. demidoff																		
E. elegantulus																		
G. moholi																		
G. senegalensus																		
G. zanzibaricus																		
O. crassicaudatus	3.823	0.053																
O. garnettii	9.646	0.002	6.649	0.011														
A. laniger	0.254	0.617	4.690	0.032	9.088	0.003												
I. Indri	0.011	0.916	4.177	0.043	10.015	0.002	0.215	0.645										
P. diadema	1.405	0.242	0.022	0.881	2.385	0.125	2.424	0.126	1.887	0.174								
P. verreauxi	1.255	0.267	0.363	0.548	4.764	0.031	2.347	0.131	1.638	0.204	0.077	0.782						
E. fulvus	6.825	0.010	1.056	0.305	2.933	0.088	7.237	0.008	7.004	0.009	0.492	0.484	1.580	0.210				
E. macaco	11.733	0.001	7.640	0.006	1.127	0.290	13.065	0.001	13.087	0.000	4.911	0.030	7.538	0.007	5.049	0.026		
E. mongoz	6.082	0.016	1.326	0.251	0.821	0.366	7.494	0.008	6.885	0.010	0.819	0.368	1.963	0.164	0.183	0.669	3.609	0.060
E. rubriventer	1.250	0.269	0.002	0.962	0.913	0.341	2.581	0.115	1.720	0.195	0.016	0.901	0.130	0.719	0.103	0.748	3.150	0.080
H. griseus	1.150	0.289	0.003	0.958	1.148	0.286	1.911	0.174	1.561	0.216	0.013	0.909	0.125	0.725	0.146	0.703	2.600	0.111
L. catta	4.736	0.034	1.166	0.282	0.397	0.530	6.303	0.015	5.748	0.019	0.770	0.384	1.726	0.193	0.247	0.620	2.636	0.108
V. variegata	4.167	0.046	1.390	0.240	0.186	0.667	5.002	0.029	4.982	0.029	0.750	0.390	1.649	0.203	0.424	0.515	1.514	0.222
L. ruficaudatus	1.932	0.171	0.011	0.917	1.729	0.191	3.273	0.077	2.577	0.114	0.033	0.857	0.244	0.623	0.182	0.670	4.772	0.032
L. tardigradus	3.678	0.061	1.821	0.180	1.120	0.292	3.807	0.057	4.441	0.039	0.485	0.489	1.433	0.236	0.240	0.625	2.629	0.109
N. bengalensis	3.706	0.061	2.044	0.155	0.267	0.607	5.370	0.026	4.870	0.031	1.508	0.226	2.335	0.132	1.417	0.235	0.007	0.934
N. coucang	4.680	0.033	0.028	0.868	4.969	0.027	6.465	0.013	5.301	0.023	0.072	0.790	0.567	0.453	0.536	0.465	9.421	0.003
P. potto	6.858	0.010	3.896	0.050	0.291	0.590	6.371	0.013	7.011	0.009	1.224	0.270	2.775	0.098	1.205	0.273	1.635	0.203

Goswami model ORBIT- PC1	*E. mongoz*		*E. rubriventer*		*H. griseus*		*L. catta*		*V. variegata*		*L. ruficaudatus*		*L. tardigradus*		*N. bengalensis*		*N. coucang*	
	F value	p value	F value	p value	F value	p value	F value	p value	F value	p value	F value	p value	F value	p value	F value	p value	F value	p value
C. major																		
C. medius																		
M. murinus																		
M. rufus																		
G. alleni																		
G. demidoff																		
E. elegantulus																		
G. moholi																		
G. senegalensus																		
G. zanzibaricus																		
O. crassicaudatus																		
O. garnettii																		
A. laniger																		
I. Indri																		
P. diadema																		
P. verreauxi																		
E. fulvus																		
E. macaco																		
E. mongoz																		
E. rubriventer	0.320	0.573																
H. griseus	0.297	0.587	0.111	0.741														
L. catta	0.018	0.894	0.100	0.753	0.291	0.592												
V. variegata	0.070	0.792	0.334	0.565	0.327	0.570	0.017	0.898										
L. ruficaudatus	0.506	0.479	0.001	0.982	0.000	0.983	0.548	0.462	0.513	0.477								
L. tardigradus	0.001	0.975	0.147	0.703	0.169	0.682	0.017	0.896	0.062	0.804	0.263	0.610						
N. bengalensis	1.075	0.303	1.349	0.251	0.826	0.368	0.797	0.376	0.416	0.521	1.550	0.220	0.520	0.475				
N. coucang	1.223	0.271	0.000	0.983	0.001	0.981	1.262	0.264	1.284	0.260	0.000	0.990	1.108	0.295	2.836	0.096		
P. potto	0.155	0.694	0.389	0.534	0.561	0.455	0.044	0.834	0.003	0.953	0.757	0.386	0.281	0.597	0.406	0.525	2.329	0.129

Goswami model ORBIT- PC2	*C. major*		*C.medius*		*M. murinus*		*M. rufus*		*G. alleni*		*G. denidoff*		*E. elegantulus*		*G. moholi*		*G.senegalensis*	
	F value	p value	F value	p value	F value	p value	F value	p value	F value	p value	F value	p value	F value	p value	F value	p value	F value	p value
C. major																		
C. medius	3.852	0.055																
M. murinus	0.852	0.358	2.627	0.108														
M. rufus	0.590	0.446	2.687	0.107	0.034	0.855												
G. alleni	0.069	0.794	2.707	0.106	0.312	0.578	0.173	0.680										
G. demidoff	0.052	0.820	3.463	0.066	0.431	0.513	0.243	0.623	0.001	0.972								
E. elegantulus	0.006	0.941	1.690	0.199	0.260	0.611	0.141	0.708	0.009	0.925	0.006	0.939						
G. moholi	2.559	0.113	0.858	0.357	0.772	0.381	1.143	0.288	1.401	0.240	2.113	0.148	0.928	0.338				
G. senegalensus	0.053	0.819	9.475	0.002	1.341	0.248	1.026	0.312	0.033	0.856	0.022	0.883	0.001	0.978	6.204	0.013		
G. zanzibaricus	0.150	0.701	1.643	0.206	0.077	0.781	0.020	0.888	0.027	0.869	0.045	0.832	0.042	0.838	0.749	0.389	0.206	0.650
O. crassicaudatus	2.229	0.138	1.928	0.167	0.346	0.557	0.705	0.403	1.035	0.311	1.798	0.182	0.708	0.401	0.239	0.626	6.255	0.013
O. garnettii	0.705	0.403	11.619	0.001	4.916	0.028	4.557	0.035	1.165	0.283	1.512	0.221	0.386	0.535	11.545	0.001	3.219	0.074
A. laniger	1.482	0.230	0.052	0.821	0.745	0.390	0.782	0.381	1.055	0.310	1.126	0.292	0.726	0.398	0.128	0.722	2.861	0.092
I. Indri	15.919	0.000	4.098	0.047	17.413	0.000	15.623	0.000	13.025	0.001	16.616	0.000	8.466	0.005	12.142	0.001	39.953	0.000
P. diadema	0.033	0.856	3.207	0.079	0.467	0.496	0.287	0.594	0.007	0.933	0.002	0.962	0.002	0.967	1.802	0.183	0.003	0.955
P. verreauxi	1.395	0.242	1.096	0.299	0.216	0.643	0.378	0.540	0.718	0.400	0.945	0.333	0.491	0.486	0.096	0.757	2.821	0.094
E. fulvus	2.028	0.156	1.848	0.176	0.312	0.577	0.635	0.426	0.943	0.333	1.709	0.192	0.706	0.402	0.214	0.644	5.156	0.024
E. macaco	1.109	0.296	1.168	0.283	0.121	0.729	0.240	0.626	0.558	0.458	0.702	0.404	0.416	0.521	0.135	0.714	1.917	0.168
E. mongoz	3.106	0.082	0.369	0.545	1.350	0.248	1.724	0.193	1.863	0.176	2.686	0.104	1.192	0.278	0.122	0.727	7.677	0.006
E. rubriventer	9.658	0.003	1.081	0.303	7.480	0.007	7.876	0.007	8.142	0.006	7.081	0.009	4.386	0.041	3.936	0.050	16.327	0.000
H. griseus	1.150	0.289	0.569	0.454	0.254	0.615	0.364	0.549	0.664	0.419	0.760	0.386	0.451	0.505	0.014	0.906	2.144	0.145
L. catta	0.331	0.567	2.483	0.120	0.076	0.783	0.014	0.906	0.076	0.783	0.108	0.744	0.084	0.773	1.039	0.310	0.441	0.508
V. variegata	4.399	0.040	0.003	0.958	3.220	0.076	3.300	0.074	3.013	0.088	4.352	0.040	1.930	0.169	1.187	0.278	12.191	0.001
L. ruficaudatus	0.725	0.399	1.727	0.195	0.001	0.980	0.033	0.856	0.296	0.589	0.297	0.587	0.198	0.658	0.456	0.501	0.973	0.325
L. tardigradus	0.487	0.489	6.228	0.016	3.985	0.049	2.906	0.094	0.712	0.403	1.258	0.265	0.262	0.611	9.115	0.003	4.027	0.046
N. bengalensis	4.096	0.049	8.763	0.005	7.539	0.007	6.963	0.011	4.838	0.033	3.677	0.059	2.056	0.158	8.359	0.005	7.710	0.006
N. coucang	0.147	0.703	4.638	0.034	0.463	0.497	0.258	0.613	0.002	0.962	0.011	0.916	0.023	0.880	2.801	0.096	0.127	0.722
P. potto	0.790	0.375	1.354	0.246	0.053	0.819	0.149	0.700	0.326	0.569	0.678	0.411	0.279	0.598	0.349	0.556	2.369	0.125

Goswami model ORBIT- PC2	*G. zanzibaricus*		*O. crassicaudatus*		*O. garnettii*		*A. laniger*		*I. indri*		*P. diadema*		*P. verreauxi*		*E. fulvus*		*E. macaco*	
	F value	p value	F value	p value	F value	p value	F value	p value	F value	p value	F value	p value	F value	p value	F value	p value	F value	p value
C. major																		
C. medius																		
M. murinus																		
M. rufus																		
G. alleni																		
G. demidoff																		
E. elegantulus																		
G. moholi																		
G. senegalensus																		
G. zanzibaricus																		
O. crassicaudatus	0.482	0.489																
O. garnettii	1.453	0.231	14.523	0.000														
A. laniger	0.577	0.451	0.363	0.548	3.949	0.049												
I. Indri	9.705	0.003	17.869	0.000	35.837	0.000	3.187	0.079										
P. diadema	0.058	0.810	1.418	0.236	1.054	0.307	1.232	0.273	14.603	0.000								
P. verreauxi	0.307	0.581	0.001	0.979	6.130	0.015	0.251	0.618	10.965	0.001	0.945	0.335						
E. fulvus	0.470	0.494	0.000	0.993	12.601	0.000	0.346	0.557	17.809	0.000	1.290	0.257	0.000	0.983				
E. macaco	0.231	0.632	0.005	0.945	4.573	0.034	0.301	0.585	10.939	0.001	0.736	0.393	0.005	0.941	0.005	0.943		
E. mongoz	1.070	0.304	0.740	0.391	12.174	0.001	0.026	0.872	9.132	0.003	2.323	0.131	0.342	0.560	0.683	0.410	0.389	0.534
E. rubriventer	4.779	0.034	5.724	0.018	16.468	0.000	1.256	0.268	0.731	0.396	8.760	0.005	4.482	0.038	5.211	0.024	4.587	0.035
H. griseus	0.292	0.591	0.025	0.875	4.105	0.045	0.131	0.719	7.077	0.010	0.837	0.365	0.012	0.911	0.022	0.882	0.029	0.865
L. catta	0.002	0.961	0.650	0.421	2.607	0.109	0.820	0.369	14.046	0.000	0.142	0.707	0.413	0.522	0.596	0.441	0.286	0.594
V. variegata	1.958	0.167	2.741	0.100	14.788	0.000	0.072	0.789	4.352	0.040	3.615	0.062	1.379	0.244	2.675	0.103	1.421	0.236
L. ruficaudatus	0.061	0.805	0.178	0.674	3.244	0.074	0.572	0.453	11.600	0.001	0.418	0.521	0.136	0.713	0.161	0.689	0.078	0.780
L. tardigradus	0.841	0.364	14.025	0.000	0.045	0.832	1.943	0.170	19.799	0.000	0.695	0.408	4.022	0.049	13.558	0.000	3.198	0.078
N. bengalensis	3.432	0.071	8.516	0.004	2.981	0.087	5.706	0.022	18.455	0.000	4.624	0.037	7.097	0.010	7.724	0.006	6.694	0.012
N. coucang	0.031	0.861	2.487	0.117	2.905	0.090	1.401	0.240	21.953	0.000	0.024	0.878	1.173	0.281	2.224	0.137	0.815	0.369
P. potto	0.141	0.708	0.094	0.759	6.465	0.012	0.280	0.598	11.269	0.001	0.472	0.493	0.037	0.848	0.097	0.755	0.011	0.917

Goswami model ORBIT- PC2	*E. mongoz*		*E. rubriventer*		*H. griseus*		*L. catta*		*V. variegata*		*L. ruficaudatus*		*L. tardigradus*		*N. bengalensis*		*N. coucang*	
	F value	p value	F value	p value	F value	p value	F value	p value	F value	p value	F value	p value	F value	p value	F value	p value	F value	p value
C. major																		
C. medius																		
M. murinus																		
M. rufus																		
G. alleni																		
G. demidoff																		
E. elegantulus																		
G. moholi																		
G. senegalensus																		
G. zanzibaricus																		
O. crassicaudatus																		
O. garnettii																		
A. laniger																		
I. Indri																		
P. diadema																		
P. verreauxi																		
E. fulvus																		
E. macaco																		
E. mongoz																		
E. rubriventer	2.833	0.096																
H. griseus	0.118	0.732	1.150	0.289														
L. catta	1.536	0.219	0.331	0.567	0.405	0.527												
V. variegata	0.529	0.469	0.967	0.329	0.685	0.411	2.916	0.092										
L. ruficaudatus	0.824	0.367	7.119	0.010	0.182	0.672	0.071	0.792	1.923	0.171								
L. tardigradus	8.609	0.004	8.291	0.006	2.237	0.141	1.697	0.198	8.788	0.004	1.851	0.180						
N. bengalensis	8.565	0.005	18.469	0.000	6.213	0.016	5.774	0.020	8.584	0.005	8.059	0.007	1.209	0.277				
N. coucang	3.599	0.060	9.429	0.003	0.931	0.337	0.090	0.764	5.902	0.017	0.331	0.567	2.612	0.109	5.427	0.022		
P. potto	0.709	0.401	3.177	0.077	0.057	0.812	0.166	0.684	2.013	0.158	0.022	0.883	6.513	0.012	3.761	0.054	0.844	0.359

Goswami model ORBIT- PC3	*C. major*		*C.medius*		*M. murinus*		*M. rufus*		*G. alleni*		*G. denidoff*		*E. elegantulus*		*G. moholi*		*G.senegalensis*	
	F value	p value	F value	p value	F value	p value	F value	p value	F value	p value	F value	p value	F value	p value	F value	p value	F value	p value
C. major																		
C. medius	0.218	0.642																
M. murinus	0.598	0.441	0.068	0.794														
M. rufus	8.042	0.007	5.190	0.027	4.949	0.028												
G. alleni	2.631	0.112	1.481	0.229	1.037	0.311	0.569	0.454										
G. demidoff	3.076	0.083	1.512	0.222	1.303	0.256	0.909	0.343	0.003	0.956								
E. elegantulus	0.126	0.724	0.004	0.947	0.011	0.917	1.675	0.201	0.487	0.488	0.582	0.447						
G. moholi	2.709	0.103	0.934	0.336	0.485	0.487	4.445	0.038	0.477	0.491	0.502	0.480	0.271	0.604				
G. senegalensus	0.044	0.834	0.171	0.680	0.811	0.369	16.621	0.000	4.017	0.046	5.956	0.015	0.145	0.704	4.103	0.044		
G. zanzibaricus	0.041	0.840	0.439	0.511	0.857	0.357	8.318	0.006	3.140	0.083	3.321	0.072	0.224	0.638	3.178	0.078	0.206	0.651
O. crassicaudatus	1.486	0.225	3.426	0.067	6.712	0.010	44.698	0.000	13.030	0.000	18.436	0.000	1.566	0.213	20.066	0.000	5.298	0.022
O. garnettii	0.796	0.374	2.338	0.129	4.584	0.034	34.755	0.000	10.525	0.002	13.935	0.000	1.111	0.294	14.267	0.000	2.742	0.099
A. laniger	3.932	0.054	5.049	0.029	8.175	0.005	11.270	0.002	6.980	0.011	10.278	0.002	3.371	0.072	12.635	0.001	11.153	0.001
I. Indri	2.510	0.118	1.502	0.225	1.261	0.264	0.152	0.698	0.040	0.841	0.075	0.785	0.646	0.424	0.723	0.397	4.111	0.044
P. diadema	1.308	0.258	0.589	0.446	0.423	0.517	0.980	0.327	0.067	0.797	0.066	0.798	0.216	0.644	0.059	0.809	2.472	0.118
P. verreauxi	2.746	0.102	1.585	0.212	1.729	0.191	0.119	0.731	0.063	0.803	0.137	0.712	0.714	0.401	1.039	0.310	6.604	0.011
E. fulvus	3.178	0.076	1.351	0.246	1.367	0.243	1.523	0.219	0.023	0.880	0.016	0.899	0.572	0.450	0.406	0.525	8.241	0.004
E. macaco	1.615	0.208	0.616	0.435	0.320	0.573	2.034	0.158	0.236	0.628	0.224	0.637	0.207	0.651	0.003	0.953	2.179	0.141
E. mongoz	2.088	0.152	0.934	0.337	0.802	0.372	1.148	0.287	0.039	0.845	0.034	0.855	0.367	0.546	0.191	0.663	4.498	0.035
E. rubriventer	5.853	0.019	4.688	0.035	3.671	0.058	0.438	0.511	1.225	0.274	1.316	0.255	1.893	0.174	3.723	0.057	7.741	0.006
H. griseus	0.764	0.387	0.202	0.655	0.041	0.839	2.580	0.114	0.539	0.466	0.487	0.487	0.046	0.830	0.103	0.749	0.834	0.362
L. catta	3.207	0.079	1.888	0.175	1.847	0.177	0.163	0.688	0.065	0.800	0.132	0.717	0.765	0.385	1.146	0.287	6.762	0.010
V. variegata	0.539	0.466	1.404	0.240	2.579	0.111	13.826	0.000	5.261	0.025	6.733	0.011	0.715	0.401	7.029	0.009	1.665	0.198
L. ruficaudatus	1.599	0.212	0.707	0.404	0.387	0.535	1.474	0.230	0.135	0.715	0.117	0.733	0.213	0.647	0.032	0.859	2.296	0.131
L. tardigradus	0.943	0.336	0.332	0.567	0.325	0.570	1.614	0.210	0.127	0.723	0.234	0.630	0.118	0.732	0.003	0.960	4.232	0.041
N. bengalensis	1.156	0.288	0.601	0.442	0.274	0.602	0.645	0.426	0.047	0.829	0.027	0.870	0.185	0.669	0.053	0.819	1.178	0.279
N. coucang	1.699	0.196	0.450	0.504	0.173	0.678	5.317	0.023	0.743	0.391	0.910	0.342	0.121	0.729	0.114	0.736	2.877	0.091
P. potto	0.687	0.409	0.087	0.768	0.003	0.958	5.675	0.018	0.916	0.340	1.486	0.224	0.018	0.894	0.495	0.483	1.493	0.223

Goswami model ORBIT- PC3	*G. zanzibaricus*		*O. crassicaudatus*		*O. garnettii*		*A. laniger*		*I. indri*		*P. diadema*		*P. verreauxi*		*E. fulvus*		*E. macaco*	
	F value	p value	F value	p value	F value	p value	F value	p value	F value	p value	F value	p value	F value	p value	F value	p value	F value	p value
C. major																		
C. medius																		
M. murinus																		
M. rufus																		
G. alleni																		
G. demidoff																		
E. elegantulus																		
G. moholi																		
G. senegalensus																		
G. zanzibaricus																		
O. crassicaudatus	0.605	0.438																
O. garnettii	0.255	0.615	0.245	0.621														
A. laniger	3.400	0.072	7.161	0.008	7.441	0.007												
I. Indri	2.851	0.097	10.725	0.001	8.825	0.004	7.551	0.008										
P. diadema	1.570	0.216	8.670	0.004	6.697	0.011	5.800	0.020	0.175	0.677								
P. verreauxi	2.868	0.095	15.591	0.000	12.196	0.001	7.766	0.007	0.002	0.961	0.236	0.628						
E. fulvus	3.151	0.077	26.618	0.000	17.608	0.000	13.238	0.000	0.139	0.710	0.036	0.849	0.310	0.578				
E. macaco	2.001	0.161	9.280	0.003	7.110	0.009	8.723	0.004	0.411	0.523	0.021	0.885	0.523	0.471	0.151	0.698		
E. mongoz	2.282	0.135	14.495	0.000	10.717	0.001	8.599	0.004	0.149	0.701	0.009	0.924	0.251	0.618	0.009	0.923	0.076	0.784
E. rubriventer	6.687	0.013	16.702	0.000	14.831	0.000	8.512	0.005	0.614	0.436	1.316	0.257	0.457	0.501	1.381	0.241	2.413	0.124
H. griseus	1.124	0.294	5.252	0.024	3.996	0.048	5.468	0.024	0.658	0.421	0.131	0.719	0.678	0.413	0.368	0.545	0.086	0.770
L. catta	3.448	0.069	17.432	0.000	13.815	0.000	8.080	0.006	0.001	0.974	0.246	0.622	0.000	0.983	0.274	0.601	0.577	0.450
V. variegata	0.241	0.625	0.000	0.984	0.066	0.798	3.207	0.079	4.855	0.031	3.293	0.074	5.658	0.020	7.604	0.006	4.096	0.046
L. ruficaudatus	2.032	0.161	9.455	0.003	7.394	0.008	6.293	0.016	0.265	0.609	0.003	0.957	0.314	0.577	0.067	0.795	0.009	0.926
L. tardigradus	1.015	0.319	16.333	0.000	10.221	0.002	4.679	0.036	0.261	0.611	0.015	0.903	0.485	0.489	0.375	0.541	0.000	0.994
N. bengalensis	1.600	0.213	4.645	0.033	3.859	0.052	4.489	0.040	0.116	0.734	0.001	0.979	0.115	0.735	0.008	0.927	0.025	0.876
N. coucang	2.067	0.154	16.506	0.000	11.221	0.001	10.731	0.002	0.984	0.323	0.190	0.664	1.446	0.232	0.938	0.334	0.086	0.770
P. potto	0.872	0.352	11.310	0.001	6.775	0.010	8.942	0.003	1.173	0.280	0.410	0.523	2.096	0.150	2.423	0.121	0.276	0.600

Goswami model ORBIT- PC3	*E. mongoz*		*E. rubriventer*		*H. griseus*		*L. catta*		*V. variegata*		*L. ruficaudatus*		*L. tardigradus*		*N. bengalensis*		*N. coucang*	
	F value	p value	F value	p value	F value	p value	F value	p value	F value	p value	F value	p value	F value	p value	F value	p value	F value	p value
C. major																		
C. medius																		
M. murinus																		
M. rufus																		
G. alleni																		
G. demidoff																		
E. elegantulus																		
G. moholi																		
G. senegalensus																		
G. zanzibaricus																		
O. crassicaudatus																		
O. garnettii																		
A. laniger																		
I. Indri																		
P. diadema																		
P. verreauxi																		
E. fulvus																		
E. macaco																		
E. mongoz																		
E. rubriventer	1.325	0.253																
H. griseus	0.242	0.624	0.764	0.387														
L. catta	0.244	0.622	3.207	0.079	0.810	0.372												
V. variegata	5.048	0.027	8.326	0.005	2.316	0.133	6.411	0.014										
L. ruficaudatus	0.026	0.871	2.017	0.162	0.137	0.712	0.355	0.554	3.800	0.056								
L. tardigradus	0.086	0.770	1.041	0.312	0.040	0.843	0.441	0.509	3.057	0.085	0.005	0.941						
N. bengalensis	0.002	0.966	1.464	0.233	0.164	0.687	0.137	0.712	2.351	0.131	0.007	0.933	0.010	0.922				
N. coucang	0.459	0.499	3.759	0.056	0.008	0.930	1.562	0.214	5.251	0.024	0.152	0.698	0.098	0.755	0.131	0.718		
P. potto	0.966	0.327	2.945	0.088	0.024	0.877	2.011	0.158	3.009	0.085	0.326	0.569	0.596	0.441	0.190	0.664	0.173	0.678

Goswami model ORBIT- PC4	*C. major*		*C.medius*		*M. murinus*		*M. rufus*		*G. alleni*		*G. denidoff*		*E. elegantulus*		*G. moholi*		*G.senegalensis*	
	F value	p value	F value	p value	F value	p value	F value	p value	F value	p value	F value	p value	F value	p value	F value	p value	F value	p value
C. major																		
C. medius	0.011	0.915																
M. murinus	1.315	0.254	1.101	0.297														
M. rufus	0.186	0.668	0.183	0.671	0.770	0.382												
G. alleni	0.695	0.409	0.434	0.513	0.117	0.734	0.196	0.660										
G. demidoff	0.105	0.746	0.034	0.854	1.967	0.163	0.517	0.474	0.712	0.401								
E. elegantulus	0.521	0.474	0.517	0.475	0.172	0.679	0.416	0.521	0.185	0.669	0.932	0.337						
G. moholi	3.487	0.065	2.670	0.105	0.542	0.463	3.020	0.085	0.955	0.331	4.506	0.036	0.018	0.893				
G. senegalensus	0.145	0.704	0.221	0.639	1.243	0.266	0.010	0.919	0.257	0.613	0.822	0.365	1.096	0.296	4.904	0.028		
G. zanzibaricus	2.567	0.116	1.598	0.212	0.350	0.556	1.833	0.182	0.881	0.353	2.180	0.144	0.007	0.934	0.001	0.973	2.390	0.124
O. crassicaudatus	2.565	0.112	1.994	0.160	0.000	0.988	1.780	0.185	0.221	0.639	3.968	0.048	0.262	0.609	1.141	0.287	3.061	0.081
O. garnettii	6.874	0.010	4.542	0.035	0.776	0.380	5.994	0.016	1.820	0.180	7.067	0.009	0.039	0.844	0.010	0.919	7.556	0.006
A. laniger	0.703	0.406	0.478	0.492	2.490	0.118	1.130	0.293	1.281	0.264	0.433	0.513	0.930	0.339	3.683	0.058	2.179	0.142
I. Indri	0.121	0.729	0.030	0.864	1.691	0.196	0.513	0.476	1.039	0.312	0.000	0.989	0.728	0.397	3.548	0.062	0.491	0.484
P. diadema	2.885	0.096	2.122	0.151	0.977	0.325	2.518	0.119	1.215	0.276	3.222	0.076	0.008	0.931	0.236	0.628	4.401	0.037
P. verreauxi	0.644	0.425	0.238	0.627	4.109	0.045	1.818	0.182	2.566	0.114	0.074	0.786	1.276	0.262	8.155	0.005	1.944	0.165
E. fulvus	1.134	0.288	1.096	0.296	0.149	0.700	0.551	0.459	0.008	0.928	2.622	0.107	0.529	0.468	2.076	0.151	1.136	0.287
E. macaco	1.741	0.191	1.360	0.247	0.109	0.742	1.183	0.280	0.376	0.542	2.066	0.153	0.050	0.824	0.073	0.787	1.717	0.191
E. mongoz	1.350	0.249	0.667	0.417	6.290	0.013	3.212	0.077	3.345	0.071	0.431	0.513	1.917	0.170	11.815	0.001	4.331	0.039
E. rubriventer	4.126	0.048	2.622	0.111	1.584	0.211	3.357	0.073	2.509	0.120	2.942	0.090	0.076	0.784	0.731	0.395	4.041	0.046
H. griseus	5.288	0.026	3.081	0.085	1.559	0.215	4.277	0.044	2.842	0.098	3.681	0.059	0.031	0.860	0.535	0.466	4.955	0.027
L. catta	4.100	0.048	2.572	0.114	0.786	0.377	3.289	0.075	1.543	0.220	3.574	0.062	0.000	0.985	0.065	0.799	4.314	0.039
V. variegata	2.089	0.154	1.016	0.317	7.143	0.009	4.143	0.046	4.586	0.036	0.726	0.396	1.872	0.176	12.223	0.001	5.181	0.024
L. ruficaudatus	0.050	0.823	0.068	0.795	0.647	0.423	0.017	0.896	0.242	0.625	0.214	0.645	0.362	0.550	2.040	0.157	0.005	0.943
L. tardigradus	0.184	0.670	0.198	0.658	0.639	0.426	0.008	0.930	0.078	0.781	0.696	0.406	0.366	0.548	3.048	0.084	0.067	0.796
N. bengalensis	0.167	0.684	0.159	0.692	0.021	0.886	0.058	0.811	0.002	0.967	0.286	0.594	0.080	0.778	0.234	0.630	0.119	0.730
N. coucang	2.986	0.087	2.617	0.109	1.931	0.167	3.449	0.066	1.328	0.252	5.373	0.022	0.102	0.750	1.031	0.312	9.311	0.003
P. potto	7.407	0.007	6.147	0.014	4.904	0.028	9.404	0.003	3.457	0.065	12.118	0.001	0.342	0.560	3.234	0.074	21.432	0.000

Goswami model ORBIT- PC4	*G. zanzibaricus*		*O. crassicaudatus*		*O. garnettii*		*A. laniger*		*I. indri*		*P. diadema*		*P. verreauxi*		*E. fulvus*		*E. macaco*	
	F value	p value	F value	p value	F value	p value	F value	p value	F value	p value	F value	p value	F value	p value	F value	p value	F value	p value
C. major																		
C. medius																		
M. murinus																		
M. rufus																		
G. alleni																		
G. demidoff																		
E. elegantulus																		
G. moholi																		
G. senegalensus																		
G. zanzibaricus																		
O. crassicaudatus	0.603	0.439																
O. garnettii	0.016	0.901	1.871	0.173														
A. laniger	2.113	0.153	3.844	0.052	5.716	0.018												
I. Indri	2.794	0.100	2.822	0.095	6.158	0.014	0.449	0.505										
P. diadema	0.115	0.736	1.752	0.188	0.528	0.469	2.420	0.127	3.167	0.080								
P. verreauxi	5.494	0.022	7.977	0.005	15.063	0.000	0.364	0.548	0.092	0.762	6.087	0.016						
E. fulvus	0.998	0.319	0.413	0.521	3.124	0.078	3.335	0.069	1.556	0.214	2.442	0.120	4.661	0.032				
E. macaco	0.061	0.805	0.180	0.672	0.078	0.780	2.448	0.122	2.090	0.152	0.361	0.550	4.376	0.039	0.515	0.474		
E. mongoz	6.547	0.012	12.975	0.000	20.578	0.000	0.181	0.671	0.396	0.531	7.902	0.006	0.192	0.662	8.646	0.004	5.994	0.016
E. rubriventer	0.573	0.453	2.427	0.122	1.491	0.225	2.737	0.105	4.292	0.042	0.137	0.713	6.733	0.012	2.655	0.105	0.903	0.345
H. griseus	0.388	0.536	2.622	0.108	1.222	0.271	3.077	0.086	5.098	0.027	0.032	0.859	9.012	0.004	2.978	0.086	0.733	0.394
L. catta	0.031	0.860	1.467	0.228	0.204	0.653	2.973	0.091	4.074	0.047	0.058	0.811	8.322	0.005	2.086	0.150	0.210	0.648
V. variegata	7.635	0.008	13.759	0.000	22.373	0.000	0.061	0.805	0.786	0.378	8.121	0.006	0.574	0.451	9.209	0.003	6.869	0.010
L. ruficaudatus	1.507	0.226	1.192	0.277	3.787	0.054	0.784	0.381	0.256	0.615	1.889	0.176	0.890	0.349	0.450	0.503	0.995	0.322
L. tardigradus	1.131	0.293	2.051	0.155	6.155	0.015	0.987	0.326	0.450	0.505	1.968	0.167	1.716	0.195	0.616	0.434	0.905	0.344
N. bengalensis	0.169	0.683	0.034	0.855	0.352	0.554	0.617	0.437	0.341	0.561	0.327	0.570	0.706	0.404	0.000	0.998	0.091	0.763
N. coucang	0.358	0.551	4.366	0.038	1.822	0.179	2.677	0.105	2.854	0.094	0.121	0.729	6.086	0.015	6.445	0.012	0.811	0.370
P. potto	1.157	0.284	13.010	0.000	5.825	0.017	5.552	0.020	6.193	0.014	0.546	0.461	13.759	0.000	16.365	0.000	2.179	0.142

Goswami model ORBIT- PC4	*E. mongoz*		*E. rubriventer*		*H. griseus*		*L. catta*		*V. variegata*		*L. ruficaudatus*		*L. tardigradus*		*N. bengalensis*		*N. coucang*	
	F value	p value	F value	p value	F value	p value	F value	p value	F value	p value	F value	p value	F value	p value	F value	p value	F value	p value
C. major																		
C. medius																		
M. murinus																		
M. rufus																		
G. alleni																		
G. demidoff																		
E. elegantulus																		
G. moholi																		
G. senegalensus																		
G. zanzibaricus																		
O. crassicaudatus																		
O. garnettii																		
A. laniger																		
I. Indri																		
P. diadema																		
P. verreauxi																		
E. fulvus																		
E. macaco																		
E. mongoz																		
E. rubriventer	7.112	0.009																
H. griseus	9.726	0.003	5.288	0.026														
L. catta	10.116	0.002	4.100	0.048	0.267	0.607												
V. variegata	0.112	0.738	8.141	0.006	11.202	0.001	11.340	0.001										
L. ruficaudatus	1.580	0.213	2.909	0.095	3.432	0.070	2.459	0.123	2.253	0.139								
L. tardigradus	3.605	0.061	2.056	0.158	2.622	0.112	2.328	0.133	3.822	0.055	0.029	0.866						
N. bengalensis	1.064	0.306	0.688	0.411	0.593	0.445	0.308	0.581	1.307	0.258	0.074	0.786	0.030	0.863				
N. coucang	9.550	0.002	0.001	0.977	0.033	0.857	0.358	0.551	8.090	0.005	2.045	0.156	4.610	0.034	0.459	0.500		
P. potto	21.193	0.000	0.018	0.892	0.229	0.633	1.274	0.261	17.904	0.000	5.032	0.026	15.052	0.000	1.136	0.288	0.112	0.739

Goswami model ORBIT- PC5	*C. major*		*C.medius*		*M. murinus*		*M. rufus*		*G. alleni*		*G. denidoff*		*E. elegantulus*		*G. moholi*		*G.senegalensis*	
	F value	p value	F value	p value	F value	p value	F value	p value	F value	p value	F value	p value	F value	p value	F value	p value	F value	p value
C. major																		
C. medius	0.000	0.989																
M. murinus	0.134	0.715	0.083	0.774														
M. rufus	0.202	0.655	0.143	0.707	0.949	0.332												
G. alleni	0.408	0.526	0.217	0.643	0.112	0.739	1.196	0.280										
G. demidoff	1.264	0.264	0.950	0.333	3.049	0.083	0.632	0.429	2.780	0.099								
E. elegantulus	0.136	0.714	0.099	0.754	0.045	0.832	0.443	0.508	0.000	0.997	1.312	0.255						
G. moholi	0.536	0.466	0.352	0.554	1.758	0.187	0.006	0.936	2.900	0.092	0.936	0.335	0.917	0.341				
G. senegalensus	1.912	0.168	1.426	0.234	4.605	0.033	0.791	0.375	4.519	0.035	0.130	0.719	2.079	0.151	0.897	0.345		
G. zanzibaricus	2.731	0.105	1.622	0.209	4.781	0.031	1.440	0.236	7.250	0.010	0.177	0.675	1.932	0.170	2.886	0.093	0.841	0.360
O. crassicaudatus	0.453	0.502	0.317	0.574	1.871	0.173	0.001	0.975	2.502	0.116	1.512	0.221	0.914	0.341	0.024	0.876	1.857	0.174
O. garnettii	0.014	0.907	0.013	0.908	0.458	0.499	0.399	0.529	0.988	0.322	2.767	0.098	0.369	0.545	0.814	0.368	4.072	0.045
A. laniger	4.281	0.044	3.111	0.084	7.279	0.008	3.277	0.077	7.060	0.011	1.903	0.172	3.266	0.076	6.681	0.011	4.725	0.031
I. Indri	5.466	0.023	4.081	0.048	9.460	0.003	4.461	0.039	8.306	0.006	2.297	0.133	4.044	0.048	7.949	0.006	5.936	0.016
P. diadema	0.105	0.748	0.075	0.785	0.534	0.467	0.007	0.932	0.900	0.348	0.560	0.456	0.327	0.570	0.036	0.849	0.656	0.419
P. verreauxi	0.146	0.703	0.100	0.753	0.717	0.399	0.021	0.886	1.401	0.241	0.882	0.350	0.445	0.507	0.079	0.780	1.014	0.315
E. fulvus	1.218	0.271	0.975	0.325	3.120	0.079	0.659	0.418	2.450	0.119	0.016	0.901	1.328	0.250	0.771	0.381	0.057	0.811
E. macaco	1.449	0.232	1.095	0.299	3.078	0.082	0.787	0.378	3.036	0.086	0.036	0.851	1.462	0.230	1.206	0.274	0.326	0.569
E. mongoz	0.402	0.528	0.318	0.574	1.313	0.254	0.083	0.774	1.247	0.268	0.189	0.665	0.633	0.428	0.098	0.755	0.108	0.743
E. rubriventer	9.683	0.003	6.290	0.015	13.650	0.000	7.315	0.009	17.077	0.000	4.202	0.044	5.998	0.017	14.776	0.000	9.407	0.002
H. griseus	0.089	0.767	0.052	0.821	0.001	0.978	0.475	0.494	0.063	0.802	1.569	0.214	0.022	0.884	1.116	0.293	2.389	0.124
L. catta	1.283	0.262	0.834	0.365	2.883	0.093	0.495	0.485	3.690	0.060	0.010	0.919	1.228	0.272	0.843	0.361	0.039	0.844
V. variegata	0.774	0.382	0.509	0.478	0.475	0.492	2.018	0.160	0.092	0.763	4.295	0.041	0.039	0.844	4.117	0.045	7.746	0.006
L. ruficaudatus	0.046	0.831	0.027	0.870	0.004	0.949	0.380	0.540	0.102	0.751	1.496	0.225	0.039	0.845	0.921	0.340	2.395	0.123
L. tardigradus	2.042	0.159	1.286	0.262	5.544	0.021	1.156	0.287	4.787	0.034	0.001	0.972	1.544	0.219	2.247	0.137	0.367	0.546
N. bengalensis	0.001	0.981	0.000	0.992	0.041	0.839	0.089	0.767	0.178	0.675	0.524	0.471	0.066	0.798	0.233	0.630	0.688	0.408
N. coucang	0.007	0.935	0.003	0.958	0.112	0.739	0.461	0.499	0.334	0.565	2.327	0.130	0.145	0.704	0.922	0.339	3.823	0.052
P. potto	1.756	0.187	1.328	0.251	4.384	0.038	0.950	0.331	3.630	0.059	0.014	0.907	1.749	0.188	1.194	0.276	0.100	0.752

Goswami model ORBIT- PC5	*G. zanzibaricus*		*O. crassicaudatus*		*O. garnettii*		*A. laniger*		*I. indri*		*P. diadema*		*P. verreauxi*		*E. fulvus*		*E. macaco*	
	F value	p value	F value	p value	F value	p value	F value	p value	F value	p value	F value	p value	F value	p value	F value	p value	F value	p value
C. major																		
C. medius																		
M. murinus																		
M. rufus																		
G. alleni																		
G. demidoff																		
E. elegantulus																		
G. moholi																		
G. senegalensus																		
G. zanzibaricus																		
O. crassicaudatus	3.187	0.077																
O. garnettii	4.736	0.032	0.859	0.355														
A. laniger	1.406	0.242	7.191	0.008	8.238	0.005												
I. Indri	1.305	0.258	9.453	0.003	10.901	0.001	0.034	0.855										
P. diadema	1.490	0.228	0.011	0.915	0.142	0.707	3.310	0.075	4.042	0.049								
P. verreauxi	2.521	0.117	0.032	0.858	0.174	0.677	5.054	0.028	5.979	0.017	0.001	0.977						
E. fulvus	0.263	0.608	1.725	0.190	3.122	0.078	2.139	0.145	2.849	0.093	0.483	0.488	0.736	0.392				
E. macaco	0.046	0.830	1.669	0.198	2.763	0.099	1.481	0.228	1.599	0.209	0.740	0.392	1.115	0.294	0.093	0.760		
E. mongoz	0.545	0.462	0.223	0.638	0.866	0.354	2.213	0.141	2.936	0.090	0.098	0.755	0.166	0.685	0.168	0.682	0.305	0.582
E. rubriventer	4.573	0.038	14.538	0.000	16.032	0.000	0.141	0.709	0.410	0.524	7.529	0.008	11.493	0.001	4.126	0.044	3.466	0.066
H. griseus	3.364	0.073	0.982	0.324	0.269	0.605	4.745	0.035	5.655	0.021	0.332	0.567	0.480	0.491	1.401	0.238	1.794	0.184
L. catta	0.376	0.542	1.171	0.281	2.415	0.123	2.460	0.123	2.749	0.102	0.516	0.475	0.877	0.352	0.000	0.997	0.081	0.776
V. variegata	6.034	0.017	4.525	0.035	2.165	0.144	6.984	0.011	9.496	0.003	1.351	0.249	1.994	0.162	4.696	0.031	4.178	0.044
L. ruficaudatus	2.742	0.105	0.857	0.356	0.184	0.669	4.126	0.048	5.307	0.025	0.242	0.625	0.352	0.555	1.475	0.226	1.666	0.201
L. tardigradus	0.254	0.617	4.436	0.037	6.894	0.010	2.148	0.150	2.849	0.096	0.881	0.352	1.679	0.200	0.052	0.819	0.038	0.845
N. bengalensis	1.425	0.239	0.172	0.679	0.010	0.920	2.695	0.108	2.843	0.097	0.059	0.809	0.078	0.781	0.415	0.520	0.690	0.409
N. coucang	3.239	0.075	1.067	0.303	0.081	0.776	5.532	0.021	7.743	0.006	0.203	0.653	0.270	0.604	2.911	0.089	2.274	0.134
P. potto	0.356	0.552	2.591	0.109	4.566	0.034	2.843	0.094	3.697	0.056	0.703	0.403	1.103	0.295	0.001	0.974	0.109	0.742

Goswami model ORBIT- PC5	*E. mongoz*		*E. rubriventer*		*H. griseus*		*L. catta*		*V. variegata*		*L. ruficaudatus*		*L. tardigradus*		*N. bengalensis*		*N. coucang*	
	F value	p value	F value	p value	F value	p value	F value	p value	F value	p value	F value	p value	F value	p value	F value	p value	F value	p value
C. major																		
C. medius																		
M. murinus																		
M. rufus																		
G. alleni																		
G. demidoff																		
E. elegantulus																		
G. moholi																		
G. senegalensus																		
G. zanzibaricus																		
O. crassicaudatus																		
O. garnettii																		
A. laniger																		
I. Indri																		
P. diadema																		
P. verreauxi																		
E. fulvus																		
E. macaco																		
E. mongoz																		
E. rubriventer	4.423	0.039																
H. griseus	0.642	0.426	0.089	0.767														
L. catta	0.103	0.749	1.283	0.262	1.765	0.189												
V. variegata	2.263	0.136	13.295	0.001	0.232	0.632	4.276	0.042										
L. ruficaudatus	0.589	0.445	8.760	0.005	0.005	0.945	1.502	0.226	0.317	0.576								
L. tardigradus	0.323	0.571	5.605	0.022	2.316	0.134	0.027	0.869	6.810	0.011	2.152	0.149						
N. bengalensis	0.169	0.682	6.125	0.017	0.036	0.850	0.600	0.442	0.301	0.585	0.016	0.901	0.689	0.411				
N. coucang	0.864	0.354	10.319	0.002	0.065	0.799	1.887	0.173	0.947	0.333	0.032	0.858	4.629	0.034	0.001	0.981		
P. potto	0.233	0.630	5.766	0.018	2.011	0.158	0.000	0.985	6.497	0.012	2.072	0.152	0.054	0.816	0.599	0.440	3.977	0.048

Goswami model ORAL- PC1	*C. major*		*C.medius*		*M. murinus*		*M. rufus*		*G. alleni*		*G. denidoff*		*E. elegantulus*		*G. moholi*		*G.senegalensis*	
	F value	p value	F value	p value	F value	p value	F value	p value	F value	p value	F value	p value	F value	p value	F value	p value	F value	p value
C. major																		
C. medius	0.457	0.502																
M. murinus	2.261	0.136	1.047	0.309														
M. rufus	4.722	0.035	3.915	0.053	1.783	0.185												
G. alleni	0.183	0.671	0.056	0.814	1.099	0.297	3.499	0.067										
G. demidoff	4.747	0.032	3.259	0.075	0.989	0.322	0.052	0.821	3.323	0.072								
E. elegantulus	0.042	0.838	0.087	0.768	0.861	0.356	2.269	0.137	0.014	0.907	2.259	0.136						
G. moholi	4.732	0.032	3.380	0.069	0.894	0.346	0.239	0.626	3.070	0.083	0.045	0.832	2.123	0.148				
G. senegalensus	2.757	0.098	1.100	0.296	0.032	0.858	3.055	0.082	1.210	0.273	1.590	0.209	1.019	0.314	1.514	0.220		
G. zanzibaricus	0.980	0.327	0.307	0.582	0.000	0.994	0.475	0.494	0.547	0.463	0.384	0.537	0.419	0.520	0.249	0.619	0.006	0.938
O. crassicaudatus	4.326	0.040	3.157	0.078	0.693	0.406	0.561	0.455	2.589	0.110	0.170	0.681	1.871	0.174	0.055	0.815	1.254	0.264
O. garnettii	7.398	0.008	6.687	0.011	3.447	0.065	0.091	0.763	5.319	0.023	0.277	0.599	3.678	0.057	0.756	0.386	5.036	0.026
A. laniger	0.001	0.979	0.449	0.506	1.848	0.177	4.158	0.047	0.220	0.641	4.332	0.041	0.050	0.824	3.975	0.049	2.190	0.140
I. Indri	1.845	0.179	5.907	0.018	11.702	0.001	17.174	0.000	4.042	0.049	16.545	0.000	1.723	0.194	17.614	0.000	14.224	0.000
P. diadema	0.013	0.908	0.613	0.437	2.210	0.140	4.774	0.033	0.326	0.571	4.862	0.030	0.090	0.765	4.529	0.036	2.611	0.108
P. verreauxi	1.983	0.164	0.705	0.404	0.000	0.994	1.038	0.312	1.097	0.299	0.705	0.403	0.767	0.384	0.484	0.488	0.017	0.897
E. fulvus	0.538	0.464	0.050	0.823	0.677	0.411	3.214	0.075	0.119	0.730	1.811	0.180	0.148	0.700	2.363	0.126	0.589	0.443
E. macaco	0.016	0.901	1.055	0.307	4.866	0.029	9.310	0.003	0.389	0.535	7.669	0.007	0.117	0.734	8.837	0.004	5.677	0.018
E. mongoz	1.407	0.239	0.668	0.416	0.000	0.999	1.166	0.283	0.663	0.418	0.682	0.411	0.568	0.453	0.648	0.422	0.026	0.872
E. rubriventer	0.412	0.524	1.179	0.283	3.019	0.086	3.633	0.062	0.798	0.376	4.363	0.040	0.518	0.475	4.605	0.034	4.430	0.037
H. griseus	6.887	0.012	5.560	0.022	2.664	0.106	0.178	0.675	5.941	0.019	0.446	0.506	3.378	0.071	0.856	0.357	4.118	0.044
L. catta	0.059	0.809	0.399	0.530	2.998	0.086	7.423	0.008	0.088	0.768	6.333	0.014	0.005	0.946	6.665	0.011	3.350	0.069
V. variegata	0.351	0.556	0.011	0.917	0.496	0.483	2.070	0.155	0.065	0.800	1.705	0.195	0.094	0.760	1.822	0.180	0.531	0.467
L. ruficaudatus	3.989	0.052	2.350	0.132	0.479	0.490	0.156	0.695	3.139	0.083	0.040	0.842	1.695	0.198	0.000	0.990	0.851	0.358
L. tardigradus	0.531	0.470	0.007	0.935	1.055	0.307	3.956	0.052	0.088	0.767	3.161	0.079	0.115	0.735	3.535	0.063	1.109	0.294
N. bengalensis	0.011	0.915	0.715	0.402	2.320	0.131	5.426	0.024	0.443	0.509	5.545	0.021	0.091	0.764	4.918	0.029	2.663	0.104
N. coucang	2.299	0.133	0.682	0.411	0.284	0.595	4.443	0.038	0.931	0.337	2.588	0.110	0.701	0.404	2.696	0.103	0.143	0.706
P. potto	0.883	0.349	0.000	0.986	2.914	0.089	10.600	0.001	0.093	0.761	6.137	0.014	0.156	0.693	7.776	0.006	2.565	0.110

Goswami model ORAL- PC1	*G. zanzibaricus*		*O. crassicaudatus*		*O. garnettii*		*A. laniger*		*I. indri*		*P. diadema*		*P. verreauxi*		*E. fulvus*		*E. macaco*	
	F value	p value	F value	p value	F value	p value	F value	p value	F value	p value	F value	p value	F value	p value	F value	p value	F value	p value
C. major																		
C. medius																		
M. murinus																		
M. rufus																		
G. alleni																		
G. demidoff																		
E. elegantulus																		
G. moholi																		
G. senegalensus																		
G. zanzibaricus																		
O. crassicaudatus	0.143	0.706																
O. garnettii	0.875	0.352	1.464	0.228														
A. laniger	1.136	0.292	3.376	0.069	5.946	0.016												
I. Indri	5.286	0.025	16.926	0.000	22.247	0.000	1.712	0.196										
P. diadema	1.322	0.256	3.897	0.051	6.651	0.011	0.009	0.927	1.461	0.231								
P. verreauxi	0.000	0.989	0.284	0.595	1.729	0.191	2.097	0.153	10.210	0.002	2.406	0.126						
E. fulvus	0.093	0.761	2.979	0.085	5.830	0.016	0.401	0.527	4.456	0.036	0.522	0.471	0.212	0.646				
E. macaco	1.388	0.242	9.201	0.003	13.862	0.000	0.007	0.932	2.051	0.156	0.000	0.991	2.922	0.091	1.506	0.221		
E. mongoz	0.000	0.996	0.540	0.463	2.637	0.107	1.104	0.297	7.481	0.007	1.351	0.249	0.000	0.995	0.609	0.436	3.405	0.068
E. rubriventer	1.308	0.258	4.691	0.032	6.502	0.012	0.362	0.550	0.000	1.000	0.331	0.568	2.369	0.129	1.526	0.218	0.521	0.472
H. griseus	1.180	0.283	1.266	0.263	0.042	0.838	7.042	0.011	22.046	0.000	7.690	0.008	2.312	0.133	3.064	0.082	10.558	0.002
L. catta	1.072	0.305	6.291	0.013	10.814	0.001	0.073	0.788	4.237	0.043	0.148	0.702	2.295	0.134	0.570	0.451	0.213	0.646
V. variegata	0.118	0.732	1.795	0.183	4.118	0.044	0.305	0.583	3.578	0.062	0.415	0.522	0.269	0.606	0.007	0.932	0.868	0.354
L. ruficaudatus	0.267	0.608	0.025	0.876	0.463	0.498	4.545	0.039	16.271	0.000	4.939	0.031	0.487	0.488	0.953	0.330	5.694	0.020
L. tardigradus	0.231	0.633	3.580	0.061	7.408	0.007	0.487	0.489	6.282	0.015	0.662	0.420	0.574	0.451	0.031	0.860	1.367	0.246
N. bengalensis	1.785	0.189	4.026	0.047	6.965	0.009	0.008	0.931	2.000	0.163	0.001	0.979	3.167	0.080	0.490	0.485	0.000	0.990
N. coucang	0.060	0.807	2.498	0.116	7.196	0.008	1.982	0.163	14.909	0.000	2.392	0.125	0.147	0.702	0.244	0.622	4.921	0.028
P. potto	0.510	0.476	9.125	0.003	15.653	0.000	0.725	0.396	10.372	0.002	0.980	0.324	1.145	0.286	0.208	0.648	2.338	0.128

Goswami model ORAL- PC1	*E. mongoz*		*E. rubriventer*		*H. griseus*		*L. catta*		*V. variegata*		*L. ruficaudatus*		*L. tardigradus*		*N. bengalensis*		*N. coucang*	
	F value	p value	F value	p value	F value	p value	F value	p value	F value	p value	F value	p value	F value	p value	F value	p value	F value	p value
C. major																		
C. medius																		
M. murinus																		
M. rufus																		
G. alleni																		
G. demidoff																		
E. elegantulus																		
G. moholi																		
G. senegalensus																		
G. zanzibaricus																		
O. crassicaudatus																		
O. garnettii																		
A. laniger																		
I. Indri																		
P. diadema																		
P. verreauxi																		
E. fulvus																		
E. macaco																		
E. mongoz																		
E. rubriventer	2.074	0.154																
H. griseus	1.643	0.204	6.887	0.012														
L. catta	1.890	0.173	0.059	0.809	10.370	0.002												
V. variegata	0.354	0.554	1.012	0.318	2.632	0.110	0.321	0.573										
L. ruficaudatus	0.286	0.594	2.947	0.092	0.815	0.371	5.637	0.021	0.939	0.336								
L. tardigradus	0.684	0.411	1.220	0.275	5.141	0.028	0.536	0.467	0.002	0.962	2.009	0.163						
N. bengalensis	1.334	0.252	0.350	0.557	10.465	0.002	0.175	0.678	0.405	0.527	8.100	0.007	0.735	0.396				
N. coucang	0.199	0.656	3.139	0.080	6.034	0.016	2.989	0.087	0.223	0.637	1.665	0.200	0.623	0.432	2.747	0.101		
P. potto	2.274	0.133	2.644	0.106	10.773	0.001	0.789	0.376	0.035	0.852	4.049	0.046	0.026	0.871	1.005	0.318	1.943	0.165

Goswami model ORAL- PC2	*C. major*		*C.medius*		*M. murinus*		*M. rufus*		*G. alleni*		*G. denidoff*		*E. elegantulus*		*G. moholi*		*G.senegalensis*	
	F value	p value	F value	p value	F value	p value	F value	p value	F value	p value	F value	p value	F value	p value	F value	p value	F value	p value
C. major																		
C. medius	0.650	0.424																
M. murinus	3.630	0.060	2.202	0.141														
M. rufus	0.189	0.665	0.551	0.461	5.622	0.020												
G. alleni	0.286	0.596	2.684	0.108	7.768	0.006	1.838	0.181										
G. demidoff	0.095	0.758	2.880	0.093	9.641	0.002	1.419	0.237	0.234	0.630								
E. elegantulus	0.512	0.477	0.036	0.850	0.465	0.497	0.413	0.523	1.668	0.202	1.702	0.195						
G. moholi	0.103	0.750	0.566	0.454	5.818	0.017	0.019	0.890	1.184	0.279	0.719	0.398	0.431	0.513				
G. senegalensus	6.703	0.010	4.831	0.029	0.415	0.520	9.923	0.002	12.599	0.000	14.274	0.000	1.211	0.272	10.327	0.001		
G. zanzibaricus	1.170	0.285	0.562	0.457	0.000	0.992	1.560	0.217	2.739	0.105	3.445	0.067	0.200	0.656	1.335	0.251	0.095	0.758
O. crassicaudatus	3.630	0.059	1.649	0.201	0.291	0.590	5.253	0.024	8.520	0.004	9.608	0.002	0.262	0.610	5.257	0.023	1.669	0.197
O. garnettii	8.234	0.005	8.052	0.005	3.119	0.079	13.640	0.000	13.639	0.000	17.833	0.000	2.506	0.116	14.307	0.000	1.856	0.174
A. laniger	2.206	0.145	1.726	0.195	0.519	0.473	3.138	0.083	3.947	0.053	5.974	0.017	0.797	0.376	3.529	0.063	0.288	0.592
I. Indri	0.020	0.887	0.607	0.439	3.991	0.048	0.095	0.759	0.633	0.429	0.314	0.577	0.489	0.487	0.029	0.864	7.074	0.008
P. diadema	0.992	0.324	0.247	0.621	0.236	0.629	1.248	0.269	2.910	0.094	3.297	0.073	0.039	0.845	0.961	0.329	0.802	0.372
P. verreauxi	1.763	0.189	0.757	0.387	0.030	0.864	2.230	0.140	4.169	0.045	4.883	0.029	0.203	0.653	2.056	0.154	0.357	0.551
E. fulvus	3.376	0.068	2.124	0.147	0.008	0.927	4.929	0.028	6.610	0.011	7.684	0.006	0.423	0.516	6.167	0.014	0.321	0.571
E. macaco	3.094	0.083	1.849	0.178	0.007	0.933	4.589	0.035	6.619	0.012	8.324	0.005	0.461	0.499	4.579	0.034	0.201	0.654
E. mongoz	0.043	0.836	1.653	0.202	9.462	0.003	0.695	0.407	0.144	0.706	0.002	0.968	0.864	0.355	0.593	0.443	17.268	0.000
E. rubriventer	0.002	0.965	0.492	0.486	2.208	0.141	0.170	0.681	0.165	0.686	0.035	0.853	0.454	0.503	0.092	0.763	3.911	0.049
H. griseus	0.654	0.423	0.012	0.913	1.256	0.265	0.612	0.438	2.516	0.119	2.687	0.105	0.011	0.916	0.554	0.459	2.880	0.091
L. catta	1.295	0.260	0.508	0.479	0.119	0.731	1.617	0.208	3.050	0.086	4.046	0.047	0.103	0.749	2.002	0.160	0.784	0.377
V. variegata	0.867	0.355	0.096	0.757	0.912	0.342	0.846	0.361	2.640	0.110	2.995	0.087	0.001	0.972	0.996	0.321	2.529	0.113
L. ruficaudatus	0.000	0.984	0.524	0.472	3.322	0.072	0.136	0.714	0.268	0.607	0.102	0.750	0.425	0.517	0.079	0.779	6.417	0.012
L. tardigradus	1.209	0.277	0.316	0.576	0.711	0.401	1.637	0.206	3.347	0.074	4.559	0.036	0.028	0.867	1.899	0.171	2.474	0.117
N. bengalensis	0.436	0.513	0.009	0.924	0.695	0.407	0.371	0.545	1.657	0.205	1.757	0.189	0.007	0.936	0.342	0.560	1.651	0.200
N. coucang	0.466	0.497	0.052	0.820	4.143	0.044	0.206	0.651	2.078	0.153	1.900	0.171	0.099	0.754	0.360	0.550	8.660	0.004
P. potto	0.280	0.598	0.092	0.761	4.120	0.044	0.073	0.787	1.350	0.247	1.091	0.298	0.108	0.743	0.178	0.673	8.498	0.004

Goswami model ORAL- PC2	*G. zanzibaricus*		*O. crassicaudatus*		*O. garnettii*		*A. laniger*		*I. indri*		*P. diadema*		*P. verreauxi*		*E. fulvus*		*E. macaco*	
	F value	p value	F value	p value	F value	p value	F value	p value	F value	p value	F value	p value	F value	p value	F value	p value	F value	p value
C. major																		
C. medius																		
M. murinus																		
M. rufus																		
G. alleni																		
G. demidoff																		
E. elegantulus																		
G. moholi																		
G. senegalensus																		
G. zanzibaricus																		
O. crassicaudatus	0.051	0.821																
O. garnettii	0.709	0.402	6.154	0.014														
A. laniger	0.190	0.665	1.171	0.281	0.032	0.857												
I. Indri	1.333	0.253	3.764	0.054	9.418	0.003	2.754	0.102										
P. diadema	0.105	0.747	0.068	0.795	2.148	0.145	0.644	0.426	1.052	0.309								
P. verreauxi	0.009	0.923	0.018	0.894	1.706	0.194	0.441	0.509	1.901	0.172	0.078	0.780						
E. fulvus	0.002	0.965	0.439	0.508	3.052	0.082	0.433	0.511	3.544	0.061	0.211	0.647	0.042	0.837				
E. macaco	0.003	0.959	0.295	0.588	2.027	0.157	0.370	0.545	3.451	0.067	0.254	0.615	0.046	0.830	0.000	0.991		
E. mongoz	1.543	0.218	10.081	0.002	18.730	0.000	3.556	0.063	0.164	0.686	1.418	0.237	2.828	0.096	13.138	0.000	6.577	0.012
E. rubriventer	1.058	0.309	2.174	0.143	4.937	0.028	1.775	0.189	0.029	0.866	0.867	0.356	1.362	0.247	1.844	0.176	2.033	0.158
H. griseus	0.425	0.518	0.852	0.358	5.246	0.024	1.343	0.252	0.630	0.430	0.149	0.702	0.506	0.480	1.108	0.294	1.150	0.287
L. catta	0.024	0.877	0.001	0.979	2.608	0.109	0.460	0.500	1.456	0.232	0.023	0.880	0.010	0.919	0.177	0.674	0.126	0.724
V. variegata	0.218	0.642	0.497	0.482	5.089	0.026	1.086	0.302	0.869	0.354	0.035	0.852	0.264	0.609	1.013	0.315	0.795	0.375
L. ruficaudatus	0.966	0.331	3.316	0.071	7.812	0.006	1.951	0.170	0.012	0.913	0.796	0.377	1.514	0.223	3.338	0.069	2.772	0.100
L. tardigradus	0.123	0.728	0.274	0.602	5.457	0.021	0.844	0.363	1.361	0.248	0.002	0.965	0.138	0.711	0.929	0.336	0.590	0.445
N. bengalensis	0.301	0.586	0.461	0.498	3.079	0.082	0.910	0.346	0.421	0.519	0.097	0.757	0.328	0.569	0.591	0.443	0.674	0.414
N. coucang	0.660	0.419	3.425	0.066	12.888	0.000	2.357	0.128	0.360	0.550	0.345	0.558	1.040	0.310	5.690	0.018	2.958	0.088
P. potto	0.544	0.462	3.496	0.063	12.167	0.001	2.104	0.149	0.188	0.665	0.302	0.584	0.900	0.344	7.656	0.006	2.727	0.100

Goswami model ORAL- PC2	*E. mongoz*		*E. rubriventer*		*H. griseus*		*L. catta*		*V. variegata*		*L. ruficaudatus*		*L. tardigradus*		*N. bengalensis*		*N. coucang*	
	F value	p value	F value	p value	F value	p value	F value	p value	F value	p value	F value	p value	F value	p value	F value	p value	F value	p value
C. major																		
C. medius																		
M. murinus																		
M. rufus																		
G. alleni																		
G. demidoff																		
E. elegantulus																		
G. moholi																		
G. senegalensus																		
G. zanzibaricus																		
O. crassicaudatus																		
O. garnettii																		
A. laniger																		
I. Indri																		
P. diadema																		
P. verreauxi																		
E. fulvus																		
E. macaco																		
E. mongoz																		
E. rubriventer	0.012	0.913																
H. griseus	1.296	0.258	0.654	0.423														
L. catta	3.244	0.075	1.295	0.260	0.289	0.593												
V. variegata	2.170	0.144	0.619	0.434	0.032	0.858	0.164	0.687										
L. ruficaudatus	0.053	0.819	0.003	0.954	0.521	0.474	1.164	0.285	0.753	0.389								
L. tardigradus	3.598	0.061	0.801	0.375	0.141	0.709	0.068	0.795	0.038	0.846	1.051	0.310						
N. bengalensis	0.742	0.392	0.401	0.530	0.000	0.991	0.165	0.686	0.017	0.898	0.343	0.561	0.072	0.789				
N. coucang	2.102	0.150	0.309	0.579	0.083	0.774	1.059	0.306	0.301	0.585	0.411	0.523	0.839	0.362	0.051	0.822		
P. potto	1.773	0.185	0.179	0.673	0.107	0.744	1.130	0.289	0.355	0.552	0.258	0.612	0.961	0.329	0.063	0.803	0.024	0.877

Goswami model ORAL- PC3	*C. major*		*C.medius*		*M. murinus*		*M. rufus*		*G. alleni*		*G. denidoff*		*E. elegantulus*		*G. moholi*		*G.senegalensis*	
	F value	p value	F value	p value	F value	p value	F value	p value	F value	p value	F value	p value	F value	p value	F value	p value	F value	p value
C. major																		
C. medius	3.659	0.062																
M. murinus	7.796	0.006	1.676	0.198														
M. rufus	4.694	0.035	0.049	0.826	1.265	0.263												
G. alleni	0.007	0.932	2.781	0.102	6.713	0.011	3.582	0.064										
G. demidoff	2.941	0.090	0.035	0.852	0.789	0.376	0.000	0.986	2.438	0.122								
E. elegantulus	0.949	0.334	0.060	0.807	0.992	0.322	0.140	0.709	0.740	0.393	0.120	0.730						
G. moholi	2.268	0.135	0.132	0.717	3.146	0.078	0.350	0.556	1.829	0.180	0.250	0.618	0.001	0.972				
G. senegalensus	3.518	0.062	0.019	0.889	3.195	0.075	0.153	0.696	2.977	0.086	0.113	0.737	0.041	0.840	0.084	0.773		
G. zanzibaricus	3.730	0.060	0.227	0.636	0.096	0.757	0.122	0.728	2.787	0.102	0.069	0.793	0.266	0.608	0.409	0.524	0.282	0.596
O. crassicaudatus	5.317	0.023	0.140	0.709	1.598	0.208	0.018	0.893	4.489	0.036	0.007	0.933	0.240	0.625	0.706	0.402	0.400	0.528
O. garnettii	7.813	0.006	1.445	0.232	0.011	0.917	1.047	0.308	6.769	0.010	0.661	0.418	0.962	0.329	2.672	0.104	2.480	0.117
A. laniger	9.853	0.003	2.528	0.118	0.323	0.571	2.206	0.144	7.508	0.009	1.288	0.260	1.527	0.222	2.803	0.098	2.666	0.104
I. Indri	2.055	0.157	0.301	0.585	2.643	0.107	0.601	0.441	1.500	0.225	0.373	0.543	0.008	0.929	0.034	0.854	0.187	0.666
P. diadema	3.510	0.067	0.165	0.686	0.207	0.650	0.071	0.791	2.718	0.106	0.042	0.838	0.226	0.636	0.395	0.531	0.260	0.611
P. verreauxi	3.713	0.058	0.024	0.878	0.767	0.383	0.001	0.977	2.883	0.094	0.001	0.970	0.114	0.737	0.191	0.663	0.068	0.795
E. fulvus	4.654	0.032	0.640	0.425	0.284	0.594	0.391	0.532	4.139	0.043	0.242	0.624	0.461	0.498	1.687	0.195	1.652	0.200
E. macaco	1.056	0.307	0.405	0.526	3.636	0.059	0.705	0.404	0.822	0.368	0.533	0.467	0.030	0.863	0.125	0.725	0.457	0.500
E. mongoz	4.749	0.032	0.651	0.422	0.162	0.688	0.413	0.522	4.070	0.047	0.270	0.605	0.477	0.491	1.600	0.208	1.578	0.210
E. rubriventer	0.655	0.422	3.493	0.067	6.985	0.010	3.977	0.051	0.672	0.417	3.777	0.055	1.723	0.195	3.563	0.062	5.555	0.019
H. griseus	6.746	0.012	1.418	0.239	0.037	0.847	1.124	0.294	5.458	0.024	0.744	0.391	0.935	0.338	2.216	0.140	2.179	0.142
L. catta	4.478	0.039	0.034	0.855	1.204	0.275	0.001	0.975	3.444	0.069	0.002	0.967	0.128	0.722	0.288	0.593	0.112	0.738
V. variegata	1.746	0.191	0.035	0.853	1.769	0.186	0.132	0.717	1.399	0.242	0.107	0.744	0.009	0.925	0.013	0.910	0.013	0.910
L. ruficaudatus	5.039	0.030	0.690	0.410	0.015	0.902	0.483	0.490	4.023	0.051	0.319	0.574	0.551	0.461	1.228	0.271	1.100	0.295
L. tardigradus	4.381	0.042	0.017	0.898	1.767	0.187	0.011	0.917	3.343	0.074	0.010	0.922	0.103	0.749	0.283	0.596	0.097	0.756
N. bengalensis	1.099	0.300	0.459	0.501	2.101	0.151	0.762	0.387	0.727	0.399	0.458	0.501	0.049	0.826	0.121	0.729	0.308	0.579
N. coucang	10.782	0.001	1.174	0.281	0.527	0.469	0.690	0.408	8.783	0.004	0.329	0.567	0.770	0.382	2.398	0.124	1.924	0.167
P. potto	2.950	0.088	0.130	0.719	5.224	0.023	0.411	0.522	2.450	0.120	0.272	0.603	0.007	0.936	0.007	0.933	0.078	0.780

Goswami model ORAL- PC3	*G. zanzibaricus*		*O. crassicaudatus*		*O. garnettii*		*A. laniger*		*I. indri*		*P. diadema*		*P. verreauxi*		*E. fulvus*		*E. macaco*	
	F value	p value	F value	p value	F value	p value	F value	p value	F value	p value	F value	p value	F value	p value	F value	p value	F value	p value
C. major																		
C. medius																		
M. murinus																		
M. rufus																		
G. alleni																		
G. demidoff																		
E. elegantulus																		
G. moholi																		
G. senegalensus																		
G. zanzibaricus																		
O. crassicaudatus	0.066	0.797																
O. garnettii	0.072	0.789	1.162	0.282														
A. laniger	0.799	0.376	1.788	0.184	0.427	0.515												
I. Indri	0.818	0.369	0.779	0.379	2.439	0.121	4.419	0.040										
P. diadema	0.007	0.933	0.036	0.850	0.166	0.684	0.927	0.341	0.694	0.408								
P. verreauxi	0.128	0.721	0.016	0.900	0.663	0.417	2.004	0.162	0.414	0.522	0.074	0.787						
E. fulvus	0.003	0.959	0.523	0.470	0.149	0.699	0.531	0.467	1.177	0.279	0.021	0.884	0.207	0.650				
E. macaco	0.572	0.452	1.327	0.251	3.281	0.072	2.795	0.099	0.019	0.891	0.598	0.442	0.435	0.511	2.304	0.130		
E. mongoz	0.007	0.933	0.520	0.472	0.086	0.769	0.498	0.483	1.322	0.253	0.034	0.855	0.263	0.609	0.006	0.940	2.028	0.157
E. rubriventer	3.018	0.089	6.120	0.015	7.579	0.007	5.562	0.023	2.806	0.099	3.236	0.078	3.843	0.054	5.534	0.020	2.228	0.140
H. griseus	0.190	0.665	1.172	0.281	0.075	0.785	0.147	0.703	2.608	0.111	0.306	0.583	0.925	0.340	0.251	0.617	2.388	0.126
L. catta	0.137	0.713	0.026	0.873	1.010	0.317	2.252	0.139	0.531	0.469	0.083	0.775	0.000	0.999	0.368	0.545	0.620	0.433
V. variegata	0.225	0.637	0.315	0.576	1.584	0.210	1.740	0.192	0.064	0.802	0.204	0.653	0.080	0.778	0.897	0.345	0.149	0.700
L. ruficaudatus	0.043	0.837	0.453	0.502	0.003	0.956	0.383	0.539	1.585	0.213	0.093	0.762	0.422	0.518	0.035	0.851	1.453	0.232
L. tardigradus	0.163	0.689	0.074	0.786	1.454	0.230	2.355	0.132	0.485	0.489	0.110	0.741	0.003	0.957	0.667	0.415	0.646	0.424
N. bengalensis	1.151	0.289	0.817	0.368	2.069	0.153	4.858	0.033	0.056	0.813	0.876	0.354	0.628	0.431	0.956	0.329	0.004	0.947
N. coucang	0.002	0.969	0.593	0.443	0.309	0.579	1.537	0.218	2.594	0.110	0.030	0.863	0.405	0.526	0.007	0.932	3.161	0.078
P. potto	0.387	0.535	1.096	0.296	3.924	0.049	2.979	0.086	0.071	0.790	0.393	0.531	0.174	0.677	3.781	0.053	0.266	0.607

Goswami model ORAL- PC3	*E. mongoz*		*E. rubriventer*		*H. griseus*		*L. catta*		*V. variegata*		*L. ruficaudatus*		*L. tardigradus*		*N. bengalensis*		*N. coucang*	
	F value	p value	F value	p value	F value	p value	F value	p value	F value	p value	F value	p value	F value	p value	F value	p value	F value	p value
C. major																		
C. medius																		
M. murinus																		
M. rufus																		
G. alleni																		
G. demidoff																		
E. elegantulus																		
G. moholi																		
G. senegalensus																		
G. zanzibaricus																		
O. crassicaudatus																		
O. garnettii																		
A. laniger																		
I. Indri																		
P. diadema																		
P. verreauxi																		
E. fulvus																		
E. macaco																		
E. mongoz																		
E. rubriventer	4.793	0.031																
H. griseus	0.187	0.666	6.746	0.012														
L. catta	0.409	0.524	4.478	0.039	1.149	0.288												
V. variegata	0.812	0.370	2.561	0.115	1.257	0.267	0.110	0.742										
L. ruficaudatus	0.019	0.890	4.077	0.049	0.063	0.803	0.508	0.479	0.669	0.416								
L. tardigradus	0.630	0.430	3.784	0.057	1.334	0.254	0.005	0.946	0.091	0.764	0.600	0.443						
N. bengalensis	1.070	0.304	1.649	0.206	2.320	0.135	0.711	0.403	0.133	0.717	1.529	0.223	0.618	0.436				
N. coucang	0.027	0.871	8.282	0.005	0.601	0.440	0.669	0.415	1.250	0.266	0.108	0.743	1.123	0.292	2.443	0.122		
P. potto	2.775	0.097	4.627	0.033	2.727	0.101	0.312	0.577	0.005	0.944	1.439	0.232	0.356	0.552	0.172	0.679	3.946	0.048

Goswami model ORAL- PC4	*C. major*		*C.medius*		*M. murinus*		*M. rufus*		*G. alleni*		*G. denidoff*		*E. elegantulus*		*G. moholi*		*G.senegalensis*	
	F value	p value	F value	p value	F value	p value	F value	p value	F value	p value	F value	p value	F value	p value	F value	p value	F value	p value
C. major																		
C. medius	3.150	0.082																
M. murinus	0.000	0.995	4.949	0.028														
M. rufus	1.979	0.166	0.370	0.546	2.994	0.087												
G. alleni	0.230	0.634	1.854	0.180	0.233	0.631	0.885	0.351										
G. demidoff	0.074	0.786	1.166	0.283	0.148	0.701	0.537	0.466	0.002	0.962								
E. elegantulus	0.183	0.670	2.650	0.109	0.251	0.618	1.894	0.174	0.539	0.466	0.354	0.553						
G. moholi	0.155	0.694	3.209	0.076	0.294	0.588	1.572	0.213	0.012	0.913	0.001	0.977	0.656	0.420				
G. senegalensus	1.059	0.305	0.987	0.322	2.474	0.117	0.151	0.698	0.294	0.588	0.385	0.535	1.802	0.181	0.845	0.359		
G. zanzibaricus	2.578	0.115	0.174	0.678	2.553	0.113	0.637	0.428	1.847	0.181	0.936	0.336	2.150	0.148	2.114	0.149	0.921	0.338
O. crassicaudatus	0.080	0.778	5.764	0.018	0.182	0.671	3.134	0.079	0.092	0.762	0.036	0.850	0.643	0.424	0.059	0.809	1.902	0.169
O. garnettii	0.719	0.398	10.430	0.002	1.452	0.230	7.791	0.006	1.775	0.185	1.408	0.237	0.013	0.908	2.844	0.094	7.415	0.007
A. laniger	3.641	0.063	0.281	0.599	3.697	0.058	0.988	0.325	2.686	0.109	1.273	0.263	2.727	0.105	3.064	0.083	1.355	0.246
I. Indri	4.079	0.048	0.210	0.648	5.285	0.023	1.015	0.317	2.736	0.103	1.656	0.201	3.376	0.070	3.954	0.049	1.666	0.198
P. diadema	9.490	0.003	2.555	0.116	8.731	0.004	4.805	0.033	8.312	0.006	3.408	0.068	5.732	0.020	8.172	0.005	4.677	0.032
P. verreauxi	0.048	0.827	2.878	0.094	0.052	0.820	1.606	0.209	0.081	0.776	0.019	0.891	0.382	0.538	0.031	0.861	0.674	0.412
E. fulvus	2.108	0.148	0.844	0.359	5.841	0.016	0.023	0.879	0.773	0.381	0.915	0.340	2.872	0.092	2.253	0.135	0.149	0.700
E. macaco	0.154	0.696	4.266	0.042	0.218	0.641	2.246	0.138	0.041	0.840	0.006	0.938	0.660	0.419	0.006	0.937	0.951	0.330
E. mongoz	7.851	0.006	1.463	0.230	16.595	0.000	3.895	0.052	5.561	0.021	4.430	0.038	6.024	0.016	11.545	0.001	6.857	0.009
E. rubriventer	1.902	0.174	0.012	0.912	1.444	0.232	0.096	0.758	1.157	0.288	0.420	0.519	1.554	0.218	1.029	0.313	0.214	0.644
H. griseus	1.405	0.242	0.587	0.447	1.485	0.226	0.056	0.814	0.536	0.468	0.258	0.613	1.415	0.239	0.727	0.396	0.011	0.915
L. catta	0.433	0.513	1.028	0.315	0.795	0.375	0.319	0.574	0.066	0.799	0.075	0.784	0.813	0.370	0.211	0.647	0.087	0.769
V. variegata	0.135	0.714	2.375	0.128	0.228	0.634	1.166	0.284	0.008	0.930	0.000	0.988	0.519	0.474	0.000	0.988	0.622	0.431
L. ruficaudatus	3.736	0.059	0.151	0.699	4.467	0.037	0.846	0.362	2.567	0.116	1.353	0.248	2.872	0.096	3.423	0.067	1.382	0.241
L. tardigradus	4.271	0.044	0.285	0.595	9.076	0.003	1.369	0.247	2.822	0.100	2.207	0.141	3.435	0.069	6.178	0.015	3.121	0.079
N. bengalensis	0.195	0.661	0.721	0.400	0.241	0.625	0.278	0.601	0.012	0.912	0.015	0.902	0.451	0.505	0.044	0.834	0.098	0.754
N. coucang	1.065	0.305	1.914	0.170	2.337	0.129	0.495	0.483	0.225	0.637	0.227	0.635	1.617	0.207	0.679	0.411	0.064	0.800
P. potto	1.611	0.206	0.160	0.689	5.192	0.024	0.034	0.853	0.714	0.399	0.971	0.326	2.097	0.150	2.260	0.134	0.513	0.474

Goswami model ORAL- PC4	*G. zanzibaricus*		*O. crassicaudatus*		*O. garnettii*		*A. laniger*		*I. indri*		*P. diadema*		*P. verreauxi*		*E. fulvus*		*E. macaco*	
	F value	p value	F value	p value	F value	p value	F value	p value	F value	p value	F value	p value	F value	p value	F value	p value	F value	p value
C. major																		
C. medius																		
M. murinus																		
M. rufus																		
G. alleni																		
G. demidoff																		
E. elegantulus																		
G. moholi																		
G. senegalensus																		
G. zanzibaricus																		
O. crassicaudatus	3.061	0.083																
O. garnettii	4.936	0.028	3.278	0.072														
A. laniger	0.001	0.981	4.536	0.035	6.974	0.009												
I. Indri	0.010	0.920	6.180	0.014	10.003	0.002	0.022	0.882										
P. diadema	0.595	0.444	11.383	0.001	13.593	0.000	0.742	0.393	1.217	0.274								
P. verreauxi	2.596	0.112	0.000	0.983	1.208	0.274	3.660	0.060	3.838	0.054	9.756	0.003						
E. fulvus	0.883	0.348	5.286	0.022	13.946	0.000	1.352	0.246	1.651	0.200	5.399	0.021	1.448	0.230				
E. macaco	2.986	0.088	0.023	0.879	2.627	0.107	4.432	0.039	5.189	0.025	12.032	0.001	0.018	0.893	2.424	0.121		
E. mongoz	0.048	0.828	20.754	0.000	25.948	0.000	0.051	0.822	0.251	0.617	0.615	0.435	7.390	0.008	9.203	0.003	13.013	0.000
E. rubriventer	0.227	0.636	1.576	0.212	3.413	0.067	0.335	0.566	0.205	0.653	2.486	0.121	1.644	0.204	0.135	0.714	1.706	0.195
H. griseus	0.912	0.344	1.410	0.237	4.558	0.035	1.378	0.246	1.290	0.260	5.884	0.019	1.049	0.310	0.018	0.894	1.195	0.278
L. catta	0.929	0.339	0.573	0.450	3.441	0.066	1.332	0.254	1.670	0.201	4.386	0.041	0.269	0.605	0.424	0.516	0.303	0.584
V. variegata	1.744	0.192	0.053	0.818	2.211	0.139	2.505	0.119	3.160	0.080	6.996	0.010	0.031	0.860	1.603	0.207	0.008	0.929
L. ruficaudatus	0.017	0.896	5.395	0.022	8.718	0.004	0.034	0.854	0.002	0.964	1.314	0.257	3.642	0.061	1.344	0.248	4.794	0.032
L. tardigradus	0.008	0.930	11.534	0.001	16.356	0.000	0.018	0.893	0.000	0.991	1.150	0.289	4.253	0.043	3.684	0.056	7.289	0.009
N. bengalensis	0.871	0.356	0.141	0.708	1.384	0.242	1.166	0.287	1.265	0.265	3.720	0.060	0.106	0.746	0.299	0.585	0.081	0.776
N. coucang	1.426	0.236	1.868	0.174	7.925	0.005	2.173	0.144	2.752	0.100	7.276	0.008	0.650	0.422	0.662	0.417	0.907	0.343
P. potto	0.307	0.580	5.151	0.024	11.201	0.001	0.473	0.493	0.553	0.458	2.359	0.127	1.228	0.269	0.297	0.586	2.207	0.139

Goswami model ORAL- PC4	*E. mongoz*		*E. rubriventer*		*H. griseus*		*L. catta*		*V. variegata*		*L. ruficaudatus*		*L. tardigradus*		*N. bengalensis*		*N. coucang*	
	F value	p value	F value	p value	F value	p value	F value	p value	F value	p value	F value	p value	F value	p value	F value	p value	F value	p value
C. major																		
C. medius																		
M. murinus																		
M. rufus																		
G. alleni																		
G. demidoff																		
E. elegantulus																		
G. moholi																		
G. senegalensus																		
G. zanzibaricus																		
O. crassicaudatus																		
O. garnettii																		
A. laniger																		
I. Indri																		
P. diadema																		
P. verreauxi																		
E. fulvus																		
E. macaco																		
E. mongoz																		
E. rubriventer	0.688	0.409																
H. griseus	3.472	0.066	1.405	0.242														
L. catta	5.084	0.027	0.433	0.513	0.103	0.750												
V. variegata	8.355	0.005	0.910	0.344	0.585	0.447	0.144	0.706										
L. ruficaudatus	0.279	0.599	0.179	0.674	1.171	0.285	1.356	0.249	2.700	0.106								
L. tardigradus	0.397	0.531	0.189	0.666	1.436	0.236	2.210	0.143	4.195	0.045	0.003	0.954						
N. bengalensis	2.697	0.105	0.411	0.525	0.138	0.712	0.009	0.926	0.031	0.861	1.071	0.307	1.223	0.275				
N. coucang	11.182	0.001	0.467	0.496	0.104	0.747	0.017	0.897	0.477	0.491	2.330	0.130	5.070	0.027	0.046	0.831		
P. potto	3.894	0.050	0.015	0.902	0.106	0.746	0.572	0.451	1.508	0.221	0.419	0.519	1.233	0.269	0.321	0.572	1.135	0.288

Goswami model ORAL- PC5	*C. major*		*C.medius*		*M. murinus*		*M. rufus*		*G. alleni*		*G. denidoff*		*E. elegantulus*		*G. moholi*		*G.senegalensis*	
	F value	p value	F value	p value	F value	p value	F value	p value	F value	p value	F value	p value	F value	p value	F value	p value	F value	p value
C. major																		
C. medius	0.019	0.890																
M. murinus	0.093	0.761	0.034	0.853														
M. rufus	2.140	0.150	3.429	0.070	5.913	0.017												
G. alleni	0.416	0.522	0.651	0.424	1.132	0.290	0.453	0.504										
G. demidoff	0.431	0.514	0.811	0.370	1.477	0.226	0.397	0.530	0.002	0.965								
E. elegantulus	0.593	0.445	0.802	0.374	1.197	0.277	0.167	0.685	0.028	0.868	0.013	0.908						
G. moholi	4.955	0.028	8.386	0.005	13.478	0.000	1.086	0.300	2.105	0.150	2.250	0.136	1.145	0.287				
G. senegalensus	4.052	0.045	7.838	0.006	12.990	0.000	0.402	0.527	1.416	0.235	1.577	0.211	0.646	0.422	0.316	0.575		
G. zanzibaricus	1.458	0.233	1.647	0.205	2.286	0.134	0.052	0.821	0.439	0.511	0.339	0.562	0.253	0.617	0.128	0.721	0.009	0.925
O. crassicaudatus	2.221	0.139	4.549	0.035	8.144	0.005	0.098	0.755	0.338	0.562	0.305	0.582	0.075	0.785	2.700	0.102	1.347	0.247
O. garnettii	0.660	0.418	1.423	0.235	2.655	0.105	0.793	0.375	0.001	0.974	0.001	0.980	0.026	0.873	4.095	0.045	2.857	0.092
A. laniger	1.515	0.225	1.660	0.204	2.199	0.142	0.020	0.887	0.240	0.627	0.136	0.713	0.076	0.784	0.726	0.396	0.289	0.591
I. Indri	4.218	0.044	5.293	0.025	6.984	0.009	0.308	0.581	1.405	0.241	1.023	0.314	0.736	0.394	0.173	0.678	0.000	0.989
P. diadema	0.163	0.688	0.271	0.605	0.452	0.503	1.196	0.279	0.110	0.742	0.100	0.753	0.247	0.621	2.934	0.090	1.971	0.162
P. verreauxi	2.763	0.101	3.506	0.065	4.653	0.033	0.067	0.796	0.778	0.381	0.569	0.452	0.374	0.543	0.363	0.548	0.049	0.825
E. fulvus	1.071	0.302	2.783	0.097	5.651	0.018	2.441	0.120	0.005	0.941	0.027	0.870	0.100	0.752	10.277	0.002	7.261	0.007
E. macaco	0.015	0.901	0.120	0.730	0.362	0.548	4.019	0.048	0.580	0.449	0.612	0.436	0.771	0.382	9.082	0.003	7.092	0.008
E. mongoz	4.817	0.031	8.557	0.004	14.701	0.000	0.708	0.403	1.795	0.184	1.852	0.176	0.895	0.347	0.122	0.728	0.058	0.810
E. rubriventer	1.661	0.204	1.752	0.191	2.226	0.139	0.014	0.906	0.416	0.522	0.263	0.609	0.205	0.652	0.265	0.608	0.055	0.815
H. griseus	0.945	0.336	1.347	0.251	2.093	0.151	0.386	0.537	0.030	0.864	0.011	0.916	0.002	0.967	2.206	0.141	1.300	0.256
L. catta	5.348	0.025	7.737	0.007	11.958	0.001	1.163	0.285	2.273	0.137	2.137	0.147	1.333	0.253	0.007	0.934	0.368	0.545
V. variegata	1.019	0.317	1.740	0.192	3.014	0.085	0.247	0.621	0.070	0.793	0.046	0.830	0.003	0.959	2.203	0.141	1.318	0.252
L. ruficaudatus	1.812	0.185	2.349	0.132	3.489	0.065	0.000	0.985	0.369	0.547	0.270	0.605	0.143	0.707	0.726	0.396	0.253	0.616
L. tardigradus	0.091	0.764	0.284	0.596	0.805	0.372	1.691	0.199	0.125	0.725	0.204	0.653	0.230	0.633	6.016	0.016	5.580	0.019
N. bengalensis	0.194	0.662	0.304	0.584	0.522	0.472	0.770	0.385	0.043	0.837	0.050	0.824	0.134	0.716	2.321	0.131	1.598	0.208
N. coucang	0.314	0.577	0.885	0.349	1.996	0.160	3.121	0.081	0.157	0.693	0.225	0.636	0.312	0.578	9.653	0.002	7.696	0.006
P. potto	2.675	0.104	5.937	0.016	11.208	0.001	0.175	0.676	0.381	0.538	0.342	0.560	0.074	0.786	3.852	0.051	2.012	0.157

Goswami model ORAL- PC5	*G. zanzibaricus*		*O. crassicaudatus*		*O. garnettii*		*A. laniger*		*I. indri*		*P. diadema*		*P. verreauxi*		*E. fulvus*		*E. macaco*	
	F value	p value	F value	p value	F value	p value	F value	p value	F value	p value	F value	p value	F value	p value	F value	p value	F value	p value
C. major																		
C. medius																		
M. murinus																		
M. rufus																		
G. alleni																		
G. demidoff																		
E. elegantulus																		
G. moholi																		
G. senegalensus																		
G. zanzibaricus																		
O. crassicaudatus	0.176	0.675																
O. garnettii	0.525	0.470	0.632	0.428														
A. laniger	0.115	0.736	0.003	0.960	0.226	0.635												
I. Indri	0.012	0.912	0.762	0.384	1.697	0.195	0.464	0.498										
P. diadema	1.135	0.292	0.855	0.357	0.133	0.716	1.204	0.278	3.221	0.077								
P. verreauxi	0.004	0.952	0.271	0.603	0.916	0.340	0.151	0.699	0.062	0.804	1.886	0.174						
E. fulvus	1.143	0.286	2.265	0.133	0.032	0.859	0.590	0.443	3.945	0.048	0.154	0.695	2.097	0.149				
E. macaco	2.108	0.151	3.949	0.049	0.980	0.324	2.041	0.157	6.477	0.013	0.139	0.710	4.025	0.048	1.660	0.199		
E. mongoz	0.041	0.840	2.187	0.141	3.699	0.056	0.509	0.478	0.028	0.868	2.789	0.099	0.158	0.692	11.062	0.001	9.566	0.003
E. rubriventer	0.013	0.910	0.089	0.767	0.404	0.526	0.074	0.787	0.088	0.768	1.396	0.243	0.007	0.936	0.903	0.343	2.204	0.142
H. griseus	0.427	0.516	0.198	0.657	0.026	0.871	0.187	0.667	1.529	0.221	0.404	0.528	0.741	0.392	0.142	0.707	1.357	0.248
L. catta	0.171	0.681	2.665	0.105	3.902	0.050	0.995	0.323	0.270	0.605	3.888	0.053	0.495	0.484	9.811	0.002	9.979	0.002
V. variegata	0.270	0.605	0.109	0.741	0.099	0.754	0.064	0.802	1.002	0.320	0.387	0.536	0.467	0.496	0.394	0.531	1.665	0.200
L. ruficaudatus	0.056	0.814	0.047	0.829	0.474	0.493	0.016	0.899	0.285	0.596	1.203	0.278	0.068	0.796	1.247	0.265	2.862	0.095
L. tardigradus	0.794	0.377	2.350	0.128	0.372	0.543	0.616	0.436	2.872	0.095	0.003	0.956	1.757	0.190	0.659	0.418	0.109	0.742
N. bengalensis	0.752	0.391	0.596	0.442	0.065	0.799	0.651	0.424	2.185	0.145	0.012	0.915	1.287	0.261	0.062	0.803	0.205	0.652
N. coucang	1.384	0.243	3.390	0.067	0.388	0.534	1.046	0.309	4.835	0.030	0.002	0.968	2.768	0.099	0.631	0.428	0.401	0.528
P. potto	0.237	0.627	0.005	0.944	0.753	0.387	0.008	0.930	1.038	0.310	0.972	0.326	0.378	0.539	3.231	0.073	4.949	0.027

Goswami model ORAL- PC5	*E. mongoz*		*E. rubriventer*		*H. griseus*		*L. catta*		*V. variegata*		*L. ruficaudatus*		*L. tardigradus*		*N. bengalensis*		*N. coucang*	
	F value	p value	F value	p value	F value	p value	F value	p value	F value	p value	F value	p value	F value	p value	F value	p value	F value	p value
C. major																		
C. medius																		
M. murinus																		
M. rufus																		
G. alleni																		
G. demidoff																		
E. elegantulus																		
G. moholi																		
G. senegalensus																		
G. zanzibaricus																		
O. crassicaudatus																		
O. garnettii																		
A. laniger																		
I. Indri																		
P. diadema																		
P. verreauxi																		
E. fulvus																		
E. macaco																		
E. mongoz																		
E. rubriventer	0.133	0.716																
H. griseus	1.894	0.173	0.945	0.336														
L. catta	0.174	0.678	5.348	0.025	2.644	0.109												
V. variegata	1.805	0.182	0.200	0.657	0.015	0.904	2.267	0.137										
L. ruficaudatus	0.458	0.501	0.019	0.892	0.315	0.578	0.883	0.351	0.163	0.687								
L. tardigradus	5.931	0.017	0.766	0.386	0.367	0.547	5.050	0.029	0.613	0.437	1.023	0.317						
N. bengalensis	2.104	0.151	0.857	0.359	0.194	0.662	2.809	0.100	0.225	0.637	0.735	0.396	0.016	0.899				
N. coucang	10.536	0.002	1.288	0.259	0.541	0.464	9.484	0.003	0.910	0.342	1.800	0.183	0.028	0.868	0.006	0.939		
P. potto	3.402	0.067	0.124	0.725	0.211	0.647	3.727	0.055	0.111	0.740	0.079	0.778	3.212	0.075	0.679	0.411	4.767	0.030

Goswami model ZYGOMATIC- PC1	*C. major*		*C.medius*		*M. murinus*		*M. rufus*		*G. alleni*		*G. denidoff*		*E. elegantulus*		*G. moholi*		*G.senegalensis*	
	F value	p value	F value	p value	F value	p value	F value	p value	F value	p value	F value	p value	F value	p value	F value	p value	F value	p value
C. major																		
C. medius	0.012	0.913																
M. murinus	0.414	0.521	0.252	0.617														
M. rufus	0.497	0.484	0.305	0.583	0.000	0.987												
G. alleni	1.375	0.247	1.047	0.311	0.216	0.643	0.373	0.544										
G. demidoff	0.049	0.826	0.106	0.745	0.926	0.338	0.925	0.339	1.921	0.170								
E. elegantulus	0.187	0.667	0.120	0.730	0.001	0.980	0.000	0.989	0.153	0.697	0.409	0.524						
G. moholi	0.060	0.808	0.111	0.739	0.915	0.340	0.773	0.381	1.506	0.223	0.003	0.954	0.387	0.535				
G. senegalensus	0.940	0.334	1.084	0.299	4.608	0.033	3.618	0.059	5.009	0.026	0.564	0.453	1.674	0.197	0.379	0.539		
G. zanzibaricus	0.006	0.939	0.001	0.982	0.236	0.628	0.285	0.596	0.942	0.337	0.076	0.783	0.116	0.735	0.083	0.774	0.863	0.354
O. crassicaudatus	0.154	0.695	0.269	0.605	2.247	0.136	1.990	0.161	3.580	0.061	0.008	0.929	0.783	0.378	0.000	0.999	1.085	0.298
O. garnettii	0.740	0.391	0.902	0.344	3.925	0.049	3.678	0.058	5.451	0.021	0.345	0.558	1.419	0.236	0.193	0.661	0.100	0.752
A. laniger	1.910	0.174	1.616	0.210	0.658	0.420	0.972	0.329	0.230	0.634	2.609	0.110	0.462	0.499	2.092	0.152	5.825	0.017
I. Indri	0.646	0.425	0.470	0.495	0.050	0.823	0.076	0.784	0.050	0.823	1.035	0.312	0.041	0.839	0.882	0.350	3.025	0.083
P. diadema	0.054	0.818	0.105	0.747	0.617	0.434	0.794	0.377	1.733	0.194	0.002	0.961	0.328	0.569	0.000	0.997	0.269	0.605
P. verreauxi	0.013	0.910	0.000	0.999	0.247	0.620	0.316	0.576	1.117	0.295	0.106	0.746	0.131	0.718	0.111	0.740	0.982	0.323
E. fulvus	0.006	0.938	0.002	0.963	0.637	0.426	0.415	0.520	1.100	0.296	0.121	0.728	0.201	0.655	0.160	0.690	2.080	0.150
E. macaco	0.030	0.863	0.004	0.950	0.200	0.655	0.206	0.651	0.811	0.371	0.153	0.697	0.095	0.759	0.162	0.688	1.230	0.269
E. mongoz	0.273	0.603	0.147	0.703	0.029	0.865	0.022	0.883	0.421	0.518	0.667	0.416	0.008	0.930	0.641	0.425	3.524	0.062
E. rubriventer	0.028	0.869	0.004	0.947	0.129	0.720	0.176	0.677	0.774	0.384	0.124	0.726	0.070	0.792	0.121	0.729	0.880	0.349
H. griseus	4.629	0.036	3.936	0.053	1.959	0.165	2.956	0.091	1.138	0.291	5.827	0.018	1.286	0.262	4.543	0.036	12.055	0.001
L. catta	0.463	0.499	0.559	0.458	1.775	0.186	1.679	0.200	2.446	0.124	0.337	0.563	0.805	0.373	0.231	0.632	0.028	0.868
V. variegata	0.214	0.645	0.289	0.593	1.133	0.290	1.101	0.298	1.836	0.181	0.110	0.741	0.545	0.463	0.066	0.798	0.022	0.884
L. ruficaudatus	0.002	0.960	0.002	0.963	0.219	0.641	0.308	0.581	1.025	0.317	0.054	0.816	0.123	0.728	0.059	0.808	0.643	0.424
L. tardigradus	0.182	0.672	0.066	0.798	0.216	0.643	0.193	0.662	1.026	0.316	0.617	0.434	0.058	0.811	0.571	0.452	5.616	0.019
N. bengalensis	1.332	0.255	1.077	0.305	0.307	0.581	0.498	0.484	0.035	0.853	1.846	0.178	0.224	0.638	1.464	0.229	4.418	0.037
N. coucang	0.707	0.403	0.830	0.365	3.019	0.085	2.758	0.100	3.931	0.050	0.440	0.508	1.202	0.276	0.286	0.593	0.003	0.958
P. potto	0.583	0.446	0.324	0.570	0.008	0.931	0.003	0.958	0.403	0.526	1.355	0.246	0.000	0.984	1.351	0.247	8.208	0.004

Goswami model ZYGOMATIC- PC1	*G. zanzibaricus*		*O. crassicaudatus*		*O. garnettii*		*A. laniger*		*I. indri*		*P. diadema*		*P. verreauxi*		*E. fulvus*		*E. macaco*	
	F value	p value	F value	p value	F value	p value	F value	p value	F value	p value	F value	p value	F value	p value	F value	p value	F value	p value
C. major																		
C. medius																		
M. murinus																		
M. rufus																		
G. alleni																		
G. demidoff																		
E. elegantulus																		
G. moholi																		
G. senegalensus																		
G. zanzibaricus																		
O. crassicaudatus	0.195	0.660																
O. garnettii	0.697	0.406	0.673	0.413														
A. laniger	1.448	0.235	4.508	0.036	6.131	0.015												
I. Indri	0.440	0.510	1.849	0.176	2.973	0.087	0.379	0.541										
P. diadema	0.077	0.782	0.000	0.996	0.156	0.694	2.237	0.141	0.909	0.344								
P. verreauxi	0.001	0.981	0.247	0.620	0.828	0.365	1.794	0.185	0.496	0.483	0.113	0.738						
E. fulvus	0.000	0.986	0.427	0.514	1.529	0.217	1.769	0.185	0.557	0.456	0.095	0.758	0.002	0.964				
E. macaco	0.007	0.936	0.349	0.556	0.994	0.320	1.428	0.236	0.373	0.543	0.141	0.708	0.004	0.950	0.014	0.905		
E. mongoz	0.143	0.707	1.586	0.210	3.093	0.081	0.982	0.325	0.137	0.712	0.487	0.487	0.146	0.703	0.321	0.572	0.100	0.753
E. rubriventer	0.007	0.934	0.268	0.606	0.767	0.383	1.295	0.261	0.325	0.571	0.128	0.722	0.005	0.945	0.011	0.916	0.000	0.993
H. griseus	3.482	0.068	10.306	0.002	13.352	0.000	0.159	0.692	1.309	0.257	4.943	0.031	4.227	0.044	4.211	0.041	3.403	0.069
L. catta	0.447	0.506	0.549	0.460	0.119	0.730	2.792	0.101	1.626	0.207	0.181	0.672	0.595	0.443	0.875	0.351	0.684	0.410
V. variegata	0.229	0.634	0.148	0.701	0.000	0.990	2.287	0.136	1.170	0.283	0.054	0.817	0.306	0.582	0.402	0.527	0.368	0.546
L. ruficaudatus	0.001	0.982	0.134	0.715	0.528	0.469	1.541	0.221	0.462	0.499	0.063	0.803	0.002	0.961	0.000	0.992	0.010	0.920
L. tardigradus	0.067	0.797	2.347	0.128	5.456	0.021	1.660	0.204	0.374	0.543	0.418	0.521	0.066	0.798	0.227	0.634	0.029	0.865
N. bengalensis	0.971	0.330	3.244	0.074	4.702	0.032	0.071	0.792	0.128	0.722	1.653	0.205	1.186	0.280	1.121	0.291	0.894	0.348
N. coucang	0.658	0.419	0.796	0.374	0.097	0.756	4.431	0.038	2.375	0.126	0.222	0.639	0.803	0.372	1.383	0.241	0.949	0.332
P. potto	0.303	0.583	4.218	0.041	7.564	0.006	1.072	0.302	0.107	0.744	0.848	0.358	0.297	0.587	1.033	0.310	0.238	0.626

Goswami model ZYGOMATIC- PC1	*E. mongoz*		*E. rubriventer*		*H. griseus*		*L. catta*		*V. variegata*		*L. ruficaudatus*		*L. tardigradus*		*N. bengalensis*		*N. coucang*	
	F value	p value	F value	p value	F value	p value	F value	p value	F value	p value	F value	p value	F value	p value	F value	p value	F value	p value
C. major																		
C. medius																		
M. murinus																		
M. rufus																		
G. alleni																		
G. demidoff																		
E. elegantulus																		
G. moholi																		
G. senegalensus																		
G. zanzibaricus																		
O. crassicaudatus																		
O. garnettii																		
A. laniger																		
I. Indri																		
P. diadema																		
P. verreauxi																		
E. fulvus																		
E. macaco																		
E. mongoz																		
E. rubriventer	0.068	0.796																
H. griseus	2.725	0.103	4.629	0.036														
L. catta	1.495	0.225	0.463	0.499	5.666	0.021												
V. variegata	0.917	0.341	0.281	0.598	4.711	0.034	0.033	0.856										
L. ruficaudatus	0.142	0.707	0.011	0.916	3.613	0.063	0.378	0.541	0.190	0.664								
L. tardigradus	0.064	0.800	0.018	0.895	4.746	0.034	1.540	0.220	0.855	0.359	0.074	0.786						
N. bengalensis	0.522	0.472	0.843	0.363	0.540	0.466	2.184	0.145	1.718	0.195	1.059	0.309	1.028	0.316				
N. coucang	2.454	0.120	0.706	0.403	9.247	0.003	0.011	0.918	0.022	0.882	0.520	0.473	3.354	0.070	3.435	0.067		
P. potto	0.020	0.889	0.148	0.701	3.160	0.077	2.774	0.098	1.666	0.199	0.271	0.604	0.357	0.551	0.525	0.470	5.144	0.024

Goswami model ZYGOMATIC- PC2	*C. major*		*C.medius*		*M. murinus*		*M. rufus*		*G. alleni*		*G. denidoff*		*E. elegantulus*		*G. moholi*		*G.senegalensis*	
	F value	p value	F value	p value	F value	p value	F value	p value	F value	p value	F value	p value	F value	p value	F value	p value	F value	p value
C. major																		
C. medius	0.074	0.787																
M. murinus	0.196	0.659	0.511	0.476														
M. rufus	0.071	0.791	0.000	0.994	0.539	0.465												
G. alleni	0.266	0.609	0.645	0.426	0.037	0.849	0.631	0.431										
G. demidoff	1.414	0.238	0.906	0.344	3.459	0.065	0.975	0.326	2.225	0.140								
E. elegantulus	0.726	0.398	1.540	0.219	0.194	0.660	1.475	0.229	0.050	0.824	3.209	0.077						
G. moholi	0.221	0.639	0.021	0.886	1.094	0.297	0.024	0.877	1.141	0.288	1.145	0.287	2.106	0.150				
G. senegalensus	1.763	0.186	0.818	0.367	5.208	0.023	0.923	0.338	3.249	0.073	0.314	0.576	4.400	0.037	0.854	0.356		
G. zanzibaricus	0.171	0.681	0.041	0.841	0.693	0.407	0.043	0.837	0.726	0.399	0.466	0.497	1.570	0.215	0.011	0.915	0.312	0.577
O. crassicaudatus	0.380	0.539	0.026	0.873	2.160	0.143	0.032	0.859	1.859	0.175	2.315	0.130	3.292	0.072	0.002	0.968	2.245	0.135
O. garnettii	1.664	0.200	0.724	0.396	4.805	0.030	0.802	0.372	3.473	0.065	0.671	0.414	5.424	0.021	0.628	0.429	0.139	0.709
A. laniger	1.656	0.205	1.598	0.212	2.403	0.125	1.516	0.224	2.658	0.110	0.040	0.842	5.264	0.026	1.460	0.230	0.436	0.510
I. Indri	0.045	0.832	0.001	0.981	0.337	0.563	0.000	0.987	0.486	0.488	0.699	0.405	1.110	0.296	0.021	0.885	0.570	0.451
P. diadema	0.029	0.866	0.015	0.905	0.344	0.559	0.012	0.912	0.529	0.470	1.022	0.315	1.408	0.240	0.073	0.787	0.976	0.324
P. verreauxi	1.012	0.318	0.635	0.428	1.925	0.168	0.632	0.429	2.266	0.137	0.142	0.707	4.340	0.041	0.468	0.495	0.001	0.979
E. fulvus	0.017	0.897	0.161	0.688	0.186	0.667	0.174	0.677	0.225	0.636	2.952	0.087	0.491	0.484	0.440	0.508	4.076	0.044
E. macaco	6.505	0.013	5.815	0.018	9.446	0.003	5.959	0.017	7.652	0.007	1.327	0.252	10.972	0.001	6.818	0.010	4.655	0.032
E. mongoz	1.871	0.175	1.193	0.278	4.005	0.048	1.259	0.265	3.183	0.078	0.034	0.855	5.041	0.027	1.243	0.267	0.139	0.710
E. rubriventer	0.002	0.963	0.093	0.762	0.098	0.755	0.087	0.770	0.195	0.661	1.065	0.305	0.595	0.444	0.209	0.648	1.163	0.282
H. griseus	0.154	0.696	0.477	0.493	0.001	0.972	0.459	0.501	0.019	0.892	1.876	0.175	0.162	0.689	0.811	0.370	2.474	0.117
L. catta	2.147	0.149	1.691	0.199	3.720	0.057	1.687	0.199	3.525	0.066	0.001	0.973	6.486	0.013	1.581	0.211	0.275	0.601
V. variegata	0.556	0.459	0.286	0.595	1.516	0.221	0.298	0.587	1.324	0.255	0.182	0.671	2.330	0.131	0.257	0.613	0.019	0.890
L. ruficaudatus	0.001	0.976	0.060	0.807	0.163	0.688	0.054	0.817	0.302	0.585	1.001	0.320	0.900	0.347	0.150	0.699	1.029	0.312
L. tardigradus	1.479	0.230	0.918	0.342	4.744	0.032	1.007	0.320	2.217	0.143	0.030	0.863	3.605	0.063	1.350	0.248	0.260	0.610
N. bengalensis	4.483	0.040	4.709	0.035	6.543	0.012	4.629	0.037	5.262	0.027	1.423	0.237	8.606	0.005	5.938	0.017	4.450	0.036
N. coucang	2.044	0.156	1.194	0.277	4.688	0.032	1.281	0.261	3.557	0.063	0.113	0.738	5.546	0.021	1.212	0.273	0.058	0.810
P. potto	5.544	0.020	3.694	0.056	12.569	0.000	4.137	0.044	6.421	0.012	0.450	0.503	7.932	0.005	5.119	0.025	3.989	0.047

Goswami model ZYGOMATIC- PC2	*G. zanzibaricus*		*O. crassicaudatus*		*O. garnettii*		*A. laniger*		*I. indri*		*P. diadema*		*P. verreauxi*		*E. fulvus*		*E. macaco*	
	F value	p value	F value	p value	F value	p value	F value	p value	F value	p value	F value	p value	F value	p value	F value	p value	F value	p value
C. major																		
C. medius																		
M. murinus																		
M. rufus																		
G. alleni																		
G. demidoff																		
E. elegantulus																		
G. moholi																		
G. senegalensus																		
G. zanzibaricus																		
O. crassicaudatus	0.029	0.864																
O. garnettii	0.195	0.660	1.900	0.170														
A. laniger	0.802	0.375	2.394	0.124	0.966	0.328												
I. Indri	0.038	0.845	0.025	0.875	0.487	0.487	1.257	0.267										
P. diadema	0.094	0.760	0.105	0.746	0.975	0.325	2.146	0.150	0.006	0.939								
P. verreauxi	0.211	0.648	0.852	0.358	0.041	0.839	0.547	0.462	0.478	0.491	0.933	0.338						
E. fulvus	0.318	0.573	0.982	0.323	3.327	0.069	1.636	0.202	0.094	0.759	0.077	0.782	1.064	0.303				
E. macaco	3.758	0.056	11.908	0.001	7.301	0.008	0.663	0.418	4.380	0.039	6.348	0.014	3.288	0.073	7.788	0.006		
E. mongoz	0.530	0.469	2.617	0.108	0.525	0.470	0.190	0.665	0.864	0.355	1.455	0.231	0.094	0.760	2.860	0.092	2.745	0.100
E. rubriventer	0.185	0.669	0.312	0.577	1.177	0.280	1.801	0.186	0.062	0.805	0.047	0.829	1.006	0.320	0.003	0.959	5.380	0.023
H. griseus	0.583	0.449	1.282	0.260	2.720	0.102	2.725	0.106	0.346	0.558	0.377	0.542	2.028	0.159	0.093	0.761	7.330	0.008
L. catta	0.752	0.390	3.100	0.081	0.837	0.362	0.119	0.731	1.199	0.277	2.217	0.142	0.263	0.610	2.541	0.112	2.180	0.144
V. variegata	0.086	0.770	0.497	0.482	0.003	0.953	0.356	0.553	0.235	0.629	0.398	0.530	0.008	0.931	0.944	0.332	2.680	0.105
L. ruficaudatus	0.153	0.698	0.221	0.639	1.079	0.301	2.118	0.153	0.036	0.851	0.022	0.884	1.050	0.309	0.017	0.897	5.735	0.019
L. tardigradus	0.390	0.535	4.312	0.040	0.880	0.350	0.111	0.740	0.655	0.422	1.057	0.309	0.081	0.777	4.930	0.028	2.380	0.127
N. bengalensis	3.062	0.087	9.620	0.002	6.477	0.012	1.018	0.319	3.989	0.051	5.321	0.026	3.584	0.063	5.731	0.018	0.218	0.642
N. coucang	0.487	0.487	2.866	0.092	0.399	0.528	0.340	0.561	0.829	0.365	1.471	0.228	0.040	0.843	3.364	0.068	3.902	0.051
P. potto	2.212	0.139	14.219	0.000	6.711	0.010	0.032	0.859	2.461	0.119	3.745	0.055	1.180	0.279	13.455	0.000	0.861	0.355

Goswami model ZYGOMATIC- PC2	*E. mongoz*		*E. rubriventer*		*H. griseus*		*L. catta*		*V. variegata*		*L. ruficaudatus*		*L. tardigradus*		*N. bengalensis*		*N. coucang*	
	F value	p value	F value	p value	F value	p value	F value	p value	F value	p value	F value	p value	F value	p value	F value	p value	F value	p value
C. major																		
C. medius																		
M. murinus																		
M. rufus																		
G. alleni																		
G. demidoff																		
E. elegantulus																		
G. moholi																		
G. senegalensus																		
G. zanzibaricus																		
O. crassicaudatus																		
O. garnettii																		
A. laniger																		
I. Indri																		
P. diadema																		
P. verreauxi																		
E. fulvus																		
E. macaco																		
E. mongoz																		
E. rubriventer	1.483	0.227																
H. griseus	2.738	0.102	0.154	0.696														
L. catta	0.032	0.858	2.147	0.149	3.334	0.073												
V. variegata	0.129	0.720	0.503	0.481	1.103	0.298	0.232	0.631										
L. ruficaudatus	1.463	0.230	0.006	0.937	0.194	0.662	2.179	0.146	0.460	0.500								
L. tardigradus	0.000	0.986	1.024	0.316	1.910	0.173	0.021	0.884	0.115	0.735	0.984	0.326						
N. bengalensis	2.859	0.095	4.355	0.043	5.501	0.023	2.474	0.122	2.455	0.123	4.798	0.034	1.802	0.186				
N. coucang	0.026	0.871	1.533	0.219	2.978	0.088	0.128	0.721	0.079	0.779	1.492	0.225	0.040	0.843	3.847	0.053		
P. potto	1.097	0.296	3.408	0.067	5.386	0.022	0.528	0.469	1.388	0.240	3.312	0.071	1.824	0.179	1.363	0.245	2.079	0.151

Goswami model ZYGOMATIC- PC3	*C. major*		*C.medius*		*M. murinus*		*M. rufus*		*G. alleni*		*G. denidoff*		*E. elegantulus*		*G. moholi*		*G.senegalensis*	
	F value	p value	F value	p value	F value	p value	F value	p value	F value	p value	F value	p value	F value	p value	F value	p value	F value	p value
C. major																		
C. medius	8.153	0.006																
M. murinus	19.253	0.000	1.458	0.230														
M. rufus	0.893	0.349	3.449	0.069	10.373	0.002												
G. alleni	1.487	0.229	0.968	0.330	4.103	0.046	0.225	0.638										
G. demidoff	1.811	0.182	1.746	0.190	8.082	0.005	0.153	0.696	0.024	0.876								
E. elegantulus	1.162	0.286	2.098	0.153	5.834	0.017	0.054	0.816	0.061	0.805	0.013	0.910						
G. moholi	4.335	0.040	2.098	0.151	9.330	0.003	0.689	0.409	0.003	0.956	0.097	0.756	0.177	0.675				
G. senegalensus	7.323	0.007	2.391	0.124	15.121	0.000	1.278	0.260	0.025	0.875	0.286	0.594	0.315	0.575	0.019	0.890		
G. zanzibaricus	0.013	0.909	7.550	0.008	15.217	0.000	0.648	0.425	1.247	0.270	1.283	0.261	0.963	0.331	3.295	0.073	4.900	0.028
O. crassicaudatus	0.483	0.488	13.591	0.000	42.696	0.000	0.764	0.384	2.014	0.158	2.424	0.122	1.038	0.310	5.578	0.019	12.796	0.000
O. garnettii	3.378	0.069	5.955	0.016	24.635	0.000	0.085	0.771	0.245	0.621	0.117	0.733	0.009	0.925	0.801	0.372	2.197	0.139
A. laniger	0.436	0.512	2.411	0.127	5.734	0.019	0.004	0.952	0.186	0.669	0.118	0.732	0.064	0.801	0.489	0.486	0.744	0.389
I. Indri	2.357	0.130	0.494	0.485	2.791	0.098	0.581	0.449	0.054	0.816	0.180	0.672	0.261	0.611	0.081	0.776	0.060	0.807
P. diadema	2.607	0.113	2.197	0.144	6.392	0.013	0.358	0.552	0.001	0.974	0.023	0.880	0.088	0.768	0.015	0.904	0.058	0.810
P. verreauxi	1.699	0.197	1.932	0.169	6.537	0.012	0.143	0.706	0.026	0.871	0.000	0.995	0.013	0.910	0.092	0.762	0.209	0.648
E. fulvus	6.571	0.011	0.935	0.335	8.638	0.004	1.559	0.213	0.143	0.706	0.644	0.423	0.498	0.481	0.242	0.623	0.297	0.586
E. macaco	0.823	0.367	3.080	0.083	9.495	0.003	0.001	0.982	0.246	0.622	0.166	0.684	0.059	0.808	0.632	0.428	1.151	0.285
E. mongoz	0.178	0.675	6.758	0.011	19.637	0.000	0.411	0.523	1.087	0.300	1.245	0.267	0.617	0.434	2.903	0.091	5.553	0.019
E. rubriventer	1.239	0.271	1.267	0.265	4.418	0.038	0.129	0.721	0.009	0.923	0.002	0.969	0.020	0.888	0.041	0.840	0.104	0.748
H. griseus	3.837	0.056	0.021	0.886	1.173	0.282	1.522	0.223	0.406	0.527	0.828	0.365	0.929	0.339	0.858	0.357	1.006	0.317
L. catta	2.596	0.113	1.494	0.226	6.533	0.012	0.405	0.527	0.001	0.982	0.051	0.821	0.107	0.744	0.001	0.973	0.025	0.874
V. variegata	9.580	0.003	0.400	0.529	0.170	0.681	4.916	0.030	1.862	0.178	3.402	0.068	3.111	0.082	4.145	0.044	5.648	0.018
L. ruficaudatus	1.389	0.245	1.222	0.274	4.356	0.040	0.171	0.681	0.004	0.953	0.007	0.932	0.036	0.851	0.022	0.883	0.067	0.796
L. tardigradus	1.268	0.266	4.162	0.046	19.039	0.000	0.000	0.986	0.250	0.620	0.239	0.626	0.053	0.818	1.060	0.306	3.183	0.076
N. bengalensis	2.275	0.139	0.533	0.469	2.528	0.115	0.584	0.448	0.056	0.813	0.167	0.684	0.291	0.592	0.091	0.763	0.063	0.802
N. coucang	4.895	0.029	1.605	0.208	9.516	0.002	0.926	0.338	0.027	0.871	0.218	0.641	0.266	0.607	0.029	0.864	0.005	0.942
P. potto	3.924	0.049	2.586	0.110	15.093	0.000	0.423	0.516	0.012	0.912	0.017	0.896	0.054	0.816	0.071	0.791	0.342	0.559

Goswami model ZYGOMATIC- PC3	*G. zanzibaricus*		*O. crassicaudatus*		*O. garnettii*		*A. laniger*		*I. indri*		*P. diadema*		*P. verreauxi*		*E. fulvus*		*E. macaco*	
	F value	p value	F value	p value	F value	p value	F value	p value	F value	p value	F value	p value	F value	p value	F value	p value	F value	p value
C. major																		
C. medius																		
M. murinus																		
M. rufus																		
G. alleni																		
G. demidoff																		
E. elegantulus																		
G. moholi																		
G. senegalensus																		
G. zanzibaricus																		
O. crassicaudatus	0.195	0.660																
O. garnettii	2.159	0.144	4.879	0.028														
A. laniger	0.343	0.561	0.262	0.609	0.081	0.776												
I. Indri	2.031	0.159	3.043	0.083	0.738	0.392	0.464	0.499										
P. diadema	2.335	0.133	2.931	0.089	0.315	0.575	0.317	0.576	0.110	0.742								
P. verreauxi	1.355	0.249	1.778	0.185	0.082	0.775	0.132	0.717	0.191	0.663	0.029	0.864						
E. fulvus	4.407	0.037	12.990	0.000	3.290	0.071	0.853	0.357	0.001	0.977	0.228	0.633	0.434	0.511				
E. macaco	0.571	0.452	0.574	0.450	0.089	0.766	0.002	0.967	0.588	0.445	0.329	0.568	0.149	0.701	1.454	0.229		
E. mongoz	0.071	0.791	0.006	0.940	1.918	0.168	0.166	0.685	1.767	0.187	1.560	0.215	1.017	0.316	5.650	0.018	0.352	0.554
E. rubriventer	1.042	0.312	1.411	0.237	0.094	0.760	0.121	0.730	0.114	0.737	0.009	0.924	0.002	0.964	0.252	0.617	0.141	0.709
H. griseus	3.450	0.069	6.404	0.013	2.593	0.110	1.110	0.298	0.190	0.665	0.759	0.388	0.863	0.356	0.362	0.548	1.564	0.215
L. catta	2.080	0.155	3.687	0.057	0.489	0.486	0.303	0.584	0.067	0.796	0.005	0.943	0.052	0.820	0.202	0.654	0.406	0.526
V. variegata	8.316	0.005	18.214	0.000	9.720	0.002	3.166	0.080	1.265	0.264	3.199	0.079	3.241	0.076	2.930	0.088	4.779	0.031
L. ruficaudatus	1.186	0.282	1.656	0.201	0.146	0.703	0.154	0.697	0.091	0.764	0.002	0.963	0.009	0.926	0.204	0.652	0.183	0.670
L. tardigradus	0.798	0.376	2.176	0.143	0.190	0.664	0.005	0.942	0.648	0.424	0.385	0.538	0.166	0.685	3.965	0.048	0.002	0.965
N. bengalensis	2.152	0.150	2.973	0.087	0.735	0.393	0.500	0.483	0.000	0.991	0.144	0.706	0.204	0.653	0.000	0.991	0.574	0.451
N. coucang	3.547	0.063	8.420	0.004	1.539	0.217	0.575	0.450	0.030	0.864	0.063	0.802	0.181	0.671	0.136	0.713	0.866	0.354
P. potto	2.512	0.115	7.396	0.007	0.602	0.439	0.260	0.611	0.195	0.660	0.007	0.933	0.013	0.909	1.080	0.299	0.411	0.522

Goswami model ZYGOMATIC- PC3	*E. mongoz*		*E. rubriventer*		*H. griseus*		*L. catta*		*V. variegata*		*L. ruficaudatus*		*L. tardigradus*		*N. bengalensis*		*N. coucang*	
	F value	p value	F value	p value	F value	p value	F value	p value	F value	p value	F value	p value	F value	p value	F value	p value	F value	p value
C. major																		
C. medius																		
M. murinus																		
M. rufus																		
G. alleni																		
G. demidoff																		
E. elegantulus																		
G. moholi																		
G. senegalensus																		
G. zanzibaricus																		
O. crassicaudatus																		
O. garnettii																		
A. laniger																		
I. Indri																		
P. diadema																		
P. verreauxi																		
E. fulvus																		
E. macaco																		
E. mongoz																		
E. rubriventer	0.801	0.374																
H. griseus	3.444	0.067	3.837	0.056														
L. catta	1.854	0.177	2.596	0.113	0.589	0.446												
V. variegata	9.317	0.003	2.170	0.146	0.374	0.543	2.835	0.097										
L. ruficaudatus	0.923	0.340	0.002	0.968	0.513	0.477	0.010	0.923	2.111	0.151								
L. tardigradus	0.737	0.393	0.135	0.715	1.715	0.196	0.536	0.467	6.532	0.013	0.179	0.674						
N. bengalensis	1.650	0.203	0.120	0.731	0.173	0.679	0.073	0.788	1.177	0.282	0.098	0.756	0.573	0.453				
N. coucang	3.760	0.055	0.090	0.764	0.626	0.431	0.031	0.862	3.637	0.059	0.062	0.804	1.765	0.187	0.033	0.856		
P. potto	2.920	0.089	0.002	0.969	1.171	0.281	0.034	0.855	5.436	0.021	0.000	0.985	1.131	0.289	0.182	0.671	0.262	0.609

Goswami model ZYGOMATIC- PC4	*C. major*		*C.medius*		*M. murinus*		*M. rufus*		*G. alleni*		*G. denidoff*		*E. elegantulus*		*G. moholi*		*G.senegalensis*	
	F value	p value	F value	p value	F value	p value	F value	p value	F value	p value	F value	p value	F value	p value	F value	p value	F value	p value
C. major																		
C. medius	2.763	0.103																
M. murinus	0.977	0.326	0.242	0.624														
M. rufus	9.058	0.004	2.505	0.119	4.391	0.039												
G. alleni	0.345	0.560	0.820	0.370	0.110	0.741	4.631	0.036										
G. demidoff	2.688	0.105	0.000	0.996	0.323	0.571	2.923	0.091	0.717	0.400								
E. elegantulus	0.787	0.379	0.152	0.698	0.002	0.966	2.630	0.110	0.125	0.725	0.148	0.702						
G. moholi	0.323	0.571	0.575	0.450	0.130	0.719	4.895	0.029	0.001	0.976	0.761	0.385	0.088	0.767				
G. senegalensus	9.958	0.002	0.531	0.467	2.968	0.086	3.205	0.075	3.201	0.075	0.705	0.402	1.188	0.277	4.174	0.042		
G. zanzibaricus	0.000	0.996	1.790	0.187	0.689	0.409	6.281	0.016	0.223	0.639	1.870	0.175	0.565	0.456	0.234	0.630	6.727	0.010
O. crassicaudatus	0.394	0.531	2.673	0.105	0.958	0.329	16.120	0.000	0.061	0.805	3.346	0.069	0.524	0.470	0.111	0.739	18.096	0.000
O. garnettii	0.000	0.999	5.020	0.027	2.642	0.106	21.005	0.000	0.577	0.449	6.184	0.014	1.377	0.243	0.800	0.372	28.016	0.000
A. laniger	1.585	0.215	0.026	0.873	0.243	0.624	0.919	0.343	0.595	0.445	0.027	0.870	0.177	0.676	0.467	0.496	0.079	0.779
I. Indri	0.226	0.636	3.230	0.077	1.443	0.232	8.437	0.005	0.842	0.363	3.099	0.082	1.321	0.254	0.724	0.397	8.506	0.004
P. diadema	0.006	0.937	2.078	0.155	0.649	0.423	7.228	0.010	0.225	0.637	1.931	0.168	0.595	0.444	0.199	0.656	6.710	0.010
P. verreauxi	0.482	0.490	0.338	0.563	0.022	0.883	3.497	0.066	0.029	0.866	0.377	0.540	0.026	0.872	0.021	0.886	2.209	0.139
E. fulvus	0.222	0.638	0.879	0.350	0.382	0.537	6.807	0.010	0.008	0.930	1.331	0.250	0.172	0.679	0.026	0.871	7.562	0.006
E. macaco	0.295	0.588	0.465	0.497	0.082	0.775	3.904	0.052	0.002	0.961	0.566	0.453	0.068	0.794	0.001	0.981	2.925	0.089
E. mongoz	4.762	0.032	0.639	0.426	2.136	0.146	0.457	0.501	1.933	0.168	0.882	0.350	0.961	0.330	2.736	0.101	0.440	0.508
E. rubriventer	0.757	0.389	3.515	0.066	2.504	0.117	7.643	0.008	1.314	0.257	4.165	0.044	1.818	0.183	1.550	0.216	11.820	0.001
H. griseus	0.327	0.570	0.428	0.516	0.048	0.827	3.261	0.077	0.007	0.935	0.441	0.509	0.054	0.818	0.003	0.959	2.256	0.135
L. catta	1.911	0.172	0.009	0.926	0.327	0.569	1.594	0.212	0.578	0.450	0.012	0.914	0.155	0.695	0.673	0.414	0.298	0.586
V. variegata	0.803	0.374	0.002	0.962	0.107	0.745	1.183	0.281	0.209	0.650	0.003	0.957	0.041	0.840	0.303	0.583	0.424	0.516
L. ruficaudatus	1.038	0.314	0.133	0.717	0.009	0.925	2.656	0.109	0.193	0.662	0.118	0.732	0.002	0.963	0.120	0.729	1.126	0.290
L. tardigradus	2.924	0.094	0.043	0.836	0.228	0.634	4.366	0.042	0.592	0.446	0.054	0.817	0.069	0.794	0.698	0.406	2.780	0.097
N. bengalensis	1.374	0.247	0.025	0.875	0.244	0.623	0.810	0.373	0.512	0.478	0.028	0.867	0.163	0.688	0.464	0.497	0.070	0.792
N. coucang	0.073	0.788	1.549	0.216	0.748	0.389	8.417	0.005	0.084	0.773	2.116	0.148	0.394	0.531	0.155	0.695	10.301	0.002
P. potto	0.256	0.614	1.894	0.171	0.848	0.358	12.313	0.001	0.048	0.827	2.678	0.103	0.400	0.528	0.107	0.744	14.934	0.000

Goswami model ZYGOMATIC- PC4	*G. zanzibaricus*		*O. crassicaudatus*		*O. garnettii*		*A. laniger*		*I. indri*		*P. diadema*		*P. verreauxi*		*E. fulvus*		*E. macaco*	
	F value	p value	F value	p value	F value	p value	F value	p value	F value	p value	F value	p value	F value	p value	F value	p value	F value	p value
C. major																		
C. medius																		
M. murinus																		
M. rufus																		
G. alleni																		
G. demidoff																		
E. elegantulus																		
G. moholi																		
G. senegalensus																		
G. zanzibaricus																		
O. crassicaudatus	0.247	0.620																
O. garnettii	0.000	0.994	1.233	0.268														
A. laniger	1.148	0.290	1.679	0.198	2.863	0.093												
I. Indri	0.167	0.684	1.121	0.292	0.375	0.541	2.141	0.149										
P. diadema	0.004	0.953	0.184	0.669	0.011	0.916	1.316	0.257	0.260	0.612								
P. verreauxi	0.352	0.555	0.255	0.615	0.970	0.326	0.314	0.577	0.954	0.332	0.339	0.563						
E. fulvus	0.154	0.695	0.022	0.882	0.719	0.397	0.638	0.425	0.565	0.453	0.115	0.735	0.078	0.780				
E. macaco	0.219	0.641	0.102	0.750	0.638	0.426	0.401	0.528	0.691	0.408	0.194	0.661	0.012	0.911	0.025	0.873		
E. mongoz	3.431	0.068	9.099	0.003	12.833	0.000	0.187	0.667	4.639	0.034	3.570	0.062	1.572	0.213	4.635	0.032	2.000	0.160
E. rubriventer	0.581	0.450	2.784	0.098	1.634	0.204	2.256	0.140	0.212	0.647	0.762	0.387	1.596	0.211	1.547	0.215	1.366	0.246
H. griseus	0.231	0.633	0.118	0.732	0.627	0.430	0.361	0.551	0.758	0.387	0.228	0.635	0.006	0.939	0.027	0.869	0.001	0.977
L. catta	1.364	0.248	2.713	0.102	4.743	0.031	0.004	0.949	2.373	0.128	1.447	0.234	0.348	0.557	1.165	0.282	0.505	0.479
V. variegata	0.615	0.436	1.135	0.289	2.133	0.147	0.018	0.893	1.160	0.285	0.613	0.436	0.128	0.721	0.614	0.434	0.218	0.642
L. ruficaudatus	0.700	0.407	0.707	0.402	1.746	0.189	0.158	0.693	1.603	0.210	0.788	0.379	0.045	0.832	0.218	0.641	0.096	0.757
L. tardigradus	1.744	0.193	5.765	0.018	11.628	0.001	0.086	0.771	3.118	0.082	1.916	0.172	0.259	0.613	1.849	0.175	0.445	0.507
N. bengalensis	1.020	0.318	1.627	0.205	2.743	0.100	0.000	0.994	1.916	0.172	1.146	0.290	0.297	0.588	0.662	0.417	0.390	0.534
N. coucang	0.048	0.826	0.063	0.802	0.212	0.646	1.022	0.315	0.417	0.520	0.027	0.869	0.239	0.626	0.084	0.772	0.132	0.717
P. potto	0.168	0.683	0.001	0.974	0.871	0.352	1.250	0.265	0.792	0.375	0.118	0.732	0.212	0.646	0.028	0.867	0.093	0.761

Goswami model ZYGOMATIC- PC4	*E. mongoz*		*E. rubriventer*		*H. griseus*		*L. catta*		*V. variegata*		*L. ruficaudatus*		*L. tardigradus*		*N. bengalensis*		*N. coucang*	
	F value	p value	F value	p value	F value	p value	F value	p value	F value	p value	F value	p value	F value	p value	F value	p value	F value	p value
C. major																		
C. medius																		
M. murinus																		
M. rufus																		
G. alleni																		
G. demidoff																		
E. elegantulus																		
G. moholi																		
G. senegalensus																		
G. zanzibaricus																		
O. crassicaudatus																		
O. garnettii																		
A. laniger																		
I. Indri																		
P. diadema																		
P. verreauxi																		
E. fulvus																		
E. macaco																		
E. mongoz																		
E. rubriventer	5.495	0.022																
H. griseus	1.453	0.232	0.327	0.570														
L. catta	0.449	0.505	1.911	0.172	0.373	0.544												
V. variegata	0.458	0.500	1.653	0.203	0.140	0.710	0.013	0.911										
L. ruficaudatus	0.897	0.347	1.952	0.169	0.082	0.776	0.127	0.723	0.028	0.868								
L. tardigradus	1.710	0.195	3.743	0.059	0.309	0.581	0.086	0.771	0.005	0.944	0.047	0.830						
N. bengalensis	0.173	0.679	2.071	0.157	0.326	0.571	0.005	0.945	0.019	0.890	0.140	0.710	0.082	0.776				
N. coucang	5.358	0.022	1.228	0.271	0.124	0.726	1.669	0.199	0.809	0.370	0.481	0.490	2.617	0.109	1.004	0.319		
P. potto	7.862	0.006	2.184	0.142	0.095	0.759	2.214	0.139	1.049	0.307	0.510	0.476	4.371	0.038	1.258	0.264	0.043	0.835

Goswami model ZYGOMATIC- PC5	*C. major*		*C.medius*		*M. murinus*		*M. rufus*		*G. alleni*		*G. denidoff*		*E. elegantulus*		*G. moholi*		*G.senegalensis*	
	F value	p value	F value	p value	F value	p value	F value	p value	F value	p value	F value	p value	F value	p value	F value	p value	F value	p value
C. major																		
C. medius	0.404	0.528																
M. murinus	0.428	0.514	0.000	0.983														
M. rufus	0.004	0.948	0.362	0.550	0.358	0.551												
G. alleni	0.866	0.357	0.118	0.733	0.083	0.774	0.857	0.359										
G. demidoff	1.498	0.225	0.359	0.551	0.439	0.509	1.404	0.239	0.057	0.813								
E. elegantulus	7.573	0.008	4.980	0.029	4.259	0.042	7.978	0.006	3.382	0.071	2.353	0.129						
G. moholi	6.186	0.015	2.585	0.111	2.481	0.117	6.023	0.016	1.127	0.291	0.576	0.449	1.926	0.168				
G. senegalensus	10.147	0.002	3.810	0.052	4.743	0.030	9.403	0.002	1.467	0.227	0.922	0.338	3.218	0.074	0.017	0.896		
G. zanzibaricus	0.175	0.678	0.024	0.877	0.029	0.865	0.145	0.705	0.211	0.648	0.484	0.489	4.801	0.033	2.802	0.097	4.170	0.042
O. crassicaudatus	2.184	0.142	0.293	0.589	0.378	0.539	1.937	0.166	0.003	0.958	0.124	0.726	5.430	0.021	2.296	0.132	4.823	0.029
O. garnettii	12.914	0.000	6.279	0.014	8.570	0.004	12.362	0.001	3.125	0.080	3.099	0.080	0.688	0.408	1.010	0.316	3.041	0.082
A. laniger	0.012	0.912	0.081	0.778	0.094	0.760	0.006	0.939	0.232	0.633	0.472	0.494	3.093	0.084	1.991	0.162	3.040	0.083
I. Indri	5.102	0.028	2.991	0.089	2.597	0.110	5.280	0.025	1.840	0.180	1.184	0.279	0.187	0.666	0.608	0.437	1.090	0.298
P. diadema	2.728	0.105	1.137	0.291	0.982	0.324	2.805	0.100	0.474	0.494	0.178	0.674	1.420	0.238	0.027	0.869	0.013	0.911
P. verreauxi	2.582	0.113	0.903	0.345	0.733	0.394	2.574	0.113	0.305	0.583	0.067	0.797	2.185	0.144	0.185	0.668	0.187	0.666
E. fulvus	5.112	0.025	2.354	0.127	4.142	0.043	4.745	0.031	1.094	0.297	1.328	0.250	0.442	0.507	0.253	0.615	0.826	0.364
E. macaco	3.266	0.075	1.600	0.210	1.892	0.171	3.225	0.076	0.793	0.376	0.613	0.436	0.528	0.469	0.092	0.762	0.249	0.619
E. mongoz	1.448	0.233	0.323	0.571	0.398	0.529	1.353	0.248	0.042	0.838	0.002	0.965	2.512	0.117	0.688	0.408	1.141	0.286
E. rubriventer	10.608	0.002	7.895	0.007	7.586	0.007	11.353	0.001	5.720	0.021	4.913	0.029	0.519	0.474	5.395	0.022	9.188	0.003
H. griseus	0.106	0.746	0.020	0.889	0.026	0.873	0.086	0.770	0.146	0.704	0.375	0.542	3.428	0.069	1.970	0.164	3.010	0.084
L. catta	6.101	0.017	3.368	0.072	3.528	0.063	6.262	0.015	1.876	0.176	1.440	0.233	0.324	0.571	0.622	0.432	1.361	0.245
V. variegata	0.030	0.862	0.085	0.771	0.125	0.724	0.017	0.896	0.256	0.615	0.691	0.408	3.742	0.057	2.675	0.105	4.754	0.030
L. ruficaudatus	0.009	0.926	0.404	0.528	0.366	0.547	0.024	0.878	0.822	0.369	1.155	0.286	6.321	0.015	4.566	0.035	6.548	0.011
L. tardigradus	1.131	0.293	0.210	0.649	0.364	0.548	1.067	0.306	0.014	0.907	0.020	0.887	2.298	0.135	1.055	0.307	2.723	0.100
N. bengalensis	1.384	0.246	0.453	0.504	0.322	0.572	1.439	0.236	0.131	0.719	0.012	0.914	1.804	0.185	0.235	0.629	0.252	0.617
N. coucang	3.590	0.061	1.105	0.296	1.299	0.256	3.395	0.069	0.305	0.582	0.081	0.776	2.877	0.093	0.384	0.537	0.555	0.457
P. potto	3.324	0.070	0.828	0.364	1.224	0.270	3.002	0.085	0.160	0.690	0.014	0.907	3.506	0.063	0.796	0.373	1.537	0.216

Goswami model ZYGOMATIC- PC5	*G. zanzibaricus*		*O. crassicaudatus*		*O. garnettii*		*A. laniger*		*I. indri*		*P. diadema*		*P. verreauxi*		*E. fulvus*		*E. macaco*	
	F value	p value	F value	p value	F value	p value	F value	p value	F value	p value	F value	p value	F value	p value	F value	p value	F value	p value
C. major																		
C. medius																		
M. murinus																		
M. rufus																		
G. alleni																		
G. demidoff																		
E. elegantulus																		
G. moholi																		
G. senegalensus																		
G. zanzibaricus																		
O. crassicaudatus	0.488	0.486																
O. garnettii	6.179	0.014	13.218	0.000														
A. laniger	0.026	0.872	0.529	0.469	3.882	0.051												
I. Indri	3.009	0.088	2.937	0.089	0.042	0.838	2.085	0.154										
P. diadema	1.247	0.270	0.790	0.376	0.777	0.380	0.902	0.347	0.522	0.472								
P. verreauxi	1.071	0.305	0.439	0.509	1.425	0.235	0.853	0.359	0.927	0.339	0.040	0.841						
E. fulvus	2.418	0.122	5.086	0.025	0.058	0.810	1.799	0.181	0.059	0.808	0.224	0.637	0.450	0.503				
E. macaco	1.689	0.198	1.852	0.176	0.101	0.751	1.313	0.255	0.105	0.746	0.110	0.741	0.278	0.600	0.013	0.908		
E. mongoz	0.446	0.506	0.089	0.766	3.555	0.061	0.441	0.508	1.288	0.259	0.216	0.643	0.092	0.763	1.523	0.219	0.689	0.408
E. rubriventer	7.291	0.010	10.776	0.001	3.498	0.064	4.545	0.038	1.252	0.267	3.362	0.073	4.811	0.032	1.978	0.161	1.893	0.173
H. griseus	0.000	0.990	0.363	0.548	4.347	0.039	0.018	0.895	2.193	0.144	0.865	0.357	0.754	0.388	1.907	0.169	1.322	0.254
L. catta	3.309	0.074	4.344	0.039	0.010	0.922	2.128	0.151	0.010	0.922	0.483	0.490	0.928	0.338	0.041	0.839	0.077	0.782
V. variegata	0.024	0.879	0.821	0.366	6.450	0.012	0.001	0.978	2.505	0.118	1.125	0.293	1.009	0.318	3.314	0.070	1.866	0.175
L. ruficaudatus	0.199	0.657	1.507	0.222	7.975	0.006	0.026	0.873	4.309	0.042	2.289	0.137	2.192	0.144	3.200	0.075	2.550	0.114
L. tardigradus	0.293	0.591	0.049	0.826	7.221	0.008	0.275	0.603	1.250	0.268	0.252	0.618	0.139	0.710	3.130	0.078	0.818	0.368
N. bengalensis	0.555	0.460	0.148	0.701	1.114	0.293	0.454	0.504	0.825	0.367	0.072	0.790	0.013	0.911	0.359	0.550	0.254	0.616
N. coucang	1.310	0.255	0.837	0.362	3.652	0.058	1.041	0.310	1.273	0.262	0.083	0.774	0.004	0.952	1.264	0.262	0.516	0.474
P. potto	1.051	0.307	0.605	0.437	7.216	0.008	0.931	0.336	1.681	0.197	0.216	0.643	0.055	0.815	2.885	0.090	0.919	0.339

Goswami model ZYGOMATIC- PC5	*E. mongoz*		*E. rubriventer*		*H. griseus*		*L. catta*		*V. variegata*		*L. ruficaudatus*		*L. tardigradus*		*N. bengalensis*		*N. coucang*	
	F value	p value	F value	p value	F value	p value	F value	p value	F value	p value	F value	p value	F value	p value	F value	p value	F value	p value
C. major																		
C. medius																		
M. murinus																		
M. rufus																		
G. alleni																		
G. demidoff																		
E. elegantulus																		
G. moholi																		
G. senegalensus																		
G. zanzibaricus																		
O. crassicaudatus																		
O. garnettii																		
A. laniger																		
I. Indri																		
P. diadema																		
P. verreauxi																		
E. fulvus																		
E. macaco																		
E. mongoz																		
E. rubriventer	5.153	0.026																
H. griseus	0.344	0.559	0.106	0.746														
L. catta	1.592	0.210	6.101	0.017	2.343	0.131												
V. variegata	0.652	0.422	5.875	0.018	0.015	0.902	3.002	0.088										
L. ruficaudatus	1.109	0.296	8.689	0.005	0.128	0.723	4.605	0.036	0.046	0.830								
L. tardigradus	0.010	0.921	4.354	0.042	0.219	0.642	1.738	0.193	0.506	0.479	0.769	0.385						
N. bengalensis	0.020	0.888	3.511	0.067	0.381	0.540	0.746	0.392	0.494	0.485	1.309	0.259	0.032	0.859				
N. coucang	0.121	0.729	6.555	0.012	0.944	0.334	1.596	0.209	1.555	0.215	2.534	0.115	0.288	0.593	0.005	0.943		
P. potto	0.034	0.854	7.930	0.006	0.792	0.375	2.422	0.122	1.553	0.214	2.179	0.142	0.184	0.669	0.004	0.950	0.073	0.787

Goswami model VAULT- PC1	*C. major*		*C.medius*		*M. murinus*		*M. rufus*		*G. alleni*		*G. denidoff*		*E. elegantulus*		*G. moholi*		*G.senegalensis*	
	F value	p value	F value	p value	F value	p value	F value	p value	F value	p value	F value	p value	F value	p value	F value	p value	F value	p value
C. major																		
C. medius	0.088	0.768																
M. murinus	0.145	0.704	0.935	0.336														
M. rufus	0.010	0.922	0.070	0.793	0.381	0.538												
G. alleni	0.493	0.486	0.477	0.493	1.183	0.279	0.641	0.427										
G. demidoff	3.752	0.056	6.228	0.015	8.804	0.004	6.094	0.016	0.269	0.606								
E. elegantulus	3.835	0.055	6.102	0.016	8.995	0.003	5.800	0.019	0.925	0.341	1.567	0.214						
G. moholi	0.920	0.340	0.894	0.347	3.164	0.077	1.206	0.275	0.044	0.835	1.661	0.200	3.981	0.049				
G. senegalensus	1.899	0.170	2.588	0.109	8.227	0.004	2.723	0.101	0.007	0.933	1.674	0.197	5.564	0.019	0.087	0.768		
G. zanzibaricus	0.290	0.593	0.193	0.663	1.052	0.308	0.357	0.553	0.099	0.755	1.591	0.211	2.432	0.125	0.052	0.820	0.213	0.645
O. crassicaudatus	0.365	0.547	1.789	0.183	0.210	0.648	0.821	0.367	1.146	0.287	9.641	0.002	9.055	0.003	4.263	0.040	17.618	0.000
O. garnettii	0.133	0.716	0.014	0.907	1.568	0.212	0.120	0.729	0.293	0.589	4.508	0.035	6.283	0.013	0.659	0.418	3.743	0.054
A. laniger	1.155	0.288	4.059	0.050	0.950	0.332	2.471	0.123	2.999	0.091	19.646	0.000	12.155	0.001	8.613	0.004	16.610	0.000
I. Indri	1.145	0.289	1.421	0.238	3.385	0.069	1.588	0.212	0.030	0.862	0.092	0.763	1.061	0.307	0.343	0.559	0.286	0.593
P. diadema	0.951	0.334	1.202	0.278	3.185	0.077	1.472	0.230	0.010	0.919	1.317	0.254	2.829	0.098	0.031	0.861	0.005	0.945
P. verreauxi	0.049	0.825	0.388	0.536	0.016	0.900	0.146	0.703	0.778	0.381	5.280	0.024	5.498	0.022	1.765	0.187	3.879	0.050
E. fulvus	0.144	0.705	0.025	0.874	1.534	0.217	0.132	0.717	0.233	0.629	3.363	0.068	5.537	0.020	0.470	0.494	2.654	0.104
E. macaco	0.346	0.558	0.283	0.596	1.802	0.182	0.421	0.518	0.041	0.840	1.115	0.293	2.425	0.123	0.017	0.897	0.209	0.648
E. mongoz	0.995	0.322	1.352	0.248	4.540	0.035	1.458	0.231	0.001	0.979	0.788	0.377	2.560	0.113	0.086	0.770	0.013	0.908
E. rubriventer	0.121	0.729	0.033	0.857	0.717	0.399	0.120	0.731	0.178	0.675	2.097	0.151	2.850	0.097	0.221	0.639	0.628	0.429
H. griseus	0.000	0.991	0.146	0.703	0.212	0.646	0.013	0.908	0.827	0.368	6.480	0.013	5.721	0.020	1.361	0.246	2.550	0.112
L. catta	0.166	0.686	0.940	0.336	0.007	0.933	0.425	0.517	1.204	0.277	9.008	0.003	7.656	0.007	3.214	0.076	7.260	0.008
V. variegata	1.285	0.262	3.961	0.051	1.287	0.259	2.469	0.121	2.659	0.108	16.130	0.000	11.955	0.001	8.200	0.005	17.969	0.000
L. ruficaudatus	0.139	0.711	0.672	0.416	0.007	0.934	0.337	0.564	1.187	0.282	6.688	0.012	5.483	0.023	2.265	0.136	3.793	0.053
L. tardigradus	5.038	0.029	10.893	0.002	18.124	0.000	8.754	0.005	1.211	0.277	4.106	0.046	0.130	0.719	8.239	0.005	20.687	0.000
N. bengalensis	0.830	0.367	2.384	0.129	0.753	0.388	1.569	0.217	2.008	0.164	11.251	0.001	7.958	0.007	5.612	0.020	10.667	0.001
N. coucang	1.020	0.315	1.549	0.216	4.771	0.031	1.498	0.224	0.016	0.900	0.131	0.718	1.219	0.272	0.318	0.574	0.467	0.495
P. potto	0.465	0.496	0.425	0.515	2.925	0.089	0.586	0.445	0.065	0.799	1.794	0.182	3.873	0.051	0.044	0.835	0.577	0.448

Goswami model VAULT- PC1	*G. zanzibaricus*		*O. crassicaudatus*		*O. garnettii*		*A. laniger*		*I. indri*		*P. diadema*		*P. verreauxi*		*E. fulvus*		*E. macaco*	
	F value	p value	F value	p value	F value	p value	F value	p value	F value	p value	F value	p value	F value	p value	F value	p value	F value	p value
C. major																		
C. medius																		
M. murinus																		
M. rufus																		
G. alleni																		
G. demidoff																		
E. elegantulus																		
G. moholi																		
G. senegalensus																		
G. zanzibaricus																		
O. crassicaudatus	1.243	0.267																
O. garnettii	0.098	0.755	5.030	0.026														
A. laniger	3.404	0.072	0.267	0.607	4.593	0.034												
I. Indri	0.331	0.567	3.979	0.048	1.368	0.244	6.148	0.016										
P. diadema	0.123	0.727	3.927	0.050	0.844	0.360	8.007	0.007	0.169	0.682								
P. verreauxi	0.602	0.441	0.197	0.658	0.575	0.450	0.789	0.378	1.952	0.166	1.700	0.197						
E. fulvus	0.067	0.796	5.261	0.023	0.006	0.938	4.257	0.040	1.155	0.284	0.637	0.426	0.586	0.445				
E. macaco	0.004	0.947	3.216	0.075	0.318	0.574	3.729	0.057	0.283	0.596	0.055	0.816	0.855	0.358	0.255	0.614		
E. mongoz	0.138	0.711	8.319	0.004	1.916	0.168	7.936	0.006	0.107	0.744	0.012	0.912	2.079	0.153	1.552	0.214	0.140	0.709
E. rubriventer	0.032	0.859	1.055	0.306	0.011	0.917	2.402	0.128	0.548	0.462	0.298	0.588	0.361	0.550	0.004	0.948	0.059	0.809
H. griseus	0.503	0.481	0.487	0.487	0.170	0.681	2.010	0.163	1.665	0.202	1.756	0.191	0.076	0.784	0.172	0.678	0.454	0.502
L. catta	1.087	0.302	0.088	0.768	1.328	0.251	0.638	0.428	3.000	0.088	3.056	0.086	0.032	0.858	1.297	0.256	1.493	0.225
V. variegata	3.065	0.085	0.507	0.478	5.644	0.019	0.023	0.879	6.278	0.014	7.036	0.010	1.006	0.319	5.451	0.020	4.420	0.038
L. ruficaudatus	0.978	0.328	0.035	0.852	0.673	0.414	0.427	0.517	2.140	0.149	2.317	0.134	0.027	0.870	0.642	0.424	0.888	0.349
L. tardigradus	3.256	0.077	26.533	0.000	20.649	0.000	16.434	0.000	2.205	0.143	5.181	0.027	8.516	0.005	19.338	0.000	5.571	0.021
N. bengalensis	2.157	0.149	0.244	0.622	3.072	0.082	0.007	0.935	4.157	0.046	4.515	0.039	0.627	0.432	3.023	0.084	2.639	0.109
N. coucang	0.238	0.627	10.024	0.002	3.021	0.084	6.411	0.013	0.001	0.970	0.139	0.710	2.125	0.148	2.768	0.097	0.383	0.537
P. potto	0.002	0.964	7.853	0.006	0.665	0.416	5.891	0.016	0.486	0.487	0.119	0.730	1.231	0.269	0.503	0.479	0.002	0.962

Goswami model VAULT- PC1	*E. mongoz*		*E. rubriventer*		*H. griseus*		*L. catta*		*V. variegata*		*L. ruficaudatus*		*L. tardigradus*		*N. bengalensis*		*N. coucang*	
	F value	p value	F value	p value	F value	p value	F value	p value	F value	p value	F value	p value	F value	p value	F value	p value	F value	p value
C. major																		
C. medius																		
M. murinus																		
M. rufus																		
G. alleni																		
G. demidoff																		
E. elegantulus																		
G. moholi																		
G. senegalensus																		
G. zanzibaricus																		
O. crassicaudatus																		
O. garnettii																		
A. laniger																		
I. Indri																		
P. diadema																		
P. verreauxi																		
E. fulvus																		
E. macaco																		
E. mongoz																		
E. rubriventer	0.356	0.553																
H. griseus	1.404	0.240	0.000	0.991														
L. catta	3.645	0.060	0.166	0.686	0.267	0.607												
V. variegata	8.846	0.004	2.492	0.119	1.885	0.175	0.847	0.361										
L. ruficaudatus	1.994	0.162	0.554	0.460	0.244	0.623	0.000	0.986	0.512	0.477								
L. tardigradus	7.637	0.007	4.122	0.048	7.431	0.009	12.198	0.001	18.769	0.000	6.354	0.015						
N. bengalensis	5.037	0.028	1.636	0.207	1.274	0.265	0.490	0.487	0.002	0.967	0.334	0.567	9.890	0.003				
N. coucang	0.146	0.703	0.483	0.489	1.327	0.252	3.450	0.066	7.866	0.006	1.721	0.193	4.463	0.037	4.304	0.041		
P. potto	0.375	0.541	0.069	0.794	0.585	0.446	2.346	0.128	7.241	0.008	1.165	0.282	13.616	0.000	4.040	0.046	1.047	0.307

Goswami model VAULT- PC2	*C. major*		*C.medius*		*M. murinus*		*M. rufus*		*G. alleni*		*G. denidoff*		*E. elegantulus*		*G. moholi*		*G.senegalensis*	
	F value	p value	F value	p value	F value	p value	F value	p value	F value	p value	F value	p value	F value	p value	F value	p value	F value	p value
C. major																		
C. medius	1.185	0.282																
M. murinus	0.676	0.413	0.033	0.857														
M. rufus	0.003	0.959	1.855	0.179	1.104	0.296												
G. alleni	2.165	0.148	0.828	0.367	0.846	0.360	2.600	0.113										
G. demidoff	1.550	0.217	0.002	0.967	0.051	0.822	2.363	0.128	1.033	0.313								
E. elegantulus	3.616	0.062	1.664	0.202	1.756	0.188	4.965	0.030	0.001	0.973	1.953	0.166						
G. moholi	0.284	0.595	0.486	0.487	0.211	0.647	0.480	0.490	1.697	0.196	0.588	0.445	3.324	0.071				
G. senegalensus	0.305	0.582	2.055	0.153	1.006	0.317	0.630	0.428	3.494	0.063	2.119	0.147	8.267	0.004	0.069	0.792		
G. zanzibaricus	0.484	0.490	0.038	0.846	0.002	0.962	0.669	0.417	0.812	0.372	0.062	0.805	1.290	0.261	0.095	0.759	0.376	0.540
O. crassicaudatus	4.093	0.045	3.434	0.066	4.346	0.039	6.940	0.009	0.021	0.884	3.555	0.061	0.081	0.776	5.874	0.016	25.610	0.000
O. garnettii	2.043	0.156	0.869	0.353	1.310	0.254	3.579	0.061	0.082	0.775	0.868	0.353	0.178	0.674	2.374	0.125	12.246	0.001
A. laniger	1.294	0.261	0.017	0.896	0.073	0.788	1.868	0.178	0.661	0.421	0.012	0.914	1.182	0.282	0.559	0.456	1.888	0.171
I. Indri	7.635	0.008	5.745	0.019	5.561	0.020	10.419	0.002	0.365	0.548	6.780	0.011	0.793	0.376	8.515	0.004	20.128	0.000
P. diadema	1.263	0.267	0.098	0.756	0.206	0.651	1.926	0.171	0.363	0.550	0.101	0.751	0.707	0.404	0.834	0.363	2.912	0.089
P. verreauxi	1.936	0.169	0.595	0.443	0.786	0.377	2.742	0.102	0.066	0.798	0.684	0.410	0.102	0.750	1.692	0.196	4.517	0.035
E. fulvus	1.053	0.306	0.082	0.775	0.226	0.635	1.871	0.173	0.337	0.562	0.065	0.799	0.799	0.372	0.789	0.375	4.109	0.043
E. macaco	1.075	0.303	0.171	0.681	0.329	0.567	1.698	0.196	0.184	0.669	0.180	0.672	0.373	0.543	0.914	0.341	3.271	0.072
E. mongoz	2.346	0.130	0.699	0.406	1.010	0.317	3.903	0.052	0.179	0.674	0.725	0.396	0.377	0.541	2.265	0.135	9.563	0.002
E. rubriventer	0.795	0.377	0.047	0.830	0.112	0.738	1.128	0.293	0.274	0.603	0.050	0.824	0.473	0.495	0.488	0.486	1.471	0.227
H. griseus	0.004	0.949	0.599	0.442	0.453	0.502	0.013	0.909	1.165	0.286	0.852	0.359	2.210	0.143	0.145	0.704	0.150	0.699
L. catta	0.094	0.760	0.274	0.603	0.172	0.679	0.168	0.684	0.817	0.370	0.389	0.534	1.715	0.195	0.004	0.948	0.012	0.914
V. variegata	4.714	0.034	3.757	0.057	4.545	0.035	6.901	0.011	0.184	0.669	4.642	0.034	0.458	0.501	6.538	0.012	18.235	0.000
L. ruficaudatus	0.806	0.374	3.899	0.054	2.985	0.087	0.904	0.346	3.881	0.055	5.200	0.025	6.484	0.014	2.453	0.121	4.065	0.045
L. tardigradus	0.022	0.882	2.739	0.104	1.977	0.163	0.015	0.902	2.442	0.125	3.562	0.063	5.899	0.018	0.881	0.350	1.928	0.167
N. bengalensis	4.306	0.044	2.256	0.140	2.177	0.144	5.662	0.021	0.019	0.891	2.786	0.099	0.053	0.819	4.008	0.048	9.408	0.002
N. coucang	2.163	0.145	1.112	0.294	1.615	0.206	3.661	0.059	0.028	0.868	1.196	0.276	0.050	0.823	2.723	0.101	11.988	0.001
P. potto	3.634	0.059	2.679	0.104	3.435	0.065	6.188	0.014	0.001	0.980	2.674	0.104	0.008	0.928	4.836	0.029	20.950	0.000

Goswami model VAULT- PC2	*G. zanzibaricus*		*O. crassicaudatus*		*O. garnettii*		*A. laniger*		*I. indri*		*P. diadema*		*P. verreauxi*		*E. fulvus*		*E. macaco*	
	F value	p value	F value	p value	F value	p value	F value	p value	F value	p value	F value	p value	F value	p value	F value	p value	F value	p value
C. major																		
C. medius																		
M. murinus																		
M. rufus																		
G. alleni																		
G. demidoff																		
E. elegantulus																		
G. moholi																		
G. senegalensus																		
G. zanzibaricus																		
O. crassicaudatus	1.655	0.201																
O. garnettii	0.508	0.478	1.786	0.183														
A. laniger	0.080	0.778	1.981	0.162	0.420	0.518												
I. Indri	3.848	0.054	0.413	0.521	1.920	0.168	4.389	0.041										
P. diadema	0.146	0.704	1.741	0.189	0.258	0.612	0.030	0.863	3.189	0.079								
P. verreauxi	0.523	0.472	0.412	0.522	0.003	0.957	0.371	0.545	1.311	0.256	0.197	0.659						
E. fulvus	0.107	0.744	4.934	0.027	0.886	0.347	0.017	0.898	3.492	0.063	0.002	0.962	0.277	0.599				
E. macaco	0.175	0.677	1.440	0.232	0.129	0.721	0.073	0.788	2.069	0.154	0.017	0.898	0.085	0.772	0.050	0.824		
E. mongoz	0.500	0.482	1.937	0.166	0.048	0.827	0.338	0.562	2.851	0.095	0.150	0.700	0.037	0.847	0.352	0.554	0.041	0.841
E. rubriventer	0.088	0.767	0.992	0.321	0.152	0.698	0.014	0.907	2.088	0.154	0.000	0.988	0.140	0.709	0.000	0.985	0.013	0.908
H. griseus	0.217	0.643	3.832	0.053	1.841	0.177	0.598	0.443	4.993	0.029	0.753	0.390	1.340	0.251	0.958	0.329	0.850	0.359
L. catta	0.061	0.805	4.038	0.047	1.667	0.199	0.288	0.593	4.431	0.039	0.449	0.506	0.979	0.326	0.677	0.412	0.598	0.442
V. variegata	2.311	0.134	0.311	0.578	1.780	0.185	2.621	0.111	0.008	0.927	2.176	0.145	0.900	0.346	3.579	0.060	1.720	0.193
L. ruficaudatus	2.117	0.152	7.181	0.008	4.647	0.033	3.784	0.058	10.960	0.002	3.498	0.067	4.258	0.043	3.325	0.070	2.939	0.091
L. tardigradus	0.779	0.382	15.162	0.000	8.434	0.004	2.286	0.137	12.437	0.001	2.716	0.105	3.585	0.063	4.673	0.032	2.841	0.096
N. bengalensis	1.749	0.193	0.001	0.976	0.359	0.550	1.731	0.196	0.372	0.544	1.011	0.320	0.253	0.617	1.056	0.306	0.554	0.459
N. coucang	0.641	0.426	0.715	0.399	0.089	0.766	0.595	0.443	1.234	0.269	0.420	0.518	0.013	0.910	1.209	0.273	0.268	0.606
P. potto	1.337	0.249	0.135	0.713	0.997	0.319	1.508	0.221	0.754	0.387	1.270	0.262	0.211	0.646	3.618	0.058	0.994	0.320

Goswami model VAULT- PC2	*E. mongoz*		*E. rubriventer*		*H. griseus*		*L. catta*		*V. variegata*		*L. ruficaudatus*		*L. tardigradus*		*N. bengalensis*		*N. coucang*	
	F value	p value	F value	p value	F value	p value	F value	p value	F value	p value	F value	p value	F value	p value	F value	p value	F value	p value
C. major																		
C. medius																		
M. murinus																		
M. rufus																		
G. alleni																		
G. demidoff																		
E. elegantulus																		
G. moholi																		
G. senegalensus																		
G. zanzibaricus																		
O. crassicaudatus																		
O. garnettii																		
A. laniger																		
I. Indri																		
P. diadema																		
P. verreauxi																		
E. fulvus																		
E. macaco																		
E. mongoz																		
E. rubriventer	0.093	0.761																
H. griseus	1.753	0.189	0.004	0.949														
L. catta	1.382	0.243	0.094	0.760	0.049	0.826												
V. variegata	2.268	0.136	1.414	0.239	3.708	0.059	3.575	0.063										
L. ruficaudatus	5.465	0.022	2.364	0.131	0.597	0.444	1.024	0.316	7.262	0.009								
L. tardigradus	7.419	0.008	1.407	0.241	0.043	0.837	0.317	0.575	9.560	0.003	0.712	0.403						
N. bengalensis	0.662	0.418	0.672	0.417	2.328	0.134	1.831	0.182	0.176	0.676	6.826	0.012	5.921	0.019				
N. coucang	0.212	0.646	0.250	0.618	1.908	0.171	1.771	0.186	1.063	0.305	4.536	0.036	7.539	0.007	0.165	0.686		
P. potto	1.196	0.275	0.730	0.394	3.446	0.065	3.524	0.062	0.638	0.426	6.811	0.010	13.930	0.000	0.022	0.882	0.303	0.583

Goswami model VAULT- PC3	*C. major*		*C.medius*		*M. murinus*		*M. rufus*		*G. alleni*		*G. denidoff*		*E. elegantulus*		*G. moholi*		*G.senegalensis*	
	F value	p value	F value	p value	F value	p value	F value	p value	F value	p value	F value	p value	F value	p value	F value	p value	F value	p value
C. major																		
C. medius	0.508	0.479																
M. murinus	0.210	0.647	2.678	0.105														
M. rufus	1.803	0.185	0.677	0.414	5.430	0.022												
G. alleni	0.296	0.589	0.005	0.946	0.869	0.354	0.456	0.503										
G. demidoff	0.005	0.942	1.390	0.242	0.319	0.573	4.041	0.048	0.505	0.479								
E. elegantulus	0.227	0.635	0.176	0.676	1.242	0.268	1.663	0.202	0.082	0.776	0.506	0.479						
G. moholi	0.044	0.835	1.989	0.162	0.174	0.677	5.239	0.024	0.795	0.375	0.031	0.860	0.861	0.356				
G. senegalensus	1.284	0.258	12.435	0.001	0.313	0.576	19.500	0.000	3.045	0.083	2.295	0.131	5.307	0.022	1.525	0.218		
G. zanzibaricus	0.067	0.797	0.217	0.643	0.581	0.448	1.342	0.252	0.136	0.714	0.169	0.682	0.032	0.859	0.339	0.562	2.611	0.108
O. crassicaudatus	1.674	0.198	9.987	0.002	1.615	0.206	13.049	0.000	2.342	0.129	3.657	0.058	4.745	0.031	2.990	0.086	2.658	0.104
O. garnettii	0.675	0.413	7.379	0.008	0.119	0.731	11.905	0.001	1.784	0.184	1.296	0.257	3.146	0.079	0.844	0.359	0.064	0.801
A. laniger	0.700	0.407	3.760	0.058	0.203	0.653	7.061	0.011	2.491	0.122	1.143	0.288	3.524	0.066	0.959	0.330	0.058	0.809
I. Indri	0.064	0.801	0.279	0.599	0.722	0.398	1.558	0.216	0.108	0.744	0.184	0.669	0.032	0.858	0.358	0.551	3.319	0.070
P. diadema	5.539	0.023	15.386	0.000	6.001	0.016	19.855	0.000	8.414	0.006	10.736	0.002	15.525	0.000	10.969	0.001	13.594	0.000
P. verreauxi	2.775	0.101	7.605	0.007	3.367	0.069	9.990	0.002	3.396	0.070	5.253	0.024	6.027	0.016	5.249	0.024	6.435	0.012
E. fulvus	0.102	0.750	3.114	0.079	0.081	0.776	6.157	0.014	0.622	0.431	0.145	0.704	0.922	0.338	0.037	0.848	1.614	0.205
E. macaco	0.553	0.460	3.816	0.054	0.182	0.670	6.646	0.012	1.344	0.250	0.982	0.324	2.165	0.145	0.752	0.388	0.029	0.866
E. mongoz	0.150	0.700	3.013	0.086	0.028	0.869	6.119	0.015	0.838	0.363	0.236	0.628	1.253	0.266	0.095	0.759	1.094	0.297
E. rubriventer	0.202	0.655	1.714	0.196	0.002	0.966	3.907	0.053	1.133	0.293	0.272	0.604	1.341	0.252	0.174	0.678	0.129	0.720
H. griseus	0.109	0.743	1.487	0.228	0.017	0.898	3.735	0.059	1.009	0.320	0.126	0.724	1.096	0.300	0.053	0.818	0.436	0.510
L. catta	4.882	0.031	13.679	0.000	5.128	0.026	17.945	0.000	7.135	0.010	9.147	0.003	12.906	0.001	9.223	0.003	10.819	0.001
V. variegata	1.886	0.175	7.162	0.009	1.368	0.245	10.941	0.002	3.538	0.065	3.341	0.071	5.889	0.018	3.105	0.081	2.017	0.157
L. ruficaudatus	0.046	0.832	0.165	0.687	0.459	0.500	0.996	0.323	0.088	0.769	0.123	0.727	0.022	0.882	0.248	0.620	2.036	0.155
L. tardigradus	0.074	0.787	0.194	0.661	1.106	0.296	1.163	0.286	0.036	0.850	0.299	0.586	0.005	0.943	0.517	0.474	7.185	0.008
N. bengalensis	1.360	0.250	4.206	0.046	1.131	0.290	6.587	0.014	2.545	0.118	2.460	0.121	4.017	0.050	2.447	0.121	1.820	0.179
N. coucang	1.057	0.307	6.669	0.011	0.873	0.352	9.352	0.003	1.678	0.199	2.322	0.130	3.296	0.072	1.895	0.171	1.139	0.287
P. potto	1.290	0.258	7.745	0.006	1.386	0.240	9.873	0.002	1.668	0.199	2.867	0.092	3.421	0.066	2.319	0.129	2.302	0.130

Goswami model VAULT- PC3	*G. zanzibaricus*		*O. crassicaudatus*		*O. garnettii*		*A. laniger*		*I. indri*		*P. diadema*		*P. verreauxi*		*E. fulvus*		*E. macaco*	
	F value	p value	F value	p value	F value	p value	F value	p value	F value	p value	F value	p value	F value	p value	F value	p value	F value	p value
C. major																		
C. medius																		
M. murinus																		
M. rufus																		
G. alleni																		
G. demidoff																		
E. elegantulus																		
G. moholi																		
G. senegalensus																		
G. zanzibaricus																		
O. crassicaudatus	2.519	0.115																
O. garnettii	1.469	0.228	2.558	0.111														
A. laniger	1.658	0.205	0.327	0.568	0.096	0.757												
I. Indri	0.000	0.992	3.571	0.061	1.923	0.168	1.554	0.218										
P. diadema	8.461	0.005	2.546	0.113	9.644	0.002	4.177	0.047	8.912	0.004								
P. verreauxi	3.682	0.059	1.443	0.232	4.622	0.033	1.680	0.200	4.630	0.035	0.000	0.995						
E. fulvus	0.388	0.534	5.199	0.023	0.930	0.336	0.549	0.460	0.550	0.459	9.644	0.002	5.753	0.017				
E. macaco	1.097	0.298	0.505	0.478	0.070	0.792	0.002	0.965	1.363	0.246	3.740	0.057	2.066	0.154	0.641	0.424		
E. mongoz	0.520	0.473	3.294	0.071	0.504	0.479	0.439	0.510	0.660	0.419	8.879	0.004	4.409	0.038	0.019	0.890	0.423	0.517
E. rubriventer	0.621	0.435	0.693	0.407	0.038	0.845	0.136	0.714	0.594	0.444	4.276	0.044	1.973	0.165	0.058	0.810	0.085	0.772
H. griseus	0.466	0.498	1.105	0.295	0.188	0.665	0.352	0.556	0.425	0.517	5.791	0.020	2.505	0.118	0.004	0.949	0.222	0.638
L. catta	7.268	0.009	1.999	0.160	7.811	0.006	3.355	0.073	7.874	0.007	0.012	0.914	0.006	0.937	8.141	0.005	3.149	0.080
V. variegata	3.188	0.079	0.034	0.853	1.642	0.202	0.512	0.477	3.469	0.067	1.575	0.214	0.753	0.388	2.528	0.113	0.524	0.471
L. ruficaudatus	0.000	0.995	2.059	0.154	1.132	0.290	1.049	0.311	0.000	0.998	5.756	0.020	3.012	0.087	0.322	0.571	0.856	0.358
L. tardigradus	0.003	0.958	7.360	0.008	4.047	0.047	1.314	0.258	0.006	0.940	8.047	0.007	4.821	0.032	1.515	0.220	1.829	0.180
N. bengalensis	2.229	0.143	0.107	0.744	1.339	0.250	0.466	0.499	2.454	0.123	0.523	0.473	0.287	0.594	1.922	0.167	0.503	0.480
N. coucang	1.697	0.196	0.087	0.769	1.124	0.291	0.110	0.741	2.396	0.125	2.627	0.108	1.506	0.222	2.931	0.088	0.187	0.666
P. potto	1.856	0.175	0.008	0.930	2.236	0.136	0.278	0.599	2.767	0.098	1.672	0.198	1.058	0.305	4.847	0.028	0.463	0.497

Goswami model VAULT- PC3	*E. mongoz*		*E. rubriventer*		*H. griseus*		*L. catta*		*V. variegata*		*L. ruficaudatus*		*L. tardigradus*		*N. bengalensis*		*N. coucang*	
	F value	p value	F value	p value	F value	p value	F value	p value	F value	p value	F value	p value	F value	p value	F value	p value	F value	p value
C. major																		
C. medius																		
M. murinus																		
M. rufus																		
G. alleni																		
G. demidoff																		
E. elegantulus																		
G. moholi																		
G. senegalensus																		
G. zanzibaricus																		
O. crassicaudatus																		
O. garnettii																		
A. laniger																		
I. Indri																		
P. diadema																		
P. verreauxi																		
E. fulvus																		
E. macaco																		
E. mongoz																		
E. rubriventer	0.029	0.866																
H. griseus	0.000	0.989	0.109	0.743														
L. catta	7.472	0.008	4.882	0.031	4.853	0.032												
V. variegata	2.212	0.140	0.923	0.340	1.443	0.234	1.212	0.275										
L. ruficaudatus	0.392	0.533	0.422	0.519	0.304	0.584	5.166	0.027	2.297	0.135								
L. tardigradus	1.175	0.282	0.509	0.479	0.377	0.542	7.353	0.009	3.456	0.068	0.003	0.958						
N. bengalensis	1.587	0.212	0.756	0.389	1.109	0.298	0.403	0.528	0.031	0.862	1.636	0.208	1.956	0.169				
N. coucang	1.780	0.185	0.363	0.548	0.632	0.429	2.133	0.147	0.128	0.721	1.372	0.245	4.409	0.038	0.186	0.668		
P. potto	2.751	0.099	0.550	0.460	0.850	0.358	1.318	0.253	0.011	0.916	1.576	0.211	6.348	0.013	0.059	0.808	0.117	0.732

Goswami model VAULT- PC4	*C. major*		*C.medius*		*M. murinus*		*M. rufus*		*G. alleni*		*G. denidoff*		*E. elegantulus*		*G. moholi*		*G.senegalensis*	
	F value	p value	F value	p value	F value	p value	F value	p value	F value	p value	F value	p value	F value	p value	F value	p value	F value	p value
C. major																		
C. medius	0.795	0.377																
M. murinus	0.996	0.321	0.028	0.869														
M. rufus	0.320	0.574	0.212	0.647	0.331	0.567												
G. alleni	2.593	0.114	1.133	0.292	0.635	0.428	2.484	0.121										
G. demidoff	4.467	0.038	2.116	0.149	1.241	0.267	3.764	0.056	0.074	0.786								
E. elegantulus	4.724	0.034	2.457	0.122	1.368	0.245	4.719	0.034	0.003	0.957	0.113	0.738						
G. moholi	8.486	0.004	5.113	0.026	2.732	0.101	8.427	0.005	0.006	0.938	0.358	0.550	0.035	0.852				
G. senegalensus	5.969	0.015	1.538	0.216	0.579	0.447	3.744	0.054	1.094	0.297	1.599	0.207	2.450	0.119	4.860	0.028		
G. zanzibaricus	3.220	0.079	1.622	0.209	1.037	0.311	3.077	0.086	0.002	0.966	0.133	0.717	0.011	0.915	0.000	0.983	1.899	0.170
O. crassicaudatus	2.359	0.127	0.330	0.567	0.095	0.758	1.190	0.277	0.740	0.391	1.503	0.222	1.754	0.188	3.707	0.056	0.329	0.567
O. garnettii	5.338	0.023	2.396	0.124	1.241	0.267	4.245	0.042	0.336	0.563	0.283	0.596	0.728	0.395	1.779	0.184	1.106	0.294
A. laniger	3.494	0.068	1.958	0.168	1.338	0.250	3.446	0.070	0.001	0.981	0.109	0.743	0.000	0.983	0.019	0.890	2.602	0.108
I. Indri	2.151	0.148	0.620	0.434	0.343	0.559	1.474	0.229	0.234	0.631	0.138	0.711	0.390	0.534	0.861	0.356	0.175	0.676
P. diadema	5.587	0.022	4.279	0.043	3.129	0.080	6.271	0.015	0.165	0.686	1.033	0.312	0.421	0.519	0.440	0.509	8.010	0.005
P. verreauxi	4.360	0.041	3.129	0.081	2.649	0.106	4.255	0.043	0.172	0.679	0.928	0.338	0.402	0.528	0.482	0.489	5.512	0.020
E. fulvus	3.890	0.050	2.415	0.122	1.804	0.180	3.172	0.076	0.021	0.885	0.008	0.928	0.035	0.852	0.152	0.697	2.478	0.116
E. macaco	4.467	0.038	2.845	0.096	2.094	0.150	4.120	0.046	0.004	0.948	0.237	0.627	0.022	0.882	0.002	0.968	3.831	0.052
E. mongoz	6.204	0.015	5.398	0.023	4.226	0.042	6.592	0.012	0.086	0.770	0.985	0.323	0.272	0.603	0.283	0.595	10.970	0.001
E. rubriventer	2.244	0.141	1.068	0.306	0.819	0.368	1.879	0.176	0.003	0.960	0.041	0.841	0.001	0.975	0.026	0.872	1.277	0.260
H. griseus	0.584	0.448	0.003	0.956	0.034	0.855	0.120	0.731	1.298	0.260	1.628	0.206	2.274	0.137	4.119	0.045	1.015	0.315
L. catta	6.251	0.015	5.273	0.025	4.242	0.042	6.993	0.010	0.407	0.526	1.938	0.167	0.971	0.328	1.282	0.260	10.934	0.001
V. variegata	2.655	0.108	1.320	0.255	0.994	0.321	2.194	0.143	0.012	0.912	0.017	0.897	0.015	0.903	0.087	0.768	1.441	0.231
L. ruficaudatus	1.943	0.170	0.669	0.417	0.405	0.526	1.512	0.225	0.094	0.761	0.008	0.928	0.119	0.731	0.302	0.584	0.434	0.511
L. tardigradus	0.141	0.709	0.491	0.486	0.798	0.374	0.041	0.839	1.681	0.201	5.134	0.026	4.264	0.043	9.613	0.003	9.088	0.003
N. bengalensis	1.011	0.320	0.124	0.726	0.047	0.829	0.526	0.472	0.476	0.494	0.472	0.494	0.810	0.372	1.638	0.204	0.035	0.852
N. coucang	3.813	0.054	2.068	0.154	1.391	0.240	3.189	0.077	0.065	0.799	0.005	0.942	0.126	0.723	0.420	0.518	1.965	0.162
P. potto	3.454	0.065	1.287	0.258	0.734	0.393	2.357	0.127	0.260	0.611	0.330	0.566	0.589	0.444	1.389	0.240	0.322	0.571

Goswami model VAULT- PC4	*G. zanzibaricus*		*O. crassicaudatus*		*O. garnettii*		*A. laniger*		*I. indri*		*P. diadema*		*P. verreauxi*		*E. fulvus*		*E. macaco*	
	F value	p value	F value	p value	F value	p value	F value	p value	F value	p value	F value	p value	F value	p value	F value	p value	F value	p value
C. major																		
C. medius																		
M. murinus																		
M. rufus																		
G. alleni																		
G. demidoff																		
E. elegantulus																		
G. moholi																		
G. senegalensus																		
G. zanzibaricus																		
O. crassicaudatus	1.298	0.257																
O. garnettii	0.605	0.438	1.651	0.200														
A. laniger	0.005	0.946	1.832	0.178	0.752	0.388												
I. Indri	0.334	0.566	0.282	0.596	0.004	0.947	0.320	0.574										
P. diadema	0.165	0.686	4.985	0.027	3.383	0.068	0.286	0.595	1.236	0.271								
P. verreauxi	0.202	0.655	3.737	0.055	2.507	0.116	0.321	0.573	1.064	0.306	0.030	0.864						
E. fulvus	0.052	0.820	2.786	0.096	0.608	0.436	0.047	0.829	0.158	0.692	0.728	0.394	0.794	0.374				
E. macaco	0.001	0.970	2.985	0.086	1.332	0.250	0.015	0.903	0.491	0.485	0.187	0.667	0.273	0.602	0.174	0.677		
E. mongoz	0.103	0.749	7.767	0.006	4.731	0.031	0.233	0.631	1.189	0.278	0.009	0.923	0.073	0.788	1.142	0.286	0.164	0.687
E. rubriventer	0.008	0.929	0.986	0.323	0.337	0.563	0.002	0.968	0.164	0.687	0.201	0.656	0.256	0.614	0.016	0.899	0.020	0.888
H. griseus	1.577	0.215	0.239	0.626	1.471	0.228	1.640	0.207	0.556	0.459	3.298	0.075	2.454	0.122	1.337	0.249	2.019	0.159
L. catta	0.481	0.491	6.764	0.010	5.214	0.024	0.738	0.394	1.927	0.170	0.162	0.689	0.024	0.876	1.600	0.207	0.661	0.419
V. variegata	0.028	0.868	1.233	0.269	0.330	0.567	0.016	0.899	0.141	0.708	0.369	0.546	0.428	0.515	0.003	0.954	0.067	0.797
L. ruficaudatus	0.120	0.731	0.404	0.526	0.045	0.833	0.087	0.770	0.034	0.855	0.542	0.465	0.500	0.482	0.016	0.901	0.148	0.701
L. tardigradus	2.635	0.111	3.184	0.077	9.287	0.003	3.613	0.064	1.825	0.182	6.949	0.011	5.117	0.027	8.099	0.005	6.019	0.016
N. bengalensis	0.596	0.444	0.005	0.946	0.260	0.611	0.580	0.451	0.085	0.772	1.520	0.224	1.261	0.266	0.433	0.511	0.814	0.370
N. coucang	0.133	0.717	2.020	0.157	0.282	0.596	0.136	0.713	0.090	0.765	1.119	0.293	1.047	0.309	0.044	0.833	0.345	0.558
P. potto	0.494	0.483	0.761	0.384	0.058	0.810	0.656	0.419	0.003	0.956	2.592	0.109	2.199	0.140	0.808	0.369	1.256	0.264

Goswami model VAULT- PC4	*E. mongoz*		*E. rubriventer*		*H. griseus*		*L. catta*		*V. variegata*		*L. ruficaudatus*		*L. tardigradus*		*N. bengalensis*		*N. coucang*	
	F value	p value	F value	p value	F value	p value	F value	p value	F value	p value	F value	p value	F value	p value	F value	p value	F value	p value
C. major																		
C. medius																		
M. murinus																		
M. rufus																		
G. alleni																		
G. demidoff																		
E. elegantulus																		
G. moholi																		
G. senegalensus																		
G. zanzibaricus																		
O. crassicaudatus																		
O. garnettii																		
A. laniger																		
I. Indri																		
P. diadema																		
P. verreauxi																		
E. fulvus																		
E. macaco																		
E. mongoz																		
E. rubriventer	0.179	0.673																
H. griseus	3.285	0.074	0.584	0.448														
L. catta	0.296	0.588	6.251	0.015	3.973	0.051												
V. variegata	0.388	0.535	0.004	0.948	1.013	0.318	0.845	0.361										
L. ruficaudatus	0.435	0.511	0.038	0.846	0.673	0.416	0.944	0.335	0.022	0.884								
L. tardigradus	11.480	0.001	2.084	0.155	0.234	0.631	8.133	0.006	3.012	0.088	1.410	0.241						
N. bengalensis	1.522	0.221	0.324	0.572	0.133	0.717	2.089	0.154	0.331	0.568	0.167	0.685	0.648	0.425				
N. coucang	1.554	0.215	0.057	0.812	1.280	0.261	2.119	0.149	0.036	0.850	0.001	0.971	6.407	0.013	0.348	0.557		
P. potto	4.089	0.045	0.342	0.560	0.782	0.378	4.109	0.044	0.374	0.541	0.065	0.800	5.907	0.016	0.105	0.747	0.405	0.525

Goswami model VAULT- PC5	*C. major*		*C.medius*		*M. murinus*		*M. rufus*		*G. alleni*		*G. denidoff*		*E. elegantulus*		*G. moholi*		*G.senegalensis*	
	F value	p value	F value	p value	F value	p value	F value	p value	F value	p value	F value	p value	F value	p value	F value	p value	F value	p value
C. major																		
C. medius	0.490	0.487																
M. murinus	0.002	0.968	0.818	0.368														
M. rufus	0.230	0.634	2.356	0.131	0.236	0.628												
G. alleni	0.101	0.752	0.052	0.820	0.105	0.746	0.633	0.430										
G. demidoff	0.039	0.845	0.650	0.423	0.082	0.776	0.884	0.350	0.057	0.812								
E. elegantulus	1.686	0.200	0.472	0.495	1.727	0.192	5.119	0.027	0.628	0.431	2.205	0.141						
G. moholi	0.083	0.774	0.670	0.415	0.134	0.714	1.309	0.255	0.051	0.821	0.007	0.932	2.659	0.106				
G. senegalensus	2.583	0.110	1.018	0.314	5.287	0.022	8.880	0.003	0.578	0.448	4.332	0.039	0.001	0.974	3.984	0.047		
G. zanzibaricus	2.023	0.162	0.932	0.339	1.981	0.163	5.088	0.028	1.048	0.311	2.805	0.098	0.246	0.622	3.580	0.062	0.292	0.590
O. crassicaudatus	0.574	0.450	0.052	0.820	1.187	0.277	3.354	0.069	0.024	0.878	0.670	0.414	1.000	0.319	0.558	0.456	3.486	0.063
O. garnettii	1.536	0.218	0.145	0.704	2.840	0.094	6.630	0.011	0.237	0.627	2.345	0.128	0.361	0.549	2.215	0.139	1.147	0.285
A. laniger	0.007	0.935	0.600	0.442	0.020	0.888	0.481	0.491	0.087	0.769	0.015	0.902	2.251	0.139	0.049	0.826	3.722	0.055
I. Indri	0.478	0.492	0.001	0.976	0.593	0.443	2.153	0.147	0.052	0.821	0.491	0.485	0.518	0.474	0.509	0.477	0.697	0.405
P. diadema	3.855	0.055	12.272	0.001	6.073	0.016	3.762	0.058	3.755	0.059	10.601	0.002	15.560	0.000	13.542	0.000	41.575	0.000
P. verreauxi	0.243	0.624	0.006	0.939	0.406	0.526	1.142	0.289	0.017	0.898	0.254	0.615	0.316	0.576	0.241	0.625	0.661	0.417
E. fulvus	0.007	0.932	0.837	0.362	0.040	0.842	0.532	0.467	0.057	0.811	0.017	0.897	1.605	0.207	0.041	0.840	8.059	0.005
E. macaco	1.125	0.292	5.584	0.021	1.747	0.189	0.580	0.449	1.351	0.249	3.324	0.071	7.292	0.008	4.086	0.045	20.829	0.000
E. mongoz	0.654	0.421	0.039	0.845	1.434	0.233	2.798	0.098	0.091	0.763	1.034	0.311	0.196	0.659	0.988	0.322	0.709	0.401
E. rubriventer	0.840	0.364	3.445	0.069	0.997	0.320	0.401	0.529	1.254	0.269	2.249	0.138	6.054	0.017	3.084	0.082	11.049	0.001
H. griseus	0.002	0.960	0.734	0.395	0.000	0.993	0.229	0.634	0.159	0.692	0.083	0.774	2.369	0.129	0.160	0.690	3.492	0.063
L. catta	0.078	0.780	0.223	0.639	0.149	0.700	0.819	0.369	0.008	0.927	0.032	0.857	1.109	0.296	0.016	0.899	2.375	0.125
V. variegata	0.025	0.874	1.161	0.285	0.019	0.889	0.135	0.714	0.219	0.642	0.220	0.640	2.694	0.105	0.348	0.557	5.845	0.016
L. ruficaudatus	0.109	0.743	0.037	0.849	0.161	0.689	0.639	0.428	0.001	0.978	0.083	0.774	0.429	0.515	0.075	0.785	0.700	0.404
L. tardigradus	2.862	0.097	2.198	0.144	5.264	0.024	8.408	0.005	1.070	0.306	6.179	0.015	0.477	0.493	7.126	0.009	1.669	0.198
N. bengalensis	2.234	0.142	1.776	0.189	3.608	0.061	4.751	0.034	1.121	0.296	4.206	0.044	0.917	0.343	5.047	0.027	2.281	0.133
N. coucang	0.762	0.385	0.182	0.671	1.895	0.171	2.812	0.097	0.145	0.704	1.364	0.245	0.029	0.865	1.297	0.257	0.112	0.738
P. potto	0.071	0.790	0.598	0.441	0.214	0.644	1.110	0.294	0.023	0.880	0.014	0.907	1.612	0.206	0.001	0.973	7.167	0.008

Goswami model VAULT- PC5	*G. zanzibaricus*		*O. crassicaudatus*		*O. garnettii*		*A. laniger*		*I. indri*		*P. diadema*		*P. verreauxi*		*E. fulvus*		*E. macaco*	
	F value	p value	F value	p value	F value	p value	F value	p value	F value	p value	F value	p value	F value	p value	F value	p value	F value	p value
C. major																		
C. medius																		
M. murinus																		
M. rufus																		
G. alleni																		
G. demidoff																		
E. elegantulus																		
G. moholi																		
G. senegalensus																		
G. zanzibaricus																		
O. crassicaudatus	1.692	0.196																
O. garnettii	1.084	0.300	0.911	0.341														
A. laniger	2.643	0.111	0.705	0.403	2.182	0.142												
I. Indri	1.077	0.304	0.022	0.883	0.122	0.727	0.544	0.464										
P. diadema	12.292	0.001	24.160	0.000	34.664	0.000	6.165	0.017	10.822	0.002								
P. verreauxi	0.607	0.439	0.003	0.957	0.130	0.719	0.251	0.618	0.003	0.960	7.052	0.010						
E. fulvus	1.888	0.171	1.390	0.239	4.031	0.046	0.000	0.998	0.474	0.492	10.376	0.001	0.348	0.556				
E. macaco	6.537	0.013	9.885	0.002	15.556	0.000	1.952	0.167	4.380	0.039	1.652	0.202	3.059	0.084	3.394	0.067		
E. mongoz	0.525	0.471	0.319	0.573	0.008	0.930	0.848	0.360	0.038	0.845	15.569	0.000	0.050	0.824	1.961	0.163	7.677	0.007
E. rubriventer	5.598	0.022	5.393	0.022	8.690	0.004	1.348	0.252	3.385	0.071	0.989	0.325	2.034	0.158	1.608	0.206	0.000	0.997
H. griseus	2.752	0.104	0.862	0.355	2.214	0.139	0.024	0.879	0.701	0.406	4.580	0.037	0.347	0.558	0.024	0.878	1.245	0.268
L. catta	1.497	0.226	0.210	0.647	1.046	0.308	0.061	0.806	0.177	0.675	7.389	0.009	0.085	0.772	0.081	0.776	2.748	0.101
V. variegata	2.937	0.092	1.623	0.205	3.667	0.058	0.085	0.772	0.977	0.326	5.158	0.027	0.569	0.453	0.116	0.734	1.282	0.261
L. ruficaudatus	0.704	0.406	0.016	0.901	0.231	0.632	0.096	0.758	0.031	0.860	4.221	0.045	0.011	0.916	0.108	0.743	1.723	0.193
L. tardigradus	0.014	0.905	6.646	0.011	4.644	0.033	4.318	0.043	1.853	0.178	24.189	0.000	1.244	0.269	8.214	0.005	15.351	0.000
N. bengalensis	0.285	0.596	4.178	0.043	3.391	0.068	2.771	0.104	1.850	0.179	10.934	0.002	1.387	0.244	4.465	0.036	8.000	0.006
N. coucang	0.204	0.653	0.868	0.353	0.132	0.716	1.022	0.315	0.143	0.706	14.423	0.000	0.153	0.696	3.107	0.079	7.870	0.006
P. potto	2.041	0.155	0.815	0.368	3.295	0.071	0.049	0.825	0.341	0.560	14.515	0.000	0.216	0.643	0.127	0.721	5.180	0.024

Goswami model VAULT- PC5	*E. mongoz*		*E. rubriventer*		*H. griseus*		*L. catta*		*V. variegata*		*L. ruficaudatus*		*L. tardigradus*		*N. bengalensis*		*N. coucang*	
	F value	p value	F value	p value	F value	p value	F value	p value	F value	p value	F value	p value	F value	p value	F value	p value	F value	p value
C. major																		
C. medius																		
M. murinus																		
M. rufus																		
G. alleni																		
G. demidoff																		
E. elegantulus																		
G. moholi																		
G. senegalensus																		
G. zanzibaricus																		
O. crassicaudatus																		
O. garnettii																		
A. laniger																		
I. Indri																		
P. diadema																		
P. verreauxi																		
E. fulvus																		
E. macaco																		
E. mongoz																		
E. rubriventer	3.982	0.049																
H. griseus	0.928	0.338	0.002	0.960														
L. catta	0.430	0.514	0.078	0.780	0.136	0.714												
V. variegata	1.645	0.203	0.831	0.365	0.014	0.905	0.280	0.598										
L. ruficaudatus	0.092	0.762	1.273	0.265	0.165	0.687	0.016	0.899	0.267	0.607								
L. tardigradus	1.968	0.164	8.316	0.006	3.994	0.051	3.052	0.086	5.823	0.019	1.045	0.312						
N. bengalensis	1.725	0.193	5.076	0.029	2.833	0.099	2.331	0.133	3.780	0.057	1.126	0.294	0.315	0.578				
N. coucang	0.096	0.758	3.772	0.055	1.042	0.310	0.647	0.423	1.879	0.173	0.172	0.679	0.939	0.335	1.089	0.300		
P. potto	1.465	0.228	2.584	0.110	0.132	0.717	0.009	0.923	0.370	0.544	0.049	0.825	8.418	0.004	4.709	0.032	2.416	0.122

Goswami model BASE- PC1	*C. major*		*C.medius*		*M. murinus*		*M. rufus*		*G. alleni*		*G. denidoff*		*E. elegantulus*		*G. moholi*		*G.senegalensis*	
	F value	p value	F value	p value	F value	p value	F value	p value	F value	p value	F value	p value	F value	p value	F value	p value	F value	p value
C. major																		
C. medius	0.001	0.980																
M. murinus	1.050	0.308	2.050	0.156														
M. rufus	0.001	0.975	0.006	0.941	1.230	0.270												
G. alleni	0.084	0.773	0.244	0.624	2.080	0.153	0.073	0.788										
G. demidoff	0.304	0.583	0.603	0.440	0.339	0.561	0.377	0.541	0.872	0.353								
E. elegantulus	0.780	0.381	2.050	0.157	0.065	0.799	0.908	0.345	1.690	0.200	0.106	0.745						
G. moholi	0.016	0.900	0.024	0.876	1.320	0.253	0.029	0.866	0.233	0.631	0.294	0.588	0.724	0.397				
G. senegalensus	0.236	0.628	0.491	0.484	1.730	0.189	0.321	0.572	1.130	0.288	0.185	0.668	0.825	0.365	0.179	0.673		
G. zanzibaricus	0.337	0.565	0.891	0.350	2.830	0.096	0.325	0.571	0.098	0.756	1.470	0.229	2.570	0.114	0.617	0.434	2.130	0.146
O. crassicaudatus	0.010	0.921	0.014	0.907	1.920	0.167	0.021	0.884	0.256	0.614	0.476	0.491	1.060	0.305	0.004	0.950	0.404	0.525
O. garnettii	0.548	0.461	1.360	0.245	6.400	0.012	0.535	0.466	0.130	0.719	3.280	0.072	4.990	0.027	1.430	0.233	5.940	0.015
A. laniger	0.121	0.729	0.243	0.624	0.317	0.575	0.157	0.694	0.386	0.537	0.008	0.930	0.114	0.737	0.116	0.734	0.045	0.832
I. Indri	0.608	0.438	1.170	0.283	0.004	0.947	0.696	0.407	1.170	0.284	0.139	0.710	0.018	0.893	0.582	0.447	0.671	0.414
P. diadema	1.560	0.218	4.840	0.032	0.014	0.905	1.760	0.190	2.850	0.098	0.502	0.481	0.189	0.666	1.510	0.222	2.220	0.138
P. verreauxi	0.648	0.424	1.560	0.216	0.151	0.698	0.772	0.383	1.530	0.221	0.052	0.820	0.016	0.900	0.640	0.425	0.662	0.417
E. fulvus	0.001	0.981	0.005	0.942	3.250	0.073	0.001	0.981	0.205	0.651	0.999	0.319	1.970	0.161	0.076	0.784	1.100	0.295
E. macaco	0.182	0.671	0.472	0.494	3.420	0.067	0.163	0.688	0.005	0.944	1.540	0.218	2.780	0.099	0.475	0.492	2.120	0.147
E. mongoz	1.460	0.230	3.560	0.063	0.001	0.976	1.720	0.193	2.980	0.088	0.457	0.500	0.083	0.773	1.880	0.173	2.890	0.090
E. rubriventer	0.120	0.730	0.332	0.567	1.570	0.213	0.105	0.747	0.007	0.934	0.718	0.399	1.530	0.221	0.214	0.645	0.806	0.370
H. griseus	0.276	0.602	0.594	0.445	0.147	0.703	0.331	0.568	0.678	0.414	0.006	0.939	0.036	0.850	0.238	0.627	0.186	0.666
L. catta	0.093	0.761	0.235	0.629	2.180	0.143	0.082	0.776	0.000	0.988	0.924	0.339	1.670	0.200	0.260	0.612	1.200	0.274
V. variegata	0.792	0.377	1.940	0.169	0.059	0.809	0.924	0.340	1.710	0.197	0.117	0.734	0.000	0.988	0.761	0.385	0.869	0.352
L. ruficaudatus	0.719	0.401	2.250	0.140	4.580	0.035	0.710	0.403	0.301	0.586	2.580	0.112	4.540	0.038	1.240	0.268	4.220	0.041
L. tardigradus	0.068	0.796	0.215	0.645	1.760	0.188	0.104	0.749	0.531	0.470	0.320	0.573	1.110	0.297	0.019	0.890	0.169	0.682
N. bengalensis	1.320	0.257	5.040	0.030	0.001	0.978	1.500	0.226	2.550	0.118	0.332	0.566	0.078	0.781	1.230	0.270	1.770	0.185
N. coucang	0.085	0.771	0.193	0.661	1.750	0.188	0.127	0.723	0.601	0.440	0.296	0.588	0.954	0.331	0.034	0.854	0.108	0.743
P. potto	0.007	0.933	0.027	0.869	3.380	0.068	0.002	0.965	0.124	0.725	1.110	0.294	1.980	0.162	0.135	0.714	1.840	0.176

Goswami model BASE- PC1	*G. zanzibaricus*		*O. crassicaudatus*		*O. garnettii*		*A. laniger*		*I. indri*		*P. diadema*		*P. verreauxi*		*E. fulvus*		*E. macaco*	
	F value	p value	F value	p value	F value	p value	F value	p value	F value	p value	F value	p value	F value	p value	F value	p value	F value	p value
C. major																		
C. medius																		
M. murinus																		
M. rufus																		
G. alleni																		
G. demidoff																		
E. elegantulus																		
G. moholi																		
G. senegalensus																		
G. zanzibaricus																		
O. crassicaudatus	0.713	0.400																
O. garnettii	0.012	0.913	1.870	0.173														
A. laniger	0.719	0.401	0.199	0.656	1.840	0.178												
I. Indri	1.750	0.191	0.788	0.376	3.070	0.082	0.132	0.718										
P. diadema	3.980	0.052	2.140	0.146	7.600	0.007	0.390	0.535	0.028	0.867								
P. verreauxi	2.370	0.128	0.984	0.323	5.070	0.026	0.073	0.787	0.052	0.820	0.322	0.572						
E. fulvus	0.758	0.385	0.062	0.804	1.800	0.181	0.491	0.484	1.390	0.240	3.720	0.055	1.890	0.171				
E. macaco	0.103	0.749	0.546	0.461	0.120	0.729	0.798	0.375	1.840	0.179	4.580	0.035	2.610	0.109	0.452	0.502		
E. mongoz	4.000	0.049	2.980	0.087	10.400	0.002	0.405	0.527	0.003	0.956	0.033	0.856	0.207	0.650	5.220	0.023	5.180	0.025
E. rubriventer	0.042	0.839	0.223	0.638	0.030	0.864	0.361	0.551	1.120	0.295	2.620	0.111	1.300	0.259	0.197	0.658	0.002	0.969
H. griseus	1.160	0.286	0.352	0.554	2.210	0.140	0.016	0.902	0.065	0.799	0.265	0.609	0.010	0.920	0.722	0.396	1.180	0.281
L. catta	0.088	0.768	0.287	0.593	0.114	0.736	0.438	0.511	1.200	0.277	2.760	0.102	1.550	0.216	0.232	0.630	0.003	0.960
V. variegata	2.580	0.114	1.110	0.293	5.070	0.026	0.125	0.724	0.015	0.902	0.168	0.684	0.020	0.889	2.050	0.154	2.810	0.097
L. ruficaudatus	0.030	0.863	1.510	0.222	0.152	0.698	1.270	0.266	2.730	0.103	6.970	0.011	4.220	0.044	1.710	0.193	0.364	0.548
L. tardigradus	1.210	0.276	0.073	0.788	3.830	0.053	0.088	0.768	0.695	0.408	2.690	0.107	0.927	0.339	0.406	0.525	1.200	0.276
N. bengalensis	3.680	0.062	1.800	0.182	7.180	0.008	0.262	0.612	0.003	0.959	0.036	0.850	0.172	0.680	3.260	0.073	4.210	0.044
N. coucang	1.300	0.258	0.107	0.745	3.890	0.050	0.093	0.762	0.685	0.410	2.260	0.136	0.820	0.367	0.475	0.491	1.250	0.266
P. potto	0.550	0.460	0.148	0.701	1.600	0.207	0.519	0.472	1.310	0.255	3.580	0.060	1.980	0.161	0.021	0.885	0.317	0.574

Goswami model BASE- PC1	*E. mongoz*		*E. rubriventer*		*H. griseus*		*L. catta*		*V. variegata*		*L. ruficaudatus*		*L. tardigradus*		*N. bengalensis*		*N. coucang*	
	F value	p value	F value	p value	F value	p value	F value	p value	F value	p value	F value	p value	F value	p value	F value	p value	F value	p value
C. major																		
C. medius																		
M. murinus																		
M. rufus																		
G. alleni																		
G. demidoff																		
E. elegantulus																		
G. moholi																		
G. senegalensus																		
G. zanzibaricus																		
O. crassicaudatus																		
O. garnettii																		
A. laniger																		
I. Indri																		
P. diadema																		
P. verreauxi																		
E. fulvus																		
E. macaco																		
E. mongoz																		
E. rubriventer	2.180	0.144																
H. griseus	0.186	0.668	0.276	0.602														
L. catta	3.050	0.084	0.093	0.761	0.710	0.403												
V. variegata	0.073	0.787	1.500	0.225	0.041	0.841	1.710	0.195										
L. ruficaudatus	7.000	0.010	0.159	0.692	1.980	0.166	0.274	0.603	4.470	0.039								
L. tardigradus	3.270	0.074	0.480	0.492	0.255	0.616	0.560	0.457	1.130	0.292	2.790	0.102						
N. bengalensis	0.000	0.998	2.440	0.125	0.159	0.692	2.440	0.125	0.065	0.799	6.820	0.012	2.340	0.133				
N. coucang	3.020	0.085	0.478	0.491	0.244	0.622	0.645	0.424	0.995	0.321	2.740	0.101	0.004	0.949	1.870	0.175		
P. potto	5.770	0.017	0.126	0.723	0.711	0.401	0.146	0.703	2.070	0.153	1.320	0.253	0.682	0.410	3.170	0.077	0.809	0.369

Goswami model BASE- PC2	*C. major*		*C.medius*		*M. murinus*		*M. rufus*		*G. alleni*		*G. denidoff*		*E. elegantulus*		*G. moholi*		*G.senegalensis*	
	F value	p value	F value	p value	F value	p value	F value	p value	F value	p value	F value	p value	F value	p value	F value	p value	F value	p value
C. major																		
C. medius	1.330	0.254																
M. murinus	0.240	0.626	0.939	0.335														
M. rufus	0.199	0.657	4.940	0.030	1.400	0.239												
G. alleni	0.055	0.816	3.070	0.086	0.804	0.372	0.053	0.819										
G. demidoff	0.710	0.402	0.248	0.620	0.225	0.636	2.730	0.102	1.750	0.190								
E. elegantulus	0.862	0.357	0.090	0.765	0.395	0.531	3.530	0.065	2.110	0.152	0.033	0.857						
G. moholi	0.026	0.873	2.980	0.088	0.725	0.396	0.114	0.737	0.013	0.911	1.700	0.195	1.800	0.182				
G. senegalensus	0.217	0.642	1.810	0.180	0.022	0.882	1.400	0.239	0.845	0.359	0.538	0.464	0.740	0.391	1.040	0.309		
G. zanzibaricus	1.810	0.185	0.265	0.609	1.580	0.212	5.980	0.018	3.690	0.061	0.793	0.376	0.573	0.452	3.050	0.084	2.170	0.142
O. crassicaudatus	0.031	0.862	4.590	0.034	1.010	0.317	0.183	0.669	0.025	0.874	2.440	0.120	2.610	0.109	0.001	0.979	1.680	0.196
O. garnettii	0.019	0.891	4.810	0.030	0.944	0.333	0.266	0.607	0.050	0.823	2.430	0.121	2.750	0.100	0.008	0.927	1.360	0.245
A. laniger	0.121	0.729	0.445	0.508	0.000	0.990	0.745	0.392	0.396	0.532	0.123	0.727	0.198	0.658	0.438	0.510	0.018	0.893
I. Indri	0.126	0.724	3.560	0.064	0.951	0.332	0.008	0.929	0.018	0.895	1.930	0.168	2.560	0.115	0.051	0.821	0.848	0.358
P. diadema	0.040	0.843	1.570	0.215	0.107	0.744	0.729	0.397	0.296	0.589	0.605	0.439	0.877	0.353	0.202	0.654	0.064	0.800
P. verreauxi	0.616	0.435	0.402	0.528	0.151	0.698	2.840	0.097	1.680	0.200	0.010	0.920	0.086	0.771	1.470	0.227	0.384	0.536
E. fulvus	4.500	0.035	0.938	0.334	4.400	0.037	9.630	0.002	8.090	0.005	2.360	0.125	1.420	0.235	11.500	0.001	11.800	0.001
E. macaco	1.760	0.188	0.049	0.825	1.330	0.250	5.050	0.027	3.570	0.063	0.486	0.487	0.239	0.626	3.770	0.055	2.510	0.114
E. mongoz	5.120	0.026	1.950	0.167	5.700	0.018	12.800	0.001	9.650	0.003	3.580	0.061	2.590	0.111	10.800	0.001	11.200	0.001
E. rubriventer	0.929	0.340	0.028	0.868	0.639	0.426	3.110	0.084	1.890	0.175	0.240	0.626	0.138	0.712	1.500	0.224	0.851	0.357
H. griseus	0.042	0.839	1.050	0.309	0.060	0.807	0.621	0.434	0.258	0.614	0.395	0.531	0.599	0.442	0.170	0.681	0.027	0.870
L. catta	0.229	0.634	0.602	0.441	0.006	0.939	1.370	0.247	0.733	0.396	0.117	0.733	0.244	0.623	0.622	0.432	0.046	0.830
V. variegata	3.390	0.071	1.160	0.285	3.630	0.059	8.700	0.004	6.210	0.016	2.250	0.137	1.680	0.200	6.310	0.014	5.710	0.018
L. ruficaudatus	0.666	0.419	0.132	0.718	0.280	0.598	3.020	0.089	1.700	0.198	0.010	0.922	0.006	0.940	1.450	0.231	0.542	0.463
L. tardigradus	0.549	0.462	0.526	0.471	0.167	0.684	2.660	0.109	1.580	0.215	0.024	0.878	0.116	0.735	2.090	0.151	0.813	0.368
N. bengalensis	1.830	0.183	0.153	0.698	1.620	0.206	6.720	0.013	4.050	0.051	0.708	0.403	0.449	0.506	3.630	0.060	2.630	0.106
N. coucang	0.830	0.365	0.450	0.504	0.276	0.600	3.220	0.076	2.160	0.145	0.003	0.953	0.070	0.792	2.770	0.099	1.180	0.278
P. potto	0.531	0.467	0.718	0.398	0.081	0.776	2.110	0.148	1.450	0.230	0.075	0.784	0.190	0.663	2.110	0.148	0.589	0.444

Goswami model BASE- PC2	*G. zanzibaricus*		*O. crassicaudatus*		*O. garnettii*		*A. laniger*		*I. indri*		*P. diadema*		*P. verreauxi*		*E. fulvus*		*E. macaco*	
	F value	p value	F value	p value	F value	p value	F value	p value	F value	p value	F value	p value	F value	p value	F value	p value	F value	p value
C. major																		
C. medius																		
M. murinus																		
M. rufus																		
G. alleni																		
G. demidoff																		
E. elegantulus																		
G. moholi																		
G. senegalensus																		
G. zanzibaricus																		
O. crassicaudatus	4.330	0.040																
O. garnettii	4.800	0.031	0.007	0.934														
A. laniger	0.778	0.382	0.635	0.427	0.603	0.439												
I. Indri	4.650	0.035	0.081	0.777	0.125	0.724	0.562	0.457										
P. diadema	2.310	0.135	0.280	0.598	0.252	0.617	0.058	0.811	0.478	0.492								
P. verreauxi	1.090	0.301	2.160	0.144	2.190	0.141	0.076	0.783	1.970	0.164	0.523	0.472						
E. fulvus	0.027	0.869	18.400	0.000	17.000	0.000	2.880	0.091	6.600	0.011	5.270	0.023	2.830	0.094				
E. macaco	0.090	0.765	5.540	0.020	5.660	0.019	0.744	0.391	3.710	0.057	1.960	0.166	0.674	0.414	0.453	0.502		
E. mongoz	0.276	0.601	17.200	0.000	17.600	0.000	3.170	0.079	9.150	0.003	6.910	0.010	4.420	0.038	0.319	0.573	1.130	0.290
E. rubriventer	0.051	0.823	2.020	0.158	2.220	0.139	0.328	0.570	2.540	0.116	1.030	0.315	0.348	0.558	0.149	0.699	0.000	0.990
H. griseus	1.730	0.195	0.226	0.636	0.210	0.648	0.033	0.856	0.431	0.514	0.001	0.972	0.335	0.564	3.380	0.068	1.350	0.250
L. catta	1.200	0.279	0.873	0.352	0.867	0.353	0.002	0.963	0.982	0.325	0.132	0.718	0.072	0.789	2.910	0.090	0.887	0.349
V. variegata	0.191	0.664	9.240	0.003	9.870	0.002	1.920	0.171	6.700	0.012	4.390	0.040	2.750	0.101	0.173	0.678	0.704	0.404
L. ruficaudatus	0.629	0.432	2.120	0.148	2.240	0.137	0.129	0.721	2.210	0.143	0.670	0.417	0.040	0.842	1.500	0.222	0.291	0.591
L. tardigradus	1.060	0.309	3.930	0.050	3.660	0.058	0.066	0.799	1.790	0.186	0.503	0.481	0.002	0.968	6.360	0.012	0.943	0.334
N. bengalensis	0.035	0.854	5.500	0.021	5.980	0.016	0.743	0.394	4.940	0.030	2.440	0.125	1.020	0.317	0.199	0.656	0.023	0.880
N. coucang	1.040	0.311	4.860	0.029	4.430	0.037	0.142	0.708	2.110	0.149	0.733	0.394	0.004	0.950	5.800	0.017	0.847	0.359
P. potto	1.160	0.282	3.720	0.055	3.120	0.079	0.043	0.836	1.340	0.248	0.373	0.542	0.026	0.872	7.960	0.005	1.200	0.275

Goswami model BASE- PC2	*E. mongoz*		*E. rubriventer*		*H. griseus*		*L. catta*		*V. variegata*		*L. ruficaudatus*		*L. tardigradus*		*N. bengalensis*		*N. coucang*	
	F value	p value	F value	p value	F value	p value	F value	p value	F value	p value	F value	p value	F value	p value	F value	p value	F value	p value
C. major																		
C. medius																		
M. murinus																		
M. rufus																		
G. alleni																		
G. demidoff																		
E. elegantulus																		
G. moholi																		
G. senegalensus																		
G. zanzibaricus																		
O. crassicaudatus																		
O. garnettii																		
A. laniger																		
I. Indri																		
P. diadema																		
P. verreauxi																		
E. fulvus																		
E. macaco																		
E. mongoz																		
E. rubriventer	0.460	0.499																
H. griseus	4.620	0.035	0.042	0.839														
L. catta	4.060	0.047	0.229	0.634	0.080	0.778												
V. variegata	0.000	0.998	0.340	0.562	3.170	0.080	2.640	0.108										
L. ruficaudatus	2.640	0.109	0.169	0.683	0.456	0.503	0.163	0.688	1.700	0.198								
L. tardigradus	6.980	0.010	0.320	0.574	0.285	0.596	0.060	0.807	3.220	0.078	0.055	0.816						
N. bengalensis	0.776	0.381	0.010	0.923	1.700	0.198	1.150	0.289	0.486	0.489	0.512	0.478	1.120	0.295				
N. coucang	6.730	0.011	0.301	0.584	0.426	0.516	0.121	0.728	3.310	0.072	0.027	0.870	0.023	0.880	1.080	0.302		
P. potto	7.500	0.007	0.386	0.535	0.205	0.651	0.022	0.882	3.600	0.060	0.111	0.739	0.039	0.843	1.320	0.253	0.138	0.711

Goswami model BASE- PC3	*C. major*		*C.medius*		*M. murinus*		*M. rufus*		*G. alleni*		*G. denidoff*		*E. elegantulus*		*G. moholi*		*G.senegalensis*	
	F value	p value	F value	p value	F value	p value	F value	p value	F value	p value	F value	p value	F value	p value	F value	p value	F value	p value
C. major																		
C. medius	0.175	0.678																
M. murinus	0.577	0.449	0.141	0.708														
M. rufus	1.990	0.164	4.690	0.035	6.630	0.012												
G. alleni	4.340	0.043	4.530	0.038	4.510	0.036	14.100	0.000										
G. demidoff	0.083	0.774	0.018	0.892	0.243	0.623	3.190	0.078	4.950	0.029								
E. elegantulus	0.002	0.962	0.349	0.557	0.966	0.328	2.880	0.095	6.980	0.011	0.163	0.687						
G. moholi	1.220	0.272	0.780	0.379	0.301	0.584	7.820	0.006	2.560	0.113	0.985	0.323	2.010	0.159				
G. senegalensus	0.703	0.403	0.217	0.642	0.000	0.999	7.430	0.007	6.420	0.012	0.392	0.532	1.240	0.267	0.538	0.464		
G. zanzibaricus	5.090	0.029	9.600	0.003	12.200	0.001	1.300	0.260	19.300	0.000	6.570	0.012	7.620	0.008	12.700	0.001	12.900	0.000
O. crassicaudatus	0.222	0.638	1.560	0.214	2.880	0.092	1.210	0.274	12.200	0.001	1.080	0.300	0.277	0.600	5.880	0.016	6.590	0.011
O. garnettii	0.143	0.706	1.320	0.253	2.560	0.112	1.800	0.182	12.700	0.001	0.839	0.361	0.164	0.686	5.310	0.023	5.110	0.025
A. laniger	2.340	0.134	2.210	0.144	2.000	0.160	9.290	0.004	0.239	0.628	2.600	0.111	3.850	0.055	0.876	0.352	3.060	0.082
I. Indri	0.237	0.628	1.010	0.320	1.790	0.184	0.940	0.336	7.480	0.008	0.622	0.432	0.283	0.596	2.620	0.108	1.880	0.172
P. diadema	2.840	0.099	6.510	0.014	9.430	0.003	0.175	0.677	16.200	0.000	4.930	0.029	4.250	0.044	11.200	0.001	12.200	0.001
P. verreauxi	0.651	0.423	2.480	0.120	4.090	0.046	0.654	0.421	12.600	0.001	1.680	0.197	0.894	0.348	6.130	0.015	5.790	0.017
E. fulvus	1.250	0.265	4.940	0.027	7.100	0.008	0.321	0.572	21.300	0.000	3.720	0.055	1.730	0.190	12.800	0.000	16.700	0.000
E. macaco	0.153	0.697	1.080	0.301	2.140	0.146	1.430	0.235	9.760	0.003	0.694	0.407	0.179	0.674	3.870	0.052	3.230	0.074
E. mongoz	0.197	0.659	1.320	0.254	2.580	0.110	1.180	0.281	10.300	0.002	0.910	0.342	0.249	0.619	4.880	0.029	4.980	0.027
E. rubriventer	0.512	0.478	1.420	0.239	2.310	0.132	0.312	0.579	6.930	0.012	0.936	0.336	0.668	0.417	2.900	0.092	2.280	0.132
H. griseus	0.444	0.508	0.148	0.702	0.019	0.890	4.470	0.039	1.890	0.176	0.226	0.636	0.739	0.394	0.069	0.794	0.023	0.879
L. catta	0.154	0.696	0.007	0.933	0.208	0.649	5.790	0.019	5.380	0.024	0.003	0.954	0.305	0.583	0.836	0.363	0.244	0.622
V. variegata	2.070	0.156	4.990	0.029	7.590	0.007	0.063	0.803	14.000	0.000	4.100	0.046	2.960	0.090	9.710	0.002	11.000	0.001
L. ruficaudatus	0.684	0.413	2.230	0.142	3.790	0.055	0.392	0.534	9.950	0.003	1.560	0.215	0.975	0.328	5.160	0.025	4.830	0.029
L. tardigradus	0.241	0.626	0.002	0.961	0.160	0.690	5.880	0.019	5.570	0.023	0.045	0.833	0.528	0.470	1.160	0.284	0.412	0.522
N. bengalensis	0.094	0.761	0.855	0.360	1.820	0.181	2.350	0.132	8.180	0.007	0.475	0.493	0.109	0.742	3.050	0.084	2.310	0.130
N. coucang	0.086	0.771	0.112	0.738	0.688	0.408	5.620	0.020	9.930	0.002	0.015	0.903	0.204	0.653	2.560	0.112	1.660	0.199
P. potto	1.170	0.280	0.867	0.353	0.294	0.588	7.460	0.007	3.110	0.080	1.140	0.286	2.040	0.155	0.004	0.950	0.971	0.325

Goswami model BASE- PC3	*G. zanzibaricus*		*O. crassicaudatus*		*O. garnettii*		*A. laniger*		*I. indri*		*P. diadema*		*P. verreauxi*		*E. fulvus*		*E. macaco*	
	F value	p value	F value	p value	F value	p value	F value	p value	F value	p value	F value	p value	F value	p value	F value	p value	F value	p value
C. major																		
C. medius																		
M. murinus																		
M. rufus																		
G. alleni																		
G. demidoff																		
E. elegantulus																		
G. moholi																		
G. senegalensus																		
G. zanzibaricus																		
O. crassicaudatus	3.870	0.051																
O. garnettii	5.270	0.024	0.044	0.834														
A. laniger	13.300	0.001	7.990	0.006	8.060	0.005												
I. Indri	3.810	0.056	0.006	0.936	0.045	0.832	4.440	0.040										
P. diadema	0.360	0.551	2.640	0.107	3.600	0.060	11.200	0.002	1.640	0.205								
P. verreauxi	3.450	0.068	0.198	0.657	0.418	0.519	8.090	0.006	0.066	0.798	1.550	0.218						
E. fulvus	2.440	0.120	1.080	0.299	1.590	0.209	15.200	0.000	0.219	0.640	1.230	0.269	0.096	0.757				
E. macaco	4.540	0.036	0.009	0.923	0.005	0.944	6.000	0.017	0.024	0.879	2.680	0.106	0.254	0.615	0.833	0.363		
E. mongoz	3.820	0.054	0.000	0.993	0.033	0.856	6.530	0.013	0.007	0.933	2.410	0.125	0.185	0.668	0.878	0.350	0.007	0.933
E. rubriventer	2.280	0.137	0.130	0.719	0.256	0.614	4.210	0.046	0.098	0.755	0.705	0.405	0.011	0.919	0.008	0.930	0.198	0.657
H. griseus	8.240	0.006	1.720	0.192	1.640	0.203	0.739	0.394	1.430	0.237	5.560	0.022	2.610	0.111	4.180	0.042	1.440	0.234
L. catta	13.300	0.001	1.080	0.301	0.934	0.336	2.610	0.112	1.110	0.297	7.350	0.009	2.380	0.127	3.430	0.066	0.909	0.343
V. variegata	0.363	0.549	2.140	0.145	2.860	0.093	9.860	0.003	1.050	0.308	0.012	0.914	1.020	0.316	0.897	0.345	2.000	0.161
L. ruficaudatus	2.700	0.107	0.263	0.609	0.495	0.483	6.260	0.016	0.127	0.722	0.984	0.326	0.019	0.892	0.014	0.908	0.331	0.567
L. tardigradus	11.400	0.001	3.410	0.067	2.720	0.102	2.780	0.102	1.230	0.272	8.760	0.005	3.770	0.056	11.300	0.001	1.730	0.192
N. bengalensis	7.810	0.008	0.046	0.831	0.004	0.947	4.650	0.037	0.080	0.779	3.480	0.069	0.429	0.515	0.983	0.323	0.015	0.904
N. coucang	11.800	0.001	2.260	0.135	1.610	0.207	5.490	0.021	0.884	0.349	9.260	0.003	3.080	0.082	8.710	0.003	1.130	0.289
P. potto	11.700	0.001	10.100	0.002	8.010	0.005	1.160	0.283	2.320	0.130	11.900	0.001	6.920	0.009	23.500	0.000	4.510	0.035

Goswami model BASE- PC3	*E. mongoz*		*E. rubriventer*		*H. griseus*		*L. catta*		*V. variegata*		*L. ruficaudatus*		*L. tardigradus*		*N. bengalensis*		*N. coucang*	
	F value	p value	F value	p value	F value	p value	F value	p value	F value	p value	F value	p value	F value	p value	F value	p value	F value	p value
C. major																		
C. medius																		
M. murinus																		
M. rufus																		
G. alleni																		
G. demidoff																		
E. elegantulus																		
G. moholi																		
G. senegalensus																		
G. zanzibaricus																		
O. crassicaudatus																		
O. garnettii																		
A. laniger																		
I. Indri																		
P. diadema																		
P. verreauxi																		
E. fulvus																		
E. macaco																		
E. mongoz																		
E. rubriventer	0.132	0.717																
H. griseus	1.530	0.220	0.444	0.508														
L. catta	1.020	0.315	0.154	0.696	0.237	0.628												
V. variegata	1.880	0.174	0.401	0.529	4.380	0.040	4.920	0.030										
L. ruficaudatus	0.245	0.622	0.000	0.995	2.360	0.131	2.480	0.121	0.601	0.441								
L. tardigradus	2.470	0.120	1.600	0.212	0.149	0.702	0.021	0.886	6.980	0.010	3.000	0.090						
N. bengalensis	0.039	0.844	0.389	0.536	1.240	0.272	0.935	0.338	2.190	0.144	0.541	0.466	1.230	0.273				
N. coucang	1.750	0.188	1.390	0.242	0.524	0.471	0.042	0.838	7.340	0.008	2.750	0.101	0.355	0.553	0.782	0.379		
P. potto	7.020	0.009	2.480	0.117	0.053	0.819	0.765	0.383	11.100	0.001	5.360	0.022	2.090	0.150	3.140	0.078	4.570	0.034

Goswami model BASE- PC4	*C. major*		*C.medius*		*M. murinus*		*M. rufus*		*G. alleni*		*G. denidoff*		*E. elegantulus*		*G. moholi*		*G.senegalensis*	
	F value	p value	F value	p value	F value	p value	F value	p value	F value	p value	F value	p value	F value	p value	F value	p value	F value	p value
C. major																		
C. medius	0.264	0.609																
M. murinus	3.020	0.086	2.760	0.100														
M. rufus	0.116	0.734	0.023	0.879	2.330	0.130												
G. alleni	0.001	0.974	0.300	0.587	3.560	0.062	0.121	0.730										
G. demidoff	0.190	0.664	0.001	0.972	2.530	0.114	0.010	0.920	0.199	0.656								
E. elegantulus	0.015	0.903	0.142	0.708	3.070	0.083	0.042	0.838	0.011	0.919	0.106	0.746						
G. moholi	0.388	0.535	2.180	0.143	9.270	0.003	1.150	0.285	0.539	0.465	1.850	0.176	0.733	0.394				
G. senegalensus	0.155	0.694	1.700	0.193	10.100	0.002	0.721	0.397	0.238	0.626	1.460	0.228	0.427	0.514	0.202	0.653		
G. zanzibaricus	1.640	0.207	1.250	0.270	0.089	0.767	1.250	0.269	1.950	0.169	1.030	0.313	1.370	0.246	4.480	0.037	4.070	0.045
O. crassicaudatus	0.008	0.929	0.444	0.507	6.690	0.011	0.132	0.717	0.003	0.957	0.326	0.569	0.008	0.928	1.380	0.241	0.920	0.338
O. garnettii	0.074	0.787	1.000	0.319	6.950	0.009	0.444	0.507	0.116	0.734	0.871	0.352	0.223	0.638	0.232	0.631	0.021	0.886
A. laniger	0.296	0.589	1.420	0.239	6.140	0.015	0.852	0.361	0.399	0.531	1.290	0.260	0.506	0.480	0.008	0.928	0.191	0.662
I. Indri	0.223	0.638	0.000	0.998	1.740	0.189	0.019	0.891	0.243	0.624	0.001	0.979	0.102	0.751	1.260	0.264	0.754	0.386
P. diadema	0.320	0.574	0.014	0.907	1.970	0.164	0.059	0.809	0.364	0.549	0.018	0.894	0.188	0.666	2.020	0.159	1.530	0.218
P. verreauxi	0.194	0.661	0.024	0.878	3.400	0.068	0.001	0.974	0.209	0.649	0.009	0.926	0.081	0.777	1.920	0.169	1.320	0.252
E. fulvus	0.261	0.610	0.033	0.857	5.700	0.018	0.001	0.969	0.275	0.601	0.014	0.907	0.136	0.712	3.670	0.057	3.440	0.065
E. macaco	0.004	0.949	0.370	0.545	4.900	0.029	0.130	0.719	0.001	0.977	0.255	0.615	0.009	0.923	0.864	0.354	0.428	0.514
E. mongoz	1.410	0.239	0.669	0.416	1.610	0.207	0.701	0.405	1.720	0.194	0.550	0.460	1.170	0.283	6.360	0.013	6.360	0.012
E. rubriventer	0.192	0.663	1.220	0.275	4.130	0.045	0.803	0.374	0.286	0.596	0.709	0.402	0.277	0.601	0.018	0.893	0.011	0.916
H. griseus	0.809	0.373	0.370	0.546	0.587	0.446	0.449	0.506	0.946	0.336	0.310	0.579	0.600	0.442	2.720	0.102	2.210	0.138
L. catta	0.569	0.454	0.149	0.701	1.230	0.270	0.221	0.640	0.655	0.422	0.138	0.711	0.407	0.526	2.620	0.109	2.130	0.146
V. variegata	4.090	0.048	4.190	0.045	0.100	0.752	3.580	0.063	4.970	0.030	3.470	0.066	3.910	0.052	10.400	0.002	10.900	0.001
L. ruficaudatus	0.153	0.697	0.008	0.929	2.350	0.128	0.003	0.954	0.165	0.687	0.002	0.963	0.068	0.795	1.420	0.237	0.980	0.323
L. tardigradus	0.451	0.505	0.064	0.801	2.820	0.096	0.119	0.732	0.542	0.465	0.074	0.786	0.355	0.554	4.240	0.042	5.640	0.019
N. bengalensis	0.040	0.843	0.117	0.734	3.220	0.076	0.025	0.874	0.036	0.851	0.074	0.787	0.005	0.946	0.988	0.323	0.611	0.435
N. coucang	0.144	0.705	0.051	0.821	4.760	0.031	0.000	0.983	0.151	0.698	0.028	0.867	0.065	0.799	2.670	0.104	2.890	0.091
P. potto	0.124	0.725	0.021	0.885	3.600	0.059	0.000	0.986	0.130	0.719	0.011	0.917	0.069	0.793	2.380	0.125	3.250	0.073

Goswami model BASE- PC4	*G. zanzibaricus*		*O. crassicaudatus*		*O. garnettii*		*A. laniger*		*I. indri*		*P. diadema*		*P. verreauxi*		*E. fulvus*		*E. macaco*	
	F value	p value	F value	p value	F value	p value	F value	p value	F value	p value	F value	p value	F value	p value	F value	p value	F value	p value
C. major																		
C. medius																		
M. murinus																		
M. rufus																		
G. alleni																		
G. demidoff																		
E. elegantulus																		
G. moholi																		
G. senegalensus																		
G. zanzibaricus																		
O. crassicaudatus	2.800	0.097																
O. garnettii	2.860	0.093	0.408	0.524														
A. laniger	2.900	0.095	0.993	0.321	0.198	0.657												
I. Indri	1.070	0.304	0.221	0.639	0.514	0.475	1.070	0.304										
P. diadema	0.896	0.349	0.499	0.481	0.956	0.330	1.360	0.249	0.011	0.916								
P. verreauxi	1.730	0.193	0.259	0.611	0.790	0.376	1.420	0.238	0.016	0.900	0.070	0.792						
E. fulvus	2.200	0.140	0.544	0.461	1.830	0.177	2.580	0.110	0.015	0.903	0.090	0.765	0.000	0.997				
E. macaco	2.490	0.119	0.001	0.978	0.212	0.646	0.681	0.412	0.238	0.627	0.441	0.509	0.233	0.631	0.352	0.553		
E. mongoz	0.496	0.483	3.050	0.083	3.910	0.050	4.240	0.043	0.395	0.531	0.340	0.561	1.030	0.312	1.600	0.208	2.240	0.137
E. rubriventer	3.540	0.066	0.326	0.569	0.025	0.875	0.033	0.857	1.230	0.272	1.310	0.258	1.090	0.300	0.959	0.329	0.323	0.571
H. griseus	0.187	0.667	1.240	0.268	1.530	0.218	1.880	0.177	0.322	0.572	0.224	0.638	0.592	0.444	0.710	0.400	1.140	0.288
L. catta	0.475	0.493	0.946	0.333	1.400	0.238	1.800	0.186	0.115	0.735	0.064	0.801	0.291	0.591	0.388	0.534	0.818	0.368
V. variegata	0.335	0.565	8.250	0.005	7.600	0.007	6.700	0.012	3.020	0.086	3.110	0.083	5.240	0.025	7.530	0.007	6.640	0.012
L. ruficaudatus	1.130	0.292	0.213	0.645	0.590	0.444	0.955	0.334	0.006	0.938	0.034	0.854	0.001	0.970	0.002	0.967	0.194	0.661
L. tardigradus	0.830	0.367	1.590	0.210	2.600	0.110	2.050	0.159	0.035	0.851	0.009	0.924	0.188	0.666	0.465	0.496	0.883	0.350
N. bengalensis	1.540	0.221	0.039	0.844	0.330	0.567	0.644	0.427	0.089	0.767	0.171	0.681	0.054	0.816	0.081	0.777	0.038	0.845
N. coucang	1.680	0.198	0.355	0.552	1.310	0.254	1.590	0.211	0.024	0.876	0.101	0.752	0.005	0.946	0.013	0.910	0.210	0.647
P. potto	1.110	0.295	0.382	0.537	1.360	0.245	1.360	0.245	0.009	0.925	0.051	0.822	0.000	0.992	0.001	0.981	0.192	0.662

Goswami model BASE- PC4	*E. mongoz*		*E. rubriventer*		*H. griseus*		*L. catta*		*V. variegata*		*L. ruficaudatus*		*L. tardigradus*		*N. bengalensis*		*N. coucang*	
	F value	p value	F value	p value	F value	p value	F value	p value	F value	p value	F value	p value	F value	p value	F value	p value	F value	p value
C. major																		
C. medius																		
M. murinus																		
M. rufus																		
G. alleni																		
G. demidoff																		
E. elegantulus																		
G. moholi																		
G. senegalensus																		
G. zanzibaricus																		
O. crassicaudatus																		
O. garnettii																		
A. laniger																		
I. Indri																		
P. diadema																		
P. verreauxi																		
E. fulvus																		
E. macaco																		
E. mongoz																		
E. rubriventer	3.070	0.084																
H. griseus	0.009	0.924	0.809	0.373														
L. catta	0.051	0.822	0.569	0.454	0.053	0.819												
V. variegata	2.910	0.092	6.430	0.014	1.150	0.287	2.060	0.155										
L. ruficaudatus	0.640	0.426	0.878	0.353	0.380	0.541	0.175	0.677	3.520	0.066								
L. tardigradus	0.408	0.525	1.270	0.265	0.169	0.683	0.036	0.849	3.800	0.056	0.087	0.770						
N. bengalensis	1.270	0.264	0.501	0.483	0.647	0.425	0.405	0.527	4.450	0.039	0.048	0.828	0.315	0.577				
N. coucang	1.560	0.214	0.648	0.423	0.583	0.447	0.351	0.555	5.920	0.017	0.009	0.927	0.491	0.485	0.032	0.858		
P. potto	1.000	0.319	0.434	0.511	0.361	0.549	0.212	0.646	4.110	0.044	0.002	0.968	0.338	0.562	0.037	0.848	0.006	0.938

Goswami model BASE- PC5	*C. major*		*C.medius*		*M. murinus*		*M. rufus*		*G. alleni*		*G. denidoff*		*E. elegantulus*		*G. moholi*		*G.senegalensis*	
	F value	p value	F value	p value	F value	p value	F value	p value	F value	p value	F value	p value	F value	p value	F value	p value	F value	p value
C. major																		
C. medius	0.939	0.337																
M. murinus	0.077	0.782	1.840	0.178														
M. rufus	2.550	0.116	6.730	0.012	1.090	0.298												
G. alleni	3.200	0.080	0.772	0.384	4.110	0.046	11.800	0.001										
G. demidoff	2.780	0.099	1.060	0.306	5.180	0.025	9.140	0.003	0.019	0.890								
E. elegantulus	0.017	0.896	1.430	0.237	0.033	0.857	1.990	0.163	3.940	0.052	4.040	0.048						
G. moholi	0.845	0.360	0.001	0.978	2.010	0.159	5.960	0.016	0.859	0.356	1.340	0.250	1.410	0.238				
G. senegalensus	3.610	0.059	1.110	0.293	8.070	0.005	14.100	0.000	0.068	0.795	0.274	0.601	5.950	0.016	1.410	0.235		
G. zanzibaricus	2.920	0.094	0.841	0.364	3.860	0.053	9.880	0.003	0.019	0.891	0.000	0.994	3.600	0.063	0.957	0.331	0.173	0.678
O. crassicaudatus	0.611	0.436	0.066	0.798	1.830	0.178	5.530	0.020	1.380	0.243	2.260	0.135	1.150	0.286	0.061	0.806	3.320	0.070
O. garnettii	0.021	0.884	1.140	0.288	0.308	0.580	2.810	0.096	3.450	0.066	4.930	0.028	0.104	0.748	1.260	0.264	8.750	0.003
A. laniger	6.880	0.012	4.020	0.051	10.100	0.002	17.000	0.000	1.180	0.284	0.965	0.329	8.900	0.004	4.960	0.028	3.910	0.050
I. Indri	3.390	0.071	1.560	0.217	4.870	0.030	8.990	0.004	0.305	0.583	0.197	0.658	4.260	0.043	1.840	0.178	0.940	0.333
P. diadema	1.460	0.233	0.257	0.614	2.750	0.101	6.240	0.016	0.058	0.810	0.151	0.699	2.110	0.152	0.345	0.558	0.017	0.897
P. verreauxi	0.035	0.853	0.619	0.434	0.272	0.603	2.400	0.126	2.260	0.138	2.940	0.090	0.113	0.738	0.677	0.412	4.440	0.036
E. fulvus	0.439	0.509	0.036	0.849	1.490	0.224	3.750	0.054	0.926	0.337	1.740	0.188	0.852	0.357	0.034	0.853	2.650	0.104
E. macaco	0.007	0.935	0.985	0.324	0.175	0.676	2.380	0.127	3.090	0.083	3.790	0.054	0.053	0.819	1.030	0.312	5.670	0.018
E. mongoz	1.900	0.172	0.651	0.422	4.440	0.037	6.980	0.010	0.002	0.962	0.043	0.835	3.040	0.085	0.925	0.338	0.060	0.807
E. rubriventer	0.474	0.495	1.830	0.183	0.241	0.625	0.066	0.798	3.450	0.070	3.600	0.061	0.392	0.534	1.990	0.161	5.220	0.023
H. griseus	0.306	0.583	0.007	0.934	0.744	0.391	2.470	0.122	0.422	0.519	0.641	0.426	0.487	0.488	0.006	0.941	0.648	0.422
L. catta	0.706	0.404	0.000	0.990	1.370	0.244	5.010	0.029	0.615	0.436	0.834	0.364	1.050	0.309	0.000	0.991	0.765	0.383
V. variegata	3.140	0.082	0.882	0.351	4.690	0.033	11.200	0.001	0.000	0.990	0.019	0.891	4.180	0.045	1.010	0.317	0.091	0.764
L. ruficaudatus	0.000	1.000	0.537	0.467	0.062	0.804	0.994	0.324	1.540	0.221	2.280	0.135	0.009	0.924	0.694	0.407	3.760	0.054
L. tardigradus	0.021	0.884	1.430	0.237	0.329	0.567	3.910	0.053	4.160	0.047	5.410	0.023	0.113	0.738	1.630	0.205	14.100	0.000
N. bengalensis	0.467	0.498	0.136	0.714	0.928	0.338	5.860	0.020	1.550	0.221	1.670	0.200	0.718	0.401	0.121	0.728	2.070	0.152
N. coucang	0.425	0.516	0.338	0.562	1.460	0.230	5.910	0.017	2.390	0.125	3.560	0.062	0.873	0.352	0.353	0.553	7.060	0.008
P. potto	0.688	0.408	0.015	0.902	2.260	0.135	5.340	0.022	1.040	0.308	2.010	0.158	1.330	0.250	0.011	0.917	3.700	0.055

Goswami model BASE- PC5	*G. zanzibaricus*		*O. crassicaudatus*		*O. garnettii*		*A. laniger*		*I. indri*		*P. diadema*		*P. verreauxi*		*E. fulvus*		*E. macaco*	
	F value	p value	F value	p value	F value	p value	F value	p value	F value	p value	F value	p value	F value	p value	F value	p value	F value	p value
C. major																		
C. medius																		
M. murinus																		
M. rufus																		
G. alleni																		
G. demidoff																		
E. elegantulus																		
G. moholi																		
G. senegalensus																		
G. zanzibaricus																		
O. crassicaudatus	1.440	0.233																
O. garnettii	3.260	0.074	1.060	0.304														
A. laniger	0.715	0.402	6.870	0.010	10.700	0.001												
I. Indri	0.160	0.691	2.490	0.117	4.430	0.037	0.119	0.732										
P. diadema	0.114	0.738	0.691	0.408	2.230	0.138	1.440	0.236	0.493	0.485								
P. verreauxi	2.180	0.145	0.492	0.484	0.006	0.937	6.620	0.013	3.050	0.085	1.290	0.261						
E. fulvus	0.986	0.322	0.002	0.969	0.929	0.336	5.060	0.026	1.840	0.176	0.499	0.481	0.410	0.523				
E. macaco	2.930	0.091	0.808	0.370	0.006	0.940	8.550	0.005	3.870	0.052	1.810	0.182	0.017	0.897	0.649	0.421		
E. mongoz	0.028	0.868	1.870	0.173	4.530	0.035	1.280	0.262	0.323	0.571	0.041	0.839	2.290	0.133	1.570	0.211	3.040	0.084
E. rubriventer	3.260	0.077	1.810	0.181	0.776	0.380	6.030	0.018	3.860	0.054	2.150	0.149	0.642	0.426	1.360	0.245	0.610	0.437
H. griseus	0.484	0.490	0.005	0.946	0.368	0.545	2.000	0.164	0.981	0.326	0.174	0.678	0.201	0.655	0.002	0.968	0.337	0.563
L. catta	0.696	0.408	0.039	0.843	0.772	0.381	3.210	0.079	1.340	0.251	0.213	0.646	0.452	0.503	0.021	0.884	0.714	0.401
V. variegata	0.017	0.896	1.670	0.199	4.080	0.046	1.330	0.254	0.326	0.570	0.074	0.786	2.610	0.110	1.160	0.284	3.480	0.065
L. ruficaudatus	1.510	0.225	0.577	0.449	0.020	0.889	4.080	0.050	2.250	0.139	0.963	0.331	0.025	0.876	0.504	0.478	0.005	0.944
L. tardigradus	3.600	0.064	1.520	0.219	0.001	0.973	11.000	0.002	4.390	0.040	2.240	0.140	0.012	0.915	1.270	0.262	0.003	0.954
N. bengalensis	1.510	0.226	0.028	0.867	0.353	0.553	5.120	0.029	2.190	0.145	0.601	0.442	0.183	0.671	0.028	0.869	0.361	0.550
N. coucang	2.300	0.133	0.153	0.696	0.638	0.426	9.480	0.003	3.420	0.067	1.270	0.263	0.248	0.620	0.155	0.694	0.502	0.480
P. potto	1.110	0.295	0.038	0.846	1.700	0.193	6.120	0.015	2.080	0.151	0.516	0.474	0.697	0.405	0.020	0.888	1.080	0.300

Goswami model BASE- PC5	*E. mongoz*		*E. rubriventer*		*H. griseus*		*L. catta*		*V. variegata*		*L. ruficaudatus*		*L. tardigradus*		*N. bengalensis*		*N. coucang*	
	F value	p value	F value	p value	F value	p value	F value	p value	F value	p value	F value	p value	F value	p value	F value	p value	F value	p value
C. major																		
C. medius																		
M. murinus																		
M. rufus																		
G. alleni																		
G. demidoff																		
E. elegantulus																		
G. moholi																		
G. senegalensus																		
G. zanzibaricus																		
O. crassicaudatus																		
O. garnettii																		
A. laniger																		
I. Indri																		
P. diadema																		
P. verreauxi																		
E. fulvus																		
E. macaco																		
E. mongoz																		
E. rubriventer	2.670	0.106																
H. griseus	0.391	0.534	0.306	0.583														
L. catta	0.493	0.484	0.706	0.404	0.005	0.946												
V. variegata	0.004	0.949	3.770	0.057	0.508	0.479	0.695	0.407										
L. ruficaudatus	1.770	0.188	0.264	0.610	0.206	0.652	0.427	0.516	1.920	0.171								
L. tardigradus	4.860	0.030	0.735	0.395	0.342	0.562	0.895	0.348	4.900	0.031	0.013	0.911						
N. bengalensis	1.090	0.300	1.300	0.261	0.022	0.882	0.093	0.762	1.640	0.206	0.208	0.651	0.483	0.491				
N. coucang	3.140	0.079	1.620	0.206	0.063	0.802	0.207	0.650	2.860	0.094	0.348	0.557	1.070	0.304	0.007	0.932		
P. potto	1.820	0.179	1.810	0.181	0.000	0.985	0.007	0.932	1.320	0.252	0.749	0.388	2.650	0.105	0.079	0.778	0.465	0.496

– Appendix 7 –

Inter-species differences in allometric scaling – Evo-maps

Evo-maps are used to illustrate where inter- and intra-species allometric patterns diverge from each other. Where branches are shown in green or red, intra-specific scalars are larger or smaller than the corresponding inter-specific scalar, respectively. In addition, the thickness of the branch represents the rate of change along that branch and the size of the circles at the tip and at the ancestral nodes are indicative of the size of the trait, in this instance the size of the difference between the slope of the intra-species regression of shape against size and the inter-species slope of the same regression.

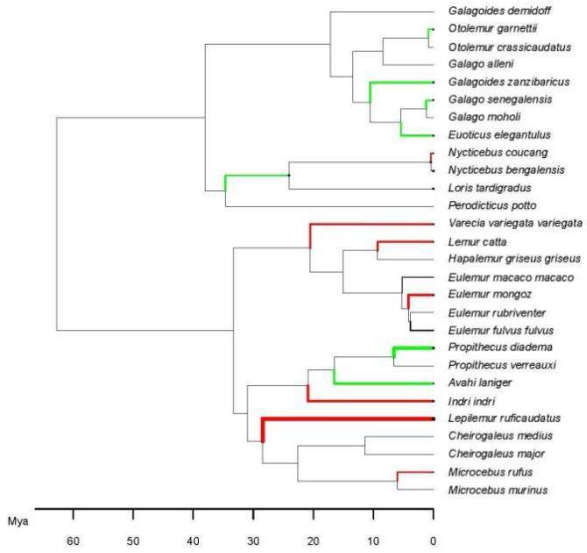

PC2

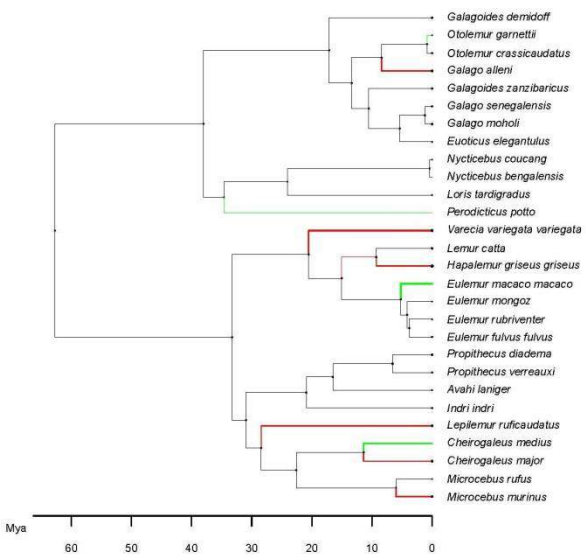

PC3

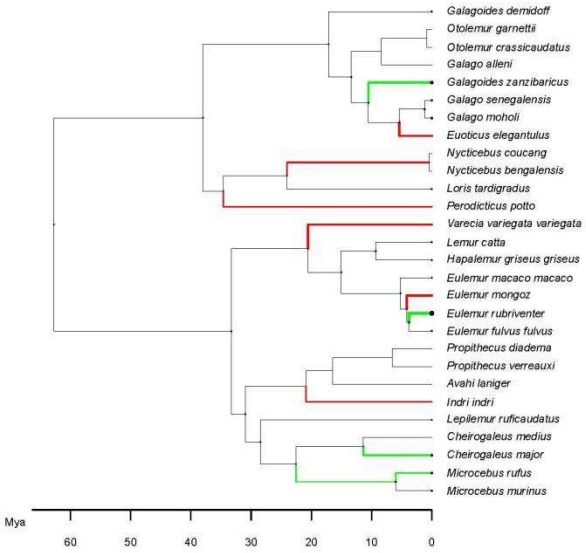

PC4

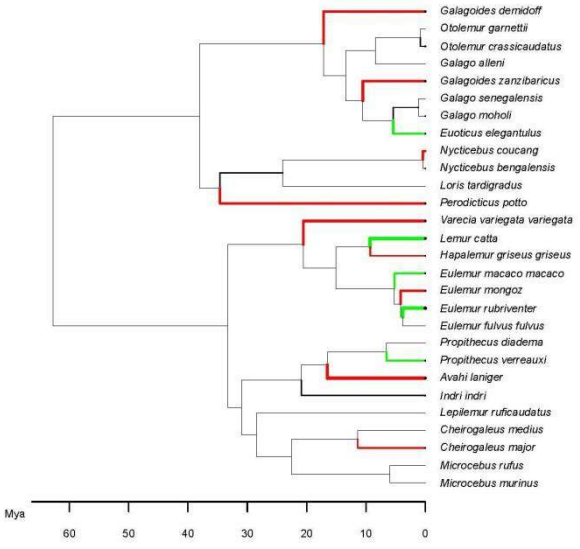

PC5

Evo-map of intra-species allometric scaling, in comparison to inter-species allometric scaling, for the whole cranium, PCs 2-5. Where green indicates that the intra-species allometric slope is more positive than the inter-species allometric slope and red that it is more negative.

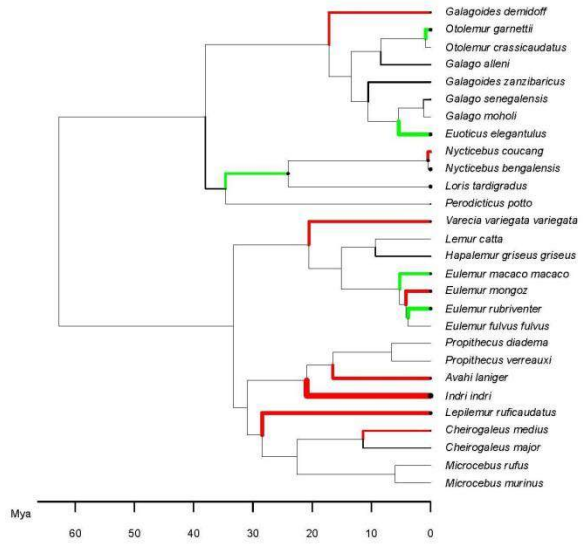

PC2

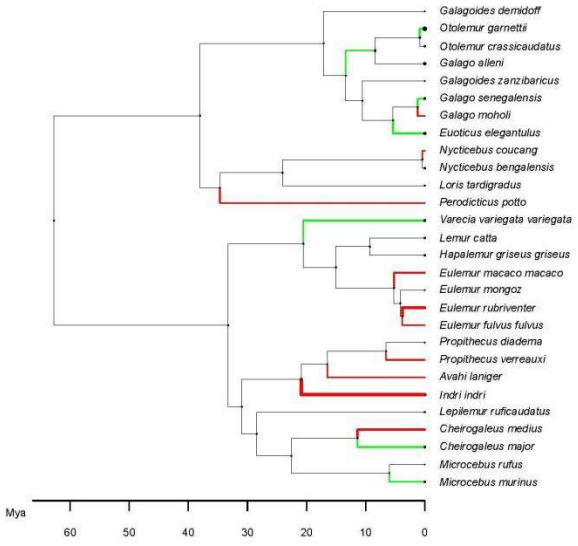

PC3

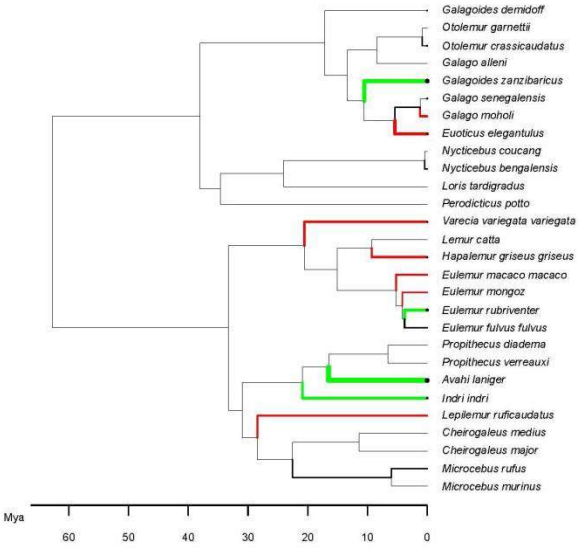

PC4

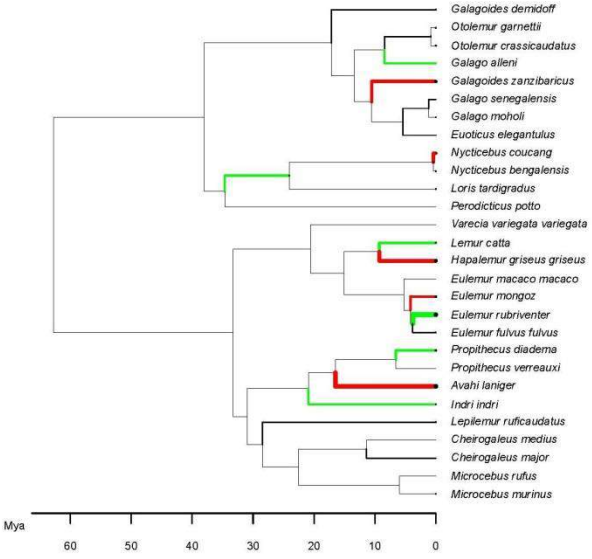

PC5

Evo-map of intra-species allometric scaling, in comparison to inter-species allometric scaling, for the 2* model Face module, PCs 2-5. Where green indicates that the intra-species allometric slope is more positive than the inter-species allometric slope and red that it is more negative.

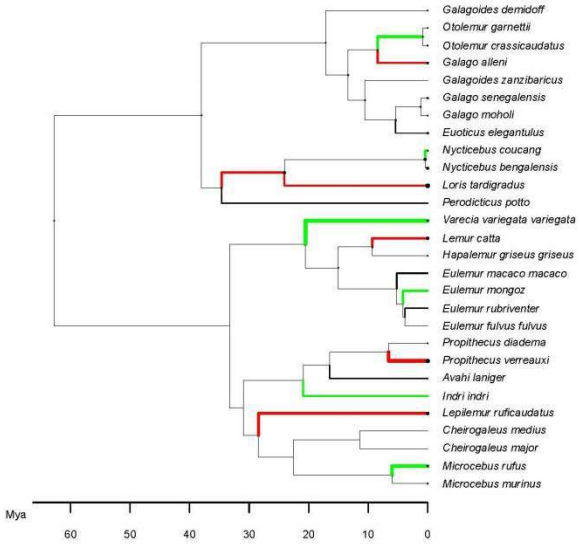

PC2

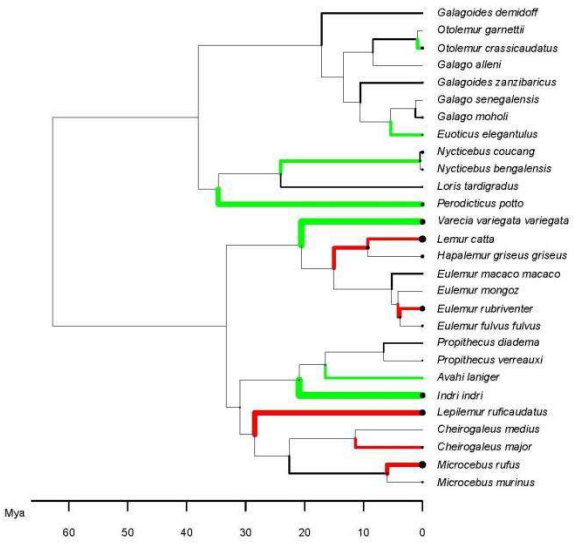

PC3

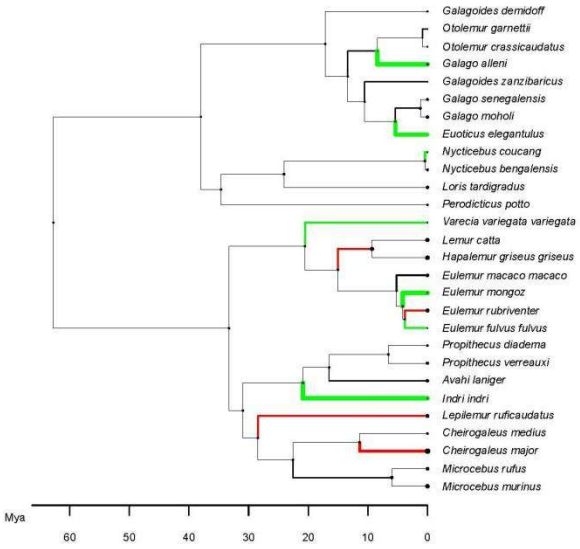

PC5

Evo-map of intra-species allometric scaling, in comparison to inter-species allometric scaling, for the 2* model Vault module, PCs 2, 3 and 5. Where green indicates that the intra-species allometric slope is more positive than the inter-species allometric slope and red that it is more negative.

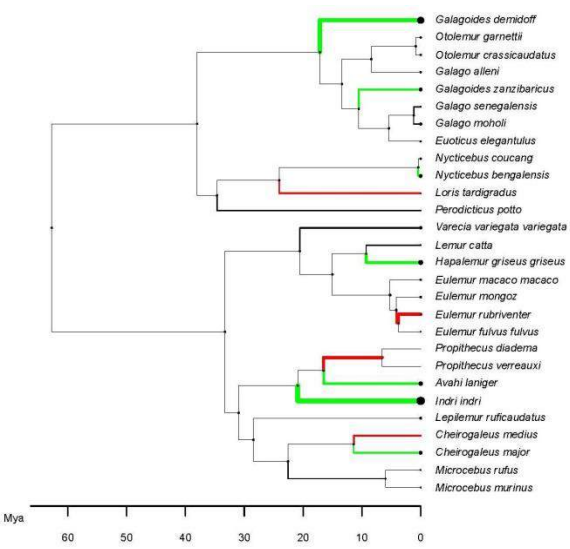

PC2

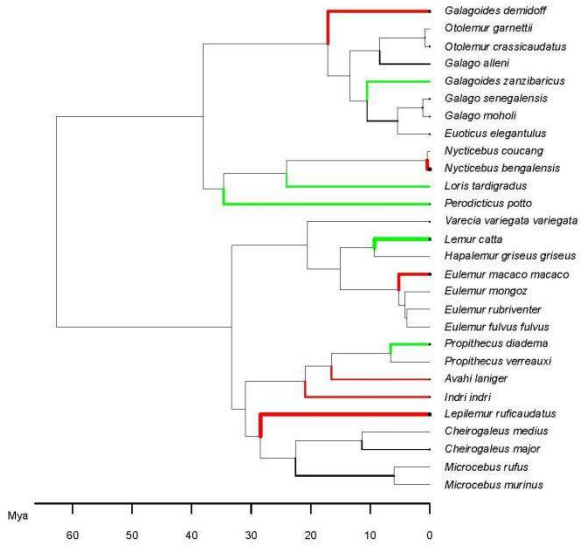

PC3

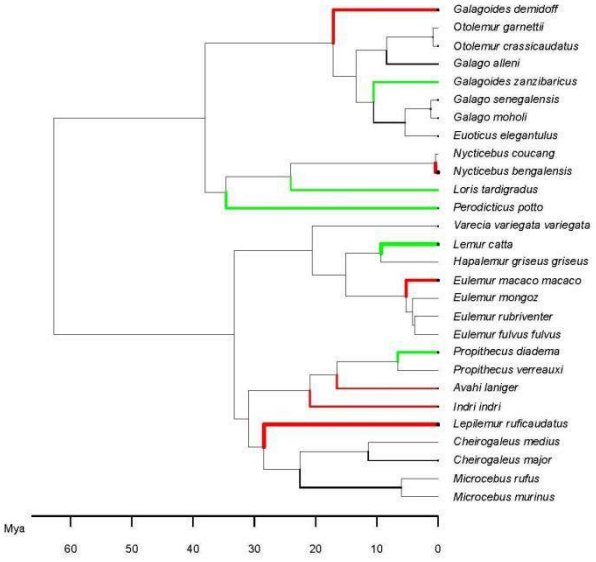

PC4

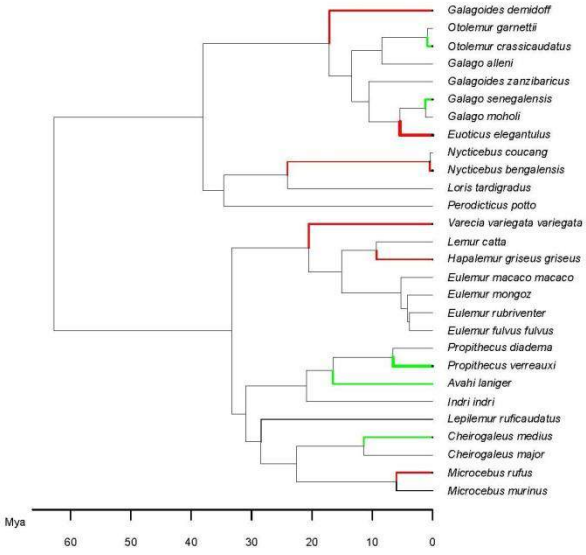

PC5

Evo-map of intra-species allometric scaling, in comparison to inter-species allometric scaling, for the Goswami model Face module, PCs 2- 5. Where green indicates that the intra-species allometric slope is more positive than the inter-species allometric slope and red that it is more negative.

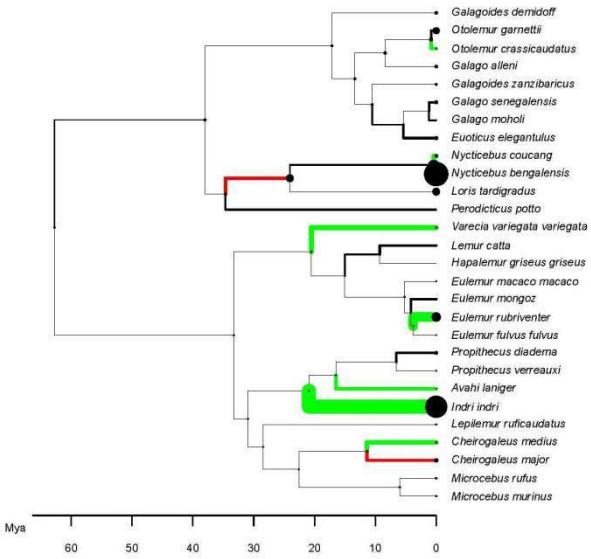

PC2

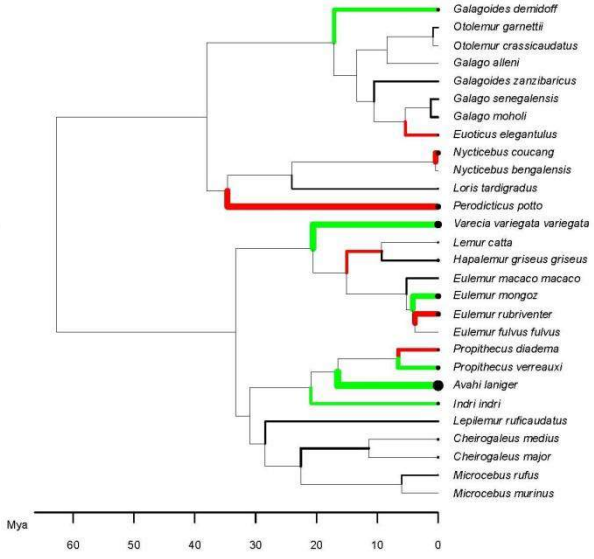

PC4

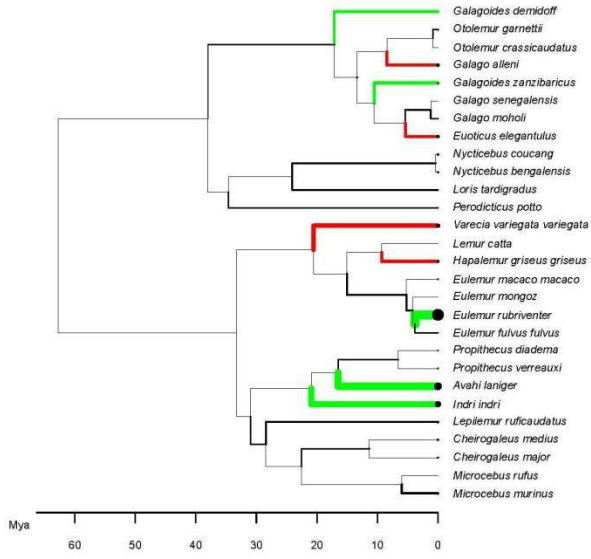

PC5

Evo-map of intra-species allometric scaling, in comparison to inter-species allometric scaling, for the Goswami model Orbit module, PCs 2, 4 and 5. Where green indicates that the intra-species allometric slope is more positive than the inter-species allometric slope and red that it is more negative.

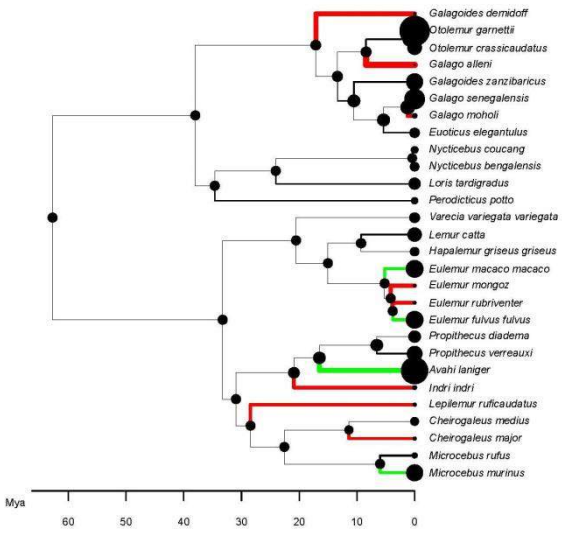

PC2

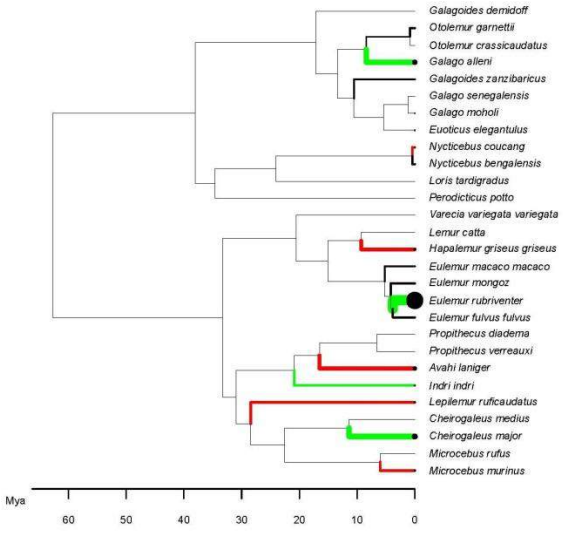

PC3

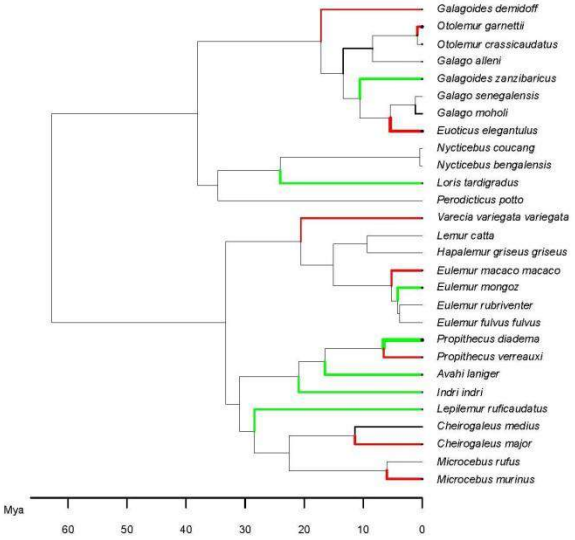

PC4

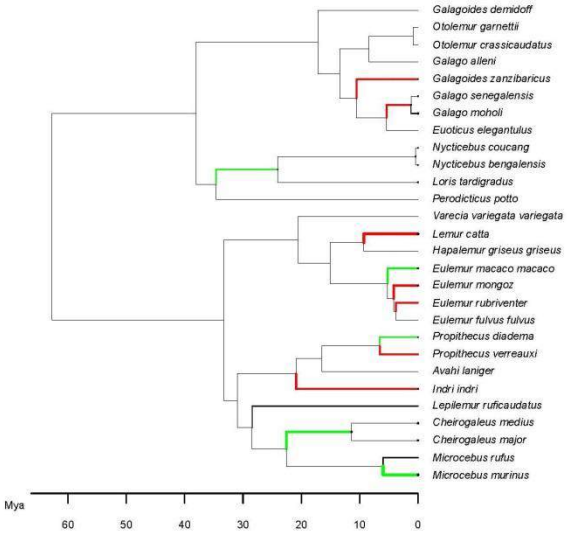

PC5

Evo-map of intra-species allometric scaling, in comparison to inter-species allometric scaling, for the Goswami model Oral module, PCs 2-5. Where green indicates that the intra-species allometric slope is more positive than the inter-species allometric slope and red that it is more negative.

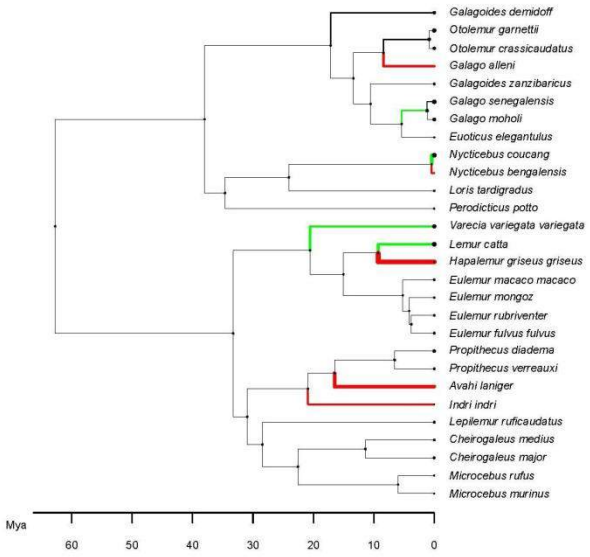

PC1

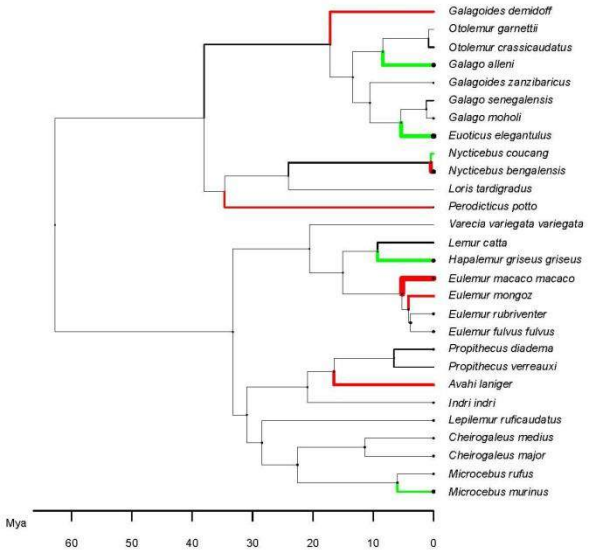

PC2

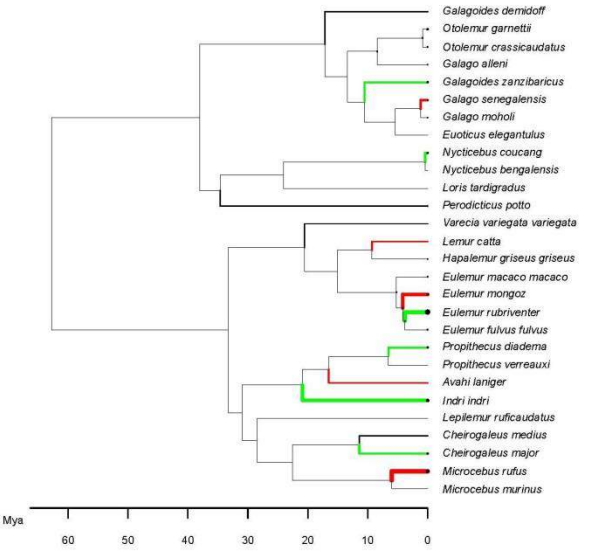

PC4

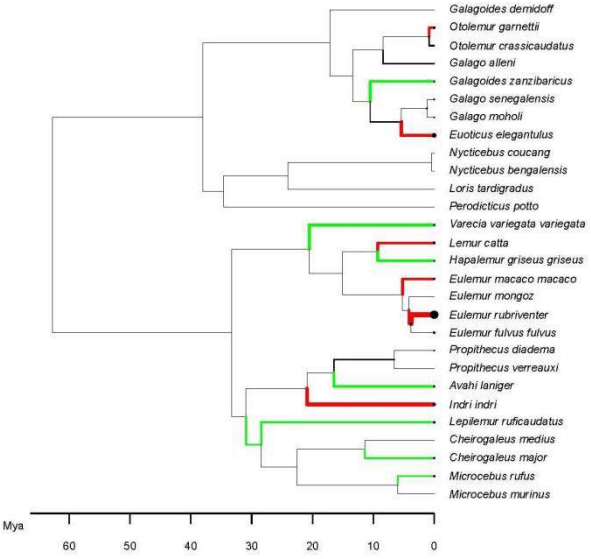

PC5

Evo-map of intra-species allometric scaling, in comparison to inter-species allometric scaling, for the Goswami model Zygomatic module, PCs 1,2,4 and 5. Where green indicates that the intra-species allometric slope is more positive than the inter-species allometric slope and red that it is more negative.

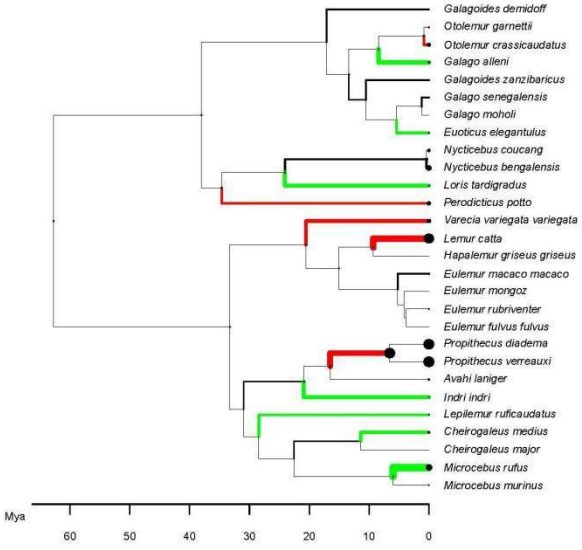

PC3

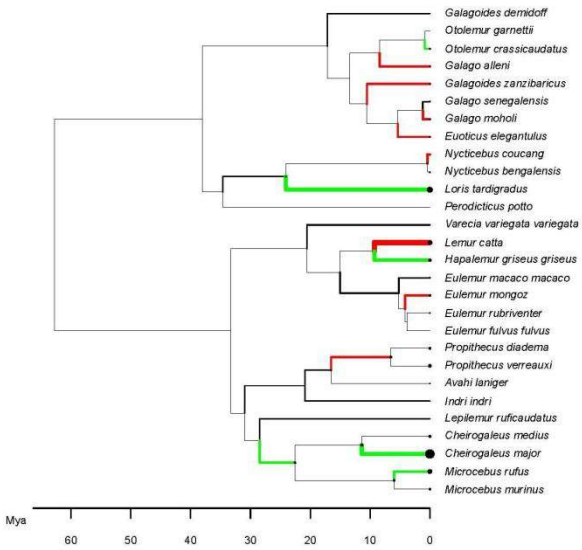

PC4

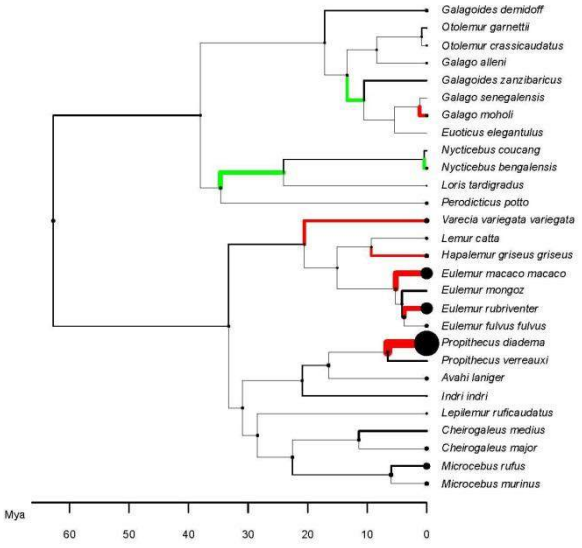

PC5

Evo-map of intra-species allometric scaling, in comparison to inter-species allometric scaling, for the Goswami model Vault module, PCs 3-5. Where green indicates that the intra-species allometric slope is more positive than the inter-species allometric slope and red that it is more negative.

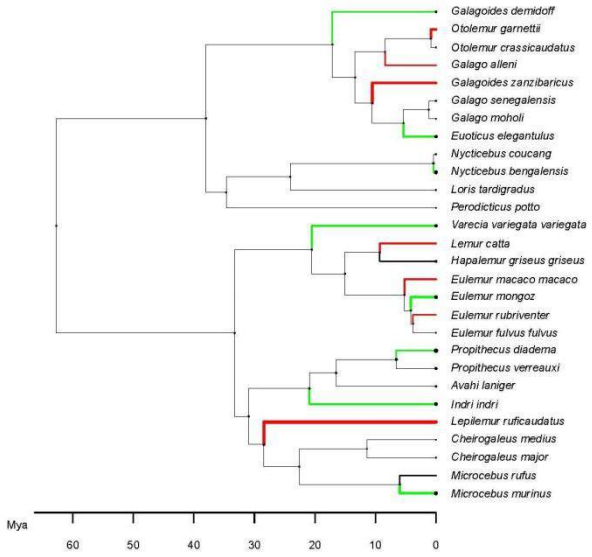

PC1

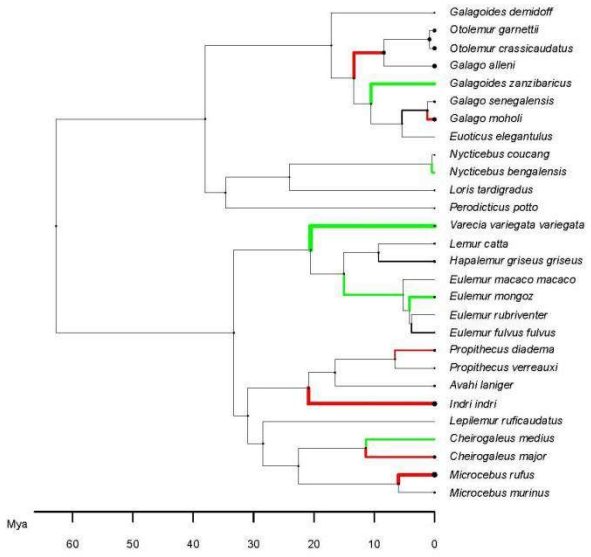

PC2

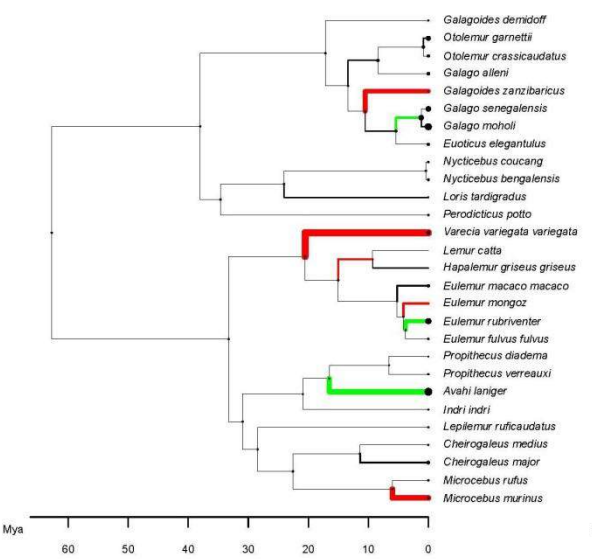

PC4

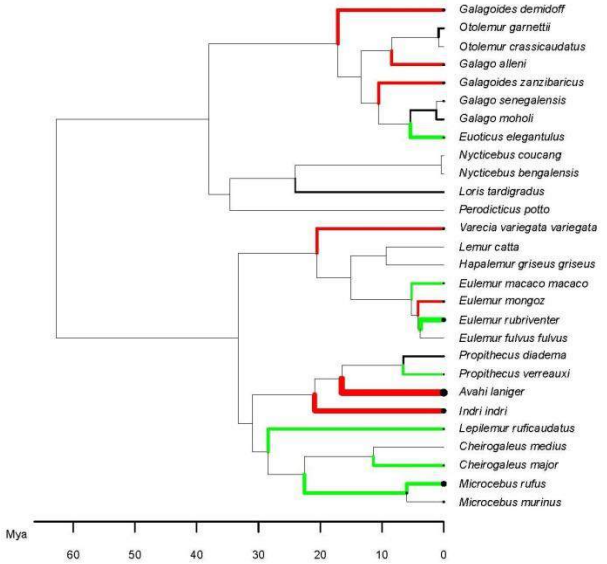

PC5

Evo-map of intra-species allometric scaling, in comparison to inter-species allometric scaling, for the Goswami model Base module, PCs 1,2,4 and 5. Where green indicates that the intra-species allometric slope is more positive than the inter-species allometric slope and red that it is more negative.